JOURNAL OF

CHROMATOGRAPHY

RNATIONAL JOURNAL ON CHROMATOGRAPHY, ELECTROPHORESIS AND RELATED METHODS

SYMPOSIUM VOLUMES

ELSEVIER

Chromatography and Modification of Nucleosides

Part C
Modified Nucleosides in Cancer and Normal Metabolism - Methods and Applications

edited by **C.W. Gehrke** *and* **K.C.T. Kuo**, *Department of Biochemistry, University of Missouri-Columbia, and Cancer Research Center, P.O. Box 1268, Columbia, MO, USA*

Chromatography and Modification of Nucleosides is a four-volume work which provides state-of-the-art chromatography and analytical methods for use in a wide spectrum of nucleic acid modification research.

The focus of Part A is the presentation of advanced methods for modification research on tRNAs, mRNAs, mtRNAs, tRNAs and DNAs. HPLC-UV, GC-MS, NMR, FT-IR and affinity chromatography approaches to nucleic acid modification studies are presented, as are nucleoside, oligonucleotide and nucleic acid isolation techniques. Part B has as its central theme the modified nucleosides of tRNA and the current analytical means for studying rRNA modifications. Modified nucleoside synthesis, function, structural conformation, biological regulation, and occurrence of modification in a wide range of tRNAs are presented, as is a chapter on DNA modification and a chapter on solid phase immunoassay for determining a particular modification.

The study of modified nucleosides in biological matrices (blood, urine) is the major thrust of Part C. As potential biological markers of disease, and for the insight that the modified nucleosides in fluids provide into the catabolism of the nucleic acids, a number of advanced methods for modified nucleoside isolation, separation, detection, characterization and measurement have been developed world-wide. Part C provides the reader with a comprehensive treatment of modified nucleosides as biochemical signals of neoplasia and normal metabolism. The final volume, Part D, will present structural characterization of unknown nucleosides as well as extensive biochemical, chemical and physical properties of RNA and DNA nucleosides, as a "database" for researchers in the field. Chromatographic methodology will be described for analysis of total modification of tRNAs and DNAs.

The chapters are written by leading scientists in their respective fields and present an up-to-date review on the roles of modified nucleosides in nucleic acids which will be extremely useful for workers in chromatography, molecular biology, genetics, biochemistry, biotechnology and the pharmaceutical industry.

JOURNAL

of

CHROMATOGRAPHY

SYMPOSIUM VOLUMES

"Duplex Bridge": main gate of Emperor's Palace in Tokyo, viewed from the front square of the palace. Tinted woodcut (anonymous, ca. 1939), probably made in celebration of 1939, which was the beginning of the 27th century of the Japanese Emperor Era.

SYMPOSIUM VOLUME

INTERNATIONAL SYMPOSIUM ON
CHROMATOGRAPHY (CIS'89)

Tokyo (Japan), October 17–20, 1990

Guest Editors

T. OKUYAMA
(Tokyo)

S. HONDA
(Higashi-Osaka)

T. HOSHINO
(Tokyo)

H. NAKAMURA
(Tokyo)

CONTENTS

INTERNATIONAL SYMPOSIUM ON CHROMATOGRAPHY (CIS'89), TOKYO, OCTOBER 17–20, 1989

FOREWORD

This volume represents the proceedings of the *CIS'89 Tokyo* symposium (Chromatography International Symposium, Tokyo, October 17–20, 1989), which was organized by the Division of Liquid Chromatography of The Japan Society for Analytical Chemistry.

About twenty years ago, some of the scientists in the Tokyo area assembled to discuss recent improvements of an amino acid analyzer. As the scope of the discussions widened, meetings were held every two months for ten years. They covered various topics in liquid chromatography (LC), such as affinity chromatography and high-performance liquid chromatography (HPLC), including applications to biological samples, novel packing materials, solvents for use in HPLC, and various items of instrumentation. After ten years of this activity, the group joined the Japan Society for Analytical Chemistry and developed into the "Discussion Group on Liquid Chromatography". It started the domestic annual meeting on LC and, some years later, the Spring Symposium on specific subjects.

For the tenth anniversary of the conference and twentieth anniversary of the group we wanted to organize an international conference and to invite many distinguished scientists from around the world. The purpose of the meeting was, of course, to increase international communication and to showcase the Japanese research frontier in chromatographic science as well as the persons and instrument companies active in it. At the same time we wanted to give young chromatographers, who would otherwise scarcely have a chance to participate in an international conference, an opportunity to overcome the language barrier and discuss chromatography in English.

In 1988 we established the Society for Chromatographic Sciences (Japan) to foster research in various aspects of LC, gas chromatography, supercritical fluid chromatography, capillary electrophoresis and all other areas of separation sciences and their industrial applications.

CIS'89 Tokyo was a complete succes, with more than 800 delegates and 54 commercial exhibitors participating. The following professional organizations lent their support:
The Japanese Biochemical Society
The Society of Synthetic Organic Chemistry
The Pharmaceutical Society of Japan
The Agricultural Chemical Society of Japan
The Japan Analytical Instrument Manufacturers' Association
The Society of Electrophoresis
The Japan Oil Chemists' Society
The Society for Sea Water Science, Japan
The Food Hygienic Society of Japan
The Society of Polymer Science, Japan
The Society for Chromatographic Sciences (Japan)
Istituto Superiore di Sanità Roma
Società Italiana di Biochimica Clinica

We would like to express our sincere thanks to those who supported our activity and

to all the members of the Organizing Committee. Special thanks are due to Dr. Heftmann for his diligent efforts in making this volume possible.

It is our hope that this kind of activity will be a signpost in international scientific cooperation, pointing the way to further international conferences on various aspects of chromatography in the near future.

Tokyo Metropolitian University, Tokyo (Japan)   T. OKUYAMA
Kinki University, Higashi-Osaka (Japan)   S. HONDA
Keio University, Tokyo (Japan)   T. HOSHINO
Tokyo University, Tokyo (Japan)   H. NAKAMURA

CHROMSYMP. 1888

Solubility parameter treatment for the characterization of the stationary phase in the reversed-phase chromatography of benzene derivatives

FUMIKO M. YAMAMOTO* and SOUJI ROKUSHIKA

Department of Chemistry, Faculty of Science, Kyoto University, Kyoto 606 (Japan)

ABSTRACT

Non-polar benzene derivatives were chromatographed on seven commercially available octadecyl columns with aqueous methanol as eluent. To interpret the differences in the retention behaviour on these columns, the role of the stationary phase was investigated by means of the solubility concept model. An apparent solubility parameter of the stationary phase, δ_s', was determined for the seven columns by using toluene as a standard solute. The values ranged from 14.32 to 14.91 $(cal/cm^3)^{1-2}$ with an 80% aqueous methanol eluent. The absolute value of the enthalpy change of solutes in the phase-transfer process, ΔH^0, was larger on C_{18} columns with a smaller δ_s'. The ΔH^0 value was predictable from the δ_s' when the physico-chemical parameters of the solute and of the mobile phase were given. The δ_s' was useful for characterizing the retention properties of the stationary phase.

INTRODUCTION

Chemically bonded octadecylsilica gel is the most popular packing material for reversed-phase chromatography. Various silica-based C_{18} materials have been provided by several manufacturers. Recently, new types of packings, such as capsule-type silica-based C_{18} materials and polymer-based C_{18} materials have become available. These C_{18} materials have different retention properties. It is well known that the retention data obtained with different columns under identical mobile phase conditions are hardly comparable. The need for characterization and classification of these materials has been expressed[1].

In reversed-phase chromatography, retention of solutes on a C_{18} column depends mainly on non-specific interactions, such as hydrophobic interactions, between the solute, mobile phase and stationary phase. The solubility concept model has been applied in semi-empirical descriptions of retention behaviour in this type of chromatography[2–6] and the polarities of solutes and mobile phases have been investigated to elucidate their role in retention. In previous papers[7,8], we expressed the polarity of the stationary phase by an apparent solubility parameter of the stationary

phase, δ'_s, by using the concept of solubility. The value of δ'_s was determined on a Nucleosil C_{18} column from chromatographic data for toluene with various compositions of methanol-containing eluents. A relationship between the δ'_s value and the methanol concentration in the mobile phase was reported[7]. In this paper, the δ'_s value was determined for seven different C_{18} columns and their characterization was studied on the basis of their δ'_s values.

EXPERIMENTAL

A Shimadzu LC-3A chromatograph including a Model SPD-2A UV detector and a Model CTO-2A column temperature controller (Shimadzu, Kyoto, Japan) was employed with a Model RI-SE51 refractometer (Showa Denko, Tokyo, Japan).

The octadecylsilica packing materials (all of particle size 5μm) used were Cosmosil C_{18} (Nacalai Tesque, Kyoto, Japan), LiChrosorb RP-18 (E. Merck, Darmstadt, F.R.G.), Spherosil XOA 600, (Rhône Poulenc, France), Nucleosil C_{18} (Macherey, Nagel & Co., Düren, F.R.G.) and Chemcosorb UH-ODS (Chemco, Osaka, Japan). These packings were slurry-packed into 25 × 0.4 cm I.D. or 15 × 0.46 cm I.D. columns, using the balanced-density technique. Asahipak ODP-50 (5 μm), with a vinyl alcohol copolymer-based structure (Asahi Chemical Industry, Tokyo, Japan), and Capcellpak C_{18} (5 μm) (Shiseido, Tokyo, Japan) were also used to compare their retention properties with those of the silica-based gels. Capcellpak C_{18} is a new type of C_{18} material prepared by coating the silica surface with a silicone polymer film and thereafter modifying the coated polymer with octadecyl groups[9].

Benzene derivatives, used as solutes, and other chemicals were purchased from Nacalai Tesque (Kyoto, Japan). Chromatography was performed with 30% or 80% aqueous methanol as the eluent at a flow-rate of 0.5 ml/min. The eluate was monitored with the UV detector for aromatic hydrocarbons and with the refractometer for n-alkanes.

RESULTS AND DISCUSSION

In the solubility concept model, the enthalpy change in the phase-transfer process. ΔH^0, is represented as the difference between the partial molar enthalpy changes, Δh^0, on dissolving a solute in the two phases. The value of Δh^0 is controlled with the molar volume and the solubility parameter. In chromatography, the enthalpy change on transferring a solute from the mobile phase to the stationary phase is represented as follows;

$$\Delta H^0 = \Delta h^0_{is} - \Delta h^0_{im} = V_i[(\delta_i - \delta_s)^2 - (\delta_i - \delta_m)^2] \tag{1}$$

where V_i is the molar volume of the solute, δ is the solubility parameter and the subscripts i, m and s refer to the solute, mobile phase and stationary phase, respectively. V_i, δ_i and δ_m are physico-chemical parameters, the values of which are obtained from non-chromatographic data[5,10]. Table I gives the values for the parameters used here. The solubility parameter of the mobile phase δ_m, was calculated from that of the pure solvent, δ_j, by using the following equation;

$$\delta_m = \Sigma v_j \delta_j \tag{2}$$

TABLE I

PHYSICO-CHEMICAL PARAMETERS FOR VARIOUS SOLUTES

Solute	V_i (cm^3)	δ_i $(cal/cm^3)^{1/2}$	Solute	V_i (cm^3)	δ_i $(cal/cm^3)^{1/2}$
n-Pentane	115.3	7.1	n-Propylbenzene	139.4	8.64
n-Hexane	130.8	7.3	Ethylbenzene	122.5	8.84
n-Heptane	146.5	7.4	Toluene	106.3	8.93
n-Octane	164.0	7.5	Benzene	88.9	9.1
n-Nonane	178.6	7.5[a]	Naphthalene	147.6	9.96
n-Amylbenzene	171.8	8.44[a]	Phenanthrene	196.7	9.8
n-Butylbenzene	156.1	8.58	Anthracene	196.7	9.9

[a] Values calculated from the heat of evaporation at 25°C by using the Hildebrand rule.

where v is the volume fraction of a constituent of the mobile phase. The values of δ_m for 30% and 80% aqueous methanol eluents were 20.83 and 16.31 $(cal/cm^3)^{1/2}$, respectively.

The stationary phase in reversed-phase chromatography is recognized as a ternary complex phase, consisting of octadecyl and unreacted silanol residues on the silica surface and a solvating layer on the residues. The polarity of such a stationary phase cannot be determined physico-chemically. However, the value of δ_s can be calculated by substituting the values of V_i, δ_i and δ_m into eqn. 1, when the ΔH^0 value for a solute is obtained experimentally from the van't Hoff plots. Thus, we determined the value of δ_s by using the retention data for toluene. The calculated δ_s was expressed as the "apparent" parameter, δ_s', which is a semi-experimental value for the polarity of the stationary phase.

Table II gives the δ_s' values for the seven different C_{18} columns with 30% and 80% aqueous methanol eluents. The δ_s' values for these C_{18} columns ranged from 14.32 to 14.91 $(cal/cm^3)^{1/2}$ with 80% aqueous methanol and from 18.24 to 19.01 $(cal/cm^3)^{1/2}$ with 30% aqueous methanol as eluent. As reported previously[7], it should be noted that the δ_s' values are larger than the solubility parameter of octadecane, which is assumed

TABLE II

δ_s' VALUES FOR VARIOUS C_{18} COLUMNS

Column	80% aqueous methanol $\delta_m = 16.31$ $(cal/cm^3)^{1/2}$	30% aqueous methanol eluent, $\delta_m = 20.83$ $(cal/cm^3)^{1/2}$
Capcellpak C_{18}	14.32	18.24
LiChrosorb RP-18	14.67	18.77
Chemcosorb UH-ODS	14.68	18.73
Nucleosil C_{18}	14.70	19.03
Cosmosil C_{18}	14.85	18.94
Spherosil XOA-600	14.88	18.75
Asahipak ODP	14.91	18.42

to be about 7 (ref. 6). The δ_s' value did not depend on the polarity of the fixed alkyl groups but on that of the complex stationary phase composed of the alkyl chains, the solvating layer on the residues. The δ_s' value changed on varying the polarity of the mobile phase, being lower with 80% than with 30% aqueous methanol.

The effect of the mobile phase composition on the δ_s' value was characteristic of the C_{18} materials. With conventional silica-based C_{18} materials, the difference in the δ_s' values under the two elution conditions ranged from 4.35 $(cal/cm^3)^{1/2}$ for Nucleosil C_{18} to 3.87 $(cal/cm^3)^{1/2}$ for Spherosil XOA. On a Capcellpak C_{18}, a capsule-type silica gel, the difference between the δ_s' values under the two elution conditions was 3.92 $(cal/cm^3)^{1/2}$. On polymer-based Asahipak ODP, the effect of the composition of the mobile phase on the δ_s' value was 3.51 $(cal/cm^3)^{1/2}$, which is smaller than those for the conventional silica-based C_{18} columns. The difference in the δ_s' values between C_{18} columns may reflect the difference in the solvation of the materials in aqueous methanol solution.

Fig. 1 shows the relationship between $-\Delta H^0$ and δ_s for benzene and n-alkylbenzenes with 80% aqueous methanol as eluent. The curves were drawn with a CAD (computer-aided design) system by substituting the values of V_i and δ_i for n-alkylbenzenes and the values of δ_m for 80% aqueous methanol into eqn. 1. The curves cross the horizontal line $(-\Delta H^0 = 0)$ at the points δ_m and $2\delta_i - \delta_m$. When the polarity of the stationary phase is higher than that of the solute, the absolute value of ΔH^0 decreases with increasing δ_s. The chromatographic conditions in this work are an example of such a case.

In Table III the experimental $-\Delta H^0$ and the calculated $-\Delta H^0$ values for n-alkylbenzenes on the various C_{18} columns are given. The experimental $-\Delta H^0$ values were evaluated from the Van 't Hoff plots of the retention data on the columns in the temperature range 40–70°C. The calculated $-\Delta H^0$ values were obtained from the plots in Fig. 1. The experimental values agreed with the calculated values, within experimental error. On the Capcellpak C_{18} and Asahipak ODP columns the absolute mean deviations were 0.75% and 1.07%, respectively. The structure of the materials,
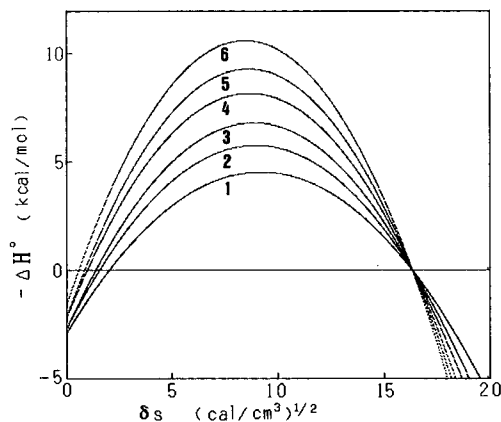
Fig. 1. Correlation curves for $-\Delta H^0$ and δ_s. Solutes: 1 = benzene; 2 = toluene; 3 = ethylbenzene; 4 = n-propylbenzene; 5 = n-butylbenzene; 6 = n-amylbenzene. Eluent: 80% aqueous methanol.

TABLE III

CHROMATOGRAPHICALLY MEASURED (obs) AND CALCULATED (cal) $-\Delta H^0$ VALUES (kcal/mol) FOR n-ALKYLBENZENES

Deviation: $|\Delta H^0(obs) - \Delta H^0(cal)| \cdot 100/\Delta H^0(obs)|$. Eluent: 80% aqueous methanol.

Solute	Capcellpak C_{18}		LiChrosorb RP-18		Chemcosorb UH-ODS		Nucleosil C_{18}	
	$-\Delta H^0(obs)$	$-\Delta H^0(cal)$	$-\Delta H^0(obs)$	$-\Delta H^0(cal)$	$-\Delta H^0(obs)$	$-\Delta H^0(cal)$	$-\Delta H^0(obs)$	$-\Delta H^0(cal)$
Benzene	2.15	2.18	1.91	1.85	1.83	1.84	1.83	1.82
Ethylbenzene	3.14	3.16	2.62	2.67	2.66	2.66	2.60	2.63
n-Propylbenzene	3.62	3.70	3.02	3.13	3.08	3.12	3.00	3.08
n-Butylbenzene	4.09	4.18	3.46	3.54	3.46	3.52	3.44	3.48
n-Amylbenzene	4.65	4.70	3.89	3.97	3.95	3.95	3.87	3.91
Av. deviation (%)	1.50		2.61		0.72		0.80	
δ_s (cal/cm^3)$^{1/2}$	14.32		14.67		14.68		14.70	

	Spherisol C_{18}		Cosmosil C_{18}		Asahipak ODP-50	
	$-\Delta H^0(obs)$	$-\Delta H^0(cal)$	$-\Delta H^0(obs)$	$-\Delta H^0(cal)$	$-\Delta H^0(obs)$	$-\Delta H^0(cal)$
Benzene	1.65	1.67	1.61	1.64	1.59	1.61
Ethylbenzene	2.40	2.41	2.36	2.37	2.30	2.32
n-Propylbenzene	2.78	2.83	2.74	2.78	2.66	2.72
n-Butylbenzene	3.18	3.19	3.18	3.13	3.10	3.07
n-Amylbenzene	3.58	3.58	3.56	3.53	3.45	3.45
Av. deviation (%)	0.75		0.59		1.07	
δ_s (cal/cm^3)$^{1/2}$	14.85		14.88		14.91	

TABLE IV

CHROMATOGRAPHICALLY MEASURED (obs) AND CALCULATED (cal) $-\Delta H^0$ VALUES (kcal/mol) FOR AROMATICS

Deviation: $|\Delta H^0(\text{obs}) - \Delta H^0(\text{cal})| \cdot 100/\Delta H^0(\text{obs})$. Eluent: 80% aqueous methanol. Values in parentheses: calculated by using V_i in the solubility concept model.

Solute	Capcellpak C_{18}		LiChrosorb RP-18		Chemcosorb UH-ODS		Nucleosil C_{18}	
	$-\Delta H^0(obs)$	$-\Delta H^0(cal)$	$-\Delta H^0(obs)$	$-\Delta H^0(cal)$	$-\Delta H^0(obs)$	$-\Delta H^0(cal)$	$-\Delta H^0(obs)$	$-\Delta H^0(cal)$
Naphthalene	3.18	3.18 (3.20)	2.68	2.71 (2.72)	2.68	2.69 (2.71)	2.68	2.66 (2.68)
Phenanthrene	4.13	4.32 (4.21)	3.58	3.67 (3.58)	3.60	3.65 (3.59)	3.52	3.61 (3.52)
Anthracene	4.41	4.24 (4.51)	3.74	3.61 (3.84)	3.76	3.59 (3.82)	3.78	3.55 (3.78)
Av. deviation (%)	2.82 (1.61)		2.37 (1.39)		2.09 (1.28)		3.13 (0.00)	
δ_s^r (cal/cm^3)$^{1/2}$	14.32		14.67		14.68		14.70	

Solute	Spherosil C_{18}		Cosmosil C_{18}		Asahipak ODP-50	
	$-\Delta H^0(obs)$	$-\Delta H^0(cal)$	$-\Delta H^0(obs)$	$-\Delta H^0(cal)$	$-\Delta H^0(obs)$	$-\Delta H^0(cal)$
Naphthalene	2.58	2.49 (2.46)	2.37	2.40 (2.42)	2.86	2.36 (2.37)
Phenanthrene	3.83	3.32 (3.23)	3.18	3.26 (3.18)	4.37	3.20 (3.12)
Anthracene	3.97	3.26 (3.47)	3.32	3.20 (3.41)	4.57	3.15 (3.35)
Av. deviation (%)	11.56 (10.97)		2.46 (1.47)		25.10 (24.02)	
δ_s^r (cal/cm^3)$^{1/2}$	14.85		14.88		14.91	
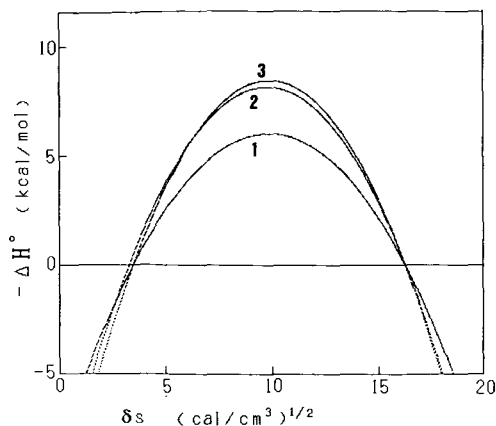
Fig. 2. Correlation curves for $-\Delta H^0$ and δ_s. Solutes: 1 = naphthalene; 2 = phenanthrene; 3 = anthracene. Eluent: 80% aqueous methanol.

whether silicone-coated silica or organic polymer-based, did not affect the $-\Delta H^0$ values for the retention of these n-alkylbenzenes.

The experimental and calculated $-\Delta H^0$ values for condensed aromatic hydrocarbons, such as naphthalene, phenanthrene and anthracene, and the absolute mean deviation on each column are given in Table IV. First, the $-\Delta H^0$ values for these aromatics were calculated by using the values of V_i in Table I, obtained by the method of Le Bas[11]. The absolute mean deviation for aromatics was larger than that for n-alkylbenzenes. This resulted from the large difference between the calculated and experimental $-\Delta H^0$ values for phenanthrene and for anthracene. The calculated $-\Delta H^0$ values for phenanthrene on the seven C_{18} columns were larger than the experimental values, whereas the calculated $-\Delta H^0$ values for anthracene were smaller than the experimental values. However, the correlation coefficients between the calculated and experimental $-\Delta H^0$ values for the retentions of these two aromatics on five columns (i.e., not including the Spherosil XOA and Asahipak ODP columns) were
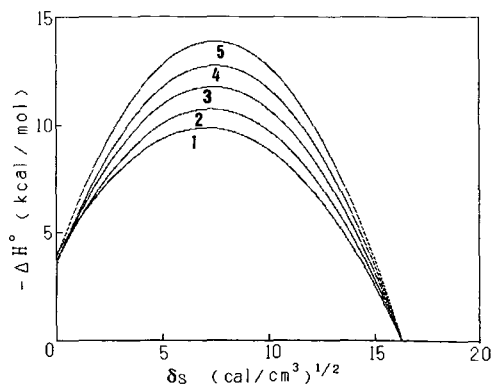
Fig. 3. Correlation curves for $-\Delta H^0$ and δ_s. Solutes: 1 = n-pentane; 2 = n-hexane; 3 = n-heptane; 4 = n-octane; 5 = n-nonane. Eluent: 80% aqueous methanol.

TABLE V

CHROMATOGRAPHICALLY MEASURED (obs) AND CALCULATED (cal) $-\Delta H^0$ VALUES (kcal/mol) FOR n-ALKANES

Deviation: $|\,\Delta H^0(\text{obs}) - \Delta H^0(\text{cal})\,|\cdot 100/\Delta H^0(\text{obs})$. Eluent: 80% aqueous methanol.

Solute	Capcellpak C_{18}		Nucleosil C_{18}		Asahipak ODP-50	
	$-\Delta H^0(obs)$	$-\Delta H^0(cal)$	$-\Delta H^0(obs)$	$-\Delta H^0(cal)$	$-\Delta H^0(obs)$	$-\Delta H^0(cal)$
n-Pentane	3.70	3.77	3.06	3.12	2.78	2.76
n-Hexane	4.13	4.17	3.42	3.46	3.06	3.07
n-Heptane	4.53	4.62	3.82	3.82	3.38	3.40
n-Octane	5.01	5.10	4.17	4.23	3.74	3.72
n-Nonane	5.44	5.55	4.61	4.60	4.05	4.06
Av. deviation (%)	1.73		0.96		0.48	
δ'_s (cal/cm^3)$^{1/2}$	14.32		14.70		14.91	

0.996 and 0.994, respectively. The deviation for the aromatics was assumed to be due to the error in the calculation of V_i values by the method of Le Bas[11].

Next, the values of V_i for the condensed aromatics were calculated by substituting the experimental $-\Delta H^0$ values into eqn. 1. We used the data for the Nucleosil C_{18} column as a standard. The V_i values obtained for naphthalene, phenanthrene and anthracene were 148.5, 191.6, and 209.4 cm^3, respectively. These V_i values differed from those obtained by the method of Le Bas by 0.6, 2.6, 6.5%, respectively. The recalculated $-\Delta H^0$ values are given in parentheses in Table IV. The absolute mean deviation for each column was improved by the recalculation. However, exceptions were found for the Spherosil XOA and Asahipak ODP columns. The experimental $-\Delta H^0$ values for the condensed aromatics on those columns were much larger than the values calculated from their δ'_s values. Hence the specific interaction may be due to the steric structure of the C_{18} materials. Fig. 2 shows the relationship between $-\Delta H^0$ for the three condensed aromatics and δ_s. Here, the recalculated V_i values were used for the molar volume of the condensed aromatics.

Fig. 3 shows the correlation curves between $-\Delta H^0$ and δ_s for n-alkanes. Table V gives the experimental and calculated $-\Delta H^0$ values for the retention of the five n-alkanes on three types of columns: Capcellpak C_{18}, Nucleosil C_{18} and Asahipak ODP. The absolute mean deviation between the experimental and calculated $-\Delta H^0$ values was sufficiently small on these three columns.

CONCLUSIONS

The polarity of the stationary phase was different for the different commercial C_{18} materials. The concentration of the organic modifier in the mobile phase also affected the polarity of the stationary phase. Seven C_{18} columns were characterized by their δ'_s values. On the C_{18} column having a larger δ'_s value, a smaller absolute value of $-\Delta H^0$ was obtained in the retention of non-polar benzene derivatives. In other words, the larger the δ'_s values, the smaller was the observed temperature effect on the retention. The $-\Delta H^0$ values for the retention of benzene derivatives were predictable from the physico-chemical parameters and the δ'_s values.

REFERENCES

1 R. E. Majors, *J. Chromatogr. Sci.*, 18 (1980) 488–511.
2 R. Tijssen, H. A. H. Billiet and P. J. Schoenmakers, *J. Chromatogr.*, 122 (1976) 185–203.
3 B. L. Karger, L. R. Snyder and C. Eon, *J. Chromatogr.*, 125 (1976) 71–88.
4 B. L. Karger, L. R. Snyder and C. Eon, *Anal. Chem.*, 50 (1978) 2126–2136.
5 T. L. Hafkenscheid and E. Tomlinson, *J. Chromatogr.*, 264 (1983) 47–62.
6 H. A. H. Billiet, P. J. Schoenmakers and L. de Galan, *J. Chromatogr.*, 218 (1984) 443–454.
7 F. M. Yamamoto, S. Rokushika and H. Hatano, *J. Chromatogr.*, 408 (1987) 21–26.
8 F. M. Yamamoto, S. Rokushika and H. Hatano, *J. Chromatogr. Sci.*, 27 (1989) 704–709.
9 Y. Ohtsu, H. Fukui, T. Kanda, K. Nakamura, M. Nakano, O. Nakata and Y. Fujiyama, *Chromatographia*, 24 (1987) 380–384.
10 H. Burrell and B. Immergut, in J. Brandrup and E. A. Immergut (Editors), *Polymer Handbook*, Wiley-Interscience, New York, 1966, p. IV-341.
11 G. Le Bas, *The Molecular Volumes of Liquid Chemical Compounds*, Longmans Green, New York, 1915.

Advances in expert systems for high-performance liquid chromatography

YUKUI ZHANG*, HANFA ZOU and PEICHANG LU

Dalian Chromatographic R & D Centre of China, Dalian Institute of Chemical Physics, Academia Sinica, 116012 Dalian (China)

ABSTRACT

The development of modules for the selection of the separation mode, stationary phase and mobile phase and for peak identification in expert systems for high-performance liquid chromatography is discussed. Both the rules and methods used in these modules and their theoretical basis are included. A program to select the separation mode and the stationary and mobile phases has been developed in which there are two modes of entry, the molecular structure of the sample and provision of the sample name. In the peak identification module, three methods for off-line peak identification, by transfer of retention values from one column to another column, by the relationship between retention values and molecular structure parameters and by the interaction index, and also a method for on-line peak identification by combination of the UV spectral parameters with the retention values, have been developed.

INTRODUCTION

In the last few years, much effort has been devoted to developing strategies for an expert system for chromatography (ESC)[1-4]. In a previous paper[1], a strategy for the development of an ESC was established that can be divided into three parts: a knowledge and chromatogram base, an inference engine and a user interface. The knowledge base consists of a set of facts and rules for the chromatographic subject. The chromatogram base contains a compilation of published chromatograms. The inference engine or rule interpreter is responsible for extracting the desired information from the knowledge base and explaining how the answer was obtained. The user interface allows interaction with the system through dialogues and a display of the reasoning results, chromatograms and explanation.

For a chromatographic analysis, the following modules should be included:
(1) selection of the sample pretreatment and detection method;
(2) selection of the separation modes and column system;
(3) optimization of operating conditions;
(4) peak identification and on-line quantification; and
(5) diagnosis of the hardware system.

A computer program package to support the ESC task modules has been developed[1], and the knowledge, rule and method for modules 3 and 5 and the on-line quantitation section in module 4 have been reported. In this paper, we discuss the selection of the mode of separation, the mobile and stationary phases in module 2 and peak identification in module 4.

SELECTION OF THE SEPARATION MODE AND THE STATIONARY AND MOBILE PHASES

The column system is the central element for the chromatographic separation of a mixture. The selection or optimization of the column dimensions and packing size, which often affect column efficiency, can be obtained from some well known relationships[5,6]. However, in most instances, the column efficiency in high-performance liquid chromatography (HPLC) is almost constant (about 10 000 plates) for a given column, and the peak capacity of such a column is about 45 at capacity factor, $k' = 5.0$[7]. Therefore, there is enough space to arrange the compounds inside the column for the separation of most samples. The key problem is the selectivity, or how to distribute the compounds to suitable positions inside the column. Chemical effects on selectivity, such as the type and amount of the mobile and stationary phases, pH and temperature, are often the most important factors.

For the selection of a column system, the following two requirements have been put forward[8]:

(1) a relative separation factor (α) value > 1.16 is needed at $k' = 0.4$, and $\alpha > 1.06$ is feasible if $k' \approx 5$;

(2) the retention of all compounds in the sample should be adjusted to be in the range $0.4 < k' < 30$.

In our opinion, reversed-phase (RP) chromatography is to be recommended for the separation mode as often as possible because it is the simplest to use, and the reproducibility of the qualitative and quantitative data is the best of all the separation modes. In order to recommend a column system, two modes of user entry have been designed to interface the computer with the user: molecular structure of the compounds and provision of the sample name. Table I lists the functional groups used for the entry of the molecular structure, each of which has associated with it the molecular structure parameters such as the Van der Waals volume and the hydrogen bonding energy.

TABLE I

FUNCTIONAL GROUPS ENTERED BY THE USER IN THE ENTRY MODE OF THE MOLECULAR STRUCTURE IN THE EXPERT SYSTEM FOR HPLC

>C<	–OH	–NH2	–SH	–Cl
≡CH	–CHO	–NH–	>S=O	–Br
>CH2	>C=O	–NO2	–S–	–I
–CH3	–COO–	–ONH	>C=S	–F
>C=C<	–COOH	–NH3+	–SOO–	–OPO2
–C≡C–	–O–	–N=O	–SO3H	–PO3H2
–C6H5	–COO⁻	–ONO–	–S–S–	–PO3H⁻
–C10H7		>N–	–SO3⁻	–CN

Before entry of the functional groups of each compound in the sample, the following questions concerning the behaviour of the sample to be analysed must be answered:

(1) how many compounds does the sample contain?;
(2) is the sample to be separated by class?;
(3) does the sample contain homologues?;
(4) does the sample contain positional isomers?;
(5) does the sample contain configurational isomers?;
(6) does the sample contain racemic components?

Question 1 should be answered by the number of compounds of interest, question 2 defines the purpose of the analytical separation, question 3 aims to enter the molecular structure as efficiently as possible because the homologues differ only in the number of methylene groups and questions 4, 5 and 6 help to define the behaviour of the sample to determine the difficulty of separating its components.

In RP-HPLC, the capacity factor of a solute is determined by the hydrophobic (or dispersive) interactions and hydrophilic interactions (mainly the hydrogen bonding interaction) simultaneously. The retention value of a solute increases with increasing hydrophobic interaction, or the number of non-polar functional groups such as CH_3, CH_2 and C_6H_5, and decreases with increasing hydrophilic interaction or the number of polar functional groups such as OH and COOH. Therefore, there is a critical value of the ratio of non-polar to polar functional groups. Solutes contained in the sample with a ratio of non-polar to polar functional groups greater than the critical value should be separated by RP chromatography, otherwise another mode of separation is recommended. Such a critical value can be roughly estimated by entering the molecular structure parameters through the user interface. For organic ions, electrostatic and hydrophobic interactions also exist simultaneously, and there is a critical value of the ratio of non-polar to polar and ionic functional groups. Such a critical value can be estimated empirically. According to the purpose of the separation and the physico-chemical behaviour of the compounds in the sample, the mode of separation can be selected by the inference engine.

From the information on the molecular structures, it is possible to determine the most difficult substance pair to be resolved in the sample. The principles of molecular interactions needed to select suitable mobile and stationary phases are as follows:

(1) For samples containing only non-polar compounds with no π-electron interactions, the selectivity and retention are determined only by the dispersive interactions, and are simultaneously changed by varying the mobile phase composition and the type of organic modifier, which means that the selectivity and retention change together. Therefore, a cheap and less toxic organic solvent is recommended for the organic modifier. If the selectivity with a given column system is insufficient to provide the α value required, the situation can be improved by selecting a solvent with a weaker dispersive interaction as the organic modifier or a packing material with a stronger dispersive interaction as the stationary phase.

(2) For samples containing compounds with selectivity determined only by the dispersive interactions, but retention by the various types of molecular interactions, a stationary phase with a strong dispersive interaction and weak or no other types of interaction is preferred. An organic solvent with a weak dispersive interaction and strong other interactions is selected as the organic modifier.

(3) When the dipole moment interaction is the main factor determining the selectivity, but the retention is determined by various types of molecular interactions, for the same reason as in rule 2, a stationary phase with a strong dipole moment interaction and weak other types of molecular interactions and an organic modifier with a weak dipole moment interaction and strong other types of molecular interactions are to be preferred. Otherwise, if the stationary phase has no or a weak dipole moment interaction, then an organic modifier with a strong dipole moment interaction and moderate other types of molecular interactions is to be preferred.

(4) When hydrogen bonding is the main factor in determining the selectivity, but the retention is determined by the various types of molecular interactions, a stationary phase with a strong hydrogen bonding interaction and weak other types of molecular interactions and an organic modifier with a weak hydrogen bonding interaction and strong other types of molecular interaction are to be preferred. If the stationary phase used has no or a weak hydrogen bonding interaction, then an organic modifier with a strong hydrogen bonding interaction and moderate other types of molecular interaction is to be preferred.

(5) When the selectivity is determined by the π-electron interaction, but the retention value is determined by various types of molecular interactions, a stationary phase with a strong π-electron interaction and weak other types of the molecular interactions and an organic modifier with a weak π-electron interaction and strong other types of molecular interaction is to be preferred. If the stationary phase used has no or a weak π-electron interaction, then an organic modifier with a strong π-electron interaction and moderate other types of molecular interaction is to be preferred.

In RP chromatography, where water is used as the weak solvent and ODS packing material is used most widely, the key problem is how to select the strong solvent[9]. In practice, methanol, acetonitrile and tetrahydrofuran are generally used. We consider that methanol alone is sufficient to separate most samples. However, if the compounds in the sample differ only in the position of a double bond, then an acetonitrile–water mixture is recommended for the mobile phase. If the compounds have very strong hydrophobic interactions and cannot be eluted even with methanol as the mobile phase, then a ternary mobile phase containing methanol–water and a solvent with a strong hydrophobic interaction such as tetrahydrofuran or acetone, or even a non-aqueous mobile phase, is recommended.

The additive reagent can be selected from the information on the functional groups contained in the compounds. If the compounds in the sample have an amino group, then addition of a suitable amount of organic amine to mobile phase is recommended in order to eliminate the strong interaction between the free silanol groups and the amino groups. If the compounds in the sample have functional groups such as phenolic OH, COOH or H_2PO_4, then a suitable amount of phosphate buffer or ammonium acetate is recommended in order to adjust the acidity in the mobile phase.

In normal-phase (NP) liquid chromatography, the interaction between the solute and the stationary phase provides the main contribution to the selectivity and retention, and hexane is generally used as the weak solvent in the mobile phase. The strong solvent is used to adjust the retention of solutes in a suitable range. Therefore, the strong solvent can be recommended according to information on the functional groups present in the solutes. Strong solvents used in normal-phase chromatography and their interaction properties have been reported by Snyder[10]. If the compounds in

the sample have the functional groups OH, COOH or NH_2, then isopropanol is recommended. If the compounds in the sample have only COO, CN, NO_2 and $C=O$ groups, ethyl acetate, acetone or acetonitrile is recommended as the strong solvent. If the compounds in the sample have only –O– and phenyl groups, diethyl ether is recommended as the strong solvent. If the compounds also have H_2PO_4, COOH or OH groups, then methanol–acetonitrile or even an aqueous solution is recommended. If the compounds have these functional groups simultaneously, the solvent can be selected using the above sequence. As an example, the results for the recommendation of the column system through the entry of molecular structure for ten bile acids and some saccharides are listed below:

Samples: ten bile acids, TUDCA, GUDCA, TCA, GCA, TCDCA, GCDCA, DCA, TDCA, TLCA and GLCA.
Entry mode: recommendation from structure.
Mode of separation: (reversed-phase) chromatography.
Column: silica-based bonded-phase C_{18}.
Mobile phase: methanol–water.
Additive agent: small amount of phosphoric acid or acetic acid.
Possibility factor: 0.9702.
Explanation: This kind of sample can be separated by RP-HPLC ($0.4 < k' < 30$). C_{18} is a common packing material for RP-HPLC. Methanol–water is sufficient to separate most samples. The acids can dissociate in RP-HPLC; the additive agent can prevent the dissociation.

Sample: saccharides of fucose, mannose and galactose.
Entry mode: recommendation from structure.
Mode of separation: (normal-phase) chromatography.
Column: silica-based bonded-phase NH_2.
Mobile phase: methanol–acetonitrile + suitable amount of water.
Additive agent: none.
Possibility factor: 0.8938.
Explanation: Sample is a strongly polar hydrophilic mixture, NP chromatography is suitable. Compounds have a strong acceptor ability for hydrogen bonding, NH_2 packing material should be selected.

CHROMATOGRAPHIC PEAK IDENTIFICATION

The other problem to be solved in an expert system of chromatography is peak identification. There are many methods[11–13] such as from retention values and mass and UV spectrometry that can be used in liquid chromatography. Here, we shall discuss the possibility of peak identification in liquid chromatography from retention values and from a combination of retention values with UV spectra.

Peak identification from retention values
It is generally observed in RP-HPLC that the retention values differ when column systems with the same mobile phase concentration but ODS packing material from different sources or even from the same source but from different batches are

used. This causes a difficulty in using retention data from the literature. In addition, the retention value is also affected by the nature of the mobile phase in a given column system. Therefore, how to transfer retention data from one ODS packing material to another with a given mobile phase and from one mobile phase to another with a given packing material is the first problem to be solved.

In another paper[14], the fundamental elution equation describing the effect of the mobile phase composition on k' is given as follows:

$$\ln k' = a + b \ln C_b + cC_b \tag{1}$$

where C_b is the volume fraction of the strong solvent and a, b and c are constants for a given chromatographic system. It has been observed that $b \ln C_b$ approaches a small constant value and is negligible in RP-HPLC, so that eqn. 1 can be simplified to

$$\ln k' = a + cC_b \tag{2}$$

The constant c is determined mainly by the properties of the mobile phase and approaches a constant for a certain solute with different ODS packing materials, and a is determined by the properties of the mobile and stationary phases. The constant c in

TABLE II

CALCULATED AND EXPERIMENTAL VALUES OF TRANSFERRED k' FOR 11 COMPOUNDS ON NUCLEOSIL C_{18} AT DIFFERENT CONCENTRATIONS OF METHANOL

Compound	k'	Methanol concentration, C_b (%)						
		95	90	85	80	70	60	50
Benzene	Exp.	0.45	0.59	0.79	1.08	1.99	3.94	7.60
	Calc.	0.42	0.58	0.80	1.10	2.08	3.93	7.43
Naphthalene	Exp.	0.72	1.02	1.51	2.29	5.29	14.16	
	Calc.	0.65	0.99	1.50	2.28	5.24	12.02	
Biphenyl	Exp.	0.85	1.29	2.03	3.40	9.24	27.90	
	Calc.	0.81	1.30	2.10	3.39	8.80	22.87	
Phenanthrene	Exp.	1.26	1.94	3.17	5.40	15.58		
	Calc.	1.15	1.92	3.20	5.33	14.82		
Anthracene	Exp.	1.32	2.08	3.47	5.91	17.29		
	Calc.	1.24	2.09	3.52	5.94	16.91		
Chrysene	Exp.	2.48	4.20	7.42	14.55	50.47		
	Calc.	2.27	4.19	7.71	14.21	48.23		
Anisole	Exp.	0.45	0.58	0.77	1.06	2.02	3.82	8.06
	Calc.	0.41	0.57	0.78	1.06	2.00	3.76	7.06
Benzyl alcohol	Exp.	0.21	0.25	0.30	0.38	0.62	1.00	1.76
	Calc.	0.20	0.26	0.33	0.42	0.67	1.10	1.79
Acetophenone	Exp.	0.33	0.39	0.48	0.63	1.09	1.93	3.76
	Calc.	0.31	0.41	0.54	0.71	1.24	2.15	3.73
p-Nitrotoluene	Exp.	0.45	0.61	0.81	1.18	2.36	5.06	11.00
	Calc.	0.40	0.57	0.81	1.16	2.34	4.72	9.54
Butyl benzoate	Exp.	0.73	1.08	1.69	2.69	7.26	21.23	
	Calc.	0.70	1.12	1.81	2.93	7.62	19.85	

the fundamental elution equation for different ODS packing materials with the same mobile phase makes it possible to transfer k' from one ODS packing material to another with different mobile phases investigated with only one isocratic experiment, from which the difference in constant a for the two kinds of ODS packing material can be determined. Table II shows data for the transfer of the capacity factor of eleven compounds from YQG-ODS to Nucleosil-ODS, where the constant c for both materials is considered to be the same and the constant a for Nucleosil-ODS can be determined by knowing constant c and $\ln k'$ after one preliminary isocratic experiment at 0.90 volume fraction of methanol on Nucleosil-ODS.

For peak identification from retention values in column systems with the same packing material and different mobile phases, a_I and c_I in the column system with mobile phase I can be correlated with a_{II} and c_{II} in the column system with mobile phase II as follows:

$$c_{II} = c' + Bc_I$$
$$a_{II} = a' + Aa_I$$

(3)

and substituting eqn. 3 into eqn. 2, we have

$$\ln k' = C + Aa_I + Bc_IC_b$$

(4)

where $C = a' + Bc_b$. Eqn. 4 can be used to predict the capacity factor of the solute in the column system with mobile phase II from data for mobile phase I. Table III lists the capacity factors of some aromatic hydrocarbons transfered from a column system with a methanol–water mobile phase to one with acetonitrile–water. Serious errors in predicting retention values may be caused by differences in the π-electron interactions and hydrogen bonding energies for methanol and acetonitrile.

TABLE III

COMPARISON OF CAPACITY FACTORS MEASURED (k'_e) IN A COLUMN SYSTEM WITH ACETONITRILE–WATER AS THE MOBILE PHASE AND DEVELOSIL-ODS AS STATIONARY PHASE WITH THOSE CALCULATED (k'_c) FROM VALUES WITH METHANOL–WATER AS THE MOBILE PHASE

Solute	Acetonitrile–water									
	95:5		90:10		80:20		70:30		60:40	
	k'_e	k'_c	k'_e	k'_c	k'_e	k'_c	k'_e	k'_c	k'_e	k'_c
Benzene	0.43	0.47	0.62	0.61	1.03	1.06	1.72	1.84	2.84	3.19
Naphthalene	0.68	0.70	0.98	0.95	1.73	1.72	3.14	3.11	5.82	5.64
Biphenyl	0.76	0.89	1.15	1.22	2.20	2.30	4.28	4.33	8.61	8.15
Phenanthrene	1.06	1.08	2.19	2.53	3.02	3.11	5.90	5.95	12.05	11.38
Anthracene	1.38	1.14	2.08	1.58	4.11	3.02	6.55	5.78	13.55	11.05
Chrysene	1.79	1.74	2.78	2.44	5.86	4.85	9.21	9.60	19.28	19.03

Peak identification from the relationship between retention values and molecular structure parameters

Peak identification from the physico-chemical parameters of the solutes in a given column system has attracted much attention. In our expert system for chromatography, a possible means of identifying the peaks using the relationship between molecular structure parameters and retention value has been established. For samples containing only non-polar compounds, the retention value is determined only by the dispersive interaction between the solute and the mobile and stationary phases. The parameters a and c in eqn. 2 increase linearly with increasing Van der Waals volume of a solute, which can be calculated by obtaining information on the molecular structure via the user interface. For example, in a column system with acetonitrile–water as the mobile phase and YCM-phenyl as the stationary phase, the relationship between a, c and the Van der Waals volume can be expressed as

$$a = 0.7444 + 0.0217 V_w$$

$$c = -1.6832 - 0.0195 V_w$$

(5)

Table IV lists the capacity factors of hydrocarbons measured experimentally and calculated from the Van der Waals volumes at different mobile phase compositions of acetonitrile–water. It can be seen from the data that the retention value data predicted from the Van der Waals volume for non-polar compounds are acceptable.

For samples containing a homologous series of compounds with the same hydrogen bonding, dipole moment and π-electron interactions, peak identification must take into account all of these interactions simultaneously. The contribution of the hydrogen bonding energy, dipole moment and π-electron interaction to the parameters a and c must be experimentally corrected for owing to the difficulty in correctly measuring the hydrogen bonding energy and the π-electron interaction. For example, for peak identification of homologous compounds such as alkylbenzenes or alcohols,

TABLE IV

COMPARISON OF EXPERIMENTAL CAPACITY FACTORS (k'_e) FOR n-ALKANES WITH THOSE CALCULATED (k'_c) FROM VAN DER WAALS VOLUMES AT DIFFERENT MOBILE PHASE COMPOSITIONS

Experimental data are from Hanai and Hubert[15].

Compound	Acetonitrile–water							
	80:20		70:30		60:40		50:50	
	k'_e	k'_c	k'_e	k'_c	k'_e	k'_c	k'_e	k'_c
Pentane	0.604	0.565	1.22	1.08	2.15	2.07	4.14	3.95
Hexane	0.679	0.653	1.41	1.31	2.66	2.62	5.52	5.24
Heptane	0.784	0.753	1.63	1.58	3.36	3.31	7.36	6.93
Octane	0.900	0.870	1.99	1.91	4.27	4.19	10.12	9.19
Decane	1.21	1.16	2.83	2.79	6.80	6.71	18.71	16.14
Dodecane	1.57	1.55	4.11	4.08	10.69	10.75	–	–

we can first input values of the parameters a and c for only one compound of each homologous series, e.g., butylbenzene and decyl alcohol as follows:

decyl alcohol: $a = 2.0175$, $c = -2.9191$, $V_w = 113.78$;
butylbenzene: $a = 2.3356$, $c = -3.1164$, $V_w = 90.20$.

The contributions of the hydrogen bonding energy, dipole moment and π-electron interaction to the parameters a and c for these two homologues can be calculated from the linear relationship between parameters a and c, and the Van der Waals volume as shown in eqn. 5:

Alcohols:
$\Delta a = 2.0175 - 0.7444 - (0.0217 \cdot 113.78) = -1.196$
$\Delta c = -2.9191 + 1.6832 + (0.0195 \cdot 113.78) = 0.9828$

Alkylbenzenes:
$\Delta a = 2.3556 - 0.7444 - (0.0217 \cdot 90.20) = -0.3468$
$\Delta c = -3.7164 + 1.6832 + (0.0195 \cdot 90.20) = 0.3257$

The contributions of the various types of molecular interactions to the parameters a and c can now be expressed as follows:

Alcohols:
$$a = 0.7444 + 0.0217V_w - 1.1967 = -0.4516 + 0.0217V_w$$

(6)

$$c = -1.6832 - 0.0195V_w + 0.9828 = -0.7004 - 0.0195V_w$$

Alkylbenzenes:
$$a = 0.7444 + 0.0217V_w - 0.3468 = 0.3976 + 0.0217V_w$$

(7)

$$c = -1.6832 - 0.0195V_w + 0.3257 = -1.3575 - 0.0195V_w$$

The data in Table V are values of the parameters a and c calculated from eqns. 6 and 7 for compounds in these homologous series. Table VI lists experimentally measured capacity factors *versus* those calculated from a and c shown in Table V with different acetonitrile–water mobile phase compositions. Comparing the calculated and experimentally measured capacity factors, the agreement is very close, hence the method developed for peak identification of homologous compounds is acceptable.

Peak identification from the interaction index
For samples containing compounds with different polar functional groups, it is difficult to identify chromatographic peaks by predicting the retention value from the molecular structure parameters because it is difficult to describe correctly the contributions of the hydrogen bonding. π-electron interaction and the molecular configuration on the retention value. These contributions must be determined experimentally in order to identify a chromatographic peak. As mentioned above, the parameter c in the fundamental elution equation reflects the mutual interaction forces

TABLE V

PARAMETERS *a* AND *c* FOR HOMOLOGUES OF *n*-ALKYL ALCOHOLS AND ALKYL-BENZENES CALCULATED BY CORRECTING FOR CONTRIBUTIONS OF HYDROGEN BONDING, DIPOLE MOMENT AND π-ELECTRON INTERACTION

Experimental data are from Hanai and Hubert[15].

Compound	a	c	Compound	a	c
Butyl alcohol	0.6855	−1.722	Toluene	1.699	−2.518
Pentyl alcohol	0.907	−1.922	Ethylbenzene	1.911	−2.717
Hexyl alcohol	1.129	−2.121	Propylbenzene	2.133	−2.917
Heptyl alcohol	1.351	−2.269	Butylbenzene	2.356	−3.116
Octyl alcohol	1.573	−2.520	Hexylbenzene	2.799	−3.515
Decyl alcohol	2.018	−2.919	Heptylbenzene	3.021	−3.715
Dodecyl alcohol	2.461	−3.318	Octylbenzene	3.243	−3.914
Tetradecyl alcohol	2.905	−3.717	Nonylbenzene	3.469	−4.114
Hexadecyl alcohol	3.350	−4.116	Decylbenzene	3.687	−4.313

between the solute and the mobile phase and is a constant for a given mobile phase. In our expert system for chromatography, the parameter c is defined as the "interaction index" and is used to identify the peak. The interaction index can be separated into

TABLE VI

COMPARISON OF EXPERIMENTALLY MEASURED CAPACITY FACTORS (k'_e) WITH THOSE CALCULATED FROM THE PARAMETERS *a* AND *c* (k'_c) SHOWN IN TABLE V AT DIFFERENT MOBILE PHASE COMPOSITIONS

Compound	Acetonitrile–water							
	80:20		70:30		60:40		50:50	
	k'_e	k'_c	k'_e	k'_c	k'_e	k'_c	k'_e	k'_c
Toluene	0.47	0.48	0.84	0.88	1.51	1.49	2.69	2.64
Ethylbenzene	0.55	0.56	1.02	0.95	1.91	1.88	3.57	3.52
Propylbenzene	0.63	0.64	1.23	1.26	2.41	2.36	4.73	4.75
Butylbenzene	0.73	0.74	1.49	1.50	3.06	2.95	6.27	6.42
Hexylbenzene	0.97	0.97	2.18	2.13	4.90	4.59	11.0	11.6
Heptylbenzene	1.12	1.11	2.63	2.54	6.19	5.80	14.6	15.6
Octylbenzene	1.29	1.27	3.19	3.04	7.85	7.29	19.3	21.1
Nonylbenzene	1.51	1.45	3.89	3.60	10.0	9.09	25.8	28.1
Decylbenzene	1.72	1.66	4.65	4.30	12.6	11.4	33.9	36.0
Butyl alcohol	0.20	0.18	0.30	0.30	0.45	0.40	0.67	0.54
Pentyl alcohol	0.23	0.22	0.37	0.36	0.57	0.54	0.88	0.76
Hexyl alcohol	0.27	0.26	0.44	0.44	0.72	0.69	1.17	1.07
Heptyl alcohol	0.34	0.31	0.58	0.55	0.98	0.88	1.65	1.47
Octyl alcohol	0.36	0.36	0.64	0.65	1.15	1.12	2.06	2.01
Decyl alcohol	0.48	0.49	0.94	0.95	1.82	1.78	3.61	3.70
Dodecyl alcohol	0.64	0.65	1.38	1.36	2.95	2.81	6.34	6.64
Tetradecyl alcohol	0.85	0.87	2.01	1.93	4.73	4.38	11.1	11.8
Hexadecyl alcohol	1.14	1.15	2.94	2.79	7.59	6.88	19.6	21.2

TABLE VII

VALUES OF V_w, μ_A^2 AND X_n FOR SOME SOLUTES AND COMPARISON OF THE CALCULATED INTERACTION INDICES WITH THOSE MEASURED IN A METHANOL–WATER MOBILE PHASE

Solute	V_w	μ_A^2	X_n	c(exp.)	c(calc.)	Error
Benzene	48.36	0.0	0.0	− 6.52	− 6.63	−0.11
Chlorobenzene	57.48	2.89	−0.76	− 8.01	− 7.85	0.16
Toluene	59.51	1.11	0.0	− 7.53	− 7.55	−0.02
p-Xylene	70.66	0.01	0.0	− 8.66	− 8.57	0.09
Phenol	52.83	4.93	−0.43	− 6.08	− 6.24	−0.16
Nitrobenzene	62.64	15.8	−2.38	− 6.84	− 7.07	−0.23
1,3,5-Trimethylbenzene	81.81	0.017	0.0	− 9.70	− 9.53	0.17
1,2,4,5-Tetramethylbenzene	92.96	0.01	0.0	−10.32	−10.50	−0.18
p-Chlorotoluene	68.99	3.69	−1.05	− 9.19	− 9.07	0.12
p-Nitrotoluene	73.79	17.6	−3.03	− 7.83	− 8.59	−0.76
p-Methylphenol	63.98	5.52	−0.55	− 7.09	− 7.23	−0.14
1,4-Dichlorobenzene	67.32	0.0	−0.25	− 9.30	− 8.71	0.59
1,4-Dihydroxybenzene	59.82	1.96	0.94	− 5.37	− 5.41	−0.04
p-Chloronitrobenzene	72.12	5.66	−0.44	− 7.65	− 7.72	−0.07
p-Chlorophenol	62.31	4.84	−0.83	− 7.69	− 7.78	−0.09
p-Chloroaniline	65.86	9.0	−1.01	− 7.05	− 7.12	−0.07
1,4-Dinitrobenzene	76.92	0.0	1.46	− 6.63	− 6.38	0.25
p-Nitroaniline	70.66	37.7	−5.22	− 6.40	− 5.90	0.50
Naphthalene	73.96	0.0	0.0	− 9.09	− 8.87	0.22
Phenanthrene	98.95	0.0	0.0	−11.15	−11.03	0.12
Anthracene	102.12	0.0	0.0	−11.42	−11.30	0.12
Pyrene	109.04	0.0	0.0	−11.75	−11.91	−0.16
Chrysene	134.64	0.0	0.0	−14.07	−14.14	−0.07

non-polar, polar and non-specific interaction indices as shown in the following equation[16]:

$$c = l_1 + l_2 V_w + l_3 \mu_A^2 + l_4 X_n \qquad (8)$$

where V_w and μ_A are the Van der Waals volume and dipole moment of the solute, respectively, X_n is the non-specific interaction energy including hydrogen bonding, π-electron interaction, etc., which can be obtained by comparison of a compound having non-specific interactions with a compound without these forces, and l_1, l_2, l_3 and l_4 are constants related to the physico-chemical behaviour of the mobile phase. Table VII lists the Van der Waals volume, dipole moment, X_n and the interaction index c measured and calculated for various solutes. The interaction index database has been established, but not yet completed.

By this method, the peak order in the published chromatograms stored in the chromatogram base in our expert system for various classes of compounds has been systematically examined.

Peak identification from UV spectra and retention values

UV detection is most widely used in HPLC. The combination of the UV

TABLE VIII

UV SPECTRAL PARAMETER *Sp* OF FIVE INTERMEDIATES OF SYNTHETIC DYESTUFFS UNDER DIFFERENT SEPARATION CONDITIONS IN ION-PAIR REVERSED-PHASE LIQUID CHROMATOGRAPHY

Solute	*Sp at different concentrations of methanol (v/v) in a mobile phase of methanol–buffer containing 20 mmol $(C_2H_7)_4$ NBr 7 mmol KH_2PO_4 and with pH 5.50*			
	0.30	*0.25*	*0.20*	*0.15*
Phenylamine-3-sulphonic acid	225.8	225.7	225.4	225.1
Phenylamine-2-sulphonic acid	248.5	248.3	247.0	248.0
4-Methylphenylamine-2-sulphonic acid	232.0	230.7	231.2	230.9
Naphthylamine-5-sulphonic acid	242.1	241.9	242.0	240.6
2-Naphthylamine-5-sulphonic acid	226.9	226.1	226.9	225.6

	Sp at different concentrations of the ion-pair reagent $(C_2H_7)_4$ NBr (mmol) in a mobile phase of methanol–buffer (0.3:0.7) with 7 mmol KH_2PO_4 and with pH 5.50		
	25	*20*	*10*
Phenylamine-3-sulphonic acid	225.9	225.4	226.4
Phenylamine-2-sulphonic acid	247.8	247.0	247.4
4-Methylphenylamine-2-sulphonic acid	231.8	231.2	231.5
Naphthylamine-5-sulphonic acid	242.2	242.0	241.4
2-Naphthylamine-5-sulphonic acid	226.3	226.9	225.1

	Sp at different pH values in a mobile phase of methanol–buffer (0.3:0.7) with 20 mmol $(C_2H_7)_4$ NBr ion-pair reagent, 7 mmol KH_2PO_4 and pH adjusted with HCl		
	5.50	*3.75*	*3.10*
Phenylamine-3-sulphonic acid	225.8	225.7	224.5
Phenylamine-2-sulphonic acid	248.5	252.2	252.7
4-Methylphenylamine-2-sulphonic acid	232.0	232.0	230.4
Naphthylamine-5-sulphonic acid	242.1	237.7	234.7
2-Naphthylamine-5-sulphonic acid	226.9	226.4	225.4

TABLE IX

UV SPECTRAL PARAMETERS *Sp*, PREDICTED CAPACITY FACTORS AND THE COMPOUND NAME IDENTIFIED BY THE ESC

Peak No.	*Sp*	*k'*	Compound name
1	208.9	1.24	1,4-Dinitrobenzene
2	196.0	2.24	Anisole
3	201.4	2.70	4-Phenylphenol
4	203.0	5.89	Naphthalene
5	186.2	6.64	Triphenylmethanol
6	191.0	9.56	Biphenyl
7	204.1	14.0	Anthracene
8	195.6	19.1	Pyrene
9	215.1	27.7	Chrysene

spectrum and the retention value is one way to identify a chromatographic peak on-line. In our expert system for chromatography, a programmable multi-wavelength UV detector has been installed, making it possible to measure the UV spectrum of a solute on-line. An identification parameter P of the UV spectrum is defined as:

$$P = Sp \cdot area$$

(9)

$$Sp = \frac{\sum\limits_{i=0}^{n} \varepsilon_{i(\lambda_i)} \lambda_i}{\int\limits_{\lambda_0}^{\lambda_n} \varepsilon_{i(\lambda)} d\lambda}$$

where *area* is the area of the UV spectrum, λ and ε are the wavelength and corresponding absorption coefficient and the summation is over a number of different wavelengths. Light is detected over the range λ_0–λ_n. For a given solute, the P and *area* are affected by many factors such as mobile phase composition, pH and amount of solute. However, Sp is determined only by ε and λ, and for a fixed wavelength range Sp is a spectral parameter indicative of the absorption of light by the solute. In a certain region, Sp is not affected by the red or blue shift of the UV spectrum with changing physico-chemical behaviour of the solution, and therefore is important for peak identification in HPLC. The reliability of the use of Sp has been investigated in ion-pair reversed-phase liquid chromatography by changing the mobile phase composition, the concentration of the ion-pair reagent and the pH value for 28 intermediates in the synthesis of dyestuffs. Table VIII lists values of Sp obtained under various separation conditions for five compounds in ion-pair reversed-phase liquid chromatography.

Sp values for the 28 synthetic dyestuff intermediates and 20 aromatic compounds have been stored in the on-line peak identification module. Table IX lists experimentally measured values of Sp and k' for nine aromatic compounds.

CONCLUSION

We have discussed the development of a module for the selection of the separation mode, the stationary phase and the mobile phase and possible approaches to a peak identification module for an HPLC expert system. In order to widen its range of application, the rules and methods for these modules should be further tested, corrected and expanded.

REFERENCES

1 P. Lu and H. Huang, *J. Chromatogr.*, 452 (1988) 175.
2 P. J. Schoenmakers and M. Mulholland, *Chromatographia*, 25 (1988) 737.
3 J. P. Bonnine and G. Guiochon, *Analusis*, 12 (1984) 175.
4 G. Musch and D. L. Massart, *J. Chromatogr.*, 370 (1986) 1.

5 G. Guiochon, in Cs. Horváth (Editor), *High Performance Liquid Chromatography*, Vol. 2, Academic Press, New York, 1980, pp. 1–56.
6 P. J. Schoenmakers, N. Dunand, A. Cleland, G. Musch and Th. Blaffert, *Chromatographia*, 26 (1988) 37.
7 P. Lu, X. Li and Y. Zhang, *J. High Resolut. Chromatogr. Chromatogr. Commun.*, 3 (1980) 609.
8 P. Lu, H. Zou, H. Haung and Y. Zhang, *Chin. J. Chromatogr.*, in press.
9 M. A. Quarry, R. L. Grob, L. R. Snyder, J. W. Dolan and M. P. Rigney, *J. Chromatogr.*, 384 (1987) 163.
10 L. R. Snyder, *J. Chromatogr. Sci.*, 16 (1978) 223.
11 K. Jinno and A. Ishigaki, *J. High Resolut. Chromatogr. Chromatogr. Commun.*, 5 (1982) 668.
12 M. J. M. Well and C. R. Clark, *J. Chromatogr.*, 244 (1982) 231.
13 Y. Zhang, H. Zou and P. Lu, *J. Chin. Chem. (Engl. Ed.)*, in press.
14 P. Lu, H. Zou and Y. Zhang, *J. Chromatogr.*, 509 (1990) 171.
15 T. Hanai and J. Hubert, *J. Chromatogr.*, 291 (1984) 81.
16 L. Chen, Y. Zhang, H. Zou and P. Lu, in X. Liang (Editor), *Proceedings of the Third Beijing Conference and Exhibition on Instrumental Analysis, 1989*, BCEIA, Beijing, 1989, D67.

CHROMSYMP. 1795

Effects of ionic strength of eluent on size analysis of sub-micrometre particles by sedimentation field-flow fractionation

YASUSHIGE MORI*

Department of Chemical Engineering, Kyoto University, Yoshida-Honmachi, Sakyo-ku, Kyoto 606 (Japan)

and

BRIAN SCARLETT and HENK G. MERKUS

Department of Chemical Process Technology, Delft University of Technology, Julianalaan 136, 2628 BL Delft (The Netherlands)

ABSTRACT

Sedimentation field-flow fractionation (SdFFF) has a high resolution over a wide range of particle size compared with other methods of sub-micrometre particle size determinations, and has the grant advantage that the fractional collection is sorted by the particle mass. However, the retention behaviour in SdFFF depends strongly on the experimental parameters, especially the ionic strength of the eluent. The sizes calculated from the experimental results of SdFFF are underestimated if an eluent with low ionic strength is used, compared with those obtained by quasi-elastic light scattering spectroscopy, owing to the interparticle repulsion. There is a maximum value of the ionic strength of the eluent for particle size analysis, because rapid flocculation of particles occurs at high electrolyte concentrations. Further, hardly any difference in the retention times was found in SdFFF using different anionic surfactant solutions as the eluent.

INTRODUCTION

Field-flow fractionation (FFF) is a single-phase chromatography-related technique in which an externally applied field is allowed to interact with suspended particles under motion in a channel. Sedimentation FFF (SdFFF) is an FFF technique that uses centrifugal force for the external field, and is well suited to the characterization and fractionation of particulate materials and soluble samples in the colloid size range.

The classical theory of FFF, developed mainly by Giddings and co-workers, was presented as a method for conversion from retention time to particle size[1-3]. Another contribution to SdFFF technology was made by Yau and Kirkland[4,5] of DuPont through the development of a commercial instrument. They also implemented a special programming technique which reduces the analysis time, and introduced

a conversion equation to obtain the size by integration of the classical theory. However, the applicability of the classical theory is limited, because the interactions among particles and the wall of the channel due to local particle concentration, surface charge of the particles and the ionic strength of the eluent are not included in this theory.

In studies of the effects of the eluent, Hoshino et al.[6] reported the unexpected prolongation of the retention at high concentrations of Aerosol OT (AOT), which was explained by the difference in the state of the interface between the channel wall and the solvent stream depending on the concentration and the kinds of the surfactants. Hansen and Giddings[4] included the particle–wall interaction in their calculation, and found that the retention time depends on the electrostatic properties of the particles and of the channel wall, by comparison of the calculation with the experimental results. We evaluated the DuPont SdFFF instrument[7], and found small effects of the surfactants in the eluent on size measurements by SdFFF, quasi-elastic light scattering (QELS) spectroscopy and transmission electron microscopy. We concluded that these small effects might be explained by the influence of the surface charge of the particles and the pH or ionic strength of the eluent.

This paper describes the importance of the ionic strength of the eluent, based on a comparison of size measurements by SdFFF and QELS spectroscopy.

THEORETICAL

In the classical theory, the retention factor R of a particle of diameter D_p is defined as the ratio of the elution time for an unretained peak, t_0, to that for particles, t_R, as usual in chromatography. The following relationship between R and λ was obtained by Hovingh et al.[8]:

$$R = t_0/t_R = 6\,\lambda\{\coth[1/(2\,\lambda)] - 2\,\lambda\} \tag{1}$$

λ is expressed by the Stokes–Einstein relationship and the force generated in a centrifuge in the case of SdFFF:

$$\lambda = 6kT/(D_p^3\pi\,\Delta\rho Gw) \tag{2}$$

where k is the Boltzmann constant, T is the absolute temperature, w is the channel thickness, G is the field strength and $\Delta\rho$ is the density difference between the particle and the eluent.

For highly retained sample components, simplifying approximations employed in obtaining eqn. 1 are valid, as shown by Giddings[9]. Caldwell[2] recommended the following second-order approximation:

$$R = 6\,\lambda\,(1 - 2\,\lambda) \qquad \text{for } R < 0.5 \tag{3}$$

In field-programmed SdFFF, the retention factor R becomes a function of time, depending on the field strength at that time:

$$t_0 = \int_0^{t_R} R(t)\,dt \tag{4}$$

The time-dependent retention $R(t)$ is still expressed by eqn. 1 if the rate of change of the field is slow so that each particle can move to the equilibrium position which is determined by the force of the field and the Brownian motion of the particle. The DuPont SdFFF instrument uses the time-delayed exponential decay force-field programming mentioned by Yau and Kirkland[4]. That form of the centrifugal force field is

$$G(t) = G_0 \qquad\qquad\qquad \text{for } t \leqslant \chi \tag{5}$$

$$G(t) = G_0 \exp[-(t - \chi)/\tau] \qquad \text{for } t > \chi \tag{6}$$

where G_0 is the initial sedimentation force field, τ is the exponential decay time constant and χ is an arbitrary delay time before decreasing the centrifugal field. In order to carry out the integration of eqn. 4, eqn. 3 can be used as the retention equation. The relationships between the retention time and the particle mass are as follows:

for $t \leqslant \chi$:
$$m = 3\phi t_R/t_0\{1 + \sqrt{1 - [4t_0/(3t_R)]}\} \tag{7}$$

for $t > \chi$:
$$m = 3\phi\tau/t_0\bigg\{(\chi - \tau)/\tau +$$

$$+ \exp[(t_R - \chi)/\tau]\bigg\}\bigg(1 + \sqrt{1 - \frac{2t_0/3\{2\chi - \tau + \tau\exp[2(t_R - \chi)/\tau]\}}{\{(\chi - \tau) + \tau \exp[(t_R - \chi)/\tau]\}^2}}\bigg) \tag{8}$$

If $\chi = \tau$, as in the DuPont SdFFF instrument, eqn. 8 is simplified[4]:

$$m = \frac{3\phi\tau}{t_0} \cdot \exp\left(\frac{t_R - \tau}{\tau}\right)\left(1 + \sqrt{1 - \frac{2t_0}{3\tau}\left\{1 + \exp\left[\frac{-2(t_R - \tau)}{\tau}\right]\right\}}\right) \tag{9}$$

where

$$\phi = kT/[G_0 w(\Delta\rho/\rho_s)] \tag{10}$$

$$m = \pi \rho_s D_p^3/6 \tag{11}$$

and ρ_s is the particle density. Eqns. 7 and 9 were used to calculate the equations for conversion from retention time to particle diameter in this paper.

EXPERIMENTAL

The DuPont SdFFF instrument was used, and the particle size was obtained by the modified calculation software based on the above theoretical consideration, which was reported previously[7]. The flow-rate during the analysis period was 2 ml/min. The

eluent was monitored with a normal UV detector at 254 nm. The delay/decay time constant, τ, was chosen to be 10 min when the instrument worked in the mode of the time-dealyed exponentially decayed programming technique (TDE mode or TDE-SdFFF)[4,5]. The non-equilibrium effects, which arise from slow mass transport between flow lines of different velocity, can be neglected if the delay/decay time constant is more than 10 min[7].

In order to measure the particle diameter by QELS spectroscopy (Model N4MD instrument; Coulter Electronics), the liquids eluted from SdFFF were each fractionated into 4-ml volumes when the detector showed signals for particles. The mean particle size and the standard deviation for the fractionated samples were obtained by the unimodal calculation procedure with this spectroscopic method. The accuracy of this measurement should be very good because of the narrow size distribution of the particles in the sample.

AOT solution (10%) (Fisher Scientific, Fair Lawn, NJ, U.S.A.) was used to prepare the eluent. The water for dilution was prepared by distillation and passage through a Milli-Q system (Millipore).

RESULTS AND DISCUSSION

Polystyrene latex

The retention times of polystyrene latex beads (G0301; Japan Synthetic Rubber, Tokyo, Japan) were measured in the TDE mode with an initial centrifugal speed of 3000 rpm using 0.1% and 0.001% AOT solution as the eluent. The mean size was calculated as 269 nm from the retention time (28.3 min) at the peak absorbance of the fractogram of the result with 0.1% ($2.2 \cdot 10^{-5}$ mol/l) AOT solution. This value is in good agreement with the mean size of the fractionated sample, 268 nm, in QELS spectroscopic analysis, which was collected from the outlet of the SdFFF instrument during the retention time period between 27.5 and 29.5 min. This is in agreement with several literature reports[10–13] that the results of size analysis by SdFFF with 0.1% AOT solution agreed well with those obtained by QELS spectroscopy or transmission electron microscopy.

However, the retention time for 0.001% ($2.2 \cdot 10^{-7}$ mol/l) AOT solution was 22.2 min. The dependence of the retention time behaviour on the AOT concentration in the eluent is the same as that reported by Hoshino *et al.*[6]. They explained this phenomenon by a change in the profile of the parabolic laminar flow in the channel and/or a change in the interaction between particles and the wall of the channel, and they suggested that the size obtained from FFF methods could be overestimated at high AOT concentrations in the eluent. However, our results with SdFFF and QELS spectroscopy indicated that particles in 0.001% AOT solution are eluted earlier than the time predicted by the classical theory.

The difference in AOT concentration causes not only a difference in the absorbed states of AOT on the particle surfaces and on the channel wall, but also differences in the ionic strength, because AOT is an anionic surfactant. Fractograms of latex (G0301) are shown in Fig. 1. The concentration of AOT in the eluent was 0.001% and sodium chloride was added in order to investigate the effect of the ionic strength of the eluent. When the sodium chloride concentration was 0.1 mol/l, the detector did not record a particle signal, which suggested particle agglomeration in the channel. Fig. 1a
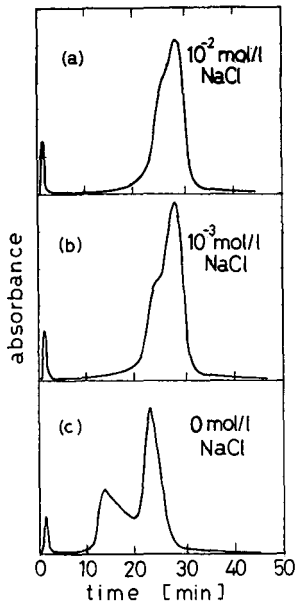
Fig. 1. Effect of the concentration of electrolyte added to 0.001% AOT solution on fractograms of polystyrene latex. TDE mode; initial centrifuge speed = 3000 rpm; delay/decay time constant = 10 min; sample concentration = 0.1 wt.-%; flow-rate = 2 ml/min.

is for 0.001% AOT and 0.01 mol/l sodium chloride. The fractogram was same as that when 0.1% AOT solution was used as the eluent without any sodium chloride added. When the concentration of sodium chloride was decreased further, the retention time of the peak absorbance became smaller, indicating a smaller particle size. The shoulder on the left-hand side of the fractogram was more pronounced at 10^{-3} than at 10^{-2} mol/l sodium chloride, and finally a double peak signal of the fractogram was obtained, as shown in Fig. 1c, when 0.001% AOT solution without sodium chloride was used as the eluent. The retention times of the peak absorbance in Fig. 1a, b and c correspond to particle sizes of 265, 262 and 220 nm, respectively. However, fractions collected at the times represented by the above peaks corresponded to particle sizes of 266, 267 and 275 nm, respectively, in QELS spectroscopic analysis.

We conclude that the difference between the sizes of the particles in SdFFF analysis shown in Fig. 1a–c is caused by the effect of the ionic strength of the eluent. With the eluent containing 0.1 mol/l sodium chloride, rapid flocculation among the particles might have occurred owing to the high concentration of electrolyte. On the other hand, the results which gave a smaller size in SdFFF analysis at low electrolyte concentration are probably due to interparticle electrostatic repulsion as a result of the long-distance effect of the electric double layer of the particles, together with the high local solid concentration. This, in turn, moves the particles further from the wall and thus results in a decrease in the retention time in SdFFF. However, interparticle forces are not experienced in QELS spectroscopic analysis, as the solid concentration is much lower.

The reason is not clear why the double peaks on the fractogram appear when

TABLE I

RETENTION TIMES OF COLLOIDAL SILICA IN VARIOUS AEROSOL OT ELUENTS

Experimental conditions: TDE mode; initial centrifuge speed = 10 000 rpm; delay/decay time constant = 10 min; sample concentration = 25% (w/w); flow-rate = 2 ml/min.

Parameter	Run No.							
	SYTON-14	SYTON-33	SYTON-10	SYTON-11	SYTON-13	SYTON-25	SYTON-27	SYTON-26
AOT (mol/l)	$2.2 \cdot 10^{-5}$	$2.2 \cdot 10^{-5}$	$2.2 \cdot 10^{-5}$	$2.2 \cdot 10^{-5}$	$2.2 \cdot 10^{-5}$	$2.2 \cdot 10^{-7}$	$2.2 \cdot 10^{-7}$	$2.2 \cdot 10^{-7}$
HCl (mol/l)	$9.9 \cdot 10^{-3}$	0	0	0	0	$1.0 \cdot 10^{-2}$	0	0
NaOH (mol/l)	0	0	0	$2.6 \cdot 10^{-4}$	$6.0 \cdot 10^{-4}$	0	0	0
NaCl (mol/l)	0	$1.0 \cdot 10^{-2}$	0	0	0	0	$1.0 \cdot 10^{-2}$	0
pH	2.0	4.0	4.0	6.0	9.7	2.0	5.5	5.7
I (mol/l)[a]	$9.9 \cdot 10^{-3}$	$1.0 \cdot 10^{-2}$	$1.0 \cdot 10^{-4}$	$2.6 \cdot 10^{-4}$	$6.0 \cdot 10^{-4}$	$1.0 \cdot 10^{-2}$	$1.0 \cdot 10^{-2}$	$2.0 \cdot 10^{-6}$
$1/k$ (nm)[b]	3.1	3.1	31	19	12	3.1	3.1	215
Retention time (min):								
1st peak	49	48	46	45	46	48	48	27
2nd peak	55	54	52	52	52	54	54	33
3rd peak	60	59	57	57	57	59	59	38
Particle size (nm):								
1st peak	83.4	80.6	75.4	73.0	75.4	80.6	80.6	40.0
2nd peak	102	92.2	92.2	92.2	92.2	98.5	98.5	48.9
3rd peak	120	116	109	109	109	116	116	57.8

[a] I = Ionic strength of the eluent.
[b] $1/k$ = Thickness of electric double layer of particle.

0.001% AOT solution without sodium chloride was used as the eluent, as shown in Fig. 1c. The particle size corresponding to the first peak in SdFFF analysis is 160 nm. In contrast, a mean size of 290 nm was obtained by QELS spectroscopy using the fractionated sample from SdFFF at the retention time of the first peak absorbance. The size indicated by QELS spectroscopy, 290 nm, is larger than the values obtained above. The large size for the first peak in QELS spectroscopy together with its smaller SdFFF retention time may be due to the lower density of this material and/or stronger repulsion forces. We require further information on the behaviour of the particle and the channel wall in different eluents if this phenomenon is to be clarified.

The relationship between the retention time of the latexes and the ionic strength of the eluent is shown in Fig. 2. These experiments were carried out with a five-component mixture of standard latex for the eluents consisting of 0.1% or 0.001% AOT solution with or without 0.01 mol/l sodium chloride. The sizes calculated from the retention times at 0.01 mol/l ionic strength, which means that the eluent with 0.01 mol/l sodium chloride added was used, were 74, 110, 182, 300 and 550 nm. The results obtained by QELS spectroscopy indicated 75, 111, 170, 296 and 598 nm, respectively. It is concluded that the size calculated from the retention time in SdFFF analysis may underestimate the true value owing to electrostatic repulsion among the particles if the ionic strength is not adjusted.

Colloidal silica

For SdFFF analysis of inorganic materials such as silica with a smaller size and a broad distribution, it is important to establish the effect of surface charge of the particles, and also the effect of the eluent composition. Both effects will appear strongly because a higher sample concentration is needed owing to the low sensitivity of the detector for smaller particles. Generally, the surface charge of inorganic particles is described in terms of zeta potential or sol stability, which are known to be strongly dependent on pH. The isoelectric point (zero point of charge) of colloidal silica is at *ca.* pH 2. At higher pH the surface charge becomes increasingly negative, until at *ca.* pH 10 dissolution occurs. SdFFF results used colloidal silica (Syton W50; Monsanto, London, U.K.) appear to be little influenced by the pH of the eluent consisting of 0.1% AOT, as indicated in Table I. The ionic strength in the eluent was calculated from the concentrations of AOT, hydrochloric acid, sodium hydroxide and
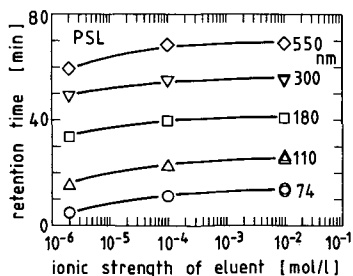
Fig. 2. Relationships between retention time and ionic strength of eluent, I, for a five-component mixture of standard latexes in TDE-SdFFF analysis. Initial centrifuge speed = 10 000 rpm; time delay/decay constant = 10 min; flow-rate = 2 ml/min. $I = 10^{-6}$ mol/l, 0.001% AOT solution; $I = 10^{-4}$ mol/l, 0.1% AOT solution; $I = 10^{-2}$ mol/l, 0.01 mol/l NaCl added to 0.1% or 0.001% AOT solution.
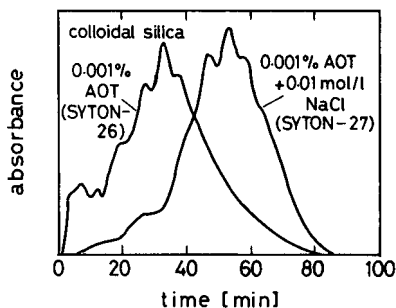
Fig. 3. Fractograms of colloidal silica in TDE-SdFFF analysis. Experimental conditions as in Table I.

sodium chloride and from the measured pH value, and then the thickness of the electric double layer of the particle, *i.e.*, the reciprocal of the Debye–Hückel parameter, was calculated (Table I). The retention time could be correlated with the ionic strength and the thickness of the electric double layer.

Run number SYTON-26, which was performed at low AOT concentration, shows a strong decrease in the retention time. When sodium chloride was added to this eluent (SYTON-27), the SdFFF retention was brought back to normal, as shown in Fig. 3 and Table I. Also, the SdFFF retention is normal at low pH near the isoelectric point (SYTON-25). Moreover, the fractions collected at the first and the third peak absorbances in these three runs show about the same mean sizes in QELS

TABLE II

RETENTION TIMES OF COLLOIDAL SILICA IN VARIOUS SURFACTANT ELUENTS

Experimental conditions as in Table I.

Parameter	Run No.					
	SYTON-23	SYTON-20	SYTON-22	SYTON-21	SYTON-32	SYTON-30
HMP^a (mol/l)	$3.3 \cdot 10^{-3}$	$3.3 \cdot 10^{-3}$	0	0	0	0
SPP^a (mol/l)	0	0	$2.2 \cdot 10^{-3}$	$2.2 \cdot 10^{-3}$	$2.2 \cdot 10^{-5}$	$2.2 \cdot 10^{-5}$
HCl (mol/l)	$1.0 \cdot 10^{-2}$	0	$1.0 \cdot 10^{-2}$	0	0	0
NaCl (mol/l)	0	0	0	0	$1.0 \cdot 10^{-2}$	0
pH	2.0	6.0	2.0	9.0	7.0	7.0
Retention time (min):						
1st peak	50	49	49	48	47	34
2nd peak	56	55	55	54	53	41
3rd peak	61	60	60	59	59	46
Particle size (nm):						
1st peak	86.2	83.4	83.4	80.6	78.0	50.6
2nd peak	105	102	102	98.5	95.3	63.9
3rd peak	124	120	120	116	116	75.4

^{a} HMP = Sodium hexametaphosphate; SPP = sodium pyrophosphate.

spectroscopic analysis, *i.e.*, 90 and 120 nm, respectively. These results indicate that the retention time depends on the ionic strength of the eluent. On the other hand, the surface charge effects of particles, that is, the effect of the pH of the eluent, may not be so significant, as shown by the same ionic strength data in Table I.

Table II shows the effect of the anionic surfactant in the eluent. Although the ionic strength could not be calculated exactly because of the lack of dissociation constants of the two surfactants, the ionic strengths in the experiments listed in Table II except run SYTON-30 are $\geqslant 10^{-2}$ mol/l. For these eluents hardly any difference in retention time was found. The ionic strength in run SYTON-30 is calculated to be of the order of 10^{-5} mol/l. The retention time in this instance is much shorter than in other instances. This fact may also indicate the importance of the ionic strength of the eluent.

REFERENCES

1 J. C. Giddings, *Sep. Sci.*, 1 (1966) 123.
2 K. D. Caldwell, in H. G. Barth (Editor), *Modern Methods of Particle Size Analysis* (*Chemical Analysis*, Vol. 73), Wiley, Chichester, 1984, Ch. 7.
3 J. Janca, *Field-Flow Fractionation*, Marcel Dekker, New York, 1987.
4 W. W. Yau and J. J. Kirkland, *Sep. Sci. Technol.*, 16 (1981) 577.
5 W. W. Yau and J. J. Kirkland, *J. Chromatogr.*, 218 (1981) 217.
6 T. Hoshino, M. Suzuki, K. Ysukawa and M. Takeuchi, *J. Chromatogr.*, 400 (1987) 361.
7 Y. Mori, H. G. Merkus and B. Scarlett, *Part. Part. Syst. Charact.*, in press.
8 M. E. Hovingh, G. H. Thompson and J. C. Giddings, *Anal. Chem.*, 42 (1970) 195.
9 J. C. Giddings, *J. Chem. Educ.*, 50 (1973) 667.
10 J. J. Kirkland, S. W. Rementer and W. W. Yau, *Anal. Chem.*, 53 (1981) 1730.
11 W. W. Yau and J. J. Kirkland, *Anal. Chem.*, 56 (1984) 1461.
12 D. A. Pitt and P. D. McGibney, personal communication.
13 J. Janca, D. Pribylova, C. Konak and B. Sedlacek, *Anal. Sci.*, 3 (1987) 297.
14 M. E. Hansen and J. C. Giddings, *Anal. Chem.*, 61 (1989) 811.

CHROMSYMP. 1886

Size-exclusion chromatography dimension for rod-like macromolecules

PAUL L. DUBIN*

Department of Chemistry, Indiana University–Purdue University at Indianapolis, Indianapolis, IN 46205-2820 (U.S.A.)

JEROME I. KAPLAN

Department of Physics, Indiana University–Purdue University at Indianapolis, Indianapolis, IN 46205-2820 (U.S.A.)

and

BING-SHOU TIAN[a] and MAMTA MEHTA

Department of Chemistry, Indiana University–Purdue University at Indianapolis, Indianapolis, IN 46205-2820 (U.S.A.)

ABSTRACT

A phenomenological approach has been taken to determine the macromolecular dimension that controls peak migration in size-exclusion chromatography. For macromolecules representative of the class of rigid rods, flexible rods, random coils, and compat ellipsoids, the dependence of the chromatographic partition coefficient, K_{SEC}, on the viscosity radius, the radius of gyration, and the contour length, respectively, was determined. Since none of these dimensions appears to control retention uniquely, a phenomenological definition of R_{SEC} was provided. This parameter progressively deviates from the hydrodynamic radius with increasing macromolecular asymmetry.

INTRODUCTION

Theoretical and experimental studies have led to a number of suggestions concerning the macromolecular dimensional parameter that controls size-exclusion chromatography (SEC). Theoretical treatments[1,2] have indicated that peak migration in SEC should be governed by the mean projection length, $\bar{X}$. However, the prediction that $\bar{X}$ controls retention has not been borne out by experiment. Thus, for example, random coil polymers appear to co-elute with globular proteins of identical $[\eta]M$, where $[\eta]$ is the intrinsic viscosity, and M the molecular weight[3,4]; and since $[\eta]M$ has different dependences on $\bar{X}$ for macromoleculaes of different shapes[5], the observation

---

[a] Present address: Department of Chemistry, Wuhan University, Wuhan, Hubei, China.

of such "universal calibration"[6] for chain polymers and globular macromolecules is not in accord with a fundamental role for $\bar{X}$. In our previous studies[7], rod-like polymers were found to be eluted earlier than random coils of identical $[\eta]M$; however, no better congruence was achieved with plots of elution volume *vs.* $\bar{X}$.

The identification of a single dimensional parameter that controls SEC, if this "R_{SEC}" indeed exists, demands comparison of data for widely varying macromolecular shapes. If studies are confined to a single structural type, virtually any dimensional parameter will prove successful. Put differently, the dependence of the chromatographic partition coefficient, K_{SEC}, on log "size" will be uniform within a particular class of conformations (*e.g.* flexible chain macromolecules) regardless of the size parameter chosen. Thus, as pointed out by Potschka[8], the preference among biochemists for the Stokes radius, R_S[9], in contrast to the viscosity radius $R_\eta \approx ([\eta]M)^{1/3}$, employed by polymer chemists[10], may be more traditional than fundamental.

In addition to $\bar{X}$, R_S and R_η, the radius of gyration R_G has also been proposed as a fundamental SEC parameter[10]. With regard to the last three quantities, it should be noted that there is no compelling reason to assume that R_{SEC} must correspond to any dimension measured in dilute solution. The earlier notion that SEC is controlled by translational diffusion appears unlikely[10] so that the choice of a diffusion-related dimension is solely a matter of convenience. It is generaly accepted that partitioning between mobile phase and pore is an equilibrium process, but this observation does not lead to the identification of R_{SEC}.

In this work, pullulan, globular proteins, DNA, and schizophyllan are chosen as representative of (non-ionic) random coil, compact ellipsoid, wormlike chain, and (non-ionic) rigid rod, respectively. The selection of the column packing (Superose) and mobile phase (pH 5.5, 0.38 M NaCl–NaH$_2$PO$_4$, 9:1) is dictated by the need to avoid electrostatic or hydrophobic solute–packing interactions, *i.e.* to ensure "ideal" SEC[11]. Comparisons of the behavior of macromolecules with different structures under such conditions allow us to examine in more detail the nature of R_{SEC}

EXPERIMENTAL

Chromatography was carried out on a Superose 6 column (Pharmacia, Uppsala, Sweden). The samples employed were globular proteins, namely thyroglobulin, apoferritin, catalase, bovine serum albumin (BSA), ovalbumin, myoglobin, and cytochrome *c*; commercial pullulan molecular weight standards; and fractions of DNA and of schizophyllan.

The chromatographic partition coefficient, K_{SEC}, was obtained as

$$K_{SEC} = (V_e - V_0)/(V_t - V_0) \tag{1}$$

where V_e is the peak elution volume, V_0 the interstitial volume, determined by the elution of Blue Dextran, and V_t the total column volume, determined from the retention of ^2H_2O.

Chromatographic conditions and procedures, and the preparation and characterization of the DNA and schizophyllan fractions are described elsewhere[7].

RESULTS AND DISCUSSION

As previously noted, "universal calibration" plots for the polymers of this study systematically diverge with increasing asymmetry, so that R_η is not the governing parameter for separation. Similarly, macromolecules with different shapes but identical $\bar{X}$ fail to co-elute[7]. Fig. 1 illustrates that the radius of gyration R_G also is not a unifying dimension. Lastly, one might speculate that rapid tumbling of rod-like solutes, such as the schizophyllan fractions, could lead them to partition as if they were spheres with effective radii $L/2$ where L is the contour length; but Fig. 2 shows this to be erroneous.

The foregoing remarks show that no previously suggested dimension uniformly governs K_{SEC} for macromolecules of widely differing shape. We now consider whether a phenomenological approach could help to identify a universal dimension, if such a concept is indeed appropriate. Geometric considerations[2,12] suggest that, for spherical macromolecules in pores of well-defined shape

$$K_{SEC} = (1 - R/r_p)^\lambda \tag{2}$$

where R and r_p are dimensions of solute and pore respectively, and λ is a constant dependent on pore geometry, namely $\lambda = 1$ for slabs, 2 for cylinders, and 3 for spherical pores. While hypothetical pore dimensions may thus be envisioned, it should be pointed out that microscopy and other techniques reveal little resemblance between the structure of real gels and such idealized models[13]. For spherical solutes, the quanity R is unambiguous; for asymmetric solutes we identify it with R_{SEC}, which is not *a priori* defined. However, as noted above, we believe that R_{SEC} does not, in general, correspond to R_η, R_G, or $\bar{X}$. The relationship between R_{SEC} and some familiar dimension, say R_η, can be defined in a very general way as

$$R_{SEC} = \alpha R_\eta^\beta \tag{3}$$
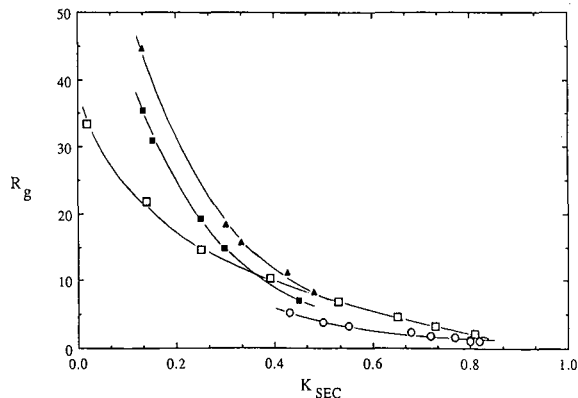
Fig. 1. Dependence of K_{SEC} on radius of gyration for pullulan ($\square$), DNA ($\blacktriangle$), schizophyllan ($\blacksquare$) and proteins ($\bigcirc$).
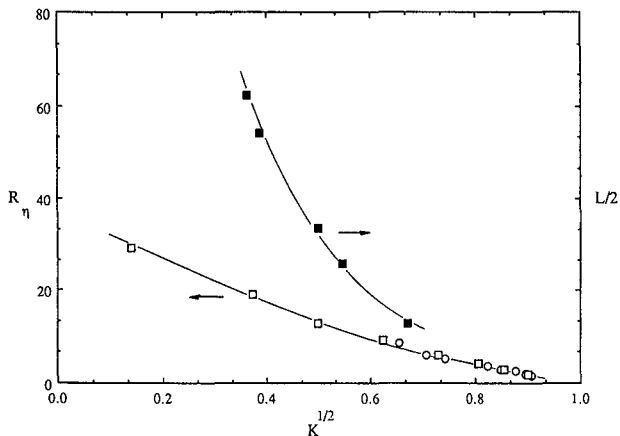
Fig. 2. Dependence of K_{SEC} of schizophyllan on $L/2$ (■) (right axis), compared to K_{SEC} vs. R_η for pullulan (□) and proteins (○) (left axis).

where α and β will depend on the shape of the macromolecule. Combining eqns. 2 and 3

$$K_{SEC} = [1 - (\alpha/r_p)R_\eta^\beta]^\lambda \tag{4}$$

The prediction of K_{SEC} thus depends on several unknown parameters. Identification of these by experiments requires the elimination of at least one unknown first. Thus, for example, if λ were known, a plot of $\ln(1 - K_{SEC}^{1/\lambda})$ vs. $\ln R_\eta$ yields β as the
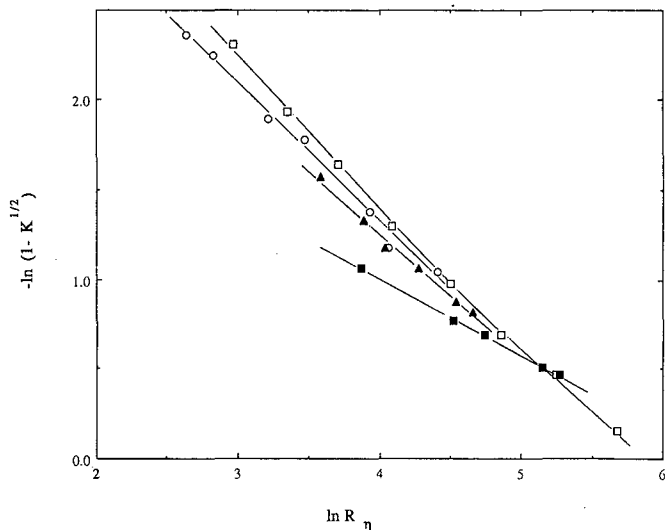
Fig. 3. Chromatographic behavior of (from right to left): pullulan (□), proteins (○), DNA (▲), and schizophyllan (■), plotted according to eqn. 4 with $\lambda = 2$.

TABLE I

FITS OF CHROMATOGRAPHIC DATA TO EQN. 4

	Pullulan	Proteins	DNA	Schizophyllan
β^a	0.85	0.75	0.69	0.43
r^b	0.998	1.00	0.996	1.00

[a] Slope of $\ln(1 - K^{1/2})$ vs. $\ln R_n$, yielding the exponent of $R_{SEC} = \alpha R_{SEC}{}^\beta$.
[b] Regression coefficient for eqn. 4.

slope. If the solute molecules were truly spherical, then $\alpha = \beta = 1$, and one may seek the value of λ which provides the best linear fit to $K^{1/\lambda}$ vs. R_n.

None of the solutes employed in this study approximate spheres, and the value of λ is difficult to define with the data in hand. We proceed with the assumption of $\lambda = 2$, for two reasons. First, we have found that the goodness of the fit of the data to the form $\ln(1 - K_{SEC}{}^{1/\lambda})$ vs. $\ln R_\eta$ is not very sensitive to the choice of λ. Second, our primary interest is to contrast the behavior of macromolecules with different degrees of asymmetry; since the data are all acquired on a single column, i.e. constant λ, useful comparisons may be made, even with residual uncertainty in λ.

Fig. 3 shows the chromatographic data plotted according to the logarithmic form of eqn. 4. Data points for $K_{SEC} < 0.1$, i.e. close to the exclusion limit, are omitted from this plot. The deviation of such data from the lines of Fig. 3 was attributed to the effect of pore-size distribution, i.e. that the mean pore diameter sampled by large solutes must be larger than the effective pore size in the middle of the calibraiton range. The linear correlation of the data is remarkably good. Values for β and the regression coefficients for the lines for pullulan, globular proteins, DNA, and schizophyllan are given in Table I. The values of β appear to deviate systematically from unity with increasing solute asymmetry, inasmuch as schizophyllan has the largest persistence length and pullulan the smallest. It is interesting to note that β for the globular proteins is intermediate between the values for pullulan and DNA. This effect may indicate that the overall structures of these proteins are better approximated by ellipsoids than spheres, but the possibility that weak non-ideal interactions with the packing distort the data cannot be ruled out.

The phenomenological treatment indicates two fruitful directions. First, the value of λ may be better defined when data are obtained with solutes of more nearly spherical structure. Second, direct insight into a separation model may be generated when comparisons are made with appropriate theoretical predictions. These issues are the subject of continued efforts.

ACKNOWLEDGEMENTS

REFERENCES

1 J. C. Giddings, E. Kucera, C. P. Russel and M. N. Meyers, *J. Phys. Chem*, 78 (1968) 397.
2 E. F. Casassa, *J. Phys. Chem.*, 75 (1971) 3929.
3 R. P. Frigon, J. K. Leypoldt, S. Uyeji and L. W. Henderson, *Anal. Chem.*, 55 (1983) 1349.
4 P. L. Dubin, J. M. Principi, B. A. Smith and M. A. Fallon, *J. Colloid Interface Sci.*, 127 (1989) 558.
5 E. F. Casassa, *Macromolecules*, 9 (1976) 182.
6 Z. Grubisic, R. Rempp and H. Benoit, *J. Polym. Sci., Part B*, 5 (1967) 753.
7 P. L. Dubin and J. M. Principi, *Macromolecules*, 22 (1989) 1891.
8 M. Potschka, *Anal. Biochem.*, 162 (1987) 47.
9 G. C. Ackers, in H. Neurath and R. L. Hill (Editors), *The Proteins*, Vol. 1, Academic Press, New York, 3rd ed., 1975, p. 1.
10 E. F. Cassasa and Y. Tagami, *Macromolecules*, 2 (1969) 14.
11 P. L. Dubin and J. M. Principi, *J. Chromatogr.*, 479 (1989) 159.
12 H. Waldmann-Meyer, *J. Chromatogr.*, 350 (1985) 1.
13 L. Hagel, in P. L. Dubin (Editor), *Aqueous Size-Exclusion Chromatography*, Elsevier, Amsterdam, 1988, Ch. 5.

CHROMSYMP. 1894

Preparation and evaluation of octadecyl-treated porous glasses

Application to the determination of methotrexate in serum

MITSUYOSHI OKAMOTO*, ISAO YOSHIDA and MAKOTO UTSUMI

Gifu Prefectural Tajimi Hospital, 5–161, Maehata cho, Tajimi, Gifu 507 (Japan)

KAZUNORI NOBUHARA

Fuji-Davison Chemical Ltd., 2-Chome, Kozoji cho, Kasugai, Aichi 487 (Japan)

and

KIYOKATSU JINNO

Toyohashi University of Technology, 1–1, Hibarigaoka, Tempaku cho, Toyohashi 440 (Japan)

ABSTRACT

The retention and selectivity of methotrexate (MTX) in serum were studied by high-performance liquid chromatography on octadecyl-treated porous glasses and silicas. From elemental analysis data for carbon, the maximum number of bonded octadecyl surface groups per gram (mean pore diameter 153 Å, specific surface area 193 m^2/g, pore volume 0.83 ml/g) in octadecyl-treated glass was calculated to be 0.131 $\times 10^{21}$. MTX in human serum could be separated on both glasses and silicas with methanol–acetate buffer mixtures as eluents.

INTRODUCTION

Chemically bonded stationary phases are the most widely used column packing materials for reversed-phase high-performance liquid chromatography (HPLC). These materials consist of organic functional groups, such as octadecyl, octyl, ethyl and phenyl groups, bonded to silicas. In previous papers[1–4], we suggested that the important parameters of silica with respect to the number of accessible alkylamino or phenyl groups per 100 $Å^2$ are the pore diameter and the specific surface area. In investigations of bioavailability, and also in pharmacokinetic and forensic science studies, several types of gel are used. Therefore, we have now considered how the chromatographic properties of octadecyl- and phenyl-modified gels are important in HPLC or micro-HPLC columns; a few reports of HPLC analyses on octadecyl-treated glass columns in physical and chemical research have been reported[5–9]. Furthermore, we studied the HPLC determination of methotrexate (MTX) in human serum.

EXPERIMENTAL

Reagents

Octadecyldimethylchlorosilane (ODS) was obtained from Petrach Systems (Bristol, PA, U.S.A.) and MTX from Sigma (Poole, U.K.). Four types of porous glasses (1G, 2G, 3G and 4G) and four types of porous silicas (1S, 2S, 3S and 4S) differing in their mean particle size, mean pore diameter, specific surface area and pore volume (Table I), were prepared in our laboratories. The other reagents and organic solvents were of analytical-reagent grade.

TABLE I

CHARACTERISTICS OF ORIGINAL GLASSES AND SILICAS

Sample[a]	Mean particle size (μm)	Mean pore diameter ($\mathring{A}$)	Specific surface area (m^2/g)	Pore volume (ml/g)
Glass 1G	5.8	153	193	0.83
Glass 2G	8.2	335	69	0.57
Glass 3G	8.5	577	57	0.84
Glass 4G	8.7	731	47	0.81
Silica 1S	8.0	164	197	1.20
Silica 2S	8.8	507	78	1.05
Silica 3S	9.7	728	52	1.11
Silica 4S	9.6	787	50	1.10

[a] The designations are for convenience and have no commercial significance.

Apparatus

HPLC measurements were carried out on a Twincle instrument (Jasco, Tokyo, Japan), equipped with a Uvidec-100 IV variable-wavelength detector (Jasco, Tokyo, Japan) and a column of 150 × 4.6 mm I.D., packed with ODS-treated glass or silica.

Stationary phase and elemental analysis

As described previously[1–4], 7 g of dried glass 1G, 2G, 3G or 4G or silica 1S, 2S, 3S or 4S were added to 70 ml of a 3.4% solution of ODS in dry toluene containing 3 ml of triethylamine. The glass or the silica suspension was refluxed for 5 h, filtered through a glass filter (1 μm), washed several times with toluene, chloroform, methanol and acetone and then dried *in vacuo* at 70°C for 2 days. The final products are listed in Table II as 1G-ODS, 2G-ODS, 3G-ODS, 4G-ODS, 1S-ODS, 2S-ODS, 3S-ODS and 4S-ODS, respectively. The characteristics of these materials are also given in Table II. The carbon contents of the treated glasses or silicas were determined by elemental analysis using an MT-3 CHN elemental analyzer (Yanagimoto, Kyoto, Japan). The specific surface areas, mean pore diameters and pore volumes of the column glasses and silicas were determined with an MOD-220 porosimeter (Carlo Erba, Milan, Italy) and an SA-1000 surface area/pore volume analyser (Shibata, Tokyo, Japan), and the data are given in Table II.

Column preparation

The column glasses or silicas were packed into stainless-steel columns (150 × 4.6 mm I.D.) by the slurry technique.

Procedure

According to the Brimmell and Sams method[10], a 25-μl volume of internal standard (aminopterin, 40 mg/l in water, with 200 μl of 1 *M* sodium hydroxide added to aid solution) was added to 225 μl of human serum in a microtube and centrifuged in a microcentrifuge at 10 000 *g* for 10 min. Acetone (250 μl) was added as protein precipitant and mixed, using a vortex mixer. The mixture was again centrifuged for 60 s. A volume of 300 μl of the supernatant was transferred to a second microtube containing 300 μl of butan-1-ol and 400 μl of diethyl ether and the procedure of mixing and centrifugation for 60 s was repeated. The supernatant was discarded, then 10–30 μl of the remaining solution were injected onto the column.

RESULTS AND DISCUSSION

Fig. 1 shows the pore diameter *vs.* pore volume plots obtained for the original glasses (glass-1G); the average pore diameter and pore volume were determined as 153 Å and 0.83 ml/g, respectively.

From the elemental analyses of glasses and silicas treated with ODS, the number of bonded octadecyl surface groups per gram or per 100 Å^2 were calculated by the previously described procedure. The results are given in Table II. As can be seen, an
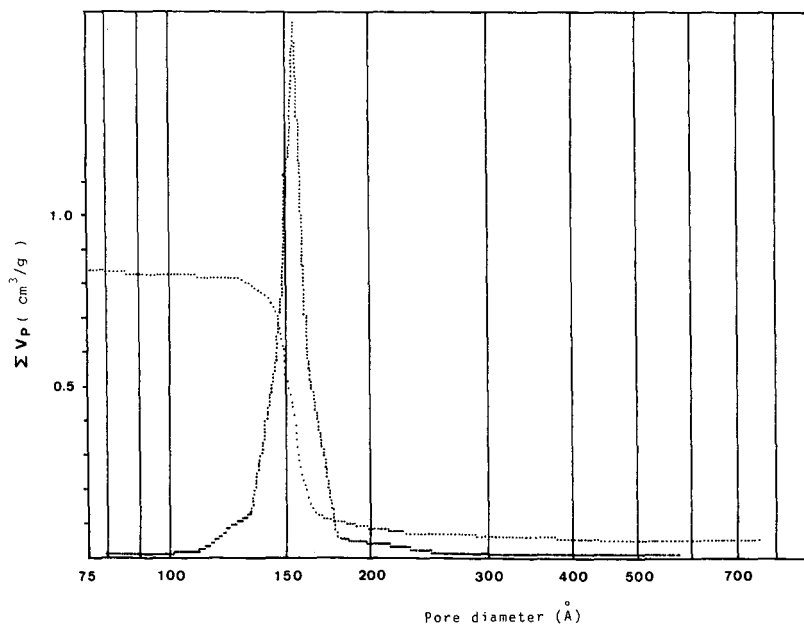
Fig. 1. Pore diameter (Å) *versus* pore volume (cm^3/g) of the original glass (glass 1G).

TABLE II

CHARACTERISTICS OF TREATED GLASSES AND SILICAS

Treated gel	Specific surface area (m^2/g)	Carbon content (%)	Average pore diameter (Å)	Pore volume (ml/g)	No. of surface groups per gram ($\times 10^{21}$)	No. of surface groups per 100 Å²
1G-ODS	107	5.73	131	0.80	0.131	1.44
2G-ODS	46.4	2.92	328	0.57	0.073	1.58
3G-ODS	43.9	2.71	530	0.70	0.068	1.55
4G-ODS	33.7	2.20	699	0.62	0.055	1.63
1S-ODS	146	11.0	130	0.81	0.276	1.89
2S-ODS	59.7	1.71	485	0.97	0.043	0.72
3S-ODS	42.7	1.44	688	0.96	0.036	0.85
4S-ODS	39.8	1.27	733	1.00	0.032	0.80

increase in the specific surface area of glass or silica increases the number of bonded surface groups per gram, but does not change the number of bonded surface groups per 100 Å².

The retention time of MTX was 13.2 min on 1G-ODS. The limit of detection for MTX was $8.0 \cdot 10^{-8}$ M, at which concentration the peak area was three times the noise level of the system. However, real minimum detectable concentration of samples, prepared as described under Experimental, was $1.5 \cdot 10^{-7}$ M.

A chromatogram for a human serum sample taken 1 h after intraveneous infusion of MTX is shown in Fig. 2, which corresponds to the experiments with 600 mg of MTX in Fig. 3. Blanks were prepared from human serum from MTX-free subjects, and no interfering peaks were observed at the retention times of the compounds of
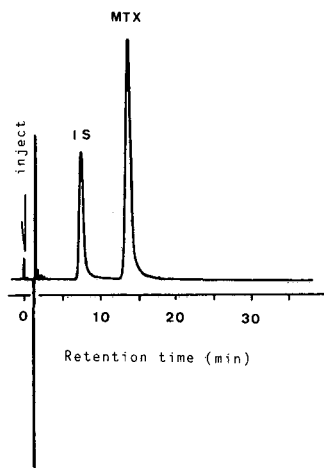
Fig. 2. Liquid chromatogram of human serum 1 h after intraveneous infusion of methotrexate. Peaks: MTX = methotrexate; IS = internal standard (aminopterin). Sample, human serum sample 1 in Fig. 3; column, 1G-ODS, 150 × 4.6 mm I.D.; mobile phase, methanol–0.01 M acetate buffer (11:39) (pH 3.8); flow-rate, 1.5 ml/min; detection, UV (305 nm).
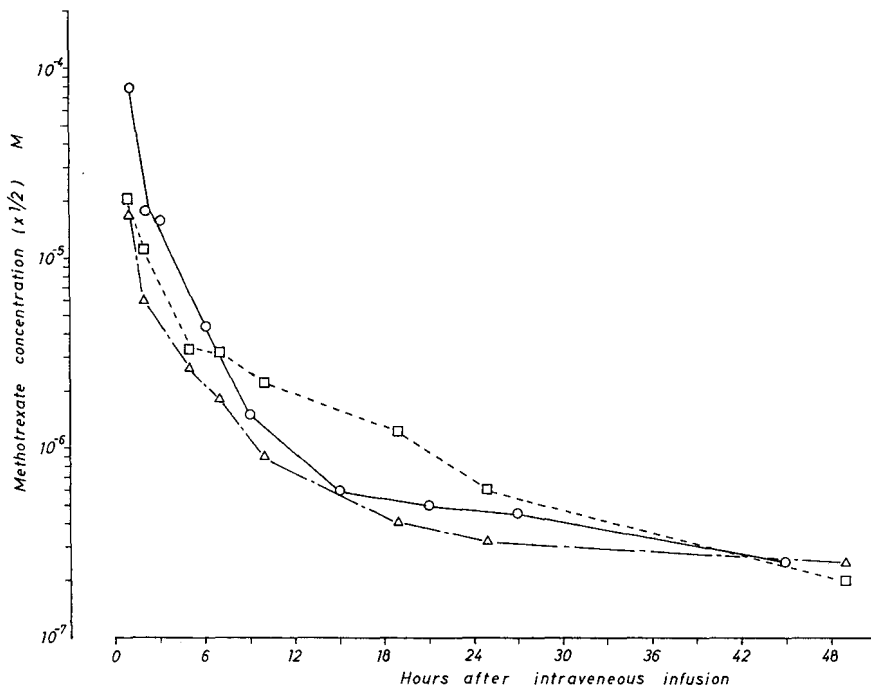
Fig. 3. Changes in methotrexate concentration in human serum with time after intraveneous infusion of 600 mg of methotrexate. Conditions and solutes as in Fig. 2. ◯ = Sample 1; △ = sample 2; ☐ = sample 3.

interest. The MTX was separated on both the glasses and silicas studied, but with different degrees of resolution and elution orders. These results show that the ODS-modified glasses could be useful column materials for HPLC.

It can be concluded that it is not sufficient to evaluate column gels only from the point of view of the carbon content of the chemically treated reversed-phase materials; one should also consider the pore-size distribution of the support glass, the bulkiness of the ligand bonded to the glass and the molecular size of the solute before any precise statement is made.

REFERENCES

1 M. Okamoto, J. Chromatogr., 202 (1980) 55.
2 M. Okamoto and H. Kishimoto, J. Chromatogr., 212 (1981) 251.
3 M. Okamoto and F. Yamada, J. Chromatogr., 247 (1982) 167.
4 M. Okamoto and F. Yamada, J. Chromatogr., 283 (1984) 61.
5 J. Rayss, A. Dawidowicz, Z. Suprynowicz and B. Buszewski, Chromatographia, 17 (1983) 437.

6 Z. Suprynowicz, J. Rayss, A. L. Dawidowicz and R. Lodknowski, *Chromatographia*, 20 (1985) 677.
7 M. Okamoto and K. Jinno, *Chromatographia*, 21 (1986) 467.
8 M. Okamoto and K. Jinno, *J. Chromatogr.*, 395 (1987) 171.
9 M. Okamoto, K. Jinno, M. Yamagami, K. Nobuhara and K. Fukushima, *J. Chromatogr.*, 396 (1987) 345.
10 P. A. Brimmell and D. J. Sams, *J. Chromatogr.*, 413 (1987) 320.

Novel silica-based strong anion exchanger for single-column ion chromatography

CHING-ERH LIN*, YONG-HWA YANG and MEI-HUI YANG

Department of Chemistry, National Taiwan University, Taipei 10764 (Taiwan)

ABSTRACT

A novel silica-based anion exchanger for single-column ion chromatography was prepared by immobilizing a quaternary ammonium salt of cyanuric chloride onto the surface of silane-modified silica-gel. A stationary phase with low capacity (0.38 mequiv./g) was obtained and effective separation of monovalent anions was achieved with a concentration of tartaric acid or *o*-phthalic acid lower than 0.5 mM on a short column prepared using a conductometric detector. Factors that can affect the retention behaviour, such as eluent species, eluent concentration and eluent pH, were examined. The results demonstrate that the retention of anions is dominantly governed by ion-exchange interactions. However, the matrix effect due to the interaction between the stationary phase and the eluent may also play an important role.

INTRODUCTION

Ion chromatography provides a means for the rapid separation and determination of mixtures of inorganic and/or organic ions in aqueous media[1-4]. In the single-column ion chromatographic method developed by Fritz and co-workers[5-8], a conductivity detector could be connected directly to a separation column employing a low-capacity ion-exchange material which allowed the use of a low concentration and, in most instances, a low equivalent conductance of the eluent so that the background conductivity could remain low. Nevertheless, eluents with high equivalent conductivity, such as potassium hydroxide, could also be used occasionally[9-11]. Further, the eluents so chosen should have a sufficiently high affinity for the ion-exchange material that the eluent anions can compete with the sample anions for the active sites on the ion-exchange surface and move the sample anions through the column.

In an attempt to design an ion-exchange material specifically for anion chromatography, Fritz and co-workers[5,6,12] synthesized a range of low-capacity anion-exchange resins. These surface-aminated macroporous ion-exchange resins do not provide adequate column efficiency for most applications because of the large particle size. In view of this, efforts have been directed towards the design of new high-efficiency resin-based ion exchangers with low ion-exchange capacities and small particle size[13].

Concurrent with the development of the resin-based ion exchangers, silica-based materials, which have better mechanical strength and do not swell in organic eluents, were also developed for anion chromatography. The silica-based anion exchangers were produced by bonding quaternary ammonium functions onto microparticle silica with low capacity (0.1–0.3 mequiv./g)[14,15]. The main drawback of the silica-based columns is that their operating pH range is limited to 2–6 owing to the dissolution problem of hydroxyl-ion attack[16], and this in turn restricts both the range of sample loadings and the choice of eluents that can be used[3]. Also, on some occasions the occurrence of system peaks in single-column ion chromatography may cause detection problems[17–19]. However, the commercial availability of silica-based columns, which show relatively high efficiencies[3,20], has led to the development of a considerable number of specialized applications[4].

In this investigation, an attempt was made to seek an alternative route to the synthesis of a silica-based strong anion exchanger. A new low-capacity anion exchanger was prepared by immobilizing a quaternary ammonium salt of cyanuric chloride onto the surface of a silane-modified silica gel. A short column was used so that the column void volume and subsequent run time could be reduced. Factors such as eluent species, eluent concentration and eluent pH, all of which may affect the retention behaviour of anions, were investigated using a conductometric detector. The results of this work may provide a useful new route to the synthesis of silica-based strong anion exchangers so that highly efficient and effective chromatographic separations can be achieved. Further, the introduction of the moiety of the trifunctional s-triazine ring to the spacer arm of the stationary phase can be further modified so that difficulties encountered with currently available silica-based anion exchangers can be minimized.

EXPERIMENTAL

Chemicals

Triethylamine and cyanuric chloride were obtained from Riedel-de Haën (Hannover, F.R.G.). The silica gel used was LiChrosorb SI 60 (particle size, 10 μm; pore size, 6 nm) obtained from E. Merck (Darmstadt, F.R.G.). Tartaric acid was purchased from J. T. Baker (Phillipsburgh, NJ, U.S.A.), o-phthalic acid from Wako (Osaka, Japan) and 3-aminopropyltriethoxysilane (APS) from Petrarch Systems (Bristol, PA, U.S.A.). Other synthesis reagents for the preparation of anion exchanger were of the highest available purity. Water was purified by ion exchange followed by a Milli-Q water purification system (Millipore, Bedford, MA, U.S.A.).

Preparation of silica-based anion exchanger

Quaternary ammonium salt of cyanuric chloride. A solution of 0.02 mol of cyanuric chloride in 30 ml of acetone was added with agitation to a 300-ml beaker containing 20 ml of acetone and 40 ml of water in an ice-bath at *ca.* 5°C, followed by dropwise addition of 2.8 ml (0.02 mol) of triethylamine. The mixed solution was reacted for 30 min. The white product was precipitated and filtered off, washed well with acetone and then dried at reduced pressure. The melting point of the product was higher than 300°C.

Silane-modified silica gel. Silica gel (3 g) dried at 150°C *in vacuo* for 18 h was

suspended in 150 ml of dry toluene, then 1.0 ml of 3-aminopropyltriethoxysilane was added. The reaction mixture was refluxed under nitrogen for 12 h with stirring. The silane-modified silica gel thus obtained was filtered, washed thoroughly with toluene, methanol and acetone successively (or Soxhlet extracted with methanol after washing with toluene), then dried in an oven at 70°C for 4 h.

Silica-based strong anion exchanger. Silane-modified silica gel (3 g) was suspended in a mixture of 100 ml water and 50 ml of acetone to which 0.88 g of the quaternary ammonium salt of cyanuric chloride was added. A solution of sodium hydrogencarbonate was slowly added to this suspension with agitation. While keeping the reaction temperature at 38°C, the reaction was terminated after 24 h and the product was filtered off, washed thoroughly with water, methanol and acetone successively, and then dried over P_2O_5 at reduced pressure for 8 h. The reaction scheme for the preparation of the anion exchanger is shown in Fig. 1. As can be seen, the moiety of the *s*-triazine ring is covalently bonded to the amino group of the silane-modified silica surface.

Elemental analyses of the strong anion exchangers were carried out. The average nitrogen and carbon contents obtained in three separate experiments were 2.71 $\pm$ 0.05% and 5.66 $\pm$ 0.01%, respectively. The anion-exchange capacity determined from the average nitrogen percentage obtained by elemental analysis was 0.38 mequiv./g. The ion-exchange capacity (I) was calculated using the equation I (mequiv./g) = [N(%) $\cdot$ 1000]/(5 $\cdot$ 14 $\cdot$ 100).

Standard solutions and eluent

Stock standard solutions of 1000 ppm of the various anions were prepared from analytical-reagent grade reagents with doubly deionized water. Potassium salts were used in all instances. Working standard solutions were obtained by diluting the stock standard solutions with deionized water. Eluents were prepared by dissolving the acid in water and, if necessary, adjusting the pH with 1 M potassium hydroxide solution. The eluents used were filtered through a 0.45-μm membrane filter and degassed by ultrasonic vibration prior to use.
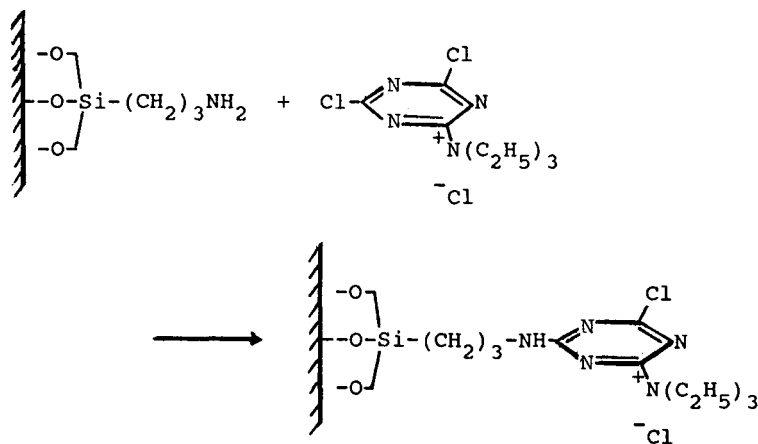
Fig. 1. Reaction scheme for the preparation of the strong anion exchanger.

Apparatus and chromatography

All ion chromatographic studies were carried out with an ion chromatographic system which consisted of a Waters Assoc. Model 510 solvent-delivery system, a U6K universal injector and a Toyo Soda Model CM-8000 conductivity detector. The integrator used was a Waters Assoc. Model 740 data module. A stainless-steel column (50 × 4 mm I.D.) was packed with isopropanol as the slurry solvent using a Chemco Model C_{pp-085} slurry-packing apparatus (Chemco Scientific, Japan) at about 350 kg/cm^2. The range of the conductometric detector was set at 0.005 and the gain at 50. The conductivity cell was maintained at 35°C. The flow-rate of the eluent was kept at 1 ml/min. The elemental analyses were carried out with a Perkin-Elmer Model 240C elemental analyser.

RESULT AND DISCUSSION

As the eluent anions compete with the sample anions during the chromato-graphic process, changes to the eluent species, eluent concentration and/or eluent pH, which may affect the retention behaviour of the sample anions, were investigated so that the retention process of the column prepared in this study could be characterized.

Effects of eluent species and eluent concentration

In order to separate the sample anions effectively, the eluent anion must be sufficiently attracted to the ion-exchange material that a very low concentration of the eluent will move sample anions to be separated through the column. However, the conductance of the eluent must also be low so that the background conductivity can remain low. As organic acids tend to have a low equivalent conductance and a wide range of pK_a values, which allow a great degree of flexibility in tailoring retention as a function of pH, organic acids and their salts are the most common eluents for anion analysis in single-column ion chromatography[4–6,21,22]. In this investigation, tartaric acid and *o*-phthalic acid were among the eluents found to be successful.

To elucidate the role of ion-exchange interactions, chromatographic data that can define the influence of eluent concentration on retention at constant pH are needed. Table I gives the adjusted retention times of some common anions detected using tartaric acid and *o*-phthalic acid as the eluents at various concentrations, while maintaining the eluent pH at 4.0. The adjusted retention time of a solute anion (t_R') is defined as $t_R' = t_R - t_0$, where t_R is the retention time of the solute anion and t_0 is the retention time of the injection peak. The interaction of the anion exchanger with the eluent anions appears to be electrostatic because an increase in eluent concentration causes a decrease in retention time, as can be seen in Table I. This is due to the increased ionic strength of the eluent. Hence the expected trend in retention as the eluent concentration is varied is clearly evident[4,18,21,23,24]. As the ion-exchange process is largely governed by electrostatic interactions, the retention is thought to be the result of the strength of this interaction, especially for inorganic anions.

As is also indicated in Table I, better separations could be achieved at eluent concentrations lower than 0.5 m*M* and the retention times of the anions were found to be longer with tartaric acid than with *o*-phthalic acid at the same concentration and pH. Therefore, tartaric acid should be a more effective eluent and the chromatographic performance of the separation of anions on the column prepared was significantly

TABLE I

ADJUSTED RETENTION TIMES OF ANIONS USING ORGANIC ACIDS AS THE ELUENT AT VARIOUS CONCENTRATIONS

Column, 50 × 4.6 mm I.D. (0.38 mequiv./g); eluent pH, 4.0; flow-rate, 1 ml/min.

Anion	Adjusted retention time (min)					
	Tartaric acid (mM)			o-Phthalic acid (mM)		
	0.1	0.25	0.5	0.1	0.25	0.5
IO_3^-	4.61	3.25	2.31	4.04	2.57	2.00
Cl^-	4.81	3.34	2.27	3.96	2.54	1.85
BrO_3^-	4.97	3.55	2.41			
Br^-	5.23	3.69	2.57	4.35	2.65	2.02
NO_2^-	5.58	4.00	2.84	4.79	3.04	2.38
ClO_3^-	5.69	4.21	2.80	4.74	3.02	2.11
NO_3^-	6.73	4.92	3.34	5.62	3.59	2.73
I^-	6.86	5.02	3.41	5.46	3.53	2.71
ClO_4^-	8.77	6.35	4.36			
SCN^-	10.2	7.42	5.03	7.83	4.80	3.71
Formate	5.28	3.91	2.80	4.75	3.23	2.44
Acetate	1.77	1.40	1.08	1.49	1.18	0.09
Propionate	1.95	1.62	1.19	1.59	1.28	1.05

improved when tartaric acid, instead of o-phthalic acid, was chosen as the eluent. The elution order of some common anions with tartaric acid at pH 4.0 was acetate < propionate < IO_3^- ≤ Cl^- < BrO_3^- < Br^- < formate < NO_2^- ≤ ClO_3^- < NO_3^- ≤ I^- < ClO_4^- < SCN^-. A typical chromatogram for the separation of acetate, Cl^-, NO_2^-, NO_3^-, ClO_4^- and SCN^- anions on a short column (50 × 4.6 mm I.D., 0.38 mequiv./g) using 0.25 mM tartaric acid as the eluent at pH 4.0 is shown in Fig. 2. Thus, anions such as NO_2^- (or ClO_3^-), NO_3^- (or I^-) and ClO_4^- can be effectively separated between Cl^- and SCN^-. On the other hand, the elution order was acetate < propionate < Cl^- ≤ IO_3^- < Br^- < ClO_3^- ≤ NO_2^- < formate < I^- ≤ NO_3^- < SCN^- when using o-phthalic acid as the eluent at pH 4.0. Reversal of the elution order was observed for some closedly eluted anions, such as IO_3^- and Cl^-, NO_2^- and ClO_3^-, and NO_3^- and I^- when the eluent was changed from tartaric acid to o-phthalic acid. This observation is not unexpected because the interactions involved in the retention of solute anions for a particular stationary phase may be different with different eluent anions. This interaction, which depends on the nature of the stationary phase and the nature of the eluent anion, influences the distribution coefficient of a solute anion and can affect the competition between the eluent anion and the sample anion for the active sites on the ion-exchange material. Therefore, the retention (or the selectivity) of an anion may vary when using different eluent anions.

The data in Table I clearly indicate that the retention times of solute anions decrease considerably when using o-phthalic acid instead of tartaric acid as the eluent under the same conditions. Apparently, the affinity of o-phthalic acid for the stationary phase is greater than that of tartaric acid. The decrease in the retention times cannot be accounted for by consideration of charge effects alone, because the fraction

0.0   7.5   (min)
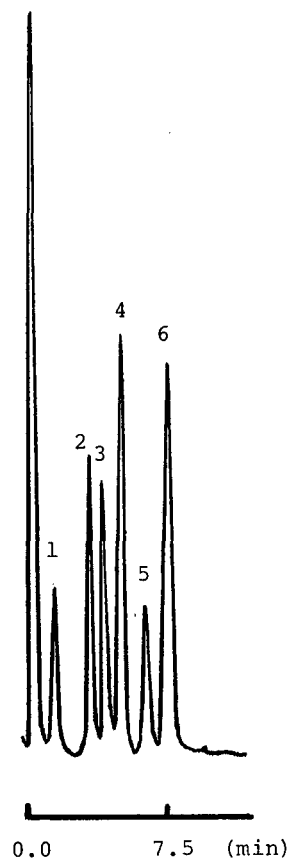
Retention Time

Fig. 2. Typical chromatogram for the separation of some common anions: 1 = acetate, 10 ppm; 2 = Cl⁻, 3 ppm; 3 = NO_2^-, 3 ppm; 4 = NO_3^-, 5 ppm; 5 = ClO_4^-, 5 ppm; 6 = SCN⁻, 10 ppm. Elution conditions: eluent, 0.25 mM tartaric acid; eluent pH, 4.0; flow-rate, 1 ml/min.

of o-phthalic acid existing as the divalent ion in the eluent solution is much smaller than that of tartaric acid at pH 4.0. We speculate that, apart from charge effects, matrix effects due to the adsorption of o-phthalic acid on the surface of the stationary phase and/or the interaction of o-phthalic acid with the s-triazine ring of the stationary phase may contribute significantly to the retention of solute anions. Indeed, it has been shown that the introduction of an s-triazine ring into the stationary phase can greatly affect the retention of aromatic compounds in HPLC[25,26].

The linear relationship between log t_R' and log [eluent] was tested for a number of anions using various concentrations of tartaric acid and o-phthalic acid at pH 4.0. The plots in Fig. 3 show the straight lines obtained. However, the slopes of these plots were found to deviate considerably from unity. In fact, the slopes obtained for inorganic anions, formate ion and low carboxylate ions are about 0.45, 0.39 and 0.31, respectively, when using tartaric acid as the eluent, whereas they are about 0.46, 0.41
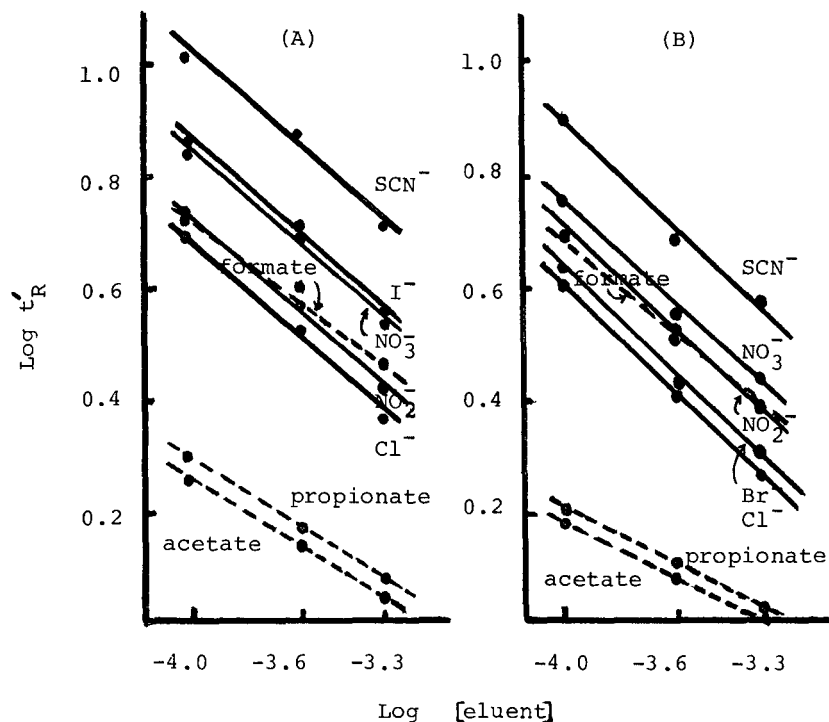
Fig. 3. Plots of log t'_R versus log [eluent] for some representative anions at pH 4.0 using (A) tartaric acid and (B) *o*-phthalic acid as the eluent. Solid lines, inorganic anions; broken lines, organic anions.

and 0.37, respectively, with *o*-phthalic acid. A similar phenomenon was observed for the hydrogencarbonate ion[27]. At the present stage of the investigation, it is not clear why the slopes are so low. However, it may imply that the charge effect is not the only contributing factor and that the matrix effect, which depends on the nature of the stationary phase, may play an important role in the retention mechanism. Perhaps other factors such as adsorption, hydrophobic interactions between the stationary phase and the eluent and acid strength should be taken into consideration in order to account for the deviation of the slope from unity[4,23,28].

It is of interest that SCN⁻ can be effectively eluted within a reasonably short time on this column. For instance, SCN⁻ was eluted in 7.83 min with 0.1 m*M* *o*-phthalic acid at pH 4.0, whereas it had a retention time of 10.2 min at a concentration of 0.1 m*M* when using tartaric acid at the same pH.

Effect of eluent pH

The elution times of anions can be greatly affected by the eluent pH because the elution power increases substantially with increasing eluent pH[4,20,21]. For example, for *o*-phthalic acid (or tartaric acid) as the eluent, the eluting power diminished when the eluent pH was above 6 (or 5). Depending on the eluent pH, some of the eluent anions are converted either into anions of lower charge or into a molecular acid[21,24]. Table II shows the effect of eluent pH on the retention of some typical anions such as

TABLE II

ADJUSTED RETENTION TIMES OF ANIONS USING ORGANIC ACID AS THE ELUENT AT DIFFERENT pH

Column, 50 × 4.6 mm I.D. (0.38 mequiv./g); eluent concentration, 0.1 mM; flow-rate, 1 ml/min.

Anion	Adjusted retention time (min)					
	Tartaric acid (pH)			o-Phthalic acid (pH)		
	4.0	4.5	5.0	4.0	4.5	5.0
IO_3^-	4.61	2.50		4.04	2.46	1.28
Cl^-	4.81	2.49	1.09	3.96	2.61	1.49
BrO_3^-	4.97	2.56	1.33	4.05	2.64	1.53
Br^-	5.23	2.66	1.23	4.35	2.93	1.61
NO_2^-	5.58	3.17	1.58	4.79	3.11	1.75
NO_3^-	6.73	3.45	1.63	5.62	3.47	1.92
I^-	6.86	3.63	1.62	5.46	3.99	2.29
ClO_4^-	8.77	4.42	2.03	6.95	4.86	2.46
SCN^-	10.2	5.18	2.45	7.83	5.59	2.88
Formate	5.28	3.62	2.13	4.75	0.51	
Acetate	1.77	1.93		1.49	2.08	1.71
Propionate	1.95	2.11		1.59	2.42	2.23

acetate, Cl^-, Br^-, NO_2^-, NO_3^-, I^-, ClO_4^- and SCN^- using tartaric acid or o-phthalic acid as the eluent. As expected, inorganic anions could be retained longer in the column when the eluent pH was decreased. Therefore, the separation of monovalent anions becomes progressively more favourable as the eluent pH decreases.

It should be noted that the retention of organic anions behaves differently from that of inorganic anions. Although the retention time of formate ion decreases with increasing eluent pH, its retention behaviour is different from that of most of the inorganic anions and other low carboxylate ions. Acetate and propionate ions are weakly retained by the column and elute early, but their retention behaviours depend on the eluent concentration and pH. For instance, with 0.5 mM o-phthalic acid as the eluent, the retention increases linearly with increasing eluent pH from 3.5 to 5.0, but with 0.1 mM o-phthalic acid, the retention first increases from pH 4.0 to 4.5, then decreases from pH 4.5 to 5.0. A pausible explanation of this behaviour can be made in terms of the effect of pH on the nature of the surface of the stationary phase, because the ionic nature of the silica surface increases slightly with increase in eluent pH from 2 to 6, and the effect on the protonation of eluent anions and organic acid anions at low eluent pH[28]. Nevertheless, the nature of the competition between the eluent anions and organic anions for the active sites of ion exchange becomes very complicated. Further study is needed in order to obtain a better understanding of the retention mechanism of organic anions.

Characteristics of the column

The strong anion exchangers prepared in this work are reproducible because the elemental analysis data obtained in three separate experiments are consistent. The

average values of the nitrogen, hydrogen and carbon contents are 2.71 ± 0.05%, 1.25 ± 0.02% and 5.66 ± 0.01%, respectively.

The anion exchangers are stable. The column was used daily to elute sample anions for 18 h at a flow-rate of 1 ml/min for at least 2 months without any noticeable changes in the band widths or the retentions of tested sample anions.

As mentioned in the Introduction, the approach of using low-capacity silica-based anion exchangers in single-column ion chromatography has the disadvantage of a limited choice of eluents. For an effective chromatographic separation of anions with a particular stationary phase, the ranges of the eluent concentration, the eluent pH and the amount of sample loading are further restricted. As the retention (or the selectivity) of anions also depends on other factors, such as the ion-exchange capacity, the functionalities of the anion exchanger and the nature of the surface of the stationary phase, in addition to the eluent species, eluent concentration and eluent pH, direct comparison between the column prepared in this work and commercially available columns, such as Vydac 302IC or Toyo Soda TSK-GEL IEX-520, is not possible owing to a lack of detailed information. However, by comparing the retention data and the chromatograms obtained in this work with those reported in the literature[18,20,21] using a commercially available column, we conclude that the efficiency of our column is as high as that of the commercial columns and the sensitivity is much better because much lower eluent concentrations and sample loadings are required. In support of the usefulness of our column, a Waters Assoc. IC PAK A column was used in our ion chromatographic system, and it was found that much larger amounts of sample were needed in order to have detectable signals, much longer retention times were observed and the resolution was not as good as with our column. For instance, with 0.25 mM tartaric acid as the eluent at pH 4.0 and at a flow-rate of 1 ml/min, iodide and thiocyanate ions were found to be retained in the column for more than 45 min, and the retention times for Cl^-, Br^-, NO_2^- and NO_3^- were 12.25, 12.27, 19.45 and 30.31 min, respectively. Therefore, the advantages of high efficiency and high sensitivity of the column prepared in this work are clearly demonstrated.

CONCLUSIONS

A new silica-based anion exchanger was successfully prepared by immobilizing a quaternary ammonium salt to cyanuric chloride onto a silane-modified silica gel for single-column ion chromatography. Effective separations of monovalent anions can be achieved with low concentrations of tartaric acid or o-phthalic acid as the eluents at $ca.$ pH 4.0. The thiocyanate anion can be eluted within a reasonably short time on the short column prepared. Better chromatographic separations can be achieved with tartaric acid than with o-phthalic acid as the eluent. The retention mechanism is dominantly governed by ion-exchange interactions. However, the matrix effect due to the interaction between the stationary phase and the eluent may play an important role in the chromatographic separation of anions.

ACKNOWLEDGEMENT

REFERENCES

1   J. S. Fritz, D. T. Gjerde and C. Pohlandt, *Ion Chromatography*, Hüthig, New York, 1982.
2   F. C. Smith, Jr., and R. C. Chang, *The Practice of Ion Chromatography*, Wiley, New York, 1983.
3   P. R. Haddad and A. L. Heckenberg, *J. Chromatogr.*, 300 (1984) 357.
4   T. H. Jupille and D. T. Gjerde, *J. Chromatogr. Sci.*, 24 (1986) 427.
5   D. T. Gjerde, J. S. Fritz and G. Schmuckler, *J. Chromatogr.*, 186 (1979) 509.
6   D. T. Gjerde, G. Schmuckler and J. S. Fritz, *J. Chromatogr.*, 187 (1980) 35.
7   J. S. Fritz, D. T. Gjerde and R. M. Becker, *Anal. Chem.*, 52 (1980) 1519.
8   D. T. Gjerde and J. S. Fritz, *Anal. Chem.*, 53 (1981) 2324.
9   T. Okada and T. Kuwamoto, *Anal. Chem.*, 55 (1983) 1001.
10 N. Hirayama and T. Kuwamoto, *J. Chromatogr.*, 447 (1988) 323.
11 T. Okada and T. Kuwamoto, *Anal. Chem.*, 57 (1985) 829.
12 R. E. Baron and J. S. Fritz, *J. Chromatogr.*, 284 (1984) 13.
13 R. W. Siergiej and N. D. Danielson, *J. Chromatogr. Sci.*, 21 (1983) 362.
14 J. E. Girard and J. A. Glatz, *Am. Lab.*, 13 (1981) 26.
15 R. L. Stevenson and K. Harrison, *Am. Lab.*, 13 (1981) 76.
16 R. W. Stout, S. I. Sivakoff, R. D. Ricker, H. C. Palmer, M. A. Jackson and T. J. Odiorne, *J. Chromatogr.*, 352 (1986) 381.
17 P. E. Jackson and P. R. Haddad, *J. Chromatogr.*, 346 (1985) 125.
18 P. R. Haddad and A. L. Heckenberg, *J. Chromatogr.*, 252 (1982) 177.
19 T. Okada and T. Kuwamoto, *Anal. Chem.*, 56 (1984) 2073.
20 S. Matsushita, Y. Tada, N. Baba and K. Hossako, *J. Chromatogr.*, 259 (1983) 459.
21 J. A. Glatz and J. E. Girard, *J. Chromatogr. Sci.*, 20 (1982) 266.
22 J. S. Fritz, D. L. Du Val and R. Barron, *Anal. Chem.*, 56 (1984) 1177.
23 G. Schmuckler, *J. Chromatogr.*, 313 (1984) 47.
24 P. R. Haddad and C. E. Cowie, *J. Chromatogr.*, 303 (1984) 321.
25 C. E. Lin, C. H. Chen, C. H. Lin, M. H. Yang and J. C. Jiang, *J. Chromatogr. Sci.*, 27 (1989) 665.
26 M. H. Yang, C. E. Lin and J. K. Fan, *Silicon Material Research Program* (*Monograph Series*, No. 1) National Science Council, Taiwan, 1986, p. 75.
27 J. S. Fritz, D. T. Gjerde and C. Pohlandt, *Ion Chromatography*, Hüthig, New York, 1982, p. 109.
28 B. A. Bidlingmeyer, J. K. del Rios and J. Korpl, *Anal. Chem.*, 54 (1982) 442.

CHROMSYMP. 1797

Characterization of an internal-surface reversed-phase silica support for liquid chromatography and its application to assays of drugs in serum

JUN HAGINAKA*, JUNKO WAKAI, NORIKO YASUDA, HIROYUKI YASUDA and YUKIO KIMURA

Faculty of Pharmaceutical Sciences, Mukogawa Women's University, 11–68, Koshien Kyuban-cho, Nishinomiya 663 (Japan)

ABSTRACT

Internal-surface reversed-phase (ISRP) silica supports having N-octanoylaminopropyl phases bound to the internal surfaces of the porous silica and N-(2,3-dihydroxypropyl)aminopropyl phases bound to the external surfaces were synthesized from silica particles differing in nominal pore diameters and specific surface areas. These ISRP supports were characterized with regard to physical and chromatographic properties. The support with an N-octanoylaminopropyl phase coverage of 485 μmol/g and an average pore diameter of 65 Å was the most suitable for the direct-injection determination of hydrophilic or hydrophobic drugs in serum or plasma. Non-steroidal anti-inflammatory (acetylsalicylic acid and salicylic acid) and tricyclic antidepressant drugs (desipramine and nortriptyline) in serum were successfully determined with this support and an acidic eluent.

INTRODUCTION

Recently, special silica supports that exclude macromolecules such as serum proteins without destructive accumulation but retain small molecules such as drugs have been designed for the direct-injection determination of drugs in biological fluids by high-performance liquid chromatography (HPLC)[1–4]. Hagestam and Pinkerton[2,5] designed a so-called internal-surface reversed-phase (ISRP) silica support having a hydrophobic oligopeptide phase and a hydrophilic diol phase, bonded to particles with a pore size of less than 80 Å, as internal and external surfaces, respectively. The widely used ISRP support designed by Hagestam and Pinkerton[2] has glycyl-L-phenylalanyl-L-phenylalanine (GFF) and diol phases as internal and external surfaces, respectively. Although direct serum injection assays have been developed for some hydrophilic substances with the GFF ISRP columns[6–8], the GFF bonded phase cannot retain certain classes of hydrophilic drugs, such as cephalosporins and penicillins, in the recommended eluent pH range of 6.0–7.5 (ref. 4).

Previously, we reported[4] the preparation of a new ISRP silica support having

N-octanoylaminopropyl and N-(2,3-dihydroxypropyl)aminopropyl phases as internal and external surfaces, respectively, by using a novel enzyme, polymyxin acylase[9]. The aim of this work was to characterize the physical and chromatographic properties of ISRP supports made from porous silicas of various pore sizes and surface areas and to apply them to the direct-injection determination of hydrophilic or hydrophobic drugs in serum.

EXPERIMENTAL

Reagents and materials

(3-Aminopropyl)trimethoxysilane was obtained from Shin-etsu Silicon Chemicals (Tokyo, Japan). Octanoyl chloride, triethylamine, glycidol (2,3-epoxy-1-propanol), acetylsalicylic acid and salicylic acid were purchased from Nacalai Tesque (Kyoto, Japan). Other reagents and organic solvents of analytical-reagent grade and control human serum (Control Serum I) were obtained from Wako (Osaka, Japan). Desipramine and nortriptyline hydrochlorides were kindly donated by Nippon Ciba-Geigy (Takarazuka, Japan) and Dainippon Pharmaceutical (Osaka, Japan),

Fig. 1. Synthetic scheme for the preparation of the new ISRP silica support.

respectively. Commercially available porous silicas with particle diameters of *ca.* 5 μm were used: Develosil-60, Develosil-90 (Nomura Chemicals, Seto, Japan) and Spherisorb (Phase Separations, Hauppage, NY, U.S.A.) with nominal pore diameters of 60, 90 and 80 Å and specific surface areas of 500, 400 and 220 m^2/g, respectively.

Water was purified with a Nanopure II unit (Barnstead, Boston, MA, U.S.A.) and used to prepare the eluent and the sample solutions.

Preparation of the ISRP silica support

The supports were synthesized as described previously[4]. Fig. 1 illustrates the synthetic scheme for the preparation of the new ISRP silica support. 3-Aminopropyl groups were attached to the base silica materials by silanization with (3-amino-propyl)trimethoxysilane. The amino groups of both the internal and external surfaces were converted to N-octanoylaminopropyl phases by reaction with octanoyl chloride in the presence of triethylamine. The octanoyl groups on the external surfaces were cleaved with a polymyxin acylase. The deacylated amino groups were converted to a diol phase by reaction with glycidol, as reported previously[4,5]. Thus ISRP silica supports having a hydrophobic N-octanoylaminopropyl phase on the internal surfaces and an N-(2,3-dihydroxypropyl)aminopropyl phase on the external surfaces were obtained.

Instrumentation

The amounts of (3-aminopropyl)trimethoxysilane and octanoyl chloride reacted were determined by elemental analysis of the prepared ISRP silicas using a CHN Corder Type MT-3 (Yanagimoto, Kyoto, Japan). The amount of octanoic acid liberated by enzyme treatment was measured by a gas chromatographic method as reported previously[4].

The prepared ISRP support was packed into 100 × 4.0 mm I.D. and 10 × 4.0 mm I.D. stainless-steel tubes for the analytical and guard columns, respectively, by conventional high-pressure slurry-packing procedures[10].

The chromatographic system consisted of a Model 880-PU pump (Japan Spectroscopic, Tokyo, Japan) equipped with a variable-wavelength detector (875-UV, Japan Spectroscopic). The precolumn (50 × 4.6 mm I.D.) packed with LC-sorb Sp-A-ODS (particle size 25–40 μm) (Chemco Scientific, Osaka, Japan) was inserted between the pump and injector to protect the analytical column from microparticles in the eluent and to saturate the eluent with silica. Samples were injected with a Sil-9A autoinjector (Shimadzu, Kyoto, Japan). The chromatograms were recorded and integrated using a Chromatopac CR-6A (Shimadzu). All separations were carried out at room temperature.

Preparation of human serum sample

Drugs were dissolved in human serum at a known concentration, and an appropriate volume of serum sample was applied to the ISRP support after filtration through a 0.22-μm membrane filter.

TABLE I

CHARACTERISTICS OF COMMERCIAL SILICA PARTICLES USED

All data are those specified by the manufacturers.

Property	Develosil-60	Develosil-90	Spherisorb
Particle diameter, d_p (μm)	5	5	5
Nominal pore diameter, d (Å)	60	90	80
Specific surface area, S (m^2/g)	500	400	220
Specific pore volume, V (cm^3/g)	0.75	0.90	—

RESULTS AND DISCUSSION

Characteristics of the prepared ISRP supports

In a previous study[4], we prepared an ISRP support having N-octanoylamino-propyl and N-(2,3-dihydroxypropyl)aminopropyl phases on the internal and external surfaces by using Devolosil-90 silica as the base silica material. The support had an N-octanoylaminopropyl phase coverage of 1000 μmol/g. We tried to design an ISRP support having a low coverage to permit the elution of hydrophobic drugs with an eluent including a small percentage of organic modifier. When the surface coverage of N-octanoylaminopropyl phases was decreased using Develosil-90 silica, the ISRP support obtained showed a lower column efficiency. Hence we prepared the ISRP support using Spherisorb silica which has a specific surface area of 220 m^2/g (about half that of Develosil-90 silica). The characteristics of the base silica materials and the prepared ISRP supports are shown in Tables I and II, respectively. The ISRP supports made from Develosil-60, Develosil-90 and Spherisorb silicas had specific N-octanoyl-aminopropyl phase coverages of 950, 1000 and 485 μmol/g, respectively, after enzymatic cleavage, which correspond to 1.9, 2.5 and 2.2 μmol/m^2, respectively. Note

TABLE II

CHARACTERISTICS OF THE ISRP SUPPORTS PREPARED

Property	Develosil-60 ISRP	Develosil-90 ISRP[a]	Spherisorb ISRP
Aminopropyl phase coverage (μmol/g)	1810	1840	514
N-Octanoylaminopropyl phase coverage (μmol/g):			
Before cleavage	1050	1110	512
After cleavage	950	1000	485
Cleavage (%)	9.5	9.0	5.3
Pore diameter (Å)	31	50	65
Number of theoretical plates[b] (plates per 10 cm)	2200	4400	3800
Capacity factor of barbital[c]	2.79	2.81	1.83

    [a] The same support as in ref. 4.

    [b] Number of theoretical plates for barbital in 100 mM phosphate buffer–acetonitrile (12:1, v/v) at 0.6 ml/min.

    [c] Capacity factor of barbital under the same conditions as in footnote *b*.
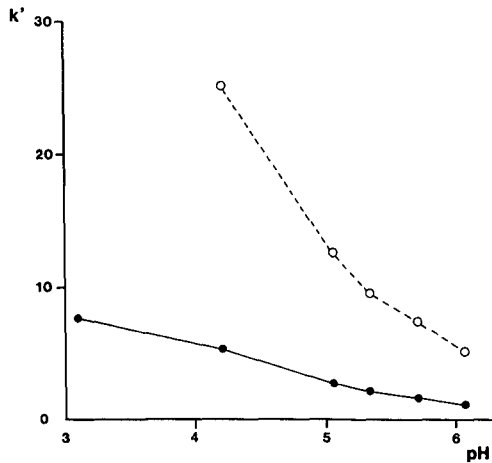
Fig. 2. Dependence of capacity factors of ($\bullet$) acetylsalicylic acid and ($\bigcirc$) salicylic acid on the eluent pH. Column, Spherisorb ISRP (100 × 4.6 mm I.D.); eluent, 100 mM phosphate buffer–acetonitrile (10:1, v/v); detection, 254 nm.

that the ISRP supports made from Develosil-90 and Spherisorb silicas have almost the same coverage per square metre of surface area. The low N-octanoylaminopropyl phase coverage of the support made from Develosil-60 could have been due to steric hindrance impeding diffusion of the silanizing and acylating reagents into some pores of the small-pore silica. The ISRP supports made from Develosil-60, Develosil-90 and
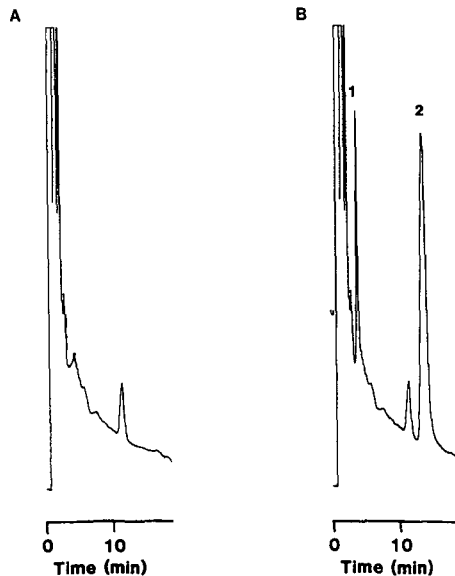
Fig. 3. Chromatograms of (A) control serum and (B) control serum spiked with (1) acetylsalicylic acid (10 μg/ml) and (2) salicylic acid (40 μg/ml). HPLC conditions: column, Spherisorb ISRP (100 × 4.6 mm I.D.); eluent, 100 mM phosphate buffer–acetonitrile (10:1, v/v) (final pH 5.1); flow-rate, 0.8 ml/min; detection, 254 nm; injection volume, 10 μl.
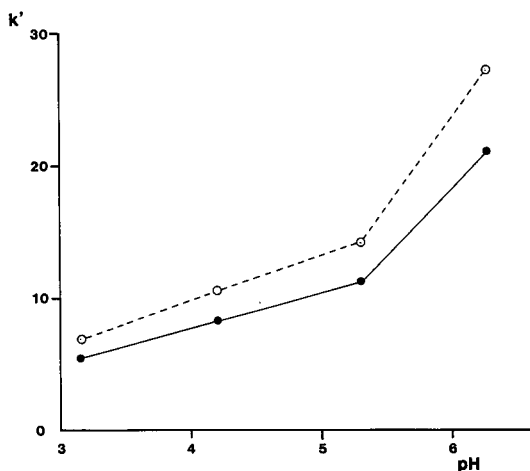
Fig. 4. Dependence of capacity factors of (●) desipramine and (○) nortriptyline on the eluent pH. Column, Spherisorb ISRP (100 × 4.6 mm I.D.); eluent, 100 m*M* phosphate buffer–acetonitrile (4:1, v/v); detection, 254 nm.

Spherisorb silicas gave capacity factors of barbital of 2.79, 2.81 and 1.83, respectively. These results indicate that the capacity of the supports is dependent on the specific N-octanoylaminopropyl phase coverage. The average pore diameters of the ISRP supports prepared from the selected silicas were less than 65 Å when measured by the
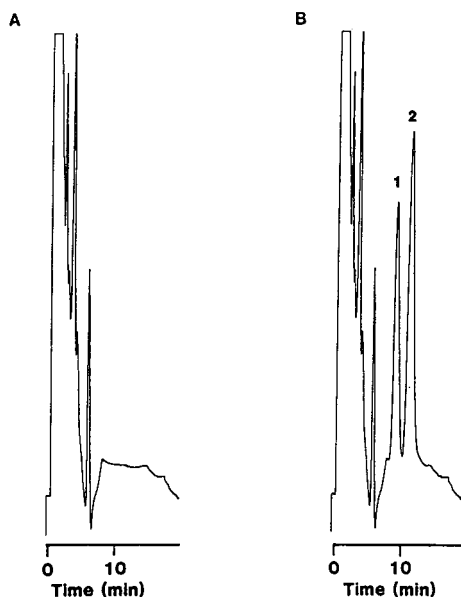
Fig. 5. Chromatograms of (A) control serum and (B) control serum spiked with (1) desipramine (5 μg/ml) and (2) nortriptyline (5 μg/ml). HPLC conditions: column, Spherisorb ISRP (100 × 4.6 mm I.D.); eluent, 100 m*M* phosphate buffer–acetonitrile (4:1, v/v) (final pH 4.2); flow-rate, 0.8 ml/min; detection, 254 nm; injection volume, 20 μl.

TABLE III

REPRODUCIBILITY AND RECOVERY OF DRUGS FROM HUMAN SERUM

The concentrations were 25 μg/ml for salicylic acid and 5 μg/ml for desipramine and nortriptyline. Relative standard deviations (R.S.D.) of five analyses.

Drug	R.S.D. (%)	Recovery (%)
Salicylic acid	1.23	101
Desipramine	4.25	99.4
Nortriptyline	2.16	101

inverse size-exclusion chromatographic method reported by Cook and Pinkerton[11]; these are small enough to exclude human serum albumin without penetrating into the pores. Although the ISRP support made from Develosil-90 silica (Table II) gave the highest column efficiency, the support made from Spherisorb silica was used for the direct-injection determination of various drugs in serum after taking into account the separation of hydrophobic drugs.

Direct-injection determination of drugs in serum

In a previous paper[4], we reported that serum proteins could be almost completely recovered from our ISRP support, while the recovery from that prepared by Pinkerton and Hagestam was low with an acidic eluent. Also, our support could be used for the direct-injection determination of drugs with an acidic eluent, whereas the latter was limited to the eluent pH range 6.0–7.5. Another aim of this study was to apply the prepared ISRP support to the direct-injection determination of hydrophilic and hydrophobic drugs with an acidic eluent.

Fig. 2 shows the pH dependence of the capacity factors of acetylsalicylic acid and salicylic acid. It can be seen that these capacity factors result from ion exclusion as the pH of the eluent increases. Hence an eluent pH of 5.1 was selected for the direct-injection determination of acetylsalicylic acid and salicylic acid in serum (Fig. 3). Fig. 4 shows the plots of the capacity factors of desipramine and nortriptyline against the pH of the eluent. As these drugs have a secondary amino group in the molecule, the capacity factors decreased with decrease in pH. As shown in Fig. 5, these drugs were separated from serum components using an eluent pH of 4.2 with a short run time. Table III gives the relative standard deviations for the assays of salicylic acid, desipramine and nortriptyline in serum and their recoveries from the serum samples. The drugs were almost completely recovered (99.4–101%) from serum with good reproducibility.

We conclude that the prepared ISRP support can also be used for direct serum injection analysis by separating hydrophilic or hydrophobic drugs with an acidic eluent.

REFERENCES

1 H. Yoshida, I. Morita, G. Tamai, T. Masujima, T. Tsuru, N. Takai and H. Imai, *Chromatographia*, 19 (1984) 466.
2 I. H. Hagestam and T. C. Pinkerton, *Anal. Chem.*, 57 (1985) 1757.

3 D. J. Gish, B. T. Hunter and B. Feibush, *J. Chromatogr.*, 433 (1988) 264.
4 J. Haginaka, N. Yasuda, J. Wakai, H. Matsunaga, H. Yasuda and Y. Kimura, *Anal. Chem.*, 61 (1989) 2445.
5 I. H. Hagestam and T. C. Pinkerton, *J. Chromatogr.*, 351 (1986) 239.
6 C. M. Dawson, T. W. M. Wang, S. J. Rainbow and T. R. Tickner, *Ann. Clin. Biochem.*, 25 (1988) 661.
7 N. Takeda, T. Niwa, K. Maeda, M. Shibata and A. Tatematsu, *J. Chromatogr.*, 431 (1988) 418.
8 N. D. Atherton, *Clin. Chem.*, 35 (1989) 975.
9 Y. Kimura and N. Yasuda, *Agric. Biol. Chem.*, 53 (1989) 497.
10 L. R. Snyder and J. J. Kirkland, *An Introduction to Modern Liquid Chromatography*, Wiley-Interscience, New York, 2nd ed., 1979, Ch. 5.
11 S. E. Cook and T. C. Pinkertron, *J. Chromatogr.*, 368 (1986) 233.

CHROMSYMP. 1895

Equilibrium of octadecylsilica gel with sodium dodecyl sulphate

SHINICHIRO HORI*, KYOKO OHTANI-SENUMA and SACHIKO OHTANI

Department of Neurochemistry, Tokyo Metropolitan Institute for Neurosciences, 2–6 Musashidai, Fuchu-city, Tokyo 183 (Japan)

and

KENJI MIYASAKA and TOSHIHIRO ISHIKAWA

New Business Development Department, Tonen Corporation, 1–1–1 Hitotsubashi, Chiyoda-ku, Tokyo 100 (Japan)

ABSTRACT

The retention times of tyrosine (Tyr), 3,4-dihydroxyphenylalanine (DOPA), 3,4-dihydroxyphenylethylamine (DA), norepinephrine (NE), epinephrine (E), homovanillic acid (HVA), 3,4-dihydroxyphenylacetic acid (DOPAC), 3-methoxy-4-hydroxymandelic acid (VMA), tryptophan (Trp), 5-hydroxytryptophan (5-HTP), serotonin (5-HT) and 5-hydroxyindoleacetic acid (5-HIAA) on octadecylsilica (ODS) gel gradually changed when the ODS gel column was washed with buffer containing sodium dodecylsulphate (0.003%). To reach the steady state, 3200 column volumes of buffer were required. The retention properties of this column correlated with the hydrophobicity of the retained materials, including Tyr, DOPA, DA, NE, E, HVA, DOPAC, VMA, Trp, 5-HTP, 5-HT and 5-HIAA. These observations are of practical importance in preparing reproducible ODS gel columns for the determination of trace amounts of materials in biological fluids.

INTRODUCTION

A solvent-generated (dynamic) ion-exchange system facilitates the separation of catecholamines, indolamine and their precursors or metabolites in biological fluids[1,2]. In the separation of materials by "soap chromatography"[2], sodium dodecyl sulphate (SDS), an anionic detergent, is adsorbed by the reversed-phase surface to form an anionic layer, thereby exhibiting properties similar to those of an ion exchanger. In experiments with an octadecyl (C_{18}) silica (ODS) gel column and a buffer containing SDS, the selectivity and resolution of some eluates on ODS gel, treated with SDS, could not be explained by the properties of an ion exchanger. For this reason, we examined the equilibration process of the ODS gel, treated with SDS, and observed a relationship between the hydrophobicity of the eluites and their retention times on the ODS gel.

EXPERIMENTAL

Materials

L-Tyrosine (Tyr), 3,4-dihydroxyphenylalanine (DOPA), 3,4-dihydroxyphenyl-ethylamine (DA), norepinephrine (NE), epinephrine (E), homovanillic acid (HVA), DL-3-methoxy-4-hydroxymandelic acid (VMA), L-tryptophan (Trp), 5-hydroxytryp-tophan (5-HTP), serotonin creatinine sulphate (5-HT) and 5-hydroxyindoleacetic acid (5-HIAA) were purchased from Nacalai Chemicals (Kyoto, Japan) and 3,4-dihydroxy-phenylacetic acid (DOPAC) from Sigma (St. Louis, MO, U.S.A.). Each compound was dissolved in 0.1 M perchloric acid to give a 100-nmol/ml solution; the solutions were stored at $-80°C$ and, just before use, were diluted to 5 nmol/ml with 0.1 M perchloric acid. The reversed-phase resin, Partisil-5 (5-μm, octadecylsilica gel), was obtained from Whatman (Maidstone, U.K.). SDS was purchased from Nacalai Chemicals. All other chemicals were of analytical-reagent grade and were used without further purification.

High-performance liquid chromatography (HPLC)

The HPLC system consisted of a sample injector (Rheodyne, Cotati, CA, U.S.A.), a Model L-6200 intelligent pump (Hitachi, Tokyo, Japan), a guard column
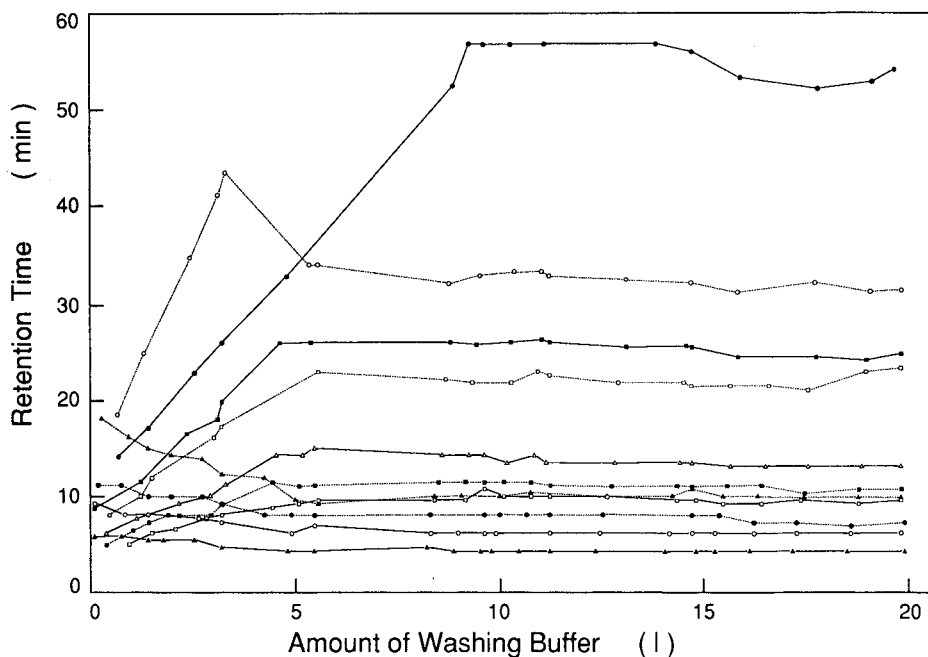
Fig. 1. Equilibrium of octadecysilica (ODS) gel column with sodium dodecyl sulphate (SDS). Stationary phase, octadecylsilica (ODS); mobile phase, 0.02 M citrate–sodium citrate buffer (pH 2.1)–3% (v/v) 1-propanol–0.2 M sodium perchlorate–0.003% SDS; flow-rate, 1 ml/min; temperature, 25°C. ●———● = 5-HT; ○– – – –○ = 5-HTP; ■———■ = DA; □– – – –□ = Tyr; △———△ = DOPA; ■– – – –■ = E; ▲– – – –▲ = NE; □———□ = HVA; ●– – – –● = 5-HIAA; ○———○ = DOPAC; ▲———▲ = VMA.

(10 mm × 4 mm I.D.), an isolation column (250 mm × 4 mm I.D.) with a column oven (25°C), a Model E-308 amperometric detector (Irica Instrument, Kyoto, Japan), a Model 7000A data analyser (System Instrument, Tokyo, Japan) and a floppy disc Model FD-10A recorder (System Instrument). The guard and isolation columns were filled with reversed-phase resin (Partisil-5) using a slurry-packing system (Nihon Seimitsu Kagaku, Tokyo, Japan). The potential of the glassy carbon working electrode of the amperometric detector was set at ±0.95 V *vs.* Ag/AgCl. This relatively high potential was necessary to detect Trp with the same sensitivity as that obtained for 5-HT and 5-HIAA (data not shown). The mobile phase was 0.02 *M* citrate–sodium citrate buffer (pH 2.1)–3% (v/v) 1-propanol–0.2 *M* sodium perchlorate–0.003% SDS.

Determination of hydrophobicity

The hydrophobicity of the materials was calculated using the hydrophobic fragmental constants[3].

RESULTS AND DISCUSSION

Equilibrium of ODS gel with SDS

The retention times on the ODS gel of catcholamines (DA, NE, E), indolamine (5-HT), their precursors (Tyr, DOPA, Trp, 5-HTP) and their metabolites (DOPAC, HVA, VMA, 5-HIAA) were gradually changed by washing the ODS gel column with the above mobile phase, as shown in Fig. 1. The amount required to attain a steady state varied depending on the material to be separated by ODS gel column
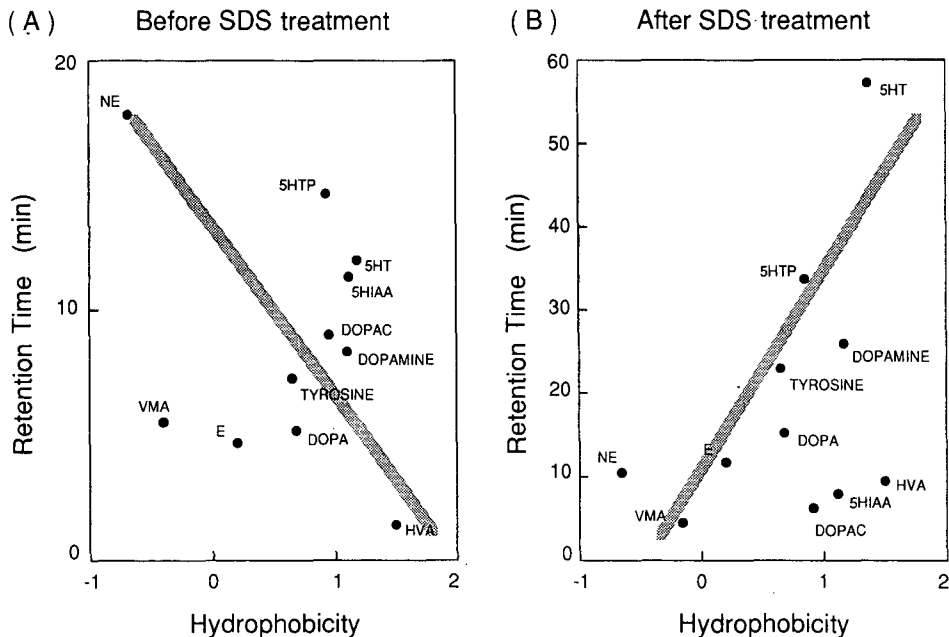
Fig. 2. Relationship between the retention time of an eluite on octadecylsilica (ODS) gel and its hydrophobicity. Stationary phase: (A) untreated ODS; (B) ODS treated with SDS. Mobile phase as in Fig. 1.

chromatography. To reach a steady state, 3200 column volumes of the buffer were required. The retention times of Tyr, DOPA, DA, E, HVA, Trp, 5-HTP and 5-HT were increased by SDS treatment, whereas those of DOPAC, NE, VMA and 5-HIAA decreased. In contrast to the data of Crombeen et al.[4], the retention time of NE decreased with SDS treatment and that of HVA increased. In the separation of materials by "soap chromatography"[2], SDS (anionic detergent) is adsorbed by the reversed-phase surface to form an anionic layer, thus exhibiting properties similar to those of an ion exchanger. As an enormous amount of the buffer containing SDS was required to attain a steady state on the ODS gel column, a change in the solid phase (ODS gel) by SDS was suspected. To examine the participation of SDS as a paired ion, the hydrophobicity of the eluite was determined and the results were compared with the retention times on the ODS gel.
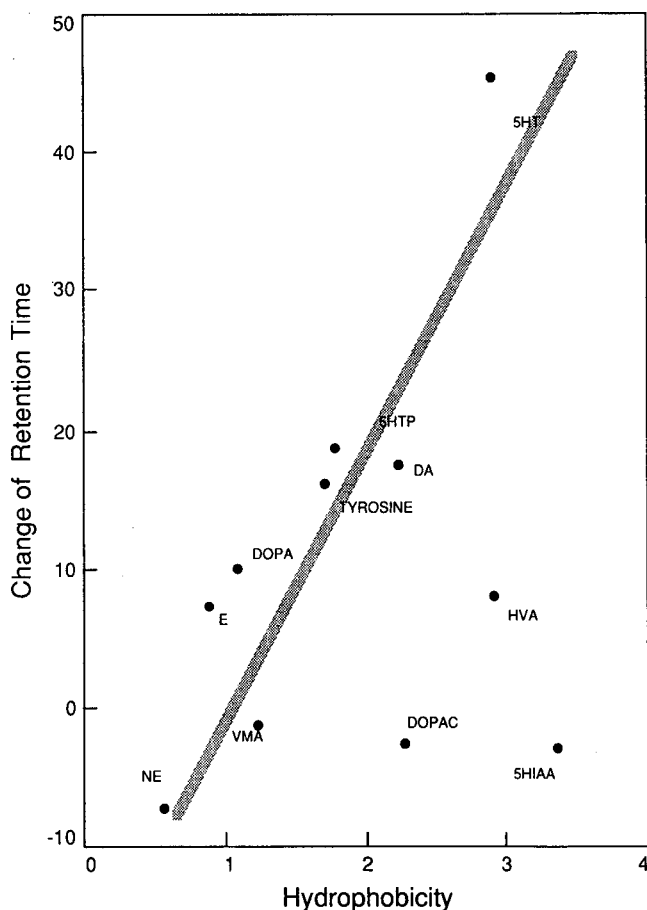
Fig. 3. Relationship between the change in retention time of an eluite on octadecysilica (ODS) gel and its hydrophobicity. The change in retention time was calculated by subtracting of the retention time of each eluite in Fig. 2A from that in Fig. 2B.
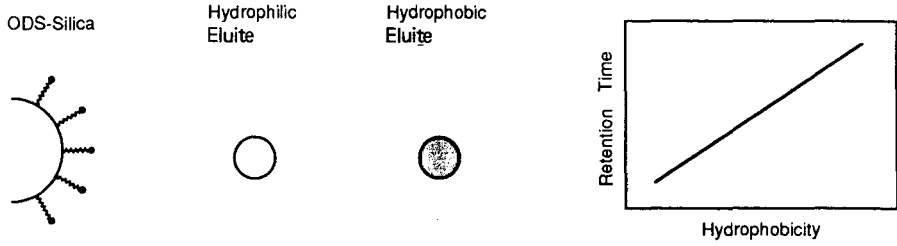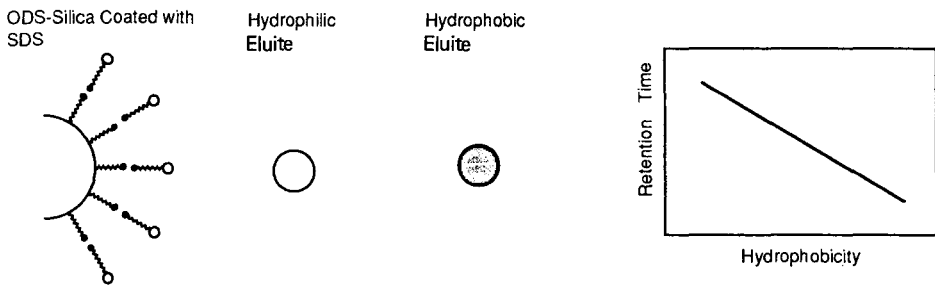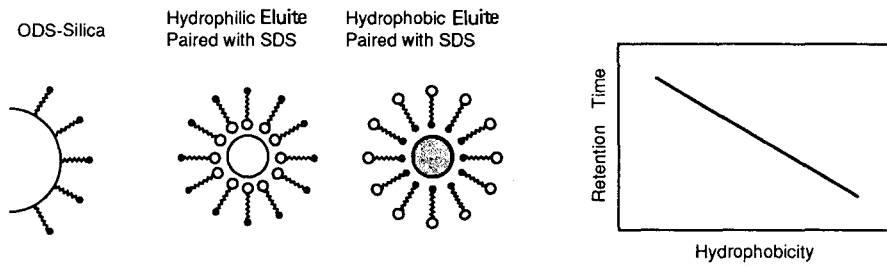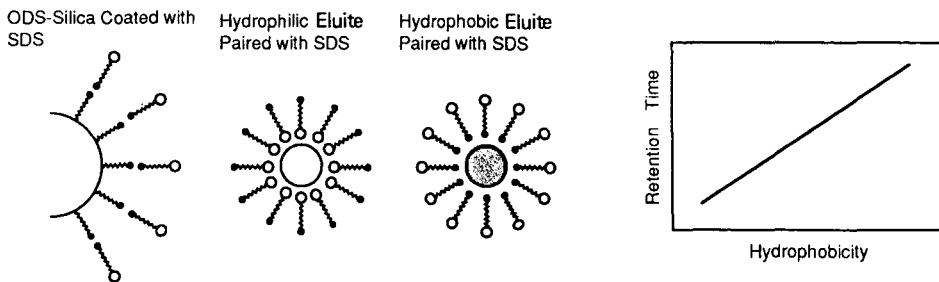
Fig. 4. Hypothetical model for the status of octadecylsilica (ODS) and eluites in solvent.

Correlation between hydrophobicity of eluites and their retention times on the ODS gel

Before treatment of the ODS gel with SDS, the increase in retention time of the eluites decreased with their hydrophobicity (Fig. 2A). After treatment of the ODS gel with SDS, the retention time increased with their hydrophobicity (Fig. 2B). Further, the difference in retention times obtained after and before SDS treatment was correlated with the hydrophobicity (Fig. 3). To explain these results, four possible conditions of the ODS gel and eluites were considered, as shown in Fig. 4: (A) ODS gel not treated with SDS (hydrophobic surface), hydrophilic and hydrophobic eluites; in this situation, an increase in hydrophobicity of the eluite should increase its retention time on the ODS gel; (B) ODS gel treated with SDS (changed to a hydrophilic surface), hydrophilic and hydrophobic eluites; in this situation, an increase in hydrophobicity of the eluite should decrease its retention time on the ODS gel; (C) ODS gel not treated with SDS (hydrophobic surface), hydrophilic, coated with SDS (changed to hydrophobic), and hydrophobic, coated with SDS (changed to hydrophilic), eluites; in this situation, an increase in hydrophobicity of the eluite should decrease its retention time on ODS gel; (D) ODS gel treated with SDS (changed to hydrophilic surface), hydrophilic, paired with SDS (changed to hydrophobic), and hydrophobic, paired with SDS (changed to hydrophilic), eluites; in this situation, an increase in hydrophobicity of the eluite should increase its retention time on the ODS gel. Our data on the relationship between retention time and hydrophobicity can be explained by conditions C and D. The eluite, dissolved in the buffer containing SDS, is readily paired with SDS, but the ODS gel is not sufficiently coated with SDS when the eluite is injected onto the ODS gel column not treated with SDS. Hence an increase in the hydrophobicity of the eluite decreased its retention time (Fig. 2A). At the steady state of the ODS gel treated with SDS (Fig. 2B), an increase in hydrophobicity of the eluite increased the retention time. Thus the selectivity and resolution on the ODS gel equilibrated with SDS (0.003%) correlates with the hydrophobicity of the eluites. These observations are of practical importance in the preparation of reproducible ODS gel columns for the determination of trace amounts of materials in biological fluids.

REFERENCES

1 K. Zech, in A. Henschen, K.-P. Hupe, F. Lottspeich and W. Voelter (Editors), *High-Performance Liquid Chromatography in Biochemistry*, VCH, Weinheim, 1985, p. 322.
2 J. H. Knox and G. R. Laird, *J. Chromatogr.*, 122 (1976) 17.
3 R. F. Rekker, in W. Th. Nauta and R. F. Rekker (Editors), *Pharmacochemistry Library, Vol. 1*, Elsevier, Amsterdam, 1977.
4 J. P. Crombeen, J. C. Kraak and H. Poppe, *J. Chromatogr.*, 167 (1978) 219.

CHROMSYMP. 1759

Method for the preparation of internal-surface reversed-phase packing materials starting from alkylsilylated silica gels

KAZUHIRO KIMATA

Kyoto Institute of Technology, Department of Polymer Science and Engineering, Matsugasaki, Sakyo-ku, Kyoto 606 (Japan)

RIYOU TSUBOI

Nacalai Tesque, Kaide-cho, Mukoh. 617 (Japan)

and

KEN HOSOYA, NOBUO TANAKA* and TAKEO ARAKI

Kyoto Institute of Technology, Department of Polymer Science and Engineering, Matsugasaki, Sakyo-ku, Kyoto 606 (Japan)

ABSTRACT

A simple method for the preparation of internal-surface reversed-phase (ISRP) packing materials was developed. Partial decomposition of alkylsilylated silica gel with an aqueous acid followed by the introduction of diol functionalities produced stationary phases possessing the properties of ISRP packing materials. The method is applicable to various types of reversed-phase packing materials irrespective of the structure of the bonded alkyl moieties. The alkyl/diol-type packing materials possess greater hydrophobic properties than other ISRP packing materials currently available for high-performance liquid chromatography. Reversed-phase separation of low-molecular-weight compounds on the alkyl/diol phase by direct injection of serum samples is demonstrated. The present packing materials prepared from relatively large particles with or without the introduction of the diol phase can also be used for open-column chromatography in the reversed-phase mode with a wide range of aqueous–organic mobile phases, as the external surfaces are wettable with water.

INTRODUCTION

Internal surface reversed-phase (ISRP) packing materials have been introduced to effect the analyses of drugs in serum or plasma by direct injection of samples[1,2]. The packing materials possess hydrophilic external surfaces and hydrophobic internal surfaces. High-molecular-weight proteins are eluted at the void volume from a column containing these packing materials without interaction with hydrophobic internal surfaces owing to steric exclusion from relatively small pores. Low-molecular-weight

compounds permeable into the pores can be separated in a reversed-phase mode. These packing materials can therefore accept the direct injection of serum or plasma without deproteinization of samples.

Currently available ISRP packing materials are prepared by the cleavage of a hydrophobic stationary phase on the external surface of the particles by the use of enzymes[1–3] or an oxygen plasma[4], or by the introduction of a hydrophilic polymer network[5] or a protein[6] over the hydrophobic surfaces, to prevent hydrophobic interactions between proteins and the stationary phase.

Methods for the preparation of ISRP materials involving enzymatic cleavage of bonded groups at the external surfaces of the particles can be applied to silica particles with relatively small pores, typically 80 Å or less, and require certain functional groups such as an amide group in the hydrophobic stationary phase in order to be cleaved by enzymes. Methods of preparation using an oxygen plasma to remove the hydrophobic stationary phase from the external surface or the introduction of hydrophilic polymers over the hydrophobic surface are not limited with respect to the structure of bonded groups. As one of the advantages of reversed-phase liquid chromatography (RPLC) is the availability of a variety of packing materials, a simple preparation method that can afford various types of stationary phases would be of value.

We report here a simple method for the preparation of ISRP packing materials, including the partial decomposition of alkylsilylated silica stationary phases. The method permits the preparation of ISRP packing materials containing various alkyl chain lengths from C_1 to C_{18} and aromatic groups. The application of the resulting packing materials to the separation of drugs in serum and for open-column chromatography is demonstrated.

EXPERIMENTAL

Equipment

The HPLC system consisted of an LC-6A pump, SIL-6A autoinjector, SPD-6A UV detector and CR-5A data processor (all from Shimadzu, Kyoto, Japan). The column temperature was maintained at 30°C with a water-bath. A Model 101 UV detector (Nacalai Tesque, Kyoto, Japan) was used to monitor the effluent in open-column liquid chromatography.

Materials

Silica gel particles, Develosil (particle size 5 μm, pore size 55.7 Å, surface area 427 m^2/g) (Nomura Chemicals, Seto, Japan) and MS gel (75 μm, 120 Å, 296 m^2/g) (Dohkai Chemicals, Fukuoka, Japan), were used for the preparation of packing materials for HPLC and for open-column chromatography, respectively.

An ISRP column with bonded phenylalanine oligomers (abbreviated to ISRP-peptide), reported by Hagestam and Pinkerton[1], was purchased from Koken (Tokyo, Japan). Other chemicals, including glycyrrhizic acid (Nacalai Tesque) and bovine serum albumin (Sigma, St. Louis, MO, U.S.A.), and LC-grade solvents were obtained commercially.

Preparation of ISRP packing materials

Silica gel particles were treated with 6 *M* hydrochloric acid at reflux temperature

for 4 h prior to a bonding reaction to remove metal impurities[7,8]. Alkylsilylation was achieved by reaction of the silica particles with alkyldimethylchlorosilanes, such as octadecyldimethylchlorosilane or octyldimethylchlorosilane, in toluene at reflux temperature for 6 h in the presence of pyridine. The details of the bonding and end-capping were given previously[9].

Alkylsilylated silica gels (10 g) were hydrolysed with 200 ml of concentrated hydrochloric acid at 100°C with rapid mechanical stirring (ca. 1000 rpm) for 5 h. The surface coverage of the resulting packing materials or the extent of the decomposition was examined chromatographically, by regularly removing the particles during the reaction and testing the retention characteristics of packed columns. After the reaction, the particles were washed successively with distilled water, tetrahydrofuran (THF) and chloroform.

In one instance, 0.8 g of octadecanol was loaded onto 4 g of C_{18} phase prior to the decomposition. In another instance, the particles were washed with THF at 5-h intervals during the decomposition process in order to wash out the hydrophobic decomposition products from the stationary phase.

Introduction of a diol functionality in the partially decomposed stationary phases was achieved by reaction of the partially hydrolysed RPLC packing materials with glycidylpropyltrimethoxysilane in water[10].

Bonding of the diol phase is not necessary for the packing materials to be used for open-column chromatography, unless samples which are expected to interact with silanols, such as polypeptides, are to be separated. Therefore, partially decomposed C_{18} phase (C_{18}-CLC) was used for open-column chromatography without bonding the diol phase.

A slurry method was used to pack stainless-steel columns (150 mm × 4.6 mm I.D.) for HPLC. Glass columns of 20 mm I.D. were packed with 75-μm particles by a gravity method using a slurry containing 30 g of packing material in 300 ml of mobile phase solvents.

Chromatographic measurements

UV detection at 280 nm was used for bovine serum albumin and at 254 nm for other compounds. Recoveries of proteins were examined by measuring the UV absorption, taking the recovery in the absence of a column as 100%.

RESULTS AND DISCUSSION

Preparation of ISRP packing materials

The proposed method for the preparation of ISRP packing materials includes the reaction of chemically bonded phases such as octadecyl- or octylsilylated silica gels with aqueous hydrochloric acid at reflux temperature for several hours. Fig. 1 shows the decomposition of a C_{18} stationary phase in 70% methanol in the presence of acids. The packing materials are wettable by the reaction medium in this instance. Decomposition of the stationary phase is achieved more effectively by using hydrochloric acid than with other acids. The hydrophobicity of the packing materials, expressed by the retention of toluene in 60% methanol on the resulting stationary phase, decreased rapidly in the early part of the reaction, then levelled off.

Similar results were obtained in the decomposition reaction in concentrated
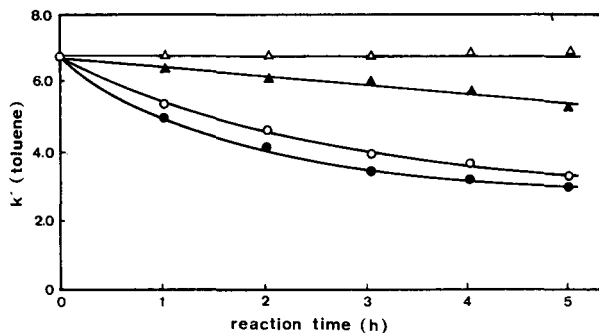
Fig. 1. Decomposition of stationary phase with acid in 70% methanol. Remaining retentivity is expressed by the k' value of toluene with each packing material in 60% methanol. Reaction mixtures contained ($\triangle$) phosphoric acid, ($\blacktriangle$) sulphuric acid, ($\bigcirc$) nitric acid or ($\bullet$) hydrochloric acid, at a concentration of 6 N.

hydrochloric acid in the absence of methanol, as shown in Fig. 2. The heterogeneous decomposition reaction gave a C_{18} phase with about 60% of the original carbon content at 5 h, without much decrease in carbon content thereafter. Washing of the reacting C_{18} phase with THF at 5-h intervals during the decomposition resulted in stationary phases with much lower carbon contents. These results indicate that the decomposition product in an aqueous reaction medium can protect the remainder of the stationary phase from further decomposition. The slower hydrolysis reaction in the presence of octadecanol supports this interpretation. This implies that it is possible to produce stationary phases with various surface coverages. It is known that many factors, including how the silicas are made, influence the stability of bonded phases[11]. Assuming similar surface chemistries of silicas at external and internal surfaces, the alkylsilyl groups at the external surfaces appeared to undergo decomposition more
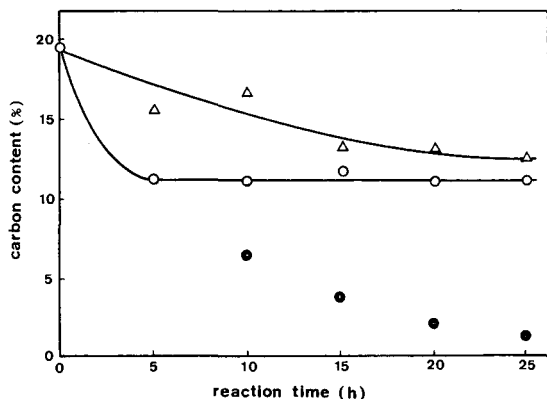
Fig. 2. Decrease in carbon content of C_{18} packing materials with decomposition in concentrated hydrochloric acid, ($\bigcirc$) without washing and ($\bullet$) with THF washing at 5 h intervals and ($\triangle$) in the presence of octadecanol without washing.

TABLE I

EFFECT OF SURFACE COVERAGE AND SILICA PORE SIZE ON THE PLANARITY RECOGNITION OF THE C_{18} PHASE

Stationary phase	Surface coverage ($\mu mol/m^2$) [carbon content, C(%), in parentheses]	Planarity recognition, $\alpha_{T/O}{}^a$	Decomposed stationary phase	Surface coverage, C(%)	Planarity recognition, $\alpha_{T/O}{}^a$
C_{18}-1[b]	3.2(19.17)	1.58	A-5[e]	15.33	1.50
C_{18}-2[b]	3.0(18.30)	1.52	A-10[e]	16.60	1.57
C_{18}-3[b]	2.9(17.79)	1.44	A-15[e]	13.18	1.59
C_{18}-4[b]	2.2(14.26)	1.33	A-20[e]	13.04	1.60
			A-25[e]	12.66	1.50
C_{18}-50[c]	2.0(17.06)	1.61	B-5[f]	11.19	1.54
C_{18}-60[d]	2.2(19.39)	1.58	B-10[f]	11.14	1.55
C_{18}-100[c]	2.6(16.94)	1.51	B-15[f]	11.73	1.59
C_{18}-300[c]	3.4(7.37)	1.45	B-20[f]	11.15	1.57
C_{18}-500[c]	2.6(2.09)	1.42	B-25[f]	11.11	1.58
			C-5[g]	11.19	1.54
			C-10[g]	6.39	1.58
			C-15[g]	3.58	1.64
			C-20[g]	2.13	1.72
			C-25[g]	1.32	1.93

[a] Retention ratio, $k'_{triphenylene}/k'_{terphenyl}$, indicating the planarity recognition of the stationary phases.

[b] Prepared by alkylsilylation of silica gel of 100 Å pore size to give the surface coverages listed.

[c] Nucleosil particles of different pore size were used for alkylsilylation to produce C_{18} phase with maximum coverage.

[d] Starting C_{18} phase prepared from silica of 60 Å pore size for decomposition reaction in concentrated HCl.

[e] Decomposition product in the presence of octadecanol shown in Fig. 2. The numbers indicate the reaction time (h).

[f] Decomposition product with HCl without other additives.

[g] The decomposition product was washed with THF at 5-h intervals starting from B-5.

easily than those at the internal surfaces. Note that the products having 60% of the original carbon content are wettable by water, whereas a C_{18} phase prepared with carbon contents of about 10–12% were not wettable by water or 40% methanol.

The results in Table I also indicate that the remaining alkylsilyl groups exist in relatively small pores. The planarity recognition by the C_{18} chains in the stationary phase, which can be indicated by the separation factor, α, between planar triphenylene and non-planar o-terphenyl[12,13], increases with increase in the surface coverage and with decrease in the pore size with ordinary C_{18} phases prepared by the alkylsilylation of silica gel, as shown in Table I. If the decomposition of a bonded phase takes place at similar rates at both the external and internal surfaces, the $\alpha_{T/O}$ values would decrease as the carbon contents decrease. However, the partially decomposed C_{18} phases obtained by acid treatment of the bonded phases gave $\alpha_{T/O}$ values much larger than C_{18} phases prepared with similar carbon contents. This tendency became pronounced as the decomposition reaction proceeded further. The results imply that the decomposition of a bonded phase takes place more slowly in smaller pores, probably owing to the

TABLE II

CARBON CONTENTS OF THE ISRP PACKING MATERIALS AND THE INTERMEDIATES

Stationary phase	Carbon content, C(%)				
	Before end-capping[a]	(Surface coverage, $\mu mol/m^2$)	End-capped[b]	Decomposed[c]	$C_{18}/diol$
ISRP $C_{18}/diol$	18.81	(2.4)	19.39	11.19	14.95
ISRP $C_8/diol$	13.27	(3.2)	14.01	6.79	9.06
ISRP $C_1/diol$	5.37	(3.9)	–	0.20	5.34
ISRP PE/diol	13.77	(3.3)	14.33	5.85	8.62
ISRP CLC	–	–	18.64	9.95	–

[a] Alkylsilylated silica gel.
[b] After end-capping, prior to decomposition.
[c] After decomposition, prior to bonding diol phase.

protection of the bonded phase by the presence of the decomposition product during the preparation of the present ISRP packing material.

Another possible explanation is the presence of air bubbles in small pores that hinder the contact between the alkylsilylated silica surface and the reaction medium. These factors seemed to lead to a faster decomposition of the stationary phases in larger pores.

Table II lists the carbon contents at each stage of the preparation of the ISRP packing materials. The original C_{18} phase (C_{18}-60) showed a lower surface coverage than stationary phases with shorter alkyl groups owing to the small pore size of 60 Å. The packing materials with smaller alkyl groups, however, lost more alkylsilyl groups on acid treatment, presumably owing to the lower hydrophobicity of the stationary phase.

TABLE III

RETENTION OF BENZENE DERIVATIVES ON ISRP PACKING MATERIALS

Stationary phase	$k' (\alpha = k'_x/k'_{benzene})$			
	Acetophenone	Methyl benzoate	Benzene	Toluene
ISRP $C_1/diol$	0.44 (1.02)	0.45 (1.04)	0.43	0.46 (1.07)
ISRP $C_8/diol$	4.03 (0.15)	9.19 (1.39)	6.62	15.29 (2.31)
ISRP PE/diol	3.38 (0.31)	5.92 (1.86)	3.18	6.38 (2.01)
ISRP $C_{18}/diol$	4.52 (0.15)	11.62 (0.39)	29.49	49.26 (1.67)
ISRP-peptide[a]	0.74 (0.80)	0.95 (1.02)	0.93	1.16 (1.26)

[a] ISRP-peptide phase described by Hagestam and Pinkerton[1]. Mobile phase: 40% methanol.

TABLE IV

EFFECT OF MOBILE PHASE COMPOSITION ON THE RECOVERY OF BSA[a]

Mobile phase	ISRP C_{18}/diol	ISRP-peptide[b]
Organic solvent[c]:		
None	87.4	97.7
CH_3CN, 10%	91.4	95.5
CH_3CN, 20%	96.2	97.0
CH_3CN, 30%	95.9	96.8
CH_3OH, 10%	93.6	96.7
CH_3OH, 20%	98.4	97.1
THF, 10%	99.5	97.5
THF, 20%	98.4	97.7
10% isopropanol+6% THF	99.7	97.5
10% isopropanol+6% THF[d]	100.2	98.4
pH[e]:		
2.76	81.1	0.6
3.77	75.6	0.9
4.41	86.2	0.9
4.91	86.9	1.1
6.02	93.7	67.7
7.00	95.3	96.8
Na_2SO_4 (mol/l)[f]:		
0.05	98.8	98.2
0.1	97.7	98.7
0.2	98.7	99.2
0.3	97.3	97.5

[a] Determined by UV absorbance at 280 nm. Sample: BSA (20 mg/ml), 100-μl injection.
[b] ISRP-peptide phase described by Hagestam and Pinkerton[1].
[c] Mobile phase: organic solvent–0.02 M phosphate buffer + 0.1 M Na_2SO_4 (pH 7).
[d] Mobile phase: organic solvent–0.1 M phosphate buffer (pH 7).
[e] Mobile phase: 15% acetonitrile–0.02 M phosphate buffer +0.1 M Na_2SO_4.
[f] Mobile phase: 15% acetonitrile–0.02 M phosphate buffer + Na_2SO_4 (pH 7).

Properties of alkyl/diol-type ISRP packing materials

Whereas ordinary stationary phases are not wettable by methanol–water mixtures with low methanol contents, the alkyl/diol-type ISRP packing materials and also partially decomposed alkylsilylated silica gels are completely wettable by water. This property is required when RPLC packing materials are to be applied in open-column chromatography, because non-wettable packing materials have problems with regard to bed stability in highly aqueous mobile phases.

The hydrophobicities of the present alkyl/diol-type ISRP packing materials are much greater than that of an ISRP packing material with bonded phenylalanine oligomers (ISRP-peptide), as indicated by the retention of benzene derivatives in Table III. The retention of these benzene derivatives on the ISRP packing materials are about 50% of those on ordinary stationary phases with maximum surface coverage when measured in 60% methanol, in fair agreement with the carbon contents after the decomposition reaction.
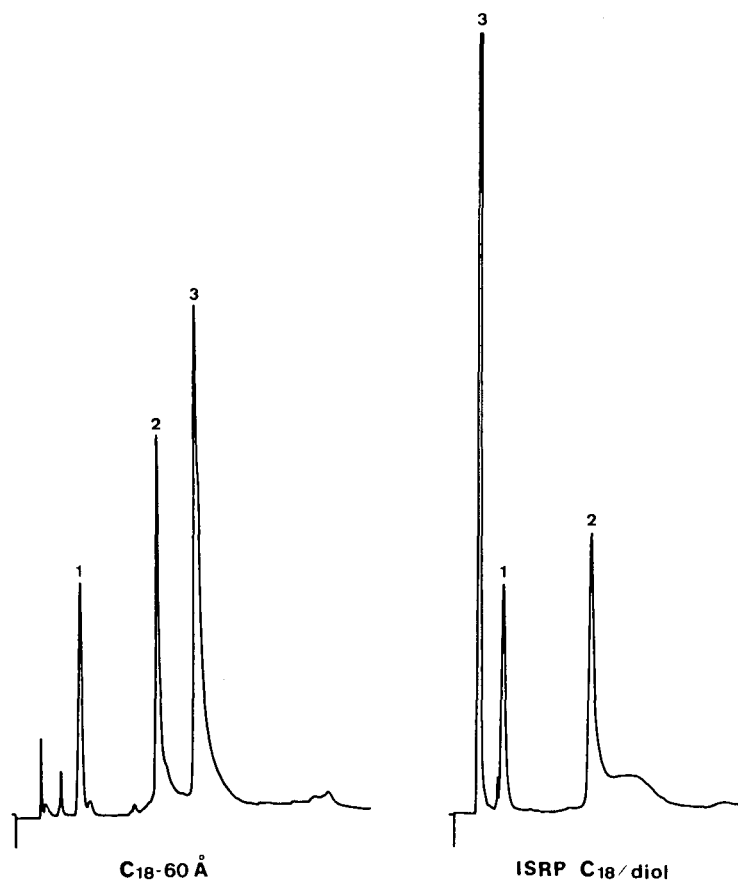
Fig. 3. Gradient elution of polypeptides with ISRP C_{18}/diol and ordinary C_{18} phase prepared from silica gel of 60 Å pore size. 1, α-Endorphin (1 mg/ml, 8 μg); 2, insulin (3 mg/ml, 9 μg); 3, bovine serum albumin (20 mg/ml, 200 μg). HPLC conditions: mobile phase, (A) 20% acetonitrile–0.02 M phosphate buffer containing 0.05 M sodium sulphate (pH 6), (B) 60% acetonitrile–0.02 M phosphate buffer containing 0.05 M sodium sulphate (pH 6) with a linear gradient from A to B in 10 min. Flow-rate, 1.0 ml/min; detection, UV (280 nm).

Injection of proteins

Table IV shows the recovery of BSA from the ISRP C_{18} and the ISRP-peptide phases. As the newly prepared ISRP alkyl/diol-type phases showed a low recovery of BSA, 10 mg of BSA were applied to the column prior to testing the recovery. Although the recovery from ISRP C_{18} was slightly lower than those from the ISRP-peptide phase with mobile phases with low contents of acetonitrile or methanol at pH 7, comparable results were obtained with mobile phases containing 10–20% or more organic solvents. Injection of BSA, 2 mg at a time, in 0.1 M phosphate buffer–iso-propanol–THF (84:10:6) at pH 7.4, onto an ordinary C_{18} phase (C_{18}-60 in Table I) resulted in a protein recovery of less than 2% until 50 mg of BSA had been injected. The recovery increased slightly thereafter, with a simultaneous increase in the column back-pressure.
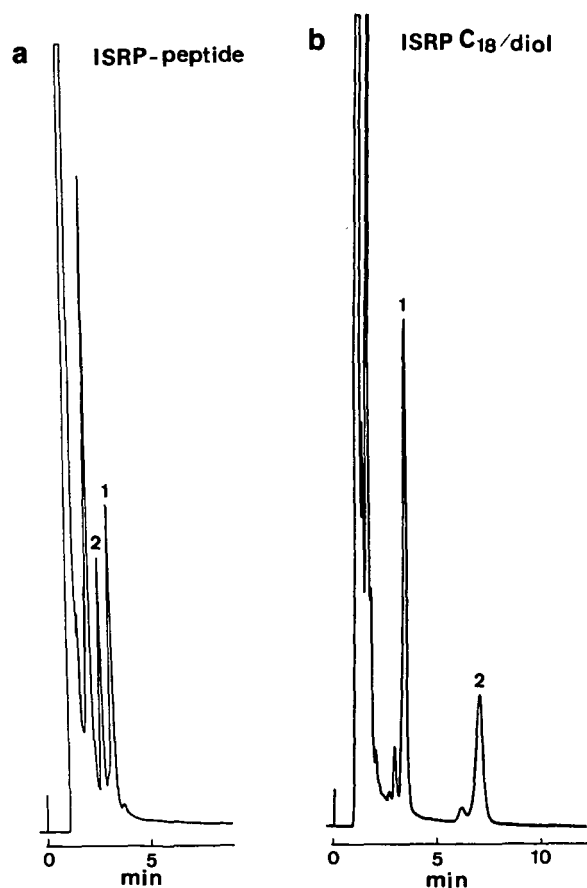
Fig. 4. Elution of human serum spiked with hydrophilic drugs using (a) ISRP-peptide phase[1] and (b) ISRP C_{18}/diol. 1, Theophylline (1 mg/ml, 1 μg); 2, barbital (1 mg/ml, 3 μg) with human serum (20 μl). HPLC conditions: (a) mobile phase 0.02 M phosphate buffer containing 0.1 M sodium sulphate (pH 7), flow-rate 1.0 ml/min, UV detection at 254 nm; (b) mobile phase 10% acetonitrile–0.02 M phosphate buffer containing 0.1 M sodium sulphate (pH 7).

At acidic pH the present ISRP materials showed much higher protein recoveries. This is due to the presence of carboxyl groups in the stationary phase in the phenylalanine oligomer-bonded phase[3]. The ionic strength of the mobile phase did not affect the protein recovery.

Fig. 3 shows that most BSA (85%) eluted from ISRP C_{18} without interacting with the hydrophobic part of the stationary phase, while smaller peptides were chromatographed in the reversed-phase mode. On the ordinary C_{18} phase, the three peptides eluted according to the molecular weight of the solutes under an acetonitrile gradient.

Fig. 4 shows the results of the injection of serum samples spiked with theophylline and barbital. Whereas the ISRP-peptide phase showed a small retention for these compounds possessing relatively small hydrophobicities, with a mobile phase not containing an organic solvent, ISRP C_{18}/diol provided an adequate separation
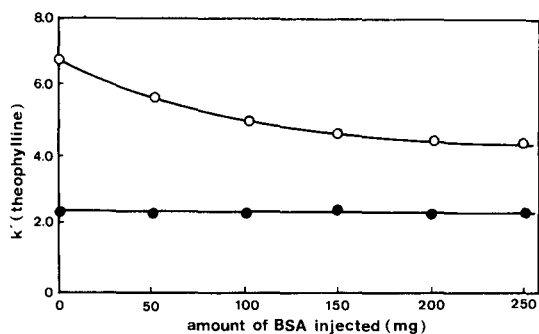
Fig. 5. Effect of BSA injection on retention of theophylline. The k' value of theophylline in 10% methanol is compared for (●) ISRP C_{18} and (○) C_{18}-60. The k' value was measured following each injection of 50 mg of BSA dissolved in 2.5 ml of distilled water onto each column.

with much longer retention with a mobile phase containing 10% acetonitrile. The greater retentivity of the alkyl/diol phases can be an advantage in such an instance.

Fig. 5. shows the variation of the retention of low-molecular-weight solutes with the injection of BSA. Whereas the ordinary C_{18} phase showed a gradual decrease in retention, the ISRP C_{18} phase showed a constant retention with up to 250 mg of BSA injected, which corresponds roughly to the total injection of 5 ml of serum. Constant k' values for theophylline and barbital were observed on ISRP C_{18}/diol in 20% acetonitrile with the injection of up to a total of 2.5 g of BSA. The experimental conditions are different from actual repeated injections of serum samples in small

TABLE V

WETTABILITY OF REVERSED-PHASE PACKING MATERIALS BY METHANOL–WATER MIXTURES

$+$ = Completely wettable; $-$ = non-wettable; $\pm$ = partially wettable.

Methanol content (%)	C_{18}-CLC	$C_{18}{}^a$	C_{18}-P^b	$C_8{}^a$	$C_1{}^a$
0	$+$	$-$	$-$	$-$	$-$
10	$+$	$-$	$-$	$-$	$-$
20	$+$	$-$	$-$	$-$	$-$
30	$+$	$-$	$-$	$-$	$-$
40	$+$	$-$	$-$	$-$	$-$
50	$+$	$-$	$\pm$	$-$	$-$
60	$+$	$-$	$+$	$-$	$\pm$
70	$+$	$+$	$+$	$+$	$+$
80	$+$	$+$	$+$	$+$	$+$
90	$+$	$+$	$+$	$+$	$+$
100	$+$	$+$	$+$	$+$	$+$

[a] Maximum surface coverage.
[b] Carbon content *ca.* 12% with end-capping.
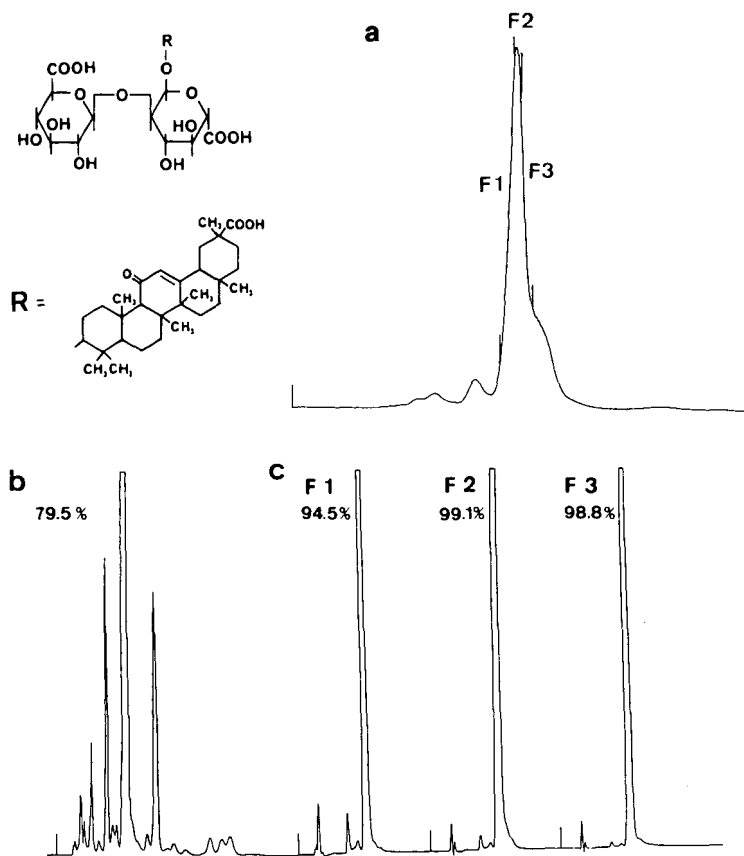
Fig. 6. Purification of glycyrrhizic acid using C_{18}-CLC packing material. (a) 20 mg of glycyrrhizic acid in 0.5 ml of mobile phase were charged. The three fractions, F1, F2 and F3, were collected from the effluent, then examined for purity by injecting into a Cosmosil C_{18} RPLC column (Nacalai Tesque) with 40% acetonitrile containing 0.1% trifluoroacetic acid as mobile phase at a flow-rate of 1.0 ml/min. (b) Prior to purification. (c) Elution of fractions F1, F2 and F3. Purity was based on the peak area with UV detection at 254 nm.

amounts. Nonetheless, the results indicate that the present ISRP materials can accept the direct injection of proteins.

Use of ISRP packing materials in open-column chromatography

Conventional RPLC packing materials are not wettable by methanol–water mixtures containing less than 60–70% of methanol. Such mobile phases cannot be used in open-column chromatography. The present ISRP packing materials with or without a diol phase is wettable by a wide range of water–organic solvent mixtures, as shown in Table V. This permits their use in open-column chromatography without the problem of disintegration of the column bed. Open-column chromatography in the reversed-phase mode will be useful when the normal-phase mode is not effective. An example is shown in Fig. 6 for the purification of glycyrrhizic acid.

By using a 20 mm I.D. column with a 30 cm bed height packed with 75-μm particles of C_{18}-CLC, the purity of glycyrrhizic acid was increased from 80% to higher than 99%. The diol bonding reaction after the decomposition of the alkyl phase is not necessary, unless solutes that are sensitive to the presence of silanols such as polypeptides and hydrogen-bond acceptors are to be chromatographed.

CONCLUSION

A simple method for the preparation of ISRP packing materials was developed by utilizing the partial decomposition of alkylsilylated stationary phases in an acidic medium followed by the introduction of a diol phase. The acid decomposition proceeded rapidly at the external surface and in the larger pores of silica particles than in smaller pores owing to the difference in the accessibility of the reagent. The method can be applied to the preparation of various types of stationary phases for a wide range Sof applications. The resulting ISRP phases can be used for the determination of drugs in serum by eluting large proteins at the void volume. The simple method also permits the preparation of packing materials for open-column reversed-phase chromatography and possibly for thin-layer chromatography with a wide range of water–organic solvent mixtures.

ACKNOWLEDGEMENTS

REFERENCES

1 I. H. Hagestam and T. C. Pinkerton, *Anal. Chem.*, 57 (1985) 1757.
2 I. H. Hagestam and T. C. Pinkerton, *J. Chromatogr.*, 351 (1986) 239.
3 J. Haginaka, N. Yasuda, J. Wakai, H. Matsunaga, H. Yasuda and Y. Kimura, *Anal. Chem.*, 61 (1989) 2445.
4 Y. Sudo, R. Miyagawa and Y. Takahata, *Chromatography*, 9, No. 2 (1988) 179.
5 H. Yoshida, I. Morita, G. Tamai, T. Masujima, T. Tsuru, N Takai and H. Imai, *Chromatographia*, 19 (1984) 466.
6 D. J. Gisch, B. T. Hunter and B. Feibush, *J. Chromatogr.*, 433 (1988) 264.
7 M. Verzele, M. De. Potter and J. Ghysels, *J. High Resolut. Chromatogr. Chromatogr. Commun.*, 2 (1979) 151.
8 Y. Ohtsu, Y. Shiojima, T. Okumura, J. Koyama, K. Nakamura, O. Nakata, K. Kimata and N. Tanaka, *J. Chromatogr.*, 481 (1989) 147.
9 K. Jinno, S. Shimura, N. Tanaka, K. Kimata, J. C. Fetzer and W. R. Biggs, *Chromatographia*, 27 (1989) 285.
10 F. E. Regnier and R. Noel, *J. Chromatogr. Sci.*, 14 (1976) 316.
11 N. Sagliano, Jr., T. R. Floyd, R. A. Hartwick, J. M. Dibussolo and N. T. Miller, *J. Chromatogr.*, 443 (1988) 155.
12 N. Tanaka, Y. Tokuda, K. Iwaguchi and M. Araki, *J. Chromatogr.*, 239 (1982) 761.
13 K. Jinno, T. Nagoshi, N. Tanaka, M. Okamoto, J. C. Fetzer and W. R. Biggs, *J. Chromatogr.*, 392 (1987) 75.

CHROMSYMP. 1816

Optical resolution of racemic compounds on chiral stationary phases of modified cellulose

YOSHITAKA FUKUI*

Fine Cellulose Production Department, Aboshi Plant, Daicel Chemical Industries, Ltd., 1239 Shinzaike, Aboshiku, Himeji 671-12 (Japan)

and

AKITO ICHIDA, TOHRU SHIBATA and KYOZO MORI

Research Centre, Daicel Chemical Industries, Ltd., 1239 Shinzaike, Aboshiku, Himeji 671-12 (Japan)

ABSTRACT

Several alcohols having chiral centres on the chain linking phenyl and hydroxyl groups were chromatographed on a chiral stationary phase, based on cellulose tris-(3,5-dimethylphenylcarbamate) (Chiralcel-OD; OD-CSP). The mobile phases used were polar and non-polar solvents consisting of *n*-hexane and acetonitrile containing 2-propanol or benzene as modifier. The solutes containing hydroxyl groups were not eluted with non-polar eluents, and enantiomeric separation was less effective with eluents containing benzene. The enantiomeric elution order was not affected by changes in eluent polarity. The results suggest that the hydroxyl group was adsorbed on OD-CSP non-stereoselectively and that the phenyl group plays an essential part in the chiral recognition of solutes by OD-CSP. With both polar and non-polar eluents the solutes are oriented toward OD-CSP in a similar conformation.

INTRODUCTION

The use of chiral stationary phases (CSPs) for the separation of enantiomers has attained increasing prominence in the past decade, but the chiral recognition mechanism on a CSP has not been clarified in most instances. The chiral separation mechanism on a polymer-type CSP is more complex than that on a monomeric type. Recently, Shibata and co-workers[1,2] and Wainer and co-workers[3,4] suggested that the enantioselectivity on cellulose derivatives is based on attractive interactions between the solute and the CSP, such as dipole stacking, hydrogen bonding and $\pi-\pi$ association. Therefore, expecting that the solute–CSP interactions could be controlled by a change in eluent polarity, we examined the chromatographic resolution of solutes containing a hydroxyl group and a phenyl group.
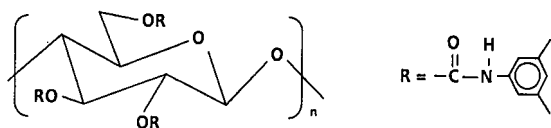
Fig. 1. Structure of the Chiralcel-OD chiral stationary phase.

EXPERIMENTAL

Chromatography was performed with a Shimadzu (Kyoto, Japan) LC-6A pump, a Shimadzu SPD-6A variable-wavelength spectrometric detector and a JASCO polarimetric detector. The CSP used for this study was cellulose tris(3,5-dimethyl-phenylcarbamate) (Fig. 1) adsorbed on macroporous silica gel (Chiralcel-OD; OD-CSP) and packed in a stainless-steel column (25 × 0.46 cm I.D.).

4-Phenyl-2-butanol,1-phenyl-2-propanol, 2-phenyl-1-propanol, 3-phenyl-1-propanol, 1-phenoxy-2-propanol, 1-phenylethanol and (3-methylbutyl)benzene were purchased from Tokyo Kasei (Tokyo, Japan) and 3-phenyl-1-butanol and 3-cyclohexyl-1-propanol from Aldrich (Milwaukee, WI, U.S.A.). The methyl ethers of 4-phenyl-2-butanol, 4-cyclohexyl-2-butanol, the methyl ether of 3-phenyl-1-butanol and 3-cyclohexyl-1-butanol were derived from the respective parent alcohols. Acetonitrile (HPLC grade), *n*-hexane, 2-propanol and benzene were purchased from Wako (Osaka, Japan).

The solutes were dissolved in the respective eluents at concentrations of 0.136 mol/l. Mobile phases were prepared so that the total concentration of modifiers was 1.3 and 2.6 M in hexane or acetonitrile, respectively. The flow-rate was set at 0.5 ml/min and the temperature was kept at 25°C. The effluent was monitored with UV and polarimetric detectors.
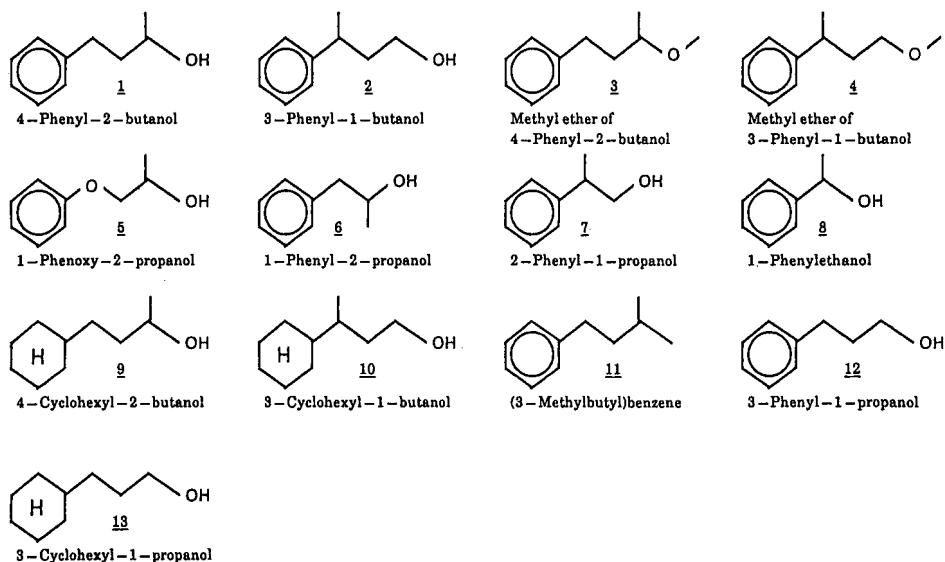
Fig. 2. The structure of the solutes used in this study.

TABLE I

CHROMATOGRAPHIC RESULTS OBTAINED WITH OD-CSP AND MOBILE PHASE CONSISTING OF 2-PROPANOL OR BENZENE MODIFIER IN HEXANE

k' = Capacity factor of first-eluted enantiomer; α = stereoselectivity; E.O. = enantiomeric elution order.

Solute	1.3 M 2-propanol in hexane			2.6 M 2-propanol in hexane			1.3 M benzene in hexane			1.3 M 2-propanol and 1.3 M benzene in hexane		
	k'	α	E.O.	k'	α	E.O.	k'	α	E.O.	k'	α	E.O.
1	1.81	1.62	−, +	1.05	1.59	−, +		Not eluted		0.90	1.36	−, +
2	1.62	1.19	−, +	0.90	1.18	−, +		Not eluted		0.88	1.15	−, +
3	0.53	2.85	−, +	0.48	2.94	−, +	1.01	1.88	−, +	0.39	1.75	−, +
4	0.43	1.43	−, +	0.39	1.44	−, +	0.70	1.59	−, +	0.34	1.27	−, +
5	2.33	2.57	−, +	1.26	2.58	−, +		Not eluted		1.07	2.37	−, +
6	1.12	1.12	+, −	0.68	1.10	+, −		Not eluted		0.67	1.04	+, −
7	1.34	1.00	+, −	0.76	1.00	+, −		Not eluted		0.65	1.00	+, −
8	1.37	1.27	+, −	0.86	1.14	+, −		Not eluted		0.85	1.14	+, −
9	0.58	1.00	−	0.54	1.00	−	−	−	−	−	−	−
10	0.43	1.00	−	−	−	−	−	−	−	−	−	−
11	0.29	−	−	0.31	−	−	0.33	−	−	0.23	−	−
12	2.19	−	−	1.35	−	−		Not eluted		1.21	−	−
13	0.42	−	−	−	−	−	−	−	−	−	−	−

RESULTS AND DISCUSSION

The structures of the solutes used to investigate the interactions with OD-CSP are shown in Fig. 2. They have polar and non-polar groups and a chiral centre on the chain linking the two functional groups. The pairs **1** and **2**, **3** and **4**, **6** and **7** or **9** and **10** have different distances between these functional groups. The chromatographic results with hexane or modifier-containing hexane and with acetonitrile or modifier-containing acetonitrile as eluents are given in Tables I and II, respectively. The percentage change in retention and stereoselectivity for each solute with hexane–modifier mixtures and acetonitrile–modifier mixtures are presented in Table III and IV, respectively.

Compounds **1, 2, 5, 6, 7, 8** and **12** were not eluted by 1.3 *M* benzene in hexane but they were eluted by 1.3 *M* 2-propanol in hexane.

Methyl ethers **3** and **4** and the hydrocarbon **11** were eluted with 1.3 *M* benzene in hexane. On the basis of these results, we suggest that the hydroxyl group of the solutes is mainly responsible for interactions with OD-CSP in a totally non-polar mobile phase. However, when the mobile phase already contained considerable amounts of a polar solvent (*e.g.*, 1.3 *M* 2-propanol in hexane and 100% acetonitrile), the k' values of the solutes decreased on addition of benzene and also on addition of 2-propanol (Tables III and IV).

The chromatographic behaviour of several solutes structurally analogous to the above was also examined, namely **11**, which has no hydroxyl group, and **9** and **13**, which have no phenyl ring. With the non-polar eluent, the k' values of **9** and **13** are slightly greater than that of **11**, but they were smaller than that of **1** (Table I). From these results it is concluded that both the hydroxyl and the phenyl group of **1** contribute to the adsorption on OD-CSP. The large k' value of **1** seems to be due to

TABLE II

CHROMATOGRAPHIC RESULTS OBTAINED WITH OD-CSP AND MOBILE PHASE CONSISTING OF ACETONITRILE OR ACETONITRILE WITH 2-PROPANOL OR BENZENE MODIFIER

k', α and E.O. as in Table I.

Solute N	Acetonitrile			1.3 M 2-propanol in acetonitrile			1.3 M benzene in acetonitrile		
	k'	α	E.O.	k'	α	E.O.	k'	α	E.O.
1	0.63	1.08	−, +	0.52	1.08	−, +	0.49	1.00	−, +
2	0.61	1.00	−, +	0.51	1.00	−, +	0.49	1.00	−, +
3	0.52	2.03	−, +	0.46	1.85	−, +	0.33	S.P.[a]	Unknown
4		Unknown			Unknown			Unknown	
5	0.55	1.59	−, +	0.45	1.57	−, +	0.40	1.34	−, +
6	0.49	1.00	+, −	0.41	1.00	+, −	0.38	1.00	Unknown
7	0.46	1.00	Unknown	0.39	1.00	+, −	0.38	1.00	Unknown
8	0.46	1.20	+, −	0.39	1.19	+, −	0.31	1.00	+, −
9		Unknown		−	−	−	−	−	−
10		Unknown		−	−	−	−	−	−
11	0.47	−	−	0.45	−	−	0.38	−	−
12	0.66	−	−	0.54	−	−	0.50	−	−
13	0.38	−	−	0.36	−	−	−	−	−

[a] Shoulder peak.

TABLE III

PERCENTAGE CHANGE IN RETENTION AND STEREOSELECTIVITY WHEN 2-PROPANOL
OR BENZENE IS ADDED TO THE ELUENT 1.3 M 2-PROPANOL IN HEXANE

$\%k'$ and $\%\alpha$ are values relative to those for 1.3 M 2-propanol in hexane as eluent in Table I being assigned
values of 100%.

Solute	1.3 M 2-propanol in hexane		2.6 M 2-propanol in hexane		1.3 M isopropanol + 1.3 M benzene in hexane	
	$\%k'$	$\%\alpha$	$\%k'$	$\%\alpha$	$\%k'$	$\%\alpha$
1	100	100	58	95	50	58
2	100	100	56	95	54	79
3	100	100	91	105	74	41
4	100	100	91	102	79	63
5	100	100	54	101	46	87
6	100	100	61	83	60	33
7	100	–	57	–	48	–
8	100	100	63	52	62	52
12	100	–	62	–	54	–

chelate formation between the hydroxyl group, the phenyl group of **1** and the xylyl
urethane group of cellulose tris(3,5-dimethylphenylcarbamate). The enantiomeric
elution order of **1–8** remained constant regardless of the solvent polarity. In each pair
of solutes, **1** and **2**, **3** and **4**, and **6** and **7**, the α value of the former is always larger than
that of the latter component, regardless of solvent polarity. These two results suggest
that the adsorptivity of solutes on OD-CSP are changed by the eluent polarity but the
stereochemical features of the complex formed when the solutes are adsorbed on
OD-CSP are not essentially affected by the eluent polarity.

Compounds **1**, **3** and **5** have similar distances between the phenyl and hydroxyl
or methoxy groups. The k' and α values of these solutes are different, but their
enantiomeric elution order is the same. On the other hand, compounds **6** and **8** have

TABLE IV

PERCENTAGE CHANGE IN RETENTION AND STEREOSELECTIVITY WHEN 2-PROPANOL
OR BENZENE IS ADDED TO THE ACETONITRILE ELUENT

$\%k'$ and $\%\alpha$ are values relative to those for acetonitrile as eluent in Table II being assigned values of 100%.

Solute	Acetonitrile		1.3 M 2-propanol in acetontrile		1.3 M benzene in acetonitrile	
	$\%k'$	$\%\alpha$	$\%k'$	$\%\alpha$	$\%k'$	$\%\alpha$
1	100	100	82	100	78	0
2	100	–	84	–	79	–
3	100	100	88	83	63	0
5	100	100	81	97	73	58
6	100	–	84	–	78	–
7	100	–	85	–	83	–
8	100	100	85	95	67	0
12	100	–	82	–	76	–

distances different from that of **1** between these groups and the enantiomeric elution order is also different from that of **1**. Both the k' and α values for **1**, **8** and **6** with non-polar eluents decrease in that order (Tables I and II). This suggests that a certain conformational flexibility and/or distance between these two functional groups is required for these compounds to fit well on the chiral recognition site of OD-CSP. The α values of solutes **1–7** were greatly decreased by the addition of benzene to the mobile phase, whereas the decrease caused by the addition of 2-propanol was much less (Tables III and IV). While solutes containing a benzene ring (**1** and **2**) were well resolved on OD-CSP, the corresponding saturated compounds **9** and **10** were not. These results indicate that the phenyl group of the solutes plays an important role in chiral recognition, presumably by π–π association with the xylyl group of cellulose tris(3,5-dimethylphenylcarbamate).

CONCLUSIONS

In the case of the solutes examined, the hydroxyl group causes strong adsorption on OD-CSP, but a major part of the adsorptive interaction seems to be non-stereo-selective. The interaction between OD-CSP and the phenyl groups of the solutes plays an essential part in chiral recognition by OD-CSP.

With these alcohols, which contain phenyl groups, the stereochemical association feature which may be formed between the solutes and OD-CSP seems to be unchanged over a wide range of solvent polarities. In solutes whose chiral centre is on the chain linking the phenyl and the hydroxyl groups, a suitable distance between the phenyl and hydroxyl groups and/or flexibility are necessary for a good fit to the chiral recognition site of OD-CSP.

ACKNOWLEDGEMENTS

REFERENCES

1 K. Torii, M. Yoshikane and T. Shibata, presented at the *32nd Meeting of the Research Group on Automatic Liquid Chromatography, Kyoto, January 1989.*
2 I. W. Wainer, R. M. Stiffin and T. Shibata, *J. Chromatogr.*, 411 (1987) 139.
3 M. H. Gaffney, R. M. Stiffin and I. W. Wainer, *Chromatographia*, 27 (1987) 15.
4 I. W. Wainer, M. C. Alembik and E. Smith, *J. Chromatogr.*, 388 (1987) 65.

CHROMSYMP. 1884

Fundamental study of hydroxyapatite high-performance liquid chromatography

II[a]. Experimental analysis on the basis of the general theory of gradient chromatography

TSUTOMU KAWASAKI*, MAKOTO NIIKURA and YURIKO KOBAYASHI

Chromatographic Research Laboratory, Koken Bioscience Institute, 3–5–18 Shimo-Ochiai, Shinjuku-Ku, Tokyo 161 (Japan)

ABSTRACT

In hydroxyapatite (HA) chromatography, competition occurs between the sample molecule and ions from the buffer for adsorption onto the crystal surface of HA. The competition mechanism for several proteins and nucleoside phosphates was analysed on the basis of the general theory of gradient chromatography that has been established recently. It was concluded that the number, x' of adsorbing sites of HA that are covered by an adsorbed molecule, in general, tends to increase slowly with increase in molecular mass, but that the correlation between molecular mass and x' is weak. The conclusion is consistent with the deduction made earlier that the stereochemical structure of the local molecular surface (which is highly characteristic of a molecule, and is intimately related to the x' value) is discerned by the regular crystal surface structure of HA. The capacity factor, k', is argued on the basis of the competition model.

INTRODUCTION

Hydroxyapatite [HA; $Ca_{10}(PO_4)_6(OH)_2$] column chromatography, a powerful technique for the separation of proteins, nucleic acids and viruses in aqueous systems, was originally introduced in 1956 by Tiselius *et al.*[2]. Between 1959 and the early 1970s, wa number of experiments were carried out by Bernardi's group with the purpose of elucidating the fundamental chromatographic mechanism. This was reviewed by Bernardi[3–5] and included the studies of other workers. In 1972, HA chromatography in the presence of a detergent was reported by Moss and Rosenblum[6]. In 1973–74, the

---

[a] For Part I, see ref. 1.

interaction mechanism between nucleic acids and HA was explored by Martinson and Wagenaar (see, *e.g.*, refs. 7 and 8). In 1978, the chromatographic properties of several types of HA prepared by using different methods were studied by Spencer[9,10] in connection with both the crystal surface structure (as observed by scanning electron microscopy) and the size of the crystallites constituting the total HA particle (as deduced from the X-ray diffraction profile). In 1984, the experimental investigation that originated in Bernardi's laboratory was continued by Gorbunoff[11,12] and Gorbunoff and Timasheff[13]. In all the experiments above, open columns were used.

In 1983, stainless-steel columns for high-performance liquid chromatography (HPLC) packed with Tiselius type HA[2] were first commercialized by Bio-Rad Labs. (Richmond, CA, U.S.A.), followed by Koken (Tokyo, Japan), and accompanied with two publications[14,15]. Slightly retarded HPLC columns packed with coral HA (constructed by aggregation of hexagonal rods) were introduced by Mitsui Toatsu Chemicals (Tokyo, Japan). The first paper reporting an HPLC column packed with spherical HA with an average diameter of about 5 μm (constructed by aggregation of microcrystals) was published in 1986 by Kawasaki *et al.*[16], followed by a second paper[17]. Almost at the same time, an independent paper on a spherical HA packed HPLC column was published by Kadoya *et al.*[18]. In parallel with the appearance of these papers[16–18], spherical HA packed columns were introduced by Koken, Tonen (Tokyo, Japan) and Asahi Optical (Tokyo, Japan). In the first, besides HA particles as presented in refs. 16 and 17, those with average diameter of *ca.* 20 μm are also produced; HPLC columns packed with these particles are also available from Regis Chemical (Morton Grove, IL, U.S.A.). The last two columns contain HA particles as presented in ref. 18. About one year later, two other types of spherical HA packed column were introduced by Tosoh (Tokyo, Japan), followed by Cica-Merck (Tokyo, Japan); the first column was accompanied by a publication[19]. HPLC columns packed with square tile-shaped HA were also introduced by Koken, accompanied by a publication[20]. (Scanning electron micrographs of Tiselius type HA, spherical HA and square tile-shaped HA developed by Koken for HPLC and that of coral HA developed by Mitsui Toatsu Chemicals will be presented in Part III[21]).

An HPLC column packed with spherical particles of strontium phosphate HA $[Sr_{10}(PO_4)_6(OH_2]$ was developed by Kawasaki *et al.*[22] and a column packed with spherical particles of fluoroapatite $[Ca_{10}(PO_4)_6F_2]$ by Sato *et al.*[23].

A new method of separating acidic and basic proteins from each other by applying double gradients of KCl (or NaCl) and phosphate buffer was introduced by Kawasaki *et al.*[15] (see below). Recently, a novel technique of chromatographing uncharged glycoside molecules on an HA column in the presence of a high concentration (*e.g.*, 70–90%) of acetonitrile was introduced by Kasai *et al.*[24]. It can be deduced[25–27] that the adsorption and desorption mechanism occurring in the presence of acetonitrile is different from that interfering in the usual aqueous system both in the absence of acetonitrile and in the presence of the inorganic salt.

The study made in Part I[1] of this series[a] together with the analysis of

---

[a] Part I was presented 5 years ago at the Conference on Liquid Chromatography, Japan, wich will be published elsewhere[1]. The reasoning with respect to the fundamental chromatographic mechanisms (see later) will be considered in detail in ref. 1.

experimental data for open-column chromatography[3-5,11-13] leads to the following fundamental mechanisms of HA chromatography when carried out in an aqueous system. In general, two types of adsorbing surface appear on an HA particle packed in the column (to the precise, on the crystallites constituting an HA particle, the latter being a polycrystal or an assembly of polycrystals). On the first and the second surface, adsorbing sites (playing roles of anion and cation exchangers, called C and P sites) are arranged with minimum interdistances of the order of magnitude of the size of a crystal unit cell, respectively (for details, see Part III[21], where it will be shown that the first and second surfaces correspond to the **a** and the **c** crystal surface, respectively).

As far as the proteins are concerned, carboxyl groups on the molecular surface are used for the adsorption of a molecule onto C sites, and phosphate groups also act as adsorption groups onto C sites in the case of phosphoproteins. On the other hand, ε-amino and guanidinyl groups are used for the adsorption onto P sites. A protein molecule can therefore be adsorbed on HA in two different ways. Thus, in the first way, the molecule is adsorbed onto C sites (existing on the first or the **a** crystal surface) by using carboxyl (and phosphate) groups and, in the second, it is adsorbed onto P sites (existing on the second or the **c** crystal surface) by using ε-amino and guanidinyl groups. Following a statistical mechanical law, a canonical or a Boltzmann distribution is realized between the two modes of adsorption. In many actual instances, however, the Boltzmann distribution is biased towards one of the two extremes, and acidic proteins that have isoelectric points lower than 7 are adsorbed mainly onto C sites, whereas basic proteins that have isoelectric points higher than 7 are adsorbed mainly onto P sites. Nucleic acids or nucleotides are adsorbed onto C sites by using phosphate groups.

Phosphate ions from the potassium or sodium phosphate buffer (called the KP or the NaP buffer; for details of the KP buffer, see Experimental) are adsorbable onto C sites whereas potassium or sodium ions from the same buffer can be adsorbed only onto P sites. Therefore, in the presence of potassium or sodium phosphate buffer in the system, competition occurs between acidic proteins (or nucleotides) and phosphate ions and between basic proteins and potassium or sodium ions for adsorption onto C and P sites, respectively. In the competition mechanism, a number, x', of crystal sites (C or P) are generally covered by a sample molecule when it is adsorbed (to be precise, covered by a local surface, or local surfaces, of the molecule), whereas a single crystal site is covered by a competing ion (for details of the competition mechanism, see refs. 25–27).

With gradient chromatography using the KP or the NaP buffer to generate a molarity gradient, the sample molecules initially adsorbed at the inlet of the column forming a narrow band are driven out of the HA surface by competing ions from the molarity gradient; the development process thus proceeds.

Chloride ions, although they are anions, are virtually unadsorbable on the HA surface, presumably owing to steric hindrance. On the basis of this mechanism, the chromatographic behaviour, "acidic" or "basic", of an arbitrary molecule can be judged from a double gradient chromatographic experiment using double gradients of KCl and KP[15]. Fig. 1a illustrates a typical example of a double gradient chromatogram for a mixture of bovine serum albumin (BSA) (with $pI = 4.7$), cytochrome c (with $pI = 9.8$–10.1) and lysozyme (with $pI = 10.5$–11.0). This was obtained by previously applying the KCl gradient after an isocratic elution in the presence of a low
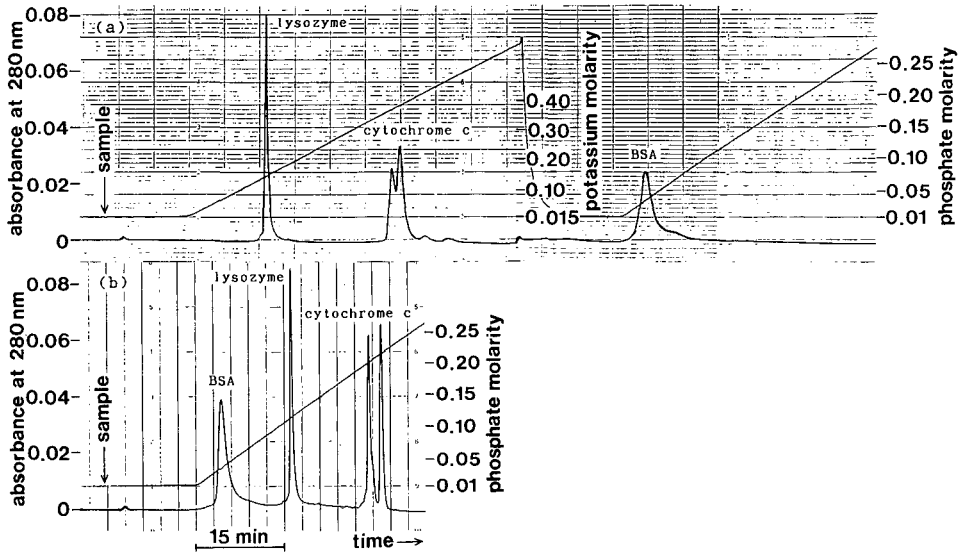
Fig. 1. (a) Double gradient chromatogram for a mixture of BSA (0.17 mg), cytochrome c (56 μg) and lysozyme (26 μg) as obtained on the KB column with $\varnothing = 6$ mm and $L = 3 + 10 = 13$ cm) packed with spherical HA type S_2. Experimental conditions: $m_{in(P)} = 10$ mM for both KCl and KP gradients; $g'_{(KCl)} = 10.4$ mM/ml [$g'_{(KCl)}$ ($\varnothing = 1$ cm) $= 3.75$ mM/ml]; $g'_{(P;KP)} = 6.94$ mM/ml [$g'_{(P;KP)}$ ($\varnothing = 1$ cm) $= 2.5$ mM/ml]; flow-rate $= 0.97$ ml/min; $P = 1.8-2.1$ MPa; $T = 24.3°$C; recovery $= 96\%$. (b) Single KP gradient chromatogram for a mixture of BSA (0.17 mg), cytochrome c (56 μg) and lysozyme (26 μg) as obtained on the same column. Experimental conditions: $m_{in(P)} = 10$ mM; $g'_{(P;KP)} = 6.94$ mM/ml [$g'_{(P;KP)}$ ($\varnothing = 1$ cm) $= 2.5$ mM/ml]; flow-rate $= 0.97$ ml/min; $P = 1.8-2.1$ MPa; $T = 24.3°$C; recovery $= 107\%$. For symbols, see Experimental and Results.

molarity (10 mM) of KP; 10 mM KP was present while the KCl gradient continued (left-hand side of Fig. 1a). The carrier solvent was again replaced with pure 10 mM KP, and the KP gradient was finally applied (right-hand side of Fig. 1a). It can be seen in Fig. 1a that BSA with an acidic pI is eluted in the second KP gradient whereas both cytochrome c and lysozyme with basic pI are eluted with the first KCl gradient. [It can be understood that the basic molecules (cytochrome c and lysozyme) that have been adsorbed on one of the two crystal surfaces (the **c** surface) are first desorbed and developed on the column, driven out of the crystal surfaces through competition with potassium ions from the first KCl gradient, while the acidic molecule (BSA) adsorbed on the other crystal surface (the **a** surface) remains on the crystal surfaces; the acidic BSA is hardly affected by the presence of the low molarity (10 mM) of KP and by the KCl gradient as chloride ions are virtually unadsorbable on both of the two types of crystal surface. BSA is desorbed from the HA surface (the **a** surface) and developed on the column, driven out of the crystal surfaces through competition with phosphate ions from the second KP gradient.] As a reference, a single KP gradient chromatogram for the same mixture is shown in Fig. 1b; this chromatogram is a superposition of the two chromatograms occurring in parallel on the basis of two different chromatographic mechanisms (see above).

The double gradient experiment was also performed for other molecules. It was confirmed that acidic molecules [DNA, ADP, ATP, adenosine tetraphosphate,

poly-L-aspartate, poly-L-glutamate, ovalbumin, pepsinogen and deoxyribonuclease I (DNase I)] are eluted in the second KP gradient whereas basic and neutral molecules [poly-L-lysine, poly-L-arginine, ribonuclease A (RNase A), trypsinogen, haemoglobin and myoglobin] are eluted in the first KCl gradient. In some instances with acidic and basic proteins, some minor components were eluted in the first KCl and the second KP gradient, respectively, however. The details of the experiments are published elsewhere[1] [in ref. 1, it was pointed out that the a surface of some commercially available spherical HA particles is damaged to a considerable extent. With these particles, acidic proteins are adsorbed so weakly on the a surface that the molecules are eluted from the column even before the second KP gradient begins in the double gradient system. In view of our experience, it is highly probable that the destruction of the surface structure occurred at least partially in the sintering process of microcrystals to make up a sphere (cf., Part III[21])].

A molecule, in general, can take a number of different configurations on the crystal surface of HA. In other words, the molecule can be adsorbed using a number of different local surfaces, each of which can face the crystal surface and can orient in different directions on the crystal surface. Again following the statistical mechanical law, a Boltzmann distribution is realized among the configurations, and the energetically most stable adsorption configuration is realized with the highest probability (cf., eqn. 37 in ref. 25). In other words, the stereochemical structure of the local molecular surface (facing the crystal surface when the molecule is in the energetically most stable configuration) can be recognized by the regularity of the crystal surface structure of HA. As a results, the molecular separation highly characteristic of HA chromatography is realized. [In contrast to HA chromatography, with the usual ion-exchange chromatography the geometrical arrangement of the adsorbing sites (called ion exchangers) on the adsorbent would fluctuate microscopically among different loci in the column since the adsorbing sites are part of an organic substrate with a more or less flexible stereochemical structure. This implies that the energetically most stable configuration of a protein molecule adsorbed on the organic substrate varies among different loci in the column, and that the charges on the total molecular surface are used rather uniformly for the reaction with the adsorbent throughout a development process on the column. HA chromatography resembles affinity chromatography in that a subtle differene in the geometrical arrangement of atoms on a local molecular surface may be discriminated by the column owing to a *regular* stereochemical structure of the adsorbent surface.]

The points in Fig. 2 are experimental plots of eluent phosphate molarity [$m_{elu(P)}$] *versus* isoelectric point (pI) for 26 proteins obtained for open-column HA chromatography with both KP and NaP systems (reproduced from refs. 5, 11–13 and 28 with slight modifications[1]. The data for both KP and NaP systems have been plotted on a common [pI, $m_{elu(P)}$] plane as the experimental conditions (*i.e.*, both the total column length and the slope of the molarity gradient) that were applied were virtually identical for the two systems, and $m_{elu(P)}$ depends only slightly on the type of univalent cation involved in the buffer[1]. It can be seen in Fig. 2 that proteins that are not eluted from the column even in the presence of 3 M CaCl$_2$ (almost corresponding to "acidic" proteins that are eluted in the second KP gradient in the double gradient system; *cf.*, Appendix I in ref. 21; see also ref. 1) tend to be eluted at lower phosphate molarities than those which are eluted from the column in the presence of less than 10 mM CaCl$_2$ (almost
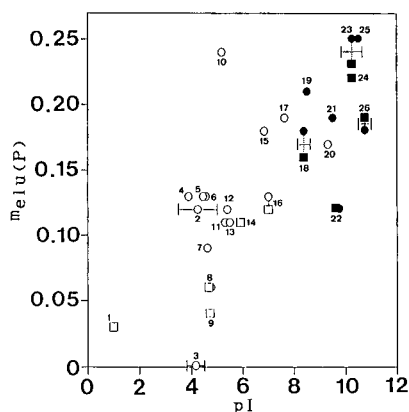
Fig. 2. Plots of $m_{elu(P)}$ *versus* pI for 26 proteins [1, pepsin; 2, Lima bean trypsin inhibitor; 3, ovamucoid; 4, pepsinogen; 5, soybean trypsin inhibitor; 6, α-lactalbumin; 7, ovalbumin; 8, bovine serum albumin; 9, deoxyribonuclease I; 10, β-lactoglobulin A; 11, carbonic anhydrase B; 12, catalase (bovine liver); 13, insulin; 14, snail acid deoxyribonuclease; 15, conalbumin; 16, myoglobin; 17, haemoglobin (horse); 18, α-chymotrypsin; 19, γ-chymotrypsin; 20, trypsinogen; 21, chymotrypsinogen; 22, ribonuclease A; 23, cytochrome c; 24, spleen acid deoxyribonuclease; 25, papaya lysozyme, 26, lysozyme (chicken)] obtained for open-column HA chromatography with both KP and NaP systems, where ø = 1 cm, L = 18–23 cm, $m_{in(P)}$ = 10 mM and $g'_{(P)}$ (ø = 1 cm) = 2.4–2.5 mM/ml (reproduced from refs. 5, 11–13 and 28 with slight modifications[1]; for symbols, see Experimental). ○ and □, "acidic" proteins that are not eluted from the column even in the presence of 3 M CaCl$_2$; ● and ■, "basic" proteins that are eluted in the presence of less than 10 mM CaCl$_2$; □ and ■, KP system; ○ and ●, NaP system.

corresponding to "basic" proteins that are eluted in the first KCl gradient in the double gradient system; *cf.*, Appendix I in ref. 21, see also ref. 1). Among the "acidic" and the "basic" proteins (*i.e.*, among the proteins obeying the same chromatographic mechanism), however, the correlation between $m_{elu(P)}$ and pI is very weak, respectively (see Fig. 2; also see Fig. 7 in Part III[21]).

The points in Fig. 3 are experimental plots (reproduced from ref. 29) of pI *versus* elution (or retention) time for a number of proteins obtained with a DEAE-5PW anion-exchange column (Tosoh) where a linear NaCl gradient was applied; the elution molarity, in general, increases linearly with an increase in elution time. It can be seen in Fig. 3 that elution time (elution molarity) is strongly correlated with pI.

Both Figs. 2 and 3 firmly support the deduction (see above) that the HA column discerns a stereochemical structure on a local surface of a protein molecule whereas the ion-exchange column is sensitive to the total charge per molecule. The possibility cannot be excluded, however, that, under certain circumstances where the secondary or the tertiary structure of the molecules under examination is fluctuating to a larger extent, a stronger correlation be realized between pI and elution molarity even in HA chromatography, In the special case when only the local molecular surface interfering in the reaction with the HA surface varies among the molecules under examination, a strong correlation might also be realized between pI and elution molarity.

Recently, a general theory of quasi-static linear gradient chromatography has been established for both small sample loads[30–32] and overloads[32–34]. Quasi-static chromatography is defined[32] as chromatography in which the rate of transition of a molecule between the mobile and the stationary phase is so high that the phase
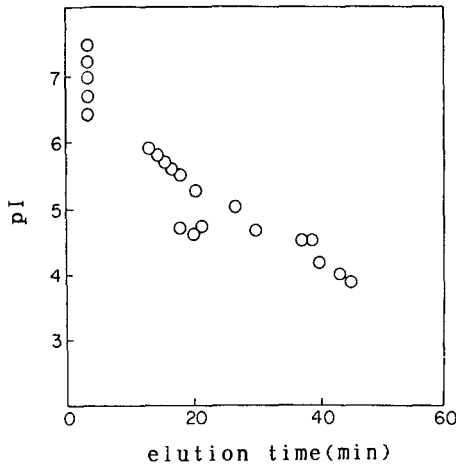
Fig. 3. Plots of p*I* *versus* elution time for a number of proteins obtained with an DEAE-5PW anion-exchange column of dimensions 10 cm × 0.78 cm I.D. (Tosoh). A linear NaCl gradient (0–0.4 *M*) was applied in the presence of 50 m*M* Tris–HCl buffer at pH 7.5 (reproduced from ref. 29).

transition effect hardly contributes to the longitudinal molecular diffusion in the column, and the longitudinal contribution of the Brownian diffusion occurring in the mobile phase is also negligible. From a practical point of view, the quasi-static condition can be assumed to hold in the usual HPLC. The fundamental structure of the theory with small sample loads is outlined schematically in the Appendix in ref. 32 (see also the first part of the Theoretical section in the presented work).

By introducing the competition mechanism (see above) into the general theory of quasi-static linear gradient chromatography, a concrete theoretical chromatogram can be calculated[30,34].

Experimental verifications of the theory of gradient chromatography into which the competition model is introduced have been made for HA chromatography carried out under both small-load[34-37] and overload[34,38] conditions. The significance of these studies is that the competition mechanism in HA chromatography has been verified on quantitative basis.

In this paper, the chromatographic behaviour of several basic and acidic proteins and nucleoside phosphates under small-load conditions on a spherical HA packed HPLC column is analysed on the basis of the theory of gradient chromatography into which the competition model is introduced. From the analysis, the adsorption configuration of the molecules on the crystal surface of HA can be deduced. Further experimental verifications of the competition model itself are added.

Most of the experimental data that were used for the analysis are original; however for some analyses, data published in earlier papers are reused (the abbreviations that are used in this paper are as follows: HA, hydroxyapatite; HPLC, high-performance liquid chromatography; ø, inside column diameter; KP or NaP, potassium or sodium phosphate buffer, respectively, at pH ≈ 6.8; *P*, pressure drop; *T*, temperature; RNase A, ribonuclease A; IgG, immunoglobulin G; DNase I, deoxyribonuclease I; BSA, bovine serum albumin).

THEORETICAL

General theory of quasi-static linear gradient chromatography with small sample loads[30-32]

Let us consider quasi-static linear gradient chromatography with small sample loads when a band of the sample molecules with an infinitesimal width is initially formed at the inlet of the column. When both the slope, g, of the molarity gradient and the total length, L, of the column are given, the theoretical chromatogram, f, for a molecular component under consideration in the sample mixture can, in general, be represented as a function of molarity, m, in the molarity gradient by eqn. 43 in ref. 30. This can be rewritten with slight modifications as

$$f(m) = \frac{1}{\sqrt{2\pi}\ \sigma(s;g)} \cdot \exp\left\{ - \frac{[m-\mu(s)]^2}{2[\sigma(s;g)]^2} \right\} \tag{1}$$

where

$$s = \int_{m_{in}}^{\mu} \frac{B'(m)}{1\ -\ B'(m)} \cdot dm \tag{2}$$

by which the function $\mu(s)$ is implicitly defined, and

$$\sigma(s;g) = \frac{\sqrt{2g\Theta_0 s}}{B'[\mu(s)]} \tag{3}$$

The physical meanings of the symbols involved in eqns. 1–3 are as follows:

$g =$ slope of the molarity gradient expressed as the increase in molarity per unit length of the column measured from the outlet to the inlet of the column. (In earlier papers[30-32], the slope, g', of the gradient expressed as the increase in molarity per unit interstitial volume of the column was considered instead of g.)

$s =$ parameter representing the difference in molarity between the inlet and the outlet of the column, defined as the product of g and the total length, L, of the column:

$$s = gL \tag{4}$$

(In refs. 30–32, s was defined as the product of g' and the total interstitial volume, L', of the column. It is evident that $g'L'$ is equal to gL.)

$m_{in} =$ initial molarity at the beginning of the molarity gradient.

$\Theta_0 =$ parameter with the dimensions of length that measures the longitudinal diffusion in the column. Θ_0 depends on the g value, the type of sample molecule and the type of solvent except in an ideal case (see ref. 31). Θ_0 is intimately related to the plate height concept[39]. (In refs. 30–32, the parameter $\Theta \equiv \Theta_0 g/g'$ was considered instead of Θ_0.)

$\mu(s) =$ elution molarity at the centre or the maximum height of the chromatographic peak, which can be considered to be a function of s (*cf.*, eqn. 2).

$\sigma(s;g) =$ standard deviation (with the dimensions of molarity) of the chromatographic peak measured in terms of the molarity range of the gradient over which the peak appears. σ can be considered to be a function of s involving the parameter g (*cf.*, eqn. 3).

$B'(m) =$ partition of sample molecules (of the chromatographic component under consideration) in the mobile phase in an elementary volume of the column in which the molarity of the gradient element is m. B', in general, increases monotonically from *ca.* 0 to 1 with increase in m. B' is related to the capacity factor, k', by the relationship $B' = 1/(1 + k')$ or $k' = (1 - B')/B'$ (*cf.*, eqn. 8).

Theory into which the competition model is introduced[30]

On the basis of the competition model where it is assumed that the adsorption of a sample molecule occurs on a single type of the adsorbent surface, the function $B'(m)$ under small-load conditions can be represented by eqn. 29 in ref. 27 (i.e., eqn. 44 in ref. 30) as

$$B'(m) = \frac{1}{1 + q \cdot (\varphi m + 1)^{-x'}} \tag{5}$$

$m =$ molarity of competing ions.

$\varphi =$ positive constant characterizing the competing ions constituting the molarity gradient. This measures the strength of adsorption of the ions onto the adsorbent surface (*cf.*, eqns. 18 and 21 in ref. 27).

$q =$ positive constant characterizing the sample molecule under consideration. This measures the strength of adsorption of the molecule on the adsorbent surface [*cf.*, eqn. 27 in ref. 27, where q is written as $q_{(\rho')}$].

$x' =$ number of adsorbing sites on the adsorbent surface covered by an adsorbed sample molecule, i.e., the number of sites on which the adsorption of competing ions is impossible owing to the presence of an adsorbed sample molecule, or the number of competing ions the adsorption of which is impossible owing to the presence of an adsorbed sample molecule. (Eqn. 5 was derived[25-27] on the basis of the assumption that a single site is covered by a competing ion when it is adsorbed. Eqn. 5 holds approximately even in the absence of this assumption, however. In this instance, the parameter x' has only the last physical meaning of the number of competing ions the adsorption of which is impossible owing to the presence of an adsorbed sample molecule.)

The prototype of eqn. 5 was first derived in an earlier paper[40], and a most reasonable method for its derivation on the basis of a grand canonical ensemble has been published recently[25-27]. The function $B'(m)$ in which account is taken of the possibility that a sample molecule can be adsorbed on two types of adsorbent surface was derived in ref. 41. However, this function is not applied here.

By introducing eqn. 5, both eqns. 2 and 3 can be rewritten concretely as

$$\mu(s) = \frac{1}{\varphi} \{[(x' + 1)\varphi qs + (\varphi m_{in} + 1)^{x'+1}]^{1/(x'+1)} - 1\} \qquad (6)$$

and

$$\sigma(s;g) = \sqrt{2g\Theta_0 s} \{1 + q[\varphi\mu(s) + 1]^{-x'}\} \qquad (7)$$

respectively. (Eqn. 6 was originally derived as eqn. 15 in ref. 35 on the basis of a primitive consideration. Eqns. 6 and 7 appear as eqns. 45 and 46, respectively, in ref. 30.)

Finally, the capacity factor, k', as a function of m can be represented by

$$k'(m) = q(\varphi m + 1)^{-x'} \qquad (8)$$

(*cf.*, eqn. 5).

EXPERIMENTAL AND RESULTS

Materials and methods

Both spherical HA particles (type S_1 or S_2 with diameters of about 5 μm; see Fig. 2b in ref. 21 for HA type S_1) and HA-packed SUS316 stainless-steel columns (KB columns; Koken) were prepared in our laboratory. [Type S_1 and S_2 particles are almost identical. Except for two experiments carried out using HA type S_2 (Fig. 1), HA type S_1 was used.] Except for one case (see below), the column I.D. was 6 mm; lengths of 0.5, 1, 3, 10 and 30 cm were prepared. The 3-cm column was used as either a precolumn or a main column. If a large overall column length was necessary , it was provided by connecting 30-cm columns in series by using fine tubes. For the purpose of preparing three components of IgG, a column of I.D. 2 cm and length 5 cm was used (see Appendix II).

The HPLC experiments were carried out at room temperature by connecting the column (or the column system) to an HPLC pump. Thus, with gradient chromatography, the sample molecules dissolved in 1 mM potassium phosphate buffer at pH $\approx$ 6.8 (*i.e.*, an equimolar mixture of K_2HPO_4 and KH_2PO_4; called KP buffer. 1 mM relates to phosphate ions in the KP buffer) was injected into the column (or the column system) by using an injector located between the HPLC pump and the column inlet; this was followed by rinsing with 1 mM KP buffer. During this process, virtually all the molecules (except denatured minor components) remained in the stationary phase (*i.e.*, on the surface of the adsorbent) in the vicinity of the column inlet forming a band. Material was then eluted using a linear molarity gradient of KP buffer. The sample elution was monitored by measuring the ultraviolet absorption (at 230, 260, 280 or 415 nm) in a flow cell. At the same time, the molarity gradient was monitored by measuring the refractive index in a special flow cell with a low angle.

With isocratic chromatography, which was carried out for the purpose of determining the R_F or the B' value of the sample molecule occurring in the presence of

KP buffers with different constant molarities, a pulse band of sample molecules was injected into two column systems with overall lengths of 13 ($= 3 + 10$) and 33 ($= 3 + 30$) cm. The difference in elution volumes at the maximum height of the molecular band between the two systems was measured. The R_F value was calculated as the ratio of the void volume involved in the column length of 20 ($= 33 - 13$) cm to the difference in elution volumes (for the void volume, see below). The R_F value should be virtually equal to B' (cf., the "first principle of chromatography in general" mentioned in Appendix III in ref. 30).

The experiment for the determination of the void volume of the column was also carried out by connecting columns (or column systems) with several overall lengths to the HPLC pump, and the pulse sucrose band dissolved in 1 mM KP was developed by using 1 mM KP as the solvent; the elution of the sucrose band was detected by measuring the refractive index in the flow cell.

The sample molecules applied in the HPLC experiments were lysozyme (from chicken egg white; P-L Biochemicals), lysozyme (from turkey egg white; Sigma), cytochrome c (from horse heart; Sigma), ribonuclease A (from bovine pancreas; Sigma), trypsinogen (from bovine pancreas; Sigma), haemoglobin (human; a gift from the Institute for Adult Diseases, Asahi Life Foundation, Tokyo, Japan), immuno-globulin G (human, with isoelectric points between 6.5 and 9; Japanese Red Cross Plasma Fractionation Centre, Tokyo, Japan), myoglobin (from sperm whale skeletal muscle; Sigma), deoxyribonuclease I (from bovine pancreas; Millipore), albumin (from bovine serum; Nutritional Biochemicals), ovalbumin (from chicken egg white; Sigma), pepsinogen (from hog stomach mucosa; Tokyo Kasei Kogyo), ADP (Sigma), ATP (Sigma) and adenosine tetraphosphate (Sigma).

Determination of the void volume of the column

The volume of the solvent (1 mM KP) at which a pulse of sucrose solution (dissolved in 1 mM KP) is eluted was measured by using HA columns with different overall lengths. On the basis of this experiment, the ratio of the void volume to the total packed volume of the HA crystals in the column was calculated to be 0.823, assuming that the migration velocity of sucrose is equal to that of the solvent.

Important experimental parameters in gradient chromatography

Before giving the results of the HPLC experiments (see the next sub-section), it is necessary to define important experimental parameters, as follows.

$m_{(P)}$ and $m_{(K^+)}$: phosphate and potassium molarities in the KP buffer, respectively. $m_{(K^+)}$ is 1.5 times $m_{(P)}$. With "acidic" molecules that compete with phosphate ions from the KP buffer for adsorption onto C sites, m (see eqns. 1, 2 and 5) represents $m_{(P)}$, i.e.,

$$m = m_{(P)} \tag{9}$$

With "basic" molecules that compete with potassium ions from the KP buffer for adsorption onto P sites, m represents $m_{(K^+)}$, i.e.,

$$m = m_{(K^+)} = 1.5m_{(P)} \tag{9'}$$

$m_{elu(P)}$: elution phosphate molarity, *i.e.*, the phosphate molarity in the KP gradient at which the maximum height of the chromatographic peak is eluted. With "acidic" and "basic" molecules, μ (eqn. 6) can be represented in terms of $m_{elu(P)}$ by the relationships

$$\mu = m_{elu(P)} \tag{10}$$

and

$$\mu = 1.5m_{elu(P)} \tag{10'}$$

respectively.

$m_{in(P)}$: initial phosphate molarity, *i.e.*, the phosphate molarity in the KP buffer occurring before the KP gradient begins. With "acidic" and "basic" molecules, m_{in} (eqn. 6) can be represented in terms of $m_{in(P)}$ by the relationships

$$m_{in} = m_{in(P)} \tag{11}$$

and

$$m_{in} = 1.5m_{in(P)} \tag{11'}$$

respectively.

$\sigma_{(P)}$: standard deviation (with the dimensions M or mM) of the chromatographic peak measured in terms of the phosphate molarity range of the KP gradient over which the peak appears. With "acidic" and "basic" molecules, σ (eqn. 7) can be represented in terms of $\sigma_{(P)}$ by the relationships

$$\sigma = \sigma_{(P)} \tag{12}$$

and

$$\sigma = 1.5\sigma_{(P)} \tag{12'}$$

respectively. For practical purposes, $\sigma_{(P)}$ is represented here as the half-width at 0.6065 times the maximum height of the experimental peak; this is identical with the standard deviation provided that the peak has a precise Gaussian shape.

L: total (overall) column length measured in centimeters.

$g'_{(P)}$ ($\emptyset = 1$ cm): reduced slope (to inside column diameter $\emptyset = 1$ cm) of the phosphate gradient [with a slope $g'_{(P)}$] in the KP gradient, measured in units of M/ml or mM/ml. $g'_{(P)}$ ($\emptyset = 1$ cm) is 0.36 ($= 0.6^2$) times as large as $g'_{(P)}$ when the column of I.D. 6 mm is used for the experiment. With "acidic" and "basic" molecules, g (eqn. 4) measured in units of M/cm or mM/cm can be represented in terms of $g'_{(P)}$ ($\emptyset = 1$ cm) by the relationships:

$$\begin{aligned} g &= (\pi/4) \cdot 0.823 \cdot g'_{(P)} \ (\emptyset = 1 \text{ cm}) \\ &= 0.646g'_{(P)} \ (\emptyset = 1 \text{ cm}) \end{aligned} \tag{13}$$

and
$$g = (\pi/4) \cdot 0.823 \cdot 1.5 \cdot g'_{(P)} \; (\o = 1 \text{ cm})$$
$$= 0.970 g'_{(P)} \; (\o = 1 \text{ cm}) \tag{13'}$$

respectively, where 0.823 represents the ratio of the void volume to the total packed volume of the HA crystals in the column that has been determined in the previous sub-section. [Similarly, the slope and the reduced slope of the KCl gradient are represented by $g'_{(KCl)}$ and $g'_{(KCl)}$ ($\o = 1$ cm), respectively ;cf., Figs. 1 and 16.]

$s_{app(P)}$: product of $g'_{(P)}$ ($\o = 1$ cm) and L. With "acidic" and "basic" molecules, s (eqn. 4) can be written in terms of $s_{app(P)}$ as

$$s = 0.646 s_{app(P)} \tag{14}$$

and

$$s = 0.970 s_{app(P)} \tag{14'}$$

respectively.

$q_{app(P)}$: experimental parameter related to q (eqns. 5–7) by the relationships

$$q = q_{app(P)}/0.646 \tag{15}$$

and

$$q = q_{app(P)}/0.970 \tag{15'}$$

with "acidic" and "basic" molecules, respectively.

The parameters φ, x' and Θ_0 in eqns. 5–7 are also used as experimental parameters. φ characterizes competing phosphate and potassium ions with chromatography of "acidic" and "basic" molecules, respectively; x' represents either the number of C sites covered by an "acidic" molecule, or the number of P sites covered by a "basic" molecule; except in an ideal case, Θ_0 depends on the g value, the type of sample molecule and the type of competing ion (see ref. 31).

Results of HPLC experiments

The samples applied in the HPLC experiments are listed in Table I, of which proteins 1–10 behave as "basic" molecules, eluted from the column with the first KCl gradient in the double gradient system; proteins 11–18 and nucleoside phosphates 19–21 behave as "acidic" molecules, eluted with the second KP gradient in the system (for the double gradient system, see Introduction). [For details, see Part I[1], where it should be recalled that myoglobin behaves partially as an "acidic" molecule in effect as the elution molarity in the KCl gradient in the double gradient system is considerably higher than the elution molarity in the KP gradient in the single gradient system (cf., Appendix I in ref. 21). For the sake of convenience, however, here we analyse the myoglobin data assuming that the protein behaves as a "basic" molecule. In connection with this problem, myoglobin (and also horse haemoglobin and trypsinogen with isoelectric points higher than 7, respectively) behaves as an "acidic"

TABLE I

SUMMARY OF RESULTS OF GRADIENT HPLC EXPERIMENTS CARRIED OUT USING A VALUE OF THE PARAMETER ϕ OF 25 M^{-1}

No.	Protein or nucleoside phosphate	Isoelectric point	Molecular mass (kDa)	Chromatographic behaviour[a]	$x'(l.l.,u.l.)$[b]	$Ln\ q_{app(P)}$	$Ln\ q$	$\mathring{m}_{(P)}$[c] (M)	$m_{elu(P)}$[d] (M)	$\Theta_0(cm)$[e] 5.0[f]	2.5[f]	1.25[f]	0.45[f]	Fig. No.
1	Lysozyme (chicken)	10.5–11.0	14.3	Basic	5.7 (4.0, 8.0)	9.5	9.5	0.115	0.113	0.004	0.005	0.008	0.013	4
2	Lysozyme (turkey)		14.2	Basic	5.7 (4.5, 8.0)	10.1	10.1	0.130	0.132		0.005	0.008		
3	Cytochrome c (in reduced state)[g]	9.8–10.6	11.7	Basic	4.8 (4.0, 6.0)	11.2	11.2	0.248	0.212	0.004	0.005	0.005	0.010	5
4	Cytochrome c (in oxidized state)[h]			Basic	4.8 (3.9, 6.0)	10.8	10.8	0.226	0.202		0.003		0.015	
5	RNase A[i]	9.7	13.7	Basic	4.3 (2.7, 6.7)	6.9	6.9	0.106	0.112					
6	Trypsinogen[i]	9.3	24.0	Basic	5.2 (3.5, 7.5)	7.7	7.7	0.091	0.097					
7	Haemoglobin[i]	7.0	64.5	Basic	5.7 (3.7, 8.0)	8.2	8.2	0.086	0.085					
8	IgG (fraction I)[j]		153	Basic	11.0 (6.4, 20.0)	11.2	11.2	0.047	0.052					
9	IgG (fraction II)[j]		153	Basic	11.0 (8.0, 15.0)	16.6	16.6	0.094	0.099		0.010		0.020	6
10	Myoglobin[i]	7.0	17.2	Basic	4.3 (2.8, 6.1)	6.6	6.6	0.097	0.093					
11	DNase I[k] (peak 1)			Acidic	8.0 (2.0, 18.0)	2.0	2.4	0.014	0.020					
12	DNase I[k] (peak 2)	4.7	28.7	Acidic	5.0 (2.1, 8.5)	3.5	3.9	0.047						
13	DNase I (peak 3)			Acidic	5.5 (3.3, 8.0)	6.3	6.7	0.095						
14	DNase I (peak 4)			Acidic	6.0 (4.1, 8.5)	8.7	9.1	0.142	0.147					

No.													
15	BSA	4.7	66.3	Acidic	6.0 (2.5, 12.0)	3.6	4.0	0.038	0.049	0.23[l]	0.30[l]	0.50[l]	7
16	Ovalbumin[i]	4.6	43.5	Acidic	8.0 (2.0, 23.0)	0.5	0.9	0.005	0.015				
17	Pepsinogen[i]	3.9	40.4	Acidic	7.0 (2.5, 15.0)	3.7	4.1	0.032	0.046				8
18	IgG (fraction III)[j]		153	Acidic	18.0 (14.0, 27.0)	25.0	25.4	0.124	0.131	0.07	0.10	0.15	9
19	ADP		0.4	Acidic	2.5 (1.2, 5.0)	2.0	2.4	0.064	0.050				
20	ATP		0.5	Acidic	2.5 (1.2, 3.5)	4.2	4.6	0.212	0.137			0.25	
21	Adenosine tetraphosphate		0.6	Acidic	2.5 (2.0, 3.5)	5.7	6.1	0.419	0.228				

[a] This was judged from the double gradient chromatography experiment using double gradients of KCl and KP (see Introduction).

[b] l.l. and u.l. represent the lower and the upper limit value of x' (i.e., $x'_{l.l}$ and $x'_{u.l.}$), respectively; see Appendix I.

[c] See Appendix III.

[d] Elution phosphate molarity obtained experimentally when $L = 13$ cm and $g'_{(P)}$ ($\emptyset = 1$ cm) $= 2.5$ mM/ml. The average value is shown when several experiments were repeated (cf., Appendix III).

[e] The Θ_0 value was not calculated for chromatographic peaks in which highly heterogeneous substances are involved or those in which molecular degradation is in progress to a large extent [both cases with ATP and adenosine tetraphosphate; cf., ref. 1 and first sub-section of Discussion).

[f] The $g'_{(P)}$ ($\emptyset = 1$ cm) value (in units of mM/ml) that was applied.

[g] This is involved in the second peak of the double peak chromatogram (cf., ref. 16).

[h] This is involved in the first peak of the double peak chromatogram (cf., ref. 16).

[i] Analysis was performed for the main peak of the chromatogram.

[j] See Appendix II.

[k] Peak 1 is the main peak; see Fig. 5 in ref. 17. The experiments were carried out by using column systems with overall lengths of 13 (= 3 + 10) and 33 (= 3 + 30) cm[17]. The precolumn part (with a length of 3 cm) of the systems, however, was packed with square tile-shaped HA or HA type F, the main part being packed with HA type S₁ (see ref. 17; for square tile-shaped HA or HA type F, see Fig. 2d in Part III[21]).

[l] The high value of Θ_0 is apparent, arising from the fact that several components are involved in a chromatographic peak.

molecule in the $CaCl_2$ system (*cf.*, Apendix I in ref. 21). It should also be noted that some "basic" components are contaminating "acidic" DNase I. The experimental analyses for RNase A, trypsinogen, haemoglobin, myoglobin, ovalbumin and pepsinogen will be performed for the main peak of the chromatogram.

The points in Fig. 4a are experimental plots (reproduced from ref. 34 of $m_{elu(P)}$ *versus* L for chicken lysozyme for four different $g'_{(P)}$ ($\emptyset = 1$ cm) values, 5.0, 2.5, 1.25 and 0.45 mM/ml. It can be seen that the profile of the experimental plot is parallel with those obtained for Tiselius type HA packed columns[35–37,42]; $m_{elu(P)}$ increases with increasing L and $g'_{(P)}$ ($\emptyset = 1$ cm) when $g'_{(P)}$ ($\emptyset = 1$ cm) and L are constant, respectively. The dependence of $m_{elu(P)}$ on L differs when the $g'_{(P)}$ ($\emptyset = 1$ cm) applied is
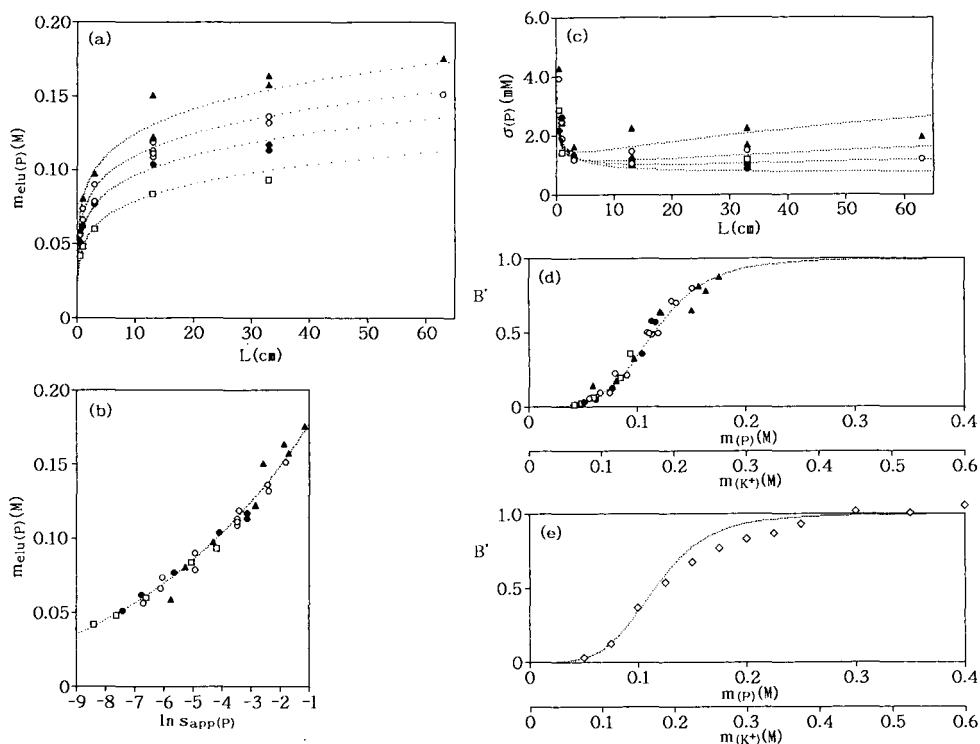
Fig. 4. Analysis of HPLC for chicken lysozyme. Points in (a)–(d): experimental plots of (a) $m_{elu(P)}$ *versus* L, (b) $m_{elu(P)}$ *versus* ln $s_{app(P)}$, (c) $\sigma_{(P)}$ *versus* L and (d) B' *versus* $m_{(P)}$ or $m_{(K^+)}$ for four different $g'_{(P)}$ ($\emptyset = 1$ cm) values: ($\blacktriangle$) 5.0, ($\bigcirc$) 2.5, ($\bullet$) 1.25 and ($\square$) 0.45 mM/ml; the corresponding sample loads are 16–30, 20–60, 30 and 50 μg. Curves in (a)–(d): theoretical curves calculated by using (a) eqn. 6, (b) eqn. 6, (c) eqn. 7 and (d) eqn. 5; in the equations, the parameters m, μ, m_{in}, σ, g, s and q have been represented in terms of $m_{(P)}$, $m_{elu(P)}$, $m_{in(P)}$, $\sigma_{(P)}$, $g'_{(P)}$ ($\emptyset = 1$ cm), $s_{app(P)}$ and $q_{app(P)}$ by using eqns. 9′–15′, respectively. With regard to the invariable parameters that are involved in the equations, the numerical values that were used for the calculation are listed in Table I. [Both the experimental plots and the theoretical curves in (a) and (b), and those for $g'_{(P)}$ ($\emptyset = 1$ cm) = 2.5 mM/ml in (c) have been reproduced from ref. 34. The experimental conditions in (a)–(d) are indicated in ref. 34, where the dependence of $m_{elu(P)}$ and $\sigma_{(P)}$ on both flow-rate and sample load are also shown.] Points in (e): experimental plots of B' *versus* $m_{(P)}$ or $m_{(K^+)}$, where B' values have been estimated from isocratic chromatography carried out under the following experimental conditions: flow-rate, 0.48–0.50 ml/min; P, 1.6–5.9 MPa; T, 22.5–27.0°C. Curve in (e): theoretical curve identical with that shown in (d).

different, giving four arrangements of the experimental points corresponding to the four values of $g'_{(P)}$ ($\o = 1$ cm) (see Fig. 4a).

The points in Fig. 4b are plots of $m_{elu(P)}$ *versus* ln $s_{app(P)}$ instead of L for the experimental points in Fig. 4a. It can be seen that the four arrangements of the experimental points on the $[L, m_{elu(P)}]$ plane (Fig. 4a) converge into a single arrangement when mapped on the $[\ln s_{app(P)}, m_{elu(P)}]$ plane.

The curve in Fig. 4b is theoretical, calculated by using eqn. 6 in which the term qs has been replaced by $q_{app(P)}s_{app(P)}$ by using both eqns. 14' and 15', and $m_{in} = 1.5$ mM since $m_{in(P)} = 1$ mM (see eqn. 11'). For $\o$, the optimum value, 25 M^{-1}, has been used (see Appendix I); this value will hereafter be used for all the calculations. For the other parameters, x' and $q_{app(P)}$, values that are shown in Table I have been applied in order to obtain a best fit with the experiment. It can be seen in Fig. 4b that the coincidence of the theoretical curve with the experimental plot is excellent, explaining a slight displacement from linearity of the arrangement of the experimental points.

The four curves in Fig. 4a were obtained by mapping the theoretical curve in Fig. 4b on the $[L, m_{elu(P)}]$ plane when $g'_{(P)}$ ($\o = 1$ cm) $= 5.0, 2.5, 1.25$ and 0.45 mM/ml, respectively.

The points in Fig. 4c are experimental plots of $\sigma_{(P)}$ *versus* L for the four $g'_{(P)}$ ($\o = 1$ cm) values in Fig. 4a where the same experimental data as used in both Fig. 4a and b were applied. The curves in Fig. 4c are theoretical, calculated by using eqn. 7 with reference to eqns. 12', 13', 14' and 15'; for the values of the parameters involved in eqn. 7, those which are shown in Table I were applied in order to obtain the best fits with the experiment.

The curve in Fig. 4d is theoretical, representing B' for chicken lysozyme as a function of $m_{(P)}$ or $m_{(K^+)}$. This was calculated by using eqn. 5 in which the values of the parameters that are shown in Table I were applied. The points in Fig. 4d correspond to the experimental points in Fig. 4a or b. Hence the theoretical curve in Fig. 4b performs a parallel transition in the abscissa direction when q or $q_{app(P)}$ varies in eqn. 6 (*cf.*, Appendix I). Therefore, the value of the parameter q which superimposes the curve on each experimental point can be estimated. By using this q value, and replacing $m_{elu(P)}$ with $m_{(P)}$ (with reference to both eqns. 9' and 10'), B' (eqn. 5) was calculated, and the position of any point in Fig. 4d was determined.

It also is possible to calculate B' values from R_F values that are obtained from isocratic chromatography carried out by using buffers with different constant molarities $m_{(P)}$ or $m_{(K^+)}$ (see the first sub-section). The points in Fig. 4e are experimental plots of B' for chicken lysozyme *versus* $m_{(P)}$ or $m_{(K^+)}$ obtained by using this method. In Fig. 4e, the theoretical curve in Fig. 4d is reproduced.

Figs. 5 and 6 represent both experimental plots and theoretical curves that correspond to those in Fig. 4 for other "basic" proteins: cytochrome c (in reduced state; Fig. 5) and fractions I and II of IgG (Fig. 6) (for IgG, see Appendix II).

Figs. 7–9 are concerned with "acidic" molecules: BSA (Fig. 7), fraction III of IgG (Fig. 8; *cf.*, Appendix II) and ADP (Fig. 9).

Fig. 10 represents mappings onto both $\{m_{(P)}$ [or $m_{(K^+)}$, ln $k'\}$ and $\{\ln m_{(P)}$ [or ln $m_{(K^+)}$], ln $k'\}$ planes of both the experimental points and the theoretical curves (calculated by using eqn. 8) for all the samples listed in Table I.

In Table I, the analytical results of all the experiments are summarized. Figs. 11 and 12 represent plots of x' *versus* molecular mass for "basic" and "acidic" substances, respectively, that are shown in Table I.
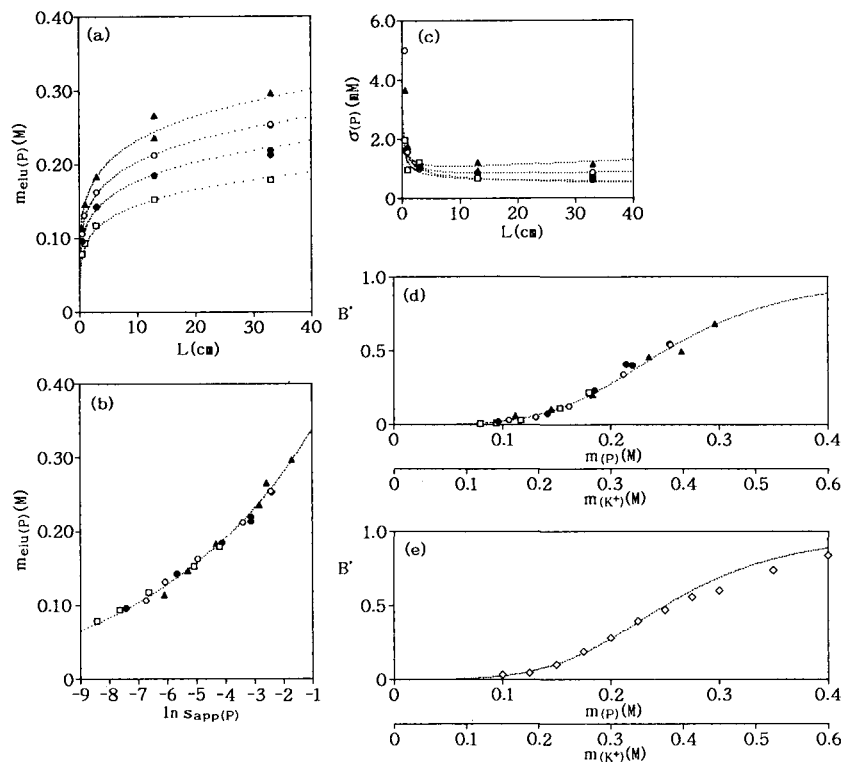
Fig. 5. Analysis of HPLC for cytochrome c in reduced state. The experiment was carried out by using the sample in which both molecules in reduced and oxidized states are involved. Points in (a)–(d): experimental plots of (a) $m_{elu(P)}$ versus L, (b) $m_{elu(P)}$ versus ln $s_{app(P)}$, (c) $\sigma_{(P)}$ versus L and (d) B' versus $m_{(P)}$ or $m_{(K^+)}$ for four different $g'_{(P)}$ ($\phi = 1$ cm) values: (▲) 5.0, (○) 2.5, (●) 1.25 and (□) 0.45 mM/ml; the corresponding total sample loads are 32–60, 40–120, 50–60 and 100–300 µg. Other experimental conditions: $m_{in(P)} = 1$ mM; flow-rate, 0.46–0.51 ml/min; P, 0.3–5.2 MPa; T, 21.0–29.7°C. Curves in (a)–(d): theoretical curves calculated by using (a) eqn. 6, (b) eqn. 6, (c) eqn. 7 and (d) eqn. 5; for details of the calculation method, see the legend for Fig. 4a–d. Points in (e): experimental plots of B' versus $m_{(P)}$ or $m_{(K^+)}$, where B' values were estimated from isocratic chromatography carried out under the following experimental conditions: flow-rate, 0.49–0.50 ml/min; P, 1.7–5.4 MPa; T, 24.2–26.5°C. Curve in (e): theoretical curve identical with that shown in (d).

·DISCUSSION

General discussion

Both Figs. 11 and 12 show a tendency for the number, x', of crystal sites (P or C) that are covered by an adsorbed molecule to increase with increase in molecular mass. The increase occurs slowly, however, and the correlation between molecular mass and x' is weak (Figs. 11 and 12). The weak correlation is consistent with the deduction that the stereochemical structure of the local molecular surface (which is highly characteristic of a molecule, and is intimately related to the x' value) is discerned by the regular crystal surface structure of HA [see Introduction; cf., Fig. 2 here and Fig. 7 in Part III[21]].

The slow increase in x' with increase in molecular mass (see above) shows that
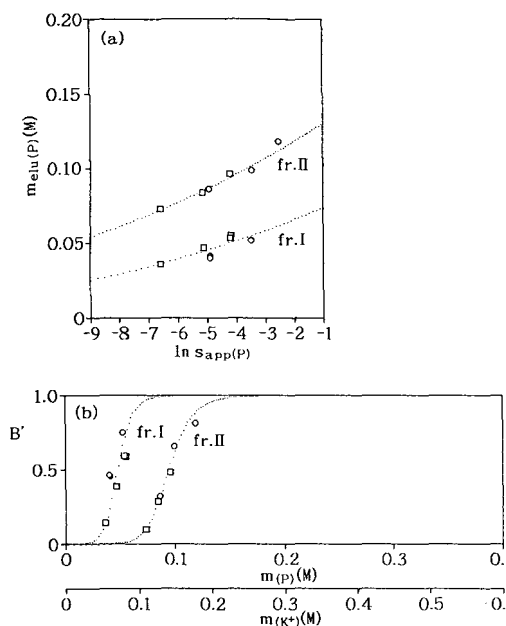
Fig. 6. Analysis of HPLC for IgG fractions I and II. Points in (a) and (b): experimental plots of (a) $m_{elu(P)}$ versus $\ln s_{app(P)}$ and (b) B' versus $m_{(P)}$ or $m_{(K^+)}$ for two different $g'_{(P)}$ ($\varnothing = 1$ cm) values: ($\bigcirc$) 2.5 and ($\square$) 0.45 mM/ml; the corresponding sample loads are 0.053–0.087 and 0.115–0.215 in units of absorbance (at 230 nm) × ml for any fraction. Other experimental conditions: $m_{in(P)} = 1$ mM; flow-rate, 0.49–0.50 ml/min; P, 0.9–4.9 MPa; T, 20.0–25.0°C. Curves in (a) and (b): theoretical curves calculated by using (a) eqn. 6 and (b) eqn. 5; for details of the calculation method, see the legend for Fig. 4a–d.

the local molecular surface that effectively keeps in contact with the crystal surface of HA does not generally increase much with increase in molecular mass. Fig. 13 depicts the approximate molecular dimensions and shapes of both lysozyme and IgG; the arrangement of P sites on the c surface of HA is also shown on the same plane. It can be seen that the molecular shape of IgG is much more complicated than that of lysozyme, and that extreme ups and downs occur on the molecular surface of IgG; this would drastically reduce the x' value for IgG. In fact, it can be seen in Table I that the x' value, 11.0 (l.l. = 6.4; u.l. = 20.0), for "basic"IgG with large molecular dimensions does not increase much in comparison with the corresponding value, 5.7 (l.l. = 4.0; u.l. = 8.0), for lysozyme with small molecular dimensions. It is now useful to consider Fig. A6 in Appendix III in ref. 44 in which are presented photographs of space-filling models of poly-L-lysine and two sodium ions that are adsorbed on the c surface of HA. A visual image of the adsorption configuration of a protein molecule on the c surface of HA can be deduced from the photographs.

It can be seen in Table I that the x' value for "acidic" IgG, 18.0 (l.l. = 14.0; u.l. = 27.0) is larger than the corresponding value for "basic" IgG. This is compatible with the deduction (mentioned in the Introduction in PartIII[21]) that two C sites are present per unit cell on the a surface of HA whereas only a single P site is present per unit cell on the c surface.

It can also be seen in Table I that the x' values for ADP, ATP and adenosine
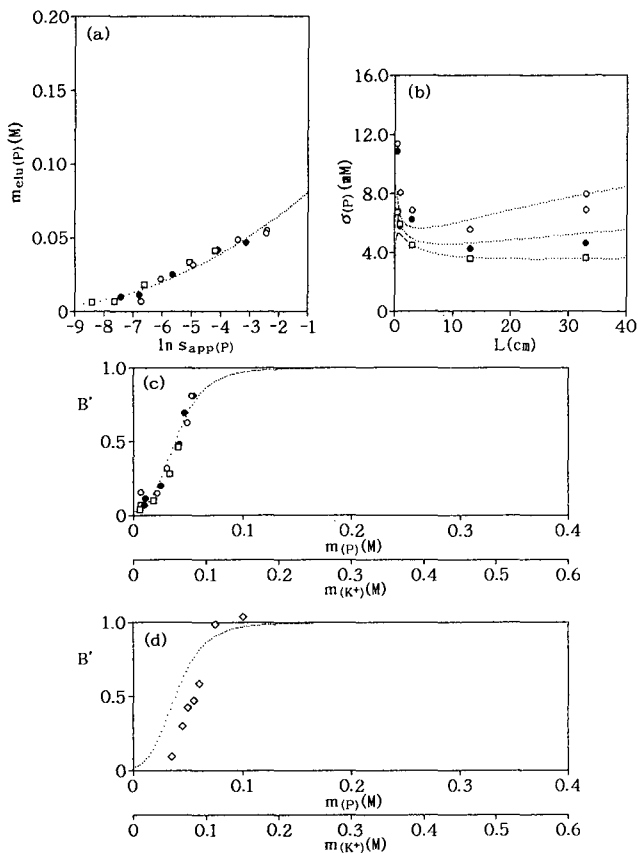
Fig. 7. Analysis of HPLC for BSA. Points in (a)–(c): experimental plots of (a) $m_{elu(P)}$ *versus* ln $s_{app(P)}$, (b) $\sigma_{(P)}$ *versus* L and (c) B' *versus* $m_{(P)}$ or $m_{(K^+)}$ for three different $g'_{(P)}$ ($\emptyset = 1$ cm) values: ($\bigcirc$) 2.5, ($\bullet$) 1.25 and ($\square$) 0.45 mM/ml; the corresponding sample loads are 120–480, 180–240 and 300–400 μg. Other experimental conditions: $m_{in(P)} = 1$ mM; flow-rate, 0.46–0.51 ml/min; P, 0.3–5.3 MPa; T, 21.5–27.2°C. Curves in (a)–(c): theoretical curves calculated by using (a) eqn. 6, (b) eqn. 7 and (c) eqn. 5; for details of the calculation method, see the legend for Fig. 4a–d, where the parameters m, μ, etc., have been replaced with $m_{(P)}$, $m_{elu(P)}$, etc., by using eqns. 9–15, and not by using eqns. 9'–15'. Points in (d): experimental plots of B' *versus* $m_{(P)}$ or $m_{(K^+)}$, where B' values were estimated from isocratic chromatography carried out under the following experimental conditions: flow-rate, 0.49–0.50 ml/min; P, 1.6–3.9 MPa; T, 23.2–26.4°C. Curve in (d): theoretical curve identical with that shown in (c).

tetraphosphate are almost equal to one another, despite the expectation that x' should increase with increase in the number of phosphate groups that are involved in the polyphosphate chain (*cf.*, ref. 45). The constant x' value perhaps is associated with the degradation of the molecule occurring on the crystal surface of HA (*cf.*, refs. 1 and 45).

It is of interest that the standard deviation, $\sigma_{(P)}$, of the chromatographic peak for proteins in general decreases rapidly with increase in the total length, L, of the column, but that $\sigma_{(P)}$ increases slowly after the first rapid decrease (Figs. 4c, 5c and 7b). With ADP with a very small x' value (see Table I), however, the first rapid decrease in $\sigma_{(P)}$ does not occur (Fig. 9c). All these results have been obtained not only
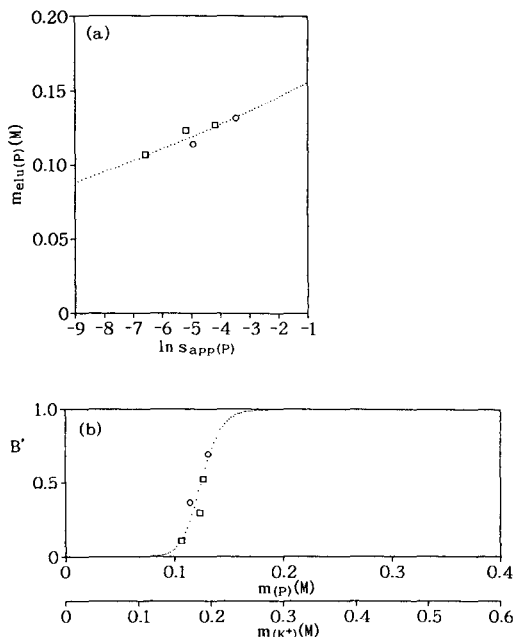
Fig. 8. Analysis of HPLC for IgG fraction III. Points in (a) and (b): experimental plots of (a) $m_{elu(P)}$ *versus* ln $s_{app(P)}$ and (b) B' *versus* $m_{(P)}$ or $m_{(K^+)}$ for two different $g'_{(P)}$ (ø = 1 cm) values: (○) 2.5 and (□) 0.45 mM/ml; the corresponding sample loads are 0.047 and 0.062 in units of absorbance (at 230 nm) × ml. Other experimental conditions: $m_{in(P)}$ = 1 mM; flow-rate, 0.49–0.50 ml/min; P, 0.9–4.5 MPa; T, 21.6–24.5°C. Curves in (a) and (b): theoretical curves calculated by using (a) eqn. 6 and (b) eqn. 5; for details of the calculation method, see the legends for Fig. 4a–d and Fig. 7.

experimentally but also theoretically. Theoretically it can further be predicted that, with molecules with extremely large x' values, the first rapid decrease in $\sigma_{(P)}$ does not occur (*cf.*, Fig. 2 in ref. 46).

Finally, it appears that the experimental plots of B' *versus* $m_{(P)}$ or $m_{(K^+)}$ obtained on the basis of isocratic chromatography tend to deviate slightly from the corresponding plots obtained on the basis of gradient chromatography (*cf.*, Fig. 4d and e, Fig. 5d and e, Fig. 7c and d, and Fig. 9d and e, respectively). It can be assumed that this arises at least partially from the fact that the effective gradient participating in the competition mechanism in chromatography is not exactly linear even though a linear molarity gradient is applied. It is activity, and not molarity, that should be exactly linear with authentically linear gradient chromatography; on proposing the activity concept, account is taken of the interaction effect of competing ions occurring not only in the bulk solution but also on the crystal surface of HA (*cf.*, ref. 27).

Capacity factor, k', with the competition model

Provided that both the sample molecule and the competing ion are adsorbed weakly onto adsorbing sites while performing the competition, then the relationship $\varphi m \ll 1$ is fulfilled (*cf.*, explanation of φ in eqn. 5), and the approximate relationship

$$\varphi m + 1 \approx e^{\varphi m} \tag{16}$$
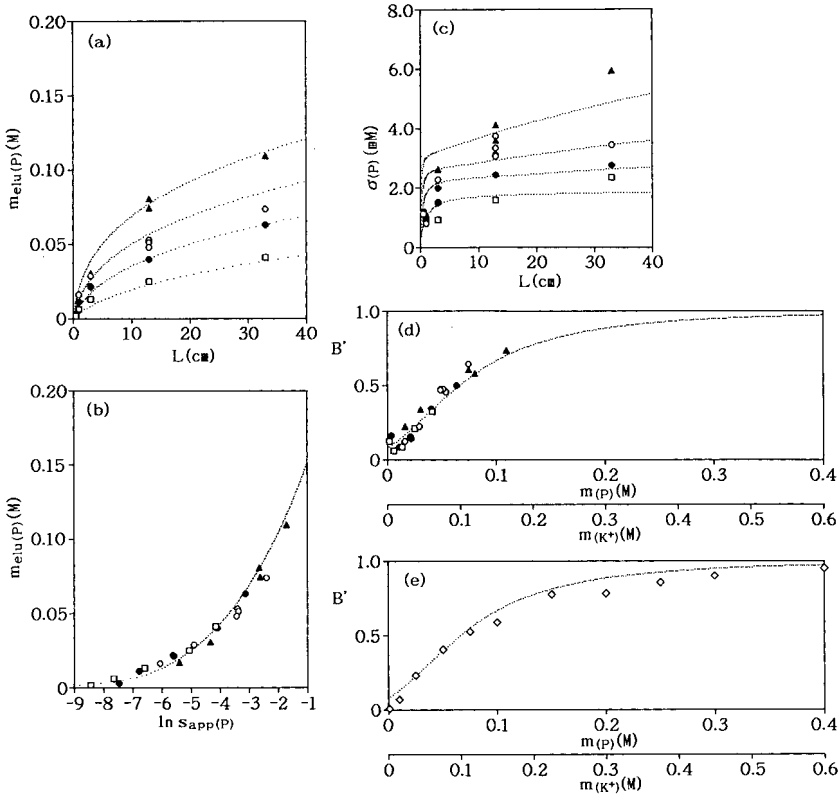
Fig. 9. Analysis of HPLC for ADP. Points in (a)–(d): experimental plots of (a) $m_{elu(P)}$ *versus* L, (b) $m_{elu(P)}$ *versus* $\ln s_{app(P)}$, (c) $\sigma_{(P)}$ *versus* L and (d) B' *versus* $m_{(P)}$ or $m_{(K^+)}$ for four different $g'_{(P)}$ ($\varnothing = 1$ cm) values: (▲) 5.0, (○) 2.5, (●) 1.25 and (□) 0.45 mM/ml; the corresponding sample loads are 0.9–4.0, ≤ 6, 1.7–10 and 5.5–15 μg. Other experimental conditions: $m_{in(P)} = 1$ mM, flow-rate, 0.45–.051 ml/min; P, 0.3–5.2 MPa; T, 20.5–27.0°C. Curves in (a)–(d): theoretical curves calculated by using (a) eqn. 6, (b) eqn. 6, (c) eqn. 7 and (d) eqn. 5; for details of the calculation method, see the legends of Fig. 4a–d and Fig. 7. Points in (e): experimental plots of B' *versus* $m_{(P)}$ or $m_{(K^+)}$, where B' values were estimated from isocratic chromatography carried out under the following experimental conditions: flow-rate, 0.49–0.51 ml/min; P, 1.5–3.9 MPa; T, 25.0–29.5°C. Curve in (e): theoretical curve identical with that shown in (d).

holds. In this instance, eqn. 8 can be rewritten as

$$\ln k'(m) \approx -x'\varphi m + \ln q \tag{17}$$

indicating that $\ln k'(m)$ decreases linearly with increase in m.

In contrast, provided that both the sample molecule and the competing ion are
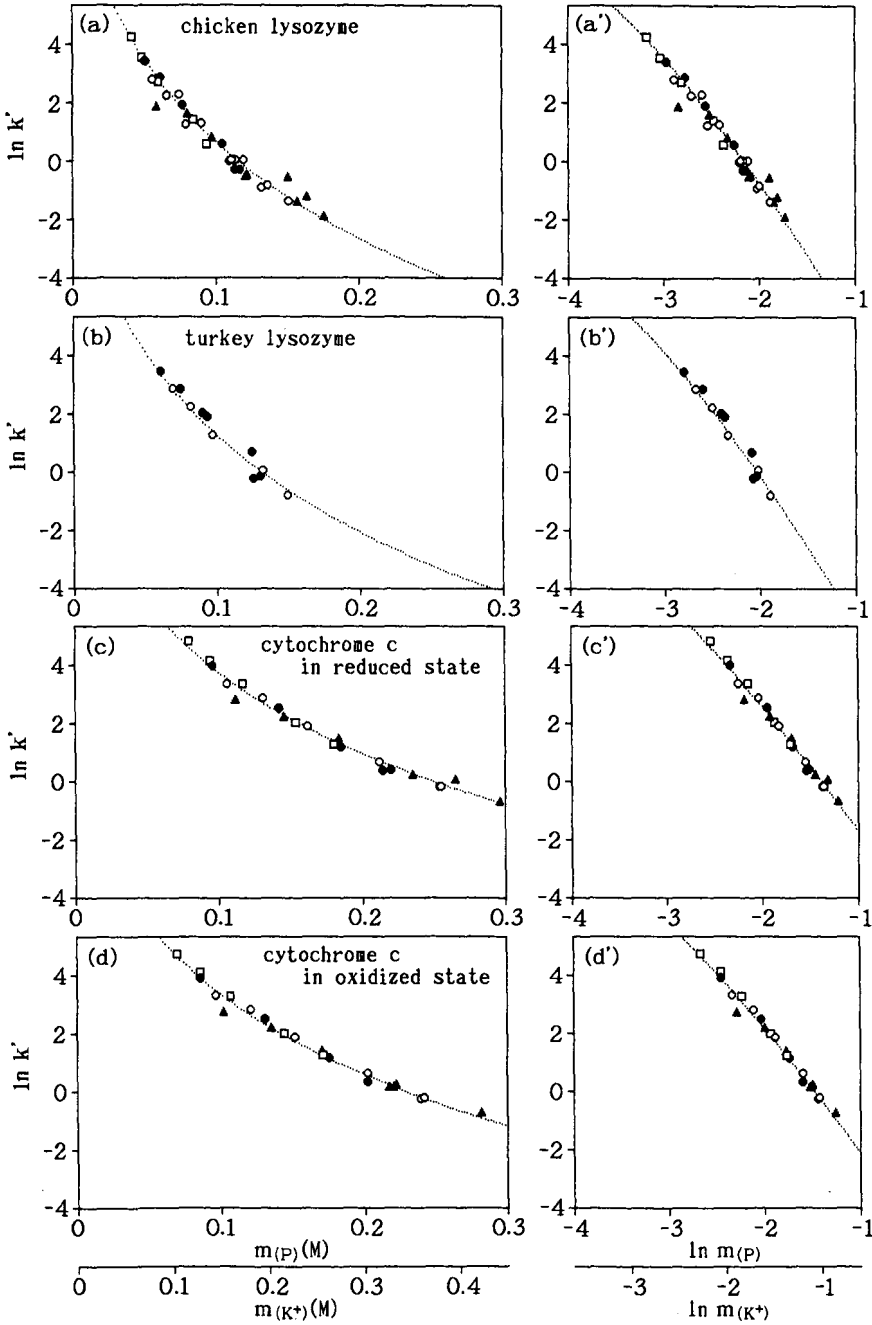
Fig. 10.
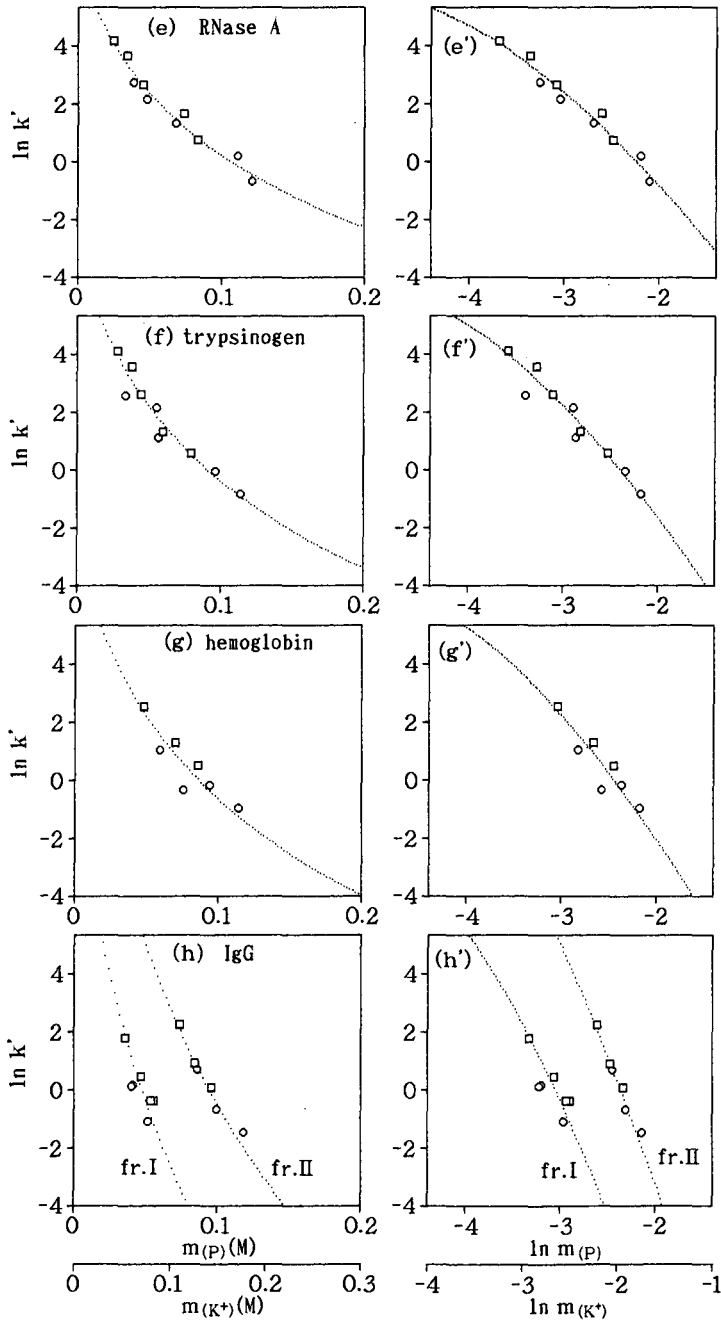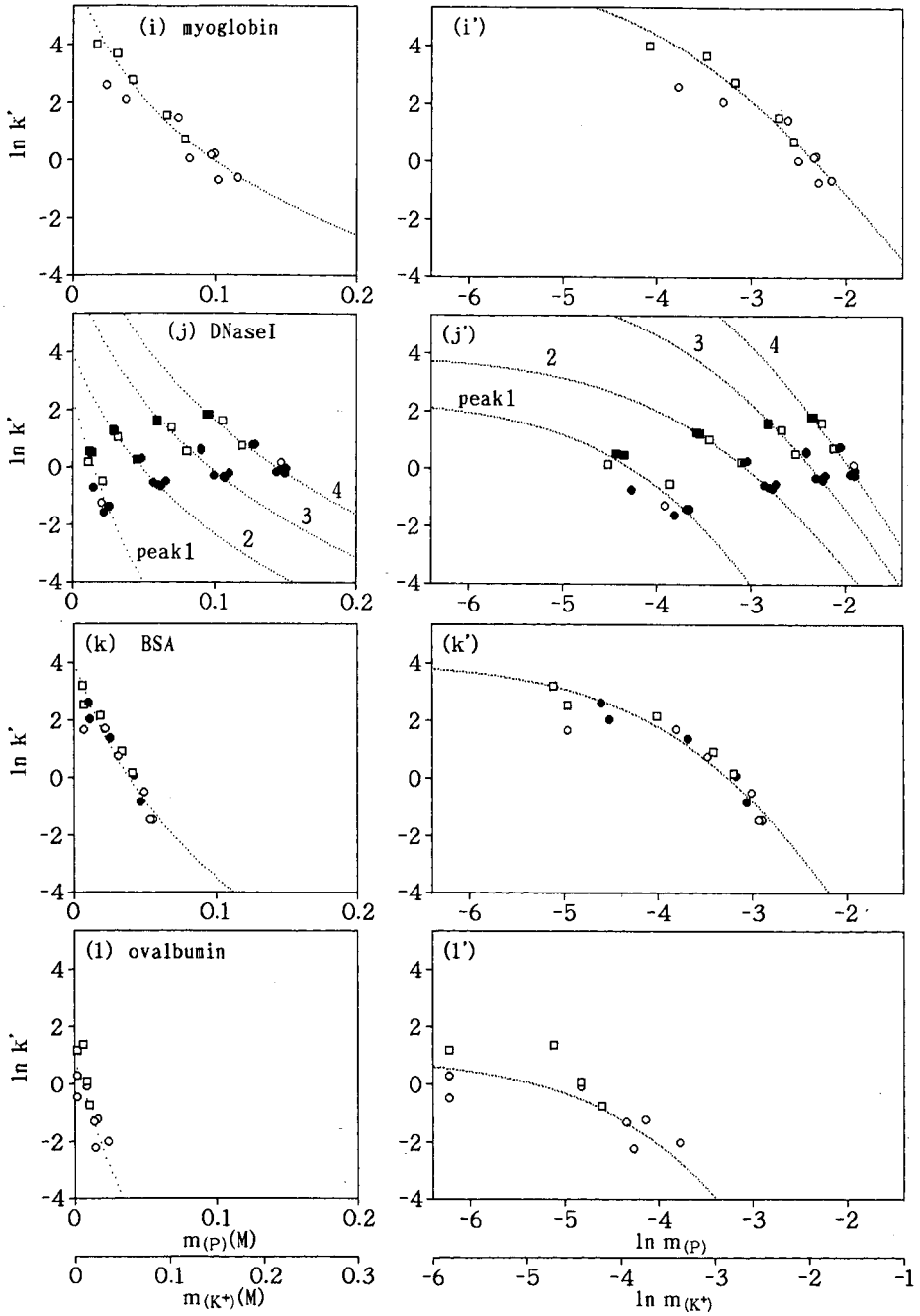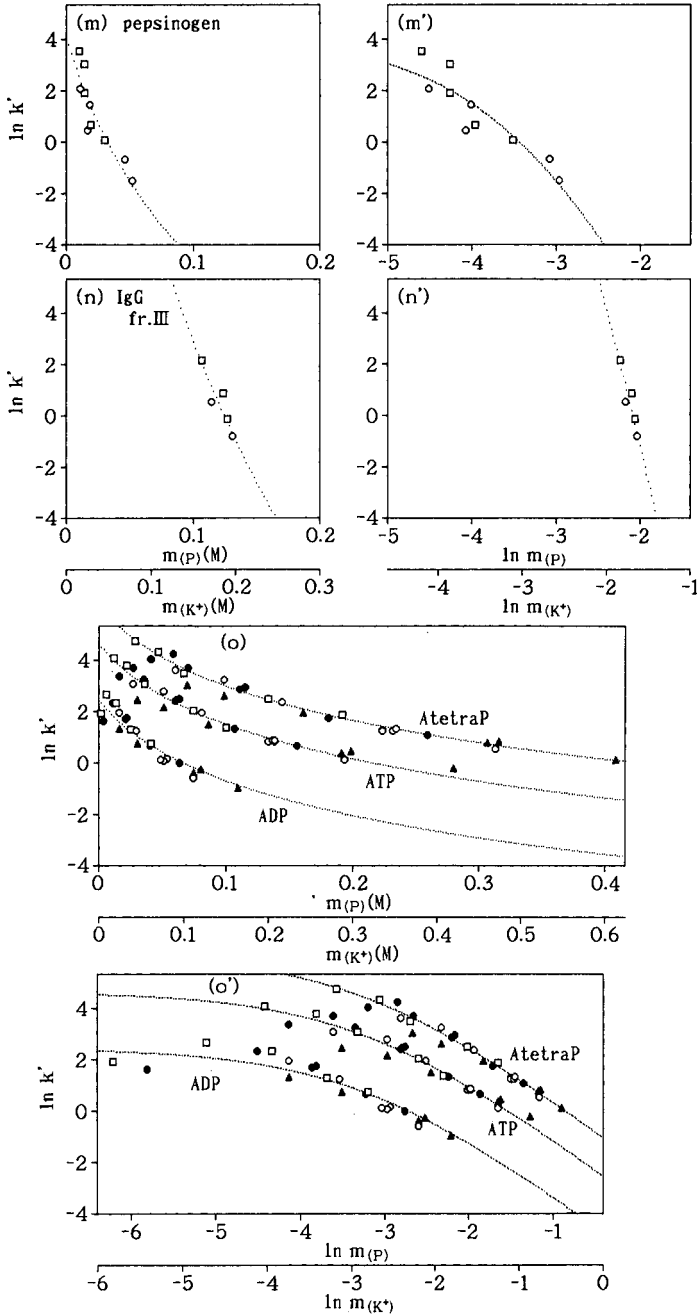
Fig. 10.

Fig. 10.

Fig. 10. Points: experimental plots of ln k' *versus* $m_{(P)}$ or $m_{(K^+)}$ (a–o) and ln k' *versus* ln $m_{(P)}$ or ln $m_{(K^+)}$ (a'–o'). All the experiments were carried out between 20.0 and 29.7°C, and the symbols ▲, ○, ●, □ and ■ correspond to the experiments performed by using $g'_{(P)}$ (∅ = 1 cm) values of 5.0, 2.5, 1.25, 0.45 and 0.15 mM/ml, respectively. Curves: theoretical curves calculated by using eqn. 8.
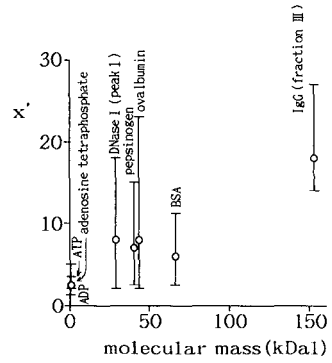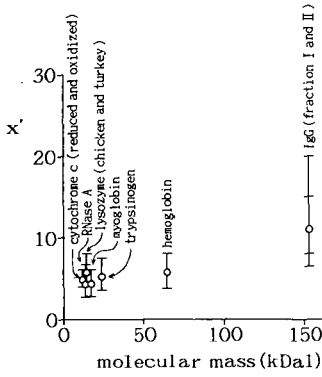
Fig. 11. Plots of x' versus molecular mass for "basic" proteins shown in Table I. kDal = kilodalton.

Fig. 12. As Fig. 11 for "acidic" substances shown in Table I.

adsorbed strongly onto adsorbing sites, then the relationship $\varphi m \gg 1$ is fulfilled (cf., explanation of φ in eqn. 5), and the approximate relationship

$$\varphi m + 1 \approx \varphi m \tag{18}$$

holds. In this instance, eqn. 8 can be rewritten as

$$\ln k'(m) \approx -x'\ln m + \ln q - x'\ln \varphi$$
$$= -x'\ln m + \ln \kappa \tag{19}$$

(cf., eqn. A2 in Appendix I), indicating that $\ln k'(m)$ decreases linearly with increase in $\ln m$.
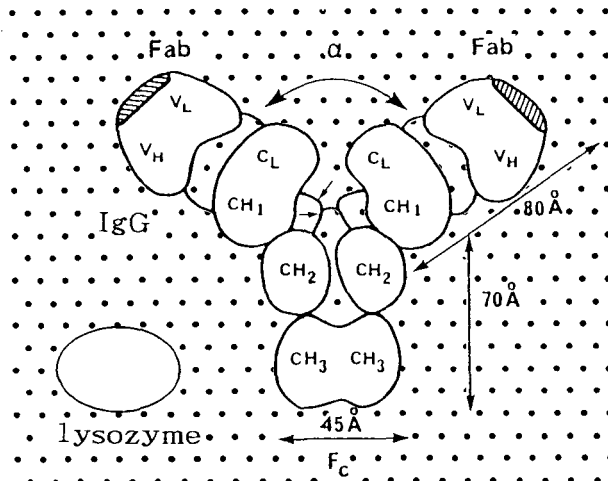
Fig. 13. Approximate molecular dimensions and shapes of lysozyme and IgG, and the arrangement of P sites on the c surface of HA; for the arrangement of P sites, see Part III[21]. (Reproduced with modifications from refs. 35 and 43.)

It can be seen in Fig. 10 that the arrangement of the experimental points on the $\{m_{(P)}$ [or $m_{(K^+)}$], $\ln k'\}$ and the $\{\ln m_{(P)}$ [or $\ln m_{(K^+)}$], $\ln k'\}$ plane, in general, deviates slightly from linearity, being concave and convex, respectively. This indicates that the adsorption of competing ions (and also that of sample molecules) onto crystal sites of HA is not extremely weak or extremely strong; it is eqn. 8, rather than eqn. 17 or 19, that coincides best with the experiment.

It should be recalled that the best theoretical curve on the $[\ln s_{app(P)}, m_{elu(P)}]$ plane was used as calibration graph for the determination of the arrangement of the experimental points on the $\{m_{(P)}$ [or $m_{(K^+)}$], $B'\}$ plane (last sub-section of Experimental and Results). This means that the arrangement of the experimental points on both $\{m_{(P)}$ [or $m_{(K^+)}$], $\ln k'\}$ and $\{\ln m_{(P)}$ [or $\ln m_{(K^+)}$], $\ln k'\}$ planes depends on the theoretical calibration graph that has been chosen on the $[\ln s_{app(P)}, m_{elu(P)}]$ plane. It has been confirmed, however, that the dependence occurs only very slightly, and that the arrangement of the experimental points on the $\{m_{(P)}$ [or $m_{(K^+)}$], $B'\}$, $\{m_{(P)}$ [or $m_{(K^+)}$], $\ln k'\}$ or $\{\ln m_{(P)}$ [or $\ln m_{(K^+)}$], $\ln k'\}$ plane is almost constant, unless the theoretical calibration graph on the $[\ln s_{app(P)}, m_{elu(P)}]$ plane deviates substantially from the experimental plot.

APPENDIX I

Evaluation of the lower and upper limit, $x'_{1.1.}$ and $x'_{u.1.}$, of the parameter x' (cf., Table I)

The theoretical curve (eqn. 6) mapped on the $(\ln s, \mu)$ or the $[\ln s_{app(P)}, m_{elu(P)}]$ plane has the following properties when $\ln s$ or $\ln s_{app(P)}$ varies within the range that is usually applied:

(a) Except when $x' = \infty$ [cf., (c)], the curve is slightly concave with positive tangential slopes.

(b) The curve performs a parallel transition towards the left when the parameter q or $q_{app(P)}$ increases.

(c) The mean tangential slope, $\bar{G}$, of the curve decreases when the parameter x' increases. When x' approaches infinity, $\bar{G}$ tends to zero, and the curve reduces to a straight line that is parallel to the $\ln s$ or the $\ln s_{app(P)}$ axis.

(d) $\bar{G}$ also decreases when the parameter φ increases. When φ approaches infinity, $\bar{G}$ tends to a finite limiting value, $\overline{G^0}_{x'}$, which depends upon x' [cf., (g)].

(e) It is possible to keep $\bar{G}$ constant either by increasing φ and decreasing x' at the same time, or by decreasing φ and increasing x' at the same time [cf., (c) and (d)]. If q or $q_{app(P)}$ is increased appropriately while performing the former operation, or if q or $q_{app(P)}$ is decreased appropriately while performing the latter operation, then the position of the curve can be kept constant [cf., (b)].

(f) When φ increases and x' decreases under the condition of a constant $\bar{G}$ [cf., (e)], then the curvature of the curve increases. Especially if φ approaches infinity and x' tends to a finite value, x'_0, while holding the relationship of $q^{1/x'} = O(\varphi)$, then both the curvature (*i.e.*, the shape) and the position of the curve are stabilized. This can be understood from the fact that, at this limit, eqn. 6 converges to

$$\mu(s) = [(x'_0 + 1) \kappa s + m_{in}^{x'_0 + 1}]^{1/(x'_0 + 1)} \tag{A1}$$

in which

$$\kappa = q\varphi^{-x'_0} \tag{A2}$$

represents a constant with a finite value.

(g) $\overline{G^0}_{x'}$ [cf., (d)] increases when x' decreases. (The increase in $\overline{G^0}_{x'}$ occurs mainly due to the increase in tangential slopes of the right-hand part of the curve.)

The lower and the upper limit of the possible x' values (written as $x'_{1.1.}$ and $x'_{u.1.}$, respectively) can be estimated on the basis of the experimental plot of $m_{elu(P)}$ versus ln $s_{app(P)}$. Thus, both $x'_{1.1.}$ and $x'_{u.1.}$ are involved in the combinations of (x', φ) that equalize the theoretical $\overline{G}$ with the experimental $\overline{G}$ while adjusting $q_{app(P)}$ or ln $q_{app(P)}$ in order for the theoretical curve to be superimposed on the experimental plot at least partially [cf.,(e)]. $x'_{1.1.}$ and $x'_{u.1.}$ are represented by the maximum and the minimum x' that give the theoretical curve a curvature stronger and weaker than that for the experimental plot, respectively [cf., (f)].

It often happens, however, that, when $x' < x'_{u.1.}$, the curvature of the theoretical curve increases only slightly with both the decrease in x' and the increase in φ. Further, the shape and the position of the curve are both stabilized rapidly when φ approaches infinity and x' tends to $x'_0 + 0$ while holding the relationship of $q^{1/x'} = O(\varphi)$ [cf., (f)]. In this instance, the curvature of the theoretical curve obtained when $x' = x'_{u.1.}$ is almost equal to that obtained when $x' = x'_0$, and it can be considered that $x'_0 = x'_{1.1.}$. [If x' decreases from $x'_{1.1.}$, then $\overline{G^0}_{x'}$ increases, i.e., $\overline{G^0}_{x'}$ deviates from the experimental $\overline{G}$; cf., (g).]

The points in Fig. 14 are experimental plots of $m_{elu(P)}$ versus ln $s_{app(P)}$ for chicken lysozyme (reproduced from Fig. 4b). Curves 1–4 are theoretical, calculated by using eqn. 6 or A1 where it has been assumed that $[x', \varphi, \ln q_{app(P)}] = (14.0, 4.0 \, M^{-1}, 7.1)$; $(8.0, 10.0 \, M^{-1}, 7.9)$; $(5.7, 25.0 \, M^{-1}, 9.5)$; and $(4.0, \infty \, M^{-1}, \infty)$, with ln $\kappa_{app(P)} \equiv \ln \kappa + \ln q_{app(P)} - \ln q (= \ln \kappa + \ln 0.970$; see eqn. 15') $= -7.0$, respectively (for κ, see eqn. A2). On the basis of the assumptions, both the mean tangential slopes $\overline{G}$ (or $\overline{G^0}_{x'}$) and the positions of the theoretical curves 1–4 are almost equal to those for the experimental plot. Further, if $x' \leqslant 5.7$, the curvature of the theoretical curve is similar to that for the experimental plot (curves 3 and 4). If $x' = 14$, however, the curvature of the theoretical curve is evidently less strong than that for the experimental plot (curve 1), from which it
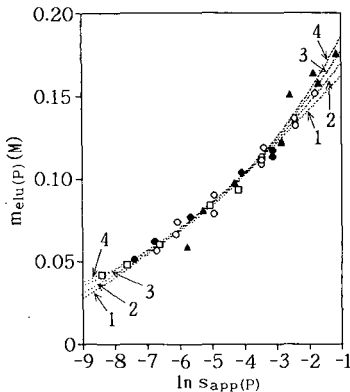
Fig. 14. Points: experimental plots of $m_{elu(P)}$ versus ln $s_{app(P)}$ for chicken lysozyme, reproduced from Fig. 4b. Curves 1–4: theoretical curves calculated by using eqn. 6 or A1 where it was assumed that $[x', \varphi, \ln q_{app(P)}]$ = $(14.0, 4.0 \, M^{-1}, 7.1)$; $(8.0, 10.0 \, M^{-1}, 7.9)$; $(5.7, 25.0 \, M^{-1}, 9.5)$; and $(4.0, \infty \, M^{-1}, \infty)$, respectively, with ln $\kappa_{app(P)} = -7.0$. For details, see text.
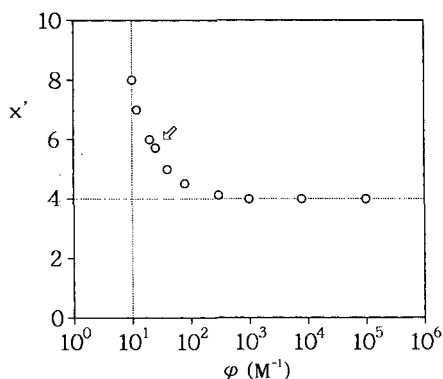
Fig. 15. Plots of x' versus φ for chicken lysozyme, where both x' and φ values were obtained from the optimum combinations of x', φ and ln $q_{\text{app}(P)}$. The vertical and horizontal dotted lines represent the lower limit value of φ and the x'_0 value, respectively. The point indicated by the arrow corresponds to the value of φ, 25 M^{-1}.

can be calculated that $x'_{\text{u.l.}} \approx 8.0$ (curve 2). $x'_{\text{l.l.}}$ can be represented by x'_0, and it can be estimated that $x'_{\text{l.l.}} = 4.0$ (curve 4).

The points in Fig. 15 are plots of x' versus φ for chicken lysozyme; both x' and φ values have been taken from the best combinations of x', φ and ln $q_{\text{app}(P)}$, three of which correspond to curves 2–4 in Fig. 14. In Fig. 15, the vertical and horizontal dotted lines represent the lower limit value of φ and the x'_0 value, respectively; the point indicated by the arrow corresponds to the value of φ, 25 M^{-1}. It can be seen in Fig. 15 that the x' value corresponding to $\varphi = 25$ M^{-1} represents a reasonable mean x' value.

For substances other than chicken lysozyme, plots similar to that shown in Fig. 15 can also be obtained. In some instances, however, it can clearly be shown that $x'_{\text{l.l.}} > x'_0$. A value of φ of 25 M^{-1} generates reasonable mean x' values for all substances.

APPENDIX II

Fractions I, II and III of IgG

Fig. 16 illustrates a double gradient chromatogram of IgG. This was obtained by previously applying a KCl gradient after an isocratic elution with 10 mM KP; 10 mM
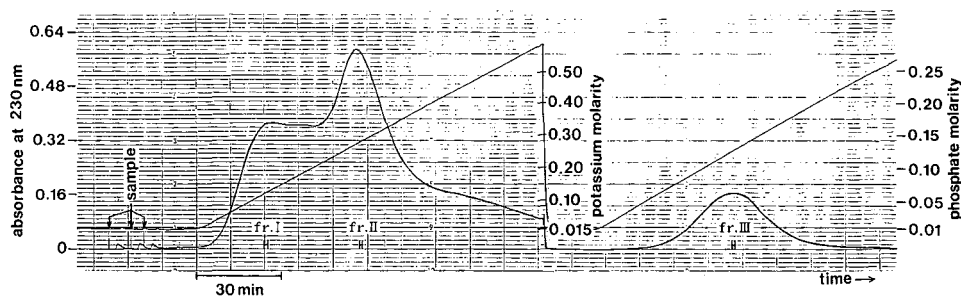
Fig. 16. Double gradient chromatogram for IgG (27 mg) as obtained on the KB column packed with HA type S₁; column 5 cm × 2 cm I.D. Experimental conditions: $m_{\text{in}(P)} = 10$ mM for both KCl and KP gradients; $g'_{\text{(KCl)}}$ (ø = 1 cm) = 3.75 mM/ml; $g'_{\text{(P;KP)}}$ (ø = 1 cm) = 2.5 mM/ml; flow-rate, 5.04 ml/min; P, 3.2–3.5 MPa; T, 24.0°C; recovery = 118%; 10 mM KP is always present in the KCl gradient.

KP was present while the KCl gradient continued (left-hand side of Fig. 16). The carrier solvent was again replaced with pure 10 mM KP, and the KP gradient was finally applied (right-hand side of Fig. 16). It can be seen that IgG is eluted partially in the first KCl gradient and partially in the second KP gradient. It can be considered (see Introduction) that IgG components that are eluted in the first and the second gradients behave as "basic" and "acidic" molecules, respectively, on the HA column. Therefore, of fractions I, II and III (see Fig. 16) that are used for the experiment (see Table I), both fractons I and II are assemblies of "basic" molecules; fraction III is an assembly of "acidic" molecules.

APPENDIX III

Relationship with the isoelectric point

In the Introduction, the correlation between the isoelectric point (pI) and the μ [or $m_{elu(P)}$] value for 26 proteins is argued (see Fig. 2). The same argument will be made in Part III[21] for the proteins listed in Table I (see Fig. 7 in ref. 21).

Eqn. 5 shows that the molarity, $\dot{m}$, of competing ions at which $B' = 1/2$ is given

by

$$\dot{m} = (q^{1/x'} - 1)/\varphi \tag{A3}$$

and, in general, it is more reasonable to consider the correlation between pI and $\dot{m}$ [or $\dot{m}_{(P)}$] than the correlation between pI and μ [or $m_{elu(P)}$] [for $\dot{m}_{(P)}$, see below].

The points in Fig. 17 are plots of $\dot{m}_{(P)}$ *versus* $m_{elu(P)}$ for the substances listed in
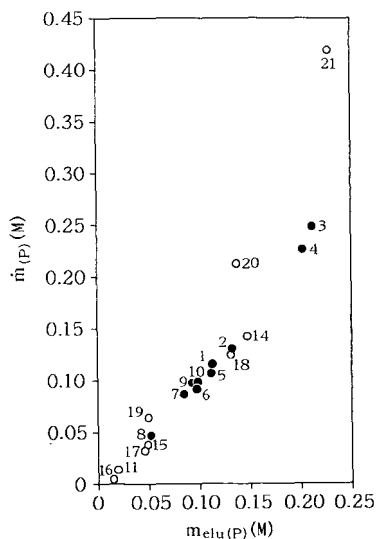
Fig. 17. Plots of $\dot{m}_{(P)}$ *versus* $m_{elu(P)}$ for the substances listed in Table I, where $m_{elu(P)}$ represents the elution molarity obtained when $L = 13$ cm and $g'_{(P)}$ (ø $= 1$ cm) $= 2.5$ mM/ml. The numbers against the experimental points are the numbers of the substances given in the first column in Table I; $\bigcirc$ and $\bullet$ correspond to "acidic" and "basic" molecules, respectively.

Table I, where $\dot{m}_{(P)}$ is related to $\dot{m}$ by the relationships $\dot{m} = \dot{m}_{(P)}$ and $\dot{m} = 1.5\dot{m}_{(P)}$ for "acidic" and "basic" molecules respectively (*cf.*, eqns. 9 and 9′); $m_{elu(P)}$ here represents othe elution molarity obtained when $L = 13$ cm and $g'_{(P)}$ ($\varnothing = 1$ cm) $= 2.5$ mM/ml, *i.e.*, when $s_{app(P)} = 32.5$ mM/cm². It can be seen in Fig. 17 that $\dot{m}_{(P)}$ is highly correlated with $m_{elu(P)}$ with respect to proteins. The correlation between pI and $\dot{m}$ [or $\dot{m}_{(P)}$] with proteins can therefore be replaced by the correlation between pI and μ [or $m_{elu(P)}$] for practical purposes.

REFERENCES

1 T. Kawasaki, *J. Chromatogr.*, submitted for publication.
2 A. Tiselius, S. Hjertén and Ö. Levin, *Arch. Biochem. Biophys.*, 65 (1956) 132.
3 G. Bernardi, *Methods Enzymol.*, 21 (1971) 95.
4 G. Bernardi, *Methods Enzymol.*, 22 (1971) 325.
5 G. Bernardi, *Methods Enzymol.*, 27 (1973) 471.
6 B. Moss and E. N. Rosenblum, *J. Biol. Chem.*, 247 (1972) 5194.
7 H. G. Martinson, *Biochemistry*, 12 (1973) 139.
8 H. G. Martinson and E. B. Wagenaar, *Biochemistry*, 13 (1974) 1641.
9 M. Spencer, *J. Chromatogr.*, 166 (1978) 423.
10 M. Spencer, *J. Chromatogr.*, 166 (1978) 435.
11 M. J. Gorbunoff, *Anal. Biochem.*, 136 (1984) 425.
12 M. J. Gorbunoff, *Anal. Biochem.*, 136 (1984) 433.
13 M. J. Gorbunoff and S. N. Timasheff, *Anal. Biochem.*, 136 (1984) 440.
14 T. Kawasaki, S. Takahashi and K. Ikeda, *Eur. J. Biochem.*, 152 (1985) 361.
15 T. Kawasaki, K. Ikeda, S. Takahashi and Y. Kuboki, *Eur. J. Biochem.*, 155 (1986) 249.
16 T. Kawasaki, W. Kobayashi, K. Ikeda, S. Takahashi and H. Monma, *Eur. J. Biochem.*, 157 (1986) 291.
17 T. Kawasaki, M. Niikura, S. Takahashi and W. Kobayashi, *Biochem. Int.*, 13 (1986) 969.
18 T. Kadoya, T. Isobe, M. Ebihara, T. Ogawa, M. Sumita, H. Kuwahara, A. Kobayashi, T. Ishikawa and T. Okuyama, *J. Liq. Chromatogr.*, 9 (1986) 3543.
19 Y. Kato, K. Nakamura and T. Hashimoto, *J. Chromatogr.*, 398 (1987) 340.
20 T. Kawasaki and W. Kobayashi, *Biochem. Int.*, 14 (1987) 55.
21 T. Kawasaki, M. Niikura and Y. Kobayashi, *J. Chromatogr.*, 515 (1990) 125.
22 T. Kawasaki, M. Niikura, S. Takahashi and W. Kobayashi, *Biochem. Int.*, 15 (1987) 1137.
23 T. Sato, T. Okuyama, T. Ogawa and M. Ebihara, *Bunseki Kagaku*, 38 (1989) 34.
24 R. Kasai, H. Yamaguchi and O. Tanaka, *J. Chromatogr.*, 407 (1987) 205.
25 T. Kawasaki, *Sep. Sci. Technol.*, 23 (1988) 601.
26 T. Kawasaki, *Sep. Sci. Technol.*, 23 (1988) 617.
27 T. Kawasaki, *Sep. Sci. Technol.*, 23 (1988) 1105.
28 G. Bernardi, M. G. Giro and C. Gaillard, *Biochim. Biophys. Acta*, 278 (1972) 409.
29 T. Isobe and T. Okuyama, *Kagaku*, Suppl., 102 (1984) 141.
30 T. Kawasaki, *Sep. Sci. Technol.*, 22 (1987) 121.
31 T. Kawasaki, *Sep. Sci. Technol.*, 23 (1988) 451.
32 T. Kawasaki, *Sep. Sci. Technol.*, 23 (1988) 2365.
33 T. Kawasaki, *Sep. Sci. Technol.*, 24 (1989) 1109.
34 T. Kawasaki and M. Niikura, *Sep. Sci. Technol.*, 25 (1990) in press.
35 T. Kawasaki, *J. Chromatogr.*, 93 (1974) 313.
36 T. Kawasaki, *Sep. Sci. Technol.*, 16 (1981) 439.
37 T. Kawasaki and S. Takahashi, *Sep. Sci. Technol.*, 23 (1988) 193.
38 T. Kawasaki, *Sep. Sci. Technol.*, 17 (1982) 407.
39 J. C. Giddings, *Dynamics of Chromatography: Part I, Principles and Theory*, Marcel Dekker, New York, 1965, p. 13.
40 T. Kawasaki, *Biopolymers*, 9 (1970) 277.
41 T. Kawasaki, *J. Chromatogr.*, 93 (1974) 337.

42 T. Kawasaki and G. Bernardi, *Biopolymers*, 9 (1970) 257.
43 R. E. Cathou, in G. W. Litman and R. A. Good (Editors), *Immunoglobulins*, Plenum Press, New York and London, 1978, p. 37.
44 T. Kawasaki, *J. Chromatogr.*, 157 (1978) 7.
45 T. Kawasaki, *J. Chromatogr.*, 151 (1978) 95.
46 T. Kawasaki, *Sep. Sci. Technol.*, 16 (1981) 439.

CHROMSYMP. 1885

Fundamental study of hydroxyapatite high-performance liquid chromatography

III[a]. Direct experimental confirmation of the existence of two types of adsorbing surface on the hydroxyapatite crystal

TSUTOMU KAWASAKI*, MAKOTO NIIKURA and YURIKO KOBAYASHI

Chromatographic Research Laboratory, Koken Bioscience Institute, 3-5-18 Shimo-Ochiai, Shinjuku-Ku, Tokyo 161 (Japan)

ABSTRACT

By using several types of hydroxyapatite (HA) with different external shapes and surface structures, adsorption and the high-performance liquid chromatographic experiments for several proteins were carried out in parallel. Direct confirmation was obtained that two types of adsorbing surface, the **a** (or **b**) and the **c** crystal surface, generally appear on the HA particle. During the chromatographic process on the column, acidic proteins with isoelectric points lower than about 7 (and also nucleic acids including other nucleotides) are mainly adsorbed on the **a** (or **b**) surface, basic proteins with isoelectric points higher than about 7 are mainly adsorbed onto the **c** surface, and these occur independently of the external crystal shape of HA that is used. It is highly probable that the surface of a domain on the HA crystal on which the molecular adsorption takes place is smooth, and that the size of the domain under consideration is larger than the size of the proteins that have been applied, *i.e.*, larger than 100–200 Å, at least with respect to the HAs that have been examined. Multilayers of protein molecules may be formed on the HA surface when the molarity of the phosphate buffer in the mobile phase is much lower than the molarity that is needed for the migration of the molecules on the column.

INTRODUCTION

The hydroxyapatite (HA) crystal usually belongs in the space group $P6_3/m$, and the crystal unit cell is characterized by the primitive vectors **a**, **b** and **c** with $\mathbf{a} \wedge \mathbf{b} = 120°$, $\mathbf{a} \wedge \mathbf{c} = \mathbf{b} \wedge \mathbf{c} = 90°$, $|\mathbf{a}| = |\mathbf{b}| = 9.42$ Å and $|\mathbf{c}| = 6.88$ Å[3,4] (see also ref. 5). In a unit cell of the ideal stoichiometric crystal, ten calcium ions (Ca^{2+}), six phosphate ions (PO_4^{3-}) and two hydroxyl ions (OH^-) are arranged in the manner

---

[a] For Parts I and II, see refs. 1 and 2, respectively.

represented in Fig. 1a. Therefore, the Ca/P molar ratio for the stoichiometric crystal is 1.67.

Fig. 2a–f show scanning electron micrographs of the surface structure of six types of HA particle to be packed in a column for high-performance liquid chromatography (HPLC). The Ca/P molar ratios for the crystals shown in Fig. 2a–f are 1.67, 1.67, 1.62, 1.57, 1.52–1.54 and 1.61–1.64, respectively. Therefore, the chemical compositions of the crystals in Fig. 2a and b are stoichiometric with respect to both calcium and phosphorus; the crystal structures of HA in Fig. 2c–f involve some defects.

The surface structure shown in Fig. 2a is quasi-ideal, and it can be identified that an HA particle is an aggregate of hexagonal rods each representing a crystallite or a micro-monocrystal. It can also be identified that the cross-sectional surface of a rod, hexagonal in shape, is an (001) surface or a c surface which is parallel to the (a, b) plane of the crystal unit cell; the six surfaces, rectangular in shape, occurring around the main axis of the rod are (100) or (010) surfaces, i.e., a or b surfaces. These are parallel to the (b, c) or the (a, c) plane of the crystal unit cell (see Fig. 1a). (The a and the b surfaces are equivalent to each other; hereafter, except in certain instances, we simply use a surface for both a and b surfaces.) Thus, on a polycrystal of the type shown in Fig. 2a, only a and c surfaces appear; the total area of the c surfaces is much smaller than that of the a surfaces.

The HA shown in Fig. 2e is an aggregate of microcrystals with a needle-like shape. From the crystal habit, it is highly probable that the c axis is parallel to the main

Fig. 1.

Fig. 1. (a) HA structure projected on the (**a**, **b**) plane along the **c** axis which is vertical to the plane of the paper. The parallelogram represents a crystal unit cell. The numerical values on the atoms represent z values, *i.e.*, coordinates along the **c** axis; z is equal to zero and unity at the lower and the upper margin of a unit cell, respectively. Calcium ions at $z = 0.00$ and 0.50 are called Ca_I ions, and those at $z = 1/4$ and $z = 3/4$ are called Ca_{II} ions. (Reproduced from ref. 3.) (b) Perspective view of Ca_{II} ions. The outline of the crystal unit cell is also drawn, where **a** is horizontally directed to the right in the plane of the paper, **b** is directed into the paper and **c** is vertical and upwards. It can be seen that there are a pair of triangular arrays of Ca_{II} ions centred on each edge (6_3 axis) of the unit cell, which lie on two mirror planes [parallel to the (**a**, **b**) plane] being at levels of $z = 1/4$ and $z = 3/4$, respectively. A pair of hydroxyl ions are also centred on each 6_3 axis, surrounded by the pair of triangular arrays of Ca_{II} ions, respectively. [Hydroxyl ions are not drawn; for the z values for the ions, see (a).] When the (**a** $= 0$, **c** $= 0$) or the (**b** $= 0$, **c** $= 0$) plane of the unit cell is on the crystal surface, one of the three Ca_{II} ions constituting a triangular array is outside the crystal; the two other Ca_{II} ions survive on the crystal surface, receding slightly behind the (**a** $= 0$, **c** $= 0$) or the (**b** $= 0$, **c** $= 0$) plane. It can be deduced that, when the HA crystal is suspended in an aqueous solution, the hydroxyl positions on the crystal surface, each inserted by two Ca_{II} ions, are void at least for an instant. (Reproduced from ref. 6. The above interpretation is given in ref. 7, however.) (c) Perspective view of Ca_I ions. It can be seen that there are two columns of Ca_I ions per unit cell along two three-fold rotatory symmetry axes, and that each column is constituted of two Ca_I ions occurring at $z = 0.00$ and 0.50 (nearly but not precisely at $z = 0$ and $1/2$, respectively). (Reproduced from ref. 6.) (d) Deduced structure of the **c** surface of HA. It can be deduced that, when the HA crystal is suspended in an aqueous solution, two types of Ca_I position appearing on the **c** surface of HA are void at least for an instant. One of them is surrounded by six oxygen atoms (upper left) and the other is surrounded by three oxygen atoms (lower right). (Reproduced from ref. 8.)

axis of the "needle", and that most of the crystal surfaces appearing around the main axis of the "needle" are **a** surfaces.

With regard to the other crystals shown in Fig. 2b–d and f, however, it is difficult to identify the crystal surface on the basis of the electron micrograph only. (For the crystal surface of HA in Fig. 2f, see the third sub-section of the Discussion.)

A comparative study of the crystal structure of HA with that of octacalcium phosphate (OCP)[9,10] in combination with a study of the degradation mechanism of polyphosphates occurring on the crystal surface of HA[10,11] leads to the deduction that the **a** (or **b**) surface which just intersects the **b** (or **a**) axis of the crystal unit cell (see
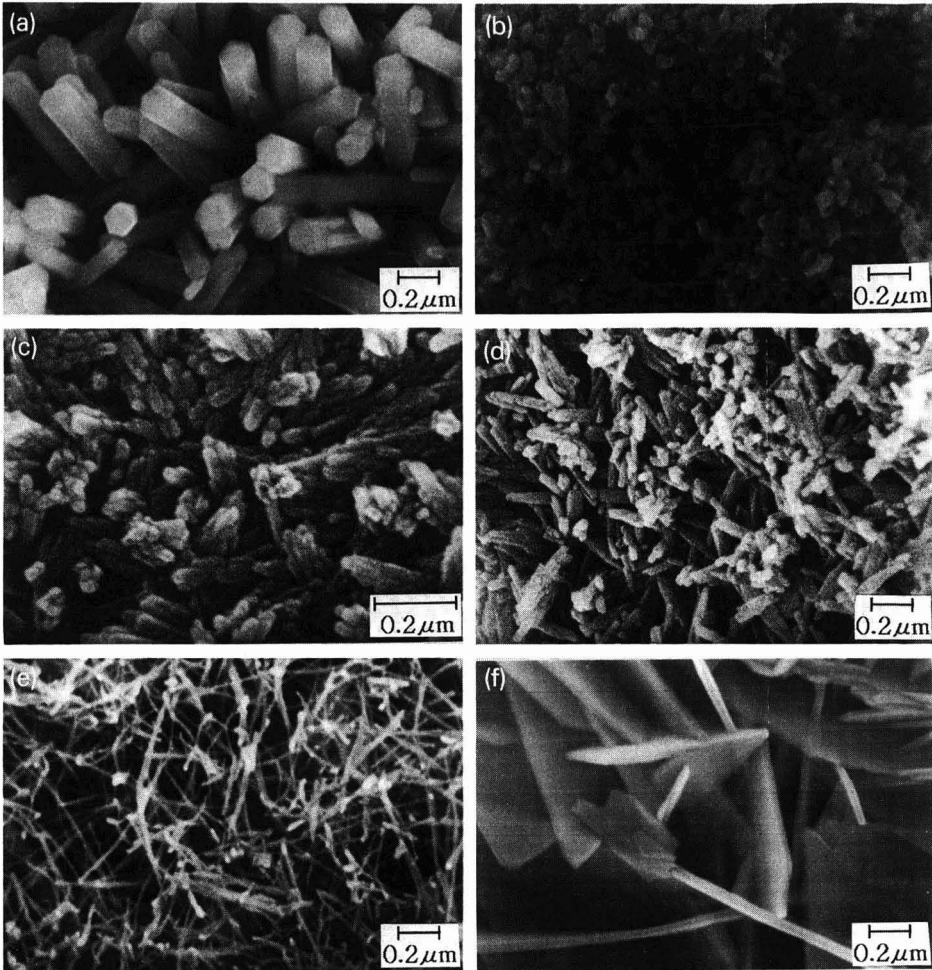
Fig. 2. Scanning electron micrographs of the surface structure of (a) coral HA with a Ca/P molar ratio of 1.67 (Mitsui Toatsu Chemicals, Tokyo, Japan), (b) spherical HA type S_1 with a Ca/P molar ratio of 1.67 (Koken), (c) HA type H with a Ca/P molar ratio of 1.62 (Koken), (d) HA type F with a Ca/P molar ratio of 1.57 (Koken), (e) potato-like HA with a Ca/P molar ratio of 1.52–1.54 (Central Glass) and (f) "rose des sables"-like HA with a Ca/P molar ratio of 1.61–1.64 (Central Glass). The entire image of HA type S_1 (b) is spherical with a diameter of about 5 μm. HA type H (c) is the Tiselius-type HA with a plate-like entire external shape. HA type F (d) has a square tile-like entire shape. The name "potato-like HA" (e) arises from the entire image of the crystal. "Rose des sables" (f) is a French word representing a gypsum "flower" produced naturally in the Sahara Desert.

Fig. 1a), in fact, appears on an HA crystal[7,10]. This means that positions at which hydroxyl ions should be present, provided that the positions are situated in the interior of the crystal, appear on the crystal surface, inserted by two Ca_{II} ions (see Fig. 1b; cf., Fig. 1a). It can be deduced[7,10] that, when the HA crystal is suspended in an aqueous solution, the hydroxyl positions on the crystal surface, each inserted by two Ca_{II} ions, are void at least for an instant, and that the two Ca_{II} ions (with positive charges) constitute an adsorbing site (see Fig. 1b). It can further be deduced[7] that the site is

identical with the chromatographic C site, or the anion exchanger on which a competing phosphate ion from the phosphate buffer and a phosphate or a carboxyl group on the sample macromolecule are adsorbable (see previous papers[1,2]). (A free phosphate ion and a phosphate group on the macromolecule would be adsorbed directly on a hydroxyl position[7,10]. The possibility cannot be excluded, however, that a carboxyl group on the macromolecule is adsorbed on a position situated in the middle of two hydroxyl positions arranged in the **c** direction on the **a** surface of HA. This is because carbonic ions may be situated at corresponding positions in the interior of the crystal, excluding hydroxyl ions[6].) An image can finally be attained that, on the **a** (or **b**) surface of HA, adsorbing C sites are arranged in a rectangular manner with the interdistance in the **b** (or **a**) direction equal to $|\mathbf{b}|$ ($= |\mathbf{a}|$) = 9.42 Å and the interdistance in the **c** direction equal to $|\mathbf{c}|/2$ = 3.44 Å (cf., Fig. 1b).

The mechanism of the adsorption of both free ions and adsorption groups of macromolecules on the crystal surface of HA resembles the first step of the epitaxial growth of the crystal (see Appendix II in ref. 8) where epitaxy consists in the growth of one crystal, in one or more particular orientations, on a substrate of another, with a near geometrical fit between the respective networks that are in contact[12]. In fact, if hydroxyl positions (C sites) on the **a** surface of HA are filled, under certain circumstances, with hydroxyl ions, then the crystal growth of HA would continue[7,10]. If hydroxyl positions are filled in an alternating manner with both phosphate ions and water molecules, then the epitaxial growth of OCP might begin on the **a** surface of HA[7,10].

It can be deduced that the **c** surface of HA is situated at the level of z = 0.00 or z = 0.50, as the exposure of another level of z on the crystal surface is only possible as compensation for the destruction of the chemical structure of crystal phosphate ions (see Appendix II in ref. 8). The levels, z = 0.00 and z = 0.50, equivalent to each other, are those where Ca_I ions should be present, provided the levels are situated in the interior of the HA crystal (see Fig. 1c; cf., Fig. 1a). It can be deduced[8] that, when the HA crystal is suspended in an aqueous solution, the Ca_I positions on the crystal surface are void at least for an instant; two types of Ca_I position appear on the **c** surface of HA, one surrounded by six negatively charged oxygen atoms belonging to three crystal phosphates and the other surrounded by three negatively charged oxygen atoms belonging to three crystal phosphates (see Fig. 1d). It can be assumed[8] that the former Ca_I position is identical with the chromatographic P site, or the cation exchanger on which a competing sodium or potassium ion from the buffer and an ε-amino or a guanidinyl group on the protein molecule are adsorbable (see previous papers[1,2]); the latter Ca_I position may constitute a weak adsorbing site. An image can finally be attained that, on the **c** surface of HA, adsorbing P sites are arranged in a hexagonal manner with the minimum interdistance in both **a** and **b** directions equal to $|\mathbf{a}|$ = $|\mathbf{b}|$ = 9.42 Å.

Of course, the possibility cannot be excluded that, owing to surface tension, the stereochemical structures of both **a** and **c** surfaces are distorted to a certain extent in comparison with the structure occurring in the interior of the crystal. It can be assumed, however, that the surface structure that has been deduced above represents the true structure to a good approximation.

In this work, by using several types of HA crystal with different external shapes and surface structures (Fig. 2a–f), adsorption and the HPLC experiments were carried

out in parallel; several proteins with different isoelectric points (pI) were used as probes. From these studies carried out with the aid of the study mentioned in the Introduction in Part II[2], a direct confirmation was obtained that, during the chromatographic process on the column, acidic proteins with p$I \lesssim 7$ (and also nucleic acids including other nucleotides) are mainly adsorbed on the **a** crystal surface, that basic proteins with p$I \gtrsim 7$ are mainly adsorbed on the **c** crystal surface and that these occur independently of the external crystal shape of HA that is used. This conclusion is consistent with the adsorption mechanism deduced from the structural study of HA with which the idea of the epitaxial crystal growth is connected (see above).

Further, profiles of the HPLC experiments obtained by using different types of HA were compared in detail. The results led to the deduction that the surface of a domain on the HA crystal on which the molecular adsorption takes place is smooth, and that the size of the domain under consideration is larger than the size of the proteins that have been applied, *i.e.*, larger than 100–200 Å. This means that the size of the crystallites that constitute the total crystal is larger than 100–200 Å, at least with respect to the HAs that have been examined.

From the analysis of overload chromatography, it can, in general, be deduced (see the last sub-section of Discussion) that a monolayer of sample molecules is formed on the crystal surface of HA when the development of the molecules is in progress on the column. On the basis of this study, the conclusion was drawn, however, that multi-layers of sample molecules may be formed on the HA surface when the molarity of the phosphate buffer in the mobile phase is much lower than that which is needed for the migration of the molecules on the column.

Concerning terminology, "acidic" and "basic" proteins are defined here as proteins that are eluted from the column with the second KP gradient and the first KCl gradient in the double gradient system, respectively (for the double gradient system, see Part II[2]; for KP, see the Experimental), whereas acidic and basic proteins mean proteins with pI values lower and higher than 7, respectively. "Acidic" and acidic proteins, and "basic" and basic proteins coincide with each other except in special cases (*cf.*, ref. 2; see also first sub-section of Discussion). (The abbreviations used in this paper are as follows: HA, hydroxyapatite; OCP, octacalcium phosphate; HPLC, high-performance liquid chromatography; ϕ, column I.D.; KP, potassium phosphate buffer, pH ≈ 6.8; P, pressure drop; T, temperature; pI, isoelectric point; BSA, bovine serum albumin; RNase A, ribonuclease A; IgG, immunoglobulin G; and m.h.h., mean height of the histogram.)

EXPERIMENTAL

In SUS316 stainless-steel columns of I.D. $\phi = 6$ mm, the following HA particles were packed: (a) coral HA constructed with hexagonal rods (Ca/P molar ratio = 1.67) (Mitsui Toatsu Chemicals, Tokyo, Japan) (see Fig. 2a), (b) spherical HA with a diameter of about 5 μm, called HA type S$_1$ (Ca/P molar ratio = 1.67) (Koken, Tokyo, Japan) (see Fig. 2b), (c) Tiselius-type plate-like HA, called HA type H (Ca/P molar ratio = 1.62) (Koken) (see Fig. 2c), (d) square tile-shaped HA, called HA type F (Ca/P molar ratio = 1.57) (Koken) (see Fig. 2d), (e) potato-like HA constructed with "needles" (Ca/P molar ratio = 1.52–1.54) (Central Glass, Tokyo, Japan) (see Fig. 2e) and (f) "rose des sables"-like HA constructed with lamellae (Ca/P molar ratio =

1.61–1.64) (Central Glass) (see Fig. 2f). For the adsorption experiments with proteins, a column of length 3 cm was used. For the HPLC experiments, columns with lengths of 3, 10 and 30 cm were prepared, and the 3-cm column was used as either a precolumn or a main column.

The adsorption experiments with proteins were carried out as follows. By using the same method as for HPLC, the sample molecules dissolved in 1 mM potassium phosphate buffer, pH $\approx$ 6.8 (composed of equimolar K_2HPO_4 and KH_2PO_4; called KP buffer), was injected, with a flow-rate of 0.5 ml/min, into a 3-cm column; this was followed by rinsing for 5–10 min with 1 mM KP buffer. In some experiments with cytochrome c, however, 1 mM KP was replaced with 50 mM KP. The column contents (*i.e.*, HA particles) were extruded from the inlet of the column by pushing them from the outlet with a rod. The cylindrical mass of the HA particles extruded from the column was cut into slices with a thickness of 2 mm; each was then suspended in 5 ml of 0.5 M KP with agitation in order to dissolve the sample molecules that had been captured on the HA surfaces into solution. The suspension was centrifuged and the absorbance of the supernatant at 230, 280 and/or 415 nm was measured in order to determine the total amount of the sample molecules that had been present in the slice.

The method used in the HPLC experiments, except preliminary double gradient HPLC, is decribed in the first sub-section of Experimental and Results in the preceding paper[2]. The sample elution was monitored by measuring the ultraviolet absorption at either 230 or 280 nm, however. With regard to the preliminary double gradient HPLC carried out by using $3 + 10 (= 13)$ cm column systems packed with coral HA, HA type S_1, HA type H, HA type F, potato-like HA and "rose des sables"-like HA, a KCl gradient, with $g'_{(KCl)}$ ($\phi = 1$ cm) $= 3.75$ mM/ml, was first applied after isocratic elution with 10 mM KP; 10 mM KP was always present while the KCl gradient continued. The carrier solvent was again replaced with pure 10 mM KP, and the KP gradient, with $g'_{(P;KP)}$ ($\phi = 1$ cm) $= 2.5$ mM/ml, was finally applied; 10 mM KP was replaced with 1 mM KP with both pepsinogen and ovalbumin, however. The final molarities of the KCl gradient in the double gradient system were nearly constant in the vicinity of 0.5 M. [For the symbols $g'_{(KCl)}$ ($\phi = 1$ cm) and $g'_{(P;KP)}$ ($\phi = 1$ cm), see the third sub-section of Experimental and Results in Part II[2].]

The sample molecules applied in the experiments were albumin (from bovine serum; Nutritional Biochemicals), lysozyme (from chicken egg white; P-L Biochemicals), pepsinogen (from hog stomach mucosa; Tokyo Kasei Kogyo), ovalbumin (from chicken egg white; Sigma, St. Louis, MO, U.S.A.), myoglobin (from sperm whale skeltal muscle; Sigma), trypsinogen (from bovine pancreas; Sigma), ribonuclease A (from bovine pancreas; Sigma), cytochrome c (from horse heart; Sigma), β-lactoglobulin A (from bovine milk; Sigma) and fractions I, II and III of immunoglobulin G (human; Japanese Red Cross Plasma Fractionation Centre, Tokyo, Japan) (for the three fractions of immunoglobulin G, see ref. 2, Appendix II).

RESULTS

Adsorption experiments on proteins: initial molecular band formed in the vicinity of the column inlet

The histograms in Fig. 3 show typical examples of the initial adsorptions of BSA (with an acidic pI of 4.7) and lysozyme (with a basic pI of 10.5–11.0) obtained in the
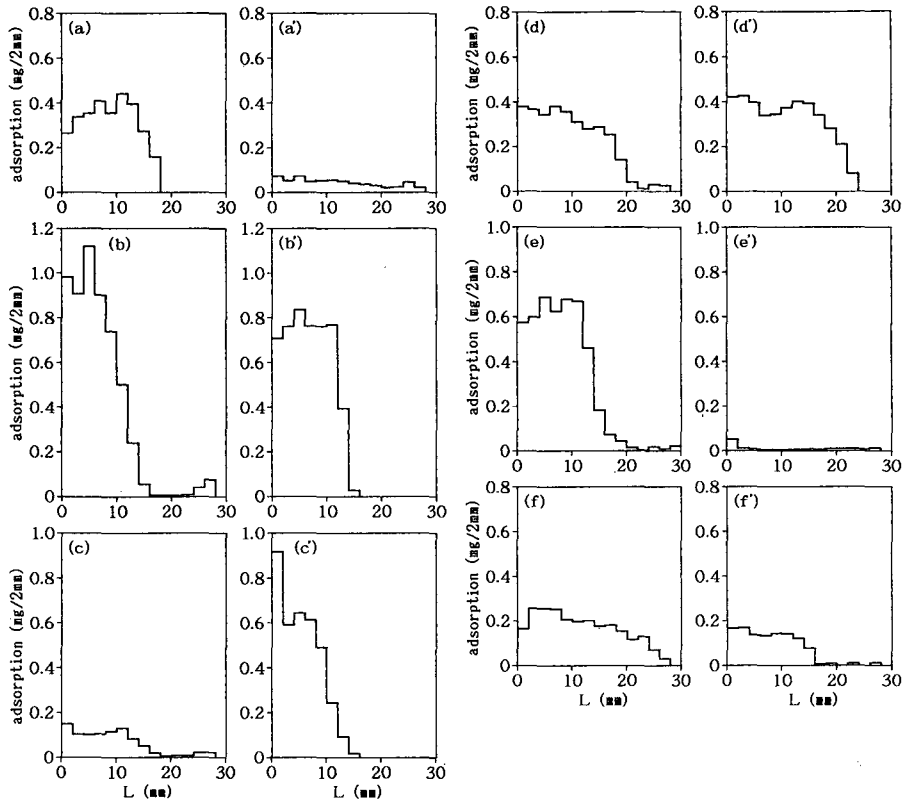
Fig. 3. Amounts of BSA (a–f) and lysozyme (a′–f′) adsorbed per 2 mm slice of the column contents (with $\phi = 6$ mm) in the presence of 1 mM KP as functions of the distance, L, from the column inlet. The types of crystal packed in the column are coral HA for (a) and (a′), HA type S_1 for (b) and (b′), HA type H for (c) and (c′), HA type F for (d) and (d′), potato-like HA for (e) and (e′) and "rose des sables"-like HA for (f) and (f′).

presence of 1 mM KP. These are drawn as functions of the distance, L, from the inlet of the columns packed with six different types of HA; the amount of molecules involved in a 2-mm slice of the column contents is represented by a portion of the histogram with a width of 2 mm (see Experimental). Hence, the histograms in Fig. 3a–f represent those for BSA obtained by using columns packed with coral HA (Fig. 2a), HA type S_1 (Fig. 2b), HA type H (Fig. 2c), HA type F (Fig. 2d), potato-like HA (Fig. 2e) and "rose des sables"-like HA (Fig. 2f), respectively. The histograms in Fig. 3a′–f′ are for lysozyme corresponding to those in Fig. 3a–f, respectively. It can be seen in Fig. 3 that, with both coral HA (constructed with hexagonal rods; Fig. 2a) and potato-like HA (constructed with "needles"; Fig. 2e), the mean height of the histogram (m.h.h.) for basic lysozyme is much smaller than that for acidic BSA [$cf.$, parts (a) and (a′) and parts (e) and (e′), respectively]. With both HA type S_1 (Fig. 2b) and "rose des sables"-like HA (Fig. 2f), the m.h.h. for lysozyme is slightly smaller than that for BSA ($cf.$, Fig. 3b and b′, and Fig. 3f and f′, respectively), in contrast to HA type F (Fig. 2d) for which the m.h.h. for BSA is slightly smaller than that for lysozyme ($cf.$, Fig. 3d and d′). With HA type H (Fig. 2c), the m.h.h. for BSA is considerably smaller than that for lysozyme ($cf.$, Fig. 3c and c′).
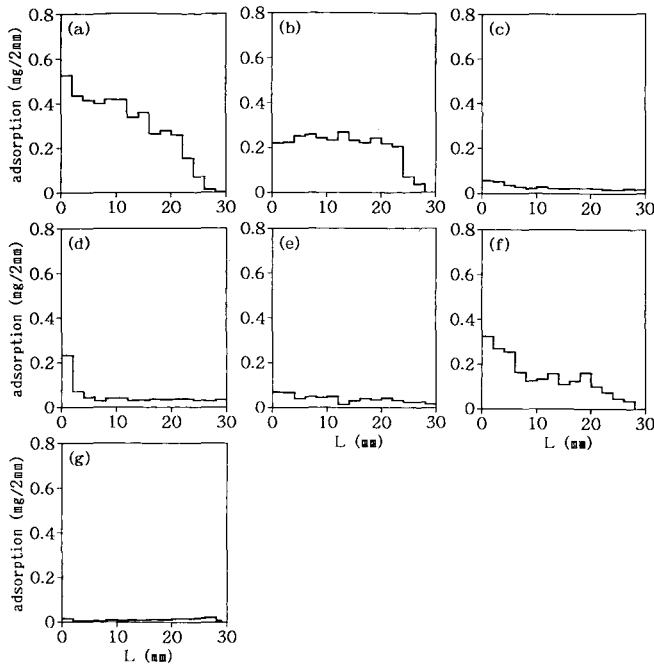
Fig. 4. As Fig. 3, obtained by using the column packed with coral HA for (a) pepsinogen, (b) ovalbumin, (c) myoglobin, (d) trypsinogen, (e) RNase A, (f) cytochrome c and (g) cytochrome c. The experiments were carried out in the presence of 1 mM KP (a–f) or 50 mM KP (g).

The histograms in Fig. 4 were obtained by using columns packed with coral HA for five other proteins: (a) pepsinogen (pI = 3.9); (b) ovalbumin (pI = 4.6); (c) myoglobin (pI = 7.0); (d) trypsinogen (pI = 9.3); (e) RNase A (pI = 9.7); and (f) and (g) cytochrome c (pI = 9.8–10.0); the histograms in Fig. 4a–f and Fig. 4g were obtained in the presences of 1 and 50 mM KP, respectively. It can be seen in Fig. 4 that the m.h.h.s for proteins with p$I \geqslant$ 7, except that for cytochrome c in the presence of 1 mM KP, are much smaller than the m.h.h.s for proteins with pI < 7.

The histograms in Fig. 5 were obtained by using columns packed with HA type S_1, and parts (a)–(g) correspond to (a)–(g) in Fig. 4, respectively. It can be seen in Fig. 5 that the m.h.h.s for all proteins are of the same order of magnitude, independent of pI. The m.h.h. for cytochrome c in the presence of 1 mM KP is exceptionally prominent, however (Fig. 5f). Fig. 5f can be compared with Fig. 4f, where the m.h.h. is exceptionally large among those for basic proteins.

The histograms in Fig. 6 were obtained in the presence of 1 mM KP by using columns packed with HA type S_1 for several types of protein mixtures. Independent histograms for the respective components of the mixture are also drawn, the amounts of the components being equal to those in the mixture. Thus, Fig. 6a and b relate to mixtures of acidic proteins, *i.e.*, a mixture of BSA and pepsinogen, and a mixture of BSA and ovalbumin, respectively. Fig. 6c is for a mixture of basic proteins, lysozyme and cytochrome c. Fig. 6d and e refer to mixtures of acidic and basic proteins, *i.e.*, a mixture of BSA and lysozyme and a mixture of BSA and cytochrome c, respectively.
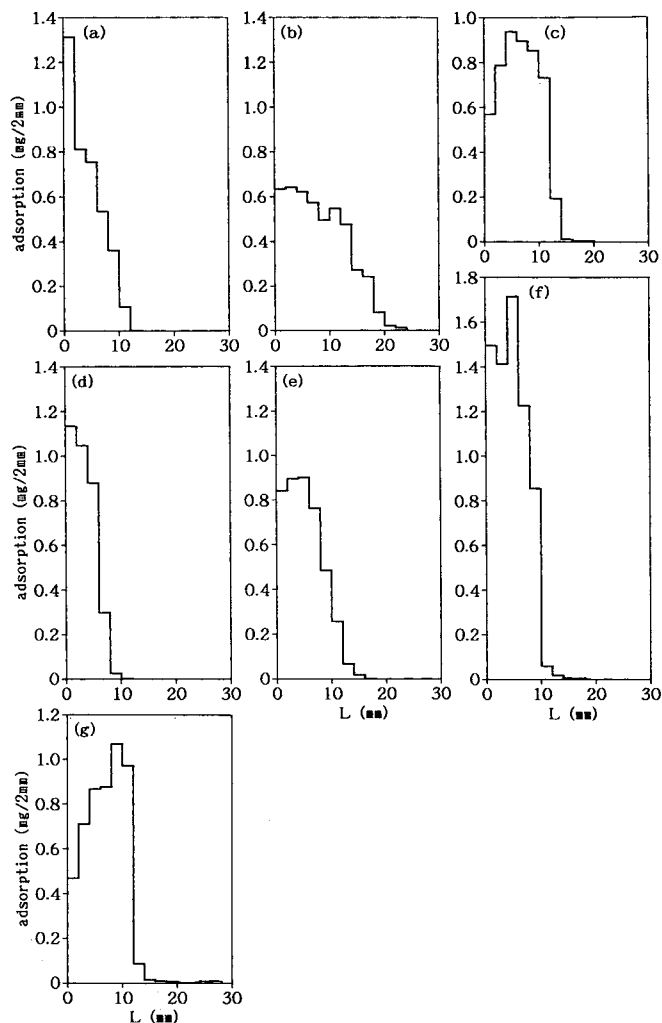
Fig. 5. As Fig. 4, obtained by using the column packed with HA type S_1.

It can be seen in Fig. 6 that, with both the mixture of acidic proteins (a and b) and the mixture of basic proteins (c), the width of the total histogram is roughly equal to the sum of the widths of the indepedent histograms for the respective components. With the mixtures of acidic and basic proteins, however, the height of the total histogram is roughly equal to the sum of the heights of the independent histograms for the respective components (see Fig. 6d and e).
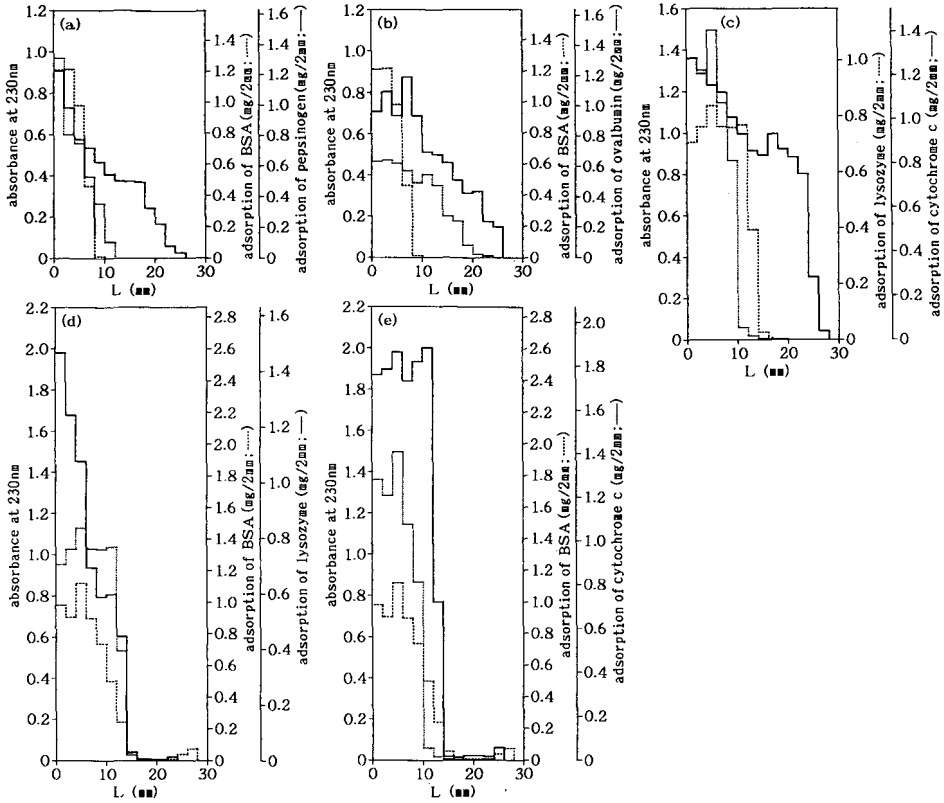
Fig. 6. As Fig. 3, obtained in the presence of 1 m*M* KP by using the column packed with HA type S_1 for mixtures of (a) BSA and pepsinogen, (b) BSA and ovalbumin, (c) lysozyme and cytochrome *c*, (d) BSA and lysozyme and (e) BSA and cytochrome *c*. (The histograms for the mixtures were drawn by using a continuous line.) Independent histograms for the respective components of the mixture are also shown, where the amounts of the components are equal to those appearing in the mixture. [The independent histograms were drawn by using two types of dotted line. Independent histograms for pepsinogen in (a), ovalbumin in (b), lysozyme in (c), BSA in (d), lysozyme in (d) and BSA in (e) are reproduced from Figs. 5a, 5b, 3b′, 3b′ and 3b, respectively.] On the left-hand ordinate, the absorbance at 230 nm of the supernatant (see Experimental) is indicated instead of the amount of molecules adsorbed per 2-mm slice of the column contents. These amounts for the respective components of the mixture in the independent histograms are indicated on the right-hand ordinate.

HPLC experiments and their analysis[a]

The proteins considered here are pepsinogen ($pI = 3.9$), ovalbumin ($pI = 4.6$), BSA ($pI = 4.7$), β-lactoglobulin A ($pI = 5.1$–5.3), myoglobin ($pI = 7.0$), trypsinogen ($pI = 9.3$), RNase A ($pI = 9.7$), cytochrome *c* ($pI = 9.8$–10.0), lysozyme ($pI = 10.5$–11.0) and fractions I, II and III of IgG; fractions I and II and fraction III are assemblies of "basic" and "acidic" molecules, respectively (for the three fractions of IgG, see Appendix II in Part II[2]).

_____

[a] See Part II[2] for double gradient chromatography, the method of analysis of the experimental results and experimental parameters that are used in this sub-section.
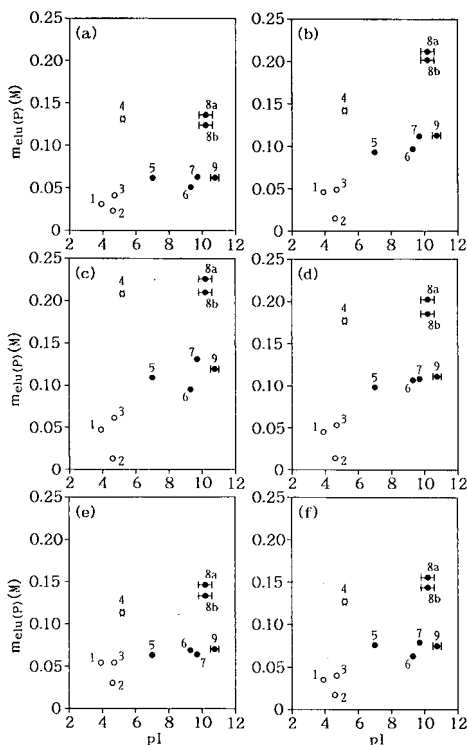
Fig. 7. Plots of $m_{elu(P)}$ versus pI for (1) pepsinogen, (2) ovalbumin, (3) BSA, (4) β-lactoglobulin A, (5) myoglobin, (6) trypsinogen, (7) RNase A, (8a) cytochrome c in reduced state, (8b) cytochrome c in oxidized state and (9) lysozyme, obtained by using columns packed with (a) coral HA, (b) HA type S_1, (c) HA type H, (d) HA type F, (c) potato-like HA and (f) "rose des sables"-like HA; $\bigcirc$ and $\bullet$ correspond to "acidic" and "basic" molecules, respectively. In all the experiments, the total length, L, of the column was fixed at 13 cm, and the slope, $g'_{(P)}$ ($\phi = 1$ cm) = 2.5 mM/ml, of the KP gradient was applied. The two points (8a and 8b) for cytochrome c in (a) were obtained by interpolation by using theoretical curves, however (cf., Fig. 8a where the theoretical curve for cytochrome c in reduced state is drawn). The points (except for β-lactoglobulin A) in (b) correspond to data shown in the tenth column in Table I in Part II[2]. Other experimental conditions: (a) sample load, 30–100 μg; flow-rate, 0.50 ml/min; P, 1.5–4.0 MPa; T, 24.5–26.5°C; (b) sample load, 25–300 μg; flow-rate, 0.49–0.51 ml/min; P, 1.3–2.4 MPa; T, 23.2–29.7°C; (c) sample load, 30–400 μg; flow-rate, 0.50–1.01 ml/min; P, $\leq$0.2 MPa; T, 24.5–27.0°C; (d) sample load, 10–275 μg; flow-rate, 0.50–1.01 ml/min; P, 0.2–0.5 MPa; T, 24.5–27.0°C; (e) sample load, 35–90 μg; flow-rate, 0.50–0.51 ml/min; P, $\leq$0.2 MPa; T, 24.0–26.0°C; and (f) sample load, 28–94 μg; flow-rate, 0.50–0.51 ml/min; P, $\leq$0.2 MPa; T, 23.0–26.2°C.

Preliminarily, double gradient HPLC of all these proteins except IgG was carried out by using columns packed with coral HA, HA type S_1, HA type H, HA type F, potato-like HA and "rose des sables"-like HA. It was confirmed that, with any type of HA, pepsinogen, ovalbumin, BSA and β-lactoglobulin A behave as "acidic" molecules, eluted from the column with the second KP gradient in the double gradient system; myoglobin, trypsinogen, RNase A, cytochrome c and lysozyme behaved as "basic" molecules, eluted with the first KCl gradient in the system (cf., Part II[2]). In some instances with both pepsinogen and ovalbumin, however, a minor proportion of the molecules was eluted with a rapid decrease in KCl molarity occurring at the end of
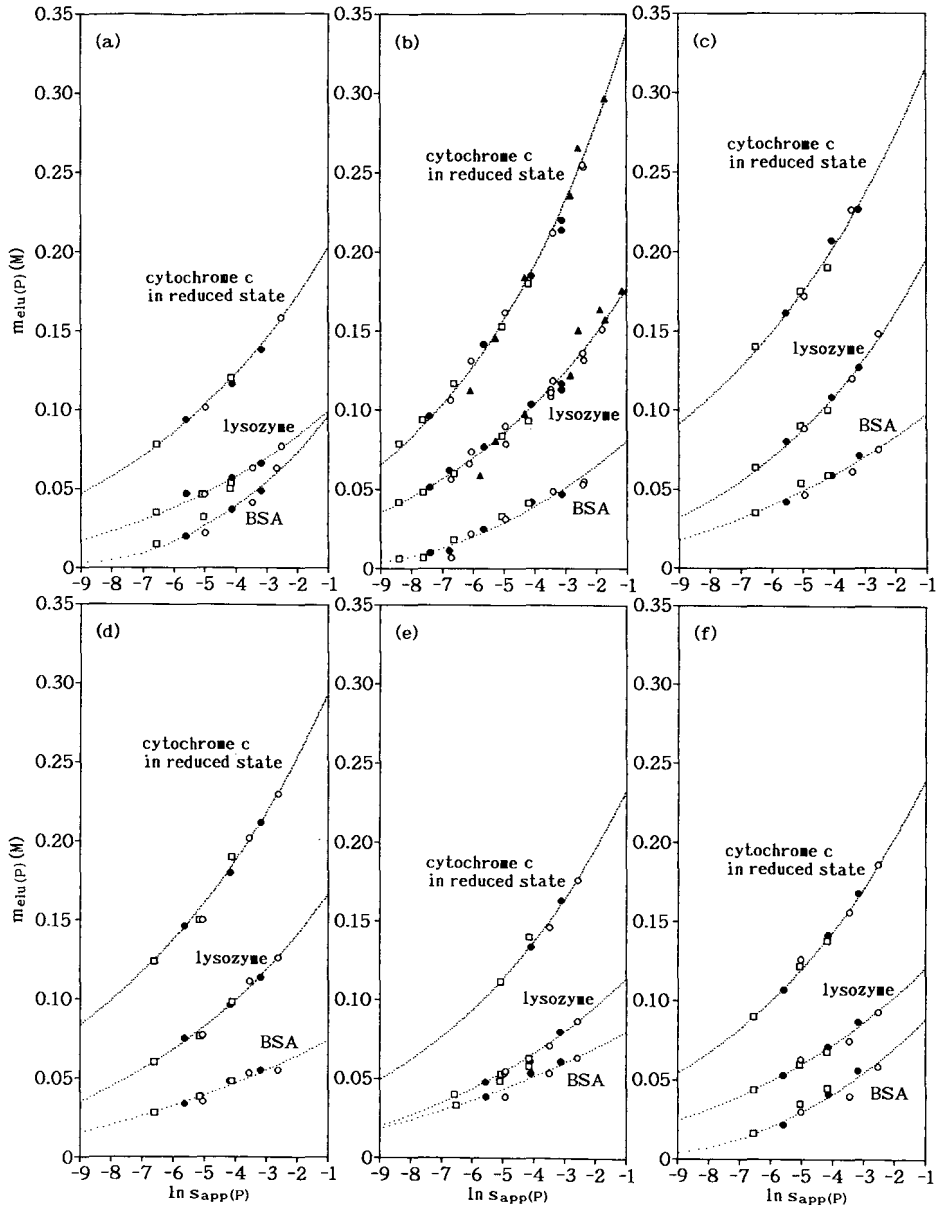
Fig. 8. Points: experimental plots of $m_{elu(P)}$ *versus* ln $s_{app(P)}$ for BSA, lysozyme and cytochrome c in reduced state, obtained by using columns packed with (a) coral HA, (b) HA type S_1, (c) HA type H, (d) HA type F, (e) potato-like HA and (f) "rose des sables"-like HA. The $g'_{(P)}$ ($\phi = 1$ cm) values applied were (▲) 5.0, (○) 2.5, (●) 1.25 and (□) 0.45 mM/ml. Other experimental conditions: (a) sample load, 30–150 μg; flow-rate, 0.46–0.52 ml/min; P, 0.1–0.6 MPa; T, 21.0–29.7°C; (b) sample load, 16–480 μg; flow-rate, 0.46–0.51 ml/min; P, 0.3–10.0 MPa; T, 21.0–29.7°C; (c) sample load, 30–200 μg; flow-rate, 0.50–0.51 ml/min; P, ≤0.4 MPa; T, 23.8–25.1°C; (d) sample load, 30–150 μg; flow-rate, 0.50 ml/min; P, 0.2–0.6 MPa; T, 23.0–26.0°C; (e) sample load, 27–150 μg; flow-rate, 0.50–0.51 ml/min; P, ≤ 0.2 MPa; T, 23.3–27.0°C; and (f) sample load, 28–145 μg; flow-rate, 0.50–0.51 ml/min; P, ≤ 0.2 MPa; T, 23.5–27.0°C. Curves: theoretical curves calculated by using eqn. 6 in ref. 2; for the parameters involved in the equation, see Table I. [Both the experimental points and the theoretical curves in (b) are reproduced from ref. 2.]

TABLE I

SUMMARY OF RESULTS OF GRADIENT HPLC EXPERIMENTS CARRIED OUT USING A VALUE OF THE PARAMETER φ OF 25 M^{-1} (Cf., FIGS. 8–10)

The analyses for pepsinogen, ovalbumin, myoglobin, trypsinogen and RNase A were performed for the main peak of the chromatogram.

Protein	HA	x'	$\ln q_{app(P)}$	Protein	HA	x'	$\ln q_{app(P)}$	Protein	HA	x'	$\ln q_{app(P)}$
"Acidic" proteins:				*"Basic" proteins:*							
BSA	Coral	4.5	2.8	Lysozyme	Coral	6.5	7.4	RNase A	Coral	5.0	5.9
	S_1	6.0	3.6		S_1	5.7	9.5		S_1	4.3	6.9
	H	8.2	6.9		H	5.0	8.7	IgG fraction I	Coral	11.0	10.4
	F	10.0	6.9		F	6.0	9.7		S_1	11.0	11.2
	Potato	10.0	7.5		Potato	6.2	7.8		H	9.5	12.4
	"Rose des sables"	5.5	3.5		"Rose des sables"	6.5	8.6		F	11.0	12.7
Ovalbumin	Coral	5.0	1.2	Cytochrome c	Coral	6.0	10.9		Potato	9.0	10.1
	S_1	8.0	0.5	(in reduced state)	S_1	4.8	11.2		"Rose des sables"	12.0	13.9
IgG fraction III	Coral	17.0	23.0		H	6.5	14.9	IgG fraction II	Coral	11.0	15.4
	S_1	18.0	25.0		F	6.5	14.4		S_1	11.0	16.6
	H	15.5	22.9		Potato	5.5	10.7		H	11.0	17.9
	F	16.0	22.7		"Rose des sables"	5.7	11.3		F	11.0	17.4
	Potato	15.0	20.5	Cytochrome c	Coral	5.5	9.6		Potato	9.0	13.3
	"Rose des sables"	19.0	26.0	(in oxidized state)	S_1	4.8	10.8		"Rose des sables"	12.0	17.9
					H	5.6	12.7				
					F	6.0	12.9				
					Potato	5.5	10.2				
					"Rose des sables"	5.7	10.8				

the first KCl gradient, presumably owing to a kinetic mechanism arising from an abrupt change in the environment (*i.e.*, the KCl molarity) (for details on the kinetic mechanism, see Part I[1]). It should be stressed that the chromatographic behaviours of all proteins are similar for all the HAs that were used.

The points in Fig. 7a–f are experimental plots of $m_{elu(P)}$ *versus* pI for the above proteins except IgG, obtained by using columns packed with (a) coral HA, (b) HA type S_1, (c) HA type H, (d) HA type F, (e) potato-like HA and (f) "rose des sables"-like HA (the plots for pepsinogen, ovalbumin, myoglobin, trypsinogen and RNase A are concerned with the main peak of the chromatogram; all the analyses for these proteins will be performed for the main peak). In all the experiments, the total length, L, of the column was fixed at 13 cm, and the slope, $g'_{(P)}$ ($\phi = 1$ cm) $= 2.5$ mM/ml, of the KP gradient was applied. It can be seen in Fig. 7 that, in general, "acidic" proteins tend to be eluted at lower phosphate molarities than "basic" proteins while keeping almost the same constellations of the plot among the "acidic" and the "basic" proteins, respectively. With coral HA, potato-like HA and "rose des sables"-like HA, however, the elution molarities of the "basic" proteins tend to decrease; as a result, the elution molarities of the "acidic" proteins and those of the "basic" proteins tend to approach each other (compare Fig. 7a, e and f with Fig. 7b, c and d).

The points in Fig. 8a–f are experimental plots of $m_{elu(P)}$ *versus* ln $s_{app(P)}$ for BSA, lysozyme and cytochrome c in reduced state, obtained by using columns packed with (a) coral HA, (b) HA type S_1, (c) HA type H, (d) HA type F, (e) potato-like HA and (f) "rose des sables"-like HA. The curves in Fig. 8 are theoretical, calculated by using eqn. 6 in Part II[2]. For the calculation, the optimum value of the parameter φ of $25\ M^{-1}$ was used; this value will hereafter be used for all the calculations (*cf.*, ref. 2). For the other experimental parameters, the values given in Table I were applied in order to obtain best fits with the experiment. It can be seen in Fig. 8 that, with (a) coral HA, (e) potato-like HA and (f) "rose des sables"-like HA the elution molarities of "basic" proteins, lysozyme and cytochrome c, tend to decrease, and they approach those of "acidic" BSA; especially the elution molarities of lysozyme are close to those of BSA.

The points in Fig. 9a and b are experimental plots of $m_{elu(P)}$ *versus* ln $s_{app(P)}$ for
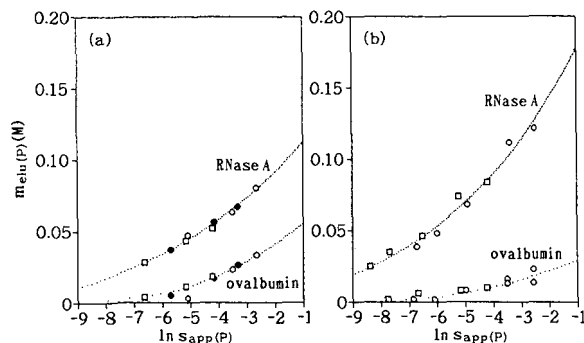
Fig. 9. Points: as Fig. 8 for ovalbumin and RNase A, obtained by using columns packed with (a) coral HA and (b) HA type S_1. The $g'_{(P)}$ ($\phi = 1$ cm) values applied were ($\bigcirc$) 2.5, ($\bullet$) 1.25 and ($\square$) 0.45 mM/ml. Other experimental conditions: (a) sample load, 35–50 μg; flow-rate, 0.50 ml/min; P, 0.1–0.5 MPa; T, 24.0–27.0°C; and (b) sample load, 25–300 μg; flow-rate, 0.50 ml/min; P, 0.5–5.0 MPa; T, 24.0–26.6°C. Curves: as Fig. 8. [Both the experimental points and the theoretical curves in (b) are reproduced from ref. 2.]
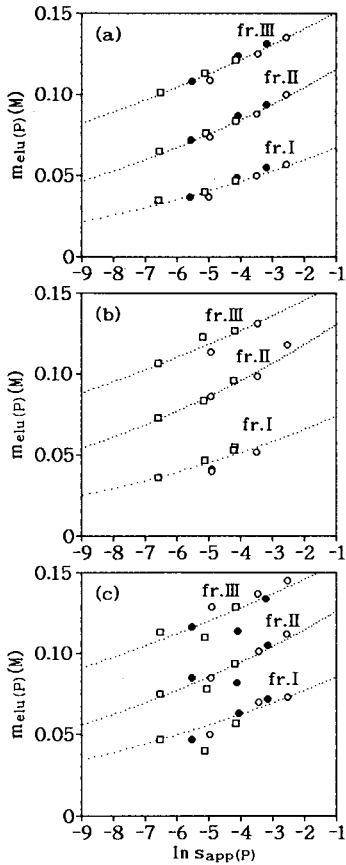
Fig. 10. Points: as Fig. 8 for fractions I, II and III of IgG, obtained by using columns packed with (a) coral HA, (b) HA type S_1 and (c) "rose des sables"-like HA. The $g'_{(P)}$ ($\phi = 1$ cm) values applied were (○) 2.5, (●) 1.25 and (□) 0.45 mM/ml. Other experimental conditions: (a) sample load, 0.033–0.114 in units of absorbance (at 230 nm) × ml; flow-rate, 0.48–0.51 ml/min; P, 0.1–0.6 MPa; T, 24.5–27.7°C; (b) sample load, 0.047–0.231 in units of absorbance (at 230 nm) × ml; flow-rate, 0.49–0.50 ml/min; P, 0.9–4.9 MPa; T, 20.0–25.0°C; and (c) sample load, 0.026–0.087 in units of absorbance (at 230 nm) × ml; flow-rate, 0.50–0.51 ml/min; P, 0.1–0.2 MPa; T, 23.5–25.8°C. Curves: as Fig. 8. [Both the experimental points and the theoretical curves in (b) are reproduced from ref. 2.]

ovalbumin and RNase A, obtained by using columns packed with (a) coral HA and (b) HA type S_1; the curves are theoretical, calculated by using the parameters given in Table I. It can be seen in Fig. 9 that the elution molarities of "acidic" ovalbumin and those of "basic" RNase A approach each other more closely with coral HA (a) than with HA type S_1 (b); this tendency is parallel with that observed for other "acidic" and "basic" proteins (see Fig. 8a and b).

The points in Fig. 10a–c are experimental plots of $m_{elu(P)}$ versus ln $s_{app(P)}$ for "basic" fractions I and II and "acidic" fraction III of IgG, obtained by using columns packed with (a) coral HA, (b) HA type S_1 and (c) "rose des sables"-like HA; the curves are theoretical, calculated by using parameters given in Table I. It can be seen in Fig. 10

that "basic" fractions I and II are eluted at lower molarities than "acidic" fraction III, and that the relative positions among the three plots for the three fractions do not depend much on the type of HA used. Similar diagrams were also obtained by using columns packed with HA type H, HA type F and potato-like HA.

DISCUSSION

*Confirmation that, during the chromatographic process on the column, acidic proteins with pI $\lesssim$ 7 (and also nucleic acids including other nucleotides) are mainly adsorbed on the **a** (or **b**) crystal surface, that basic proteins with pI $\gtrsim$ 7 are mainly adsorbed on the **c** crystal surface and that these occur independently of the external crystal shape of HA that is used*

The above confirmation can be obtained from the following three considerations. First, in the double gradient system, acidic proteins (ovalbumin, BSA and β-lactoglobulin A) are eluted with the second KP gradient whereas basic (and neutral) proteins (myoglobin, trypsinogen, RNase A, cytochrome c and lysozyme) are eluted with the first KCl gradient; this occurs independently of the external crystal shape of HA used (preliminary experiment in the second sub-section of Results). The behaviour of DNA and nucleoside phosphates in the double gradient system is parallel with that of acidic proteins (see Part I[1]). Further, the constellation of the $m_{elu(P)}$ *versus* pI plot among the acidic proteins and the constellation of the same plot among the basic (and neutral) proteins are both almost parallel for all the HAs used, with different external shapes (Fig. 7; for slight differences in the constellation among different HAs, see the third sub-section). These data indicate that, with HA with any external shape, the crystal surface on which acidic proteins (and nucleic acids, including other nucleotides) are adsorbed is different from the surface on which basic (and neutral) proteins are adsorbed, and that the two common adsorbing surfaces appear independently of the external crystal shape of HA (*cf.*, Introduction in Part II[2]; for some related arguments, see Appendix I).

Second, with regard to coral HA constructed with hexagonal rods (Fig. 2a), only **a** and **c** surfaces appear on the crystal, and the total· area of the **c** surfaces is much smaller than that of the **a** surfaces (see Introduction). On the other hand, the m.h.h.s with coral HA for basic (and neutral) proteins (lysozyme, myoglobin, trypsinogen, RNase A and cytochrome c) are generally much smaller than those for acidic proteins (BSA, pepsinogen and ovalbumin) (Figs. 3a and a' and 4a–e and g) except for cytochrome c in the presence of 1 mM KP (Fig. 4f). These data indicate that, with coral HA, acidic proteins are (mainly) adsorbed on the **a** surface whereas basic (and neutral) proteins are (mainly) adsorbed on the **c** surface; the exceptional behaviour of cytochrome c occurring in the presence of 1 mM KP will be discussed in the last sub-section.

With regard to potato-like HA constructed with "needles" (Fig. 2e) also, it is highly probable that the **a** surface appears in a major proportion (see Introduction) whereas the m.h.h. for basic lysozyme is much smaller than that for acidic BSA (Fig. 3e and e'). The situation is parallel with that with coral HA (see above).

With regard to the other HAs [HA type S$_1$ (Fig. 2b), HA type H (Fig. 2c), HA type F (Fig. 2d) and "rose des sables"-like HA (Fig. 2f)], it is difficult to identify the crystal surface on the basis of the electron micrograph only (see Introduction).

However, it does not appear that the ratio between **a** and **c** surface areas is extremely biased except for "rose des sables"-like HA (for "rose des sables"-like HA in Fig. 2f, see the third sub-section). In fact, the ratios between m.h.h.s for acidic and basic proteins are not extremely biased with HA type S_1, HA type F and "rose des sables"-like HA (compare Fig. 3b and b', d and d', and f and f', respectively; see also Fig. 5). As far as HA type H is concerned, however, the m.h.h. for acidic BSA is considerably smaller than that for basic lysozyme (Fig. 3c and c').

All these data, together with the first part of the confirmation, indicate that acidic proteins, or more generally proteins with p$I \lesssim 7$ and nucleic acids including other nucleotides, are mainly adsorbed on the **a** surface whereas proteins with p$I \gtrsim 7$ are mainly adsorbed on the **c** surface; these occur independently of the external crystal shape of HA.

Third, the width of the total histogram for mixtures of acidic proteins (a mixture of BSA and pepsinogen and a mixture of BSA and ovalbumin) is roughly equal to the sum of the widths of the independent histograms for the respective components of the mixtures (Fig. 6a and b). The width of the total histogram for a mixture of basic proteins (lysozyme and cytochrome c) is also roughly equal to the sum of the widths of the independent histograms for the respective components of the mixture (Fig. 6c). These data indicate that acidic proteins are adsorbed on a common surface of HA and that basic proteins are also adsorbed on a common surface. With mixtures of acidic and basic proteins (a mixture of BSA and lysozyme and a mixture of BSA and cytochrome c), however, the height of the total histograms is roughly equal to the sum of the heights of the independent histograms for the respective components of the mixtures (Fig. 6d and e). These data indicate that acidic and basic proteins are adsorbed on different crystal surfaces of HA. The conclusions support those obtained in both the first and second parts of the confirmation.

Relationship with the crystal surface structure deduced from the structural study of HA

It should be recalled that the appearances of both the **a** and the **c** surfaces on the HA crystal can also be deduced from the structural study of HA with which the idea of the epitaxial crystal growth is connected (see Introduction). It should be emphasized that, from this study, the conclusion has been drawn that anion exchangers with positive charges (or adsorbing C sites) should be present on the **a** surface whereas cation exchangers with negative charges (or adsorbing P sites) should be present on the **c** surface (see Introduction). The conclusion is consistent with the considerations in the first sub-section and also those in Part I[1] (*cf.*, Introduction in Part II[2]): with HA chromatography, competition occurs between acidic proteins (or nucleic acids including other nucleotides) and phosphate ions from the buffer, and between basic proteins and cations from the buffer for adsorption on the **a** and the **c** surface of HA, respectively.

Comparison of detailed profiles of the HPLC experiments carried out by using different types of HA

In general, acidic proteins tend to be eluted at lower phosphate molarities than basic proteins (Fig. 7; see also Fig. 2 in Part II[2]). With coral HA, potato-like HA and "rose des sables"-like HA, however, the elution molarities of "basic" proteins tend to decrease and the elution molarities of "acidic" proteins and those of "basic" proteins

tend to approach each other (compare Fig. 7a, e and f with Fig. 7b, c and d, Fig. 8a, e and f with Fig. 8b, c and d, and Fig. 9a with Fig. 9b), except for IgG, the elution profile of which does not depend much on the type of HA used (Fig. 10). The elution profiles of the proteins, including the exceptional behaviour of IgG, can be explained qualitatively by the fact that, with both coral HA and potato-like HA, the total area of the **c** surfaces on which the adsorption of "basic" proteins occurs is much smaller than the total area of the **a** surfaces on which the adsorption of "acidic" proteins occurs (see Appendix II; for "rose des sables"-like HA, see below).

Monma et al.[13] performed an electron diffraction analysis of an HA crystal with an external shape very similar to that of "rose des sables"-like HA, the surface of which is covered by lamellae (Fig. 2f). They reported that the flat surface of a lamella corresponds to the (100) or the **a** surface as deduced from the electron diffraction pattern. It is therefore highly probable that the flat surface of a lamella of "rose des sables"-like HA also corresponds to the **a** surface, and that the major proportion of the total surface of the lamella is occupied by the **a** surface. This deduction appears to be compatible with the fact that, with "rose des sables"-like HA also, the elution molarities of "basic" proteins tend to decrease (Figs. 7f and 8f) in parallel with both cases for coral HA and potato-like HA (Figs. 7a and e, and 8a and e). As far as the adsorption experiment is concerned, however, the m.h.h. for "acidic" BSA is only slightly larger than that for "basic" lysozyme with "rose des sables"-like HA (Fig. 3f and f′); this can be compared with both cases for coral HA and potato-like HA in which the m.h.h. for "acidic" BSA is much larger than that for "basic" lysozyme (Fig. 3a, a′, e and e′). This experimental result implies that, on the total surface of "rose des sables"-like HA, non-lamellar structures are also involved in part. Consistent with this deduction, non-lamellar structures can be found on the crystal surface of "rose des sables"-like HA by careful examination of the electron micrograph (not shown). In order to continue the argument, further experimental data are needed.

Table I summarizes both x' and $\ln q_{app(P)}$ values calculated on the basis of Figs. 8–10 for several proteins with different types of HA; for IgG with HA type H, HA type F and potato-like HA, additional data were used for the calculations. All the calculations were performed in order for the theoretical curve (represented by eqn. 6 in Part II[2]) to coincide best with the experimental plot by using the optimum value of the parameter φ of 25 M^{-1} (for the value of φ, see ref. 2). It can be seen in Table I that, except for BSA and ovalbumin, the x' value, representing the number of adsorbing sites (C or P) on the HA surface covered by an adsorbed sample molecule[2], is nearly constant, independent of the type of HA used. The considerable fluctuations in the x' value that occur with both BSA and ovalbumin are artifacts, arising from the difficulty in carrying out precise evaluations of the parameter when the molecule is eluted with low phosphate molarities (see Figs. 8 and 9).

The constellation of the $m_{elu(P)}$ versus pI plot among the "acidic" proteins and the constellation of the same plot among the "basic" proteins, both representing only weak correlations (if they exist) between $m_{elu(P)}$ and pI, are almost parallel among different types of HA (Fig. 7; cf., first sub-section). This, together with the fact that x' is nearly constant, independent of the type of HA (except for the fluctuations arising from the artifact; see above), leads to the deduction that the surface of a domain on the HA crystal on which the molecular adsorption takes place is fairly smooth, and that the size of the domain under consideration is larger than the size of the proteins that

have been applied. The size of the smooth domain is larger than 100–200 Å, the size of IgG (the largest molecule that has been applied; see Fig. 13 in Part II[2]). This means that the size of the crystallites that constitute the total crystal is larger than 100–200 Å. It should be recalled that the chromatographic properties of several types of HA prepared by using different methods were studied by Spencer[14] in connection with both the crystal surface structure (as observed by scanning electron microscopy) and the size of the crystallites constituting the total HA particle (as deduced from the X-ray diffraction profile). On the basis of some reasonable assumption, he deduced that the elution phosphate molarity of tRNA (with the longest dimension of about 90 Å for one of the smaller species) increases with increase in the smallest dimension of the crystallite faces if it is less than 110 Å; if it exceeds 110 Å, the elution molarity of tRNA is virtually constant, independent of the crystallite size[14]. This suggests that, for optimum binding, the smallest dimension of the crystallite faces needs to exceed the size of the molecule[14].

It can be seen in Table I that the x' values of 15.0–19.0 for "acidic" IgG are larger than the corresponding values of 9.0–12.0 for "basic" IgG's. As pointed out in Part II[2], this is compatible with the deduction that two C sites are present per unit cell on the **a** surface of HA whereas only a single P site is present per unit cell on the **c** surface (see Introduction); the size of the smooth domain on the HA surface where the molecular adsorption takes place is larger than the size of an IgG molecule (see above). [It should be recalled that the x' values were calculated by using the optimum value of the parameter φ of 25 M^{-1}. If the lower or the upper limit value of φ is assumed, the x' values deviate considerably from the values that are given in Table I (see Table I in Part II[2] and also Figs. 11 and 12 in Part II[2]). The ratios among the x' values for different proteins are kept virtually constant if the φ value varies, however.]

The constellation of the $m_{elu(P)}$ *versus* pI plot is slightly different among the different HAs that were used (Fig. 7). This, together with the slight fluctuation in the x' value (in addition to that arising from the artifact; see Table I), might reflect certain minor defects in the crystal surface structure which might occur in different manners on the smooth domains of the surfaces of different types of HA. It does not appear, however, that the non-stoichiometric Ca/P molar ratio in some HAs (see Introduction) is effectively related to the defect in the crystal surface structure under consideration; this is because no direct correlation has so far been found between the chromatographic properties of HA and the Ca/P molar ratio. [At the 8th Conference on Liquid Chromatography, Tokyo (1987), the influence of the Ca/P molar ratio on the elution molarity of proteins was reported orally by Inoue *et al.* No proof was given, however, concerning whether or not the elution molarity is *directly* influenced by the Ca/P molar ratio of HA. The possibility cannot be excluded that a slight change in the Ca/P molar ratio occurring on the crystal surface of HA affects the network structure of water molecules that keep in contact with the HA crystal, and that this brings about a slight change in the elution molarity of proteins. Also, no detailed investigation on the surface structure of HAs that were used in this study was performed.] In Part I[1], it was pointed out that the **a** surface of some commercially available spherical HA particles is damaged to a considerable extent.

Exceptional adsorption of cytochrome c in the presence of 1 mM KP

With coral HA, the m.h.h.s for basic (and neutral) proteins occurring in the

presence of 1 mM KP are generally much smaller than those for acidic proteins occurring in the presence of 1 mM KP (Figs. 3a and a', and 4a–e); the m.h.h. for basic cytochrome c in the presence of 1 mM KP is exceptionally large (Fig. 4f). The m.h.h. for cytochrome c in the presence of 50 mM KP is as small as those for the other basic proteins occurring in the presence of 1 mM KP, however (Fig. 4g). With HA type S_1, the m.h.h.s for all the proteins in the presence of 1 mM KP (Figs. 3b and b', and 5a–f) and the m.h.h. for cytochrome c in the presence of 50 mM KP (Fig. 5g) are of the same order of magnitude. The m.h.h. for cytochrome c in the presence of 1 mM KP is exceptionally prominent, however (Fig. 5f).

It can be considered that the exceptionally large m.h.h.s for cytochrome c in the presence of 1 mM KP (Figs. 4f and 5f) are connected with the fact that the molarity of the KP buffer used, 1 mM, is exceptionally *much* lower than the molarity at which the transition of the B' value from *ca.* 0 to 1 begins (see Fig. 5d and e in Part II[2]). In fact, with regard to the other proteins that were examined (BSA, lysozyme, pepsinogen, ovalbumin, myoglobin, trypsinogen and RNase A), 1 mM is close to the molarity at which the transition of the B' value begins (*cf.*, Fig. 4d and e, and Fig. 7c and d in Part II[2] for HA type S_1; the statement was also confirmed for the other types of HA). A molarity of 50 mM with cytochrome c is also close to that at which the transition of the B' value begins (*cf.*, Fig. 5d and e in Part II[2] for HA type S_1; the statement was also confirmed for the other types of HA).

In an earlier paper[15], it was pointed out that, when the development of the molecules is in progress under overload conditions, repulsive forces reside among sample molecules that remain on the adsorbent surfaces in the column. This means that the surface of any molecule in the stationary state keeps in contact with the adsorbent surface at least partially when the development of the molecules is in progress in the column. In other words, the formation of multi-layers of molecules on the adsorbent surface is impossible at least when the development of the molecules is in progress in the column; this is because it is repulsive forces, and not attractive forces, that reside among molecules in the stationary state (see above). It was demonstrated previously[16] that the chromatographic behaviour of chicken and turkey lysozymes and a mixture of them under overload conditions can be explained quantitatively by assuming the participation of repulsive molecular interactions.

The development of molecules on the HA column is possible only when B' is larger than *ca.* 0 (*cf.*, the "first principle of chromatography in general" mentioned in Appendix III in ref. 17) or when the molarity of the KP buffer is higher than the molarity at which the transition of the B' value from *ca.* 0 to 1 begins. This means that the m.h.h.s for BSA, lysozyme, pepsinogen, ovalbumin, trypsinogen and RNase A occurring in the presence of 1 mM KP and also the m.h.h. for cytochrome c occurring in the presence of 50 mM KP are all close to those that should be realized when the maximum possible number of molecules is adsorbed on the HA surface, fulfilling the condition that the surface of any molecule keeps in contact with the crystal surface of HA at least partially.

It can be deduced that the large m.h.h. for cytochrome c occurring in the presence of 1 mM KP (Figs. 4f and 5f) arises from the formation of multi-layers on the crystal surface of HA due to weak attractive interactions among molecules. With an increase in KP molarity from 1 to 50 mM, the multi-layers would be released as the molecules in the layers are fixed only weakly to one another. It can also be deduced that

a single layer finally survives in which all the molecules keep in contact with the crystal surface owing to strong attractive forces towards the crystal surface of HA; repulsive forces reside among the molecules that keep in contact with the crystal surface (see above).

APPENDIX I

To the argument for the first step of the confirmation in the first sub-section under Discussion, it should be added that the chromatographic behaviour of proteins as a function of pI changes continuously at about p$I \approx 7$, although it occurs very abruptly (see first sub-section of Discussion and the Introduction in Part II[2]). In fact, it was pointed out in Part I[1] that the elution molarity, $m_{elu(KCl)}$, of myoglobin (with a neutral pI of 7) in the KCl gradient system is 2.3 times higher than the potassium elution molarity, $m_{elu(K^+;KP)}$, in the KP gradient system under certain experimental conditions. This means that, although myoglobin behaves as a "basic" molecule in the double gradient system, mainly adsorbed to one of the two surfaces of HA where basic molecules should be adsorbed (i.e., the c surface), it is partially adsorbed on the other surface where acidic molecules should be adsorbed (i.e., the a surface); the Boltzmann distribution between the two manners of adsorption is not extremely biased towards one of them with this neutral protein (see Introduction in Part II[2]). Slight increases in $m_{elu(KCl)}$ in comparison with $m_{elu(K^+;KP)}$ were also observed for cytochrome c, haemoglobin, trypsinogen and RNase A (for details, see Part I[1]). This indicates that, even with basic proteins, a minor proportion of molecules are adsorbed on the crystal surface where acidic molecules should be adsorbed (i.e., the a surface). Parallel tendencies were reconfirmed in the preliminary experiment in the second sub-section of Results and also for fractions I and II of IgG in the double gradient experiment reported in Appendix II in Part II[2].

It should also be added that the chromatographic behaviour of proteins as a function of pI in the $CaCl_2$ system is fundamentally almost parallel to the behaviour in the KCl system (cf., Introduction in Part II[2]). Both myoglobin and trypsinogen, which behave as "basic" molecules in the KCl system, behave as "acidic" molecules in the $CaCl_2$ system, however[1]. Further, the adsorption of "acidic" proteins on the HA surface is generally stabilized in the presence of calcium ions in the mobile phase[1]. It can be suggested that, when a carboxyl group of the molecule has been adsorbed on a C site constructed with two crystal calcium ions (see Introduction), a calcium ion from the mobile phase is also fixed on the C site, completing a triangular array of calcium ions around the carboxyl group (cf., Fig. 1b). The structure constructed with three calcium ions and a carboxyl group would resemble the corresponding structure in the interior of the crystal occurring when one (or two) hydroxyl ion(s) is (are) replaced by a carbonic ion (cf., Introduction). On the basis of this mechanism, the adsorption of a carboxyl group on a C site would be stabilized in the presence of calcium ions in the mobile phase. It can also be suggested that the behaviour of both myoglobin and trypsinogen as "acidic" molecules in the presence of calcium ions in the mobile phase (see above) is intimately related to this adsorption mechanism.

APPENDIX II

The elution molarity, $m_{elu(P)}$ or μ, in gradient chromatography can be represented by eqn. 6 in Part II[2]. The parameter q in this equation [intimately related to the parameter $q_{app(P)}$ in Table I; cf., eqns. 15 and 15' in ref. 2], is defined by both eqns. 27 and 28 in ref. 18 as

$$q = An_0/V \tag{1}$$

where A is a positive constant, n_0 the total number of adsorbing sites (C or P) on the HA surfaces involved in an elementary volume of the column, and V the total volume of the interstitial part of the elementary volume [in ref. 18, q is written as $q_{(\rho')}$, however].

It can now be understood that, with both the coral HA packed column and the potato-like HA packed column, the n_0/V value with respect to P sites existing on the c surface of HA is much smaller than the corresponding value with respect to C sites existing on the a surface. On the basis of eqn. 6 in ref. 2, it can be shown that, in general, the elution molarity, $m_{elu(P)}$, decreases with decrease in the n_0/V value. It can also be shown that, provided that the $m_{elu(P)}$ value is kept within the same order of magnitude, the dependence of $m_{elu(P)}$ on n_0/V decreases with increase in x', which is also involved in eqn. 6 in ref. 2; when $x' = \infty$, then $m_{elu(P)}$ is independent of n_0/V. The decrease in the dependence of $m_{elu(P)}$ on n_0/V with increase in x' is intimately related to the fact that the transition of the B' value (cf., eqn. 5 in ref. 2) from ca. 0 to 1 that occurs with an increase in the phosphate or potassium molarity, $m_{(P)}$ or $m_{(K^+)}$, becomes sharp with an increase in x', provided that the transition occurs within a molarity range of the same order of magnitude (cf., Figs. 4–9 in ref. 2).

It can be seen in Table I that the x' values of 15.0–19.0 for "acidic" IgG are considerably larger than the corresponding values of 4.5–10.0 for the other "acidic" proteins, and that the x' values of 9.0–12.0 for "basic" IgGs are also considerably larger than the corresponding values of 4.3–6.5, for the other "basic" proteins. The theory gives a qualitative explanation for why the elution molarities of "basic" proteins other than IgG tend to decrease with both coral HA and potato-like HA (and also, perhaps, with "rose des sables"-like HA), and why the elution molarities of "acidic" proteins other than IgG and those of "basic" proteins other than IgG tend to approach each other with these HAs. The theory also explains why the elution profile of IgG with large x' values does not depend much on the type of HA used.

REFERENCES

1 T. Kawasaki, J. Chromatogr., submitted for publication.
2 T. Kawasaki, M. Niikura and Y. Kobayashi, J. Chromatogr., 515 (1990) 91.
3 M. I. Kay, R. A. Young and A. S. Posner, Nature (London), 204 (1964) 1050.

 4 K. Sudarsanan and R. A. Young, *Acta Crystallogr., Sect. B*, 25 (1969) 1534.

 5 J. C. Elliott, P. E. Mackie and R. A. Young, *Science*, 180 (1973) 1055.

 6 R. A. Young, *Colloq. Int. CNRS*, No. 230 (1973) 21.

 7 T. Kawasaki, *J. Chromatogr.*, 151 (1978) 95.

 8 T. Kawasaki, *J. Chromatogr.*, 157 (1978) 7.

 9 W. E. Brown, *Nature (London)*, 196 (1962) 1048.

10 D. R. Taves and R. C. Reedy, *Calcif. Tissue Res.*, 3 (1969) 284.

11 S. M. Krane and M. J. Glimcher, *J. Biol. Chem.*, 237 (1962) 2991.

12 K. Lonsdale, *Nature (London)*, 217 (1968) 56.

13 H. Monma, S. Ueno, M. Tsutsumi and T. Kanazawa, *Yogyo-Kagaku-Shi*, 86 (1978) 28.

14 M. Spencer, *J. Chromatogr.*, 166 (1978) 423.

15 T. Kawasaki, *Sep. Sci. Technol.*, 24 (1989) 1109.

16 T. Kawasaki and M. Niikura, *Sep. Sci. Technol.*, 25 (1990) in press.

17 T. Kawasaki, *Sep. Sci. Technol.*, 22 (1987) 121.

18 T. Kawasaki, *Sep. Sci. Technol.*, 23 (1988) 1105.

Titania and zirconia: possible new ceramic microparticulates for high-performance liquid chromatography

MASAHIRO KAWAHARA, HIROSHI NAKAMURA* and TERUMI NAKAJIMA

Department of Analytical Chemistry, Faculty of Pharmaceutical Sciences, University of Tokyo, 7–3–1, Hongo, Tokyo 113 (Japan)

ABSTRACT

The adsorptive properties of various new ceramics as column packing materials for high-performance liquid chromatography were evaluated by a newly developed method. Screening of many new ceramics revealed that titania and zirconia have much greater adsorption capacities than silica gel. The adsorptive properties of titania and zirconia columns were found to be different from those of silica gel in chromatography. Further, titania and zirconia proved to have a high resistance to both alkaline and acidic eluents. Applications of these new ceramics columns to the separation of biogenic substances were also studied.

INTRODUCTION

Silica gel and its derivatives have been the predominant column packing materials in modern liquid chromatography, owing to their high resolution[1]. However, their use is limited to the pH range 2.5–7.5 in view of the chemical stability of the silica gel matrices[2]. Recently, new ceramics have been introduced for diverse purposes, *e.g.*, as heat-resistant materials, sensor elements and mechanical parts, owing to their ability to withstand heat, mechanical shock and the effects of various chemicals[3]. The advantageous characteristics of the new ceramics indicate that they should also be usable as packing materials for high-performance liquid chromatography (HPLC). We previously evaluated the adsorptive properties of some new ceramics by determining their adsorption isotherms[4], which indicated that titania and zirconia are promising column packing materials. Therefore, columns of these two new ceramics were investigated for their separating abilities in adsorption chromatography, and applied to the separation of some biogenic substances. In this paper, the separation of ribonucleosides and deoxyribonucleosides on titania and zirconia columns are described.

EXPERIMENTAL

Materials

Reagents and solvents were of analytical-reagent grade. Silica gel (LiChrosorb Si 60, particle size 5 μm) was purchased from E. Merck (Darmstadt, F.R.G.). Zirconia (non-porous, mean particle size 3 μm) and titania (rutyl type, 1–2 μm) were purchased from Soekawa Chemical (Tokyo, Japan). Titania microbeads (anatase type, porous, pore volume 0.3 ml/g, surface area 45 m^2/g, particle size 5–15 μm) were kindly donated by Catalysts & Chemicals Industries (Tokyo, Japan). Ribonucleosides (adenosine, guanosine, cytidine and uridine) and deoxyribonucleosides (thymidine, 2'-deoxy-adenosine, 2'-deoxyguanosine, 2'-deoxycytidine and 2'-deoxyuridine) were purchased from Sigma (St. Louis, MO, U.S.A.).

Measurement of adsorption isotherms

The adsorption isotherms for p-hydroxybenzoic acid (p-HBA) in hexane–2-propanol (9:1) on the various ceramics were determined by the shake-flask method[4].

HPLC system

A Trirotar-VI (Jasco, Tokyo, Japan) HPLC system was used. The column packing materials were suspended in glycerol–methanol (1:1, v/v) and packed in a stainless-steel tube (100 mm × 4 mm I.D.) by the slurry packing method at a constant pressure of 450 kg/cm^2.

Endurance test

A 100-mg amount of each ceramic, silica gel (LiChrosorb Si 60, 5 μm), titania (microbeads, 5–15 μm) and zirconia (3 μm), was placed in a test-tube and 10 ml of either 1 or 0.1 M hydrochloric acid or 50 mM or 0.5 M sodium hydroxide solution were added. After the tube had been shaken at 40°C for 48 h, the solvent was removed by centrifuging at 1000 g for 10 min. The resulting residue was washed with distilled water followed by a similar centrifugation. After the ceramic material had been dried at 110°C for 2 h, it was weighed.

RESULTS AND DISCUSSION

Evaluation of ceramics

The adsorption isotherms of the various ceramics were measured and the amount of p-HBA adsorbed per unit weight of the adsorbent (C_S, nmol/mg) and the concentration of p-HBA in the supernatant (C_M, μM) were determined. The adsorption isotherms in the liquid phase are commonly represented by either the Henry equation (eqn. 1), the Langmuir equation (eqn. 2) or the Freundrich equation (eqn. 3)[5,6].

$$C_S = K_d C_M \tag{1}$$

where K_d is the distribution constant.

$$C_S = A Q_m C_M/(1 + A C_M) \tag{2}$$

where A is related to the affinity of the adsorbent and Q_m indicates the maximum capacity of the adsorbent. To determine these parameters, following two linearized forms are employed:

$$C_M/C_S = (1/Q_m)C_M + 1/(AQ_m) \qquad (2a)$$
$$1/C_S = (1/A)(1/Q_m)(1/C_M) + 1/Q_m \qquad (2b)$$

$$C_S = KC_M^{1/n} \qquad (3)$$

where K is the capacity of the adsorbent when $C_M = 1$ and n is related to both the adsorption activity and the distribution of adsorption points; a large value of n indicates a higher ratio of the adsorption points with larger heats of adsorption.

Fig. 1 shows the adsorption isotherms on silica gel, titania and zirconia analysed by the four isotherm quations. Table I gives the values of the parameters and the correlation coefficients (r) of these four isotherms. It was found that these isotherms were best fitted by the Freundrich equation (eqn. 3). The Freundrich equation also gave good representation for other ceramics. Therefore, the adsorptive properties of
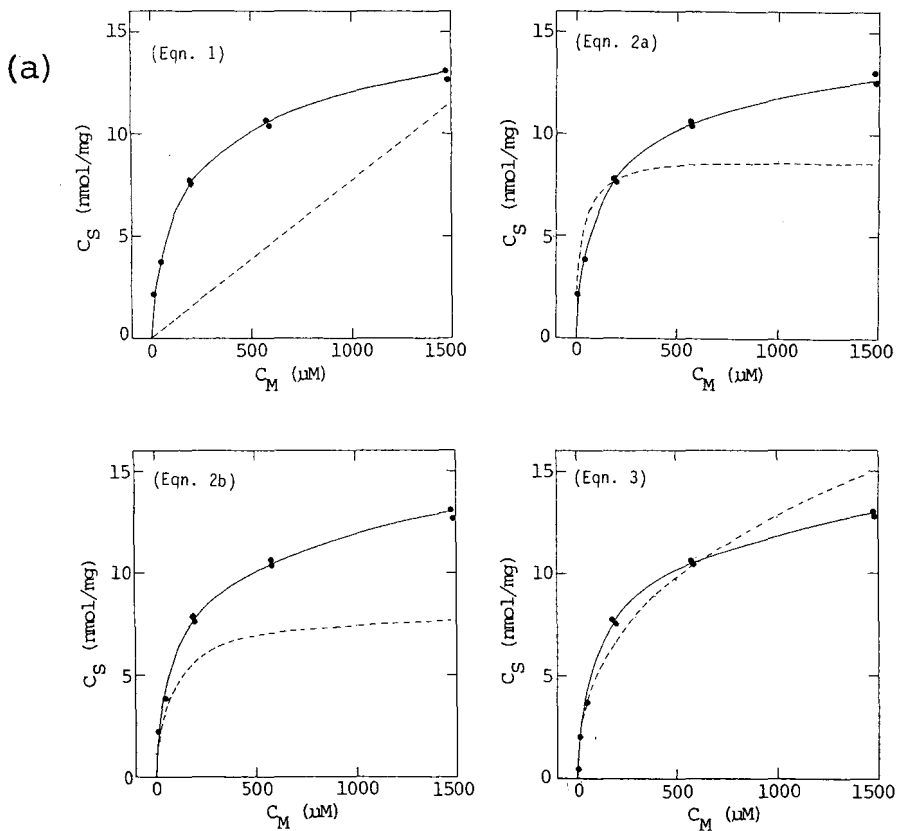
Fig. 1.

the ceramics were subsequently determined from the parameters of the Freundrich equation. As shown in Table I, the values of the capacity parameter K for silica gel (LiChrosorb Si 60), titania and ziconia were 0.567, 12.1 and 15.0, respectively, and the values of the activity parameter n were 2.16, 3.79 and 4.14, respectively. These results indicate that titania and zirconia have much larger adsorption capacities than silica gel. The rutyl type of titania showed a smaller adsorption capacity than the anatase type employed in this work.

Further, titania and zirconia were found to possess a high resistance to both alkaline and acidic eluents (Table II). These two new ceramics did not dissolve in either 1 M hydrochloric acid or 0.5 M sodium hydroxide solution on shaking at 40°C for 48 h, whereas silica gel dissolved completely in 0.5 M sodium hydroxide solution.

Separation profiles of titania and zirconia

Titania and zirconia were packed into columns (100 mm × 4 mm I.D.) and their properties in adsorption chromatography were investigated. In Fig. 2, the values of the capacity factor (k') of methyl paraben in eluents with various ratios of hexane and 2-propanol were compared using the three columns. These results indicate that titania and zirconia columns also act as adsorbents in normal-phase chromatography, and
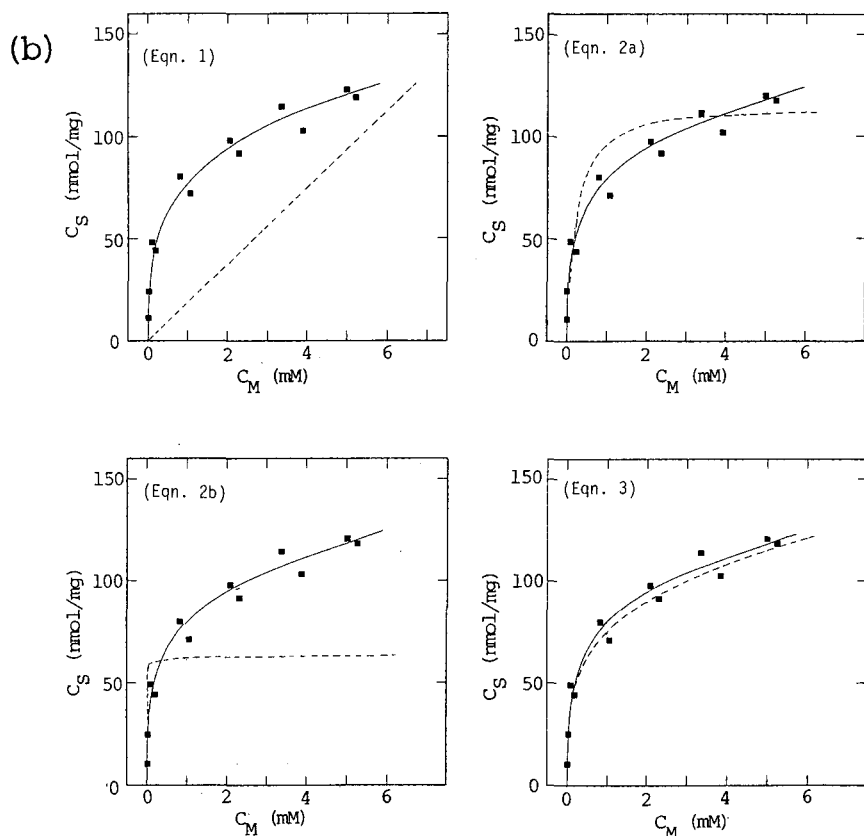
Fig. 1.

that the adsorption was greater on the zirconia column than on the titania and silica gel columns, which is supported by the values of the parameter K in the Freundrich equation. However, the effect of water was severe on the zirconia column and the k' value was found to become small with an eluent containing even a small amount of water.

Fig. 3 shows the separation profiles of parabens with hexane–2-propanol–water (95:4.5:0.5) as eluent on silica gel, titania and zirconia columns. In all instances hexyl, propyl and methyl paraben were eluted in that order. These results suggest that titania and zirconia are actually usable as column packing materials. The recoveries with titania and zirconia seemed to be almost the same as that with silica gel, judging from the peak areas of the solutes. The theoretical plate numbers measured with methyl paraben for silica gel, titania and zirconia were 56 000, 12 000 and 11 000 per metre, respectively. The column efficiencies of titania and zirconia are expected to be improved by using uniform and smaller particle sizes.

The capacity factors (k') of various compounds were compared under the above elution conditions and it was found that the elution order of acidic compounds and
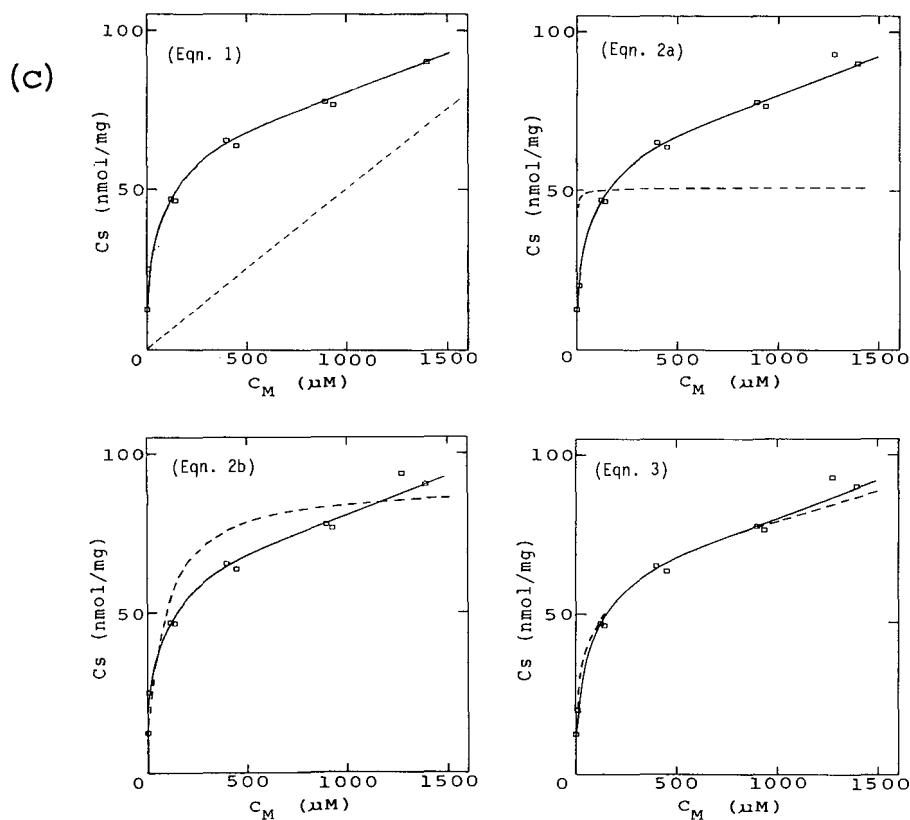
Fig. 1. Adsorption isotherms of (a) silica gel, (b) titania and (c) zirconia as analysed by the four equations. Solid lines, experimental isotherms; dashed lines, theoretical isotherms.

TABLE I

SUMMARY OF PARAMETERS OF ISOTHERM EQUATIONS

Material	Henry (eqn. 1)		Langmuir (eqn. 2a)			Langmuir (eqn. 2b)			Freundrich (eqn. 3)		
	K_d (l/g)	r	A	Q_m ($nmol/mg$)	r	A	Q_m ($nmol/mg$)	r	K	n	r
Silica gel (Lichrosorb Si 60)	$7.77 \cdot 10^{-3}$	0.874	$3.62 \cdot 10^{-2}$	8.89	0.986	$1.18 \cdot 10^{-2}$	8.04	0.996	$5.67 \cdot 10^{-1}$	2.16	0.980
Titania	$1.88 \cdot 10^{-2}$	0.893	$4.56 \cdot 10^{-3}$	117	0.987	$3.21 \cdot 10^{-1}$	61.3	0.914	12.1	3.79	0.992
Zirconia	$5.17 \cdot 10^{-2}$	0.926	$8.57 \cdot 10^{-1}$	50.8	0.856	$1.26 \cdot 10^{-2}$	90.6	0.989	15.0	4.14	0.997

TABLE II

RESULTS OF ENDURANCE TEST ON NEW CERAMICS

Material	Recovery (%)[a]			
	1 M HCl	0.1 M HCl	0.05 M NaOH	0.5 M NaOH
Silica gel	95.5	96.3	73.0	0
Titania	100	99.0	98.2	101
Zirconia	100	99.5	100	101

[a] After shaking in 10 ml of the medium at 40°C for 48 h.

basic compounds was reversed on titania and zirconia columns, *i.e.*, acidic compounds eluted later than basic compounds[7]. This suggests that the adsorption mechanisms with titania and zirconia are different from that with silica gel. This effect should be advantageous in the analysis of basic compounds, which show peak tailing on the usual silica-based columns owing to anionic free silanol groups.

It was possible to use titania and zirconia columns with water-rich eluents such as acetonitrile–water. Table III gives the k' values for various compounds using acetonitrile–water (97.5:2.5) as eluent on silica gel, titania and zirconia columns. The results also indicate that the elution order of pyridine and phenol is reversed on titania and zirconia columns. Further, the k' values of three similar compounds, caffeine, theophylline and theobromine, were very different on the titania and silica gel columns. These unique adsorptive properties of titania and zirconia may be useful in the separation of compounds that are difficult to separate on the usual column packings. Therefore, titania and zirconia columns were applied to the separation of biogenic substances, including nucleosides.

Fig. 4 shows the separation profiles of a mixture of ribonucleosides (uridine,
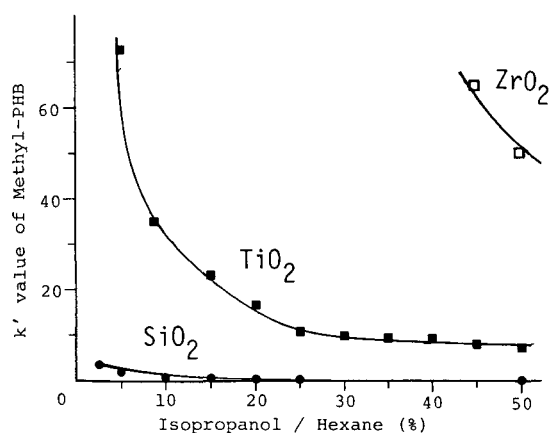
Fig. 2. k' Value of methyl paraben as a function of 2-propanol concentration in hexane (eluent). Column, 100 mm × 4 mm I.D.; column temperature, 40°C; flow-rate, 0.5 ml/min. ● = Silica gel; ■ = titania; □ = zirconia.
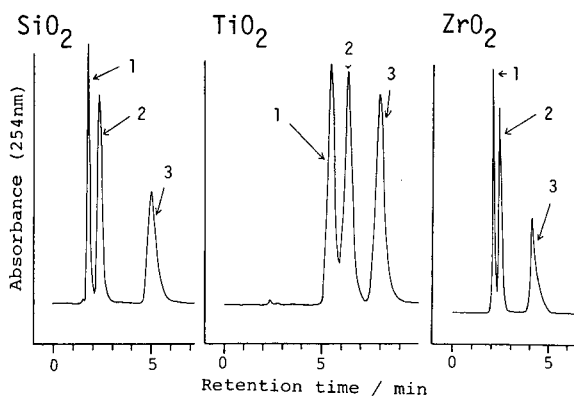
Fig. 3. Chromatograms of parabens on (a) silica gel, (b) titania and (c) zirconia columns. Column 100 mm × 4 mm I.D.; column temperature, 40°C; flow-rate, 0.5 ml/min; eluent, hexane–2-propanol–water (95:4.5:0.5). Peaks: 1 = hexyl paraben; 2 = propyl paraben; 3 = methyl paraben.

guanosine, cytidine and adenosine) and deoxyribonucleosides (thymidine, 2′-deoxy-uridine, 2′-deoxycytidine, 2′-deoxyguanosine and 2′-deoxyadenosine) with gradient elution from acetonitrile to 20% acetonitrile on silica gel, titania and zirconia columns. Although, deoxyribonucleosides were eluted rapidly from the titania and zirconia columns as sharp peaks, ribonucleosides were adsorbed strongly and were eluted later as broad peaks. However, ribonucleosides and deoxyribonucleosides eluted at similar retention times on the silica gel column. On the titania column, ribonucleosides and deoxyribonucleosides were also separated with 2 mM Tris–HCl buffer (pH 7.0) as the eluent[8]. It is noteworthy that ribonucleosides and deoxyribonucleosides have very similar structures, differing only in the 2′-positions of the sugar moieties, but their behaviours on titania and zirconia are obviously different. This suggests the possibility of chelation of Ti^{IV} or Zr^{IV} to compounds having a vicinal hydroxyl group. Some kinds

TABLE III

k' VALUES OF VARIOUS COMPOUNDS ON THE THREE COLUMNS

Column, 100 mm × 4 mm I.D.; column temperature, 40°C; eluent, acetonitrile–water (97.5:2.5); flow-rate, 1.0 ml/min.

Compound	Column		
	Silica gel	Titania	Zirconia
Benzene	0.00	0.00	0.00
Phenol	0.03	2.81	0.32
Pyridine	1.00	0.36	0.05
Aniline	0.08	0.10	0.02
Methyl paraben	0.08	12.5	2.39
Caffeine	1.24	0.25	0.05
Theophylline	1.97	>30	2.44
Theobromine	2.56	20.0	11.3
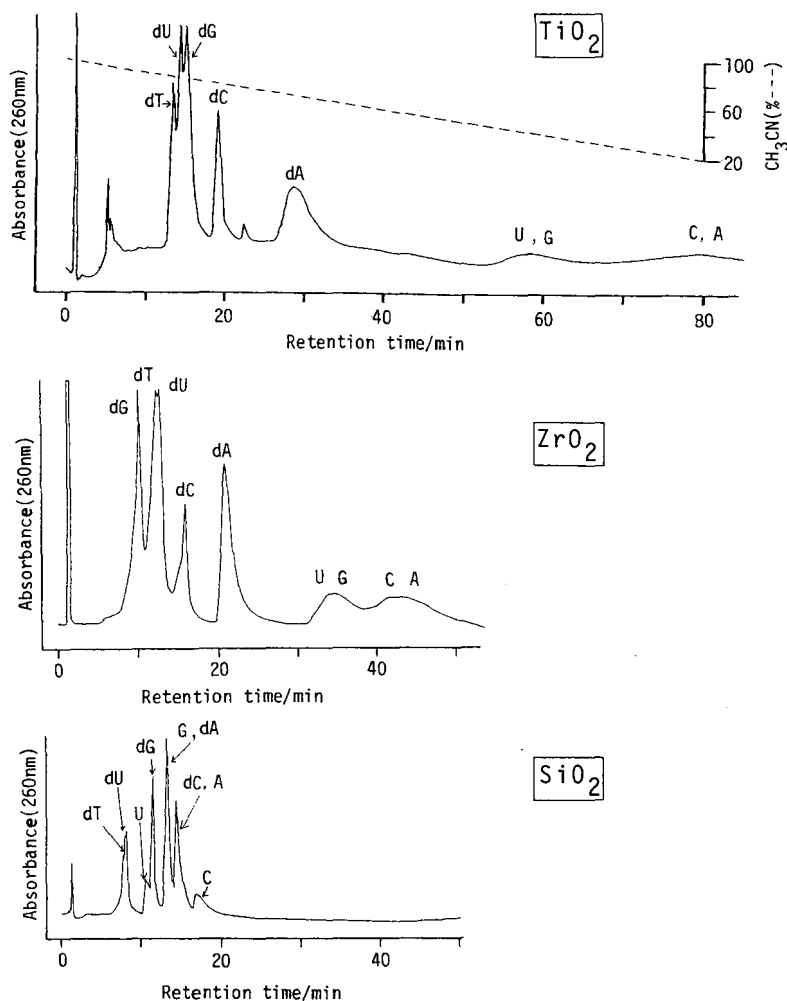
Fig. 4. Chromatograms of nucleosides on (a) titania, (b) zirconia and (c) silica gel columns. Column, 100 mm × 4 mm I.D.; column temperature, 40°C; flow-rate, 1.0 ml/min; eluent A, acetonitrile; eluent B, acetonitrile–water (20:80); elution programme, linear gradient from eluent A to B in 80 min. Peaks: dT = thymidine; dU = 2'-deoxyuridine; dG = 2'-deoxyguanosine; dC = 2'-deoxycytidine; dA = 2'-deoxyadenosine; U = uridine; G = guanosine; C = cytidine; A = adenosine.

of boronate gels[9-11] have been employed both for the group separation of ribonucleosides and deoxyribonucleosides and for the enrichment of compounds having a vicinal hydroxy group. Investigations on the adsorption mechanisms of titania and zirconia are now in progress, including the relationship between crystallographic and chromatographic properties.

In conclusion, new titania and zirconia ceramics have been found to have at least three advantages as column packing materials for modern LC: (1) titania and zirconia possess a high resistance to both alkaline and acidic eluents; (2) they show unique adsorption profiles, adsorb acidic compounds strongly rather than basic compounds;

and (3) they easily permit the separation of compounds such as ribonucleosides and deoxyribonucleosides which are not separable on the usual column packings.

The titania and zirconia columns are also expected to be useful in a two-dimensional HPLC separation system in combination with a different separation mode such as reversed-phase HPLC on ODS-silica. Application of the new ceramics to the separation of various biogenic substances will be reported in the near future.

ACKNOWLEDGEMENTS

REFERENCES

1 W. S. Hancock and J. T. Sparrow, *HPLC Analysis of Biological Compounds*, Marcel Dekker, New York, 1984.
2 J. L. Glajch, J. J. Kirkland and J. Kohler, *J. Chromatogr.*, 384 (1987) 81.
3 G. Adachi, K. Sibayama and T. Minami (Editors), *Sentanbunnya ni Okeru Zairvo Gijyutu*, Kagaku Doujin, Kyoto, 1984.
4 M. Kawahara, H. Nakamura and T. Nakajima, *Anal. Sci.*, 4 (1988) 671.
5 J.-X. Huang and C. Horváth, *J. Chromatogr.*, 406 (1987) 285.
6 P. K. Gessner and M. M. Hasan, *J. Pharm. Sci.*, 76 (1987) 319.
7 M. Kawahara, H. Nakamura and T. Nakajima, *Anal. Sci.*, 5 (1989) 485.
8 M. Kawahara, H. Nakamura and T. Nakajima, *Anal. Sci.*, 5 (1989) 763.
9 M. Glad and S. Ohlson, *J. Chromatogr.*, 200 (1980) 254.
10 E. H. Pfadenhauer and S.-D. Tong, *J. Chromatogr.*, 162 (1979) 585.
11 S. Hjerten and D. Yang, *J. Chromatogr.*, 316 (1984) 301.

CHROMSYMP. 1867

Effect of pore size on the surface excess isotherm of silica packings

KAZUE TANI* and YOSHIHITO SUZUKI

Faculty of Engineering, Yamanashi University, Takeda 4–3–11, Kofu 400 (Japan)

ABSTRACT

Silicas with pore diameters ranging from 100 to 300 Å were used as packing materials in order to evaluate the surface excess isotherms of organic modifiers in binary aqueous systems. The method is based on the measurement of the retention volumes of labelled components of the eluent. The isotherms obtained were compared with each other in order to investigate the effect of pore size on the surface excess isotherm.

INTRODUCTION

The study of chemically modified surfaces for use in liquid chromatography is a matter of great interest. A variety of techniques for probing chemically modified surfaces have been employed, including fluorescence[1], infrared[2–5], and nuclear magnetic[5–10] spectrometry. Information obtained by these techniques has provided important insights into surface–ligand structures and interactions, bonded layer solvation and segmental and total chain mobility.

It is well known that the organic solvent is enriched in the bonded phase in reversed-phase liquid chromatography. The amount of enriched modifier can be determined as the surface excess amount. The surface excess amount of a given component is defined as the difference between the amount of component actually present in the system and that which would be present in a reference system if the bulk concentrations in the adjoining phases were maintained up to a chosen geometrical dividing surface[11]. Therefore, the surface excess amount can be used as a measure of the comparison of the chemically modified surface. The surface excess isotherm is accessible to direct experimental determination. General relationships for calculating the surface excess amount from chromatographic retention data were given by Riedo and Kováts[12]. Chromatographic methods to determine the surface excess isotherms were based on measurements of the retention volumes of concentration steps (frontal analysis)[13–15] and labelled components of the eluent[16] and solvent disturbance peaks[17–19].

In order to make it possible to use the surface excess isotherm as a measure of the comparison of chemically modified surfaces with various pore sizes, it is necessary to

investigate the influence of pore size on the surface excess isotherm. In this work, we explored whether the pore sizes of column packings influence their surface excess isotherms or not. The silicas were used as packing materials in order to investigate the net effect of the pore size on the exclusion of the chemically bonded phase. The surface excess isotherms of organic modifiers on these packings were evaluated in binary aqueous systems. The method was based on measurements of the retention volumes of labelled components of the eluent.

EXPERIMENTAL

Apparatus

The liquid chromatograph was constructed from a Model 880-UP pump (Jasco, Tokyo, Japan), a Rheodyne Model 7125 injector and a Shodex RI SE-51 differential refractive index detector (Showa Denko, Tokyo, Japan). A constant-temperature water-bath (Model TM108M; Toyo, Tokyo, Japan) was used to maintain the column temperature, which was measured with an alumel–chromel thermocouple. The chromatograms were recorded on a Chromatopac CR1A (Shimadzu, Kyoto, Japan).

Chemicals and materials

Liquid chromatographic grade solvents and deuterated compounds were obtained from Nacalai Tesque (Kyoto, Japan). Silicas with pore diameters ranging from 100 to 300 Å were used as packing materials. The silicas used were Vydac 101TPB (300 Å) (Separation Group, Hesperia, CA, U.S.A.) and Shiseido's silicagel (120 and 300 Å) and Super Micro Bead silica gel (100, 150 and 300 Å) (Fuji-Davison Chemical, Kasugai, Japan). They were packed by means of the balanced slurry technique into 250 × 4.6 mm I.D. stainless-steel tubes in our laboratory. Data on the column packings are summarized in Table I.

TABLE I

PHYSICAL PROPERTIES OF SILICA MATERIALS

Silica	Particle diameter (μm)	Pore diameter ($\mathring{A}$)	Area (m^2/g)	Pore volume (ml/g)	pH
Super Micro Bead[a]					
100 Å	5.9	108	385	1.04	5.1
150 Å	5.7	167	181	1.08	5.7
300 Å	5.1	321	95	1.07	5.6
Shiseido's silica gel[b]					
120 Å	5	124	264	0.80	
300 Å	5	274	168	1.39	
Vydac 101TPB[b]					
	5	303	75	0.59	

[a] Data provided by manufacturer.
[b] Data determined by Y. Shiojima of Shiseido.

Procedures

The retention volumes of labelled components of the eluent were obtained from the flow-rate and retention time, t_R. The nominal flow-rate used throughout the study was 1 ml/min. The actual flow-rate was measured by collecting the column eluent in a 10-ml volumetric flask and recording the collection time. The sample concentration was chosen to be as low as possible while maintaining a suitable signal-to-noise ratio in refractive index detection. Eluents of appropriate compositions were prepared by weighing. The column materials were removed from each column after chromatographic measurements and washed with methanol, dried under reduced pressure and weighed.

Surface excess amounts

Quantitative definitions for the adsorption of binary liquid mixtures at solid–liquid interfaces in terms of surface excess amounts were given by Everett[11]. Riedo and Kováts[12] derived general relationships for calculating their surface excess amounts from chromatographic retention data.

The necessary expressions for calculating points on the adsorption isotherms are taken from ref. 12. The surface concentration of component 2 is given by

$$\Gamma_2^{(n)} = (V_{R,2^*} - V_{R,1^*})x_2^l x_1^l / S v_m \tag{1}$$

where $\Gamma_2^{(n)}$ is the areal reduced surface excess of component 2 and x_1^l and x_2^l are the mole fraction of components 1 and 2 in the eluent. V_R is the retention volume, S is the surface area of silica and v_m is the mean molar volume of the eluent at

$$v_m = v_1 x_1^l + v_2 x_2^l \tag{2}$$

the composition x_1^l, and v_1 and v_2 are the partial molar volumes of components 1 and 2. The asterisk refers to labelled components of the element, 1* or 2*. The areal reduced surface excess of component 1 is

$$\Gamma_1^{(n)} = -\Gamma_2^{(n)} \tag{3}$$

Layer model

When dealing with an actual system, it is not sufficient to obtain the surface excess isotherm, because it only represents the total change of the system and does not refer to the actual amount of a component present in the mobile phase and adsorbed phase. Therefore, the layer model[11] was used to calculate the composition of the adsorbed phase and determine the absolute amount adsorbed.

Assuming that the adsorbed phase consists of t layers of molecules on a plane smooth homogeneous surface, the mole fraction, x_2^s, of component 2 in the surface phase is given by

$$x_2^s = \frac{t x_2^l + a_1^0 \Gamma_2^{(n)}}{t - (a_2^0 - a_1^0)\Gamma_2^{(n)}} \tag{4}$$

TABLE II

VALUES OF t_{min} SATISFYING THE CRITERIA

Silica	t_{min}	
	CH_3CN-H_2O	CH_3OH-H_2O
Super Micro Bead:		
100 Å	3	1
150 Å	3	1
300 Å	3	1
Shiseido's silica gel:		
120 Å	3	1
300 Å	3	1
Vydac 101TPB		
	5	2

where a_1^0 and a_2^0 are the molar cross-sectional areas of components 1 and 2, which can be calculated from the molar volumes, v_1 and v_2, using the equation $a_i^0 = 9200(v_i)^{2/3}$, $(i=1,2)$. Using these a_i^0 values and the experimental surface excess data, $\Gamma_2^{(n)}$, the minimum number of layers, t_{min}, was calculated by satisfying the criteria that the values of x_2^s calculated do not exceed unity, and x_2^s always increased with x_2^l, i.e., $(\partial x_2^s / \partial x_2^l) > 0$. The values of t_{min} are given in Table II. x_2^s was calculated using eqn.

Fig. 1. Surface excess amount of acetonitrile adsorbed at 30°C from an aqueous mixture on Super Micro Bead silica gel plotted against the mole fraction of acetonitrile. Pore size: ● = 100 Å; ○ = 150 Å; ◆ = 300 Å.

4 with values of t_{min}. In this study, components 1 and 2 correspond to water and organic modifier, respectively.

RESULTS AND DISCUSSION

The method of calculation of adsorption isotherms is based on the existence of solutes which are in every respect identical with components of the eluent with the exception of one property permitting their detection. These solutes were approximated by deuterated compounds, which we used as the solutes in this study although it is certainly not true that they are in every respect identical with non-deuterated compounds.

Acetonitrile–water and methanol–water systems were studied on six column packings at 30°C. In Figs. 1–4, the areal reduced surface excess amounts are plotted against the mole fraction, x_2^l. The negative values of the surface excess amount mean that the adsorbed phase on the silica surface holds a much larger amount of water than the mobile phase. It can be seen from Figs. 1–4 that the value of the surface excess amount is similar among the column packings from the same manufacturer. These results do not reveal a distinct effect of pore size on the surface excess isotherm. It seems reasonable to assume that the difference in pore size has no influence on the surface excess isotherm. It is necessary to take into account the pore distribution and structure. However, the effect of pore distribution might be negligible because the pore size of the silica materials used in this study extends from 100 to 300 Å. With regard to pore structure, it is not apparent whether it influences the surface excess isotherm or not, because there is no information relating to the pore structure. Figs. 5 and 6 show the surface excess isotherms of silicas with pore size 300 Å from different manufacturers. The results suggests that the surface excess isotherm is influenced by the
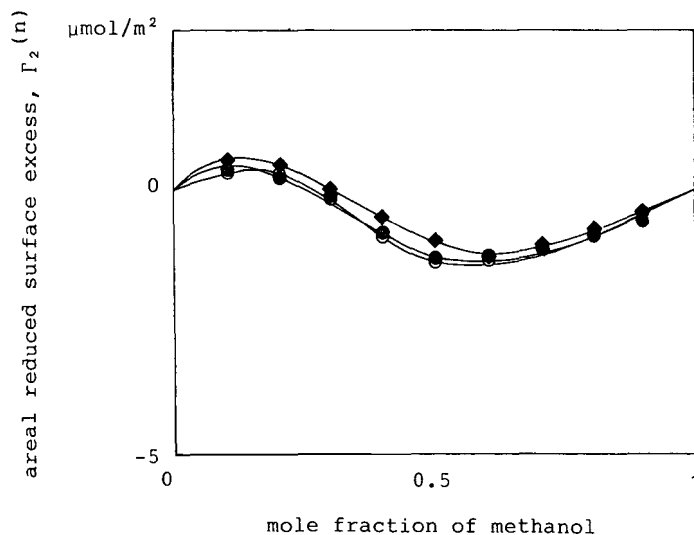
Fig. 2. Surface excess amount of methanol adsorbed at 30°C from an aqueous mixture on Super Micro Bead silica gel plotted against the mole fraction of methanol. Symbols as in Fig. 1.
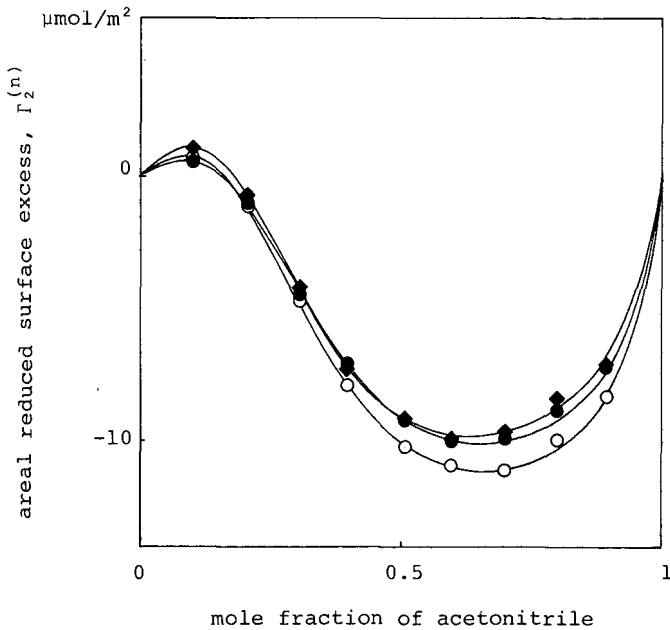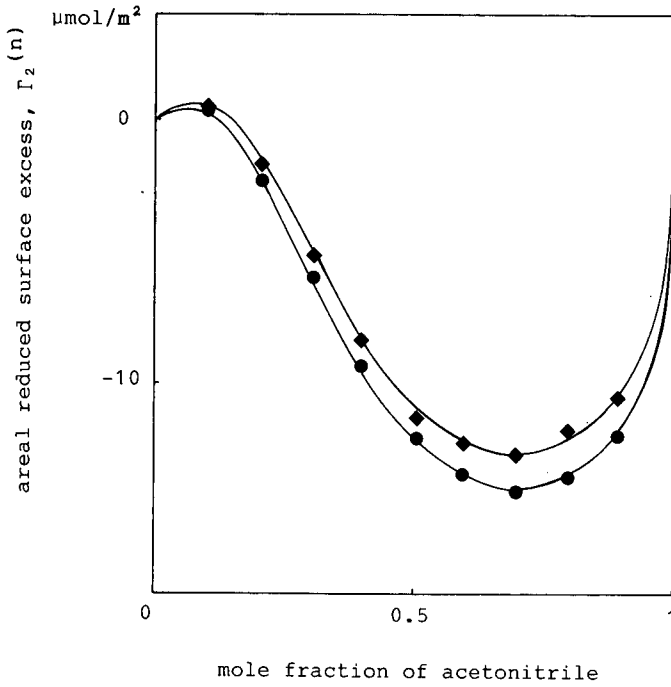
Fig. 3. Surface excess amount of acetonitrile adsorbed at 30°C from an aqueous mixture on Shiseido's silica gel plotted against the mole fraction of acetonitrile. Pore size: ● = 120 Å; ◆ = 300 Å.
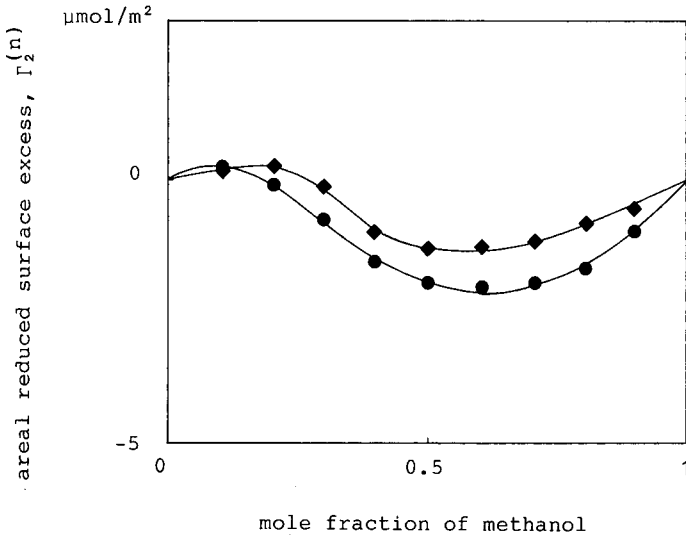
Fig. 4. Surface excess amount of methanol adsorbed at 30°C from an aqueous mixture on Shiseido's silica gel plotted against the mole fraction of methanol. Symbols as in Fig. 3.
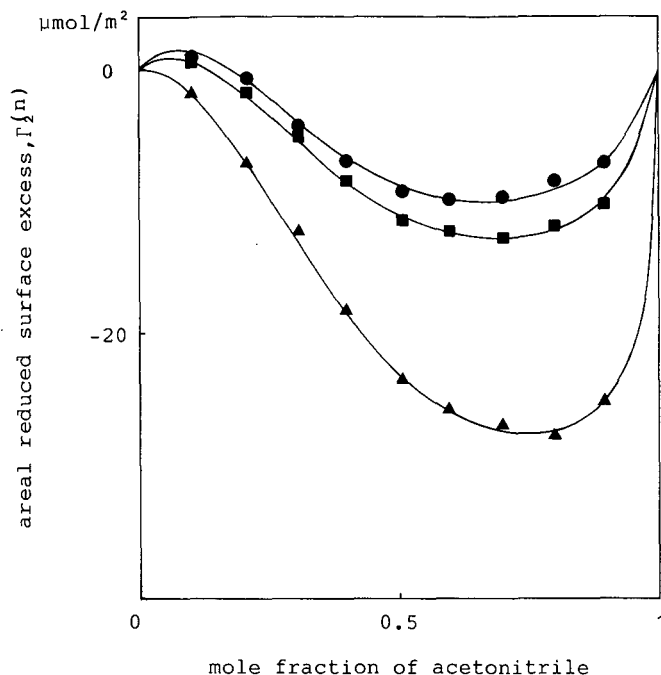
Fig. 5. Surface excess amount of acetonitrile adsorbed at 30°C from an aqueous mixture on silicas with pore size 300 Å plotted against the mole fraction of acetonitrile. ●, Super Micro Bead silica gel; ■, Shiseido's silica gel; ▲, Vydac 101TPB.

substrate rather than pore size. It seems that the difference in the substrate is based on the number of the silanol groups, which plays an important role in the adsorption of water from an aqueous mixture on the silica surface, or the difference in the pore structure. Vydac 101TPB, which shows a large surface excess amount as can be seen in Figs. 5 and 6, is presumed to have a larger number of the silanol groups than the other packing materials, or a unique pore structure. Similarly, the values of t_{min} given in Table II are greater on Vydac 101TPB than on the other silicas. The compositions of the adsorbed phase on the silica surfaces are given by eqn. 4. The data for the silicas with pore size 300 Å are given in Tables III and IV. The mole fractions of organic modifier in the adsorbed phase on Super Micro Bead silica gel, Shiseido's silica gel and Vydac 101TPB decrease in that order, regardless of the pore diameter, and are smaller than those in the mobile phase except for a few values, as shown in Tables III and IV. Comparison of these data indicates that the silica substrates are significantly different from one another.

Comparison of Fig. 1 with Fig. 2 or Fig. 3 with Fig. 4 indicates that the surface excess amount of water is much greater in aqueous acetonitrile than in aqueous methanol. In previous work[20], we found that acetonitrile was more preferentially adsorbed on the chemically modified surface than methanol in aqueous mixtures. These results and the values of t_{min} given in Table II indicate the difference in the miscible states between the acetonitrile–water and methanol–water systems. In the
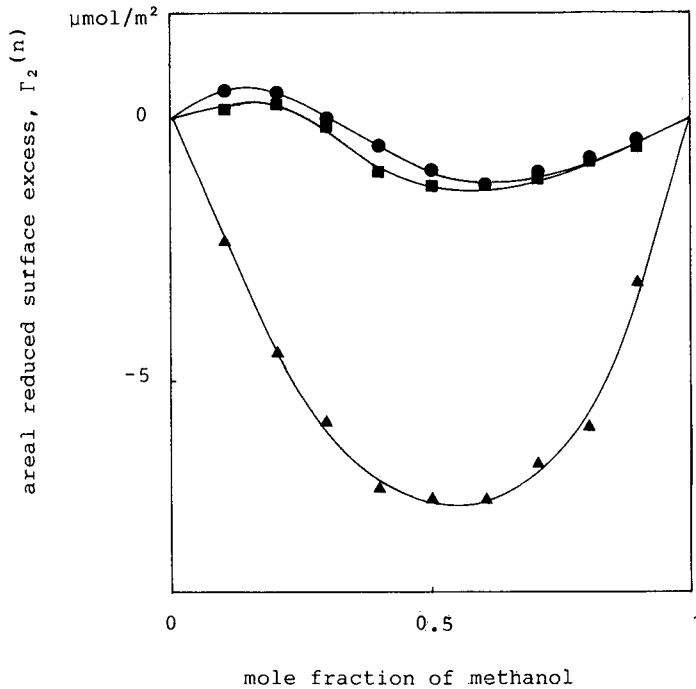
Fig. 6. Surface excess amount of methanol adsorbed at 30°C from an aqueous mixture on silicas with pore size 300 Å plotted against the mole fraction of methanol. Symbol as in Fig. 5.

acetonitrile–water system, the weak association between acetonitrile and water seems to promote the adsorption of water on the silica surface or acetonitrile on the chemically modified surface because silica has a strong affinity for water through hydrogen bonding with silanol groups, and the chemically modified surface prefers an

TABLE III

COMPOSITION OF THE ADSORBED PHASE ON THE SILICAS WITH PORE SIZE 300 Å FOR THE ACETONITRILE (2)–WATER (1) SYSTEM

x_2^l	x_2^s		
	Super Micro Bead	Shiseido's silica gel	Vydac 101 TPB
0.893	0.643	0.544	0.432
0.798	0.524	0.435	0.327
0.697	0.407	0.334	0.263
0.595	0.317	0.265	0.201
0.506	0.260	0.213	0.160
0.397	0.210	0.185	0.133
0.305	0.198	0.176	0.128
0.205	0.186	0.162	0.105
0.099	0.124	0.110	0.074

TABLE IV

COMPOSITION OF THE ADSORBED PHASE ON THE SILICAS WITH PORE SIZE 300 Å FOR THE METHANOL (2)–WATER (1) SYSTEM

x_2^l	x_2^s		
	Super Micro Bead	Shiseido's silica gel	Vydac 101TPB
0.898	0.856	0.842	0.746
0.805	0.734	0.724	0.545
0.706	0.611	0.599	0.433
0.603	0.493	0.493	0.320
0.500	0.420	0.393	0.233
0.398	0.357	0.319	0.151
0.297	0.298	0.286	0.103
0.202	0.237	0.222	0.056
0.103	0.139	0.115	0.028

organic solvent to water owing to the non-polarity of bonded hydrocarbon chains. In aqueous methanol, the low surface excess amount might be due to keeping a strongly associated state of methanol and water as a result of strong hydrogen bonding.

In conclusion, the data obtained from this study suggest that the surface excess isotherm on the silica surface was influenced by the substrate itself rather than pore size. This means that the surface excess isotherm can be used as a measure of the comparison of chemically modified surfaces. Further, the surface excess isotherm reflects the difference of the miscible states between acetonitrile–water and methanol–water systems. Therefore, the comparison of isotherms may be useful in studying the state of binary mobile phases.

REFERENCES

1 C. H. Lochmüller, A. S. Colborn, M. L. Hunnicutt and J. M. Harris, *Anal. Chem.*, 55 (1983) 1344–1348.
2 B. R. Suffolk and R. K. Gilpin, *Anal. Chem.*, 57 (1985) 596–601.
3 B. R. Suffolk and R. K. Gilpin, *J. Chromatogr. Sci*, 24 (1986) 423–426.
4 L. C. Sander, J. B. Callis and L. R. Field, *Anal. Chem.*, 55 (1983) 1068–1075.
5 D. E. Leyden, D. . Kendall, L. W. Burggraf, F. J. Pern and M. DeBello, *Anal. Chem.*, 54 (1982) 101–105.
6 M. E. Gangoda and R. K. Gilpin, *J. Magn. Reson.*, 53 (1983) 140–143.
7 R. K. Gilpin and M. E. Gangoda, *Anal. Chem.*, 56 (1984) 1470–1473.
8 R. K. Gilpin and M. E. Gangoda, *J. Magn. Reson.*, 64 (1985) 408–413.
9 M. E. Gangoda, R. K. Gilpin and B. M. Fung, *J. Magn. Reson.*, 74 (1987) 134–138.
10 J. J. Kirkland, J. L. Glajch and R. D. Farlee, *Anal. Chem.*, 61 (1989) 2–11.
11 D. H. Everett, *Pure. Appl. Chem.*, 58 (1986) 967–984.

12 F. Riedo and E. Sz. Kováts, *J. Chromatogr.*, 239 (1982) 1–28.
13 H. L. Wang, J. L. Duda and C. J. Radke, *J. Colloid Interface Sci.*, 66 (1978) 153–165.
14 F. Köster and G. H. Findenegg, *Chromatographia*, 15 (1982) 743–747.
15 C. S. Koch, F. Köster and G. H. Findenegg, *J. Chromatogr.*, 406 (1987) 257–273.
16 N. Le Ha, J. Ungvaral and E.sz. Kováts, *Anal. Chem.*, 54 (1982) 2410–2421.
17 R. M. McCormick and B. L. Karger, *Anal. Chem.*, 52 (1980) 2249–2257.
18 E. H. Slaats, W. Markovski, J. Fekete and H. Poppe, *J. Chromatogr.*, 207 (1981) 299–323.
19 J. H. Knox and R. Kaliszan, *J. Chromatogr.*, 349 (1985) 211–234.
20 K. Tani and Y. Suzuki, *J. Chromatogr. Sci.*, 27 (1989) 698–703.

CHROMSYMP. 1783

Copper(II)–iminodiacetic acid chelating resin as a stationary phase in the immobilized metal ion affinity chromatography of some aromatic amines

YU LIU and SHILIN YU*

Department of Applied Chemistry, Beijing Institute of Chemical Technology, 15 Beisanhuan East Road, Changyang District, Beijing 100029 (China)

ABSTRACT

Styrene–divinylbenzene copolymer 60–80 mesh was used as the matrix and ground to a reasonable particle size in a colloid mill. Small and uniform particles (5–15 μm) can be obtained in a laboratory-made continuous acetone elutriation device. After elutriation the iminodiacetic acid (IDA) chelating resin was synthesized, and the infrared spectrum of the product indicated that the synthetic reaction is effective. The Cu(II)-modified IDA chelating resin was used as a stationary phase in high-performance immobilized metal ion affinity chromatography, packed into a column by the high-pressure slurry-packing technique. Methanol, to which ammonia was added as a competitive ligand, was used as the mobile phase for the separation of aromatic amines. The retention value of aromatic amines depends mainly on their basicity and molecular size. The results showed that some aromatic amines can be separated with the Cu(II)–IDA column.

INTRODUCTION

Ligand-exchange chromatography or metal chelate affinity chromatography, which was introduced by Helfferich[1] and Porath and co-workers[2,3], was more recently renamed immobilized metal ion affinity chromatography (IMAC)[4,5]. It has been widely applied to the analysis of biomolecules such as amino acids, proteins and peptides[6–10], and also molecules of small size[11].

IMAC is a versatile separation method based on interfacial interactions between sample molecules in solution and metal ions fixed to a chelating ligand which is covalently coupled to a solid support. The simplest chelating ligand is iminodiacetic acid (IDA), bonded to an insoluble matrix of biological (agarose gel)[4], inorganic (silica gel)[6,7] or synthetic organic polymers (TSK gel G5000PW)[8–10], and relatively stable coordinate compounds with heavy metal ions are formed.

A buffer solution or salt solution is often used as the mobile phase in IMAC. In some instances, modifiers such as chelators, detergents or organic solvents may be added to the buffer to improve the chromatographic selectivity.

Shimomura *et al.*[12] used 200–400 mesh Chelex 100–Ni(II) as the stationary phase for the separation of aliphatic amines using classical column chromatography. In our work, an attempt was made to prepare IDA chelating resin on a styrene–divinylbenzene (S–DVB) copolymer matrix of small particle size (5–15 μm) using a new method. The Cu(II)-modified IDA chelating resin was used as the stationary phase in high-performance IMAC for the separation of aromatic amines.

EXPERIMENTAL

Apparatus

The grinding and elutriation of S–DVB copolymer were carried out in a Model JTM-50 colloid mill and a laboratory-made continuous elutriation device, respectively. The particle size was measured in a Model S-250 III scanning electron microscope. The identification of IDA resin was made by IR spectroscopy (Nicolet Model 60SX-B) and elemental analysis (Carlo Erba Model 1106 analyser). The adsorption properties of IDA resin for metal ions were determined by atomic absorption spectrometry (Model WFD-Y spectrometer). A slurry-packing apparatus (CHEMCO Model 124A) was employed for column packing. The chromatographic separations were carried out on a liquid chromatograph (Shimadzu Model LC-1) equipped with a reciprocating single-piston pump (Model LC-6A) and a UV detector (Model SPD-1, 254 nm).

Grinding and elutriation of S–DVB copolymer

The 60–80-mesh GDX-101 S–DVB copolymer was immersed in aqueous acetone for 30 min, then ground for 5 min twice in a colloid mill (160 V, a.c.). Finally, a suspension was obtained.

According to Stokes' law, particles of different size can be ranged by varying the velocity of a fluid[13,14]. Using a laboratory-made continuous acetone elutriation device (Fig. 1), narrow-sized fractions of S–DVB copolymer were obtained. As the flow-rate
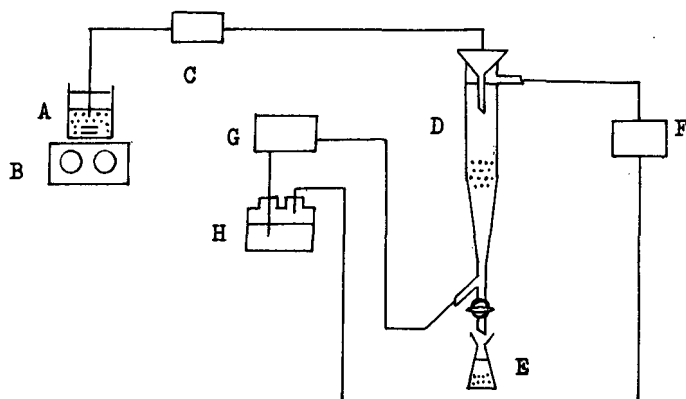
Fig. 1. Apparatus for continuous elutriation. A = Feed supply; B = magnetic stirrer; C = slurry pump; D = elutriation column; E = bottom product receiver; F = filter (overhead product receiver); G = peristaltic pump; H = acetone reservoir.

of acetone was 0.5 ml/min the small and uniform particles (5–15 μm) can be screened out.

Both the grinding and screening steps were examined by scanning electron microscopy.

Synthetic procedures for IDA–S–DVB chelating resin

The 5–15-μm GDX-101 was chloromethylated with chloromethyl methyl ether in the presence of anhydrous zinc(II) chloride. After washing and drying under vacuum, the chloromethylated copolymer (S–DVB–CH$_2$Cl) was immersed in dimethylformamide (DMF) for 4 h at room temperature, diethanolamine was added with gentle stirring at 110°C on oil-bath and reflux distillation was performed for 7 h. The gel [S–DVB–CH$_2$N(CH$_2$CH$_2$OH)$_2$] was filtered on a Buchner funnel and washed with 5% dilute hydrochloric acid, water and 95% ethanol, sucked dry and then returned to the reaction flask. At 50°C, 33% nitric acid containing a small amount of iron(III) chloride was added to the gel in the reaction flask, with slow stirring, followed by reflux distillation for 4 h at 95°C. The product gel (IDA–S–DVB chelating resin) was cooled, washed thoroughly on a Buchner funnel with water until the washings were neutral, then washed again with 95% ethanol and dried at room temperature.

Preparation of Cu(II)–IDA column

The IDA chelating resin in a methanol–butanol–carbon tetrachloride (5:10:25) slurry was packed into a 250 mm × 2 mm I.D. stainless-steel column by the high-pressure slurry packing technique.

First the column was washed with methanol, then copper(II) ions were loaded on the column by pumping 0.01 M copper nitrate solution at 0.5 ml/min. The copper nitrate solution was equilibrated with the chelating resin for 4 h. In order to ensure no leakage of metal ion in the experimental work, the column was washed with methanol to removing excess copper(II).

RESULTS AND DISCUSSION

The infrared spectrum of the product [S–DVB–CH$_2$N(CH$_2$COOH)$_2$, IDA] (Fig. 2) shows the strongest hydroxyl stretching absorption peak at 3435 cm^{-1}, a strong carbonyl stretching absorption peak at 1700 cm^{-1}, a stronger C–N stretching band around 1170 cm^{-1} and a weak C–O stretching band around 1420 cm^{-1}. Therefore, it was concluded that the synthetic reaction is effective.

The elemental composition of IDA resin is C 59.55, H 7.89, N 2.69 and O 29.87%. The functional group (IDA) content calculated from elemental analysis is 2.11 mmol/g (S–DVB).

The IDA chelating resin can absorb many divalent metal ions. The absorption capacity (at pH 5) for Cu^{2+}, Ni^{2+}, Co^{2+} and Zn^{2+} is 2.00, 1.18, 0.75 and 0.61 mmol/g, respectively. The rate of chelation between IDA resin and metal ions is so rapid that chemical equilibrium, under operating conditions, can almost be attained in 5 min.

The distribution coefficient of Cu^{2+} on the IDA resin increases with increasing pH, but at higher pH (>6), the distribution coefficient decreases rapidly with increasing pH owing to the formation of an amino complex. The ionic strength of the solution does not affect the distribution coefficient because the IDA resin possesses
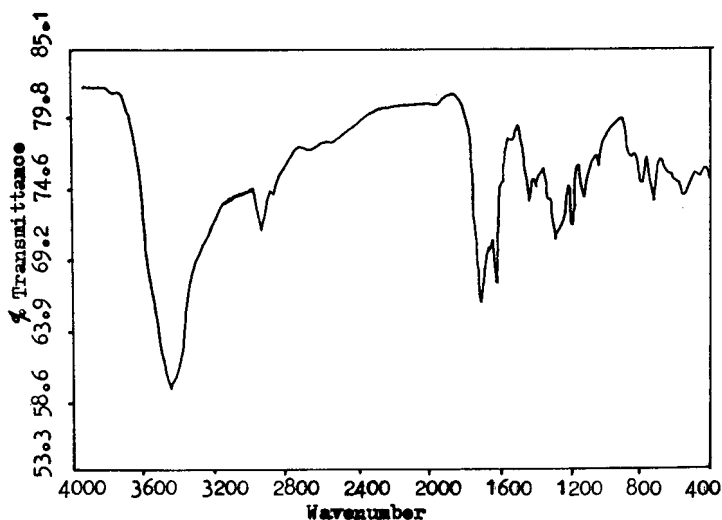
Fig. 2. Infrared spectrum of IDA chelating resin.

a strong chelating tendency towards heavy metal ions. The strong binding of copper ion to the IDA chelating groups minimizes the bleeding of copper ion (about 10^{-8}–10^{-7} M) from the column, and the Cu(II)–IDA column is stable.

The S–DVB matrix cannot be operated under high pressure (>200 kg/cm^2) as the apparent column efficiency decreases. Some aromatic amines appear to have a very high affinity to copper(II) ion, and are difficult to elute by using methanol as the mobile phase. We therefore added ammonia to the mobile phase as a competitive ligand, and examined the effect of the ammonia ligand concentration on the capacity factor of sample ($k'\alpha[NH_3]^{-1}$, Table I).

The retention values of aromatic amine depend mainly on their basicity[15]. As the affinity action of amines for copper(II) ion increases with increasing basicity of the

TABLE I

CAPACITY FACTORS (k') OF AROMATIC AMINES ON THE CU(II)–IDA COLUMN

Compound	Mobile phase	
	Methanol	Methanol + 0.3 mM NH$_3$
Aniline	3.98	2.10
N-Methylaniline	1.84	1.28
N,N-Dimethylaniline	0.62	0.30
2,4-Dimethylaniline	4.24	2.51
o-Nitroaniline	4.15	2.44
m-Nitroaniline	5.67	4.23
p-Nitroaniline	5.77	4.36
Pyridine	13.50	6.64
8-Hydroxyquinoline	6.31	4.98

amines, the retention value increases. On the other hand, steric hindrance will also affect the affinity action, and the retention value depends on the above two factors.

CONCLUSION

The results indicate that the Cu(II)–IDA chelating resin column has advantageous properties for use in IMAC, and may be applied to the analysis of aromatic amines. If the high-pressure resistance of the S–DVB matrix could be improved by the synthesis of highly cross–linked S–DVB copolymer, an effective column for use under high pressures could be developed. Such a column should be useful for the separation and analysis of biomacromolecular samples.

REFERENCES

1 F. Helfferich, *Nature (London)*, 189 (1961) 1001.
2 J. Porath, J. Carlsson, I. Olsson and G. Belfrage, *Nature (London)*, 258 (1975) 598.
3 A. Hubert and J. Porath, *J. Chromatogr.*, 198 (1980) 247.
4 J. Porath and B. Olin, *Biochemistry*, 22 (1983) 1621.
5 J. Porath, *Trends Anal. Chem.*, 7(7) (1988) 254.
6 Z. El Rassi and C. Horvath, *J. Chromatogr.*, 359 (1986) 241.
7 A. Figueroa, C. Corradini, B. Feibush and B. L. Karger, *J. Chromatogr.*, 371 (1986) 335.
8 Y. Kato, K. Nakamura and T. Hashimoto, *J. Chromatogr.*, 354 (1986) 511.
9 M. Belew, T. T. Yip, L. Andersson and R. Ehrnstrom, *Anal. Biochem.*, 164 (1987) 457.
10 J. Porath, *J. Chromatogr.*, 443 (1988) 3.
11 A. Foucault and R. Rosset, *Bio-Sciences*, 6, No. 4 (1987) 93.
12 K. Shimomura, L. Dickson and H. F. Walton, *Anal. Chim. Acta*, 37 (1967) 102.
13 C. D. Scott, *Anal. Biochem.*, 24 (1968) 292.
14 S. Coppi, G. Blo and A. Betti, *J. Chromatogr.*, 388 (1987) 135.
15 D. K. Singh and A. Darbari, *Chromatographia*, 23 (1987) 93.

CHROMSYMP. 1916

Characteristics of C$_4$- and C$_8$-bonded vinyl alcohol copolymer gels for reversed-phase high-performance liquid chromatography

TOMOKO OHTANI*, YUICHI TAMURA, MASAO KASAI, TAKATERU UCHIDA, YUZO YANAGIHARA and KOHJI NOGUCHI

Gel Separation Development Department, Asahi Chemical Industry Co. Ltd., 1–3–2, Yakoo, Kawasaki-ku, Kawasaki-shi, Kanagawa-ken 210 (Japan)

ABSTRACT

The fundamental characteristics of C$_4$- and C$_8$-bonded polymer (C4P and C8P) gels developed for reversed-phase high-performance liquid chromatography and obtained by introduction of butyryl and octanoyl groups, respectively, at the hydroxyl groups of vinyl alcohol copolymers were investigated and compared with the characteristics of a previously developed C$_{18}$-bonded polymer (ODP) gel obtained in a similar manner and with those of commercial C$_4$-, C$_8$- and C$_{18}$-bonded silica gels.

For both alkyl alcohols and standard proteins, the retention strength on the polymer gels clearly increased with increasing number of carbons in the bonded alkyl group and thus in the order C4P, C8P, ODP. The C4P and C8P gels, like the ODP gel and in clear contrast to the silica gels, displayed excellent tolerance towards acidic, alkaline and buffered eluents. They also exhibited minimal shrinking and swelling effects with variations in eluent polarity, as measured by their solvent regain.

INTRODUCTION

In reversed-phase liquid chromatography (RP-LC), which is now predominant in high-performance liquid chromatographic (HPLC) applications, columns have generally been packed with C$_{18}$-bonded polymer or silica gels.

Asahipak ODP-50, a commercially available column packed with a hard gel composed of rigid polymers with octadecyl (C$_{18}$) groups, is known to display little shrinkage and swelling with varying eluent polarity, unlike conventional polymer-based gel columns, and to equal or exceed conventional octadecylsilica (ODS) columns in separation effficiency. It is also known to display excellent tolerance to both acidic and alkaline elution, in contrast to the generally poor chemical stability and short service life of ODS columns[1,2].

In recent years, the need has grown for weakly hydrophobic gels which would allow more efficient analysis of peptides and proteins. C$_1$-, C$_4$- and C$_8$-bonded silica

gels, with relatively short alkyl groups, have partially met this need, but have also displayed a tendency for even lower chemical stability than the ODS gels and thus are restricted to a narrow range of chromatographic conditions[3,4].

The C_4- and C_8-bonded polymer (C4P and C8P) gels investigated in this study were therefore developed to meet the requirement for weak hydrophobicity while displaying a broader tolerance to eluent pH and composition.

EXPERIMENTAL

C4P and C8P gels were obtained by reaction of *n*-butyryl and *n*-octanoyl chloride, respectively, with the hydroxyl group of a vinyl alcohol copolymer gel having an average particle size of 5 μm. The resulting increases in carbon content were 6% and 10% of the final gel weight, respectively, as determined from the gel weight before and after the reaction. The C4P and C8P gels were packed in stainless-steel columns (150 mm $\times$ 4.6 mm I.D.).

Commercially available columns used for comparisons (all 150 mm $\times$ 4.6 mm I.D.), were the C_{18}-bonded polymer-based ODP-50 (ODP) and the silica-based Vydac 214TP (C_4) and 218TP (C_8), YMC-AP802 (C_4), AP202 (C_8) and AP302 (C_{18}).

Solvent regain was calculated as $SR = [(W_1 - W_2)/d]/W_2$, where d is the solvent density, W_1 is the measured weight of the gel following immersion in the solvent and centrifugion for removal of excess solvent and W_2 is the measured weight of the gel following its subsequent drying.

The chromatographic equipment consisted of Model 543 degassers (Showa Denko, Tokyo, Japan), 880-PU pump (Japan Spectroscopic, Tokyo, Japan), a Reodyne Model 7125 injector, a Model 875 UV detector (Japan Spectroscopic) and a Model SE-61 refractive index detector (Showa Denko).

Chemicals were obtained from Wako (Osaka, Japan). Organic solvents were of HPLC grade. Alkyl alcohols from Wako, peptides from Peptide Kenkyujo (Osaka, Japan) and proteins from Sigma (St. Louis, MO, U.S.A.) were used without further purification as samples.

RESULTS

Gel properties

The particle size, carbon content attributable to alkyl groups and solvent regain of the C4P, C8P and ODP gels are given in Table I.

The SR for a given solvent is a measure of the amount of solvent retained in the gel and is thus an indirect representation of the gel's pore volume when immersed in that solvent. In most gels, solvents of different polarities tend to result in marked differences in SR and thus in pore volume, with a corresponding swelling or shrinking of the gel.

For both the C4P and the C8P gel, the difference between SR values in distilled water and acetonitrile was even smaller than that observed for the ODP gel. In view of the known tolerance of the ODP gel to varying solvent polarities, the C4P and C8P gels may also be expected to be amenable to a broad range of eluents.

TABLE I

CHARACTERISTICS OF C4P, C8P AND ODP GELS

Gel	Particle size (μm)	Carbon content (%)	Solvent regain (SR) (ml/g)	
			Distilled water	Acetonitrile
C4P	5	6	1.01	1.06
C8P	5	10	0.86	0.92
ODP	5	17	0.68	0.75

TABLE II

k' AND N VALUES OF THE C4P, C8P AND ODP COLUMNS

k' and N were determined with 10 μl of 1% analyte solution using methanol–water (80:20) as eluent; flow-rate, 0.6 ml/min; detector, refractive index; temperature, 30°C.

Compound	C4P		C8P		ODP	
	k'	N	k'	N	k'	N
Ethylene glycol		3800		3500		3500
C_4H_9OH	0.12	4000	0.16	4300	0.19	4200
$C_6H_{13}OH$	0.21	4300	0.31	4100	0.40	4700
$C_8H_{17}OH$	0.34	4200	0.57	4500	0.82	5900
$C_{10}H_{21}OH$	0.51	4200	0.98	5200	1.65	6900
$C_{12}H_{25}OH$	0.75	4500	1.69	6100	3.43	7700
$C_{14}H_{29}OH$	1.08	4400	2.90	7700	7.34	8000

TABLE III

k' AND N VALUES OF SILICA-BASED COLUMNS

Conditions as in Table II.

Compound	Vydac 214TP (300 Å, C_4)		YMC-AP202 (300 Å, C_8)		Vydac 218TP (300 Å, C_{18})	
	k'	N	k'	N	k'	N
Ethylene glycol				3900		3500
C_4H_9OH	0.04		0.08	4200	0.08	3400
$C_6H_{13}OH$	0.08		0.18	5000	0.17	3200
$C_8H_{17}OH$	0.14	8500	0.37	5100	0.38	3600
$C_{10}H_{21}OH$	0.23	8100	0.72	5900	0.89	3600
$C_{12}H_{25}OH$	0.39	8500	1.38	7200	2.31	2700
$C_{14}H_{29}OH$	0.65	6100	2.60	9700	7.09	1200
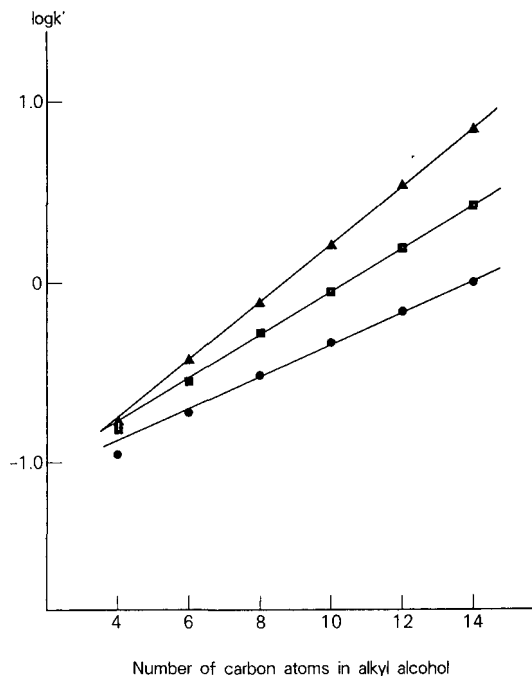
Fig. 1. Relationship between logarithm of capacity factor and carbon number in alkyl alcohol. Columns: (●) C4P; (■) C8P; (▲) ODP. Sample: *n*-alkyl alcohol ($n = 4, 6, 8, 10, 12, 14$). Eluent: methanol–distilled water (80:20). Flow-rate: 0.6 ml/min.

Retention strength

The capacity factors (k') and numbers of theoretical plates (N) measured for a series of alkyl alcohols in methanol–water (80:20) are given in Table II for the C4P, C8P and ODP columns and in Table III for the silica-based columns. The k' values were calculated as $k' = (V_r - V_o)/V_o$, where V_r is the retention volume of the analyte and V_o is the retention volume of ethylene glycol. As shown in Fig. 1, a close correlation between the k' value and the number of carbon atoms in the alkyl alcohol was observed for all three of the polymer-based gels. Among these gels, the k' value was also observed to rise with increasing number of carbons in the bonded alkyl group, in accordance with Martin's rule; the retention strength was clearly lowest on the C_4-, intermediate on the C_8- and highest on the C_{18}-bonded polymer gel. Similar tendencies were observed for the silica-based gel columns.

As indicated by the chromatograms in Fig. 2, a similar tendency for retention strength to increase with increasing number of carbons in the bonded alkyl group was observed for the standard proteins on the polymer-based gels and on the two silica-based gels which were tested. The differences in retention strength between the C4P, C8P and ODP gels, however, were substantially larger and far more consistent than those between the two silica-based gels.

Stability in acidic and alkaline eluents

Fig. 3 shows chromatograms obtained for a mixture of uracil, methyl benzoate,
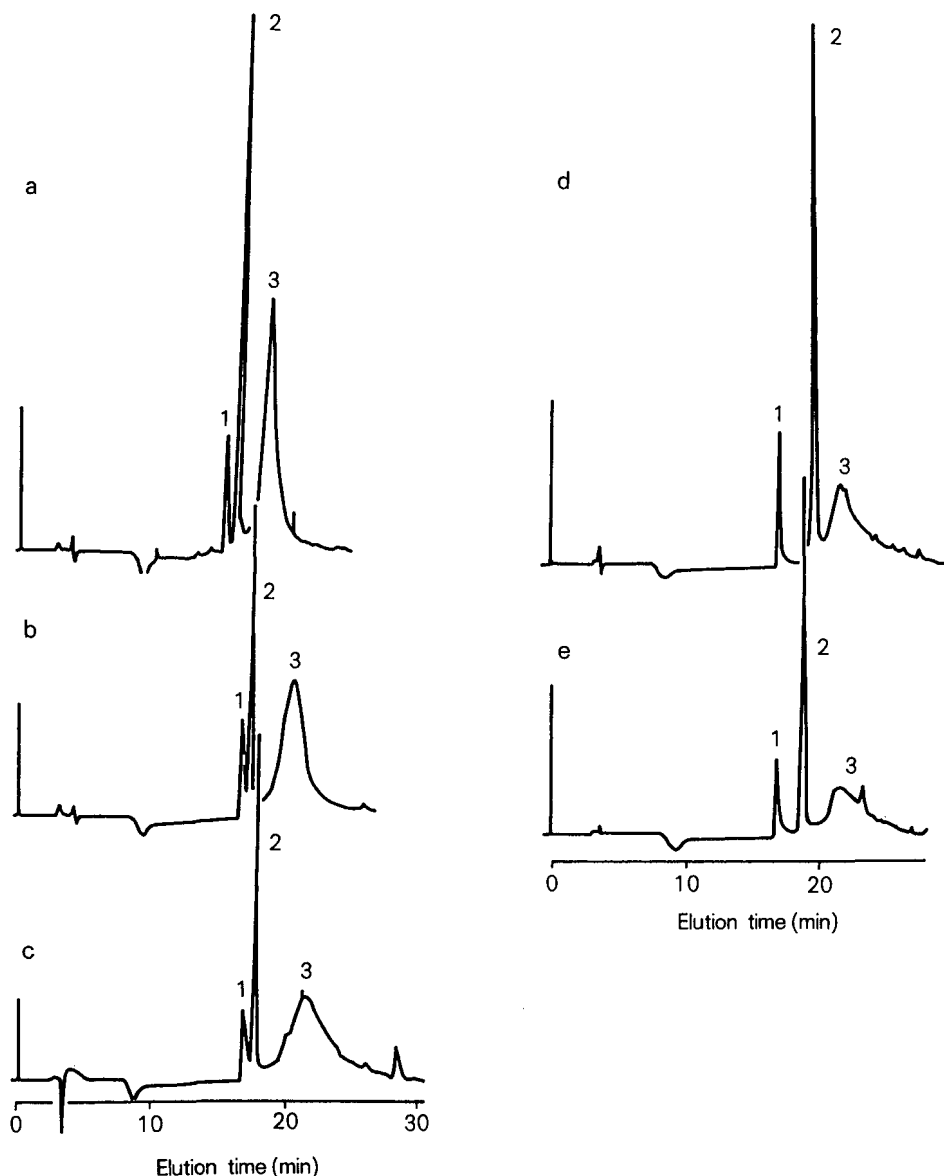
Fig. 2. Chromatograms of standard proteins on columns (a) C4P, (b) C8P, (c) ODP, (d) YMC-AP802 and (e) YMC-AP202. Sample: 1, BSA; 2, chymotrypsinogen A; 3, ferritin. Eluent: A, 0.1% TFA–acetonitrile (90:10); B, 0.1% TFA–acetonitrile (5:95); linear gradient from A to B in 30 min. Flow-rate: 0.6 ml/min. Detector: UV at 280 nm. Temperature: 30°C.

butyl benzoate and hexyl benzoate on the C4P column before and after its exposure to passage of an acidic solution (0.1% trifluoroacetic acid, pH 2) for 140 h. Fig. 4 shows those obtained before and after passage of an alkaline solution (100 mM sodium phosphate buffer, pH 9) for 140 h. No decrease in column efficiency occurred
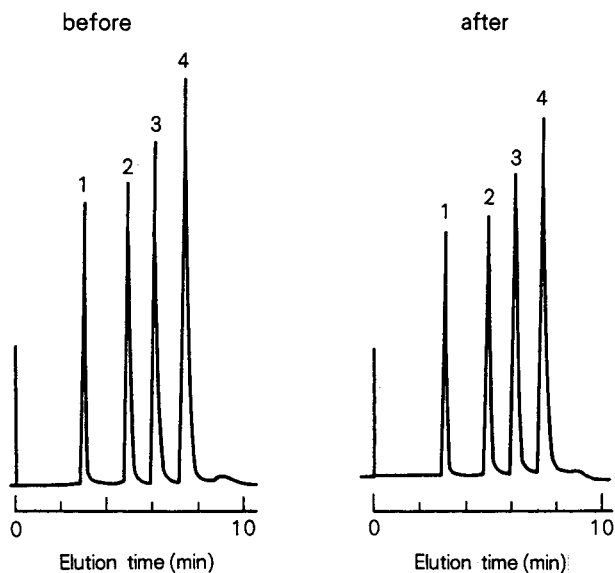
Fig. 3. Chromatograms obtained with C4P before and after passage of acidic solution [0.1% TFA (pH 2.0); flow-rate, 0.6 ml/min, 140 h]. Eluent: acetonitrile–distilled water (65:35). Flow-rate: 0.6 ml/min. Detector: UV at 254 nm. Temperature: 30°C. Peaks: 1 = uracil; 2 = methyl benzoate; 3 = butyl benzoate; 4 = hexyl benzoate.
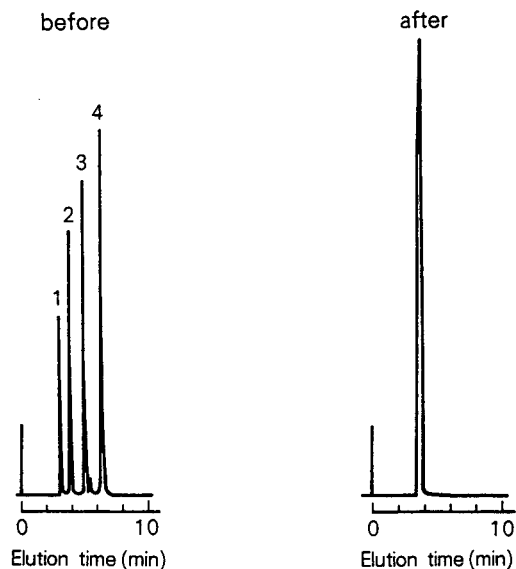
Fig. 4. Chromatograms obtained with C4P before and after passage of alkaline solution [100 mM sodium phosphate buffer (pH 9.0); flow-rate, 0.6 ml/min, 140 h]. Conditions as in Fig. 3.
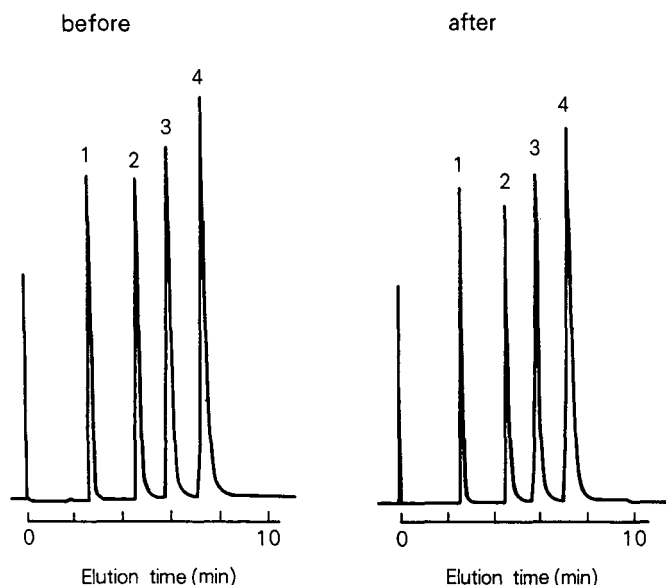
Fig. 5. Chromatograms obtained with YMC-AP802 before and after passage of acidic solution. Conditions as in Fig. 3.

in either instance. These results indicate that the C4P column and presumably the C8P column, like the ODP column, are highly stable in eluents throughout the pH range 2–9.

Silica-based columns are generally known to decrease rapidly in efficiency under acidic conditions and therefore were not tested with solutions of high pH in this study. One C4-bonded silica gel column (YMC-AP802) was tested (Fig. 5), by exposure to a solution of pH 2 in the same manner as described above. The results indicate that this gel is unstable in strongly acidic eluents and also in alkaline eluents, presumably because of separation of its alkyl groups from the base silica.

CONCLUSION

The C4P and C8P gels investigated were developed in order to eliminate the disadvantages of conventional C_1-, C_4- and C_8-bonded silica gels utilized in RP-LC. C_8- and particularly C_4-bonded silica gels are generally known to exhibit short service life under alkaline conditions, because of their tendency for solubility at pH 8 or higher[4]. This study has shown that C_4-bonded silica gel may also exhibit a serious loss in retention strength on exposure to highly acidic solutions, apparently because of separation between the bonded alkyl groups and the silica.

The results indicate that the problem of gel stability has been eliminated with the C4P and C8P gels, owing to the utilization of a vinyl alcohol copolymer rather than silica as the gel base, and that both acidic and alkaline eluents, in a far wider pH range than was previously possible, can be readily used with columns containing these gels.

Among the polymer-based gels, the retention strength for both alkyl alcohols and standard proteins was clearly lowest on the C4P, intermediate on the C8P and highest on the ODP gel, in close correspondence with the number of carbons in their bonded alkyl groups. The C_4-, C_8- and C_{18}-bonded silica gels exhibited a similar tendency for low-molecular-weight samples, but for some of the high-molecular-weight samples showed little or no such tendency.

The C4P and C8P gels may be expected to lead to a substantially expanded range of protein and peptide analyses by RP-LC.

ACKNOWLEDGEMENT

REFERENCES

1 Y. Yanagihara, K. Yasukawa, Y. Tamura, T. Uchida and K. Noguchi, *Chromatographia*, 24 (1987) 701.
2 K. Yasukawa, Y. Tamura, T. Uchida and K. Noguchi, *J. Chromatogr.*, 410 (1987) 129.
3 L. Glajch, J. J. Kirkland and J. Kohler, *J. Chromatogr.*, 384 (1987) 81.
4 N. Tanaka, *Protein, Nucleic Acid and Enzyme*, 31 (1986) 1.

CHROMSYMP. 1919

Separation of anionic and cationic compounds of biomedical interest by high-performance liquid chromatography on porous graphitic carbon

GUANGHUA GU and C.K. LIM*

Division of Clinical Cell Biology, MRC Clinical Research Centre, Watford Road, Harrow, Middlesex HA1 3UJ (U.K.)

ABSTRACT

The separation of small, ionizable compounds of biomedical interest on porous graphitic carbon is described. The retention of anionic compounds is dominated by electronic interaction between the solute and the delocalized electron clouds on the graphitized carbon, while cationic compounds are mainly retained by reversed-phase interaction with the hydrophobic carbon surface. Anionic and cationic compounds can be separated simultaneously with a mobile phase containing an electronic modifier (*e.g.*, trifluoroacetic acid) and an organic modifier (*e.g.*, acetonitrile) for elution. Examples of applications include the measurement of oxalic acid in urine, the determination of creatine and creatinine in urine and in serum, the separation of basic drugs (remoxipride and FLA 981) and the simultaneous analysis of pertechnetate anion and the cationic technetium–amine complexes.

INTRODUCTION

Porous graphitic carbon (PGC) is a new column packing available recently for high-performance liquid chromatography (HPLC)[1–3]. It was considered a "pure" reversed-phase material because it contains no unreacted silanols but only hydrophobic carbon surfaces. It is stable to strong acids and alkalis and therefore eluents at any pH can be used. In addition to the extremely hydrophobic nature, PGC is also unique in possessing a conduction band of delocalized electrons. Thus, retention on PGC is usually a mixture of hydrophobic and electronic interactions. The study by Bassler *et al.*[4] on the retention behaviour of 24 substituted aromatic compounds under non-polar solvent conditions has concluded that direct electronic interactions can arise from both the mixing of the HOMO and LUMO orbitals of the solute with the electronic distribution of PGC or from charge transfer between the solute and PGC. Using the separation of TcO_4^- and ReO_4^- as an example, Lim[5] has demonstrated that electronic-interaction chromatography (EIC), based totally on electronic interaction, is also possible.

The aim of the present study is to exploit further the extreme hydrophobicity and

the electronic properties of PGC for the separation of small anionic and cationic compounds of biomedical interest, particularly compounds which are difficult or impossible to retain on ODS silicas.

EXPERIMENTAL

Materials and reagents

Creatine, creatinine, ethylenediamine, stannous tartrate and oxalic acid were from Sigma (Poole, U.K.). Trifluoroacetic acid (TFA), hydrochloric acid and sodium chloride were AnalaR grade from BDH (Poole, U.K.). 1,5,8,12-Tetraazadodecane was from Aldrich (Gillingham, U.K.). Remoxipride and FLA 981 were gifts (to Dr. N. Veall) from Astra Läkemedel (Södertälje, Sweden). Acetonitrile was of HPLC grade from Rathburn (Walker, U.K.).

Preparation of technetium–amine complexes

The method of Emery and Lim[6] was used. Sodium pertechnetate was eluted from an Ultratechnekow FM generator (Malinckrodt Diagnostia, The Netherlands). The eluate was diluted with 0.9% sodium chloride to give a working solution of 0.2–1 mCi/ml. A saturated solution of stannous tartrate (as the reductant) was made by adding the solid to nitrogen-purged 0.01 M hydrochloric acid. The solution was filtered through a Millex GS 0.22-μm filter (Millipore, Watford, U.K.) into a nitrogenfilled vial and constantly purged with nitrogen. Ethylenediamine and 1,5,8,12-tetraazadodecane solutions (20–50 mM) were made up in water. The reaction was carried out by mixing 1 ml of ligand solution, 1 ml of sodium pertechnetate working solution and 1 ml of filtered stannous tartrate solution in a capped vial. The mixture was shaken and allowed to stand at room temperature for 20 min.

Preparation of urine sample for oxalic acid measurement

A Varian UK (Walton-on-Thames, U.K.) AASP Vac-Elut system was used with C_8 AASP extraction cartridges for sample preparation. Urine (500 μl) was vortex-mixed with 200 μl of 10% TFA. The mixture was loaded rapidly under positive nitrogen pressure onto the C_8 cartridge, which had previously been washed successively with 0.5 ml of methanol and 1 ml of water. The eluate was collected. The cartridge was then washed with 300 μl of 10% TFA and the eluate was again collected. A 10–20-μl volume of the pooled eluate was injected into the PGC column for oxalic acid separation and quantitation.

Preparation of urine sample for determination of creatine and creatinine

Urine (100 μl) was mixed with 0.1% TFA (100 μl) and loaded onto a C_8 AASP extraction cartridge, which had been pre-conditioned by washing with 0.5 ml of methanol, followed by 1 ml of 0.1% TFA. The eluate was collected. The cartridge was then washed with 1 ml of 0.1% TFA and the eluate was again collected. A 10–20-μl volume of the pooled eluate was used for HPLC analysis.

Preparation of serum sample for creatine and creatinine analysis

Serum (200 μl) was vortex-mixed with 500 μl of 10% TFA and centrifuged at. 3000 g for 5 min. The supernatant was loaded onto a C_8 AASP extraction cartridge and

the eluate was collected. The cartridge was washed with 1 ml of 0.1% TFA and the eluate was again collected. A 100-μl volume of the pooled eluate was injected into the HPLC column for analysis.

HPLC

A Varian Model 5000 liquid chromatograph was used with a Varian UV-100 variable-wavelength detector and/or a laboratory-built radiometric detector for the detection of technetium complexes[6]. The separations were carried out on a 10 cm × 4.6 mm I.D. Hypercarb column (Shandon Scientific, Runcorn, Cheshire, U.K.) With 0.1–1% TFA with or without acetonitrile as mobile phases. The flow-rate was 1 ml/min for all separations. The particle diameter of PGC was 7 μm with a surface area of 150 m^{52}/g,a mean pore diameter of 300 Å and a particle porosity of 70%.

RESULTS AND DISCUSSION

Separation of oxalic acid by EIC

In an earlier study on the separation of the inorganic anions pertechnetate (TcO_4^-) and perrhenate (ReO_4^-), it was demonstrated conclusively that retention was exclusively a result of electronic intereaction between solutes and the delocalized electrons on PGC[5]. In order to find out whether EIC can also be extended to the separation of organic molecules, the separation of oxalic acid was investigated. Oxalic acid was chosen, because it is clinically important and is difficult to retain on ODS silicas. It also possesses lone pairs of electrons on the carboxyl groups, ideal for studying electronic interaction.

Like the oxo-anions of Tc and Re, oxalic acid could not be eluted with water as mobile phase and addition of an organic modifier (acetonitrile) had no effect. Since oxalic acid ionizes completely in water, it cannot be retained on a reversed-phase column without ion pairing or ion suppression. Also, there are no ion-exchange sites on PGC. Thus total retention of oxalic acid with water as eluent can only be due to electronic interaction. This was confirmed by addition of TFA, an electronic modifier[5], to the mobile phase, when oxalic acid was eluted as a sharp peak. It is now clear that to separate anionic compounds on PGC, an electronic modifier (competitor) rather than an organic modifier is of prime importance. The retention of oxalic acid decreases with increasing electronic modifier concentration. This provides further evidence in support of an electronic-interaction mechanism.

Separation of oxalic acid in urine

Oxalic acid in urine can be separated from endogenous impurities with 0.08% TFA as mobile phase (Fig. 1). Sample preparation, particularly removal of hydrophobic compounds which will contaminate the column, is essential for the analysis of biological fluids on PGC. For urinary oxalic acid, this can simply be carried out by loading acidified urine onto a silica-based reversed-phase extraction cartridge, which will remove most hydrophobic components but allow the hydrophilic oxalic acid to pass straight through. Urine samples must be acidified to pH 0.5 or below with 10% TFA or concentrated hydrochloric acid before loading onto the cartridge. This prevents the precipitation of oxalic acid (mainly as the Ca^{2+} and Mg^{2+} salts) and will also dissolve any salts that have already formed in the urine sample. The recovery was
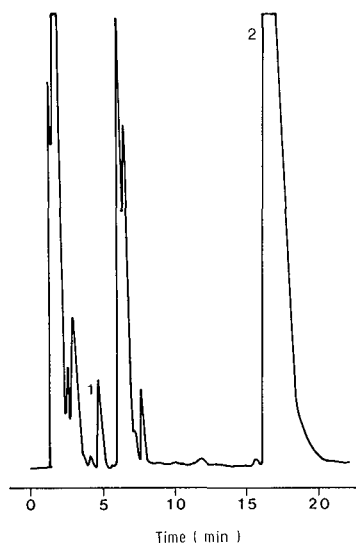
Fig. 1. Chromatography of oxalic acidin human urine. Eluent, 0.08% TFA; flow-rate, 1 ml/min; detector, 210 nm, 0.1 a.u.f.s. Peaks: (1) oxalic acid; (2) creatinine.

virtually 100%. The detection limit at 210 nm and 0.1 a.u.f.s. was 0.3 μg injected (signal-to-noise ratio of 3), which is adequate for the determination of oxalic acid in normal and in pathological urine.

Separation of creatine and creatinine in body fluids

Although many HPLC methods are described for the separation of creatinine in body fluids, very few are suitable for the simultaneous determination of creatine and creatinine[7]. Creatine is difficult to retain on ODS columns and it is often eluted together with other early-eluted interfering compounds. However, creatine and creatinine are expected to be retained much more strongly on the highly hydrophobic PGC column.

The separation of creatine and creatinine with 3% (v/v) acetonitrile in 0.1% TFA as the mobile phase is shown in Fig. 2. The study on the relationship between TFA concentration and capacity ratios (k') of creatine and creatinine (Fig. 3) indicates that retention was based mainly on reversed-phase ion-pair chromatography. The k' value increased with increasing TFA (ion-pairing agent) concentration. There was probably also a slight electronic interaction involved in the retention of these compounds, as at low TFA concentrations (below 0.01%) increasing the TFA concentration caused a small drop in k' (Fig. 3). At higher TFA concentration (above 0.05%), however, ion-pairing predominated. With 3% (v/v) acetonitrile in water as eluent, resolution was poor. The percentage acetonitrile content of the mobile phase can also be used to control the retention and resolution of creatine and creatinine, as shown in Fig. 4. The effect is that, as expected for reversed-phase chromatography, k' decreases with increasing organic modifier content.

From the above retention behaviour studies, it was concluded that 3% (v/v) acetonitrile in 0.1% TFA is the optimal system for the separation of creatine and
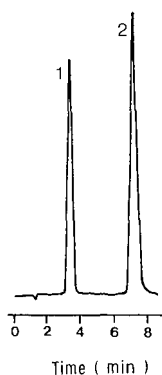
Fig. 2. Separation of creatine (1) and creatinine (2) on porous graphitic carbon. Eluent, 3% (v/v) acetonitrile in 0.1% TFA; flow-rate, 1 ml/min; detector, 210 nm.

creatinine in urine (Fig. 5a and b) and in serum (Fig. 5c). Removal of hydrophobic contaminants was again effected by a C_8 extraction cartridge, in which creatine and creatinine were not retained (see Experimental). The recoveries were virtualy 100%. The detection limits for creatine and creatinine were 20 and 10 ng injected, respectively.

Separation of remoxipride and FLA 981

Remoxipride and FLA 981 (Fig. 6) are potential neuroleptic agents[8]. These basic drugs were well known to behave badly with severe peak tailing and broadening on silica-based reversed-phase columns[9] because of partial ionization and interaction with residual silanol groups, despite the inclusion of a silanol masking agent in the mobile phase. An example is shown in Fig. 7.

The major advantages of PGC column over silica-based materials are that it contains no silanol groups and is stable at high pH. It is therefore commonly believed that PGC is an ideal reversed-phase packing for the chromatography of basic
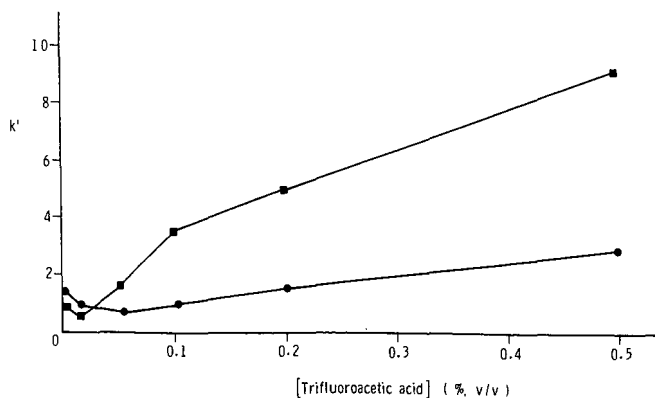
Fig. 3. Relationship between TFA concentration and capacity ratios of creatine (●) and creatinine (■).
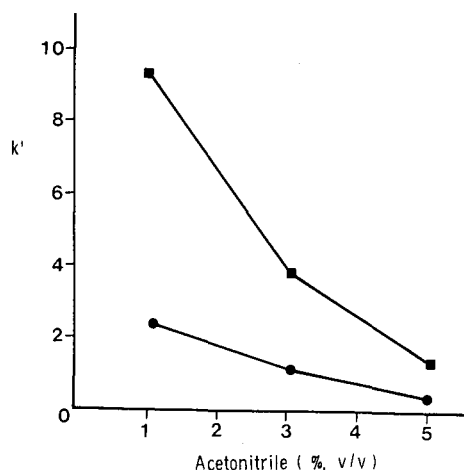
Fig. 4. Relation between percentage acetonitrile content of the mobile phase and retention of creatine (●) and creatinine (■).

compounds by ion-suppression at high pH. However, suppression of ionization greatly increases the hydrophobicity of the solute, and this can lead to strong interaction with the highly hydrophobic carbon surface, resulting in excessive retention.

A better approach to the separation of basic compounds on PGC is the use of a mobile phase containing TFA as eluent. TFA can function as an ion-pairing agent for bases, but, unlike long-chain ion-pairing agents it does not confer strong
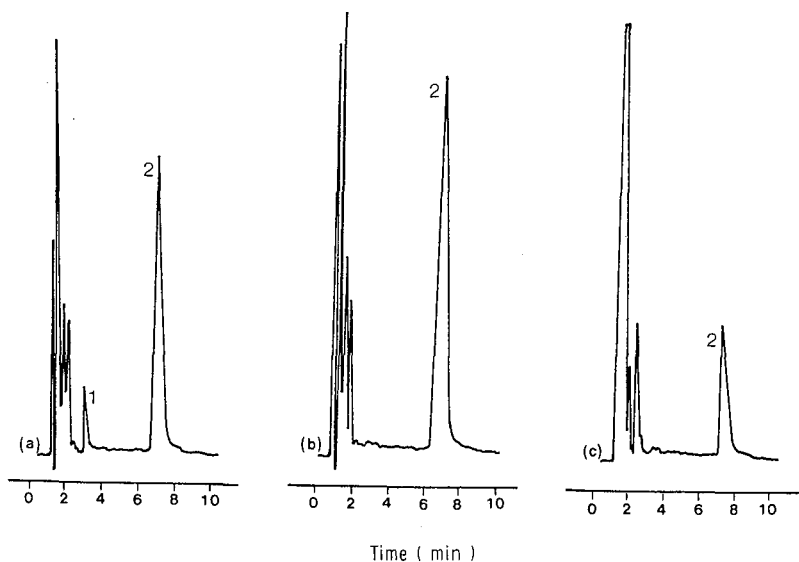
Fig. 5. Separation of creatine (1) and creatinine (2) in body fluids. (a) Baby urine; (b) adult urine; (c) adult serum. Eluent, 3% (v/v) acetonitrile in 0.1% TFA; flow-rate, 1 ml/min; detector, 210 nm, 0.1 a.u.f.s.
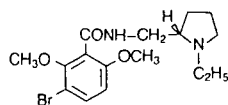
Remoxipride
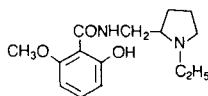
FLA 981

Fig. 6. Structures of remoxipride and FLA 981.

hydrophobicity on the solute. The separations of remoxipride and FLA 981 by ion suppression at pH 10 (50% acetonitrile in 0.1 M ammonium hydroxide) and by ion pairing with TFA (50% acetonitrile in 0.1% TFA) are shown in Fig. 8a and b, respectively. The superiority of the TFA mobile phase system is clearly demonstrated, remoxipride and FLA 981 being eluted within convenient retention times. With ion suppression, excessive retention was observed for both compounds and FLA 981 could not be eluted at 50% acetonitrile concentration.

Simultaneous separation of the oxo-anion of technetium and cationic ^{99m}technetium–amine complexes

Pertechnetate (TcO$_4^-$), the oxo-anion of technetium, is the starting material for the preparation of many radiopharmaceuticals[10], and cationic ^{99m}technetium–amine complexes are typical examples[11]. To monitor the radiochemical purity of these potential imaging agents and to study their stability and metabolic fate, a chromato-
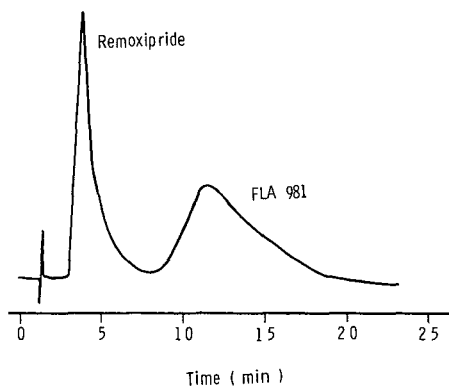
Fig. 7. Separation of remoxipride and FLA 981 on 5-μm Hypersil ODS (10 cm × 5 mm). Eluent, 50% (v/v) acetonitrile in water, containing 1% triethylamine; flow-rate, 1 ml/min; detector, 254 nm.
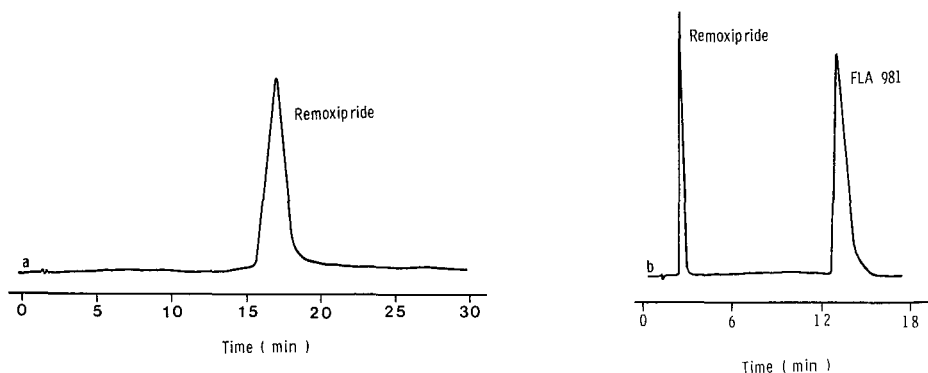
Fig. 8. Separation of remoxipride and FLA 981 on porous graphitic carbon. (a) With 50% (v/v) acetonitrile in 0.1 M ammonium hydroxide (pH 10) as eluent; (b) with 50% (v/v) acetonitrile in 0.1% TFA as mobile phase; flow-rate, 1 ml/min; detector, 254 nm.

graphic system capable of simultaneously separating anionic and cationic compounds is required. Previous studies[6] have shown that this is possible on a PGC column with TFA and acetonitrile as mobile phase.

The separation of TcO_4^- and the cationic complexes dioxo(bisethylenediaminato)technetium and dioxo(1,5,8,12-tetraazadodecane)technetium (Fig. 9) is shown Fig. 10a and b. TcO_4^- was retained exclusively by electronic interaction while the cationic complexes were retained by reversed-phase interaction. It is therefore possible to control the separation precisely according to the nature of application by altering the TFA concentration or acetonitrile content in the mobile phase. TFA functions as an electronic modifier and has a significant effect on the retention of TcO_4^- (Fig. 10a and b). The acetonitrile content in the mobile phase, on the other hand, affected the retention of the cationic complexes but not the anionic TcO_4^-.

The electronic modifier strengths of acetates have been studied and the order TFA > sodium acetate > acetic acid was observed. Acetic acid is a weak electronic modifier and requires a concentration of above 5% (v/v) for elution of TcO_4^-. Sodium acetate ionizes better than acetic acid and is also a stronger electronic modifier, because the lone-pair electrons on the carboxyl group are more available for electronic interaction. TFA is a strong carboxylic acid, which ionizes easily to provide lone-pair electrons for interaction. Its electronic-modifier strength is thus the strongest among the acetates.
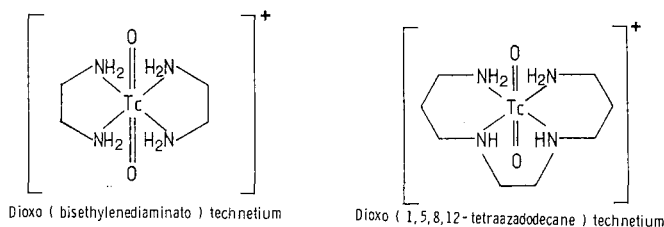
Fig. 9. Structures of dioxo(bisethylenediaminato)technetium and dioxo(1,5,8,12-tetraazadodecane)technetium cations.
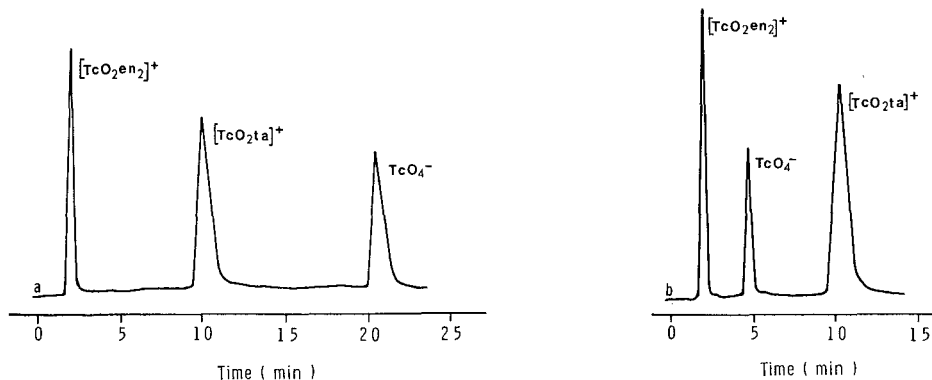
Fig. 10. Separation of pertechnetate (TcO_4^-), dioxo(bisethylenediaminato)technetium, $[TcO_2en_2]^+$, and dioxo(1,5,8,12-tetraazadodecane)technetium, $[TcO_2ta]^+$, on porous graphitic carbon. (a) With 2% (v/v) acetonitrile in 0.1% TFA as eluent; (b) with 2% acetonitrile in 1% TFA as eluent; flow-rate, 1 ml/min; detector, radiometric.

CONCLUSIONS

Retention on PGC is usually a mixture of reversed-phase and electronic interactions, although pure EIC is also possible. Retention of anionic compounds is dominated by electronic interaction and the mobile phase must contain an electronic modifier with or without an organic modifier. For the separation of cationic compounds, ion suppression with basic eluents at high pH increases the hydrophobicity of the solute, resulting in excessive retention on the highly hydrophobic carbon surface. Hydrophobic ion-pairing agents also lead to strong retention of cationic compounds for the same reason.

TFA is a universal mobile phase additive for chromatography of ionic compounds on PGC. It is an excellent electronic modifier, which can also function as an ion-pairing agent that does not confer excessive hydrophobicity on the solute. Sticking to one mobile phase additive will improve the reproducibility of separation on PGC.

To avoid excessive contamination, sample preparation is essential when biomedical samples are analysed on PGC. It is recommended that, after a separation, the column be washed with a gradient of TFA in acetonitrile or methanol in order to remove both ionic and hydrophobic contaminants. The column is then stored in methanol or aqueous methanol.

REFERENCES

1 M. T. Gilbert, J. H. Knox and B. Kaur, Chromatographia, 16 (1982) 138.
2 J. H. Knox and B. Kaur, J. Chromatogr., 352 (1986) 3.
3 J. H. Knox and B. Kaur, Eur. Chromatogr. News, 1 (1987) 12.
4 B. J. Bassler, E. Garfunkel, R. A. Hartwick and R. Kaliszan, J. Chromatogr., 461 (1989) 139.
5 C. K. Lim, Biomed. Chromatogr., 3 (1989) 92.
6 M. F. Emery and C. K. Lim, J. Chromatogr., 479 (1989) 212.
7 S.-M. Huang and Y.-C. Huang, J. Chromatogr., 429 (1988) 235.

8 L. Florvall and S.-O. Ogren, *J. Med. Chem.*, 25 (1982) 1280.
9 A. C. Veltkamp, H. Das, R. W. Frei and U. A. Th. Brinkman, *J. Chromatogr.*, 384 (1987) 357.
10 W. A. Voklert, D. E. Troutner and R. A. Holmes, *Int. J. Appl. Isot.*, 33 (1982) 891.
11 P. Bläuenstein, G. Pfeiffer, P. A. Schubiger, G. Anderegg, K. Zollinger, K. May, Z. Proso, E. Ianovici
    and P. Lerch, *Int. J. Appl. Radiat. Isot.*, 36 (1985) 315.

CHROMSYMP. 1899

Binding capacities of hydroxyapatite for globular proteins

SENYA INOUE* and NOBUYUKI OHTAKI

Central Research Laboratory, Kanto Chemical Co., Inc., 1-7-1, Inari Soka-City, Saitama 340 (Japan)

ABSTRACT

The binding capacities of hydroxyapatite (HAP) for globular proteins depended on the effective surface area for adsorption, described as $(S_{BET} - S_p)px$, where S_{BET} is the BET surface area, S_p is the accumulation of surface areas based on small pores which the tested protein cannot enter, p is the proportion of the area of the adsorbing surface connected with basic or acidic proteins and x is the proportion of the area of the active part of each type of adsorbing surface. The values of px and $(S_{BET} - S_p)$ varied with the preparation methods and condition of HAP.

INTRODUCTION

The hydroxyapatite (HAP) crystal has two types of main adsorbing surfaces which are related to the binding of basic and acidic proteins[1,2]. The proportion of the area of each type of adsorbing surface, the state of the adsorbing surface and the BET surface area are considered to be affected by the preparation methods and condition of HAP. For example, HAP crystallized in aqueous solution tends to grow along the c axis and the surfaces parallel to the $\{10\bar{1}0\}$ planes develop mostly on the crystal surface[3-5]. On the other hand, spherical and sintered polycrystalline HAPs have been developed during the last few years with improvements in their mechanical strength for use as packing materials[6-9]. Based on their preparation methods it is considered that they have almost equal proportions of the areas of each type of adsorbing surface. Further, polycrystalline HAP surfaces have lattice defects due to the presence of grain boundaries and some deficiencies of lattice hydroxyl groups, which affect the completeness of the surface state[10]. These differences in surface state are suggested to affect the binding capacities for proteins. Hence the binding capacities of HAP cannot be interpreted solely from the dependence on surface areas measured by the BET method.

In this work we studied the effect of the surface states of HAP on the binding capacities for globular proteins. Spherical HAPs with different surface states were prepared by the spray method and heat treatments at various temperatures in air. For comparison of the effects of preparation methods on surface states, commercially available HAPs prepared by wet processes were also tested. Surface states were

determined by X-ray diffraction analysis, differential thermal and thermogravimetric analysis, infrared spectrophotometry and scanning electron microscopy (SEM).

EXPERIMENTAL

HAP packing materials

Spherical HAP packing materials (HAP-1–5) were prepared as follows. HAP crystals with diameters of the order of 0.1 μm as starting material were precipitated by mixing a $Ca(NO_3)_2$–CH_3OH–H_2O solution and an H_3PO_4–CH_3OH–H_2O solution. The HAP slurry thus obtained was then spray-pyrolysed. The droplets when sprayed into a flame were instantaneously dried and sintered into spherical and porous polycrystals by heat of combustion of the vaporized CH_3OH. These spherical and sintered HAP packing materials were heat treated at 700–1000°C for 4 h in air to change the physical and chemical properties of the HAP surface. HAP-6 and -7 were prepared by wet processes. Table I summarizes the properties of the HAP samples tested. Fig. 1 illustrates the scanning electron microscopy (SEM) photographs of the surfaces of these HAPs.

Proteins

The proteins used are listed in Table II. Bovine serum albumin (BSA) and lysozyme were obtained from Merck (Darmstadt, F.R.G.) and all other proteins from Sigma (St. Louis, MO, U.S.A.). They were all globular proteins with a frictional ratio range of 1.1–1.3.

Binding capacities

Seven samples of HAP with different surface states were packed in 100 mm × 8 mm I.D. stainless-steel columns. The maximum amount of proteins loaded

TABLE I

PROPERTIES OF HYDROXYAPATITES USED

For details of preparations and measurements, see Experimental.

Sample	Preparation	Phase	BET surface area (m²/g)	Weight loss[a] (%)	Intensity of OH⁻ frequency[b]	
					New sample	Sample used for HPLC
HAP-1	Spray method	HAP	21.8	0	100	100 × 1.04[c]
HAP-2	Heating of HAP-1 at 700°C	HAP	18.0	0.8	96	96 × 1.04
HAP-3	Heating of HAP-1 at 800°C	HAP	14.4	1.3	84	84 × 1.09
HAP-4	Heating of HAP-1 at 900°C	HAP	6.4	1.4	72	72 × 1.12
HAP-5	Heating of HAP-1 at 1000°C	HAP + α-TCP	1.9	1.7	45	45 × 1.31
HAP-6	Wet process	HAP	7.8	–	–	–
HAP-7	Wet process	HAP	32.4	–	–	–

[a] Calculated by $[(W_0 - W)/W_0] \cdot 100$, where W_0 and W are weight of HAP-1 before and after heating at a given temperature.

[b] Intensity (arbitrary units) of the hydroxyl stretching frequency at 3572 cm⁻¹.

[c] The intensity of the OH⁻ frequency (= 104 in arbitrary units) of the sample used for HPLC increased by 4% compared to that (= 100) of the new sample. This is similar for the other HAP samples.
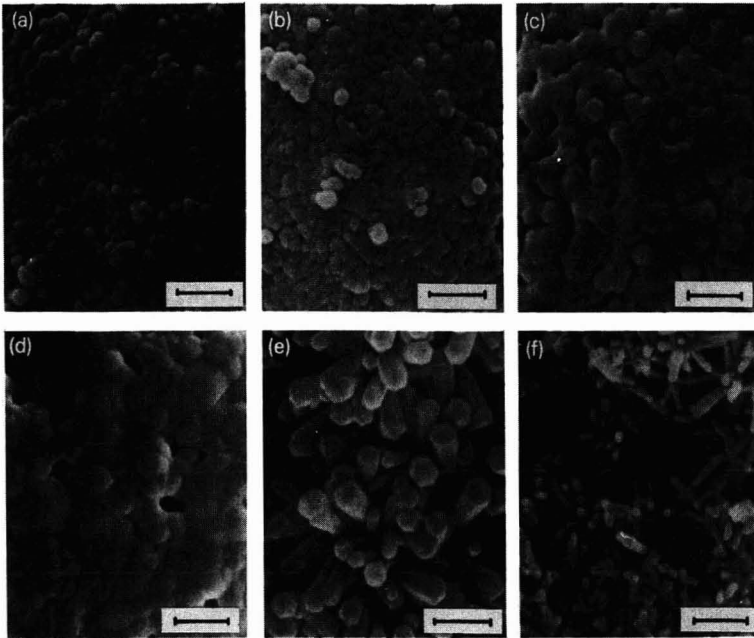
Fig. 1. SEM photographs of hydroxyapatite packing materials used: (a) HAP-1; (b) HAP-3; (c) HAP-4; (d) HAP-5; (e) HAP-6; (f) HAP-7. Photograph of HAP-2 was omitted; the surface state of HAP-2 by SEM observation was very similar to that of HAP-1. The bars indicate 0.5 μm.

(binding capacity) on HAP were measured by the following method. Various amounts of protein dissolved in 10 mM sodium phosphate buffer solution (pH 6.8; $H_2PO_4^-/HPO_4^{2-}$ molar ratio = 12:7) were applied to the column. The column was then eluted with 10 mM pure sodium phosphate buffer solution (pH 6.8) at a flow-rate of 1 ml/min for 30 min. As the 10 mM phosphate concentration in the buffer solvent cannot elute any of the adsorbed proteins used in this study, no peak appears when the loaded proteins are all adsorbed on HAP. When the limiting load is exceeded, peaks due to excess and unbound proteins can be detected.

TABLE II

PROTEINS USED

Most data on molecular weight (M), frictional ratio (f/f_0) and partial specific volume of the molecule ($\bar{v}$) were taken from ref. 11. Stokes radius (r) was calculated using eqn. 2. pI = isoelectric point.

Protein	Source	pI	M ($\cdot 10^4$)	f/f_0	$\bar{v}$	r ($\mathring{A}$)
Serum albumin	Bovine serum	4.7–4.9	6.6	1.288	0.733	34.5
Trypsin inhibitor	Soy bean	4.3–4.6	2.1–2.2	1.2–1.3	0.70–0.74	21.6–24.2
Transferrin	Human serum	5.2	8–9	1.23–1.37	0.73	35.1–40.6
Myoglobin	Horse muscle	7.3	1.78	1.105	0.741	19.2
α-Chymotrypsinogen A	Bovine pancreas	9.5	2.57	1.193	0.721	23.2
Ribonuclease A	Bovine pancreas	9.5–9.6	1.37	1.066	0.707	16.7
Lysozyme	Chicken egg	11.0–11.4	1.43	1.21	0.703	19.2

Surface areas

Total surface areas were measured by the BET method. The accumulation of surface areas based on small pores existing in the HAP were determined by the Cranston–Inkley method[12], assuming a cylindrical pore shape. In the Appendix, the calculation method is briefly explained. They were measured by nitrogen adsorption at 77 K.

Phases and X-ray scattering intensities

Crystalline phases of samples and X-ray scattering intensities of $(10\bar{1}0)$ and (0002) reflections of HAP were obtained on a Rigaku Denki diffractometer with Cu-Kα radiation and a graphite monochromator.

Hydroxyl groups

The intensities of the hydroxyl stretching frequency (3572 cm^{-1}) of powdered HAP samples in CaF$_2$ discs (5 mg per 500 mg of CaF$_2$) were measured by the diffuse reflectance method on a Perkin-Elmer Fourier transform (FT)/IR spectrophotometer.

Determination of the surface area available for adsorption

The binding capacities for proteins are related to the surface area necessary for the adsorption of protein molecules on HAP. Assuming the shape of the protein molecules to be a sphere with a Stokes radius, that no interactions occur among them and that there is monolayer adsorption on HAP, the surface area occupied by the maximum amount of globular proteins adsorbed on the HAP surface (S_{capa}) can be estimated from the equation

S_{capa} = (surface area occupied by one protein molecule) × (the maximum number of protein molecules adsorbed on HAP surface).

The surface area occupied by one protein molecule with a Stokes radius r can be calculated as $2\sqrt{3}r^2$, assuming closed-packed adsorption of the protein molecules on the HAP surface. Therefore, we obtain

$$S_{capa} = 2\sqrt{3}r^2 \ (W_{capa} \ N_0/M) \tag{1}$$

where W_{capa} is the maximum amount of protein adsorbed on the HAP surface (binding capacity), N_0 is Avogadro's number and M is the molecular weight of the protein. The Stokes radius is represented by

$$r = (f/f_0) \ (3\bar{v}M/4N_0)^{1/3} \tag{2}$$

where f/f_0 is the ratio of the frictional coefficient for the flow of a molecule to that of a hydrodynamically equivalent sphere and $\bar{v}$ is the partial specific volume of the molecule.

On the other hand, we consider two types of protein, namely basic and acidic with relatively basic and acidic isoelectric points, respectively, and we assume that all surfaces appearing on an HAP crystal belong to either type of adsorbing surface. The first type of adsorbing surfase is that on which negatively charged adsorbing sites are

arranged and basic proteins are mainly adsorbed. Such main surfaces are those parallel to the $\{0001\}$ planes. The second type of adsorbing surface is that on which positively charged adsorbing sites are arranged and acidic proteins are mainly adsorbed. Such main surfaces are those parallel to the $\{10\bar{1}0\}$ planes.

If HAP packing materials have neither pores nor lattice defects and all surfaces are active for adsorption of proteins, we can relate S_{capa} with S_{BET} as follows:

$$S_{capa} = S_{BET}p' \tag{3}$$

where S_{BET} is the total surface area of HAP measured by the BET method and p' represents the proportion of the area of the first or second type of adsorbing surface. ·

However, there are some inactive parts for adsorption on actual HAP crystals owing to the presence of small pores which the tested protein cannot enter. It is assumed that the pores are present uniformly on the HAP crystal surfaces. It is also assumed that the distribution of the pore size occurring in connection with the first type of adsorbing surface is equal to that occurring in connection with the second type of adsorbing surface. In addition to the inactive area that occurs owing to the presence of pores, another type of inactive area exists in the crystal surface structure, owing to lattice defects such as grain boundaries and some deficiencies of lattice OH^- groups. It is assumed that, on each type of adsorbing surface, the distribution of the lattice defects existing on the inside of the pores is equal to that existing on the outside. With these assumptions, S_{capa} for the HAP material on which both pores and lattice defects are present can be described by

$$S_{capa} = (S_{BET} - S_p)px \tag{4}$$

where S_p is the accumulation of surface areas based on small pores existing in the HAP material which the tested protein cannot enter, and p represents the proportion of the area of the first or second type of adsorbing surface under consideration on which pores are present. With the above-mentioned assumptions, the relationship

$$p' = p \tag{5}$$

is fulfilled. The parameter x represents the proportion of the area of the active part of the first or second type of adsorbing surface under consideration on which lattice defects are present. Hence px represents the proportion of the area of the active part of the $S_{BET} - S_p$ surface area for adsorption of basic proteins or acidic proteins. ($S_{BET} - S_p$) px can be considered to be the effective surface area for adsorption of proteins. In this paper, we assume that the minimum pore diameter in which a protein can enter is $2r$. S_p depends on the molecular size of the tested proteins. The parameters p and x are independent of S_p under the above-mentioned assumptions, and they vary with the method of preparation of HAP. The parameter p means p_1 or p_2 where $p_1 + p_2 = 1$ and the subscripts 1 and 2 are used to denote the first and second type of adsorbing surface, respectively. As the effect of a deficiency of lattice OH^- groups on an adsorbing surface is different between $\{0001\}$ and $\{10\bar{1}0\}$ planes, x depends on the type of protein used as a probe. Consequently, from eqns. 1 and 4,

$$px = S_{capa}/(S_{BET} - S_p) = 2\sqrt{3}r^2 (W_{capa}N_0/M)/(S_{BET} - S_p) \qquad (6)$$

S_{BET}, S_p and W_{capa} are known from experiments and r and M are fixed for each kind of protein. Hence px can be calculated from eqn. 6.

HAP packing materials have a certain constant value of p which depends on the preparation method. If the surface state of HAP changes with the preparation conditions, some variation of px must be recognized, mainly because of a change in x.

RESULTS AND DISCUSSION

Effect of heat treatment on HAP surface state

Fig. 2 plots the relative changes of both $S_{BET} - S_p$ and the binding capacities (W_{capa}) of spherical HAPs on heat treatment for lysozyme and BSA. The decrease in W_{capa} for lysozyme was found to have almost the same tendency as that of $S_{BET} - S_p$. However, the decrease in W_{capa} for BSA was greater than that of $S_{BET} - S_p$ for HAP samples heat treated below 900°C. With HAP-5 (heat treated at 1000°C), W_{capa} for BSA was found to increase considerably, although $S_{BET} - S_p$ still decreased. Therefore, the relative change in W_{capa} on heat treatment of HAP could not be explained only by the decrease in $S_{BET} - S_p$. Table III gives the data on binding capacities and surface states of spherical HAPs heat treated at various temperatures. As can be seen, both px and $S_{BET} - S_p$ for HAP samples heat treated below 900°C, calculated by eqn. 6, decreased with increase in temperature. In contrast, the px value of HAP-5 for BSA increased.

The parameters p and x were separately calculated as follows. The value of p_1x(Lys) of HAP-1 was 0.51 for lysozyme whereas p_2x(BSA) was 0.25 for BSA, where x(Lys) and x(BSA) signify the x for lysozyme and BSA, respectively. Thus the range of p was determined to be $0.51 \leqslant p_1 \leqslant 0.75$ and $0.25 \leqslant p_2 \leqslant 0.49$ from the relationships $x \leqslant 1$ and $p_1 + p_2 = 1$. As HAP-1 is sintered bodies of polycrystals and has some inactive surface for adsorption due to grain boundaries and other lattice defects, it is reasonable to evaluate that the maximum value of x is, in real situations of the order of 0.9 or less. In addition, from the HAP crystal structure, the effect of a deficiency of lattice OH^- groups on the state of the adsorbing surface is considered to be more harmful on
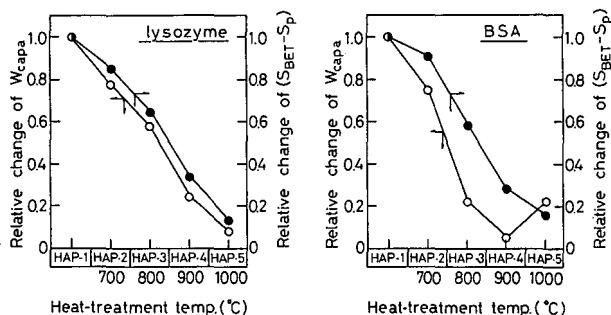

Fig. 2. Relative changes in binding capacities (W_{capa}) and $S_{BET} - S_p$ for lysozyme and bovine serum albumin on heat treatment of HAP-1. The relative change was calculated by dividing W_{capa} or $S_{BET} - S_p$ of HAP heat treated at given temperatures by that of HAP-1.

TABLE III

BINDING CAPACITIES AND PROPERTIES OF SPHERICAL HAP HEAT TREATED AT VARI-OUS TEMPERATURES

For details of the measurements of W_{capa} and $S_{BET} - S_p$, see Experimental. S_{capa} and px were calculated using eqns. 1 and 4, respectively.

Protein	Sample	W_{capa} (mg/g)	S_{capa} (m²/g)	$S_{BET} - S_p$ (m²/g)	$p_1 x(Lys)$	p_1	$x(Lys)$
Lysozyme	HAP-1	12.26	6.57	12.9	0.51	0.6	0.85
	HAP-2	9.60	5.14	11.0	0.47	0.6	0.78
	HAP-3	7.11	3.81	8.3	0.46	0.6	0.77
	HAP-4	2.99	1.60	4.3	0.37	0.6	0.62
	HAP-5	1.04	0.56	1.7	0.33	0.5	0.66

Protein	Sample	W_{capa} (mg/g)	S_{capa} (m²/g)	$S_{BET} - S_p$ (m²/g)	$p_2 x(BSA)$	p_2	$x(BSA)$
BSA	HAP-1	5.38	2.01	7.9	0.25	0.4	0.63
	HAP-2	4.02	1.51	7.2	0.21	0.4	0.53
	HAP-3	1.16	0.43	4.6	0.09	0.4	0.23
	HAP-4	0.26	0.10	2.2	0.05	0.4	0.13
	HAP-5	1.19	0.45	1.3	0.35	0.5	0.70

$\{10\bar{1}0\}$ than on $\{0001\}$ planes. Thus, $x(BSA) < x(Lys)$ is realized. Hence the range of p was limited to be $0.56 < p_1 < 0.67$ and $0.33 < p_2 < 0.44$. From these inequalities, p values for HAP-1 were estimated to be 0.6 for p_1 and 0.4 for p_2 with an uncertainty of about ± 0.05.

The X-ray diffraction analysis indicated that the HAP phase of HAP-1–4 did not decompose, as shown in Table I. Further, their intensity ratio, $I_{0002}/I_{10\bar{1}0}$, was found not to change significantly. Hence the value of p was considered to remain almost constant for heat treatments below 900°C.

The value of x of HAP-1–4 for lysozyme and BSA decreased with increasing treatment temperature. The change was particularly large for BSA. For example, only 13% of the adsorbing surface was available for BSA in HAP-4. From the weight loss in thermogravimetric analysis and the decrease in intensity of the hydroxyl stretching frequency ($3572 \, cm^{-1}$) in FT-IR analysis, which occurred to heat-treated HAP samples as shown in Table I, the decrease in x can be interpreted by the lattice defects caused by some hydroxyl deficiencies in a crystal. The deficiencies of lattice OH^- groups were extended with increasing heat-treatment temperature. According to the FT-IR analysis of HAP-1–4 after being used for high-performance liquid chromatographic (HPLC) measurements, it was found that the intensities of the hydroxyl stretching frequency increased by about 4–12% compared to that of the new material. These results indicate that, once a loss of lattice OH^- groups has occurred during heat treatment, its complete recovery could not take place although OH^- groups were partly taken into HAP crystals from the phosphate buffer solution.

The p and x values for HAP-5 were similarly determined as follows. As measured by FT-IR spectrophotometry, as many as 55% of the OH^- groups were lost from the crystal surface of HAP-1 during heating at 1000°C. A high deficiency of OH^- groups is

known to cause decomposition of the HAP crystal[10]. In fact, slight decomposition to
α-tricalcium phosphate (α-TCP) in HAP-5 was detected by X-ray diffraction analysis.
α-TCP is reported to change to HAP again in aqueous solution[13]. In this experiment,
the main peak of α-TCP produced in HAP-5, which was weakly detected by X-ray
diffraction analysis, had almost disappeared after the material had been used for
HPLC. The planes most commonly developed on the crystal exterior in the first stage
of crystallization of HAP are those described by the Miller indices $\{10\bar{1}0\}$. Hence p_2 of
HAP-5 is considered to become greater than that of HAP-1 because of the generation
of new HAP surfaces due to dissolution of α-TCP. From the data on px for HAP-5, the
range of p for HAP-5 was determined to be $0.33 \leqslant p_1 \leqslant 0.65$ and $0.35 \leqslant p_2 \leqslant 0.67$
using the procedure used for HAP-1. This range is clearly different from that for
HAP-1. Further, from the above experimental analysis, it was considered that p_2 for
HAP-5 $> p_2$ for HAP-1 and p_1 for HAP-5 $< p_1$ for HAP-1. Hence the range of p was
limited to $0.4 < p_1 < 0.6$ and $0.4 < p_2 < 0.6$. From these inequalities p values for
HAP-5 were estimated to be approximately $p_1 = p_2 = 0.5$.

An increase in the x values of HAP-5 was also observed. This may be due to the
repairing of the HAP-5 surface when it is used in the phosphate buffer solution. This
was supported by the experimental result that the recovery of the intensity of the OH^-
frequency was so large compared with other HAP samples that it reached about 30%.
This result can also be seen in Table I.

Change of px by protein types

From the above assumption that the same type of proteins adsorb on the same
adsorbing surface of HAP, it is expected that the px values would be almost the same
among the same type of proteins but would vary with the protein types. The px values
of HAP-3 for each protein used were determined by capacity measurements and are
given in Table IV. As expected, similar values of px were obtained among the same type
of proteins. The values of px were about 0.51 for basic proteins and 0.14 for acidic
proteins.

The x values of HAP-3 for basic proteins (about 0.8–0.9) were higher than those
for acidic proteins (about 0.4 or less). The reason may be that the repair of the
adsorbing surface for basic proteins is better than that for acidic proteins in
a phosphate buffer solution, although both adsorbing surfaces are damaged by heat
treatment.

$S_{BET} - S_p$ of HAP-3 is plotted against pore diameter and S_{capa} is plotted against
protein size in Fig. 3. S_{capa} of HAP-3 for each protein tested lay according to protein
type on two curved lines, which were the $(S_{BET} - S_p)px$ expressed as a function of pore
diameter. This indicates that S_{capa} of a globular protein of known size and type can be
obtained from Fig. 3. Thus, W_{capa} of HAP-3 for the protein can be determined by
calculation using eqn. 1, without measurement, substituting S_{capa} obtained from Fig. 3.

Effect of preparation method on surface state

For comparison of the effect of preparation methods on the surface state of
HAP, HAP-6 and -7 prepared by wet processes were tested. The values of W_{capa} of
these HAP samples for lysozyme and BSA were measured, and px, p and x were then
calculated by the above-mentioned method (Table V).

There was a difference in p between HAP-6 and HAP-1. With HAP-6, p_1 for

TABLE IV

BINDING CAPACITIES AND PROPERTIES OF HAP-3 SURFACE FOR GLOBULAR PROTEINS

Protein	r (Å)	W_{capa} (mg/g)	S_{capa} (m^2/g)	$S_{BET} - S_p$ (m^2/g)	px	p	x
Transferrin	37.9	1.72	0.60	4.3	0.14	0.4	0.35
Bovine serum albumin	34.5	1.16	0.43	4.6	0.09	0.4	0.23
Trypsin inhibitor	22.9	2.16	1.10	7.1	0.15	0.4	0.38
Myoglobin	19.2	3.23	1.39	8.3	0.17	0.4	0.43
α-Chymotrypsinogen A	23.2	8.19	3.57	7.0	0.51	0.6	0.85
Lysozyme	19.2	7.11	3.81	8.3	0.46	0.6	0.77
Ribonuclease A	16.7	12.3	5.20	9.5	0.55	0.6	0.92

lysozyme (basic protein) was small whereas p_2 for BSA (acidic protein) was so large that it reached 83% of $S_{BET} - S_p$. This was supported by SEM observations. Most surfaces appearing on a hexagonal pillar-shaped HAP-6 crystal (Fig. 1e) were considered to belong to those parallel to the $\{10\bar{1}0\}$ planes.

HAP-7 was considered to be prepared by a wet process different from that for HAP-6. It consisted of very fine pillar-shaped crystals as shown in Fig. 1f. The proportion of the area of the active part of the $S_{BET} - S_p$ surface, px, was very small (about 0.2) for both protein types. The calculated p ranges were too large to calculate p and x separately. Hence in this instance some additional information from other experiments is necessary for the determination of reasonable p values.
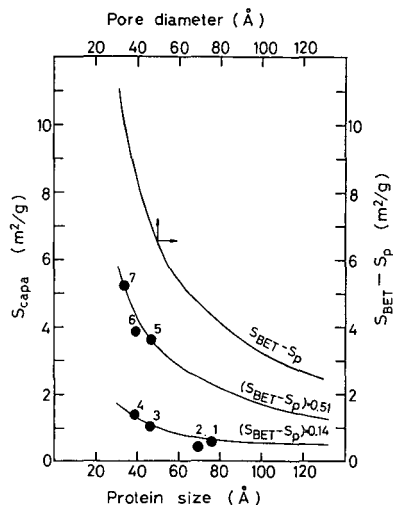
Fig. 3. Relationship between $S_{BET} - S_p$ and pore diameter of HAP-3 and relationship between S_{capa} for tested protein and protein size for HAP-3. Depending on protein type, S_{capa} of HAP-3 for the tested proteins lay on either of the curved lines which show $(S_{BET} - S_p)px$ as a function of pore diameter; px is 0.51 for basic proteins and 0.14 for acidic proteins. Proteins: 1 = transferrin; 2 = BSA; 3 = trypsin inhibitor; 4 = myoglobin; 5 = α-chymotrypsinogen A; 6 = lysozyme; 7 = ribonuclease A.

TABLE V

BINDING CAPACITIES AND PROPERTIES OF THE SURFACE OF HAP-6 AND HAP-7

Sample	Protein	W_{capa} (mg/g)	S_{capa} (m²/g)	$S_{BET}-S_p$ (m²/g)	px	p	x
HAP-6	Lysozyme	1.70	0.91	5.54	0.16	0.17	0.94
	BSA	8.50	3.19	3.85	0.83	0.83	1.00
HAP-7	Lysozyme	8.53	4.57	23.3	0.20	$(0.5)^a$	$(0.40)^a$
	BSA	7.75	2.90	15.4	0.19	$(0.5)^a$	$(0.38)^a$

[a] Low reliability. The range of p was too large to calculate the exact value of p in the case of HAP-7.

Correlation between W_{capa} and S_{BET}

In order to examine whether W_{capa} depends on S_{BET} of HAP, the values of W_{capa} and S_{BET} among the HAP samples were compared. For instance, W_{capa} of HAP-6 for BSA was not very different from that of HAP-7, but S_{BET} of HAP-6 was only about one quarter of that of HAP-7. Further, in spite of the fact that the value of S_{BET} of HAP-1 was smaller than that of HAP-7, W_{capa} of HAP-1 for lysozyme was larger than that of HAP-7. Other similar experimental results were also obtained. Hence no correlation was found between W_{capa} for globular proteins and S_{BET} of HAP.

CONCLUSION

The state of the adsorbing surface of HAP could be established from the effective surface area described as $(S_{BET} - S_p)\,px$. The binding capacities for globular proteins could be related to the effective surface area, not to the BET surface area, as follows:

$$W_{capa} = (M/2\sqrt{3}r^2 N_0)\,(S_{BET} - S_p)px \equiv A(S_{BET} - S_p)\,px$$

where $A \equiv M/2\sqrt{3}r^2 N_0$ is fixed for each protein.

The proportion of the area of the active part of the $S_{BET} - S_p$ surface area for adsorption, px, was similar among the same type of proteins but varied with the protein type, which was expected from the idea that the same adsorbing surface was related to the adsorption of the same type of proteins.

The px values obtained in this study contained some inaccuracies. This may be due to the errors accompanying the measurements of S_{BET}, S_p and W_{capa} and the uncertainty in the calculation of S_{capa}. For the determination of S_{capa}, for example, if we take into consideration the repulsive interactions which actually exist among proteins adsorbed on HAP, S_{capa} becomes larger than that calculated by eqn. 1. This results in x being calculated to be higher than the value given in this study. Further, S_{capa} becomes different if we calculate the surface area occupied by one protein molecule based on the shape of an ellipsoid. Although the numerical values themselves have some uncertainties such as this, it is still true that px is dependent on the preparation methods, the preparation conditions and also the protein types.

APPENDIX

The Cranston–Inkley method[12] is an improved method of deriving pore-size distributions from adsorption isotherms. It can be summarized as follows.

We consider an adsorption step from a relative pressure P_r to a pressure $P_{r+\delta r}$. It is assumed that pores in this range become filled with condensate, whereas in the pores having radii larger than $r+\delta r$ the thickness of the adsorbed layer on their walls increases from t_r to $t_r+\delta t$. Thus, $v_r\delta r$, the volume of nitrogen adsorbed between P_r and $P_{r+\delta r}$, is given by

$$v_r\delta r = \frac{(r - t_r)^2}{r^2} V_r\delta r + \delta t \int_{r+\delta r}^{\infty} \frac{(r - t_r)}{r} \cdot \frac{2V_r}{r} \cdot dr \tag{A1}$$

where $V_r\delta r$ is the total volume of pores having radii between r and $r+\delta r$. The first term on the right-hand side represents the volume of nitrogen due to the effect of capillary condensation and the second term represents the volume of nitrogen due to the effect of multi-layer adsorption.

We then consider a finite adsorption step from pressure P_1 (corresponding to radius r_1) to pressure P_2 (corresponding to r_2). Further, assuming V_r is sensibly constant over the range r_1 to r_2, eqn. A1 becomes

$$v_{12} = \frac{V_{12}}{r_2 - r_1} \int_{r_1}^{r_2} \frac{(r - t_1)^2}{r^2} \cdot dr + (t_2 - t_1) \int_{r_2}^{\infty} \frac{V_r (2r - t_1 - t_2)}{r^2} \cdot dr \tag{A2}$$

where V_{12} is the volume of pores having radii between r_1 and r_2. Rearranging this equation gives

$$V_{12} = R_{12} \left(v_{12} - k_{12} \int_{r_2}^{\infty} \frac{r - t_{12}}{2r^2} \cdot V_r dr \right) \tag{A3}$$

where $R_{12} = (r_2 - r_1) \Big/ \int_{r_1}^{r_2} [(r - t_1)^2/r^2] dr$, $k_{12} = 4 (t_2 - t_1)$, and $t_{12} = 1/2 (t_1 + t_2)$. v_{12} can be derived from experimental measurements.

It is convenient to replace the integral term in eqn. A3 by a summation term of all pore increments and to use pore diameter instead of pore radius. Thus, eqn. A3 becomes

$$V_{12} = R_{12} \left(v_{12} - k_{12} \sum_{d_2 + \frac{1}{2}\Delta d}^{d_{max}} \frac{d - 2t_{12}}{d^2} \cdot V_d \Delta d \right) \tag{A4}$$

R_{12}, k_{12} and the function $(d-2t)/d^2$ for mean values of t and d have been tabulated for standard pore diameter increments[12]. Thus, S_{12} (surface area in units of m^2/g) can be calculated from eqn. A4 by using the relationship

$$S_{12} = 4aV_{12} \cdot 10^4/d'$$

where a is the ratio of the density of gaseous nitrogen at NTP to that of liquid nitrogen and d' is the mean pore diameter between d_1 and d_2 (Å). The reader is referred to the original paper[12] for the exact details of the calculations.

In our work, the S_p value for each tested protein based on pores existing in the HAP was obtained by accumulating the S_{12} values over a range of pore diameters which is smaller than the size of the tested protein molecule.

REFERENCES

1 T. Kawasaki, *J. Chromatogr.*, 151 (1978) 95.
2 T. Kawasaki, *J. Chromatogr.*, 157 (1978) 7.
3 M. Kukura, L. C. Bell, A. M. Posner and J. P. Quirk, *J. Phys. Chem.*, 76 (1972) 900.
4 A. L. Boskey and A. S. Posner, *J. Phys. Chem.*, 80 (1976) 40.
5 D. M. Roy, L. E. Drafall and R. Roy, in A. M. Alper (Editor), *Refractory Materials,* Vol. 6-V, Academic Press, New York, 1978, pp. 187–206.
6 T. Kawasaki, W. Kobayashi, K. Ikeda, S. Takahashi and H. Monma, *Eur. J. Biochem.*, 157 (1986) 291.
7 Y. Kato, K. Nakamura and T. Hashimoto, *J. Chromatogr.*, 398 (1987) 340.
8 S. Inoue and A. Ono, *U.S. Pat.*, 4 711 769 (1987).
9 N. Tagaya, H. Kuwahara, T. Hashimoto, N. Komatsu, K. Fukamachi and T. Maeshima, *U.S. Pat.*, 4 794 171 (1988).
10 S. Shimabayashi and M. Nakagaki, *Nippon Kagaku Kaishi,* (1978) 326.
11 H. A. Sober (Editor), *Handbook of Biochemistry,* CRC Press, Cleveland, OH, 1973, p. C-10.
12 R. W. Cranston and F. A. Inkley, *Adv. Catal.*, 9 (1957) 143.
13 H. Monma and T. Kanazawa, *Yogyo Kyokai Shi*, 84 (1976) 209.

Porous glass sheets for use in thin-layer chromatography

MASANORI YOSHIOKA*, HIROKO ARAKI and MIWAKO KOBAYASHI

Faculty of Pharmaceutical Sciences, Setsunan University, 45–1, Nagaotoge-cho, Hirakata, Osaka, 573-01 (Japan)

FUMIKO KANEUCHI, MADOKA SEKI and TADASHI MIYAZAKI

Japan Spectroscopic Co., Ltd. (JASCO), 2967–5, Ishikawa-cho, Hachioji, Tokyo, 192 (Japan)

and

TAKESHI UTSUKI, TAKAO YAGINUMA and MASAAKI NAKANO

Ise Chemical Industries Co., Ltd., 2–7–12, Yaesu, Chuo-ku, Tokyo, 104 (Japan)

ABSTRACT

Porous glass was made from a mixture of 45–70% SiO_2, 8–30% B_2O_3, 8–25% CaO, 5–15% Al_2O_3, 3–8% Na_2O + 1–5% K_2O and 0–8% MgO. The mixture was heated at 600–850°C for 20 h and cut into square sheets of 5 cm × 5 cm × 0.5 mm. Each sheet was leached with 1 M hydrochloric acid at 80–90°C for 4–16 h to make it porous. The surface of each sheet was examined with a scanning electron micrograph. The various sheets with pore diameters from 110 to 1200 nm were developed with a few common solvents for thin-layer chromatography (TLC). The larger the pore diameters, the shorter were the developing times with the solvents. A sheet of 700 nm pore diameter required only a few minutes and showed good separations, and was adopted in the subsequent TLC study.

Twenty Dns-amino acids were applied to the sheet and detected by their fluorescence at picomole levels. Free amino acids were also applied and derivatized to fluorescent compounds with fluorescamine, and were detected at 100-pmol levels. Inorganic cations and anions at concentrations down to nanomole levels were applied and sensitively detected by colour reactions.

The fluorescence spectrum of DNS-alanine on the sheet was measured directly. A Fourier transform IR spectrum of phenacetin *in situ* on the sheet was obtained, and was reliable in the region of wavenumber from 1550 to 4000 cm^{-1}. The sheet is very stable towards strong acids, alkalis and mechanical scratching. It has no supporting matrix, although the conventional thin layers have, and showed a sharp front line without a necklace effect.

INTRODUCTION

In thin-layer chromatography (TLC), originated by Stahl[1,2], fine particles of silica gel, several tens of micrometres in diameter, are coated in a layer less than 1 mm

thick on a supporting matrix such as glass or plastics. In place of silica gel, alumina crystalline cellulose and polyamide can be used. Recently, these particles have been made much smaller and refined to increase the resolution in so-called high-performance TLC.

These thin layers are very good for separation, but several problems arise when other functions need to be improved. Various kinds of binders are necessary to coat the particles on the matrix and, even if the particles are completely coated with the binders, they are apt to scrape during handling, especially spotting. Separations are sometimes affected by the boundary between the thin layer and its supporting matrix. When a separated zone is preparatively extracted with a solvent, fine powders from the particles remain in the extract. When the zone is measured spectrophotometrically *in situ*, it is difficult to obtain a detailed spectrum owing to the high background of the surface of the layer.

In this study, we aimed not only to solve the above problems, but also to prepare more technologically advanced thin layers. Recently, porous glass has been produced and used in high-performance liquid chromatography[3] and we thought that a porous glass sheet could act both as the separation layer and the supporting matrix in TLC. Sheets of various diameters were prepared and examined for their versatility. Separation profiles were determined for 5-dimethylaminonaphthalene-1-sulphonyl (Dns) amino acids, free amino acids and inorganic ions. For their detection, we examined several new methods such as chemical reactions, direct measurements of fluorescence and Fourier transform (FT) IR spectrometry on the sheets.

EXPERIMENTAL

Reagents

Dns-Amino acids were obtained from Pierce (Rockford, IL, U.S.A.). Twenty L-amino acids were obtained from Wako (Osaka, Japan). Glycine, cysteine, histidine, arginine and lysine were in the hydrochloride form. Inorganic ions in the following forms were also obtained from Wako: $MgCl_2 \cdot 6H_2O$, $AlCl_3 \cdot 6H_2O$, $CaCl_2 \cdot 2H_2O$, VCl_3, $CrCl_3 \cdot 6H_2O$, $MnCl_2 \cdot 4H_2O$, $FeCl_2 \cdot nH_2O$, $FeCl_3 \cdot 6H_2O$, $CoCl_2 \cdot 6H_2O$, $NiCl_2 \cdot 6H_2O$, $CuCl_2 \cdot 2H_2O$, $ZnCl_2$, $GeCl_4$, As_2O_3, $SeCl_4$, $SrCl_2 \cdot 6H_2O$, $YCl_3 \cdot 6H_2O$, $ZrCl_2O \cdot 8H_2O$, $PbCl_2$, $AgNO_3$, $CdCl_2 \cdot 2.5H_2O$, $InCl_3 \cdot 4H_2O$, $SnCl_2 \cdot 2H_2O$, $SbCl_3$, $TeCl_4$, $CeCl_3 \cdot 7H_2O$, $TbCl_3 \cdot xH_2O$, $YbCl_3 \cdot 6H_2O$, $IrCl_4$, $H_2PtCl_6 \cdot 6H_2O$, $HAuCl_4 \cdot 4H_2O$, $HgCl_2$, $TlCl$, $PbCl_2$, $BiCl_3$, NaF, $NaCl$, KI, $KBrO_3$, KIO_3, $K_2B_4O_7 \cdot 4H_2O$, $Na_2C_2O_4$, $NaNO_2$, KNO_3, $Na_3PO_4 \cdot 12H_2O$, Na_2SO_4, $Na_2S_2O_3 \cdot 5H_2O$, $NaSCN$, K_2CrO_4, $K_2Cr_2O_7$, $K_4Fe(CN)_6 \cdot 3H_2O$, $K_3Fe(CN)_6$ and Na_2CO_3. Fluorescamine was obtained from Nippon Roche (Kamakura, Japan). Dithizone and 8-hydroxyquinoline were obtained from Wako.

Reagent solutions

For spraying the sheets, solutions of 0.05% dithizone in chloroform, 1% 8-hydroxyquinoline in methanol, 25% ammonia, 0.1% silver nitrate and $7.5 \cdot 10^{-5}$ *M* fluorescamine in acetone were prepared.

Preparation of new glass sheets

The glass consisted of 45–70% SiO_2, 8–30% B_2O_3, 8–25% CaO, 5–15% Al_2O_3,

3–8% Na_2O + 1–5% K_2O and 0–8% MgO. The mixture was heated at 600–800°C for 20 h to effect a phase separation and the product was cut into square sheets of 5 cm × 5 cm × 0.5 mm. Each sheet was leached with 1 M hydrochloric acid at 80–90°C for 4–16 h to etch the B_2O_3 phase to make it porous, washed with water and dried.

TLC

For spotting sample solutions, a 1-μl glass capillary (32 mm × 0.1 mm I.D.) (Microcaps) was cut to one tenth of the original length, *i.e.*, 3.2 mm long. The small tip of the capillary was connected with a silicon tube of 0.5 mm I.D. The tip was dipped into the sample solution and 0.1 μl was sucked into it. This solution was applied to the sheet by pushing the silicon tube, dried and developed with a solvent. Dns-Amino acids were dissolved in 95% ethanol to give $1 \cdot 10^{-6}$ M solutions. The Dns-amino acids were located by irradiation with a UV lamp at 366 nm. The fluorescence spectrum of Dns-Ala, 7 μl of a solution of which was spotted on the sheet, was measured with an FP-770 fluorescence spectrophotometer (JASCO).

Amino acids were dissolved in a small aliquot of 0.1 M hydrochloric acid and diluted with water to make $1 \cdot 10^{-3}$ M solutions. The glass sheet used for the free amino acids was reheated at 600°C for 5 h to change the silanol groups to siloxanes. For detection, the developed sheet was immersed in a fluorescamine solution in acetone.

Each inorganic cation was dissolved in 0.1 M hydrochloric acid and diluted with water to 0.01 M. For detection, the developed sheet was sprayed with 1% 8-hydroxyquinoline or 0.05% dithizone.

Each inorganic anion was dissolved in 5% sodium carbonate solution to make 0.05–1 M solutions. For detection, the sheet was sprayed with 0.1% silver nitrate solution and irradiated with the UV lamp.

Phenacetin was dissolved in chloroform to make a 0.1 M solution and 7 μl of the solution were spotted on the sheet and dried. An FT-IR spectrum of the spot was measured *in situ* with a Model 8000 FT-IR spectrometer (JASCO).

RESULTS

An electron micrograph of a glass sheet is shown in Fig. 1. The pore edge of diameter 1000 nm was so thin and sharp that it was fragile in comparison with that of 500 nm. The larger the pore sizes, the shorter were the developing times with normal solvents, as shown in Fig. 2. The sheet of pore size 700 nm took only a few minutes, showed good separations and was adopted in the subsequent TLC studies. The sheet was further cut into half to make the developing time shorter and more economical. The development was carried out in a small sample bottle in a few minutes.

The separation of twenty Dns-amino acids was tried with two solvents as shown in Fig. 3. Their fluorescences were seen at the same places on both sides of the sheet. It should be possible to identify an unknown sample by locating it at the same place on the front side as for a standard on the other side. It was also possible to obtain a fluorescence spectrum of Dns-Ala on the sheet, as shown in Fig. 4. The spectrum almost corresponded to that taken in a solvent.

Twenty free amino acids were separated as shown in Fig. 5. The separations of structurally related compounds were dependent on their sizes, as shown by Gly, Ala and Val.
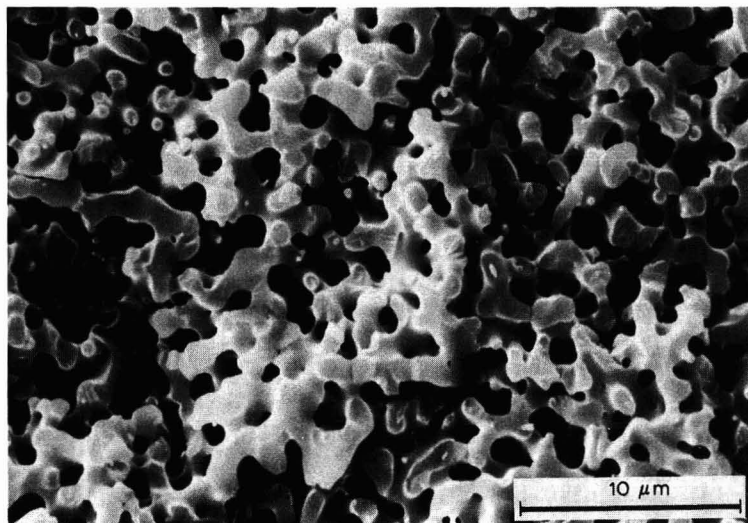
Fig. 1. Electron micrograph of glass sheet (700 nm).

A good FT-IR spectrum of the thin layer was obtained, as shown in Fig. 6. The spectrum was reliable for wavenumbers in the range above 1550 cm^{-1}.

The cations were well separated by two solvent systems, as shown in Fig. 7. The visible colours or the fluorescence were almost the same as those in conventional TLC using a crystalline cellulose or silica gel. However, no shrinkage of the sheet with strong acid was observed.

The sheets for the anions were developed with two solvent systems as shown in Fig. 8. The colours of the spots obtained with 0.1% silver nitrate solution and UV irradiation were sensitive and clear. This kind of UV irradiation effect was not found on silica gel plates. The separation on the sheet was characteristic, as shown in Fig. 9, where a small difference in the solvent composition led to a large difference in the separation.
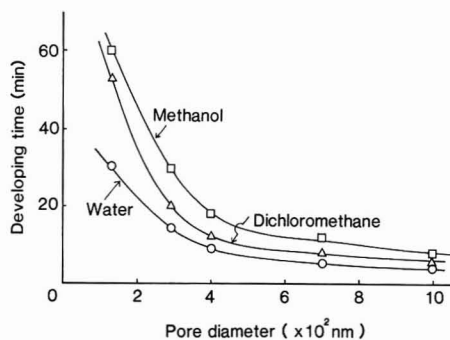
Fig. 2. Relationship between pore size and developing time. The sheets were developed to 4.5 cm with the three solvents indicated.
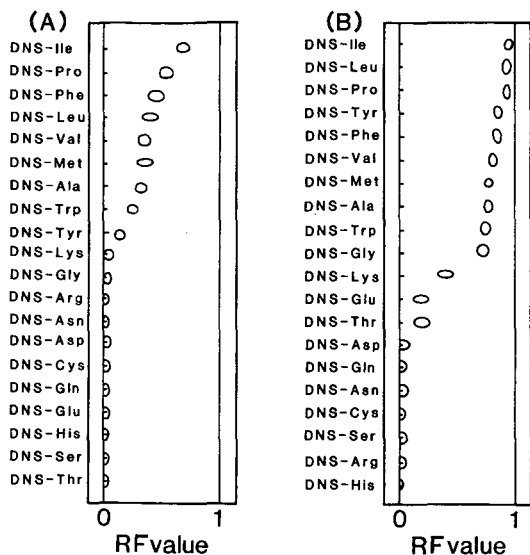
Fig. 3. Chromatograms of twenty Dns (DNS)-amino acids on a sheet of pore size 700 nm developed with (A) chloroform and (B) benzene–acetic acid (19:1, v/v).

Fig. 4. Excitation and fluorescence spectra of Dns-Ala on a sheet.

Fig. 5. Chromatogram of 100 pmol of amino acids on a reheated sheet (2.5 cm × 5 cm) developed with *n*-butanol–acetic acid–water (10:1:1, v/v/v) and detected with fluorescamine. Pro (dotted circle) was detected with ninhydrin.
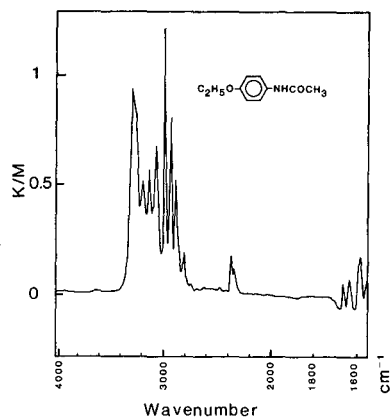
Fig. 6. FT-IR spectrum of 0.7 μg of phenacetin on the sheet. K/M means the Kubelka–Munk format.

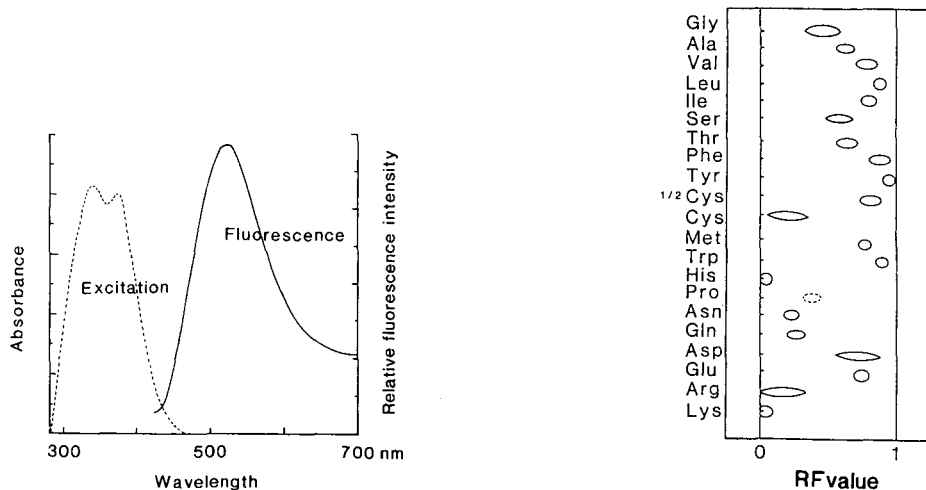|	Dithizone	Oxine	Oxine upon UV
Mg		Yellow	Yellowish green
Al		Yellow	Yellowish green
Ca		Light yellow	Yellow
V	Brown		Dark
Cr	Reddish orange		Dark
Mn	Pink	Yellow	Dark
Fe²⁺	Brown	Grey	Dark
Fe³⁺	Brown	Grey	Dark
Co	Purple	Yellow	Dark
Ni	Purple	Yellow	Dark
Cu	Brown	Yellow	
Zn	Reddish purple	Light yellow	Orange
Ge		Light yellow	Orange
As			
Se	Brown		
Sr	Yellow	Light yellow	Yellow
Y			White
Zr		Yellow	Brown
Pd		Yellow	Orange
Ag	Green		Yellow
Cd	Reddish orange	Brown	Dark
In	Orange	Ligth yellow	Yellow
Sn	Pink		
Sb	Purple	Yellow	Orange
Te	Orange		
Ce	Orange		Dark
Tb	Yellowish brown		Dark
Yb		Yellow	Dark
Ir		Yellow	Dark
Pt	Brown	Brown	Dark
Au	Reddish orange	Brown	Dark
Hg	Orangish brown	Brown	Dark
Tl	Orange	Yellow	Dark brown
Pb			Dark
Bi	Reddish orange		
	Pink	Yellow	Dark

Fig. 7. Chromatograms of metal ions developed with (A) *n*-butanol–benzene–1 M HNO₃–1 M HCl (75:69:4:2, v/v) and (B) acetone–3 M HCl (99:1, v/v). Colours with dithizone, oxine and oxine upon UV are given at the right-hand side.

(A)   **(B)**

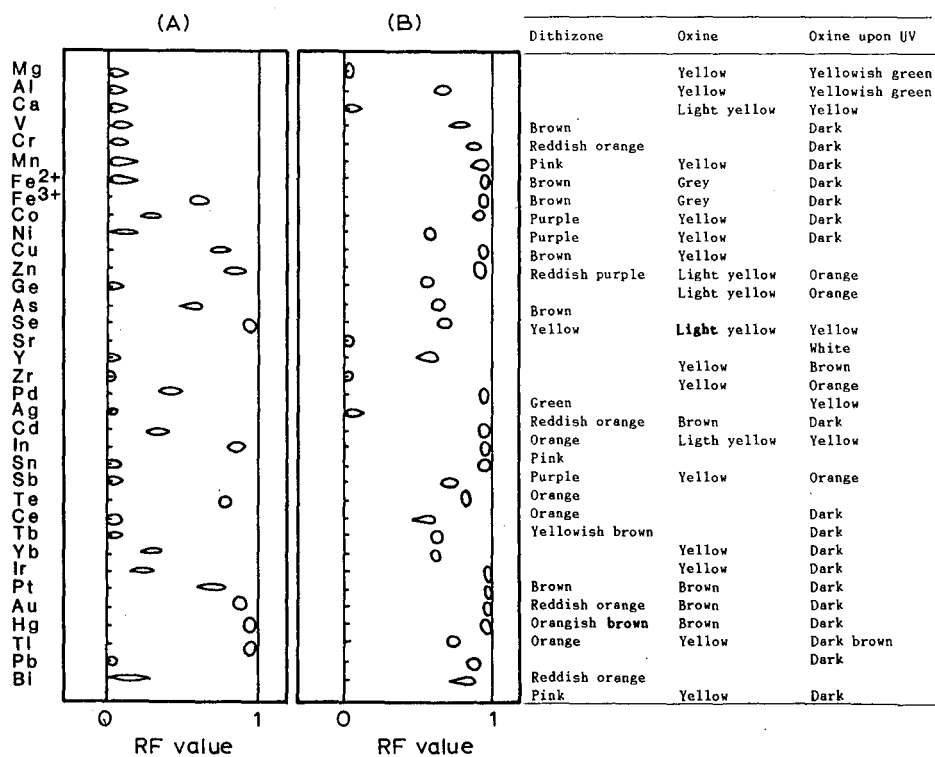|	AgNO₃	AgNO₃ upon UV
F⁻		Dark
Cl⁻	Grey	Dark
Br⁻	Grey	Dark
I⁻	Grey	Dark
BrO₃⁻	Grey	
IO₃⁻		Dark
BO₂⁻		Dark
C₂O₄²⁻	Grey	Dark
NO₂⁻		Dark
NO₃⁻	Grey	Dark
PO₄³⁻	Bluish grey	Dark
SO₄²⁻	Grey	
S₂O₃²⁻	Brown	Dark
SCN⁻	Brown	Dark
CrO₄²⁻	Reddish brown	Dark
Cr₂O₇²⁻	Reddish brown	Dark
Fe(CN)₆⁴⁻	Yellow(A),Grey(B)	Dark
Fe(CN)₆³⁻	Orange brown	Dark
CO₃²⁻	Orange	

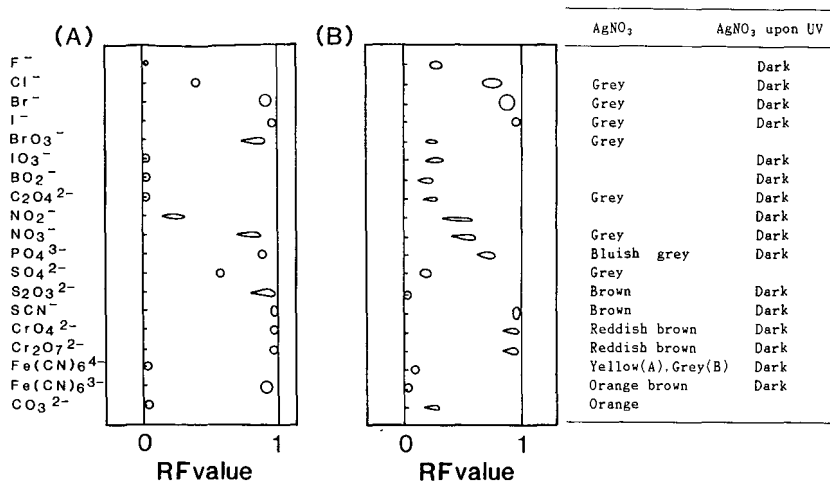0   1   0   1
RF value   **RF value**

Fig. 8. Chromatograms of anions developed with (A) acetone–water (96:4, v/v) and (B) n-butanol saturated with water. Colours with AgNO₃ and AgNO₃ upon UV are given at the right-hand side.

100 %   98 %   96 %   94 %   92 %

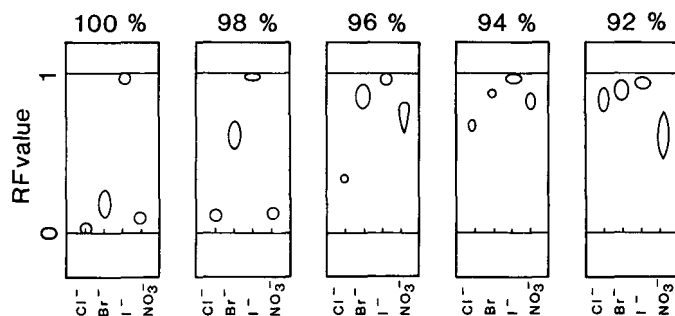RFvalue

Cl⁻ Br⁻ I⁻ NO₃⁻

Fig. 9. Chromatograms of anions developed with various concentrations of acetone in water.

DISCUSSION

Satisfactory TLC of representative compounds was achieved on the porous glass sheets. The spots appear broader than those on conventional plates. The separation characteristics on the sheets such as the R_F values and the broadening did not vary much with the pore diameters, although the broadening on the sheet of pore size 700 nm was larger.

The principle of the separation has not been elucidated. However, the higher the R_F values, the larger were the molecular weights of the related compounds, as shown in the chromatograms for the halogens (Fig. 8), amino acids (Fig. 5) and Dns-amino acids (Fig. 3) such as Leu, Val, Ala and Gly. In addition, silanols on the sheet and interactions between the solutes and the solvent seem to influence the separation.

It is possible to measure the fluorescence and FT-IR spectra *in situ* on the sheet. The spectrum is influenced by the environment of the solute on the surface. For identification, the spectrum of a standard must be taken on the same sheet. The

application is still limited, since at wavenumbers below 1550 cm^{-1} the influence of silanol groups is so great that correction with the background is impossible. Previously, FT-IR spectra were measured by Chalmers et al.[4] after the sample had been extracted with a solvent from the zone on the layer. With the present type of sheet, extraction is unnecessary and the recovery therefore need not be considered. Zuber et al.[5] measured FT-IR spectra in situ on a silica gel plate, but below 1550 cm^{-1} the background due to silanols was high and above 1550 cm^{-1} the influence of the surface was too high to obtain clear signals. In this respect the glass sheet is superior.

It is possible to achieve fine separations by using more developing solvents and to detect nanomole levels of inorganic cation except Mg^{2+} and Ca^{2+} at the 10-nmol level. For the anions, 10-nmol levels are also detectable. These sensitivities are higher than those reported by Nakamura and Tamura[6], who detected these ions on a thin layer containing a mixture of fluorescent compounds, but not those of specific colour reactions for the respective ions. The sensitivities for the fluorescence of the Dns-amino acids and fluorescamine derivatives on the sheet are 1000 times higher than those for the above colour reactions and slightly higher than those for fluorescence reported by Spivak et al.[7] and Nakamura and Pisano[8], judging from the detection limits given.

The sheet is mechanically strong compared with conventional thin layers of powders coated on the matrix. It is also more stable against acids and alkalis so that shrinkage of the sheet does not occur during the separations of inorganic compounds and detection. The detection on the sheet is based completely on "dry" chemistry, as the spot is developed, dried and reacted with a spray reagent. The volume per gram of the sheet is 0.39 ml/g, making a large specific surface area of 6.6 m^2/g, which accelerates the reduction of Ag^+ on the UV irradiation as shown in Fig. 8. The sheet whould be useful for the study of this kind of dry chemistry. The equivalence of the front and rear sides of the sheets is another merit. The boundary between the thin layer and the matrix gives rise to a necklace effect of the front of the developing solvent in conventional TLC, but on the glass sheet the front line is straight and does not show such an effect.

It is easy to cut the sheet with a cutter and to extract the separated zone using a solvent, as the surface of the glass is so strong that no powder is introduced into the extracted residue. The spectra measured in situ on the sheet show fine detail. The glass sheets under investigation are expensive and it is undesirable to dispose of them like conventional plates. The sheets should be washable with strong acids and organic solvents and hence can be reused. With further development the high performance and function of these sheets should lead to ideal thin layers for TLC.

REFERENCES

1 E. Stahl, Pharmazie, 11 (1956) 633.
2 E. Stahl, Arch. Pharm., 292 (1959) 411.
3 Y. Matsushima, Y. Nagata, K. Takakusagi, M. Niyomura and N. Takai, J. Chromatogr., 332 (1985) 265.
4 J. M. Chalmers, M. W. Mackenzie and J. L. Sharp, Anal. Chem., 59 (1987) 415.
5 G. E. Zuber, R. J. Warren, P. P. Begosh and E. L. O'Donnell, Anal. Chem., 56 (1984) 2935.
6 H. Nakamura and Z. Tamura, Bunseki Kagaku, 22 (1973) 1356.
7 V. A. Spivak, V. M. Orlov, V. V. Shcherbukhin and Ya. M. Varshavsky, Anal. Biochem., 35 (1970) 227.
8 N. Nakamura and J. J. Pisano, J. Chromatogr., 121 (1976) 79.

CHROMSYMP. 1819

Constant-potential amperometric detector for carbohydrates at a nickel(III) oxide electrode for micro-scale flow-injection analysis and high-performance liquid chromatography

MASASHI GOTO*

Department of Pharmaceutical Analytical Chemistry, Gifu Pharmaceutical University, 5–6–1 Mitahora-Higashi, Gifu 502 (Japan)

and

HIROYOSHI MIYAHARA and DAIDO ISHII

Department of Applied Chemistry, Faculty of Engineering, Nagoya University, Chikusa-ku, Nagoya 464 (Japan)

ABSTRACT

A constant-potential amperometric detector for carbohydrates based on oxidation at an active nickel(III) oxide electrode for micro flow-injection analysis (micro-FIA) and micro high-performance liquid chromatography (micro-HPLC) was developed. The active nickel(III) oxide is formed *in situ* on the electrode surface at potentials near *ca.* 0.5 V *vs.* Ag/AgCl. The nickel(III) surface acts as a strong oxidant and reacts with the carbohydrate by hydrogen atom abstraction to yield a radical. A tubular-type electrolytic cell was constructed by inserting nickel wire of diameter 25 or 50 μm and length *ca.* 5 mm into the fused-silica tube (50 or 100 μm I.D.). The effective cell volume was less than *ca.* 30 nl. The cell was successfully applied to the detection of various sugars such as aldopentoses, aldohexoses, ketohexoses, sugar alcohols, disaccharides and trisaccharides. The detection limit of micro-FIA was 0.1 ng (signal-to-noise ratio = 3) for glucose.

INTRODUCTION

Liquid chromatography has become a well established technique for the separation of carbohydrates. Unfortunately, the absence of a strongly absorbing chromophore in carbohydrates restricts the use of direct UV–visible detection. Refractive index detection, the most generally used mode, often lacks sensitivity. Recently, improvements in sensitivity have been attempted by the development of electrochemical detectors based on the direct or catalytic electrooxidation of carbohydrates in highly basic solution[1–13]. In order to reduce the large overpotential for carbohydrate oxidation, various working electrode materials have been used. Electrochemical detectors for carbohydrates can be divided into two groups. The first

group employs platinum[1-3] or gold[4-7] electrodes on which the carbohydrates adsorb and subsequently undergo relatively facile dehydrogenation/oxidation. However, because of the surface cleaning and regeneration steps necessary to obtain a stable response, simple constant-potential operation is not possible, and double- or triple-pulse potential waveforms are required. The detection limits for carbohydrates with platinum and gold electrodes are about 100 and 10 ng, respectively. The second group employs catalytic electrodes using an oxidizable metal such as nickel[8-10], copper[11] and silver[11], or containing a surface-attached electron-transfer mediator such as cobalt phthalocyanine[12,13]. For these, the lowest detection limits (1 ng for monosaccharides and 5 ng for oligosaccharides) have been found with nickel electrodes. More recently, a copper-based chemically modified electrode has been developed for a constant-potential amperometric detector[14]. Such an electrode was prepared by coating a glassy carbon electrode with a copper(II) layer that catalyses the oxidation of carbohydrates when a potential sufficiently positive to generate copper(III) is applied. Detection limits at the subnanogram level (0.22 ng for glucose) have been reported with this type of detector. However, none of the electrochemical detectors reported are suitable for micro-scale flow-injection analysis (micro-FIA) or high-performance liquid chromatography (micro-HPLC) because of the relatively large cell volume.

    In this work, an electrolytic cell with an extremely small volume for a constant-potential amperometric detector based on oxidation at an active nickel(III) oxide electrode was constructed by using a nickel wire of diameter 25 or 50 μm and applied in micro-FIA and micro-HPLC.

EXPERIMENTAL

Reagents
    Stock solutions of 21 kinds of carbohydrates, purchased from Wako or Aldrich, were prepared fresh daily in deionized water and, just prior to use, were adjusted to the desired concentration. Supporting electrolyte solution was prepared from carbonate-free sodium hydroxide and deionized water.

Apparatus
    Cyclic voltammetry (CV) was performed with a new cyclic voltammetric analyser (Yanagimoto, VMA-010) and an *X-Y* recorder (Yokogawa, 3086). A schematic diagram of the micro-HPLC apparatus is shown in Fig. 1. A micro-feeder (Azuma Denki, FM-2) and two micro-syringes (Ito, GAN-050) were used for feeding the mobile phase (carrier) and the electrolyte solution to reduce pulsations in the flow. A micro-valve injector (Nihon Bunko, ML-422; 20 nl) was used for sample injection. The fundamental construction of the tubular-type electrolytic cell, which is similar to that of a carbon fibre working electrode[15], is shown in Fig. 2. A nickel wire of diameter 25 or 50 μm and length 5mm was inserted into the fused-silica tube (50 or 100 μm I.D., respectively) to serve as the working electrode. A silver/silver chloride and a platinum counter electrode were placed outside the tube near the outlet of the solution. The effective cell volume was less than *ca.* 30 nl.

    A voltammetric detector (Yanagimoto, VMD-101) and a recorder (Yokogawa, 3056) were used for constant-potential amperometry. The electrolytic cell was
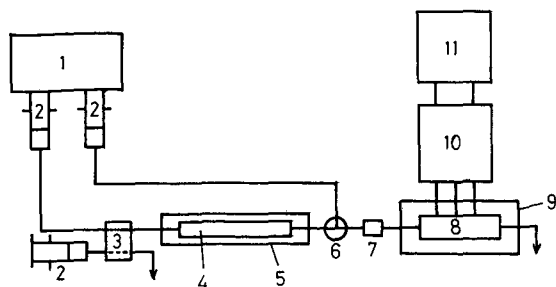
Fig. 1. Schematic diagram of apparatus for micro-HPLC. 1 = Micro-feeder; 2 = micro-syringe; 3 = valve injector (0.02 μl); 4 = micro-separation column; 5 = water-bath; 6 = mixing joint; 7 = mixing column; 8 = electrolytic flow cell; 9 = heater; 10 = potentiostat; 11 = recorder.

thermostated by using a column heater (Sugai Kagaku, U-620). Laboratory-made micro-separation columns packed with Shodex Ionpak KS-801 (247 mm $\times$ 0.35 mm I.D. + 217 mm $\times$ 0.35 mm I.D.) and SAX (100 mm $\times$ 0.25 mm I.D. + 100 mm $\times$ 0.25 mm I.D.) were used for size-exclusion and ion-exchange chromatography of carbohydrates, respectively. For ion-exchange chromatography, the electrolyte solution was mixed before the column instead of after the column. Micro-FIA experiments were carried out by removing the micro-separation columns.
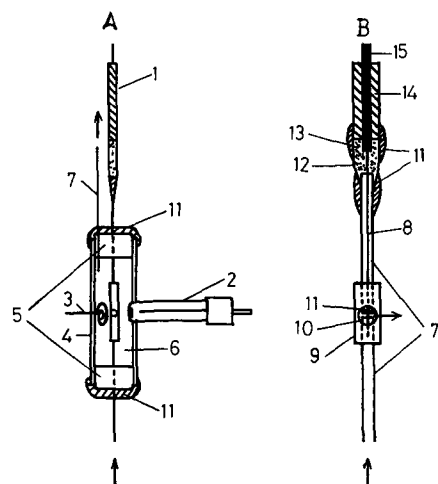

Fig. 2. Structure of electrolytic flow cell of tubular type. (A) Whole cell; (B) detail of working micro-electrode. 1 = Working electrode; 2 = reference electrode (Ag/AgCl); 3 = counter electrode (Pt wire); 4 = acrylic tube; 5 = rubber cup; 6 = electrolyte solution (mobile phase); 7 = fused-silica tube (50 or 100 μm I.D.); 8 = Ni wire (diameter 25 or 50 μm, length 5 mm); 9 = PTFE tube (0.1 mm I.D., 2 mm O.D.); 10 = hole; 11 = adhesive resin; 12 = glass pipette; 13 = silver paste; 14 = insulator; 15 = electric wire.
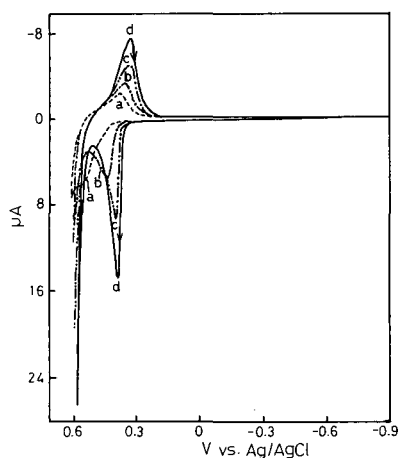
Fig. 3. Consecutive cyclic voltammograms of nickel micro-electrode itself in 0.5 *M* NaOH. Order of potential scans: (a) 1st; (b) 2nd; (c) 5th; (d) multiple scans. Working electrode, Ni wire (diameter 50 μm, length 5 mm); potential scan rate, 100 mV/s.
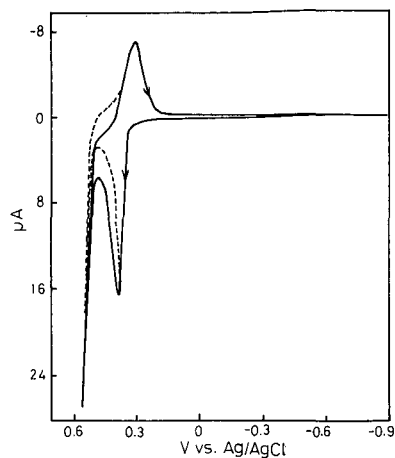
Fig. 4. Cyclic voltammogram of glucose in 0.5 *M* NaOH using a nickel working micro-electrode. Solid line, 1.0 m*M* glucose; dashed line, 0 m*M* glucose. Potential scan rate, 100 mV/s.

RESULTS AND DISCUSSION

Electrochemistry

Cyclic voltammograms obtained for the nickel micro-electrode itself immersed in oxygen-free 0.5 *M* NaOH are shown in Fig. 3. During the first scan in the anodic direction, a single, broad oxidation wave with a peak potential of 0.55 V (*vs.* Ag/AgCl) was observed. This may be due to the oxidation of metallic nickel to a nickel(II) compound. On subsequent scans, this wave gradually increased and shifted to the negative potential side. After more than ten scans, a steady-state cyclic voltammogram, which shows an oxidation wave with a peak potential of 0.38 V and a re-reduction wave with a peak potential of 0.32 V, was observed. The peak height of the oxidation wave at the steady state was proportional to the potential scan rate. This indicates that the wave is due not to the soluble species but to the absorbed species on the electrode. The peak potential of the oxidation wave at the steady state was changed to the negative side at the rate of 60 mV/pH with increasing NaOH concentration in the medium, indicating that OH$^-$ is involved in the electrode reaction. In conclusion, the peaks in the steady-state voltammogram correspond to the nearly reversible oneelectron reaction between $Ni(OH)_2$ and $NiO(OH)$. Addition of glucose to the above NaOH solution produced a clear increase in the oxidation current, whereas the re-reduction current was almost the same as that obtained without glucose (see Fig. 4). This suggests that nickel in contact with NaOH solution becomes covered with a layer of nickel(II) hydroxide mainly by electrooxidation, from which, at a high enough applied potential, $NiO(OH)$ is formed. Acting as a catalyst, this nickel(III) compound may oxidize carbohydrates such as glucose and $NiO(OH)$ itself is reduced to $Ni(OH)_2$, which again will be oxidized by the applied potential to give an increased oxidation current, as pointed out by Fleischmann et al.[16].

Micro-FIA

On the basis of the above CV results, it seemed likely that the amperometric detection of carbohydrates in flow analysis might be able to be carried out at relatively low potentials on the nickel(III) oxide electrode. The hydrodynamic voltammograms for glucose and lactose obtained on the nickel(III) oxide micro-electrode (diameter 25 μm, length 5 mm) are shown in Fig. 5. In this instance, pure water and 0.25 M sodium hydroxide solution were used as the carrier and the electrolyte solution, respectively, each at a flow-rate of 1.1 μl/min and 0.02 μl of each sample being injected. The maximum electrode responses were observed at a working electrode potential of 0.63 V (*vs.* Ag/AgCl), independent of species, and oxygen generation began to occur at about 0.60 V as shown in the dashed line. In order to obtain high sensitivity, a potential of 0.57 V, at which the ratio of peak current to background current was maximum, was chosen as a suitable applied potential for amperometry in this work.

The effect of the flow-rates of the carrier and electrolyte solutions on the electrode response is shown in Fig. 6. In this instance, the ratio of the flow-rate of the carrier (pure water) to that of the electrolyte solution was kept at 1:1 and 1.0 M sodium hydroxide solution was used as the electrolyte solution. The electrode response tended to increase with decreasing flow-rate and to become nearly constant at flow-rates higher than about 2.8 μl/min. This indicates that a longer contact time of the sample with the electrode is preferable. With respect to the time of analysis, a flow-rate of 1.1 μl/min was chosen as the most suitable for both the carrier and electrolyte solution in further work.

The effect of alkali concentration in the electrolyte solution on the electrode response was investigated. It was found that the electrode response was a maximum at a sodium hydroxide concentration of about 0.25 M, and the background current
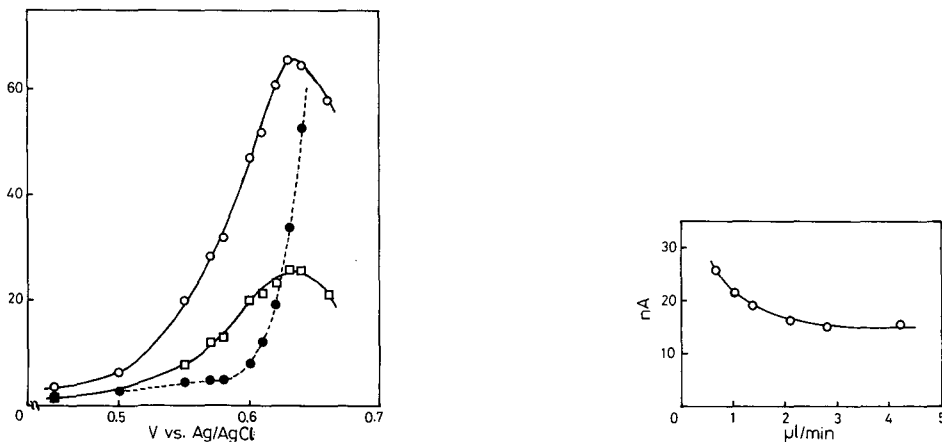

Fig. 5. Relationship between applied potential and peak height in micro-FIA. ($\bigcirc$) 10 mM Glucose sample; ($\square$) 10 mM lactose sample; ($\bullet$) background current. Injection volume, 0.02 μl; flow-rates of water and 0.25 M NaOH, both 1.1 μl/min; working electrode, Ni wire (diameter 25 μm, length 5 mm).

Fig. 6. Effect of flow-rates of carrier (pure water) and electrolyte solution on peak height. Sample, 10 mM glucose; injection volume, 0.02 μl; applied potential, 0.57 V *vs.* Ag/AgCl; NaOH concentration in electrolyte solution, 1.0 M.
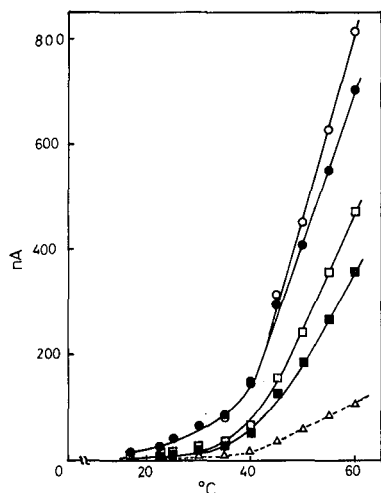
Fig. 7. Effect of detection temperature on peak height. (○) Glucose; (●) arabinose; (□) lactose; (■) raffinose; (△) background current. Concentration of sample, 10 mM each; injection volume, 0.02 μl; applied potential. 0.57 V vs. Ag/AgCl; flow-rates of water and 0.25 M NaOH, both 1.1 μl/min.
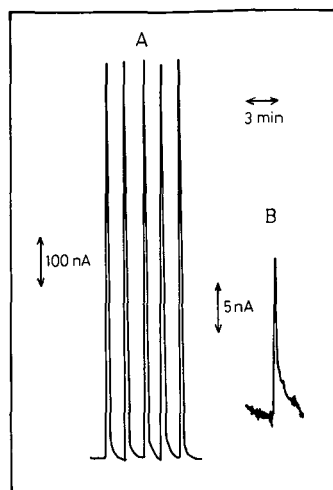
Fig. 8. Typical responses of glucose in micro-FIA. (A) 10 mM; (B) 0.1 mM. Injection volume, 0.02 μl; applied potential, 0.57 V vs. Ag/AgCl; flow-rates of water and 0.25 M NaOH, both 1.1 μl/min; detection temperature, 60°C.

increased linearly with increasing sodium hydroxide concentration. A sodium hydroxide concentration in the electrolyte solution of 0.25 M was therefore used in further work.

When the temperature of the detector was increased from 17 to 60°C, the electrode response increased dramatically, as shown in Fig. 7. This indicates that the chemical oxidation of carbohydrates by nickel(III) oxide is the rate-limiting step in the proposed detection mode and the temperature increase accelerates the reaction rate. Operation at higher temperatures required a back-pressure to prevent gas production in solution. In the cell construction shown in Fig. 2, gas production did not occur at temperatures up to 60°C. Typical responses of glucose at different concentrations in micro-FIA at a detection temperature of 60°C are shown in Fig. 8. The detection limits aof glucose at 30 and 60°C were 0.35 and 0.10 ng (signal-to-noise ratio = 3), respectively, and the peak currents at 30 and 60°C were proportional to the amount of glucose up to 90 ng (25 mM for a sample size of 0.02 μl) and 18 ng (5mM for a sample size of 0.02 μl), respectively. A glucose detection limit of 0.1 ng with the proposed micro-detector compares favourably with those for conventional detectors with platinum[2], gold[7], nickel[10], cobalt phthalocyanine[13] and copper-based chemically modified[14] electrodes. For example, Neuburger and Johnson[17] described a coulo-metric variation of the commercially available pulsed amperometric detector with a gold electrode which improved the glucose detection capability from 315 to 9 ng. This corresponds to a figure of merit 90 times poorer than that obtained here.

The relative standard deviations for the determination of carbohydrates at the 10 mM level with the proposed detector were about 1.5%. The relative intensities with

TABLE I

RELATIVE INTENSITIES OF RESPONSES FOR VARIOUS CARBOHYDRATES IN MICRO-FIA

Applied potential, 0.57 V *vs.* Ag/AgCl; flow-rates of water and 0.25 M NaOH, both 1.1 μl/min; detection temperature, 30°C.

Species	Compound	Relative intensity
Aldopentoses	Xylose	0.89
	Ribose	0.92
	Arabinose	0.92
Aldohexoses	Glucose	1.00
	Mannose	0.70
	Allose	0.99
	Galactose	1.01
Ketohexoses	Fructose	0.64
	Sorbose	0.60
Deoxysugars	2-Deoxyribose	0.11
	2-Deoxyglucose	0.12
	Fucose (6-deoxygalactose)	0.56
	Rhamnose (6-deoxymannose)	0.30
Sugar alcohols	Ribitol	0.98
	Sorbitol	1.17
	Mannitol	0.96
Glycoside	Methyl-D-glucoside	0.28
Disaccharides	Lactose	0.43
	Sucrose	0.35
	Trehalose	0.23
Trisaccharide	Raffinose	0.33

respect to glucose in equal molar concentrations of the responses for various carbohydrates at a detection temperature of 30°C are summarized in Table I. The relative intensity tended to decrease in the order mono-, di- and trisaccharides. It is clear that the proposed detector can detect not only reducible sugars, but also non-reducible sugars containing sugar alchols.

Micro-HPLC

The proposed detector was applied to the detection of carbohydrates separated by micro-HPLC with the micro-separation columns described under Experimental with different separation modes. The results are shown in Fig. 9. In both instances the nickel wire of diameter 25 μm and length 5 mm was used as the working electrode, and the detection temperature, the total flow-rate and the sodium hydroxide concentration of the solution in the detector were kept at 60°C, 2.1 μl/min and 0.13 M, respectively. Pure water and 0.13 M sodium hydroxide solution were used as the mobile phases for the size-exclusion and ion-exchange modes, respectively. The separation columns for the size-exclusion and ion-exchange modes were kept at 80 and 30°C, respectively, by using a water-bath. It should be noted that the elution orders of the samples investigated were the opposite in the two separation modes. It became clear that the proposed detector is useful for micro-HPLC of carbohydrates in both separation modes.

The proposed detector was successfully applied to several real samples such as
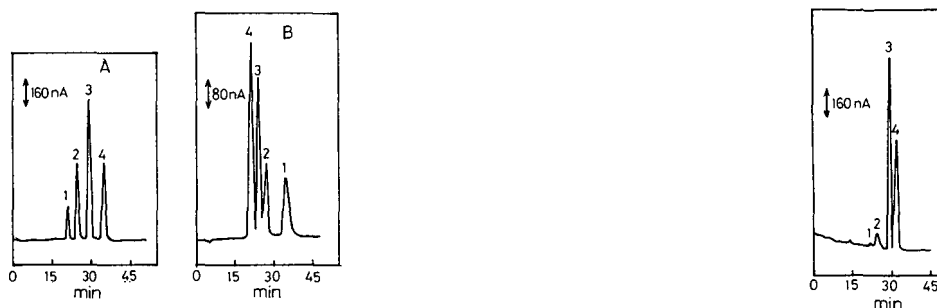
Fig. 9. Application to the detection of sugars separated by micro-HPLC in different modes. (A) Size-exclusion mode. Column, Shodex Ionpak KS-801 (247 mm × 0.35 mm I.D. + 217 mm × 0.35 mm I.D.); column temperature, 80°C. (B) Ion-exchange mode. Column, SAX (100 mm × 0.25 mm I.D. + 100 mm × 0.25 mm I.D.); column temperature, 30°C. Peaks: 1 = raffinose; 2 = lactose; 3 = glucose; 4 = arabinose. Amount of sample injected, 1.0 nmol each; flow-rates of water and 0.25 M NaOH, both 1.1 μl/min; detection temperature, 60°C.

Fig. 10. Application to the detection of sugars in a real sample. Sample, 0.02 μl of 4.40% honey; column, Shodex Ionpak KS-801 (247 mm × 0.35 mm I.D. + 217 mm × 0.35 mm I.D.); column temperature, 80°C. Peaks: 1 = raffinose; 2 = sucrose; 3 = glucose; 4 = fructose.

honey, cola and orange juice. Fig. 10 shows a typical chromatogram obtained for honey. In this instance, the sample was diluted with distilled water and injected directly onto the micro-column without any pretreatment. Hence the proposed detector can be applied to real samples without interferences from other analytes and eluent matrices present.

REFERENCES

1 S. Hughes and D. C. Johnson, *Anal. Chim. Acta*, 132 (1981) 11.
2 S. Hughes and D. C. Johnson, *J. Agric. Food Chem.*, 30 (1982) 712.
3 S. Hughes and D. C. Johnson, *Anal. Chim. Acta*, 149 (1983) 1.
4 G. G. Neuburger and D. C. Johnson, *Anal. Chem.*, 59 (1987) 203.
5 P. Edwards and K. K. Haak, *Am. Lab.*, April (1983) 78.
6 R. D. Rocklin and C. A. Pohl, *J. Liq. Chromatogr.*, 6 (1983) 1577.
7 G. G. Neuburger and D. C. Johnson, *Anal. Chem.*, 59 (1987) 150.
8 K. G. Schick, V. G. Magearu and C. O. Huber, *Clin. Chem.*, 24 (1978) 448.
9 W. Buchberger, K. Winsauer and C. H. Breitwieser, *Fresenius' Z. Anal. Chem.*, 315 (1983) 518.
10 R. E. Reim and R. M. Van Effen, *Anal. Chem.*, 58 (1986) 3203.
11 Y. B. Vassilev, O. K. Khazova and N. N. Nikolaeva, *J. Electroanal. Chem.*, 196 (1985) 127.
12 L. M. Santos and R. P. Baldwin, *Anal. Chem.*, 59 (1987) 1766.
13 L. M. Santos and R. P. Baldwin, *Anal. Chim. Acta*, 206 (1988) 85.
14 S. V. Prabhu and R. P. Baldwin, *Anal. Chem.*, 61 (1989) 852.
15 M. Goto, K. Shimada, T. Takeuchi and D. Ishii, *Anal. Sci.*, 4 (1988) 17.
16 M. Fleischmann, K. Korinek and D. Pletcher, *J. Chem. Soc., Perkin Trans.*, 2 (1972) 1396.
17 G. G. Neuburger and D. C. Johnson, *Anal. Chim. Acta*, 192 (1987) 205.

Enantiomeric resolution by micellar electrokinetic chromatography with chiral surfactants

KOJI OTSUKA*

Department of Industrial Chemistry, Osaka Prefectural College of Technology, Saiwai-cho, Neyagawa, Osaka 572 (Japan)

and

SHIGERU TERABE[a]

Department of Industrial Chemistry, Faculty of Engineering, Kyoto University, Sakyo-ku, Kyoto 606 (Japan)

ABSTRACT

Enantiomeric resolution of phenylthiohydantoin (PTH)-amino acids by micellar electrokinetic chromatography using chiral surfactants was studied. As a chiral surfactant, digitonin, which is a non-ionic compound, was used with anionic sodium dodecyl sulphate (SDS) to form mixed micelles. Under acidic conditions (pH 3.0), PTH derivatives of six amino acids (tryptophane, norleucine, norvaline, valine, α-aminobutyric acid and alanine) were separated from each other and optically resolved with a 25 mM digitonin–50 mM SDS solution, although a long separation time was required. The use of an anionic chiral surfactant, sodium N-dodecanoyl-L-valinate, was also examined under neutral conditions. In this instance, the same enantiomers as above except PTH-DL-Ala were resolved in a shorter time.

INTRODUCTION

Electrokinetic chromatography (EKC)[1] is a recently developed high-resolution separation method which is a branch of high-performance capillary electrophoresis (HPCE)[2–4] based on chromatographic principles using homogeneous solutions. EKC has the unique characteristic that both neutral analytes and charged solutes can be separated electrophoretically. Among various modes of EKC, micellar EKC (MEKC)[5,6], which uses micellar solutions of ionic surfactants, has become the most popular method for separating small neutral molecules and the fundamental characteristics of MEKC have been published[6,7].

Optical resolution of chiral compounds is a major application of chromatography, and a number of studies on chiral separations by chromatographic techniques have appeared. Zare and co-workers first reported the resolution of racemic mixtures

---

[a] Present address: Department of Material Science, Himeji Institute of Technology, 2167 Shosha, Himeji, Hyogo 671-22, Japan.

of dansylated DL-amino acids by EKC with copper(II)–L-histidine[8] or copper(II)–aspartame complexes[9]. Recently, papers on optical resolution by MEKC without any additives such as metal ions have been published, chiral micelles of various bile salts[10,11] and a mixed micelle of an N-acyl-L-amino acid with sodium dodecyl sulphate (SDS)[12] being used to achieve chiral recognition.

In this paper, preliminary results on the enantiomeric resolution of phenylthiohydantoin-DL-amino acids (PTH-DL-AA) by MEKC with chiral surfactants are described. As a chiral surfactant we first used digitonin, which is a glycoside of digitogenin. As digitonin is electrically neutral, SDS was added to digitonin solutions to form mixed micelles having negative charges, and some PTH-DL-AA were successfully separated from each other and optically resolved. As another chiral surfactant, sodium N-dodecanoyl-L-valinate was used without making mixed micelles, and some PTH-DL-AA were also separated and optically resolved.

EXPERIMENTAL

Digitonin, the structure is shown in Fig. 1, was purchased from Wako (Osaka, Japan), and it is soluble in water. Although the digitonin used was of analytical-reagent grade, its purity was not examined. Sodium dodecyl sulphate (SDS) was obtained from Nacalai Tesque (Kyoto, Japan) and sodium N-dodecanoyl-L-valinate (SDVal) from Ajinomoto (Tokyo, Japan). All the reagents were used as received. PTH-DL-AA, obtained from Wako, were used as acetonitrile solutions with concentrations of *ca.* 1 mg/ml. Chromatographic solutions were prepared by dissolving digitonin and SDS or SDVal in 50 mM phosphate buffers adjusted to an appropriate pH. Sudan IV was obtained from Eastman Kodak (Rochester, NY, U.S.A.).

An untreated fused-silica capillary tube (Scientific Glass Engineering, Ringwood, Victoria, Australia) (630 mm × 0.05 mm I.D.) was used as a separation column, in which 490 mm from the injection end UV absorption was measured by a Jasco (Tokyo, Japan) UVIDEC-100-III spectrophotometric detector. As a regulated high-voltage power supply, an HepLL-30P0.08-LS (Matsusada Precision Devices,
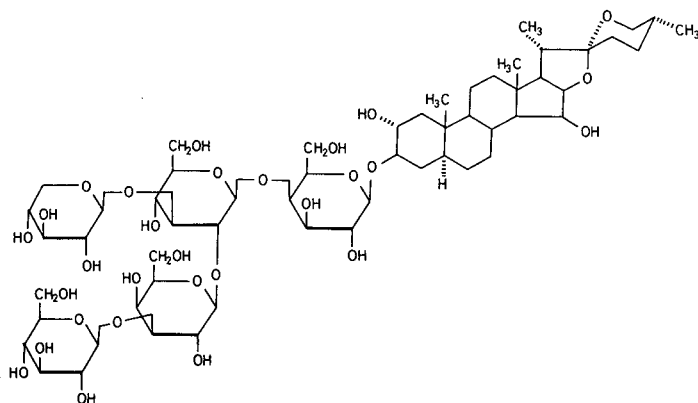

Fig. 1. Structure of digitonin.

Kusatsu, Shiga, Japan) was used. For data processing, a Chromatopac C-R3A (Shimadzu, Kyoto, Japan) was used. All experiments were carried out in the constant-voltage mode at ambient temperature.

RESULTS AND DISCUSSION

Digitonin–SDS solutions

First, we used a 25 mM digitonin–50 mM SDS solution of pH 7.0. Under these conditions, no enantiomeric resolution was achieved for any PTH-DL-AA. In this instance the electroosmotic velocity was large compared with the electrophoretic velocity of the digitonin–SDS mixed micelle, and hence the migration-time range was narrow and sufficient resolution could not be attained[6].

To suppress the electroosmotic flow and to extend the migration-time range, we used an acidic micellar solution (pH 3.0). The effects of pH on electrokinetic velocities, such as the electroosmotic velocity, electrophoretic velocity of the micelle and migrating velocity of the micelle, and on the chromatographic parameters in MEKC in the presence of SDS solutions have been reported previously[13]. Under the acidic conditions, PTH derivatives of six amino acids [tryptophane (Trp), norleucine (Nle), norvaline (Nva), valine (Val), α-aminobutyric acid (Aba) and alanine (Ala)] were separated from each other and each PTH-DL-AA was optically resolved as shown in Fig. 2, where a 25 mM digitonin–50 mM SDS mixed micellar solution of pH 3.0 was used, although a long separation time was required. Peak assignment of each enantiomer was not achieved. Here, the direction of migration of the mixed micelle was towards the positive electrode and was the opposite of the electroosmotic flow. As for other PTH derivatives, methionine was optically resolved, but serine was not resolved. The effect of concentrations of digitonin and SDS will be reported elsewhere.

Capacity factors, $\tilde{k}'$, defined as in previous papers[5,6], for each peak in Fig. 2, are
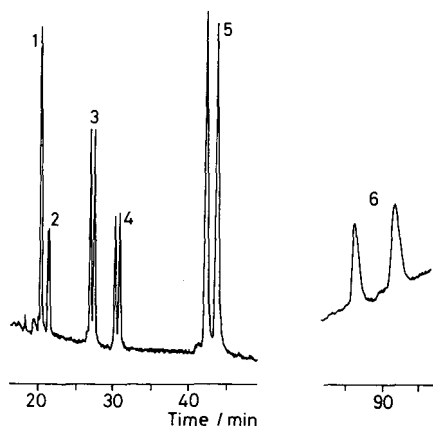

Fig. 2. Micellar electrokinetic chromatogram of six PTH derivatives of DL-amino acids. Corresponding amino acids: 1 = Trp; 2 = Nle; 3 = Nva; 4 = Val; 5 = Aba; 6 = Ala. Micellar solution, 25 mM digitonin–50 mM SDS (pH 3.0); separation tube, 630 × 0.05 mm I.D.; length of the tube used for separation, 490 mm; total applied voltage, 20 kV; current, 34 μA; detection wavelength, 260 nm; temperature, ambient.

TABLE I

CAPACITY FACTORS, SEPARATION FACTORS AND RESOLUTION OF SOME PTH DERIVA-
TIVES OF DL-AMINO ACIDS

Conditions as in Fig. 2 (for digitonin–SDS) and Fig. 3 (for SDVal).

Solute	Digitonin–SDS				SDVal			
	$\tilde{k}'_1$	$\tilde{k}'_2$	α	R_s	$\tilde{k}'_1$	$\tilde{k}'_2$	α	R_s
Trp	38.8	44.5	1.15	0.54	2.4	3.7	1.56	8.01
Nle	18.3	20.5	1.12	0.83	5.3	8.1	1.54	8.58
Nva	5.2	5.5	1.06	1.49	0.6	0.8	1.46	5.28
Val	3.9	4.1	1.04	1.53	0.8	0.9	1.17	3.14
Aba	2.3	2.4	1.04	1.92	0.4	0.5	1.08	0.85
Ala	1.3	1.3	1.03	3.20				

given in Table I. In this instance, methanol and Sudan IV were used to measure the
migration times of the aqueous phase (or the bulk solution), t_0, and of the micelle, t_{mc},
respectively. Here, t_0 and t_{mc} were found to be 24 and -19.5 min, respectively (the sign
of the migration time was discussed previously[13]: a positive value means that the
migration direction is from the positive to the negative electrode, and *vice versa*). As
shown in Table I, the larger is $\tilde{k}'$, the shorter the migration time becomes[13]. As all the
PTH-DL-AA separated in Fig. 2 are derivatized from monoaminomonocarboxylic
acids and hence have no charge under the experimental conditions used, the calculated
capacity factors can be considered as actual values. The validity of the calculation of $\tilde{k}'$
was confirmed as follows: three alkyl *p*-hydroxybenzoates, in which the carbon
number, n of the alcohol residue ranged from 2 to 4, were injected under the same
conditions as given in Fig. 2 and logarithms of the observed $\tilde{k}'$ values were plotted
against n. A good linear relationship was observed and, therefore, the values of $\tilde{k}'$
calculated seem to be reliable. Methyl *p*-hydroxybenzoate ($n = 1$) was not detected
owing to its very long migration time.

The separation factor, α, which is equal to $\tilde{k}'_2/\tilde{k}'_1$, and the resolution, R_s, between
enantiomers for each PTH derivative are also given in Table I. In MEKC, resolution is
related to the chromatographic parameters through[6]

$$R_s = \frac{\sqrt{N}}{4} \cdot \frac{\alpha - 1}{\alpha} \cdot \frac{\tilde{k}'_2}{1 + \tilde{k}'_2} \cdot \frac{1 - (t_0/t_{mc})}{1 + (t_0/t_{mc})\tilde{k}'_1} \tag{1}$$

where N is the theoretical plate number and R_s given in Table I was calculated by eqn.
1. It should be noted that in eqn. 1 (and also in the calculation of the separation factor)
the capacity factors are taken as $\tilde{k}'_1 > \tilde{k}'_2$ in the case when the electroosmotic flow and
the migration direction of the solute are opposite. For the case in Fig. 2, maximum
resolution should be attained for the solute of $\tilde{k}' = -t_{mc}/t_0$ or 0.81 (ref. 13), provided
that N and α are constant, although the solute having that $\tilde{k}'$ value will not migrate in
the capillary. The fact that R_s for the pairs of Val, Aba and Ala becomes larger in that
order, whereas the α values remain almost constant, clearly shows the effect of the
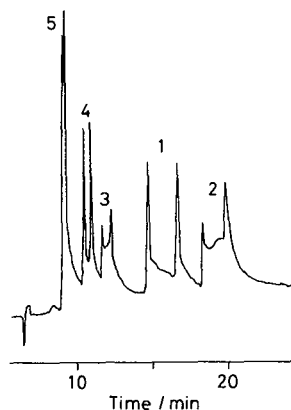product of the last two terms in eqn. 1, because its value increases in that order.

Fig. 3. Micellar electrokinetic chromatogram of five PTH derivatives of DL-amino acids. Micellar solution, 20 mM SDVal (pH 7.0); current, 38 μA; other conditions and peak numbers as in Fig. 2.

SD Val solutions

The use of SDVal in MEKC for chiral separations has been reported by Dobashi *et al.*[12]. In their study, SDS was added to SDVal solutions to form mixed micelles, and SDVal–SDS comicellar solutions containing methanol were also employed. In this study, however, we used SDVal solutions without any other surfactants or organic modifiers. Separation was carried out under neutral conditions or pH 7.0, where the SDVal micelle has negative charges.

As shown in Fig. 3, five pairs of enantiomers described above but not PTH-DL-Ala were resolved using a 20 mM SDVal solution in a much shorter time than in Fig. 2. For all peaks, especially Nva and Nle, much worse peak shapes than in Fig. 2 were observed. Unfortunately, the reason has not been clarified and is being investigated. Washing the capillary with sodium hydroxide solution, methanol or acetone was examined but no improvement in peak shape was obtained.

For the chromatogram in Fig. 3, the capacity factor for each peak, the separation factor and the resolution between each pair of enantiomers were calculated and are given in Table I. The reproducibility of the chromatogram for the sample shown in Fig. 3 was not good, especially with regard to baseline fluctuation and peak shape.

CONCLUSIONS

In conclusion, enantiomeric resolution by MEKC using chiral surfactants without any additives such as metal ions or chelating reagents was successfully achieved, although the resolution needs to be improved and the separation time reduced. The mixed micelle of digitonin, a neutral chiral surfactant, with anionic SDS can be used under acidic conditions, and SDVal, an anionic chiral surfactant, is also found to be useful in neutral solutions. Application of these MEKC systems to other chiral compounds is being investigated.

ACKNOWLEDGEMENTS

REFERENCES

1 S. Terabe, *Trends Anal. Chem.*, 8 (1989) 129.
2 F. E. P. Mikkers, F. M. Everaerts and Th. P. E. M. Verheggen, *J. Chromatogr.*, 169 (1979) 11.
3 J. W. Jorgenson and K. D. Lukacs, *Anal. Chem.*, 53 (1981) 1298.
4 S. Hjertén, *J. Chromatogr.*, 270 (1983) 1.
5 S. Terabe, K. Otsuka, K. Ichikawa, A. Tsuchiya and T. Ando, *Anal. Chem.*, 56 (1984) 111.
6 S. Terabe, K. Otsuka and T. Ando, *Anal. Chem.*, 57 (1985) 834.
7 S. Terabe, K. Otsuka and T. Ando, *Anal. Chem.*, 61 (1989) 251.
8 E. Gassmann, J. E. Kuo and R. N. Zare, *Science (Washington, D.C.)*, 230 (1985) 813.
9 P. Gozel, E. Gassmann, H. Michelsen and R. N. Zare, *Anal. Chem.*, 59 (1987) 44.
10 S. Terabe, M. Shibata and Y. Miyashita, *J. Chromatogr.*, 480 (1989) 403.
11 H. Nishi, T. Fukuyama, M. Matsuo and S. Terabe, *J. Microcolumn Sep.*, 1 (1989) 234.
12 A. Dobashi, T. Ono, S. Hara and J. Yamaguchi, *Anal. Chem.*, 61 (1989) 1984.
13 K. Otsuka and S. Terabe, *J. Microcolumn Sep.*, 1 (1989) 150.

Ferroceneboronic acid as a derivatization reagent for the determination of brassinosteroids by high-performance liquid chromatography with electrochemical detection

KEIJI GAMOH* and HIROMICHI SAWAMOTO

Faculty of Education, Kochi University, Akebono-cho, Kochi-shi 780 (Japan)

SUGURU KAKATSUTO

Department of Chemistry, Joetsu University of Education, Joetsu-shi, Niigata 943 (Japan)

and

YOSHIYUKI WATABE and HIROMI ARIMOTO

Analytical Applications Department, Shimadzu Corp., Kuwabara-cho, Nakagyo-ku, Kyoto 604 (Japan)

ABSTRACT

A micro-scale method for the determination of brassinosteroids as ferroceneboronates by high-performance liquid chromatography with electrochemical detection has been developed. Ferroceneboronic acid (FBA) proved to be satisfactory for use in the derivatization of brassinosteroids with respect to reactivity and sensitivity. The steroids were readily condensed with FBA under mild conditions to provide the corresponding boronates, exhibiting maximum sensitivity at $+0.6$ V *vs.* a silver–silver chloride reference electrode with a detection limit of 25 pg for brassinolide. The method was successfully applied to the determination of natural brassinosteroids in a plant. Brassinolide, dolichosterone, norcastasterone and castasterone were identified in the pollen of sunflower (*Helianthus annuus* L.).

INTRODUCTION

High-performance liquid chromatography (HPLC) is useful for the separation and determination of trace amounts of various biologically active compounds in many kinds of natural products. Since the discovery of brassinolide as a plant-growth hormonal steroid[1], a number of related steroids, brassinosteroids, have been found to occur in a wide variety of higher plans[2]. Because of their remarkable biological activities and the very small amounts contained in plants[2], micro-scale methods have been necessary for the screening and identification of brassinosteroids in plants. In a previous paper, we described the microdetermination of brassinosteroids using labelling with 1-naphthaleneboronic acid[3], 9-phenanthreneboronic acid[4], 1-cyanoisoindole-2-*m*-phenylboronic acid[5] or dansylaminophenylboronic acid[6]. The boronic acid derivatives were very useful labelling reagents for brassinosteroids which have two

sets of vicinal diol functional groups, in the A ring and in the side-chain. Further interest in brassinosteroid analysis prompted us to investigate electrochemical detection in hope of developing a more sensitive and selective method.

Shimada and co-workers[7,8] reported that ferrocene reagents, e.g., N-succinimidyl 3-ferrocenylpropionate or ferrocenoyl azide, were very useful for the precolumn labelling of amines or alcoholic hydroxyl compounds for HPLC with electrochemical detection. The ferrocene derivatives are readily oxidizable and selectively detected in the presence of other electroactive compounds. Brooks and Cole[9,10] have already proposed ferroceneboronic acid (FBA) for the precolumn labelling of glycol compounds for gas chromatography with electron-capture detection. However, this reagent does not appear to have been used in HPLC analysis. In this paper, we describe a micro-scale method for the determination of brassinosteroids as ferroceneboronate derivatives by HPLC with electrochemical detection and its application to the identification of brassinosteroids in plant extracts.

EXPERIMENTAL

Chemicals

Authentic brassinosteroids, 28-norbrassinolide, brassinolide, dolichosterone, 28-norcastasterone, 28-homobrassinolide, castasterone and 28-homocastasterone, were synthesized in our laboratory[11–13]. FBA was purchased from Tokyo Kasei (Tokyo, Japan). All other reagents were of analytical-reagent grade.

Plant material and the bioactive brassinosteroid fraction[4]

The bee-collected pollen of sunflower (*Helianthus annuus* L.) was obtained from China and was kindly supplied by Nippon Kayaku (Tokyo, Japan). Identification of the pollen was carried out by microscopic examination. The bioactive brassinosteroid fraction was obtained from the pollen as described previously[14].

Derivatization

The standard mixture or the biologically active brassinosteroid fraction was dissolved in 100 μl of acetonitrile and 100 μl of FBA (1 mg/ml) in 1% (v/v) pyridine–acetonitrile were added. The mixture was heated at 70°C for 10 min. After cooling, several microlitres of the solution were injected directly into the analytical column.

HPLC analysis

A Shimadzu Model LC-6A chromatograph equipped with a Shimadzu Model L-ECD-6A electrochemical detector using a glassy carbon working electrode was employed. A reversed-phase Shim-pack CLC-ODS(M) (5 μm) column (250 mm × 4.6 mm I.D.) was used at 45°C. Samples were injected into the column using a Rheodyne Model 7125 rotary valve syringe-loading injector. The optimum mobile phase for the separation of the brassinosteroid ferroceneboronates was a mixture of acetonitrile and water containing 1 M sodium perchlorate at a flow-rate of 1.0 ml/min.

RESULTS AND DISCUSSION

HPLC analysis

On treatment with FBA, the authentic brassinosteroids were quantitatively derivatized in 10 min. In previous studies[3-6], the chromatographic behaviour of brassinosteroids as their boronate derivatives on a reversed-phase column was investigated. Using the data obtained, the separation of brassinosteroid ferroceneboronates could be performed successfully on a reversed-phase column using aqueous acetonitrile containing sodium perchlorate as a mobile phase. When sodium acetate solution was used as the mobile phase, a poor detection limit was observed. As shown in Fig. 1, the hydrodynamic voltammogram of the brassinolide ferroceneboronate derivative showed a constant value above $+0.6$ V *vs.* a silver–silver chloride reference electrode owing to oxidation of the ferrocenyl moiety. The authentic brassinosteroid ferroceneboronates were clearly separated by HPLC on the Shim-pack CLC-ODS(M) reversed-phase column, as illustrated in Fig. 2a. The amounts of these steroids are 10 ng each.

We examined the detection limits of these brassinosteroid derivatives using the ODS column and acetonitrile–water (85:15) containing 1 M sodium perchlorate as the mobile phase. The method with FBA gave a detection limit for brassinolide of 25 pg per injection with a signal-to-noise ratio of 3. A two-fold increase in detectability was observed in comparison with the fluorimetric detection of phenanthreneboronates[4]. The detection limits of the derivatives with electrochemical detection were found to be comparable to those of the other derivatives with fluorimetric detection[5,6]. The relationships between the peak areas and the amounts of the individual brassinosteroids were linear from 50 pg to 5 ng. The ferroceneboronates were found to be stable for 2 months in solution in pyridine–acetonitrile at 0°C.
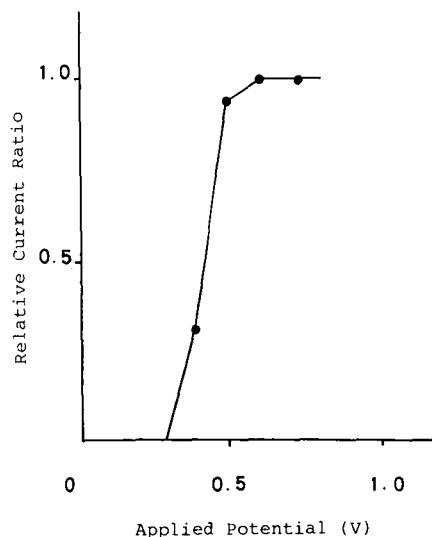

Fig. 1. Hydrodynamic voltammogram of brassinolide ferroceneboronate. The maximum response of the derivative is arbitrarily taken as 1.0.
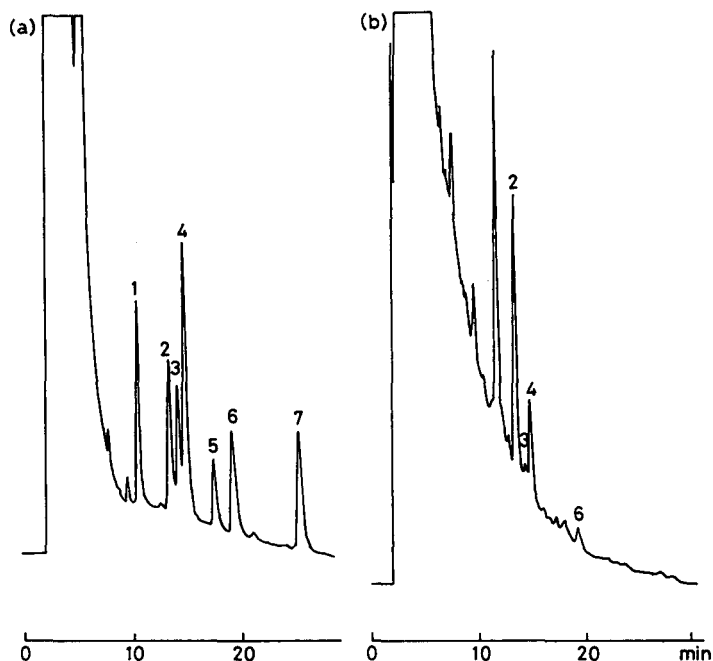
Fig. 2. Chromatograms of brassinosteroid ferroceneboronates. (a) A mixture of authentic samples; (b) biologically active fraction extracted from the pollen of sunflower. Peaks: 1 = norbrassinolide; 2 = brassinolide; 3 = dolichosterone; 4 = norcastasterone; 5 = homobrassinolide; 6 = castasterone; 7 = homocastasterone. Conditions: Shim-pack CLC-ODS(M) column; mobile phase, acetonitrile–water (85:15) containing 1 M NaClO$_4$; flow-rate, 1.0 ml/min; temperature, 40°C.

Application

The method was applied to the identification and quantification of brassino-steroids in the pollen of sunflower. The biologically active fraction obtained from the pollen as described previously[14] was derivatized with FBA as described above and analysed by HPLC. As shown in Fig. 2b, brassinolide, dolichosterone, norcastasterone and castasterone were identified in the pollen. The structures of these steroids are shown in Fig. 3. The amounts of these brassinosteroids were determined by using authentic samples for calibration, and the results, except for dolichosterone, were in good agreement with those obtained previously using fluorescence–HPLC with 9-phenanthreneboronic acid derivatization and gas chromatography–mass spectrom-
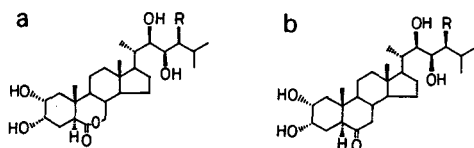

Fig. 3. Structures of brassinosteroids identified in the pollen of sunflower. (a) R = CH$_3$: brassinolide; (b) R = CH$_2$: dolichosterone; R = H$_2$: norcastasterone; R = CH$_3$: castasterone.

etry[14]. Although dolichosterone was not identified and determined in the same pollen in the previous study[14], the chromatographic data obtained by the present method suggest the presence of dolichosterone in the pollen. Hence it seems that FBA may be a very useful and selective reagent for the derivatization of brassinosteroids.

A recovery test was carried out by adding a mixture of 2 ng of brassinolide and 5 ng of castasterone to the divided bioactive fraction. The samples ere derivatized as described above and analysed by HPLC. The recovery of the added compounds was than $>95\%$ ($n = 4$; relative standard deviation $= 1.8\%$). It is evident from these data that the proposed analytical procedure is satisfactory in both accuracy and precision.

In conclusion, this paper is the first report of the application of HPLC with electrochemical detection using FBA as a derivatization reagent for the determination of brassinosteroids. We have demonstrated its usefulness in the identification and quantification of several brassinosteroids in sunflower pollen. As the ferrocene-boronates were found to be highly sensitive, specific and suitable derivatives, this method is ideally suited to sample-limitted natural product analysis and may be suitable for use by agricultural and biological chemists interested in small amounts of natural brassinosteroids and their trace analysis.

REFERENCES

1 M. D. Grove, G. F. Spencer, W. K. Rohwedder, N. B. Mandava, J. F. Worley, J. D. Warthen, Jr., G. L. Steffens, J. L. Flippen-Anderson and J. C. Cook, Jr., *Nature (London)*, 281 (1979) 216.
2 G. Adam and V. Marguardt, *Phytochemistry*, 25 (1986) 1787.
3 K. Gamoh, T. Kitsuwa, S. Takatsuto, Y. Fujimoto and N. Ikekawa, *Anal. Sci.*, 4 (1988) 533.
4 K. Gamoh, K. Omote, N. Okamoto and S. Takatsuto, *J. Chromatogr.*, 469 (1989) 424.
5 K. Gamoh and S. Takatsuto, *Anal. Chim. Acta*, 222 (1989) 201.
6 K. Gamoh, K. Omote, S. Takatsuto and I. Tejima, *Anal. Chim. Acta*, 228 (1990) 101.
7 M. Tanaka, K. Shimada and T. Nambara, *J. Chromatogr.*, 292 (1984) 410.
8 K. Shimada, S. Orii, M. Tanaka and T. Nambara, *J. Chromatogr.*, 352 (1986) 32.
9 C. J. W. Brooks and W. J. Cole, *J. Chromatogr.*, 362 (1986) 113.
10 C. J. W. Brooks and W. J. Cole, *J. Chromatogr.*, 399 (1987) 207.
11 S. Takatsuto and N. Ikekawa, *J. Chem. Soc., Perkin Trans. I*, (1983) 2133.
12 S. Takatsuto and N. Ikekawa, *Chem. Pharm. Bull.*, 30 (1982) 4181.
13 S. Takatsuto, N. Yazawa, M. Ishiguro, M. Morisaki and N. Ikekawa, *J. Chem. Soc., Perkin Trans. I*, (1984) 139.
14 S. Takatsuto, T. Yokota, K. Omote, K. Gamoh and N. Takahashi, *Agric. Biol. Chem.*, 53 (1989) 2177.

Chiral separation of diltiazem, trimetoquinol and related compounds by micellar electrokinetic chromatography with bile salts

HIROYUKI NISHI*, TSUKASA FUKUYAMA and MASAAKI MATSUO

Analytical Chemistry Research Laboratory, Tanabe Seiyaku, Co., Ltd., 16–89, Kashima 3-chome, Yodoga-wa-ku, Osaka 532 (Japan)

and

SHIGERU TERABE

Department of Material Science, Faculty of Science, Himeji Institute of Technology, 2167 Shosha, Himeji 671-22 (Japan)

ABSTRACT

The separation of optically isomeric diltiazem hydrochloride, trimetoquinol hydrochloride and related compounds by micellar electrokinetic chromatography was investigated employing four bile salts as chiral surfactants. The chiral separation of diltiazem hydrochloride and trimetoquinol hydrochloride was successfully achieved by use of sodium taurodeoxycholate under neutral conditions, although enantiomers of carboline derivatives A and B and 2,2'-dihydroxy-1,1'-dinaphthyl were resolved with all the bile salts under conditions from neutral to alkaline. The chiral separation of diltiazem-related compounds was affected by the structure of the samples in addition to the effects of bile salt structures and pH of the buffer solutions. Application to the optical purity testing of trimetoquinol hydrochloride by the area percentage method is described. A possible chiral separation mechanism is briefly mentioned.

INTRODUCTION

Micellar electrokinetic chromatography (micellar EKC or MEKC) has been developed for the separation of non-ionic compounds by the use of capillary zone electrophoresis (CZE). This method is based on micellar solubilization and electrophoretic migration of the micelle[1-3], that is, the solutes are separated by the differential distribution between the micelle and the surrounding aqueous phase and the differential migration of the two phases. Hence this method can be classified as an individual kind of chromatographic technique from the viewpoint of the separation principle, although it is performed with the same apparatus as in CZE.

Micellar EKC has many advantages for the separation of drugs in addition to high theoretical plate numbers. The selectivity has been much improved, even for the

separation of water-soluble ionic compounds, *e.g.*, water-soluble vitamins[4] and β-lactam antibiotics[5], in comparison with CZE, although some of these solutes can be separated by the usual CZE. Moreover, corticosteroids and benzothiazepin analogues, which are insoluble in water or lipophilic and are not separated by CZE, have been successfully separated by this method[6]. The determination of drugs in preparations by the internal standard method has also been studied with the same reproducibility as in HPLC[6-10]. The determination of antibiotics in human plasma by micellar EKC was successful using a direct sample injection method[11-13]. The plasma proteins, which can interfere with the drug analysis, were solubilized by the micelle employed and hence eluted later than the drugs. That is, pretreatment of the plasma sample such as deproteinization or extraction was not necessary in micellar EKC. Separations of closely related isotopic compounds have also been successfully achieved by micellar EKC[14,15].

Recently, chiral separation by EKC has been investigated, using various techniques. In micellar EKC, chiral separation was achieved by employing a chiral surfactant such as bile salts[16,17] or by using a mixed micelle of sodium dodecyl sulphate (SDS) and some chiral additives such as N,N-didecyl-L-alanine in the presence of copper(II)[18] or digitonin[19]. Chiral separation of dansylated DL-amino acids was achieved by EKC with cyclodextrin derivatives, which have ionic groups in the molecules, based on inclusion formation[3].

In a previous paper, we described the chiral separation of carboline derivatives A and B and 2,2'-dihydroxy-1,1'-dinaphthyl by micellar EKC with bile salts, discussing the effects of pH and bile salts species on the chiral recognition[17]. These solutes were successfully separated with all the bile salts employed at pH 7.0 and 9.0. Chiral separation of dansylated DL-amino acids has been also successfully achieved by micellar EKC using bile salts[16]. In that work, the separation was successful with sodium taurodeoxycholate (STDC) at pH 3.0 or 7.0, and the best chiral separation of these solutes was accomplished with acidic (pH 3.0) buffer solutions. A tentative separation mechanism was also described.

In this paper, we describe the chiral separation of some drugs, especially diltiazem hydrochloride, trimetoquinol hydrochloride and related compounds, by micellar EKC with bile salts, which are readily available chiral surfactants. Enantiomers of diltiazem hydrochloride and trimetoquinol hydrochloride were successfully separated with STDC under neutral conditions, based on the differential solubilization of each isomer to the bile salt micelle. The effects of bile salt species, the pH of buffer solutions and the structure of samples are also described. This method was successfully applied to the purity testing of trimetoquinol hydrochloride.

EXPERIMENTAL

Apparatus

Separation was performed in a 650 mm × 50 μm I.D. (effective length 500 mm) fused-silica capillary tube (Scientific Glass Engineering, Ringwood, Victoria, Australia). A high voltage (up to + 25 kV) was applied with a Model HJLL-25PO d.c. power supply (Matsusada Precision Devices, Kusatsu, Shiga, Japan). Detection was achieved by measuring the on-column UV adsorption at 210 nm with a Uvidec-100-VI (Jasco, Tokyo, Japan) with a time constant of 0.05 s. A Chromatopac C-R5A

(Shimadzu, Kyoto, Japan) was used for data processing. The micellar EKC apparatus used was the same as described previously[4].

Reagents and samples

Sodium cholate (SC), sodium taurocholate (STC), sodium deoxycholate (SDC) and sodium taurodeoxycholate (STDC), purchased from Nacalai Tesque (Kyoto, Japan), were dissolved in 0.02 M phosphate–borate buffer of pH 7.0 or 9.0 at a concentration 0.05 M and these micellar solutions were passed through a membrane filter (0.45 μm) prior to use. Sudan III from Nacalai Tesque was used as a tracer of the micelle[2]. All other reagents and solvents were of analytical-reagent grade from Katayama Kagaku (Osaka, Japan) and used without further purification.

The structures of diltiazem hydrochloride [(*SS*)-form], its related compounds, trimetoquinol hydrochloride [(*S*)-form] from Tanabe Seiyaku (Osaka, Japan) and tetrahydropapaveroline from Aldrich (Milwaukee, WI, U.S.A.) are given in Tables I and II. Diltiazem hydrochloride is a calcium antagonist with coronary vasodilatory activity. Trimetoquinol hydrochloride is a bronchodilator. Antipodes of diltiazem hydrochloride, its related compounds (except for D7 and D8) and trimetoquinol hydrochloride were obtained from Tanabe Seiyaku. Enantiomers of 2,2'-dihydroxy-1,1'-dinaphthyl, 2,2,2-trifluoro-1-(9-anthryl)ethanol, purchased from Nacalai Tesque, and carboline derivatives A and B, which are new hepatoprotective agents synthesized at Tanabe Seiyaku, were also studied. These solutes were dissolved in water or methanol at concentrations of 0.2 mg/ml (D2 and D10) and 1 mg/ml (others) to give adequate peak heights. A known amount of racemic trimetoquinol hydrochloride was added to (*S*)-trimetoquinol hydrochloride in the optical purity testing.
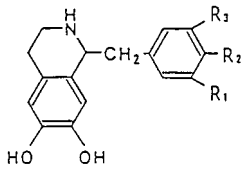
TABLE I

STRUCTURE OF DILTIAZEM HYDROCHLORIDE AND RELATED COMPOUNDS
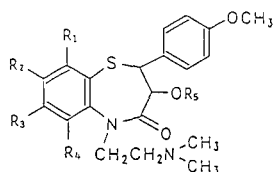
Solute	R_1	R_2	R_3	R_4	R_5
D1 (diltiazem)	H	H	H	H	$COCH_3$
D2	H	H	H	H	H
D3	Cl	H	H	H	$COCH_3$
D4	Cl	H	H	H	H
D5	H	Cl	H	H	$COCH_3$
D6	H	Cl	H	H	H
D7	H	H	Cl	H	$COCH_3$
D8	H	H	Cl	H	H
D9	H	H	H	Cl	$COCH_3$
D10	H	H	H	Cl	H

TABLE II

STRUCTURE OF TRIMETOQUINAL AND TETRAHYDROPAPAVEROLINE

Compound	R_1	R_2	R_3
Trimetoquinol	OCH_3	OCH_3	OCH_3
Tetrahydropapaveroline	OH	OH	H

Procedure

A sample solution was introduced into the positive end of the tube by siphoning (about 10 cm height, 5–10 s) and micellar EKC was performed at ambient temperature (*ca.* 20°C). The injection volume in the system was of the order of 1 nl. The detailed procedure has been described previously[4].

In order to obtain a good peak shape, enantioselectivity and reproducibility of the migration times, it was necessary to wash the capillary tube with an alkaline solution as follows: the capillary was filled with a 0.1 M potassium hydroxide solution with a manually operated syringe and allowed to stand for 30 min, flushed with water and allowed to stand for 5 min, then finally filled with the working solution. The capillary tube was washed out every week.

RESULTS AND DISCUSSION

Chiral separation with bile salts

The structure of the bile salts employed in this study is given in Table III. Bile salts form small or primary micelles with up to ten monomers by the hydrophobic

TABLE III

STRUCTURE OF BILE SALTS
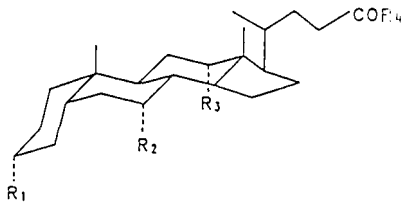
Bile salt	Abbreviation	R_1	R_2	R_3	R_4
Sodium cholate	SC	OH	OH	OH	ONa
Sodium taurocholate	STC	OH	OH	OH	$NHCH_2CH_2SO_3Na$
Sodium deoxycholate	SDC	OH	H	OH	ONa
Sodium taurodeoxycholate	STDC	OH	H	OH	$NHCH_2CH_2SO_3Na$

interaction between the non-polar faces of the monomers[20]. This may be considered as one of the reasons for the characteristic solubilization capability of the bile salt micelle[6,21] in comparison with long-chain alkyl-type surfactants such as SDS. The enantiomeric separation of diltiazem hydrochloride, trimetoquinol hydrochloride, carboline derivatives A and B, 2,2'-dihydroxy-1,1'-dinaphthyl and 2,2,2-trifluoro-1-(9-anthryl)ethanol was investigated with four kinds of bile salts (0.05 M) under the neutral (pH 7.0) and alkaline (pH 9.0) conditions. Chiral separation was successfully achieved except for 2,2,2-trifluoro-1-(9-anthryl)ethanol and the detailed chiral separation of carboline derivatives A and B and 2,2'-dihydroxy-1,1'-dinaphthyl was reported previously[17]. From the results, it was concluded that the structure of bile salts and the buffer pH significantly affect the recognition of enantiomers.

Chiral separation of diltiazem and related compounds

The chiral separation of diltiazem hydrochloride and related compounds (Table I) was investigated with neutral (pH 7.0) and alkaline (pH 9.0) buffer solutions of the four bile salts. Enantiomers of diltiazem hydrochloride were resolved with only STDC
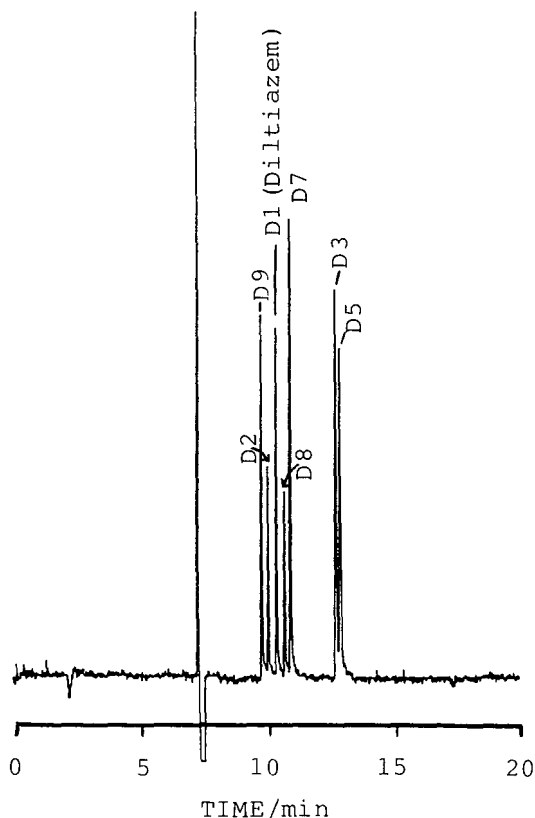

Fig. 1. Micellar EKC separation of seven diltiazem analogues. Samples are indicated with the abbreviations in Table I. Conditions: buffer, 0.05 M STC in 0.02 M phosphate–borate buffer solution of pH 7.0; separation tube, 650 mm × 0.05 mm I.D. (effective length, 500 mm); applied voltage, 20 kV; detection, 210 nm; temperature, ambient.

solutions of pH 7.0. Chiral separation of its related compounds was also successful under the same conditions, except for samples D5 and D6. Under the other conditions, enantiomers of D3 were partially resolved with the SC solution of pH 9.0 and those of D9 and D10 with the STDC solution of pH 9.0.

Migration of the solutes at pH 7.0 occurs in the order D9, D1 (diltiazem), D7, D3 and D5 in all the bile salt solutions, although D1 migrated faster than D9 at pH 9.0. Each deacetyl form migrated faster than the corresponding acetyl form because of an increase in hydrophilicity, although separation between the acetyl form D5 and its deacetyl form D6 was not achieved with the 0.05 *M* bile salt employed. A typical chromatogram of a mixture of seven diltiazem derivatives with a 0.05 *M* STC solution
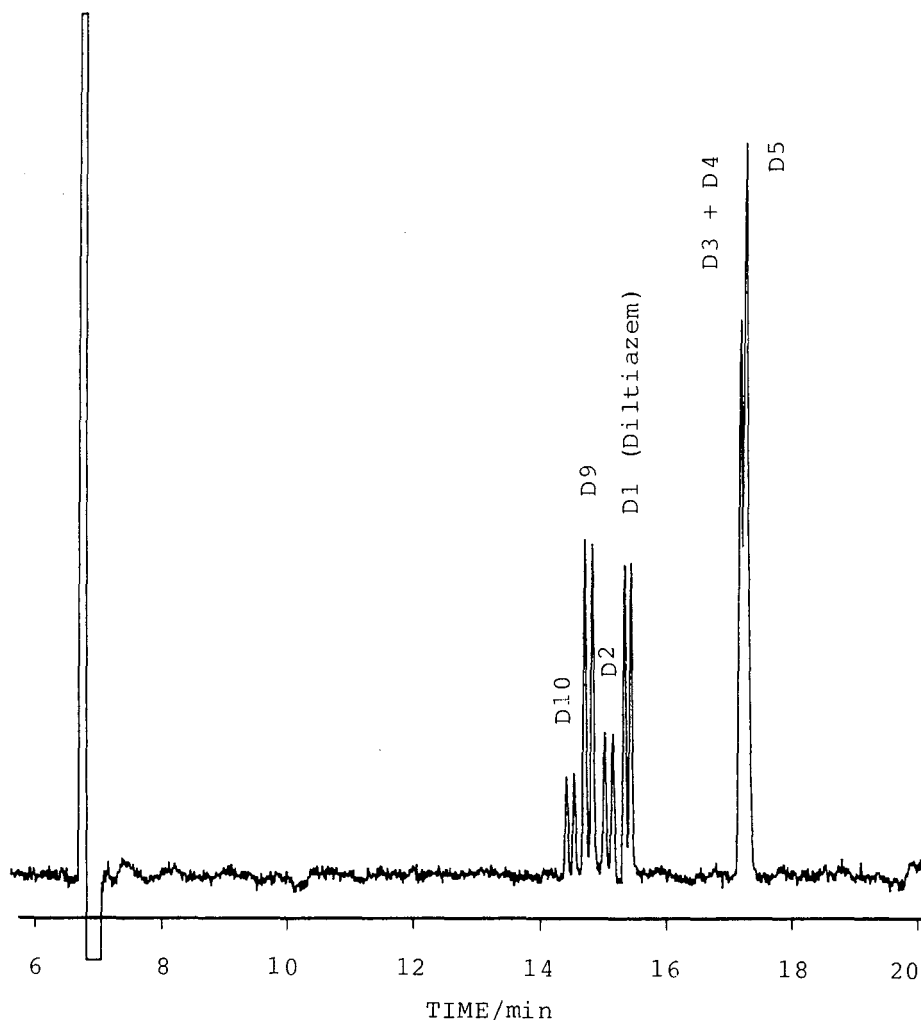
Fig. 2. Chiral separation of diltiazem hydrochloride and related compounds. Samples are indicated with the abbreviations in Table I. Buffer, 0.05 *M* STDC in 0.02 *M* phosphate–borate buffer solution solution of pH 7.0. Other conditions as in Fig. 1.

of pH 7.0 is shown in Fig. 1. Under these conditions, D6 and D10 overlapped with their acetyl forms (D5 and D9) and D4 migrated slightly faster than D3. Chiral separation was not achieved at all.

A successful chiral separation of seven enantiomeric diltiazem-related compounds with STDC solutuons of pH 7.0 is shown in Fig. 2. The migration times, capacity factors ($\tilde{k}'$) and separation factors ($\alpha = \tilde{k}'_2/\tilde{k}'_1$) of the solutes shown in Fig. 2 are summarized in Table IV. In micellar EKC, the capacity factor of an electrically neutral solute is given by[2]

$$\tilde{k}' = \frac{t_R - t_0}{t_0(1 - t_R/t_{mc})} \tag{1}$$

where t_0, t_R and t_{mc} are the migration times of an unincorporated solute, the sample and the micelle, respectively. We employed methanol as a tracer of the electroosmotic flow and Sudan III as that of the micelle. Enantiomers of D1, D2, D9 and D10 were successfully resolved and those of D3 and D4, which eluted with the same migration times, were partially resolved with α values around 1.04. Chiral separation of D5 was not successful.

From these results, D5, which has a chlorine atom in the R_2 position (see Table I), has some unfavourable substituents for the chiral recognition in comparison with D1 (diltiazem, no chlorine) or D9, which has a chlorine atom in the R_4 position. The results that D6 (deacetyl form) could not be separated from its acetyl form D5, and the insufficient chiral separation of D3 and D4, each of which has a chlorine atom in the R_1 position, also support the above consideration. That is, it was difficult to recognize enantiomers of diltiazem-related compounds which have some hydrophobic groups in the R_1 or R_2 position with the bile salt micelles. The longer migration times of D3 and D5 compared with those of D1 and D9, which were successfully separated (see Fig. 2), indicate that the region around the R_1, R_2 and p-methoxybenzyl part may be the area of interaction of diltiazem-related compounds with the non-polar part of the bile salt micelle. Solubilization of D3 and D5, in which hydrogen atoms in the R_1 or R_2 position are replaced by chlorine atoms, more than D1 and D9, on the other hand, may reduce the chiral recognition.

TABLE IV

MIGRATION TIMES, CAPACITY FACTORS AND SEPARATION FACTORS OF DILTIAZEM HYDROCHLORIDE AND RELATED COMPOUNDS

0.05 M STDC at pH 7.0; applied voltage, 20 kV; t_0, 6.62 min; t_{mc}, 18.81 min.

Solute	t_{R1} (min)	t_{R2} (min)	$\tilde{k}'_1$	$\tilde{k}'_2$	α
D10	14.06	14.17	4.45	4.62	1.04
D9	14.33	14.44	4.89	5.08	1.04
D2	14.64	14.76	5.46	5.71	1.05
D1 (diltiazem)	14.94	15.05	6.11	6.37	1.04
D4	16.80	16.86	14.39	14.92	1.04
D3	16.80	16.86	14.39	14.92	1.04
D5	16.86	—	14.92	—	—

Chiral separation of trimetoquinol and tetrahydropapaveroline

Enantiomers of trimetoquinol hydrochloride were successfully resolved and those of tetrahydropapaveroline, which is a biosynthetic precursor of morphine and has a similar structure to that of trimetoquinol hydrochloride, were partially resolved with a 0.05 M STDC solution of pH 7.0. A typical chromatogram of these solutes is shown in Fig. 3. Calculated $\tilde{k}'$ and α values are summarized in Table V. The capacity factors of these solutes are relatively small compared with those of diltiazem-related compounds and it can be expected that the chiral separation of tetrahydropapaveroline will be improved with increase in the k' value through an increase in surfactant concentration. In micellar EKC, the resolution equation is given by[2]
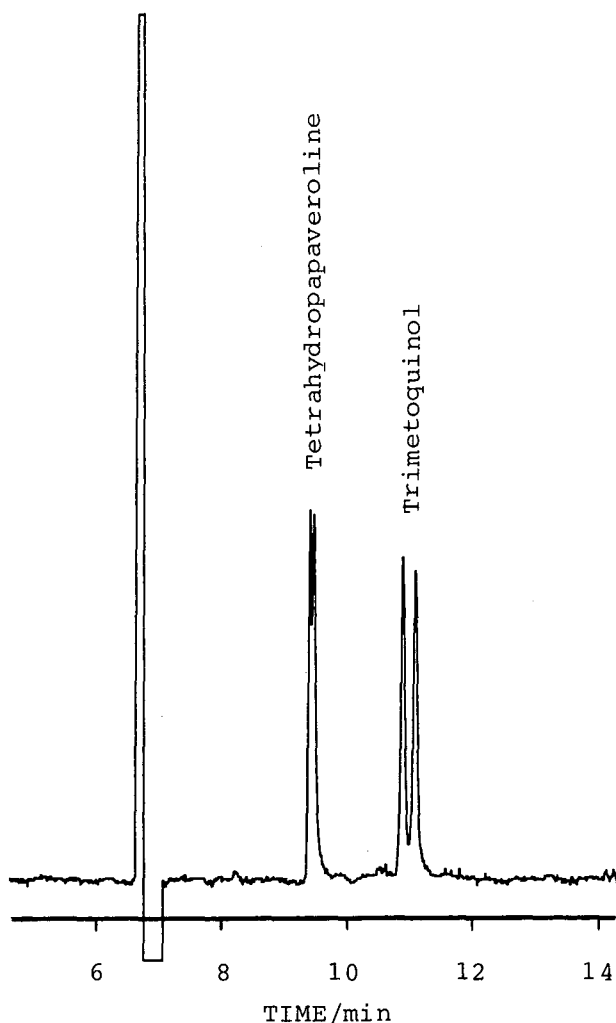
Fig. 3. Chiral separation of trimetoquinol hydrochloride and tetrahydropapaveroline. Conditions as in Fig. 2.

TABLE V

MIGRATION TIMES, CAPACITY FACTORS AND SEPARATION FACTORS OF TRIMETO-
QUINOL HYDROCHLORIDE, TETRAHYDROPAPAVEROLINE AND DINAPHTHYL

0.05 M STDC at pH 7.0; applied voltage, 20 kV; t_0, 6.62 min; t_{mc}, 18.81 min.

Solute	t_{R1} (min)	t_{R2} (min)	$\tilde{k}'_1$	$\tilde{k}'_2$	α
Tetrahydropapaveroline	9.36	9.42	0.82	0.85	1.03
Trimetoquinol	10.84	11.04	1.50	1.62	1.07
2,2'-Dihydroxy-1,1'-dinaphthyl	17.72	18.03	28.94	41.56	1.44

$$R_s = \frac{\sqrt{N}}{4}\left(\frac{\alpha - 1}{\alpha}\right)\left(\frac{\tilde{k}'_2}{1 + \tilde{k}'_2}\right)\left[\frac{1 - t_0/t_{mc}}{1 + (t_0/t_{mc})\tilde{k}'_1}\right] \qquad (2)$$

where N is the theoretical plate number of the solute. The last term on the right-hand side is additional to that in the usual HPLC and hence R_s depends considerably on this
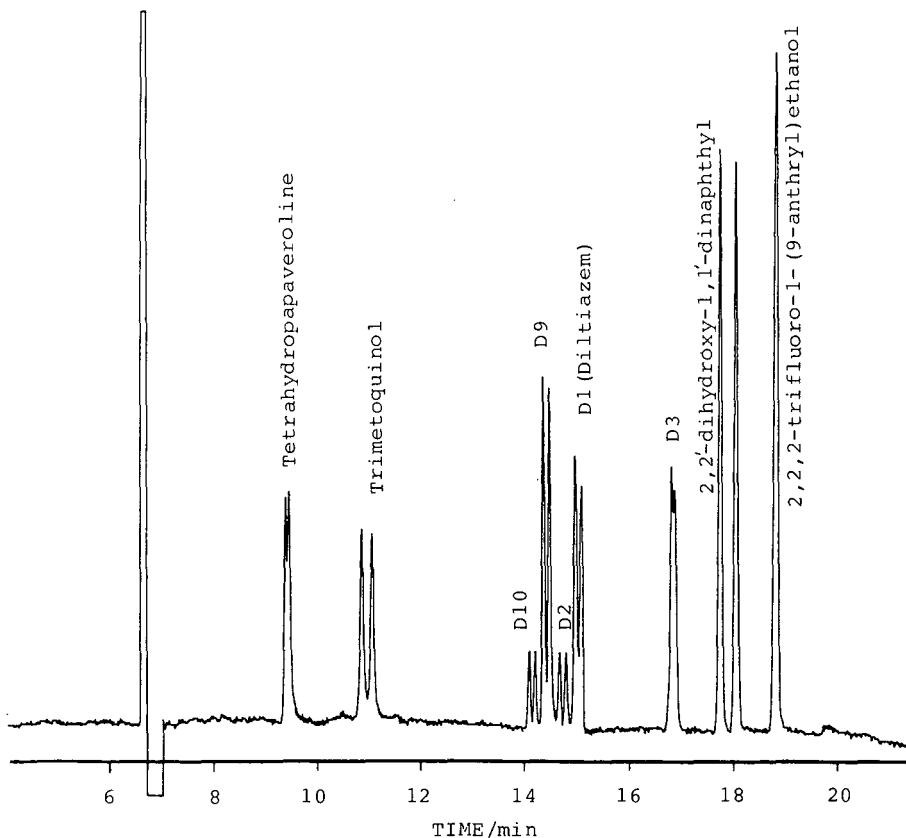
Fig. 4. Chiral separation of trimetoquinol hydrochloride, tetrahydropapaveroline, five diltiazem-related compounds, 2,2'-dihydroxy-1,1'-dinaphthyl and 2,2,2-trifluoro-1-(9-anthryl)ethanol. Conditions as in Fig. 2.

term. With bile salts, the maximum resolution should be obtained when the $\tilde{k}'$ values are between 1 and 2 from the value $t_0/t_{mc} = 0.35$ at a constant N value[2]. The capacity factor of trimetoquinol hydrochloride fitted the above range.

However, to separate several solutes in one run, a 0.05 M concentration was sufficient. A typical chiral separation of nine enantiomeric compounds is shown in Fig. 4, in which t_0 (electroosmotic flow) and t_{mc} were *ca.* 6.6 and 18.8 min, respectively. The $\tilde{k}'$ and α values of 2,2'-dihydroxy-1,1'-dinaphthyl are given in Table V. Enantiomers of 2,2,2-trifluoro-1-(9-anthryl)ethanol migrated with the same velocity as Sudan III, indicating that it was totally solubilized into the micelle, and were not separated.

Application to the optical purity testing of trimetoquinol hydrochloride was also investigated. Typical chromatograms are shown in Fig. 5. Down to 1% of the minor enantiomer [(R)-form] of the major enantiomer of trimetoquinol hydrochloride [(S)-form] could be detected directly by micellar EKC at a signal-to-noise ratio of 3. The optical purity of five actual batches determined by this method were all more than 99% (not detected).

In conclusion, chiral separation by micellar EKC with anionic bile salts is successful when the solutes have a relatively rigid conformation, probably owing to the rigid structure of the bile salt molecule. Enantiomeric compounds, which are positively charged or basic, will be more effectively resolved because of increasing ionic interaction between the solute and the anionic bile salt micelle. However, it will be difficult to predict whether enantiomers can be successfully separated or not because a small difference in the solute structure significantly affects the chiral recognition. In addition to bile salts, other chiral surfactants will be used in micellar EKC similarly to
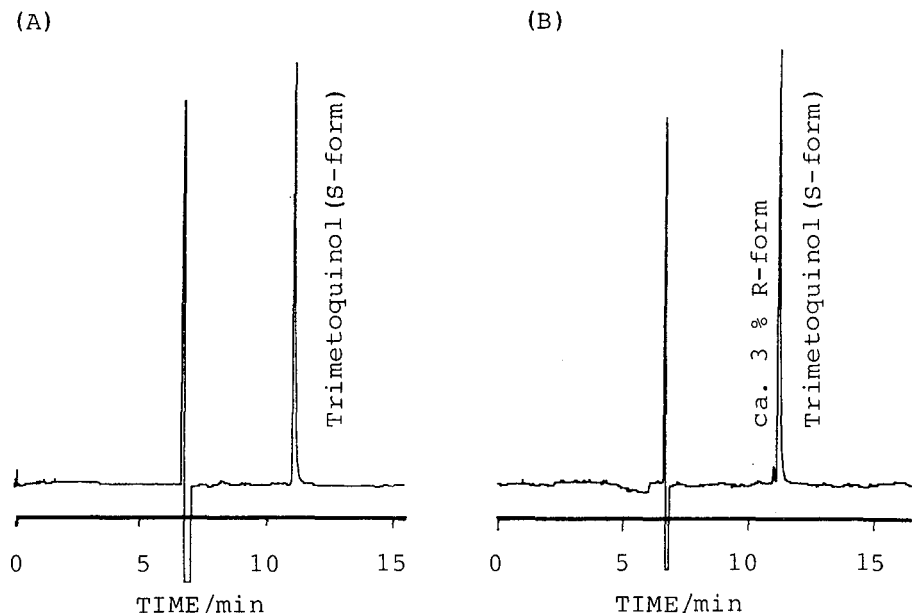

Fig. 5. Optical purity testing of trimetoquinol hydrochloride. (A) Authentic trimetoquinol hydrochloride [(S)-form] and (B) *ca.* 3% of (R)-form added to A. Conditions as in Fig. 3.

the use of chiral mobile phases in HPLC. Micellar EKC will be widely applied in the future to the direct chiral separation of drugs by use of new chiral surfactants or SDS micelles, mixed with a chiral additive.

REFERENCES

1 S. Terabe, K. Otsuka, K. Ichikawa, A. Tsuchiya and T. Ando, *Anal. Chem.*, 56 (1984) 111.
2 S. Terabe, K. Otsuka and T. Ando, *Anal. Chem.*, 57 (1985) 834.
3 S. Terabe, *Trends Anal. Chem.*, 8 (1989) 129.
4 H. Nishi, N. Tsumagari, T. Kakimoto and S. Terabe, *J. Chromatogr.*, 465 (1989) 331.
5 H. Nishi, N. Tsumagari, T. Kakimoto and S. Terabe, *J. Chromatogr.*, 477 (1989) 259.
6 H. Nishi, T. Fukuyama, M. Matsuo and S. Terabe, *J. Chromatogr.*, 513 (1990) 279.
7 H. Nishi, T. Fukuyama, M. Matsuo and S. Terabe, *J. Pharm. Sci.*, 79 (1990) in press.
8 K. Otsuka, S. Terabe and T. Ando, *J. Chromatogr.*, 396 (1987) 350.
9 S. Fujiwara and S. Honda, *Anal. Chem.*, 59 (1987) 2773.
10 S. Fujiwara, S. Iwase and S. Honda, *J. Chromatogr.*, 447 (1988) 133.
11 T. Nakagawa, Y. Oda, A. Shibukawa and H. Tanake, *Chem. Pharm. Bull.*, 36 (1988) 1622.
12 T. Nakagawa, Y. Oda, A. Shibukawa, H. Fukuda and H. Tanaka, *Chem. Pharm. Bull.*, 37 (1989) 707.
13 H. Nishi, T. Fukuyama and M. Matsuo, *J. Chromatogr.*, 515 (1990) 245.
14 M. M. Bushey and J. W. Jorgenson, *Anal. Chem.*, 61 (1989) 491.
15 M. M. Bushey and J. W. Jorgenson, *J. Microcolumn Sep.*, 1 (1989) 125.
16 S. Terabe, M. Shibata and Y. Miyashita, *J. Chromatogr.*, 480 (1989) 403.
17 H. Nishi, T. Fukuyama, M. Matsuo and S. Terabe, *J. Microcolumn Sep.*, 1 (1989) 234.
18 A. S. Cohen, A. Paulus and B. L. Karger, *Chromatographia*, 24 (1987) 15.
19 K. Otsuka and S. Terabe, *J. Chromatogr.*, 515 (1990) 221.
20 D. Attwood and A. T. Florence, *Surfactant Systems. Their Chemistry, Pharmacy and Biology*, Chapman and Hall, London, 1983, pp. 185–196.
21 H. Nishi, T. Fukuyama, M. Matsuo and S. Terabe, *J. Chromatogr.*, 498 (1990) 313.

CHROMSYMP. 1780

Separation and determination of aspoxicillin in human plasma by micellar electrokinetic chromatography with direct sample injection

HIROYUKI NISHI*, TSUKASA FUKUYAMA and MASAAKI MATSUO

Analytical Chemistry Research Laboratory, Tanabe Seiyaku, Co., Ltd., 16–89, Kashima 3-chome, Yodogawa-ku, Osaka 532 (Japan)

ABSTRACT

Both the separation and determination of aspoxicillin in human plasma by micellar electrokinetic chromatography (MEKC) were investigated. Selectivity in the separation of seven penicillin antibiotics was improved by using MEKC in comparison with capillary zone electrophoresis. Plasma proteins, which might interfere with drug analysis in conventional chromatography, were solubilized by the micelles employed in MEKC and eluted later than the drugs. This permitted the determination of the drugs in plasma by a direct sample injection method. One analysis of a plasma sample was performed within *ca.* 20 min without pretreatment. Good linearity and recovery were also obtained in the range of plasma levels usually encountered in clinical analysis with a correlation coefficient $r = 0.999$ and 94–104% recovery. The limit of detection for aspoxicillin was 1.3 μg ml^{-1} at a signal-to-noise ratio of 3.

INTRODUCTION

Micellar electrokinetic chromatography (MEKC) is a new type of separation method[1,2] based on micellar partitioning of the solute and electrophoretic migration of the micelle, and can be classified as an individual kind of chromatography on the basis of its separation principle, although it is performed with the same apparatus as capillary zone electrophoresis (CZE). Although this technique is called micellar electrokinetic capillary chromatography (MECC)[3], the term micellar EKC or MEKC will be used in order to stress that the partition mechanism in electrokinetic chromatography (EKC) has a wider scope than micellar solubilization as described elsewhere[4].

MEKC has many attractive advantages in addition to the capability of electrophoretic separation of electrically neutral substances. The selectivity and peak shapes are even better for the separation of ionic substances[5,6], although some of them can be separated by conventional CZE. Closely related isotopic compounds have been successfully separated by MEKC[7,8]. Chiral separation of some amino acid deriva-

tives[9,10] and drugs[11,12] has also been achieved by MEKC with a mixed micelle of sodium dodecyl sulphate (SDS) and a chiral additive or with chiral cholate micelles. The application of MEKC to the determination of drugs in preparations has been well studied by using an internal standard method[13-16] with the same reproducibility as in high-performance liquid chromatography (HPLC). Purity testing by the area percentage method has also been reported[16].

In a previous paper, we reported the migration behaviour of penicillins and cephalosporins in MEKC with sodium dodecyl sulphate (SDS) and sodium N-lauroyl-N-methyltaurate[6]. The selectivity was greatly improved for these ionic substances by MEKC in comparison with CZE.

In this paper, we describe the separation and determination of aspoxicillin in human plasma by MEKC with SDS. Aspoxicillin is a new broad-spectrum semi-synthetic penicillin, which has a amino acid residue N^4-methyl-D-asparagine in the molecule[17,18]. The determination of aspoxicillin in human serum, urine and bile by HPLC[19] and by bioassay[20] has been reported elsewhere. In MEKC, plasma proteins, which might interfere with drug analysis, are solubilized by the micelle, and hence elute later than the drugs. Consequently, a direct palsma sample injection can be performed without any pretreatment such as deproteinization or extraction. Nakagawa and co-workers[21,22] first reported the determination of drugs in plasma by MEKC using a direct injection method.

EXPERIMENTAL

Apparatus

An untreated fused-silica capillary tube (Scientific Glass Engineering, Ringwood, Victoria, Australia) with dimensions of 650 mm × 50 μm I.D. (effective length 500 mm) was used as a separation tube. Detection of separated solutes was achieved by on-column UV absorption measurement at 210 nm using a Uvidec-100-VI (Jasco, Tokyo, Japan) with a time constant of 0.05 s. A Chromatopac C-R5A (Shimadzu, Kyoto, Japan) was used for data processing. A high voltage was applied with a Model HJLL-25PO d.c. power supply (Matsusada Precision Devices, Kasatsu, Japan), which delivered up to +25 kV. Other instruments were the same as described previously[5].

Reagents and samples

SDS was purchased from Nacalai Tesque (Kyoto, Japan). Aspoxicillin (ASPC) was obtained from Tanabe Seiyaku (Osaka, Japan). Benzylpenicillin, ampicillin, carbenicillin, sulbenicillin, piperacillin and amoxicillin were obtained either commercially or from the National Institute of Hygienic Sciences (Tokyo, Japan), and were used as test samples. The structure of each penicillin is shown in Fig. 1 together with that of acetaminophen from Wako (Osaka, Japan), which was used as an internal standard (I.S.). All other reagents and solvents, of analytical-reagent grade, were obtained from Katayama Kagaku (Osaka, Japan) and used without further purification.

SDS was dissolved in a buffer solution prepared by mixing a 0.02 M sodium dihydrogen phosphate solution with a 0.02 M sodium tetraborate solution to give the appropriate pH value, and the micellar solutions were passed through a 0.45-μm membrane filter (Gelman Science Japan, Tokyo, Japan) and degassed by sonication before use. The samples were dissolved in water at a concentration of $ca.$ 1 mg ml^{-1} to

Fig. 1. Structures of penicillins and acetaminophen.
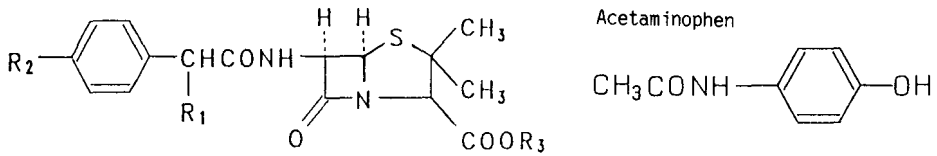
Penicillins	Symbol	R_1	R_2	R_3
Benzylpenicillin	1	H	H	K
Ampicillin	2	NH_2	H	Na
Carbenicillin	3	COONa	H	Na
Sulbenicillin	4	SO_3Na	H	Na
Piperacillin	5	*1)	H	Na
Aspoxicillin	6	*2)	OH	H
Amoxicillin	7	NH_2	OH	H

give adequate peak heights for separation studies. Human plasma was prepared from fresh human blood in the usual manner. Known amounts of aspoxicillin and I.S. were dissolved in human plasma or water for concentration studies (for concentrations, see later).

Procedure

    A sample solution was introduced manually into the positive end of the capillary tube by siphoning (about a 10-cm height for 5–10 s) as described previously[5] and MEKC was performed at ambient temperature (*ca.* 20°C).

    The capillary tube was flushed with the operating buffer solution once per five runs by using a syringe and washed with an alkaline solution daily, usually at the end of an experiment as follows: the capillary tube was filled manually with 0.1 *M* potassium hydroxide solution using a syringe and allowed to stand for 30 min, flushed with water and allowed to stand for a further 5 min, then finally filled with the working buffer solution.

RESULTS AND DISCUSSION

CZE of seven penicillin antibiotics

The separation of seven penicillins by CZE was investigated with a 0.02 *M* phosphate–borate buffer solution of pH 7 ∼ 9, in which all the solutes must be completely ionized. A typical electropherogram at pH 8.5 is shown in Fig. 2A. All the solutes migrated toward the negative electrode, that is, the electroosmotic velocity was always higher than the electrophoretic velocity of any solute employed under the above experimental conditions. Although these ionic antibiotics can be separated by conventional CZE, their migration times are similar, except for carbenicillin and sulbenicillin, and the separation was not successful. This is because that these solutes, except for carbenicillin and sulbenicillin, have similar structures (molecular weights) and electric charges (one carboxyl group), leading to the similar electrophoretic mobilities. Carbenicillin and sulbenicillin, which have additional anionic groups in molecules, are retarded more strongly than other solutes by the electrophoretic effect. The migration times of carbenicillin and sulbenicillin are also similar. These results show that the migration of the solutes in CZE depends greatly on the electric charge in the buffer solution used, in which the solutes are completely ionized. Acetaminophen migrated with the same velocity as methanol, which is a tracer of the electroosmotic velocity[2], because this is electrically neutral.

The buffer pH and composition were very critical in relation to peak symmetry of the solutes. In the pH range examined, the peak symmetry of each solute, especially carbenicillin and sulbenicillin, was improved with increasing pH. Mikkers *et al.*[23] suggested that unsymmetrical peaks are usually generated when the electrophoretic mobilities of the solute and that of the buffer constituent are different.
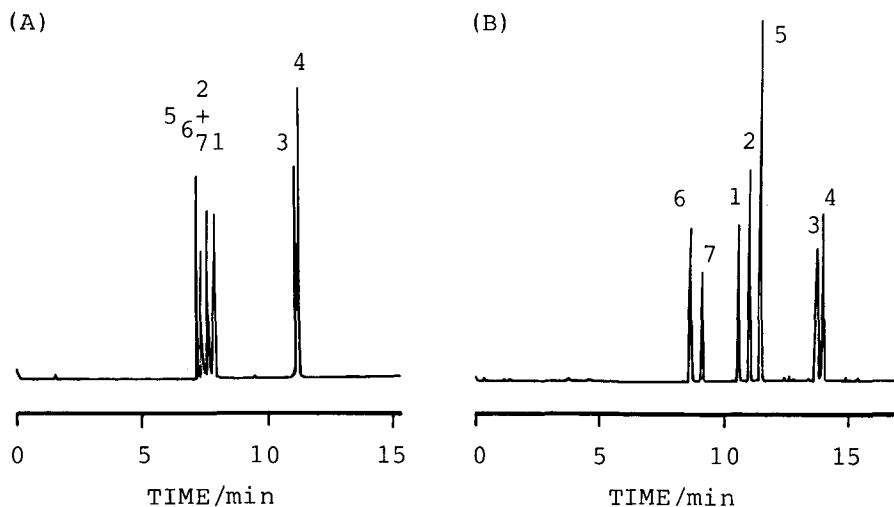

Fig. 2. Separation of seven penicillins by (A) CZE and (B) MEKC. (A) 0.02 *M* phosphate–borate buffer of pH 8.5; (B) 0.1 *M* SDS added to A. Applied voltage, 20 kV; temperature, ambient; detection, 210 nm; attenuation, 0.04 a.u.f.s. Sample numbers are given in Fig. 1.
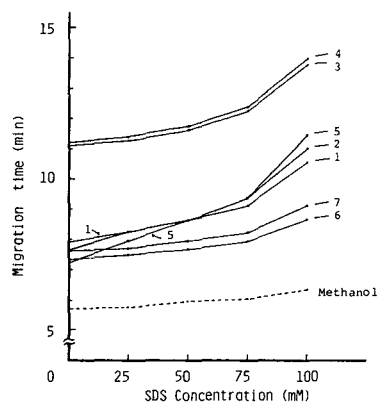
Fig. 3. Effect of SDS concentration on the migration times of penicillins. Buffer, 0.02 M phosphate–borate buffer (pH 8.5). Other conditions as in Fig. 2.

MEKC of seven penicillin antibiotics

The effect of SDS concentration on the migration time of the solutes using a phosphate–borate buffer solution of pH 8.5, in which all the solutes are completely ionized, is shown in Fig. 3. The migration time increased gradually with increasing SDS concentration. The solubilization into the micelle or interaction with the micelle of the solutes probably increased with increase in SDS concentration even for these ionic solutes, as was observed previously[6]. The change in the migration time of piperacillin was remarkable, indicating that this was more readily incorporated into the SDS micelle owing to its high lipophilicity. A typical chromatogram at 0.1 M SDS is shown in Fig. 2B, showing an improvement in the selectivity in comparison with CZE (Fig. 2A).

The pH dependence of the migration times of seven penicillins and acetaminophen (I.S.) was examined using 0.05 M SDS solutions in the pH range 7–9 (Fig. 4).
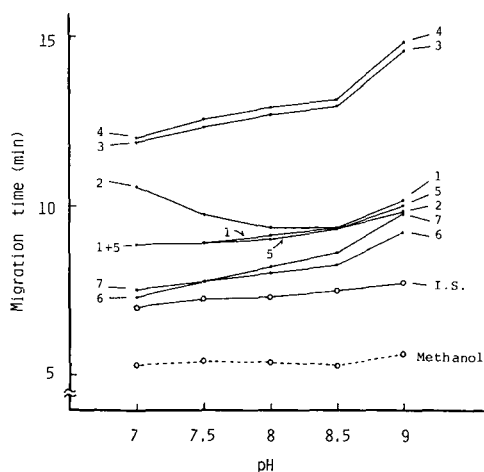

Fig. 4. pH dependence of the migration time of penicillins and acetaminophen (I.S.) in MEKC. Buffer, 0.02 M phosphate–borate buffer containing 0.05 M SDS. Other conditions as in Fig. 2.

The migration time of each solute except ampicillin increased with increasing pH, although those of methanol (electroosmotic velocity) and acetaminophen remained almost constant. It can be seen that the range of migration times increased. This can be ascribed to the increase in the electrophoretic velocity of the micelle with increasing pH[24]. For ampicillin, however, the migration time decreased from pH 7 to 8.5 and increased from pH 8.5 to 9. This may be due to the amino group in ampicillin.

MEKC of human plasma sample

The migration times of aspoxicillin, acetaminophen and methanol, which is considered as a tracer of the electroosmotic velocity, and the range of the migration times of blood proteins as a function of SDS concentration in a phosphate–borate buffer solution of pH 8.5 are shown in Fig. 5. In CZE, where SDS was absent, aspoxicillin coeluted with proteins. Acetaminophen migrated with the same velocity as that of methanol because it is electrically neutral under the above experimental conditions. After a plasma sample had been injected in CZE mode, aspoxicillin and acetaminophen, even in the standard solution, which was prepared by dissolving each standard compound in water, migrated with slower velocities in the following run. This was probably due to the adsorption of plasma proteins on the inside surface of the fused-silica capillary tube, leading to a decrease in the electroosmotic velocity. Therefore, it was necessary to wash the capillary tube with an alkaline solution to regenerate the capillary tube (surface) or to avoid such a phenomenon after the injection of plasma samples in the CZE mode.

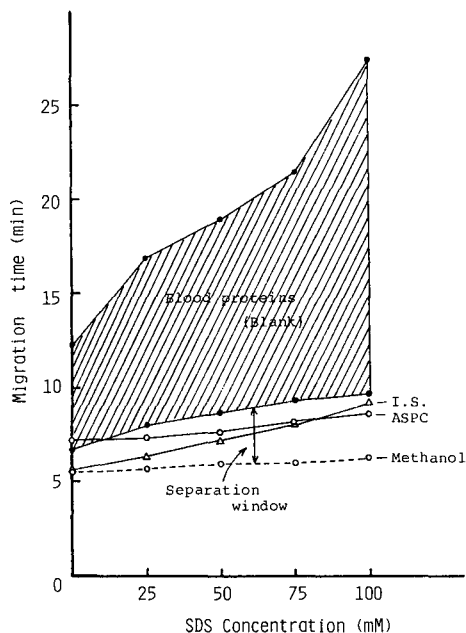The complete separation of aspoxicillin and acetaminophen from the protein

Fig. 5. Effect of SDS concentration in the migration times of aspoxicillin (ASPC), acetaminophen (I.S.) and plasma proteins. Other conditions as in Fig. 3.

peaks was attained through the addition of SDS, that is, by MEKC. The migration time of plasma proteins increased with increase in concentration of SDS, as shown in Fig. 5. Plasma proteins were probably solubilized by the SDS micelles because the SDS concentration in the buffer solution is above the critical micellar concentration (CMC)[25]. Hence the proteins migrated later than the drugs. That is, the plasma proteins are solubilized by SDS and they acquire a strong negative charge and are consequently retarded strongly by the electrophoretic force operating in the opposite direction. In this way, the adsorption of plasma proteins on the capillary tube, which was encountered in CZE, was prevented in MEKC[21,22]. This permitted the determination of the drugs in plasma by a direct sample injection method, similar to micellar chromatography in HPLC developed by Armstrong[26] and Dorsey[27]. Typical MEKC results for a standad solution containing 50 μg ml^{-1} of aspoxicillin and 25 μg ml^{-1} of acetaminophen, blank plasma and plasma spiked with aspoxicillin and acetaminophen at the same concentration as in the standard solution are shown in Fig. 6, where an operating buffer solution of pH 8.5 containing 0.05 M SDS was used.

In MEKC, where SDS was added to the buffer solution, the migration times of aspoxicillin and acetaminophen of the plasma samples were consistent with those for the standard samples (aqueous solution) and these values were almost constant from run to run and from day to day. Good reproducibility of the migration time of each solute was obtained without frequent capillary washing (see below). The effect of SDS concentration on the migration time of acetaminophen, which is electrically neutral, was greater than that of aspoxicillin, which is ionized (Fig. 5).

In this method, in order to obtain a good separation, the drugs and I.S. substances should migrate more rapidly than the first-eluted plasma protein, or within the separation window (see Fig. 5) without coelution with blank plasma peaks shown in Fig. 6B. The SDS concentration, which is above the CMC, has to be adjusted to avoid such coelution. A buffer solution containing 0.05 M SDS was employed for concentration studies from the above investigations and with a relatively short analysis time.

Quantitation

Quantitation of aspoxicillin in human plasma was performed by the internal standard method using a buffer solution of pH 8.5 containing 0.05 M SDS. The reproducibility of the migration time and peak-area ratios of standards and spiked plasma samples was determined by repeated injections ($n = 5-9$) (Tables I and II). The calculated relative standard deviations (R.S.D.) of 0.25–0.97% for migration times and 2.7–4.9% for peak-area ratios are comparable to those obtained in previous studies[13-16]. The calibration graph for aspoxicillin in water over the concentration range 25–300 μg ml^{-1}, which covers the plasma levels encountered in clinical analysis[19], shows excellent linearity with a correlation coefficient $r = 0.999$ and passes through the origin. The detection limit of aspoxicillin, calculated from the peak height for a standard solution containing 25 μg ml^{-1} of aspoxicillin, was *ca.* 1.3 μg ml^{-1} at a signal-to-noise ratio of 3.

The recovery was also examined over the concentration range 50–250 μg ml^{-1} (Table III). The average recovery with repeated injections ($n = 5-6$) was 94–104%. Hence the total amount of bound together with unbound aspoxicillin could be determined by this method.
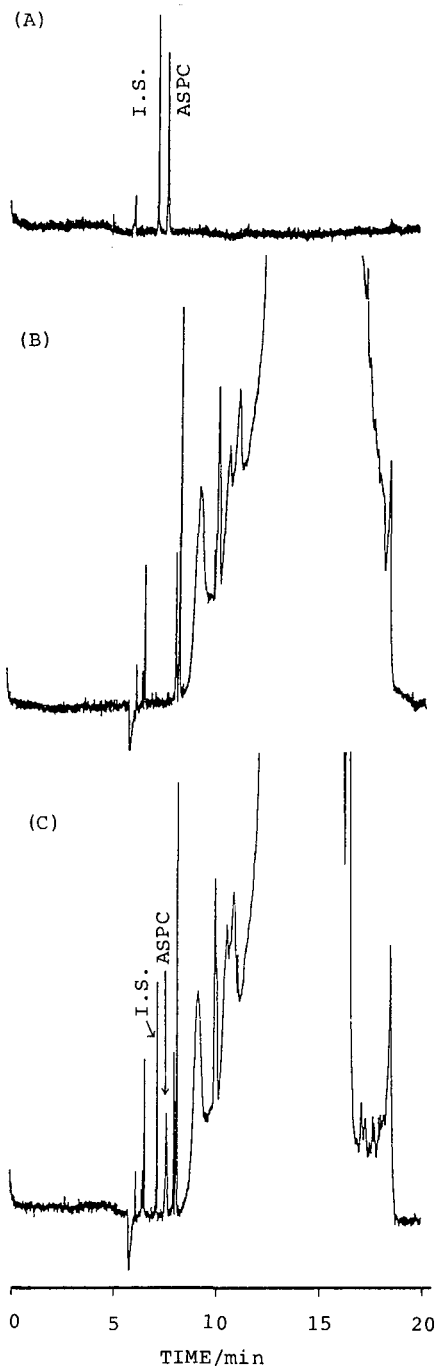
Fig. 6. MEKC separation of aspoxicillin (ASPC) and acetaminophen (I.S.). (A) Standard solution; (B) blank plasma; (C) plasma spiked with ASPC and I.S. Buffer, 0.02 M phosphate–borate buffer (pH 8.5) containing 0.05 M SDS. Other conditions as in Fig. 2.

TABLE I

REPRODUCIBILITY OF MIGRATION TIMES

Concentration ($\mu g\ ml^{-1}$)	Solvent	n	Acetaminophen		Aspoxicillin	
			t_R (min)	R.S.D. (%)	t_R (min)	R.S.D. (%)
50	Water	9	7.17	0.85	7.62	0.73
50	Plasma	9	7.31	0.97	7.75	0.88
100	Plasma	5	7.26	0.83	7.71	0.75
150	Plasma	5	7.35	0.89	7.78	0.96
200	Plasma	5	7.30	0.27	7.74	0.25
250	Plasma	5	7.41	0.35	7.83	0.48

TABLE II

REPRODUCIBILITY OF PEAK-AREA RATIOS

Concentration ($\mu g\ ml^{-1}$)	Solvent	n	R.S.D. (%)
50	Water	9	4.07
50	Plasma	9	3.90
100	Plasma	5	4.92
150	Plasma	5	4.48
200	Plasma	5	3.66
250	Plasma	5	2.73

TABLE III

RECOVERY TEST

Aspoxicillin added to plasma ($\mu g\ ml^{-1}$)	n	Recovery (%)
50	6	94.3
100	5	103.9
150	6	100.1
200	5	103.4
250	5	97.7

TABLE IV

THEORETICAL PLATE NUMBERS

Concentration ($\mu g\ ml^{-1}$)	Water		Plasma	
	I.S.[a]	ASPC[b]	I.S.[a]	ASPC[b]
50	276 000	98 000	256 000	39 100
100	267 000	104 000	267 000	42 500
150	245 000	89 900	272 000	46 300
200	279 000	98 800	277 000	46 200
250	275 000	96 700	277 000	51 800

[a] Acetaminophen.
[b] Aspoxicillin.

The theoretical plate numbers (N) calculated for aspoxicillin and acetaminophen in water and plasma samples over the concentration 50–250 μg ml^{-1} are summarized in Table IV. The N value for aspoxicillin at a given concentration in a plasma sample was half that obtained in water (standard solution) (see Fig. 6A and C). However, the migration time and peak-area ratios were not affected (Tables I and II). In contrast, the N value of acetaminophen did not change between water and plasma samples. These results indicate that a higher protein binding of aspoxicillin than acetaminophen caused a slower release of aspoxicillin from proteins, which resulted in the broadening of the aspoxicillin peak.

In conclusion, MEKC improved the separation of ionic penicillins in comparison with CZE, in addition to the high separation efficiency. Under the experimental conditions of an effective capillary tube length of 500 mm and a voltage of 20 kV, one analysis of a plasma sample was performed within *ca.* 20 min without pretreatment such as deproteinization and extraction. Recently, a few commercial instruments have become available, but it will be necessary to develop an ultra-microinjector which allows quantitative and reproducible injection or highly sensitive detectors for the assay of drugs in body fluids.

ACKNOWLEDGEMENTS

REFERENCES

1 S. Terabe, K. Otsuka, K. Ichikawa, A. Tsuchiya and T. Ando, *Anal. Chem.*, 56 (1984) 111.
2 S. Terabe, K. Otsuka and T. Ando, *Anal. Chem.*, 57 (1985) 834.
3 D. E. Burton, M. J. Sepaniak and M. P. Maskarinec, *Chromatographia*, 21 (1986) 583.
4 S. Terabe, *Trends Anal. Chem.*, 8 (1989) 129.
5 H. Nishi, N. Tsumagari, T. Kakimoto and S. Terabe, *J. Chromatogr.*, 465 (1989) 331.
6 H. Nishi, N. Tsumagari, T. Kakimoto and S. Terabe, *J. Chromatogr.*, 477 (1989) 259.
7 M. M. Bushey and J. W. Jorgenson, *Anal. Chem.*, 61 (1989) 491.
8 M. M. Bushey and J. W. Jorgenson, *J. Microcolumn Sep.*, 1 (1989) 125.
9 A. S. Cohen, A. Paulus and B. L. Karger, *Chromatographia*, 24 (1987) 15.
10 S. Terabe, M. Shibata and Y. Miyashita, *J. Chromatogr.*, 480 (1989) 403.
11 H. Nishi, T. Fukuyama, M. Matsuo and S. Terabe, *J. Microcolumn Sep.*, 1 (1989) 234.
12 H. Nishi, T. Fukuyama, M. Matsuo and S. Terabe, *J. Chromatogr.*, 515 (1990) 233.
13 K. Otsuka, S. Terabe and T. Ando, *J. Chromatogr.*, 396 (1987) 350.
14 S. Fujiwara and S. Honda, *Anal. Chem.*, 59 (1987) 2773.
15 H. Nishi, T. Fukuyama, M. Matsuo and S. Terabe, *J. Pharm. Sci.*, 79 (1990) in press.
16 H. Nishi, T. Fukuyama, M. Matsuo and S. Terabe, *J. Chromatogr.*, 513 (1990) 279.
17 M. Wagatsuma, M. Seto, T. Miyagishima, M. Kawazu, T. Yamaguchi and S. Ohshima, *J. Antibiot.*, 36 (1983) 147.
18 S. Okuno, I. Maezawa, Y. Sakuma, T. Matsushita and T. Yamaguchi, *J. Antibiot.*, 41 (1988) 239.
19 T. Yanagida, Y. Kojima, K. Yamasaki, I. Daira and T. Ishikawa, *Chemotherapy*, 32 (1984) 112.
20 K. Tani, I. Maezawa, Y. Sakuma, N. Ishii, H. Yoshida, T. Yamaguchi, M. Ichikawa, M. Itoh, T. Ehara, M. Inoue and T. Ishikawa, *Chemotherapy*, 32 (1984) 99.
21 T. Nakagawa, Y. Oda, A. Shibukawa and H. Tanaka, *Chem. Pharm. Bull.*, 36 (1988) 1622.
22 T. Nakagawa, Y. Oda, A. Shibukawa, H. Fukuda and H. Tanaka, *Chem. Pharm. Bull.*, 37 (1989) 707.

23 F. E. P. Mikkers, F. M. Everaerts and Th. P. E. M. Verheggen, *J. Chromatogr.*, 169 (1979) 11.
24 S. Terabe, H. Utsumi, K. Otsuka, T. Ando, T. Inomata, S. Kuze and Y. Hanaoka, *J. High Resolut. Chromatogr. Chromatogr. Commun.*, 9 (1986) 666.
25 W. L. Hinze, *Ordered Media in Chemical Separations (ACS Symposium Series*, No. 342), American Chemical Society, Washington, DC, 1987, p. 4.
26 D. W. Armstrong, *Anal. Chem.*, 59 (1987) 84A.
27 J. G. Dorsey, *Advances in Chromatography*, Vol. 27, Marcel Dekker, New York and Basle, 1988, pp. 167–214.

CHROMSYMP. 1773

High-performance liquid chromatography of thiols with differential pulse polarographic detection of the catalytic hydrogen evolution current

XUE-XIN QIAN, KUNIO NAGASHIMA* and TOSHIYUKI HOBO

Department of Industrial Chemistry, Faculty of Technology, Tokyo Metropolitan University, 2-1-1 Fukasa-wa, Setagaya-ku, Tokyo 158 (Japan)

and

YUE-YIN GUO and CHIAKI YAMAGUCHI

Senshu Scientific Co. Ltd., 3-31-10 Igusa, Suginami-ku, Tokyo 167 (Japan)

ABSTRACT

SH and SS groups in organic compounds were sensitively detected in NH_3–NH_4Cl (0.24 M)–Co^{2+} (5 · 10^{-4} M) solution by differential-pulse polarography (DPP). A new type of flow-through cell was developed and used to combine the polarograph with a high-performance liquid chromatograph. The experimental conditions for polarography and chromatography were studied and the effectiveness of the cell was also evaluated. The chromatogram obtained showed that this combined system works very well for the detection of thiols. The sensitivity was similar to that given by UV detection but was not handicapped by the wavelength. As a negative potential was used, the coexistence of other species did not cause large interferences.

INTRODUCTION

Thiols and corresponding disulphides constitute an important group of organosulphur compounds owing to their abundance and properties[1], but biochemical and environmental studies have been limited because of shortcomings in the existing analytical techniques[2]. For the determination of thiols, the usual method applied is chromatography with UV or fluorescence detection. The main disadvantage of UV spectrophotometric detection is its limited wavelength range and that of fluorimetric detection is that it detects only fluorescent substances. On the other hand, the linking of electrochemical detection with high-performance liquid chromatography (HPLC) has advantages for the measurement of various sulphur-containing compounds[3]. Shea[4] applied polarographic detection with a platinum electrode covered with thin mercury membrane to hydrophilic thiols in sediment pore water or marine water, the detection limit being 2 pmol. However, the electrode has to be checked every day and the mercury membrane peels off even in weakly alkaline

solution. A dual-electrode detector was developed by Laura and Shoup[5]. Both thiols and disulphides can be detected by using the series mode. However, complete conversion of disulphides has to be ensured, which is difficult.

SH and SS groups can be sensitively detected by measuring the "Brdička current" in NH_3/NH_4Cl solution containing Co^{2+} or Ni^{2+} ions[6], but so far it has been seldom used with HPLC, mainly because of the difficulty of making a suitable flow-through cell for HPLC. The object of this study was to develop a new type of flow-through cell which is well suited for combining polarography with HPLC for the application of Brdicka current detection to the determination of SH groups.

EXPERIMENTAL

Chemicals

L-Cysteine, reduced glutathione, thiomalic acid, α-thioglycerol and mercapto-ethanol were obtained from Tokyo Kasei (Tokyo, Japan), ammonia solution and solvents (HPLC grade) from Kanto (Tokyo, Japan), cobalt dichloride from Showa (Tokyo, Japan) and the ion-pair reagent, sodium trichloroacetate, from Nacalai Chemicals (Kyoto, Japan). The water used for the preparation of the mobile phase and electrolyte was deionized by passage through a mixed-bed resin in a Milli-Q laboratory water purification system (Millipore).

Equipment

The HPLC–differential pulse polarographic (DPP) system consisted of an SSC-3100-J pump (Senshu, Tokyo, Japan) and either a Model SSC-3000A-2 UV detector (Senshu) or a P-1100 polarographic analyser (Yanagimoto, Kyoto, Japan) equipped with a P-1000ST dropping mercury electrode (DME) stand. The controls were set as follows: current range, 5 μA/V; modulation amplitude, 50 mV; drop time, 1 s; and potential scan rate (when required), 5 mV/s.

Polarographic peaks were measured with a three-electrode system consisting of a platinum metal electrode, a saturated calomel reference electrode (SCE MR-P2) and a DME as the working electrode. The electrode characteristics were m (*i.e.* flow-rate of mercury) = 1.989 mg/s, pulse interval 50 ms and pulse sampling time 20 ms. All measurements were made at room temperature.

Peristaltic pumps were used to send carrier solution and Co^{2+} mixing solution into the flow-through cell via thin PTFE tubing (0.5 mm I.D.) and wide glass tubing (4 mm I.D.), respectively. The columns used were Capcell SG-ODS (250 mm × 4.6 mm I.D.), obtained from Shiseido (Tokyo, Japan), Senshu Pak ODS-N-1251 and Senshu Pak ODS-H-1251 (250 mm × 4.6 mm I.D.), obtained from Senshu and TSKgel-120T (200 mm × 4.6 mm I.D.), obtained from Tosoh (Tokyo, Japan).

Construction of flow-through cell

An effective flow-through cell must have a small effective determination volume[7], in other words, the volume around the DME should be as small as possible. As shown in Fig. 1, the newly designed flow cell was made with glass tubing of 4 mm I.D. There are three holes in the cell through which three electrodes (working, reference and counter) were inserted. From one end of the cell PTFE tubing of 0.5 mm I.D. was inserted exending to a position very close to the DME. Sample solution was introduced
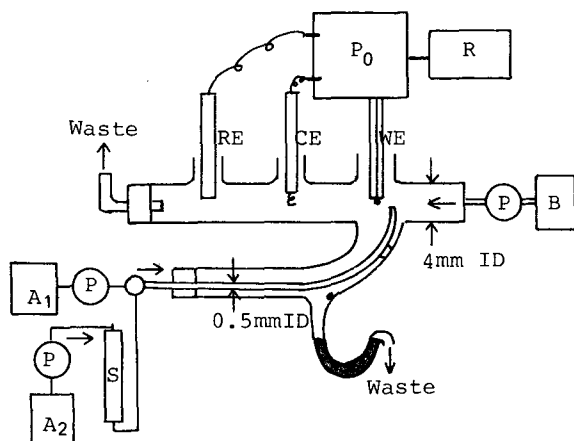
Fig. 1. Flow-through cell and HPLC–DPP system. A_1, $B = NH_3-NH_4Cl-CH_3OH-Co^{2+}$ solution; A_2 = $NH_3-NH_4Cl-CH_3OH$ solution; Po = polarograph; S = separation column; P = pump; RE = reference electrode; CE = counter electrode; WE = working electrode.

through this thin tubing and when it flowed out of the outlet (1 ml/min) it immediately diffused to the surface of the mercury drop and an electrode reaction occurred. The sample solution was carried away from the DME and removed from the cell by the carrier solution (2.5 ml/min) which was flowing in through the wide glass tubing which came from another inlet of the cell. Accumulated mercury supports the liquid line, which ensures the flow of carrier solution through the electrodes.

Because the outlet of thin tubing was very close to the electrode drop and because the inside diameter of the tubing was very small, the electrode reaction in fact occurred in a very small effective determination volume (*ca.* 3 μl). The volume could be hypothetically calculated using three values, the maximum radius of drop (0.33 mm), the distance between the drop and the tubing outlet (2.0 mm) and the radius of the tubing outlet (0.25 mm). In addition, as the glass tubing had an I.D. of 4 mm, turbulence did not occur.

Because the sample solution flows out upwards to the DME, there was a larger surface area for receiving diffusing sample ions than in the previous design, which received sample ions diffused from only one side. The structure was beneficial for enhancing the intensity of current detected.

This flow cel could be easily made in the laboratory and is believed to be applicable to other electrodes such as the hanging mercury drop electrode or the mercury membrane- covered platinum electrode. Moreover, the flow cell could be easily connected to the HPLC column.

HPLC–DPP procedure

Mobile phase solution (solution A_2) (1.0 ml/min), carrier solution (solution B) (2.5 ml/min) and Co^{2+} mixing solution (solution A_1) (0.5 ml/min) are pumped into the flow-through cell to obtain a stable baseline, then the sample solution is injected into the mobile phase. After separation, the compounds immediately diffuse to the surface of DME and the Brdička current is recorded. Waste solution and mercury are drained
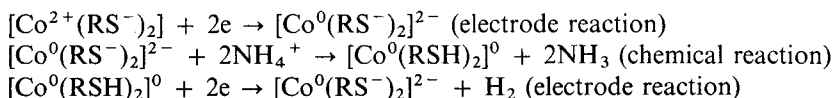
from the other two outlets of the cell. Because the concentrations of common components of solutions A_1, A_2 and B are identical, the electrode reaction is not affected by the heterogeneous mixing.

RESULTS AND DISCUSSION

Brdička current and Brdička reaction

The Brdička current is a catalytic hydrogen evolution current given by SH and SS groups in NH_3–NH_4Cl solution in the presence of Co^{2+}. It is characterized by double waves with a special peak form in a negative potential range and by the extreme sensitivity for the determination of SH and SS groups. The Brdička current of dithiouracil in the DPP mode is shown in Fig. 2.

The Brdička reaction can be represented as follows[8]:

$$[Co^{2+}(RS^-)_2] + 2e \rightarrow [Co^0(RS^-)_2]^{2-} \text{ (electrode reaction)}$$
$$[Co^0(RS^-)_2]^{2-} + 2NH_4^+ \rightarrow [Co^0(RSH)_2]^0 + 2NH_3 \text{ (chemical reaction)}$$
$$[Co^0(RSH)_2]^0 + 2e \rightarrow [Co^0(RS^-)_2]^{2-} + H_2 \text{ (electrode reaction)}$$

In the Brdička reaction, the second electrode reaction produces the double waves. $[Co^0(RSH)_2]^0$ acts as a catalyst and NH_4^+ provides protons. For the investigation of the Brdička reaction, we studied seven kinds of SH-containing compounds. They showed two potential ranges for producing a Brdička current, -1.20 to -1.30 V and -1.50 to -1.70 V (potentials corresponding to the top of the peaks). No compound was detected in the range -1.35 to -1.45 V. This result coincided with that for proteins containing SH groups. The detection potential of the thiols are given in Table I.

pH and concentrations of NH_4^+ and Co^{2+} ions

As discussed, the formation of active $[Co^0(RSH)_2]^0$ by the reaction between $[Co^0(RS^-)_2]^{2-}$ and NH_4^+ ions lead to the production of NH_3, which can partially escape from the solution. As a result, the reaction can proceed continuously. The Brdička reaction in fact occurs in a weakly alkaline solution and a certain concentration of NH_4^+ is required. The effect of pH an $[NH_4^+]$ on the Brdička reaction were investigated and the results are shown in Fig. 3. It can be seen that the strongest
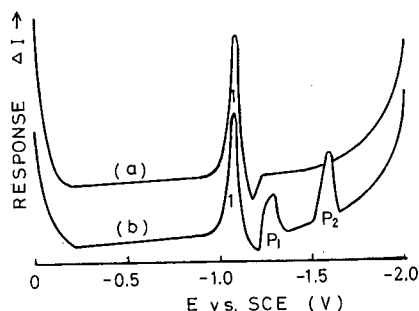

Fig. 2. Differential-pulse polarograms of dithiouracil obtained batchwise. (a) 0 M; (b) $1 \cdot 10^{-5}$ M. 1 = Reduction current of Co^{2+}; P_1, P_2 = Brdička current of dithiouracil.

TABLE I

DETECTION POTENTIALS (E_p) AND PEAK HEIGHTS (P) FOR SOME THIOLS

Thiols	E_{p1} (V vs SCE)	E_{p2} (V vs SCE)	P_1 (mm)	P_2 (mm)
Dithiouracil	-1.30	-1.60	36	121
Thionalide	-1.25	-1.50	150	88
Thiomalic acid	-1.25	-1.55	17	38
L-Cysteine	-1.30	-1.59	79	98
α-Thioglycerol	n.d.[a]	-1.70	0	84
2-Meraptoethanol	-1.20	-1.60	15	55
Glutathione	-1.25	-1.60	80	23

[a] Not detected.

Brdička current is obtained when the pH is 9.47 and [NH_4^+] is 0.265 M. The results were obtained by detecting thionalide; other thiols showed small differences in the intensity of the current at the same concentration but gave similar curves. Fig. 3 also shows the effect of Co^{2+} concentration on the intensity of the Brdička current. Similar to reports[6,8] on proteins containing SH groups, the current intensity increased with increase in the concentration of Co^{2+}. At Co^{2+} concentrations above $5 \cdot 10^{-4}$ M, the current intensity showed no noticeable increase. A Co^{2+} concentration of $5 \cdot 10^{-4}$
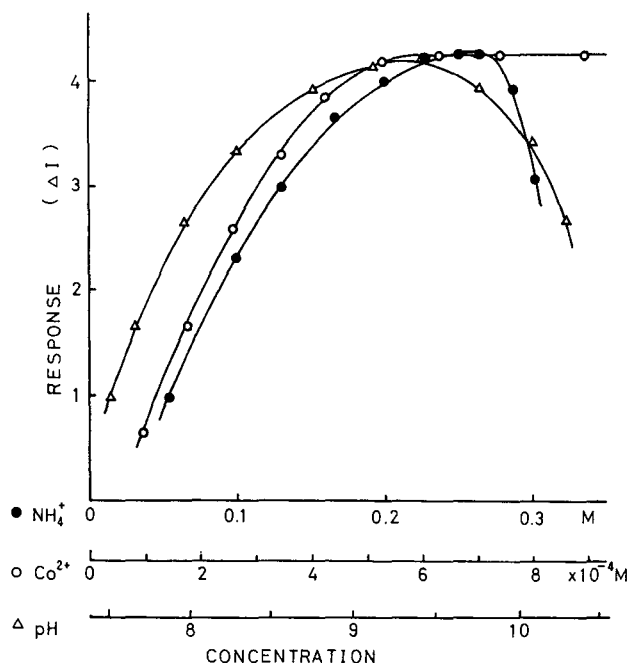
Fig. 3. Effects of (●) [NH_4^+], (○) [Co^{2+}] and (△) pH on response of thionalide. $1 \cdot 10^{-5}$ M thionalide in 20% ethanol solution.

M was therefore selected for use. As with pH and $[NH_4^+]$, the effects of $[Co^{2+}]$ for all the thiols studied are very similar.

The detection limit for thionalide was $2 \cdot 10^{-9}$ *M* under the optimum experimental conditions.

Separation of thiols

In studies of the separation of thiols by HPLC, most workers have concluded that reversed-phase columns and an acidic pH were appropriate[3,9–13]. Accordingly, we selected reversed-phase columns for thiol separation. In this case, the pH has to be considered, because a pH of 9.47 was needed for electrochemical detection.

To investigate the applicability of the HPLC–DPP analytical system, we chose several thiols with different retention times. We first used a general ODS column coupled with a UV detector, and found that even though only water was used as the mobile phase, thiols could be separated very well. Mixing of the eluent with Co^{2+} solution was carried out after separation because Co^{2+} has strong absorption properties which may lead to peak tailing. The results showed that Co^{2+} greatly affected the Brdička reaction and reliable polarograms could not be obtained. Accordingly, the electrolyte solution was used as the mobile phase.

The addition of Co^{2+} ions was carried out after separation and was found to have no effect on the Brdička reaction. Because an alkaline mobile phase was used, a general ODS column could not be used, so a Capcell SG-ODS column, which can be used over a wide pH range (2–10), was used. With this column and mobile phase, good separations were obtained. The capacity factors (k') decreased very little in comparison with those obtained with water as the mobile phase and a general ODS column.

Improvement of separation and peak shapes

Methanol and an ion-pair reagent [trichloroacetate (TCA)] were added to the mobile phase and their effects on k' and the Brdička reaction were studied. It was found that even a very small amount of methanol (0.1%) increased k' considerably, but at methanol concentrations above 0.5% k' began to decrease. The addition of methanol had no effect on the Brdička current. A concentration of 0.5% v/v) methanol was therefore selected. The ion-pairing reagent TCA had no effect on the separation or the Brdička reaction of thiols so it was not subsequently employed.

The effect of flow-rate was als investigated. In our HPLC–DPP flow system, with three flow lines the most important is the flow-rate of the mobile phase because the tubing for the HPLC system and the tubing inserted in the cell are very narrow (I.D. 0.25 and 0.5 mm). A small increase in flow-rate will therefore lead to a large increase in linear velocity, which has considerable effects both on mixing of the eluent with Co^{2+} solution and diffusion of the sample to the electrode surface. It was found that at mobile phase flow-rates above 1.2 ml/min the Brdička current decreased substantially and the peak width increased. At flow-rates below 1.0 ml/min, good diffusion of sample to the electrode could not be obtained, which led to a decrease in the intensity of the Brdička current. Hence a mobile phase flow-rate of 1.0 ml/min was selected and, to correspond with this flow-rate, 0.5 and 2.5 ml/min were selected for the Co^{2+} mixing solution and carrier solution, respectively.

A chromatogram of an aqueous solution containing thiomalic acid, L-cysteine, α-thioglycerol and 2-mercaptoethanol is shown in Fig. 4. The chromatogram shows
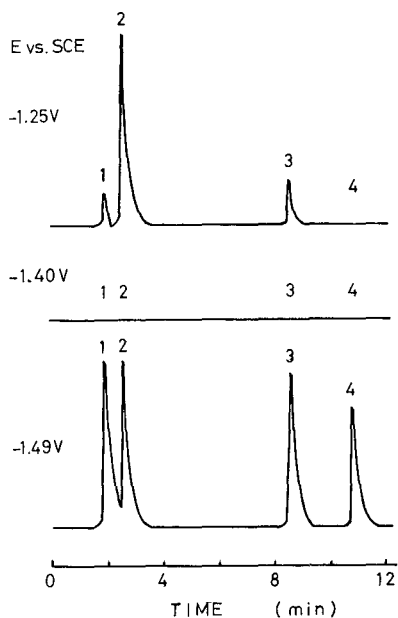
Fig. 4. Chromatograms obtained with the HPLC–DPP system with detection potentials of -1.25 V (top), -1.40 V (centre) and -1.49 V (bottom). Peaks: 1 = thiomalic acid; 2 = L-cysteine; 3 = α-thioglycerol; 4 = 2-mercaptoethanol. Concentration of each thiol, $1 \cdot 10^{-5}$ M; Sample size, 10 l. Column: Capcell SG-ODS (250 mm × 4.6 mm I.D.). Mobile phase (A_2): NH_3–NH_4Cl (0.24 M)–CH_3OH (0.5%), 1.0 ml/min. Co^{2+} mixing solution (A_1): NH_3–NH_4Cl (0.24 M)–CH_3OH (0.5%)–Co^{2+} (1.5 $\cdot$ 10^{-4} M), 0.5 ml/min. Carrier solution (B): NH_3–NH_4Cl (0.24 M)–CH_3OH (0.5%)–Co^{2+} (5 $\cdot$ 10^{-4} M), 2.5 ml/min.

a good separation of these four thiols. It is interesting that a change in detection potential leads large changes in the chromatogram. When the potential was -1.49 V, all four thiols could be detected. When -1.25 V was used, the peak height of L-cysteine did not change, but those of thiomalic acid and α-thioglycerol decreased considerably and the Brdička current of 2-mercaptoethanol could not be detected. When a detection potential of -1.40 V was used, no Brdička current for any of the thiols could be detected.

DPP can be used as a more selective method than other polarographic modes. Very small changes in the of detection potential have a large effect on the peak height and the intensity of the Brdička current. Although it is difficult to obtain the maximum Brdička current for each thiol in the sample mixture at a fixed detection potential, the latter can be adjusted to obtain the strongest Brdička current for a particular thiol.

The chromatograms shown in Fig. 5 were obtained by UV (254 nm) detection and with the HPLC–DPP system. Studies showed that glutathione has no absorption at 254 nm, but at a detection potential of -1.25 V it could be detected by the HPLC–DPP system. This means that the HPLC–DPP system can detect thiols or disulphides which have no UV absorption but give a Brdička current. Of course, at this potential (-1.25 V), mercaptoethanol could not be detected, as discussed with regard to Fig. 4. A detection potential of -1.49 V was also used, but glutathione gave a very small peak, the Brdička current intensity at -1.25 V being only one quarter of that at -1.49 V.
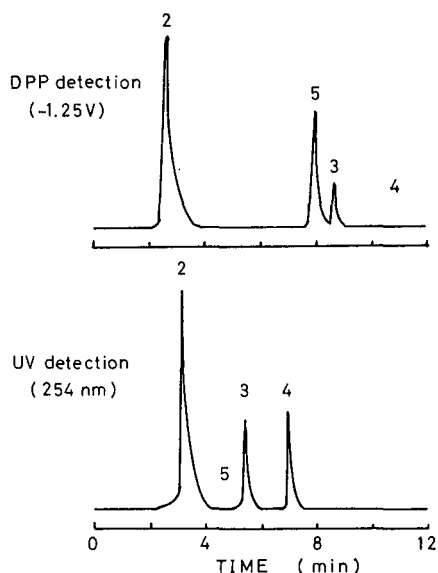
Fig. 5. Chromatograms of thiols with (top) DPP and (bottom) UV detection. Peaks: 2–4 as in Fig. 4; 5 = glutathione. Experimental conditions for DPP detection as in Fig. 4. For UV detection: column, TSK gel-120 T (250 m × 4.6 mm I.D.); mobile phase, CH_3OH (1%), 1.0 ml/min; concentration of each thiol, $1 \cdot 10^{-5}$ M; sample size, 10 μl.

CONCLUSION

In this basic investigation of the use of a Brdička current measurement cell in HPLC detection, it was clearly shown that thiols can be detected selectively, and the sensitivity is comparable to that of UV detection. Further, it was shown that the Brdička current can also differentiate thiol by selection of an appropriate applied potential. This system is expected to have wide application in biological, clinical and environmental chemistry.

REFERENCES

1 A. Przyjazny, J. Chromatogr., 292 (1984) 189–196.
2 K. Mopper and D. Delmas, Anal. Chem., 56 (1984) 2557–2560.
3 D. Perrett and S. Rudge, J. Chromatogr., 294 (1984) 380–384.
4 D. Shea, Anal. Chem., 60 (1988) 1449–1454.
5 A. Laura and R. E. Shoup, Anal. Chem., 55 (1983) 8–12.
6 P. W. Alexander and M. H. Shah, Talanta, 26 (1979) 97–102.
7 W. Kutner, J. Debowski and W. Kemula, J. Chromatogr., 191 (1980) 47–60.
8 M. Senda, T. Ikeda, K. Kano and I. Tokimitsu, Bioelectrochem. Bioenerg., 9 (1982) 253–263.
9 T. Toyooka and K. Imai, J. Chromatogr., 282 (1983) 495–500.
10 B. Debowska and K. Smochocka, J. Chromatogr., 455 (1988) 336–343.
11 M. Sogami and S. Era, J. Chromatogr., 332 (1985) 19–27.
12 G. Yamashita and D. L. Rabenstein, J. Chromatogr., 491 (1989) 341–354.
13 D. Sybilska, K. Duszczyk and M. Przasnyski, J. Chromatogr., 298 (1984) 352–355.

CHROMSYMP. 1910

Detection and identification modes for the highly sensitive and simultaneous determination of various biogenic amines by coulometric high-performance liquid chromatography

HIROSHI TAKEDA*

Department of Pharmacology, Tokyo Medical College, 6–1–1 Shinjuku, Shinjuku-ku, Tokyo 160 (Japan)

TERUHIKO MATSUMIYA

Department of Pharmacology, School of Medicine, Tokai University, Bohseidai, Isehara, Kanagawa 259–11 (Japan)

and

TAKESHI SHIBUYA

Department of Pharmacology, Tokyo Medical College, 6–1–1 Shinjuku, Shinjuku-ku, Tokyo 160 (Japan)

ABSTRACT

Detection and identification modes for the rapid, selective, highly sensitive and simultaneous determination of catecholamines, indoleamines and related metabolites by high-performance liquid chromatography (HPLC) with series of coulometric working electrodes (CWE) were investigated. Five detection modes were examined: (1) oxidative single mode using a single CWE, (2) oxidative screen mode using a series of two CWE, (3) redox mode using a series of two CWE, (4) redox–reductive screen mode using a series of three CWE and (5) redox–reductive screen mode using a series of four CWE. For the highly sensitive detection of catechol compounds, oxidative single, redox and redox–reductive screen modes were suitable. Oxidative single and oxidative screen modes were better than the other modes for indole and o-methylated catechol compounds. For the selective detection of these compounds, however, the redox–reductive screen mode was best. The specific ratio obtained in HPLC with the redox or redox–reductive screen mode is useful as an index for identification purposes. These findings suggest that HPLC with the redox–reductive screen mode of detection is applicable to neuroscience studies.

INTRODUCTION

Since high-performance liquid chromatography with electrochemical detection (HPLC–ED) for the determination of catecholamine and its metabolites was introduced by Refshauge *et al.*[1] in 1974, this assay method has become widely accepted and applied to measuring neurochemical compounds, such as monoamines[2–5] and their metabolites[3,6,7] and precursors[3,4] in biological samples.

The combination of a thin-layer single amperometric detector with reversed-

phase HPLC separation techniques is used for the analysis of neurochemical compounds, but it is not necessarily satisfactory with respect to sensitivity, selectivity and reproducibility for the measurement of neurochemical compounds by the direct injection of crude biologial samples into the HPLC–ED apparatus[8,9]. More recently, the use of HPLC with dual or multiple coulometric detectors for the simultaneous determination of catecholamines, indoleamines and their major metabolites and precursors in crude perchloric acid extracts of brain tissues and unprocessed cerebrospinal fluid was reported[10–14].

In this study, suitable detection and identification modes for the rapid, selective, highly sensitive and simultaneous determination of catecholamines (norepinephrine, epinephrine and dopamine), indoleamine (serotonin) and related metabolites (4-hydroxy-3-methoxyphenylglycol, 3,4-dihydroxyphenylacetic acid, homovanillic acid, 3-methoxytyramine and 5-hydroxyindole-3-acetic acid) by HPLC with coulometric detectors were investigated in detail.

EXPERIMENTAL

Reagents

All reagents were purchased at the highest available purity and used without further purification. 3-Hydroxytyramine hydrochloride (dopamine, DA), 5-hydroxyindole-3-acetic acid (5-HIAA), 4-hydroxy-3-methoxyphenylacetic acid (homovanillic acid, HVA), 5-hydroxytryptamine hydrochloride (serotonin, 5-HT), 3-methoxytyramine hydrochloride (3-MT), 4-hydroxy-3-methoxyphenylglycol (MHPG), epinephrine (E), norepinephrine (NE) and deoxyepinephrine hydrochloride (DEP) were purchased from Sigma. 3,4-Dihydroxyphenylacetic acid (DOPAC) and 5-hydroxy-Nω-methyltryptamine oxalate (n-MET) were obtained from Aldrich. Analytical-reagent grade chemicals for sample preparation and chromatography were obtained from Katayama Chemical and Nakarai Chemicals.

Sample preparation

Male Sprague–Dawley rats (Charles River Japan) weighing 270–300 g were killed by decapitation and the brains were rapidly removed. The brains were dissected on a dry, ice-cooled aluminium plate according to the method of Glowinski and Iversen[15]. In this study, striatum tissue samples were used. After dissection, tissue samples were immediately placed in liquid nitrogen and frozen until extraction.

Extraction was based on the procedure of Ikarashi and Maruyama[5]. Dissected tissue was weighed and was initially added to a mixture consisting of 1 ml of 0.1 M perchloric acid, 30 μl of 0.1 M ethylenediaminetetraacetic acid, 30 μl of 1 M sodium hydrogen sulphite and 200 ng each of DEP and n-MET as internal standards. The mixture was then homogenized with an ultrasonic cell disruptor (Sonifier Model 200, Branson) at 13% power output (20 W) at 0°C for 30 s and centrifuged at 20 000 g for 15 min at 0°C. The supernatant layer was filtered through a 0.45-μm Millipore filter to separate the insoluble residue. A portion of the supernatant (*ca.* 100 μl) was then carefully transferred to a small tube and further centrifuged at 20 000 g for 2 min using a Beckman Microfuge. An aliquot of the supernatant was injected into the HPLC–ED system.

HPLC–ED system

The HPLC–ED system is shown schematically in Fig. 1. The HPLC system consisted of a Model LC-6A solvent delivery system (Shimazu) equipped with an extra damper, a Model 7125 sample injector (Rheodyne) with a 100-μl sample-holding loop, in-line filter unit (0.20-μm graphite filter) (ESA) and a μBondapak C_{18} (10 μm) reversed-phase column (300 mm × 3.9 mm I.D.) (Waters Assoc.). A Model BX-7000A column heater (Ishido) maintained the analytical column at a constant temperature (23°C).

Electrochemical detection was performed with a coulometric detection system consisting of four coulometric high-efficiency flow-through cells in series: a Model 5010 analytical cell with dual coulometric working electrodes [test electrode 1, T_1 (efficiency 100%); test electrode 2, T_2 (efficiency 100%)] (ESA)[10–14]; a Model 5011 high-sensitivity analytical cell containing dual coulometric working electrodes [test electrode 3, T_3 (efficiency 100%); test electrode 4, T_4 (efficiency 70%)] (ESA)[11–14]; and a Model 5100A control module (ESA). The four coulometric working electrodes (T_1–T_4) were connected in series by installing a Model 5010 analytical cell before a Model 5011 high-sensitivity analytical cell.
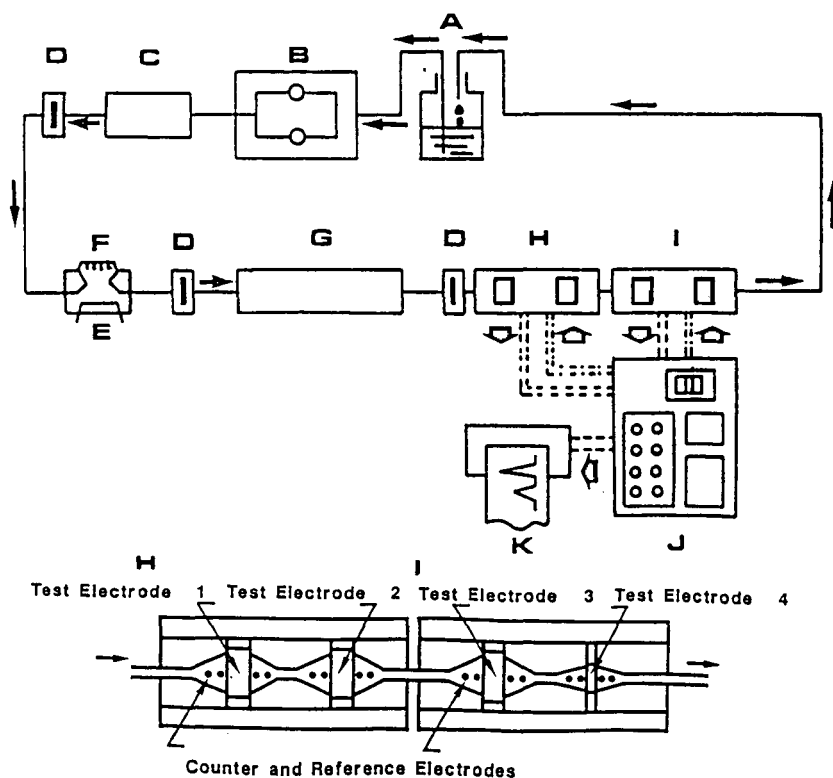
Fig. 1. HPLC–ED system for the simultaneous determination of catecholamines, indoleamines and related metabolites. A = mobile phase; B = pump; C = damper; D = in-line filter; E = injection valve; F = sampling loop; G = analytical column; H = Model 5010 analytical cell (ESA); I = Model 5011 high-sensitivity analytical cell (ESA); J = Model 5100A control module (ESA); K = recorder.

Data analysis was performed with four recorders connected to T_1, T_2, T_3 and T_4. For good separation of catecholamines, indoleamine, related metabolites and internal standards (eleven compounds), a mobile phase consisting of mixed 0.04 M phosphate–0.04 M citrate buffer (pH 3.0) containing 7.5 mM sodium 1-heptanesul-
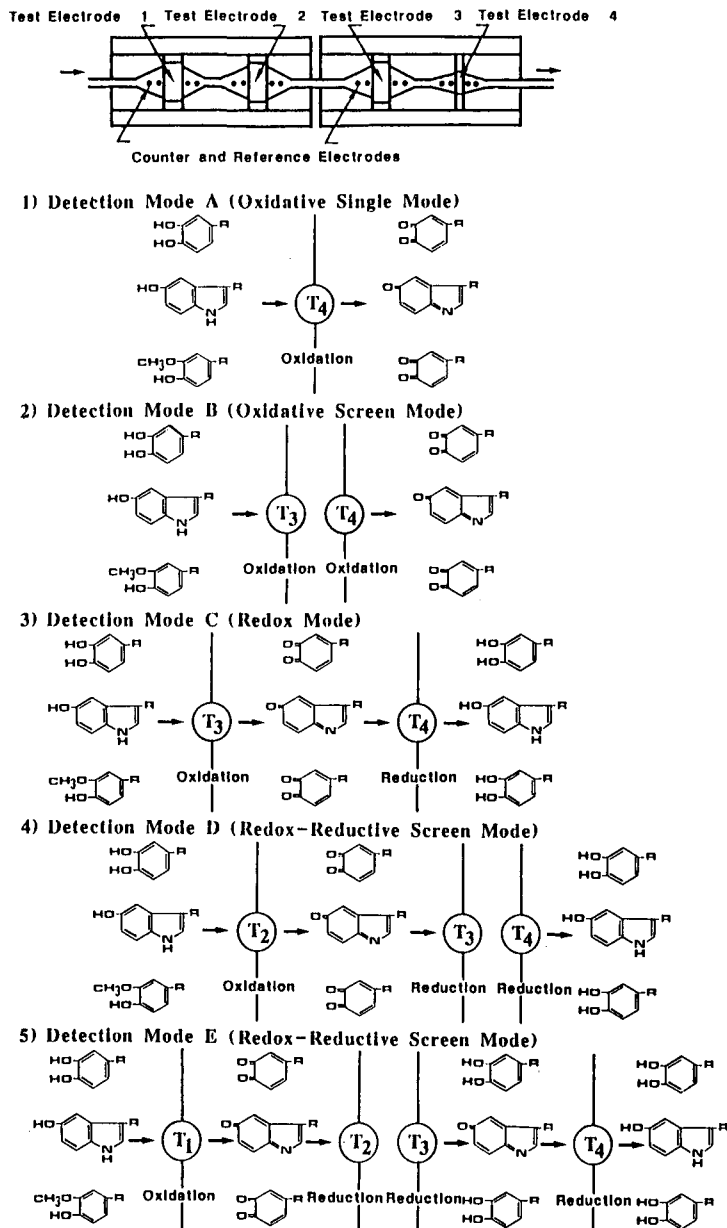
Fig. 2. Detection system and modes for the simultaneous determination of catecholamines, indoleamines and related metabolites. T_1, T_2, T_3 and T_4: test electrodes 1, 2, 3 and 4, respectively.
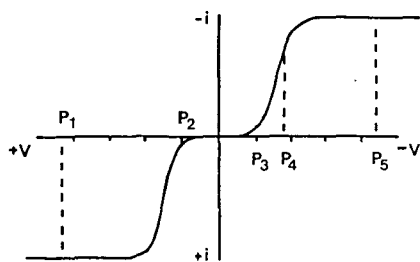
Fig. 3. Oxidation and reduction current–voltage curve. P_1, P_2, P_3, P_4 and P_5 are potentials (see text).

phonate, 0.08 mM ethylenediaminetetraacetic acid, 11.7% methanol and 4.7% acetonitrile was used. The mobile phase flow-rate was maintained at 1.0 ml/min. Mobile phase was also circulated in the HPLC–ED system and was exchanged when marked changes in the back-current occurred.

Electrochemical detection modes

The principles of the five electrochemical detection modes examined are illustrated in Fig. 2 and a schematic illustration of the oxidation and reduction current–voltage curve for determination of the applied potentials of each coulometric working electrode used in the five detection modes is shown in Fig. 3.

(1) Detection mode A (oxidative single mode using a single coulometric working electrode). The oxidative single mode was performed using only T_4. The potential of T_4 was set at P_1, corresponding to the top of the oxidation current–voltage curve for the analyte, to measure these compounds.

(2) Detection mode B (oxidation screen mode using a series of two coulometric working electrodes). T_3 and T_4 were used to perform the oxidative screen mode. The first electrode (T_3) was set at P_2, near the low end of the oxidation current–voltage curve for the analyte, to remove compounds having a lower oxidation potential than the analyte. The potential of the second electrode (T_4) was set at P_1, corresponding to the top of the curve for the measurement of the analyte.

(3) Detection mode C (redox mode using a series of two coulometric working electrodes). In the redox mode, T_3 and T_4 were used. The potential of the first electrode (T_3) was set at P_1, corresponding to the top of the oxidation current–voltage curve for the analyte, to oxidize these compounds completely. The second electrode (T_4) was set at P_5, corresponding to the top of the reduction current–voltage curve for the measurement of the analyte.

(4) Detection mode D (redox–reductive screen mode using a series of three coulometric working electrodes). The redox–reductive screen mode was performed using T_2, T_3 and T_4. The first electrode (T_2) was set at P_1, corresponding to the top of the oxidation current–voltage curve for the analyte, to oxidize these compounds completely. The second (T_3) and third electrodes (T_4) were set at different reduction potentials. The potential of T_3 was set at P_3, near the low end of the reduction current–voltage curve for the analyte, to remove compounds having a lower reduction potential than these compounds and the potential of T_4 was set at P_5, corresponding to the top of the curve for actual measurement of the analyte.

(5) Detection mode E (redox–reductive screen mode using a series of four coulometric working electrodes). The redox–reductive screen mode was performed using T_1, T_2, T_3 and T_4. The first electrode (T_1) was set at P_1, corresponding to the top of oxidation current–voltage curve for analyte, to oxidize these compounds completely

The second electrode (T_2) was set at P_3, near the low end of the reduction current–voltage curve for the analyte, to remove compounds having a lower reduction potential than these compounds. For measurement of the analyte, the third (T_3) and fourth (T_4) electrodes were set at different reduction potentials, P_4 and P_5, respectively.

Identification modes

Two identification modes were examined for the selective determination of catecholamines, indolamines and related metabolites by direct injection of crude biological samples into the HPLC–ED apparatus. The principle of the two identification modes is illustrated in Fig. 4.

Identification mode A. In this mode, identification of peaks on the chromatogram was performed on the basis of retention time.

1) Identification Mode A (Retention time)

2) Identification Mode B (Specific ratio)
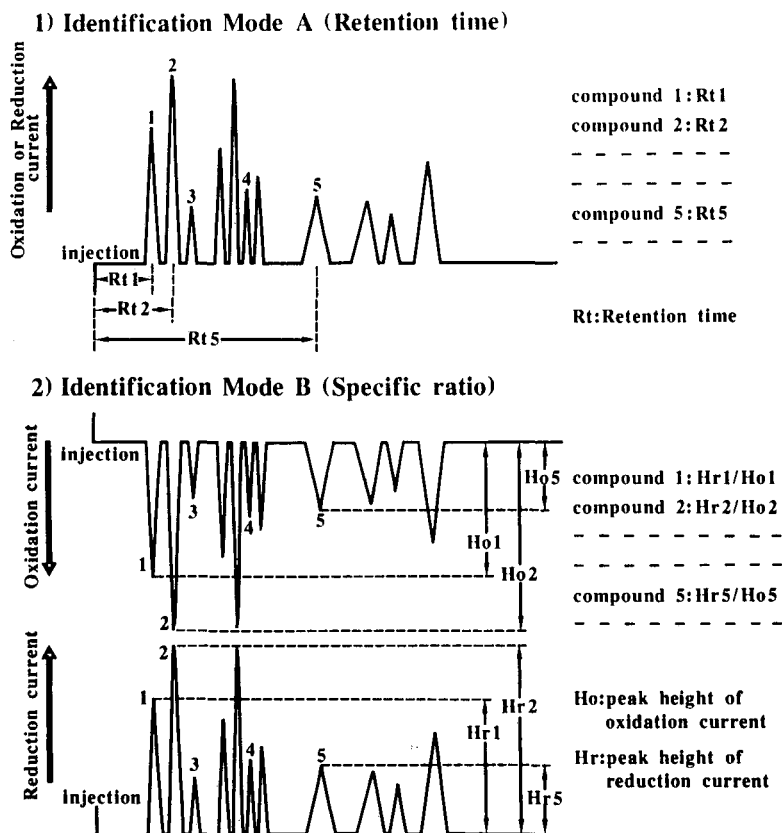
Fig. 4. Identification modes for the selective determination of catecholamines, indoleamines and related metabolites.

Identification mode B. The specific ratio of the reduction current response to the oxidation current response monitored in detection mode C or D was used for the identification of peaks on the chromatogram.

RESULTS

Applied potential

For determination of the optimum potentials for each coulometric working electrode (T_1, T_2, T_3 and T_4) in the five electrochemical detection modes, current–voltage curves for catecholamines, indoleamines and related metabolites were investigated.

Oxidation and reduction current–voltage curves for catecholamines, indoleamines and related metabolites in T_1, T_2 or T_3 (coulometric working electrodes of 100% efficiency) are shown in Figs. 5 and 6. The oxidation current responses for catechol (DA, NE, E, DOPAC, DEP), indole (5-HT, 5-HIAA, n-MET) and *o*-methylated catechol compounds (3-MT, HVA, MHPG) were over +0.00, +0.10 and +0.25 V, respectively. The maximum current responses for catechol and indole compounds were obtained in the range +0.15 to +0.40 V, followed by decreases in
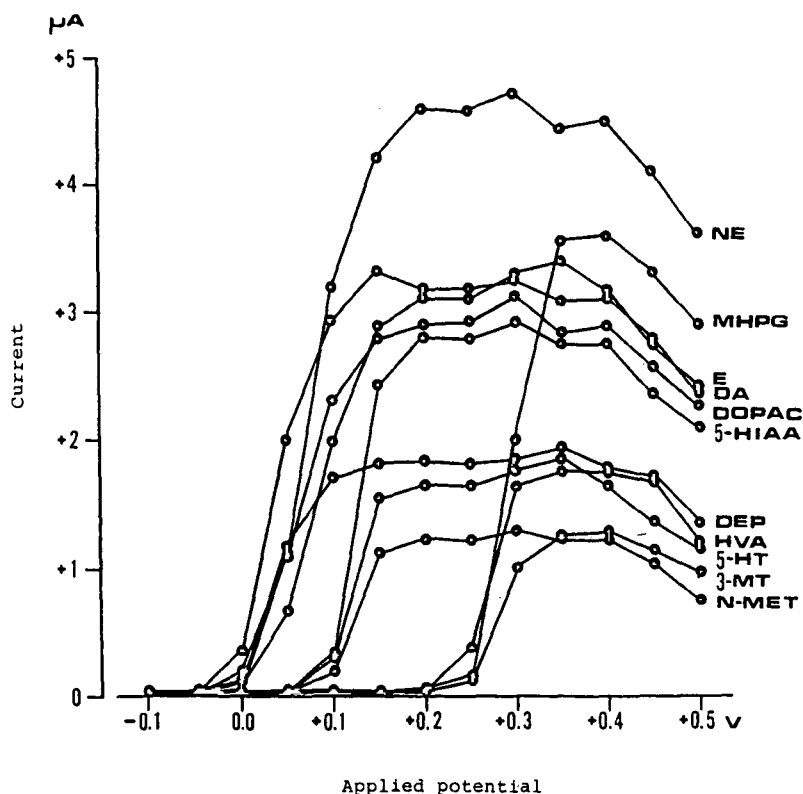
Applied potential

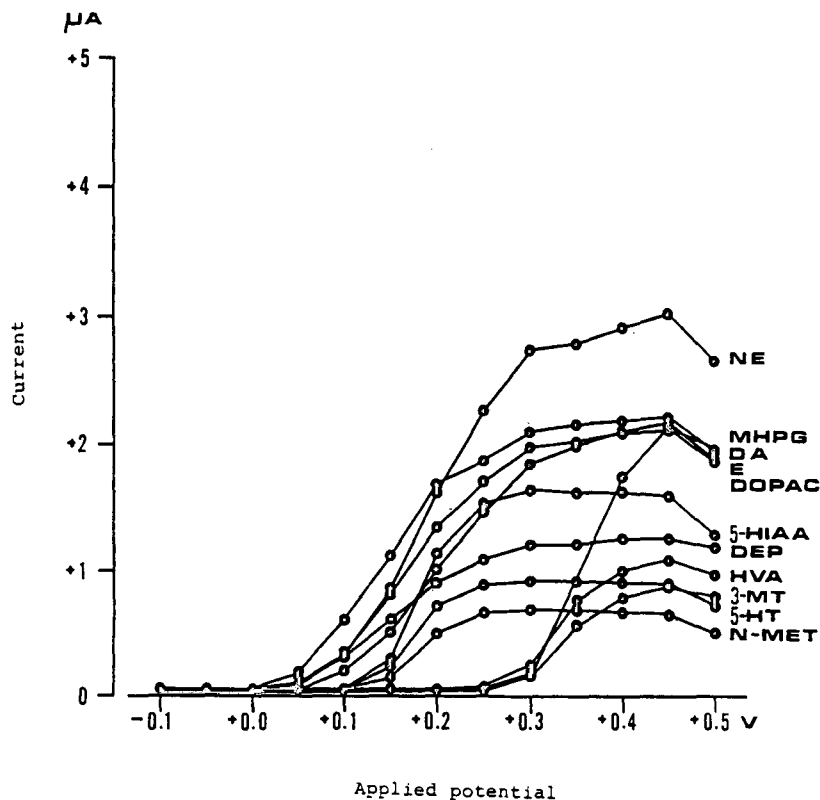Fig. 5. Relationship between applied oxidative potentials and reaction currents in coulometric working electrode of 100% efficiency.
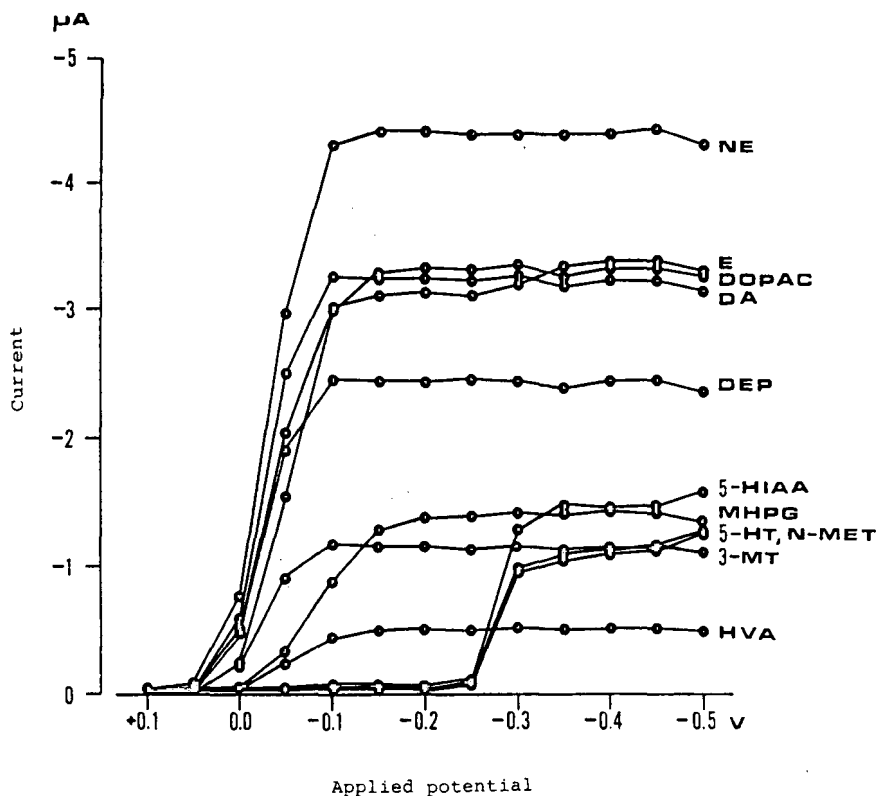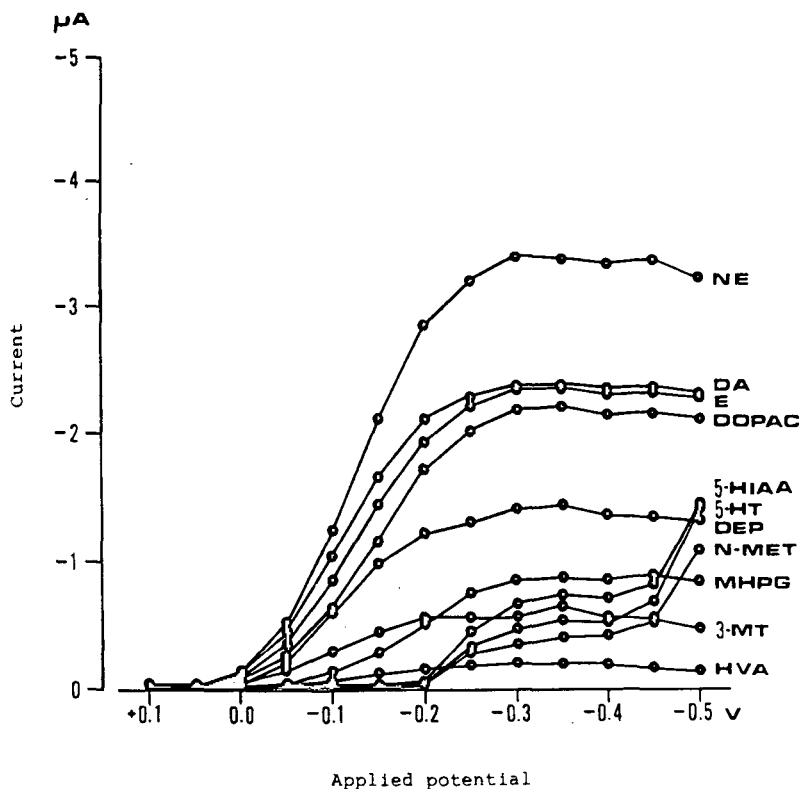
Fig. 6. Relationship between applied reductive potentials and reaction currents in coulometric working electrode of 100% efficiency.

these responses. The oxidation current responses for o-methylated catechol compounds were maximum in the range $+0.35$ to $+0.40$ V (Fig. 5).

Reduction current responses for catechol and o-methylated catechol compounds were detected below -0.00 V, and stable maximum responses were obtained in the range -0.10 to -0.45 V. Current responses for indole compounds were below -0.25 V and these responses were maximum in the range -0.30 to -0.45 V (Fig. 6).

The oxidation and reduction current–voltage curves in T_4 (coulometric working electrode of 70% efficiency) are shown in Figs. 7 and 8. Oxidation current responses for catechol, indole and o-methylated catechol compounds were detected over $+0.05$, $+0.15$ and $+0.30$ V, respectively.

Current responses for catechol and indole compounds were maximum in the ranges $+0.30$ to $+0.45$ and $+0.25$ to $+0.45$ V, respectively, followed by decreases in these responses. Maximum current responses for o-methylated catechol compounds were obtained in the range $+0.40$ to $+0.45$ V (Fig. 7). Reduction current responses for catechol and o-methylated catechol compounds were maximum in the range -0.25 to -0.50 V and those for indole compounds in the range -0.30 to -0.45 V, followed by increases in these responses (Fig. 8).

Fig. 7. Relationship between applied oxidative potentials and reaction currents in coulometric working electrode of 70% efficiency.

From these results, the optimum applied potentials for each coulometric working electrode in the five electrochemical detection modes were as follows: (1) the potential of T_4 in detection mode A was $+0.35$ V; (2) the potentials of T_3 and T_4 in detection mode B were $+0.00$ and $+0.35$ V, respectively; (3) the potentials of T_3 and T_4 in detection mode C were $+0.35$ and -0.35 V, respectively; (4) the potentials of T_2, T_3 and T_4 in detection mode D were $+0.35$, $+0.05$ and -0.35 V, respectively; and (5) the potentials of T_1, T_2, T_3 and T_4 in detection mode E were $+0.35$, $+0.05$, -0.15 and -0.35 V, respectively.

Detection modes

The characteristics of the five electrochemical detection modes examined are shown in Table I. In all detection modes, a linear and close correlation between the current responses of catecholamines, indoleamines and related metabolites and their amounts in the range 0.5–5000 pg was observed. Also, assay limits for the simultaneous determination of these compounds were in the high femtogram to low picogram range. The current responses of catechol compounds obtained in detection modes A, C, D and E were larger than in detection mode B. On the other hand, the

Fig. 8. Relationship between applied reductive potentials and reaction currents in coulometric working electrode of 70% efficiency.

current responses of indole and *o*-methylated catechol compounds in detection modes C, D and E were small compared with those in detection mode A or B.

Identification modes

The retention times of catecholamines, indoleamines and related metabolites under the HPLC–ED conditions employed were as follows: MHPG, 4.32 $\pm$ 0.16 (mean $\pm$ S.D., $n = 5$); NE, 4.94 $\pm$ 0.26; E, 5.58 $\pm$ 0.30; DOPAC, 7.56 $\pm$ 0.33; DA, 8.98 $\pm$ 0.55; DEP, 10.10 $\pm$ 0.64; 5-HIAA, 11.40 $\pm$ 0.85; HVA, 15.05 $\pm$ 0.99; 3-MT, 17.59 $\pm$ 1.14; 5-HT, 20.40 $\pm$ 1.45; and n-MET, 23.32 $\pm$ 1.42 min.

The specific ratios (all $\times$ 10^{-2}) of the reduction current response to the oxidation current response of each analyte monitored in detection mode C were 23.9 $\pm$ 2.0 MHPG) (mean $\pm$ S.D., $n = 5$), 75.8 $\pm$ 2.6 (NE), 74.2 $\pm$ 0.7 (E), 70.4 $\pm$ 0.3 (DOPAC), 73.1 $\pm$ 0.3 (DA), 73.5 $\pm$ 1.5 (DEP), 24.8 $\pm$ 0.8 (5-HIAA), 9.6 $\pm$ 0.4 (HVA), 41.9 $\pm$ 1.8 (3-MT), 29.6 $\pm$ 1.7 (5-HT) and 28.5 $\pm$ 0.4 (n-MET). In detection mode D, these ratios (all $\times$ 10^{-2}) were 49.3 $\pm$ 0.8 (MHPG), 63.8 $\pm$ 0.2 (NE), 64.3 $\pm$ 0.4 (E), 62.2 $\pm$ 0.7 (DOPAC), 67.5 $\pm$ 1.2 (DA), 66.0 $\pm$ 0.7 (DEP), 41.9 $\pm$ 0.3 (5-HIAA), 18.1 $\pm$ 0.4 (HVA), 51.4 $\pm$ 0.6 (3-MT), 38.1 $\pm$ 1.1 (5-HT) and 37.8 $\pm$ 0.9 (n-MET).

TABLE I

CHARACTERISTICS OF DETECTION MODES

Parameter	Detection mode					
	A (oxidative single mode)	B (oxidative screen mode)	C (redox mode)	D (redox–reductive screen mode)	E (redox–reductive screen mode)	
Assay limit (pg)	0.5–2.0 pg	0.5–2.5 pg	0.5–6.0 pg	0.5–5.0 pg	1.0–8.0 pg	
Linearity (γ) (0.5–5000 pg)	0.9987–0.9998	0.9992–0.9997	0.9997–0.9999	0.9994–0.9999	0.9996–0.9999	
Compound (500 pg)	Response (current, μA)					
	T_4	T_4	T_4	T_4	T_3	T_4
MHPG	0.11	0.12	−0.04	−0.06	−0.06	−0.004
NE	0.22	0.09	−0.22	−0.17	−0.14	−0.004
E	0.17	0.08	−0.17	−0.15	−0.11	−0.03
DOPAC	0.16	0.05	−0.17	−0.13	−0.12	−0.003
DA	0.15	0.01	−0.16	−0.15	−0.11	−0.003
DEP	0.12	0.01	−0.12	−0.11	−0.08	−0.004
5-HIAA	0.09	0.09	−0.04	−0.02	—	−0.02
HVA	0.07	0.07	−0.02	−0.02	−0.03	−0.001
3-MT	0.06	0.07	−0.04	−0.05	−0.04	−0.001
5-HT	0.06	0.07	−0.03	−0.04	—	−0.03
n-MET	0.06	0.06	−0.03	−0.04	—	−0.03

The values of the specific ratios were different depending on the detection mode employed, but these values were stable compared with the retention times.

Chromatograms

Excellent chromatograms of catecholamines, indoleamines and related metabolites were obtained within 25 min in all HPLC–ED systems with detection mode A, B, C, D or E. In the HPLC–ED system with detection modes other than A, the large "void volume" signal on the chromatogram which was typically observed with direct injection of perchloric acid extracts was markedly reduced. A representative chromatogram obtained by direct injection of a perchloric acid extract of rat striatum.tissue into the HPLC–ED system with detection mode D is shown in Fig. 9. The retention times for each peak on this chromatogram were as follows: 4.29 (MHPG), 4.88 (NE), 5.31 (E), 7.49 (DOPAC), 8.68 (DA), 10.02 (DEP), 11.28 (5-HIAA), 14.91 (HVA).
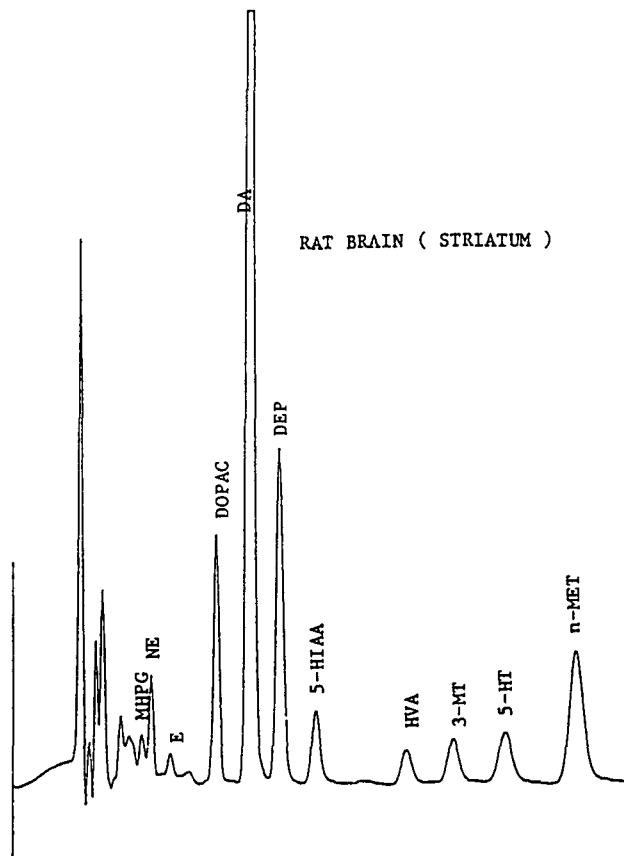
Fig. 9. Representative chromatogram obtained by direct injection of perchloric acid extract of rat striatum tissue into the HPLC–ED system with detection mode D. Mobile phase, mixed 0.04 M phosphate–0.04 M citrate buffer, (pH 3.0) containing 7.5 mM sodium 1-heptanesulphonate, 0.08 mM ethylenediaminetetraacetic acid, 11.7% methanol and 4.7% acetonitrile; flow-rate, 1.0 ml/min; column, μBondapak C_{18} (300 mm × 3.9 mm I.D.). Applied potential: test electrode 2, +0.35 V; test electrode 3, +0.05 V; test electrode 4, −0.35 V.

16.43 (3-MT), 19.87 (5-HT) and 22.82 min (n-MET). The specific ratios (all $\times 10^{-2}$) were as follows: 50.7 (MHPG), 64.5 (NE), 64.2 (E), 62.1 (DOPAC),67.3 (DA), 66.1 (DEP), 41.7 (5-HIAA), 17.9 (HVA), 50.8 (3-MT), 37.9 (5-HT) and 37.6 (n-MET). There were no significant differences between these retention times and specific ratios of the sample peaks on the chromatogram shown in Fig. 9 and those obtained with authentic standards.

DISCUSSION

Assessment of the neurochemical functions of biogenic amines requires a quantitative assay with high sensitivity, selectivity, reproducibility and reliability for the determination of these compounds and their related metabolites and precursors in a single sample. HPLC–ED has become a widely accepted technique for this purpose[1–14]. Several single amperometric electrode detection methods are currently using the quantitative HPLC of the monoamines and their metabolites and precursors in urine, blood, cerebrospinal fluid and brain. However, through experience with developing and applying these methods, certain limitations and areas for improvement have become apparent[8,9]. Major shortcomings and problems are related to detection limits in the high picogram to low nanogram range and the inability to detect the presence of co-eluting substances adequately.

Recently, a system was reported using HPLC with a series of coulometric detectors for the simultaneous determination of catecholamines, indoleamines and their major metabolites and precursors in unprocessed cerebrospinal fluid and crude perchloric acid extracts of brain tissues[10–14]. This greatly enhanced the sensitivity, selectivity and reproducibility of these analyses.

In this study, we investigated the suitable detection and identification modes for the rapid, selective, highly sensitive and simultaneous determination of catechol-amines, indoleamines and related metabolites by direct injection of crude perchloric acid extracts of brain tissues into the HPLC system with coulometric detectors. The results obtained suggest that the detection of these compounds is possible by using all the detection modes examined. In particular, for the highly sensitive detection of catechol compounds (NE, E, DA, DOPAC, DEP), the oxidative single, redox and redox–reductive screen modes are suitable. The oxidative single and oxidative screen modes are better than other modes for indole (5-HT, 5-HIAA, n-MET) and o-methylated catechol compounds (MHPG, HVA, 3-MT). For the selective and simultaneous detection of these compounds in crude perchloric acid extracts of brain tissues, however, the redox–reductive screen mode using a series of three coulometric working electrodes is the best of the five detection modes examined.

In this detection mode, the first high-efficiency coulometric working electrode is set at $+0.35$ V to oxidize most of the analyte eluting from the column. This improves the selectivity by eliminating the detection of non-reversible compounds at subsequent electrodes operated in the reductive mode. That is, all compounds that can be completely oxidized at $+0.35$ V and cannot be subsequently reduced do not appear in the analysis with the recording electrode set at -0.35 V. Second, oxidation of the column effluent greatly reduced baseline drift and virtually eliminates the large void currents routinely observed with amperometric detectors following direct injections of crude samples into an HPLC apparatus. The second coulometric working electrode is

set at $+0.05$ V to eliminate the detection at subsequent recording electrodes of reversible compounds having a lower reduction potential than the analyte. The third electrode is set at -0.35 V for actual measurement of the analyte.

The results obtained suggest that both retention time and specific ratios are suitable as indices for the identification of each peak in a chromatogram. However, the retention time changes depending on the chromatographic conditions and the specific ratio differs depending on the detection mode employed. Also, the results for specific ratios suggest that they depend on the redox property of each catecholamine, indoleamine or related metabolite. The values may therefore become an important factor, yielding information about peak composition and purity. Careful investigations should be made of the significance of these specific ratios. It is possible to identify peaks by comparing the specific ratios of sample peaks with those obtained with authentic standards.

In conclusion, HPLC with the redox–reductive screen detection mode using a series of three coulometric working electrodes is applicable to the highly sensitive, selective and simultaneous determination of catecholamines, indoleamines and related metabolites by direct injection of crude biological samples.

REFERENCES

1 C. Refshauge, P. T. Kissinger, R. Dreiling, L. Blank, R. Freeman and R. N. Adams, *Life Sci.*, 14 (1974) 311.
2 S. Sasa and C. Blank, *Anal. Chim. Acta*, 104 (1979) 29.
3 I. N. Mefford and J. D. Barchas, *J. Chromatogr.*, 181 (1980) 187.
4 J.Wagner, P. Vitali, M. G. Palhreyman, M. Zraika and S. Huot, *J. Neurochem.*, 38 (1982) 1241.
5 Y. Ikarashi and Y. Maruyama, *Biogenic Amines*, 2 (1985) 101.
6 F. Hefti, *Life Sci.*, 25 (1979) 775.
7 O. Magnusson, L.B. Nilsson and D. Westerlund, *J. Chromatogr.*, 221 (1980) 237.
8 P. J. Langlais, W. J. McEntee and E. D. Bird, *Clin. Chem.*, 26 (1980) 786.
9 P. J. Langlais, E. D. Bird and W. J. McEntee, *Ann. Neurol.*, 12 (1982) 48.
10 J. Dutrieu and Y. A. Delmotte, *Fresenius Z. Anal. Chem.*, 314 (1983) 416.
11 P. J. Langlais, E. D. Bird and W. R. Matson, *Clin. Chem.*, 30 (1984) 1046.
12 W. R. Matson, P. J. Langlais, L. Volicer, P. H. Gamache, E. D. Bird and K. A. Mark, *Clin. Chem.*, 30 (1984) 1477.
13 I. C. Kilpatrick, M. W. Jones and O. T. Phillipson, *J. Neurochem.*, 46 (1986) 1865.
14 H. Sugiyama, T. Fujita, Y. Shin, H. Takeda, K. Sakamoto and R. Ikeda, *Jpn. J. Pharmacol.*, 46 (1988) 252p.
15 J. Glowinski and L. L. Iversen, *J. Neurochem.*, 13 (1966) 655.

CHROMSYMP. 1777

Evaluation of ammonium acetate as a volatile buffer for high-performance hydrophobic-interaction chromatography

TADAO KONISHI and MASAFUMI KAMADA

Kanto Chemical Co., Inc., 3–2–8 Nihonbashi Honcho, Chuo-ku, Tokyo 103 (Japan)

and

HIROSHI NAKAMURA*

Department of Analytical Chemistry, Faculty of Pharmaceutical Sciences, University of Tokyo, 7–3–1, Hongo, Bunkyo-ku, Tokyo 113 (Japan)

ABSTRACT

Hydrophobic-interaction chromatography (HIC) is a widely used technique for the separation of proteins without denaturation. In HIC, although, ammonium sulphate or sodium sulphate buffer is generally used as an eluent, volatile buffers such as ammonium acetate and ammonium formate seem to be advantageous in order to simplify the subsequent procedures including desalting. Therefore, the applicability of ammonium acetate buffer was evaluated, as a representative of volatile buffers for HIC, with respect to effects on the retention and peak broadening of proteins. Several proteins were successfully separated under the optimized conditions using volatile ammonium acetate buffer.

INTRODUCTION

In hydrophobic-interaction chromatography (HIC), a salt gradient elution of ammonium sulphate or sodium sulphate is widely used[1–5]. However, with such non-volatile buffers, extensive desalting procedures are usually required after the separation. On the other hand, volatile buffers such as ammonium acetate and ammonium formate seem to be advantageous in order to simplify the subsequent procedures including desalting. This simplification would be especially helpful for the preparative separation and purification of proteins, which are also a practically important aspect of HIC. Hitherto, volatile buffers have often been used in reversed-phase and ion-exchange chromatography[6,7]. However, they have not been used in HIC except in one instance[8]. In a previous study[9], volatile ammonium acetate, ammonium formate and ammonium carbonate buffers were evaluated in comparison with non-volatile ammonium sulphate buffer for the separation of proteins by HIC on a macroporous polymer having butyl groups, Polyspher BUTYL. Although proteins showed weaker retention in volatile buffers than in ammonium sulphate buffer, the separation of proteins was successfully achieved with volatile buffers. In this work,

ammonium acetate buffer was chosen as a representative of volatile buffers and the influence of pH and salt concentration on the chromatographic behaviour of proteins was investigated in detail using Polyspher BUTYL.

EXPERIMENTAL

Reagents

Analytical-reagent grade ammonium acetate was obtained from Kanto Chemical (Tokyo, Japan). Water was purified with a Milli-Q system (Millipore, Bedford, MA, U.S.A.). Ovalbumin from hen egg white, myoglobin from horse skeletal muscle, haemoglobin from bovine erythrocyte and α-chymotrypsinogen A from bovine pancreas were purchased from Sigma (St. Louis, MO, U.S.A.). Bovine serum albumin (BSA), cytochrome *c* from horse heart, lysozyme from hen egg white and ribonuclease from bovine pancreas were obtained from E. Merck (Darmstadt, F.R.G.). These proteins were used without further purification, and were dissolved in 0.1 M ammonium acetate (pH 7.0) to make stock solutions (10 mg/ml).

High-performance liquid chromatographic apparatus

The gradient liquid chromatograph consisted of an L-6000 and an L-6200 intelligent pump (Hitachi, Tokyo, Japan) equipped with a high-pressure gradient programmer controlled by an internal CRT computer, a Hitachi L-4000 UV detector and a Hitachi D-2000 data processor. Generally, a 10-μl aliquot of the stock solution was injected through a Rheodyne Model 7125 sample injector with a 20-μl loop. The proteins were separated on Cica-Merck Polyspher BUTYL (10 μm) column (100 mm × 7.8 mm I.D.) (Kanto Chemical) by a 30-min linear gradient elution with a decreasing concentration of ammonium acetate (1.0–4.0 M to 0.1 M) at a flow-rate of 1.0 ml/min and were detected at 280 nm.

RESULTS AND DISCUSSION

Effect of salt concentration

The gradient elution with a decreasing concentration of ammonium acetate was performed in 30 min. The initial salt concentration was changed and the effects on retention times and peak shapes of various proteins were evaluated. The final concentration of ammonium acetate and pH were fixed at 0.1 M and 7.0, respectively, throughout this work. Fig. 1 shows the relationships between the initial concentration and the retention of proteins. Naturally, the retention became stronger with increase in the initial salt concentration. Although haemoglobin and ovalbumin showed broad peaks with higher initial concentrations, the peak shapes of α-chymotrypsinogen A and lysozyme were improved when higher initial concentrations were used.

Effect of pH

The effect of pH on the retention of proteins was examined by gradient elution from 2.0 to 0.1 M ammonium acetate. The results are summarized in Fig. 2. Generally, the retentions seemed to become stronger with increase in pH, except for the acidic proteins ovalbumin and BSA. The retention of ovalbumin (pI 4.6–5.0) and BSA (pI 4.7–4.9) was greatest at pH 5 with the broadest peaks. In contrast, haemoglobin and
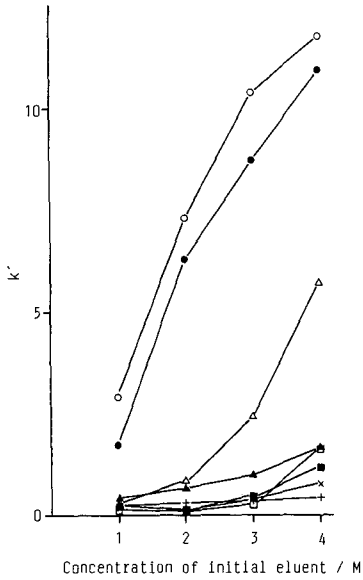
Fig. 1. Effect of concentration of initial eluent (eluent A, ammonium acetate buffer, pH 7.0) on capacity factor (k') of proteins. Eluent B, 0.1 M ammonium acetate (pH 7.0); linear gradient, from 0% to 100% eluent B in 30 min; column, Polyspher BUTYL (10 μm) (100 mm × 7.8 mm I.D.); column temperature, ambient; flow-rate, 1.0 ml/min; detection, UV (280 nm). ○ = α-Chymotrypsinogen A; ● = lysozyme; △ = haemoglobin; ▲ = ribonuclease; □ = BSA; ■ = ovalbumin; × = myoglobin; + = cytochrome c.
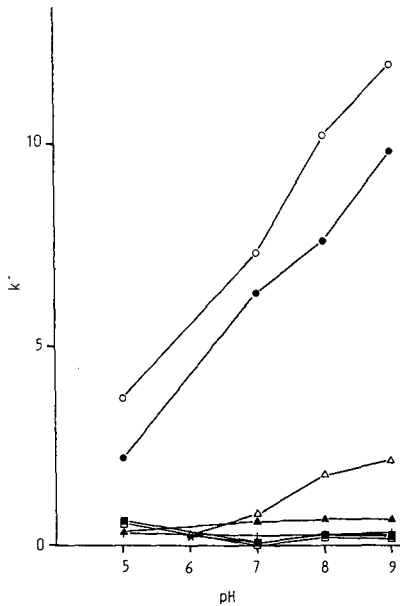
Fig. 2. Effect of pH on capacity factor (k') of proteins. Eluent A, 2.0 M ammonium acetate; eluent B, 0.1 M ammonium acetate. Other conditions and symbols as in Fig. 1.

basic proteins, α-chymotrypsinogen A (pI 9.2–9.3) and lysozyme (pI 11.0–11.4), were most strongly retained at pH 9. In HIC, it is generally considered that proteins are most strongly retained at pH values near their pI values. The results in this work showed agreement with this, though the results also suggest that the peak broadening is greatest at pH values near the pI values of proteins.

Optimization of conditions

      Based on the above results, the conditions were optimized for the HIC separation of four proteins, cytochrome c, haemoglobin, lysozyme and α-chymotrypsinogen A. The chromatogram obtained is shown in Fig. 3. The results suggest that HIC separation using volatile ammonium acetate buffer can be successfully performed if the initial concentration and pH are properly selected with respect to the pI values of the proteins to be separated. Miller *et al.*[8] evaluated the application of several buffers in HIC and size-exclusion chromatography, including ammonium sulphate and volatile ammonium acetate buffer. Unlike our results obtained on Polyspher BUTYL, they concluded that ammonium acetate buffer cannot be used as an eluent for HIC on a column with an ether-bonded stationary phase because proteins are not retained. This discrepancy in the applicability of ammonium acetate as an eluent for HIC suggests that the effectiveness of volatile buffers is limited to situations where both the stationary phase and the proteins have some hydrophobic character. In fact, the retention of proteins with lower concentrations of ammonium acetate buffer was very weak also in this work because of insufficient hydrophobicity of the proteins, although ammonium acetate was found to be usable for HIC with a high initial concentration in gradient elution. In combination with more hydrophobic stationary phases than that
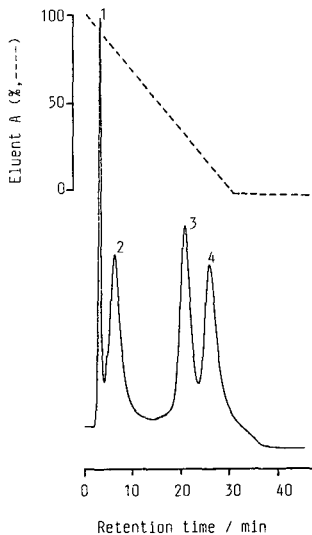
Fig. 3. Separation of proteins by HIC using ammonium acetate as the eluent. Eluent A, 2.0 M ammonium acetate (pH 8.0); eluent B, 0.1 M ammonium acetate (pH 8.0); other conditions as in Fig. 1. Peaks: 1 = cytochrome c (40 μg); 2 = haemoglobin (100 μg); 3 = lysozyme (20 μg); 4 = α-chymotrypsinogen A (40 μg).

employed here, HIC using volatile buffers should find wide applicability and become a practically useful tool for the preparative separation and purification of proteins.

REFERENCES

1 S. Hjerten, K. Yao, K. Eriksson and B. Johansson, *J. Chromatogr.*, 359 (1986) 99.
2 Y. Kato, T. Kitamura and T. Hashimoto, *J. Liq. Chromatogr.*, 9 (1986) 3209.
3 Z. E. Rassi and C. Horvath, *J. Liq. Chromatogr*, 9 (1986) 3245.
4 T. Ueda, Y. Yasui and Y. Ishida, *Chromatographia*, 24 (1987) 427.
5 P. T. Padfield and R. M. Case, *Anal. Biochem.*, 171 (1988) 294.
6 C. K. Lim and T. J. Peters, *J. Chromatogr.*, 316 (1984) 397.
7 K. Majumder, P. K. Latha and S. K. Brahmachari, *J. Chromatogr.*, 355 (1986) 328.
8 N. T. Miller, B. Feibush and B. L. Karger, *J. Chromatogr.*, 316 (1985) 519.
9 H. Nakamura, T. Konishi and M. Kamada, *Anal. Sci.*, 6 (1990) 137.

CHROMSYMP. 1926

Sample introduction and elution method for preparative supercritical fluid chromatography

YOSHIO YAMAUCHI*, MIKI KUWAJIMA and MUNEO SAITO

JASCO, Japan Spectroscopic Co., Ltd., 2967–5, Ishikawa-cho, Hachioji City, Tokyo 192 (Japan)

ABSTRACT

The loading capacity in preparative supercritical fluid chromatography with different injection and elution methods was investigated. With the ordinary valve injection method using a syringe, the maximum loading capacity onto a column (250 mm × 10 mm I.D.) packed with 5-μm silica gel was only a few milligrams. However, this value was increased by a factor of ten (a few hundred milligrams) for a column (125 mm × 10 mm I.D.) packed with 10–20 μm silica gel using a programmed extraction–elution method employing a small extraction vessel (1 ml) connected to the column and stepwise pressure gradient elution.

INTRODUCTION

The advantage of preparative supercritical fluid chromatography (SFC) is that the supercritical carbon dioxide mobile phase becomes gaseous under normal ambient conditions, permitting the easy separation of solutes simply by pressure reduction. Therefore, even though the solute concentration in the mobile phase is lower than that in LC, a low-concentration or broad peak can be fractionated efficiently without removing a solvent by evaporation as required in preparative liquid chromatography (LC).

There are two approaches to the establishment of preparative SFC. The first is to enlarge the dimensions of the column and peripheral devices in proportion to the required sample loading capacity[1-3]. The other approach is to increase the column lodading capacity by improving the sample introduction and elution method.

In SFC and LC, the maximum loading capacity for a compound is restricted by the solubility of the compound in the mobile phase. Solubilities in supercritical carbon dioxide are generally very low (*e.g.*, a few percent even for a favourable compound) compared with those in liquid solvents. Therefore, the capacity is lower in SFC than in LC as long as the conventional elution method is employed. Hence, the most crucial point is to increase the sample loading capacity by improving the sample introduction and elution method.

We have previously reported a programmed extraction–elution method which significantly increased the loading capacity by nearly 20% of the stationary phase

mass[4,5]. This paper describes a comparison of the maximum sample loading capacity by the programmed extraction–elution method with that obtained by the ordinary valve injection method.

EXPERIMENTAL

Materials
        Coffee (UCC Original Blend, Ueshima Coffee, Kobe, Japan) was purchased from a grocery store.
        Carbon dioxide (standard grade) was purchased from Toyoko Kagaku (Kanagawa, Japan) and was used as the mobile phase. A test mixture was prepared by dissolving naphthalene and anthracene (Wako, Osaka, Japan) in dichloromethane.
        The columns used were a Jasco SuperPak SIL (250 mm × 4.6 mm I.D.) packed with 5-μm silica gel, referred to as column A, a SuperMegaPak SIL column (250 mm × 10 mm I.D.) packed with 5-μm silica gel, referred to as column B, and a Super-MegaPak SIL column (125 mm × 10 mm I.D.) dry-packed with 10–20 μm silica gel, referred to as column C.

Apparatus
        A Jasco Super-200 system 3[6–8] was used. A Model 7125 injection valve (Rheodyne, Cotati, CA, U.S.A.) was used in the ordinary valve injection method. An extraction vessel was used for the programmed (stepwise pressure gradient elution) extraction-elution method as described previously[4].

RESULTS AND DISCUSSION

Ordinary valve injection method
        Before investigating the sample loading capacity on columns A and B, the optimum flow-rates were established with reference to the *H–u* curves (*H* = plate height, *u* = linear velocity) shown in Fig. 1. They were found to be 3.0 and 5.0 ml/min for columns A (4.6 mm I.D.) and B (10 mm I.D.), respectively. Preparative SFC was carried out using these optimum flow-rates.
        Fig. 2 shows the chromatograms of the test mixture containing various amounts (0.01, 0.60, 1.5, 3.0 and 6.0 mg each) of naphthalene and anthracene separated on column B. When column B was loaded with 0.30 mg of the compounds the peaks started to tail, and with more than 0.60 mg their shapes were distorted and split into two parts, exhibiting an overloaded state.
        This may be due to a partial increase in the solvating power of the dichloromethane used as a sample solvent and overloading of the stationary phase. The sample solubility in dichloromethane is higher than that in supercritical carbon dioxide. Therefore, when an excessive amount of the sample solutes dissolved in dichloromethane was injected, the solutes were introduced into the column as an oversaturated solute band in the mobile phase. Dichloromethane accompanied part of the solute as it moved in the column, but soon it moved faster than this solute band. This caused the band to be left as oversaturated in the mobile phase. The remainder was adsorbed on the stationary phase up to saturation. In this way, the solutes saturated in the stationary phase travelled immediately after the over-saturated solute band,
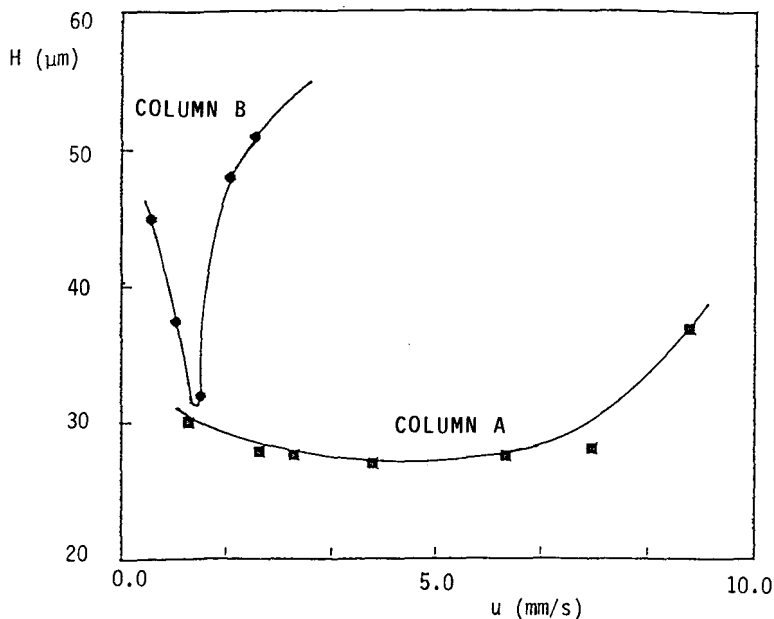
Fig. 1. *H–u* curves for columns A and B. Conditions: mobile phase, carbon dioxide; column temperature, 40°C; back-pressure, 20 MPa; detection, UV at 300 nm; Sample, anthracene.

resulting in a Gaussian peak shape adjoining a trapezoid with a logarithmic increase and an exponential decay.

The results of the programmed extraction–elution method, in which no solvent was used for dissolving the sample solutes, support the above interpretation because such peaks were not observed.

Programmed extraction–elution method (column C)

Fig. 3 shows a chromatogram of the test mixture obtained by the programmed extraction–elution method with a stepwise pressure gradient. The test mixture containing 100 mg of each of the compounds was loaded as a solid material using a 1-ml extraction vessel. Naphthalene was eluted in 30 min at 60°C and 10 MPa, whereas anthracene was retained in the column. By changing the back-pressure to 25 MPa, anthracene then started to elute. With this method, the mixture of 100 mg each of naphthalene and anthracene was separated completely.

At 10 MPa 60°C, the compounds were extracted in the vessel and flowed into the column without the aid of an organic solvent as in the ordinary valve injection method discussed above. With this method, the elution profile of naphthalene was a simple logarithmic increase and exponential decay.

However, the elution profile of anthracene was not as simple as that of naphthalene, and was wavy. This may be due to the low solubility of the compound in supercritical carbon dioxide, which caused variations in concentration resulting from the change in surface area during the extraction process.

It is remarkable that even though the column used (column C) was packed with 10–20 μm material and had only 1000 plates and the amounts of sample injected were
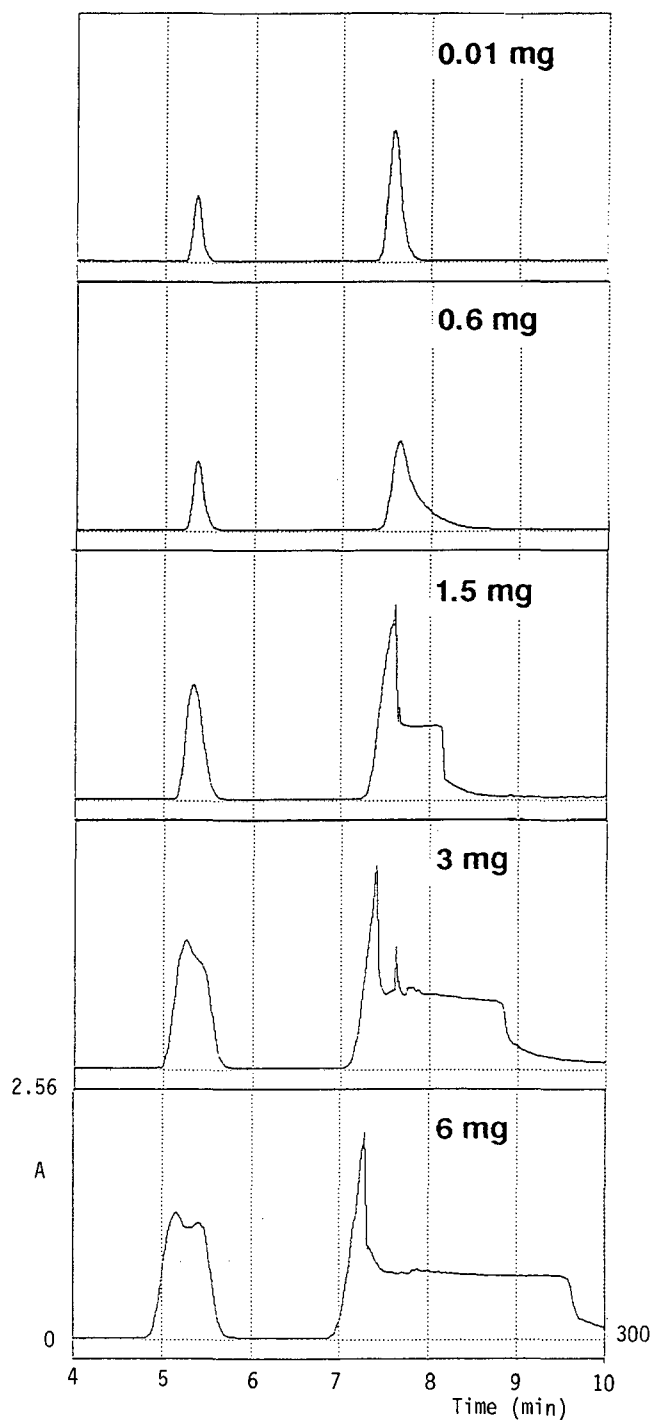
Fig. 2. Chromatograms for various sample loadings on column B. Conditions: carbon dioxide flow-rate, 5.0 ml/min (at − 5°C); column temperature, 40°C; back-pressure, 20 MPa.
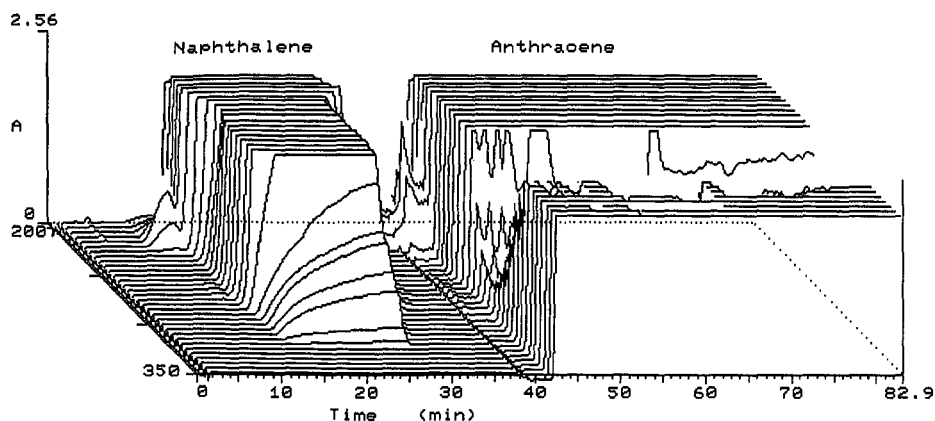
Fig. 3. Preparative chromatogram obtained with the programmed extraction–elution method using column C. Conditions: carbon dioxide flow-rate, 5.0 ml/min (at −5°C); column temperature, 60°C; back-pressure, 10 MPa for 0–30 min and 25 MPa for 30–120 min; sample, naphthalene and anthracene (100 mg of each).

about ten times higher than those in the valve injection method using a highly efficient column (column B, having 10 000 plates), the two compounds were completely separated.

Practical applications to fractionation of coffee extract

SFC fractionation of coffee powder was performed with the proposed method. A 3.50-g amount of coffee powder was loaded in the 10-ml extraction vessel and column C was used for separation and fractionation of the extract. The column outlet pressure was kept at 20 MPa for the first 40 min, then ethanol was added at a
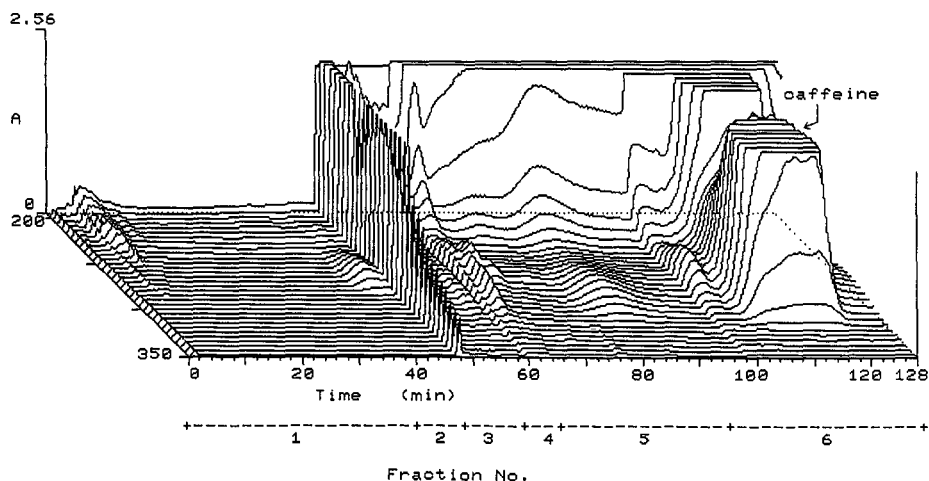
Fig. 4. Preparative chromatogram of coffee extract obtained with the programmed extraction/elution method. See text for details.
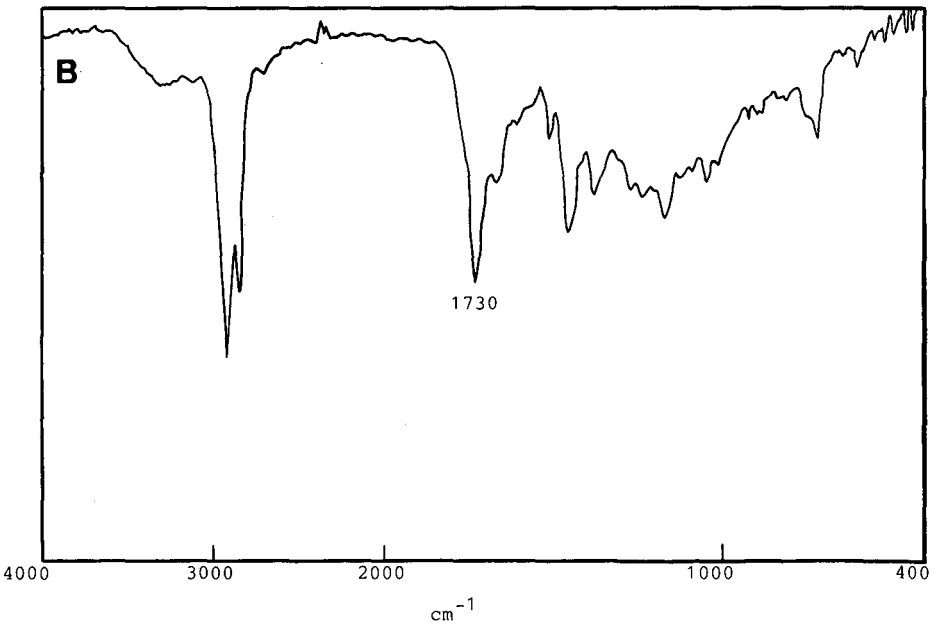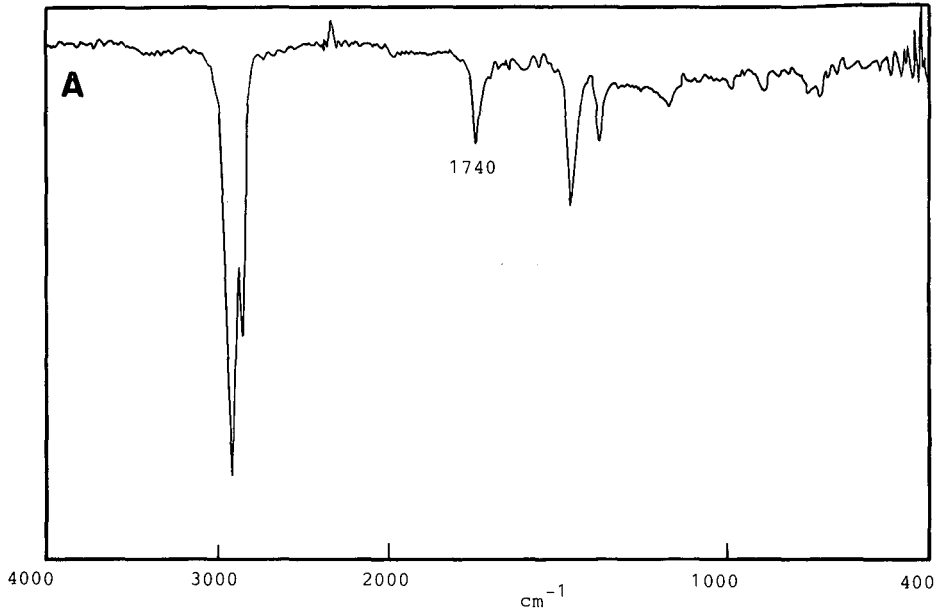
Fig. 5.
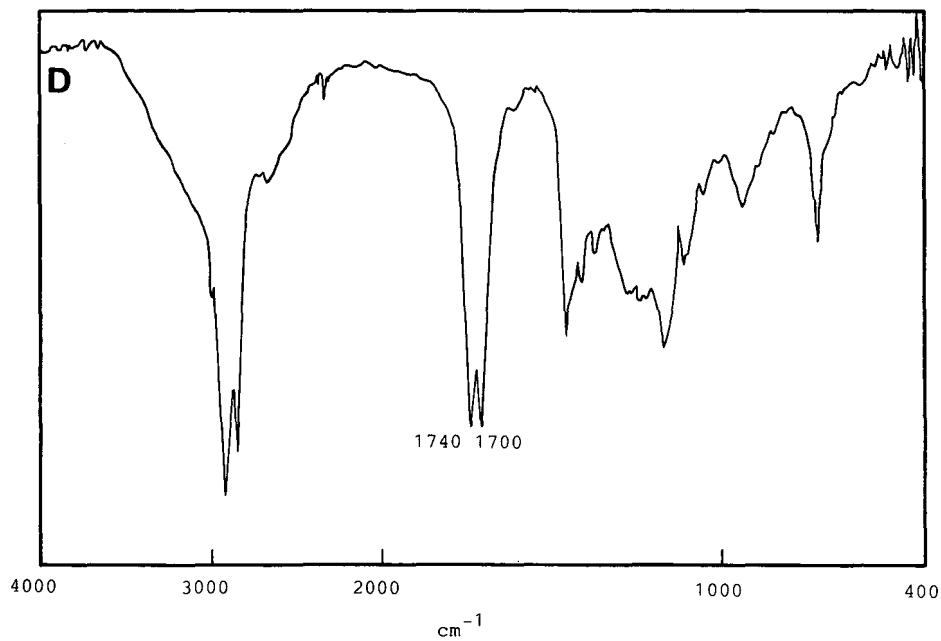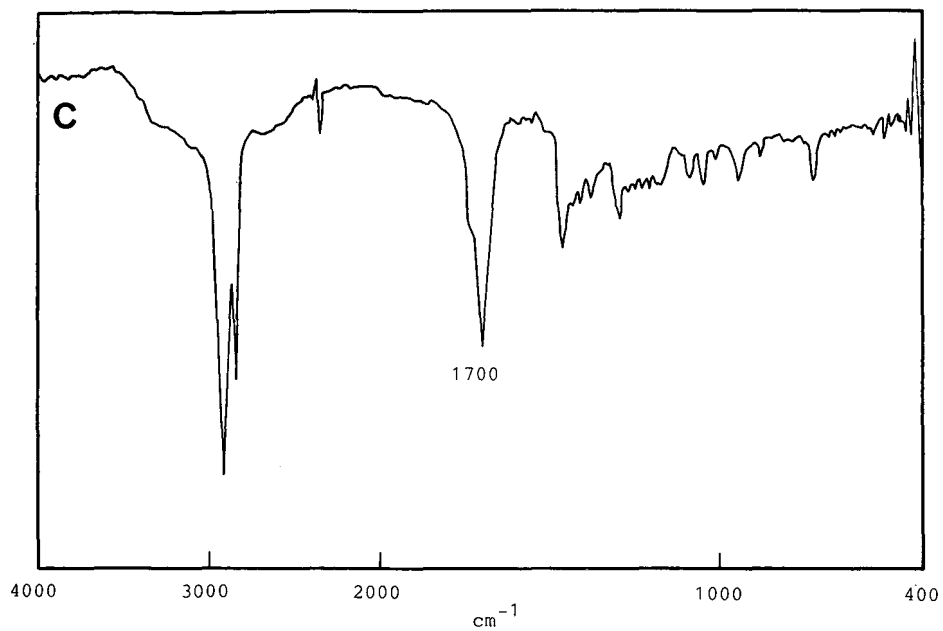
Fig. 5.
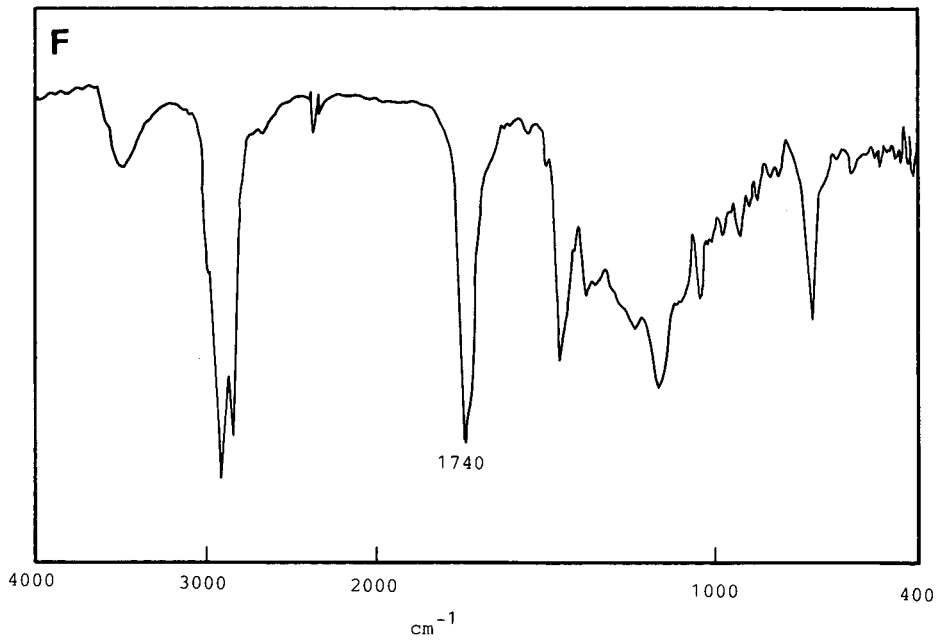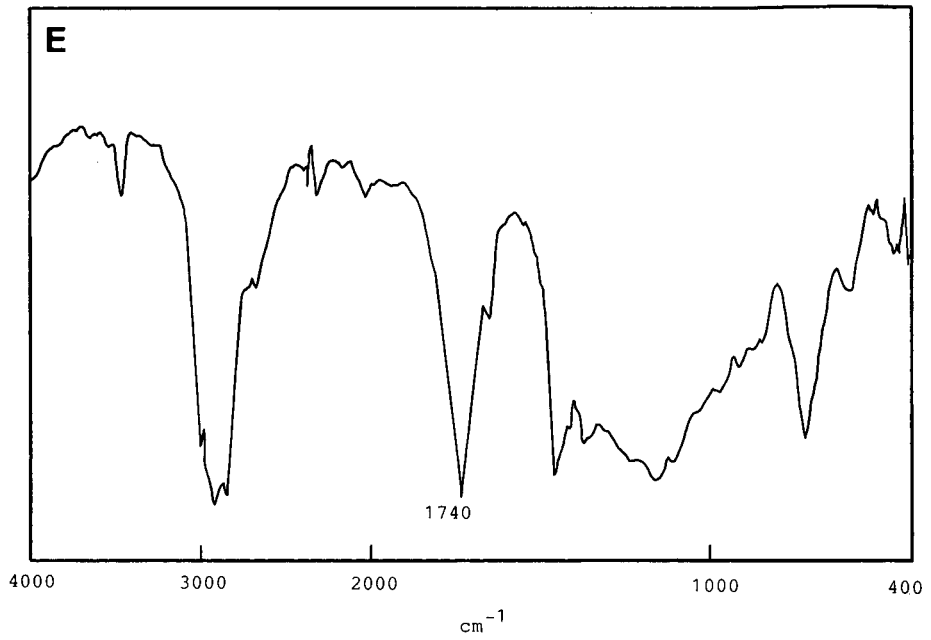
Fig. 5. IR spectra of each fraction in Fig. 4. (A) Fraction 1; (B) fraction 2; (C) fraction 3; (D) fraction 4; (E) fraction 5; (F) fraction 6.

flow-rate of 0.05 ml/min for 10 min, then increased stepwise to 0.1 ml/min, maintained at this level for 45 min, and finally increased to 0.2 ml/min for 30 min. The carbon dioxide flow-rate was kept constant at 6.0 ml/min ($-5°C$) and the column temperature was also constant at 60°C.

Fig. 4 shows the three-dimensional elution profile of the coffee extracts obtained by the above preparative SFC run. The numbers shown under the time axis are the time frames and the corresponding fractions collected with reference to real-time UV spectrum monitoring. The amount extracted was measured to be 190 mg by weighing the sample before and after the run.

Fraction 1, weighing 1.3 mg, was oil. It smelled completely off-flavour from coffee flavor. The IR spectrum shown in Fig. 5A, suggested that this fraction contained substances having long alkyl chains and keto groups.

Fraction 2 was a flavour component and was collected as an ethanolic solution. It smelled like deeply roasted coffee with a bitter taste. The IR spectrum shown in Fig. 5B suggested that this fraction contained fatty acid esters. Fraction 3 was also a flavour component smelled like coffee flavour with an acidic taste. The IR spectrum shown in Fig. 5C suggested that this fraction contained fatty acids. Fraction 4 was also a flavour component and smelled similar to fraction 3. The IR spectrum shown in Fig. 5D suggested that this fraction contained two types of substances, fatty acids and triglycerides.

Fraction 5, weighing 100 mg, was oil without a smell. The IR spectrum shown in Fig. 5E suggested that the main constituent was triglyceride. Fraction 6, weighing 72.4 mg, was also oil without a smell. The IR spectrum shown in Fig. 5F suggested that the main constituent was triglyceride containing caffeine. Caffeine was identified by SFC analysis monitored with a multi-wavelength UV detector.

CONCLUSION

The programmed extraction–elution method offers a high loading capacity in preparative SFC. In addition, even a solid sample can be applied without dissolution in a solvent. Insoluble components of the sample remain in the extraction vessel, and such components can readily be extracted and separated by LC. A delicate change in the mobile phase strength can be achieved rapidly and precisely by simply varying the density of the fluid. It is not easy to change the mobile phase strength in LC as quickly as in SFC, and LC cannot be applied to the programmed extraction–elution method.

Theoretical aspects of this method are currently under investigation.

REFERENCES

1 R. E. Jentoft and T. H. Gouw, *Anal. Chem.*, 44 (1972) 681.
2 W. Hartmann and E. Klesper, *J. Polym. Sci., Polym. Lett. Ed.*, 15 (1977) 713.
3 M. Perrut and P. Jusforgues, *Entropie*, 132 (1985) 3.
4 Y. Yamauchi and M. Saito, in M. Perrut (Editor), *Proceedings of the International Symposium on Supercritical Fluids*, Nice, 1988, p. 501.
5 Y. Yamauchi and M. Saito, *J. Chromatogr.*, 550 (1990) 237.
6 M. Saito, Y. Yamauchi, H. Kashiwazaki and M. Sugawara, *Chromatographia*, 25 (1988) 801.
7 M. Saito, Y. Yamauchi, K. Inomata and W. Kottkamp, *J. Chromatogr. Sci.*, 27 (1989) 79.
8 T. Imahashi, Y. Yamauchi and S. Saito, *Bunseki Kagaku*, 39 (1990) 79.

CHROMSYMP. 1769

Enrichment of eicosapentaenoic acid and docosahexaenoic acid esters from esterified fish oil by programmed extraction–elution with supercritical carbon dioxide

SAKAE HIGASHIDATE*, YOSHIO YAMAUCHI and MUNEO SAITO

JASCO, Japan Spectroscopic Co., Ltd., 2967–5 Ishikawa-cho, Hachioji City, Tokyo 192 (Japan)

ABSTRACT

Methyl esters of eicosapentaenoic acid (EPA) and docosahexaenoic acid (DHA) in esterified fish oil were extracted by supercritical fluid extraction with carbon dioxide and directly introduced into a silica gel column coated with silver nitrate. Supercritical fluid chromatography with carbon dioxide was then performed by changing stepwise the pressure of the column outlet. The EPA and DHA methyl esters thus separated were fractionated by reducing the pressure of column effluent to atmospheric. In this way, EPA and DHA methyl esters were enriched from 12% to 93% and from 13% to 82%, respectively.

INTRODUCTION

Recent studies have revealed that polyunsaturated fatty acids can prevent diseases such as arteriosclerosis and myocardial infarction by lowering the concentration of lipids and cholesterol in blood. This stimulated considerable interest in the enrichment of these fatty acids, especially, eicosapentaenoic acid (EPA) and docosahexaenoic acid (DHA). It is known that fish oil is a rich source of such fatty acids. These polyunsaturated fatty acids exist in the form of triglycerides.

A number of methods have been developed to isolate EPA and DHA from esterified fish oil, including molecular distillation[1], liquid chromatography (LC)[2–5], supercritical fluid extraction (SFE) with carbon dioxide[6,7] and supercritical fluid chromatography (SFC) with carbon dioxide[8]. SFE with carbon dioxide permits operation at moderate temperatures and treatment of samples without exposure to oxygen; this advantage prevents compounds with many $C = C$ double bonds from being oxidized by oxygen and from being degraded by heat. Further, SFE allows fractionation by simply reducing the pressure of carbon dioxide to atmospheric; this results in precipitation of solutes because of a significant decrease in their solubility. However, a simple SFE system does not have sufficient selectivity to obtain highly purified EPA and DHA. Therefore, SFE in combination with other techniques was examined previously, *e.g.*, SFE–reflux column[6,9] and SFE–urea adduction[10].

In LC, it is known that a silica gel column coated with silver nitrate is very suitable for separation of alkenes with *cis* configurations from *n*-alkanes, because *cis*-alkenes form silver chelates that are adsorbed on the stationary phase more strongly than *n*-alkanes. The use of this technique for the concentration of esters of EPA and DHA has been reported[11,12]. If the compounds behave in the same way in supercritical carbon dioxide mobile phase, then SFC using a silver nitrate-coated silica gel column can enrich EPA and DHA esters efficiently. Such a separation system will have the advantages of both SFE and LC.

EXPERIMENTAL

Materials

Fish oil was derived from sardines (Hokkaido, Japan). Hydrogen chloride–methanol solution (Reagent 10) was obtained from Tokyo Kasei (Tokyo, Japan) and silver nitrate from Wako (Osaka, Japan). Silica gel (10–20 μm, 90 Å) was purchased from Nomura Kagaku (Aichi, Japan). Standard-grade carbon dioxide was obtained from Toyoko Kagaku (Kanagawa, Japan) and was used as the extraction medium and mobile phase. The fish oil was esterified with the hydrogen chloride–methanol solution in the usual way[13].

The separation column was prepared as follows. A 1-g amount of silver nitrate
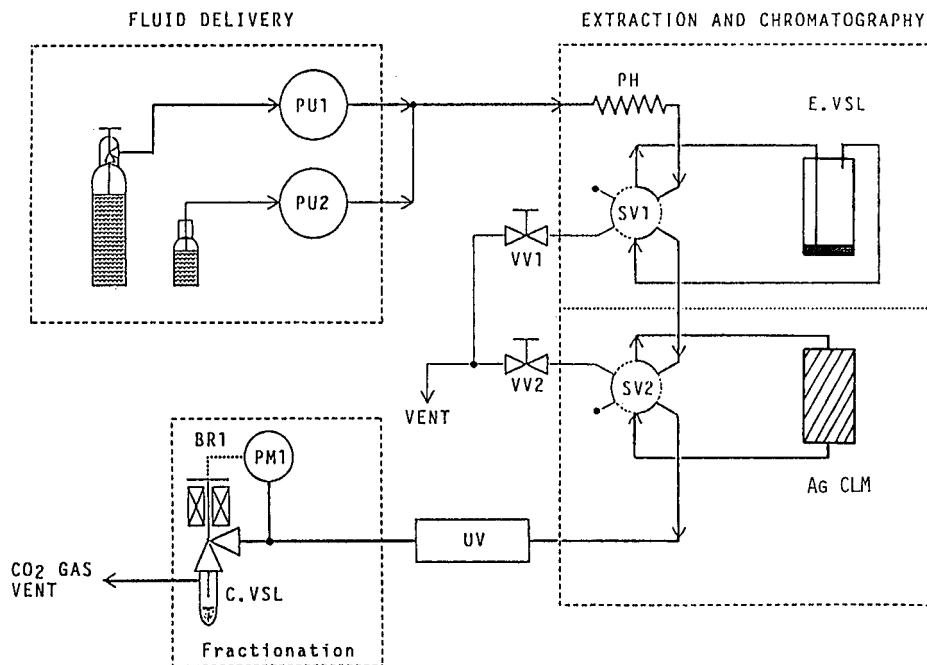
Fig. 1. Schematic diagram of the system. Components: PU1 = CO_2 pump; PU2 = modifier pump; PH = preheating coil; SV1 and SV2 = six-way switching valves; E.VSL = extraction vessel; Ag CLM = separation column; UV = photodiode-array UV detector; PM1 = pressure transducer; BR1 = back-pressure regulator; C.VSL = collection vessel.

dissolved in 50 ml of acetonitrile was added to 10 g of silica gel and the mixture was evaporated to dryness at 40°C. A 6-g amount of the residue obtained was packed into a stainless-steel tube (125 mm × 10 mm I.D.).

Apparatus

A Jasco (Tokyo, Japan) Super-200 System 3 (Fig. 1) was used. It consisted of three sections: fluid delivery, extraction and chromatography, and fractionation. The fluid-delivery section included two pumps, which delivered liquid carbon dioxide and a modifier solvent separately. In the extraction and chromatography section, programmed extraction–elution was performed with supercritical carbon dioxide modified with ethanol. The column effluent was monitored with a Jasco Multi-330 photodiode-array multi-wavelength UV detector. The fractionation section included a back-pressure regulator, which kept the pressure of the extraction vessel and the column at a desired value[14]. The column effluent flowing through the regulator reduced its pressure to atmospheric and thereby the solubility of the solutes in the effluent was reduced virtually to zero. In this way, the solutes were deposited and collected in the collection vessel.

An HP 5890A capillary gas chromatograph (Hewlett-Packard, Avondale, PA, U.S.A) was used for the determination of the EPA and DHA methyl ester contents in each step. Each fraction was dissolved in *n*-hexane or dichloromethane at a concentration of 10 or 20 mg/ml and a 1-μl portion was injected into the column.

SFE and SFC

A 0.5-ml volume (445 mg) of the esterified fish oil was placed in the extraction vessel (E.VSL), which was then connected to the separation column (SEP.CLM) by a switching valve (SV1) and SFE was performed for 20 min at 8 MPa and 40°C. The flow-rate of liquid carbon dioxide was 9 g/min. Thus, the extract from the fish oil was directly introduced into the separation column.

When the extraction was completed, the extraction vessel was bypassed by the switching valve (SV1), then SFC was performed by a programmed extraction–elution method. The pressure of the back-pressure regulator (BR1) was changed stepwise to 8, 12 and 20 MPa and ethanol was delivered as a modifier[15,16]. In this way, the column effluent was fractionated into five portions: fraction 1 (8 MPa, 0–110 min), fraction 2 (8 MPa, 110–180 min), fraction 3 (12 MPa, 180–250 min), fraction 4 (20 MPa, 250–310 min) and fraction 5 (20 MPa, 310–370 min). In the last fractionation, the flow-rate of liquid carbon dioxide was changed from 9 to 5 g/min and at the same time the modifier was added to the carbon dioxide at a flow-rate of 0.1 ml/min.

RESULTS AND DISCUSSION

The extraction vessel was used in order to introduce only constituents of the esterified fish oil that are soluble in supercritical carbon dioxide into the separation column. This was successful in the fractionation of EPA and DHA methyl esters. However, direct injection of the esterified fish oil was unsuccesful in this fractionation, because constituents of the esterified fish oil insoluble in supercritical carbon dioxide precipitated and covered the stationary phase, resulting in a decrease in the selectivity of the column.
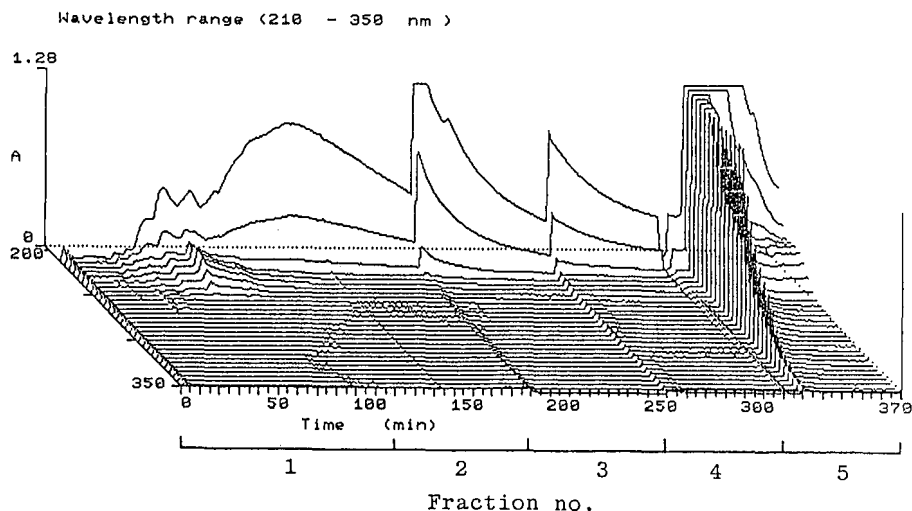
Fig. 2. Three-dimensional chromatogram obtained from SFC of esterified fish oil. The numbers under the time axis correspond to fraction numbers.

A three-dimensional chromatogram obtained from SFC of the esterified fish oil is shown in Fig. 2. Fractionation was achieved by means of real-time monitoring of the column effluent.

The gas–liquid chromatogram of the esterified fish oil is shown in Fig. 3. Peaks of fatty acid methyl esters from C_{14} to C_{22} appear. The peak areas of EPA and DHA methyl esters relative to those of all the other peaks except the solvent peak were 12% and 13%, respectively.

Each fraction obtained was of oil. The gas–liquid chromatograms of fractions 1–5 are shown in Figs. 4–8. Each chromatogram indicates the EPA and DHA methyl ester contents of the corresponding fraction. Fraction 1 (8MPa, 0–110 min) included mainly C_{16} and C_{18} fatty acid methyl esters. However, EPA and DHA methyl esters were not detected by gas–liquid chromatographic (GLC) analysis. Fraction 2 (8MPa, 110–180 min) included 57% of EPA methyl ester and 39% of other fatty acid methyl esters from C_{16} to C_{18}. Fraction 3 (12 MPa, 180–250 min) included 93% of EPA methyl ester. However, DHA methyl ester was not detected by GLC. Fraction 4 (20 MPa, 250–310 min) included 46% of EPA methyl ester and 18% of DHA methyl ester. Fraction 5 (20 MPa, 310–370 min), which was obtained with addition of the modifier (ethanol), included 82% of DHA methyl ester. However, EPA methyl ester was not detected by GLC. Because the solvent power of supercritical carbon dioxide increases with increase in its pressure or with addition of a modifier, these GLC results indicate that adsorption of fatty acid methyl esters on the stationary phase increases with increase in the number of C=C double bonds.

The amount of each fraction, the EPA and DHA methyl ester contents of the fraction and the recoveries of these esters are given in Table I. SFE of 0.5 ml (445 mg) of the esterified fish oil yielded 352 mg of oil. The contents of both EPA and DHA
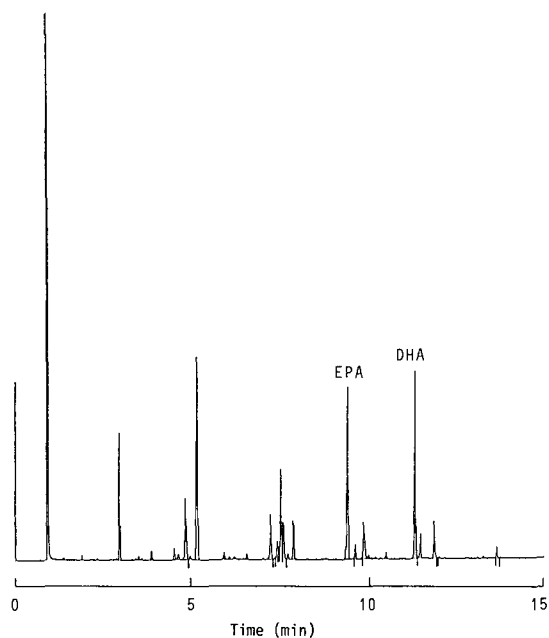
Fig. 3. GLC of esterified fish oil. Conditions: column, HP-1 (cross-linked methylsilicone, 20 m × 0.2 mm I.D.; Hewlett-Packard); detector, flame ionization; column temperature, initial 200°C, held for 5 min, increased at 10°C/min to 300°C; injection volume, 1 μl (splitting ratio = 1:100); injection temperature, 300°C; carrier gas, helium at 180 kPa.
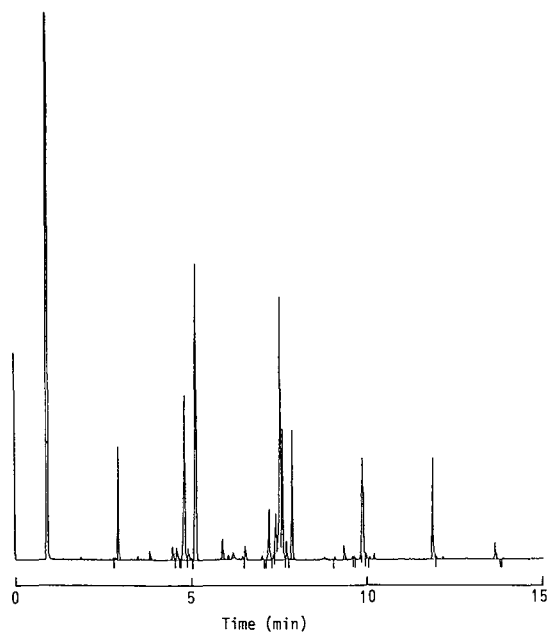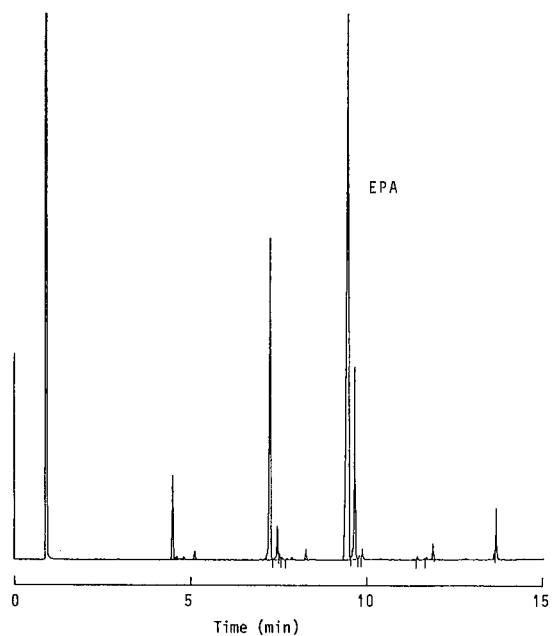

Fig. 4. GLC of fraction 1. Conditions as in Fig. 3.
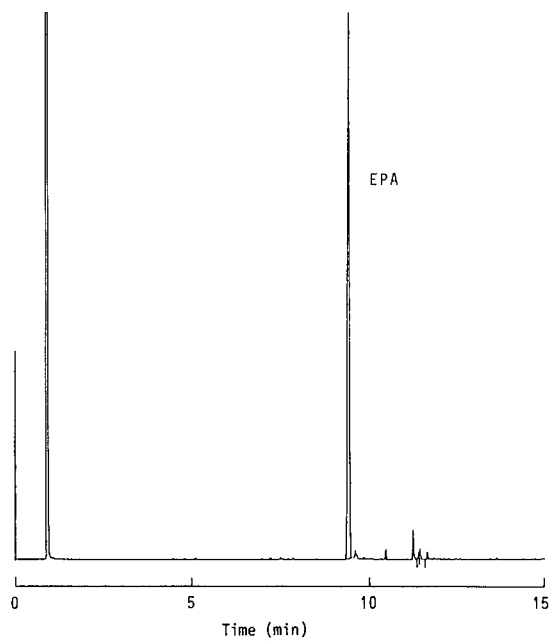
Fig. 5. GLC of fraction 2. Conditions as in Fig. 3.

Fig. 6. GLC of fraction 3. Conditions as in Fig. 3.
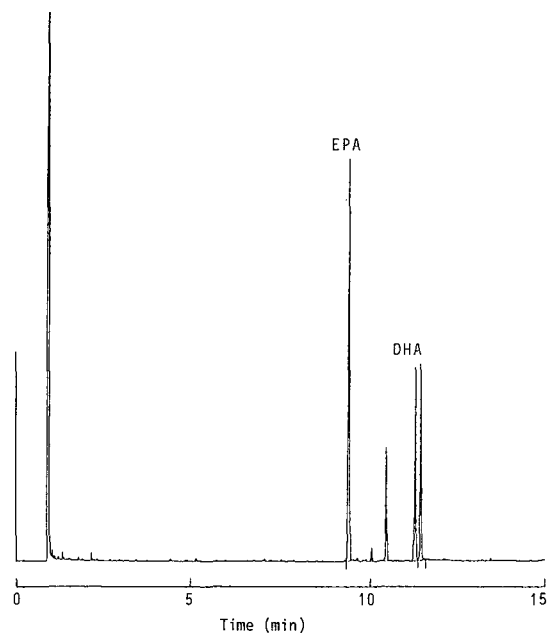
Fig. 7. GLC of fraction 4. Conditions as in Fig. 3.
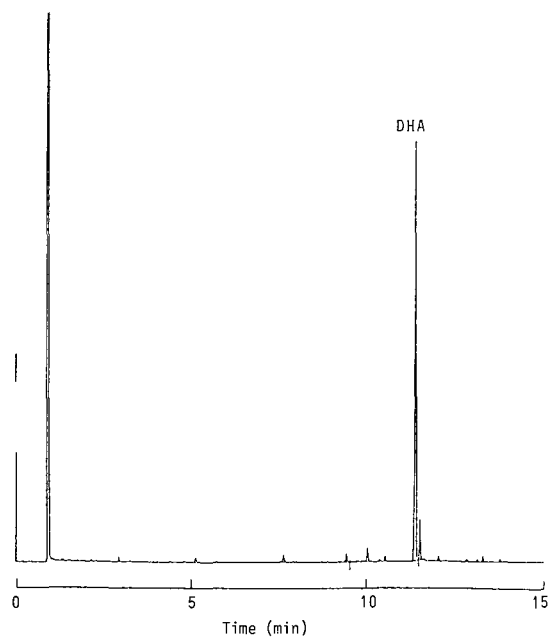
Fig. 8. GLC of fraction 5. Conditions as in Fig. 3.

TABLE I

EPA AND DHA METHYL ESTER CONTENTS IN EACH STEP AND THEIR RECOVERIES

Starting material or fraction	EPA content (recovery, %[a])	DHA content (recovery, %[a])	Amount (mg)
Fish oil	12% (53.4 mg, 100%)	13% (57.9 mg, 100%)	445
SFE fraction	13% (45.8 mg, 86%)	13% (45.8 mg, 79%)	352
SFC fraction No.:			
1	–	–	88.9
2	57% (7.5 mg, 14%)	–	13.1
3	93% (11.3 mg, 21%)	–	12.2
4	46% (1.2 mg, 2%)	18% (0.5 mg, 1%)	2.6
5	–	82% (39.2 mg, 68%)	47.8
Total	12% (20.0 mg, 37%)	24% (39.7 mg, 69%)	164.6

$$[a] \ Recovery \ (\%) = \frac{amount \ of \ EPA \ (DHA) \ ester \ in \ each \ fraction}{amount \ of \ EPA \ (DHA) \ ester \ in \ the \ esterified \ fish \ oil} \cdot 100.$$

methyl esters in this oil were shown to be 13% by GLC. With reference to the amount of EPA methyl ester included in the esterified fish oil (53.4 mg, 12% of 445 mg), the total amount of EPA methyl ester obtained by SFC (fractions 2, 3 and 4) was 20 mg; the recovery was 37%. This low recovery may be due to the EPA methyl ester being sprayed out of the regulator outlet nozzle and taken by gaseous carbon dioxide to the vent line in collection. This recovery can be increased by adding a small amount of ethanol to supercritical carbon dioxide containing EPA methyl ester just upstream of the regulator. With this arrangement the compound can be collected as an ethanolic solution. The recovery of DHA methyl ester was then calculated to be 69%.

Although the separation column was loaded with esterified fish oil weighing nearly 6% of the weight of the stationary phase, 11.3 mg of highly purified EPA methyl ester and 39.2 mg of highly purified DHA methyl ester were obtained by using a 125 mm × 10 mm I.D. column. This result indicates that the stationary phase has a good selectivity for polyunsaturated fatty acid methyl esters, and that the separation column has a high loading capacity in spite of its small dimensions.

In conclusion, the programmed extraction–elution method provided the isolation of highly purified EPA and DHA methyl esters; preconcentration of these esters with urea was not needed before SFC. In this method, solute–fluid separation was performed by simply reducing the pressure of carbon dioxide to atmospheric; fractionation in LC need to be followed by removal of the solvents used for elution, such as methanol, acetonitrile and water.

ACKNOWLEDGEMENT

REFERENCES

1 W. Stoffel and E. H. Ahrens, Jr., *J. Lipid Res.*, 1 (1960) 139.
2 J. L. Gellerman and H. Schlenk, *J. Protozool.*, 12 (1965) 178.
3 J. M. Beebe, P. R. Bown and J. G. Turcotte, presented at the *3rd Washington Symposium on Preparative Scale Liquid Chromatography, Washington, DC, May 4–5, 1987.*
4 H. J. Wille, H. Traitler and M. Kelly, *Rev. Fr. Corps Gras*, 34 (1987) 69.
5 M. Perrut, *LC·GC*, 6 (1988) 914.
6 W. Eisenbach, *Ber. Bunsenges. Phys. Chem.*, 88 (1984) 882.
7 V. J. Krukonis, presented at the *75th Annual Meeting of the American Oil Chemists' Society, Dallas, April 29–May 3, 1984.*
8 M. Perrut, C. Berger and P. Jusforgues, presented at the *2nd Symposium on Preparative and Up-Scale Chromatography, Baden-Baden, February 1–3, 1988.*
9 W. Nilson, J. K. Hudson, J. S. Stout and E. J. Gauglitz, presented at the *77th Annual Meeting of the American Oil Chemists' Society, Honolulu, HI, May 19, 1986.*
10 K. Arai and S. Saito, presented at *World Congress III of Chemical Engineering, Tokyo, 1986.*
11 O. S. Privett and E. C. Nickell, *J. Am. Oil. Chem. Soc.*, 40 (1963) 189.
12 A. Gosh, M. Hogue and J. Dutta, *J. Chromatogr.*, 69 (1972) 207.
13 W. Stoffel, H. Chu and E. H. Ahrens, *Anal. Chem.*, 31 (1990) 237.
14 M. Saito, Y. Yamauchi, H. Kashiwazaki and M. Sugawara, *Chromatographia*, 25 (9) (1988) 801.
15 M. Saito, Y. Yamauchi, K. Inomata and W. Kottkamp, *J. Chromatogr. Sci.*, 27 (1988) 741.
16 Y. Yamauchi and M. Saito, *J. Chromatogr.*, 505 (1990) 237.

Phenols as internal standards in reversed-phase high-performance liquid chromatography in pharmaceutical analysis

SHIRO YAMAUCHI* and HIDEO MORI

Analytical Development, Formulation Research Institute, Otsuka Pharmaceutical Co., Ltd., 463–10 Kagasuno, Kawauchi-cho, Tokushima 771-01 (Japan)

ABSTRACT

To find a series of compounds for use as internal standards in reversed-phase high-performance liquid chromatography, about 70 commerically available phenols were chromatographed under various conditions. The stationary phases used were hydrocarbon chemically bonded silica gels (phenyl, C_8 and C_{18} columns). The mobile phases consisted of 10–60% aqueous–organic solutions (organic solvents, methanol, acetonitrile, tetrahydrofuran and mixtures thereof; aqueous phases, water, buffer solutions of pH 2 and 7, 20 mM sodium sulphate or water containing 5 mM of counter ion). A series of 30 phenol derivatives showed a constant order of elution regardless of the separation conditions and are useful as potential internal standards.

INTRODUCTION

Reversed-phase high-performance liquid chromatography (RP-HPLC) using hydrocarbon chemically bonded silica gels has widely been used for the determination of a large number of drugs and chemicals. An internal standard technique has often been employed for the determination of drug substances and finished drug products as errors in the analytical measurements are usually reduced.

Finding a suitable internal standard, however, is empirical and often involves extensive trial-and-error experiments[1]. Moreover, an internal standard chosen for a particular set of conditions is sometimes useless under other conditions and a new one must be found again. The reason is that the retention times of target compounds vary and the profiles for their impurities or degradation products are often inconsistent. If a series of commercially available compounds that elute every few minutes with a consistent order under different separating conditions could be found, then choosing an internal standard would be facilitated because a new one could be found promptly as required among the established series.

With similar aims, systematic approaches to finding internal standards were reported by Verzele *et al.*[2] using anilides and by Kikta and Stange[3] using alkyl aryl

ketones. However, most of the anilides selected were not commercially available and the alkyl aryl ketones were not applicable to the analysis of compounds that elute with mobile phases containing less than 50% of methanol.

There have been many studies aimed at finding standard compounds for retention indices applicable to the identification of drugs, such as Smith's work on alkyl aryl ketones[4,5], Baker and Ma's work on 2-ketoalkanes[6] and Bogusz and Aderjan's work on 1-nitroalkanes[7]. These studies were successful at finding scales of retention indices, and these reference standards for retention index scaling also seem to be useful as internal standards. Wells and Clark[8-10] also reported the retention behaviours of alkylbenzamides, but most of them are not commercially available.

As retention behaviour is very dependent on chemical structure[11,12], we considered that compounds with a fixed functional group that serves as a retention time determinant should be explored. Alkyl 4-hydroxybenzoates, which are a group of phenol derivatives, are often used as internal standards in official analytical methods for pharmaceutical products[13]. Retention behaviours of phenol derivatives have been reported by Miyake et al.[11], Hanai and Hubert[14] and Callmer et al.[15], and it is well known that phenol derivatives are eluted with a wide range of mobile phases. We therefore selected them as model compounds in a search for widely applicable internal standards.

In addition, many phenol derivatives are soluble in aqueous organic solvents and have dissociation constants (pK_a) higher than 7.5. This property is of great importance as the pH of mobile phases in RP-HPLC using chemically bonded silica gel as stationary phases is usually kept within the range 2–7 (ref. 16). Phenols respond well to UV spectrophotometric detectors, which are widely used in HPLC. Other advantages of phenols are that they are commercially available in high purity and are generally inexpensive. This is an important point as the analytical methods developed by us are often used in different locations.

With the aim of finding a series of compounds as practical internal standards useful for quality control analyses, we studied the chromatographic behaviour of commercial phenols with estimated pK_a values of more than 7 (refs. 17 and 18). We report here studies that resulted in finding a series of 30 phenol derivatives that are potential internal standards in RP-HPLC.

EXPERIMENTAL

Chromatographic apparatus

Two HPLC systems were used. One consisted of a Model 510 solvent delivery system, a WISP 710A automatic sample injection system and a Model 440 fixed-wavelength UV detector (Waters Assoc., Milford, MA, U.S.A.). The detector was set at 254 and 280 nm. The other consisted of a Model M600 solvent delivery system, a WISP 710B automatic sample injection system and a Model 481 variable-wavelength UV detector operated at 254 nm (Waters Assoc.). Chromatograms were recorded on either a Chromatopak C-R3A integrator (Shimadzu, Kyoto, Japan) or a SIC 7000A integrator (System Instruments, Tokyo, Japan).

Chemicals

All phenol derivatives were obtained from Tokyo Kasei (Tokyo, Japan) or

Wako (Osaka, Japan) and used without further purification. PIC B-8 reagent for ion-pair chromatography was obtained from Waters Assoc.

Analytical columns

The commercially available prepacked columns shown in Table I were used.

Mobile phase

LC-grade methanol (MeOH; Me = CH$_3$), acetonitrile (ACN) and tetrahydrofuran (THF) were used. Water was deionized and purified with a Milli-R/Q water purifier (Millipore, Bedford, MA, U.S.A.).

The mobile phases were 10–60% aqueous organic solutions consisting of the above organic solvents or mixtures thereof and aqueous phases which were water, 10 mM KH$_2$PO$_4$ solution (pH 2), 10 mM Na$_2$HPO$_4$ solution (pH 7), 20 mM sodium sulphate solution (ionic strength 0.06) or water containing a counter ion (5 mM octylsulphonate). The 10 mM KH$_2$PO$_4$ and 10 mM Na$_2$HPO$_4$ solutions were adjusted to pH 2–7 with 85% phosphoric acid.

Sample preparation and chromatographic procedure

A 50-mg amount of each phenol derivative was weighed accurately and dissolved in methanol to make exactly 100 ml (0.05% solution). A 10-μl volume of each sample solution was injected for HPLC determination. The flow-rate was adjusted to between 0.5 and 1.0 ml/min to keep the column pressure below 2000 p.s.i. at about 25°C.

The retention behaviours were evaluated by correlations of the logarithmic plots of capacity factors under different conditions. The retention time of uracil was taken as t_0 and was used to determine the capacity factors of the phenol derivatives.

RESULTS AND DISCUSSION

The phenol derivatives listed in Table II were chromatographed under various HPLC conditions as summarized in Table III. These conditions were set up to examine the effects of the separation conditions on the chromatographic behaviours of the phenols, *e.g.*, the structure of the bonded group, the degree of unreacted silanol groups

TABLE I

ANALYTICAL COLUMNS USED

Stationary phase	Dimensions	Manufacturer
Nucleosil 5C$_{18}$ (5 μm)	15 cm × 4.6 mm I.D.	Macherey, Nagel & Co. (Düren, F.R.G.)
YMC Pack ODS-A, A-302 (5 μm)	15 cm × 4.6 mm I.D.	Yamamura Chemical (Kyoto, Japan)
μBondapak C$_{18}$ (10 μm)	30 cm × 3.9 mm I.D.	Waters Assoc. (Milford, MA, U.S.A.)
Chemcosorb 5-ODS-H (5 μm)	15 cm × 4.6 mm I.D.	Chemco Scientific (Tokyo, Japan)
Zorbax ODS (5 μm)	25 cm × 4.6 mm I.D.	DuPont (Wilmington, DE, U.S.A.)
Cosmosil 5Ph (5 μm)	15 cm × 4.6 mm I.D.	Nakarai Tesque (Kyoto, Japan)
Chemcosorb 10C$_8$ (10 μm)	15 cm × 4.6 mm I.D.	Chemco Scientific

TABLE II

PHENOL DERIVATIVES USED

The structure and name of each phenol are expressed using abbreviations of substituents: Me = CH_3-; Et = C_2H_5-; iso-Pr = $(CH_3)_2CH-$; n-Pr = $CH_3(CH_2)_2-$; sec.-Bu = $CH_3CH_2CH(CH_3)-$; n-Bu = $CH_3(CH_2)_3-$; tert.-Bu = $(CH_3)_3C-$; iso-Am = $(CH_3)_2CH(CH_2)_2-$; n-Hex = $CH_3(CH_2)_5-$; n-Hep = $CH_3(CH_2)_6-$; Oc = $CH_3(CH_2)_3CH(C_2H_5)CH_2-$; n-No = $CH_3(CH_2)_8-$; Ph = C_6H_5-.

2-OMe	3-OMe	4-OMe	2-OEt
4-On-Bu	2-OCH$_2$Ph	4-OCH$_2$Ph	4-iso-Pro
4-tert.-Bu	2,3-Me$_2$	2,4-Me$_2$	2,6-Me$_2$
2-CH$_2$Ph	4-Ph	2,3,5-Me$_3$	2-tert.-Bu-4-OMe
3-Me-6-tert.-Bu	2-Me-4-OH	2-CH$_2$OH	H
4-CH$_2$OH	2-NHCOMe	3-NHCOMe	4-NHCOMe
3-OH	3-OH-5-Me	2-OMe-4-CHO	4-Cl
4-Br	2,3-Cl$_2$	2,4-Cl$_2$	2,5-Cl$_2$
2,4-Br$_2$	2,4,6-Cl$_3$	4-Cl-2-NO$_2$	2-NO$_2$
3-NO$_2$	4-NO$_2$	2-CN	4-CN
2-COMe	3-COMe	4-COMe	4-COEt
4-COn-Bu	2-CHO	3-CHO	4-CHO
2-COOMe	2-COOEt	2-COOiso-Pr	2-COOsec.-Bu
2-COOn-Bu	2-COOPh	2-COOCH$_2$Ph	4-COOMe
4-COOEt	4-COOiso-Pr	• 4-COOn-Pr	4-COOiso-Bu
4-COOsec.-Bu	4-COOn-Bu	4-COOPh	4-COOCH$_2$Ph
4-COOiso-Am	4-COOn-Am	4-COOn-Hex	4-COOn-Hep
4-COOOc	4-COOn-No		

TABLE III

HPLC CONDITIONS EMPLOYED FOR EVALUATING THE CHROMATOGRAPHIC BEHAVIOUR OF PHENOLS: INFLUENCE OF ANALYTICAL COLUMNS AND MOBILE PHASES

Stationary phase				Mobile phase
Material	Bonded group	Carbon content (%)[a]	End-capping	
Nucleosil 5C$_{18}$	C$_{18}$	14	Treated	ACN–water (10:90, 20:80, 30:70, 40:60, 50::50, 60:40)
				MeOH–water (40:60, 50:50, 60:40)
				ACN–MeOH–water (20:20:60)
				ACN–THF–water (25:5:70)
				ACN–MeOH–THF–water (10:10:10:70)
				ACN–20 mM Na$_2$SO$_4$ (30:70)
				ACN–10 mM phosphate buffer (pH 2.5) (30:70)
				ACN–10 mM phosphate buffer (pH 7.0) (30:70)
				ACN–5 mM octylsulphonic acid (30:70)
YMC Pack ODS-A, A-302	C$_{18}$	17	Treated	ACN–water (20:80, 30:70, 40:60, 50:50)
μBondapak C$_{18}$	C$_{18}$	10	Treated	ACN–water (30:70)
Chemcosorb 5-ODS-H	C$_{18}$	20	Treated	ACN–water (30:70)
Zorbax ODS	C$_{18}$	10	Untreated	ACN–water (30:70)
Cosmosil 5Ph	C$_6$H$_5$	9	Treated	ACN–water (30:70), MeOH–water (30:70)
Chemcosorb 10C$_8$	C$_8$	9.5	Treated	ACN–water (30:70)

[a] Values taken from manufacturers' catalogues.

of the stationary phases, type and content of organic solvents in mobile phases, pH and ionic strength of the mobile phases[19] and counter ion added to the mobile phases.

The capacity factors of all the phenols decreased with increase in concentration of organic solvent in the mobile phase, and increased in order of the hydrophobicity of the bonded alkyl group ($C_{18} > C_8 >$ phenyl). These results seem to agree with general retention tendencies in RP-HPLC.

Many phenols were rejected as candidates for internal standards, as they showed undesirable peak shapes such as leading or tailing or impurity peaks of more than 1%. The phenols of which the capacity factors varied with pH, ionic strength or counter ion of the mobile phase were also rejected. In addition, phenols with deviations from the correlation line for logarithmic plots were rejected. However, three bicyclic compounds (4-hydroxybiphenyl, 4-hydroxybenzophenone and benzyl 4-hydroxybenzoate) were not rejected as the deviations from the correlation line for logarithmic plots, due to an increase in π–π interactions between the compounds and phenyl stationary phase, were only small.

Finally a series of 30 phenol derivatives were selected and are listed in Table IV. Typical elution patterns of these phenols are shown in Fig. 1 [operating conditions: column, Nucleosil $5C_{18}$ (15 cm × 4.6 mm I.D.); mobile phase, ACN–water (20:80, 30:70, 40:60, 50:50, 60:40); flow-rate, 1.0 ml/min]. These phenols elute every 2–5 min within a 20-min operating period.

We applied this series of 30 selected phenols as potential internal standards to the determination of a new antibacterial agent, OPC-7251. The operating conditions indicated in Fig. 2 were set to separate all impurities and degradation products. OPC-7251 showed a retention time of about 8 min under these conditions. It is therefore desirable that an internal standard should have a retention time of about 10–20 min. As the acetonitrile concentration in the mobile phase was 35%, we referred to the second and third columns of Fig. 1 and selected ethyl 4-hydroxybenzoate,

TABLE IV

SERIES OF 30 PHENOL DERIVATIVES SELECTED AS POTENTIAL INTERNAL STANDARDS IN RP-HPLC

Derivative	Substituent	Derivative	Substituent
4-Hydroxyacetanilide	4-NHCOMe	2,3-Dichlorophenol	2,3-Cl$_2$
3-Hydroxyacetanilide	3-NHCOMe	2,5-Dichlorophenol	2,5-Cl$_2$
2-Hydroxyacetanilide	2-NHCOMe	4-Isopropylphenol	4-iso-Pr
4-Hydroxyacetophenone	4-COMe	sec.-Butyl 4-hydroxybenzoate	4-COOsec.-Bu
3-Hydroxyacetophenone	3-COMe	4-Hydroxybiphenyl	4-Ph
Methyl 4-hydroxybenzoate	4-COOMe	n-Butyl 4-hydroxybenzoate	4-COOn-Bu
4-Hydroxypropionphenone	4-COEt	4-tert.-Butylphenol	4-tert.-Bu
3-Nitrophenol	3-NO$_2$	Benzyl 4-hydroxybenzoate	4-COOCH$_2$Ph
Ethyl 4-hydroxybenzoate	4-COOEt	Thymol	3-Me-6-iso-Pr
4-Chlorophenol	4-Cl	Isoamyl 4-hydroxybenzoate	4-COOiso-Am
4-Bromophenol	4-Br	n-Amyl 4-hydroxybenzoate	4-COOn-Am
4-Hydroxybenzophenone	4-COPh	n-Hexyl 4-hydroxybenzoate	4-COOn-Hex
Isopropyl 4-hydroxybenzoate	4-COOiso-Pr	n-Heptyl 4-hydroxybenzoate	4-COOn-Hep
n-Propyl 4-hydroxybenzoate	4-COOn-Pr	2-Ethylhexyl 4-hydroxybenzoate	4-COOOc
4-Hydroxyvalerophenone	4-COn-Bu	n-Nonyl 4-hydroxybenzoate	4-COOn-No

Mobile Phases

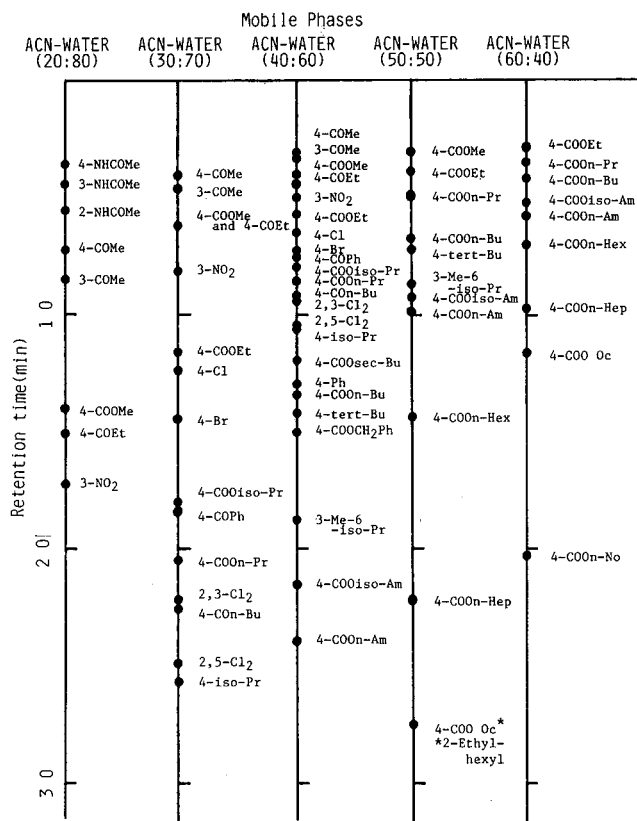| ACN–WATER (20:80)	ACN–WATER (30:70)	ACN–WATER (40:60)	ACN–WATER (50:50)	ACN–WATER (60:40)

Fig. 1. Typical elution patterns of selected phenols. Column, Nucleosil $5C_{18}$ (5 μm) (15 cm × 4.6 mm I.D.); mobile phase, ACN–water (20:80 to 60:40); flow-rate, 1.0 ml/min; t_0 was found to be 1.9 min. All phenols are expressed using abbreviations of substituents (see Tables II and IV).

4-bromophenol, 4-hydroxybenzophenone, isopropyl 4-hydroxybenzoate, n-propyl 4-hydroxybenzoate and 4-hydroxyvalerophenone as candidates for the internal standard. These compounds were chromatographed under the conditions shown in Fig. 2. 4-Bromophenol, 4-hydroxybenzophenone, n-propyl 4-hydroxybenzoate and 4-hydroxyvalerophenone were well separated from OPC-7251 and did not overlap with any related substances. 4-Bromophenol showed the shortest retention time of these four compounds and was therefore selected as the internal standard. Sample solutions were prepared so that each injection contained 0.2–1.2 μg of OPC-7251 and 4.5–5.5 μg of the internal standard in 10 μl. A calibration graph was plotted of relative peak area *versus* the amount of OPC-7251 (μg). Over this range, the calibration graph showed excellent linearity (correlation coefficient 0.99999) and the precision was 0.4% (relative standard deviation). Sample solutions were found to be stable for at least 6 days at room temperature without precautions. The relative retention of OPC-7251 with respect to the internal standard was consistent even when using three C_{18} columns supplied by different manufacturers.
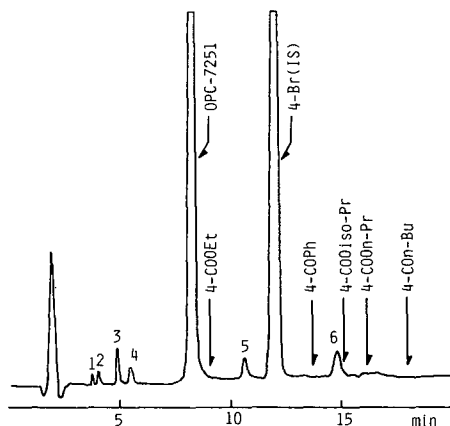
Fig. 2. Typical chromatogram showing the separation of OPC-7251 and 4-bromophenol as an internal standard spiked with 0.5% of substances related to OPC-7251 (1–6). Candidate phenols for the internal standard are expressed using abbreviations of substituents (see Tables II and IV). Column, TSKgel ODS 80 (5 μm) (15 cm × 4.6 mm I.D.); mobile phase, ACN–water–acetic acid (70:130:1); flow-rate, 1.0 ml/min; detection, 280 nm.

CONCLUSION

About 70 commercial phenol derivatives were chromatographed under various RP-HPLC conditions in order to find a series of compounds as candidates for internal standards. Of these, 30 were selected from logarithmic plots of capacity factors and other chromatographic parameters. These 30 phenols maintain an almost constant elution order under different operating conditions which are typical for RP-HPLC methods commonly used in analytical and quality control laboratories.

REFERENCES

1 C. Guillemin, J. Gressin and M. Caude, *J. High Resolut. Chromatogr. Chromatogr. Commun.*, 3 (1982) 128.
2 M. Verzele, L. Use and M. Van Kerrebroeck, *J. Chromatogr.*, 289 (1984) 333.
3 E. J. Kikta, Jr. and A. E. Stange, *J. Chromatogr.*, 138 (1977) 41.
4 R. M. Smith, *J. Chromatogr.*, 236 (1982) 313.
5 R. M. Smith, *Trends Anal. Chem.*, 7 (1984) 186.
6 J. K. Baker and C.-Y. Ma, *J. Chromatogr.*, 169 (1979) 107.
7 M. Bogusz and R. Aderjan, *J. Chromatogr.*, 435 (1988) 43.
8 M. J. M. Wells and C. R. Clark, *J. Chromatogr.*, 235 (1982) 31.
9 M. J. M. Wells and C. R. Clark, *J. Chromatogr.*, 243 (1982) 263.
10 M. J. M. Wells and C. R. Clark, *J. Chromatogr.*, 244 (1982) 231.
11 K. Miyake, N. Mizuno and H. Terada, *Chem. Pharm. Bull.*, 34 (1986) 4787.
12 N. Tanaka, H. Goodell and B. L. Karger, *J. Chromatogr.*, 158 (1978) 233.
13 N. Kyokai (Editor), *Pharmacopoeia of Japan*, Hirokawa Press, Tokyo, 11th ed., 1986.
14 T. Hanai and J. Hubert, *J. High Resolut. Chromatogr. Chromatogr. Commun.*, 6 (1983) 20.
15 K. Callmer, L.-E. Edholm and B. E. F. Smith, *J. Chromatogr.*, 136 (1977) 45.
16 S. Hara, S. Mori and T. Hanai, *Kuromatogurafi-Bunri Sisutemu (Chromatographic Separation System*; in Japanese), Maruzen, Tokyo, 1981, p. 177.
17 G.-Z. Ceng, *Acta Chim. Sin.*, 32 (1966) 107.
18 P. D. Bolton, K. A. Fleming and F. M. Hall, *J. Am. Chem. Soc.*, 94 (1972) 1033.
19 J. L. M. van de Venne and J. L. H. M. Hendrikx, *J. Chromatogr.*, 167 (1978) 1.

Automated high-resolution two-dimensional liquid chromatographic system for the rapid and sensitive separation of complex peptide mixtures

KUNIE MATSUOKA, MASATO TAOKA, TOSHIAKI ISOBE* and TSUNEO OKUYAMA

Department of Chemistry, Faculty of Science, Tokyo Metropolitan University, Setagaya-ku, Tokyo 158 (Japan)

and

YOSHIO KATO

Central Research Laboratory, TOSOH Manufacturing Co., Ltd., Sinnanyo-shi, Yamaguchi 753 (Japan)

ABSTRACT

An automated two-dimensional liquid chromatographic system for the rapid and sensitive separation of complex peptide mixtures is presented. The method presents an application of the column-switching technique, and performs sequential anion-exchange and reversed-phase chromatography under a programme directed by a computer-assisted controller. To facilitate rapid and sensitive separations, short analytical columns (3.5 cm in length) packed with non-porous packing materials of small particle size (2.5 μm) were selected for both dimensional separations, and the dead volumes of the flow system were reduced to the minimum. With this system, complex peptide mixtures such as a crude peptide fraction prepared from brain extracts were resolved into *ca.* 150 peaks within 80 min, with a detection limit of 10 ng. The method can be used for the systematic analysis of biologically active peptides and for the micro-scale separation of peptide fragments in the strategy of protein and gene sequence analysis.

INTRODUCTION

Two-dimensional high-performance liquid chromatographic (2D HPLC) is an application of the column-switching technique, which performs sequential chromatography on two different columns. The automated system for this method developed by Takahashi and co-workers[1,2] and by us[3] consists of two columns with different separation modes connected in tandem through a tee-tube or a column-switching valve, two independent flow systems for each column and a computer-assisted controller for regulation of the total system (see refs. 4 and 5 for reviews). Both of these systems employ ion-exchange and reversed-phase chromatography for the first- and second-dimensional separations, respectively, and separate peptides and proteins by

two independent parameters, first by charge and second by hydrophobicity, which is correlated strongly with the molecular weight[6]. Hence the separation principle of the 2D-HPLC technique resembles two-dimensional electrophoresis, which is widely used for the systematic separation of complex protein mixtures.

Like two-dimensional electrophoresis, the automated 2D HPLC system exhibits excellent resolution and reproducibility when applied to the systematic separation of proteins in crude tissue or cell extracts[4,5] and to the total separation of peptides produced by enzymatic digestions of very large proteins such as ceruloplasmin[1] or genetic variants of human serum albumin[2]. Other advantages of this system are easy operation and quantification and the simultaneous recovery of isolated proteins or peptides. The system is flexible, and various types of separation are possible depending on the purpose and the complexity of the sample mixture, *e.g.*, by modification of the elution conditions and number of separation cycles, or by replacing the columns with larger or smaller diameter columns or with columns having different separation specificites.

In our standard system, focused particularly on the separation of acidic proteins in the brain, we used a polymer-based TSK-gel DEAE-5PW column (75 mm × 7.5 mm I.D.; particle size 10 μm, pore diameter 1000 Å) and a polymer-based TSK-gel Phenyl-5PWRP column (75 mm × 4.6 mm I.D.; particle size 10 μm, pore diameter 1000 Å) for the first- and second-dimensional separations, because of their weak hydrophobic nature and excellent durability in both acidic and alkaline conditions. This system separates crude tissue or cell extracts into *ca.* 200 proteins by a single operation of chromatography. Takahashi and co-workers[1,2] constucted their peptide separation system with convensional silica-based DEAE and octadecyl columns of 15–25 cm × 4.6 mm I.D., and separated tryptic digests of ceruloplasmin or serum albumin into *ca.* 300 peaks. Both systems required about 12 h for the total analysis.

Here, we present a 2D HPLC system for the more rapid and sensitive separation of complex peptide mixtures. The system can separate more than 100 peptides within 80 min, using micro-amounts of samples.

EXPERIMENTAL

Materials

Calmodulin and D59 protein were purified from bovine brain extracts essentially as previously described[7,8]. A crude mixture of brain peptides was obtained by passing the brain extract through a molecular sieve ultrafiltration membrane (Ultrafree C3-LGC, molecular cut 10 000; Millipore, Bedford, MA, U.S.A.).

The sources of enzymes and reagents were as follows: trypsin, treated with 1-(tosylamido-2-phenyl)ethyl chloromethyl ketone (TPCK) (Cooper Biomedical, Malvern, PA, U.S.A.); lysylendopeptidase (Wako, Osaka, Japan); chymotrypsin (Sigma, St. Louis, MO, U.S.A.); trifluoroacetic acid (TFA) (Sequanal grade) and urea (biochemical grade) (Wako); 4-vinylpyridine (Tokyo Kasei Industries, Tokyo, Japan); and acetonitrile (chromatography grade) (Merck, Darmstadt, F.R.G.). All other reagents were of analytical-reagent grade from Wako. Water was distilled, passed through a mixedbed ion-exchange resin and redistilled before use.

TSK-gel DEAE-NPR (3.5 cm × 4.6 mm I.D.) column and TSK-gel octadecyl-NPR (3.5 cm × 4.6 mm I.D.) column were products of TOSOH (Yamaguchi, Japan).

Proteolytic digestion

    Before digestion, D59 protein was reduced and pyridylethylated in 2 *M* Tris–acetate buffer (pH 7.6) containing 8 *M* urea and 1% (v/v) ethylenediaminetetraacetic acid[9]. The pyridylethylated protein was then digested with lysylendopeptidase or chymotrypsin (enzyme-to-substrate ratio = 1:100) in 0.1 *M* ammonium hydrogen-carbonate solution (pH 8.0) at 37°C for 7 h (lysylendopeptidase) or 20 h (chymo-trypsin). Tryptic digestion of calmodulin was performed at 37°C for 5 h using TPCK-treated trypsin (enzyme-to-substrate ratio = 1:100).

Apparatus and performance of the 2D HPLC system

    The automated 2D HPLC system is illustrated in Fig. 1. The system was constructed from Model 8010 HPLC assemblies provided by TOSOH. An anion-exchange DEAE-NPR column (Cl) is connected in tandem with a reversed-phase octadecyl-NPR column (C2) through a six-way electrical column-switching valve (Model MV-8010). For each column, programmed elution is performed with a Model SC-8010 controller (SC). The controller regulates two dual-plunger pumps (Model CCPM; P11–P12 and p21–P22) to perform a series of stepwise elutions for Cl and to perform repetitive gradient elution for C2. The stepwise elution of the first-dimen-sional anion-exchange chromatography and the gradient elution of the second-di-mensional reversed-phase chromatography are synchronized by time-dependent control of the flow system.

    The 2D HPLC was performed as follows. On starting the programme, columns C1 and C2 are equilibrated with B1 (25 m*M* Tris–HCl buffer, pH 7.5) and B3 [0.1% trifluoroacetic acid (TFA)] respectively at a flow-rate of 1.0 ml/min. After 10 min P2 is stopped and the column switching valve moves to connect C1 and C2. Analysis is started by applying a sample mixture through a sample injecter (I) followed by elution of C1 with B1 for 3 min. During this time the eluent flows directly into C2. P1 is stopped; simultaneously, P2 starts pumping at a flow-rate of 1.0 ml/min with a linear gradient from B3 to B4 (0 to 50% acetonitrile in 0.1% TFA unless mentioned
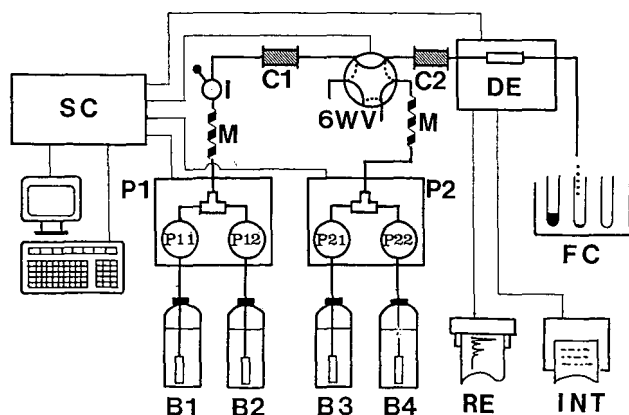
Fig. 1. Schematic diagram of the 2D HPLC system for micro-scale separation of peptides. The system is similar in principle to that described previously[4,5], except for columns C1 and C2 and some modifications to the flow system for micro-scale separation. Details are explained in the text.

otherwise in the figure legends) in 10 min. When the gradient elution has finished, C2 is equilibrated again with B3 for 3 min and then P2 is stopped. At this stage the first cycle of the 2D HPLC is completed. P1 then starts to elute peptides stepwise again from C1 by introducing and mixing a portion of buffer B2 (0.4 M Tris–HCl buffer, pH 7.5) into B1. After applying the eluent to C2, the second reversed-phase chromatography is repeated exactly as in the first cycle. These procedures are repeated for a programmed number of cyles, changing the mixing ratio of B1 and B2.

The eluent was monitored at 210 nm with a 1-cm light path (cell volume 12 μl) with a Model UV-8010 detector (DE) connected to an FBR-2 recorder (RE) and a PR-8010 integrator. When necessary, the eluent was collected in an FC-8000 peak collecter (FC). In order to reduce the dead volumes of the system, a conventional 2-ml volume dynamic mixer was replaced by an on-line coil solvent mixer (M; 1 m × 0.6 mm I.D.) and the tube connecting the outlet of the second column and the detector was reduced in volume to 1.2 μl to avoid diffusion of the eluent.

Amino acid analysis and nomenclature of peptides

The amino acid composition was determined on a Model 800 amino acid analyser (JASCO, Tokyo, Japan) after hydrolysis of peptides with 6 M hydrochloric acid containing 5% (v/v) phenol for 20–24 h in evacuated, sealed tubes. The calmodulin peptides are numbered by the fragmentation method used (T for trypsin) followed by the residue numbers starting from the N-terminus of the complete amino acid sequence[10].

RESULTS AND DISCUSSION

Separation of tryptic peptides of bovine calmodulin

Calmodulin is an acidic calcium-binding protein found in all eukaryotic cells. It contains 148 amino acids and has the potential to yield 12 tryptic peptides[10]. The micro 2D HPLC separation of the tryptic digest of calmodulin using a 10-μg sample (600 pmol) resulted in seventeen well resolved peptide fragments (Fig. 2). Of these, eight major fragments were collected from HPLC, subjected to amino acid analysis after hydrolysis with 6 M hydrochloric acid (see Experimental) and their positions in the primary sequence were identified on the basis of the amino acid composition and the published sequence. The identified peptides (shown in Fig. 2) included all of the peptides expected from tryptic cleavage of calmodulin, except for very small peptides T31–37, T76–77, T78–86, T87–90 and a free lysine. Two peptides, T1–30 and T107–148, were the fragments generated by incomplete tryptic cleavage.

Determination of the hydrophobicity by the method of Sasagawa *et al.*[11] indicated that all peptides identified in Fig. 2 had a hydrophobicity (ln H) greater than 1.9, whereas others had a value of less than 1.4. Therefore, we expected that the four small peptides mentioned above and a free lysine would not be retained on the reversed-phase column during the first-dimensional ion-exchange chromatography. The retention time of each identified peptide was linearly related to its hydrophobicity (correlation coefficient = 0.97), suggesting that the present system could separate peptides having hydrophobicities of ln H > 1.5.

Fig. 3 shows a 2D HPLC profile in which 1 μg of the same digest of calmodulin was analysed by increasing the detector sensitivity 10-fold over that for standard
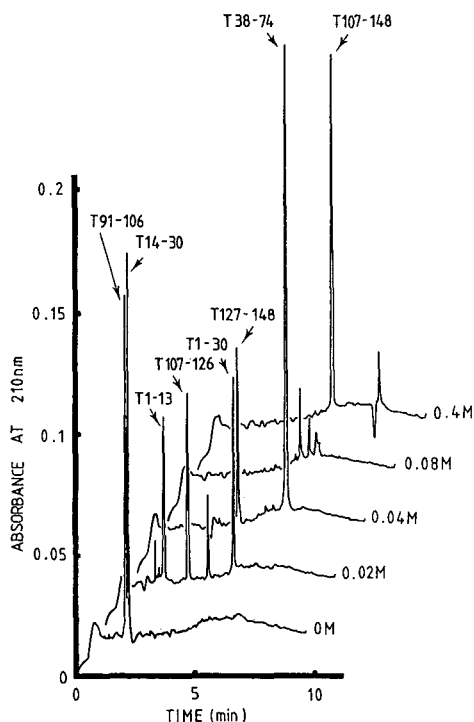
Fig. 2. Tryptic peptide map of bovine brain calmodulin obtained by automated 2D HPLC. The tryptic digest (10 μg) was applied to the system and eluted under the standard conditions described in the text. Each horizontal profile represents the result of the second-dimensional reversed-phase chromatography of a peptide fraction eluted from the first-dimensional anion-exchange column. The sodium chloride concentration for the stepwise elution of the anion-exchange column is shown on the right side of each profile. Peptides are identified according to the nomenclature described under Experimental.

conditions. At this sensitivity, the signal-to-noise ratio was considerably reduced by the appearance of many small peaks detected at an early stage of gradient elution and a very broad peak observed around 5 min. However, the peptide fragments that were identified in the standard analysis (Fig. 2) were still clearly distinguishable from the baseline. From this profile, the detection limit of the present system was estimated to be 10 ng. Peptide separation at this level of sensitivity is valuable for many biologically interesting proteins that are available in only limited amounts for identification, characterization and comparison with other proteins on the basis of primary structure. The method should be applicable to a wide range of such proteins, because the amount required (1–10 μg) is compatible with the currently available, most efficient protein separation techniques such as 2D electrophoresis or 2D HPLC and also other micro protein chemical techniques such as the *in situ* protease digestion of a protein blotted onto a nitrocellulose membrane[12].

Separation of proteolytic fragments of D59 protein

   D59 protein is an acidic protein (pI = 4.1) with an apparent molecular weight of 59 000 daltons as estimated by 2D electrophoresis in the presence of sodium dodecyl
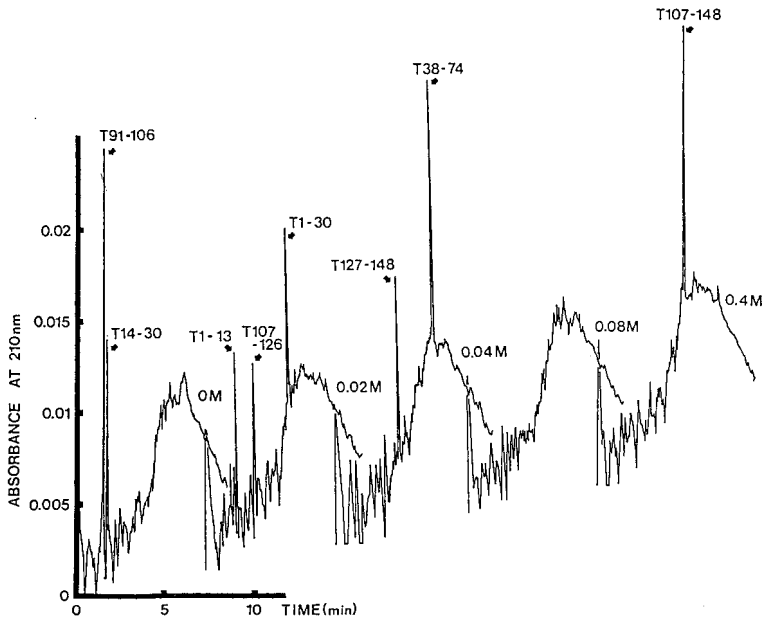
Fig. 3. High-sensitivity analysis of the tryptic digest of calmodulin. A 1-μg amount of the digest was separated under the same conditions as in Fig. 2, except that the detector sensitivity was set at 0.02 a.u.f.s. at 210 nm. To avoid complication the time-axis is indicated only for the first chromatogram.
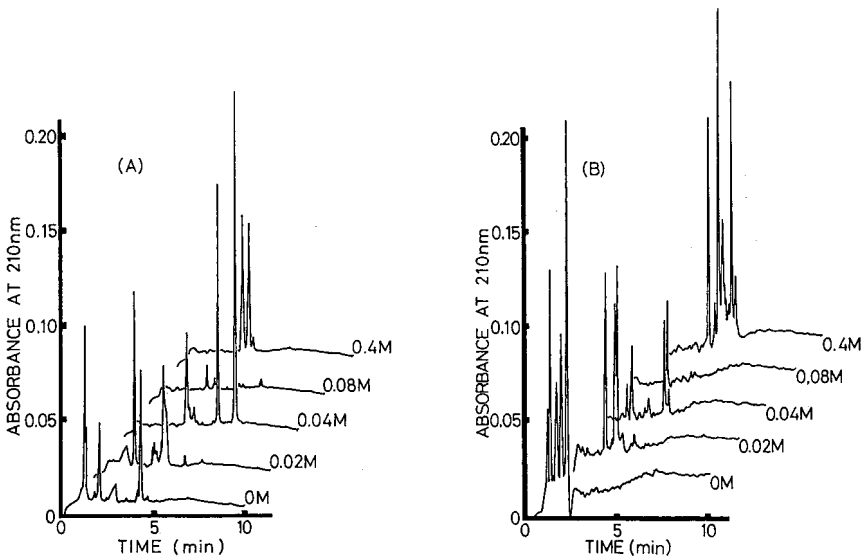
Fig. 4. Elution profile of peptide fragments of bovine brain D59 protein produced by cleavage with (A) lysylendopeptidase and (B) chymotrypsin. The digests (20 μg each) were separated by 2D HPLC under the conditions described in the text.

sulphate. This protein has been isolated during systematic studies of brain proteins but its biological function is unknown. In order to characterize this protein in further detail, the pyridylethylated D59 was cleaved by lysylendopeptidase and chymotrypsin and the peptide fragments generated were separated by 2D HPLC. As shown in Fig. 4, 20–30 fragments were detected for each digest using 20 μg (300 pmol) of protein. The number of fragments detected was less than that expected from the estimated molecular weight of this protein, probably because the large number of lysine or hydrophobic residues in D59 led to the generation of large numbers of very small fragments on lysylendopeptidase or chymotryptic digestion that did not bind to the reversed-phase column.

Subsequent protein chemical analysis proved that most of the fragments isolated by 2D HPLC had sufficient purity for the determination of their amino acid composition and sequence. Because computer-assisted searches of sequence databases showed that the determined peptide sequences of D59 did not show significant homologies with any protein with a known amino acid sequence, we assumed that D59 was one of the brain proteins that had not been described. The determined sequences were used as probes for gene cloning of this protein.

Separation of a crude peptide mixture prepared from brain

The brain tissue contains many biogenic peptides important for neural function and homeostatis. Because of the complexity of the brain extract, however, the isolation
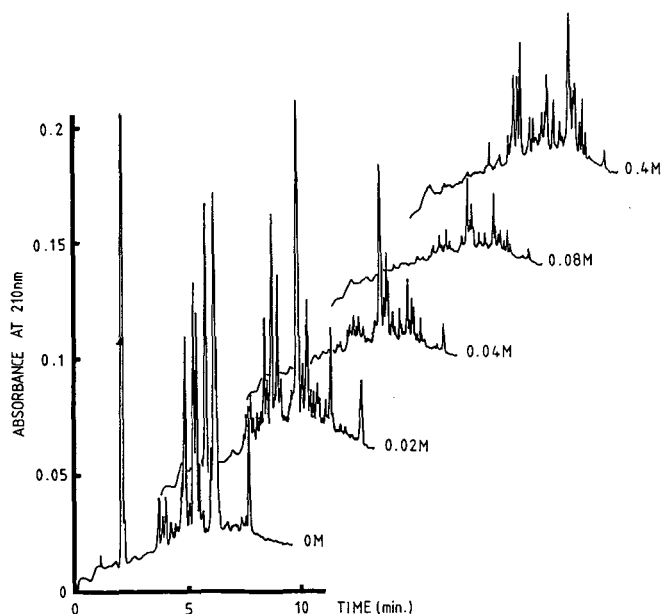
Fig. 5. Separation of crude peptide mixture extracted from brain tissue. A crude peptide fraction was prepared from bovine brain extracts as described under Experimental and an aliquot (40 μg of peptide) was analysed directly with the 2D HPLC system. The analytical conditions were as described in the text, except that the second-dimensional reversed-phase chromatography was performed with a gradient from 20% to 60% acetonitrile in 0.1% TFA.

of such components has generally been achieved by tedious multi-step purification procedures that often result in low recoveries. To test the resolution of the 2D HPLC technique, a crude peptide fraction was prepared by filtration of the brain extracts through a molecular sieve membrane (see Experimental) and an aliquot of filtrate was applied directly to the automated 2D HPLC system. The separation was achieved by repeating both the ion-exchange and reversed-phase chromatograhic processes five times within 80 min. As shown in Fig. 5, the peptide fraction was resolved into *ca.* 150 peaks by a single operation of chromatography. Although these peaks were not . characterized in detail, this suggests that the system presented should be useful for the isolation of biologically important peptides which are present in small amounts in the brain and other tissue extracts or in physiological fluids such as serum and urine.

ACKNOWLEDGEMENTS

REFERENCES

 1 N. Takahashi, N. Ishioka, Y. Tanahashi and F. W. Putnam, *J. Chromatogr.*, 326 (1985) 407.
 2 N. Takahashi, Y. Takahashi, N. Ishioka, B. Blumberg and F. W. Putnam, *J. Chromatogr.*, 359 (1986) 181.
 3 T. Isobe, K. Uchida, M. Taoka, T. Manabe and T. Okuyama, *Anal. Biochem.*, submitted for publication.
 4 N. Takahashi, T. Isobe and F. W. Putnam, in M. T. W. Hearn (Editor), *HPLC of Proteins, Peptides, and Polynucleotides,* Verlag Chemie, New York, NY, in press.
 5 T. Isobe, N. Takahashi and F. W. Putnam, in R. S. Hodges and C. Mant (Editors), *HPLC of Peptides and Proteins: Separation, Analyis, and Conformation,* CRC Press, Boca Raton, FL, in press.
 6 T. Ichimura, Y. Amano, T. Isobe and T. Okuyama, *Bunseki Kagaku*, 34 (1985) 653.
 7 T. Isobe, T. Nakajima and T. Okuyama, *Biochim. Biophys. Acta*, 494 (1977) 222.
 8 N. Ishioka, T. Isobe, T. Kadoya, T. Okuyama and T. Nakajima, *J. Biochem. (Tokyo)*, 94 (1984) 611.
 9 J. F. Cavins and M. Friedman, *Anal. Biochem.*, 35 (1970) 489.
10 K. Kasai, Y. Kato, T. Isobe, H. Kawasaki and T. Okuyama, *Biomed. Res.*, 1 (1980) 248.
11 T. Sasagawa, T. Okuyama and D. C. Teller, *J. Chromatogr.*, 240 (1982) 329.
12 R. H. Aebersold, J. Leavitt, R. A. Saavedra, L. E. Food and S. B. H. Kent, *Proc. Natl. Acad. Sci. U.S.A.*, 84 (1987) 6970.

CHROMSYMP. 1815

Direct sample injection into the high-performance liquid chromatographic column in theophylline monitoring

YUKIMITSU KOUNO and CHIYOJI ISHIKURA

Bohsei Pharmacy Co., Isehara, Kanagawa 259-11 (Japan)

NORIYUKI TAKAHASHI

Department of Pharmacy, Tokyo Medical College Hospital, Shinjuku-ku, Tokyo 160 (Japan)

and

MASATO HOMMA and KITARO OKA*

Division of Clinical Pharmacology, Tokyo College of Pharmacy, Hachioji, Tokyo 192-03 (Japan)

ABSTRACT

A small diatomaceous earth column was used for direct sample injection into a high-performance liquid chromatographic (HPLC) column for theophylline monitoring. The original design of this device has been improved so as to make it easily usable and disposable following use. It consists of a diatomaceous earth-packed polystyrene tube, the inner surface of which is coated with PTFE, having a capacity of *ca.* 5 μl of plasma or serum sample, and a stainless-steel needle for introducing an extract into the HPLC sample injector. Using this device together with an optimized injection solvent mixture, an accurate determination of theophylline can be carried out at low cost. The results obtained were comparable to those given by an immunological method, such as fluorescence polarization immunoassay.

INTRODUCTION

A direct sample injection technique for high-performance liquid chromatography (HPLC) developed by Pinkerton *et al.*[1] has been applied to the determination of drug concentrations in human plasma[2-4]. Because of its complete elimination of clean-up procedures, it seems difficult to improve void-peak spreading for baseline separation. Disposable clean-up tools, such as Sep-Pak cartridges developed by Waters Assoc. (Milford, MA, U.S.A.) and Extrelut (Merck, Darmstadt, F.R.G.), have been widely used for conventional HPLC. However, no method has generally been available that could provide optimum conditions for extraction. Recently, a diatomaceous earth column has been developed for the extraction of various compounds in human biofluids. Optimizing the solvent polarity of binary mixtures for extraction[5-7] and compound determination by silica gel chromatography have become much easier and more accurate[8-13]. Recently, we have reported a syringe-type minicolumn for direct injection of plasma into HPLC columns[14]. This device, which we named Ex-

trashot, rendered tedious sample pretreatment unnecessary. This paper describes an improved Extrashot which is designed to be disposable following use. It can be easily applied to therapeutic drug monitoring such as theophylline in asthmatic patients. The results obtained so far show close agreement with those given by conventional immunoassay.

EXPERIMENTAL

Extrashot apparatus

The newly designed Extrashot, shown in Fig. 1A, consists of the following components: 1, stainless-steel needle fitted to an ordinary syringe-loading sample injector such as a Rheodyne type; 2, minicolumn holder made of polystyrene; 3, minicolumn tube made of PTFE; 4, filter-papers; and 5, 45-μl minicolumn containing diatomaceous earth granules. The diatomaceous earth granules are prepared from
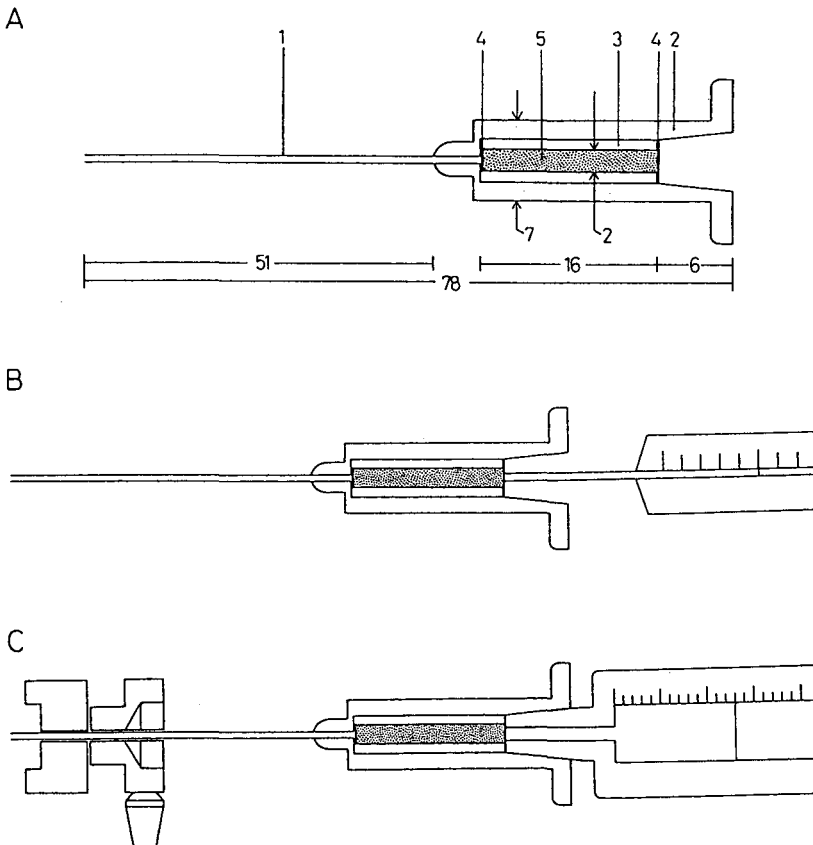
Fig. 1. (A) Overall view of the Extrashot. 1 = Application needle; 2 = minicolumn holder made of polystyrene; 3 = minicolumn tube made of PTFE; 4 = filter; 5 = support material. Sizes in mm. (B) Sample loading by a microsyringe. (C) Solvent introduction into the HPLC system through the Extrashot.

Celite powder No. 545 (Johns Manville, Denver, CO, U.S.A.) by precipitation in distilled water. The granule particle size is 50–100 μm and 1 ml of granules weighs about 0.58 g.

Sample loading

A 5-μl aliquot of plasma or serum is loaded onto the surface of the packed material through the filter-paper by a microsyringe as illustrated in Fig. 1B. The aqueous sample is absorbed and continuously retained by the granules. The sample as an aqueous phase occupies about 11% of the dead volume of the Extrashot.

Solvent introduction

After the sample has been loaded, the Extrashot was attached to an ordinary syringe-loading sample injector of the HPLC system (Fig. 1C), followed by a 130-μl portion of the extraction–injection solvent over a period of 5–10 s by a tuberculin test glass syringe.

HPLC

The HPLC system consisted of a continuous-flow solvent-delivery system (BIP-I; Jasco, Tokyo, Japan), a UV detector (Uvidec-100V; Jasco), a syringe-loading sample injector (Model 7125; Rheodyne, Cotati, CA, U.S.A.), and a single pen recorder (RC-150; Jasco). The sample injector was equipped with a 100-μl loop by which the extract from the device is loaded. The analytical column (125 mm × 4 mm I.D.) was packed with silica gel (LiChrosorb Si 60, particle size 5 μm) (Merck, Darmstadt, F.R.G.). This column was treated with 100 μl of 1% sulphuric acid and excess of distilled water until the effluent was neutral. Methanol and finally chromatographic solvent mixtures were then introduced. Sulphuric acid treatment was conducted once prior to first use so that the surface pH was slightly below 7, at which the theoretical plate number of acidic compounds such as theophylline exceeds 3000 per column. The solvent system for the theophylline determination was water–acetic acid–ethanol–dichloromethane (0.2:0.2:4:95.6, v/v) at a flow-rate of 1.0 ml/min. The UV detector was set at 275 nm for theophylline analysis.

Optimization of solvent for Extrashot

Binary solvent mixtures were used for extraction–injection by Extrashot. To attain critical frontal extraction of the target molecule, a strong solvent component such as ethanol and a non-polar component such as dichloromethane or *n*-hexane were used. The optimum solvent composition was determined by a preliminary experiment using a larger diatomaceous earth column of 4 ml inner volume and 0.5 ml of water, these dimensions being about 100 times those of the Extrashot. Using this column, a solvent composition *vs.* capacity factor curve was obtained to find a suitable solvent composition with minimum polarity by which the target molecule could be extracted and other polar compounds eliminated.

Calibration

Direct peak-height calibration was used. The amount of sample is small and, consequently, the addition of an internal standard is neither possible nor necessary prior to the analysis. Peak heights at various concentrations, such as 1, 5, 10, 20, and

30 μg/ml, gave the correlation equation $y = 0.0853x + 0.2040$ ($r = 0.9994$; $p < 0.001$), where y is the concentration of theophylline (μg/ml) and x is observed peak height (mm) at 0.02 a.u.f.s.

Solvents and reagents

Organic solvents and other reagents were of analytical-reagent grade and purchased from Wako (Osaka, Japan). Theophylline kit II (TDX) for fluorescense polarization immunoassay (FPIA) with an automated system was obtained from Dinabot (Tokyo, Japan).

RESULTS

The accuracy and efficiency of the device were assessed on the basis of plasma concentrations of theophylline. Test plasma mixtures at various concentrations were prepared from a blood sample from a healthy male volunteer.

Loading capacity of Extrashot

This parameter was found to be 5 μl when operating the device manually with a tuberculin test syringe for solvent delivery and varied according to the flow-rate, being higher at a slower rate. It was thus considered that, at an operating capacity of 5 μl, the aqueous phase would not leak out into the HPLC system.

Optimization of extraction solvent

The solvent composition *vs.* capacity factor curve shown in Fig. 2 was obtained using theophylline and a binary solvent mixture of ethanol and dichloromethane. Frontal extraction of theophylline from distilled water was successfully carried out when the ethanol content of the mixture exceeded 3%. Extraction–injection using plasma specimens containing theophylline at various concentrations was then observed. Repeated peak-height measurements at theophylline concentrations between 1 and 20 μg/ml showed good reproducibility with a 4% ethanol concentration. The relative standard deviation for peak height was less than 3.5% ($p < 0.001$) at any concentration, such as 1, 5, 10 and 20 μg/ml. A typical chromatogram is shown in Fig. 3.
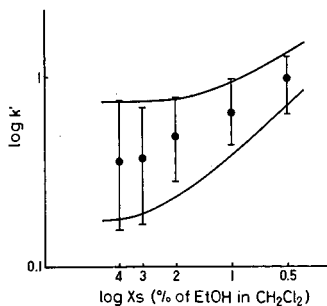
Fig. 2. Solvent composition (X_s; %, v/v) *vs.* capacity factors (k') and peak widths obtained with the diatomaceous earth column of 4 ml inner volume. The points indicate the top of the extraction peak and the bars the peak width. One k' unit corresponds to 4 ml of each solvent. EtOH = Ethanol.
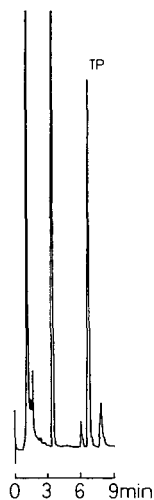
Fig. 3. Typical chromatogram of theophylline determination by Extrashot HPLC. The plasma specimen was obtained from an asthmatic patient. TP = theophylline corresponding to 5 μg/ml.
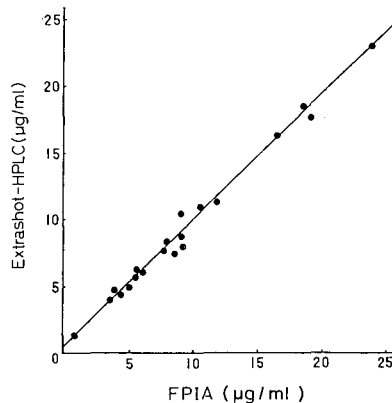
Fig. 4. Extrashot HPLC vs. FPIA for theophylline determination. $y = 0.9375x + 0.6240$ ($r = 0.9939, p < 0.001$).

Comparison of Extrashot HPLC with FPIA

This comparison showed the two methods to give essentially the same results, as is evident from Fig. 4. The results obtained by FPIA were about 1.07 times those given by Extrashot HPLC. In the therapeutic range of theophylline between 10 and 20 μg/ml, the results were comparable, FPIA being only about 3% higher.

DISCUSSION

Conventional experiments for selecting an extraction solvent for biofluids are usually performed on a trial-and-error basis. However, our extraction-monitoring procedure using a diatomaceous earth column constitutes a new method for optimizing a solvent system prior to HPLC determination[6]. A rapid-flow fractionation (RFF) column system set up by this extraction monitoring has been found to be clinically suitable for the monitoring of various drugs[8-13]. The use of combined extraction monitoring and RFF has been found to be ideal for optimizing extraction conditions such as solvent choice, control of solvent polarity, volume of solvent and extraction flow-rate.

With regard to solvent polarity for extraction, it is of primary importance that the polarity of the solvent mixture be the minimum necessary for extracting the target molecule and eliminating other polar compounds[6]. Adhering to this principle, critical frontal extraction has been successfully carried out with a minimum volume of extract. Further, a solvent can be easily introduced into an RFF column by nitrogen at a pressure as low as 1 kg/cm^2. An appropriate flow-rate as fast as 1 ml/s is possible

through the use of a gauge control. Hence the time required for sample treatment is considerably shortened. With the minimum column size, the desired flow-rate can be secured by manually operating the solvent-delivery syringe. These considerations served as the basis for the design of this improved Extrashot[14]. The outstanding features of this device are its ease of use and disposability following use.

The plasma- or serum-loading capacity of the Extrashot is as much as 5 μl. This volume of blood from asthmatic patients administered theophylline daily contains only 50 ng of this drug. This amount is ten times greater than the detection limit of our HPLC system. Therefore, in this study, the UV detector was operated at a sensitivity of 0.01–0.02 a.u.f.s., permitting the analysis of more dilute samples.

Solvent polarity was optimized so that a quantitative amount of the drug could be extracted and introduced into the 100-μl loop of the HPLC injector. The volume of eluent from the Extrashot was about 90–100 μl following the administration of a 130-μl aliquot of solvent. The theophylline recovery was 94 ± 3% at 1 μg/ml and 97 ± 3% at 20 μg/ml, being higher than 95% at therapeutic concentrations. The drug was contained in a minimum volume of solvent with the least possible polarity. Using this solvent system, more polar components in plasma specimens are prevented from being extracted, so that their elimination is thus achieved. It is for this reason that the chromatograms obtained were much cleaner and more accurate than those obtained by the usual pretreatment.

Day-to-day variations in peak height can be easily corrected by injection an authentic specimen once prior to an analytical run. The relative standard deviations for determinations at various concentrations were less than 5% and the results were in good agreement with those given by FPIA, as shown in Fig. 3.

CONCLUSION

The improved Extrashot is a disposable device for direct plasma extraction–injection with conventional HPLC. The method is convenient and inexpensive for therapeutic drug monitoring at a community hospital. The Extrashot should also be applicable for determining concentrations of other drugs in blood provided that at least 1 μg/ml is present.

ACKNOWLEDGEMENTS

REFERENCES

1 T. C. Pinkerton, T. D. Miller, S. E. Cook, J. D. Perry, J. D. Rateike and T. J. Szczerba, *Biomed. Chromatogr.*, 1 (1986) 96–105.
2 T. C. Pinkerton and I. H. Hagestam, *Anal. Chem.*, 57 (1985) 1757–1763.
3 T. C. Pinkerton, J. A. Perry and J. D. Rateike, *J. Chromatogr.*, 367 (1986) 412–418.
4 T. Nakagawa, A. Shibukawa, N. Shimono, T. Kawashima, H. Tanaka and J. Haginaka, *J. Chromatogr.*, 420 (1987) 297–311.

5 K. Oka, K. Minagawa, S. Hara, M. Noguchi, Y. Matsuoka, M. Kono and S. Irimajiri, *Anal. Chem.*, 56 (1984) 24–27.
6 K. Oka, N. Ohki, M. Noguchi, Y. Matsuoka, S. Irimajiri, M. Abe and T. Takizawa, *Anal. Chem.*, 56 (1984) 2614–2617.
7 K. Oka, T. Ijitsu, K. Minagawa, S. Hara and M. Noguchi, *J. Chromatogr.*, 339 (1985) 253–261.
8 K. Oka, S. Aoshima and M. Noguchi, *J. Chromatogr.*, 345 (1985) 419–424.
9 K. Oka, M. Noguchi, T. Kitamura and S. Shima, *Clin. Chem.*, 33 (1987) 1639–1642.
10 K. Oka, T. Hirano and M. Noguchi, *J. Chromatogr.*, 423 (1987) 285–291.
11 K. Oka, T. Hirano and M. Noguchi, *Clin. Chem.*, 34 (1988) 557–559.
12 K. Oka, K. Hosoda, T. Hirano, E. Sakurai and M. Kozaki, *J. Chromatogr.*, 490 (1989) 145–154.
13 X. Kang and K. Oka, *Yakugaku Zasshi*, 109 (1989) 274–279.
14 M. Homma, K. Oka and N. Takahashi, *Anal. Chem.*, 61 (1989) 784–787.

High-performance liquid chromatography with a 3α-hydroxysteroid dehydrogenase postcolumn reactor and isoluminol–microperoxidase chemiluminescence detection

MASAKO MAEDA, SHINGO SHIMADA and AKIO TSUJI*

School of Pharmaceutical Sciences, Showa University, Hatanodai, Shinagawa-ku, Tokyo 142 (Japan)

ABSTRACT

A high-performance liquid chromatographic system with chemiluminescence detection for the determination of bile acids has been developed. Immobilized 3α-hydroxysteroid dehydrogenase was used as a postcolumn reactor and the generated NADH in the eluent was monitored by the chemiluminescence reaction of NADH using a 1-methoxy-5-methylphenazinium methylsulphate–isoluminol–microperoxidase system. A good separation of unconjugated bile acids and their glycine and taurine conjugates could be achieved with a reversed-phase column (Bilepak II) and acetonitrile–methanol–30 mM ammonium acetate as the eluent. The detection limit was about 2 pmol for each bileacid.

INTRODUCTION

In recent years, considerable attention has been focused on the development of high-performance liquid chromatography (HPLC) for the analysis of various biological substances, in particular polar and unstable compounds. HPLC is suitable for the separation and determination of unconjugated and conjugated bile acids without prior hydrolysis and/or solvolysis[1]. However, the sensitivity of HPLC using refractometric or ultraviolet spectrometric detection is low for the determination of bile acids in normal human serum. The most significant improvements in the sensitivity of HPLC methods for bile acid determination have been with the use of pre- or postcolumn derivatization and fluorimetric or enzymatic detection. In previous papers we described HPLC methods using 1-bromoacetylpyrene[2] and dansylhydrazine[3] as fluorescent precolumn reagents and an HPLC method using an immobilized 3α-hydroxysteroid dehydrogenase (3α-HSD) column combined with electrochemical detection[4].

Recently, the use of chemi- and bioluminescence analysis has been introduced into biochemistry and clinical chemistry because of their high sensitivity[5]. Several applications of chemiluminescence detection in HPLC have been reported using the peroxyoxalate–hydrogen peroxide[6] and lucigenin[7,8] chemiluminescence reaction

systems. We have also developed HPLC methods using isoluminol derivative–hydrogen peroxide[9] and phenacyl derivative–lucigenin[10] chemiluminescence detection for the assay of amines and carboxylic acids.

In this study, we have developed an HPLC method for bile acids using a 3α-HSD enzyme reactor and isoluminol–microperoxidase chemiluminescence detection.

EXPERIMENTAL

Materials

Cholic acid, chenodeoxycholic acid, deoxycholic acid, ursodeoxycholic acid, lithocholic acid and their glycine and taurine conjugates were purchased from Sigma (St. Louis, MO, U.S.A.). NAD^+ and NADH were obtained from Boehringer Mannheim–Yamanouchi (Tokyo, Japan), 1-methoxy-5-methylphenazinium methylsulphate (1-MPMS) from Nacalai Tesque (Kyoto, Japan) and isoluminol (IL) from Tokyo Chemical Industry (Tokyo, Japan). 3α-Hydroxysteroid dehydrogenase (3α-HSD) (grade II) and microperoxidase (m-POD) were purchased from Sigma. Amino glass beads used as the solid phase of the immobilized enzyme were Amino Propyl-CPG 180 A from Electro-Nucleonics (Fairfield, NJ, U.S.A.) and Sep-Pak C_{18} cartridges from Millipore (Milford, MA, U.S.A.). All other chemicals were of analytical-reagent grade from commercial sources.

Bile acid stock solution. Each bile acid was dissolved in methanol and made up to 10 μmol/ml with methanol.

NAD^+ *solution.* A 0.9-mM NAD^+ solution was prepared by dissolving NAD^+ in 10 mM KH_2PO_4 containing 1 mM Na_2EDTA (pH 7.77).

1-MPMS solution. This solution was prepared by dissolving 1-MPMS in redistilled water (4 μg/ml).

IL–m-POD solution. This solution contained $2.4 \cdot 10^{-4}$ M IL and $1 \cdot 10^{-6}$ M m-POD in 0.4 M carbonate buffer (pH 9.5).

Immobilized 3α-HSD column. 3α-HSD was coupled to amino glass beads by the glutaraldehyde method as described previously[4] and packed into a stainless-steel column (25 mm × 4.6 mm I.D.).

Apparatus and chromatographic conditions

A schematic diagram of the apparatus is shown in Fig. 1. It consisted of a Model CCPM 8000 chromatograph (Tosoh, Tokyo, Japan), a JASCO (Tokyo, Japan) Bilepak-II (5 μm) column (100 mm × 5 mm I.D.) and a JASCO Model 825 CL chemiluminescence detector.

The mobile phases were acetonitrile–methanol–30 mM ammonium acetate [(A) 30:30:40 (pH 7.10) and (B) 20:20:60 (pH 6.80)], with isocratic elution with B for 5 min and then linear gradient elution from 100% B to 100% A in 32 min at a flow-rate of 1.0 ml/min. The eluent from the column was mixed with NAD^+ solution (1 ml/min). 1-MPMS solution and IL–m-POD solution were mixed into the eluent from the immobilized 3α-HSD column by pumps at a flow-rate of 1.0 ml/min. The generated chemiluminescence was monitored with the chemiluminescence detector.

Sample preparation

Extraction of bile acids from bile. Bile (20 μl) was diluted using 0.05 M phosphate
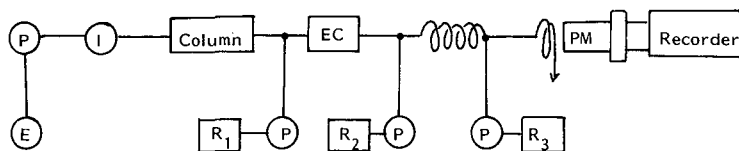
Fig. 1. HPLC system with chemiluminescence detection for the assay of bile acids. P = Pump; E = eluent; I = injection valve; column = Bilepak-II; EC = Enzymepak-3α-HSD; R_1 = 0.9 mM NAD$^+$–10 mM KH$_2$PO$_4$–1 mM Na$_2$EDTA (pH 7.77), flow-rate 1.5 ml/min; R_2 = 1-MPMS (4 μg/ml), flow-rate 1.0 ml/min; R_3 = isoluminol (2.4 · 10^{-4} M)–m-POD (1.0 · 10^{-6} M), flow-rate 1.0 ml/min. Mobile phase: acetonitrile–methanol–30 mM ammonium acetate [(A) 30:30:40 (pH 7.10) and (B) 20:20:60 (pH 6.80)] with isocratic elution with B for 5 min followed by linear gradient elution from 100% B to 100% A in 32 min at a flow-rate of 1.0 ml/min.

buffer (pH 7.0) containing internal standard (I.S.). The diluted bile (1.0 ml) was applied to a Sep-Pak C$_{18}$ column. After washing with 2% methanol (2 ml), the bile acids were eluted with 90% ethanol (5 ml). The solvent was evaporated under a stream of nitrogen at 40°C. The residue was dissolved in methanol (1 ml) and the solution evaporated to dryness under a stream of nitrogen. The residue was dissolved in methanol 100 μl and a 10-μl portion was injected into the HPLC system.

Extraction of bile acids from serum. Serum (500 μl) was mixed with methanol (3 ml) and ultrasonicated for 15 min. The mixture was centrifuged at 1200 g for 10 min at 4°C, the supernatant was transferred into a test-tube and the precipitated residue was extracted with methanol (2 ml) in the same manner. The combined supernatant was evaporated to dryness under a stream of nitrogen. The residue was dissolved by adding 0.05 M phosphate buffer (pH 7.0) and applied to a Sep-Pak C$_{18}$ column, after which bile acids were extracted in the same manner as above.

Recovery test

A synthetic mixture of 500 pmol of each bile acid containing I.S. was added to 20 μl of normal bile or 500 μl of normal serum and then assayed by the proposed method. Recoveries were calculated against a pure standard bile acid mixture carried through the procedure.

RESULTS AND DISCUSSION

Recently, we reported a highly sensitive chemiluminescent assay of NADH and NADPH based on the chemiluminescence reaction using an electron mediator and isoluminol–microperoxidase[11], and also developed a flow system for the assay of total bile acids in serum by using an enzyme column containing immobilized 3α-HSD on amino glass beads. In this study, we have developed an HPLC method with chemiluminescence detection for the assay of individual bile acids based on the flow detection system.

The assay principle is illustrated schematically in Fig. 2. This method utilizes an immobilized 3α-HSD enzyme column reactor in a flow mode that converts the 3α-hydroxyl group of bile acid to the corresponding 3-oxo bile acids in the presence of
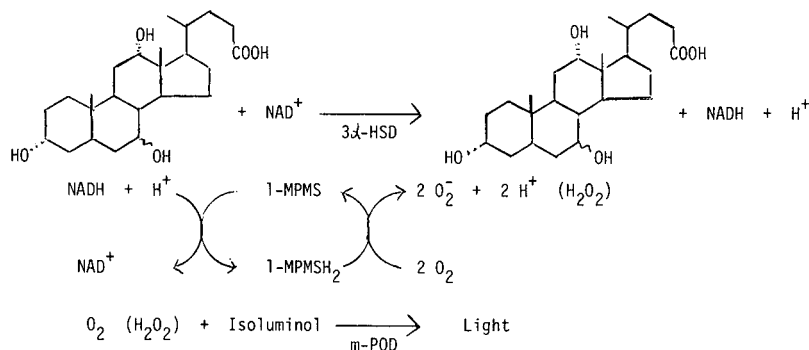
Fig. 2. Principle for the assay of bile acids using 3α-HSD and NADH chemiluminescence reaction.

NAD^+ after chromatographic separation by HPLC on an ODS column. In the enzyme column reactor NADH is generated and monitored by the chemiluminescence reaction with 1-MPMS–IL–m-POD.

Several parameters were examined in order to determine the optimum conditions for the enzymatic reaction of bile acids by using the flow system without the separation column shown in Fig. 1.

The first step of this method is the enzymatic oxidation of bile acids to 3-oxo bile acids in the immobilized 3α-HSD enzyme column reactor. Fig. 3 shows the effects of the concentration and flow-rate of NAD^+ solution on the chemiluminescence intensity (peak height in the chromatogram). The peak height increased with increasing concentration and flow-rate and reached a maximum at 0.9 mM NAD^+ concentration and a flow-rate of 1.5 ml/min; therefore, these conditions were adopted for the method.

The second step is the reaction of NADH with 1-MPMS in the reaction coil. The concentration of 1-MPMS solution and the length of the reaction coil were examined. As shown in Fig. 4, the maximum peak occurred at a 1-MPMS concentration
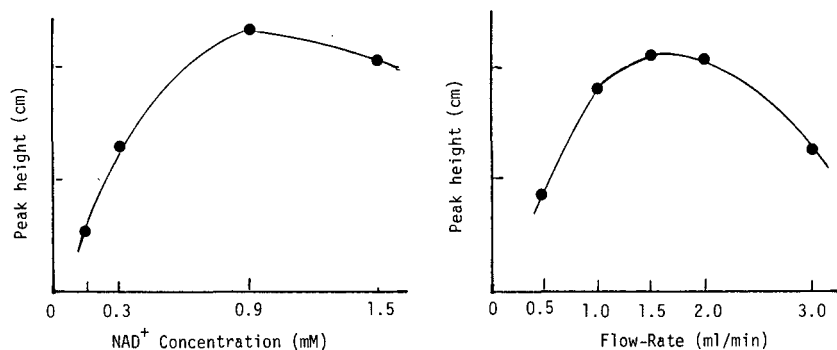
Fig. 3. Effects of the concentration and the flow-rate of NAD^+ solution on chemiluminescence intensity. Sample used: glycoursodeoxycholic acid (300 pmol).
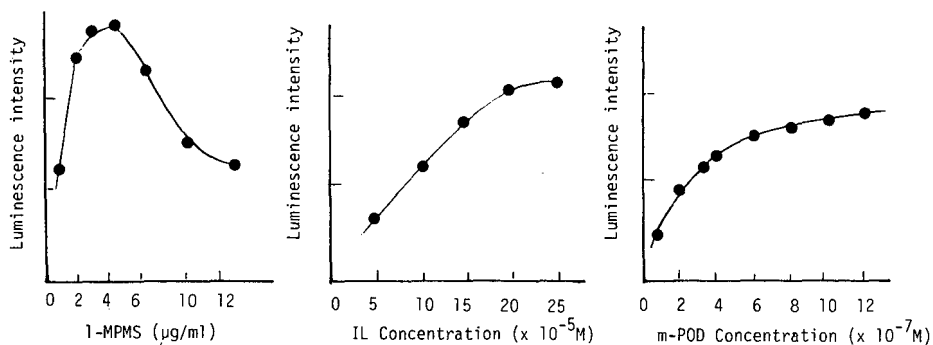
Fig. 4. Effects of the concentrations of 1-MPMS, isoluminol and microperoxidase solutions on chemiluminescence intensity.

3–4 μg/ml and the sensitivity decreased sharply on either side of this concentration; therefore 4 μg/ml 1-MPMS solution was used. The reaction rate of NADH with oxygen depends on the electron mediator used. In this system, 1-MPMS was used because the reaction rate was faster than with other electron mediators and 1-MPMS was stable towards light. The chemiluminescence intensity increase with increasing length of reaction coil, but the peak band became wider. Therefore, a 12-m reaction coil was used as a compromise between sensitivity and separation efficiency.

The last step is the chemiluminescence reaction of hydrogen peroxide with IL and m-POD. As shown in Fig. 4, the chemiluminescence intensity increased with increasing concentration of IL and m-POD and reached a nearly constant value at concentrations of $2 \cdot 10^{-4}$ and $1 \cdot 10^{-6}$ M, respectively. Therefore, these conditions were selected for the method.
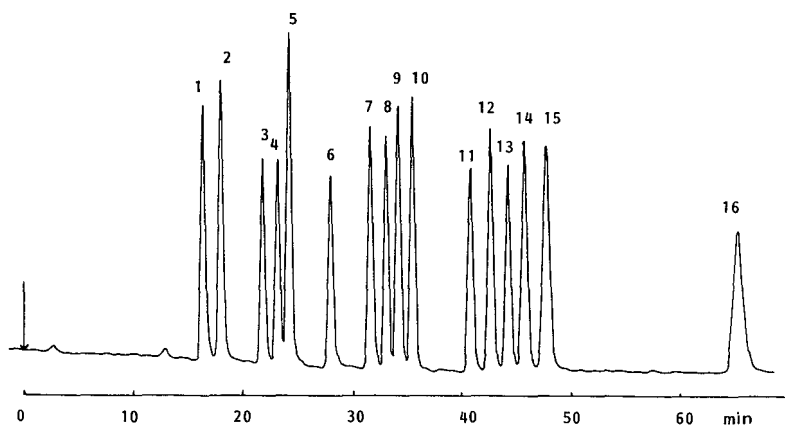
Fig. 5. Typical chromatogram of bile acids obtained with the proposed method. Peaks: 1 = GUDC; 2 = TUDCA; 3 = GCA; 4 = TCA; 5 = UDCA; 6 = CA; 7 = GCDCA; 8 = TCDCA; 9 = GDCA; 10 = TDCA; 11 = CDCA; 12 = DCA; 13 = GLCA; 14 = TLCA; 15 = I.S.; 16 = LCA [CA = cholic acid, DCA = deoxycholic acid, CDCA = chenodeoxycholic acid, UDCA = ursodeoxycholic acid, LCA = lithocholic acid, G = glyco-, T = tauro-, I.S. = internal standard (5α-pregnane-3α,17α,20α-triol)].

The chromatographic conditions were examined in order to obtain a complete separation of all unconjugated bile acids and their glycine and taurine conjugates. From the results, the gradient elution mode and the acetonitrile–methanol–30 mM ammonium acetate as the mobile phase were selected. A typical chromatogram is shown in Fig. 5. All the bile acids were completely separated from each other. Calibration graphs were costructed from the chromatograms obtained by injecting a standard mixture of bile acids and I.S. and were linear for all the bile acids over the range 10–500 pmol. The detection limit was about 2 pmol per injection (signal-to-noise ratio = 2). This value is comparable to those obtained with previous methods[2–4], with fluorescence prederivatization and electrochemical detection. The relative standard deviations at 250 and 500 pmol ranged from 0.9 to 13.2% and from 1.5 to 9.4%, respectively.

In order to determine the recovery for each bile acid, standard solutions of bile acids were added to normal bile and serum and assayed using the HPLC system after extraction as described under Experimental. The mean recoveries of each bile acid (n = 5) ranged from 85.1 to 112.1% for bile and from 93.7 to 103.7% for serum.

The applicability of the method to clinical samples was examined by the assay of bile acids in bile and serum samples from patients. Typical chromatograms for patients with liver cancer and chirrhosis are shown in Fig. 6. Characteristic patterns of individual serum bile acids were observed in patients with these diseases. Unconjugated bile acids and glycine and taurine conjugates were significally elevated in patients with liver chirrhosis and carcinoma. The results suggested that the method may
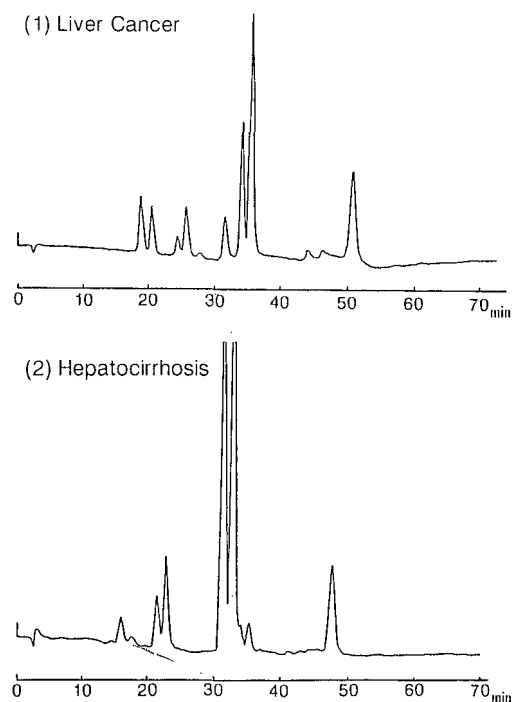
Fig. 6. Typical chromatograms of bile acids in serum from patients.

provide more precise information on the metabolic profile of bile acids in patients with various diseases, including hepatobiliary diseases.

CONCLUSION

The HPLC of bile acids using the immobilized 3α-HSD enzyme reactor and the NADH chemiluminescence reaction for detection is sensitive enough for the determination of bile acids in human serum. This metod has advantages over previous HPLC methods as since unconjugated bile acids and their glycine and taurine conjugates can be determined simultaneously in a single step using a simple linear methanol gradient without prior fractionation of the sample and prior hydrolysis of the conjugatad bile acids. Although the complicated detection system using three pumps is a disadvantage, this problem may be overcome by improving the system for the delivery of the postcolumn reagent solutions.

ACKNOWLEDGEMENTS

REFERENCES

1 T. Nambera and J. Goto, in K. D. R. Setchell, D. Kritchevsky and P. P. Nair (Editors), *The Bile Acids*, Vol. 4, Plenum Press, New York, 1988, Ch. 2, p. 43.
2 S. Kamada, M. Maeda and A. Tsuji, *J. Chromatogr.*, 272 (1983) 29.
3 T. Kawasaki, M. Maeda and A. Tsuji, *J. Chromatogr.*, 272 (1983) 261.
4 S. Kamada, M. Maeda, A. Tsuji, Y. Umezawa and T. Kurahashi, *J. Chromatogr.*, 239 (1982) 773.
5 L. J. Kricka and T. J. N. Carter (Editors), *Clinical and Biochemical Luminescence*, Marcel Dekker, New York, 1982.
6 K. Imai, K. Miyaguchi and K. Honda, in K. V. Dyke (Editor), *Bioluminescence and Chemiluminescence: Instruments and Applications*, Vol. II, CRC Press, Boca Raton, FL, 1986, Ch. 5, p. 65.
7 R. L. Veazey and T. A. Nieman, *J. Chromatogr.*, 200 (1980) 153.
8 L. L. Klopf and T. A. Nieman, *Anal. Chem.*, 57 (1985) 46.
9 T. Kawasaki, M. Maeda and A. Tsuji, *J. Chromatogr.*, 328 (1985) 121.
10 M. Maeda and A. Tsuji, *J. Chromatogr.*, 352 (1986) 213.
11 K. Tanabe, T. Kawasaki, M. Maeda and A. Tsuji, *Bunseki Kagaku*, 36 (1987) 82.

Polymeric dimethylaminopyridinium reagents for derivatization of weak nucleophiles in high-performance liquid chromatography–ultraviolet/fluorescence detection

CHUN XIN GAO and IRA S. KRULL*

Department of Chemistry and The Barnett Institute (341MU), Northeastern University, Boston, MA 02115 (U.S.A.)

ABSTRACT

This paper introduces a novel polymeric dimethylaminopyridinium 9-fluorenyl-methoxycarbonyl reagent for off-line derivatizations of *weak* nucleophiles in high-performance liquid chromatography. The method of synthesis and characterization of the polymeric reagent via loading determinations is presented and discussed. Derivatization conditions (solvent, time, and temperature) for primary and secondary alcohols were optimized. As one application, off-line derivatizations of 2-chloro-1-propanol, a potential carcinogen in foodstuffs, were carried out with this polymeric reagent with single-blind and standard addition techniques. A specific sample treatment procedure was also developed. The accuracy and precision of the method were determined and data were statistically evaluated.

INTRODUCTION

There are many important natural or man-made organic compounds that contain hydroxyl or thiol functionalities[1,2]. Virtually all such analytes must be derivatized prior to the application of any chromatographic method, mainly because of their often limited volatility [gas chromatography (GC)], poor chromatographic properties [thin-layer chromatography, high-performance liquid chromatography (HPLC)], and especially their limited detectability by all common detection techniques[3]. There are several classes of successful derivatizing reagents for soft nucleophiles, such as alkyl, acyl and silyl reagents, and a large number of reports exist on the use of such reagents for the successful derivatization of hydroxyl, sulfhydryl and/or carboxyl groups. Most of these reagents enhance detectability and sensitivity[4–6]. Almost all derivatizations have been performed in solution, requiring sample preparation, sample work-up, and lengthy reaction times at elevated temperatures.

We have described several polymeric reagents for strong nucleophiles in earlier publications[7–11]. It was shown that the use of solid-phase reagents in HPLC has many advantages over solution reactions. However, none of these polymeric reagents were useful for the derivatization of soft nucleophiles.

There are very few examples in the literature of any successful solid-supported reagents for soft nucleophiles. Only Rosenfeld and co-workers[12–15] have described useful approaches for alcohols or carboxylic acids. However, these reagents were physically adsorbed on a solid support, for off-line reactions in GC, and none of them were covalently bonded solid-phase reagents that could be used off-line or on-line in HPLC. Thus, all derivatizations of these and other classes of weak nucleophiles are performed by solution reactions. They are generally inefficient and time-consuming. Thus, there is a great need for the development and application of faster and more efficient derivatizing reagents for alcohols, thiols, and related soft nucleophile classes, especially solid-phase-attached reagents for off-line and on-line HPLC applications.

In 1967, Litvinenko and Kirichenko[16] discovered that by replacing pyridine as the general base catalyst by 4-dimethylaminopyridine (DMAP) for the solution benzoylation of a m-chloroaniline reaction they could realize an increase in the overall rate of the reaction by $ca.$ 10^4 times. In separate studies, Steglish and Hofle[17] described in 1969 the strong catalytic effect of DMAP in preparative-scale acylation. Since then, a large number of papers have been published in which advantage was taken of the high catalytic activity of DMAP. With acetic anhydrides of acyl halides, for example, for acylating sterically hindered secondary alcohols, such as 1-methylcyclohexanol, 1-ethylcyclohexanol, linalool, 5,5-dimethoxy-2-methyl-3-pentyn-2-ol[18], cis-4-(1-hydroxypropyl)-2-methylcyclohexanone[19], and 1-hydroxycholesterol[20]. DMAP has also been used for acylating sterically hindered hydroxyl groups in carbohydrates, such as methyl sibirosaminide[21] and related sugar derivatives[22]. All of these acylation have been performed under very mild conditions (room temperature, one-half to several hours) with high yields (87–93%).

The enormous increase in acylation rates and the quantitative conversions possible with DMAP as the catalyst have made its use attractive for heterogeneous reactions as well. Hierl et $al.$[23] reported that DMAP was covalently attached to poly(ethyleneimines), which then showed significant catalytic effects in the hydrolysis of nitrophenyl acylates. Shinkai et $al.$[24] described the use of polymer-bound DMAP as an effective catalyst for ester synthesis. Another research group in Japan has also reported a rapid amide synthesis, with high purity, using acid anhydrides with polymer-bound DMAP as the catalyst[25]. A French research group has published a paper showing that polystyrene-supported DMAP exhibited good catalytic activity in acylations of methylcyclohexanol[26].

Patchornik and co-workers[27,28] have described a method for the synthesis of peptides in a "two-polymer system" by using polymer-bound DMAP salts. This work demonstrated the applicability of polymer-bound DMAP as a storable acylium "bank", and its versatility for peptide synthesis was demonstrated. The acylation of amino acids by the acyl-DMAP support was faster than that of the corresponding polymeric o-nitrobenzophenone activated esters, reported earlier by the same group. All of these heterogeneous acylations were aided by the polymer-supported DMAP, and were carried out successfully in terms of batch syntheses in high purity, high yields and diminished reaction times. However, none of these homogeneous or heterogeneous acylation reactions aided by DMAP were related to any analytical or HPLC applications or interfacing.

We have synthesized a polymer-attached DMAP reagent, containing a 9-fluorenylmethoxycarbonyl (FMOC) detector sensitive tag, for the derivatization of

strong and *weak* nucleophiles. This has led to significant improvements in the detectability of primary and secondary alcohols, simplicity, and overall rates of reaction for off-line derivatizations in HPLC. In this paper we discuss the method of synthesis, characterization of the polymeric reagent via loading determinations, and optimization of derivatization conditions (solvent, time and temperature). A number of primary and secondary alcohols were derivatized, as a mixture, and separated under optimized conditions. These peaks could be well separated within 20 min isocratically, by reversed-phase HPLC with resolution (R_s) values of 1.1–1.5.

As one of the possible applications, a method of determination of 2-chloro-1-propanol (CP) in foodstuffs has been developed using "single-blind spiking" and standard addition techniques. CP is used as an important chemical intermediate in the polymer industry[29]. It may be found in wheat products after fumigation with propylene oxide, which reacts with moisture and chlorine from the natural inorganic chloride content of foodstuffs to form the corresponding CP. When CP was identified as a potential carcinogen, it became very significant to monitor it in foodstuffs and environmental samples. There have been a few publications, in the past two decades, describing analytical methods for CP: a chemical method involves the hydrolysis of the distillation product and titration of any chloride liberated from the expected CP[30], and several GC methods were used for the determination of CP in foodstuffs[31–33]. It was reported that the chromatographic performance and sensitivity of these methods were poor. There is no current HPLC method for CP in the literature.

Validated by "single-blind spiking" experiments, our method may become the first HPLC method for quantitation of CP in wheat flour. The accuracy and precision of the method were: standard deviation $< \pm 1.9$, relative standard deviation $< \pm 9.1\%$, and relative error $< 10\%$ for a CP concentration range of 10–50 ppm. The smallest detectable amount of CP recovered from wheat flour was *ca.* 150 ppb[a] after derivatization with this reagent.

EXPERIMENTAL

Chemicals

Macroporous chloromethylstyrene–divinylbenzene copolymer (4% cross-linked, 200–400 mesh, 4.2 mequiv. Cl/g) was obtained from Bio-Rad Labs. (Richmond, CA, U.S.A.). 4-Chloropyridine hydrochloride (99%) and CP were from Aldrich (Milwaukee, WI, U.S.A.), and methylamine (gas at room temperature, 97%) was from Fluka (Ronkonkoma, NY, U.S.A.). Other chemicals were obtained with the highest purity available from Aldrich and J. T. Baker (Phillipsburg, NJ, U.S.A.). HPLC solvents were obtained from EM Science (Cherry Hill, NJ, U.S.A.), (Omnisolv HPLC grade). All HPLC solvents were used after filtration through a 0.45-μm solvent filter (GVWP; Millipore, Bedford, MA, U.S.A.) and degassed under vacuum with stirring.

Apparatus

The HPLC system consisted of a Waters Model 6000A solvent delivery system (Waters Chromatography Division, Millipore, Milford, MA, U.S.A.), a Rheodyne

---

[a] Throughout this article, the American billion (10^9) is meant.
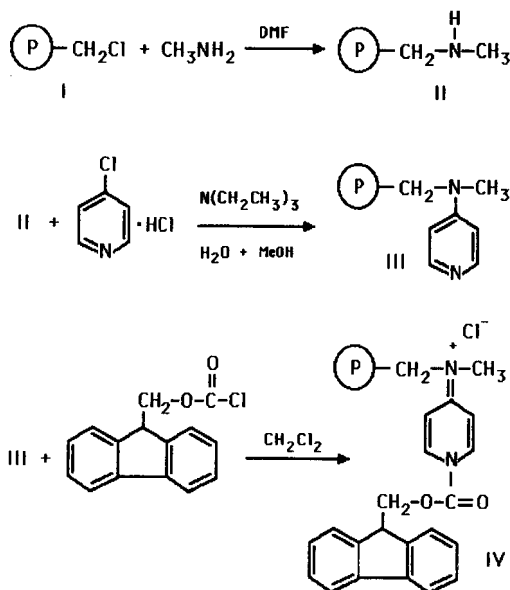
Fig. 1. Synthesis of polymeric DMAP/FMOC reagent. 1 = Chloromethyl styrene–divinylbenzene copolymer; II = polymeric N-methylene methylamine; III = polymeric DMAP; IV = polymeric DMAP/FMOC reagent. DMF = Dimethylformamide; MeOH = methanol.

Model 7010 injection valve with 10- and 20-μl sample loops (Rainin, Emeryville, CA, U.S.A.), a EM Science LiChrospher C_{18} reversed-phase column, 250 mm × 4.0 mm I.D., 5-μm particle size, a Waters Model 480 variable-wavelength UV–VIS detector, a Hitachi Model F1000 fluorescence spectrophotometer, and a Hitachi Model D-2000 ChromatoIntegrator (Hitachi, Naka Works, Mito City, Japan).

The instrumentation used to characterize the synthesized, purified standards consisted of a Varian 300 MHz nuclear magnetic resonance (NMR) spectrometer (Varian Assoc., Palo Alto, CA, U.S.A.), a Perkin-Elmer (PE) Model 599B infrared (IR) spectrophotometer (Perkin-Elmer, Norwalk, CT, U.S.A.), and a Thomas capillary melting point apparatus (Arthur H. Thomas Co., Philadelphia, PA, U.S.A.).

Synthesis of polymeric DMAP/FMOC reagent

The dry polymer (I, Fig. 1) (10 g) was suspended in 15 ml N,N-dimethylform-amide (DMF) and saturated with methylamine gas at 0°C. The vessel was sealed and agitated for 1 day. The polymer was washed successively in dioxane (3 × 30 ml), ethanol (3 × 30 ml), 2 *M* sodium hydroxide–2-propanol (1:1) (3 × 30 ml), water (until eluate neutral), ethanol (3 × 30 ml), and diethyl ether (2 × 30 ml). After drying in vacuum, a white product, polymeric N-methylene methylamine (II, Fig. 1) was obtained.

This product (3.5 g) was swelled in a mixture of water (1 ml), ethanol (2 ml) and triethylamine (5 ml). The excess solvent was evaporated until the polymer was slightly wet. This mixture was transferred to a pressure vessel (obtained from Ace Glass,

Vineland, NJ, U.S.A.), sealed, and heated for 4 days at 140°C. The polymer was washed as before, and unreacted amino groups were blocked by acetylation. This reaction was carried out by treating the polymer with acetic anhydride–dichloromethane (1:1) (5 ml) with stirring at room temperature for 1 h. The polymer was then washed with 2 × 10 ml, as above. The washed polymer was dried to constant weight at 140°C. The product, polymer-bound dimethylaminopyridine (DMAP) (III) was obtained (light brown, 3.4 g).

The anhydrous DMAP polymer (3 g) (III) was swelled in anhydrous dichloromethane and treated with excess FMOC-Cl (3 g) at room temperature with stirring for 1 h. The polymer product .was filtered and washed with dichloromethane under anhydrous conditions until the washings contained negligible amounts of FMOC-Cl (blank tests by HPLC). The polymer was dried under vacuum at room temperature. The final, polymeric DMAP/FMOC reagent (IV) was obtained (light brown, 3.1 g).

Loading determination of the final polymeric reagent

Because the hydrolysis product of the fluorenyl tag was unstable under strong basic hydrolysis conditions[8], a pH-controlled (sodium carbonate buffer) hydrolysis procedure was then developed.

Hydrolysis procedure. The final polymeric reagent (IV), 0.2 g, was suspended in 20 ml of acetonitrile–sodium carbonate (4.1 mM in water) (50:50, v/v). A round-bottom flask (25 ml), containing the mixture, was placed into a water bath at constant temperature (70°C) for 1 h. After it had cooled to room temperature, the mixture was filtered, and washed with a 1:1 mixture of acetonitrile–0.2% HCl, and made to the
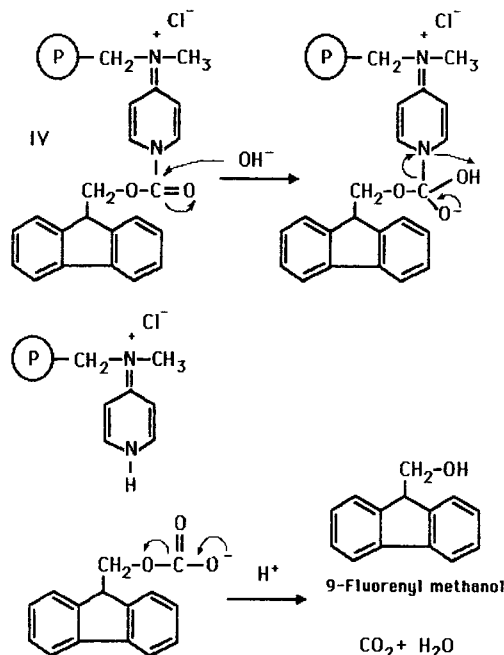
Fig. 2. Hydrolysis of the polymeric DMAP/FMOC reagent.

mark of a 10-ml volumetric flask. After dilution with the same acetonitrile–0.2% HCl mixture, 10 μl of the dilute solution was injected into the HPLC column.

Calibration plot for FMOC methanol. FMOC methanol was the final hydrolysis product (Fig. 2), and this was confirmed by quantitative HPLC–fluorescence detection (FL) *vs.* an authentic standard of FMOC methanol, which is commercially available. A calibration plot of 5–100 ppm of FMOC methanol was constructed to determine the load of final FMOC tag on the polymeric reagent (IV).

Recovery studies. FMOC methanol (100 μg) was added to the polymeric reagent intermediate III (0.3 g). The polymer-containing FMOC methanol was then treated, following the procedures described above. The final solution (20 μl) was injected into the HPLC column for quantitation of the recovered FMOC methanol. HPLC conditions: acetonitrile–0.1% aqueous acetic acid, pH 4 (70:30), 1.0 ml/min, LiChrospher C_{18}, 5 μm, 250 × 4.0 mm I.D., FL excitation wavelength 265 nm, emission wavelength 320 nm.

Elemental analysis for the polymeric reagent

Starting polymer I, polymer intermediate III, and final polymeric reagent IV were dried to constant weight. Three vials, containing 20 mg of each polymer product, were sealed and sent to Galbraith Labs. (Knoxville, TN, U.S.A.) for elemental analysis. Results of the elemental analysis were: starting material I (%C = 79.41, %H = 6.77, %N = <0.10), intermediate III (%C = 86.40, %H = 7.49, %N = 4.53), and final polymeric reagent IV (%C = 79.20, %H = 7.29, %N = 3.69).

Preparation and characterization of the external standards

FMOC-Cl (1.00 g, 3.87 mmol) was added into a 50-ml round-bottom flask containing excess ethanol or 2-propanol (5 ml) and 0.5 ml pyridine and kept at room temperature for 1 h with stirring. Afterwards, the excess solvent was evaporated, methanol (5 ml) was added to dissolve the product, and the mixture was heated to 60°C while distilled water was added dropwise until a turbidity appeared. The suspended mixture was kept at 5°C for crystallization. Pure ethanol FMOC derivative (white crystals) was obtained by recrystallization. Because the 2-propanol FMOC derivative was an oil at room temperature, preparative HPLC was used for purification (Waters μPorasil column, 300 × 7.8 mm I.D., *n*-hexane–2-propanol (90:10), 1.5 ml/min, FL excitation wavelength 265 nm, emission wavelength 320 nm). After purification, ethanol and 2-propanol FMOC derivative standards were characterized on the basis of NMR, IR, HPLC–UV/FL and melting point.

Off-line derivatization of alcohols

The substrate (primary or secondary alcohols, 100 ppm) in chloroform was added via a gas-tight syringe to the polymeric reagent (30 mg) in a closed vial. The capped vial, sealed with Parafilm, was placed in a constant-temperature Al_2O_3 bath at 60°C for 20 min (Fig. 3). The reaction mixture was rinsed with acetonitrile into a 1-ml volumetric flask under positive pressure, and 20 μl of this solution was injected into the HPLC column.

Determination of CP in wheat flour

Single blind spiking. CP solutions in chloroform were added to 1 g of wheat flour,
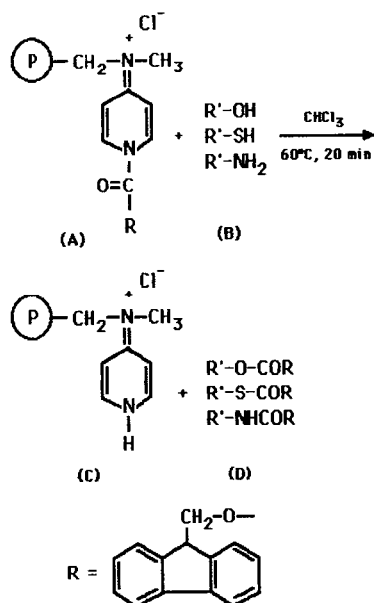
Fig. 3. Derivatization of nucleophiles with polymeric DMAP/FMOC reagent. A = Polymeric reagent; B = nucleophilic substrates; C = polymer backbone; D = derivatives of interest.

at three different concentrations, by another analyst. These spiked samples were then analyzed as samples containing CP at trace levels.

   Sample extraction. Each spiked sample was extracted with 100 ml chloroform. After filtration through Waters Millex-SR filters (0.5 μm) to remove suspended wheat flour particles, the extract was ready for analysis.

Standard addition

   Two different concentrations of CP (20 and 40 ppm in chloroform) were prepared as a set. To each spiked wheat flour sample two additional concentration levels of CP were added. One spiked flour sample without standard addition was used as a blank. These three samples represented one original wheat flour sample. Each derivatized sample was injected into the HPLC system in triplicate. Three-point calibration plots were constructed for the quantitation of CP in individual wheat flour samples.

RESULTS AND DISCUSSION

Nature of the polymeric DMAP/FMOC reagent

   For derivatizing weak nucleophiles, the polymeric reagent should be extremely reactive. The polymeric reagent was intentionally designed to meet this need. Having a quaternary ammonium group in the para position, via a double bond (immonium ion), to the nitrogen containing the FMOC tag, the reagent IV (Fig. 1) is present as a loosely-bound ion pair. The reagent is very labile and highly reactive towards virtually all nucleophiles. However, the polymeric reagent is very sensitive to moisture

and polar solvents. Thus, on-line derivatizations met with failure in both normal- and reversed-phase modes, even when a switching valve was used for selecting derivatization solvents. Nevertheless, the polymeric reagent was very stable when stored at low temperature (5°C) under anhydrous conditions.

FMOC-Cl was again chosen as the tag because: (1) the detection properties of the tag are well known, as discussed in previous papers[8,10]; (2) in the acid chloride form, it can be well retained by the polymeric DMAP backbone[26,27]; and (3) it is commercially available from several manufacturers in high purity and at low cost.

The load, determined by the pH-controlled hydrolysis was 0.2 mequiv./g. Within experimental error, this number agreed with that calculated from the elemental analysis (0.3 mequiv./g). All these numbers were within the normal range of loads quoted in the literature[26,27], indicating that the correct synthetic route was followed, and that the desired polymeric reagent was obtained.

General mechanism of acylation reactions with DMAP

In all acyl-transfer reactions, it is assumed that there are three functions of DMAP. First, it serves as a Brønsted base, B, which can produce an anion, Y^-, from a substance H–Y.

$$H-Y + B \rightleftharpoons Y^- + H-B$$
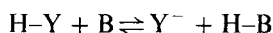
This anion is a better nucleophile than H–Y, and therefore reacts more rapidly with the electrophilic acylating reagent. The extent of general base catalysis depends on the relative basicities of B and Y^-, *i.e.*, on the position of the acid–base equilibrium.

Second, it has been shown that the nucleophilic and sterically hindered base DMAP tends to attack the acylation reagent with formation of a salt-like intermediate. For example, carboxylic anhydrides and pyridine yield small amounts of N-acylpyridinium carboxylates, which, because of their charge, are more capable of transferring an acyl group to a nucleophile than the anhydride itself[33,34]. Even acyl halides react more slowly with nucleophiles than this acylium salt[33]. The extent of this nucleophilic catalysis depends on the reactivity and concentration of the acylium salt, which is, in turn, determined by the position of the equilibrium. However, as a referee has indicated, DMAP does not *always* lead to an increase in the rate of acylation reactions.

Third, once the DMAP salt is formed, it would be stable in solution and on a polymer support[27,28]. It has been estimated that the DMAP salt is about 25 kJ/mol lower in energy than the starting materials[35]. This large shift in equilibrium is caused by a lowering in energy due to the mesomeric stabilization of the N-acyl-4-dialkyl-amino pyridinium ion (Fig. 4). The mesomeric resonance structures do indeed contribute significantly to the stabilization of this anion, and this has been demonstrated by its NMR spectrum[35].

Mechanism of acylation reaction with polymeric DMAP/FMOC reagent

We believe there is a tetrahedral addition/elimination mechanism and a diffusion-controlled process in this heterogeneous reaction. In view of the above concepts and evidence, the polymeric DMAP/FMOC reagent is highly activated by the fact that: (1) the neighboring anion may act as a base catalyst in acetylation reactions; (2) the inductive effect caused by the delocalization of electrons through the pyridine ring
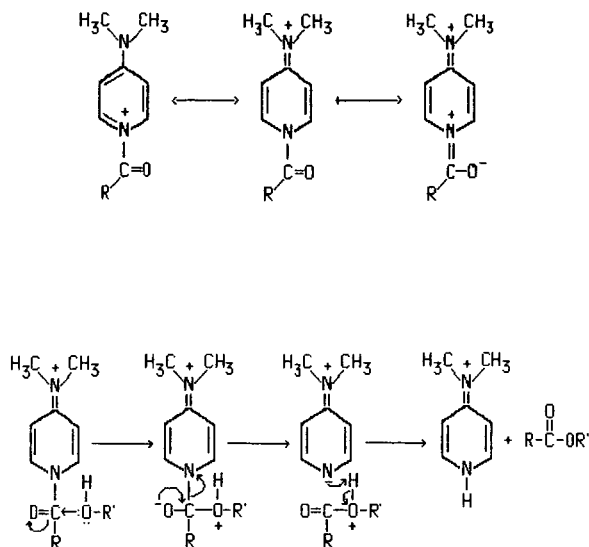
Fig. 4. Resonance structure of DMAP and the mechanism of its reaction with alcohols.

to the quaternary ammonium site makes the carbonyl carbon more electro-positive, susceptible to nucleophilic attack; and (3) attack by a nucleophile occurs at the carbonyl group, with transfer of the pair of electrons to nitrogen, resonance stabilized through the pyridine ring, eventually onto the quaternary nitrogen cation. With strong delocalization, the pyridinium ion may act as a good leaving group, perhaps one of the best imaginable, similar to that derived from the o-nitrobenzophenone phenoxide anion, as described in our earlier publications[8–11]. Thus, it would be expected, by analogy with all solution and polymeric reactions for DMAP already described, that IV should possess even higher reactivity than any of our previously described immobilized reagents.

Characterization of external standards

Simple primary and secondary alcohols (ethanol and 2-propanol) were chosen as the representative weak nucleophiles for evaluation of the polymeric reagent. Authentic tagged standards for each alcohol were synthesized and purified (see Experimental). This was followed by analytical and physical property measurements (HPLC–UV/FL, NMR, IR, melting point and elemental analysis), in order to prove structures. All data are shown in Table I.

All of the analytical and structural data were fully consistent with the expected structures, suggesting that correct and pure FMOC alcohol derivatives were obtained from the synthesis and purification. These compounds were then used as external standards to determine the extent of reactions with the polymeric reagent, under varying conditions.

Solvent optimization

As indicated in the literature[35], the degree of solvation has a strong effect on the

TABLE I

PHYSICAL AND SPECTRAL PROPERTIES OF FMOC ETHANOL AND 2-PROPANOL DERIVA-
TIVES

HPLC conditions: 10-μl injection of 5 ppm of each standard in acetonitrile; acetonitrile–methanol–water
(60:20:20), 1.5 ml/min, FL excitation wavelength 265 nm, emission wavelength 320 nm.

Property	FMOC ethanol	FMOC 2-propanol
Molecular weight	269	282
Melting point (°C)	56°C	liquid at 25°C
HPLC–FL	4.25 min	5.03 min
Elemental analysis[a]	C 76.1% (75.9%); H 6.0% (5.8%)	
NMR	–CH$_3$, 3H (triplet), 1.4 ppm	–(CH$_3$)$_2$, 6H (doublet), 1.3 ppm
	–CH$_2$–, 2H (multiplet), 4.2 ppm	–CH$_2$–, 2H (doublet), 4.4 ppm
	–CH$_2$–, 2H (doublet) 4.4 ppm	–CH–, 1H (multiplet), 4.9 ppm
	Aromatic 8H (multiplet), 7.5 ppm	Aromatic 8H (multiplet) 7.5 ppm
IR	Aromatic C–H stretch, 3040/cm	Aromatic C–H stretch, 3040/cm
	Aliphatic C–H stretch, 2960/cm	Aliphatic C–H stretch, 2960/cm
	Carbonyl C=O vibration, 1750/cm	Carbonyl C=O vibration, 1750/cm
	Ester C–O stretch, 1250/cm	Ester C–O stretch, 1250/cm
		Dimethyl C–H stretch, 1290/cm

[a] Numbers in parentheses are theoretical values.

reactivity of the DMAP reagent. Using an arbitrary, initial setting for temperature and
time, four solvents were evaluated for optimum derivatization yield (Table II).

As expected, the derivatizations of ethanol with the polymeric DMAP/FMOC
reagent proceeded much better in less polar solvents. This can be understood in view of
the fact that the N-acylpyridinium ion pairs do not react themselves, but only
dissociate and solvate in polar solvents, with charges further apart. More separated
charges would decrease the mesomeric stabilization of the reagent, leading to
decreased reactivity. In less polar solvents, charges on the reagent become less spread,
and thus increasing mesomeric stabilization of the N-acylpyridinium ions results. This
leads to an increased expansion of the ion pair, and this, in turn, activates the carbonyl
carbon and facilitates attack of a nucleophile.

Among the solvents tested, chloroform provided the highest derivatization yield.
It was therefore used as derivatization solvent throughout the study. After derivatiza-

TABLE II

SOLVENT OPTIMIZATION FOR OFF-LINE DERIVATIZATIONS OF ETHANOL WITH POLY-
MERIC DMAP/FMOC REAGENT

Conditions: 60°C, 20 min, 100 ppm ethanol; acetonitrile–water (60:40), 1.5 ml/min, LiChrospher C$_{18}$, 5 μm,
250 × 4.0 mm I.D., FL excitation wavelength 265 nm, emission wavelength 320 nm.

Solvent	Derivatization (%) (average ± S.D.)
Acetonitrile	7.8 ± 0.6 (n = 6)
Dioxane	10.1 ± 1.1 (n = 6)
Dichloromethane	27.8 ± 4.7 (n = 9)
Chloroform	30.4 ± 3.2 (n = 9)
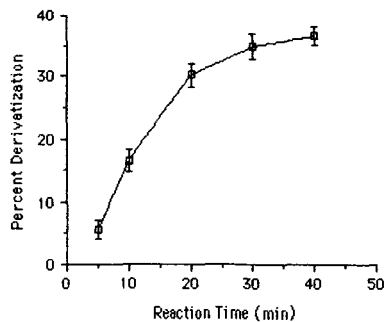
Fig. 5. Optimization of reaction time for off-line solid-phase derivatizations of ethanol. Reaction temperature 60°C; times: 5–40 min; acetonitrile–water (60:40), 1.4 ml/min, LiChrospher C_{18}, 5 μm, 250 × 4.0 mm I.D., FL excitation wavelength 265 nm, emission wavelength 320 nm.

tion in chloroform, acetonitrile was used as washing solvent in view of its good dissolving ability for the derivative and its compatibility with reversed-phase mobile phases.

Time optimization

Using chloroform as the best derivatizing solvent, off-line derivatizations of ethanol were attempted at room temperature. Low yields of derivatizations were obtained. Thus, a higher temperature was needed for more efficient reaction. This is true, especially for a heterogeneous reaction, where the rate of molecular collision/diffusion is highly increased with temperature, leading to a faster reaction. Since chloroform has a low boiling point (62°C), the temperature of 60°C was fixed for the optimization of reaction time and for all experiments throughout the study.

Holding the temperature constant at 60°C, the reaction time was then varied from 5 to 40 min. The results (Fig. 5) show a plot of percent derivatizations *vs.* reaction times. More than 30% derivatization for ethanol was obtained after 20 min at 60°C. Low-percent conversions for these alcohols may be due to high energy barriers in the reaction pathway to the product, leading to a decrease in reaction rates. The frequency factor, *A*, for alcohols, especially for secondary alcohols, may be inherently small, resulting in unfavorable orientation and slow collision rates in the reaction.

This may explain why it is always difficult to derivatize weak nucleophiles, even in solution reactions with highly reactive reagents. Higher-percent derivatization yields can be obtained by using longer reaction times, owing to an increase in collision probability. However, these low-percent derivatizations were still acceptable, because the method was highly sensitive and the results were reproducible. In addition, short reaction times could provide a great saving in analysis time and could reduce the chance of decomposition of the derivatives. Thus, the final, practical derivatization conditions used throughout were: chloroform as derivatizing solvent, acetonitrile as washing solvent, 60°C, and 20 min reaction times. Fig. 6 shows typical chromatograms of ethanol, derivatized with the polymeric DMAP/FMOC reagent, off-line, under optimized conditions, with confirmation by the external standard. Baseline separation and symmetric peaks were obtained.
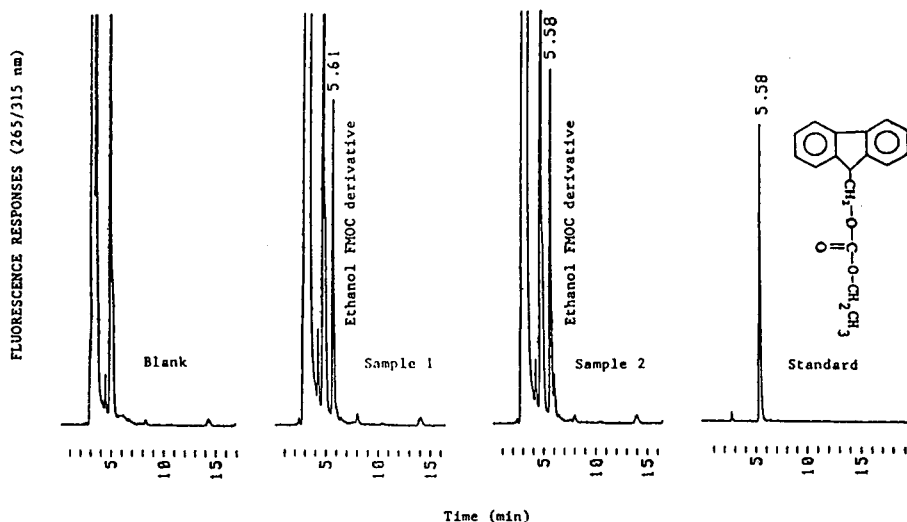
Fig. 6. Chromatograms of ethanol derivatized with polymeric reagent and of the external standard. Conditions: ethanol in dichloromethane (100 ppm), 60°C for 20 min, 10-μl injections for samples and the standard (20 ppm); other conditions as in Fig. 5.

Derivatizations of nucleophiles with the polymeric reagent under optimized conditions

To evaluate the reactivity of the polymeric reagent towards different nucleophiles, further off-line solid-phase derivatizations of strong and weak nucleophiles were investigated under optimized conditions. Ethanol, 2-propanol, and propylamine were prepared in chloroform separately (each at 100 ppm). Off-line derivatizations for individual nucleophiles were then followed at 60°C for 20 min. The results are given in Table III.

The polymeric DMAP/FMOC reagent was very reactive, in view of high-percent yields for a strong nucleophile, propylamine, and lower-percent yields for weak nucleophiles, both primary and secondary alcohols, under optimized conditions. Compared to the percent derivatizations obtained under the same conditions, difficulties were realized in derivatizing weak alcohol nucleophiles (less reactive). It is very clear that alcohols, especially secondary ones, do not show very high reactivity when compared with primary amines. Therefore, it was the reactivity of the analyte,

TABLE III

DERIVATIZATIONS OF DIFFERENT NUCLEOPHILES WITH THE POLYMERIC REAGENT UNDER OPTIMIZED CONDITIONS

60°C for 20 min, off-line derivatizations of separate nucleophiles (each at 100 ppm).

Substrate	Derivatization (%) (average ± S.D., n = 9)
Propylamine	84.2 ± 2.1
Ethanol	31.5 ± 1.5
2-Propanol	7.8 ± 0.7

but not of the polymeric reagent, that dominated the yields in these particular reactions.

Regeneration of the polymeric reagent

Since this solid-phase reagent was a stoichiometric type, a prolonged, continuous usage for a given amount of material resulted in a gradual decrease in percent derivatizations and overall reactivity. Since only the FMOC tag was consumed in reactions with nucleophiles, this left the activated pyridine site on the polymeric support (Fig. 1, III). It was possible to generate the spent polymeric reagent, using the same, last synthetic step initially employed to prepare reagent IV (Fig. 1). Since the pyridinium ion was left after the reaction, the spent polymeric reagent (100 mg) was then washed with a basic mixture, 50% aqueous acetonitrile, 4.2 mM Na$_2$CO$_3$, to remove all unreacted tags. The recovered polymeric intermediate, III, was then obtained. The regeneration (tagging) of the intermediate was performed using the conditions described in the Experimental section. The percent derivatizations with this batch before intentional consumption of tag and after regeneration were measured under optimized off-line reaction conditions (Table IV).

The final reactivity, as evidenced by percent derivatization, was almost equal to that of the fresh reagent. This result suggested that the reactivity of the polymeric reagent could be regenerated by just a simple, one-step tagging reaction. This experiment showed a very significant feature. If the spent reagent is intended to be used again with the original reactivity, it is not necessary to repeat the synthetic procedures from the beginning, but rather to repeat the very last, tagging step of the overall synthetic scheme (Fig. 1). The reagent reactivity could be easily regenerated, leading to simplification of the reagent recycling process and lower cost per analysis.

Shelf-life determination

One of the advantages of using solid-phase reagents is that they obviate the preparation of reagent solutions. The polymeric reagent can be stored at 5°C for prolonged periods of time between use without decrease in reactivity. The shelf-life stability of this polymeric reagent was determined. Percent derivatizations were determined immediately after synthesis of a fresh batch of the polymeric reagent and after it had been stored at room temperature, on the laboratory shelf. The results in Table V suggest that there was very little change in reactivity or percent derivatizations after at least four months of such storage.

TABLE IV

REGENERATION OF POLYMERIC DMAP/FMOC REAGENT

Conditions as in Table II.

Reagent status	Substrate	Derivatization (%) (average $\pm$ S.D., n = 9)
Fresh	Ethanol	28.9 $\pm$ 3.0
	2-Propanol	7.1 $\pm$ 0.6
Base washed	Ethanol	Not detectable
	2-Propanol	Not detectable
Regenerated	Ethanol	27.8 $\pm$ 2.8
	2-Propanol	6.7 $\pm$ 0.5

TABLE V

DETERMINATION OF SHELF-LIFE STABILITY FOR THE POLYMERIC DMAP/FMOC RE-AGENT

Mobile phase: acetonitrile–water (60:40); other conditions as in Table II.

Storage status	Substrate	Derivatization (%) (average ± S.D., n = 9)
Fresh	Ethanol	30.4 ± 3.1
	2-Propanol	7.8 ± 0.3
Four months	Ethanol	28.9 ± 3.0
	2-Propanol	7.1 ± 0.5

Calibration plots for alcohol derivatives and detection limits

This study was performed to understand the working concentration range over which the FL responses would be linear. Calibration plots of FMOC alcohol standard derivatives were constructed, using concentrations *vs.* FL response.

Ethanol and 2-propanol FMOC derivatives were prepared separately at various concentrations (10–15 000 ppb in acetonitrile). Three injections were made for each concentration, and linear calibration plots were then obtained with line equations ($y = -0.1748 + 0.9496x$, $r = 1.00$ and $y = -0.2324 + 0.9066x$, $r = 1.00$). This concentration range was within the normal concentration range for all analytes investigated. These calibration plots were linear, providing validated measurements via external standards.

The fluorescence detector was set at the maximum excitation and emission wavelengths (265/320 nm). Using a signal-to-noise ratio of 2:1, the detection limits of the FMOC alcohol derivatives were 10 ppb and 15 ppb, for the ethanol and 2-propanol FMOC derivative, respectively. The sensitivity of the method is comparable with those reported in the literature[12–16].

Separation of a mixture of alcohols after off-line derivatization

We demonstrated that a variety of typical primary and secondary alcohols could be simultaneously derivatized by a single cartridge of polymeric reagent. In this study, five different alcohols (methoxyethanol, ethanol, 2-propanol, 1-pentanol and 1,8-octanediol) were reacted as a mixture, off-line, under optimized conditions, and derivatives were detected by HPLC–FL. Typical chromatograms for the final derivative mixture are shown in Fig. 7. All five alcohols could be simultaneously derivatized and separated within 16 min. Baseline resolutions were obtained with R_s 1.3–1.5.

A mixture of another class of compounds, nitro alcohols, was also derivatized and separated successfully, using the polymeric reagent under optimized conditions. These compounds are well known as important chemical intermediates in the chemical industry and as bactericides in environmental applications. Baseline separation was also obtained for 2-ethyl-2-nitro-1-propanol (ENP) and 2-nitro-2-methyl-1-propanol (NMP), with R_s value 1.4. The result is shown in Fig. 8.

This method was versatile, and was further validated by the results obtained from the derivatization and separation of additional alcohol substrates. These
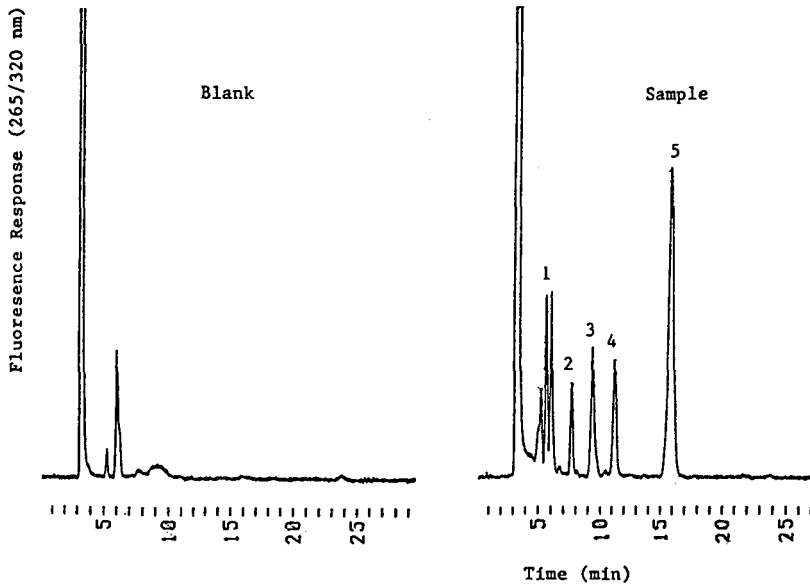
Fig. 7. Chromatograms for off-line solid-phase derivatization of a typical alcohol mixture. Peaks: 1 = methoxyethanol, 100 ppm; 2 = ethanol, 100 ppm; 3 = 2-propanol, 400 ppm; 4 = 1-pentanol, 100 ppm; 5 = 1,8-octanediol, 200 ppm. Mobile phase, acetonitrile–methanol–water (50:10:40); other conditions as in Fig. 5.
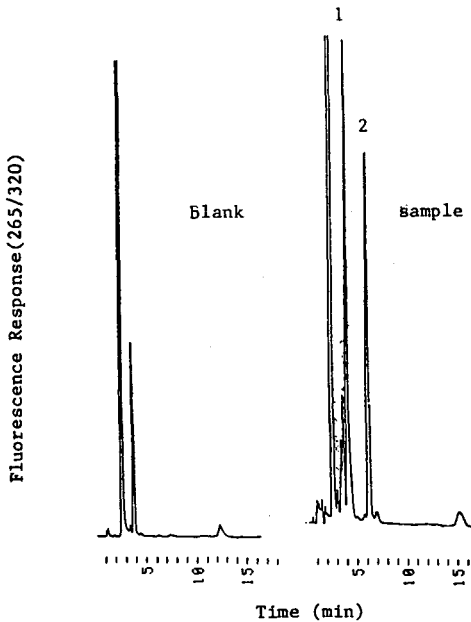
Fig. 8. Chromatograms for off-line solid-phase derivatization of a nitro alcohol mixture. Peaks: 1 = ENP, 200 ppm; 2 = NMP, 200 ppm. Conditions as in Fig. 5.

examples are but a few of the imaginable applications to many important compounds containing hydroxyl groups. We believe that most alcohol-like compounds, especially with primary hydroxyl groups, can be derivatized with this polymeric DMAP/FMOC reagent, and the resulting derivatives can be separated by either normal- or reversed-phase HPLC.

Derivatization of CP with the polymeric reagent

As an application of this polymeric reagent to actual samples, the determination of CP in wheat flour was performed. As stated in the Introduction, this is a potential carcinogen occurring in foodstuffs after fumigation. Because the current GC methods suffer from poor column performance and poor specificity, and there is no HPLC method in the literature for the determination of this compound, it was important for us to develop a new HPLC approach using the polymeric reagent, for the derivatization and quantitation of CP in a complex matrix.

First, we accomplished off-line derivatizations of standard CP after dissolving it in chloroform, using the polymeric reagent under optimized conditions. A single peak was observed, as compared with blanks analyzed under identical conditions (Fig. 9). The peak height for the suspected CP derivative increased with increasing concentration levels of CP derivatized, off-line, with good reproducibility. This confirmed that CP could be derivatized and separated under these conditions.
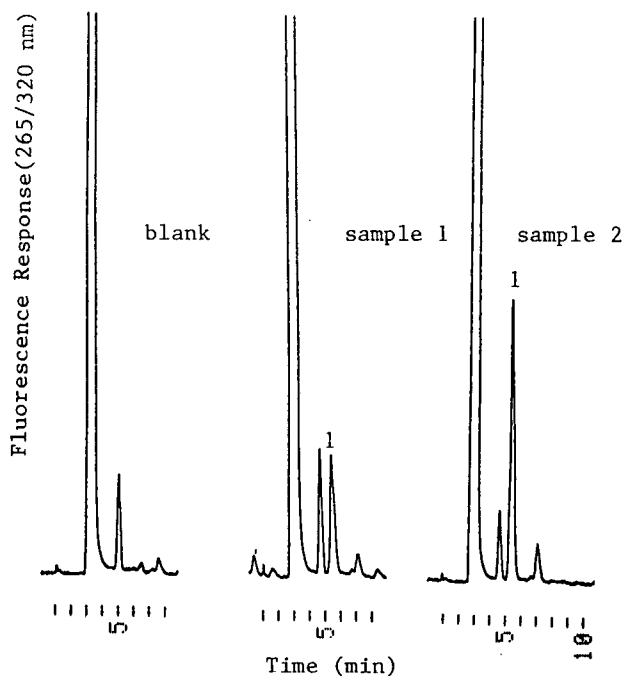
Fig. 9. Chromatogram of CP FMOC derivative after solid-phase derivatization. Peak: 1 = CP FMOC derivative. Conditions as in Fig. 5.

Recovery experiment

Wheat flour sample work-up involved only extraction. Good recovery for CP from the matrix is always desirable, although the recovery is taken into account when the standard addition technique is used. This experiment was designed to show a valid sampling method and sampling efficiency. The concentrations of CP standard (50 ppm in chloroform) before and after addition to wheat flour, followed by the extraction, were determined using the same off-line derivatization conditions. The recovery was 92 ± 3% (*n* = 3), indicating a high sampling efficiency.

Determining minimum detectable amount of CP in wheat flour

To demonstrate the sensitivity of the method for CP recovered from wheat flour, CP standards at different concentrations (0.15–1 ppm in series) were prepared and derivatized off-line, with the polymeric reagent under optimized conditions (60°C for 20 min). Each resulting solution was injected in triplicate into the HPLC system for quantitation. Peak heights and noise levels were measured for each CP concentration tested. The minimum amount of CP that could be derivatized, using the polymeric reagent and FL detection, was 150 ± 15 ppb (*n* = 6) with signal-to-noise ratio 3:1 (Fig. 10). The results showed high sensitivity or low detection limits of the method for the determination of CP in a complex matrix. These detection limits are lower than or comparable to those reported in the literature[29–35].
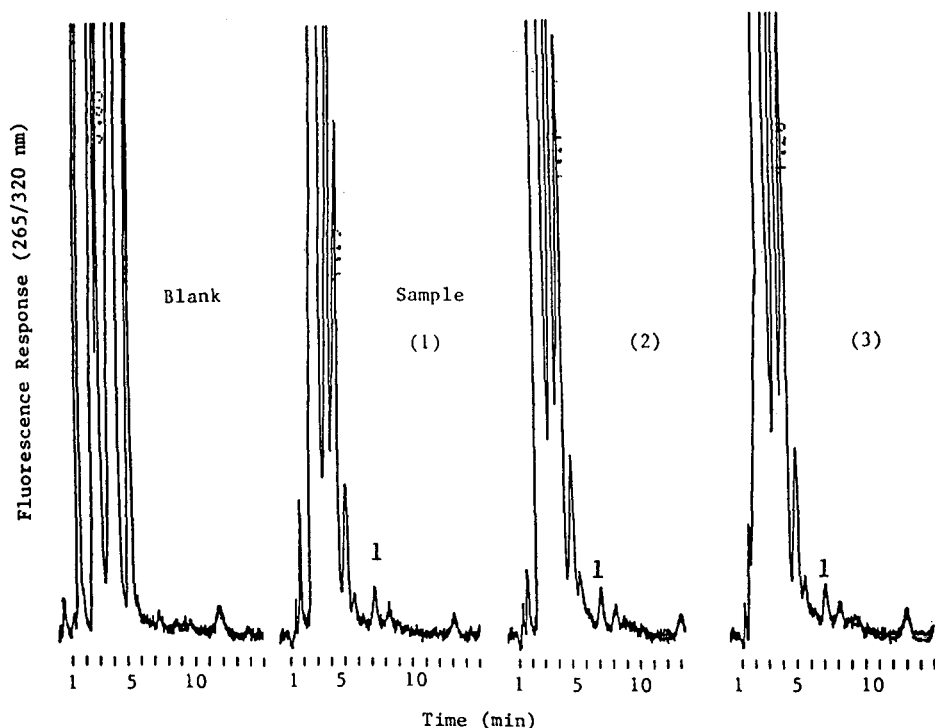
Fig. 10. Chromatogram of minimum detectable amount of CP in wheat flour after derivatization with the polymeric reagent. Peak: 1 = CP, at 150 ppb. Conditions as in Fig. 5.
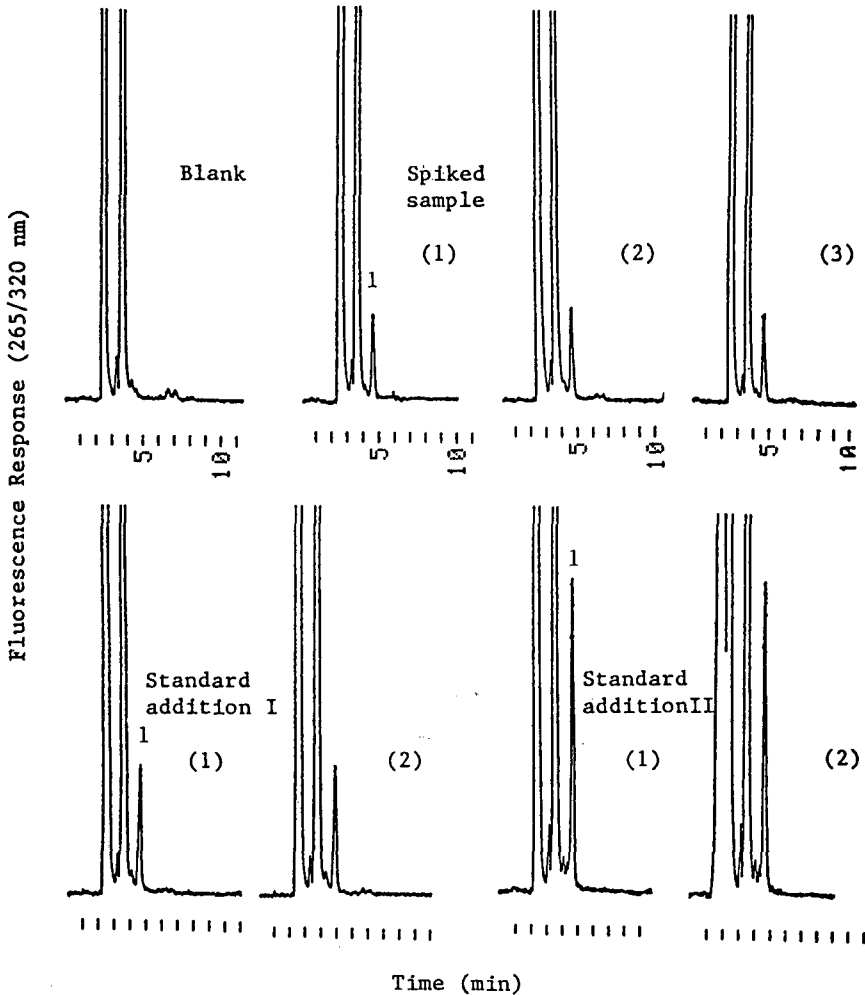
Fig. 11. Chromatograms of CP in wheat flour, derivatized with polymeric reagent and quantitated via standard addition. Peak: 1 = CP FMOC derivative. Reaction detection conditions as in Fig. 5.

Quantitation of CP in wheat flour via standard addition

CP in wheat flour was determined using single-blind spiking procedures. With a minimum of sample work-up (Experimental), off-line solid-phase derivatization, reversed-phase separation, and final FL detection could be accomplished in 45 min per analysis. A standard addition method was used for final quantitation. This could take into account the matrix effect and percent derivatization yields for the analyte, leading to reliable results with good precision and accuracy.

Fig. 11 illustrates typical HPLC–FL chromatograms for one of the spiked wheat flour samples and standard-addition results (increased peak heights), with off-line solid phase derivatization under optimized conditions. Peak symmetry was excellent. Baseline separation with good reproducibility and stability was obtained for each

TABLE VI

DETERMINATION OF 2-CHLORO-1-PROPANOL SPIKED IN WHEAT FLOUR BY STANDARD-ADDITION TECHNIQUE

Reaction detection conditions: 60°C for 10 min. R.S.D. = Relative standard deviation = (S.D./X) × 100, $n = 9$; R.E. = Relative error = (value found − true value)/true value × 100.

Spike level (ppm)	Found (ppm)	R.S.D. (%)	R.E. (%)
10	11.0	9.1	+10
15	13.9	8.6	−7.3
30	28.1	7.1	−6.3

wheat flour sample. Most interferences in the wheat flour sample were removed after extraction and filtration. Finally, by carefully choosing the mobile phase composition, any interfering derivatized and/or underivatized impurity could be eluted with the solvent front, or as earlier-eluted peaks, totally separated from the CP FMOC derivative of interest.

Each wheat flour sample (with standard added samples as a set of three) was injected in triplicate. Three-point calibration plots were then constructed for each spiked wheat flour sample. The quantitation results are given in Table VI. The relative standard deviations (R.S.D.) were <9.1%, indicating good reproducibilities for these spiked wheat flour samples. These errors could be further reduced with more careful sample handling, preparation, and spiking. R.S.D. values were comparable to those for other CP assays in the literature[29-35]. Accuracy of the method is evident from the relative errors, which were less than 10%.

A polymeric DMAP chiral reagent for enantiomer recognition

We have prepared the first polymeric DMAP chiral reagent containing the FMOC-L-proline tagging species. This polymeric chiral reagent has been characterized via hydrolysis and elemental analysis. The polymeric chiral reagent was used successfully, off-line, for the derivatizations of chiral primary alcohols, such as (±)-cyclohexenyl-4-methanol. The expected diastereomers were formed and confirmed by external standards prepared via solution reactions. The resulting diastereomers were separated by normal-phase TLC. We are now optimizing reaction conditions, such as solvent, temperature, time, and so forth, to increase percent derivatizations towards chiral or achiral alcohols. The resulting diastereomers should be separable using reversed- or normal-phase HPLC.

REFERENCES

1 E. O. A. Haahti and H. M. Fales, *J. Lipid Res.*, 8 (1967) 131.
2 M. A. Carey and A. F. Persinger, *J. Chromatogr. Sci.*, 10 (1972) 537.
3 D. R. Knapp, *Handbook of Analytical Derivatization Reactions*, Wiley, New York, 1979, pp. 27–29.
4 R. B. Watts and R. G. O. Kekwick, *J. Chromatogr.*, 88 (1974) 15.
5 M. Donike, *J. Chromatogr.*, 78 (1973) 273.
6 M. Donike, *J. Chromatogr.*, 42 (1969) 103.
7 C. X. Gao, T. Y. Chou, S. T. Colgan, I. S. Krull, C. Dorschel and B. Bidlingmeyer, *J. Chromatogr. Sci.*, 26 (1988) 449.
8 C. X. Gao, I. S. Krull and T. Trainor, *J. Chromatogr.*, 463 (1989) 192.
9 C. X. Gao and I. S. Krull, *J. Pharm. Biomed. Anal.*, 7 (1989) 1183.
10 C. X. Gao, T. Y. Chou and I. S. Krull, *Anal. Chem.*, 61 (1989) 1538.
11 T. Y. Chou, C. X. Gao and I. S. Krull, *Anal. Chem.*, 61 (1989) 1548.
12 J. Rosenfeld, *Anal. Lett.*, 10 (1977) 917.
13 J. M. Rosenfeld and R. A. McLeod in D. J. Harvey, W. Paton and G. G. Nahas (Editors), *Marihuana '84: Proceedings of the Oxford Symposium on Cannabis*, IRL Press, Oxford, 1985, p. 151.
14 J. M. Rosenfeld, M. Mureika-Russell and A. Phatak, *J. Chromatogr.*, 283 (1984) 127.
15 J. Rosenfeld, *The Cannabinoids: Chemical, Pharmacologic, and Therapeutic Aspects*, Academic Press, New York, 1984, p. 151.
16 L. M. Litvinenko and A. I. Kirichenko, *Dokl. Akad. Nauk SSSR, Ser. Khim.*, 176 (1967) 97; *Chem. Abstr.*, 68 (1968) 68325u.
17 W. Steglish and G. Hofle, *Angew. Chem., Int. Ed. Engl.*, 8 (1969) 981.
18 G. Hofle and W. Steglish, *Synthesis*, (1972) 619.
19 J. E. McMurry, J. H. Musser, M. S. Ahmad and L. C. Blaszczak, *J. Org. Chem.*, 40 (1975) 1829.
20 D. H. R. Barton, R. H. Hesse, M. M. Pechet and E. Rizzardo, *J. Am. Chem. Soc.*, 95 (1973) 2748.
21 A. S. Mesentsev and V. V. Kuljaeva, *Tetrahedron Lett.*, (1973) 2225.
22 H. Paulsen and H. Homhne, *Carbohydr. Res.*, 58 (1977) 484.
23 M. A. Hierl, E. P. Gamson and I. M. Klots, *J. Am. Chem. Soc.*, 26 (1979) 6020.
24 S. Shinkai, H. Tsuji, Y. Hara and O. Manabe, *Bull. Chem. Soc. Japan*, 54 (1981) 631.
25 S. Takimoto, T. Kamikihara, Y. Kodera and H. Ohta, *Fukuoka Daigaku Rigaku Shuho*, 15 (1985) 89.
26 F. Guendouz and R. Jacquier, *Tetrahedron Lett.*, 25 (1984) 4521.
27 Y. Shai, K. A. Jacobson and A. Patchornik, *J. Am. Chem. Soc.*, 107 (1985) 4249.
28 A. Patchornik, *ChemTech*, Jan. (1987) 58.
29 F. Wesley, F. Rourke and O. Darbishire, *J. Food Sci.*, 36 (1965) 1037.
30 E. H. Pfeiffer and H. Dunkelberg, *Food Cosmetic Toxicol.*, 18 (1980) 115.
31 E. P. Ragelis, B. S. Fisher and B. A. Klimeck, *J. Assoc. Off. Anal. Chem.*, 49 (1966) 963.
32 E. P. Ragelis, B. S. Fisher, B. A. Klimeck and C. Johnson, *J. Assoc. Off. Anal. Chem.*, 51 (1968) 709.
33 W. von E. Doering and W. E. McEwen, *J. Am. Chem. Soc.*, 73 (1951) 2104.
34 A. R. Fersht and W. P. Jencks, *J. Am. Chem. Soc.*, 92 (1970) 5432.
35 G. Hofle, W. Steglish and H. Vorbruggen, *Angew. Chem., Int. Ed. Engl.*, 17 (1978) 569.

CHROMSYMP. 1890

Use of a focusing cylindrical lens for increasing sensitivity in the optical detector of a capillary flow-through cell

TAKAO TSUDA* and YASUFUMI KOBAYASHI

Department of Applied Chemistry, Nagoya Institute of Technology, Gokiso-cho, Showa-ku, Nagoya 466 (Japan)

ABSTRACT

In capillary column liquid chromatography, a cylindrical flow-through cell is often used in absorbance detection. The cross-sectional shape of the cylindrical flow-through cell perpendicular to the light beam is rectangular. Therefore, the optimum shape of the focused light beam is also rectangular. The use of a cylindrical lens to obtain a rectangular light beam, thus increasing the sensitivity of the UV detector more than 10-fold, is described.

INTRODUCTION

For optimum results, the cell volume of a UV absorbance detector should be extremely small in capillary column liquid chromatography and capillary electrophoresis. This cell volume is much smaller than the volume of conventional liquid chromatographic cells. It is very important to achieve high sensitivity when using such a small cell for detecting trace components separated in the capillary column. Preservation of flow dynamics and separation efficiency in capillary high-performance liquid chromatography or capillary electrophoresis demands a cylindrical detector flow-through cell (CF cell)[1–4]. In most experiments with capillary columns, a cylindrical cell has been used. Theoretical and geometrical treatments[3] and refractive index of CF cells[5] have been extensively discussed. A cylindrical cell is usually oriented perpendicular to the light beam and its path length is therefore equal to the capillary inner diameter (*e.g.*, 0.1–0.01 mm) and its cross-section perpendicular to the light beam is rectangular. For optimum sensitivity, the cell length perpendicular to the light beam should be increased until the decrease in separation efficiency becomes *ca.* 5%. Both the light path length and cross-sectional area of the CF cell are considerably smaller than those used in conventional liquid chromatography (*ca.* 1% of the size). The stability of the photocell and photomultiplier in the UV detector depend on the amount of light reaching the photocell and the area illuminated. Both of these factors for CF cells used with capillary columns are extremely small in comparison with cells for conventional columns. As a result, CF cells for capillary columns exhibit baseline instability.

As mentioned above, the cross-sectional shape of the cylindrical flow-through cell is rectangular. Therefore, for optimum results the shape of the focused light beam should also be rectangular. To produce a rectangular shape, we used a cylindrial lens for focusing the light. We examined the effects of a cylindrical lens both on sensitivity and the signal-to-noise ratio, and describe the use of relatively wide slits in conjunction with the cylindrical lens.

EXPERIMENTAL

The liquid chromatographic system consisted of a pump (Microfeeder MF-2; Azuma Denki Kogyo, Tokyo, Japan), and injector (Model 7520, 0.02 μl; Rheodyne, Cotati, CA, U.S.A.), an open-tubular capillary column (60 cm × 50 μm I.D.) of fused-silica capillary tubing with an unmodified surface (Shinwa Kakou, Kyoto, Japan) and either a UV double-beam detector at 254 nm (light source, deuterium lamp; arrangement of light path, two mirrors and a grating; type, SPD-1; Shimadzu, Kyoto, Japan) or a fluorescence detector with excitation at 345 nm and emission at 520 nm (RF-535; Shimadzu). Methanol at a flow-rate of 4.19 μl/min was used as the eluent and dansylated alanine in methanol solution (10^{-3} M) as a sample. One end of the column itself was used as the cylindrical flow-through cell. The polyimide coating at the end of the column was removed by using a micro-flame. A focusing cylindrical plano-convex lens (focal length 15 mm, size 10 × 10 mm, made of synthetic quartz, Model CLSQ-1010-15P; Sigma Kohki, Irima-gun, Saitama, Japan) was connected to the cell housing, shown in Fig. 1, at the UV absorption detector. The lens was moved in the
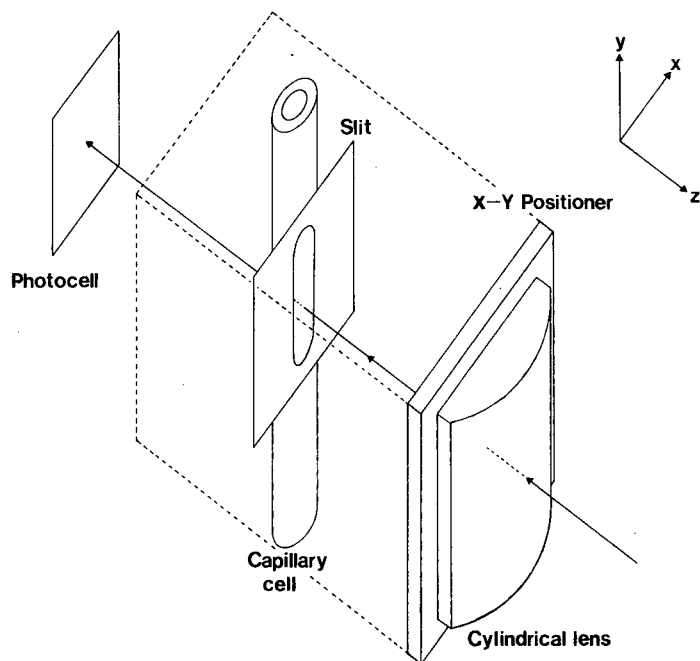
Fig. 1. Schematic diagram of the device for UV absorption detection.

X and Y directions by means of a manual positioner (Sigma Kohki). A slit was positioned in one of two locations. In one configuration, the slit was attached to the outside wall of the CF cell, as shown in Fig. 1. The slit was 50 μm wide and 0.8 mm long (kindly donated by Yokogawa Denki, Tokyo, Japan). This size is commonly used in capillary electrophoresis experiments.

In a second configuration, a slit (0.8 mm wide) was attached to the surface of the cylindrical lens (In Fig. 1, the slit on the CF cell was removed and the second slit was attached to the cylindrical lens). With this configuration, we could use a wider slit owing to the magnification of the CF cell by the cylindrical lens.

With fluorescence detection using an instrument with a xenon lamp, made for liquid chromatography, a long CF cell (5 mm) was used to provide sufficient sensitivity. The positioning of the CF cell and the slit were checked with a visible laser beam. The response of the detector was recorded with a data handling instrument (CR-4A; Shimadzu). All reagents used were of analytical-reagent grade.

RESULTS AND DISCUSSION

The focusing cylindrical lens attached to the cell housing was adjusted by an x–y positioner until the response of the photocell was maximized. The distance between the lens and the CF cell (z axis) was set approximately equal to the focal length of the lens. The cell image had a width of 0.8 mm when the cell inner diameter and the magnification of the lens were 50 μm and 16, respectively. A slit was positioned either on the outside wall of the CF cell or on the surface of the lens. The positioning of the lens in front of the CF cell offers several advantages. First, by using a cylindrical lens, we are able to focus most of the light beam on the capillary flow-through cell. Therefore, by focusing, the beam is 16 times more intense than it would be without using the lens. Second, the light beam is focused on a line drawn vertically through the centre of the capillary cell by the cylindrical lens. Third, we can use a wider slit, *e.g.*, 0.8 mm, for the CF cell of 50 μm I.D. if we position the slit on the surface of the lens. This slit is less expensive to produce and easier to position than the slit mounted on the CF cell.

The schematic arrangement for UV detection is shown in Fig. 1. The slit, which is a rectangle 50 μm wide and 0.8 mm long, is attached to the outside wall of a capillary tube by epoxy adhesive. The positioning of the slit is carefully accomplished under a microscope. With the slit in place, chromatograms obtained with and without the cylindrical lens are shown in Fig. 2, and count numbers of peaks are shown in Table I. From these we conclude that we have obtained peak heights with the lens which are eleven times larger than those obtained without the lens under the same conditions. By using a cylindrical lens to focus the light beam we can obtain a higher sensitivity as a result of the first two advantages above. The use of a cylindrical lens instead of a simple focusing plano-convex lens for focusing the ligh beam is considerably superior for the CF cell because the rectangular shape of the focused light beam by a cylindrical lens corresponds to the rectangular shape of the CF cell. Therefore, we can focus a much greater portion of the light beam on the cell by using a cylindrical lens than we can by using a simple focusing plano-convex lens.

Using a UV detector we examined the effect on the response and signal-to-noise ratio of a slit positioned on the surface of the cylindrical lens. The peak heights with the
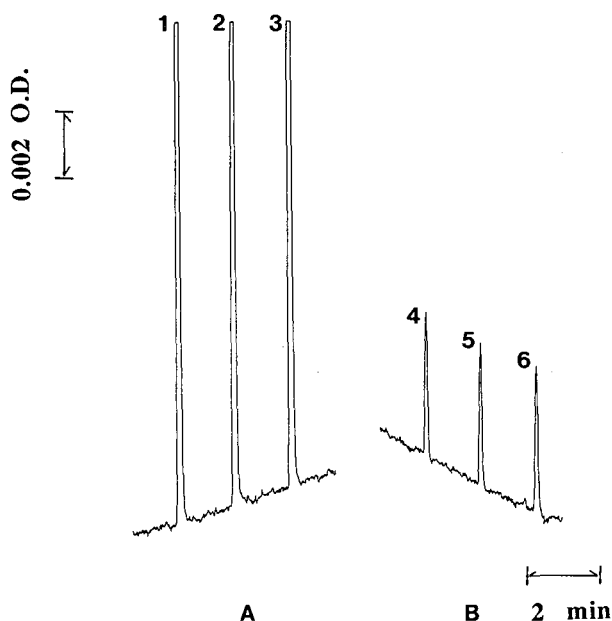
Fig. 2. Comparison of peaks obtained with and without a cylindrical lens (0.02 a.u.f.s.). Peaks 1–3 were obtained with and peaks 4–6 without a cylindrical lens.

slit in place were more than ten times greater than those when no slit was used. As the coherence of the light beam from the deuterium lamp is not good, stray light is a problem when we position the slit away from the cell, such as on the lens surface. Although a slit which is positioned directly on the outside wall of the cell is very effective for excluding stray light, it is much more difficult to position than a slit of large width located on the lens.

In summary, improved detection sensitivity can be achieved by using a cylindrical lens and a slit positioned either on the capillary flow-through cell or directly on the surface of the lens. The slit is easier to make (wider) and position on the surface of

TABLE I

PEAK HEIGHT AND PEAK AREA (COUNT NUMBER)

The count numbers were obtained by a data handling instrument.

Arrangement	Peak No.[a]	Peak height	Peak area
With	1	4869	24632
cylindrical	2	4922	25376
lens	3	4947	24746
Without	4	425	2246
cylindrical	5	425	2109
lens	6	435	2331

[a] Peak numbers correspond to Fig. 2.

the lens than a slit that is positioned on the cell. On the other hand, the slit positioned directly on the cell eliminates more stray light.

The use of a cylindrical lens in conjunction with a slit is also effective for improving fluorescence detection. In this instance, we could place a cylindrical lens in front of the cell housing and a second cylindrical lens, for collecting the fluorescent light, mounted on the flow-through cell, but oriented 90° from the first lens. This second lens would have a slit placed on the lens and a cut filter (passing wavelengths longer than 440 nm) placed in front of the photomultiplier. The sample was 0.2 μl of 10^{-6} M dansylated alanine in methanol. By using this device, the noise level decreased by one third (the height of the noise on the strip chart improved from 9 to 3 mm). The peak heights with this device were 14.5 cm and without it 17.5 cm. Therefore the signal-to-noise ratio was improved by a factor of about 2.5. The present device is useful for both capillary liquid chromatography and capillary electrophoresis.

In ordinary commercial instruments made for liquid chromatography, the focusing area of the light beam is about 1 mm^2. Therefore, it is necessary to focus the light beam when we use a capillary flow-through cell of 50 μm I.D. For this purpose we can use either a plano-convex lens or a cylindrical lens. There are certain advantages in using a cylindrical instead of a plano-convex lens. First, the shape of the light beam is rectangular. Second, intense light does not destroy the fluorophor owing to the smaller amount of light intensity per unit area if the total amount of light is equal for both a plano-convex and a cylindrical cell device. Third, saturation of fluorescence might be less likely when using a cylindrical lens. There are also disadvantages in using a cylindrical lens. The cell length is longer than that when a plano-convex lens is used. In this study we used a CF cell 0.8 mm in length. In ordinary capillary zone electrophoresis and micro-column liquid chromatography, the decrease in theoretical plate number might be less than 5% under the above conditions[6].

Hence the most favorable arrangement would utilize both a cylindrical and a plano-convex lens for focusing a light beam on a capillary flow-through cell.

REFERENCES

1 T. Tsuda, K. Hibi, T. Nakanishi, T. Takeuchi and D. Ishii, *J. Chromatogr.*, 158 (1981) 227–232.
2 F. J. Yang, *J. High Resolut. Chromatogr. Chromatogr. Commun.*, 4 (1981) 83–85.
3 M. Novotny, in P. Kucera (Editor), *Microcolumn High-Performance Liquid Chromatography (Journal of Chromatography Library*, Vol. 28), Elsevier, Amsterdam, 1984, Ch. 7.
4 J. W. Jorgenson, *Anal. Chem.*, 58 (1986) 743A–760A.
5 R. E. Synovec, *Anal. Chem.*, 59 (1987) 2877–2884.
6 S. Terabe, K. Otsuka and A. Ando, *Anal. Chem.*, 61 (1989) 251–260.

Direct injection of blood samples into a high-performance liquid chromatographic adenine analyser to measure adenine, adenosine and the adenine nucleotides with fluorescence detection

HIROYUKI FUJIMORI*

Faculty of Pharmaceutical Sciences, Setsunan University, 45–1, Nagaotoge-cho, Hirakata, Osaka 573-01 (Japan)

TOORU SASAKI, KIYOKATSU HIBI and MASAAKI SENDA

JASCO, Japan Spectroscopic Co., Ltd., 2967–5, Ishikawa-cho, Hachioji City, Tokyo 192 (Japan)

and

MASANORI YOSHIOKA

Faculty of Pharmaceutical Sciences, Setsunan University, 45–1, Nagaotoge-cho, Hirakata, Osaka 573-01 (Japan)

ABSTRACT

Adenine (Ade), adenosine (Ado) and its nucleotides such as AMP, cAMP, ADP and ATP in blood or plasma were determined by a high-performance liquid chromatographic (HPLC) adenine analyser with fluorescence detection. In order to inject samples directly into the HPLC system without pretreatment except dilution, the analyser consisted of two systems each, having three columns (pre-, mini- and analytical). A precolumn with an inlet filter of pore size 40 μm was common to both systems and packed with Butyl-Toyopearl 650-M to remove hydrophobic compounds and blood cell membranes. In the system for analysis of the nucleotides, a mini-column of Hitachi anion-exchange gel 3013-N was used for adsorbing AMP, cAMP, ADP and ATP. The adsorbed nucleotides were separated by the Hitachi gel 3013-N analytical column. In the other system for analysis of Ado and Ade, they were adsorbed on a Develosil ODS-5 mini-column and separated by an Asahipak GS-320H size-exclusion analytical column. The adenine compounds in each eluate were derivatized on-line in a 15-m reaction coil at 115°C with bromoacetaldehyde as the fluorescent reagent in each mobile phase for the analytical column, and detected by spectrofluorimetry.

ATP, ADP and AMP were accurately determined by the direct injection of hamster, rat and human whole blood. Authentic Ade and Ado were well separated and Ado in human plasma was determined, but it was difficult to determine it in rat plasma owing to interference from an unknown compound.

INTRODUCTION

ATP, ADP, AMP, cAMP, adenosine (Ado) and adenine (Ade) are involved in a series of metabolic pathways in biological systems, not only producing carriers of high energy but also playing important roles as chemical mediators[1].

Yoshioka and co-workers[2-5] reported that adenine compounds were converted with bromoacetaldehyde as a fluorescent reagent into fluorescent derivatives, which were systematically determined by high-performance liquid chromatography (HPLC) with fluorescence detection. In one system described by Yoshioka and co-workers[2,4,5], adenine compounds from biological samples such as blood and cultured cells were extracted with perchloric acid and then prederivatized with the aldehyde. In the other system[3], the extracted compounds were separated and derivatized on-line with a prototype analyser. In these analyses, pretreatment of the samples was essential in order to maintain the efficiency of the columns. The conditions for pretreatment were critical to prevent the degradation of adenine nucleotides.

In this study, we tried to develop methods for the direct injection of biological samples, including cells, into the prototype analyser without any pretreatment such as deproteinization, except sample dilution. The method consisted of two systems, one for analyses of anionic compounds such as ATP, ADP, cAMP and AMP, and the other for analyses of the neutral compounds such as Ado and Ade.

EXPERIMENTAL

Materials

Bromoacetaldehyde was prepared and crystallized according to the method of Schukovskaya *et al.*[6]. Butyl-Toyopearl 650-M (BT 650-M) (44-88 μm) was purchased from Tosoh (Tokyo, Japan). Hitachi gel 3013-N (3 μm), consisting of particles of macroreticular anion-exchange resin that had been sieved from the original size of mean diameter 5 μm, was kindly provided by Hitachi (Tokyo, Japan). Develosil ODS-5 (ODS-5) (5 μm) was kindly provided by Mr. M. Nomura (Nomura Chemical, Aichi, Japan). Asahipak GS-320H for size exclusion was donated by Asahi Chemical Industry (Kanagawa, Japan).

All adenine compounds were dissolved in 0.1 M phosphate buffer (pH 7.0) to make 0.5–10 μM standard solutions and stored at $-80°C$ until HPLC analysis. β-Nicotinamide adenine dinucleotide (NAD), flavine adenine dinucleotide (FAD) and adenosine-5'-diphosphoribose (ADP-ribose), obtained from Sigma (St. Louis, MO, U.S.A.), were dissolved in 0.1 M phosphate buffer to make 10 μM solutions. Other chemicals were of analytical-reagent grade.

Columns

For the determination of the nucleotides, a common precolumn (3 cm × 4.6 mm I.D.) with an inlet filter of pore size 40 μm was packed with BT 650-M to remove cell debris and proteins, and a mini-column (1 cm × 4.0 mm I.D.) to adsorb only the nucleotides and an analytical column (5 cm × 4.6 mm I.D.) were packed with Hitachi gel 3013-N. For determination of Ade and Ado, a precolumn packed with BT 650-M was used, a mini-column (3 cm × 4.6 mm I.D.) to adsorb Ade and Ado was packed with ODS-5 and the analytical column (25 cm × 7.6 mm I.D.) was packed with

Asahipak GS-320H. The inlet and outlet filters of the columns, except the precolumn, were equipped with filters of pore size 2 μm.

Analyser system for determination of adenine nucleotides

A flow diagram of the analyser is shown in Fig. 1. The precolumn at ambient temperature was equilibrated with 10–20% (v/v) acetonitrile in water as eluent I and the mini-column and the analytical column were equilibrated with a mixed solution of 0.008–0.1 M bromoacetaldehyde (finally selected as 0.05 M), 0.15 M sodium chloride and 15% acetonitrile containing 0.025 M citrate buffer (pH 4.0) (eluent II). Just before the sample injection, the pre- and mini-columns were connected with each other. After a 10-μl sample injection, eluent I was passed through the precolumn into the mini-column at a flow-rate of 0.1–0.5 ml/min for 2–10 min (optimally 0.3 ml/min for 4 min) to adsorb the nucleotides on the mini-column. Then the mini-column was connected with the analytical column maintained at 45°C and eluted with eluent II at a flow-rate of 0.3 ml/min. The eluate was heated in a reaction coil of 3–18 m × 0.25 mm I.D. at 70–125°C (15 m at 115°C was finally selected) with an FIU Reaction Unit RU-150F (Jasco) which was filled with polyethylene glycol 400, and detected using a Model 820-FP spectrofluorimeter (Jasco). The wavelengths of excitation and emission were set at 254 and 400 nm, respectively. One division of relative fluorescence intensity (RFI) corresponded to 1.5 mV. The chart speed of the recorder was set at 0.5 cm/min.

Analyser system for determination of Ade and Ado

The flow diagram of the analyser is as shown in Fig. 1. The pre- and mini-columns at ambient temperature were equilibrated with 0–7% (v/v) acetonitrile as eluent I'. The analytical column maintained at 40°C was equilibrated with 0.05 M bromoacetaldehyde–0.15 M sodium chloride–15% acetonitrile containing 0.025 M citrate buffer (pH 5.0) (eluent II'). After a 10-μl sample injection, Ado and Ade were adsorbed on the mini-column by passing eluent I' at a flow-rate of 0.3 ml/min for 2–6 min (finally selected as 4 min). After the adsorption, the mini-column was connected
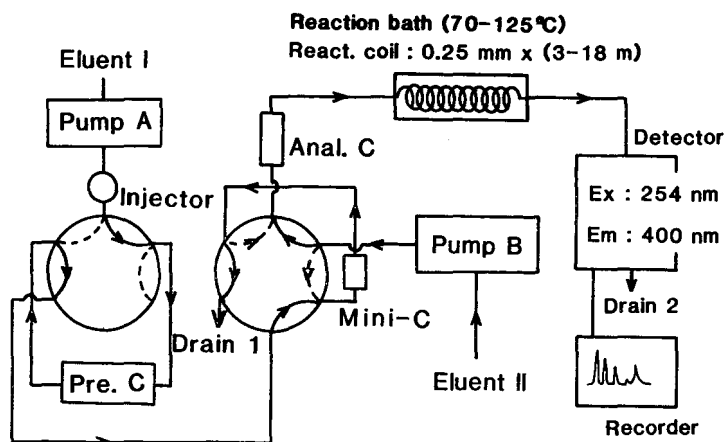
Fig. 1. Schematic diagram of the analyser.

with the analytical column and eluted with eluent II′ containing bromoacetaldehyde at a flow-rate of 0.5 ml/min. The eluate was heated and monitored as described above. The chart speed of the recorder was set at 0.3 cm/min.

Determination of adenine compounds in blood and plasma

Hamster or rat whole blood from a common carotid vein or human whole blood from a brachial vein was taken by using a 1-ml plastic disposable syringe rinsed with 1 ml of physiological saline (0.9%) containing heparin (100 U/ml). To measure systematically the nucleotides in the whole blood, 5 μl of the blood were diluted 10–100-fold with 0.32 M sucrose and 10 μl of the diluted solution (net injection volume of 0.1–1 μl of the blood) was injected into the analyser system.

Blood from a healthy human volunteer's (10 ml) was withdrawn from a brachial vein into a 50-ml plastic disposable syringe containing 10 ml of a mixed solution of 20 U heparin, 0.01% (w/v) dipyridamol and 10 mM manganese chloride. The blood was centrifuged at 600 g for 5 min at 4°C and the resulting supernatant plasma was stored at −80°C until use. To determine Ado and Ade, 10 μl of the plasma were injected into the analyser system.

RESULTS

The adenine nucleotides were well separated by the analyser system and eluted from the Hitachi gel 3013-N analytical column in the order AMP, cAMP, ADP and ATP, as shown in Fig. 2. The analytical time was *ca.* 26 min. Ade and Ado were not detected by the present analyser system despite injecting large amounts (100 nmol each) of Ade and Ado as they were not adsorbed on the mini-column. Hence the developed system was specific for determination of the adenine nucleotides, as expected.

The effect of the acetonitrile concentration in eluent I on the peak heights of
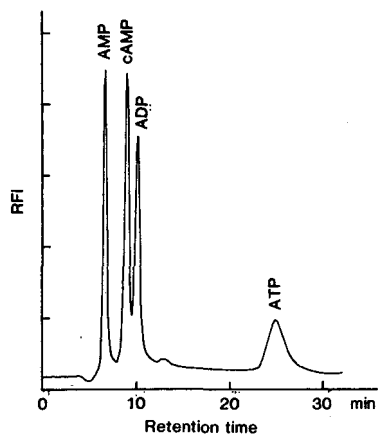
Fig. 2. Chromatogram of authentic adenine compounds obtained with the analyser for nucleotides. A 10-μl volume of 3 μM adenine compounds in 0.1 M phosphate buffer (pH 7.0) was injected into the analyser system. The retention time means the time elapsed just after the connection of the mini- with the analytical column.

ATP, ADP and AMP was examined in the range 10–20%. As all the peaks at 15% acetonitrile were the heighest, this concentration was adopted. A flow-rate of eluent I of 0.3 ml/min gave the best results in the range 0.2–0.5 ml/min. The retention times of the nucleotides remained constant with variation in the flow-rate of eluent I, because their retention times were completely dependent on the flow-rate of eluent II for the analysis. The peak height of AMP was constant during 4 min of adsorption, but decreased as a function of adsorbing time between 4 and 10 min, whereas the peak heights of cAMP, ADP and ATP still remained constant after 10 min. Calibration graphs for AMP, cAMP, ADP and ATP were linear from 0.5 to 100 pmol injected. By direct injection of 10 μl of rat whole blood diluted 20-fold with 0.32 M sucrose, the highest peaks of AMP, ADP and ATP at 4-min adsorption were also obtained under the optimum conditions established. Judging from these results, 15% acetonitrile in the eluent I, a flow-rate of 0.3 ml/min and an adsorption time of 4 min were selected as optimum for the pre- and mini-columns.

Derivatization of the nucleotides eluted from the analytical column was examined. The peak heights of the nucleotides almost reached plateaux at *ca.* 0.05 M bromoacetaldehyde in eluent II when the 10-m reaction coil was used at 120°C, as shown in Fig. 3. Fig. 4 shows the effect of the length of the reaction coil on the analysis. Judging from the heights of peaks and the analytical time, 15 m was selected as the optimum length. The effect of the temperature of the reaction coil on the derivatization is shown in Fig. 5. The peak heights of cAMP, ADP and ATP, but not AMP, were maximum at a heating temperature of 110°C in the range 70–125°C examined, without changing their retention times. Therefore, 115°C was selected for the subsequent experiments.

The adenine nucleotides in hamster whole blood were determined under the optimum conditions developed above, as shown in Fig. 6. From the calibration graphs for the authentic adenine compounds, the concentrations of ATP, ADP and AMP in the whole blood were calculated to be 813, 129 and 8 μmol/l, respectively. The unknown peaks 1 and 2 were assumed to be adenine-related compounds, because
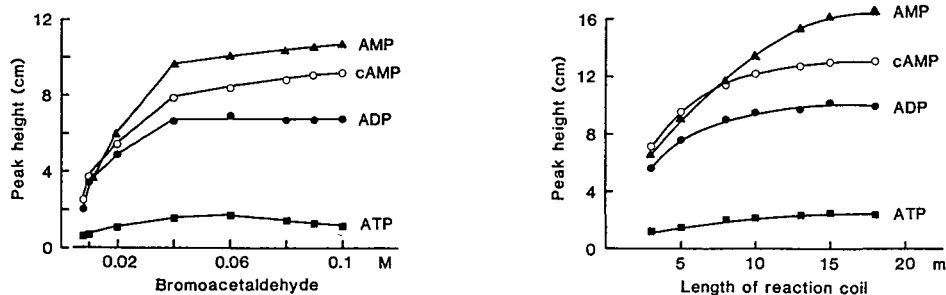
Fig. 3. Effect of bromoacetaldehyde concentration on peak heights. A 40-pmol amount of the adenines was injected into the analyser system. Eluent I was passed through the precolumn into the mini-column at a flow-rate of 0.3 ml/min for 4 min. The eluate was heated in a 10-m reaction coil at 120°C. Data points: ▲ = AMP; ○ = cAMP; ● = ADP; ■ = ATP.

Fig. 4. Effect of length of reaction coil on peak heights. A 40-pmol amount of the adenines was injected and eluted with eluent II containing 0.05 M bromoacetaldehyde. The other condition and data points were the same as in Fig. 3, except the length of the coil.
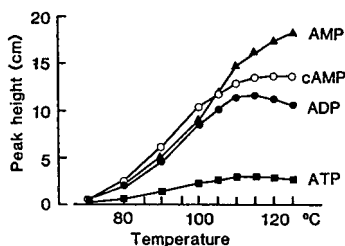
Fig. 5. Effect of heating temperature on peak heights. The length of the reaction coil was 15 m and the other conditions were the same as in Fig. 4, except the heating temperature. Data points as in Fig. 3.
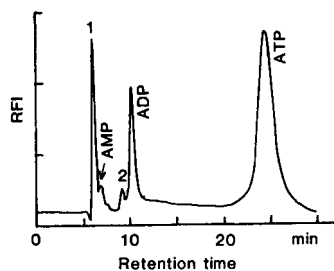
Fig. 6. Chromatogram of hamster whole blood. Peaks 1 and 2 are unknown compounds.

the fluorescent reaction and detection were selective for adenine bases. As the retention times of NAD, FAD and ADP-ribose and also cAMP corresponded to the unknown peak 2, cAMP was difficult to determine. The nucleotides in hamster whole blood were also determined at 35-min intervals during 140-min storage (Table I). The total concentration of AMP, ADP and ATP and the concentration of ATP decreased to 69 and 63% of the original concentrations, respectively. However, the concentration of AMP and the value of the "energy charge" (EC) were constant during 140 min of storage. Table II gives the concentrations of ATP and ADP in whole blood determined with the present analyser system and with the previously described prederivatization method[2,4,5]. The values obtained with the present system were reasonable.

In the other system, Ado and Ade were well separated by the analyser system and the analytical time was *ca.* 30 min, as shown in Fig. 7. Ado and Ade were adsorbed on the mini-column packed with ODS-5 using 0–5% acetonitrile as eluent I′ but the amounts adsorbed were markedly decreased when 6 and 7% acetonitrile were used. When the acetonitrile content in eluent I′ was lower than 2%, ATP, ADP and

TABLE I

CHANGES IN LEVELS OF ADENINE NUCLEOTIDES IN HAMSTER WHOLE BLOOD DURING STORAGE

The hamster whole blood was diluted 20-fold with 0.32 M sucrose and stored at 4°C. This set of experiments was performed three times with similar results.

Time (min)	Concentration in whole blood ($\mu mol/l$)			Total adenines[a] ($\mu mol/l$)	EC^b
	ATP	ADP	AMP		
0	8	129	812	949	0.92
35	10	192	717	919	0.88
70	11	217	671	899	0.87
105	12	192	545	749	0.86
140	10	137	512	659	0.88

[a] AMP + ADP + ATP.
[b] EC (energy charge) is calculated from the concentrations (ATP + 0.5 ADP)/(AMP + ADP + ATP).

TABLE II

COMPARISON OF LEVELS OF ATP AND ADP IN VARIOUS WHOLE BLOODS DETERMINED BY THE PRESENT AND PREDERIVATIZATION METHODS

As reported previously by Yoshioka and co-workers[2,4,5], adenine compounds in each whole blood were extracted with perchloric acid, prederivatized with bromoacetaldehyde and analysed by HPLC. The values represent means ± S.D. of three and five experiments using the present and the prederivatization methods, respectively.

Method	Concentration in whole blood ($\mu mol/l$)					
	Hamster		Rat		Human	
	ATP	ADP	ATP	ADP	ATP	ADP
Present	810 ± 33	130 ± 4.9	600 ± 27	115 ± 5.3	750 ± 35	110 ± 5.3
Prederivatization	780 ± 32	140 ± 6.0	580 ± 26	120 ± 6.0	700 ± 32	100 ± 5.0

ATP were also adsorbed on ODS-5. Hence a 5% acetonitrile content was optimum for selective adsorption.

When the 1 cm × 4.6 mm I.D. column was used as the mini-column, the pH of eluent I' containing 5% acetonitrile was a critical factor for the adsorption of Ado and Ade. At pH 4, ATP, ADP and AMP and also Ado and Ade were adsorbed on the column, but only Ado and Ade were selectively adsorbed at pH 7.4. Judging from these results, 5% acetonitrile in 2 mM phosphate buffer (pH 7.4) was selected as optimum for eluent I'. The peak height of Ado reached a plateau from 3 to 6 min
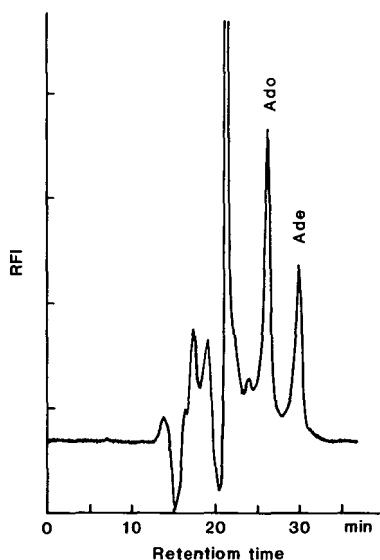
Fig. 7. Chromatogram of authentic adenine compounds obtained with the analyser for Ado and Ade. A 30-pmol amount of the adenines was injected into the analyser system. Eluent I, 5% acetonitrile in 2 mM phosphate buffer (pH 7.4), was passed through the precolumn into the mini-column at a flow-rate of 0.3 ml/min for 4 min. The other conditions were the same as optimized with the analyser for the nucleotides.
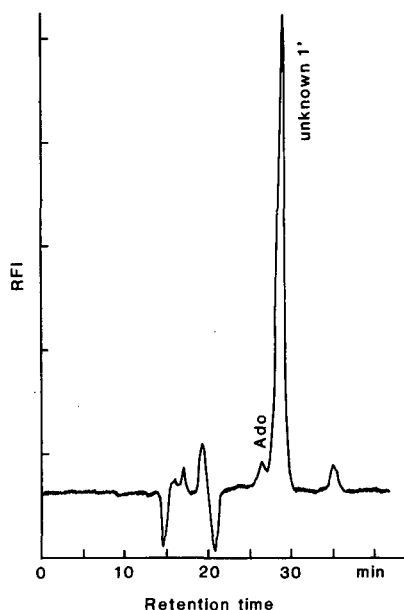
Fig. 8 Chromatogram of human plasma.

adsorption after the sample injection. On the other hand, the peak of Ade after 4 min of adsorption was the highest in the period 2–6-min. As both the pre- and mini-columns should be well equilibrated with eluent I′, timing of the column switching from connection of the mini- with the analytical column to connection of the pre- with the mini-column was a critical factor for the successive determination of Ado and Ade. As the peak heights of Ado and Ade were nearly same from 3 to 9 min after the connection of the mini- with the analytical column, the timing of the column switching was selected to be 5 min. The calibration graphs were linear over the range 5–50 pmol of Ade and Ado injected.

Under the conditions established above, Ado and Ade in healthy human plasma were determined and the results are shown in Fig. 8. The concentration of Ado was *ca.* 0.3 μmol/l and no Ade could be detected. It was difficult to determine the content of Ado in rat plasma by the large intereference from the unknown peak 1′, which was also observed in human plasma. However, NAD, FAD and ADP-ribose passed through the mini-column, and did not appear in the chromatogram. Hence the system was specific for the determination of Ado and Ade.

DISCUSSION

Tamai *et al.*[7-9] established individual methods for the determination of hydrophobic, moderately hydrophobic and hydrophilic drugs in whole blood by direct injection of the blood into HPLC systems. For the determination of hydrophilic drugs, they introduced BT 650-M in a precolumn equipped with an inlet filter of pore size 40 μm, allowing blood cells to pass into the column and cell debris, cell mem-

branes and proteins to be trapped in the column. The adsorbed materials such as proteins, lipids and cell debris on the BT 650-M precolumn were removed by washing with 0.5% sodium dodecylsulphate and then methanol after the direct injection of 200 μl of whole blood into the HPLC system[9].

Adenine compounds are relatively hydrophilic, and the introduction of BT 650-M as the precolumn was adequate for development of the present system. In this study, 0.1–1 μl of the whole blood was sufficient to determine the contents of adenine compounds based on the high sensitivity of the fluorescence detection and the selectivity of derivatization with bromoacetaldehyde. Cytosine and guanine compounds also react with bromoacetaldehyde, but the relative fluorescence intensities of their products are 100 times lower than those of adenine derivatives and they are therefore, virtually not detectable in the chromatograms. The yield of the fluorescent derivatization in the reaction coil was not calculated, but the peak heights of the nucleotides reached plateaux at 115°C, as shown in Fig. 5, suggesting that the yield is high enough for quantitative determination. Judging from the reproducibility of the peak heights of each nucleotide, the system was stable for at least 100 injections without regeneration of the pre- and mini-columns. In our system, polymerized bromoacetaldehyde and the adsorbed compounds such as lipids and proteins are washed out after every 50 sample injections with 50% methanol.

As pointed out by Hartwick and Brown[10], sample preparation in HPLC is very critical when determining the actual nucleotide contents. ATP and ADP are easily metabolized during sample preparation. The concentrations of ATP and ADP in the dilute human blood analysed with the present system were 750 and 110 μM, respectively, which are close to those obtained by the prederivatization method described previously[4,5]. The ATP concentration in rat whole blood obtained by our methods (Table II) was higher than the 521 μmol/l obtained with UV detection[11]. By direct injection of hamster whole blood into the analyser system, a high EC value (0.92) was obtained. Hence the analyser for the nucleotides is useful for assessing the EC values of various cells or clinical samples.

Ado is a metabolic product of ATP and a mediator of coronary vasodilatation[12], hormonal secretion[13], cyclic nucleotide formation[14–16], neurotransmission[17] and immune response[18,19]. Several methods for measuring Ado with enzymatic spectrophotometric[20], radiochemical[21], fluorimetric[22], enzymatic isotope dilution[23], radioligand binding[24] and radioimmunological[25] techniques have been reported. HPLC has been used for the determination of Ado and Ade in plasma[26,27]. As the Ado content in plasma is very low, an ODS column such as Sep-Pak C_{18} has commonly been used to concentrate Ado from plasma, but elution of Ado from the Sep-Pak C_{18} and evaporation of the eluate were time consuming. Boos et al.[28] developed effective column-switching techniques for the direct injection of biological fluids such as human serum, urine and breast milk into a high-performance affinity chromatograph using phenylboronic acid bonded precolumn material. Ado was clearly separated from the other ribonucleosides by the automated on-line analysis of ribonucleosides with UV detection. However, a large amount of serum (500 μl) was required. From the clinical point of view, the system should be set up for small amounts of biological samples.

In this study, the Ado concentration in normal human plasma was found to be about 0.3 μmol/l, which corresponds closely with the levels of 0.29[25], 0.51[26], 0.35[28] and 0.28 μmol/l[29] reported previously.

In our system, an unexpected appearance of an unknown peak which intereferes with the determination of Ado was found with the plasma samples, particularly rat plasma. When the plasma and blood cells were separated immediately by centrifugation, the unknown compound was detected in the chromatogram of the plasma whereas no such peak could be detected in that of the blood cells, indicating that the unknown compound exists mainly in the plasma. The unknown compound was stable against the endogenous adenosine deaminase. Deoxyadenosine corresponded to the retention time of the unknown peak 1' but was completely degradaded in the rat plasma (data not shown). Characterization of the compound is being undertaken and will be described elsewhere. Using our analyser system, Ado in crude hepatic mitochondria from guinea pig was accurately determined (data not shown).

The analyser for Ado and Ade was stable for at least *ca.* 15 sample determinations without washing the BT 650-M and ODS-5 columns with a higher concentration of the acetonitrile or other washing solutions.

For the simultaneous determination of Ade and Ado with the nucleotides, a new packing material for the mini-column that will adsorb Ado and Ade in the presence of bromoacetaldehyde would be required. Further, development of a micro-injection method for $0.01-0.1-\mu l$ volumes would also be required for the real direct injection of biological samples into the analyser.

REFERENCES

1 J. L. Gordon, *Biochem. J.,* 233 (1986) 309.
2 M. Yoshioka, K. Nishidate, H. Iizuka, A. Nakamura, M. M. El-Merzabani, Z. Tamura and T. Miyazaki, *J. Chromatogr.,* 309 (1984) 63.
3 M. Yoshioka, Z. Tamura, M. Senda and T. Miyazaki, *J. Chromatogr.,* 344 (1985) 345.
4 M. Yoshioka, K. Yamada, M. M. Abu-Zeid, H. Fujimori, A. Fuke, K. Hirai, A. Goto, M. Ishii, T. Sugimoto and H. Parvez, *J. Chromatogr.,* 400 (1987) 133.
5 M. Yoshioka, K. Yamada, M. M. Abu-Zeid, H. Fujimori, A. Fuke, K. Hirai, A. Goto, M. Ishii, T. Sugimoto and H. Parvez, *Supercritical Fluid Chromatography and Micro-HPLC,* VSP, Utrecht, 1989, p. 181.
6 L. L. Schukovskaya, S. N. Ushakov and N. K. Galania, *Izv. Akad. Nauk SSSR, Otd. Khim. Nauk,* (1962) 1692.
7 G. Tamai, H. Yoshida and H. Imai, *J. Chromatogr.,* 423 (1987) 163.
8 G. Tamai, H. Yoshida and H. Imai, *J. Chromatogr.,* 423 (1987) 147.
9 G. Tamai, H. Yoshida and H. Imai, *J. Chromatogr.,* 423 (1987) 155.
10 R. A. Hartwick and P. R. Brown, *J. Chromatogr.,* 112 (1975) 651.
11 K. Shimizu, S. Kawazoe, M. Shiraishi and T. Asahi, *Yakugaku Zasshi,* 103 (1983) 1323.
12 R. M. Berne, *Am. J. Physiol.,* 204 (1963) 317.
13 J. Wolff and G. H. Cook, *J. Biol. Chem.,* 252 (1977) 687.
14 H. Shimuzu, C. R. Creveling and J. Daly, *Proc. Natl. Acad. Sci. U.S.A.,* 65 (1970) 1033.
15 C. Londos and J. Wolff, *Proc. Natl. Acad. Sci. U.S.A.,* 74 (1977) 5482.
16 M. Saito, *Biochim. Biophys. Acta,* 498 (1977) 316.
17 J. Daly, *Physiological and Regulatory Functions of Adenosine and Adenine Nucleotides,* Raven Press, New York, 1979, p. 229.

18 E. R. Giblett, J. E. Anderson, F. Cohen, B. Pollara and H. J. Meuwissen, *Lancet*, 2 (1972) 1067.
19 G. C. Mills, F. C. Schmalstieg, K. B. Trimmer, A. S. Goldman and R. M. Goldblum, *Proc. Natl. Acad. Sci. U.S.A.*, 73 (1976) 2867.
20 H. M. Kalckar, *J. Biol. Chem.*, 167 (1947) 429.
21 E. Randerath, C.-T. Yu and K. Randerath, *Anal. Biochem.*, 48 (1972) 172.
22 G. Avigad and S. Damle, *Anal. Biochem.*, 50 (1972) 321.
23 D. H. Namm and J. P. Leader, *Anal. Biochem.*, 58 (1974) 511.
24 P. A. Olsson, C. J. Davis, M. K. Gentry and R. B. Vomacka, *Anal. Biochem.*, 85 (1978) 132.
25 T. Sato, A. Kuninaka, H. Yoshino and M. Ui, *Anal. Biochem.*, 121 (1982) 409.
26 M. C. Capogrossi, M. R. Holdiness and Z. H. Israili, *J. Chromatogr.*, 227 (1982) 168.
27 E. K. Jackson and A. Ohnishi, *Hypertension*, 10 (1987) 189.
28 K.-S. Boos, B. Wilmers, E. Schlimme and R. Sauerbrey, *J. Chromatogr.*, 456 (1988) 93.
29 J. Ontyd and J. Schrader, *J. Chromatogr.*, 307 (1984) 404.

CHROMSYMP. 1764

Purification of D_2 dopamine receptor by photoaffinity labelling, high-performance liquid chromatography and preparative sodium dodecyl sulphate polyacrylamide gel electrophoresis

HIROSHI USUI* and YASUO TAKAHASHI

Department of Neuropharmacology, Brain Research Institute, Niigata University, Niigata 951 (Japan)

NAOKI MAEDA and HIROMI MITUI

Department of Biology, Faculty of Science, Niigata University, Niigata 950 (Japan)

TOSHIAKI ISOBE and TSUNEO OKUYAMA

Department of Chemistry, Faculty of Science, Tokyo Metropolitan University, Tokyo 158 (Japan)

and

YOSHIKO NISHIZAWA and SHIGENOBU HAYASHI

National Saigata Hospital, Saigata, Niigata Prefecture 949-31 (Japan)

ABSTRACT

[^{125}I]N-azidophenethylspiperone ([^{125}I]azido-NAPS) was used as a photoaffinity ligand for bovine D_2 dopamine receptor. On photolysis, [^{125}I]azido-NAPS was covalently incorporated into a major band of 94 kDa in bovine striatal membrane as assessed by autoradiography after sodium dodecyl sulphate polyacrylamide gel electrophoresis (SDS-PAGE) (10% acrylamide gel). The labelled D_2 receptor protein from striatal membrane was solubilized and subjected to HPLC using gel filtration (TSK G3000SW) and hydroxyapatite gel (Pentax SH2010C), followed by two steps of preparative SDS-PAGE. The D_2 receptor protein could be obtained as a single major polypeptide on SDS-PAGE by either silver staining or autoradiography.

INTRODUCTION

Dopamine is a typical neurotransmitter in the central nervous system. Brain dopamine receptor has been classified into two groups, D_1 and D_2, based on their affinity toward dopaminergic ligands and the relationship to adenylate cyclase. D_1 receptor is linked to adenylate cyclase, whereas D_2 receptor is either negatively or not directly linked to this enzyme, but has not yet been fully characterized. D_2 dopamine receptor is of particular interest because it is associated with certain clinical conditions, *e.g.*, schizophrenia and Parkinson's disease, or their drug treatment[1,2]. Purification of this receptor has remained a formidable task owing to the minute amounts available

and the instability of ligand binding activity. Recently, several papers have reported the purification of D_2 dopamine receptor[3-8]. However, few studies have succeeded in showing this receptor protein as an apparent single polypeptide on sodium dodecyl sulphate polyacrylamide gel electrophoresis (SDS-PAGE).

A high-affinity radioiodinated probe of D_2 dopamine receptor, $[^{125}I]N$-azido-phenethylspiperone ($[^{125}I]$azido-NAPS), has been synthesized and used for the characterization of D_2 dopamine receptor[9-12]. We photolabelled the D_2 dopamine receptor of bovine striatal membrane with this ligand, and found that the labelled D_2 dopamine receptor protein showed an unusual mobility on SDS-PAGE. We utilized this characteristic for the purification of this protein. The D_2 dopamine receptor protein was purified to an apparent homogeneous polypeptide by high-performance liquid chromatography (HPLC) and preparative SDS-PAGE, using photoaffinity-labelled receptor protein as a tracer.

This method, described here, was simple and efficient in comparison with the other purification procedures reported previously.

EXPERIMENTAL

Chemicals and reagents

$[^{125}I]$Azido-NAPS (2200 Ci/mmol) were purchased from New England Nuclear (Boston, MA, U.S.A.) and $[^3H]$spiperone (85 Ci/mmol) from Amersham (Amersham, U.K.). The following drugs were obtained from Research Biochemical (Natick, MA, U.S.A.): (+)- and (−)-butaclamol, haloperidol, sulpiride, mianserin, propranolol and SCH23390. E-64 was obtained from Taisho Pharmaceutical (Tokyo, Japan). Leupeptin and phenylmethylsulphonyl fluoride (PMSF) were purchased from Boehringer (Mannheim, F.R.G.). All other chemicals were of the highest available purity.

Preparation of bovine synaptic membranes

Fresh bovine brains were obtained from a local slaughterhouse. Bovine striata were dissected out, weighted and frozen at $-80°C$ until used. All subsequent steps were performed at $0-4°C$. The striata were minced and homogenized with a Waring blender followed by a Potter–Elvehjem homogenizer in buffer A [0.25 M sucrose–10 mM Tris-HCl (pH 7.4)–2 mM EDTA–0.5 mM PMSF–1 μg/ml pepstatin–1 μg/ml leupeptin–1 μg/ml E-64]. The homogenate was centrifuged at 870 g for 10 min and the supernatant was recentrifuged at 17 600 g for 35 min. The pellet was then suspended in buffer B [10 mM Tris–HCl (pH 7.4)–2 mM EDTA–0.5 mM PMSF–1 μg/ml pepstatin–1 μg/ml leupeptin–1 μg/ml E-64] for osmotic shock, followed by centrifugation at 17 600 g for 35 min. The resulting pellet was resuspended and homogenized in buffer B, then the sucrose concentration of this preparation was adjusted to 0.8 M. The sample was layered over 1.3 M sucrose and centrifuged at 70 000 g for 2 h. The resulting band above the 1.3 M sucrose phase was collected, homogenized and stored at $-80°C$ until further use.

Photoaffinity labelling

The stored bovine synaptic preparation was washed and suspended in buffer C [50 mM Tris–HCl (pH 7.4)–100 mM NaCl–2 mM MgCl$_2$–0.5 mM PMSF–1 μg/ml pepstatin–1 μg/ml leupeptin–1 μg/ml E-64]. This preparation (2 mg of protein) was

incubated (in the dark) with [^{125}I]azido-NAPS (*ca.* 30 pmol) for 2 h at 37°C in a final volume of 1 ml and processed for photolysis. Samples were irradiated for 5 min with a Hitachi 700-W mercury lamp at a distance of 20 cm, transferred to a 1.5-ml Eppendorf microfuge tube and sedimented at 17 500 *g* for 30 min. The resulting pellet was stored at −80°C. For analysis of the labelled band, samples were dissolved in sample buffer containing 10% SDS and 1% *β*-mercaptoethanol (*β*-ME) with gentle stirring for 1–2 h at room temperature and electrophoresed[13]. After the gel had dried, autoradiography was performed with intensifying screens for 1–2 days at −80°C. For large-scale preparation, we used 10-fold larger volumes than those described above.

Gel permeation chromatography

The membrane preparation labelled with [^{125}I]azido-NAPS was mixed with unlabelled preparation and solubilized with 10 m*M* phosphate buffer (pH 6.6) containing 10% SDS and 1% *β*-ME. The solubilized sample was chromatographed on a TSK G3000SW molecular exclusion column (60 cm × 7.5 mm I.D.) (Tosoh, Tokyo, Japan) at a flow-rate of 3 ml/min at 22°C using a Hitachi Model L6000 HPLC pump and a model L4000 UV detector. The mobile phase was 10 m*M* phosphate buffer (pH 6.6)–3% SDS. The continuous protein profile of the column eluate was monitored by measuring the absorbance at 280 nm. The column eluate was fractionated (3 ml each) and the radioactivity of each fraction was determined with a *γ*-scintillation counter.

Hydroxyapatite chromatography

A Pentax SH2010C HPLC column (10 cm × 21.5 mm I.D.) (Asahi Optical Industry, Tokyo, Japan) was used for hydroxyapatite chromatography. After gel permeation chromatography, the fractions containing photolabelled receptor protein were collected and diluted with two volumes of 10 m*M* phosphate buffer (pH 6.6). The sample was loaded on a hydroxyapatite HPLC column at flow-rate of 2.5 ml/min at 22°C. The mobile phase was a 10–500 m*M* linear gradient of phosphate buffer (pH 6.6)–1% SDS. The absorbance of the column eluate was monitored at 280 nm. The column eluate was fractionated (2.5 ml) and the radioactivity of each fraction was determined with a *γ*-scintillation counter.

SDS-PAGE

SDS-PAGE was carried out according to the procedure described by Laemmli[13]. For analytical SDS-PAGE, a 1.0-mm thick slab gel was used, whereas a 3.0-mm thick slab gel was used for preparative SDS-PAGE. Sample preparation for preparative SDS-PAGE was carried out as follows: the fractions containing photo-labelled receptor protein in the hydroxyapatite HPLC eluate were collected, dialysed against 25 m*M* Tris–HCl buffer (pH 6.8) containing 0.1% SDS and concentrated using a CentriCell centrifuge ultrafilter (Polysciences, Warrington, PA, U.S.A.). The buffer composition of this sample was adjusted to that of the SDS-PAGE sample buffer [62.5 m*M* Tris–HCl (pH 6.8)–1% SDS–10% glycerol–1% *β*-ME] and then applied to a 3.0-mm thick slab gel containing 4% acrylamide stacking gel and 6% acrylamide separation gel. Electrophoresis was carried out overnight with electrophoresis buffer [25 m*M* Tris–HCl (pH 8.9)–192 m*M* glycine–0.1% SDS]. After the molecular marker had been stained with Coomassie Brilliant Blue R-250 (CBB), the gel containing photolabelled protein was cut off at the proper position assessed with a standard

molecular marker. The gel was then loaded directly on the stacking gel (4% acrylamide) and the second SDS-PAGE (12% acrylamide preparation gel) was performed. After electrophoresis, the receptor protein was electroeluted from the 12% acrylamide gel using Biotrap BT-1000 (Schleicher & Schüll, Keene, NH, U.S.A.). The resulting sample was stored at $-80°C$.

Binding assay
    Binding assays of bovine synaptic membranes were carried out according to the procedure described by Ramwani and Mishra[3] with slight modification. The total binding of [^{3}H]spiperone to the preparation was determined in a 1.0-ml assay volume containing 1 nM [^{3}H]spiperone, whereas non-specific binding was determined in a parallel assay in the presence of 1 μM ($+$)-butaclamol. Specific binding is defined as the difference in counts detected in the absence and presence of 1 μM ($+$)-butaclamol.

Protein determination
    Proteins were determined by the method of Lowry *et al.*[14] with bovine serum albumin as a standard.

RESULTS

Preparation of bovine synaptic membrane
    Bovine synaptic membrane was prepared from 150 g of bovine striata (fifteen cows). The amount of the total membrane protein was 750 mg–1.0 g when it was determined by the Lowry *et al.* method. When a ligand binding assay was performed, the membrane preparation exhibited a maximum specific binding (B_{max}) of 460 fmol/mg and an equilibrium dissociation constant (K_D) of 0.26 nM by Scatchard analysis (data not shown).

Photoaffinity labelling
    The bovine synaptic membrane preparation was photoaffinity labelled with [^{125}I]azido-NAPS, electrophoresed and rendered visible by autoradiography. [^{125}I]-Azido-NAPS was incorporated into a major polypeptide of $M_r \approx 94\ 000$ (10% acrylamide gel). This photoaffinity labelling was blocked by dopaminergic ligands such as ($+$)-butaclamol, haloperidol and sulpiride, whereas it was not blocked by mianserin (serotonin S_2 receptor antagonist), propanolol (adrenergic receptor antagonist) and SCH23390 (dopamine D_1 receptor specific antagonist) (Fig. 1). Therefore, the broad band of $M_r \approx 94\ 000$ represents the D_2 dopamine receptor protein; this finding coincides with those in other reports[9,10,12]. We measured the radioactivity of the acrylamide gel containing labelled polypeptide of $M_r \approx 94\ 000$, and calculated the uptake rate of [^{125}I]azido-NAPS from the specific radioactivity of this ligand and a maximum specific binding (B_{max}) of the membrane preparation. We estimated that [^{125}I]azido-NAPS incorporated to about 2% of D_2 dopamine receptor protein in the synaptic membrane preparation.
    We found that the labelled polypeptide of $M_r \approx 94\ 000$ has an unusual mobility on SDS-PAGE, *viz.*, the mobility of this polypeptide relative to that of the molecular marker protein varied with the acrylamide concentration of the separation gel. The apparent molecular weight of this polypeptide in each acrylamide concentration was
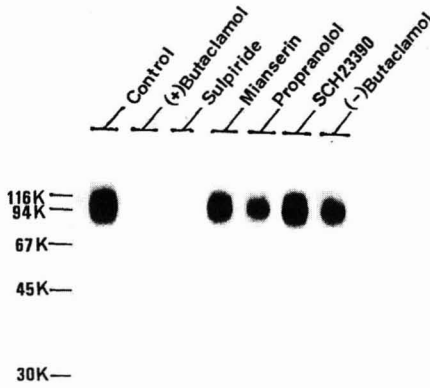
Fig. 1. Selectivity and specificity of the photoaffinity labelling of bovine striatal membrane with [^{125}I]azido-NAPS. The membrane preparation was photoaffinity labelled with [^{125}I]azido-NAPS alone (control) or in the presence of the indicated competing ligand (100 nM). Samples were then solubilized, electrophoresed on 10% acrylamide gel and rendered visible by autoradiography.

estimated roughly as 78 000 (6%), 88 000 (7.5%), 94 000 (10%) and 130 000 (12%) from the electrophoretic mobility of the middle portion of the broad band (Fig. 2). When CBB staining was performed, the other proteins in the membrane preparation were stained in a constant position, even if the acrylamide concentration was changed.
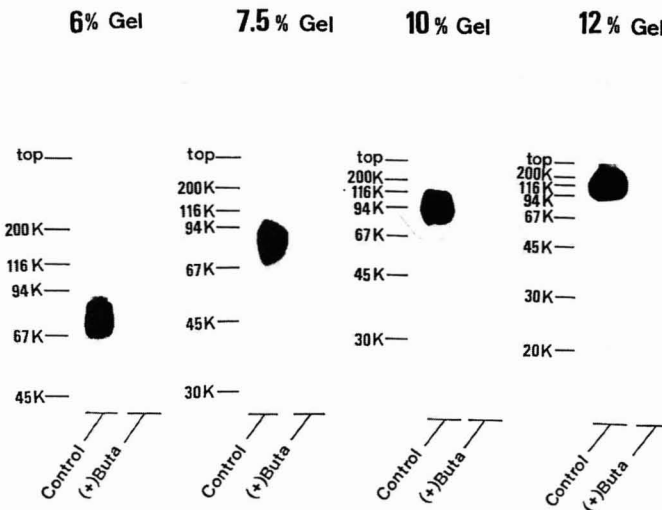
Fig. 2. SDS-PAGE pattern of the labelling with [^{125}I]azido-NAPS at several acrylamide concentrations. Membranes were photolabelled with [^{125}I]azido-NAPS alone (control) and in the presence of 100 nM (+)-butaclamol [(+)Buta]. Samples were then electrophoresed on different acrylamide gels as indicated, and rendered visible by autoradiography. Each gel contains the 4% acrylamide stacking gel and different acrylamide (6%, 7.5%, 10% or 12%) preparation gels.

Therefore, the shift of the mobility on SDS-PAGE seemed to be characteristic for D_2 dopamine receptor protein.

Gel permeation chromatography

The photoaffinity-labelled membrane preparation was solubilized and chromatographed on size-exclusion HPLC columns as described under Experimental. The elution profile of the protein and specific labelling in gel permeation HPLC is shown in Fig. 3a. Specific binding was determined by subtracting the counts in the eluate prelabelled in the absence and presence of 1 μM (+)-butaclamol in a parallel
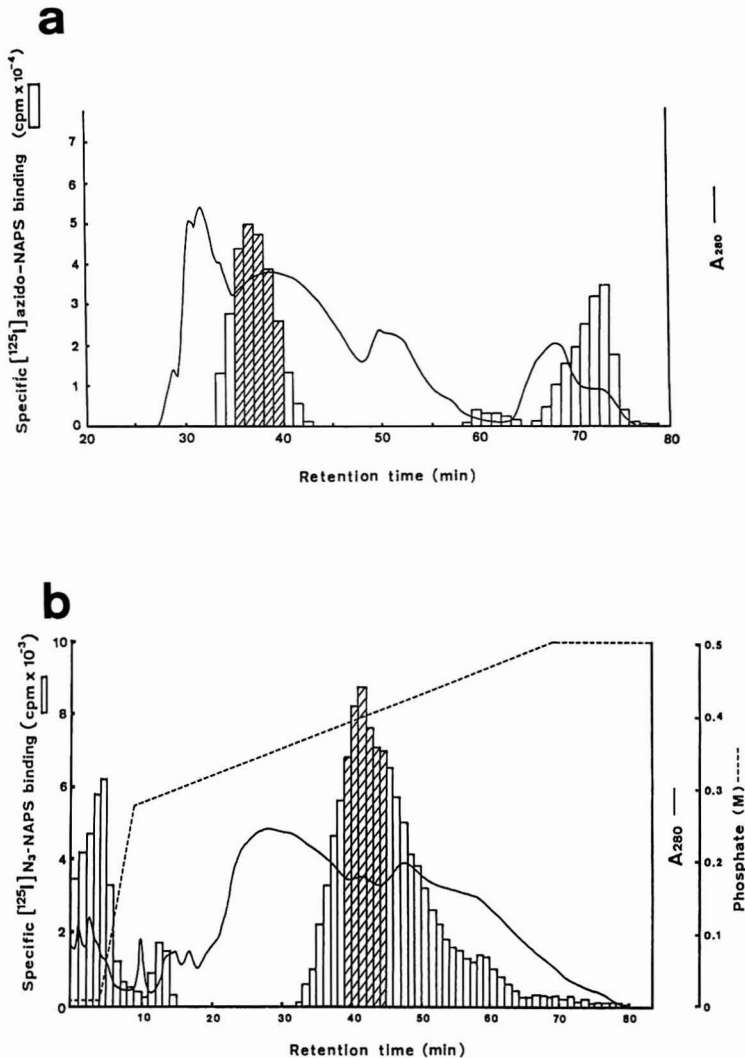
Fig. 3. Elution profile of protein and specific labelling in (a) gel permeation-HPLC and (b) hydroxyapatite HPLC. The solid line indicates the absorbance at 280 nm and the histogram indicates the radioactivity of each fraction. The fractions indicated on the histogram with an oblique line were applied to the next step.

experiment. The peak of specifically labelled receptor protein with [^{125}I]azido-NAPS consistently eluted at a retention time of 37.0 ± 4.0 min ($n = 40$). We analysed this fraction and detected the labelled polypeptide of $M_r \approx 94\,000$ by SDS-PAGE (10% acrylamide gel), followed by autoradiography. On the other hand, the labelled polypeptide was not detected in the minor radioactive peaks eluted later. These peaks may contain the free radioactive ligand and degraded low-molecular-weight substances. Fractions 35–39, which actually contains the D_2 dopamine receptor protein, were collected and applied to the next step. The recovery of membrane protein was determined by the Lowry *et al.* method, and the recovery of D_2 dopamine receptor protein was assessed by counting the radioactivity of [^{125}I]azido-NAPS using a γ-scintillation counter. The recovery of the protein and the ligand binding activity in this step were about 20% and 80%, respectively, resulting in about a 4-fold purification.

Hydroxyapatite chromatography

In Pentax SH2010C hydroxyapatite chromatography, the labelled protein with [^{125}I]azido-NAPS was eluted as a broad peak in about 0.4 M phosphate buffer (Fig. 3b). Specific binding was determined by the difference in a parallel experiment in the absence and presence of (+)-butaclamol, and confirmed by autoradiography after SDS-PAGE. Fractions 39–44, which contained the D_2 receptor protein, were collected, dialysed and concentrated using the CentriCell. The sample was then applied to the two steps of preparative SDS-PAGE. The recovery of the protein and ligand binding activity in the hydroxyapatite chromatography step were 11% and 31%,
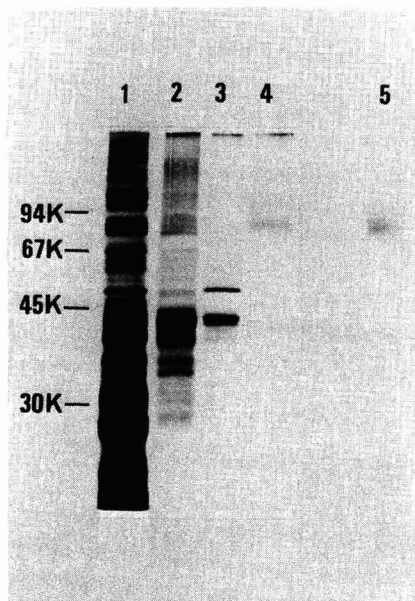
Fig. 4. SDS-PAGE pattern of the preparation of each purification step. Lanes 1–4 were made visible by silver staining and lane 5 by autoradiography. Lane 1, solubilization of bovine synaptic membrane; 2, gel permeation HPLC; 3, hydroxyapatite HPLC; 4 and 5, two steps of preparative SDS-PAGE.

TABLE I

PURIFICATION OF D_2 DOPAMINE RECEPTOR

Preparation	Specific [^3H]spiperone binding				
	Binding (cpm) (A)	Protein (mg) (B)	(A)/(B) (cpm/mg)	Purification (-fold)	Yield (%)
SDS solubilized	264 900	100	2650	1	100
Gel filtration HPLC eluate	204 200	22	9280	3.5	77
Hydroxyapatite HPLC eluate	63 400	2.5	25 360	9.6	24
Preparative SDS-PAGE eluate	23 000	0.0007	$3.54 \cdot 10^7$	13 400	8.7

respectively, when they were determined by the same methods as those in gel permeation chromatography. This step resulted in about a 3-fold purification. `

Preparative SDS-PAGE

The partially purified sample obtained by gel permeation chromatography and hydroxyapatite chromatography was applied to the two steps of preparative SDS-PAGE. After electrophoresis on 6% acrylamide preparation gel, the gel was cut off at the position of M_r 60 000–90 000, which contained photolabelled protein. This gel was loaded on 12% acrylamide preparation gel, electrophoresed and then gel was cut off at the position above M_r 94 000. The labelled protein was electroeluted by Biotrap BT-1000 with high efficiency. This sequential preparative SDS-PAGE step was very effective for the purification of D_2 dopamine receptor. We could obtain D_2 dopamine receptor protein as an apparent single polypeptide by analytical SDS-PAGE followed by silver staining. Further, autoradiography exhibited a single band at the same position as that detected by silver staining (Fig. 4).

The recovery of receptor protein in this step could not be determined by the Lowry et al. method, because it was undetectable. However, it was determined approximately from the staining density compared with those of various doses of the standard marker proteins after SDS-PAGE. Moreover, it could be estimated based on the recovery of the radioactivity of [^{125}I]azido-NAPS, which incorporated about 2% of D_2 dopamine receptor protein, because the preparation obtained by this step exhibited a nearly pure polypeptide by silver staining after SDS-PAGE. We calculated the recovery of the receptor protein to be about 28%, resulting in about a 1400-fold purification in this step. The series of purification procedures finally resulted in a *ca.* 13 400-fold purification of the receptor protein, with a recovery and specific activity of 9% and 5400 pmol/mg of protein, respectively (Table I).

DISCUSSION

The polypeptide of $M_r \approx 94\,000$, assessed by SDS-PAGE (10% acrylamide gel), was photolabelled with [^{125}I]azido-NAPS, with an appropriate pharmacological profile of D_2 dopamine receptor. The relative mobility of this photolabelled D_2

dopamine receptor on SDS-PAGE varied when the acrylamide concentration of the separation gel was changed from 6% to 12%. The apparent molecular weight of the polypeptide at each acrylamide concentration was calculated to be *ca.* 78 000 (6%), 88 000 (7.5%), 94 000 (10%) and 130 000 (12%). The D$_2$ dopamine receptor has an affinity to wheat germ lectin[15]. Sequential exoglycosidase (neuraminidase)–endo-glycosidase (glycopeptidase-F) treatment altered the electrophoretic mobility of the 94-kDa labelled band to *ca.* 43 kDa (data not shown)[11,12,16]. Therefore, the D$_2$ dopamine receptor protein obviously contains an aspartate-linked polyglycoside chain. The decrease in mobility on SDS-PAGE seemed to be caused by a large polyglycoside chain of D$_2$ dopamine receptor. The exact reason for the variation of the mobility that was observed on changing the acrylamide concentration is still unclear, but it seems that changes in hydration and steric structure contribute to this phenomenon. Recently, it was reported that an opiate receptor, which also has an affinity to wheat germ lectin, exhibited a similar strange mobility on SDS-PAGE[17].

We utilized this unusual character for the purification of D$_2$ dopamine receptor using preparative SDS-PAGE. In order to solve the problem of the limited volume of loading in SDS-PAGE, we employed partial purification steps with gel permeation HPLC and hydroxyapatite HPLC prior to the preparative SDS-PAGE. Bovine synaptic membrane was solubilized by SDS, subjected to gel permeation HPLC and hydroxyapatite HPLC and separated by sequential SDS-PAGE (6% acrylamide gel and 12% acrylamide gel; 3-mm thick slab gel). This procedure resulted in about a 13 400-fold purification with about 9% recovery. Further, D$_2$ dopamine receptor protein was detected as an apparent single polypeptide, assessed by silver staining and autoradiography after SDS-PAGE. The degree of purification of the D$_2$ dopamine receptor by our procedure is similar to those reported recently by the other workers[6,7].

The direct detection of the binding activity of purified receptor protein is difficult because of the presence of SDS in all purification steps. However, we concluded that the purified polypeptide is the D$_2$ dopamine receptor, because we could observe the photolabelled band with [^{125}I]azido-NAPS, which was blocked by several drugs with an appropriate pharmacological profile, at the same position by autoradiography as that shown by silver staining. [^{125}I]Azido-NAPS is a specific antagonist to D$_2$ dopamine receptor.

We would emphasize the advantages of this method over previous purification procedures that it is simple and reproducible and we could obtain high recoveries of receptor protein. The general procedure for the purification of receptor protein is as follows: the receptor protein is solubilized with mild detergent while holding an intact ligand binding activity, and then applied to ligand-affinity chromatography and to fixed lectin-affinity chromatography. However, with ligand-affinity chromatography, which is a highly efficient procedure for receptor purification, it is difficult to obtain a reproducible result. We attempted the ligand-affinity chromatography [with a halo-peridol-Sepharose column, carboxymethyleneoximinospiperone(CMOS)-Sepharose column, etc.] according to several previous reports[3,5,7], but could not obtain satisfactory results. This is probably due to the difficulty in finding the exact conditions necessary to exclude non-specific absorption on an affinity column. Moreover, even if the receptor protein was successfully purified to a single polypeptide according to these procedures, the recovery of receptor protein was usually below 1%. Therefore, it is difficult to prepare a sufficient amount of purified receptor protein for determination of the amino acid sequence by the procedures reported previously.

The purification procedure described here is simple and efficient in comparison with previous purification procedures. If necessary, we can use an additional step of reversed-phase HPLC with an acidic mobile phase, which seems to be effective for the separation of the membrane proteins. The purified protein obtained by this method did not have ligand-binding activity, but can be used for the determination of the amino acid sequence of this protein. When the partial amino acid sequence of the 94-kDa protein was determined, the cloning and expression of cDNA for this protein also seemed possible in the animal cell. The primary amino acid sequence and the characterization of the expressed protein in the animal cell will confirm that the purified 94-kDa protein is indeed the D_2 dopamine receptor. A similar purification procedure, using photolabelled receptor protein as a tracer, should be useful for the receptor proteins other than D_2 dopamine receptor.

ACKNOWLEDGEMENT

REFERENCES

1 L. L. Iversen, *Trends Biochem. Sci.*, 1 (1976) 121.
2 P. Seeman, *Pharmacol. Rev.*, 32 (1980) 229.
3 J. Ramwani and R. K. Mishra, *J. Biol. Chem.*, 261 (1986) 8894.
4 L. Antonian, E. Antonian, R. B. Murphy and D. I. Schuster, *Life Sci.*, 38 (1986) 1847.
5 S. E. Senogles, N. Amlaiky, A. L. Johnson and M. G. Caron, *Biochemistry*, 25 (1986) 749.
6 Z. Elazar, H. Kanety, C. David and S. Fuchs, *Biochem. Biophys. Res. Commun.*, 156 (1988) 602.
7 R. A. Williamson, S. Worrall, P. L. Chazot and P. G. Strange, *EMBO J.*, 7 (1988) 4129.
8 S. E. Senogles, N. Amlaiky, P. Falardeau and M. G. Caron, *J. Biol. Chem.*, 263 (1988) 18996.
9 N. Amlaiky and M. G. Caron, *J. Biol. Chem.*, 260 (1985) 1983.
10 N. Amlaiky and M. G. Caron, *J. Neurochem.*, 47 (1986) 196.
11 D. E. Grigoriadis, H. B. Niznik, K. R. Jarvie and P. Seeman, *FEBS Lett.*, 227 (1988) 220.
12 K. R. Jarvie, H. B. Nuznik, N. H. Bzowej and P. Seeman, *J. Biochem.*, 104 (1988) 791.
13 U. K. Laemmli, *Nature (London)*, 227 (1970) 680.
14 O. H. Lowry, N. J. Rosebrough, A. L. Farr and R. J. Randall, *J. Biol. Chem.*, 193 (1951) 265.
15 W. M. Abbott and P. G. Strange, *Biosci. Rep*, 5 (1985) 303.
16 K. R. Jarvie, H. B. Nizik and P. Seeman, *Mol. Pharmacol.*, 34 (1988) 91.
17 H. Ueda, Kyoto University, Kyoto, personal communication.

CHROMSYMP. 1896

Separation of amphetamines by supercritical fluid chromatography

JEAN-LUC VEUTHEY* and WERNER HAERDI

Département de Chimie Minérale, Analytique et Appliquée, Université de Genève, 30 Quai E. Ansermet, 1211 Genève 4 (Switzerland)

ABSTRACT

The separation of polar compounds by supercritical fluid chromatography (SFC) is difficult, especially with amine compounds. In this study a derivatization method was used to obtain apolar compounds and also to block the amine functions. The target compounds were amphetamines and the derivatizing agent was the 9-fluorenylmethyl chloroformate. This reagent reacts with primary and secondary amines to form UV-absorbing apolar complexes which permits selective and sensitive detection methods. This method allowed the SFC separation of five amphetamines in less than 5 min.

INTRODUCTION

Supercritical fluid chromatography (SFC) with packed or capillary columns has been developed for the analysis of organic apolar and moderatly polar compounds with carbon dioxide as mobile phase[1], but only a few results have been reported for polar compounds and particularly basic compounds[2], owing to the apolar nature of carbon dioxide. However, the analysis of amines by chromatography is a challenge, as gas chromatography (GC) is limited to volatile and thermally stable compounds and high-performance liquid chromatography (HPLC) involves a long analysis time and lacks a universal detector. SFC could be an efficient alternative technique for the analysis of these compounds[3], because it offers faster separations and higher efficiencies per unit time than HPLC.

The separation of primary and secondary amines is difficult by SFC with carbon dioxide as the mobile phase on a packed column for two reasons: amines react with carbon dioxide and a strong silanol–analyte interaction induces significant peak tailing. There are various ways of overcoming these difficulties. (1) The most commonly used method is the addition of a polar modifier to mask the silanol groups and to enhance the solvent polarity. However, when this is done, SFC may no longer have an advantage over HPLC, and in many instances separation is achieved by subcritical chromatography[4]. (2) The use of columns specially prepared for the separation of basic compounds, such as polymer-encapsulated stationary phases with

aliphatic groups[5] or cross-linked cyanopropyl-bonded phase silica[6], eliminates the silanol–amine interactions and improves the separation efficiency, but it does not eliminate the carbon dioxide–amine reaction. (3) A polar supercritical fluid, such as ammonia, has been used instead of carbon dioxide, but it requires stationary phases such as n-octyl or n-nonyl polysiloxane and a special device (sample introduction valve equipped with a rotor made of Valcon H material, ferrules in graphite or Kel-F material, etc.) to work with such a corrosive medium[7–9]. Sulphur hexafluoride (SF_6), alone[10–12] or mixed with ammonia[13] has not been used extensively, owing to its weak solvating power. (4) The derivatization of polar to apolar or less polar compounds by masking the ionizable functions would permit the use of conventional packed columns with carbon dioxide as supercritical fluid[14,15].

In this study, the last-mentioned procedure was chosen for the separation of amphetamines by SFC. The continuing abuse of amphetamine and related compounds as stimulants has led to the development of many GC and HPLC for their determination. Currently, HPLC is the most commonly used technique for amphetamine analysis, as the sample preparation with aqueous samples is not laborious. In order to overcome the weak UV absorbance and the slight natural fluorescence of amphetamines, several derivatization procedures have been reported[16,17]. Both primary and secondary amines react with many reagents, which permits selective and sensitive detection methods. These derivatization procedures can be employed before SFC analysis. The aim of this study was to use 9-fluorenylmethyl chloroformate (FMOC-Cl) as a derivatizing agent for the separation of amphetamines before SFC separation to improve the chromatographic performance and the resolution per unit time relative to conventional HPLC procedures.

EXPERIMENTAL

Apparatus

The apparatus used for this study included a Varian 2500 chromatograph (Varian, Palo Alto, CA, U.S.A.), modified for SFC operations. Cooling of the pump head with cold ethanol (0°C) is necessary to improve the pump efficiency. Temperature control of the fluid and the chromatographic columns was achieved by using an oven (Crocosil; Varian). The injector was a Rheodyne 7125 six-way switching valve with a 10-μl loop. A Varian UV 2550 spectrophotometer was used with a detection cell modified in order to withstand pressures up to 350 bar. The pressure in the system was monitored by a back-pressure regulator (Model 26-3220-24004; Tescom, Minneapolis, MN, U.S.A.). A Kontron (Zurich, Switzerland) Model 414-T pump was used as a modifier pump.

Materials

The carbon dioxide (technical grade) was contained in a cylinder with an eductor tube (Polygaz, Geneva, Switzerland). Methanol, 2-propanol and acetonitrile were of HPLC grade (Romil, Shepshed, U.K.). Solvent mixing of the cabon dioxide and the modifier was accomplished by using a static mixer, incorporated in the liquid chromatograph.

The chromatographic columns were stainless-steel columns (30 cm × 0.39 cm I.D.) packed with Hypersil ODS (10 μm) and Hypersil APS (5 μm) (Shadon, Runcorn,

Cheshire, U.K.) and a commercial Nucleosil-100 bare silica (5 μm) (20 cm $\times$ 0.4 cm I.D.) (Macherey, Nagel & Co., Duren, F.R.G.).

Methylamphetamine chlorohydrate and amphetamine sulphate were obtained from Sigma (St. Louis, MO, U.S.A.) and phenethylamine, ephedrine, norephedrine and FMOC-Cl from Fluka (Buchs, Switzerland). Stock solutions of each amphetamine were 10^{-2} M in 0.1 M hydrochloric acid and were stored in the dark at 5°C. A stock solution of 150 mg of FMOC-Cl in 100 ml of acetone was stored at 5°C.

Derivatization procedure

The derivatization procedure for the amino acids and the amines has been described in detail by Einarsson and co-workers[18,19]. The sample (250 μl), buffered at pH 9.50 (below pH 9.0 the derivatization of amphetamines is incomplete), was mixed with 250 μl of the FMOC-Cl solution, placed in a 1-ml reaction vial and allowed to react for 10 min, then extracted with dichloromethane. The organic layer, containing the FMOC–amphetamine complexes, was injected into the HPLC system.

RESULTS AND DISCUSSION

In a previous study[14], amino acids were derivatized with FMOC-Cl reagent prior to SFC separation. Here, this reagent was used for amine separation, in particular for the amphetamines, where it forms an apolar complex that can be readily eluted with a supercritical mobile phase. The extraction procedure was modified so as to collect the complex in the organic layer. Dichloromethane was chosen as the solvent, owing to its higher density than water (so no evaporation occurs during the experiment) and its compatibility with carbon dioxide.

Chromatography was performed on bare silica octadecyl-bonded silica and aminopropyl-bonded silica with methanol, 2-propanol and acetonitrile as polar modifiers.

Influence of polar modifier

The results obtained on the three columns showed that a polar modifier is necessary to elute the FMOC–amphetamine complexes, otherwise no elution occurs. The capacity factors decrease with increasing percentage of the polar modifier in carbon dioxide. Methanol was the modifier that increased the polarity of the mobile phase most and yielded the fastest elution times of amphetamine complexes. A methanol concentration in carbon dioxide of 2.4% (v/v) is sufficient to elute and resolve a mixture of five amphetamines in less than 5 min on a bare silica, as shown in Fig. 1. Under the same conditions, 2-propanol has a lower eluting power; further, methylamphetamine and amphetamine are not resolved, even with a low percentage of modifier, as shown in Fig. 2. Acetonitrile was also tested as a modifier, but poor results were obtained (band broadening, long retention times and poor efficiency). These results indicate that modifiers increase the solubilities of solutes in the mobile phase according to their eluting strength (methanol 0.73, 2-propanol 0.63, acetonitrile 0.50)[20]. Further, as shown previously[14], modifiers also play a role as silanol masking agents.

The effects of pressure and temperature were also investigated to modify the mobile phase density (in the presence of a polar modifier). The capacity factors of all
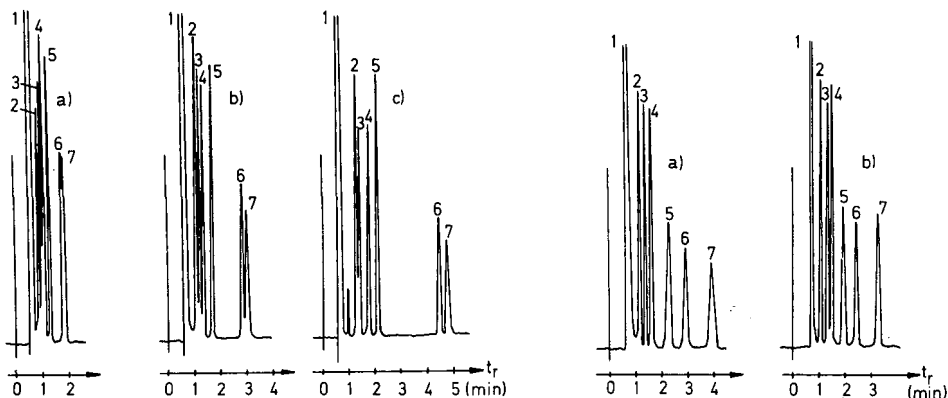
Fig. 1. Separation of five FMOC–amphetamines on Nucleosil-100 (5 μm) bare silica (15 cm × 0.4 cm I.D.) as a function of the percentage of methanol in CO_2: (a) 7.0%; (b) 4.8%; (c) 2.4%. CO_2 flow-rate, 4 ml/min; mean pressure, 200 bar; temperature, 40°C; detector, 269 nm. Solutes: 1 = acetone; 2 = methylamphetamine; 3 = amphetamine; 4 = phenethylamine; 5 = FMOC-Cl; 6 = ephedrine; 7 = norephedrine.

Fig. 2. Separation of five FMOC–amphetamines on bare silica as a function of the percentage of 2-propanol in CO_2: (a) 7.0%; (b) 4.8%. Other conditions and solutes as in Fig. 1.

the solutes were found to decrease with increasing density, whereas the selectivity remained changed. Hence the mobile phase density has a slight influence on the solvating power in comparison with the nature and concentration of the polar modifier.

Influence of stationary phase

As mentioned earlier, satisfactory separations of amphetamines are obtained on bare silica with methanol or 2-propanol as polar modifiers. A comparison of these results with those of HPLC[16,17], obtained with derivatization, on bare and reversed-phase silicas shows that SFC separation gives a shorter analytical time (3 min instead of 10 min to separate the five amphetamines) and a higher selectivity per unit time (*i.e.*, α divided by the mean retention times), as shown in Table I. On octadecyl-bonded silica, all compounds are eluted very rapidly by SFC, and no resolution was obtained even with 2-propanol as polar modifier. This result may be explained by the smaller number of silanol groups available on this stationary phase.

Aminopropyl-bonded silica gave results similar to those obtained with bare silica and good amphetamine separations. In this instance, with both modifiers (methanol and 2-propanol), all compounds were eluted and resolved in less than 4 min, as shown in Fig. 3. Further, in comparison with results obtained on bare silica, ephedrine and norephedrine are better separated (Table I). The amino functions bonded to the silica induce an additional interaction with the hydroxyl groups of ephedrine and norephedrine. Thus, aminopropyl silica is preferably used for ephedrine–norephedrine separation; otherwise, bare silica and methanol give efficient and rapid separations, as shown previously.

The order of elution is identical on both stationary phases and follows the adsorption energies, as in normal-phase liquid chromatography[20]; only the selec-

TABLE I

RETENTION TIMES (t_r) IN MINUTES AND SELECTIVITIES (α) OF AMPHETAMINES, DERIV-ATIZED WITH FMOC-Cl, AS A FUNCTION OF THE STATIONARY PHASE AND THE POLAR MODIFIER UNDER OPTIMUM CHROMATOGRAPHIC CONDITIONS

Optimum conditions: CO_2 flow-rate, 4 ml/min; modifier concentration, 4.8%; mean pressure, 200 bar; temperature, 40°C; detection, 269 nm.

Solute[a]	Parameter	Bare silica		Aminopropyl silica	
		Methanol	2-Propanol	Methanol	2-Propanol
MA	t_r	1.12	1.25	1.10	1.33
	α	1.21	1.00	1.66	1.55
AMP	t_r	1.22	1.25	1.35	1.64
	α	1.28	1.45	1.24	1.38
PEA	t_r	1.38	1.50	1.50	1.97
	α	3.05	3.81	2.15	2.77
E	t_r	2.88	3.75	2.40	4.09
	α	1.07	1.06	1.48	1.60
NE	t_r	3.03	3.92	3.20	6.09

[a] MA = methylamphetamine; AMP = amphetamine; PEA = phenethylamine; E = ephedrine; NE = norephedrine.

tivities are slightly different, as shown in Table I. This may be due to the fact that the functional group bonded to the silica induces a steric hindrance of some silanol functions and modifies slightly the main silanol–analyte interaction.

These findings indicate that the separation of amphetamines by SFC is governed principally by an interaction with the silanol groups of the silica, which can be partically hindered with a functional group or masked by a polar modifier. Polar
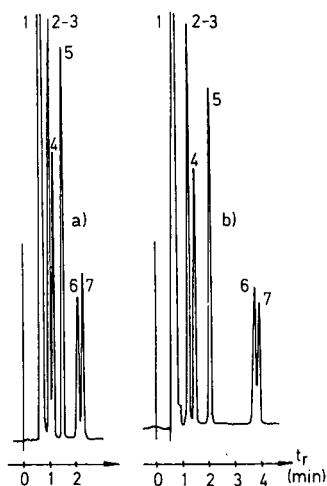
Fig. 3. Separation of five FMOC–amphetamines on Hypersil APS (5 μm) aminopropyl-bonded silica (30 cm × 0.39 cm I.D.) with (a) 7.0% of 2-propanol and (b) 4.8% of methanol. Other conditions and solutes as in Fig. 1.

modifiers also play the role of solubilizing agents for the complexes in the mobile phase.

All chromatograms show the presence of a FMOC-Cl excess peak. This excess can be easily removed by adding a hydrophilic amino acid, such as valine, which consumes this reagent during the derivatization process. The FMOC–valine charged complex may then be extracted in the aqueous layer. The injection of the aqueous solution shows that FMOC–amphetamine complex peaks are absent in this layer. This procedure was not used routinely, because the FMOC-Cl peak does not interfere with any amphetamine peaks.

In conclusion, these preliminary results obtained for amphetamine separations by SFC are satisfactory. Very rapid, efficient elution (no peak tailing) of the uncharged FMOC–amphetamine complexes, on conventional polar silicas is possible under supercritical conditions. The derivatization of amines to apolar complexes therefore has great potential in SFC. These qualitative results must now be developed for quantitative analyses.

The FMOC-Cl reagent was chosen because of the simple derivatization procedure and because, on addition of a methyl group, it becomes a chiral reagent, which is commercially available as FLEC[14]. Work is now in progress to separate amphetamine enantiomers in the same way.

ACKNOWLEDGEMENTS

REFERENCES

1 R. M. Smith (Editor), *Supercritical Fluid Chromatography*, Royal Society of Chemistry, London, 1988.
2 S. M. Fields and K. Grolimund, *J. High Resolut. Chromatogr. Chromatogr. Commun.*, 11 (1988) 727.
3 M. Ashraf-Khorassani and L. T. Taylor, *J. Chromatogr. Sci.*, 26 (1988) 331.
4 J. L. Janicot, M. Caude and R. Rosset, *J. Chromatogr.*, 437 (1988) 351.
5 H. Engelhardt, A. Gross, R. Mertens and M. Petersen, *J. Chromatogr.*, 477 (1989) 169.
6 M. Ashraf-Khorassani, L. T. Taylor and R. A. Henry, *Anal. Chem.*, 60 (1988) 1529.
7 K. Grolimund, W. P. Jackson, M. Joppich, W. Nussbaum, K. Anton and H. M. Widmer, in D. Ishii, K. Jinno and P. Sandra (Editors), *Proceedings of the Seventh International Symposium on Capillary Chromatography, May 11–14, 1986, Gifu*, University of Nagoya Press, Nagoya, 1986.
8 J. C. Kuei, K. E. Markides and M. L. Lee, *J. High Resolut. Chromatogr. Chromatogr. Commun.*, 10 (1987) 257.
9 P. J. Schoenmakers and F. C. C. J. G. Verhoeven, *Trends Anal. Chem.*, 6 (1987) 10.
10 J. C. Giddings, M. N. Myers, L. McLaren and R. A. Keller, *Science*, 162 (1968) 67.
11 J. W. Hellgeth, M. G. Fessehaie and L. T. Taylor, *Chromatographia*, 25 (1988) 172.
12 S. M. Field and K. Grolimund, *J. Chromatogr.*, 472 (1989) 197.
13 J. L. Veuthey, J. L. Janicot, M. Caude and R. Rosset, *J. Chromatogr.*, 499 (1990) 637.
14 J. L. Veuthey, M. Caude and R. Rosset, *Chromatographia*, 27 (1989) 105.
15 M. Ashraf-Khorassani, M. G. Fessehaie, L. T. Taylor, T. A. Berger and J. F Deye, *J. High Resolut. Chromatogr. Chromatogr. Commun.*, 11 (1988) 352.
16 B. M. Farrell and T. M. Jefferies, *J. Chromatogr.*, 272 (1983) 111.
17 K. Hayakawa, K. Hasegawa, N. Imaizumi, O. S. Wong and M. Miyazaki, *J. Chromatogr.*, 464 (1989) 343.
18 S. Einarsson, B. Josefsson and S. Lagerkvist, *J. Chromatogr.*, 282 (1983) 609.
19 S. Einarsson, S. Folestad, B. Josefsson and S. Lagerkvist, *Anal. Chem.*, 58 (1986) 1638.
20 L. R. Snyder, *Principles of Adsorption Chromatography*, Marcel Dekker, New York, 1968.

Determination of malonaldehyde in oxidized biological materials by high-performance liquid chromatography

M. TOMITA* and T. OKUYAMA

Department of Legal Medicine, Kawasaki Medical School, 577 Matsushima, Kurashiki City, Okayama 701–01 (Japan)

and

S. KAWAI

Gifu Pharmaceutical University, 6–1 Mitahora-higashi, 5 chome, Gifu 502 (Japan)

ABSTRACT

A high-performance liquid chromatographic (HPLC) method was used to determine the level of malonaldehyde (MA) in materials containing unsaturated fatty acids and rat liver microsomes peroxidized *in vitro*. The detection limit was 8.3 pmol for fatty acid samples and 25 pmol for microsomal samples. The method was specific to MA and the relative standard deviation was 4.34–5.14%. The recovery of MA was about 100%. In general, the MA values in oxidized materials obtained by the proposed HPLC method were lower than those obtained by the thiobarbituric acid method, although similar results were obtained with both methods for microsomal samples oxidized by NADPH. The effect of temperature on the HPLC results was investigated and it was found that the MA values obtained by derivatization at 25°C, followed by separation using HPLC, reflected the situation of the peroxidation more accurately.

INTRODUCTION

Lipid peroxidation, the oxidative deterioration of polyunsaturated lipids, has been implicated in diverse pathological conditions including drug toxicities, various liver disorders, cardiac ischaemia, thermal injury and ageing. The most widely used method for the determination of the level of malonaldehyde (MA), which is a degradation product of peroxidized lipids, is based on its reaction with thiobarbituric acid (TBA test). The TBA test, however, is not specific for MA, as many other substances which are also formed in the peroxidation process give positive reactions with TBA[1–4]. The reaction factors employed in the TBA test also raise the possibility of generating MA as an artifact[5,6]. Recently, we[7] and others[8] developed an HPLC method using 2,4-dinitrophenylhydrazine (DNPH) as a derivatizing reagent. The reaction was specific to MA and proceeded readily at room temperature.

In this study, we attempted to determine MA as MA–DNPH in various

peroxidized samples containing unsaturated fatty acids and rat liver microsomes. The values obtained by the conventional TBA and the high-performance liquid chromatographic (HPLC) methods were compared and the effect of the temperature employed in the reaction of MA and DNPH for the HPLC method was examined.

EXPERIMENTAL

Reagents and materials

Arachidonic acid, linolenic acid, thiobarbituric acid (TBA) and *tert.*-butyl hydroperoxide (*t*-BOOH) were obtained from Sigma (St. Louis, MO, U.S.A.). HPLC-grade acetonitrile was purchased from Nacalai Tesque (Kyoto, Japan). 2,4-Dinitrophenylhydrazine (DNPH), 1,1,3,3-tetraethoxypropane and 2-nitroresorcinol were obtained from Tokyo Kasei (Tokyo, Japan). Microsomes were prepared from rat liver homogenates made in iced 1.15% KCl solution by differential centrifugation[9]. Protein was determined by the method of Lowry *et al.*[10]. All other reagents were of analytical-reagent grade.

Lipid peroxidation

The ascorbate-induced system for the fatty acids contained *ca.* 70 μmol of each fatty acid, 100 μM $FeSO_4$, 1 mM KH_2PO_4, 0.4 mM ascorbate and 0.5% Triton X-100 in 2.0 ml of reaction mixture. The mixtures were incubated at 56°C for 2 h. For microsomes, 200-μl samples, 50 μM $FeSO_4$, 1 mM KCl and 0.4 mM ascorbate in 1.0 ml of air-saturated 0.1 M phosphate buffer (pH 7.5) were incubated at 56°C for 2 h. The *t*-BOOH-induced system contained *ca.* 70 μmol of each fatty acid, 100 μM $FeSO_4$, 1 mM *t*-BOOH and 0.5% Triton X-100 in 2.0 ml of reaction mixture. The mixtures were incubated at 56°C for 1 h. The NADPH-induced system for microsomes contained 100-μl samples, 50 μM $FeCl_3$, 4 mM ADP, 1 mM KCl and 0.4 mM NADPH in 1.0 ml of the above buffer, and the mixtures were incubated at 37°C for 1 h.

Measurement of MA

The MA formed was determined by the TBA method of Uchiyama and Mihara[11] and by the HPLC procedure. In the TBA method, extraction was carried out with *n*-butanol and then the absorbance of the organic phase was measured at 532 nm. Calibration graphs were prepared using MA obtained by the acid hydrolysis of 1,1,3,3-tetraethoxypropane. The HPLC method was as follows; for the fatty acid peroxidation systems, a 0.1-ml volume of peroxidized sample was reacted with 0.5 ml of DNPH solution (0.5 mg/ml in 1 M HCl) containing an appropriate amount of 2-nitroresorcinol as internal standard (IS) at room temperature (25°C) for 1 h or in boiling water-bath (100°C) for 10 min. An aliquot of the reaction mixture was injected into the HPLC column. For microsomal peroxidation systems, a 0.3-ml volume of peroxidized sample was reacted with 0.3 ml of DNPH solution (2.5 mg/ml in 1 M HCl) containing an appropriate amount of 2-nitroresorcinol at 25°C for 1 h. After centrifugation (5000 g for 10 min), an aliquot of the supernatant was injected. MA was calculated from an independently prepared calibration graph.

HPLC

A Model 6A high-performance liquid chromatograph (Shimadzu, Kyoto,

Japan) equipped with a UV spectrophotometric detector set at 310 nm was used for quantification of MA. The HPLC separations were performed on a Cosmosil 5 C_{18} packed column (250 × 4.6 mm I.D.; Nacalai Tesque) with a mobile phase consisting of acetonitrile–0.01 M hydrochloric acid (45:55, v/v) at a flow-rate of 1.5 ml/min at room temperature.

RESULTS AND DISCUSSION

We have previously described an HPLC method for determining MA in serum[7]. The technique, which uses DNPH as a derivatizing reagent, is simple, sensitive and specific. Therefore, we used this method to determine the MA levels in materials containing unsaturated fatty acids and microsomes, but without alkali treatment. The effect of protein on the recovery of MA added to the various concentrations of bovine serum albumin solution is shown in Fig. 1. As the concentration in *in vitro* systems was below 0.5%, the recovery was almost 100% without alkali hydrolysis. In the materials containing fatty acids, the MA–DNPH formed is possible soluble in coexisting fatty acids. For this reason, we studied the recovery of MA using an authentic synthesized MA–DNPH (Fig. 2). In the absence of Triton X-100, the peaks corresponding to both MA–DNPH and IS decreased and the recovery of MA–DNPH calculated from the peak height was about 40%. However, on adding Triton X-100 to the reaction mixture, about 100% of the MA–DNPH was recovered. Under these conditions, the
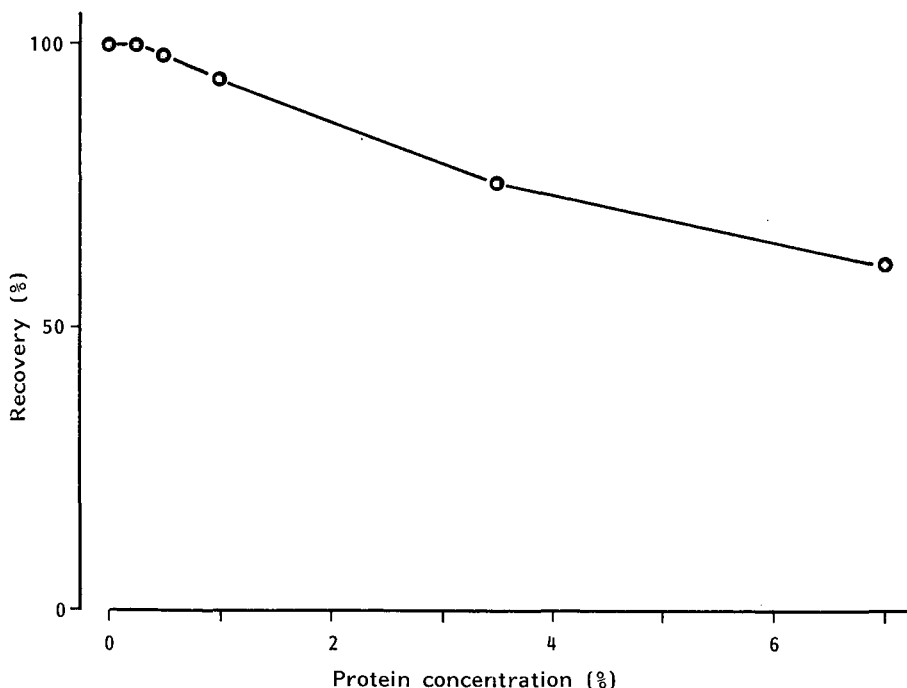
Fig. 1. Effect of protein concentration on the recovery of added MA. Samples containing 3.6 μg/ml of MA with various concentrations of bovine serum albumin were incubated with the same volume of DNPH aqueous solution at 25°C for 1 h.
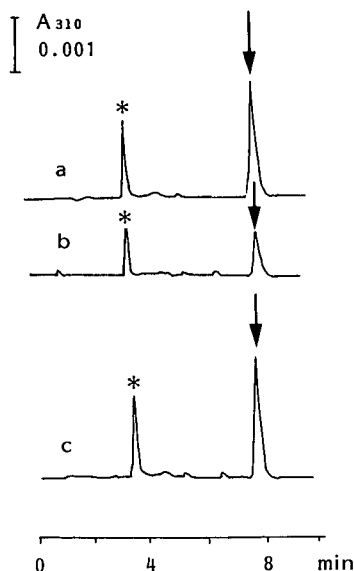
Fig. 2. Recovery of MA-DNPH (arrowed peaks) in aqueous solutions containing linolenic acid. (a) MA-DNPH aqueous solution (6 μg/ml) with 1.6 μg of 2-nitroresorcinol as IS; (b) as (a) with 0.2% linolenic acid added; (c) as (b) with 0.1% Triton X-100 added. Asterisks indicate IS. The volume of all samples was the same.

calibration graphs for both fatty acids and microsomes were linear up to 18 μg/ml of MA. The detection limits with a 20-μl injection were 8.3 and 25 pmol for fatty acids and microsomes, respectively. The relative standard deviations from the 1:5 incubation samples containing 1.44 and 3.6 μg/ml of MA were 4.73% and 5.14% ($n = 10$), respectively, and that from the 1:1 incubation samples containing 1.44 μg/ml of MA was 4.34% ($n = 10$). Incubation at 100°C increased the peak height for MA–DNPH to about 1.2 times that at 25°C. HPLC profiles for the materials containing arachidonic acid or microsomes peroxidized *in vitro* are shown in Fig. 3. The retention times for IS and MA–DNPH were *ca.* 3.5 and 7.8 min, respectively. The peak at *ca* 4.5 min represented unreacted DNPH. The peak at *ca.* 7.8 min was specific to MA, as shown in Fig. 3.

　　Table I shows the formation of MA from the unsaturated fatty acids in the oxidation system containing ascorbate. In this system, the MA values determined by the HPLC method were 20–25% of those obtained by the TBA method in the control assay and 60% in the oxidation system. The TBA method is not specific to MA[1-4]. In addition, it is well known that MA is produced at high temperatures and under acidic conditions[6]. Therefore, using the HPLC method, we investigated the effect of heat on the production of MA. As shown in Table I, no difference was found between the MA values obtained at 25 and at 100°C for either of the fatty acid samples. Hence it is obvious that TBA reacts with substances other than MA in fairly large amounts. The MA values in the peroxidized samples obtained by the TBA method increased to 2–3 times those in non-oxidized samples. The increase obtained by the HPLC method was 5–7 times greater. Hence the effect of peroxidation observed with the HPLC method was greater than that measured by the TBA method. Similar results were obtained with
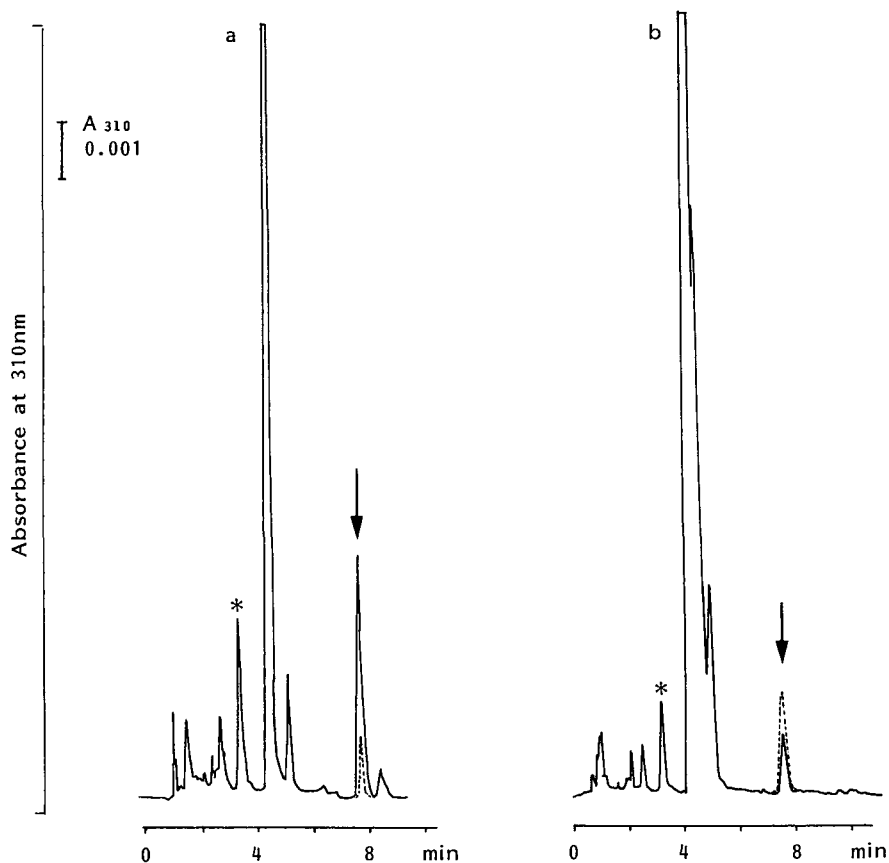
Fig. 3. Elution profile of MA-DNPH (arrowed peaks) for (a) arachidonic acid oxidized by the ascorbate system and (b) rat liver microsome oxidized by the NADPH system. The dashed line in (a) indicates the profile of the control assay and that in (b) indicates the profile of the oxidation system to which 6 nmol MA had been added. Asterisks indicate IS.

TABLE I

MA LEVELS FOUND IN ASCORBATE-INDUCED SYSTEMS CONTAINING FATTY ACIDS BY THE TBA AND HPLC METHODS

Data represent the mean values $\pm$ S.D. of three different experiments performed in duplicate. Values are expressed as nmol/ml. Samples incubated at 56°C for 2 h without ascorbate acted as the control.

Method	Arachidonic acid		Linolenic acid	
	Control	Peroxidized	Control	Peroxidized
TBA	76.9 ± 4.4	161.8 ± 2.5^b	66.1 ± 7.6	154.3 ± 0.4^a
HPLC (room temperature)	19.3 ± 1.5	95.4 ± 0.7^b	13.1 ± 0.8	91.5 ± 3.9^b
HPLC (boiling)	18.9 ± 1.0	100.6 ± 2.5^b	12.8 ± 2.2	94.9 ± 4.0^b

[a] Significantly different from control values, $p < 0.01$.
[b] Significantly different from control values, $p < 0.001$.

TABLE II

MA LEVELS FOUND IN *t*-BOOH-INDUCED SYSTEMS CONTAINING FATTY ACIDS BY THE TBA AND HPLC METHODS

Data represent the mean values ± S.D. of three different experiments performed in duplicate. Values are expressed as nmol/ml. Samples incubated at 56°C for 1 h without *t*-BOOH acted as the control.

Method	Arachidonic acid		Linolenic acid	
	Control	Peroxidized	Control	Peroxidized
TBA	36.1 ± 0.4	103.3 ± 14.7[a]	55.0 ± 5.8	122.8 ± 5.0[c]
HPLC (room temperature)	5.6 ± 1.1	17.8 ± 2.6[b]	9.6 ± 0.1	33.3 ± 1.4[c]
HPLC (boiling)	9.6 ± 1.4	55.3 ± 4.0[b]	9.7 ± 1.0	51.9 ± 4.2[c]

[a] Significantly different from control values, $p < 0.05$.
[b] Significantly different from control values, $p < 0.01$.
[c] Significantly different from control values, $p < 0.001$.

the *t*-BOOH-induced peroxidation system (Table II). The MA levels obtained by the HPLC method were 15–27% of those obtained by the TBA method in the control assay and 17–54% of those in the oxidation system. In this system, a significant difference in MA levels was observed between derivatizations at 25 and at 100°C. This is probably due to the effect of *t*-BOOH under the heating conditions employed in the DNPH derivatization reaction. As shown in Tables I and II, the MA values determined by the HPLC method were lower than those obtained by the TBA method. These results suggest that the proposed method with derivatization performed at 25°C, not 100°C, can determine MA levels selectively and accurately, whereas the TBA method tends to overestimate. These results are in agreement with those of other workers[12–14]. However, many investigators have presented conflicting results for MA values in lipid peroxidation[14–17]. In this study, we found that the MA values obtained by the HPLC method increased during lipid peroxidation and that this increase could be taken as an index of lipid peroxidation.

Lipid peroxidation has been proposed as a mechanism of tissue damage. NADPH- and ascorbate-induced lipid peroxidation of microsomes have been studied

TABLE III

MA LEVELS FOUND IN NADPH- AND ASCORBATE-TREATED MICROSOMES BY THE TBA AND HPLC METHODS

Data represent the mean values ± S.D. of three different experiments performed in duplicate. Values are expressed as nmol/mg protein. Microsomes incubated without NADPH (37°C for 1 h) or ascorbate (56°C for 2 h) acted as the controls.

Method	NADPH-induced		Ascorbate-induced	
	Control	Peroxidized	Control	Peroxidized
TBA	0.58 ± 0.05	13.21 ± 0.32[a]	2.29 ± 0.14	7.43 ± 0.48[b]
HPLC	trace	13.10 ± 0.35[b]	1.36 ± 0.13	5.25 ± 0.38[b]

[a] Significantly different from control values, $p < 0.01$.
[b] Significantly different from control values, $p < 0.001$.

in detail[18-20], with the TBA method being the method most commonly used. We applied the proposed HPLC method to the determination of MA in microsomal samples peroxidized *in vitro* (Table III). The difference in MA values in the two control assays depends on the differences in the incubation conditions. Kikugawa *et al.*[14], using the lipid fraction from the oxidized microsomes, reported that the MA contents in oxidized lipids were too low to be taken into account. Our results, however, showed a significant increase in the MA values in both oxidation systems. The value obtained by HPLC was the same as that obtained by the TBA method in the oxidation system containing NADPH. Although similar yields of MA by the HPLC and TBA methods were not obtained in other systems, the results have been reported by Janero and Burghardt[17,21]. These data support the view that the MA values in the NADPH system represent the major TBA reactive product in the microsomal lipid oxidized. However, MA is not the only decomposition product, as a variety of molecules can be generated from lipid peroxide breakdown. The MA value obtained by HPLC was 60–70% of that measured by the TBA method in the system containing ascorbate. The correlation between MA values obtained by HPLC and the TBA method depends on the peroxidation conditions[17]. Accordingly, we are convinced that the HPLC value is a good quantitative index of lipid peroxidation and hope that this method will encourage others to carry out more detailed studies on lipid peroxidation.

REFERENCES

1 R. Marcuse and L. Johansson, *J. Am. Oil Chem. Soc.*, 50 (1973) 387.
2 H. Esterbauer, K. H. Cheeseman, M. U. Dianzani, G. Poli and T. F. Slater, *Biochem J.*, 208 (1982) 129.
3 J. M. C. Gutteridge and D. Toeg, *Int. J. Biochem.*, 14 (1982) 891.
4 H. Kosugi and K. Kikugawa, *Lipids*, 20 (1985) 915.
5 W. A. Pryor, J. P. Stanley and E. Blair, *Lipids*, 11 (1976) 370.
6 T. Asakawa and S. Matsushita, *Lipids*, 14 (1979) 401.
7 S. Kawai, K. Kasashima and M. Tomita, *J. Chromatogr.*, 495 (1989) 235.
8 T. Ekström, P. Garberg, B. Egestad and J. Högberg, *Chem.-Biol. Interact.*, 66 (1988) 177.
9 S. Shaw, E. Jayatilleke and C. S. Lieber, *Biochem. Biophys. Res. Commun.*, 118 (1984) 233.
10 O. H. Lowry, N. J. Rosebrough, A. L. Farr and R. J. Randall, *J. Biol. Chem.*, 193 (1951) 265.
11 M. Uchiyama and M. Mihara, *Anal. Biochem.*, 86 (1978) 271.
12 R. P. Bird, S. S. O. Hung, M. Hadley and H. H. Draper, *Anal. Biochem.*, 128 (1983) 240.
13 M. Beljean-Leymarie and E. Bruna, *Anal. Biochem.*, 173 (1988) 174.
14 K. Kikugawa, T. Kato and A. Iwata, *Anal. Biochem.*, 174 (1988) 512.
15 T. Hirayama, N. Yamada, M. Nohara and S. Fukui, *J. Assoc. Off. Anal. Chem.*, 66 (1983) 304.
16 H.-S. Lee and A. S. Csallany, *Lipids*, 22 (1987) 104.
17 D. R. Janero and B. Burghardt, *Lipids*, 24 (1989) 125.
18 J. A. Buege and S. D. Aust, *Methods Enzymol.*, 52 (1978) 302.
19 D. J. Kornbrust and R. D. Mavis, *Mol. Pharmacol.*, 17 (1980) 400.
20 T. P. A. Devasagayam, *FEBS Lett.*, 199 (1986) 203.
21 D. R. Janero and B. Burghardt, *Lipids*, 23 (1988) 452.

Separation of membrane protein–sodium dodecyl sulphate complexes by high-performance liquid chromatography on hydroxyapatite

TAKAAKI HIRANUMA*, TSUNEYOSHI HORIGOME and HIROSHI SUGANO

Department of Biochemistry, Faculty of Science, Niigata University, 2-Igarashi, Niigata 950-21 (Japan)

ABSTRACT

The analytical conditions for the high-performance liquid chromatography of protein–sodium dodecyl sulphate complexes on ceramic hydroxyapatite were optimized for the purification of membrane proteins and the microanalysis of membrane protein mixtures. About 12 mg of erythrocyte membrane protein could be separated by ceramic hydroxyapatite chromatography at one time and about 0.8 mg of purified anion carrier protein was obtained on one-step purification. Erythrocyte membrane proteins could be analysed with buffers not containing dithiothreitol and detection at 230 nm. A two-step method, *i.e.*, combined diethylaminoethyl and hydroxyapatite chromatography, made it possible to separate many membrane proteins.

INTRODUCTION

High-performance liquid chromatography (HPLC) is one of the most useful methods for the separation and analysis of proteins. Recently, many soluble proteins have been purified by HPLC. However, with membrane proteins, solubilization of the samples is necessary prior to separation or analysis by HPLC. Various detergents have been used for membrane solubilization, depending on the purpose of the experiment.[1] However, most of the detergents used could not solubilize whole membrane proteins, *e.g.*, some intrinsic and high-molecular-weight proteins could not be solubilized by detergents other than sodium dodecyl sulphate (SDS). Therefore, the development of a chromatographic method for the separation of membrane proteins dissolved in SDS is very important for the analysis of whole membrane proteins.

Moss and Rosenblum[2] studied the separation of protein–SDS complexes by conventional hydroxyapatite chromatography. We have improved the resolution of their method by using a ceramic hydroxyapatite HPLC column and applied the modified method to membrane protein analysis[3]. The retention times of protein–SDS complexes increased with increasing hydrophobicity of the proteins. Whole membrane proteins were well separated with this method.

In this study, we examined the conditions for ceramic hydroxyapatite HPLC

for the microanalysis and preparative separation of membrane protein–SDS complexes. The two-step separation of whole membrane proteins was also examined through the combination of this method with ion-exchange chromatography.

EXPERIMENTAL

Materials

All reagents except 3-(tetradecyldimethylammonio)-1-propanesulphonate (Zwittergent 14) were purchased from Wako (Osaka, Japan). Zwittergent 14 was synthesized by the method of Gonenne and Ernst[4]. Biochemical-grade SDS was used.

Membrane preparations

Rat erythrocyte membranes and rat liver rough microsomal membranes were prepared according to the methods reported previously[3]. The rat brain myelin fraction was prepared by the method of Norton and Poduslo[5].

Buffers for HPLC

Buffer A was 0.01 M sodium phosphate buffer (pH 6.5) containing 1.0% SDS and 0.1 mM calcium chloride. Buffer B was 0.5 M sodium phosphate buffer (pH 6.5) containing 1.0% SDS and 7.5 μM calcium chloride. Buffers A' and B' were buffers A and B containing 0.5 mM dithiothreitol, respectively. Buffer C was 20 mM Tris–HCl buffer (pH 8.0) containing 0.4% Zwittergent 14. Buffer D was 20 mM Tris–HCl buffer (pH 8.0) containing 0.4% Zwittergent 14 and 1.0 M sodium chloride.

Columns used for HPLC

The columns used for hydroxyapatite HPLC were Hibar RT 100-8 hydroxy-apatite-MP (100 mm × 8.0 mm I.D.), (Cica-Merck, Tokyo, Japan) and TSKgel HA-1000 (75 mm × 7.5 mm I.D.) (Tosoh, Tokyo, Japan). A TSKgel DEAE-5 PW column (75 mm × 7.5 mm I.D.) (Tosoh) was used for anion-exchange chromatography.

HPLC apparatus

Chromatographic equipment consisting of a model L-5000 LC controller, Model 655A-11 and 655A-12 pumps, a Model 655A variable-wavelength UV monitor, a Model D-2500 chromato-integrator (Hitachi, Tokyo, Japan), an injector with a 1-ml loop (Rheodyne, Cotati, CA, U.S.A.) and a fraction collector (LKB, Bromma, Sweden) was used.

Solubilization of membrane proteins

To a 140-μl aliquot of a protein solution (5.5 mg protein/ml buffer A) were added 50 μl of 10% SDS and 10 μl of 2-mercaptoethanol, followed by incubation at 37°C for 1 h. The solution was diluted with an equal volume of buffer A or A' and then centrifuged at 8500 g for 10 min. A 250-μl aliquot of the supernatant was applied to a ceramic hydroxyapatite column. In exchange chromatography, Zwittergent 14 and 40 mM Tris–HCl (pH 8.0) were used instead of SDS and buffer A.

Standard conditions for ceramic hydroxyapatite HPLC

Rat erythrocyte membrane protein–SDS complexes (0.48 mg of protein) were applied to a TSK gel HA-1000 column equilibrated with buffer A', followed by elution with a 69-min linear gradient from 55 to 100% of buffer B' at 30°C. The flow-rate was 0.6 ml/min.

Two-step separation of membrane proteins

First step. A TSK gel-5PW column was equilibrated with buffer C. Rat erythrocyte membrane protein (4.5 mg) solubilized as above was applied to the column, followed by elution with a 120-min linear gradient, from 0 to 100%, of buffer D at a flow-rate of 1.0 ml/min. The column temperature was maintained at 30°C and the effluent was monitored by measuring the absorbance at 280 nm. The eluted sample was separated into ten fractions, as shown in Fig. 6A.

Second step. Each fraction was separated by hydroxyapatite HPLC in the presence of SDS. In the case of fraction 1, a 1.8-ml aliquot (1/5 volume) of the fraction was added to 1.35 ml of 10% SDS, 0.27 ml of 2-mercaptoethanol and 1.98 ml of buffer A, followed by incubation at 37°C for 1 h. After centrifugation at 8500 g for 10 min, a 5-ml aliquot of the supernatant was applied to a hydroxyapatite column. After washing with buffer A for 5 min the sample was eluted under the standard conditions except that a linear gradient from 50 to 95% of buffer B was used.

SDS–polyacrylamide gel electrophoresis (SDS-PAGE)

To 20-μl of each fraction was added concentrated dithiothreitol solution (final concentration 24 mM), followed by incubation at 37°C for 1 h. Prior to application of the sample to a gel, sulphydryl groups in the sample were blocked with iodoacetamide[6]. An aliquot of each fraction of the column eluent was analysed by SDS-PAGE according to the method of Laemmli[7]. Linear gradient acrylamide gels (4–15 or 6–15%) were used. After electrophoresis, the gels were stained with silver according to a modification of the method of Morrissey, as reported previously[8]. M, P, B, A and C denote the positions of molecular weight marker proteins: M = myosin (MW 205 000); P = phosphorylase b (MW 97 400); B = bovine serum albumin (MW 66 000); A = actin (MW 42 000); and C = carbonic anhydrase (MW 29 000).

RESULTS AND DISCUSSION

Preparative hydroxyapatite chromatography

When the usual amount of rat erythrocyte membrane protein–SDS complexes was applied to a ceramic hydroxyapatite column and eluted with buffers containing 1% SDS, good resolution was obtained, as can be seen in Fig. 1. Most proteins were bound on the column, and then not only low but also high-molecular-weight proteins such as the α- and β-chains of spectrin were eluted as sharp peaks with a phosphate buffer concentration gradient. These results show that this method is useful for separating and analysing membrane proteins which cannot be separated by ion-exchange or reversed-phase chromatography.

As a basis for the preparative separation of membrane proteins, the amount of membrane protein that can be applied to a column was examined using rat erythrocyte membranes. As can be seen in Fig. 2, with an increase in the amount of applied
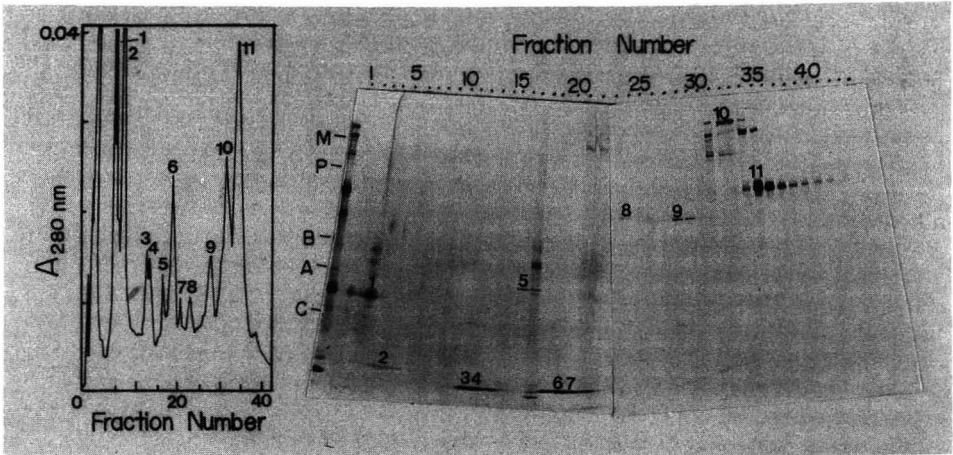
Fig. 1. Separation of erythrocyte membrane protein–SDS complexes by ceramic hydroxyapatite HPLC. Left: rat erythrocyte membrane protein–SDS complexes (0.48 mg of protein) were separated under the standard conditions. The eluate was collected in 1.8-ml (Nos. 1–4) or 0.9-ml fractions (Nos. 5–44). Right: the fractions were analysed by SDS-PAGE under the standard conditions. Proteins numbered in the gel are as follows: 1,2 = unknown; 3,4 = haemoglobin α_1- and α_2-chains; 5 = actin; 6,7 = haemoglobin β_1- and β_2-chains; 8 = band 4.1; 9 = band 4.2; 10 = spectrin α-chain; 11 = anion carrier protein.

protein, the separation of each membrane protein became poorer, the protein–SDS complexes were eluted faster and the tailing of peaks increased. When 24 mg of protein were applied, part of the sample protein could not be adsorbed on the column, being eluted in the flow-through fraction (data not shown). These results suggested that the amount of sample should be kept at less than 12 mg of protein.

Generally, a decrease in the flow-rate increases the resolution in the chromatography of macromolecules such as proteins. A protein–SDS complex has a Stoke's radius larger than that of the respective native globular protein. Therefore, we chose a lower flow-rate of 0.3 ml/min for the preparative separation of rat erythrocyte mem-
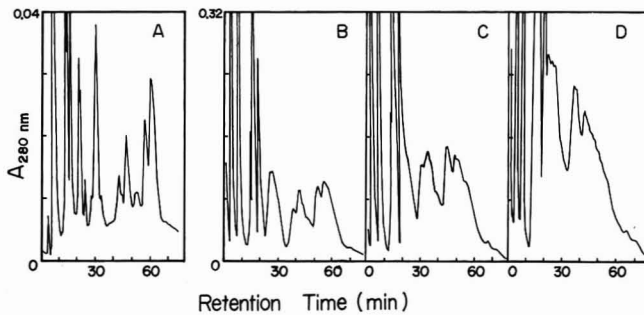
Fig. 2. Loadability of the hydroxyapatite column. Various amounts of rat erythrocyte membrane proteins were separated with a Hibar RT 100-8 hydroxyapatite-MP column under the standard conditions except that a 47–92% buffer B' gradient was used. Amounts of rat erythrocyte membrane proteins: A, 0.48; B, 3.0; C, 6.0; D, 12 mg.
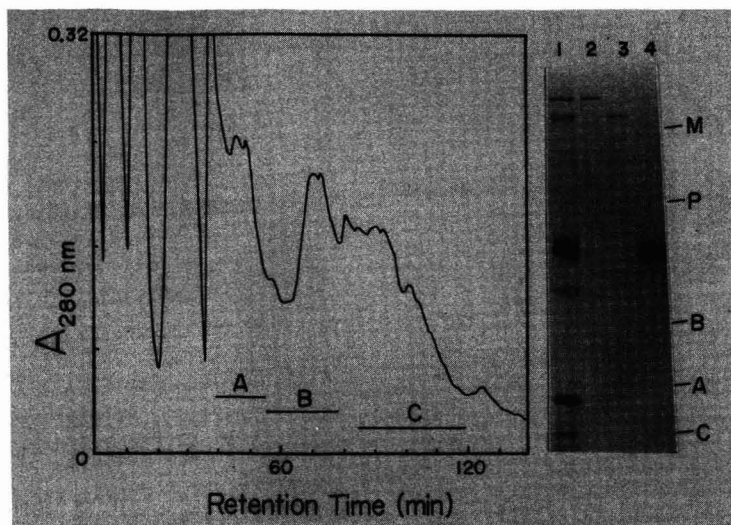
Fig. 3. Purification of spectrin α-chain, spectrin β-chain and anion carrier protein from erythrocyte membranes by hydroxyapatite HPLC. Left: rat erythrocyte membrane (12 mg of protein) was separated with a 138-min linear gradient and a flow-rate of 0.3 ml/min. Other conditions as in Fig. 2. The eluate was collected in 0.9-ml fractions. Right: SDS-PAGE of the isolated spectrin α-chain, spectrin β-chain and anion carrier protein fractions. Aliquots of the A, B and C fractions (left) which contained spectrin α-chain, spectrin β-chain and anion carrier protein, respectively, were subjected to SDS-PAGE and then the gel was stained with silver. Lanes: 1 = rat erythrocyte membrane protein; 2 = fraction A; 3 = fraction B; 4 = fraction C. Marker proteins as in Fig. 1.

brane proteins (Fig. 3). The eluate was analysed by SDS-PAGE and it was shown that all the peaks that appeared at 80–110 min were anion carrier protein. Therefore, fractions were collected as shown in Fig. 3. Fraction A, B and C contained spectrin α-chain, spectrin β-chain and anion carrier protein as the main components, the contents being 84, 71 and 95%, respectively. About 0.7, 0.6 and 0.8 mg of protein were obtained from these fractions through the one-step purification. This method could be applied to the purification of other membrane proteins with little changes in the gradient.

Microanalysis of membrane proteins

Under the standard conditions, samples were analysed using buffers containing dithiothreitol to prevent the oxidation of sulphydryl groups during the analysis. Therefore, the absorbance at 280 nm had to be used for protein detection because buffers containing dithiothreitol absorb light of wavelength shorter than 240 nm. However, the use of a shorter wavelength was necessary to increase the sensitivity. We therefore attempted to separate erythrocyte membrane proteins with buffers not containing dithiothreitol and with detection at 230 nm (Fig. 4). It was found that dithiothreitol in the elution buffer could be omitted without any change in the elution pattern (compare Fig. 4A and C). Pretreatment of a sample with iodoacetamide to block sulphydryl groups in the sample also had no effect on the pattern. The use of the absorbance at 230 nm made it possible to reduce the sample amount to 100 μg of
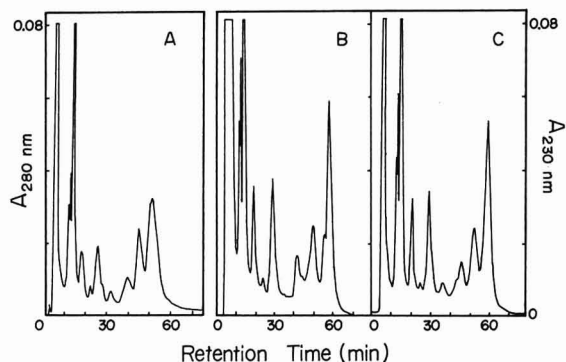
Fig. 4. Influence of omission of dithiothreitol from the elution buffer on the elution pattern. Rat erythrocyte membrane protein–SDS complexes were separated under the standard conditions except that buffers A and B were used instead of buffers A' and B', and chromatography was performed at room temperature. Buffer A not containing dithiothreitol but with 24.4 μM of sodium azide added was used in B and C. The amounts of samples were (A) 480, (B) 96 and (C) 96 μg. The sample in B was treated with iodoacetamide to block sulphydryl groups prior to analysis[6].

protein (Fig. 4). Correction of the baseline was also attempted because some lots of the second buffer showed a slightly higher absorbance than that of the first, and the baseline increased during analysis. Cytidine shows some absorbance in the ultraviolet region and does not adsorb to hydroxyapatite. Therefore, the baseline was corrected by the addition of a suitable amount of cytidine to the first buffer when necessary. The addition of an adequate amount of cytidine reduced the change in the baseline during analysis and as little as 24 μg of protein could be analysed constantly (Fig. 5). This sample amount is comparable to that necessary for SDS-PAGE analysis with Coomassie blue staining. This method was applied to the analysis of proteins of erythrocyte membrane, a myelin fraction and a rough microsomal membrane fraction, good
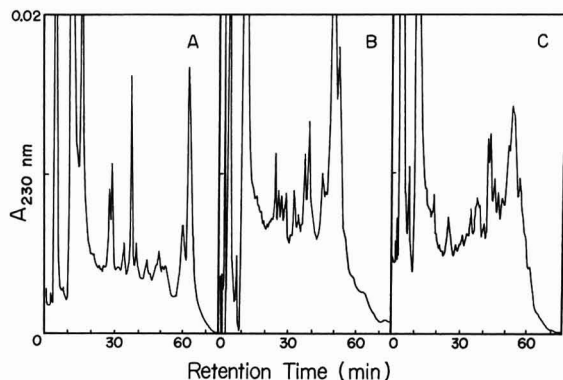
Fig. 5. Microanalysis of membrane proteins. Samples were separated by ceramic hydroxyapatite chromatography under the standard conditions except that a 50–95% buffer B gradient was used. Samples containing 24 μg of protein of (A) rat erythrocyte membrane, (B) rat brain myelin fraction and (C) rat liver rough microsomal membrane were analysed.

Retention Time (min)
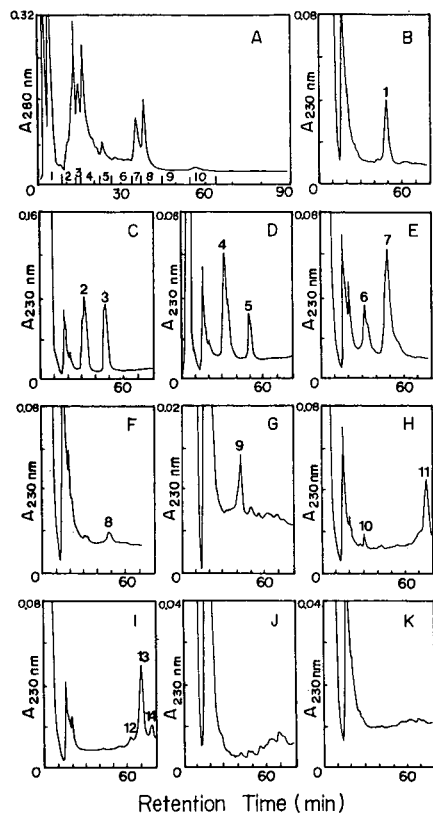
Fig. 6. Two-step purification of membrane proteins. (A) Anion-exchange HPLC of erythrocyte membrane proteins. Rat erythrocyte membrane proteins (4.5 mg) were solubilized with Zwittergent 14 and separated with a TSKgel DEAE-5PW column. The eluate was fractionated into ten fractions, as shown. (B–K) Hydroxyapatite HPLC of fractions 1–10, respectively. Fractions were treated with SDS and analysed by TSKgel HA-1000 column chromatography. Proteins separated as peaks 1–14 in B–K were as follows: 1, 3, 5 and 7 = haemoglobin β_1- and β_2-chains; 2, 4 and 6 = haemoglobin α_1- and α_2-chains; 8 = unknown; 9 = actin; 10 = 30 000 dalton protein; 11 = spectrin β-chain; 12 = unknown; 13 = spectrin α-chain; 14 = spectrin β-chain.

resolution being obtained in all instances (Fig. 5). Sodium azide could also be used instead of cytidine for correction of the baseline (see Fig. 4B and C).

Two-step analysis of erythrocyte membrane proteins

Although the above method showed very high resolution, it was not sufficient to separate all proteins in a complex protein mixture from each other. Therefore, a two-step separation method was examined. It is known that in the hydroxyapatite chromatography of protein–SDS complexes there is a positive correlation of the retention time with lõg (molecular mass) and Log Σ (hydrophobicity of amino acids), but not with the isoelectric point[3]. Therefore, we chose ion-exchange chromatography, the separation mode of which is different from that of the above chromatography, as the fractionation step prior to hydroxyapatite chromatography. Erythrocyte

membranes were solubilized with Zwittergent 14 and then fractionated into ten fractions by DEAE column chromatography (Fig. 6A). Then the fractions were analysed by hydroxyapatite chromatography.

As expected, the combination of DEAE and hydroxyapatite chromatography allowed a better separation of membrane proteins from each other than the one-step method. This two-step method will be useful for the analysis of more complex membrane protein mixtures. In this system, Zwittergent 14 was used to solubilize the erythrocyte membrane proteins. However, one of the intrinsic membrane proteins, anion carrier protein, could not be solubilized completely by the detergent. Hence improvements in the solubilization conditions are needed to make this method more suitable for whole membrane protein analysis. Investigations along these lines are in progress.

REFERENCES

1 G. W. Welling, R. van der Zee and S. Welling-Wester, *J. Chromatogr.*, 418 (1987) 223.
2 B. Moss and E. N. Rosenblum, *J. Biol. Chem.*, 247 (1972) 5194.
3 T. Horigome, T. Hiranuma and H. Sugano, *Eur. J. Biochem.*, 186 (1989) 63.
4 A. Gonenne and R. Ernst, *Anal. Biochem.*, 87 (1978) 28.
5 W. T. Norton and S. E. Poduslo, *J. Neurochem.*, 21 (1973) 749.
6 F. Hashimoto, T. Horigome, M. Kanbayashi, K. Yoshida and H. Sugano, *Anal. Biochem.*, 129 (1983) 192.
7 U. K. Laemmli, *Nature (London)*, 227 (1970) 680.
8 T. Horigome, T. S. Golding, V. E. Quarmby, D. B. Lubahn, Sr., K. McCarty and K. S. Korach *Endocrinology*, 121 (1987) 2099.

CHROMSYMP. 1927

Analysis of proteins by high-performance liquid chromatography with circular dichroism spectrophotometric detection

YASUYUKI KUROSU, TORU SASAKI, TAKASHI TAKAKUWA, NOBUYUKI SAKAYANAGI, KIYOKATSU HIBI and MASAAKI SENDA

JASCO, Japan Spectroscopic Co., Ltd., 2967–5, Ishikawa-cho, Hachioji City, Tokyo 192 (Japan)

ABSTRACT

High-performance liquid chromatography combined with circular dichroism spectrophotometry (HPLC–CD) for the separation and conformational analysis of proteins is described. The HPLC–CD measurement of proteins was performed easily and reproducibly with a gradient elution method by using a micro-flow cell unit. Reversed-phase chromatography and hydroxyapatite chromatography of proteins with this system were demonstrated. In addition, the influence of salts, surfactants and the interaction of packing materials on the secondary structure of proteins during HPLC was investigated and the α-helix content of protein was calculated by using a secondary structure estimation program.

INTRODUCTION

High-performance liquid chromatography (HPLC) is now routinely applied to the separation of proteins owing to its high resolution and rapid separation capability. However, the biological activity of a protein is often reduced or lost during the HPLC separation process.

The biological activity of a protein is related to its conformational structure. Therefore, it has been desirable to have a detector which can sensitively monitor the conformational structure. NMR, X-ray diffraction and circular dichroism (CD) are well known methods for the conformational analysis of proteins. Although NMR and X-ray diffraction offer a high resolution capability, NMR analysis requires too much sample and it is very difficult to use as an on-line monitor for an HPLC system. With X-ray diffraction analysis, it is impossible to measure a protein in solution. Of the three methods, CD is the most useful for the conformational analysis of proteins in combination with a separation method. A CD spectrophotometer allows the determination of the secondary structure, which is a conformational structure, of a protein in solution with higher sensitivity than NMR. Therefore, if a CD spectrophotometer can be used as an on-line monitor with an HPLC system, such a system (HPLC–CD)

would be a powerful tool for the separation and conformational analysis of proteins.

In the early 1980s, preliminary studies on HPLC–CD were reported[1–3]. However, they examined the applicability of HPLC–CD systems only to low-molecular-weight chiral substances. More recently, we reported[4,5] an HPLC–CD system for protein analysis based on gel filtration chromatography (GFC) and a highly sensitive CD system which was equipped with a micro-flow cell. We have now extended the HPLC section of the system to reversed-phase (RP) HPLC and hydroxyapatite chromatography (HAC) with gradient elution, and have investigated the influences of salts, surfactants and stationary phase materials on the secondary structure in protein separation.

EXPERIMENTAL

Materials

All proteins and tyrosine were purchased from Sigma (St. Louis, MO, U.S.A.). Surfactants {sodium dodecyl sulphate (SDS), Tween 20 and 3-[(3-cholamidopropyl) dimethylammonio]-1-propanesulphonate, (CHAPS)} were purchased from Wako (Osaka, Japan). For GFC, Biofine GFC SI-150K [particle size 7 μm, exclusion size 1 · 10^5 dalton (protein level), column dimensions 300 mm × 7.5 mm I.D., packing material silica), for HAC, Biofine HAC-5CP (particle size 5 μm, column dimensions 100 mm × 7.5 mm I.D.), RP-HPLC, Biofine RPC-SC18 (particle size 7 μm, column dimensions 250 mm × 4.6 mm I.D.), were used. All column were obtained from JASCO (Tokyo, Japan). Other reagents were purchased from Wako.

Apparatus

HPLC was carried out on a JASCO 800 Series HPLC system with a Multi-320 multi-wavelength UV detector (195–350 nm) (JASCO) and a Model J-600 CD spectrophotometer with a micro-flow cell device attached. Both detectors were connected in series to give an HPLC–UV–CD system.

Preparation of protein solution

Each protein solution was prepared by dissolution in the same solvent as the eluent (concentration 0.01–1%, w/v) except for RP-HPLC, where water was used. In the gradient elution method, the first eluent was used. The solution was stored for about 1 h at 0°C and then HPLC was performed.

Chromatographic procedure and CD measurement

The effluent was first monitored at 195–350 nm by using the multi-wavelength UV detector, and subsequently monitored at 220 nm by using the CD spectrophotometer [spectral band-width (SBW) 2 nm; time constant (TC) 2 s]. The on-line CD spectrum was measured with the following procedures. The pump delivery was stopped at each chromatographic peak top monitored by CD and at the same time the injector valve was set to the intermediate position to stop the eluent flow completely (stopped-flow method). Then each CD spectrum under the operating conditions of SBW = 2 nm, TC = 0.5 s, scan speed = 50 nm/min and a computer of average transient (CAT) = 5 was measured within 10 min. After completion of one CD measurement, the pump delivery was restarted to continue the elution. The CD chro-

matogram and on-line CD spectra were obtained by performing measurements separately. As a reference for the CD spectrum, the effluent at the same retention time as each eluted protein was used.

HPLC was performed under the following conditions. For RP-HPLC, the column was Biofine RPC-SC18; eluent, linear gradient of acetonitrile (10–60%) in 0.1% trifluoroacetic acid (TFA) for 20 min; flow-rate, 1.0 ml/min; and column temperature, room temperature. For HAC, the column was Biofine HAC-5CP; eluent, linear gradient of sodium phosphate (10–300 mM) in the presence or absence of 0.1% Tween 20 for 20 min; flow-rate, 1.0 ml/min; and column temperature, room temperature. For GFC, the column was Biofine GFC SI-150K; eluent, (A) 50 mM Tris–HCl (pH 7.2) or (B) 50 mM Tris–HCl + 300 mM sodium chloride (pH 7.2) in the presence or absence of surfactant; flow-rate, 1.0 ml/min; and column temperature, room temperature. For flow-injection analysis (FIA), the same conditions as in GFC were adopted, except for the column.

Secondary structure estimation (SSE) of proteins

After smoothing by fast Fourier transformation (FFT), secondary structure estimation of proteins was performed by an SSE program (JASCO protein SSE program). This program provides the four fractions of the secondary structure of α-helix, β-form, β-turn and unordered form of protein conformation.

RESULTS AND DISCUSSION

HPLC–CD for RP-HPLC and HAC using the gradient elution method

HPLC–CD measurements of some proteins were performed using RP-HPLC with a linear gradient of acetonitrile (10–60%) for 20 min (Fig. 1) and HAC with a linear gradient of sodium phosphate (10–300 mM) for 20 min (Fig. 2). The amount of each protein charged was 50 μg [total injection volume, 150 μl (RP-HPLC) and 100 μl (HAC)], which was suitable for CD detection. As a reference for the CD spectrum, the effluent at the same retention time as each eluted protein was used. Although the reference is not completely identical, no difference was observed between CD spectra which were repeatedly measured three times.

Fig. 1 shows (A) the CD chromatogram at 220 nm, (B) the UV chromatogram at 280 and 350 nm and (C) the CD spectra (192–250 nm) of proteins on RP-HPLC. This mode allows proteins to be substantially denatured because of the high concentration of the organic solvent. For example, myoglobin was changed into an apoprotein part (peak 3, first) and a haeme part (peak 3, second). The haeme peak, which did not have a secondary structure such as proteins, was not monitored by CD. The apoprotein peak was determined from both the UV and CD spectra and amino acid analysis (data not shown).

Fig. 2 shows (A) the CD chromatogram at 220 nm, (B) the UV chromatogram at 280 and 350 nm in the absence of Tween 20, and the CD spectra (192–250 nm) of (C-1) myoglobin and (C-2) cytochrome c in the absence (solid lines) and presence (dashed and dotted lines) of Tween 20 on HAC. The separation and the CD spectra of cytochrome c were greatly influenced by Tween 20. Two peaks appeared in the presence of Tween 20 on HAC. As shown Fig. 2(C-2), each CD spectrum was very different from that in the absence of Tween 20. In contrast, the CD spectra of myoglo-
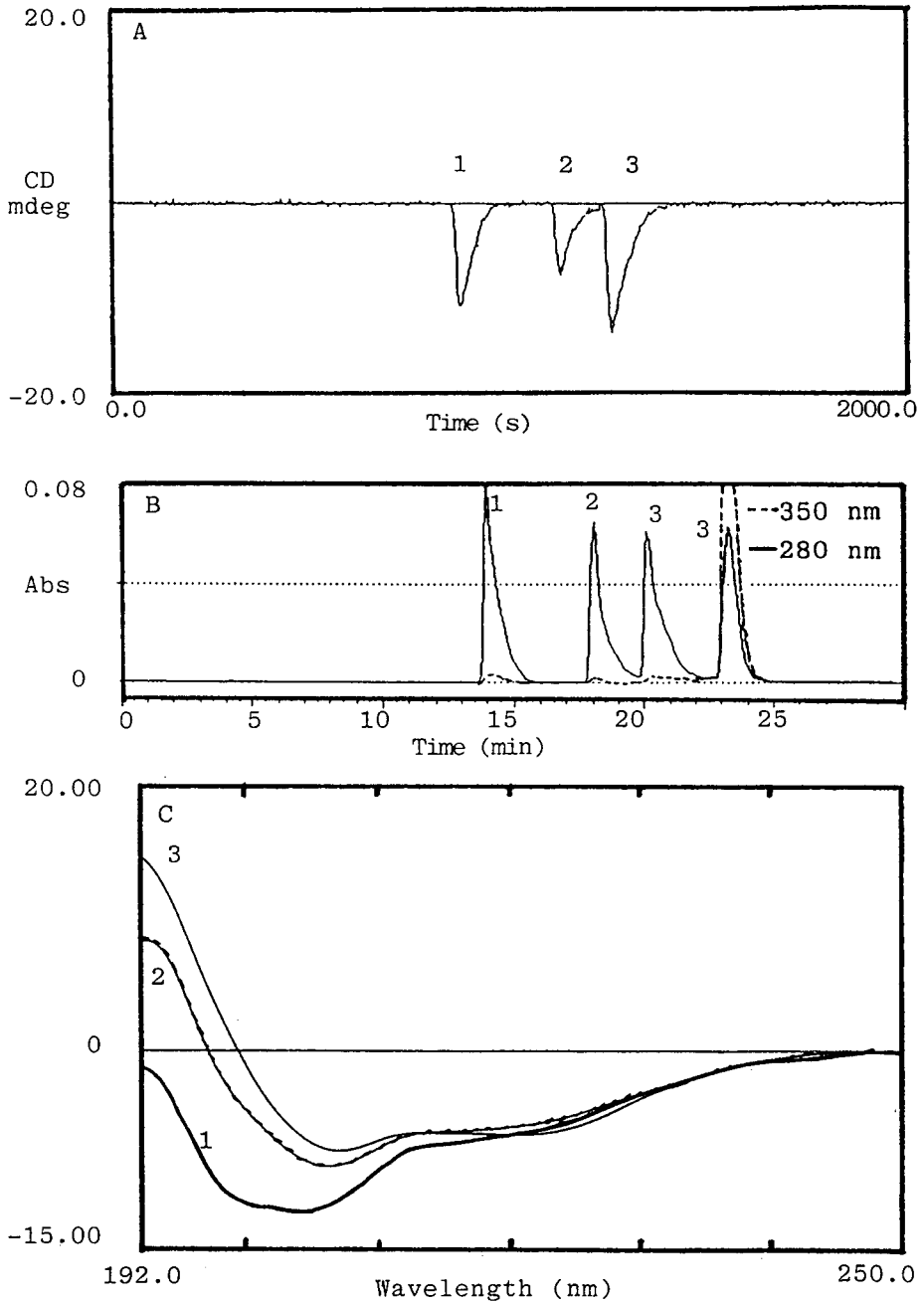
Fig. 1. RP-HPLC of proteins by using the described HPLC–CD system. (A) CD chromatogram; (B) UV chromatogram; (C) CD spectra with the stopped-flow method. Sample: 1 = ribonuclease A; 2 = transferrin; 3 = myoglobin. Chromatographic conditions as described under Experimental.
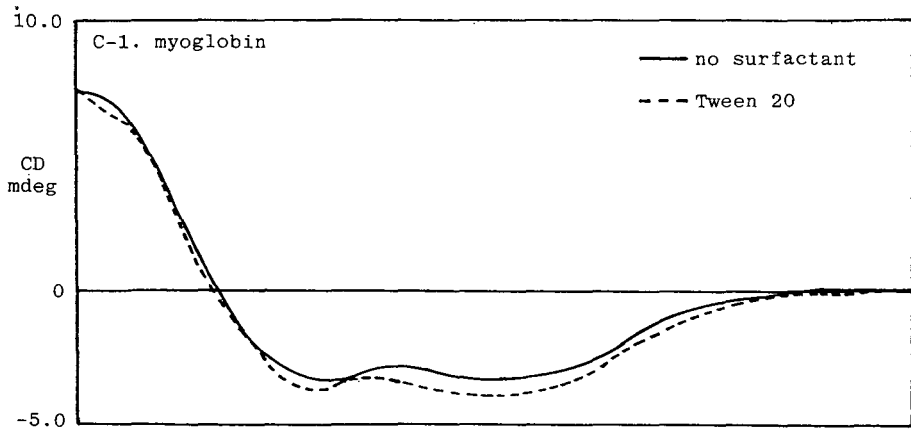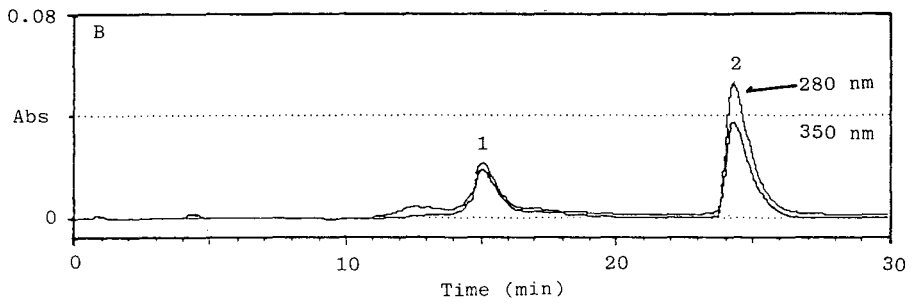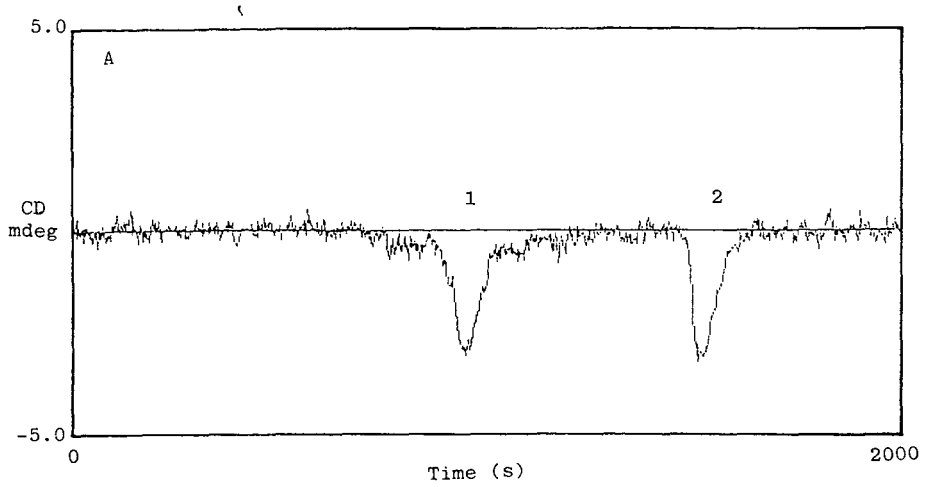
Fig. 2.
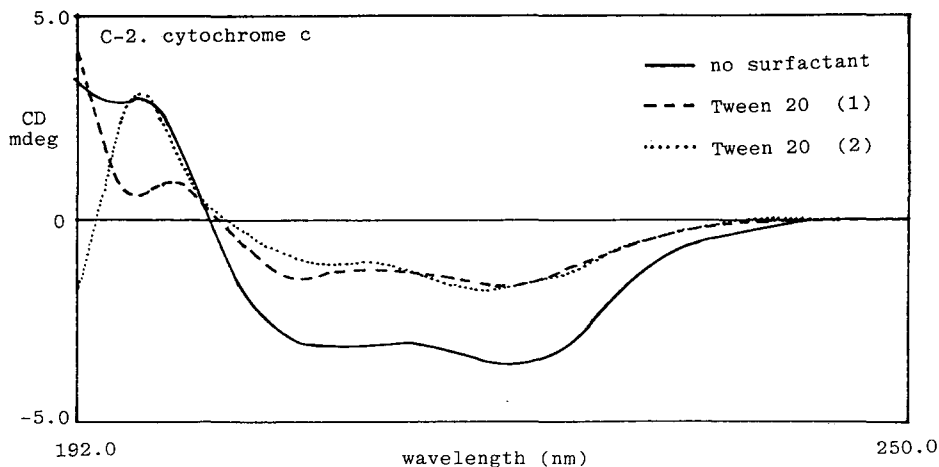
Fig. 2. HAC of proteins by using the described HPLC–CD system. (A) CD chromatogram; (B) UV chromatogram; (C) CD spectra of (C-1) myoglobin and (C-2) cytochrome c with the stopped-flow method. Sample: 1 = myoglobin; 2 = cytochrome c. Chromatographic conditions as described under Experimental. The CD and UV chromatograms and CD spectra (solid lines) were obtained in the absence of Tween 20. Dashed and dotted lines represent the CD spectra obtained during HAC in the presence of 0.1% Tween 20 (C-1 and C-2). With cytochrome c, two peaks appeared on HAC in the presence of 0.1% Tween 20.

bin in the absence and presence of Tween 20 were only slightly different. The HPLC–CD measurement could be performed by the gradient elution method with not only sodium phosphate (10–300 mM) but also sodium chloride (0–500 mM), which was confirmed by ion-exchange chromatography (IEC) (data not shown). Hence it was demonstrated that HPLC–CD could be performed with the gradient elution method using several separation modes.

Effect of packing materials on α-helix content of proteins

The biological activity of a protein is often reduced or lost during the HPLC separation process. Although the nature of the eluent is known to cause denaturation, we presumed that the packing materials may also be related to denaturation. As FIA can be considered to represent HPLC without an analytical column, in FIA proteins could not be influenced by interactions with packing materials. Therefore, a comparison of GFC with FIA will demonstrate the influence of the packing materials on the conformational structure of proteins under the same chromatographic conditions.

We adopted the α-helix content, which is one factor of secondary structure, to determine the conformational structure, because it was expected to be the most stable conformation in comparison with the β-form, β-turn, etc. The estimation was performed with the SSE program.

As shown Table I, lysozyme was not eluted by 50 mM Tris–HCl (pH 7.2) (solvent A) in GFC. However, It was eluted by 50 mM Tris–HCl + 300 mM sodium chloride (pH 7.2) (solvent B) in GFC. This result indicates a strong interaction between the packing materials and lysozyme in a buffer of weak ionic strength. In myoglobin, although it was eluted by both solvents A and B, the α-helix content with

TABLE I

EFFECT OF PACKING MATERIALS ON THE α-HELIX CONTENT OF PROTEINS

Eluent: A, 50 mM Tris–HCl (pH 7.2); B, 50 mM Tris + 300 mM NaCl (pH 7.2). Other conditions as described under Experimental. The α-helix content was calculated with the SSE program.

Protein	Eluent	α-Helix content (%)	
		FIA	GFC
Lysozyme	A	35.4	Not eluted
	B	38.4	34.9
Myoglobin	A	62.0	57.4
	B	63.1	62.9
Transferrin	A	48.9	40.1
	B	48.2	42.3
Haemoglobin	A	56.1	57.6
	B	56.4	57.7

solvent A in GFC was slightly decreased in comparison with that with solvent A on FIA. In transferrin, when GFC was performed, the α-helix contents with both solvents A and B were decreased in comparison with FIA. In haemoglobin, the α-helix content was not influenced by the nature of the solvent and packing materials. In general, ionic strength is not related to α-helix content in FIA, but it is related to it in GFC, which causes a slight interaction. The results showed no influence of the concentration of sodium chloride (at least in the range 0–300 mM) on denaturation. However, the influence of the packing materials on denaturation was suggested during HPLC in the HPLC–CD analysis.

Effect of surfactants on α-helix content of proteins

As shown in Fig. 2, the presence of a surfactant affected HAC. Generally the chromatographic resolution and reproducibility is reduced by the presence of surfactants. In addition, surfactants cause denaturation of active proteins. However, surfactants are very useful for the solubilization of insoluble proteins, e.g., membrane proteins. SDS (strong for solubilization, ionic), Tween 20 (medium, non-ionic) and

TABLE II

EFFECT OF SURFACTANTS ON THE α-HELIX CONTENT OF PROTEINS

Eluent: A, 50 mM Tris–HCl (pH 7.2). Other conditions as described under Experimental. The α-helix content was calculated with the SSE program.

Eluent	α-Helix content (%)			
	Lysozyme	Myoglobin	Transferrin	Haemoglobin
A	26.2	63.1	48.2	56.4
A–0.1% SDS	23.4	55.6	42.7	52.8
A–0.1% Tween 20	23.9	64.5	47.0	58.9
A–0.1% CHAPS	23.7	63.5	51.9	57.2

CHAPS (weak, amphoteric) were used as surfactants. This investigation was performed by FIA and the use of the SSE program.

As shown Table II, the α-helix content of lysozyme was reduced by all the surfactants used. However, those of myoglobin, transferrin and haemoglobin were hardly changed by Tween 20 and CHAPS. CHAPS in fact caused the α-helix contents of myoglobin, transferrin and haemoglobin to increase slightly.

In addition, the influence of concentration of Tween 20 and SDS on the α-helix content was investigated (data not shown). The results observed were as expected: in myoglobin, the α-helix content was influenced by the concentration of SDS (strong surfactant) and not influenced by that of Tween 20 (medium surfactant). Similar results were obtained on GFC by the presence of SDS. However, the degree of denaturation was enhanced as compared with that on FIA. The α-helix contents of transferrin, myoglobin and lysozyme, with those obtained by FIA under the same conditions in parentheses were 36.6 (42.7), 43.9 (55.6) and 24.5% (23.4%), respectively. The results suggested that both SDS and the packing materials caused denaturation during HPLC. In lysozyme, although the values were almost unchanged, it may represent the limit of denaturation because of the rigid protein structure (lysozyme has four disulphide bonds).

CONCLUSION

As demonstrated, the HPLC–CD system could be easily applied to the analysis of the conformation of proteins during HPLC using a gradient elution method, *e.g.*, RP-HPLC with an organic solvent or HAC with a buffer containing salts.

In addition, the influence of surfactants and packing materials on the secondary structure was observed by using this system during HPLC. Salts such as sodium chloride in the concentration range 0–300 mM did not cause denaturation of some standard proteins sodium chloride.

This method will permit theoretical studies of the behaviour of active proteins during HPLC, and in the future, the relationship between the structure of proteins and their activity during HPLC will be studied using this system.

REFERENCES

1 A. F. Drake, J. M. Gould and S. F. Mason, *J. Chromatogr.*, 202 (1980) 239.
2 S. A. Westwood, D. E. Games and L. Sheen, *J. Chromatogr.*, 204 (1981) 103.
3 P. Salvadori, C. Rosini and C. Bertucci, *J. Org. Chem.*, 49 (1984) 5050.
4 T. Takakuwa, Y. Kurosu, N. Sakayanagi, F. Kaneuchi, N. Takeuchi, A. Wada and M. Senda, *J. Liq. Chromatogr.*, 10 (1987) 2759.
5 Y. Kurosu and T. Takakuwa, *Bunkou Kenkyu*, 36 (1987) 413.

CHROMSYMP. 1880

Review

Applications of high-performance liquid chromatography in bacteriology

I. Determination of metabolites

C. LUCARELLI*

Istituto Superiore di Sanità, V. le R. Elene, 299 00161 Rome (Italy)

and

L. RADIN, R. CORIO and C. EFTIMIADI

Istituto di Microbiologia, Università di Genova, Genova (Italy)

CONTENTS

1. INTRODUCTION

     Recent studies on the chemistry of bacterial cells have dealt with both the analysis of the structural components and the determination of the metabolic end-products. A wide range of instrumental techniques, including gas chromatography and high-performance liquid chromatography (HPLC), are currently available in chemical bacteriology. The purpose of this review is to summarize work concerning the bacterial identification by HPLC analysis of spent culture media, to discuss in detail some aspects of the chromatographic procedures and to evaluate the potential of HPLC for application to the analysis of body fluids. In particular, this review deals with the chemotaxonomic approach to the identification of pathogenic bacteria for clinical purposes. The primary interest is the application of HPLC to the determina-

tion of metabolic end-products derived from anaerobic bacteria. A brief survey of the HPLC monitoring of bacterial fermentations for the food industry is also given. The analysis of the structural components of the bacterial cell will be dealt with in the second part of the review.

1.1. Bacterial identification

An important area of microbiological studies is the taxonomic arrangement of the various bacterial species considered pathogenic for humans. Their classification is a preliminary step, which is strictly related to the problem of microorganism identification. In clinical specimens, the correct identification of the bacterial species responsible for infective processes in various areas of the human body is necessary to formulate correctly the aetiological diagnosis of infection. Therefore, identification is the central step of a triad (classification, identification and diagnosis) whose mutual relationships must be kept in mind when dealing with clinical microbiological problems.

1.2. Chemotaxonomy

Chemotaxonomy has been defined as the study of chemical variations in living organisms and the use of chemical characters in classification and identification[1].

As the morphological and physiological characteristics appeared to be insufficient to classify correctly some bacterial species, particularly anaerobes, attention has increasingly been directed to chemical methods capable of providing reliable characters in bacterial classification.

The application of chemotaxonomic techniques may bring more objectivity into the field of bacterial identification. The discovery of specific chemical markers can make bacterial identification more practical. Demonstration of specific markers may also reduce the variability of the results obtained from different laboratories performing physiological and biochemical identification tests. The chemotaxonomic approach can provide a better classification of bacteria, facilitating the identification of clinically important microorganisms[2–10].

Knowledge of the taxonomic characters of anaerobic bacteria has included the main structural components of the bacterial cell and the metabolites produced or utilized by these microorganisms. In fact, the chemotaxonomic approach has involved the elucidation of the cell wall structure, the determination of cellular fatty acids and DNA base composition and, more frequently, the qualitative and quantitative profile of exocellular short-chain acids[11,12]. Major applications include the analysis of some important macromolecules (peptidoglycan, lipopolysaccharide, DNA)[13] and the determination of relatively simple molecules (carboxylic acids, monosaccharides, amino acids, amines).

2. DETERMINATION OF EXOCELLULAR METABOLITES

The application of instrumental methods to the identification of anaerobic bacteria has involved mainly gas chromatography (GC)[14], a very sensitive and rapid technique which has proved useful for the diagnosis of infectious diseases[15–17]. The term GC–chemotaxonomy[18] has been used to describe the application of GC methods to the determination of metabolic products for the identification of a microorganism on the basis of chromatographic profiles of carboxylic acids, alcohols and amines.

In recent years, the use of HPLC to determine bacterial metabolites, especially short-chain acids including keto acids, hydroxy acids and phenolic acids, has become increasingly popular[19,20].

2.1. Short-chain acids

As the metabolism of anaerobic bacteria is characterized by a profile of acid end-products which is typical for each species, the determination of short-chain acids in culture media after growth of anaerobic bacteria is useful for the identification of these microorganisms. Also, the GC determination of short-chain acids in clinical specimens has been used for the presumptive identification of anaerobic infections[21]. GC procedures require separate treatment of samples for different classes of acids: volatile fatty acids can be chromatographed directly from the acidified cultural medium or after extraction with organic solvents, whereas non-volatile fatty acids require simple derivatization to methyl esters prior to GC analysis. On the other hand, GC often appears to have greater resolution, specificity and sensitivity than HPLC. Moreover, the continuous advances made in GC technology are not usually utilized in routine anaerobic analyses.

Technological improvements in HPLC instrumentation, especially of column selectivity and detector sensitivity, have shown that the HPLC determination of acidic metabolites is a suitable alternative to the GC method[19,20]. The flexibility of HPLC techniques in acidic metabolite analysis is evidenced by the following examples. In particular, the analytical possibilities deriving from the selection of a suitable column and especially from modification of the physico-chemical characteristics of the mobile phase are illustrated. Different modes of separation for the HPLC determination of carboxylic acids, including ion-pair chromatography, solvophobic chromatography and ion-exchange chromatography, were reviewed by Schwarzenbach[22]. Short-chain aliphatic acids are separated as such (without prior derivatization)[23,24] or as their phenacyl derivatives[25] on reversed phases. In the ion-pair chromatographic separation of dihydroxybenzoic acids on LiChrosorb RP-18 with 0.05 M phosphoric acid–methanol (7:3) + 0.005 M hexylamine, the pH is a very important parameter as it determines the concentration of the ionic form of the solutes. Quaternary ammonium salts dissolved in buffered water–methanol (as mobile phase) have also been used[26]. In solvophobic chromatography, the addition of acids or acidic buffers to the mobile phase lowers the pH and suppresses the ionization of the acidic functional groups of the solutes. Retention is the result of hydrophobic interactions between the hydrocarbon moiety of the solute and the octadecyl chains of the stationary phase. Separations are based on the hydrophobic properties of the solutes. The capacity factor of a solute is determined by the concentration of the organic modifier in the mobile phase. The separation selectivity can be affected by either the pH of the mobile phase or the nature of the organic modifier. To suppress the ionization of dicarboxylic acids, the addition of acidic buffers, such as sodium or potassium phosphate, sodium hydrogensulphate or sodium chlorate, has also been successfully used[27,28].

Ion-exchange materials have been used in many applications as stationary phases for the liquid chromatography of carboxylic acids. Owing to the development of new ion-exchange materials of small particle size and narrow size range, which are stable at higher pressures, improvements in the column efficiency and reductions in retention times were possible. Therefore, prepacked columns filled with efficient

ion-exchange materials became commercially available and columns of the HPX series (Bio-Rad Labs.) were used for organic acid separations[29,30]. When subjected to ion-moderated partition chromatography[31], the acids of the citric acid cycle elute according to their increasing pK_a values. Partition chromatographic separations on ion-exchange resins of aromatic carboxylic acids have also been described[32]. Separations of carboxylic acids on cation-exchange resin columns adopted ion-exclusion chromatography coupled with ultraviolet monitoring of the effluent[33,34] or with conductimetric detection[35]. Dilute mineral acids[36] or dilute mineral acids modified with acetonitrile[37] were used as mobile phases for ion-exclusion chromatography.

A comparison between the GC and HPLC determination of acidic metabolism indicates that both techniques present some advantages and disadvantages, whose relative importance depends on the specific application. When simple analysis of volatile acids is required, the superior sensitivity of capillary GC with a flame ionization detector indicates that the use of this technique is preferable. When, on the other hand, the analysis of ionic, non-volatile or thermally labile compounds is necessary, HPLC has the following advantages: no need for methylation of non-volatile acids, the possibility of determining both volatile and non-volatile acids in a single chromatographic run and high sensitivity for aromatic acid determination.

2.1.1. Applications. One of the first applications of HPLC to bacterial metabolites concerned the fermentation products of several *Clostridium* species[36]. Sample preparation for HPLC analysis required only membrane filtration. Separation was performed on an Aminex column with $6.5 \cdot 10^{-3}$ M sulphuric acid. The effects of eluent concentration and column temperature on the retention times of various organic compounds were described. Effluents were monitored with refractive index (RI) and ultraviolet (UV) detectors. Alcohols absorb very little UV light above 200 nm. As pyruvic and fumaric acids absorb strongly at 210 nm, UV absorbance is suitable for detecting these compounds. The other organic acids yielded moderate UV and RI responses. HPLC traces of peptone–yeast extract–glucose cultures of *Clostridium* species were shown.

The acid metabolites present in cultures of a group of clinically significant anaerobic bacteria, including *Peptostreptococcus anaerobius, Bacteroides fragilis* and *Clostridium difficile*, have been successfully determined[37]. This method involved organic acid extraction with diethyl ether–sodium hydroxide from bacterial culture supernatants. The double extraction improved the reliability of the procedure by selectively removing the acids from potentially interfering compounds. Separation was performed on an Aminex HPX-87H column using $3.5 \cdot 10^{-3}$ M sulphuric acid–10.8% acetonitrile as the mobile phase, and effluents were monitored at 210 nm. *B. fragilis* and *C. difficile* cultures contained acids which had not been detected by commonly employed GC procedures. In fact, α-ketoglutaric, *p*-hydroxyphenylacetic and phenyl-acetic acids were determined in the extracts of *B. fragilis*, and *p*-hydroxyphenyl acetic, phenylacetic, 3-phenylpropionic and indoleacetic acids together with *p*-cresol in those of *C. difficile*.

Adams *et al.*[38] presented the results of the application of the HPLC procedure of Guerrant *et al.*[37] to the analysis of acid products from cultures of *Clostridia, Salmonellae* and *Lactobacilli*. Chromatograms of culture extracts of *Clostridium perfringens, Clostridium difficile* grown in cooked-meat medium, *Salmonella sofia,*

Salmonella infantis, Salmonella typhimurium, Lactobacillus casei and *Lactobacillus fermentum* grown anaerobically in peptone–yeast extract–glucose medium were shown. The acid profiles of bacterial cultures showed that considerable differences existed among the genera and among the species tested. The procedure has the greatest value when used qualitatively, as in the development of profiles of microbial metabolites for quality control purposes, and when used semi-quantitatively as an aid to bacterial identification.

Another example of the applicability of HPLC to the determination of exocellular acid metabolites has involved black-pigmented *Bacteroides*. The organic acids produced by eight oral *Bacteroides* species were determined by HPLC, after extraction with diethyl ether–sodium hydroxide[39]. The chromatographic profiles were typical of the individual species examined: *Bacteroides gingivalis* produced phenylacetic and *p*-hydroxyphenylacetic acids, *Bacteroides intermedius* produced major amounts of succinic and formic acids. These results indicate that the application of HPLC to the determination of the organic acids produced by oral *Bacteroides* is very useful for classifying these bacteria. The capacity factors of the carboxylic acids of a standard mixture under the same chromatographic conditions as described in ref. 39 are reported in Table 1. The chromatographic profiles of acidic end-products from two *Bacteroides* species are shown in Fig. 1.

The production of volatile and non-volatile fatty acids has been revealed with an Aminex column, for the rapid identification of *Clostridium, Bacteroides, Fusobacterium, Peptostreptococcus, Peptococcus, Veillonella* and *Propionibacterium* species[40]. The results illustrated the usefulness of HPLC in determining acidic end-products as an additional means for rapid differentiation between closely related anaerobic bacterial species. Pyruvic and malonic acids were found in some species of all the genera with the exception of *Fusobacterium*. Butyric acid was produced by all the species of *Clostridium, Fusobacterium, Peptococcus, Peptostreptococcus* and *Veillonella*. Butyric acid was most often detected when *Clostridium* or *Fusobacterium*

TABLE 1

CAPACITY FACTORS OF CARBOXYLIC ACIDS IN THE HPLC ANALYSIS OF A STANDARD MIXTURE

Chromatographic conditions: column, Aminex HPX-87H (30 cm × 7.8 mm I.D.); mobile phase, $3.5 \cdot 10^{-3}$ *M* sulphuric acid–10.8% acetonitrile; flow-rate, 0.4 ml/min; detector, spectrophotometer at 210 nm and 0.08 a.u.f.s.

Carboxylic acid	k'	Carboxylic acid	k'
Oxalic	0.122	Propionic	1.677
α-Ketoglutaric	0.433	Isobutyric	1.933
Pyruvic	0.555	Butyric	2.111
Malonic	0.622	Isovaleric	2.411
Methylmalonic	0.755	Valeric	3.000
Succinic	0.788	*p*-Hydroxyphenylacetic	3.222
Lactic	1.000	Isocaproic	3.455
Fumaric	1.233	Caproic	4.422
Formic	1.288	Phenylacetic	5.011
Acetic	1.366		
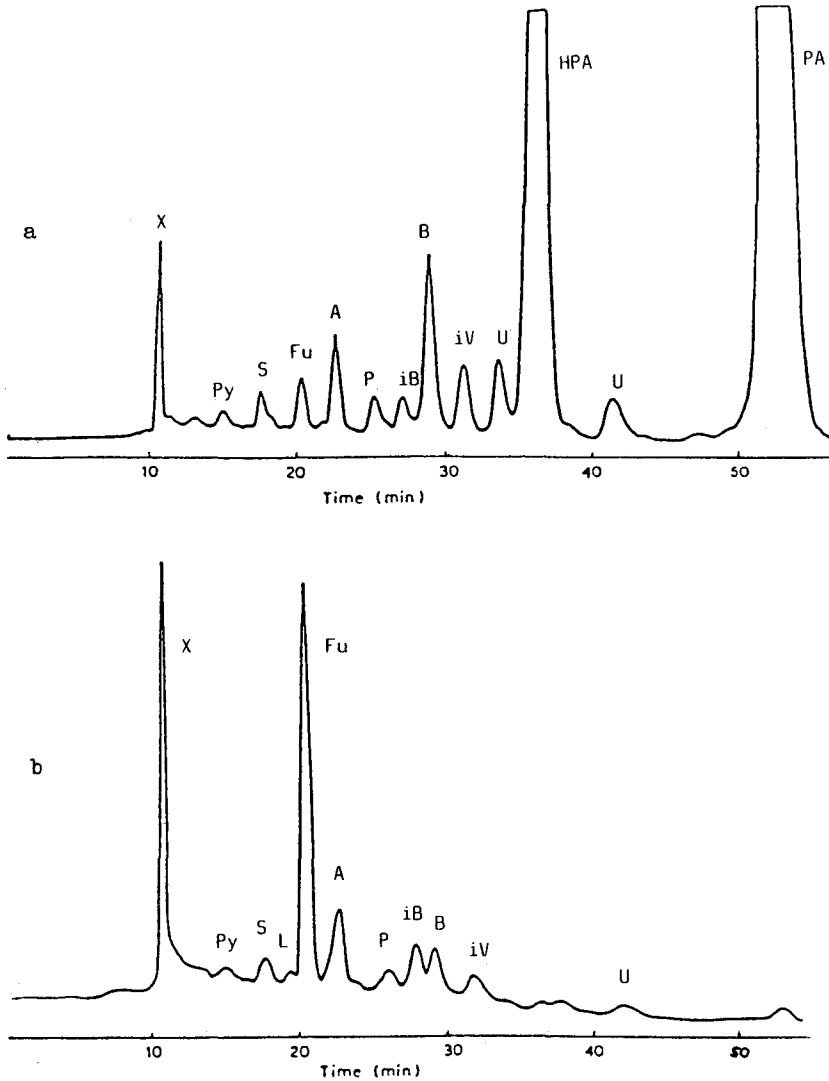
Fig. 1. HPLC of short-chain acids produced by (a) *Bacteroides gingivalis* and (b) *Bacteroides endodontalis*.
X = solvent and non-adsorbed components. Acids: Py = pyruvic; S = succinic; L = lactic; Fu = fumaric;
A = acetic; P = propionic; iB = isobutyric; B = butyric; iV = isovaleric; HPA = *p*-hydroxyphenylacetic;
PA = phenylacetic. U = unidentified components.

species were present in blood cultures[41]. Large amounts of phenylacetic acid were
produced by 75% of *Bacteroides* species; phenylacetic acid was produced also by a few
species of *Clostridium* and *Fusobacterium*. Large amounts of caprylic acid were
detected only in *Clostridium tetani* cultures. The detection of 4-methylvaleric acid in
stool specimens was proposed as a screening test to reveal *Clostridium difficile*
involvement in diarrhoeal disease[42,43]. Although the presence of isocaproic acid is, in
principle, not sufficient to distinguish *in vitro C. difficile* from other *Clostridia* species

which also produced this acid, the detection of isocaproic acid *in vivo* in patients suffering from diarrhoeal disease can be considered a specific marker of the presence of *C.difficile*.

Bacterial growth conditions, treatment of culture supernatants and operating conditions employed by several workers[36–40,44,45] in the HPLC determination of carboxylic acids from different bacteria are summarized in Table 2. Very important factors are composition of the medium and incubation time. As these factors significantly affect short-chain acid production by microorganisms[46–48], it is difficult to compare the results obtained by different workers. There is no universally accepted ideal growth medium for microorganisms, which differ widely in their individual growth requirements. For qualitative analysis the choice of a growth medium may be important. As the proportions of individual products vary considerably during growth, standard incubation times should be adhered to. Krausse and Ullmann[45] used a 48–72-h incubation time for anaerobes in Schaedler broth, while other workers used 24–48-h incubation in peptone–yeast extract–glucose broth[36,37]. The use of a defined medium can often solve the problem of media variability, but this is almost a "mirage" in the case of fastidious microorganisms[15]. Unfortunately, a synthetic medium with a defined chemical composition for cultivating most anaerobic bacteria has not yet been formulated by microbiologists. This drawback constitutes a limit to the whole subsequent analytical procedure, including treatment of culture supernatant and HPLC analysis. In our experience, the utilization of a synthetic medium originally developed by Socransky *et al.*[49] to cultivate *Bacteroides gingivalis* appears to be very promising: chromatograms of spent cultures obtained on a yearly basis proved to be virtually identical, as the relative standard deviation of individual acids ranged from 2 to 5% (unpublished results). Preliminary experiments with this type of medium indicate that it can be successfully utilized to analyse other species of anaerobic bacteria. From these considerations it appears that most of the efforts to standardize growth conditions for HPLC experiments should be directed to the development of a new synthetic medium capable of allowing the satisfactory growth of all anaerobic species of clinical interest. Treatments of the culture supernatants prior to the HPLC analysis differ from one another: single or double extraction procedures provide different recoveries of the carboxylic acids and affect the final quantitative data. The recoveries of selected acids in water extracted with diethyl ether were determined by Adams *et al.*[38]. The values ranged from 22% for pyruvic acid to 72% for isovaleric acid. The recoveries of known concentrations of acids after double extraction with diethyl ether–sodium hydroxide from water were determined by Corio *et al.*[50]: the values for volatile fatty acids decreased with increasing carbon chain length (from 40% for acetic acid to 12% for isovaleric acid). This behaviour was opposite to that mentioned above involving extraction with diethyl ether alone. These data indicate that different extraction procedures can give rise to different results. The values for non-volatile acids were in the range 32–36%, with the exception of succinic acid (15%). As the yields for some acids were too low, it would be useful to examine alternative methods, *e.g.*, solid-phase extraction, for the sample treatment prior to HPLC analysis.

The addition of acetonitrile to the mobile phase as an organic modifier differentiates some HPLC procedures[37–39] from the other methods listed. Changes in acetonitrile concentration cause a shift in the retention time of some compounds. For

TABLE 2

CHROMATOGRAPHIC CONDITIONS IN THE HPLC DETERMINATION OF CARBOXYLIC ACIDS PRODUCED BY SEVERAL BACTERIAL SPECIES

Bacteria	Growth[a]	Treatment	Mobile phase	Temperature (°C)	Flow-rate (ml/min)	Detection	Ref.
Clostridium	PYG 24–48 h	Filtration	6.5 mM H_2SO_4	30	0.7	RI/UV	36
Peptostreptococcus, Bacteroides, Clostridium	PYG 24–48 h	Extraction with diethyl ether–NaOH	3.5 mM H_2SO_4–10.8% CH_3CN	20	0.5	UV, 210 nm	37
Clostridium, Salmonella, Lactobacillus	CMM PYG 4 d PYG 4 d	Extraction with diethyl ether–NaOH	3 mM H_2SO_4–CH_3CN (90:10)	50	0.6	UV, 210 nm	38
Bacteroides	BM 6 d	Extraction with diethyl ether–NaOH	3.5 mM H_2SO_4–10.8% CH_3CN	20	0.4	UV, 210 nm	39
Azospirillum, Desulfovibrio	Salts	—	2.25 mM H_2SO_4	85	0.8	UV, 210 nm	44
Campylobacter	Schaedler 72 h	Extraction with diethyl ether	6.5 mM H_2SO_4	20	0.8	UV, 210 nm	45
Clostridium, Bacteroides, Fusobacterium, Peptostreptococcus, Peptococcus, Veillonella, Propionibacterium	Schaedler 48–72 h	Extraction with diethyl ether	6.5 mM H_2SO_4	22	0.8	UV, 210 nm	40

[a] PYG = Peptone-yeast extract-glucose; CMM = cooked meat medium; BM = bacteroides medium.

example as the concentration of acetonitrile was decreased from 10.8 to 5%, as described by Guerrant et al.[37], the retention times of fumaric and p-hydroxyphenyl acetic acids increased more than those of other acids, facilitating the identification of the former acids. Separation of the acids was optimized by adjusting the concentrations of sulphuric acid and acetonitrile in the eluent. The separation of some acids which elute close together with $6.5 \cdot 10^{-3}$ M sulphuric acid alone (succinic–lactic, fumaric–formic–acetic, p-hydroxyphenylacetic–2-methylvaleric, caprylic–phenylacetic)[40] could be optimized by manipulating the eluent pH, by adjusting the organic modifier concentration and by changing the column temperature. The values of column temperature and flow-rate employed by several workers cover wide ranges. It is important to point out that it will be useful in the future to select optimum conditions for each chromatographic variable. Standardization of the chromatographic conditions will make it possible to compare the qualitative and quantitative data obtained by different laboratories.

2.2. Substrates utilized by bacteria

A new approach that has proved useful for taxonomic and identification purposes in clinical laboratories is based on establishing the utilization of a complex mixture of defined substrates by bacteria.

2.2.1. Carbohydrates.
An improved procedure for determining carbohydrates, alcohols and organic acids in fermentation mixtures metabolized by intestinal microflora has been described[51]. A fermentation mixture containing four carbohydrates was incubated at 37°C for 24 h. The compounds were separated on an Aminex HPX-87H column with 0.028 M sulphuric acid. Effluents were monitored with UV and RI detectors in series. The metabolic profiles for the fermentation of glucose, fructose, lactose and sucrose by several intestinal microorganisms (*Escherichia coli, Klebsiella pneumoniae* and *Streptococcus faecalis*) were characterized and compared. The fermentation patterns indicated that all three microorganisms produced acetic acid from the four sugars studied. Additionally, levulinic acid was formed by *E. coli* and formic acid by *S. faecalis*. The sucrose fermentation pattern of *E. coli* was different from those of the other three sugars. The concentrations of both the sugars metabolized and the analytes produced were calculated. All three microorganisms metabolized glucose to a higher degree than did the other three sugars.

The chromatograms for the fermentation of lactose by *E. coli* using RI or UV detection were shown. When the 0- and 24-h samples were compared, a decrease in the amount of lactose and an increase in the amounts of lactic, acetic, levulinic, isobutyric, butyric and isovaleric acids were found.

The applicability of HPLC to the rapid identification of *Bacteroides* species has been evaluated by analysing the effects of their glycosidase patterns on the composition of a defined chemical medium after aerobic incubation[52]. The defined chemical medium contained six carbohydrates and lyxose was added as an internal standard. Each *Bacteroides* isolate was inoculated into the medium and incubated at 37°C for 1 h. After centrifugation, the supernatants were injected into an Aminex HPX-87H column to determine carbohydrates and acid metabolic products. *Bacteroides fragilis* metabolized some carbohydrates (raffinose, lactose, glucose) and produced seven new peaks (B–H). Peaks B and C were identified as succinic and lactic acid, respectively. The production of peak H was a metabolic feature of *B. fragilis*,

TABLE 3

CAPACITY FACTORS OF CARBOHYDRATES SELECTED FOR THE PREPARATION OF CONTROL MEDIUM

Chromatographic conditions: column, Aminex HPX-87H (30 cm × 7.8 mm I.D.); mobile phase, $3.5 \cdot 10^{-3}$ M sulphuric acid; flow-rate, 0.4 ml/min; detector, spectrophotometer at 196 nm and 0.04 a.u.f.s.

Carbohydrate	k′	Carbohydrate	k′
Raffinose	0.088	Galactose	0.544
Cellobiose	0.188	Xylose	0.555
Trehalose	0.188	Rhamnose	0.588
Maltose	0.200	Lyxose	0.622
Lactose	0.222	Arabinose	0.733
Glucose	0.422	Salicin	1.655
Mannose	0.522		

which could be distinguished from the other *Bacteroides* species. The capacity factors of carbohydrates to be selected for the preparation of control medium under the same chromatographic conditions as described in ref. 52 are reported in Table 3. The HPLC profiles of both the defined chemical medium and *Bacteroides thetaiotaomicron* supernatant after aerobic incubation are shown in Fig. 2.

Polystyrene–divinylbenzene cation-exchange resins with a metallic counter ion and water as the eluent proved useful for the separation of carbohydrates, whereas the hydrogen form with an acidic eluent was employed for carbohydrate[53–56] and organic acid analysis[57,58]. HPLC separation of carbohydrates, alcohols, aldehydes, ketones and carboxylic acids on a cation-exchange resin in the hydrogen form was described by Pecina *et al.*[59]. The chromatographic behaviour of 63 substances of the above classes on an HPX-87H column was investigated. The effects of column temperature on the capacity factors of the examined compounds were described. The column temperature appeared to be a very important parameter for optimizing the separation of these substances. Optimized separations of carbohydrates, acids, aldehydes, ketones and alcohols were described. Operating conditions for the HPLC separation of monosaccharides and disaccharides were reviewed by Robards and Whitelaw[60].

2.2.2. Amino acids. In a study of numerous species of *Clostridium*[61], the isolated strains were inoculated into a chemically defined medium, containing primarily ten amino acids, and incubated aerobically at 37°C for 1 h. After centrifugation, the supernatants were derivatized with *o*-phthalaldehyde for 1 min in the presence of saturated boric acid. Samples were injected into an Ultrasphere-ODS column and effluents were monitored at 340 nm by spectrophotometry. Elution was performed with 30 mM sodium phosphate (pH 6.5), programming a 25–70% methanol gradient. The total time required for chromatographic analysis was *ca.* 50 min. A chromatogram of the medium after incubation with *Clostridium sordelii* showed that this microorganism metabolized many of the components of the control medium and produced seven new peaks (A–G). The chromatographic profile showed both the utilization of defined substrates (as demonstrated by the elimination of the peak corresponding to an amino acid) and the appearance of new peaks corresponding to compounds produced by the metabolism of the amino acids contained in the medium. Multiple
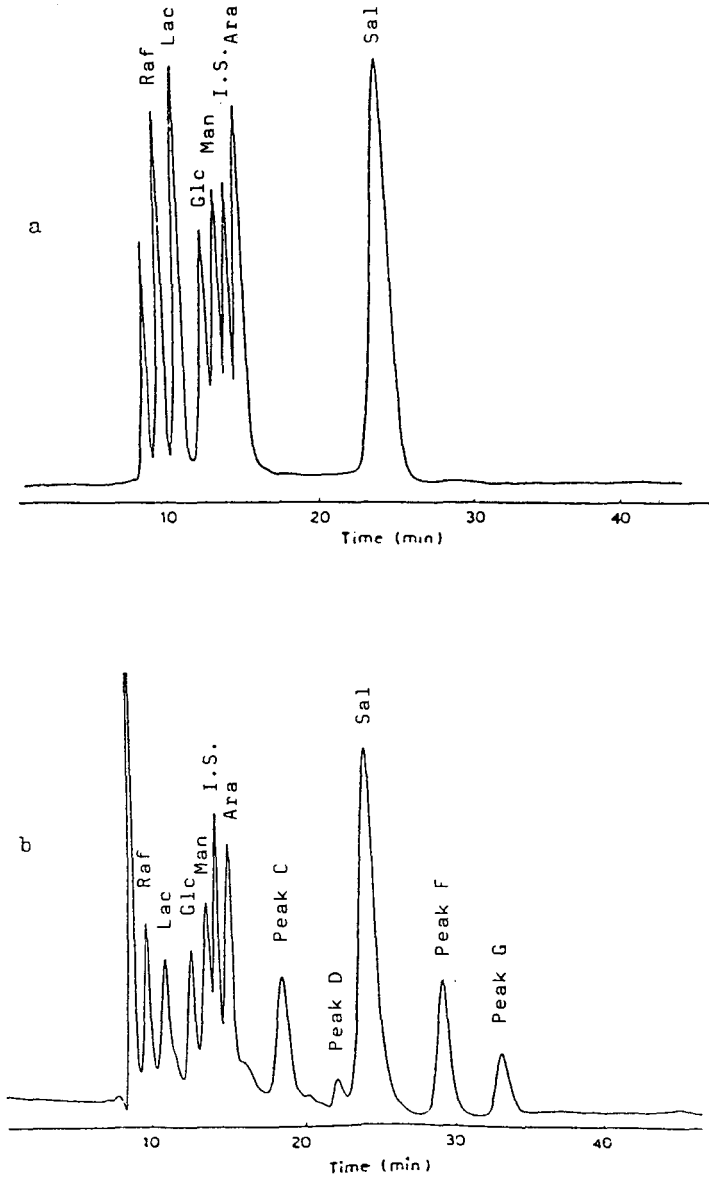
Fig. 2. HPLC profile of (a) the defined chemical medium and (b) *Bacteroides thetaiotaomicron* supernatant after aerobic incubation. Raf = Raffinose; Lac = lactose; Glc = glucose; Man = mannose; Ara = arabinose; Sal = salicin; internal standard (I.S.) = lyxose; peak C = latic; D = acetic; F = isobutyric; G = butyric.

isolates of various *Clostridium* species gave consistent patterns of medium utilization that could be used for identification. *Clostridium sordelii* was the only indole-positive t*Clostridium* species that produced peak D and also a very large peak E. These features can be used for distinguishing *Clostridium sordelii* from the other clostridial species.

Harpold and Wasilauskas[62] evaluated HPLC for the rapid identification of obligately anaerobic Gram-positive cocci by using the same method as described above. Chromatograms of a derivatized *P. anaerobius* supernatant and of a derivatized *G. anaerobia* supernatant after 1 h of incubation were shown. Medium utilization indices for *Peptostreptococcus* species (*micros, magnus, anaerobius asaccharolyticus, prevotii*) and *Staphylococcus saccharolyticus* were calculated. *P. magnus* utilized only serylleucine. *P. anaerobius* utilized serine, alanine, serylleucine, phenylalanine and leucine. A scheme for identifying Gram-positive anaerobic cocci was proposed on the basis of the differential utilization of some amino acids (phenylalanine, histidine, serine).

These positive experiments prompted Radin *et al.* [63] to apply this method to *Bacteroides* species. Some profiles representative of the most significant species, belonging to the *B. fragilis* group were shown. Even if the metabolic activities involved in the amino acid utilization appear to be much more reduced for *Bacteroides* than *Clostridium,* it was possible to propose a scheme which affords the correct identification of the examined microorganism within about 2 h. It is important to emphasize that, for the species belonging to the *B.fragilis* group, incubation can occur in aerobiosis and the time of incubation can be reduced to 30 min. In conclusion, one can say that this identification approach is rapid and reliable. The capacity factors of amino acids under the same chromatographic conditions as described in ref. 63 are reported in Table 4.

The operating conditions employed in the HPLC determination of different substrates (carbohydrates and amino acids) and their metabolic end-products by several bacterial species are summarized in Table 5.

2.3. Perspectives of HPLC in diagnostic bacteriology

The application of instrumental chromatographic techniques for diagnostic purposes has extensively involved the GC analysis of biological fluids from different areas of the human body. A chromatographic profile might be valuable if it demonstrated that the disease process was originally infectious or non-infectious. Brooks[15] pointed out that the direct analysis of biological fluids is the ultimate goal in

TABLE 4

CAPACITY FACTORS OF AMINO ACIDS IN THE HPLC ANALYSIS OF DERIVATIZED UNINOCULATED CONTROL MEDIUM

Chromatographic conditions: column, Ultrasphere-ODS (15 cm × 4.6 mm I.D.); mobile phase, gradient from 25 to 70% methanol in 30 mM sodium phosphate (pH 6.5); flow-rate, 1 ml/min; detector, spectrophotometer at 340 nm.

Amino acid	k'	Amino acid	k'
Asparagine	3.391	Alanine	11.43
Serine	4.913	Tryptophan	14.73
Glutamine	6.043	Valine	15.30
Histidine	6.304	Phenylalanine	15.73
Glycine	8.695	Leucine	17.39
Arginine	9.130	Lysine	19.26

the GC identification of a specific infectious disease. Many pathogenic micro-organisms that grow slowly or with difficulty might be identified so that a more appropriate therapy could be started much earlier.

The use of HPLC for the analysis of clinical specimens presents some technical drawbacks in comparison with GC. There is a pitfall in the direct injection of biological samples, owing to the possibility of clogging the capillary which connects the injector to the analytical column. In contrast, samples subjected to filtration, extraction with organic solvents or concentration by solid-phase extraction are suitable for HPLC analysis.

The identification of components present in biological fluids is a much more demanding task than identifying metabolites produced by microorganisms in spent culture media. In fact, clinical specimens, in most instances, are difficult to obtain, whereas the amount of spent culture media is usually unlimited. The types of components found in pathological body fluids are often less predictable than metabolites produced by bacteria in spent culture media. The components detected in biological fluids may derive not only from the metabolism of the infecting micro-organism but also from the host response to infection. Determining reproducible HPLC profiles from various sources will provide specific information that will help in identifying a particular disease.

While many reports have dealt with the use of GC for diagnostic purposes, application of HPLC to the analysis of clinical specimens are limited to only a few specific cases.

HPLC has been used for the determination of histamine and other biological amines in sputum samples from patients with asthma, pneumonia, chronic bronchitis and cystic fibrosis[64,65]. Separation was performed on a Spherisorb 3 ODS column with 0.2 M sodium acetate and tetrahydrofuran (75:25), adjusted to pH 5.1 with hydrochloric acid. Detection of the o-phthalaldehyde-derivatized amines was achieved using a fluorescence spectrometer (emission at 430 nm and excitation at 350 nm). The results of HPLC analysis strongly supported the hypothesis that bacteria might contribute to the presence of histamine in sputum from patients with infective lung disease. Sputum bacteriology for both chronic bronchitis and cystic fibrosis samples revealed the presence of *Pseudomonas aeruginosa, Haemophilus influenzae* and *Staphylococcus aureus*, together with anaerobic species in the former disease and *H. influenzae* in the latter[65].

Another very interesting application of HPLC in clinical bacteriology is in the analysis of gingival crevicular fluid, which is considered a promising medium for the detection of chemical markers of periodontal disease activity[66]. Gingival crevicular fluid contains a large number of components derived not only from the host tissues but also from the sub-gingival bacterial plaque; hence a wide range of molecules may be evaluated as potential markers. The metabolism of sugars and amino acids by the microbial community in periodontal pockets produces an array of both acidic and basic end-products. The concentration of acidic metabolites in sub-gingival plaque has been evaluated to be in the millimolar range. The aim of this approach was to provide the clinician with a rapid and sensitive means of diagnosis of active periodontal breakdown. The detection of a characteristic end-product profile and/or of a specific marker in clinical samples can be utilized to indicate the presence of both a quiescent or active microflora in the infected site. The limitation of this approach is that only

TABLE 5

CHROMATOGRAPHIC CONDITIONS IN THE HPLC DETERMINATION OF SUBSTRATES FOR SEVERAL BACTERIAL SPECIES

Bacteria	Substrate	Column	Mobile phase	Temperature (°C)	Flow-rate (ml/min)	Detection	Ref.
–	–	Aminex HPX-87H	0.005M H$_2$SO$_4$	70	0.7	RI	59
E. coli, K. pneumoniae, S. faecalis	Carbohydrates	Aminex HPX-87H	0.028 M H$_2$SO$_4$	40		UV + RI	51
B. fragilis	Carbohydrates	Aminex HPX-87H	$3.5 \cdot 10^{-3}$ M H$_2$SO$_4$	20	0.3	UV, 196 nm	52
Clostridium	Amino acids	Ultrasphere-ODS	25–70% methanol	–	1	UV, 340 nm	61
Peptostreptococcus	Amino acids	Ultrasphere-ODS	25–70% methanol	–	1	UV, 340 nm	62

(sub)microlitre amounts of gingival fluid can be retrieved; this means that analytical techniques requiring both minimum sample handling and detection of these metabolites in a single run, must be used. Detection methods have been developed, using HPLC[67], luciferase-linked enzyme assays[68], GC[69] and isotachophoresis[70]. The use of HPLC is attractive as different classes of acids, including phenolic acids, can be determined in a single analysis. However, the detection methods for bacterial end-products, such as hydroxy acids, dicarboxylic acids and amines, at concentrations present in gingival crevicular fluid, require considerable modification in order to be useful in diagnostic laboratories. We are currently evaluating the potential of HPLC in this area where detection of millimolar concentrations in sub-microlitre volumes is necessary. Further improvements in HPLC technology will be necessary to determine picomole amounts of most of these molecules. At present, electron-capture GC seems capable of offering some advantages over the available HPLC procedures.

One of the features of HPLC is that, whereas selectivity is achieved in the separation step on the analytical column, sensitivity and improved selectivity can be achieved in the detection step. When comparing HPLC and GC analysis, the inherent differences between the two methods affect the selectivity of the separation and of the detection system. As far as the separation in GC is concerned, it is the volatility of the compounds that determines the selectivity of the chromatographic procedure; on the other hand, solubility of chemical compounds in the mobile phase is the major determinant in HPLC. It should be noted that in HPLC the mobile phase can be selected in such a way as to improve the solubility of the substances under study and therefore to increase selectivity. A similar flexibility is achieved in GC by selecting a polar or non-polar stationary phase from a wider array of commercially available types. In terms of detectors, both GC and HPLC present the possibility of using different detection systems. Mass spectrometric, photodiode-array, fluorescence, electrochemical and electron-capture detectors all improve selectivity, facilitating peak identification; when applying these techniques, peak identification is not based solely on retention times.

The type of detector to be used should be selected according to the amounts of the substances to be analysed and the nature of the compounds to be determined. In general, UV and fluorescence methods are suitable for the more sensitive detection of substances, *e.g.*, from nanomoles to 10 pmol. As not all substances show UV or fluorescence properties, chemical derivatization can be used to obtain these properties to increase the sensitivity[71–77]. An example is most aliphatic acids, which are normally detected at the millimole level only, whereas their detection limit can reach the nanomole level when they are derivatized. Labelling of substances with reagents that afford structures with UV bands is the most popular means of derivatization. Phenyl, *p*-bromophenacyl bromide, 2-naphthacyl bromide and other types of reagents for precolumn labelling of carboxylic acids have been reported[78,79].

The application of labelling procedures to bacterial metabolites could improve the HPLC analysis of biological fluids from different sources, as suggested by the results of Tsuchiya *et al.*[80]. They determined the fatty acid composition of phospholipids from several oral *Streptococci*, following derivatization with a fluorescent reagent (4-bromomethyl-7-acetoxycoumarin). These results showed that the HPLC method was at least 500 times more sensitive than GC with flame ionization detection but less sensitive (50%) than GC with electron-capture detection. By

analogy, the application of similar labelling procedures to the HPLC analysis of bacterial metabolites in biological fluids could provide sensitivity comparable to GC with frequency pulse-modulated electron-capture detection as proposed by Edman and Brooks[4] for the diagnosis of infectious diseases. All these considerations suggest that HPLC is potentially useful in bacteriological laboratories, especially for the diagnosis of anaerobic infections.

3. BACTERIAL FERMENTATIONS

An important application of HPLC procedures is the monitoring of bacterial fermentations during the industrial preparation of various food products (beer, wine, cheese, yogurt, sauces). Qualitative data are often sufficient for these applications; however, HPLC analysis carried out under controlled conditions can provide excellent quantitative data.

The chromatographic profile of a sample of soya sauce obtained from a mixed fermentation, including *Lactobacilli*, yeasts and fungi, was considered a useful indicator of product integrity and stability. A peak present in the final part of the chromatogram was assigned to benzoic acid, an additive commonly employed for the storage of some food products[38].

4. METABOLITES ASSOCIATED WITH THE PURINE AND PYRIMIDINE PATHWAYS

The biological importance of purine compounds is emphasized by their occurrence in nucleic acids and their participation in biosynthetic reactions involving nucleotides. A number of methods for the HPLC analysis of free bases, nucleosides and nucleotides has been published. Isocratic separations on ion-exchange columns[81] have proved to be more time consuming than analyses performed by reversed-phase HPLC[82,83]. Mechanisms of RP-HPLC retention, structure–retention relationhips of purines and pyrimidines in reversed-phase systems, effects of mobile phase on purine and pyrimidine retention characteristics and ion-pairing techniques were reviewed by Scoble and Brown[84]. The roles of the mobile phase parameters pH, organic modifier and ionic strength were examined in reversed-phase chromatographic systems[85].

As the retention times of purines are highly affected by changes in pH using reversed-phase systems[86], various pH values of potassium phosphate buffers were tested in an HPLC separation of purines (adenine, 6,8-dihydroxypurine, 2-hydroxypurine, hypoxanthine, purine, uric acid, xanthine) and their anaerobic and aerobic degradation products (4-ureido-5-imidazolecarboxylic acid, 4-amino-5-imidazolecarboxylic acid, 4-aminoimidazole, formiminoglycine, allantoin, ureidoglycolate) using UV detection at 205 nm[87]. The best resolution of purines and their anaerobic degradation products was achieved at pH 3.7, whereas the separation of uric acid and its aerobic degradation products was achieved at pH 3.1.

Interesting applications have involved the determination of the pathway of purine degradation by *Clostridium purinolyticum*[87,88], the study of the metabolism of a xanthine drug by microorganisms[89] and the determination of ribonucleoside triphosphates in *Escherichia coli*[90]. The degradation of purines by aerobic microorganisms starts from uric acid by a pathway yielding allantoin, allantoic acid, ureidoglycolate and finally urea and glyoxylate[91]. HPLC was used to determine the

pathway of adenine degradation by *Clostridium purinolyticum*, a species of obligate purine-fermenting bacteria[92]. The decomposition of adenine by cell-free extracts of *C. purinolyticum*, was found to proceed via hypoxanthine, xanthine and imidazole derivatives. The strict dependance on selenium compounds for the growth of this anaerobic species was thought to be due to the presence of some selenoenzymes which have key functions in the catabolic breakdown of purines and energy generation[93]. The possibility of a purine ring cleavage in the imidazole moiety yielding pyrimidine derivatives has been investigated[88]. *C. purinolyticum* decomposed uric acid via pyrimidine derivatives under selenium starvation conditions, producing acetate, formate, glycine, ammonia and carbon dioxide. The results of the HPLC determination of uric acid, 4,5-diaminouracil and 6,7-dimethyllumazine[88] showed that under selenium starvation conditions an alternative pathway is used for uric acid decomposition. The discovery of the new pathway led to the speculation that some sort of diabetes, induced by the pyrimidine alloxan[94], might be due to a microbiological origin of this compound.

An HPLC method has been developed for the determination of pentoxifylline and its major metabolites in microbial extracts[89]. Pentoxifylline is widely used in the treatment of patients with cerebrovascular and peripheral vascular diseases[95]. Seven metabolites of pentoxifylline have been identified in mammals, including man[96]; the major metabolites are a secondary alcohol and two carboxylic acids[97]. The strategy of microbial models of mammalian metabolism[98] was planned to seek microorganisms that metabolize pentoxifylline in a manner similar to mammals. The developed procedure was used for investigating the metabolism of pentoxifylline by *Nocardia corallina*. Initial extraction of acidified media with dichloromethane-2-propanol (4:1) was required. HPLC with a methanol–0.02 M phosphoric acid (pH 5.0) (3:7) mobile phase and UV detection at 275 nm permitted detection of $\mu g/ml$ concentrations of the xanthine compounds. This technique was previously used to determine pentoxifylline and secondary alcohol metabolite in plasma[99] and carboxylic acid metabolites in urine[100].

A correlation between the accumulation of pyrophosphate and the increased level of ribonucleoside triphosphates in *Escherichia coli* in the presence of some inhibitors (6-azauracil, 6-mercaptopurine, 5-fluorouracil and hydroxyurea) of nucleic acid synthesis was demonstrated by Kukko and Kallio[90]. Ribonucleoside triphosphate concentrations were determined by HPLC using isocratic elution with 0.2 M sodium phosphate (pH 6.0)–0.025 M tetrabutylammonium hydroxide–10% methanol and detection at 260 nm.

The results obtained in the applications mentioned above indicate that reversed-phase HPLC can be useful not only for monitoring the activities of purine-metabolizing enzymes but also for studying the metabolism of purine drugs.

5. ACKNOWLEDGEMENT

6. ABSTRACT

The chemotaxonomic approach to the identification of pathogenic bacteria for clinical purposes is surveyed. Primary interest is focused on the applications of HPLC to the determination of metabolic products from anaerobic bacteria. The use of HPLC is attractive as different classes of short-chain acids can be determined in a single analysis. Chromatographic conditions are extensively described, emphasizing the effects of changing variables on the HPLC profiles of analytes. The application of labelling procedures to bacterial metabolites can markedly increase the sensitivity of the analysis of pathological fluids. HPLC appears to be potentially useful in clinical bacteriology for the diagnosis of anaerobic infections.

REFERENCES

1 M. Goodfellow and D. E. Minnikin, in M. Goodfellow and D. E. Minnikin (Editors), *Chemical Methods in Bacterial Systematics*, Academic Press, London, 1985, pp. 1–15.
2 M. Goodfellow and R. G. Board (Editors), *Microbiological Classification and Identification,* Academic Press, London, 1980.
3 D. B. Drucker, *Microbiological Applications of Gas Chromatography*, Cambridge University Press, Cambridge, 1981.
4 D. C. Edman and J. B. Brooks, *J. Chromatogr.*, 274 (1983) 1.
5 N. R. Krieg (Editor), *Bergey's Manual of Systematic Bacteriology*, Vol. 1, Williams and Wilkins, Baltimore, 1984.
6 G. Gottschalk (Editor), *Methods in Microbiology*, Vol. 18, Academic Press, London, 1985.
7 I. Brondz, *Dr. Thesis,* University of Oslo, Oslo, 1985.
8 M. Goodfellow and D. E. Minnikin (Editors), *Chemical Methods in Bacterial Systematics*, Academic Press, London, 1985.
9 I. Brondz and I. Olsen, *J. Chromatogr.*, 380 (1986) 1.
10 I. Brondz and I. Olsen, *J. Chromatogr.*, 379 (1986) 367.
11 H. N. Shah and M. D. Collins, *J. Appl. Bacteriol.*, 55 (1983) 403.
12 H. N. Shah, R. A. Nash, J. M. Hardie, D. A. Wheetman, D. A. Geddes and T. W. McFarlane, in M. Goodfellow and D. E. Minnikin (Editors), *Chemical Methods in Bacterial Systematics*, Academic Press, London, 1985, pp. 317–340.
13 R. C. Seid, H. Schneider, S. Bondarew and R. A. Boykins, *Anal. Biochem.*,124 (1982) 320.
14 L. V. Holdeman, E. P. Cato and W. E. C. Moore, *Anaerobe Laboratory Manual*, Virginia Polytechnic Institute and State University, Blacksburg, VA, 4th ed., 1977.
15 J. B. Brooks, *Adv. Chromatogr.*, 15 (1977) 1.
16 D. C. Edman, R. B. Craven and J. B. Brooks, *CRC Crit. Rev. Clin. Lab. Sci.*, 14 (1981) 133.
17 C. W. Moss, *J. Chromatogr.*, 203 (1981) 337.
18 D. B. Drucker, in J. R. Norris (Editor), *Methods in Microbiology*, Vol. 9, Academic Press, New York, 1976, p. 52.
19 E. Postaire, F. Schnirer and J. C. Darbord, *Bull. Inst. Pasteur*, 86 (1988) 145.
20 D. B. Drucker, *Microbiological Applications of High-Performance Liquid Chromatography*, Cambridge University Press, Cambridge, 1987.
21 S. L. Gorbach, J. W. Mayhew, J. G. Bartlett, H. Thadepalli and A. B. Onderdonk, *J. Clin. Invest.*, 57 (1976) 478.
22 R. Schwarzenbach, *J. Chromatogr.*, 251 (1982) 339.
23 B. Libert, *J. Chromatogr.*, 210 (1981) 540.
24 C. Droz and H. Tanner, *Schweiz. Z. Obst. Weinbau*, 118 (1982) 434.
25 R. L. Patience and J. D. Thomas, *J. Chromatogr.*, 249 (1982) 183.
26 P. Jandere and H. Engelhardt, *Chromatographia*, 13 (1980) 18.
27 B. S. Buslig, C. W. Wilson and P. E. Shaw, *J. Agric. Food Chem.*, 30 (1982) 342.
28 K. G. Wahlund, *J. Chromatogr.*, 218 (1981) 671.
29 D. N. Buchanan and J. G. Thoene, *Anal. Biochem.*, 124 (1982) 108.
30 N. Kubadinow, *Zuckerindustrie*, 107 (1982) 1107.

31 F. G. R. Reyes, R. E. Wrolstad and C. J. Cornwell, *J. Assoc. Off. Anal. Chem.*, 65 (1982) 126.
32 L. M. Jahangir and O. Samuelson, *Anal. Chim. Acta*, 92 (1977) 329.
33 V. T. Turkelson and M. Richards, *Anal. Chem.*, 50 (1978) 1420.
34 R. T. Marsili, *J. Chromatogr. Sci.*, 19 (1981) 451.
35 P. R. Monk and P. G. Iland, *Food Technol. Aust.*, 36 (1984) 16.
36 G. G. Ehrlich, D. F. Goerlitz, J. H. Bourell, G. V. Eisen and E. M. Godsy, *Appl. Environ. Microbiol.*, 42 (1981) 878.
37 G. O. Guerrant, M. A. Lambert and C. W. Moss, *J. Clin. Microbiol.*, 16 (1982) 355.
38 R. F. Adams, R. L. Jones and P. L. Conway, *J. Chromatogr.*, 336 (1984) 125.
39 L. Radin, A. Costa, M. van Steenbergen, J. De Graaff and G. A. Botta, *IV Convegno delle Sezioni Liguri, Genoa, 1984,* Associazone Microbiologi Clinici Italiani, Tecnostampa, Reggio Emilia, 1986, p. 267.
40 R. Krausse and U. Ullmann, *Zentralbl. Bakteriol. Parasitenkd. Infektionskr. Hyg., Abt. 1 Orig., Reihe A,* 265 (1987) 340.
41 R. S. Edson, J. E. Rosenblatt, J. A. Washington and J. B. Stewart, *J. Clin. Microbiol.*, 6 (1982) 1059.
42 J. B. Brooks, O. L. Nunez-Montiel, B. J. Wycoff and C. W. Moss, *J. Clin. Microbiol.*, 20 (1984) 539.
43 C. Potvliege, M. Labbe' and E. Yourassowsky, *Lancet,* ii (1981) 1105.
44 W. H. Loh, N. Santoro, R. H. Miller and O. H. Tuovinen, *J. Gen. Microbiol.*, 130 (1984) 1051.
45 R. Krausse and U. Ullmann, *Zbl. Bakteriol. Parasitenkd. Infektionskr. Hyg., Abt. 1 Orig., Reihe A,* 260 (1985) 342.
46 J. W. Mayhew, A. B. Onderdonk and S. L. Gorbach, *Appl. Microbiol.*, 4 (1975) 472.
47 P. N. Levett and K. D. Phillips, *J. Clin. Pathol.*, 38 (1985) 82.
48 A. E. van den Bogaard, M. J. Hazen and C. P. van Boven, *J. Clin. Microbiol.*, 3 (1986) 523.
49 S. S. Socransky, J. L. Dzink and C. M. Smith, *J. Clin. Microbiol.*, 22 (1985) 303.
50 R. Corio, P. A. Dusi, L. Radin and C. Lucarelli, in Emmezeta (Editor), *20th National Congress, Italian Society of Clinical Biochemistry, Rome,* La Grafica Briantea, Como, 1988, p. 117.
51 L. F. Ross and D. C. Chapital, *J. Chromatogr. Sci.*, 25 (1987) 112.
52 L. Radin, A. Arzese, C. Lucarelli and G. A. Botta, *J. Chromatogr.*, 459 (1988) 331.
53 M. E. Cieslak and W. C. Herwig, *J. Am. Soc. Brew. Chem.*, 40 (1982) 43.
54 K. M. Brobst and H. D. Scobell, *Starke*, 34 (1982) 117.
55 F. E. Wentz, A. D. Marcy and M. G. Gray, *J. Chromatogr. Sci.*, 20 (1982) 349.
56 J. C. du Preez and J. P. van der Walt, *Biotechnol. Lett.*, 5 (1983) 357.
57 L. A. Th. Verhaar and B. F. M. Kuster, *J. Chromatogr.*, 210 (1981) 279.
58 K. Brunt, *J. Chromatogr.*, 246 (1982) 145.
59 R. Pecina, G. Bonn, E. Burtscher and O. Bobleter, *J. Chromatogr.*, 287 (1984) 245.
60 K. Robards and M. Whitelaw, *J. Chromatogr.*, 373 (1986) 81.
61 D. J. Harpold, B. L. Wasilauskas and M. L. O'Connor, *J. Clin. Microbiol.*, 22 (1985) 962.
62 D. J. Harpold and B. L. Wasilauskas, *J. Clin. Microbiol.*, 25 (1987) 996.
63 L. Radin, R. Corio and G. A. Botta, *Biochim. Clin.*, 13 (1989) 993.
64 J. L. Devalia, B. D. Sheinman and R. J. Davies, *J. Chromatogr.*, 343 (1985) 407.
65 B. D. Sheinman, J. L. Devalia, S. J. Crook ad R. J. Davies, *Agents Actions*, 17 (1985) 449.
66 M. A. Curtis, I. R. Gillett, G. S. Griffiths, M. F. J. Maiden, J. A. C. Sterne, D. T. Wilson, J. M. A. Wilton and N. W. Johnson, *J. Clin. Periodontol.*, 16 (1989) 1.
67 M. A. Curtis and C. W. Kemp, in B. Guggenheim (Editor), *Cariology Today*, Karger, Basle, 1983, p. 212.
68 S. Robrish, M. A. Curtis, S. A. Sharer and W. H. Bowen, *Anal. Biochem.*, 136 (1984) 503.
69 G. A. Botta, L. Radin, A. Costa and G. Blasi, *J. Periodont. Res.*, 20 (1985) 450.
70 W. M. Edgar, M. W. J. Dodds and S. M. Higham, *Biochem. Soc. Trans.*, 14 (1986) 977.
71 J. F. Lawrence, *Organic Trace Analysis by Liquid Chromatography,* Academic Press, New York, 1981, Ch. 7.
72 R. E. Majors, H. G. Barth and C. H. Lochmüller, *Anal. Chem.*, 54 (1982) 323R.
73 R. E. Majors, H. G. Barth and C. H. Lochmüller, *Anal. Chem.*, 56 (1984) 300R.
74 H. Lingeman, W. J. M. Underberg, A. Takadate and A. Hulshoff, *J. Liq. Chromatogr.*, 8 (1985) 789.
75 D. Perrett and S. R. Rudge, *J. Pharm. Biomed. Anal.*, 3 (1985) 3.
76 I. S. Krull, C. M. Selavka, C. Duda and W. Jacobs, *J. Liq. Chromatogr.*, 8 (1985) 2845.
77 K. Imai and T. Toyo'oka, in R. W. Frei and K. Zech (Editors), *Selective Sample Handling and Detection in High-Performance Liquid Chromatography,* Part A, Elsevier, Amsterdam, 1988, p. 209.

78 R. L. Patience and J. D. Thomas, *J. Chromatogr.*, 249 (1982) 183.
79 P. C. Bossle, J. J. Martin, E. W. Sarver and H. Z. Sommer, *J. Chromatogr.*, 267 (1983) 209.
80 H. Tsuchiya, M. Sato, I. Namikawa, T. Hayashi, M. Tatsumi and N. Takagi, *J. Clin. Microbiol.*, 24 (1986) 81.
81 E. Nissinen, *Anal. Biochem.*, 106 (1980) 497.
82 N. D. Brown, J. A. Kintzios and S. E. Koetitz, *J. Chromatogr.*, 177 (1979) 170.
83 W. E. Wung and S. B. Howell, *Clin. Chem.*, 26 (1980) 1704.
84 H. A. Scoble and P. R. Brown, in Cs. Horváth (Editor), *High-Performance Liquid Chromatography —Advances and Perspectives*, Vol. 3, Academic Press, New York, 1983, p. 1.
85 M. Zakaria, P. R. Brown and E. Grushka, in A. Zlatkis, R. Segura and L. S. Ettre (Editors), *Advances in Chromatography 1981*, University of Houston, Houston, TX, 1981, pp. 451–471.
86 P. R. Brown, A. M. Krstulovic and R. A. Hartwick, *Adv. Exp. Med. Biol.*, 76A (1977) 610.
87 P. Duerre and J. R. Andreesen, *Anal. Biochem.*, 123 (1982) 32.
88 P. Duerre and J. R. Andreesen, *Arch. Microbiol.*, 131 (1982) 255.
89 R. V. Smith, S. K. Yang, P. J. Davis and M. T. Bauza, *J. Chromatogr.*, 281 (1983) 281.
90 E. Kukko and T. Kallio, *Biochem. Int.*, 8 (1984) 1.
91 G. D. Vogels and C. van der Drift, *Bacteriol. Rev.*, 40 (1976) 403.
92 P. Duerre, W. Andersch and J. R. Andreesen, *Int. J. Syst. Bacteriol.*, 31 (1981) 184.
93 P. Duerre and J. R. Andreesen, *J. Gen. Microbiol.*, 128 (1982) 1457.
94 M. Pojek and B. Rocic, *Experientia*, 36 (1980) 78.
95 H. Denck, *Arzneim.-Forsch.*, 23 (1973) 571.
96 H. J. Hinze, G. Bedessem and A. Soder, *Arzneim.-Forsch.*, 22 (1972) 1144.
97 H. J. Hinze, *Arzneim.-Forsch.*, 22 (1972) 1492.
98 R. V. Smith and J. P. Rosazza, *J. Nat. Prod.*, 46 (1983) 79.
99 D. A. Chivers, D. J. Birkett and J. O. Miners, *J. Chromatogr.*, 225 (1981) 261.
100 J. Chamberlain and K. W. Jolley, Hoechst U.K., personal communication, 1981.

CHROMSYMP. 1793

Determination of free catecholamines in human urine by direct injection of urine into a liquid chromatographic column-switching system with fluorimetric detection

TOKUICHIRO SEKI*

College of Bio-Medical Technology, Osaka University, 1–1, Machikaneyama-cho, Toyonaka-shi, Osaka 560 (Japan)

and

YUZO YANAGIHARA and KOHJI NOGUCHI

Asahi Chemical Industry Co. Ltd., 1–3–2, Yakoo, Kawasaki-ku, Kawasaki-shi, Kanagawa 210 (Japan)

ABSTRACT

An ion-exchange chromatographic method combined with ion exclusion was developed for the determination of free catecholamines in human urine. Catecholamines were separated by ion exclusion from most acidic and neutral impurities by filtration through an anion-exchange column with a hydrophilic matrix (Asahipak ES-502N) and the excluded catecholamines were separated by ion-exchange chromatography on a column of weakly acidic ion exchanger with a hydrophilic matrix (Asahipak ES-502C), connected in series to the Asahipak ES-502N column with a four-way automatic valve. A sodium succinate–borate buffer of pH 6.7 (0.035 mol of succinic acid, 0.0075 mol of borate and 0.5 mmol of ethylenediaminetetraacetate were dissolved in 1 kg of water and the pH of the solution was adjusted to 6.7 with sodium hydroxide) was used as the mobile phase, and the temperature of both columns was kept at 30°C.

The catecholamines in the eluate were determined fluorimetrically by post-column derivatization with glycylglycine. A diluted urine sample was injected directly onto the first column. The first column was back-flushed with the mobile phase for 52.5 min after the elution of the catecholamines from the first to the second column. Then the columns were washed with the mobile phase for 10 min in the normal direction before the next sample was injected into the first column. Samples could be analysed every 70 min and 5 pmol/ml of epinephrine, 5 pmol/ml of norepinephrine and 25 pmol/ml of dopamine in human urine could be determined.

INTRODUCTION

The determination of catecholamines in human urine by high-performance liquid chromatography consists of three steps, namely prepurification of catechol-

amines, separation of the catecholamines by ion-exchange or ion-pair chromato-
graphy and detection with electrochemical or fluorimetric methods. Various methods
for prepurification based on purification on alumina[1,2], phenylboronate[3,4] and
cation-exchange columns[5-7] have been automated and the equipment for prepurifi-
cation has been coupled to high-performance liquid chromatographs[2,4,7]. These
automated systems require multiple solvents for the adsorption and elution of the
catecholamines and regeneration of the adsorbent in the precolumn, in addition to the
mobile phase(s) for the elution of catecholamines from the analytical column, and the
systems can be complex and expensive.

On the other hand, we have found that a urine sample filtered through a column
of QAE-Sephadex A-25 gave a lower background fluorescence when the sample was
analysed on a weakly acidic ion exchanger with a hydrophilic matric (Asahipak
ES-502C) using a sodium succinate–borate buffer as described previously[8]. Therefore,
we tried to separate a basic fraction containing catecholamines from acidic and neutral
components in a urine sample by filtering it through a column of anion exchanger with
a hydrophilic matrix (Asahipak ES-502N) with a sodium succinate–borate buffer of
pH 6.7. The excluded fraction was transferred to a cation-exchange column (Asahipak
ES-502C) using a four-way valve, eluted with the same sodium succinate–borate buffer
as that used for filtration and detected fluorimetrically. This method requires a single
buffer for exclusion and elution of catecholamines from Asahipak ES-502N and
Asahipak ES-502C. Therefore, the whole process can be easily automated and
catecholamines in a diluted acidic urine sample could be successfully determined.

EXPERIMENTAL

Materials

Epinephrine bitartrate, norepinephrine bitartrate and dopamine hydrochloride
were purchased from Sigma (St. Louis, MO, U.S.A.) and glycylglycine from Nakarai
Chemicals (Kyoto,Japan). Other chemicals were of analytical-reagent grade from
Yashima Pharmaceutical (Osaka, Japan). Stock solutions of amines (1 mM) were
prepared in 0.01 M hydrochloric acid, and were diluted in 0.035 M succinate buffer
(pH 3.5) containing 0.5 mM ethylenediaminetetraacetate to give standard solutions of
various concentrations.

Apparatus

The liquid chromatograph with automatic column switching valves involved
two constant-flow pumps (Trirotar III and V; Jasco, Tokyo, Japan), an automatic
injector (Model KSST-60J; Kyowa Seimitsu, Tokyo, Japan), two ion-exchange
columns (Asahipak ES-502N and Asahipak 502C; Asahi Chemical Industries,
Kanagawa, Japan), an automatic six-way valve (Model 821-09; Jasco), an automatic
four-way valve (Model MVA-4U7H; Sanuki Kohgyoh, Tokyo, Japan), a dual-head
pump (Model SP-024-2; Jasco), a coil of PTFE tubing (50 m × 0.5 mm I.D.),
a spectrofluorimeter (Model 821-FP; Jasco) and a recorder (Model RC-125; Jasco).
They were assembled as shown in Fig. 1.

Sample injection and the switching events were controlled by a combination of
three timer units. The first timer unit (T_1), equipped with a programmable timer
(Model KS-1500; Koizumi Computer, Kobe, Japan), repeats on and off modes of
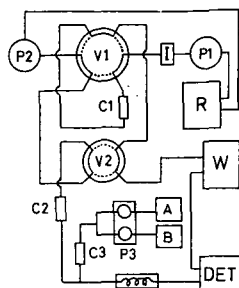
Fig. 1. Diagram of column-switching equipment. P_1 = Trirotar III; P_2 = Trirotar V; P_3 = dual-head pump; I = Automatic injector; V_1 = six-way automatic valve; V_2 = four-way automatic valve; C_1 = Asahipak ES-502N column (10 × 0.76 cm I.D.); C_2 = Asahipak ES-502C column (10 × 0.76 cm I.D.); C_3 = Shodex DS-613 column (15 × 0.6 cm I.D.); DET = spectrofluorimeter and recorder; R = mobile phase reservoir; A = reagent A reservoir; B = reagent B reservoir; W = waste. Full line in V_1 represents position B and dotted line position A, and full line in V_2 represents position L and dotted line position R. The temperature of C_1 and C_2 was kept at 30°C.

electric supply (100 V a.c.), at preset time intervals to the relay circuit of T_1 which controls the automatic injector and four-way valve (V_2), and to the second and third timer units. The second timer unit (T_2) controls V_2 and the third timer unit (T_3) controls the six-way automatic valve (V_1). T_2 is equipped with a motor timer with a maximum graded time of 6 min (Model SYS-6M; Omron Tateisi Electronics, Kyoto, Japan) and T_3 is equipped a motor timer with a maximum graded time of 12 min (Model SYS-12M; Omron Tateisi Electronics).

Mobile phase and reagents

A sodium succinate–borate buffer of pH 6.7 (0.035 and 0.0075 *M*, respectively, containing 0.5 m*M* ethylenediaminetetraacetate) was used as the mobile phase at a flow-rate of 1.5 ml/min. Reagent A was a solution of 0.1 *M* glycylglycine (pH 6.5) containing 0.1 *M* boric acid and 0.05 *M* tartaric acid and reagent B was 0.25 *M* potassium borate buffer of pH 8.3 containing hexacyanoferrate(III) (0.01%, w/v). They were filtered through a membrane filter (pore size 0.45 μm) and degassed under vacuum before use. Water of ultrapure grade, prepared by reverse osmosis (ROpure 40; Barnstead, Boston, MA, U.S.A.), ion exchange and charcoal adsorption of organic matter (NANOpure-II; Barnstead) was used to prepare these solutions.

Sample preparation

Urine was mixed with 1% of its volume of 6 *M* hydrochloric acid and kept in a refrigerator. It was analysed within 2 weeks. The acidified urine was diluted with 0.5 m*M* disodium ethylenediaminetetraacetate solution. The dilution was 5–20-fold, and the diluted urine was centrifuged at 13 000 *g* for 15 min at 5°C. It was filtered through a disposable membrane filter (ACRO LC3A, 0.45 μm; Gelman Sciences, Ann Arbor, MI, U.S.A.) and poured into a plastic vial.

Column switching and detection

Valves V_1 and V_2 were positioned at B and L (full line in Fig. 1) so that the mobile phase pumped by P_1 flowed through the anion-exchange column (C_1) to waste

TABLE I

TIMING AND SEQUENCE OF EVENTS OF AUTOMATED COLUMN SWITCHING FOR THE DETERMINATION CATECHOLAMINES IN HUMAN URINE

Time (min)	On–off of timers			Position of valves		Events
	T_1	T_2	T_3	V_1	V_2	
0	On	On	On	B	L	Sample injection onto C_1
3	On	Off	On	B	R	Connection of C_1 and C_2
7.5	On	Off	Off	A	R	Backflush of C_1 and elution of basic fraction from C_2
60	Off	Reset	Reset	B	L	End of backflush of C_1
70	On	On	On	B	L	Injection of next sample

and the mobile phase pumped by P_2 flowed through the cation-exchange column (C_2) to the post-labelling detector. When switch T_1 was turned on, sample was injected onto C_1, from which basic compounds were excluded. At 3 min after injection, V_2 rotated to position R (dotted line in Fig. 1) and C_1 and C_2 were connected. At 7.5 min after injection, V_1 rotated to position A (dotted line in Fig. 1). The mobile phase pumped by P_1 eluted the basic fraction transferred to C_2 from C_1, and at the same time C_1 was backflushed by the mobile phase pumped by P_2. At 60 min after injection, V_1 turned back to the original position B and V_2 to position L, and 10 min later the next sample was injected onto C_1 (Table I).

Catecholamines in the eluate from C_1 were determined by fluorimetry. Eluate was mixed with an equal mixture of reagents A and B. Each reagent was pumped at a flow-rate of 0.45 ml/min with a dual-head pump and mixed by using a T-shaped connector. The mixture of reagents was filtered through a guard column (15 × 0.6 cm I.D.) packed with 5-μm Shodex DS-613 polystyrene gel (Showa Denko, Tokyo, Japan) to remove fine particles that would cause background noise when passing through the flow cell. The mixture of reagents and the eluate was heated at 70°C in a PTFE tube immersed in a water-bath. The fluorescence was measured with a spectrofluorimeter with excitation at 350 nm and emission at 500 nm. The width of the slits was 18 nm for excitation radiation and 30 nm for emitted radiation.

RESULTS AND DISCUSSION

Elution patterns of a standard sample and a diluted urine sample are shown in Figs. 2 and 3, respectively. When the concentration of boric acid in the mobile phase was increased, the separation of norepinephrine from metanephrine and the separation of dopamine from the impurities which were eluted just after the dopamine peak was improved. However, under these conditions epinephrine was eluted closer to the main impurity peaks eluted before epinephrine. The separation of epinephrine from impurity peaks also became worse when a mobile phase of lower pH was used. Based on these observations, optimum pH and concentrations of the components of the mobile phase were selected. With some batches of Asahipak ES-502C the separation of dopamine from impurity peaks was unsatisfactory. In that event, the use of a mobile
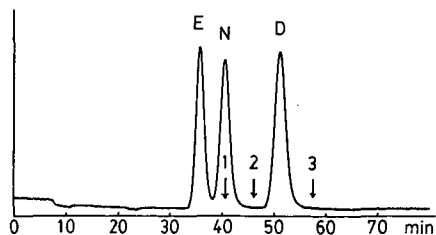
Fig. 2. Elution of standard catecholamines. A 300-μl volume of a solution containing 20 pmol/ml of epinephrine (E), 20 pmol/ml of norepinephrine (N) and 100 pmol/ml of dopamine (D) was injected. Arrows indicate the retention times of (1) metanephrine, (2) normetanephrine and (3) 3-methoxytyramine.

phase of lower succinate concentration (0.030 M) and of higher borate concentration (0.008 M) gave a better result. When the separation of metanephrine from norepinephrine is needed, the use of a mobile phase with a higher borate concentration (0.011 M) and a lower succinate concentration (0.030 M) can be used. Metanephrine is eluted after norepinephrine, but the normetanephrine peak overlaps that of dopamine. As the detection limit of metanephrine by the present post-labelling method is 1 nmol/ml, the presence of metanephrine in a urine sample will not affect the determination of norepinephrine by direct injection of a diluted urine sample.
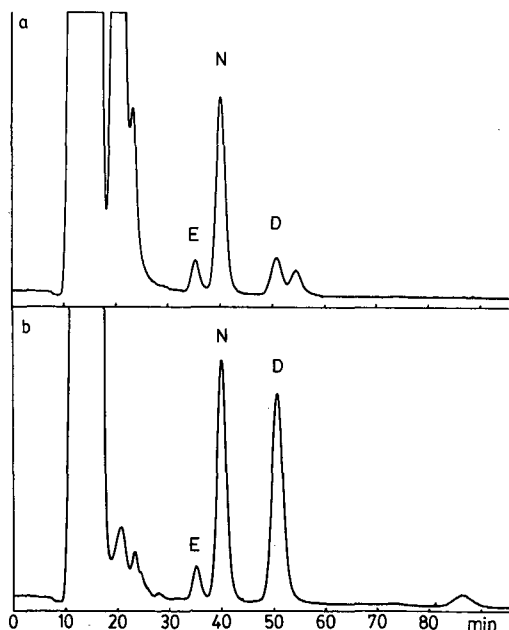
Fig. 3. Elution of diluted urine samples. (a) In the elution patterns of some samples impurity peak(s) were observed just after the dopamine peak, and (b) most of the samples analysed yielded a peak with a retention time of 86 min. When the next sample was injected at 70 min after the first sample, the peak with a retention time of 86 min of the first sample overlapped the large impurity peaks of the second sample.

Urine samples diluted 5–20-fold (pH 2–4) were analysed and 5 pmol/ml of epinephrine, 5 pmol/ml of norepinephrine and 25 pmol/ml of dopamine in urine could be determined. The reproducibility was evaluated by performing six replicate analyse of a normal urine sample diluted 10-fold. The relative standard deviation for epinephrine was 3.2% at a mean concentration of 6.5 pmol/ml, for norepinephrine 1.1% at a mean concentration of 52 pmol/ml and for dopamine 2.7% at a mean concentration of 240 pmol/ml. The correlations between the concentration of catecholamines as determined by the present method (x) and the internal standard method[9] (y) were as follows: for epinephrine, $y = 0.996x - 1.14$ ($r = 0.998$); for norepinephrine, $y = 0.966x + 2.98$ ($r = 0.999$); and for dopamine, $y = 0.932x + 56.1$ ($r = 0.998$) ($n = 17$). These results indicate that the method will be useful for the direct determination of free catecholamines in human urine samples.

REFERENCES

1 H. Tsuchiya, T. Koike and T. Hayashi, *Anal. Chim. Acta*, 281 (1989) 119.
2 M. Goto, T. Nakayama and D. Ishii, *J. Chromatogr.*, 226 (1981) 33.
3 S. Higa, T. Suzuki, A. Hayashi, I. Tsuge and Y. Yamamura, *Anal. Biochem.*, 77 (1977) 18.
4 P. Edlund and D. Westerlund, *J. Pharm. Biomed. Anal.*, 2 (1984) 315.
5 T. Huang, J. Wall and P. Kabra, *J. Chromatogr.*, 452 (1988) 409.
6 T. Seki and H. Wada, *J. Chromatogr.*, 114 (1975) 227.
7 A. Yamatodani and H. Wada, *Clin. Chem.*, 27 (1981) 1983.
8 T. Seki, Y. Yamaguchi, K. Noguchi and Y. Yanagihara, *J. Chem. Soc. Jpn.*, (1986) 1040.
9 T. Seki, Y. Yamaguchi, K. Noguchi and Y. Yanagihara, *J. Chromatogr.*, 332 (1985) 9.

CHROMSYMP. 1800

Enantiomer separation of pyrethroid insecticides by high-performance liquid chromatography with chiral stationary phases

NAOBUMI ÔI*, HAJIMU KITAHARA and REIKO KIRA

Sumika Chemical Analysis Service, Ltd., 3-1-135 Kasugade-naka, Konohana-ku, Osaka 554 (Japan)

ABSTRACT

The separation of enantiomers of pyrethroid insecticide esters by high-performance liquid chromatography was studied using some recently developed chiral stationary phases. Improved resolution was obtained for compounds with a variety of acid and alcohol moieties containing one to three chiral centres.

INTRODUCTION

As the individual isomers of chiral pyrethroid insecticide esters have widely differing biological activities, it is important to be able to determine the amount of each enantiomer. High-performance liquid chromatography (HPLC) with chiral stationary phases is a very useful technique for the analysis of these enantiomers, because it is a rapid, non-destructive technique in which there is little chance of epimerization during the course of analysis.

Many attempts have been made to apply HPLC with chiral stationary phases to the direct separation of pyrethroid enantiomers. Okamoto *et al.*[1] resolved the isomers of phenothrin on a chiral polymer column. Chapman[2] and Papadopoulou-Mourkidou[3] separated isomers of pyrethroids based on α-cyano-3-phenoxybenzyl alcohol, and Doi *et al.*[4] obtained separations of pyrethroids with no α-cyano group in the alcohol moiety using Pirkle-type columns[5,6]. Cayley and Simpson[7] made a more systematic study of the separation of pyrethroid isomers with a covalently bonded Pirkle-type stationary phase. Useful separation were reported for various pyrethroids, but unfortunately the separations of many compounds were incomplete.

Recently, we have developed[8,9] urea-derivative chiral stationary phases derived from (*S*)-1-(α-naphthyl)ethylamine with (*S*)-valine and (*S*)-*tert.*-leucine chemically bonded to 3-aminopropylsilanized silica (I and II), which are efficient for the separation of racemic ester compounds. We have also developed[10] a modified Pirkle-type column with (*R*)-N-(3,5-dinitrobenzoyl)-1-naphthylglycine ionically bonded to 3-aminopropylsilanized silica (III), and found that this phase could resolve some ester racemates.
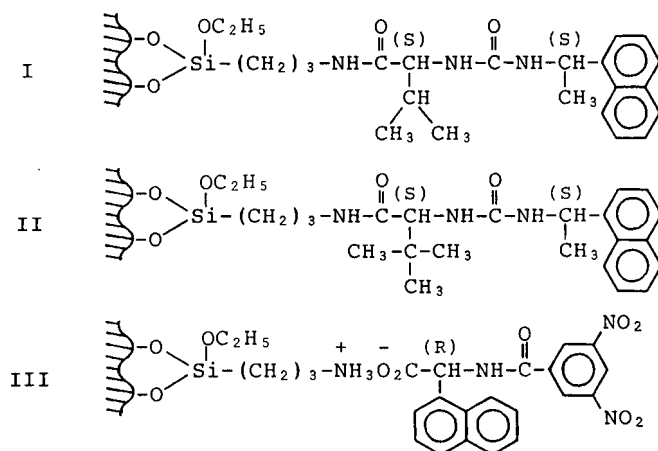
TABLE I

PYRETHROIDS USED

Common name	Systematic name	Isomers	Total number of isomers
Terallethrin	(RS)-3-Allyl-2-methyl-4-oxocyclopent-2-enyl 2,2,3,3-tetramethylcyclo-propanecarboxylate	(αRS)	2
Fenpropathrin	(RS)-α-Cyano-3-phenoxybenzyl 2,2,3,3-tetramethylcyclopropanecarboxylate	(αRS)	2
Resmethrin	5-Benzyl-3-furylmethyl (1RS)-cis,trans-2,2-dimethyl-3-(2-methylprop-1-enyl)-cyclopropanecarboxylate	(1RS)cis,trans	4
Permethrin	3-Phenoxybenzyl (1RS)-cis,trans-3-(2,2-dichlorovinyl)-2,2-dimethyl-cyclopropanecarboxylate	(1RS)cis,trans	4
Phenothrin	3-Phenoxybenzyl (1RS)-cis,trans-2,2-dimethyl-3-(2-methylprop-1-enyl)cyclopropanecarboxylate	(1RS)cis,trans	4
Tetramethrin	3,4,5,6-Tetrahydrophthalimidomethyl (1RS)-cis,trans-2,2-dimethyl-3-(2-methylprop-1-enyl)cyclopropanecarboxylate	(1RS)cis,trans	4
Fenvalerate	(RS)-α-Cyano-3-phenoxybenzyl (RS)-2-(4-chlorophenyl)-3-methylbutyrate	(αRS)(RS)	4
Cypermethrin	(RS)-α-Cyano-3-phenoxybenzyl (1RS)-cis,trans-3-(2,2-dichlorovinyl-2,2-dimethylcyclopropanecarboxylate	(αRS) (1RS)cis, trans	8
Allethrin	(RS)-3-Allyl-2-methyl-4-oxocyclopent-2-enyl (1RS)-cis,trans-2,2-dimethyl-3-(2-methylprop-1-enyl)cyclopropanecarboxylate	(αRS)(1RS)cis,trans	8
Bioallethrin	(RS)-3-Allyl-2-methyl-4-oxocyclopent-2-enyl (1R)-trans-2,2-dimethyl-3-(2-methylprop-1-enyl)cyclopropanecarboxylate	(αRS)(1R)trans	2

In this paper we present some improved results obtained for the separation of pyrethroid isomers by HPLC with the chiral stationary phases I–III.

EXPERIMENTAL

Chiral stationary phases I–III were prepared by the method described previously[8,9]. Stainless-steel columns (250 × 4 mm I.D.) were slurry packed with these phases using a conventional technique[11]. These columns are available from Sumika Chemical Analysis Service (Osaka, Japan), as SUMICHIRAL OA-4000, OA-4600 and OA-2500I respectively. SUMICHIRAL OA-2000 [(R)-N-(3,5-dinotrobenzoyl)phenylglycine chemically bonded to 3-aminopropylsilanized silica] and SUMICHIRAL OA-4700 [urea derivative derived from (R)-1-(α-naphthyl)ethylamine with (S)-tert.-

(a)

(b)

(c)

(d)

(e)

(f)

(g)
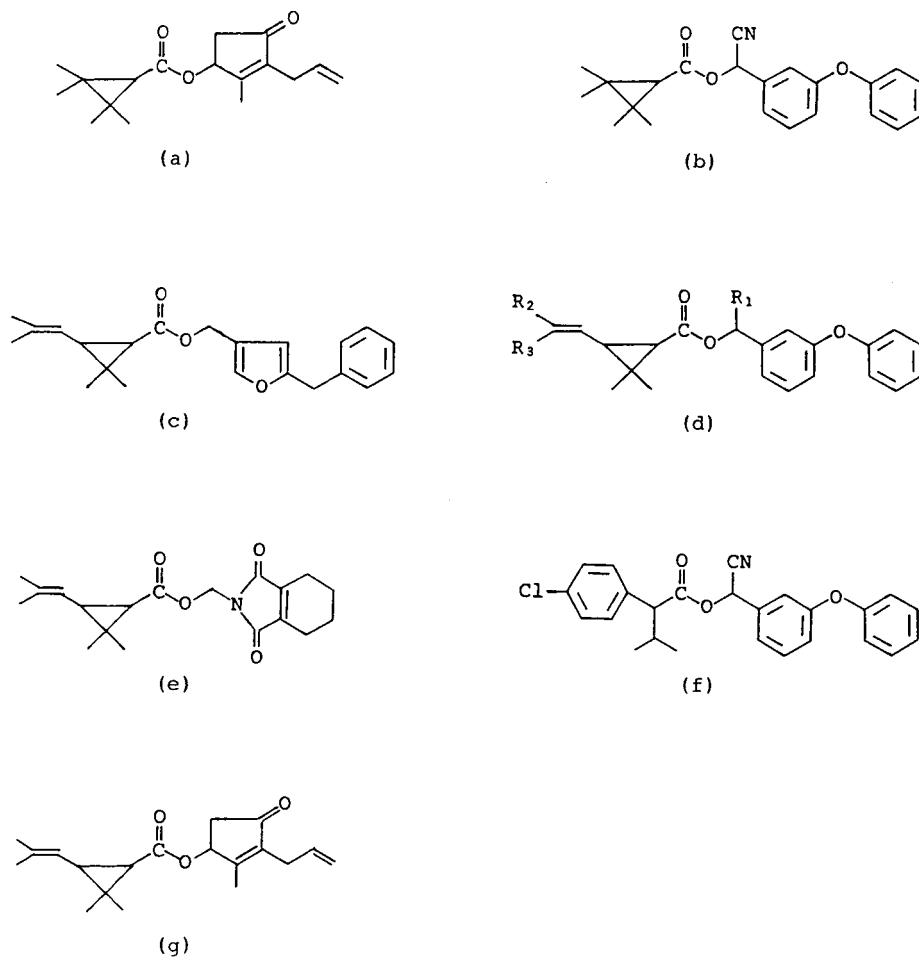
Fig. 1. Structures of pyrethroids: (a) terallethrin; (b) fenpropathrin; (c) resmethrin; (d) $R_1 = H$, $R_2 = R_3 = Cl$, permethrin; $R_1 = H$, $R_2 = R_3 = CH_3$, phenothrin; $R_1 = CN$, $R_2 = R_3 = Cl$, cypermethrin; (e) tetramethrin; (f) fenvalerate; (g) allethrin and bioallethrin.

leucine chemically bonded to 3-aminopropylsilanized silica] columns were also used for the separation of fenvalerate and cypermethrin isomers, respectively. The experiments were carried out using a Waters Assoc. Model 510 high-performance liquid chromatograph equipped with a variable-wavelength ultraviolet detector operated at 230 nm.

The common and chemical names of the pyrethroid insecticides used are summarized in Table I and their structures are shown in Fig. 1. We have adopted the names as given by Cayley and Simpson[7]. These compounds were kindly provided by Sumitomo Chemical (Osaka, Japan). All other chemicals were purchased from Wako (Osaka, Japan).

TABLE II

HPLC ENANTIOMER SEPARATION OF PYRETHROID INSECTICIDES

Elution orders of isomers were established by the injection of the pure isomers individually. Mobile phase: (A) hexane–1,2-dichloroethane–ethanol (500:30:0.15); (B) hexane–1,2-dichloroethane–ethanol (500:10:0.05); (C) hexane–1,2-dichloroethane (500:1). A flow-rate of 1.0 ml/min was typically used for the 250 × 4 mm I.D. column at room temperature. An injection volume of 1 μl (1 mg/ml) was typically used. k'_1, k'_2 = Capacity factors of first- and second-eluted isomer; α = separation factor (k'_2/k'_1).

Compound	Isomers	Phase	Mobile phase	k'_1/k'_2	α
Terallethrin	$\alpha S/\alpha R$	I	A	5.32/ 6.19	1.16
Fenpropathrin	$\alpha R/\alpha S$	II	B	3.00/ 3.77	1.26
Resmethrin	(1R)cis/(1S)cis	III	C	9.79/10.53	1.08
	(1R)trans/(1S)trans			11.43/12.05	1.05
Permethrin	(1R)cis/(1S)cis	III	C	8.20/ 9.24	1.13
	(1R)trans/(1S)trans			14.69/15.25	1.04
Phenothrin	(1R)cis/(1S)cis	III	C	4.98/ 5.42	1.09
	(1R)trans/(1S)trans			6.13/ 6.49	1.06
Tetramethrin	(1R)cis/(1S)cis	III	A	22.32/24.10	1.08
	(1R)trans/(1S)trans			25.98/26.87	1.03
Fenvalerate	(αR) (S)/(αS) (R)	III	A	7.77/11.25	1.45
	(αS) (S)/(αR) (R)			10.05/13.42	1.34
	(αR) (S)/(αS) (R)	OA-2000	A	7.55/ 8.35	1.11
	(αS) (S)/(αR) (R)			8.98/10.42	1.16
Cypermethrin	(αR) (1R)cis/(αS) (1S)cis	II	B	4.91/ 6.16	1.25
	(αR) (1S)cis/(αS) (1R)cis			6.51/ 6.91	1.06
	(αR) (1R)trans/(αS) (1S)trans			7.50/ 9.17	1.22
	(αR) (1S)trans/(αS) (1R)trans			9.-17/9.96	1.09
	(αR) (1R)cis/(αS)(1S)cis	OA-4700	B	4.76/ 5.05	1.06
	(αR) (1S)cis/(αS) (1R)cis			6.04/ 6.27	1.04
	(αR) (1R)trans/(αS)(1S)trans			7.10/ 7.47	1.05
	(αR) (1S)trans/(αS) (1R)trans			8.55/ 8.78	1.03
	(αR) (1R)cis/(αS) (1S)cis	II +	B	4.03/ 4.59	1.14
	(αR) (1S)cis/(αS) (1R)cis	OA-4700		5.23/ 5.47	1.05
	(αR) (1R)trans/(αS) (1S)(1R)trans			6.06/ 6.80	1.12
	(αR) (1S)trans/(αS) (1R)trans			7.42/ 7.79	1.05
Allethrin	(αS) (1R)cis/(αR) (1S)cis	II	A	4.54/ 5.87	1.29
	(αS) (1S)cis/(αR) (1R)cis			4.87/ 5.52	1.13
	(αS) (1R)trans/(αR) (1S)trans			5.05/ 6.14	1.28
	(αS) (1S)trans/(αR) (1R)trans			5.28/ 6.14	1.16

RESULTS AND DISCUSSION

The chromatographic results are summarized in Table II.

The chiral stationary phases I–III are all efficient for the enantiomer separation of pyrethroid insecticide esters, but the enantioselectivities differ for the individual compounds. Hence a good choice of the stationary phase is important for practical analysis. It is also important to use a suitable mobile phase for the efficient separation of isomers, because the polarity of the mobile phase sensitively affects the capacity factors (k') and the separation factors (α) of solutes.

The two isomers of terallethrin and fenpropathrin, which contain one asymmetric carbon atom in the alcohol moiety, were completely separated with the phases I and II. Typical chromatogram are shown in Figs. 2 and 3.

Resmethrin, permethrin, phenothrin and tetramethrin, which contain two asymmetric carbon atoms in the acid moiety, were resolved into their four isomers with phase III. A typical example of a chromatogram is shown in Fig. 4. Separations of these compounds were comparable to those achieved by Doi et al.[4] using a Pirkle-type column.

A useful separation of the four isomers of fenvalerate, each of which contain one asymmetric carbon atom in the alcohol and acid moiety, was obtained by Cayley et al.[7] and Papadopoulou-Mourkidou[3] using a Pirkle-type phase. We achieved a better separation with phase III than that with SUMICHIRAL OA-2000 Pirkle-type
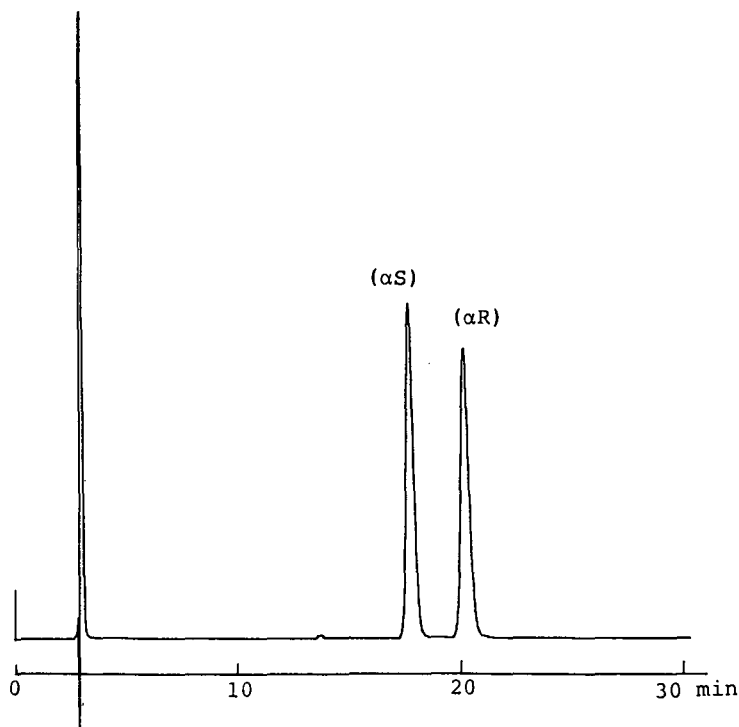
Fig. 2. Separation of terallethrin isomers with phase I. Chromatographic conditions as in Table II.
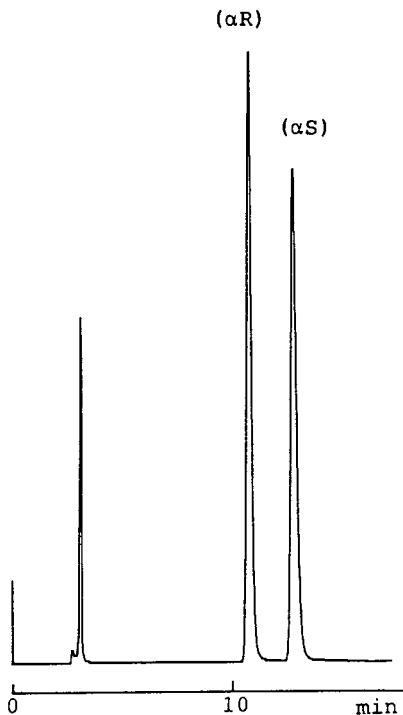
Fig. 3. Separation of fenpropathrin isomers with phase II. Chromatographic conditions as in Table II.

phase, as shown in Fig. 5. It is interesting that the elution orders of the four isomers are different on these two phases: $(\alpha R)(S)$, $(\alpha S)(R)$, $(\alpha S)(S)$, $(\alpha R)(R)$ on SUMICHIRAL OA-2000 and $(\alpha R)(S)$, $(\alpha S)(S)$, $(\alpha S)(R)$, $(\alpha R)(R)$ on the phase III. This result may be due to the large difference in enantioselectivity between the two phases. The separation factors for two enantiomer pairs $(\alpha R)(S)$ and $(\alpha S)(R)$ and $(\alpha S)(S)$ and $(\alpha R)(R)$, were 1.11 and 1.16, respectively, on SUMICHIRAL OA-2000 and 1.45 and 1.34, respectively, on the phase III.

The separation of the eight isomers of cypermethrin, which contain one chiral centre in the alcohol moiety and two chiral centres in the acid moiety, was difficult using a Prikle-type column[2,7]. The separation with phases I–III was also incomplete.
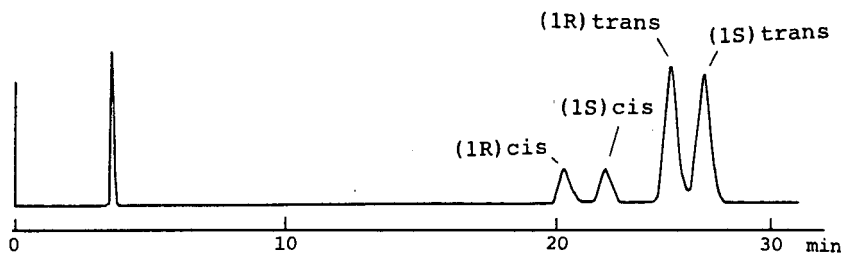
Fig. 4. Separation of phenothrin isomers with phase III. Chromatographic conditions as in Table II.
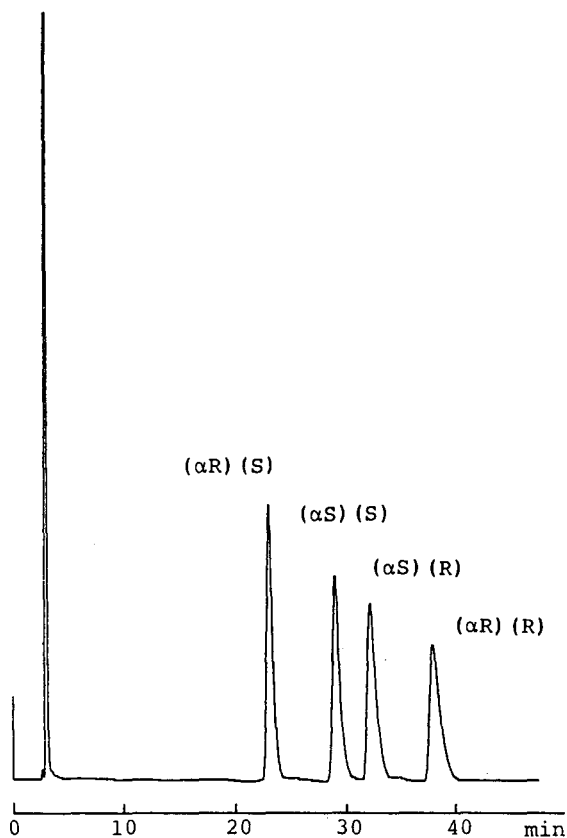
Fig. 5. Separation of fenvalerate isomers with phase III. Chromatographic conditions as in Table II.

However, the chromatogram obtained with phase II (Fig. 6a) shows that the enantio-selectivity of this phase is essentially sufficient for the separation of four enantiomer pairs, and the adjacent peaks of two diastereomeric isomers [(αS)(1S)trans and (αR)-(1S)trans] unfortunately overlap. We have found that the combination of two chiral stationary phases, phase II and SUMICHIRAL OA-4700, afforded a sufficient separation of the eight isomers of cypermethrin as shown in Fig. 6b. The good selectivity of SUMICHIRAL OA-4700 for the diastereomeric isomers may contribute to the successul separation of the eight isomers.

Cayley and Simpson[7] indicated that a mixture of the eight isomers of allethrin, which has a chiral alcohol moiety with no α-cyano group, was only partially resolved using a Pirkle-type column. However, an efficient separation of allethrin into eight isomers was acomplished with phase II, as shown in Fig. 7a. The chromatogram of bioallethrin (Fig. 7b) clearly shows that this compound consists of the (αS)(1R)trans and (αR)(1R)trans diastereomeric pair.
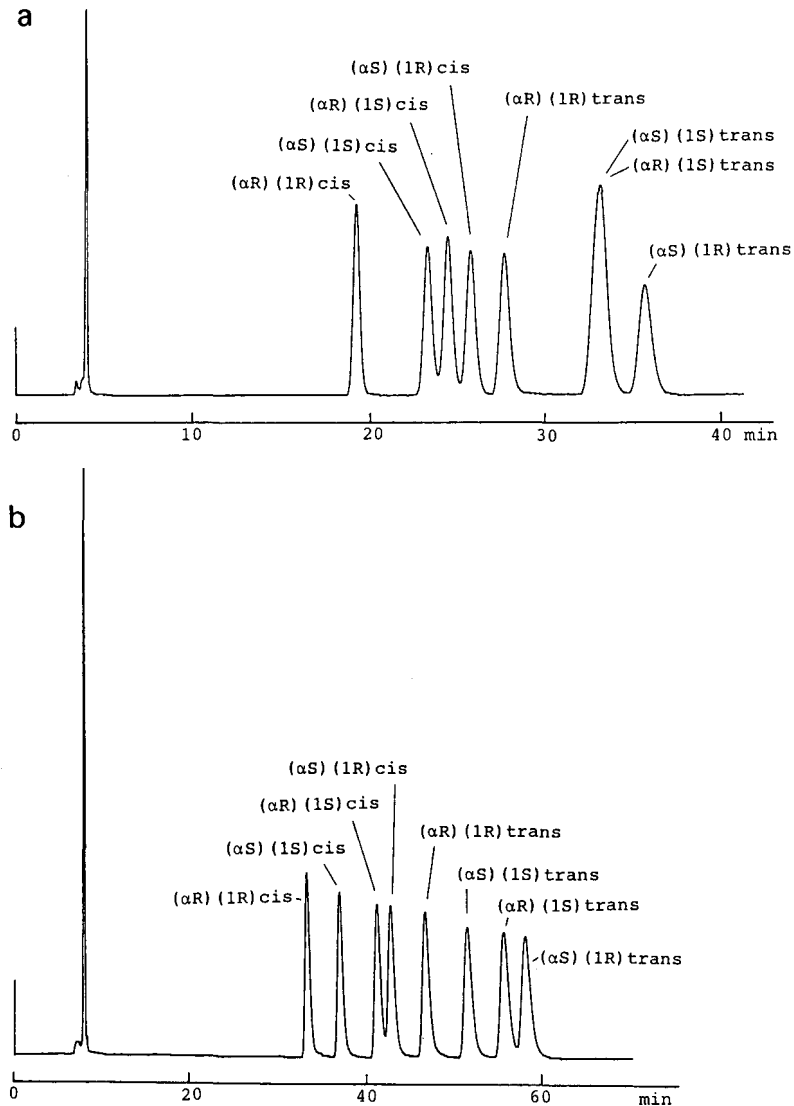
Fig. 6. Separation of cypermethrin isomers: (a) with phase II; (b) with phase II and SUMICHIRAL OA-4700 in series. Chromatographic conditions as in Table II.

CONCLUSION

It was found that chiral stationary phases I–III are very efficient for the enantiomer separation of pyrethroid insecticides. HPLC with these chiral phases is very promising for the enantiomer analysis of technical preparations, formulations and residues of various pyrethroid esters.
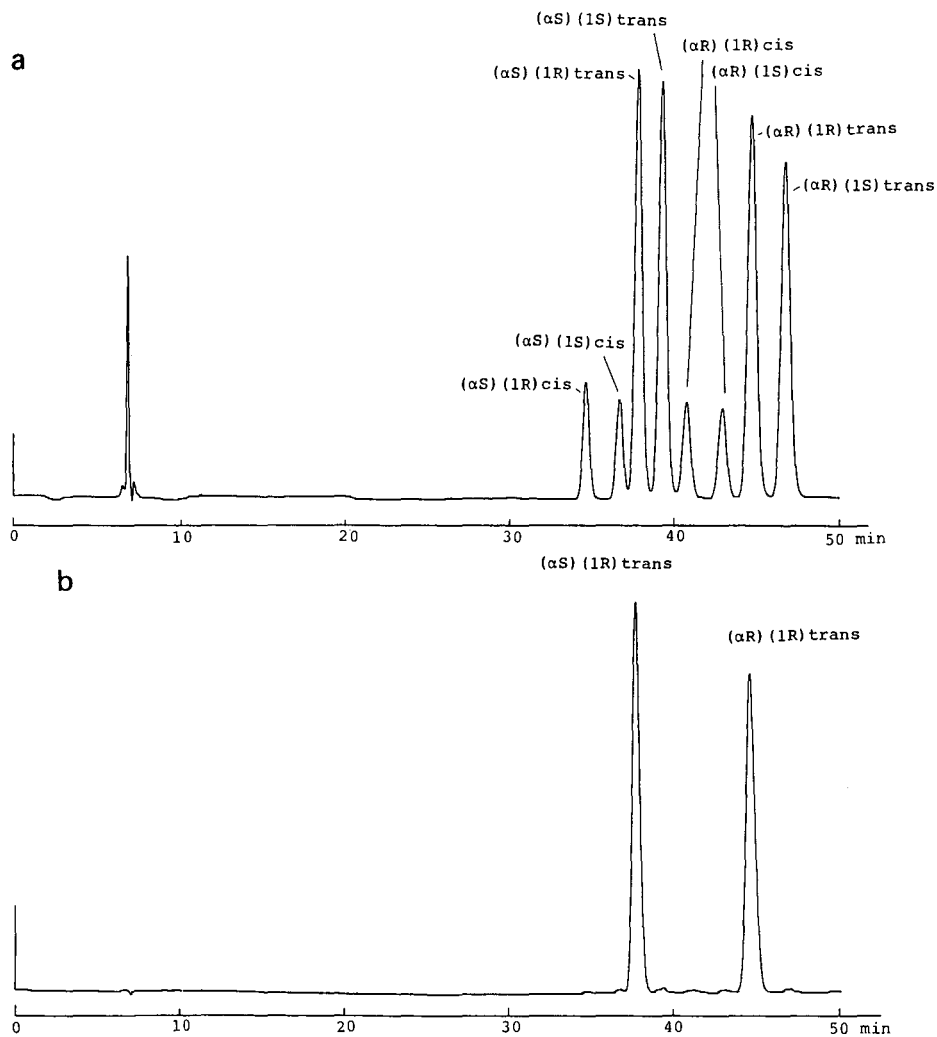
Fig. 7. Separation of (a) allethrin and (b) bioallethrin isomers with phase II. Chromatographic conditions as in Table II.

ACKNOWLEDGEMENT

The authors thank Sumito Chemical for providing the pyrethroid insecticides.

REFERENCES

1 Y. Okamoto, S. Honda, I. Okamoto and H. Yuki, *J. Am. Chem. Soc.*, 103 (1981) 69.
2 R. A. Chapman, *J. Chromatogr.*, 258 (1983) 175.
3 E. Papadopoulou-Mourkidou, *Chromatographia*, 20 (1985) 376.
4 T. Doi, S. Sakaue and M. Horiba, *J. Assoc. Off. Anal. Chem.*, 68 (1985) 911.

5 W. H. Pirkle, D. W. House and J. M. Finn, *J. Chromatogr.*, 192 (1980) 143.
6 W. H. Pirkle and J. M. Finn, *J. Org. Chem.*, 46 (1981) 2935.
7 G. R. Cayley and B. W. Simpson, *J. Chromatogr.*, 356 (1986) 123.
8 N. Ôi and H. Kitahara, *J. Liq. Chromatogr.*, 9 (1986) 511.
9 N. Ôi, H. Kitahara and R. Kira, in preparation.
10 N. Ôi, H. Kitahara, Y. Matsumoto, H. Nakajima and Y. Horikawa, *J. Chromatogr.*, 462 (1989) 382.
11 S. Hara and A. Dobashi, *J. Chromatogr.*, 186 (1979) 543.

Electrochemical detection of dipeptides and dipeptide amides

HWEIYAN TSAI and STEPHEN G. WEBER*

Department of Chemistry, University of Pittsburgh, Pittsburgh, PA 15260 (U.S.A.)

ABSTRACT

A postcolumn reagent is used to create electroactive species from non-electroactive peptides. The reagent, based on the classical biuret reagent, consists of Cu(II), tartrate, bicarbonate and base. The detection is by dual electrode electrochemical detection. N-Acetylated dipeptides are oxidized at pH 12 and low potential. Dipeptides and carboxy terminal dipeptide amides give useful signals at lower pH. The dipeptide amides react with Cu(II) as do the tripeptides to yield the electronic spectrum and electrochemistry of the biuret complex. The complexes formed from the dipeptides are reversibly oxidized at potentials greater than 0.85 V *vs.* Ag/AgCl, 3 *M* NaCl. Analytically useful signals are obtained for the dipeptide amides at sensitivities equivalent to the sensitivities for longer peptides, 3–5 nA/μM, while the sensitivities for the dipeptides are about an order of magnitude lower.

INTRODUCTION

Recently[1] it has been shown that the classical biuret reaction[2] can be used in the electrochemical detection of peptides. The complex between Cu(II) and the peptide is formed in a weakly basic solution containing tartrate to stabilize the copper. The electrochemical activity results from the ease of oxidation of the Cu(II) complex thus formed[3]. The advantage of this procedure over other procedures that are based on amine specific reagent chemistry[4–10] or specific amino acid determination[11–19] are several. The amine specific reagents are not peptide selective. There are many more amines in human body fluids and other biological media than there are peptides. As a consequence a heavy burden is placed on chromatography for the required selectivity for trace peptide determinations. Furthermore, some peptides have no primary amine. Peptides that do not contain lysine and that have a pyroglutamate residue on the amine terminus or the amine terminus of which has been acetylated or formylated will not react with the primary and secondary amine specific reagents. Amino acid specific detection schemes can be very useful if the peptide sought is characterized by the presence of a particular amino acid. For example, the electrochemical detection of the opioid peptides[15] is conveniently carried out because of the presence of the oxidizable tyrosine residue. However, this approach suffers from the obvious problem that it is restricted to those peptides containing the detectable amino acid. The proce-

dure using the biuret reagent is selective for the peptide bond. Detection limits of 0.25 pmol for small (3–6 amino acid-containing) peptides can be obtained using dual electrode electrochemical detection following the formation of the biuret complex in a postcolumn reactor.

In previous work[1] it was shown that the dipeptide glycyl–alanine (GA) was no more reactive than amino acids in this detection scheme, whereas the tripeptide glycyl–glycyl–glycine (G_3) was several thousand times more sensitively detected than non-electroactive amino acids. As a consequence, it would seem that, unfortunately, the selectivity of this detection scheme is restricted to tripeptides and longer peptides.

Margerum et al.[20] have carefully studied the influence of deprotonation of model copper peptide complexes on electrochemical activity of the complex. In Table I the data from Margerum's work have been abstracted into a convenient form. The table contains data for four derivatives of a simple tripeptide G_3. These are: the native peptide; the carboxyterminal amide; the N-formylated tripeptide; and the N-formylated carboxyterminal amide. The table shows that there is roughly an inverse relationship between the pH required to remove the last proton necessary for complex formation and the half-wave potential of the resulting complex. Thus, the simple tripeptide is fully formed in mild base (pH > 8.7) but requires a potential of 0.70 V (vs. Ag/AgCl, 3 M NaCl) for its oxidation. Contrarily, only at a pH > 12.1 would the biuret complex from the N-formylated carboxyterminal amide be fully formed, but its oxidation would occur at the relatively modest potential of 0.27 V. Intermediate are the N-formyl compound and the carboxyterminal amide.

The biuret reaction is given by dipeptide carboxyterminal amides (for example G–G amide)[20]. This work will show that the post-column reaction of dipeptide amides and dipeptides to form Cu(II) complexes and electrochemical detection of those complexes is possible for dipeptides and dipeptide amides with good sensitivity and only possible with acetylated dipeptides at extreme potentials and pH values.

EXPERIMENTAL

Reagents
    The following reagents were used without further purification: potassium phosphate monobasic GR crystals (EM Science, Cherry Hill, NJ, U.S.A.), acetonitrile (HPLC grade) and phosphoric acid (EM Science), sodium carbonate anhydrous and

TABLE I

pK_{last} AND $E°$ (vs. Ag/AgCl, 3 M NaCl) FOR G_3 DERIVATIVES

From ref. 20

Amine terminus	Carboxyl terminus			
	$-COO^-$		$-CONH_2$	
	pK_{last}	$E°$	pK_{last}	$E°$
H_2N-	6.72	0.70	8.69	0.42
HCOHN–	9.2	0.55	10.1	0.27

sodium bicarbonate (Fisher Scientific, Pittsburgh, PA, U.S.A.), sodium hydroxide pellets (J. T. Baker, Phillipsburgh, NJ, U.S.A.), L-α-Asp-L-Phe, L-α-Asp-L-Phe amide and L-Ala-L-Ala-L-Ala(A_3) (Sigma, St. Louis, MO, U.S.A.), Z-Gly-L-Phe (Z = carbobenzoxy), Z-Gly-L-Phe-NH$_2$, Gly-L-Phe and Gly-L-Phe-NH$_2$ · (CH$_3$COOH) (Peptide Institute, Japan), N-acetyl-Gly-L-Leu, N-Acetyl-Gly-L-Leu-NH$_2$, Gly-L-Leu and Gly-L-Leu-NH$_2$ · HCl (Research Plus, NJ, U.S.A.). Single letter abbreviations for the amino acids will be used hereafter: A = Ala, D = Asp, F = Phe, G = Gly, L = Leu. Potassium sodium tartrate (Aldrich, Milwaukee, WI, U.S.A.) was recrystallized from water before use. Water was doubly deionized and passed through an activated carbon bed before distillation in a Corning system.

Two reagent systems were used for chromatography. The mobile phase contained 25 mM KH$_2$PO$_4$ in acetonitrile–water (10:90) with added H$_3$PO$_4$ (around 2 g/l) to adjust the pH to 2.6. Postcolumn reagents contained 0.1 mM copper sulfate, 2 mM potassium sodium tartrate and 200 mM sodium bicarbonate except where mentioned. Sodium hydroxide and/or sodium carbonate were added in order to adjust to different pH values. These solutions were filtered through nylon 66 filters (pore size 0.2 μm, purchased from Rainin, Woburn, MA, U.S.A.) before use.

Instrumentation

A Waters Model 510 pump was used to pump the postcolumn reagents and a Waters Model M-45 was used to pump the mobile phase. These two pumps were operated by a Waters automated gradient controller in isocratic mode at a flow-rate of 2.0 ml/min. The mixing ratio was mobile phase–post-column reagents 40:60 (except where mentioned.)

A reversed-phase column, Waters Nova Pak-C$_{18}$ was placed between the injector and mixing tee in the system. The detector was a glassy carbon dual electrode, Bioanalytical systems LC-17A electrochemical detector (W. Lafayette, IN, U.S.A.). A Bioanalytical system model LC-4B potentiostat was used to control the potential and measure the anode current. The cathode current-to-voltage converter was laboratory made. The pH was measured with an ORION Research pH meter and Fisher Scientific glass electrode.

RESULTS AND DISCUSSION

N-Terminal blocked dipeptides

An N-terminal blocked peptide, whether it is an amide, *e.g.* N-formyl, N-acetyl, pyroglutamyl (a lactam), or a carbamate, *e.g.* a carbobenzyloxy derivative, will have a less basic amine-terminal nitrogen than the native peptide. The three coordinating groups in an N-acetyl dipeptide are the N-terminal amide, the peptide amide and the terminal carboxyl group. An OH$^-$ fills out the coordination sphere of Cu(II)[20]. The weakly basic amide is more acidic than the corresponding amine, and can be deprotonated to form the amido nitrogen (RCON̄R') in the presence of base and Cu(II). In comparison to the amine, the amide requires a higher pH for complex formation (donor strength is RCON̄R' > R-NH$_2$ > RCONHR'), but once formed is easier to oxidize because the strongly donating amido nitrogen stabilizes the Cu(III).

The following compounds were chromatographed: N-acetyl-GL, N-acetyl-GL-NH$_2$, Z-GF, Z-GF-NH$_2$. The postcolumn reagent (using 50 mM NaHCO$_3$) was
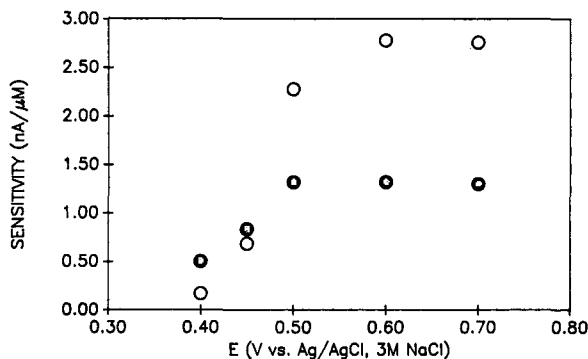
Fig. 1. Hydrodynamic voltammograms (anodic peak current *vs.* potential) for A$_3$(○) and N-acetyl-GL-NH$_2$(●). The sensitivities are calculated by dividing the peak current obtained by the injected concentration. Chromatographic conditions: total flow-rate, 1.7 ml/min; final pH = 12.7 ± 0.1; mobile phase [using 25 mM KH$_2$PO$_4$ in acetonitrile–water (10:90)]–postcolumn reagent (60:40) (using 0.2 mM Cu^{2+}, 4 mM tartrate 0.5 M NaHCO$_3$, 1.0 M NaOH). The injected volumes were 20 μl (containing 10 μM A$_3$, 10 μM N-acetyl-GL-NH$_2$ and 25 μM N-acetyl-GL).

added with a volume fraction 0.5 to achieve a pH around 10.7–10.8, a volume fraction of 0.6 to achieve a pH of 11.6 ± 0.1 and a high pH and large buffer capacity postcolumn reagent (containing 0.5 M NaHCO$_3$, 1.0 M NaOH) was added with a volume fraction 0.4 (total flow-rate 1.7 ml/min) to achieve a pH of 12.7 ± 0.1. No signal was detected in the potential range 0.6–0.8 V for all but the N-acetyl-GL-NH$_2$. The sensitivity (nA/μM) at the cathode for this compound was 0 at pH 10.7 and at pH 11.6 ± 0.1 was (potential) 0.005 (0.6), 0.003 (0.7), 0.017 (0.8). Hydrodynamic voltammograms for a control tripeptide, A$_3$, and N-acetyl-GL-NH$_2$ at pH 12.7 ± 0.01 are shown in Fig. 1. The collection efficiencies for all potentials were about 0.25. Even at this pH, there was no response from N-acetyl-GL, Z-GF-NH$_2$ and Z-GF. Thus, although it is possible to detect the N-terminal blocked dipeptide amides, it is not possible, with the current system, to determine N-terminal blocked dipeptides with a free carboxy terminus.

Free N-terminal dipeptides

Dipeptide amides yield the biuret reaction[20]. The coordinating groups are the free amino, two amide nitrogens and a hydroxide. The complex between GG-NH$_2$ and Cu(II) can be formed at a pH of 9.2, and is oxidizable with an $E°$ of 0.67[20]. Other dipeptide-based compounds that give the biuret reaction have not been reported, to our knowledge. The simple dipeptides do react with Cu(II). For example DF, in a solution containing an excess of Cu(II) in basic tartrate, yields a broad absorbance band with $\lambda_{max} \approx$ 660 nm. After heating (*ca.* 70°C, *ca.* 15 min) the band sharpens and increases in intensity, demonstrating a $\lambda_{max} \approx$ 640 nm. If the donor ligands are –NH$_2$, amido, carboxylate and hydroxide, one would predict[20] a λ_{max} around 610 nm. The biuret reaction, as exemplified by the complex formed between DF-NH$_2$ and Cu(II), has a $\lambda_{max} \approx$ 560 nm. Thus, the dipeptide coordinates with the Cu(II), but with two of the four ligands, carboxylate and hydroxide, not being significant stabilizers of the Cu(III) oxidation state, the complex may be difficult to oxidize.
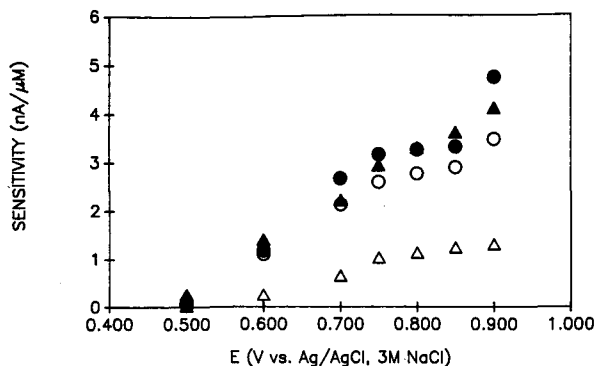
Fig. 2. Hydrodynamic voltammograms for A_3($\bigcirc$), GF-NH$_2$($\bullet$), GL-NH$_2$($\triangle$) and DF-NH$_2$($\blacktriangle$). Chromatographic conditions: total flow-rate 2.0 ml/min; final pH = 10.0 ± 0.1; mobile phase [using 25 mM KH$_2$PO$_4$ in acetonitrile-water (10:90)]–postcolumn reagent (40:60) (containing 0.1 mM CuSO$_4$, 2 mM tartrate, 0.2 M NaHO$_3$, 0.15 M NaOH). The injected volumes were 20 μl. Injections of dipeptide amides were of 5 μM solutions and 25 μM solutions of dipeptides were used. All injections contained 5 μM A$_3$.

Hydrodynamic voltammograms for a control tripeptide, A_3, and the dipeptide amides DF-NH$_2$, GF-NH$_2$, GL-NH$_2$ are shown in Fig. 2, and those for the dipeptides GF, DF and GL are shown in Fig. 3. The half wave potential for the dipeptide amides are the same as for A_3, about 0.65 V. Also the sensitivities for three of the four compounds are similar. The sensitivity for GL-NH$_2$ is significantly lower than others, which indicates an unusual behavior. However, at 0.90 V a very large peak appears in the anodic chromatogram, but not in the cathodic chromatogram of GL-NH$_2$. There is obviously an impurity in the GL-NH$_2$ solid.

The dipeptides give analytically useful signals at 0.9 V, but not at lower potentials. The shift of $E_{1/2}$ to a higher potential has been discussed in terms of the ligands. At such high potentials, the background problem becomes significant at the anode, but the behavior at the cathode is better.

The sensitivities shown in Fig. 2 are somewhat lower than those reported earlier[1]; 8 nA/μM at the anode. The lower values (3–5 nA/μM) reported here are the result
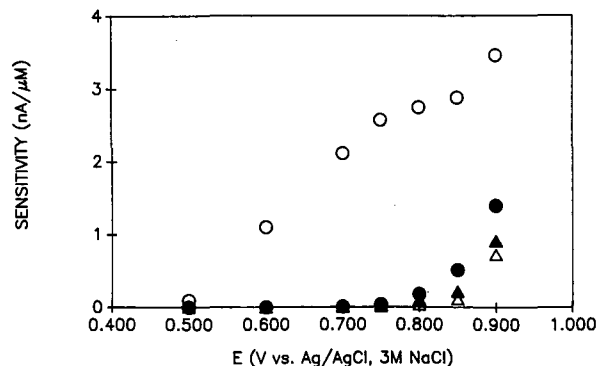
Fig. 3. Hydrodynamic voltammograms for A_3($\bigcirc$), GF ($\bullet$), GL ($\triangle$) and DF($\blacktriangle$). The chromatographic conditions are the same as in Fig. 2.

TABLE II

COLLECTION EFFICIENCIES

The chromatographic conditions are the same as in Fig. 2.

Peptide	Potential						
	0.5	0.6	0.7	0.75	0.8	0.85	0.9
A_3	–	0.24	0.25	0.27	0.28	0.28	0.24
GF-NH$_2$	–	0.24	0.26	0.29	0.27	0.26	0.15
GL-NH$_2$	–	0.25	0.27	0.27	0.27	0.26	0.24
DF-NH$_2$	0.29	0.30	0.31	0.30	0.31	0.31	0.30
GF	–	–	–	0.11	0.11	0.11	0.08
GL	–	–	–	–	0.02	0.10	0.09
DF	–	–	–	0.12	0.12	0.17	0.19

of greater dilution of the mobile phase by the postcolumn reagent in the current experiments. Although a variety of ratios have been used, they have been approximately mobile phase–postcolumn reagent (50:50). With the previous pressure-driven apparatus the ratio was about 9:1. By using a more concentrated reagent a lower mixing ratio could be used, with a resulting small increase in sensitivity.
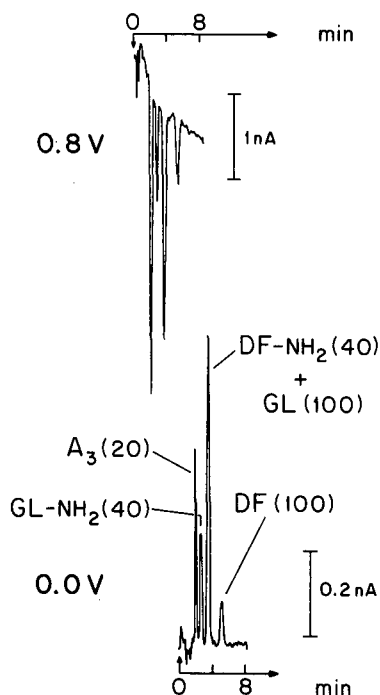
Fig. 4. A chromatogram of peptides. Mobile phase–postcolumn reagent ratio (40:60), flow-rate is 2.0 ml/min. The peaks (masses in pg) are A_3 (20); GL-NH$_2$ (40); DF-NH$_2$ and GL (40 and 100); DF (100). The top trace is the response of the anode and the bottom one is the response of the cathode.

Collection efficiencies have been determined for the analytes discussed. The collection efficiencies, ratios of cathodic to anodic current, should be around 0.35 for the geometry of this electrode system[1] if the oxidized product is perfectly stable. The values observed in Table II for A_3 and the amides are within the range of values previously seen for a variety of larger peptides, 0.25–0.30[1]. The collection efficiencies for the dipeptides are markedly lower and somewhat sensitive to potential.

The combination of lower anodic current and lower collection efficiency, the former by about a factor of four and the latter by about a factor of two to three, makes cathodic detection of the dipeptides about an order of magnitude less sensitive than the detection of higher peptides.

A chromatogram of peptides is shown in Fig. 4, the top trace is the response of the anode and the bottom one is the response of the cathode. This mixture of dipeptides, derivatives and the tripeptide was separated with a flow-rate of 0.8 ml/min [KH_2PO_4 in acetonitrile–water (10:90), pH 2.6 $\pm$ 0.1] and was mixed with 1.2 ml/min postcolumn reagent (containing 0.1 mM $CuSO_4$, 2 mM tartrate, 50 mM $NaHCO_3$, 100 mM Na_2CO_3, pH = 10.10 $\pm$ 0.1). The final pH was 9.7.

REFERENCES

1 A. M. Warner and S. G. Weber, *Anal. Chem.*, 61 (1989) 2664.
2 A. G. Gornall, C. J. Bardawill and M. M. David, *J. Biol. Chem.*, 177 (1949) 751.
3 D. W. Margerum, *Pure Appl. Chem.*, 55 (1983) 23.
4 A. F. Spatola and D. E. Benovitz, *J. Chromatogr.*, 327 (1985) 165.
5 I. Molnár and C. Horváth, *J. Chromatogr.*, 142 (1977) 623.
6 Y. Hirago and T. Kinoshita, *J. Chromatogr.*, 226 (1981) 43.
7 L. A. Sternson, in R. W. Frei and J. F. Lawrence (Editors), *Chemical Derivatization in Analytical Chemistry*, Vol. 1, Plenum, New York, 1981, Ch. 3, p. 127.
8 S. Udenfriend, S. Stein, P. Böhlen, W. Dairman, W. Leimgruber and M. Weigele, *Science (Washington, D.C.)*, 178 (1972) 871.
9 W. Vogt, E. Egler, W. Sommer, F. Eisenbeiss and H. D. Meyer, *J. Chromatogr.*, 400 (1987) 83.
10 P. deMontigny, T. F. Stobaugh, R. S. Givens, R. G. Carlson, K. Srinivasachar, L. A. Sternson and T. Higuchi, *Anal. Chem.*, 59 (1987) 1096.
11 R. H. Haschemeyer and A. D. V. Haschemeyer, *Proteins A Guide to Study by Physical and Chemical Methods*, Wiley, New York, 1973, Ch. 9, p. 217.
12 L. Allison and R. E. Shoup, *Anal. Chem.*, 55 (1983) 8.
13 L. H. Fleming and N. C. Reynolds, Jr., *J. Chromatogr.*, 375 (1986) 65.
14 J. T. Bretz and P. R. Brown, *J. Chromatogr. Sci.*, 26 (1988) 310.
15 G. W. Bennet, J. V. Johnson and C. A. Marsden, *IBRO Handb. Ser. (Neuropeptides)*, 11 (1989) 125.
16 A. L. Drumheller, A. Bachelard, S. St. Pierre and F. B. Jolicoeur, *J. Liq. Chromatogr.*, 8 (1985) 1829.
17 A. Sauter and M. Frick, *J. Chromatogr.*, 297 (1984) 215.
18 M. W. White, *J. Chromatogr.*, 262 (1983) 420.
19 S. Mousa and D. Couri, *J. Chromatogr.*, 267 (1983) 191.
20 D. W. Margerum, L. F. Wong, F. P. Bossu, K. L. Chellappa, J. J. Czarnecki, S. T. Kirksey, Jr. and T. A. Neubecker, in K. N. Raymond (Editor), *Bioinorganic Chemistry, II (ACS Symposium Series*, No. 162), American Chemical Society, Washington, DC, 1977, p. 281.

CHROMSYMP. 1850

Determination of methamphetamine, amphetamine and piperidine in human urine by high-performance liquid chromatography with chemiluminescence detection

KAZUICHI HAYAKAWA*, NORIKO IMAIZUMI, HIROMI ISHIKURA and ERIKO MINOGA-WA

Department of Hygienic Chemistry, Faculty of Pharmaceutical Sciences, Kanazawa University, 13–1 Tak-ara-machi, Kanazawa 920 (Japan)

NARIAKI TAKAYAMA and HIROSHI KOBAYASHI

Forensic Science Laboratory, Ishikawa Prefectural Police Headquarters, 2–1–1 Hirosaka, Kanazawa 920 (Japan)

and

MOTOICHI MIYAZAKI

Department of Hygienic Chemistry, Faculty of Pharmaceutical Sciences, Kanazawa University, 13–1 Tak-ara-machi, Kanazawa 920 (Japan)

ABSTRACT

A high-performance liquid chromatographic method for the determination of trace levels of methamphetamine, amphetamine and piperidine in human urine is reported. The three compounds, extracted into diethyl ether from alkaline urine, were derivatized with dansyl chloride, then separated on a reversed-phase column and detected by chemiluminescence after reaction with bis(2,4,6-trichlorophenyl) oxalate and hydrogen peroxide. The corresponding peaks obtained from human urine were identified as the dansyl derivatives by mass spectrometry. Methamphetamine levels as low as $2 \cdot 10^{-10}$ M in urine were determined. The sensitivity of the method is higher than that of Simon's reagent test and gas chromatography.

INTRODUCTION

The abuse of methamphetamine (MA) is a serious drug problem in Japan. Administration of MA has usually been proved by the detection of MA in urine, because a large fraction of the MA administered is excreted into urine as MA itself. Many methods have been developed for the determination of MA and related compounds, including colour tests, UV spectrometry, immunological methods, thin-layer chromatography, gas chromatography (GC), GC–mass spectrometry (MS) and high-performance liquid chromatography (HPLC). In these methods, Simon's reagent test has commonly been used as a simple and selective colour test[1], and both

GC[2-4] and GC–MS[5] have been used as highly sensitive methods. HPLC with UV detection has not been widely used in the determination of MA in biological fluids because of its low sensitivity[6-8]. However, both fluorescence and electrochemical detection have been used for the determination of MA and its hydroxylates by HPLC[9-11].

The reliability of the detection of MA in suspected human urine is obtained by satisfying the following two requirements. The first is that MA must be detected by more than two different and sensitive methods; a sensitive method comparable to GC or GC–MS is necessary. Second, the method should indicate that MA has not been added artificially but excreted into the suspected human urine; the simultaneous determination of MA, its metabolites and, if possible, some urinary compounds is necessary.

We have previously reported the determination method of MA and related compounds by HPLC with chemiluminescence detection[12]. The sensitivity of chemiluminescence detection for primary or secondary amines was much higher than fluorescence detection by using dansyl chloride[13] or naphthalenedialdehyde[12] as derivatizing reagents. The high sensitivity of the method with dansylation satisfies the first of the requirements. The interesting fact was that chromatograms of suspected human urine samples usually showed three major peaks that had the same retention times as dansyl-MA, dansyl-amphetamine (A) and dansyl-piperidine (P). A is a metabolite of MA[14] and P is a compound usually contained in human urine[15]. If the three peaks are identified as dansyl-MA, -A and -P, the second requirement described above is satisfied.

The purposes of this work were to identify dansyl-MA, -A and -P in the corresponding peaks from suspected human urine and to demonstrate several potential advantages of the present method.

EXPERIMENTAL

Chemicals

MA (hydrochloride), A (sulphate) and P were purchased from Dainippon Pharmaceutical (Osaka, Japan), Takeda Pharmaceutical (Osaka, Japan) and Nacalai Tesque (Kyoto, Japan), respectively. All other chemicals were of analytical-reagent grade or better and used without further purification.

HPLC

The pre-treatment procedures for human urine were as follows. To 2 ml of urine in a tube, 0.2 ml of 10% sodium hydroxide solution and 2.0 ml of diethyl ether were added and the mixture was shaken vigorously for 2 min. After centrifugation (1000 g, 10 min), the ether layer was collected. The extraction with diethyl ether was repeated again and the two extracts were combined. If the concentration of MA was not high enough, the ether extract (4 ml) was dried in a stream of nitrogen after the addition of a drop of diethyl ether containing 0.1 M acetic acid.

For dansylation, to 0.1 ml of the ether extract (4 ml) or to the evaporated residue, 1.0 ml (1.1 ml for the latter) of 10 mM carbonate buffer (pH 9.0) and 0.9 ml of acetone containing 1.0 mM dansyl chloride were added successively, and the mixture was incubated at 45°C for 1 h. An aliquot of the solution was injected into the HPLC system.

The HPLC system was as described previously report[12] except that a Jasco (Hachioji, Tokyo, Japan) 880-PU post-column pump and a Soma (Hinode, Tokyo, Japan) S-3400 chemiluminescence monitor (spiral flow cell, 100 μl) were used.

The mobile phase was acetonitrile–water (7:3, v/v) containing 1 mM imidazole, with a pH of 7.0 adjusted with nitric acid. The chemilumigenic reagent solution was acetonitrile solution containing 0.5 mM bis(2,4,6-trichlorophenyl)oxalate (TCPO) and 0.15 M hydrogen peroxide. Other operating conditions were as in the previous study[12].

Mass spectrometry

The HPLC fractionation for the three peaks used the same system as described above except that the loop volume of the injector was 100 μl and a fraction collector was attached just after the analytical column through a switching valve. Acetonitrile–water (7:3, v/v) was used as the mobile phase. After pretreatment (extraction and derivatization) of suspected human urine as described above, an aliquot (100 μl) of the sample solution was injected into the HPLC system. The fractions of the three peaks corresponding to dansyl-MA, -A and -P were collected. The injection of urine was repeated five times.

Electron impact (EI) mass spectra were obtained using a Shimadzu QP-1000 instrument. The ionization voltage and current were 200 eV and 60 μA, respectively.

Simon's reagent test

To 5.0 ml of urine in a tube, 0.5 ml of 10% sodium hydroxide solution and 5.0 ml of diethyl ether were added and the mixture was shaken vigorously for 2 min. After centrifugation (1000 g, 10 min), the ether layer was dehydrated with about 1 g of sodium sulphate and decanted. After addition of several drops of acetic acid, the solution was dried in a stream of nitrogen. An aliquot of the precipitate was dissolved in several drops of methanol and spotted on a paper. At the same point of the paper, 20% sodium carbonate, acetaldehyde–ethanol (1:1, v/v) and 1% sodium nitroprusside were spotted successively. If a positive purple-blue coloration was observed, the sample was applied to thin-layer chromatography and the spot of the same R_F value as MA was checked by the same coloration test.

GC

The same residue of the ether extracts obtained for Simon's reagent test was used for GC. Volumes of 200 μl each of ethyl acetate and trifluoroacetic anhydride were added to the residue and the mixture was incubated at 55°C for 1 h. After drying under a flow of nitrogen, the residue was dissolved in ethyl acetate containing diphenyl-methane as an internal standard.

The conditions for GC were as follows: apparatus, Shimadzu GC-14A; column, Chromosorb W coated with 2% OV-17 (1.1 m × 2.6 mm I.D.); carrier gas, helium (30 ml/min); detector, flame ionization; column temperature, 130°C; injection port temperature, 160°C; and injection volume, 1 μl. Trifluoroacetyl (TFA) derivatives of A and MA and the internal standard eluted at 2.1, 3.7 and 4.5 min, respectively. TFA-P was eluted too fast to be separated from the large peak of the solvent front.

RESULTS AND DISCUSSION

Typical chromatograms of suspected and control human urine samples

Typical chromatograms of a standard solution and suspected and control human urine are shown in Fig. 1. Peaks of dansyl-A, -P and -MA were observed at 11.9, 12.7 and 18.8 min, respectively, in the standard chromatogram (A). Three peaks (labelled I, II and III from the earliest) were found in the chromatogram of the suspected human urine (B) at the same retention times as the three standards. The concentrations of MA and P were calculated to be $1.6 \cdot 10^{-3}$ and $2.9 \cdot 10^{-2}$ M, respectively, in the urine, assuming that peaks I and II are dansyl-A and -MA, respectively. In the chromatogram of the control human urine (C), which showed peak II, no interfering peaks were observed at the retention times of peaks I and II. Further, all other suspected human urine samples tested showed the same three peaks and all control human urine samples showed only peak II.

Peak identification by MS

In previous work, imidazole buffer was used as a catalyst to enhance the generation of chemiluminescence in the TCPO–hydrogen peroxide system[16]. However, the buffer was removed from the mobile phase in the fractionation experiment in order to reduce its interference in MS analysis. The retention times of the three dansyl derivatives were not changed by the removal of imidazole buffer, although their peak heights in chemiluminescence detection became smaller. The three standard peaks (dansyl-A, -P and -MA) and the corresponding three peaks (I, II and III) fractionated from suspected human urine (No. 40) were characterized by MS as in Table I. All characteristic fragment peaks in each standard fraction were observed in the corresponding fractions from the urine with similar relative intensities. The possible
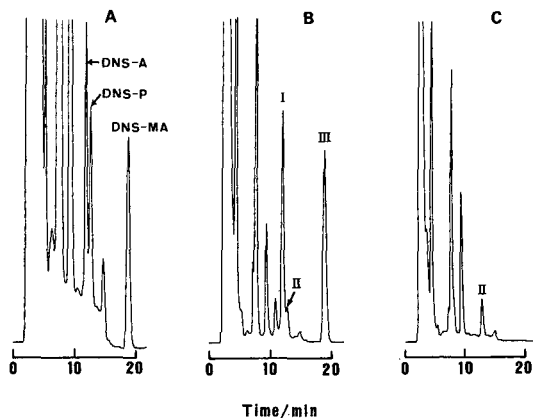
Fig. 1. Typical chromatograms of suspected human urine and control human urine. Analytical column, Inertsil ODS-2; detector, Soma S-3400 with range 64; mobile phase, acetonitrile–water (7:3, v/v) containing 1 mM imidazole (pH adjusted at 7.0 with nitric acid); chemiluminescence reagent solution, acetonitrile containing 0.5 mM TCPO and 0.15 M hydrogen peroxide. (A) Standard solution of dansyl (DNS)-MA, -A and -P (each $1.0 \cdot 10^{-6}$ M; attenuation of integrator, 5); (B) suspected human urine diluted 100-fold (attenuation 4 before 16 min and 8 thereafter); (C) control human urine (attenuation 9). For other conditions, see text.

TABLE I

m/z VALUES OF CHARACTERISTIC MASS FRAGMENTS

Standard		Suspected human urine	
Peak	*m/z (relative intensity)*	Peak	*m/z (relative intensity)*
Dansyl-A	91(11), 154(10), 170(100), 234(15), 277(16), 368(23)	I	91(15), 154(43), 170(100), 234(10), 277(10), 368(11)
Dansyl-P	170(100), 318(22)	II	170(100), 318(20)
Dansyl-MA	91(8), 154(10), 170(100), 234(14), 291(38), 382(8)	III	91(11), 154(9), 170(100), 234(16), 291(43), 382(8)

degradations of the three compounds are shown in Fig. 2. These results suggested that peaks I, II and III were mainly dansyl-A, -P and -MA, respectively.

Purification and enrichment

Sample purification is necessary in the simultaneous determination of MA, A and P in order to remove interfering compounds such as peptides and proteins which react with dansyl chloride. For the purification of MA or A in urine, extraction with organic solvents[17,18], extraction with an ion-pair reagent[19,20], headspace purification[4] and column treatment[6,21] have been reported. We reported previously that MA was easily extracted into diethyl ether from urine by the addition of sodium hydroxide and that there was no interfering peak in the determination of dansyl-MA by HPLC with chemiluminescence detection[12]. Therefore, the optimum conditions for diethyl ether extraction from alkaline urine were examined in this work for the purification of the three compounds. The percentage extraction of the three compounds increased with increase in the concentration of sodium hydroxide, and both MA and A were extracted quantitatively at pH > 9. This result was in agreement with the fact that the pK_a values of alkylamines are generally over 9. The extraction of P was lower than those of MA and A at every pH, and was as low as 50% at concentrations of sodium hydroxide over 10%. The high pK_a of piperidine (11.1) might be considered as a reason. Although the low extraction efficiency may decrease the accuracy, the determination of P is not as important as those of MA and A, as the purpose of the

DNS–MA MW382   **DNS–A** MW368   **DNS–P** MW318
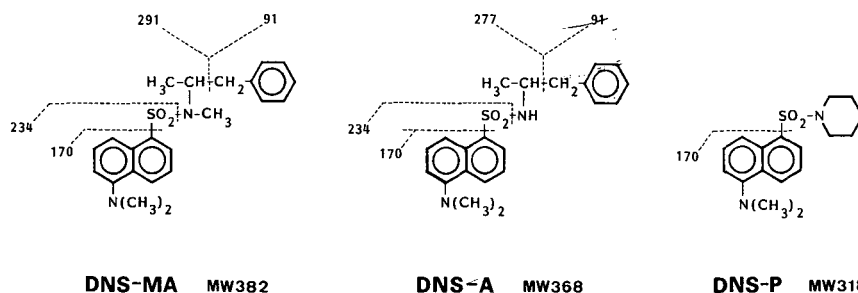
Fig. 2. Possible fragments of dansyl derivatives identified by electron impact MS. MW = Molecular weight.

TABLE II

EFFECT OF ACETIC ACID ON RECOVERIES OF METHAMPHETAMINE (MA) AND PIPER-
IDINE (P) IN DIETHYL ETHER BY ENRICHMENT WITH A STREAM OF NITROGEN

Each value is the mean $\pm$ standard deviation (%) ($n = 4$).

Addition	Recovery (%)			
	MA		P	
	$5 \cdot 10^{-8} M$	$5 \cdot 10^{-10} M$	$5 \cdot 10^{-8} M$	$5 \cdot 10^{-10} M$
None	100 ± 3.0	55 ± 5.4	73 ± 1.7	59 ± 3.9
Acetic acid	97 ± 3.9	92 ± 6.2	100 ± 2.2	100 ± 14.1

detection of P was to show that the sample solution tested was urine. Hence
a concentration of sodium hydroxide of 10% was adopted in subsequent experiments.

The recoveries of both MA and A were over 99% at concentrations of $5.0 \cdot 10^{-7}$
M, which are almost the same as those in the previous study[12]. Linear calibration
graphs were also observed in the range $2 \cdot 10^{-8}$–$2 \cdot 10^{-5}$ M in urine with a correlation
coefficient of 0.996 for MA and 0.994 for A. If 0.1 ml of the diethyl ether extracts was
subjected to dansylation, both MA and A at levels as low as $8 \cdot 10^{-9}$ M could be
detected in urine as the detection limits (signal-to-noise ratio $= 3$) were $4 \cdot 10^{-15}$
mol[12]. Although the sensitivity of the present method is comparable to that of
GC–MS, enrichment is necessary in order to determine trace levels of MA and
A accurately. The use of a stream of nitrogen is a well known and easy enrichment
technique. However, the recoveries of MA and P from diethyl ether alone decreased at
lower concentrations because of the higher volatility of the compounds whose amino
groups were unprotonated. To decrease the loss, a small amount of acetic acid was
added to the diethyl ether. Without the addition of a drop of diethyl ether containing
0.1 M acetic acid, the recoveries of MA at $5 \cdot 10^{-10}$ M and of P at both $5 \cdot 10^{-8}$ and
$5 \cdot 10^{-10}$ M were low. However, the addition of a drop of diethyl ether containing 0.1
M acetic acid increased the recoveries of MA and P to 92% and 100%, respectively, as
shown in Table II. Using the enrichment technique, MA at levels as low as $2 \cdot 10^{-10}$
M was detected in aqueous solution. A linear calibration graph for MA with
a correlation efficient of 0.988 was observed in the range $5 \cdot 10^{-10}$–$1 \cdot 10^{-7}$ M. This
technique was effective for the determination of MA at concentrations less than $1 \cdot
10^{-7}$ M in urine.

The enrichment technique was applied to suspected human urine (No. 9) in
which MA was not detected either by Simon's reagent test nor by GC. The peak of
dansyl-MA was not large enough to be quantified without any enrichment, as shown in
Fig. 3A. The peak size was increased about 40-fold by the enrichment, although a small
peak was observed near the peak of dansyl-MA, as shown in Fig. 3B. The
concentration of MA in the urine was calculated to be $1.3 \cdot 10^{-8}$ M. However, the peak
of dansyl-A could not be detected in the same chromatogram because the level of
A was usually much lower than that of MA, as shown in Table III.
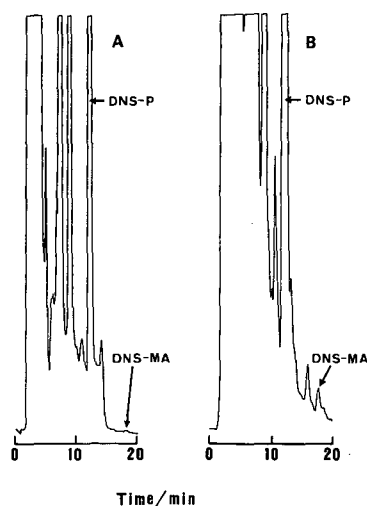
Fig. 3. Chromatograms of suspected human urine (No. 9) (A) without and (B) with enrichment by a stream of nitrogen. Range of the detector, 8; attenuation of the integrator, 6. For other conditions, see Fig. 1.

Comparison with other methods

Both Simon's reagent test and GC are popular detection methods for MA. Therefore, analytical results for the three compounds in several suspected human urine samples obtained by Simon's reagent test, GC and the present HPLC method are compared in Table III. Simon's reagent test, with a detection limit of $6 \cdot 10^{-8}$–$7 \cdot 10^{-7}$ mol, detected MA but did not detect A as the reagent is sensitive to only secondary amines. GC with a flame ionization detector determined TFA derivatives of both MA and A simultaneously and had the same sensitivity for MA as Simon's reagent test. The sensitivity to these compounds of GC with an electron-capture detector might be

TABLE III

COMPARISON OF RESULTS FOR MA, A AND P IN SUSPECTED HUMAN URINE SAMPLES OBTAINED BY THE PRESENT HPLC METHOD, SIMON'S REAGENT TEST AND GC

Urine No.	MA (mol/l)			A (mol/l)		P (mol/l)	
	Simon's reagent	GC	HPLC	GC	HPLC	GC	HPLC
40	D[a]	$1.2 \cdot 10^{-3}$	$1.3 \cdot 10^{-3}$	$2.6 \cdot 10^{-5}$	$3.5 \cdot 10^{-5}$	ND[a]	$7.3 \cdot 10^{-5}$
44	D	$1.9 \cdot 10^{-4}$	$1.7 \cdot 10^{-4}$	$5.0 \cdot 10^{-6}$	$3.0 \cdot 10^{-6}$	ND	$2.8 \cdot 10^{-5}$
41	D	$1.0 \cdot 10^{-4}$	$9.9 \cdot 10^{-5}$	$6.7 \cdot 10^{-6}$	$7.5 \cdot 10^{-6}$	ND	$1.4 \cdot 10^{-5}$
42	D	$6.7 \cdot 10^{-5}$	$8.3 \cdot 10^{-5}$	$3.8 \cdot 10^{-6}$	$3.3 \cdot 10^{-6}$	ND	$2.8 \cdot 10^{-5}$
43	ND	ND	$4.2 \cdot 10^{-8}$	ND	ND	ND	$2.4 \cdot 10^{-6}$
39	ND	ND	$3.6 \cdot 10^{-8}$	ND	ND	ND	$2.8 \cdot 10^{-5}$

[a] D = Detected; ND = not detected.

increased by a factor of about 100–1000. The retention of TFA-P was too weak to be determined under the conditions used. In contrast to these two methods, the present method determined MA, A and P simultaneously, and its sensitivity was much higher than those of the other two methods.

The concentrations of MA determined by the present method were very close to those given by GC. The differences in the concentrations of A between the two methods seemed to be larger than those of MA, possibly became the concentrations of A were much lower than MA in all samples. The concentrations of P in six suspected human urine samples were detected in the range $2.4 \cdot 10^{-6} – 7.3 \cdot 10^{-5} M$. The level was comparable to the normal value $(1.46 \cdot 10^{-5} M)$. These results indicate the high reliability of the present method for the simultaneous determination of MA, A and P in human urine. The precision of the method might be improved by the use of an internal standard. The previous study[12] suggested that the dansyl derivatives of both phenylbutylamine and N-methylphenethylamine eluted between dansyl-P and -MA, and dansyl-N-isopropylbenzylamine was eluted after dansyl-MA. These amines are considered to be suitable internal standards for addition to urine.

REFERENCES

1 F. Feigl, *Spot Tests in Organic Analysis*, Elsevier, Amsterdam, 1956, p. 260.
2 G. Belvedere, S. Caccia, A. Frigerio and A. Jori, *J. Chromatogr.*, 84 (1973) 353.
3 M. Terada, S. Yoshimura, T. Yamamoto, T. Yoshida and Y. Kuroiwa, *Eisei Kagaku*, 29 (1983) 143.
4 H. Tsuchihashi, K. Nakajima, H. Ono, A. Matsushita and M. Nishikawa, *Eisei Kagaku*, 34 (1988) 146.
5 T. Yamamoto, M. Terada, S. Yoshimura, T. Sato, H. Kitagawa, T. Yoshida, H. Aoki and Y. Kuroiwa, *Eisei Kagaku*, 27 (1981) 331.
6 N. Takayama, H. Kobayashi and A. Tsuji, *Eisei Kagaku*, 30 (1984) 14.
7 K. Slais, M. W. F. Nielen, U. A. Th. Brinkman and R. W. Frei, *J. Chromatogr.*, 393 (1987) 57.
8 Y. Hosoi, *Eisei Kagaku*, 33 (1987) 170.
9 B. M. Farrell and T. M. Jefferies, *J. Chromatogr.*, 272 (1983) 111.
10 K. Ishikawa, J. Martinez and J. McGauch, *J. Chromatogr.*, 306 (1984) 394.
11 K. Shimosato, M. Tomita and I. Ijiri, *J. Chromatogr.*, 377 (1986) 279.
12 K. Hayakawa, K. Hasegawa, N. Imaizumi, O. S. Wong and M. Miyazaki, *J. Chromatogr.*, 464 (1989) 343.
13 S. Kobayashi, K. Imai, *Anal. Chem.*, 52 (1980) 424.
14 T. Baba and H. Yoshimura, *Forensic Toxicol. News*, 6 (1988) 7.
15 Y. Okano, T. Kadota, M. Naka, J. Nagata, S. Ijima, A. Matsuda, H. Iwamura, T. Hitoshi, K. Takahama and T. Miyata, *J. Pharmacobio-Dyn.*, 8 (1985) 487.
16 N. Imaizumi, K. Hayakawa and M. Miyazaki, *Analyst (London)*, 114 (1989) 161.
17 Y. Yamamoto, A. Fukui and K. Kondo, *Jpn. J. Legal Med.*, 33 (1979) 105.
18 T. Mitsui and Y. Fujimura, *Bunseki Kagaku*, 64 (1988) T27.
19 S. Motomizu, M. Iwachi and K. Toei, *Bunseki*, 64 (1980) 234.
20 M. Syoyama and T. Sano, *Eisei Kagaku*, 31 (1985) 410.
21 I. Une, M. Yashiki, J. Yamauchi and T. Kojima, *Jpn. J. Legal Med.*, 37 (1983) 63.

CHROMSYMP. 1779

Rapid determination by high-performance liquid chromatography of free fatty acids released from rat platelets after derivatization with monodansylcadaverine

YONG MOON LEE, HIROSHI NAKAMURA* and TERUMI NAKAJIMA

Department of Analytical Chemistry, Faculty of Pharmaceutical Sciences, University of Tokyo, 7-3-1 Hongo, Bunkyo-ku, Tokyo 113 (Japan)

ABSTRACT

The release of free fatty acids from rat platelets, triggered by thrombin stimulation, was monitored by high-performance liquid chromatography (HPLC) after precolumn derivatization with monodansylcadaverine (MDC). A rapid filtration procedure was devised for the precise determination of free fatty acids released from aggregated platelets, instead of the conventional method using a stop solution or enzyme reactions. The fatty acids thus collected were derivatized with MDC in the presence of diethyl phosphorocyanidate (DEPC). The simultaneous separation of MDC derivatives of fatty acids was achieved on a reversed-phase TSKgel ODS-80$_{TM}$ column within 60 min by linear gradient elution, using 0.2 M Tris–HCl buffer (pH 7.8)–methanol (50:50, v/v) and acetonitrile. The MDC derivatives were detected with excitation and emission wavelengths of 340 and 518 nm, respectively. The amounts of liberated fatty acids were in the range from 45.0 pmol for myristoleic acid ($C_{14:1}$) to 395.0 pmol for palmitic acid ($C_{16:0}$) per $1.9 \cdot 10^7$ platelets.

INTRODUCTION

Various labelling reagents have been developed for the trace determination of carboxylic materials. Fluorogenic derivatization reagents are especially effective in providing high sensitivities for the detection of biologically active carboxylic acids[1-4].

Recently, a new derivatization method was introduced for the sensitive determination of carboxylic acids with monodansylcadaverine (MDC) as a fluorophore[5] (Fig. 1). The method exceeds the conventional methods in rapidity of derivatization and in sensitivity and it has been successfully employed in the determination of fatty acids in rabbit blood plasma[6].

Blood platelets, stimulated by adenosine diphosphate (ADP), collagen, thrombin, etc., aggregate rapidly. This leads to a dynamic change in the fatty acid composition of membrane phospholipids, caused by activated phospholipases which liberate
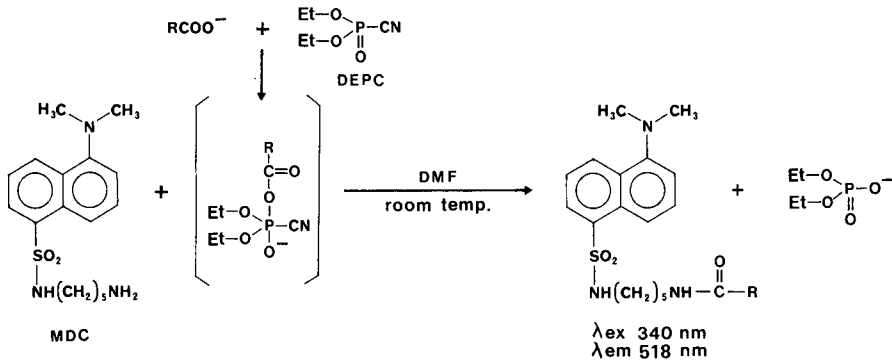
Fig. 1. Derivatization of carboxylic acids with monodansylcadaverine (MDC). DEPC = Diethyl phosphorocyanidate; DMF = N,N-dimethylformamide; Et = ethyl; λ_{ex} = excitation maximum; λ_{em} = emission maximum.

saturated and unsaturated fatty acids from the *sn*-1 and/or *sn*-2 sites in membrane phospholipids.

In this work, stimuli-induced free fatty acids in activated platelets were determined by high-performance liquid chromatography (HPLC) after derivatization with MDC.

EXPERIMENTAL

Chemicals

Saturated fatty acids ($C_{12:0}$–$C_{20:0}$) were obtained from Tokyo Kasei (Tokyo, Japan). Arachidonic acid ($C_{20:4}$) was purchased from Sigma (St. Louis, MO, U.S.A.) and other unsaturated fatty acids from Nacalai Tesque (Kyoto, Japan). MDC was purchased from Sigma and purified with absolute ethanol prior to use. Diethyl phosphorocyanidate (DEPC) was obtained from Wako (Osaka, Japan), and the fraction collected by distillation at 88–89°C under reduced pressure (*ca.* 8 mmHg) was used. All other reagents were of analytical-reagent grade.

Instrumentation

A Jasco (Tokyo, Japan) Trirotar-VI high-performance liquid chromatograph equipped with a reversed-phase TSKgel ODS-80$_{TM}$ column (250 mm × 4.6 mm I.D.) (Tosoh, Tokyo, Japan) was used. An FP-210 spectrofluorimeter (Jasco) equipped with a 15-μl micro-flow cell was used as a monitor.

Preparation of washed rat platelets

Wistar rats (male, *ca.* 250 g) were purchased from Saitama Zikken Doubutsu (Saitama, Japan). Volumes of 10 ml of blood were collected from the heart under diethyl ether anaesthesia by the use of a disposable polypropylene syringe (20 ml) containing 2 ml of ACD buffer (anticoagulant; 65 mM citric acid–85 mM sodium citrate–2.0 g per 100 ml glucose). To prevent the blood from coagulating, the syringe was shaken gently to mix the blood with the anticoagulant. After removing the sy-

ringe needle, the blood was transferred slowly to a Polyspits tube (10 × 1.4 cm I.D.) (Iwaki, Tokyo, Japan) with a PTFE cap and then centrifuged at 250 g for 10 min at room temperature. The upper phase, platelet-rich plasma, was collected and centrifuged at 800 g for 15 min. Precipitated platelets were washed with 3 ml of Tyrode–N-(2-hydroxyethyl)piperazine-N'-2-ethanesulphonic acid (HEPES) buffer (pH 7.2; 137 mM NaCl–2.7 mM KCl–10 mM HEPES–0.1% glucose) and centrifuged at 500 g for 10 min. Washing was repeated twice and then the number of platelets was adjusted to $1.9 \cdot 10^7$/ml by diluting with Tyrode–HEPES buffer.

Stimulation of washed rat platelets

A 1-ml volume of washed rat platelet suspension was transferred to a Polyspits tube with a PTFE cap. Platelets were stimulated in the presence of 2 mM calcium chloride by the addition of 2.5 units/ml of thrombin at 7°C.

Isolation of free fatty acids in platelets

After incubation at 37°C for 4 min, 100 pmol of margaric acid ($C_{17:0}$), dissolved in 50 μl of methanol, were added as an internal standard. The platelet pellets were removed quickly by passing the mixture through a membrane filter kit (pore size 0.45 μm, HA type) (Millipore, Milford, MA, U.S.A.), which was previously connected to a vacuum aspirator. The aqueous layer, collected in a glass test-tube, was acidified with 10 μl of 20% hydrochloric acid and then extracted with 2 ml of chloroform–methanol (1:1, v/v) followed by 1 ml of chloroform. After centrifugation at 800 g for 10 min, the lower organic layer was separated, combined and evaporated under a flow of nitrogen. The amounts of free fatty acids were determined by the following procedures.

Derivatization procedure

After the residue containing the fatty acids had been dissolved in 50 μl of N,N-dimethylformamide (DMF), 50 μl of 12 mM MDC in DMF and then 2 μl of DEPC were added. The reaction mixture was stirred for 10 s, allowed to stand at room temperature for 15 min, and then directly injected into the HPLC system.

HPLC conditions

The simultaneous separation of MDC derivatives of fatty acids was achieved by linear gradient elution using 0.2 M Tris–HCl buffer (pH 7.8)–methanol (50:50, v/v) (eluent A) and acetonitrile (eluent B). The initial condition was set at 50% each of eluents A and B and the proportion of B was increased to 90% in 60 min. The flow-rate was set at 1.0 ml/min. The column temperature was maintained at 40°C. The MDC derivatives of fatty acids were detected with an excitation wavelength of 340 nm and an emission wavelength of 518 nm.

RESULTS AND DISCUSSION

Although the complete mechanism of platelet activation is not yet known, the liberation of fatty acids from membrane phospholipids and the subsequent oxygenation of some fatty acids by cyclooxygenase or lipoxygenase are well known. Therefore the determination of liberated fatty acids is essential to the understanding of stimuli–response phenomena occurring in the cell membrane. With the procedure

described under Experimental, the extraction recoveries of fatty acids with chloro-form–methanol (1:1, v/v) were more than 95% at the 100-pmol level. Further, the derivatization yield of arachidic acid ($C_{20:0}$) with MDC exceeded 95%. We reported previously that the MDC-labelled free fatty acids in rabbit plasma could be separated completely using the HPLC conditions described under Experimental[6]. By using this HPLC method, free fatty acids liberated from rat platelets were determined in this work at picomole levels. Fig. 2 shows typical HPLC patterns which illustrate stimuli-induced changes in intracellular free fatty acids of washed platelets with and without thrombin stimulation. As shown in Table I, the levels of all free fatty acids were increased after stimulation in comparison with intracellular levels. Saturated fatty acids generally show larger increases than unsaturated fatty acids; the net amounts of the increased levels were 169.3 pmol for myristic acid ($C_{14:0}$), 395.0 pmol for palmitic acid ($C_{16:0}$) and 106.6 pmol for stearic acid ($C_{18:0}$). The increased amounts of oleic acid ($C_{18:1}$) and linoleic acid (C18:2) were larger than those of the other unsaturated fatty acids. The large increase in saturated fatty acids supports the theory that the sn-1 site of phospholipids is mostly occupied by such saturated fatty acids, as they are liberated by means of hydrolysis by stimulated phospholipases. Especially palmitic acid ($C_{16:0}$) is known to occcupy ca. 62% of the total carboxylic acids in phosphatidylcholine (PC), which is the most abundant phospholipid in rat platelet membrane[7].

However, arachidonic acid ($C_{20:4}$) was not detected in the free form, although it is known to be liberated by phospholipase A_2 during platelet aggregation. Probably
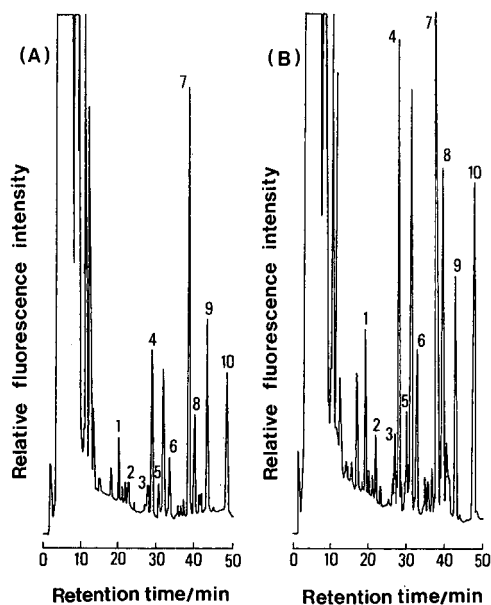
Fig. 2. HPLC profiles of MDC-labelled intracellular fatty acids in washed rat platelets (A) before and (B) after thrombin-induced aggregation. Peaks: 1 = $C_{12:0}$; 2 = $C_{14:1}$; 3 = $C_{18:3}$; 4 = $C_{14:0}$; 5 = $C_{16:1}$; 6 = $C_{18:2}$; 7 = $C_{16:0}$; 8 = $C_{18:1}$; 9 = $C_{17:0}$; (internal standard); 10 = $C_{18:0}$. For HPLC conditions, see Experimental.

TABLE I

CHANGES IN FREE FATTY ACID CONTENT OF WASHED RAT PLATELETS FOLLOWING
THROMBIN-INDUCED AGGREGATION

Free fatty acid[a]	Aggregated by thrombin (pmol fatty acids per $1.9 \cdot 10^7$ platelets)		
	Before	After	Increase
12:0	111.1	165.4	54.3
14:1	80.3	125.3	45.0
18:3	68.9	120.9	52.0
14:0	177.7	347.0	169.3
16:1	55.0	126.4	71.4
18:2	70.2	161.3	91.1
16:0	381.8	776.8	395.0
18:1	133.5	336.0	202.5
18:0	146.3	252.9	106.6

[a] Fatty acids are designated by chain length:number of double bonds.

liberated arachidonic acid is converted quickly to its oxidized metabolites through the cyclooxygenase and/or lipoxygenase pathways. On the other hand, a peak which was eluted earlier than arachidonic acid appeared and tended to increase like free fatty acids after thrombin stimulation (Fig. 2). To identify the unknown peak, the incubation mixture (Fig. 2B) was mixed with the same volume of the MDC derivatives
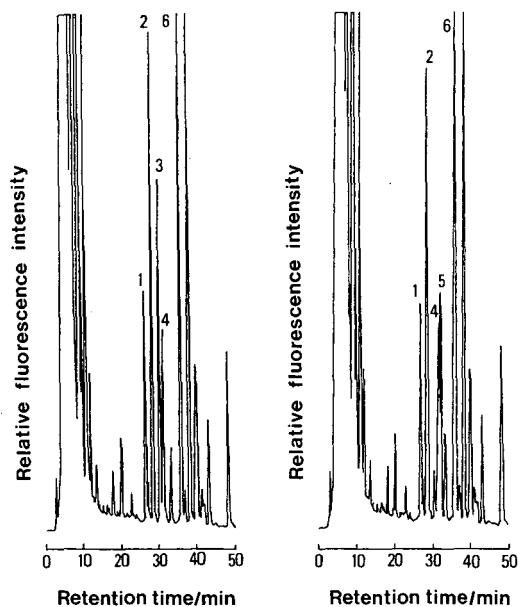
Fig. 3. Mixed chromatograms of MDC derivatives of fatty acids released from rat platelets with those of authentic compounds. The incubation mixture illustrated in Fig. 2B was spiked with a mixture of (A) $C_{20:5}$, $C_{14:0}$, $C_{22:6}$ and $C_{20:3}$ or (B) $C_{20:5}$, $C_{14:0}$, $C_{20:4}$ and $C_{20:3}$. Peaks: $1 = C_{20:5}$; $2 = C_{14:0}$; $3 = C_{22:6}$; $4 =$ unknown; $5 = C_{20:4}$; $6 = C_{20:3}$. HPLC conditions as in Fig. 1.
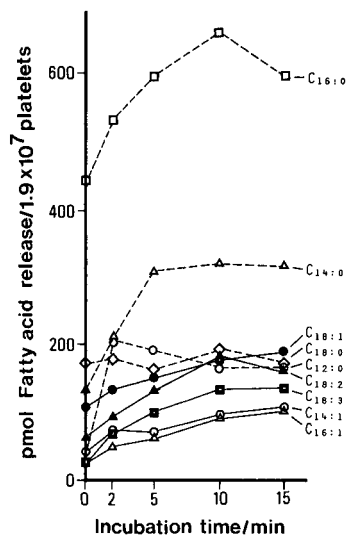
Fig. 4. Time courses of fatty acid release from washed rat platelets after thrombin stimulation.

of authentic fatty acids and injected into the HPLC system. The resulting mixed chromatograms are shown in Fig. 3. This unknown peak was eluted between docosa-hexaenoic acid ($C_{22:6}$) (Fig. 3A) and arachidonic acid (Fig. 3B). Therefore, it seems to be an oxidized intermediate of arachidonic acid associated with the oxygenase pathways. The identity of the unknown peak is under investigation.

The detection limit of this method was reported[5] to be 0.1 pmol at a signal-to-noise ratio of 3. In this study, application of this method with such high sensitivity was adequate for determining the free fatty acids at the intracellular level of 10^7 platelets.

Fig. 4 illustrates the changes in the liberated free fatty acids 2, 5, 10 and 15 min after the addition of thrombin at an incubation temperature of 25°C. A larger increase in palmitic acid ($C_{16:0}$) and stearic acid ($C_{14:0}$) was observed and reached maximum values 10 min after thrombin stimulation. The other fatty acids were observed to increase slightly, and arachidonic acid also was not observed.

As stated above, the present HPLC method, involving the use of MDC as a labelling fluorophore, was useful in the determination of the fatty acids liberated from platelets owing to its high sensitivity. Although Ikeda and Matsumoto[8] reported a precolumn derivatization method for the determination of released fatty acids from washed rat platelets with fluorescent 9-aminophenanthrene, their HPLC conditions and extraction procedure for fatty acids were inadequate for a precise determination. By using the membrane filter method developed here, the aggregated platelets were removed quickly from the reaction mixture. Hence the precise quantification achieved can be attributed to the reactivity of MDC with carboxylic acids and the rapid extraction system mentioned above. Therefore, this method will permit the precise determination of the total changes in released fatty acids originating from various biological reactions. However, the roles of the liberated fatty acids from activated platelets and their metabolites related to membrane flexibility remain to be elucidated in the future.

REFERENCES

1 H. Tsuchiya, T. Hayashi and M. Sato, *J. Chromatogr.*, 309 (1984) 43.
2 N. Nimura and T. Kinoshita, *Anal. Lett.*, 13 (1980) 191.
3 W. D. Watkins and M. B. Peterson, *Anal. Biochem.*, 124 (1982) 30.
4 M. Yamaguchi, S. Hara, R. Matsunaga, M. Nakamura and Y. Ohkura, *J. Chromatogr.*, 346 (1985) 227.
5 Y. M. Lee, H. Nakamura and T. Nakajima, *Anal. Sci.*, 5 (1989) 209.
6 Y. M. Lee, H. Nakamura and T. Nakajima, *Anal. Sci.*, 5 (1989) 681.
7 T. W. Weiner and H. Sprecher, *Biochim. Biophys. Acta*, 792 (1984) 293.
8 M. Ikeda and U. Matsumoto, *Res. Commun. Chem. Pathol. Pharmacol.*, 60 (1988) 235.

CHROMSYMP. 1856

Separation of peptide diastereomers by reversed-phase high-performance liquid chromatography and its applications

IV^a. New derivatization reagent for the enantiomeric analysis of α- and β-amino acids

TAKASHI YAMADA*, SONOKO NONOMURA, HIROYUKI FUJIWARA, TOSHIFUMI MIYA-ZAWA and SHIGERU KUWATA

Department of Chemistry, Faculty of Science, Konan University, 8-9-1 Okamoto, Higashinada-ku, Kobe 658 (Japan)

ABSTRACT

A new derivatization reagent, (Z–L-Val–Aib–Gly–ONSu, Z = benzyloxycarbonyl; Aib = α-aminoisobutyric acid; ONSu = N-oxysuccinimide), was developed for the enantiomeric analysis of various amino acids, including unusual α-amino acids having a long or bulky alkyl side-chain or a substituted phenyl or heteroaromatic ring and β-substituted β-amino acids. The diastereomers derived from various amino acids and this chiral reagent were well resolved by reversed-phase high-performance liquid chromatography using aqueous methanol as the eluent. As it is generally considered that in chiral derivatization for the separation of enantiomers the chiral centres in the diastereomeric derivatives should be as close as possible to each other, it is surprising that the above diastereomers, which have two chiral centres separated by nine bonds, can be well separated. This can be explained by the conformational difference between the L–L and L–D isomers.

INTRODUCTION

It is very important to analyze, both qualitatively and quantitatively, enantiomers of amino acids, *e.g.*, for examining the optical purity of unusual amino acids that have been optically resolved or synthesized asymmetrically, or for determining the absolute configuration of constituent amino acids of naturally occurring peptides, especially antibiotics and toxins. For the purpose of finding good derivatives applicable to such enantiomeric analysis, we have investigated the separation behaviour of diastereomers of various peptides by reversed-phase high-performance

---

^{a} For Part III, see ref. 1.

liquid chromatography (RP-HPLC). Although the separation of amino acid enantiomers without prior derivatization by the use of chiral stationary phases may provide the most promising method, the separation of diastereomers produced by a precolumn derivatization with chiral reagents, by means of ordinary stationary phases, is still useful, particularly when the same instrument must be routinely used for various investigations and, hence, the use of special columns and eluents is not advantageous[2].

Recently we found that diastereomers of protected tetrapeptides (1) containing two achiral amino acids (X and Y) between two chiral amino acids exhibit marked separation, particularly when X is an α,α-dialkylated glycine such as α-aminoisobutyric acid (Aib) and Y is glycine (Gly)[4].
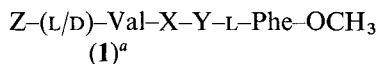
Z–(L/D)–Val–X–Y–L–Phe–OCH$_3$
(1)[a]

It is generally considered that in chiral derivatization for the separation of enantiomers, the two chiral centres in the diastereomeric derivatives should be as close as possible to each other in order to maximize the difference in chromatographic properties; in general, three bonds separate the two centres, and derivatives having distances exceeding four bonds are not often useful[5]. From this point of view, it is surprising that the separation of diastereomers of 1 is excellent in spite of the fact that two chiral centres in 1 are separated by nine bonds.

In this study, taking account of the excellent separation of diastereomers of the tetrapeptide (1) in which X–Y = Aib–Gly, a new derivatization reagent (2) (where ONSu = N-oxysuccinimide) has been successfully developed for the enantiomeric analysis of various α- and β-amino acids by RP-HPLC.

Z–L–Val–Aib–Gly–ONSu
(2)
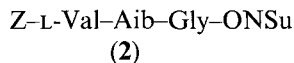
EXPERIMENTAL

Apparatus

The HPLC system used was constructed with a Shimadzu (Kyoto, Japan) Model LC-3A pumping system, a Rheodyne (Cotati, CA, U.S.A.) Model 7125 sample injector with a 20-μl loop and a Shimadzu Model SPD-2A UV detector (monitoring at 254 nm). A column (150 mm × 4.6 mm I.D.) packed with Cosmosil 5C$_{18}$ (Nacalai Tesque, Kyoto, Japan) was used, the temperature of which was maintained at 30°C by a thermostated bath. HPLC data were processed with a Shimadzu C-R2AX Chromatopac. The mobile phase was 65% aq. methanol at a flow-rate of 1 μl/ml, unless stated otherwise.

---

[a] Abbreviations according to the IUPAC–IUB Commission[3] are used: Z = benzyloxycarbonyl; Hep = heptyline (2-aminoheptanoic acid); Tle = *t*-leucine; Mle = γ-methylleucine; ONSu = N-oxysuccinimide; pNA = *p*-nitroanilide; DCC = dicyclohexylcarbodiimide; HOBt = 1-hydroxybenzotriazole.

Chemicals

α-Amino acids were obtained from Wako Jun-yaku (Osaka, Japan), Tanabe Seiyaku (Osaka, Japan), Aldrich (Milwaukee, WI, U.S.A.) and Sigma (St. Louis, MO, U.S.A.). Methanol was distilled and water was deionized and then glass distilled.

β-Amino acids were prepared as follows: optically active L-β-amino acids were prepared from L-α-amino acids by the Arndt–Eistert reaction[6,7]. Racemic β-(substituted phenyl)-β-alanines were prepared by addition of hydroxylamine to the corresponding substituted cinnamic acids[8].

Synthesis of derivatization reagent, Z–L–Val–Aib–Gly–ONSu (2)

Z–Aib and Gly–OCH$_3$ · HCl were coupled in the presence of triethylamine in dichloromethane by the DCC–HOBt method. The resulting Z–Aib–Gly–OCH$_3$ was debenzyloxycarbonylated with 25% hydrobromic acid–acetic acid and coupled with Z–L–Val by the method described above. Z–L-Val–Aib–Gly–OCH$_3$ was hydrolysed in methanol under alkaline conditions and then the N-Z-tripeptide was coupled with N-hydroxysuccinimide by using DCC in dioxane–ethyl acetate (1:1). The crude product (2) was recrystallized from ethyl acetate; m.p. 120–121°C, $[\alpha]_D^{25}$ + 3.8° (c 1, methanol).

Derivatization

An amino acid (50 μmol) was dissolved into 7% methanolic HCl (1 ml) and the solution was stirred at 80–90°C in a water-bath for 1 h. After the solution had been concentrated under the reduced pressure, the residual methyl ester hydrochloride, the reagent (2) (27 mg, 55 μmol) and 0.5 ml of a freshly prepared solution of triethylamine (50 μmol) in dichloromethane were mixed and stirred at room temperature for 2–3 h. An aliquot (0.5–1.0) μl of the reaction mixture was injected into the liquid chromatograph. A typical chromatogram is shown in Fig. 1.

RESULTS AND DISCUSSION

The separation of diastereomers of tetrapeptides (3) containing various amino acids at the C-terminal was examined. Table I summarizes the HPLC data for diastereomers of 3. HPLC analysis was carried out using the conditions described under Experimental.

Z–L-Val–Aib–Gly–(L/D)-amino acid–OCH$_3$
(3)
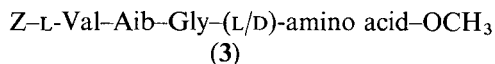
Excellent separations of diastereomers were obtained for all peptides (3) examined, except when the amino acid is Pro. Interestingly, for amino acids with an alkyl side-chain, the more bulky the side-chain the shorter is the retention time of 3 and the better is the separation of diastereomers. When the amino acid has a polar side-chain, the separation of diastereomers is poor because of rapid elution in 65% methanol, but baseline separation is still exhibited. Every L–D isomer is eluted faster than the corresponding L–L isomer. As shown in Table I, excellent separations are obtained for some unusual amino acids having a long alkyl side-chain (Hep) or a bulky side-chain
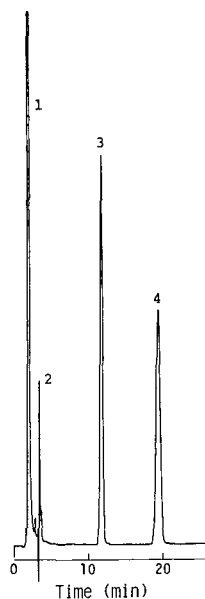
Fig. 1. Chromatogram of the reaction mixture of Z–L–Val–Aib–Gly–ONSu (**2**) and DL-Phe–OCH$_3$. See Experimental for details of reaction and chromatographic conditions. Peaks: 1 = excess **2** + HOSu + DL-Phe–OCH$_3$; 2 = CH$_2$Cl$_2$; 3 = Z–L–Val–Aib–Gly–D–Phe–OCH$_3$; 4 = Z–L–Val–Aib–Gly–L–Phe–OCH$_3$.

TABLE I

SEPARATION OF DIASTEREOMERS OF Z–L–Val–Aib–Gly–(L/D)-AMINO ACID–OCH$_3$ (3)

k' = Capacity factor; α = separation factor.

Amino acid		k'	α	Amino acid		k'	α
Ala	(D)	1.69	1.34	Pro	(D)	1.70	1.00
	(L)	2.26			(L)	1.70	
Abu	(D)	2.49	1.47	Phg	(D)	4.56	1.22
	(L)	3.66			(L)	5.57	
Nva	(D)	4.20	1.54	Phe	(D)	6.09	1.77
	(L)	6.47			(L)	10.79	
Val	(D)	3.82	1.65	Ser	(D)	1.07	1.16
	(L)	6.32			(L)	1.24	
Nle	(D)	6.92	1.63	Thr	(D)	1.44	1.22
	(L)	11.28			(L)	1.76	
Leu	(D)	6.52	1.66	Asp[a]	(D)	1.85	1.16
	(L)	10.80			(L)	2.14	
Ile	(D)	6.12	1.68	Glu[a]	(D)	2.30	1.19
	(L)	10.35			(L)	2.73	
Tle	(D)	5.61	1.75	Tyr	(D)	1.87	1.74
	(L)	9.81			(L)	3.26	
Hep	(D)	11.48	1.66	Met	(D)	3.68	1.42
	(L)	19.03			(L)	5.24	
Mle	(D)	9.06	1.72	Trp	(D)	4.72	1.61
	(L)	15.58			(L)	7.58	

[a] Dimethyl ester.

TABLE II

FORMATION OF THE DIASTEREOMERS OF TETRAPEPTIDES (3) IN THE REACTIONS BE-
TWEEN Z–L-Val–Aib–Gly–ONSu (2) AND DL-Phe–OCH$_3$

For reactions conditions, see Experimental.

Parameter	Reaction time					
	15 min	45 min	90 min	3 h	6 h	22 h
Ratio of the peak area of the L–D isomer to that of the internal standard[a]	1.341	1.369	1.410	1.342	1.377	1.400
Ratio of the peak area of the L–L isomer to that of the internal standard[a]	1.316	1.357	1.416	1.368	1.368	1.386
L–D/L–L	1.02	1.01	1.00	0.98	1.01	1.01
L–L (%)	49.5	49.8	50.1	50.5	49.9	49.8

[a] Z–L-Leu–pNA (1.0 mg) was used as an internal standard.

TABLE III

CHIRAL SEPARATION OF UNUSUAL AROMATIC AMINO ACIDS AFTER DERIVATIZA-
TION WITH Z–L-Val–Aib–Gly–ONSu (2)
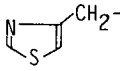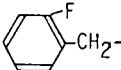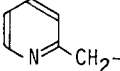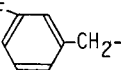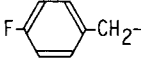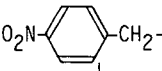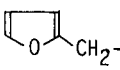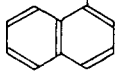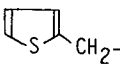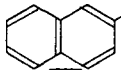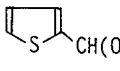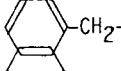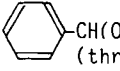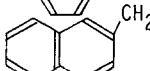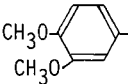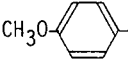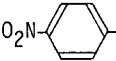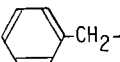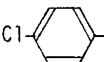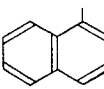
Amino acid: NH–CH–COO, with side chain R (R bonded to CH).

R		k'	α	R		k'	α
thiazole–CH$_2$–		1.99 / 2.78	1.40	2-fluorophenyl–CH$_2$–		5.79 / 10.63	1.83
pyridine–CH$_2$–		2.33 / 3.31	1.42	3-fluorophenyl–CH$_2$–		6.21 / 11.09	1.79
benzothiophene		3.48 / 4.19	1.20	4-fluorophenyl–CH$_2$–		6.17 / 11.30	1.83
benzothiophene		3.74 / 4.72	1.26	4-nitrophenyl–CH$_2$–		5.18 / 9.56	1.84
benzofuran–CH$_2$–		3.31 / 4.95	1.50	naphthyl		9.18 / 12.42	1.35
benzothiophene–CH$_2$–	(D) (L)	4.63 / 7.32	1.58	naphthyl	(D) (L)	10.13 / 12.91	1.27
benzothiophene–CH(OH)–		2.52 / 3.16	1.26	anthracene–CH$_2$–	(D) (L)	13.26 / 25.75	1.94
phenyl–CH(OH)– (threo)		2.91 / 3.67	1.26	phenanthrene–CH$_2$–	(D) (L)	13.15 / 26.37	2.00

TABLE IV

CHIRAL SEPARATION OF β-SUBSTITUTED β-AMINO ACIDS AFTER DERIVATIZATION WITH Z-L-Val-Aib-Gly-ONSu (2)

$$\overset{R}{\underset{|}{\;}}$$

β-Amino acid: NHCHCH₂COO.

R		k'	α	R		k'	α
CH₃–	(D)	2.05	1.15	CH₃O–⟨⟩– (with CH₃O–)		3.22	1.12
	(L)	2.35				3.59	
(CH₃)₂CH–	(D)	5.00	1.36	CH₃O–⟨⟩–		4.98	1.14
	(L)	6.79				5.65	
(CH₃)₂CHCH₂–	(D)	8.41	1.22	O₂N–⟨⟩–		5.04	1.28
	(L)	10.29				6.44	
CH₃CH₂(CH₃)CH–	(D)	8.23	1.44	⟨⟩–	(D)	5.67	1.11
	(L)	11.86			(L)	6.31	
⟨⟩–CH₂–	(D)	7.89	1.32	Cl–⟨⟩–		10.39	1.22
	(L)	10.41				12.72	
(furyl)		3.55	1.06	(naphthyl)		14.48	1.26
		3.77				18.29	
(thienyl)		4.74	1.07				
		5.09					

(Tle, Mle). These results stimulated us to investigate the utility of the tripeptide N-hydroxysuccinimide ester (**2**) as a chiral derivatization reagent for the enantiomeric analysis of unusual amino acids. This reagent can be easily prepared by the conventional method for peptide synthesis, easily purified by recrystallization and stored in the dry state.
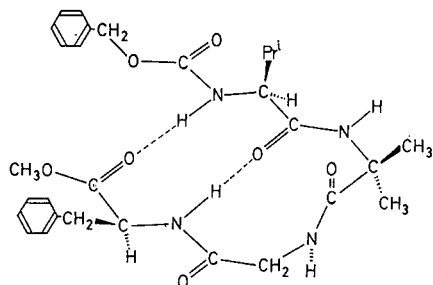
Fig. 2. Proposed conformation (A) for the L–L isomer of **3**.

The derivatization reaction of amino acid methyl ester and the reagent (2) takes place almost quantitatively within 1–2 h, and the ratio of the peak areas of the diastereomeric derivatives does not depend on the reaction time (Table II). Satisfactory chromatograms can be obtained in most instances by direct injection of the reaction mixture into the liquid chromatograph, because of the rapid elution of all of the unreacted reagents and by-products (Fig. 1), although better chromatograms can be obtained after the usual washing of the reaction mixture.

This method was applied to the chiral separation of various unusual aromatic amino acids. The results are given in Table III. Every diastereomeric pair of **3** is well separated.

Investigation by NMR and circular dichroism measurements revealed that the marked separation of diastereomers of **3** could be explained by the conformational difference between the L–L and L–D isomers: the L–L isomer of **3** prefers the β-turn conformation (A) with two parallel intramolecular hydrogen bonds in less polar aprotic solvents, as shown in Fig. 2, whereas the corresponding L–D isomer adopts a different β-turn conformation (B) with only an intramolecular hydrogen bond between the Val C = O and amino acid NH groups[4,9]. This is also the case under HPLC conditions, particularly at the instant of contact with the hydrophobic surface of octadecylated stationary phase. Conformation A of the L–L isomer can interact more strongly with the stationary phase than conformation B of the L–D isomer, because hydrophilic groups in conformation A are less exposed outside than those in conformation B and the two hydrophobic side-chains in the L–L isomer are closer than those in the D–L isomer.

We tried to apply the reagent (2) to the enantiomeric analysis of β-amino acids. Various β-substituted β-amino acids were converted into the peptides (4) and analysed by the same procedure as described above.

$$Z-L-Val-Aib-Gly-(L/D)-\beta\text{-amino acid}-OCH_3$$
$$(4)$$
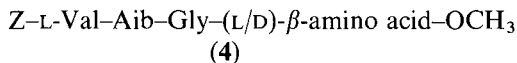
The results are summarized in Table IV. The separation of diastereomers of **4** is sufficient to be used for enantiomeric analysis, although the separation is less than that for α-amino acids. In this case too, every L–D isomer is eluted in advance of the corresponding L–L isomer. Recently, Griffith *et al.*[10] reported a good method for the HPLC separation of enantiomers of β-amino acids using a chiral stationary phase, but convenient methods using precolumn derivatization for the enantiomeric analysis of β-amino acids have rarely been reported. We therefore believe that our method will be useful for the enantiomeric analysis of not only α but also β-amino acids.

REFERENCES

1 T. Yamada, K. Dejima, M. Shimamura, T. Miyazawa and S. Kuwata, *Chem. Express*, 4 (1989) 729.
2 S. Görög, B. Herényi and M. Lőw, *J. Chromatogr.*, 353 (1986) 417.
3 IUPAC–IUB Commission, *J. Biol. Chem.*, 247 (1972) 977.
4 T. Yamada, M. Nakao. K. Tsuda, S. Nonomura. T. Miyazawa, S. Kuwata and M. Sugiura, in T. Shiba and S. Sakakibara (Editors), *Peptide Chemistry 1987*, Protein Research Foundation, Osaka, 1988, p. 97.
5 S. G. Allenmark, *Chromatographic Enantioseparation: Methods and Applications*, Ellis Horwood, Chichester, 1988, p. 51.
6 J.-M. Cassel, A. Furst and W. Meier, *Helv. Chim. Acta*, 59 (1976) 1917.
7 C. N. C. Drey, in B. Weinstein (Editor), *Chemistry and Biochemistry of Amino Acids, Peptides, and Proteins*, Vol. 4, Marcel Dekker, New York, 1977, Ch. 5.
8 R. E. Steiger, *Org. Synth.*, Coll. Vol. III (1955) 91.
9 T. Yamada, M. Nakao, T. Yanagi, T. Miyazawa, S. Kuwata and M. Sugiura, in E. Bayer and G. Jung (Editors), *Peptides 1988*, Walter de Gruyter, Berlin, 1989, p. 301.
10 O. W. Griffith, E. B. Campbell, W. H. Pirkle, A. Tsipouras and M. H. Hyun, *J. Chromatogr.*, 362 (1986) 345.

Isolation and characterization of recombinant eel growth hormone expressed in *Escherichia coli*

SEIJI SUGIMOTO*, KAZUO YAMAGUCHI and YOSHIHARU YOKOO

Tokyo Research Laboratories, Kyowa Hakko Kogyo Co., Ltd., 3–6–6 Asahimachi, Machidashi, Tokyo 194 (Japan)

ABSTRACT

To obtain information about the microheterogeneity of recombinant protein, recombinant eel growth hormone II (EGH) analogues expressed in *Escherichia coli* were isolated and characterized. The modification was classified into three types: monodeamidation of Asn, oxidation of Met and N-terminal formylation. Monodeamidated EGH was isolated by ion-exchange chromatography. The major deamidation site (Asn147) was determined by peptide mapping using the substrate specificity of trypsin. Oxidized EGH and N-terminal-formylated EGH were isolated by reversed-phase high-performance liquid chromatography. Oxidized EGH was identified by amino acid composition analysis and N-terminal-formylated peptide by mass spectrometry.

INTRODUCTION

Growth hormones (GH) complementary deoxyribonucleic acid (cDNA) have been isolated from several vertebrate species[1-6] and some of these GH were produced by recombinant techniques in *Escherichia coli*[1-3,7]. Human GH has been applied for dwarfism, bovine GH is being developed as an animal medicine for growth promotion and to increase milk production and fish GH is expected to be applied in fish culture[8,9].

Eel GH (EGH) was isolated from eel pituitaries by Kishida *et al.*[10] and the primary structure of EGH was determined by Kishida *et al.*[9] and Yamaguchi *et al.*[11]. Molecular cloning of EGH cDNA and its expression in *Escherichia coli* were performed by Saito *et al.*[12]. The refolding and purification process of *Escherichia coli* derived EGH was established and its growth-promoting activity *in vivo* was confirmed by Sugimoto *et al.*[13].

Recombinant protein medicines for humans and other vertebrates should be highly purified and uniform in structure for safety and efficacy. However, several methods have revealed that small amounts of analogues exist in purified recombinant protein preparations[14,15]. It is very important to detect and determine such analogues in order to prevent their appearance and to separate them.

We have found minor analogues in purified recombinant EGH by several

analytical methods. In this study, native EGH and five analogues were isolated and their structures were established.

EXPERIMENTAL

Materials

Trypsin-TPCK was purchased from Worthington (Freehold, NJ, U.S.A.), α-chymotrypsin from Sigma (St. Louis, MO, U.S.A.) and *Achromobacter* protease I from Wako (Osaka, Japan). DEAE Toyopearl 650 M for ion-exchange chromatography and a TSK gel ODS 120T reversed-phase high-performance liquid chromatographic (RP-HPLC) column (30 cm × 4.6 mm I.D.) were obtained from Tosoh (Tokyo, Japan), YM-10 ultrafiltration membrane from Amicon (Danvers, MA, U.S.A.), TEFCO-gel for sodium dodecyl sulphate polyacrylamide gel electrophoresis (SDS-PAGE) from TEFCO (Tokyo, Japan), Determiner NH_3 ammonia assay kit from Kyowa Medex (Tokyo, Japan) and a protein assay kit from Bio-Rad Labs. (Richmond, CA, U.S.A.).

Preparation of recombinant EGH Lot E-21-0

Recombinant EGH expressed in *Escherichia coli* as inclusion bodies was refolded and purified more than 95% pure, judging from gel filtration HPLC and SDS-PAGE[13]. The percentage purity was based on the peak areas of the chromatogram and of the scanning profile of the SDS-PAGE gel. The refolding and purification process was as follows: *Escherichia coli* cells containing EGH inclusion bodies were harvested from 6 l of broth and broken by passage through a Manton Gaulin homogenizer. The resulting homogenate was centrifuged at 8000 *g* for 40 min at 4°C and a 20-g pellet was solubilized by stirring for 5 days at 4°C in 2 l of 5 *M* guanidine hydrochloride–50 m*M* Tris–0.005% Tween 80 at pH 8.0. The solution was centrifuged, as above, to remove any insoluble materials and then dialysed against 60 l of 10 m*M* Tris–HCl buffer (pH 8.0) three times at 4°C. The dialysate was clarified by centrifugation. The supernatant, containing 890 mg of protein, was loaded onto a DEAE Toyopearl 650M column (25 cm × 7 cm I.D.) equilibrated with 10 m*M* Tris–HCl buffer (pH 8.0) and eluted with a linear gradient from 0 to 250 m*M* NaCl in 10 m*M* Tris–HCl buffer (pH 8.0) in a 3-l volume. The flow-rate was 1 l/h. Pooled fractions, containing 360 mg of protein, were concentrated to 0.5 mg/ml on a YM-10 filter. The final sample was poured into 5-ml glas containers and freeze-dried. Each container was sealed with a plastic cap and stored at 4°C with desiccant. The contents of each container of EGH Lot E-21-0 were redissolved in 5 ml of ice-cold water just before use.

Rechromatography on DEAE Toyopearl

A 50-mg amount of EGH Lot E-21-0 was redissolved, dialysed against 10 l of 10 m*M* Tris–HCl buffer (pH 8.0) at 4°C and loaded onto a DEAE Toyopearl 650M column (14 cm × 3 cm I.D.) equilibrated with 10 m*M* Tris–HCl buffer (pH 8.0). Following washing with 100 ml of equilibration buffer, EGH was eluted with an NaCl gradient (from 0 to 250 m*M* in equilibration buffer) in 600 ml at a flow-rate of 50 ml/h. The volume of each fraction was 4 ml.

PAGE

PAGE at pH 9.5 and staining with Coomassie brilliant blue were carried out essentially as described by Davis[16], using TEFCO gel. The stacking gels contained 4% (w/v) acrylamide and the separation gels 14% (w/v) acrylamide. EGH fragment fractions from RP-HPLC were evaporated and redissolved in the sample buffer.

RP-HPLC

RP-HPLC was carried out on a TSK gel ODS-120T column (30 cm × 4.6 mm I.D.) with a JASCO Tri Rotar SR2 HPLC system. Linear gradient elutions from 40 to 70% acetonitrile in 0.1% trifluoroacetic acid (TFA) for EGH analogue separation and from 0 to 70% acetonitrile in 0.1% TFA for peptide mapping were performed in 60 min. The column oven temperature was kept at 35°C. The flow-rate was 0.7 ml/min. UV detection was carried out at 220 nm.

Amino acid composition analysis

Hydrolysis of protein and peptide was performed in 6 M HCl at 110°C for 22 h. Amino acid analysis was carried out by the Waters Pico Tag method of Bidlingmeyer *et al.*[17]. Amino acid standard solution was obtained from Wako.

N-Terminal sequence analysis

N-Terminal sequence analysis was performed with a gas-phase sequencer (Applied Biosystems Model 470A). EGH analogues and EGH fragment fractions from RP-HPLC were concentrated to about 0.1 ml and applied to the sequencer.

Enzymatic digestion

Digestion of EGH and its fragments was carried out with trypsin-TPCK, *Achromobacter* protease I (API) and α-chymotrypsin at pH 8.0 and 37°C for 4 h. The ratio of substrate to enzyme was 100:1 (w/w). The digestion was stopped by acidification to pH 2–3 with 1 M HCl.

Deamidation

Deamidation of EGH and its fragment was performed in 25 mM Tris–HCl buffer (pH 10) containing 250 mM NaCl at 37°C for 2 days. Detection of ammonia was carried out with the Determiner NH_3[18,19]. EGH fragment fractions from RP-HPLC were evaporated and redissolved in 10 mM Tris–HCl buffer (pH 8.0).

Mass spectrometry

Secondary ion mass spectra were obtained with a Hitachi M-80 B spectrometer. EGH fragment fractions from RP-HPLC were freeze-dried and redissolved in acetic acid and mixed with glycerol.

Protein concentration determination

Assay of protein was carried out with the Bio-Rad[20] protein assay kit. Bovine serum albumin was used as a standard.

RESULTS AND DISCUSSION

Isolation of EGH analogues

EGH preparation Lot E-21-0 was 95% pure (see Experimental for calculation) judging from gel filtration HPLC and SDS-PAGE[13]. Analogues of EGH, however, were detected in EGH Lot E-21-0 by PAGE (Fig. 1, lane a) and RP-HPLC (Fig. 2c). Here we call the EGH analogues corresponding to bands A and B in PAGE (Fig. 1, lane a) EGH-A and EGH-B, respectively, and EGH analogues corresponding to peaks α, β and γ in RP-HPLC (Fig. 2c) EGH-α, EGH-β and EGH-γ, respectively. The contents of both EGH-A and EGH-B were 50% and those of EGH-α, EGH-β and EGH-γ were 5%, 85% and 10%, respectively. Natural EGH derived from eel pituitaries[10] had the same mobility as EGH-A in PAGE and the same retention time as EGH-β in RP-HPLC (data not shown).

To separate EGH-A and EGH-B, EGH Lot E-21-0 was dialysed against 10 mM Tris–HCl buffer (pH 8.0) and rechromatographed on DEAE Toyopearl (Fig. 3). A slower flow-rate and a gentle gradient gave a good resolution. EGHs were eluted in two peaks, the first and second corresponding to bands A and B in PAGE (Fig. 1, lanes b and c), respectively. As it was found that both EGH-A and EGH-B were divided into three peaks (α, β and γ) (Fig. 2a and b), a total of five analogues (EGH-A-α, EGH-A-γ, EGH-B-α, EGH-B-β and EGH-B-γ) were detected in addition to native EGH (EGH-A-β). The contents of the analogues were 2.5% for EGH-A-α and EGH-B-α, 42.5% for EGH-A-β and EGH-B-β and 5% for EGH-A-γ and EGH-B-γ.

It is suggested that the modification causing heterogeneity in hydrophobicity among α, β and γ was independent of the modification causing heterogeneity in charge between A and B, because both the retention times and compositions of EGH-A-α, EGH-A-β and EGH-A-γ in RP-HPLC were identical with those of EGH-B-α, EGH-B-β and EGH-B-γ, respectively (Fig. 2). This indicates that each analogue can be characterized from the difference between EGH-A (mixture of EGH-A-α, EGH-A-β
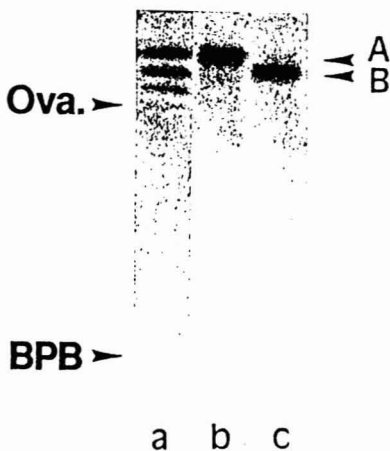
Fig. 1. PAGE of recombinant EGH. Recombinant EGH preparation Lot E-21-0 (lane a) was rechromatographed on DEAE Toyopearl (Fig. 3) and fractionated into two pools, EGH-A (lane b) and EGH-B (lane c). Ova. and BPB indicate the mobilities of ovalbumin and bromophenol blue, respectively.
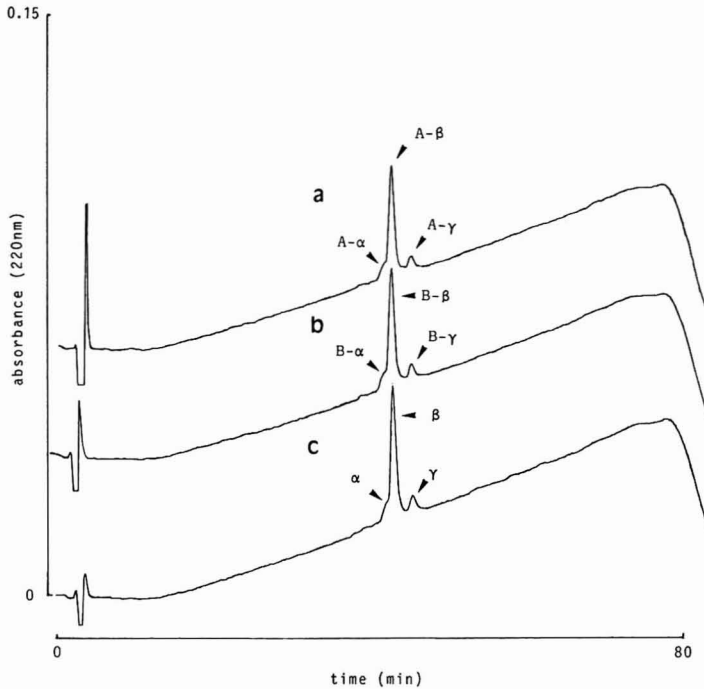
Fig. 2. RP-HPLC of recombinant EGH. EGH-A (a) and EGH-B (b) in addition to recombinant EGH preparation Lot E-21-0 (c) were divided into three peaks, α, β and γ. The peaks corresponding to α, β and γ in EGH-A are referred to as A-α, A-β and A-γ, respectively. Peaks in EGH-B were named in the same way. EGH analogues corresponding to peaks A-α, A-β, A-γ, B-α, B-β and B-γ are referred to as EGH-A-α, EGH-A-β, EGH-A-γ, EGH-B-α, EGH-B-β and EGH-B-γ, respectively. No measurable peak was seen in a blank chromatogram.

and EGH-A-γ) and EGH-B (mixture of EGH-B-α, EGH-B-β and EGH-B-γ) and that between EGH-α (mixture of EGH-A-α and EGH-B-α), EGH-β (mixture of EGH-A-β and EGH-B-β) and EGH-γ (mixture of EGH-A-γ and EGH-B-γ). To determine the difference between EGH-A and EGH-B, we used EGH-A and EGH-B, which were
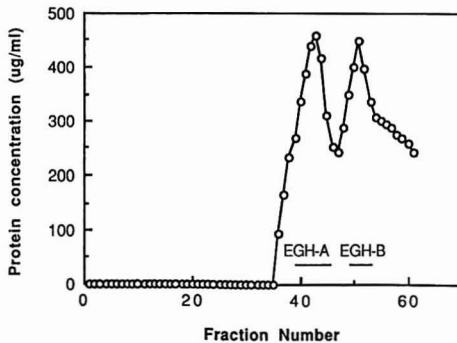
Fig. 3. Ion-exchange chromatography of recombinant EGH preparation Lot E-21-0 on DEAE Toyopearl. For conditions, see Experimental. Bars indicate the pooled fractions as EGH-A and EGH-B.

fractionated by DEAE chromatography. To determine the difference between EGH-α, EGH-β and EGH-γ, we used EGH-α, EGH-β and EGH-γ, which were fractionated by RP-HPLC.

Each analogue was denatured under reducing conditions and refolded as above to clarify whether these analogues were caused by different types of disulphide bond formation or by conformational changes of the peptide chain. No changes were observed, indicating that these analogues were formed in some other way.

Characterization of EGH-A and EGH-B

Heterogeneity of human and bovine GH in PAGE was reported by Lewis *et al.*[21]. They and others[21–27] suggested that deamidation was a possible cause of the electrophoretic heterogeneity of preparations of GH. That conclusion was based on the facts that (1) ammonia is liberated when the GH are exposed to an alkaline medium; (2) no change in amino acid composition occurs, nor are new end terminal amino acids detected in altered samples; (3) heterogeneity is not seen when the electrophoresis is carried out at pH 4, indicating suppression of ionization of carboxyl groups; (4) the converted forms have the same molecular weight as the major band; and (5) proteolytic inhibitors failed to prevent the alteration.

EGH-A was treated at alkaline pH to examine the deamidation of EGH. Band B in PAGE was formed, releasing a stoichiometric amount of ammonia (Fig. 4). As this suggests that EGH-B is a deamidated form of EGH-A, peptide mapping was performed to determine the deamidation site.

Tryptic mapping of EGH Lot E-21-0 had been performed in a previous study[13]. Peaks were assigned to fragments from EGH and it was confirmed that disulphide bonds were formed at the same position as human GH.

The tryptic mapping patterns of both EGH-A and EGH-B by RP-HPLC were
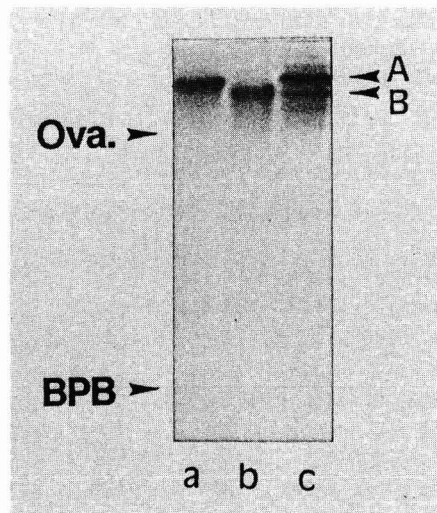
Fig. 4. PAGE of deamidated EGH-A. Lane a, EGH-A; lane b, EGH-B; lane c, EGH-A treated at alkaline pH. Ova. and BPB indicate the mobilities of ovalbumin and bromophenol blue, respectively. For treatment conditions, see Experimental.
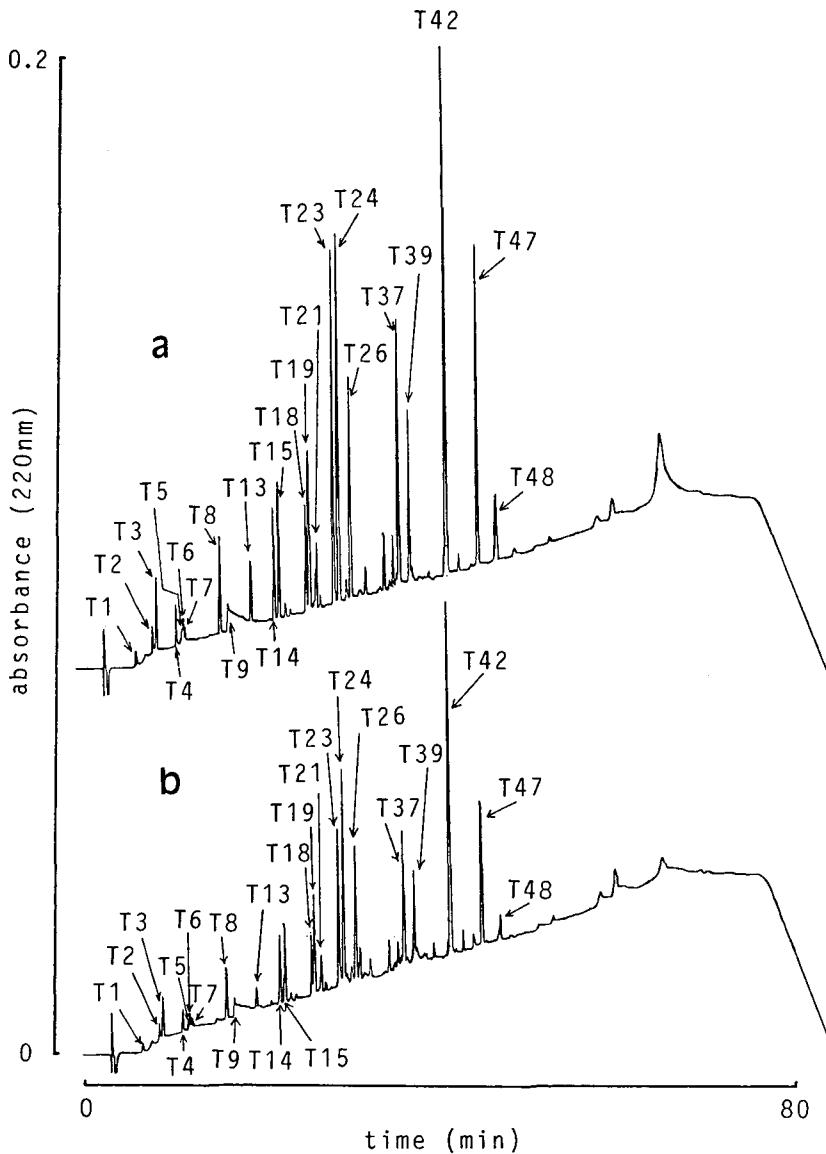
Fig. 5. Tryptic mapping by RP-HPLC of (a) EGH-A and (b) EGH-B. Volumes of 20 µl of digests were injected. Correspondence between peaks and fragments was confirmed previously[13]. No measurable peaks was seen in a blank chromatogram. For conditions of enzymatic digestion and mapping by RP-HPLC, see Experimental.

almost the same (Fig. 5). Each fragment peak had the same retention time within ± 12 s. One peak (T13) of the tryptic peptide of EGH-B, however, were markedly smaller than that of EGH-A. It is assumed that N- and/or C-terminal peptide bonds of the peptide derived from EGH-B were not hydrolysed completely. The peptide from
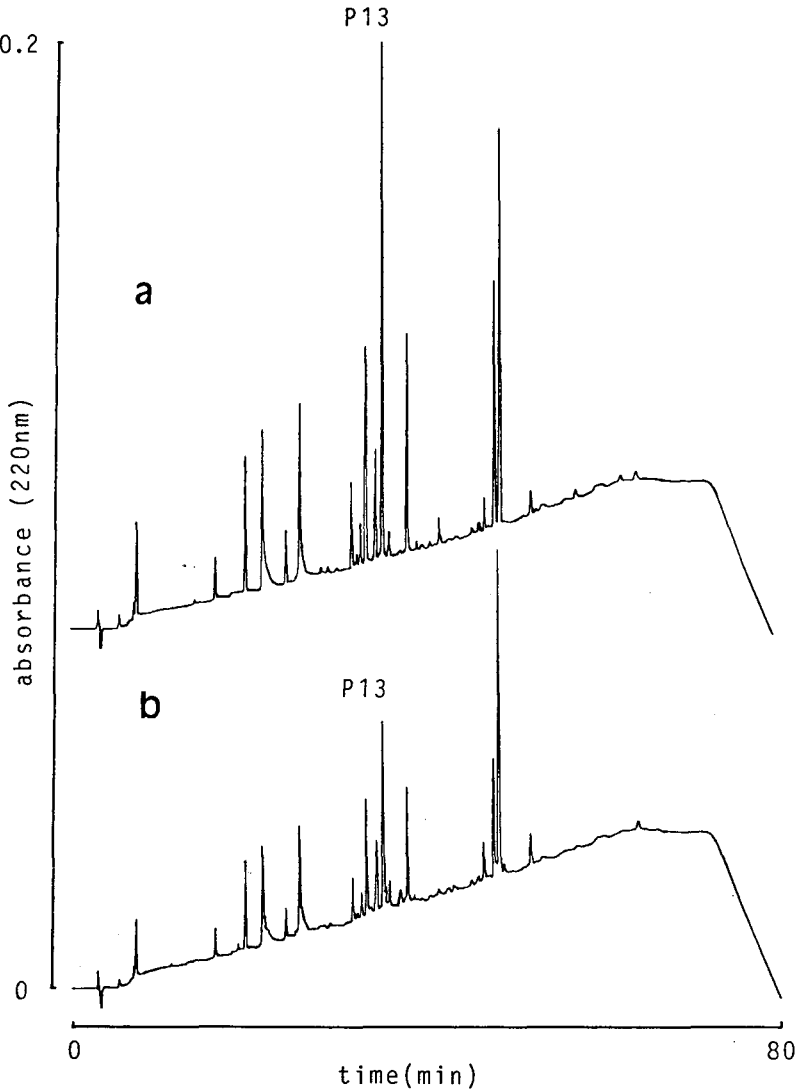
Fig. 6. API mapping by RP-HPLC of (a) EGH-A and (b) EGH-B. Volumes of 20 μl of digests were injected. No measurable peak was seen in a blank chromatogram. For conditions of enzymatic digestion and mapping by RP-HPLC, see Experimental.

EGH-A and EGH-B (Val122–Lys153), which includes tryptic peptide T13 (Asn147–Lys153), was isolated as peak P13 using lysyl endopeptidase API (Fig. 6). Amino acid analysis of all peaks from API mapping of EGH-B revealed no other peak corresponding to the fragment including peptide (Val122–Lys153).

The peaks P13 for EGH-A and EGH-B were further digested by trypsin (Fig. 7). The digest of peak P13 from EGH-B showed one more peak (PT5) in addition to peaks PT1–PT4 from EGH-A. Although amino acid analysis revealed that peak PT5
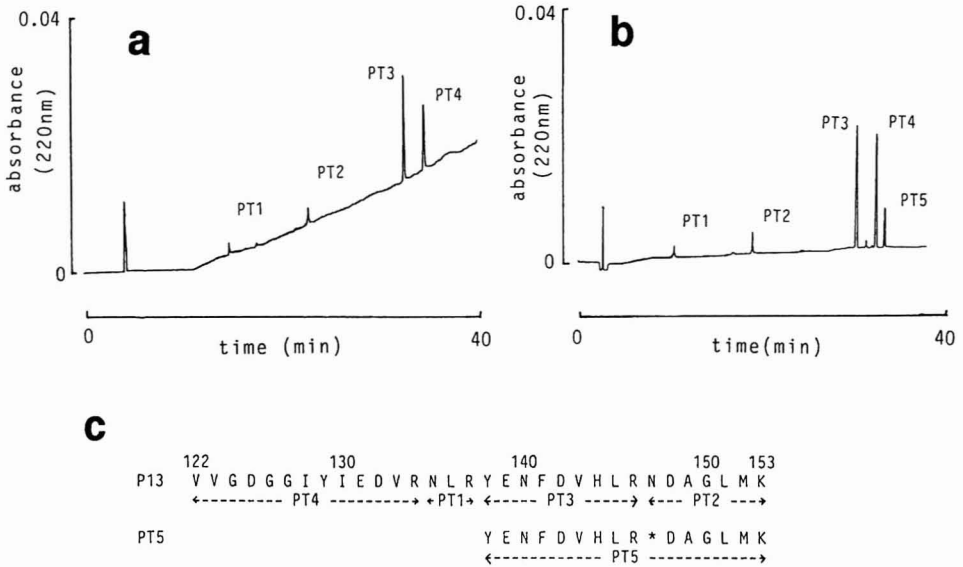
Fig. 7. Tryptic mapping of API peptide P13 (Val122–Lys153). (a) Fingerprint of the peptide from EGH-A; (b) from EGH-B. No measurable peak was seen in a blank chromatogram. For conditions, see Experimental. (c) Amino acid sequence of the peptide. The asterisk indicates an isoAsp residue.

correspond to peptide (Tyr138–Lys153), N-terminal sequence analysis of peak PT5 stopped at Asn147. As the Edman degradation reaction was continued but the remaining sequence was missed, some modification was detected in the backbone peptide bond of Asn147, other than in the side-chain of that residue. These data suggested that deamidation of Asn147 to an isoaspartyl residue occured.

To clarify the deamidation of peptide (Val122–Lys153), the peptide from EGH-A was treated at alkaline pH and compared with the peptide from EGH-A and EGH-B by PAGE (Fig. 8). Two bands, X and Y, appeared for the peptide from EGH-B whereas a single band, X, was observed for EGH-A. Band X was converted to band Y, releasing a stoichiometric amount of ammonia.

These results suggested that EGH-B is the deamidated form of EGH-A and that the main component of EGH-B was deamidated EGH at Asn147. Based on the height of the peak PT1–PT5 in the mapping experiment, 25–30% of EGH-B was deamidated at Asn147. Given that EGH-B showed a single band on PAGE, EGH-B is apparently a mixture of monodeamidated EGH at some sites.

It has been reported that an acidic amino acid residue just before or after Arg and Lys interrupts cleavage of peptide bonds after those basic residues in trypsin digestions[28–30]. Hence it was concluded that conversion of Asn147 to IsoAsp interrupts enzymatic cleavage of the peptide bond between Lys146 and Asn147.

To determine a modification site, peptide mapping is useful. However, deamidated peptide was retained at the same time as non-deamidated peptide on RP-HPLC and all cleaved peptide can not be detected by PAGE and ion-exchange HPLC, because the charges of the peptides are variable. For these reasons it is difficult
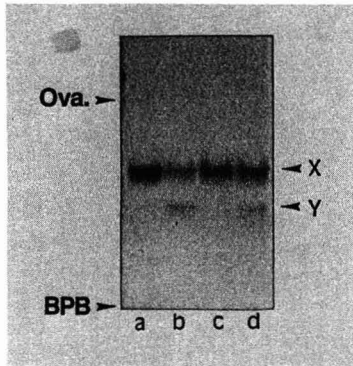
Fig. 8. PAGE of peak P13 from API mapping of EGH. Lane a: P13 from EGH-A; lane b: P13 from EGH-B; lane c: P13 from EGH-A, treated at alkaline pH at −20°C as a control; lane d: P13 from EGH-A, treated at alkaline pH at 37°C. Ova. and BPB indicate the mobilities of ovalbumin and bromophenol blue, respectively. For conditions of alkaline pH treatment, see Experimental.

to find the deamidation sites. Fortunately, Asn and Gln occur before or after Lys and Arg at selected positions in EGH. Here we successfully determined the one deamidation site using the substrate specificity of trypsin.

Characterization of EGH-α, EGH-β and EGH-γ

Amino acid composition was analysed for EGH-α, -β and -γ. One Met residue of EGH-α was oxidized to methionine sulphoxide whereas in EGH-β and -γ it was not.

Amino acid analysis of EGH Lot E-21-0 was unable to detect the conversion of Met to methionine sulphoxide because of the low content of the oxidized EGH. Separation of EGH-α was effective in establishing the oxidation of Met.

In N-terminal amino acid sequence analysis, the N-terminal sequence study of EGH-γ was blocked whereas EGH-α and -β started with an additional Met. N-Terminal API peptide of EGH-γ was further digested with chymotrypsin (data not shown). Mass spectra of N-terminal chymotryptic peptides of EGH-γ indicated that N-terminal additional Met was formylated (Fig. 9).

These results indicate that about 10% of EGH was formylated. It is also impossible to detect a 10% decrease in recovery by N-terminal sequence analysis. Separation of EGH-γ was effective in detecting the N-terminal blocked form of EGH. It has been reported that the formyl group is removed by deformylase[31]. The mechanism of inclusion body formation after expression is not clear, but it may be caused by a low level of deformylase or insufficient time for deformylation. EGH-β was not oxidized at Met nor formylated at the N-terminal position.

Although at most seven analogues could be formed by three types of independent modifications other than native EGH, oxidized and formylated EGH with and without deamidation were not detected. These analogues might be retained at almost the same position as EGH-β in RP-HPLC and/or the content might be less than 1%.

In conclusion, native EGH and EGH analogues have been characterized by
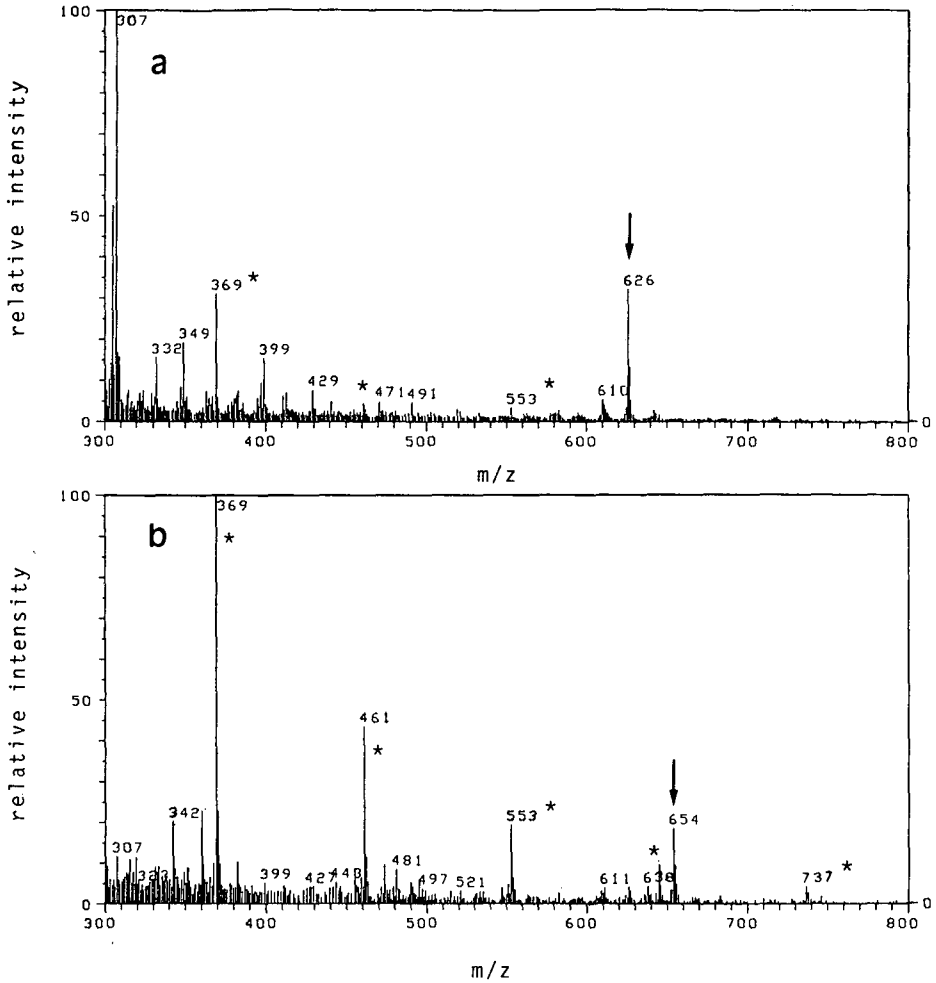
Fig. 9. Secondary ion mass spectra of N-terminal chymotryptic fragment of (a) EGH-β and (b) EGH-γ. Arrows indicate M$^+$. The peak at m/z 626 in (a) corresponds to the N-terminal fragment Met–Ile–Ser–Leu–Tyr and m/z 654 in b to the N-terminal fragment formylMet–Ile–Ser–Leu–Tyr. Signals marked with asterisks were derived from glycerol.

a combination of separations and proteolytic digestions. The modifications can be classified into three types: deamidation of Asn, oxidation of Met and formylation of N-terminal Met. EGH-A-β was the native structure and five other analogues were modified in one or two positions.

Recently, uniformity of recombinant protein medicine has become important and high purity is needed. To confirm the uniformity for recombinant proteins, SDS-PAGE and gel filtration–HPLC analysis have been routinely used. However, these techniques are inadequate for mixtures of analogues as in EGH preparation.

Here we have shown the importance of PAGE and RP-HPLC for the detection and isolation of analogues and the usefulness of peptide mapping, mass spectrometry, amino acid analysis and N-terminal sequence analysis for the determination of the modifications.

REFERENCES

1 D. V. Goeddel, H. L. Heyneker, T. Hozumi, R. Arentzen, K. Itakura, D. G. Yansura, M. J. Ross, G. Miozzari, R. Crea and P. H. Seeburg, *Nature (London)*, 281 (1979) 544.
2 E. Kechet, A. Rosner, Y. Bernstein, M. Gorecki and H. Aviv, *Nucleic Acids Res.*, 9 (1981) 19.
3 S. Sekine, T. Mizukami, T. Nishi, Y. Kuwana, A. Saito, M. Sato, S. Itoh and H. Kawauchi, *Proc. Natl. Acad. Sci. U.S.A.*, 82 (1985) 4306.
4 N. Sato, K. Watanabe, K. Murata, M. Sakaguchi, Y. Kariya, S. Kimura, M. Nonaka and A. Kimura, *Biochim. Biophys. Acta*, 949 (1988) 35.
5 M. Watahiki, M. Tanaka, N. Masuda, M. Yamakawa, Y. Yoneda and K. Nakashima, *Gen. Comp. Endocrinol.*, 70 (1988) 401.
6 M. Watahiki, M. Yamamoto, M. Yamakawa, M. Tanaka and K. Nakashima, *J. Biol. Chem.*, 264 (1989) 312.
7 P. H. Seeburg, S. Sias, J. Adelman, H. A. DeBoer, J. Hayflick, P. Jhurani, D. V. Goeddel and H. L. Heyneker, *DNA*, 2 (1983) 37.
8 H. Kawauchi, S. Moriyama, A. Yasuda, K. Yamaguchi, K. Shirahata, J. Kubota and T. Hirano, *Arch. Biochem. Biophys.*, 244 (1986) 542.
9 M. Kishida, T. Hirano, J. Kubota, S. Hasegawa, H. Kawauchi, K. Yamaguchi and K. Shirahata, *Gen. Comp. Endocrinol.*, 65 (1987) 478.
10 M. Kishida, J. Kubota, T. Hirano, K. Yamaguchi and K. Shirahata, *Zool Sci.*, 2 (1985) 974.
11 K. Yamaguchi, A. Yasuda, M. Kishida, T. Hirano, H. Sano and H. Kawauchi, *Gen. Comp. Endocrinol.*, 66 (1987) 447.
12 A. Saito, S. Sekine, Y. Komatsu, M. Sato, T. Hirano and S. Itoh, *Gene*, 73 (1988) 545.
13 S. Sugimoto, Y. Yokoo, Y. Inui and T. Hirano, in preparation.
14 P. T. Wingfield and P. Graber, *J. Chromatogr.*, 387 (1987) 291.
15 P. T. Wingfield, R. J. Mattaliano, H. R. MacDonald, S. Craig, G. M. Clore, A. M. Gronenborn and U. Schmeissner, *Protein Eng.*, 1 (1987) 413.
16 B. J. Davis, *Ann. N.Y. Acad. Sci.*, 121 (1964) 404.
17 B. A. Bidlingmeyer, S. A. Cohen and T. L. Tarvin, *J. Chromatogr.*, 336 (1984) 93.
18 A. Mondzac, G. E. Ehrlich and J. E. Seegmiller, *J. Lab. Clin. Med.*, 66 (1965) 526.
19 I. Kaidoh, S. Satoh, K. Suzuki, F. Yusa, T. Ikeda, Y. Kosaka, M. Toriya, M. Ono, S. Tanaka and T. Yoshida, *Seibutsu Shiryo Bunseki*, 1 (1979) 89.
20 M. Bradford, *Anal. Biochem.*, 72 (1976) 248.
21 U. J. Lewis, E. V. Cheever and W. C. Hopkins, *Biochim. Biophys. Acta*, 214 (1970) 498.
22 U. J. Lewis and E. V. Cheever, *J. Biol. Chem.*, 240 (1965) 247.
23 E. V. Cheever and U. J. Lewis, *Endocrinology*, 85 (1969) 465.
24 N.-S. Jiang and S. Howard, *Fed. Proc. Fed. Am. Soc. Exp. Biol.*, 25 (1966) 348.
25 F. Reusser, *Arch. Biochem. Biophys.*, 106 (1964) 410.
26 M. Sluyser and C. H. Li, *Arch. Biochem. Biophys.*, 104 (1964) 50.
27 B. B. Saxena and P. H. Henneman, *Biochem. J.*, 100 (1966) 711.
28 W. A. Schroeder, J. R. Shelton, J. B. Shelton, J. Cormick and R. T. Jones, *Biochemistry*, 2 (1963) 992.
29 T. Koide and T. Ikenaka, *Eur. J. Biochem.*, 32 (1973) 417.
30 C. H. W. Hirs, S. Moore and W. H. Stein, *J. Biol. Chem.*, 219 (1956) 623.
31 J. M. Adams, *J. Mol. Biol.*, 33 (1968) 571.

Determination of pseudouridine in human urine and serum by high-performance liquid chromatography with post-column fluorescence derivatization

YOSHIHIKO UMEGAE, HITOSHI NOHTA and YOSUKE OHKURA*

Faculty of Pharmaceutical Sciences, Kyushu University 62, Maidashi, Higashi-ku, Fukuoka 812 (Japan)

ABSTRACT

A selective and sensitive method for the determination of psuedouridine in human urine and serum is described. The method is based on high-performance liquid chromatography with post-column fluorescence derivatization. Pseudouridine and 5-fluorouridine (internal standard) in a 10-fold diluted urine sample or a deproteinized serum sample are separated on a reversed-phase column (TSK gel ODS-80$_{TM}$) with isocratic elution and successively subjected to derivatization involving periodate oxidation followed by fluorescence reaction with *meso*-1,2-bis(4-methoxyphenyl)ethylenediamine. The detection limit for pseudouridine is 4 pmol in a 100-μl injection volume.

INTRODUCTION

Urinary excretion of modified nucleosides which result from the enzymatic degradation of ribonuleic acid (RNA), especially from transfer-RNA, has been found to increase in a variety of neoplastic diseases[1-4], and pseudouridine is a nucleoside that increases most frequently[4-7]. Therefore, pseudouridine in urine can be utilized as a tumour marker for the diagnosis and follow-up of the diseases. Pseudouridine in serum has also been measured[6,8,9].

Most of currently available methods for the determination of pseudouridine are based on liquid chromatography with UV detection. Although these methods are fairly sensitive, they are not very selective and thus require complicated clean-up using boronate gel chromatography[2-8] or high-performance liquid chromatography (HPLC) on two reversed-phased columns[10].

In a previous paper[11], we reported that 1,2-bis(4-methoxyphenyl)ethylenediamine (p-MOED) reacted sensitively and selectively with ribonucleosides and ribonucleotides in an acidic medium after periodate oxidation to produce fluorescent derivatives.

The purpose of this study was to establish a highly sensitive and selective HPLC method for the determination of pseudouridine in human urine and serum, based on

HPLC separation on a reversed-phased column followed by post-column derivatization utilizing the above-mentioned fluorescence reaction. 5-Fluorouridine was used as an internal standard.

EXPERIMENTAL

Reagents and solutions

p-MOED was synthesized as described previously[12]. Pseudouridine and 5-fluorouridine were purchased from Sigma (St. Louis, MO, U.S.A.). All other chemicals were of analytical-reagent grade. Deionized, distilled water was used.

Urine and serum samples were obtained from healthy subjects in the absence of preservative or anticoagulant, and kept frozen at $-20°C$ until used. Sodium phosphate buffers (10 mM, pH 5.0) containing 4 and 2% (v/v) of methanol were used as HPLC mobile phases for urine and serum samples, respectively. p-MOED solution (20 mM) was prepared in 0.14 M perchloric acid containing 68% (v/v) of ethanol. Sodium periodate solution (2 mM) was prepared in water. Both p-MOED and sodium periodate solutions were used for fluorescence derivatization.

HPLC system and its operation

Fig. 1 shows a schematic diagram of the HPLC system constructed for the determination of pseudouridine. A 100-µl aliquot of sample solution was injected into a CCPM chromatograph (Tosoh, Tokyo, Japan) equipped with a Rheodyne 7125 syringe-loading sample injector valve (100-µl loop) and a TSK gel ODS-80$_{TM}$ column (particle size 5 µm; 150 × 4.6 mm I.D.) (Tosoh). The mobile phase was pumped at a flow-rate of 0.5 ml/min. The column temperature was ambient (25 ± 2°C). The column eluate was first passed through a Tosoh UV-8010 detector (254 nm; flow cell, 10.7 µl) if it was required to monitor the absorbance in comparison with fluorescence
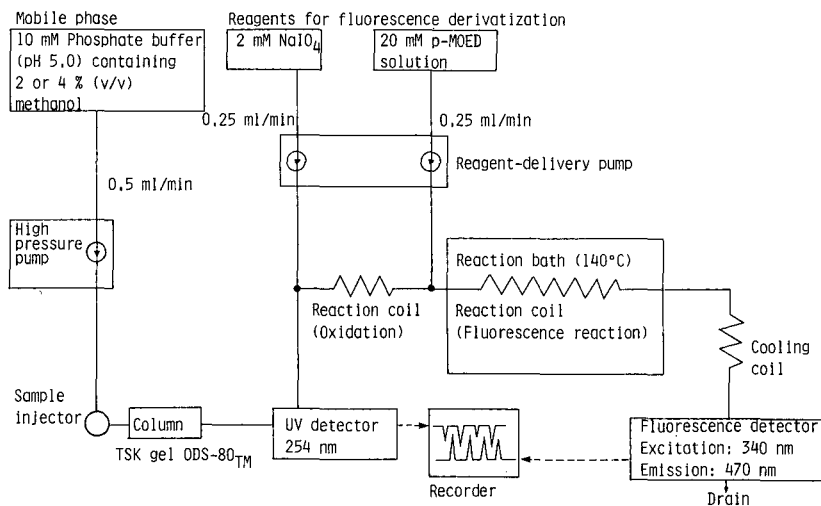
Fig. 1. Schematic diagram of the HPLC system.

detection. Sodium periodate solution was then added to the eluate stream by means of an SSP PM 1024 pump (Sanuki Kogyo, Tokyo, Japan) at a flow-rate of 0.25 ml/min, and the mixture was passed through a reaction coil (1 m × 0.5 mm I.D. stainless-steel tube) for oxidation. The p-MOED solution was added to the stream at a flow-rate of 0.25 ml/min. The mixture was then heated in a reaction coil (20 m × 0.5 mm I.D. stainless-steel tube) placed in a Shimadzu (Tokyo, Japan) CRB-6A reaction bath (140°C) to develop the fluorescence and the reaction mixture was passed through an air-cooling coil (1 m × 0.25 mm I.D. stainless-steel tube). The fluorescence intensity of the last effluent was monitored at 470 nm emission with excitation at 340 nm (both spectral band widths 20 nm) using a Tosoh FS-8000 spectrofluorimeter equipped with a flow cell (15 μl). Peak height was used for quantification.

HPLC sample preparation

Urine sample. To 100 μl of urine, 100 μl of 500 nmol/ml 5-fluorouridine (internal standard) and 800 μl of water were added. A 100-μl aliquot of the mixture was used for HPLC. Urinary creatinine was measured by using a creatinine test kit (Wako, Osaka, Japan).

Serum sample. To 0.5 ml of serum were added 0.5 ml each of 50 nmol/ml 5-fluorouridine solution and 2.0 M perchloric acid and the mixture was centrifuged at 1000 g for 10 min at 4°C. To 0.5 ml of the supernatant were added 65 μl of 2 M potassium carbonate solution and the mixture was briefly centrifuged. A 100-μl aliquot of the supernatant was subjected to HPLC.

RESULTS AND DISCUSSION

HPLC conditions

Fig. 2 shows a chromatogram obtained by fluorescence detection with a standard mixture of pseudouridine and 5-fluorouridine using sodium phosphate buffer (10 mM, pH 5.0) containing 4% (v/v) methanol as the mobile phase (retention times
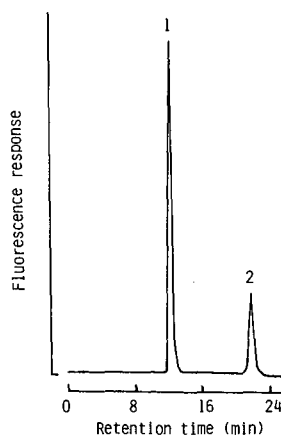
Fig. 2. Chromatogram obtained with a standard mixture of pseudouridine and 5-fluorouridine (fluorescence detection). Mobile phase: 10 mM sodium phosphate buffer (pH 5.0) containing 4% (v/v) of methanol. Peaks: 1 = pseudouridine; 2 = 5-fluorouridine. Concentrations: 2.0 nmol/ml each.

12.0 and 21.6 min, respectively). The eluates from peaks 1 and 2 both have fluorescence excitation and emission maxima at 340 and 470 nm, respectively.

The retention times of pseudouridine and 5-fluorourdine decreased with increasing concentration of methanol in the mobile phase. At a concentration greater than 5% (v/v) the pseudouridine peak overlapped with an early eluting large peak for unknown substance(s) in urine or serum (see Figs. 3A and 4A). In the absence of methanol, much longer times were required for the elution of pseudouridine and 5-fluorouridine (retention times 16.0 and 34.0 min, respectively). Methanol concentrations of 4 and 2% (v/v) were the most satisfactory for urine and serum samples, respectively. Although the sodium phosphate concentration only slightly affected the retention times in the range 10–100 mM, the background fluorescence intensity increased with increasing concentration of phosphate; 10 mM gave the highest signal-to-noise ratio. The pH of 10 mM sodium phosphate buffer had no effect on the retention times of the peaks in the range 3.0–7.0; pH 5.0 was employed.

Post-column fluorescence derivatization

Sodium periodate concentrations ranging from 1 to 3 mM yielded the highest peaks for pseudouridine and 5-fluorouridine; the selected concentration of 2 mM gave reproducible results. Perchloric acid, which was the acid required for the fluorescence reaction, provided almost maximum peak heights for both compounds in the concentration range 0.05–0.15 M in the p-MOED solution; 0.14 M was used. Water-miscible organic solvents such as methanol, ethanol and acetonitrile served to accelerate the fluorescence reaction. Of these solvents, ethanol was most effective in the concentration range 60–80% (v/v) in the p-MOED solution; 68% (v/v) was selected as optimum. The highest peaks were attained at p-MOED concentrations of 15–25 mM; 20 mM was employed.

A reaction coil (0.5 mm I.D.) length of 1 m for the oxidation, was the most satisfactory. Almost maximum and constant peak heights were achieved when a reaction coil (0.5 mm I.D.) of 15–25 m was used for the fluorescence reaction; a 20-m reaction coil was recommended in the HPLC system. Higher temperatures allowed the peak heights to increase more rapidly up to *ca.* 150°C. A temperature higher than 150°C caused background noise in the chromatogram owing to gas-bubble formation in the reaction coil; 140°C was optimum.

Determination of pseudouridine in urine and serum

5-Fluorouridine, an artificial nucleoside, was employed as an internal standard. Fig. 3 depicts typical chromatograms obtained with human urine. Chromatogram A, obtained with fluorescence detection, is much simpler than B, obtained with UV detection. This indicates that fluorescence detection is fairly selective for the nucleosides. Although urine contains diverse modified nucleosides (other than pseudouridine) that could react with p-MOED to afford fluorescent compounds, they did not interfere with the assay of pseudouridine because their concentrations were much lower than that of pseudouridine. The peak component pseudouridine was identified on the basis of the retention time in comparison with the standard solution and also by co-chromatography of the standard and the samples.

Fig. 4 shows typical chromatograms obtained for human serum with fluorescence and UV detection. The recommended deproteinization procedure, which used
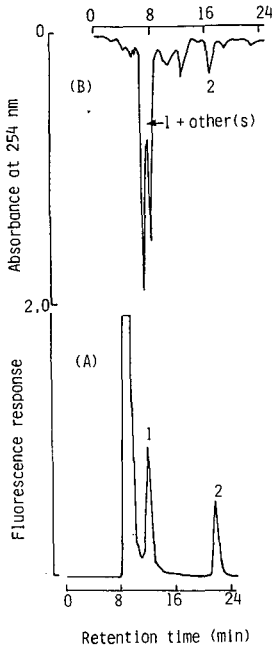
Fig. 3. Chromatograms obtained with (A) fluorescence and (b) UV detection in the HPLC of pseudouridine in·human urine. Mobile phase: 10 mM sodium phosphate buffer (pH 5.0) containing 4% (v/v) of methanol. Peaks: 1 = pseudouridine (238 nmol/ml); 2 = 5-fluorouridine (internal standard) (500 nmol/ml); others = unidentified.
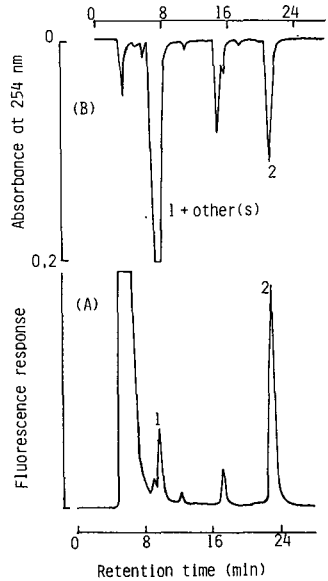
Fig. 4. Chromatograms obtained with (A) fluorescence and (B) UV detection in the HPLC of pseudouridine in human serum. Mobile phase: 10 mM sodium phosphate buffer (pH 5.0) containing 2% (v/v) of methanol. Peaks: 1 = pseudouridine (2.50 nmol/ml); 2 = 5-fluorouridine (internal standard) (50.0 nmol/ml); others = unidentified.

TABLE I

URINARY EXCRETION OF PSEUDOURIDINE FROM HEALTHY PERSONS

Sex[a]	Age (years)	Concentration[b] (nmol/μmol creatinine)
M	42	19.2
M	31	17.0
F	28	27.1
F	26	23.2
M	25	19.5
M	24	16.3
M	23	19.2
F	23	20.4
F	22	26.6
F	21	19.7
	Mean ± S.D. 20.8 ± 3.5	

[a] M = Male; F = female.
[b] Measured using 24-h urine samples.

TABLE II

CONCENTRATIONS OF PSEUDOURIDINE IN SERA FROM HEALTHY PERSONS

Sex	Age (years)	Concentration (nmol/ml)
M	59	2.93
M	32	1.84
M	28	2.02
M	26	2.01
M	26	2.50
M	26	1.78
M	23	1.65
F	26	1.64
F	24	1.20
F	21	2.50
	Mean ± S.D.	2.01 ± 0.48

perchloric acid, provided complete recoveries (99 ± 2%; mean ± relative standard deviation, $n = 5$) of pseudouridine asnd 5-fluorouridine added to 500 μl of serum sample in amounts of 4 nmol each. Other deproteinization methods (trichloroacetic acid, acetonitrile and ultrafiltration through a Millipore Ultrafree C3TK membrane) gave poor recoveries.

Linear relationships were observed between the amounts (y, nmol) of pseudouridine obtained by the internal standard method and the amounts (x, nmol) added in the range 0.5–50 nmol to 100 μl of urine ($y = 1.002x - 0.17$, $r = 0.999$) and 0.1–4 nmol to 0.5 ml of serum ($y = 1.003x - 0.06$, $r = 0.998$). The limits of detection (signal-to-noise ratio $= 3$) for pseudouridine in urine and serum were 40 and 8 pmol/ml (both corresponded to 4 pmol per 100-μl injection volume), respectively. The relative standard deviations in replicate determinations ($n = 10$) of pseudouridine were 2.2 and 2.7% at mean concentrations of 233 and 1.6 nmol/ml in urine and serum, respectively.

The amounts of pseudouridine in urine and serum from healthy persons assayed by this method are given in Tables I and II, respectively. The values are in good agreement with previously reported data[8–10].

This method is sensitive and so selective that it does not require complicated clean-up procedures. Therefore, this method should be useful for the diagnosis and follow-up of neoplastic diseases and for the biomedical investigation of modified nucleosides.

REFERENCES

1 T. P. Waalkes, C. W. Gehrke, R. W. Zumwalt, S. T. Chang, D. B. Lakings, D. C. Tormey, D. L. Ahmann and C. G. Moertel, Cancer, 36 (1975) 390.
2 T. P. Waalkes, M. D. Aeloff, D. S. Ettinger, K. B. Woo, C. W. Gehrke, K. C. Kuo and E. Borek, Cancer, 50 (1982) 2457.
3 S. Tamura, Y. Amuro, T. Nakano, J. Fujii, Y. Moriwaki, T. Yamamoto, T. Hada and K. Higashino, Cancer, 57 (1986) 1571.
4 J. Speer, C. W. Gehrke, K. C. Kuo, T. P. Waalkes and E. Borek, Cancer, 44 (1979) 2120.

5 K. C. Kuo, C. W. Gehrke, R. A. McCune, T. P. Waalkes and E. Borek, *J. Chromatogr.*, 145 (1978) 383.
6 T. Russo, A. Colonna, F. Salvatore, F. Cimiso, S. Brides and C. Gurge, *Cancer Res.*, 44 (1984) 2567.
7 S. Tamura, J. Fujii, T. Nakano, T. Hada and K. Higashino, *Clin. Chim. Acta,* 154 (1986) 125.
8 A. Colonna, T. Russo, F. Esposito, F. Salvatore and F. Cimino, *Anal. Biochem.,* 130 (1983) 19.
9 L. Levine, T. P. Waalkes and L. Stolbach, *J. Natl. Cancer Inst.,* 54 (1975) 341.
10 T. Yamamoto, K. Higashino, S. Tamura, H. Fujioka, Y. Amuro and T. Hada, *Anal. Biochem.,* 170 (1988) 387.
11 Y. Umegae, H. Nohta and Y. Ohkura, *Chem. Pharm. Bull.,* 38 (1989) 452.
12 F. Vogtle and E. Goldshmitt, *Chem. Ber.,* 109 (1976) 1.

Identification of a new minor iridoid glycoside in *Symplocos glauca* by thermospray liquid chromatography–mass spectrometry

JUNKO IIDA*, MORIMASA HAYASHI and TAKESHI MURATA

Shimadzu Corporation, Analytical Applications Department 1, Nishinokyo-kuwabaracho, Nakagyo-ku, Kyoto 604 (Japan)

and

MASAMI ONO, KENICHIRO INOUE and TETSURO FUJITA

Kyoto University, Faculty of Pharmaceutical Sciences, Sakyo-ku, Kyoto 606 (Japan)

ABSTRACT

Iridoid glycosides in *Symplocos glauca* were identified by thermospray liquid chromatography–mass spectrometry. The conditions for optimization of the separation of iridoid glycosides were investigated. The mass spectra obtained gave qualitative information concerning both the aglycone and sugar moieties and also the molecular weights. Methanol extracts from the leaves of *S. glauca* were analysed for iridoid glycosides. Not only major but also minor components could be separated and identified from the mass spectra and mass chromatograms. A new minor component in *S. glauca* was tentatively identified as 6-dihydroverbenalin.

INTRODUCTION

Ethnopharmacological studies have revealed a wide variety of naturally occurring substances of plant origin which are used in Chinese and other folk remedies. These folk preparations are often effective antipyretics, anti-inflammatories, tranquillizers and laxatives, and contain a number of iridoid glycosides which appear to play an important role in their efficacy. The identification of iridoid glyosides has been attempted using several analytical methods, and some molecular weight determinations based on mass spectrometry have been reported. However, the successful isolation and identification of these glycosides has been hampered by their highly polar and thermally labile nature. These characteristics have limited MS applications to identifications that rely mostly on field desorption (FD) and fast atom bombardment (FAB) techniques[1–5]. With both techniques, isolation and purification of target components is a prerequisite.

Liquid chromatography–mass spectrometry (LC–MS) has been applied to the separation and MS characterization of known glycosides using moving-belt[6] and frit
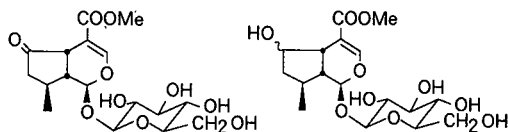
Fig. 1. Structural formulae of verbenalin (left) and 6-dihydroverbenalin (right). Me = Methyl.

FAB[7] techniques. However, these methods do not appear suitable for the identification of unknown glycosides when present in trace amounts.

We have been investigating iridoid glyosides in various medicinal plants using thermospray (TSP) LC–MS. Spectra obtained from extracts of *Symplocos glauca* suggested the presence of a minor glycoside which is closely related to the known substance verbenalin (Fig. 1). LC separation conditions were examined in order to provide a clearer separation of this unknown trace component, which was subsequently tentatively identified as 6-dihydroverbenalin (Fig. 1).

EXPERIMENTAL

Materials

Fresh chopped leaves of *S. glauca* (10 g) were extracted by shaking with hot methanol (3 × 20 ml) and the combined extracts were evaporated to dryness *in vacuo*. The residue was taken up in water and insoluble substances were removed by filtration through a layer of Celite. The filtrate was evaporated to dryness *in vacuo* and residue was taken up in methanol just prior to measurement.

Verbenalin standard was isolated and purified in the following way. Fresh leaves of *S. glauca* (11.87 g) were extracted by shaking with hot methanol (5 × 18 ml) and the combined extracts were concentrated to 30 ml *in vacuo*. After filtration through Celite, the filtrate was saturated with water and concentrated to 11.1 ml *in vacuo*, then filtered through Celite to remove precipitates. Dry yeast (55.5 mg) was suspended in the filtrate, which was subsequently allowed to stand overnight at 30°C to decompose sugars. After filtration of the reaction mixture through Celite, the solvent was removed *in vacuo*. The residue (51.66 mg) was recrystallized from ethanol to afford pure verbenalin (25 mg). The purity of the verbenalin obtained was confirmed by melting point, elemental analysis, refractive index and NMR measurements.

Chemicals and reagents

Ammoniom acetate (special grade) and acetic acid (special grade) were purchased from Wako (Osaka, Japan) and was used as received. Pure water obtained with a Toraypure system (Toray, Tokyo, Japan) was used in the mobile phase. All other chemicals and reagents were of analytical-reagent or chromatographic grade.

Liquid chromatography–mass spectrometry

The mobile phase established by examination of LC separations consisted of solution A [0.1 *M* ammonium acetate–acetic acid buffer (pH 4.7)] and solution B [0.2 *M* ammonium acetate–acetic acid buffer (pH 4.7)–acetonitrile (1:1, v/v)]. Linear binary gradient elution was used (0 to 50% solution B in 20 min, then held for 10 min) at a total flow-rate of 1.0 ml/min through the column [Shimadzu Shim-pack

CLC-ODS(M), 150 mm × 4.6 mm I.D.]. Solutions A and B were degassed prior to use and were delivered by a pair of Shimadzu LC-6A pumps. A 10-μl volume of the extract from *S. glauca* was injected with a Rheodyne Model 7124 injector. The column oven temperature was 45°C. A UV detector (Shimadzu SPD-6AV) equipped with a high-pressure-resistant UV cell (maximum pressure 400 kg/cm^2) was fitted in series between the column and the mass spectrometer and UV absorbance was detected together with mass spectrometric acquisition. The UV absorbance of the verbenalin standard was measured with a Shimadzu UV-1600 instrument and the liquid chromatograph's UV detector was set at 240 nm (λ_{max} of verbenalin).

The LC eluate was introduced into a Shimadzu LCMS-QP1000 mass spectrometer equipped with a Vestec thermospray interface. The thermospray ionization mode was used for ionization. The ion source block temperature was 240°C according to previous results[8]. The measurement mass range was m/z 170–800.

RESULTS AND DISCUSSION

Only verbenalin has been reported as an iridoid glycoside in *S glauca*. The verbenalin standard and the extract from *S. glauca* were analysed using the mobile phase composition 0.1 *M* ammonium acetate–acetic acid buffer (pH 4.7)–acetonitrile (70:30, v/v). On the mass spectrum of the verbenalin standard (Fig. 2a), the [M + H]$^+$ ion, the proton adduct ion of the aglycone ([A + H]$^+$, A = aglycone) and the ammonium adduct ion of the aglycone ([A + NH$_4$]$^+$) were observed at m/z 389, 227 and 244, respectively. An ion cleaving at the glycoside bond appeared at m/z 209 and an ion derived from the sugar moiety was observed at m/z 180. Closer examination of the mass spectra of the verbenalin standard and the major peak corresponding to verbenalin in the extract (Fig. 2b) revealed stronger relative intensities of m/z 229 (the isotopic ion of [A + H]$^+$ 227), m/z 391 (the isotopic ion of [M + H]$^+$ 389) and m/z 211 (the isotopic ion of m/z 209) for the latter than those of the standard, while the relative intensities of m/z 228 ([A + H]$^+$ 227 + 1 u), m/z 390 ([M + H]$^+$ 389 + 1 u) and m/z 210 (m/z 209 + 1 u) were almost the same on the two mass spectra. These results
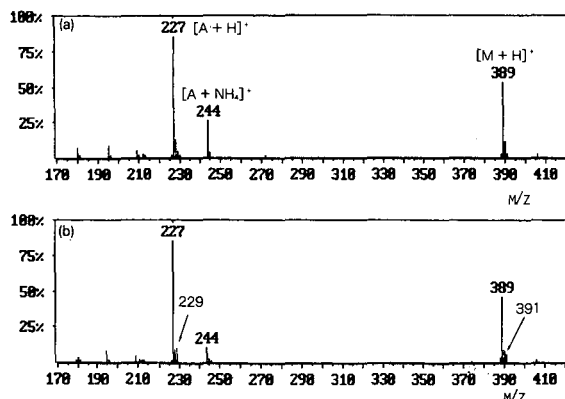
Fig. 2. Mass spectra of (a) the verbenalin standard and (b) the major peak corresponding to verbenalin in the extract. Mobile phase: 0.1 *M* ammonium acetate–acetic acid buffer (pH 4.7)–acetonitrile (70:30, v/v).

suggest that some other compounds which have a 2 a.m.u. higher mass number than verbenalin co-eluted with verbenalin in the major peak of the extract. In order to verify the existence of these unknowns, the LC separation conditions were investigated. Considering the previous study of *S. glauca* and the mass spectrum of the extract, the amount of the unknowns was expected to be small. As there is a possibility that minor components may not be detected under isocratic conditions, gradient elution was investigated.

In the examination of the gradient conditions for TSP LC–MS, attention was paid to maintaining the concentration of the electrolytes in the mobile phase constant while increasing the ratio of the aqueous solution. When using TSP LC–MS, electrolytes such as ammonium acetate are added to the mobile phase in order to promote the ion–molecular reaction, which is the main ionization mechanism in TSP LC–MS[9,10]. As the concentration of the electrolytes influences the ionization efficacy, it should be kept constant during measurements. On the other hand, a mobile phase that includes a low proportion of organic solvent and a high proportion of aqueous solution is preferable for ionization efficacy. From this viewpoint, of methanol and acetonitrile, which are commonly used in reversed-phase chromatography as organic modifiers, the latter is more suitable because it has a greater eluting ability. Considering that ammonium acetate dissolves slightly in acetonitrile, solution A [0.1 M ammonium acetate–acetic acid buffer (pH 4.7)] and solution B [0.2 M ammonium acetate–acetic acid buffer (pH 4.7)–acetonitrile (1:1, v/v)] were used. By changing the concentration of solution B from 0 to 50% linearly over 20 min, and then holding for 10 min, the major component (verbenalin) and other components could be separated satisfactorily.

The chromatogram of the extract from *S. glauca* detected by measuring the UV absorbance under the conditions mentioned above is shown in Fig. 3a and the total ion chromatogram obtained is shown in Fig. 3b. The amount of sample injected was equivalant to 0.11 mg of the leaf. The mass spectra of peaks 4 and 6 are shown in Fig. 4a
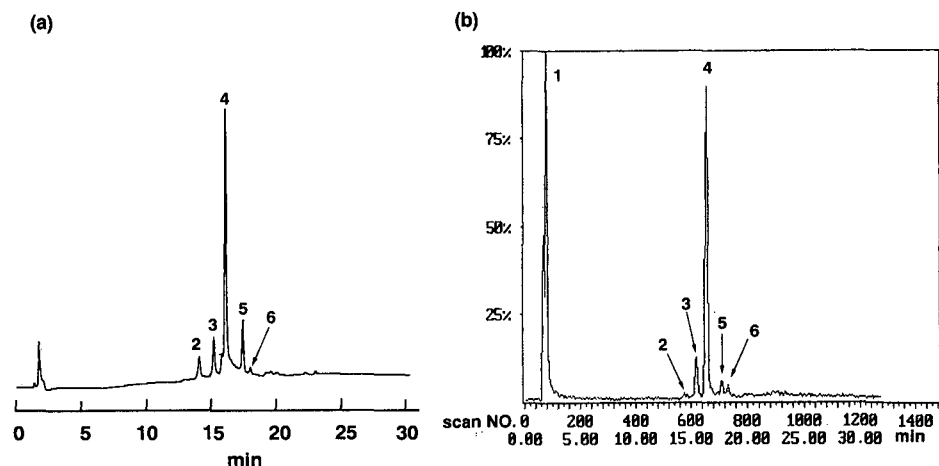
Fig. 3. (a) Chromatogram of the extract from the leaf of *S. glauca* (UV detection at 240 nm). (b) Total ion chromatogram of the extract from the leaf of *S. glauca*.
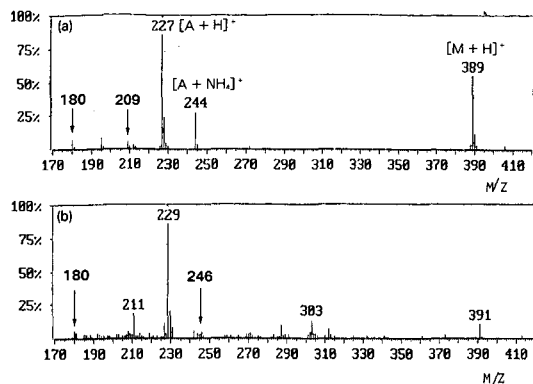
Fig. 4. Mass spectra of (a) peak 4 (verbenalin) and (b) peak 6 in Fig. 2b. A = Aglycone.

and b, respectively. Fig. 4a was in agreement with the mass spectrum of the verbenalin standard. In Fig. 4b, the peak of m/z 229, which is identical with the 2 a.m.u. shifted ion of the base peak of verbenalin (m/z 227), appeared as the base peak ion.

Further, peaks at m/z 391 and 211, which are identical with the 2 a.m.u. shifted ion of the $[M + H]^+$ ion and the diagnostic fragment ion, respectively, are observed. The 2 a.m.u. shifted ion from $[A + NH_4]^+$ (m/z 244) of verbenalin is also observed at m/z 246, although the intensity is weak. Whereas the quasimolecular ion and fragment ions from the aglycone moiety in Fig. 4b are shifted 2 a.m.u. from the corresponding ions in Fig. 4a, the ion from the sugar moiety appeared at m/z 180 in both Fig. 4a and b and is the characteristic ion of a monosaccharide.

Fig. 5 shows mass chromatograms produced by quasimolecular ions and fragment ions from the aglycone moieties of peaks 4 and 6. It was therefore confirmed that m/z 229, 391, 246 and 211 are all derived from peak 6. The compound shows UV absorption at 240 nm and the retention time is close to that of verbenalin. Based on these facts and considering the biosynthetic pathway of the congener, $i.e.$, verbenalin,
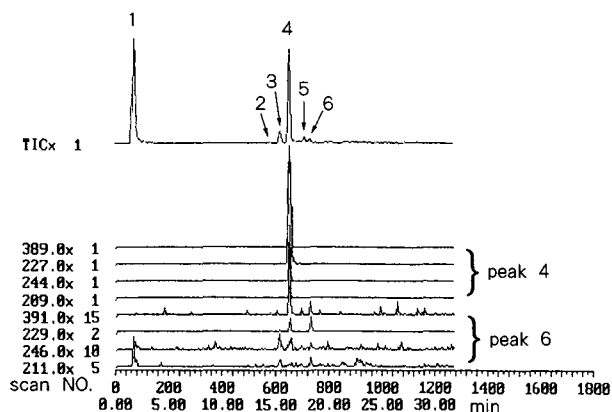
Fig. 5. Mass chromatograms produced by characteristic ions of peaks 4 and 6. × 1, etc. indicates intensity scale magnification factor.

peak 6 was presumed to be 6-dihydroverbenalin. In the structure of this compound, the ketone group of verbenalin is reduced to hydroxyl groups. As there is no possibility of reduction during the extraction procedure, this compound can be regarded as present in *S. glauca*. 6-Dihydroverbenalin is a new iridoid glycoside which has not been found in any plants hitherto. Verification of this trace component by other methods will be investigated in further work. It was recognized from the mass spectrum that peak 1, which was not detected by UV measurement but appeared in Fig. 2b, is a saccharide. Judging from their mass spectra, peaks 2, 3 and 5 are not iridoid glycosides.

CONCLUSION

TSP LC–MS has been applied satisfactorily to highly polar and thermally labile compounds such as iridoid glycosides. This method gives information about both molecular weight and structure. By optimization of the separation conditions, it was possible to identify a new component even though it was present in only trace amounts in a complex plant extract sample.

REFERENCES

1 G. King, H. Rimper and D. Hunkler, *Phytochemistry*, 26 (1987) 423.
2 B. Gering, P. Junior and M. Wichtel, *Phytochemistry*, 26 (1987) 753.
3 Y. Takeda, S. Tsuchida and T. Fujita, *Phytochemistry*, 26 (1987) 2303.
4 F. Asai, M. Mizuno, M. Iinuma, T. Takeda, C. Phengklai, A. Anada and T. Nakanishi, *Phytochemistry*, 41 (1987) 349.
5 H. Inoue, Y. Takeda, A. Kanomi, H. Nishiyama, T. Okuda and C. Purff, *Phytochemistry*, 27 (1988) 2591.
6 D. E. Games, M. A. McDowall, K. Levsen, K. H. Shafer, P. Dobberstein and J. L. Gower, *Biomed. Environ. Mass Spectrom.*, 11 (1984) 87.
7 M. Hattori, Y. Kawata, N. Kakiuchi, K. Matsuura and T. Namba, *Syoyakugaku Zasshi*, 43 (1988) 2591.
8 J. Iida, M. Hayashi, M. Ono, K. Inoue and T. Fujita, *Chem. Pharm. Bull.*, submitted for publication.
9 C. Fenselau, D. J. Liberate, J. A. Yerger, R. J. Cotter and A. L. Yergey, *Anal. Chem.*, 56 (1984) 2759.
10 R. D. Voyksner, E. D. Bush and D. Brent, *Biomed. Environ. Mass Spectrom.*, 14 (1987) 524.

CHROMSYMP. 1755

Supercritical fluid extraction and chromatography of cholesterol in food samples

C. P. ONG, H. K. LEE and S. F. Y. LI*

Department of Chemistry, National University of Singapore, 10 Kent Ridge Crescent, Singapore 0511 (Singapore)

ABSTRACT

A method based on supercritical fluid chromatography is presented which can be used for the determination of cholesterol in certain foods. The method involves the extraction with supercritical carbon dioxide and analysis of the extracts using a capillary column with supercritical carbon dioxide as mobile phase and flame ionization detection. Quantification is achieved using cholesteryl chloroacetate as an internal standard.

INTRODUCTION

In recent years, appplications of supercritical fluid chromatography (SFC) have been rapidly increasing[1,2]. Among the attributes of SFC are a high separation efficiency, appplicability to thermally labile compounds, compatibility with a wide range of detectors and flexibility in pressure, temperature and density control. Supercritical fluid extraction (SFE) has also attracted considerable interest as it is relatively easy to implement simultaneous control of volatility and solubility simply by programming the pressure and temperature or density and temperature simultaneously during an experimental run.

In both SFC and SFE, carbon dioxide is frequently employed as the mobile phase and as the extraction solvent, respectively, primarily owing to its inert properties, its compatibility with universal detectors (*e.g.*, the flame ionization detector) and its availability in high purity. In addition, carbon dioxide is supercritical at moderate temperature (*ca.* 31.1°C) and pressure (*ca.* 72.8 atm), thus making it a suitable choice from an instrumentation point of view. Further, SFE utilizing carbon dioxide is a solvent-free type of extraction where no toxic solvents are required and the carbon dioxide used can be easily removed by reducing the pressure.

The aim of this study was to investigate the applicability of SFC for the determination of cholesterol. Cholesterol was chosen as a test material because there are a number of inherent difficulties associated with its determination using conventional chromatographic techniques. Derivatization is often required to improve the detec-

tion in the liquid chromatographic analysis of cholesterol[3]. Even though gas chromatography has been successfully carried out[4], a high temperature is required (*ca*. 260–300°C). Although cholesterol can be determined at lower temperatures by a number of other methods[5–9], these methods are either inaccurate or time consuming. Further, cholesterol is of great interest in both the food and medical sciences. It has been implicated in vascular pathology including coronary disease and there is therefore a need for a sensitive and accurate quantitative procedure for its determination[10].

In this paper, we report a simple technique based on SFC for the determination of cholesterol in food samples. The efficiency of a supercritical carbon dioxide ectraction method was compared with that of a Soxhlet extraction procedure employing *n*-hexane as the extraction solvent.

EXPERIMENTAL

The experiments were performed with a Model SFC 3000 system (Carlo Erba), equipped with a flame ionization detector. The column was a SE-52 fused-silica capillary column (10 m × 100 μm I.D., coating thickness 0.45 μm). Tapered restrictors rated nominally at 8 ml/min (J&W Scientific) were connected after the column for pressure reduction. Injections were made with an air-actuated Valco VICI injection valve equipped with a 1-μl loop. The injection time was 1 s. The chromatographic data were collected and analysed with a Hewlett-Packard Model 3390A integrator. The temperatures of the injection port, splitting outlet and detector were set at 40, 250 and 320°C, respectively. All runs were performed isothermally at 85°C. The pressure programming was from 14 to 20 MPa in 60 min.

All chemicals were of analytical-reagent grade or better. The standard and calibration solutions were prepared in HPLC-grade hexane (J. T. Baker). The standard solution contained 650 ppm each of cholesterol and the seven derivatives.

In order to select an appropriate internal standard, seven cholesteryl derivatives were analysed together with cholesterol in preliminary runs. The seven derivatives used were cholesteryl chloride, bromide, chloroacetate, *n*-hexanoate, *n*-heptanoate, caprylate and benzoate. The criteria for the choice of the internal standard were that it should not have a retention time too close to that of cholesterol and that it should elute witin a reasonably short time.

The design of the SFE system used in this study has been described elsewhere[11]. For the SFE of egg yolk samples, the pressure of carbon dioxide was kept constant at 17.7 MPa and the temperature at 45°C. An extraction time of 1 h was used. For the Soxhlet extraction procedure, *n*-hexane was used as the solvent and the extraction time was 7 h. In both instances the extraction times used were obtained by periodically analysing the extracts until no further improvement in the extraction efficiency could be obtained with further increases in the extraction time. For the calculation of the extraction efficiency of each type of extraction procedure, the recoveries of cholesterol and the internal standard from spiked glass-wool were determined. To illustrate further the applicability of the procedure to food samples, experiments were performed to extract cholesterol from egg yolk. The amount of egg yolk used for each extraction was 0.2 g and the amount of internal standard added to each sample was 0.03 g. The extracts were collected in a heated stainless-steel collector[11] and then dissolved in 100 ml of *n*-hexane. The solutions were evaporated to dryness under reduced pres-

sure. Subsequently, the dried extracts were dissolved in 4 ml of *n*-hexane for chromatographic analysis.

RESULTS AND DISCUSSION

Fig. 1 illustrates the chromatogram obtained for cholesterol and the seven cholesteryl derivatives. Based on the results, cholesteryl chloroacetate was chosen as the internal standard as it satisfied both of the selection criteria. The amounts injected were within the linearity range of the detector. The R^2 values of the linear fittings for cholesterol and cholesteryl were 0.9980 and 0.9995, respectively. Peak area reproducibility was within 2% relative standard deviation (R.S.D.) and retention reproducibility within 0.15% R.S.D. These values were obtained using manual injection in the splitless mode and with an identical flow restrictor. The detection limits for both cholesterol and cholesteryl chloroacetate were 25 ppm at a signal-to-noise ratio of 3.

In Table I the extraction efficiencies and levels of cholesterol in two egg yolk samples are given. The extraction efficiencies were obtained based on the recoveries of the internal standard in each sample. The levels of cholesterol shown were corrected for the efficiency of the respective extraction procedure and each value represents at least duplicate extractions. A typical chromatogram for an extracted egg yolk sample is illustrated in Fig. 2.

From the results in Table I, it can be seen that SFE is a more effective extraction method than the conventional Soxhlet procedure. The small difference in the amount of cholesterol determined were due to inhomogeneity of the sample, as two eggs were used. Although in both extraction methods recoveries as high as 98% could be achieved, SFE required only 1 h whereas Soxhlet extraction required 7 h. Compared with the extraction procedure employed by Hurst *et al.*[12], which involved hydrolysing the samples with potassium hydroxide, followed by a number of subsequent steps, SFE is much simpler and has been found to be capable of yielding superior extraction
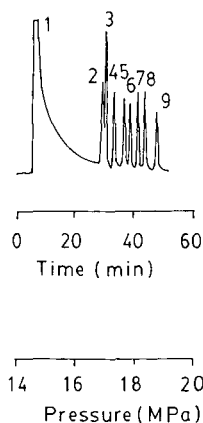
Fig. 1. Typical chromatogram for cholesterol and cholesteryl derivatives obtained under the following conditions: mobile phase, carbon dioxide; linear pressure programme from 14 to 20 MPa in 60 min; oven temperature, 85°C; injector temperature, 40°C; detector temperature, 320°C. Peaks: 1 = *n*-hexane; 2 = cholesterol; 3 = cholesteryl chloride; 4 = cholesteryl bromide; 5 = cholesteryl chloroacetate; 6 = cholesteryl *n*-hexanoate; 7 = cholesteryl *n*-heptanoate; 8 = cholesteryl caprylate; 9 = cholesteryl benzoate.

C. P. ONG, H. K. LEE, S. F. Y. LI

TABLE I

COMPARISON OF RESULTS OF EXTRACTION USING SFE AND SOXHLET EXTRACTION

Extraction method	Efficiency (%)	Cholesterol in 100 g of egg yolk (mg)
SFE	98.0	1447 ± 1.7
Soxhlet	98.0	1380 ± 2.0
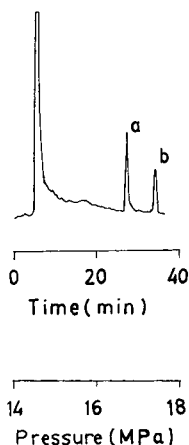
Fig. 2. Typical chromatogram of an extracted egg yolk sample. Chromatographic conditions as in Fig. 1. Peaks: a = cholesterol; b = cholesteryl chloroacetate.

efficiencies for cholesterol. Bearing in mind that the extraction selectivity and efficiency can be further improved by using pressure and temperature programming for the extraction of complicated samples, it is believed that it will be possible to develop the potential of SFE as a powerful alternative to many conventional extraction procedures.

CONCLUSION

The possibility of using low temperatures in SFC, as shown here, makes it a very attractive technique especially in the analysis of thermally labile compounds. Similarly in SFE the operating temperature required can be as low as 35°C for the extraction of cholesterol. This would mean that during the extraction procedure other thermally labile components in the food samples, such as protein, vitamins and various nutrients, would not be destroyed. For some applications where it is necessary to preserve the materials of the matrix for further analysis, SFE can be used advantageously. Further, it is worth noting that in the present procedure, minimum sample preparation is required. It is only necessary to dissolve the samples in an appropriate solvent. With the possibility of performing simultaneous pressure and temperature or density and temperature programming, there is ample flexibility in selecting the chro-

matographic and extraction conditions. It is therefore possible to develop a rapid and reliable method for the routine determination of cholesterol in biological samples using supercritical fluid technology.

REFERENCES

1 M. Novotny, S. R. Springston, P. A. Peaden, J. C. Fjeldsted and M. L. Lee, *Anal. Chem.*, 53 (1981) 407A.
2 R. D. Smith, W. D. Felix, J. C. Fjeldsted and M. L. Lee, *Anal. Chem.*, 54 (1982) 1883.
3 K. Sugino, J. Terao, H. Murakami and S. Matshushita, *J. Agric. Food Chem.*, 34 (1986) 36.
4 T. S. Hor, S. F. Y. Li and H. K. Lee, *SNIC Bull.* 16 (1988) 41.
5 C. C. Allain, L. S. Poon, C. S. G. Chan, W. Richmond and P. C. Fu, *Clin. Chem.*, 34 (1974) 470.
6 G. R. Cooper, S. J. Myers and E. J. Sampson, *Clin. Chem.*, 34 (1988) B95.
7 I. W. Duncan, P. H. Culbreth and C. A. Burtis, *J. Chromatogr.*, 162 (1979) 281.
8 L. Orgen, L. Csiky, L. Risinger, L. Nilsson and G. Johansson, *Anal. Chim. Acta*, 117 (1980) 71.
9 C. J. Shen, L. S. Chen and A. J. Sheppard, *J. Assoc. Off. Anal Chem.*, 65 (1982) 1222.
10 A. R. Newman, *Anal. Chem.*, 61 (1989) 663A.
11 C. P. Ong, H. K. Lee and S. F. Y. Li, presented at the *10th Australian Analytical Conference, Brisbane, August 28–September 2, 1989.*
12 W. J. Hurst, M. D. Aleo and R. A. Martin, Jr., *J. Agric. Food Chem.*, 33 (1985) 820.

CHROMSYMP. 1859

Supercritical fluid extraction and chromatography of steroids with Freon-22

S. F. Y. LI*, C. P. ONG, M. L. LEE and H. K. LEE

Department of Chemistry, National University of Singapore, 10 Kent Ridge Crescent, Singapore 0511 (Singapore)

ABSTRACT

   The use of Freon-22 in supercritical fluid extraction and chromatography was investigated. For the extraction of steroids, the extraction efficiency with supercritical Freon-22 was found to be significantly better than that with supercritical carbon dioxide and the extraction time required was much shorter. Preliminary results for the chromatographic analysis of steroids also indicated that polar compounds could be eluted much more easily with Freon-22 than carbon dioxide as the mobile phase.

INTRODUCTION

   Until now carbon dioxide has been the most widely used supercritical fluid for supercritical fluid extraction (SFE) and supercritical fluid chromatography (SFC), mainly owing to its inert properties, its compatibility with universal detectors (*e.g.*, flame ionization detector) and its availability in high purity. In addition, carbon dioxide is supercritical at moderate temperature and pressure, thus making it a suitable choice from an instrumentation point of view. However, a severe limitation is that it is relatively non-polar and consequently the extraction and chromatography of highly polar substances are relatively difficult. Attempts have been made to use alternative supercritical fluids[1,2] and to add polar modifiers to carbon dioxide[3–5] to extend the polarity range. However, the use of these alternatives has not been entirely satisfactory. For instance, when ammonia is used, the effects of corrosion and possible chemical reactions with the analytes have to be considered. The most commonly used modifier, methanol, not only has a very high critical temperature but also is flammable and therefore a flame ionization detector cannot be employed.
   Freons have been used successfully in a few SFC applications[6]. In this investigation, chlorodifluoromethane (Freon-22) was selected based on considerations of the physical and chemical properties of a wide range of supercritical fluids. Table I compares the properties of carbon dioxide, methanol and selected Freons. It is noteworthy that the critical temperature of Freon-22 is much lower than that of methanol. Further, the dipole moment of Freon-22 is not only much higher than that of carbon dioxide and the other Freons but is also similar to that of methanol.

TABLE I

COMPARISON PROPERTIES OF CARBON DIOXIDE, METHANOL AND FREON-22

Compound	Critical temperature, T_c (K)	Critical pressure, P_c (atm)	Dipole moment (Debye)
Carbon dioxide	31.3	72.9	0.0
Methanol	239.5	81.0	1.7
Freon-11	198.1	43.5	0.5
Freon-12	111.7	39.4	0.2
Freon-22	96.1	49.1	1.4

Therefore, the polarity range that can be covered by Freon-22 would be much greater than that by carbon dioxide. From an environmental point of view, Freon-22 has a much lower ozone-depleting and global warming potential than Freon-11 and -12 and has been suggested as their substitute in certain applications[7].

In this investigation, we evaluated the use of Freon-22 as an SFE solvent and the feasibility of using it as an alternative to or modifier of carbon dioxide in the SFC of polar compounds. As test substances seven steroids were studied.

EXPERIMENTAL

SFC experiments using carbon dioxide were performed with a Model SFC 3000 system (Carlo Erba), equipped with a flame ionization detector. Fused-silica capillary columns, SE-52 (column I, 10 m × 100 μm I.D., coating thickness 0.45 μm) and RSL-300 (column II, 12.5 m × 100 μm I.D., coating thickness 0.20 μm) were used. Tapered restrictors rated nominally at 8 ml/min (J&W Scientific) were connected after the column for pressure reduction. The actual flow-rate measured using a bubble flow meter was 8 ml/min at a detector temperature of 320°C. Injections were made with an air-actuated Valco VICI injection valve with a 1-μl loop. The injection time was 1 s. The chromatographic data were collected and analysed with a Hewlett-Packard Model 3390A integrator. The temperatures of the injection port, splitting outlet and detector were set at 45, 250 and 320°C, respectively.

The preliminary results for the SFC analysis using Freon-22 were obtained on a laboratory-built instrument. A Shimadzu LC-6A pump was fitted with a laboratory-made cooling jacket around the pump head. The temperature of the cooling jacket was maintained at 5°C by a refrigerating circulator consisting of a Thermomix 1442D temperature controller and a Frigomix-S cooling unit (Braun). A Hewlett-Packard 5790 GC oven was used to control the column temperature. A Rheodyne 7520 micro-injection valve fitted with a 0.5-μl injection loop was used for sample introduction. A Carlo Erbo Micro-UVis 20 detector was used for detection. The wavelength was set at 254 nm. An RSL-300 capillary column (10 m × 100 μm I.D., coating thickness 0.2 μm) was used for the analysis. A tapered restrictor fabricated in our laboratory with a measured flow-rate of 34 ml/min at 40°C was used for flow restriction and the tip of the restrictor during the chromatographic runs was immersed

in methanol to prevent blocking of the restrictor. A chart recorder (Houston Instruments) was used to record the chromatograms.

The seven steroids (Fig. 1) were obtained from Fluka and were of purum or puriss grade. Standard solutions were prepared in HPLC-grade methanol (J. T. Baker). The concentrations of estrone, testosterone, 17α-methyltestosterone and 17α-hydroxyprogesterone were 500 ppm and those of estriol, cortisone and hydrocortisone were 1000 ppm.

CP-grade carbon dioxide (British Oxygen) of 100% purity was used for the chromatographic work and purified-grade carbon dioxide for the extraction. Freon-22 was supplied by Atochem and had a purity exceeding 99.8%.

The design of the supercritical fluid extraction system has been described elsewhere[8-10]. The extraction pressures were 13.8, 15.2 and 18.0. MPa. For carbon

ESTRONE (270)
$C_{18}H_{22}O_2$

TESTOSTERONE (288)
$C_{19}H_{28}O_2$

ESTRIOL (288)
$C_{18}H_{24}O_3$

17α-METHYLTESTOSTERONE (320)
$C_{20}H_{30}O_2$

17α-HYDROXYPROGESTERONE (330)
$C_{21}H_{30}O_3$

CORTISONE (360)
$C_{21}H_{28}O_5$

HYDROCORTISONE (362)
$C_{21}H_{30}O_5$
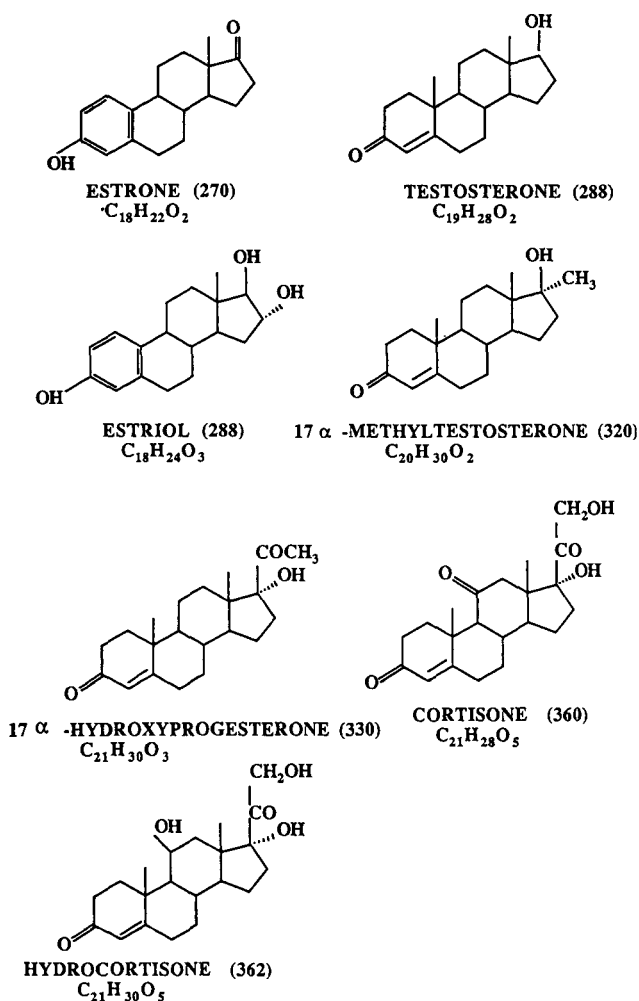
Fig. 1. Structures of the seven steroids studied.

dioxide an extraction time of 30 min was used and the temperature was maintained at 50°C, whereas for Freon-22 the extraction time was 15 min and the temperature was maintained at 100°C. For the Soxhlet extraction procedure, methanol was used as the solvent and the extraction time was extended to 7 h. In the latter instance, the extracts were periodically analysed until no further improvement in the extraction efficiency could be obtained with further increases in the extraction times. For the calculation of the extraction efficiency of each type of extraction procedure, the recoveries of estrone from spiked glass-wool were determined.

RESULTS AND DISCUSSION

The result of the supercritical fluid extraction studies are illustrated in Fig. 2. Although the extraction time for carbon dioxide was twice that of Freon-22, the recoveries obtained were much lower. Further, very little improvement could be made by increasing the extraction pressure to 18 MPa and a maximum recovery of only 16% was obtained. However, with Freon-22, 100% recovery could be achieved within 15 min. The results indicated that Freon-22 was not only capable of achieving higher extraction efficiencies but also required a shorter time. In Fig. 3, the results of the Soxhlet extraction procedure are shown. It can be seen that in order to obtain 100% recovery, an extraction time of more than 7 h would be needed. Therefore, the SFE procedure using supercritical Freon-22 would provide a significant reduction in analysis time.

Figs. 4 and 5 illustrate the chromatograms of the seven steroids obtained with pure carbon dioxide as the mobile phase using columns I and II respectively. For column I, which is the non-polar column, the selectivity was insufficient to separate testosterone and methyltestosterone. Estriol was not eluted even after an analysis time of more than 1 h at a column temperature of 115°C. However, with column II, which is of medium polarity, complete separation of all seven peaks was achieved using pure carbon dioxide as the mobile phase and the retention times obtained were not excessively long. Therefore, the use of a highly polar mobile phase did not seem necessary. However, to explore the potential of employing Freon-22 for SFC analysis,
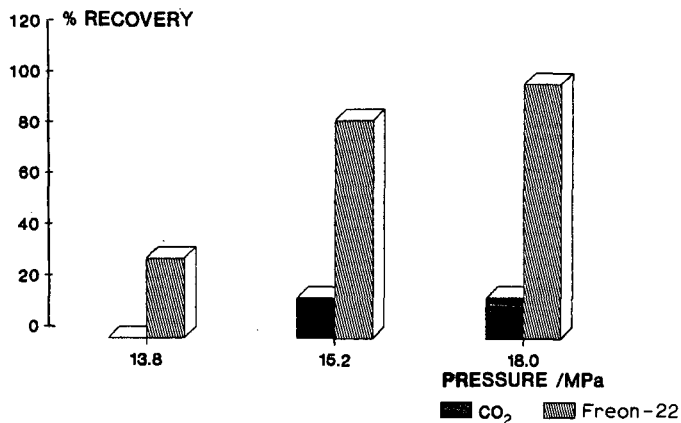
Fig. 2. Results of supercritical fluid extraction. Extraction times: carbon dioxide, 30 min; Freon-22, 15 min.
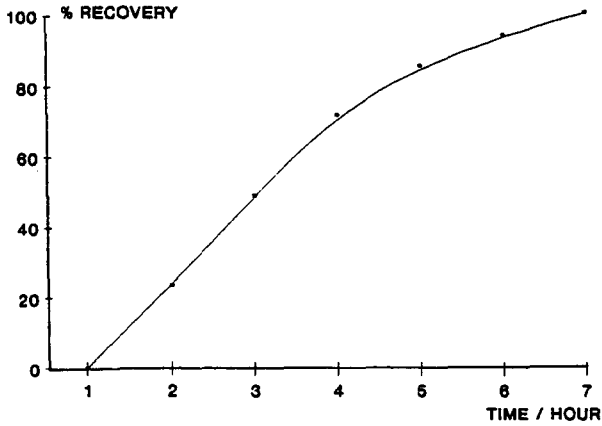
Fig. 3. Results of Soxhlet extraction using methanol.

some preliminary results were obtained to illustrate the faster elution times obtainable compared with carbon dioxide. The compound selected for this investigation was testosterone. The chromatograms obtained are shown in Fig. 6. The results show that the elution of testosterone with Freon-22 was much faster than that with carbon
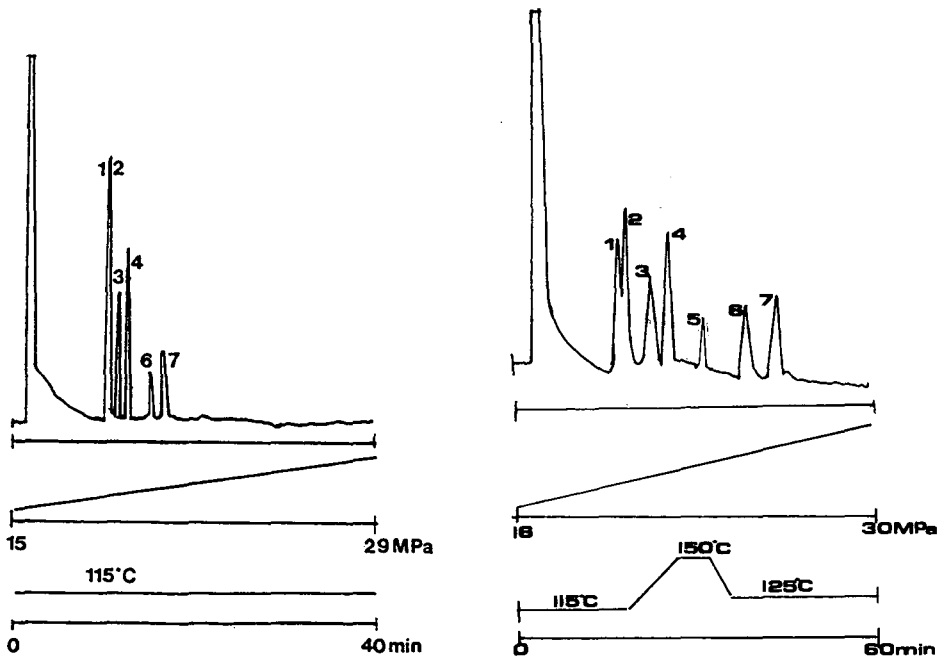
Fig. 4. Chromatogram of steroids obtained using column I and carbon dioxide as mobile phase. Peaks: 1 = testosterone; 2 = 17α-methyltestosterone; 3 = estrone; 4 = estriol; 5 = 17α-hydroxyprogesterone (not detected); 6 = cortisone; 7 = hydrocortisone.

Fig. 5. Chromatogram of steroids obtained using column II and carbon dioxide as mobile phase. Peaks as in Fig. 4.
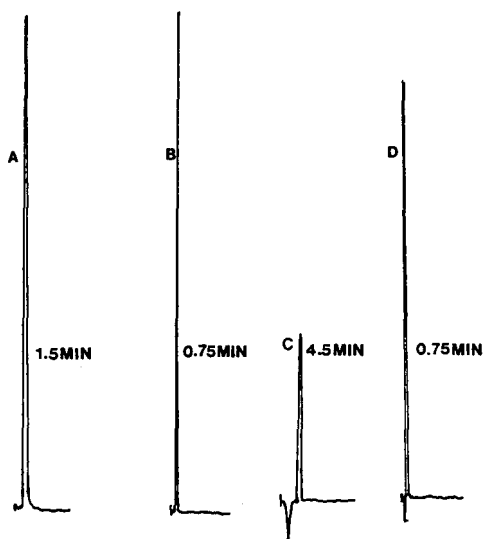
Fig. 6. Chromatograms for testosterone obtained using (A) Freon-22 at 5 MPa, (B) Freon-22 at 10 MPa, (C) carbon dioxide at 15 MPa and (D) carbon dioxide at 20 MPa.

dioxide. A lower operating pressure can be used to obtain similar or shorter retention times. These observations are consistent with the results of the extraction studies. Further, it was noted that with Freon-22 as mobile phase, peaks with higher signal-to-noise ratios were obtained. Therefore, a higher detection sensitivity could be achieved using Freon-22 with UV detection at 254 nm. In Fig. 6, chromatograms A and B were obtained using Freon-22 and the concentration of testosterone employed was 833 ppm, whereas chromatograms C and D were obtained using carbon dioxide with 2500 ppm of testosterone. Also, the UV cut-off for Freon-22 was found to be similar to that of methanol and therefore no solvent peak was observed. With carbon dioxide, a small negative peak was noted, indicating that the absorbance of supercritical carbon dioxide may be slightly higher than that of methanol. As 254 nm is the most widely used setting for UV detection, the enhanced sensitivity would certainly help to maximize the potential of SFC as a chromatographic technique.

Further work is being carried out to explore applications of Freon-22 in other supercritical fluid separation processes. However, from the promising results obtained so far, it can be concluded that there are significant advantages in using supercritical Freon-22 as a substitute for carbon dioxide in SFE and SFC.

REFERENCES

1 C. Fujimoto,T. Watannabe and K. Jinno, J. Chromatogr. Sci., 27 (1989) 325.
2 Y. Hirata, J. Chromatogr., 315 (1984) 39.
3 D. E. Raynie, S. M. Fields, N. M. Djordevic, K. E. Markides and M. L. Lee, J. High Resolut. Chromatogr. Chromatogr. Commun., 11 (1989) 51.
4 T. A. Berger, J. F. Dye, M. Ashrof-Khorassani and L. T. Taylor, J. Chromatogr. Sci., 27 (1989) 105.
5 S. Hara, A. Dobashi, K. Konoshita, T. Hondo, M. Saito and M. Senda, J. Chromatogr., 371 (1986) 153.
6 D. Leyendecker, D. Leyendecker, F. P. Schmitz and E. Klesper, J. Liq. Chromatogr., 10 (1987) 1917.
7 P. S. Zurer, Chem. Eng. News, July 24 (1989) 7.
8 C. P. Ong, H. K. Lee and S. F. Y. Li, paper presented at the 10th Australia Analytical Conference, August 28–September 2, 1989, Brisbane.
9 C. P. Ong, H. M. Ong, S. F. Y. Li and H. K. Lee, J. Microcolumn Sep., (1990) in press.
10 C. P. Ong, H. K. Lee and S. F. Y. Li, J. Chromatogr., 515 (1990) 509.

CHROMSYMP. 1784

High-performance liquid chromatography of proteins on a ceramic hydroxyapatite with volatile buffers

TOSHIHIKO KADOYA

Pharmaceutical Laboratory, Kirin Brewery Co., Ltd., Soujamachi 1-2-2, Maebashi, Gunma 371 (Japan)

ABSTRACT

Volatile solutions were applied as eluents in the hydroxyapatite high-perform-ance liquid chromatography (HPLC) of proteins and the elution behaviour was in-vestigated. Four standard proteins were loaded on a ceramic hydroxyapatite column for HPLC and eluted with linear gradients of seven volatile solutions. Hydroxyapa-tite HPLC using ammonium hydrogencarbonate solution seems to be the best al-ternative although the resolution and recovery of proteins were lower than those obtained with a phosphate buffer system. The system was applied to the purification of a monoclonal antibody and of an enzyme in small amounts.

INTRODUCTION

Since the original work by Hjerten and co-workers[1,2], high-performance liquid chromatography (HPLC) on hydroxyapatite has sometimes been used for the specific separation of proteins[3-8]. However, operation with the conventional type of hydroxyapatite was difficult because of the fragility of the crystals and the difficulty of obtaining a uniform quality from batch to batch. Recently, the hydroxyapatite columns for HPLC have become commercially available, and this has led to effective methods for the purification of proteins[9-13]. Fang *et al.*[14] demonstrated the separation of proteins in very small amounts using a microbore column packed with ceramic hydroxyapatite beads with diameters as small as 2 μm.

In the purification of proteins, the samples sometimes need to be concentrated or to be desalted. Operations such as ultrafiltration or dialysis, however, may cause losses of proteins, especially with very small amounts of proteins. Volatile electrolytes are attractive in these cases, because they can be removed by freeze-drying. When desalting is performed with gel filtration chromatography, a volatile electrolyte is sometimes used to increase the ionic strength.

In hydroxyapatite chromatography, phosphate buffer is ordinarily used for elution. In this study, seven volatile solution systems were applied to the hydroxy-apatite HPLC of proteins and the elution behaviour was investigated. Although these

systems showed lower resolution and recoveries of proteins than when phosphate buffer was used, the HPLC with ammonium hydrogencarbonate gave the best separation among the volatile solutions examined.

EXPERIMENTAL

Reagents and materials

Hydrochloric acid and ammonia solution were purchased from Kokusan Kagaku (Tokyo, Japan). Other reagents were purchased from Nakarai Tesque (Kyoto, Japan). Myoglobin (equine heart), lysozyme (chicken egg), chymotrypsinogen A (bovine pancreas) and cytochrome c (equine heart) were obtained from Serva (Heidelberg, F.R.G.). Acetylcholinesterase (electric eel) was purchased from Sigma (St. Louis, MO, U.S.A.).

Ascites fluid containing immunoglobulin M (IgM) monoclonal antibody produced by BALB/c mouse was passed through a 0.22-μm filter (Millipore, Bedford, MA, U.S.A.) prior to HPLC separation.

Apparatus

Pentax SH-0410F (100 mm × 4.6 mm I.D., particle size 2 μm) (Asahi Optical, Tokyo, Japan) hydroxyapatite columns were used with a precolumn of hydroxyapatite (10 mm × 4.6 mm I.D., particle size 10 μm).

A Hitachi (Tokyo, Japan) HPLC system consisting of L-6210 and L6010 pumps, a dynamic mixer, a ceramic injector and an L-4000 UV detector connected to a recorder was used.

Standard chromatographic procedure

Sample proteins were introduced onto a column of hydroxyapatite and eluted with a 30-min linear gradient at a flow-rate of 0.25 ml/min. The seven volatile solution systems used were 10–500 mM ammonium hydrogencarbonate (pH 8.0), 10–500 mM ammonium formate (pH 8.0), 10–500 mM ammonium acetate (pH 8.0), 10–500 mM ethylenediamine–acetic acid (pH 8.0), 10–500 mM ethylenediamine–HCl (pH 8.0), 10–1000 mM triethanolamine–acetic acid (pH 8.0) and 10–1000 mM triethanolamine–HCl (pH 8.0). All separations were conducted at room temperature. The effluent was monitored by measuring the absorbance at 280 nm. After completion of each chromatographic run, the column was re-equilibrated for 16–20 min with the initial solvent before the next cycle run. All the elution buffers were prepared immediately before use.

Measurement of acetylcholinesterase activity

Acetylcholinesterase activity was measured by a fluorimetric method using acetylthiocholine iodide (Wako, Osaka, Japan) as a substrate and 7-diethylamino-3-(4'-maleimidylphenyl)-4-methylcoumarin (Molecular Probes, Eugene, OR, U.S.A.) as a fluorescence reagent.

Sodium dodecyl sulphate–polyacrylamide gel electrophoresis (SDS-PAGE)

The eluate from the column was lyophilized and analysed by SDS-PAGE (10–15% polyacrylamide gradient gel) in the presence of a reductant using the Phast System (Pharmacia, Uppsala, Sweden).

RESULTS AND DISCUSSION

Seven volatile solutions were applied to hydroxyapatite HPLC for the elution of proteins and the elution behaviours were investigated using four purified proteins, myoglobin, chymotrypsinogen A, lysozyme and cytochrome *c*.

The protein mixture was loaded on the column and eluted with a 30-min linear gradient. The chromatograms are shown in Fig. 1. For comparison, a chromatogram obtained with sodium phosphate buffer is shown in Fig. 1A. Compared with the use of phosphate buffer, HPLC using the volatile solutions gave lower resolution and recoveries of proteins. The proteins were not eluted with triethanolamine systems and
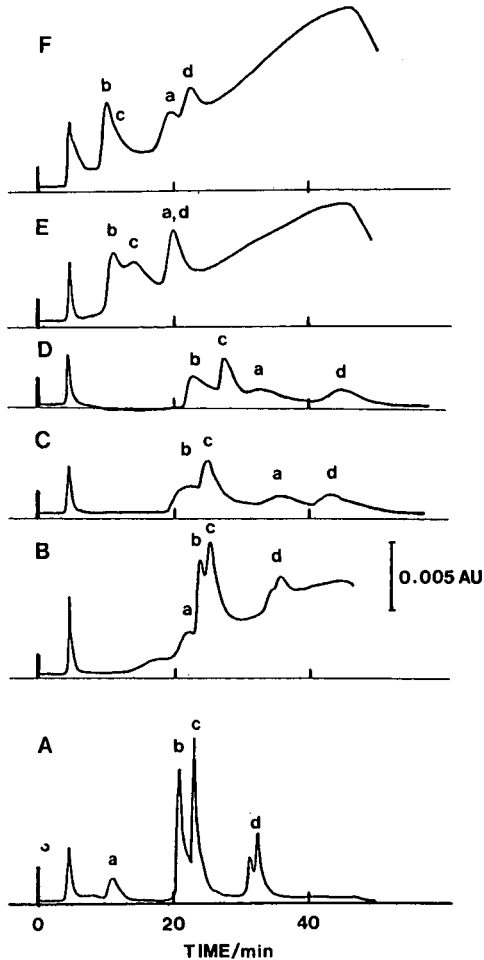
Fig. 1. Hydroxyapatite HPLC of a protein mixture (1.5–3 μg of each protein) using various volatile solutions for elution: (A) sodium phosphate (pH 8.0) (10–250 m*M*); (B) ammonium hydrogencarbonate (pH 8.0) (10–500 m*M*); (C) ammonium formate (pH 8.0) (10–500 m*M*); (D) ammonium acetate (pH 8.0) (10–500 m*M*); (E) ethylenediamine–acetic acid (pH 8.0) (10–500 m*M*); (F) ethylenediamine–HCl (pH 8.0) (10–500 m*M*). Peaks: a = myoglobin; b = lysozyme; c = chymotrypsinogen A; d = cytochrome *c*.
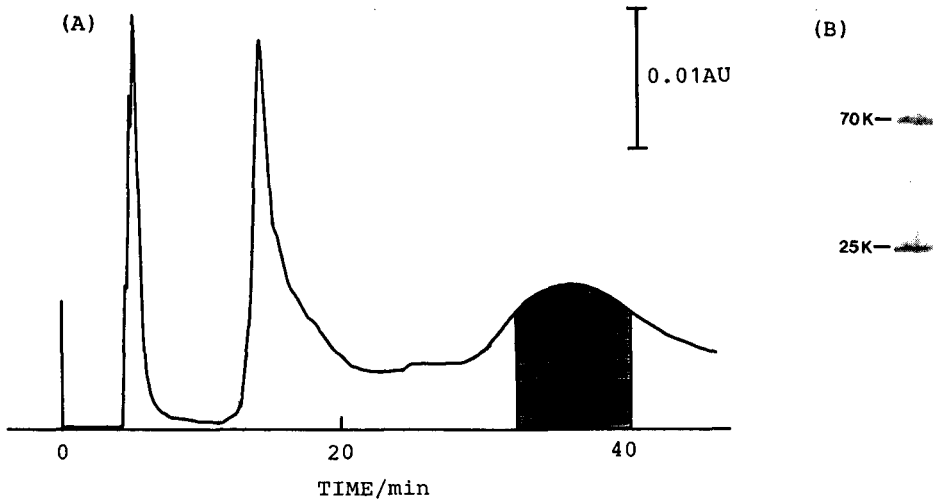
Fig. 2. Purification of IgM monoclonal antibody from mouse ascites fluid by hydroxyapatite HPLC using ammonium hydrogencarbonate solution for elution. Mouse ascites fluid (5 μl) was loaded onto the column and eluted by a 30-min linear gradient of ammonium hydrogencarbonate (pH 8.0) from 10 to 1000 mM. The column effluent in the shaded portion in A was collected and analysed by SDS-PAGE (B). K = kilodalton.

in the other systems the protein recoveries, calculated from the areas of the eluted peaks, were 40–80%, whereas with the phosphate buffer system the recovery was more than 90%. In the systems in Fig. 1C–F, myoglobin was retained on the column more tightly than in the other systems (Fig. 1A and B). Also, cytochrome c was eluted as one broad peak (Fig. 1C–F), whereas it was eluted as two peaks with phosphate buffer (Fig. 1A) or ammonium hydrogencarbonate (Fig. 1B). The reason for this difference in retention behaviour is not clear, but the solutions might affect the structures of these proteins. Among the systems tested, ammonium hydrogencarbonate seems to be the best alternative. This solution also has the advantage that the base and the acid are equally volatile and the residue after lyophilization is neither strongly acidic nor alkaline.
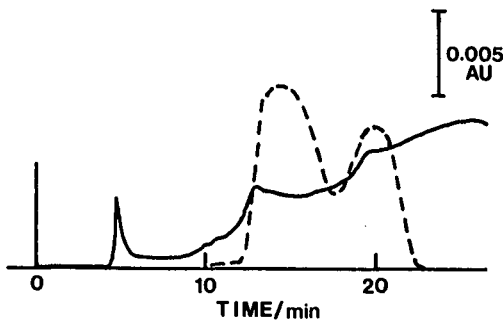
Fig. 3. Purification of acetylcholinesterase by hydroxyapatite HPLC using ammonium hydrogencarbonate solution for elution. A commercial sample of acetylcholinesterase (*ca.* 500 ng) was aplied to the column and eluted by a 20-min linear gradient of ammonium hydrogencarbonate (pH 8.0) from 10 to 500 mM. The broken line represents the activity of acetylcholinesterase.

IgM monoclonal antibody was purified from ascites fluid on the hydroxyapatite column using ammonium hydrogencarbonate solution for elution. A 5-μl volume of ascites fluid was applied to the column and eluted with a 30-min linear gradient of ammonium hydrogencarbonate from 10 to 1000 mM. The effluent was fractionated and lyophilized, and then analysed by SDS-PAGE and enzyme-linked immunosorbent assay (ELISA). The results are shown in Fig. 2. IgM monoclonal antibody was eluted as a broad peak (Fig. 2A), which preserved the immunoreactivity. The results of SDS-PAGE (Fig. 2B) suggested that the antibody was highly purified. Fig. 3 shows the separation of a commercial crude sample (*ca.* 500 ng) of acetylcholinesterase by hydroxyapatite HPLC with ammonium hydrogencarbonate. The effluent from the column was collected and lyophilized, and the activity was measured. Acetylcholinesterase activity was found in two peaks eluting at *ca.* 14 min and *ca.* 20 min. The recovery of the activity was about 70%.

In the purification of very small amounts of proteins, the concentration or desalting step may cause losses of proteins. Hydroxyapatite HPLC of proteins using volatile solutions for elution appears to be a useful tool for the purification of very small amounts of proteins.

REFERENCES

1 A. Tiselius, S. Hjerten and O. Levin, *Arch. Biochem. Biophys.*, 65 (1956) 132.
2 S. Hjerten, *Biochim. Biophys. Acta*, 31 (1959) 216.
3 G. Bernardi, *Methods Enzymol.*, 22 (1971) 325.
4 B. Moss and E. N. Rosenblum, *J. Biol. Chem.*, 247 (1972) 5194.
5 G. Bernardi, *Methods Enzymol.*, 27 (1973) 471.
6 M. F. Yeh and J. M. Trela, *J. Biol. Chem.*, 251 (1976) 3134.
7 G. M. Kostner and A. Holasek, *Biochim. Biophys. Acta*, 488 (1977) 417.
8 W. Love, D. Millay and J. S. Huston, *Arch. Biochem. Biophys.*, 207 (1981) 300.
9 T. Kadoya, T. Isobe, M. Ebihara, T. Ogawa, M. Sumita, H. Kuwahara, A. Kobayashi, T. Ishikawa and T. Okuyama, *J. Liq. Chromatogr.*, 9 (1986) 3543.
10 T. Kadoya, T. Ogawa, H. Kuwahara and T. Okuyama, *J. Liq. Chromatogr.*, 11 (1988) 2951.
11 T. Kawasaki, W. Kobayashi, K. Ikeda, S. Takahashi and H. Monma, *Eur. J. Biochem.*, 157 (1986) 291.
12 Y. Kato, K. Nakamura and T. Hashimoto, *J. Chromatogr.*, 398 (1987) 340.
13 S. Hjerten, J. Lindeberg and B. Shopova, *J. Chromatogr.*, 440 (1988) 305.
14 Y.-I. Fang, T. Hiroi and T. Okuyama, in *Proceedings of the 7th Conference on Liquid Chromatography, Tokyo, October 28–30, 1986*, Division of Liquid Chromatography of the Japan Society for Analytical Chemistry, Tokyo, 1986, p. 65.

CHROMSYMP. 1803

o-Phthalaldehyde post-column derivatization for the determination of gizzerosine in fish meal by high-performance liquid chromatography

HIROYUKI MURAKITA* and TAKESHI GOTOH

Analytical Applications Department, Shimadzu Corporation, 1–63–1, Shibasaki, Chofu, Tokyo (Japan)

ABSTRACT

A method for the fluorimetric determination of gizzerosine by high-performance liquid chromatography was developed. *o*-Phthalaldehyde reagent without thiol was used for derivatization. A higher selectivity for gizzerosine was obtained with this reagent than with *o*-phthalaldehyde reagent containing thiol. This method will be useful for the determination of gizzerosine in fish meal.

INTRODUCTION

Gizzerosine [2-amino-9-(4-imidazolyl)-7-azanonanoic acid] from fish meal has been found to be the cause of gizzard erosion in chicks[1]. It is assumed that gizzerosine is formed by the reaction between the ε-amino group of lysine and histidine when heated[1]. It is now important to be able to determine gizzerosine in fish meal for quality control purposes.

Fluorimetric detection of gizzerosine after reaction with *o*-phthalaldehyde and high-performance liquid chromatography (HPLC) has been reported[2–4]. The *o*-phthalaldehyde reagent contained thiol, as frequently used for the detection of amino acids and amines. However, the selectivity for gizzerosine is not satisfactory and the purification procedure before injection is time consuming. In this work we used *o*-phthalaldehyde reagent without thiol in order to obtain higher selectivity.

EXPERIMENTAL

Apparatus

A Shimadzu LC-9A high-performance liquid chromatograph equipped with an RF-535 fluorimetric detector, a SIL-6B sample injector and a CTO-6A column oven were used. Another LC-9A pump was used to deliver reaction reagent. The reaction tube set in the CTO-6A oven was a stainless-steel tube (7 m × 0.3 mm I.D.).

Chemicals

Distilled water was of HPLC grade. *o*-Phthalaldehyde was of biochemical grade and citric acid, boric acid, phosphoric acid, sodium hydroxide and polyoxyethylene lauryl ether were of analytical-reagent grade. All reagents were purchased from Wako (Osaka, Japan). Gizzerosine standard and fish meal were kindly donated by the National Federation of Agricultural Cooperative Associations (Tokyo, Japan).

Chromatographic conditions

The strong cation exchanger Shim-pack ISC-07/S1504 (150 mm × 4 mm I.D.), obtained from Shimadzu (Kyoto, Japan), was used. The mobile phase was 30 mM sodium borate buffer (pH 9.8) at a flow-rate of 0.4 ml/min. The *o*-phthalaldehyde reagent was 15 mM citric acid containing 0.08% *o*-phthalaldehyde and 0.4% polyoxyethylene lauryl ether; the ether was used to keep the surface of the reaction tube clean. The flow-rate was 0.2 ml/min. The column temperature and reaction temperature were both 45°C.

Sample pretreatment

A 200-mg amount of fish meal was hydrolysed with 2 ml of 6 M hydrochloric acid at 110°C for 22 h. The sample was then filtered and evaporated under reduced pressure to remove the acid. The residue was dissolved in 2 ml of 10 mM sodium phosphate buffer (pH 2.6) and 200 μl of the solution were applied to a Bond Elut C_{18} column (catalogue No. 607101, packing volume 100 mg) obtained from Analytichem International (Harbor City, CA, U.S.A.) and the eluate was collected. A 200-μl volume
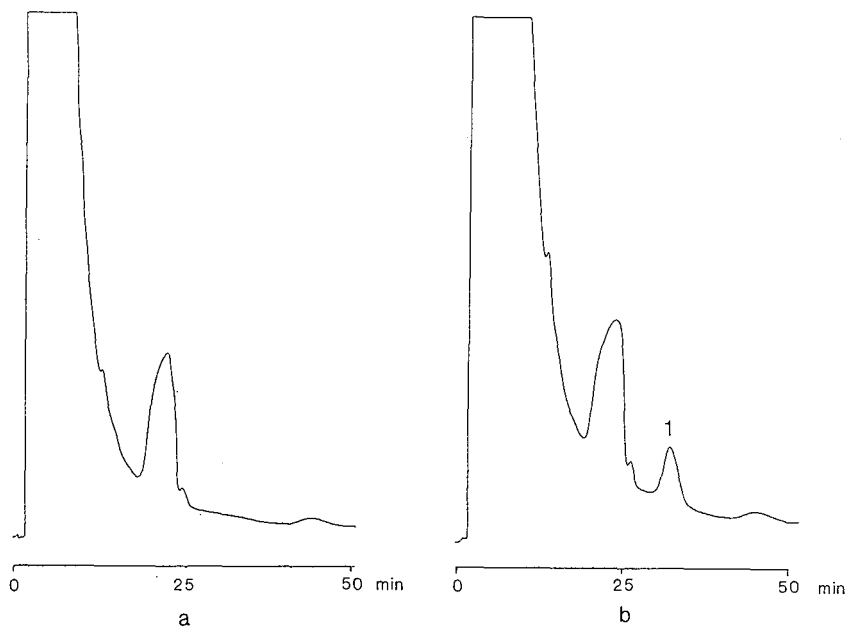
Fig. 1. Chromatograms of fish meal samples containing 65% of crude protein obtained using *o*-phthalaldehyde reagent as described. (a) Blank; (b) with 10 ppm of gizzerosine added. Peak 1 = gizzerosine.

Fig. 2. Chromatograms of a fish meal sample and a standard sample using o-phthalaldehyde reagent containing thiol. (a) Fish meal (blank) (same sample as in Fig. 1a); (b) standard sample. Peak 1 = gizzerosine (10 ng), corresponding to 10 ppm in fish meal.

of water was then applied and the eluate was collected in the same vial. A 20-μl volume of the eluate (400 μl) was injected.

RESULTS AND DISCUSSION

The optimum wavelengths were 320 nm (excitation) and 410 nm (emission). The optimum reaction pH was $ca.$ 8.0. Chromatograms of fish meals (crude protein 65%) are shown in Fig. 1 (a) blank; (b) with 10 ppm of gizzerosine added]. Another fish meal sample (crude protein 60%) was tried and no interference peak was observed. Fish meals that induced heavy gizzard erosion in chicks contained 20 ppm of gizzerosine[2]. The detection limit was $ca.$ 0.5 ppm in fish meal. The detector response was linear up to 1000 ng. The linear regression equation for the calibration graph was $y = 3912x - 331$ ($r = 0.999$), where $y =$ peak area (μVs) and $x =$ amount of sample (ng). The mean retention time and recovery at 10 ppm were 30.2 min and 98.2% ($n = 5$), respectively, with relative standard deviations of 1.8% and 1.5%, respectively. The reagent is selective to gizzerosine, compared with the o-phthalaldehyde reagent containing thiol.

The aminoethylimidazolyl group of gizzerosine is assumed to react with o-phthalaldehyde and produce a fluorescent compound[5]. Fig. 2 shows the chromatograms (standard sample and fish meal) obtained using o-phthalaldehyde reagent containing thiol. An interference peak was observed.

REFERENCES

1 T. Okasaki, T. Noguchi, K. Igarashi, Y. Sakagami, H. Seto, K. Mori, H. Naito, T. Masumura and M. Sugahara, *Agric. Biol. Chem.*, 47 (1983) 2949.
2 Y. Ito, T. Noguchi and H. Naito, *Anal. Biochem.*, 151 (1985) 28.
3 T. Wada, T. Hishiyama and J. Ueno, *Sci. Feeds,* 32 (1987) 342.
4 Y. Ohta, H. Ohashi, S. Enomoto and Y. Machida, *Agric. Biol. Chem.*, 52 (1988)2817.
5 P. A. Shore, A. Burkhalter and V H. Corn, *J. Pharmacol. Exp. Ther.*, 127 (1959) 182.

CHROMSYMP. 1917

Application of high-performance liquid chromatography in establishing an accurate index of blood glucose control

TADAO HOSHINO*, YUKO TAKAHASHI and MIKIKO SUZUKI

Pharmaceutical Institute, School of Medicine, Keio University, 35-Shinanomachi, Shinjuku-ku, Tokyo 160 (Japan)

ABSTRACT

A chromatographic method utilizing a carboxymethylated poly(vinyl alcohol) resin for a more accurate determination of stable haemoglobin A_{1c} (St-A_{1c}) has been developed. The complete separation between St-A_{1c}, labile HbA_{1c} (L-A_{1c}) and HbF was achieved by gradient elution with sodium chloride in phosphate buffer. This high resolution permits accurate quantitation of St-A_{1c}, even in the presence of high levels of HbF or L-A_{1c}. In 142 subjects with normal fasting plasma glucose and normal response to a 75-g oral glucose tolerance test, the reference interval of St-A_{1c} was 2.80–3.98%.

INTRODUCTION

Haemoglobin A_{1c} (HbA_{1c}) is considered to be a reliable indicator of long-term blood glucose regulation in diabetic subjects. However, the measured value of HbA_{1c} often changes, paralleling short-term fluctuations of blood glucose levels, and shows unexpectedly high levels[1,2]. Goldstein *et al.*[1] have shown that these acute changes depend on the concentration of labile A_{1c} (L-A_{1c}), which is not separated from stable A_{1c} (St-A_{1c}) by chromatography. Therefore, it was necessary to remove L-A_{1c} by incubation of erythrocytes in saline or by other methods prior to HbA_{1c} assay[3]. Recently, many attempts have been made to improve the high-performance liquid chromatographic (HPLC) techniques used, and the resolution and accuracy of commercially available analysers for HbA_{1c} have been improved. However, the measured value does not yet reflect accurately the integrated level of blood glucose.

We have previously developed a liquid chromatographic method, based on an IEX-530 column, which enabled us to establish that HbA_{1c} consisted of six sub-fraction[4,5]. Although this method could measure L-A_{1c} and St-A_{1c} simultaneously, the resolution between the two peaks had a value of 0.49, and was still too poor for performing accurate measurements. More recently, we have employed a carboxymethylated poly(vinyl alcohol) resin for the analysis of HbA_{1c}, and it provided better resolution than that of the earlier chromatographic method. In this paper we report the improved method and some applications.

EXPERIMENTAL

Apparatus

The chromatographic apparatus was obtained from Japan Spectroscopic Co. (Tokyo, Japan). The HPLC system was composed of a Trirotar VI pump, a system controller, a DG-3510 in-line degasser, a TU-300 column oven, a VL-614 sample injector and a Uvidec-100-VI variable-wavelength detector, equipped with a Model 7000A intelligent integrator (System Instruments, Tokyo, Japan). All flow lines were made of PTFE tubing (0.5 mm I.D.), except in the pump and injector. The column temperature was thermostatically controlled by passing water through the column jacket.

Reagents

All chemicals used for elution buffer and sample preparation were of special grade, purchased from Wako (Osaka, Japan). The weak and strong eluting buffers used were (A) 30 mM sodium phosphate contaning 0.01% sodium azide and (B) 30 mM sodium phosphate containing 0.6 M sodium chloride and 0.01% sodium azide. The pH was adjusted to 5.0–6.5 by adding the appropriate volume of 0.1 M sodium hydroxide solution. The water used was tap water purified with a system consisting of a Milli-Q/R and a Milli-Q filter (Millipore, Bedford, MA, U.S.A.).

Sample preparation

Blood samples from fasting subjects were obtained by venipuncture and placed in tubes containing EDTA or heparin. Haemolysates were prepared by a modification of the method of Trivelli et al.[26]. Blood was centrifuged at 800 g for 10 min and the packed erythrocytes were washed three times with four volumes of saline. The washed cells were lysed with four volumes of purified water and an equal volume of carbon tetrachloride was added. After vigorous mixing, cellular debris and carbon tetrachloride were settled by centrifugation under the same conditions. The haemolysate was analysed immediately or stored at −80°C until analysed. All of these procedures were carried out at 4°C.

To prepare a control haemolysate, which was used to study the elution behaviour of haemoglobin components, packed erythrocytes were incubated with 5% glucose in isotonic phophate buffer (pH 7.0) for 1 h at 37°C prior to the saline washing.

For in vitro studies on the fluctuations of HbA$_{1c}$, packed erythrocytes and haemoglobin A$_0$ fraction, which was obtained by HPLC fractionation of the haemolysate, were incubated with 10% glucose at 37°C for 2 h or with saline at room temperature for 1 day.

Column preparation

Packing material based on carboxymethylated poly(vinyl alcohol) (DVT-119; exclusion limit = 30 000 daltons, particle size = 9 μm; ion-exchange capacity = 0.8 mequiv./g) was provided by Asahi Kasei Industries (Kawasaki, Japan). Dry resin (1 g) was dispersed in an adequate volume of buffer B and degassed by sonication under reduced pressure. The degassed slurry was pumped into a Pyrex glass column (150 × 8 mm I.D.) with a removable water-jacket and adjustable plunger. The packed resin reached a height of 50 mm.

RESULTS AND DISCUSSION

The elution behaviour of the haemoglobin components on the DVT-119 column was observed by using isoelectric elution at various pH and ionic strength values. The control haemolysate was used for this study. At pH > 6.0, St-A_{1c} was eluted together with other haemoglobin components but is was not eluted at pH < 5.0. The ionic strength of the mobile phase was also critical. At 0.12 M NaCl St-A_{1c} was eluted together with L-A_{1c}. As the ionic strength decreased from 0.12 to 0.06 M NaCl, the resolution of St-A_{1c} and L-A_{1c} was increased, but the k' value increased to more than 12.0. Moreover, HbA_0 is more readily retained than HbA_{1c} by cation-exchange. Therefore, we used an elution gradient consisting of buffers A and B (both at pH 5.5).

A chromatogram of a control haemolysate is shown in Fig. 1. The column was equilibrated with buffer A–buffer B (90:10). A 4-μl volume of haemolysate was injected into the column and eluted with the followed gradient: 10% B for 2 min; 10 to 12% B in 8 min; 12 to 15% B in 8 min; 15 to 20% B in 6 min; 20 to 40% B in 18 min; 40 to 80% B in 12 min and 80 to 100% B in 2 min. The flow-rate was 1.0 ml/min and the eluate was monitored at 415 nm. The column temperature was kept at 24°C. Before the next injection, the column had to be equilibrated with 10% buffer B for at least 20 min. Eight haemoglobin components were obtained from 4 μl of haemolysate and were arbitrarily numbered 1–8.

The identification of the peaks was carried out as described previously[4]. Fraction 3 was alkali-resistant and was eluted at the same position as foetal haemoglobin. Fractions 4 and 5 were identified as L-A_{1c} and St-A_{1c}, respectively. St-A_{1c} was well separated from HbF, and the resolution value of St-A_{1c} and L-A_{1c} was 0.98.

The influence of blood glucose fluctuations on the levels of haemoglobin components, as measured with our HPLC method, was investigated. The results are
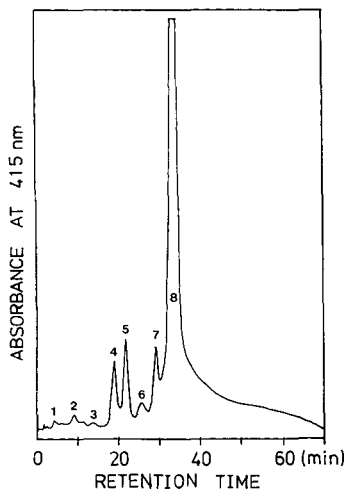
Fig. 1. Chromatogram of a control haemolysate on carboxymethylated poly(vinyl alcohol) resin. A 4-μl sample was applied to the column and eluted with a sodium chloride gradient (see text.) Four peaks were identified: 3 = HbF; 4 = L-A_{1c}; 5 = St-A_{1c}; 8 = HbA_0.
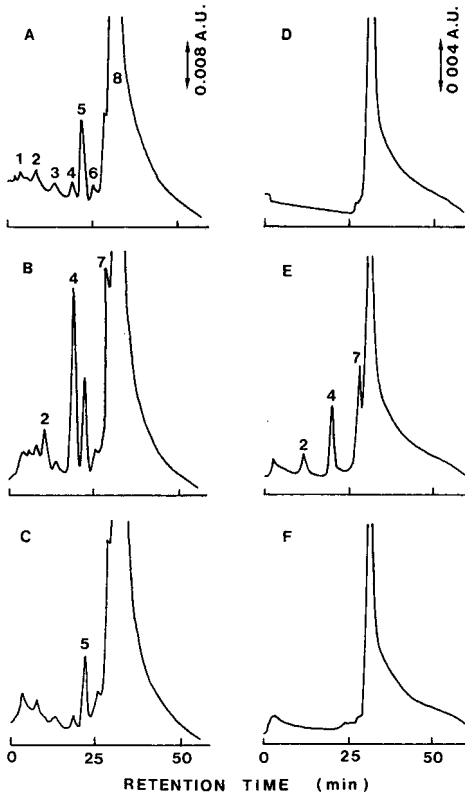
Fig. 2. Acute changes of L-A_{1c} *in vitro*. (A) Normal adult blood; (B) normal adult blood after incubation with 10% glucose at 37°C for 2 h; (C) normal adult blood after washing with saline for 1 day at room temperature; (D) HbA_0 fraction; (E) HbA_0 fraction after incubation with glucose; (F) HbA_0 fraction after following wash with saline.

shown in Fig. 2. Haemolysate from a healthy person and the HbA_0 fraction obtained by HPLC in advance were incubated in 10% glucose at 37°C for 2 h, then further dialysed against saline for 1 day at room temperature. The elution pattern of fraction 5 was hardly affected by incubation in glucose or dialysis against saline. In contrast, fractions 2, 4 and 7 increased after incubation in glucose and decreased after dialysis against saline (Fig. 2A, B, C). In the case of a HbA_0 fraction containing no fraction 2, 4 and 7 components (Fig. 2D), after incubation with glucose Fractions 2, 4 and 7 newly appeared, as shown in Fig. 2E. These peaks disappeared when the HbA_0 fraction was further dialysed against saline for 1 day. Fraction 4 of the haemolysate sample decreased after dialysis against saline, but did not disappear, as in the HbA_0 fraction sample (Fig. 2E). It may represent various other forms of haemoglobin which are eluted together with L-A_{1c} in fraction 4. These results suggest that in patients who have wide fluctuations of blood glucose, the levels of fractions 2, 4 and 7 can be highly variable. In contrast, the level of fraction 5 is very stable. Therefore, to obtain an accurate reflection of long-term blood glucose control, it may be necessary to measure only St-A_{1c}. This method enabled us to measure St-A_{1c}, distinguished from L-A_{1c} and

HbF, without pretreatment to remove L-A_{1c}. In 142 subjects with normal fasting plasma glucose and normal response to a 75-g oral glucose tolerance test, the range of St-A_{1c} levels (mean ± 2S.D.) was 2.80–3.98%.

One of the advantages of the method presented here is an improvement in the purity of St-A_{1c}. This is clearly illustrated in the chromatographic patterns of haemoglobin samples from normal subjects and patients, as shown in Fig. 3. In diabetic patients the level of fraction 5 was high and uninfluenced by incubation with glucose or dialysis against saline (Fig. 3B).

Fig. 3C is a chromatogram of a haemolysate from a normal subject, which shows high level of fraction 3. This peak was identified as HbF by its alkaline resistance and elution behaviour. Samples showing elevated HbF values, as in Fig. 3C, accounted for about 6% of all the samples analysed. Even in these instances the method made it possible to determine St-A_{1c} accurately.

An elevation of fractions 4 and 7 in the haemolysate from patients with renal failure was observed, as shown in Fig. 3D. Increases in these fractions were also observed when glucose incubation of erythrocytes was carried out as stated above. However, in this instance, the blood glucose levels of the patients were within the normal range. Hence the increase was not due to hyperglycaemia. Whereas L-A_{1c} disappeared after saline incubation of erythrocytes or dialysis of a haemolysate before measurement, the amounts of these fractions hardly decreased. Hence it seems that carbamylated haemoglobins which is formed by combination of haemoglobin and cyanic acid, originating from urea, was eluted in the same position as L-A_{1c}. Several other investigators have reported that in patients with renal failure HbA_1 or HbA_{1c} was often observed to be present in large amounts in site of normal blood glucose levels[7,8]. These unreasonable results are considered to be caused by a failure to separate fraction 4, whose amount increases in cases of renal failure, from HbA_1 or HbA_{1c} by their method.

A chromatogram of haemoglobin from a patient with β-thalassaemia is shown in Fig. 3E. It was different from that from a normal person. HbS was eluted after HbA_0
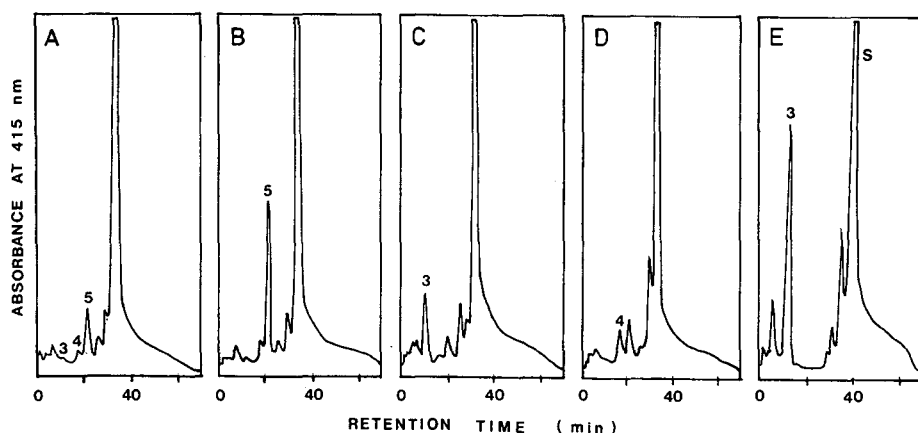
Fig. 3. Separations of haemoglobins from normal persons and patients. (A) Normal adult; (B) diabetic subject; (C) normal subject with high level of HbF; (D) patient with renal failure; (E) patient with β-thalassaemia.

and the amount of HbF was found to be high. Although this method was not designed for the detection of abnormal haemoglobins, it is considered that it could be a useful method for this purpose with further modification of the chromatographic conditions.

In summary, the chromatographic method developed here gave excellent resolution between L-A_{1c} and St-A_{1c}. This made it possible to determine St-A_{1c} levels accurately in normal persons and patients. This method enables characteristic chromatographic patterns of haemoglobin in patients to be obtained. However, there is a minor problem concerning custom-made columns and the difficulty that might arise with some clinical applications.

Prepacked CM columns, ES-502C (Asahi Kasei Industries) IEX-530CM (TOSOH, Tokyo, Japan), which are now commercially available, gave similar chromatographic patterns of haemoglobin in normal persons and patients to those obtained with the custom-made column packed with DVT-119. However, the resolution between St-A_{1c} and L-A_{1c} was very poor in the prepacked columns compared with that from the custom-made column.

REFERENCES

1 D. E. Goldstein, S. B. Peth, J. D. England, R. L. Hess and J. D. Costa, *Diabetes*, 29 (1980) 623–628.
2 P. A. Sevendsen, J. S. Christiansen, U. Soegaard, B. S. Welinder and J. Nerup, *Diabetologia*, 19 (1980) 130–136.
3 D. M. Nathan, E. S. Avezzano and J. L. Palmer, *Diabetes*, 30 (1981) 700–701.
4 T. Hoshino, M. Ueki and S. Amemiya, *Proc. Symp. Chem. Physiol. Pathol.*, 21 (1981) 103–109.
5 T. Hoshino, S. Amemiya, M. Ueki, K. Kato and S. Toyoshima, *Tohoku J. Exp. Med.*, 141 (Suppl.) (1983) 85–90.
6 L. A. Trivelli, H. M. Ranney and H. T. Lai, *N. Engl. J. Med.*, 284 (1971) 353–357.
7 G. Schernthaner, H. K. Stummvoll and M. M. Muller, *Lancet*, i (1979) 774.
8 M. Oimomi, K. Ishikawa, T. Kawasaki, S. Kubota, K. Takagi, G. Tanke, Y. Yoshimura and S. Baba, *Jpn. J. Nephrol.*, 25 (1983) 1343–1347.

Isolation and identification of urinary nucleosides

Applications of high-performance liquid chromatographic methods to the synthesis of 5'-deoxyxanthosine and the simultaneous determination of 5,6-dihydrouridine and pseudouridine

KATSUYUKI NAKANO* and TOSHIO YASAKA

Perfect Liberty (PL) Comprehensive Research Institute, 1 Kamiyamacho, Tondabayashi, Osaka 584 (Japan)

KARL H. SCHRAM, MARK L. J. REIMER and THOMAS D. McCLURE

Department of Pharmaceutical Sciences, College of Pharmacy, University of Arizona, Tucson, AZ 85721 (U.S.A.)

and

TERUTOSHI NAKAO and HIDEKI YAMAMOTO

Department of Surgery, PL Hospital, 2182 Shindo, Tondabayashi, Osaka 584 (Japan)

ABSTRACT

Modified nucleosides from pooled normal human urine were extracted using a boronate affinity gel column and fractionated by reversed-phase high-performance liquid chromatography (RP-HPLC). The major constituents in each of the 30 RP-HPLC fractions were determined by gas chromatography–mass spectrometry of the trimethylsilyl derivatives of the fractions. The same RP-HPLC method was used in the synthesis of 5'-deoxyxanthosine from authentic 5'-deoxyadenosine. In addition, the simultaneous determination of urinary 5,6-dihydrouridine (D) and pseudouridine (Ψ) was carried out by RP-HPLC using two ODS columns in series. The level of D in pooled normal urine was 4.87 nmol/μmol creatinine. The RP-HPLC method was applied to the measurement of D and Ψ levels in urines collected before and after surgery from four patients with gastrointestinal cancer. A large decline in both nucleoside levels in urines after surgery was observed in three of the four cancer patients.

INTRODUCTION

Modified nucleosides excreted in human urine have been studied to examine their biomedical significance as possible biomarkers of cancer[1–7] and certain immunodeficiency diseases[8], including AIDS[9,10]. In human urine, about 20 out of

more than 40 urinary nucleosides are known to be derived from tRNAs. Among them, several modified nucleosides occurring at comparatively high levels such as pseudo-uridine (Ψ), 1-methyladenosine (m^1A), 1-methylinosine (m^1I), N^2-methylguanosine (m^2G) and N^2,N^2-dimethylguanosine (m_2^2G), have frequently been used to examine the differences between urinary nucleoside levels of cancer patients and normal subjects. Studies monitoring the correlation between urinary levels of these nucleosides and the degree of tumour involvement or response to therapy have also been performed[2–7,11].

In addition, more than ten urinary modified nucleosides derived from other biochemical processes not related to tRNA have been found. Recently, the presence of the unusual nucleosides 5'-deoxyinosine (5'-dI)[12], 5'-deoxy-5'-methylthioadenosine sulphoxide[12,13] and 7-β-D-ribofuranosylhypoxanthine[14] in human urine has been reported. The origin of these nucleosides is not known to occur from any biochemical metabolism. Chheda *et al.*[12] suggested that one possible source of 5'-dI in mammals appeared to be 5'-deoxyadenosine (5'-dA), which is liberated from coenzyme-vitamin B_{12}, adenosylcobalamin.

Through our collaborative studies on the isolation and identification of urinary nucleosides in human urines, 3-methyluridine (m^3U)[15] and the novel nucleoside 5'-deoxyxanthosine (5'-dX)[16] were detected by means of gas chromatography–mass spectrometry (GC–MS) analysis following partial purification by boronate gel affinity chromatography and reversed-phase high-performance liquid chromatography (RP-HPLC). In addition, 5,6-dihydrouridine (D) was recently identified in pooled normal human urine by GC–MS[17]. Although D is present in the tRNAs of most organisms, and is second in abundance to Ψ among the modified nucleosides in tRNAs, there was little evidence of the presence of D in human urines; a thin-layer chromatographic method has been used for the determination of D in tRNAs[18,19] and LC–MS for the detection of D in human urine[20].

In this paper, we describe methods used for the isolation and identification of nucleosides in pooled normal human urines, the RP-HPLC analysis of 5'-dX synthesized from authentic 5'-dA and the simultaneous determination of urinary D and Ψ by another RP-HPLC method.

EXPERIMENTAL

Chemicals and standards

Ammonium acetate, formic acid, methanol (HPLC grade) and acetonitrile (HPLC grade) were purchased from Wako (Osaka, Japan), A Wako Creatinine Test Kit using the Jaffe method was used for the measurement of urinary creatinine. Authentic samples of D, m^1A, Ψ, 5'-dA, purine nucleoside phosphorylase (PNP; N3003, from bovine spleen) and xanthine oxidase (XO; X1875) were purchased from Sigma (St. Louis, MO, U.S.A.). A milli-Q reagent water system (Millipore, Bedford, MA, U.S.A.) was used for water purification.

Urine collection

For the isolation of urinary nucleosides, a 188-ml aliquot of pooled normal urine obtained from more than 300 apparently normal male and female subjects at the PL Osaka Health Control Centre was centrifuged to remove particulate matter and stored at $-20°C$ prior to analysis.

Urine samples (24-h) were collected 4 or 5 days before and 8 or 9 days after surgical operations on two gastric cancer patients and two sigmoid colon cancer patients at the PL Hospital, and used for the determination of urinary D and Ψ.

The case history of cancer patients is briefly summarized as follows. Case No. 1: sigmoid colon cancer (well differentiated adenocarcinoma); stage, Dukes A; resection, absolutely curative; carcinoembryonic antigen (CEA), 1.8 ng/ml (pre-surgery), 1.0 ng/ml (post-surgery). Case No. 2: gastric cancer (moderately differentiated tubular adenocarcinoma); stage, Ia (TNM classification of International Union Against Cancer); resection, absolutely curative; CEA, 2.3 ng/ml (pre-surgery), 2.9 ng/ml (post-surgery). Case No. 3: gastric cancer (signet-ring cell carcinoma, scirrhous type); stage, IV (TNM classification); resection, absolutely non-curative; CEA, not quantitated (pre-surgery), 13.6 ng/ml (post-surgery). Case No. 4: sigmoid colon cancer (mucinous carcinoma); stage, Dukes B; resection, absolutely curative; CEA, 2.9 ng/ml (pre-surgery), 0.8 ng/ml (post-surgery).

Boronate gel affinity chromatography

The boronate gel affinity chromatographic methods used to isolate the urinary nucleosides were a modification of a published procedure[11]. Affi-gel 601 (Bio-Rad Labs., Richmond, CA, U.S.A.) possessing a specific affinity for *cis*-hydroxyl groups was packed in a plastic column (60 × 9 mm I.D.; 1.66 ml bed volume) and equilibrated with 20 ml of 0.25 M ammonium acetate (pH 8.8). A 20-ml aliquot of urine adjusted to pH 8.8 with 4 ml of 2.5 M ammonium acetate (pH 9.5) was centrifuged to remove precipitable material and its supernatant was loaded onto the column. The sample tube and column were then washed with 3 and 7 ml of 0.25 M ammonium acetate (pH 8.8) and the nucleosides were eluted with 7 ml of 0.2 M formic acid. The eluate was evaporated under reduced pressure and the residue dissolved in 1 ml of water for HPLC purification. However, in the experiments for the determination of urinary D, the boronate column extract was lyophilized. The sample was passed through an ultrafiltration membrane filter (Nihon Millipore Kogyo, Yonezawa, Japan) just before the HPLC fractionation in order to remove macromolecules.

RP-HPLC fractionation of urinary nucleosides

The RP-HPLC conditions for fractionation of the urinary nucleosides were as follows: an LC-6A HPLC instrument (Shimadzu, Kyoto, Japan); two pumps; an SCL-6A system controller; an SPD-6AV UV–VIS detector; a C-R6A Chromatopac integrator; a Develosil ODS-5 (5 μm) column (250 × 4.6 mm I.D.) (Nomura Chemicals, Nagoya, Japan); a Develosil ODS (15–30 μm) precolumn (50 × 4.0 mm I.D.); linear gradient elution from water at 0 min to methanol–water 13:87 (v/v) at 25 min, methanol–water 45:55 (v/v) at 35 min and water at 40 min; flow-rate 1.1 ml/min; sample injection volume 300 or 350 μl; and UV detection at 260 nm (0.64 a.u.f.s.). A total of 30 HPLC fractions were collected and lyophilized for GC–MS analysis.

Preparation of reference sample 5'-dX from 5'-dA

A reference sample of 5'-dI was prepared by the deamination of 5'-dA with sodium nitrite[21]. A 10-mg amount of authentic 5'-dA was dissolved in 4 ml of 3.5 M acetic acid and treated with 4 ml of 4 M sodium nitrite at 25°C for 2.5 h. The product was purified and isolated using the RP-HPLC method as described above, and the

structure of the sample was confirmed by comparing the GC–MS analysis of the trimethylsilyl (TMS) derivative with data from the literature[12].

5-Deoxyribose-1-phosphate (5-dR-1-P) was obtained by the enzymatic cleavage of 5′-dI using a modification of a literature method[22]. The reaction mixture for the preparation of 5-dR-1-P contained 0.6 mmol 5′-dI, 2.5 units of PNP, p 0.125 units of XO and 50 mM potassium phosphate buffer (pH 7.5 adjusted using 5 M sodium hydroxide) in a total volume of 5 ml. Prior to the reaction, the two enzymes had been dialysed against 50 mM phosphate buffer (pH 7.5) to remove ammonium sulphate. The reaction was allowed to proceed for 12 h at 23°C on a rotary shaker. Following the reaction, the enzymes were removed by an ultrafiltration membrane. Inorganic phosphate was precipitated by strictly maintaining the pH between 8 and 9 through the addition of either saturated barium hydroxide or 1 M barium acetate. The mixture containing 5-dR-1-P was used without further purification in the synthesis of 5′-deoxyguanosine (5′-dG).

5′-dG was prepared[22] by the reaction of 140 μmol of guanine with 80 μmol of 5-dR-1-P in the presence of 4 units of PNP in 10 mM Tris–HCl (pH 7.5) in a total volume of 20 ml. The reaction was carried out at 23°C for 5 h on a rotary shaker. 5′-dG was isolated using RP-HPLC and the structure of the product was confirmed by GC–MS. 5′-dG was then deaminated using sodium nitrite as described earlier[21]. Attempts to couple xanthine directly to 5-dR-1-P using PNP were unsuccessful.

GC–MS analysis

The methods and results of the GC–MS analyses for the TMS derivatives of the RP-HPLC nucleoside fractions have been described elsewhere[15–17].

RP-HPLC analysis of urinary D and Ψ

For the determination of urinary D and Ψ, two Capcell Pak C_{18} (5 μm) columns (250 × 4.6 mm I.D.) (Shiseido, Tokyo, Japan) were used in series. The urinary nucleoside samples were analysed using isocratic elution with water alone at a flow-rate of 0.8 ml/min. After 20 min the columns were washed with a gradient of acetonitrile–water. UV detection was performed at 230 nm (0.04 a.u.f.s.). A precolumn (20 × 4.6 mm I.D.) packed with 15–30-μm Develosil ODS was fitted between the injector and the analytical column.

RESULTS AND DISCUSSION

HPLC analysis of urinary nucleosides

Urinary nucleosides extracted with the boronate gel column were fractionated by RP-HPLC. Water–methanol was adopted as mobile phase for RP-HPLC to simplify sample preparation for the subsequent GC–MS analysis. Fig. 1 shows a typical RP-HPLC trace for urinary nucleoside extract. A total of 30 peaks present in pooled normal urine were numbered as shown in Fig. 1.

GC–MS analyses of these HPLC fractions revealed that some of the fractions included well known nucleosides and bases as major constituents: HPLC fraction No. 1, m^{1}A; No. 2, Ψ; No. 2.5, hypoxanthine; No. 3, uric acid; No. 4, uridine (U); No. 9, inosine (I); No. 10, 1-ribosylpyridin-4-one-3-carboxamide (4,3-PCNR) + guanosine (G); No. 11, m^{3}U[15]; No. 12, m^{1}I; No. 14, m^{1}G; No. 15, adenosine (A) + xanthosine (X); No. 16, m$^2_2$G; and No. 18, 5′-dX[16].
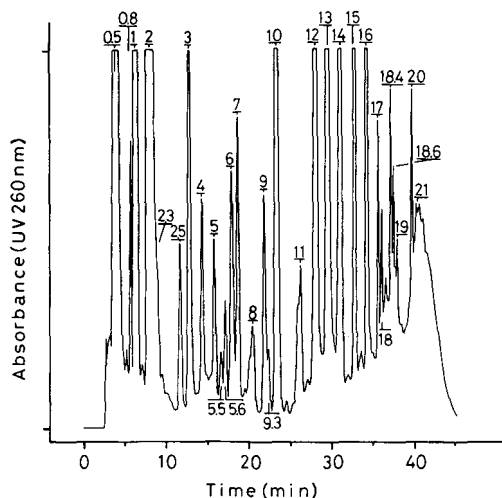
Fig. 1. Preparatory HPLC separation of a nucleoside sample in pooled normal human urine. Injection volume: 350 μl of nucleoside sample, corresponding to nucleosides present in 7 ml of original urine. UV detection at 260 nm (0.64 a.u.f.s.). For other chromatographic conditions, see Experimental.

Several unknown nucleosides were also revealed by the GC–MS analysis of the HPLC fractions. The structures of these unknown nucleosides are now under investigation.

The RP-HPLC fraction No. 1 (retention time 6.6 min) exhibited an absorption maximum at 257 nm, corresponding to the λ_{max} of m[1]A. However, as reported previously[17], the GC–MS examination of HPLC fraction No. 1 indicated the presence of D in addition to m[1]A. The presence of D was also confirmed in HPLC fraction No. 2, which contained Ψ as a major nucleoside. From this evidence, D was considered to be eluted between peaks 1 and 2 detected at 260 nm.

HPLC analysis for the preparation of 5'-dX

For the identification of urinary 5'-dX, the nucleoside was synthesized from an authentic sample of 5'-dA. Fig. 2 shows the RP-HPLC traces of an authentic 5'-dA and 5'-dI formed by sodium nitrite deamination of 5'-dA.

Fig. 3 shows the RP-HPLC separation of enzymatically synthesized 5'-dG and 5'-dX resulting from deamination of 5'-dG. 5'-dG and 5'-dX were purified by RP-HPLC and confirmed by GC–MS[16,23]. The UV absorption spectra of the 5'-dX thus obtained and the reference sample of X are shown in Fig. 4. Significant differences between the spectrum of 5'-dX and that of X were observed.

RP-HPLC analysis of urinary D and Ψ

Because D was not resolved from m[1]A and Ψ under the HPLC conditions in Fig. 1, the HPLC determination of urinary D was further developed. As D does not exhibit UV absorption around 260 nm, 230 nm (corresponding to the λ_{min} of Ψ) was selected as the detection wavelength for urinary D. The following HPLC conditions for the separation of D and Ψ were examined using mainly a Develosil ODS column: cations, anions, pH, ionic strength of buffers, organic solvents used as mobile phase, column
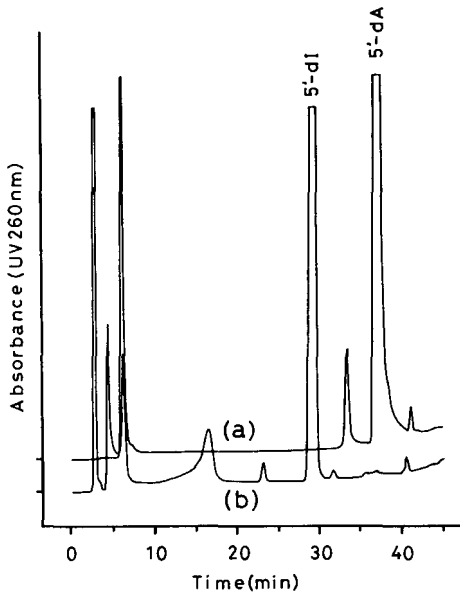
Fig. 2. HPLC separation of authentic sample of 0.995 · 10^{-2} M 5'-deoxyadenosine in 3.5 M acetic acid (a) and 5'-deoxyinosine in the reaction mixture prepared by deamination of 5'-deoxyadenosine with sodium nitrite (b). UV detection at 260 nm (0.04 a.u.f.s.). Injection volume: 5 μl. For other chromatographic conditions, see Experimental.
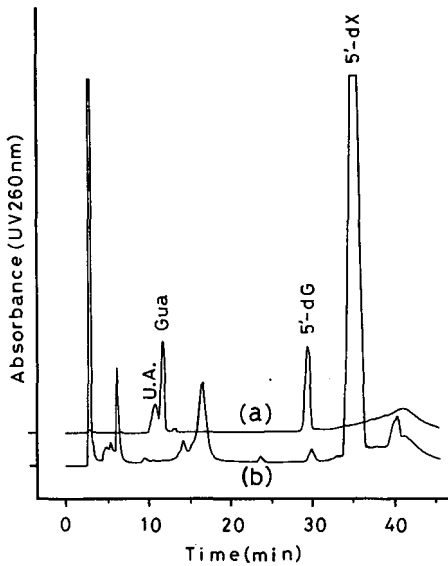
Fig. 3. HPLC separation of 5'-deoxyguanosine in the reaction mixture of 5-deoxyribose-1-phosphate and guanosine catalysed by purine nucleoside phosphorylase (a) and 5'-deoxyxanthosine in the reaction mixture prepared by deamination of 5'-deoxyguanosine with sodium nitrite (b). UV detection at 260 nm (0.04 a.u.f.s.). Injection volume: (a) 20 μl and (b) 5 μl. For other chromatographic conditions, see Experimental.
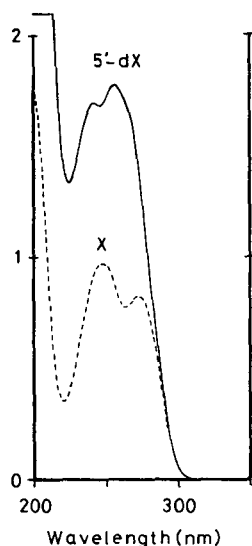
Fig. 4. Absorption spectra of 5′-deoxyxanthosine in water (solid line) and $1.0 \cdot 10^{-4}$ M authentic xanthosine in 0.01 M KH$_2$PO$_4$, pH 6.1 (broken line).

temperature, counter ions for ion-pair techniques; and stationary phases in columns from several suppliers.

When the reversed-phase column was used, elution with water alone as the mobile phase gave a fairly good separation; the use of buffers and organic solvents shortened the retention times of both D and Ψ compared with those obtained using water alone. However, the use of a single column did not provide a sufficient separation of the two nucleosides.

Finally, the use of two Capcell Pak C$_{18}$ columns in series gave an adequate separation for the quantitative analysis of urinary D and Ψ. Fig. 5 shows a chromatographic separation of D (retention time 14.4 min) and Ψ (retention time 15.7 min) in a nucleoside sample from 40 μl of pooled normal human urine, and a chromatogram of a nucleoside sample co-injected with an authentic sample of D. HPLC detection at 230 nm showed equal peak heights (or areas) for authentic samples of D and Ψ prepared at the same concentrations.

The recovery of authentic D using boronate gel column extraction of an aqueous solution of D was found to be 100%. After repeated analyses of standard solutions of D and Ψ with several known concentrations, a calibration graph was obtained to determine the levels of urinary D and Ψ using an external standard method. Both plots resulted in straight lines passing through the origin for samples concentrations up to 10 nmol.

Urinary D and Ψ levels of cancer patients

Fig. 6 shows a chromatogram of D and Ψ in nucleoside samples from urines collected before and after a surgical operation on a patient with malignant gastric cancer. In the analysis, the creatinine level (Jaffe method) in 20 μl of pre-operative
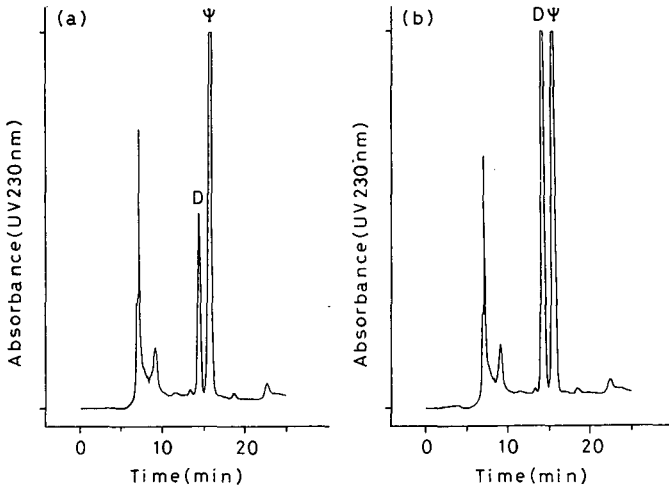
Fig. 5. HPLC separation of 5,6-dihydrouridine and pseudouridine in a nucleoside sample from pooled normal human urine (a) and a nucleoside sample co-injected with 4.06 nmol of authentic 5,6-dihydrouridine (b). Injection volume: 10 μl of nucleoside sample, corresponding to nucleoside present in 40 μl of original urine. UV detection at 230 nm (0.04 a.u.f.s.). Column conditions and elution gradients are given under Experimental.

sample injected (corresponding to 80 μl of original urine) was the same as that in the pooled normal human urine shown in Fig. 5, but that in the post-operative sample was about two-thirds of that level.

The levels of D and Ψ in urines collected before and after surgery from four
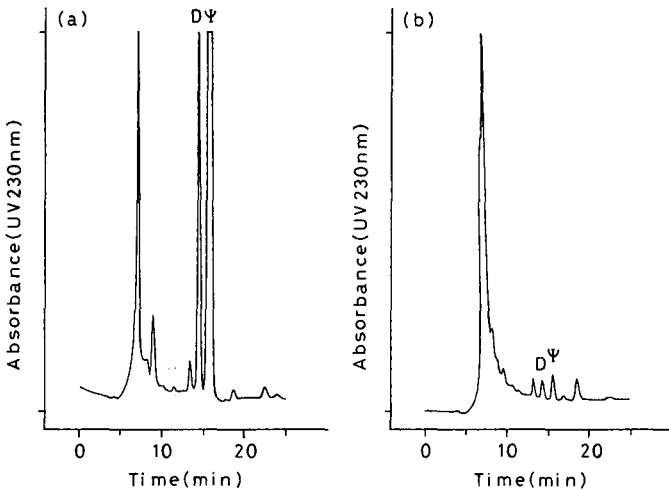
Fig. 6. HPLC separation of 5,6-dihydrouridine and pseudouridine in a nucleoside sample from urines collected before (a) and after (b) surgical procedures on a patient with malignant gastric cancer. Injection volume: 20 μl, corresponding to nucleoside present in 80 μl of original urine. UV detection at 230 nm (0.04 a.u.f.s.). Column conditions and elution gradients are given under Experimental.
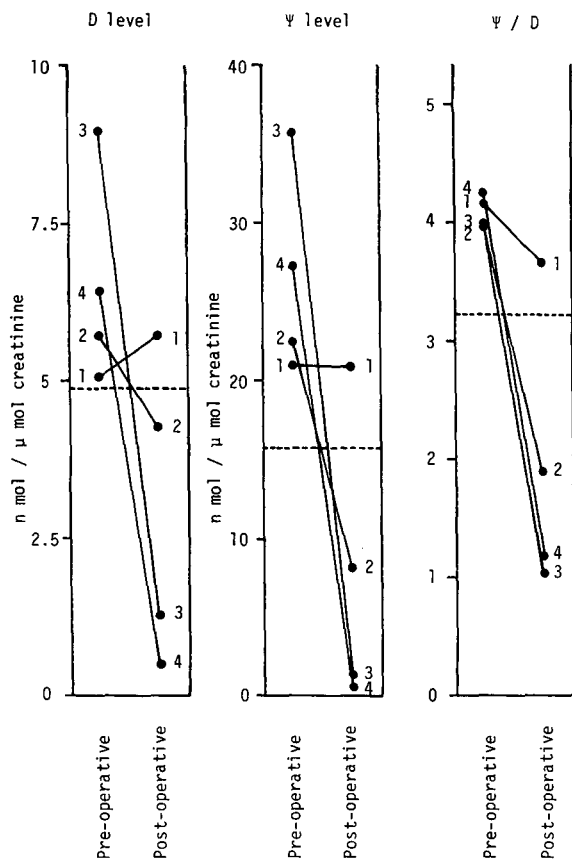
Fig. 7. Levels of urinary 5,6-dihydrouridine (D) and pseudouridine (Ψ) and Ψ/D molar ratio in four pre- and post-operative patients with gastrointestinal cancer. The broken lines indicate data from pooled normal human urine. The numbers 1–4 correspond to the case numbers given under Experimental.

patients with malignant gastrointestinal cancer were determined by the RP-HPLC method described above, and then normalized by the urinary creatinine level of each urine sample. Fig. 7 shows a comparison of normalized urinary D and Ψ levels and the Ψ/D ratio in the pre- and post-operative cancer patients. Compared with our previous report[11], a large decrease in both nucleoside levels in urines after surgery was observed in three of the cancer patients (Nos. 2–4 in Fig. 7) in a comparatively advanced stage. The other cancer case (No. 1 in Fig. 7), exhibiting no significant change in urinary D and Ψ levels, was diagnosed as a early stage of sigmoid colon cancer. These results seem to indicate a direct relationship between the change in urinary D and Ψ levels before and after surgical operation and the cancer burden or the turnover rate of cancer cells.

In this experiment, the rates of change of D levels before and after surgery appear to be almost the same as those of the Ψ levels. The decrease in the Ψ/D molar ratio after surgery compared with that before surgery, as seen in Fig. 7, suggests that tRNAs in cancer cells have a higher molar content of Ψ than D.

ACKNOWLEDGEMENTS

REFERENCES

 1 C. W. Gehrke, K. C. Kuo, T. P. Waalkes and E. Borek, *Cancer Res.*, 39 (1979) 1150.
 2 J. Speer, C. W. Gehrke, K. C. Kuo, T. P. Waalkes and E. Borek, *Cancer*, 44 (1979) 2120.
 3 D. A. Heldman, M. R. Grever, C. E. Speicher and R. W. Trewyn, *J. Lab. Clin. Med.*, 101 (1983) 783.
 4 E. Borek, O. K. Sharma and T. P. Waalkes, *Recent Results Cancer Res.*, 84 (1983) 301.
 5 F. Salvatore, A. Colonna, F. Costanzo, T. Russo, F. Esposito and F. Cimino, *Recent Results Cancer Res.*, 84 (1983) 360.
 6 T. P. Waalkes, M. D. Abeloff, D. S. Ettinger, K. B. Woo, C. W. Gehrke, K. C. Kuo and E. Borek, *Eur. J. Cancer Clin. Oncol.*, 18 (1982) 1267.
 7 T. Rasmuson, G. R. Björk, L. Damber, S. E. Holm, L. Jacobsson, A. Jeppsson, T. Stigbrand and G. Westman, *Acta Radiol. Oncol.*, 22 (1983) 209.
 8 G. C. Mills, F. C. Schwalstieg and R. M. Goldblum, *Biochem. Med.*, 34 (1985) 37.
 9 F. Esposito, T. Russo, R. Ammendola, A. Duilio, F. Salvatore and F. Cimino, *Cancer Res.*, 45 (1985) 6260.
10 E. Borek, O. K. Sharma, F. L. Buschman, D. L. Cohen, K. A. Penley, F. N. Judson, B. S. Dobozin, C. R. Horsburgh, Jr. and C. H. Kirkpatrick, *Cancer Res.*, 46 (1986) 2557.
11 K. Nakano, K. Shindo, T. Yasaka and H. Yamamoto, *J. Chromatogr.*, 332 (1985) 127; 343 (1985) 21.
12 G. B. Chheda, H. B. Patrzyc, A. K. Bhargava, P. F. Crain, S. K. Sethi, J. A. McCloskey and S. P. Dutta, *Nucleosides Nucleotides*, 6 (1987) 597.
13 J. S. Mills, G. C. Mills and D. J. McAdoo, *Nucleosides Nucleotides*, 2 (1983) 465.
14 G. B. Chheda, S. P. Dutta, A. Mittelman, J. A. Montgomery, S. K. Sethi, J. A. McCloskey and H. B. Patrzyc, *Cancer Res.*, 45 (1985) 5958.
15 T. D. McClure, K. H. Schram, K. Nakano and T. Yasaka, *Nucleosides Nucleotides*, 8 (1989) 1417.
16 T. D. McClure, K. H. Schram, K. Nakano and T. Yasaka, *Nucleosides Nucleotides*, 8 (1989) 1399.
17 M. L. J. Reimer, K. H. Schram, K. Nakano and T. Yasaka, *Anal. Biochem.*, 181 (1989) 302.
18 P. Cerutti, Y. Kondo, W. R. Landis and B. Witkop, *J. Am. Chem. Soc.*, 90 (1968) 771.
19 W.-C. Tseng, D. Medina ad K. Randerath, *Cancer Res.*, 38 (1978) 1250.
20 E. L. Esmans, P. Geboes, Y. Luyten and E. C. Alderweireldt, *Biomed. Mass Spectrom.*, 12 (1985) 241.
21 R. E. Holmes and R. K. Robins, *J. Am. Chem. Soc.*, 87 (1965) 1772.
22 J. D. Stoeckler, C. Cambor and R. E. Parks, *Biochemistry*, 19 (1980) 102.
23 M. L. J. Reimer, T. D. McClure and K. H. Schram, *Biomed. Environ. Mass Spectrom.*, 17 (1989) 533.

CHROMSYMP. 1887

Simple method for determination of the cephalosporin DQ-2556 in biological fluids by high-performance liquid chromatography

KYUICHI MATSUBAYASHI*, MARIKO YOSHIOKA and HARUO TACHIZAWA

Research Institute, Daiichi Pharmaceutical Co., Ltd., 1-16-13 Kitakasai, Edogawa-ku, Tokyo 134 (Japan)

ABSTRACT

A sensitive method for the determination of DQ-2556 by high-performance liquid chromatography was established. The limits of detection for serum and urine were 0.1 and 2 μg/ml, respectively. Two clean-up procedures for serum samples were developed. In the first, deproteinization with 10% trichloroacetic acid was used and the recovery was 68.5%. In the other, ultrafiltration under acidic conditions was employed and the recovery was 85.1%. The former procedure is economical but complicated, whereas the latter is simple and labour-saving, but a special ultrafiltration tube is required. This situation offers a flexible choice, depending on the conditions of the laboratory.

INTRODUCTION

DQ-2556, (6R,7R)-7-[(Z)-2-(2-aminothiazol-4-yl)-2-(methoxyimino)acetamido]-3-[4-(oxazol-5-yl)-1-pyridinio]methyl-8-oxo-5-thia-1-azabicyclo[4.2.0]oct-2-ene-2-carboxylate (**I**), a new cephalosporin, has a broad antibacterial spectrum, including activity against *Pseudomonas aeruginosa*[1], and is currently under clinical trials in Japan. It is difficult to develop a method for the determination of **I** in biological samples because of its high hydrophilicity. As a part of a study on the pharmacokinetics of the drug, a sensitive high-performance liquid chromatographic (HPLC) method was developed for routine use. A large number of samples must be analysed in a short period in clinical trials to evaluate the pharmacokinetics of a drug and to plan subsequent trials. This paper offers both a traditional and a labour-saving procedure for the clean-up of serum samples.

EXPERIMENTAL

Chemicals and reagents
The sulphate of compound **I** was synthesized by the Research Institute, Daiichi Pharmaceutical (Tokyo, Japan)[2] and S-p-nitrobenzyl-L-cysteine (**II**) was prepared by

DQ-2556 (I)

S-p-Nitrobenzyl-L-cysteine
(II)

3-Amino-4-methylbenzoic acid
(III)
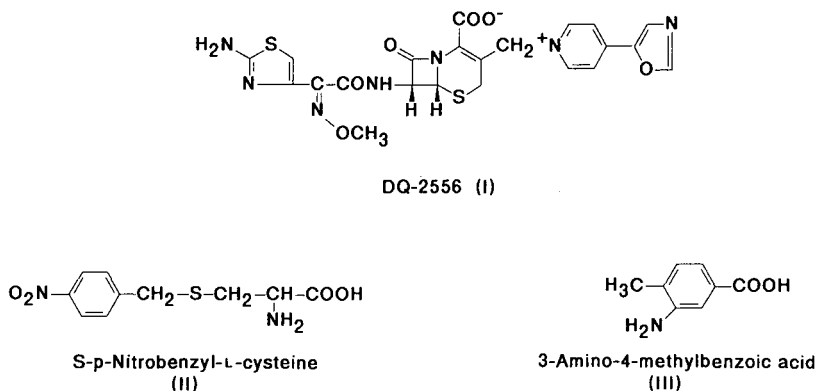
Fig. 1. Structures of DQ-2556 and internal standards.

the method of Berse *et al.*[3] with slight modifications. The sources of other materials used were as follows: 3-amino-4-methylbenzoic acid (**III**) and trichloroacetic acid from Tokyo Kasei Kogyo (Tokyo, Japan), ultrafiltration tubes (Ultrafree C3TK, molecular weight cut-off 30 000 Da) from Nihon Millipore (Tokyo, Japan) and lyophilized human serum (Consera) from Nissui Seiyaku (Tokyo, Japan). The lyophilized serum was dissolved in distilled water just before use as a control serum. Serum was obtained from healthy volunteers by a doctor with informed consent. Chemicals and solvents were of analytical-reagent grade.

HPLC apparatus and conditions

HPLC analysis was performed with an SP8700 solvent delivery system (Spectra Physics, San Jose, CA, U.S.A.), equipped with a Type AS-48 automatic sample injector, fitted with a 50-μl loop (Tosoh, Tokyo, Japan) and a Model 638-41 variable-wavelength UV detector (Hitachi, Tokyo, Japan). The detector was coupled with a FACOM S-3300 computer system (Fujitsu, Tokyo, Japan). The chromatographic system was equipped with a precolumn, fitted with an MPLC New Guard Cartridge RP-8 (Brownlee Labs., Santa Clara, CA, U.S.A.) and a stainless-steel column (15 cm × 4.6 mm I.D.) packed with 5-μm octadecylsilica (TSK gel ODS-80TM) (Tosoh). The mobile phase was acetonitrile–0.02 M acetic acid (8:92, v/v) and the flow-rate was 1.2 ml/min for serum. The retention times were 9, 18 and 14 min for **I**, **II** and **III**, respectively. For urine, the mobile phase was acetonitrile–water (11:89, v/v) and the flow-rate was 0.8 ml/min. The retention times were 8 and 17 min for **I** and **II**, respectively.

Sample preparation

Serum. In procedure A, to 0.5 ml of serum in a 10-ml glass centrifuge tube, 0.5 ml of a 10% solution of trichloroacetic acid, containing **II** at a concentration of 100 μg/ml, was added and mixed on a vortex mixer for 1 min. After centrifugation at 1500 g at 4°C for 10 min, the supernatant was transferred to another centrifuge tube. The supernatant was extracted with 7 ml of diethyl ether and centrifuged (1500 g, 10 min, 4°C). The organic layer was discarded and the aqueous layer was transferred to 1-ml

sample tube. The tube was set on the automatic sample injector and a 50-μl portion was analysed by HPLC.

In procedure B, a 0.2-ml portion of serum was transferred to the inner cell of the ultrafiltration tube, the bottom of which was made of an ultrafiltration membrane. and acidified with 0.2 ml of 3 M acetic acid containing 150 μg/ml of **III** as the interna: standard. After centrifugation for 2 h at 5000 g at 4°C, the inner cell was discarded and the outer tube, which contained the collected filtrate at the bottom, was set on the tray of an automatic sample injector.

Urine. Urine samples were diluted 5-fold with distilled water, if necessary, and centrifuged. To 0.25 ml of urine, 0.25 ml of a 40 μg/ml (for samples in which the concentrations of **I** were $\leqslant 80$ μg/ml) or 400 μg/ml (for samples in which the concentrations of **I** were > 80 μg/ml) solution of **II** was added and a 50-μl portion of the mixture was injected into the HPLC system.

Calibration graph

The standard serum samples were prepared by dissolving **I** in control serum at concentrations of 0.30, 0.59, 1.19, 2.37, 4.74, 9.48, 18.96, 37.93, 75.86, 151.7 and 303.4 μg/ml. Three 0.5-ml portions of standard sample at each concentration were processed as described in the sample preparation section. A calibration graph was obtained by plotting the peak-area ratios (**I/II** or **I/III**) against the concentrations of **I** in the standard samples.

Standard urine samples were prepared by dissolving **I** at concentrations of 2.54, 5.07, 10.14, 20.29, 40.58 and 81.15 μg/ml or 25.4, 50.7, 101.4, 202.9, 405.8 and 811.5 μg/ml. Three 0.25-ml portions of the standard samples were treated as described in the sample preparation section. The calibration graph was obtained in the same way as for serum.

Recovery in serum sample preparation

The absolute recovery in the serum sample clean-up procedure A was measured as follows. Blank serum was spiked with **I** at concentrations in the range 0.3–303.4 μg/ml. A 0.5-ml volume of each sample was processed as described in the sample preparation section. An aqueous solution with the same concentration of **I** as the serum was processed in the same manner. The peak area of **I** observed in the chromatogram of the serum sample was compared with that observed in the chromatogram of the aqueous solution.

For procedure B, the recovery was examined as follows. Blank serum was spiked with **I** in the same manner as in procedure A, and 0.2 ml of each sample was processed as described in procedure B in the sample preparation section. The peak area of **I** observed in the chromatogram of the serum sample was compared with that of the standard solution. The standard solution was a mixture of equal volumes of 3 M acetic acid and an aqueous solution of **I** in which the concentration of **I** was the same as that of the spiked serum sample. The recovery was also examined in the case in which 3 M acetic acid in the procedure was replaced with 0.2 M acetate buffer of different pH or with different concentrations of acetic acid.

RESULTS AND DISCUSSION

Chromatographic conditions

Compound I showed tailing in the chromatogram when Nucleosil $5C_{18}$ was used as the stationary phase. It has both a quaternary amine group and a carboxyl group in the molecule, and electrostatic interactions between these ionized functional groups and silanol groups on the stationary phase are considered to be responsible for the tailing. The stationary phase was then changed to end-capped octadecylsilica, TSK gel ODS-80TM, in which silanol groups are fully silylated. Compound I was eluted as a sharp and symmetrical peak (Figs. 2 and 3). Serum samples were analysed by HPLC with an acidic eluent in order to elute the interfering substances in serum earlier than I. Urine samples could also be analysed in neutral medium with a mixture of acetonitrile and water as eluent. Modification of the eluent with acidic buffer was not effective, because urinary components were eluted near the retention time of I.

The chromatogram was monitored at 306 nm because the solution of I had an absorption maximum at this wavelength and the baseline was clear, whereas at 254 nm some interfering peaks were detected in the chromatogram.

Clean-up procedures for serum samples

Procedure A. The most frequently used clean-up procedures for cephalosporins in biological samples are extraction with organic solvents and precipitation of serum proteins by an organic solvent or trichloroacetic acid[4]. As the attempt to extract I was not successful on account of its high hydrophilicity, a precipitation procedure was chosen for clean-up. Precipitation of serum proteins with methanol or acetonitrile was not satisfactory, giving a fluffy precipitate in the supernatant when it was allowed to stand in the automatic sample injector. Therefore, a procedure consisting of precipitation with trichloroacetic acid and diethyl ether wash was developed. The internal standard for this procedure was expected not only to absorb at 306 nm but also
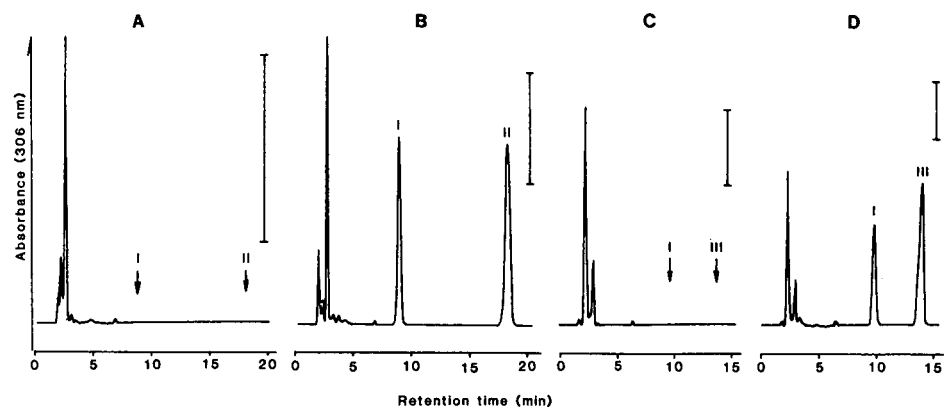
Fig. 2. Chromatograms of serum samples. (A) and (C) control; (B) spiked with 19.0 μg/ml of DQ-2556 and 100 μg/ml of S-*p*-nitrobenzyl-L-cysteine (II); (D) spiked with 20.6 μg/ml of DQ-2556 (I) and 150 μg/ml of 3-amino-4-methylbenzoic acid (III). Samples were processed by procedure A [(A) and (B)] or by procedure B [(C) and (D)]. Bars represent 0.1 absorbance.
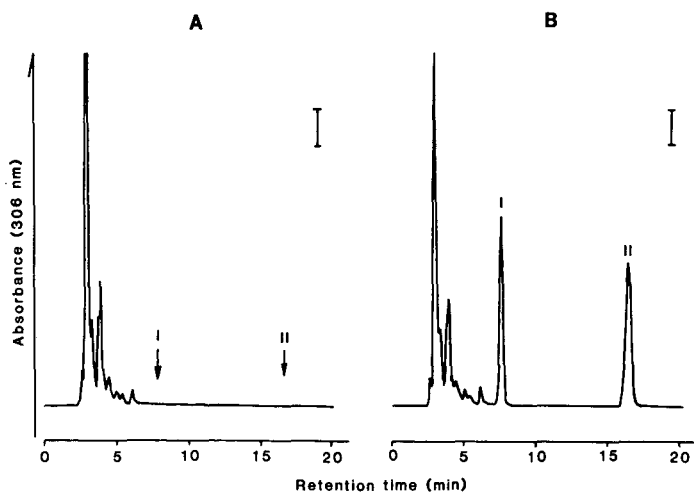
Fig. 3. Chromatograms of urine samples. (A) Control; (B) spiked with 101 μg/ml of DQ-2556 (**I**) and 400 μg/ml of *S*-*p*-nitrobenzyl-L-cysteine (**II**). Bars represent 0.1 absorbance.

to be hydrophilic so as not to be extracted with diethyl ether. Among many compounds tested, L-γ-glutamyl-*p*-nitroanilide, sulphathiazole and **II** were found to have acceptable chromatographic characeristics. Although the first two were commercially available, they were not sufficiently stable in the samples, even at low temperature (8°C). The UV spectrum of **II** showed a maximum absorbance at 280 nm, but even at 306 nm the absorbance was fairly large. This compound was stable for at least 2 days in acidic solutions of the prepared samples.

    Procedure B. As a large number of samples must be analysed in a short period in clinical trials, it is better if the clean-up procedure is more labour saving. Ultrafiltration is a simple and frequently used method for deproteinization, like precipitation with trichloroacetic acid[5]. However, the bound fraction of the drug to serum protein should

TABLE I

RECOVERY OF DQ-2556 AND 3-AMINO-4-METHYLBENZOIC ACID (**III**) FROM SERUM UNDER DIFFERENT ACIDIC CONDITIONS AFTER ULTRAFILTRATION

The serum was made acidic by the addition of an equal volume of acetate buffer or of acetic acid. Concentrations in the serum: DQ-2556 = 30 μg/ml; **III** = 150 μg/ml.

Added solution	Recovery (mean ± S.D.) (%)	
	DQ-2556	III
0.2 M acetate buffer (pH 5)	64.5 ± 2.6	51.1 ± 0.7
0.2 M acetate buffer (pH 4)	65.0 ± 1.1	51.1 ± 1.2
0.2 M acetate buffer (pH 3)	68.1 ± 0.4	56.8 ± 0.9
0.2 M acetic acid	70.2 ± 2.3	57.5 ± 0.6
1.0 M acetic acid	77.0 ± 2.7	89.1 ± 1.8
3.0 M acetic acid	85.1 ± 1.7	99.1 ± 1.1

be dissociated prior to ultrafiltration. Haginaka et al.[6] showed that cephalosporin bound to serum proteins is dissociated by acidification of the serum.

The recovery of I from human serum at various pH values is summarized in Table I. It increases as the serum is made more acidic. The recovery of I reached 85.1% on addition of an equal volume of 3 M acetic acid to the serum, and the pH of the filtrate was less than 3 under these conditions. When solutions of I and II in distilled water were treated in the same way as serum, the recoveries were 94.6% and 101.4%, respectively. These data showed that a small amount of I (<6%) might be adsorbed on the ultrafiltration membrane. Although a higher recovery was expected under more acidic conditions, these conditions were employed because the acidity of sample recommended by the maker of the column was pH 2 or above. The internal standard did not have to be hydrophilic, because this procedure involved no extraction steps. When III, which is commercially available, was used as the internal standard, the analysis time was shortened, as its retention time was shorter than that of II.

Linearity, recovery and precision

It was expected that serum samples in clinical trials would contain widely different concentrations of I. Therefore, calibration graphs were developed at two levels of sensitivity for I (0.30–5 and 5–300 μg/ml) in procedure A. Linear relationships were observed in both ranges, and the correlation coefficients for low and high levels were 0.9998 and 0.9997, respectively. In procedure B, the calibration graph was linear in the range 0.3–330 μg/ml and the correlation coefficient was 0.9991. The relative

TABLE II

ACCURACY AND PRECISION OF THE PROPOSED METHODS FOR THE DETERMINATION OF DQ-2556 IN SERUM

Procedure	Concentration (μg/ml)		Accuracy [(found/added) · 100]	Precision, R.S.D. (%)
	Added	Found (mean ± S.D.)		
A	*Intra-assay (n = 5):*			
	0.59	0.61 ± 0.02	103.4	3.8
	2.37	2.43 ± 0.06	103.8	2.4
	9.48	9.42 ± 0.17	99.4	1.8
	37.93	36.74 ± 0.54	96.9	1.5
	151.71	149.89 ± 2.70	98.8	1.8
B	*Intra-assay (n = 5):*			
	0.32	0.31 ± 0.01	96.9	2.9
	1.29	1.31 ± 0.01	101.6	0.8
	5.15	5.10 ± 0.13	99.0	2.5
	20.60	20.48 ± 0.53	99.4	2.6
	82.40	80.85 ± 2.07	98.1	2.6
	Inter-assay (n = 10):			
	0.39	0.39 ± 0.02	98.9	6.1
	3.13	3.10 ± 0.11	98.9	3.5
	12.50	12.38 ± 0.17	99.1	1.4
	50.0	49.79 ± 0.73	99.6	1.5
	100.0	100.14 ± 0.34	100.1	0.3

TABLE III

ACCURACY AND PRECISION OF THE PROPOSED METHODS FOR THE DETERMINATION OF DQ-2556 IN URINE

Concentration (μg/ml)		Accuracy [(found/added) · 100]	Precision, R.S.D. (%)
Added	Found (mean ± S.D.)		
Intra-assay (n = 5):			
2.54	2.62 ± 0.13	103.1	5.1
5.07	5.11 ± 0.15	100.8	2.9
20.29	19.71 ± 0.54	97.1	2.7
40.58	39.53 ± 0.79	97.4	2.0
81.15	79.55 ± 2.05	98.0	2.6
202.9	206.7 ± 2.04	101.9	1.0
811.5	813.9 ± 5.58	100.3	0.7
Inter-assay (n = 9):			
3.13	2.96 ± 0.24	94.7	7.9
12.5	12.53 ± 0.23	100.2	1.8
50.0	50.53 ± 0.20	101.6	0.4
100.0	99.77 ± 0.18	99.8	0.2

recovery (accuracy) and the precision, defined as the relative standard deviation (R.S.D.), are summarized in Table II. The R.S.D. values were less than 4% in both procedures in intra-assay and less than 6% in inter-assay comparisons. The absolute recoveries in procedures A and B were $68.5 \pm 1.1\%$ and $85.1 \pm 1.7\%$, respectively, at a concentration of 20 μg/ml and they were almost constant over the concentration range of the standard samples. The lyophilized serum could be used as a control serum in the preparation of standard samples without any difficulties after dissolution in distilled water.

Calibration graphs for urine were prepared at two levels of sensitivity for I (2.5–100 and 100–800 μg/ml) in a similar way as for serum. The plotted data were well described by linear relationships with correlation coefficients for low and high levels of 0.9998 and 0.9999, respectively. The R.S.D. values were less than 3%, except at low concentration (Table III). The limits of detection were 0.1 μg/ml in serum and 2 μg/ml in urine at a signal-to-noise ratio of 3.

Comparative evaluation of clean-up procedures

Two clean-up procedures for serum samples were developed. In the first precipitation of serum proteins with trichloroacetic acid is used. Although only ordinary reagents, common solvents and no expensive materials are used, careful handling of the sample is required. The second procedure is very simple and requires only the addition of serum and 3 M acetic acid to the ultrafiltration tube and centrifugation, but the tubes are expensive. Hence the choice depends on the conditions of the laboratory.

The applicability of procedure B to the determination of other β-lactam antibiotics was confirmed by preliminary experiments in which the recoveries of some carbapenem compounds were over 94%. Recently, a similar procedure was success-

fully applied in the HPLC assay of a new cephalosporin, BMY-28100[7]. This procedure might be useful for the assay of β-lactams, although the effects of extremely low concentrations of serum proteins in patients with hypoalbuminaemia and the strong protein binding of drugs on the recoveries remain to be clarified.

REFERENCES

1 T. Fujimoto, T. Otani, R. Nakajima, T. Une and Y. Osada, *Antimicrob. Agents Chemother.*, 30 (1986) 611.
2 A. Ejima, T. Hayano, T. Ebata, T. Nagahara, H. Koda, H. Tagawa and M. Furukawa, *J. Antibiot.*, 40 (1987) 43.
3 C. Berse, R. Boucher and L. Piché, *J. Org. Chem.*, 22 (1957) 805.
4 R. D. Toothaker, D. S. Wright and L. A. Pachla, *Antimicrob. Agents Chemother.*, 31 (1987) 1157.
5 R. D. McDowall, *J. Chromatogr.*, 492 (1989) 3.
6 J. Haginaka, J. Wakai, H. Yasuda and T. Nakagawa, *Anal. Chem.*, 59 (1987) 2732.
7 H. Nakanomyo, M. Kidono, M. Shiraya, T. Shimizu, K. Ishikawa, K. Deguchi, S. Fukuyama and Y. Nishimura, *Chemotherapy (Tokyo)*, 37 (S-3) (1989) 141.

CHROMSYMP. 1846

Application of supercritical fluid chromatography and supercritical fluid extraction to the measurement of hydroperoxides in foods

K. SUGIYAMA*, T. SHIOKAWA and T. MORIYA

Research Institute, Morinaga and Company, Ltd., 1–1 Shimosueyoshi, 2-Chome, Tsurumi-ku, Yokohama 230 (Japan)

ABSTRACT

The applicability of supercritical fluid extraction (SFE) and supercritical fluid chromatography (SFC) for determining lipid peroxide levels in foods containing fats and oils was investigated. Lipid peroxide levels determined by SFC and SFE–SFC were compared with peroxide values (POVs) determined by conventional methods. The retention behaviour with respect to oil components in both the mobile phase of supercritical carbon dioxide modified with ethanol and the stationary phase of silica gel is similar to the retention behaviour in normal-phase high-performance liquid chromatography.

SFC was found to be useful for measuring hydroperoxide compounds in small amounts of sample extracted from peanut oil with diethyl ether. The peak areas of peroxide compounds are in good agreement ($r = 0.9923$) with POV determinations made by potentiometry.

Coupled SFE–SFC provides useful qualitative and quantitative information, and can therefore serve as a simple high-speed method for extracting and separating hydroperoxide compounds. Compared with conventional methods, coupled SFE–SFC offers an advantage with regard to sample preparation by eliminating the need for preextraction when using solid samples.

INTRODUCTION

Detecting the presence of peroxide compounds and determining the lipid peroxide value (POV) in foods containing fats and oils are of great interest because peroxide compounds accelerate the deterioration of the taste and appearance of food. Lipid peroxide compounds are also known to have adverse physiological activity *in vivo*. Lipid peroxide levels are currently determined using the official method of the Japan Oil Chemists' Society (JOCS)[1]. This is an iodimetric titration method based on the stoichiometric reaction between lipid hydroperoxide and potassium iodide. However, the method is relatively insensitive and sometimes yields inconsistent results because

it is difficult to determine the exact titration end-point when the lipid level is low or when the sample is coloured.

Reliable POV determinations can be made with potentiometry[2,3]. In addition high-performance liquid chromatography (HPLC) has been used to measure levels of hydroperoxide compounds[4-13]. However, the results were not completely satisfactory because these HPLC systems employed either a UV or refractive index detector. The former, although highly sensitive, is effective in detecting hydroperoxide compounds only at a wavelength of 235 nm, where the conjugated double bond in these compounds gives rise to maximum absorption. The latter, although capable of measuring a wide range of compounds, even those without UV absorption bands, is relatively insensitive.

Supercritical fluid extraction (SFE) and supercritical fluid chromatography (SFC) using carbon dioxide are known to be very suitable methods for the extraction and separation of labile compounds, because sample compounds can be extracted and chromatographed in an oxygen-free environment at relatively low temperatures. In addition, coupled SFE–SFC may offer a great advantage over conventional methods with regard to sample preparation. The reason is that a coupled SFE–SFC system is capable of accepting solid samples, thus eliminating the need for pre-extraction using a Soxhlet extraction system which is currently required in all conventional methods. We investigated the applicability of the above techniques to the determination of lipid peroxide levels in goods, and the results were compared with POVs determined by conventional methods.

EXPERIMENTAL

Materials

Peanut oil samples were prepared from peanuts commonly used as ingredients in confectionary products. The peanuts were ground and sieved to a 30-mesh fineness and then extracted with diethyl ether (Tabata, Chiba, Japan). Oils containing various POV levels were obtained by storing the ground peanut samples at 63°C for 45–450 h prior to extraction.

Peanut samples for coupled SFE–SFC measurements were ground and sieved to a 60-mesh fineness in order to reduce the extraction time.

Reagents and column

Food-additive grade carbon dioxide (Showa Tansan, Tokyo, Japan) was used as the mobile phase and as the extraction medium for the SFC and SFE–SFC analyses. HPLC-grade ethanol was used as a modifier for the SFC mobile phase. A Super-Pak SIL (5-μm silica gel) (JASCO, Hachioji, Japan) column (250 mm × 4.6 mm I.D.) was used for SFC separation. Stigmasterol was used as an internal standard for determining the lipid peroxide compounds in SFC.

Special-reagent-grade sodium thiosulphate, potassium iodide and diethyl ether were used in the potentiometric measurements. Unless indicated otherwise, all chemicals were purchased from Wako (Osaka, Japan).

Apparatus

A JASCO Super-100 SFE–SFC system with a MULTI-320 wavelength UV
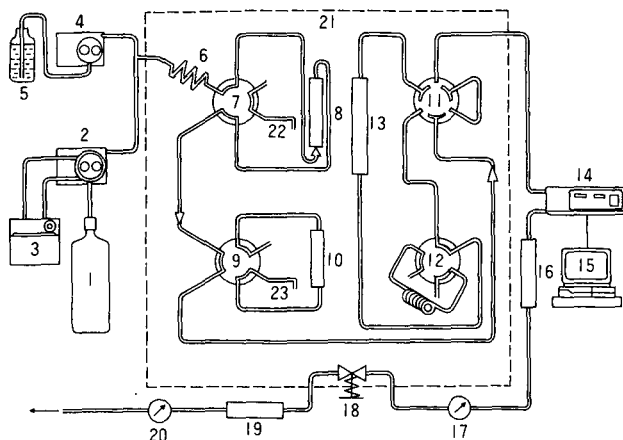
Fig. 1. Schematic diagram of coupled SFE–SFC system. 1 = Carbon dioxide cylinder; 2 = liquefied carbon dioxide delivery pump; 3 = coolant circulating bath; 4 = modifier delivery pump; 5 = modifier solvent reservoir; 6 = heat-exchange coil; 7 = six-way valve for bypassing extraction vessel; 8 = extraction vessel; 9 = six-way valve for bypassing trap vessel; 10 = extract trap vessel; 11 = six-way valve for bypassing injector and separation column; 12 = injector; 13 = separation column; 14 = multi-wavelength detector; 15 = detector data processor; 16 = extract trap column; 17 = back-pressure gauge; 18 = back-pressure regulator; 19 = trap for mass flow meter; 20 = mass flow meter; 21 = oven. (From ref. 14).

detector was used for SFC and SFE–SFC[14]. A schematic diagram of the system is shown in Fig. 1. The volume of the extract trap vessel used for the extraction was 25 ml (50 mm × 8.0 mm I.D.). An AUT-1 automatic titrator (TOA Electronics, Tokyo, Japan) was used for the potentiometric determinations.

Procedures

SFC measurement. Samples for SFC were prepared by weighing 0.1-g samples of fats and oils dissolved in 1 ml of *n*-hexane in 3-ml vials capped with silicone rubber. A 20-μl volume of sample solution was injected into the SFC system. The results of SFC measurements were expressed in terms of peak areas of absorbance at 230 nm.

SFE–SFC measurement. Extraction and chromatography were carried out in a single process using a coupled SFE–SFC system to determine the levels of lipid peroxide compounds in the ground peanut samples. Peanut powder (40 mg) was placed in the extraction vessel (50 mm × 8.0 mm I.D.) and 52.5 μg of stigmasterol in 30 μl of *n*-hexane were added as an internal standard. The extraction was carried out with supercritical carbon dioxide containing 5% ethanol at a pressure of 140 kg/cm^2 at 40°C for 7 min using the constant-pressure delivery mode. During the extraction, the extraction vessel was simply pressurized with carbon dioxide and thus extraction was performed using the stop-flow method.

After 7 min had elapsed, the six-way valve 9 was switched to trap the extracted compounds in the extract trap vessel (10), which contained carbon dioxide gas at atmospheric pressure. When the system pressure had stabilized, indicating that transfer of the extract was complete, the six-way valve 7 was switched to by-pass the extraction vessel 8. Then, six-way valve 11 was switched so that the separation column (13) was included in the flow line in order to equilibrate the system under SFC

conditions at a pressure of 120 kg/cm² at 40°C with a carbon dioxide flow-rate of 4.0 ml/min as a liquid at −5°C and an ethanol flow-rate of 0.3 ml/min.

Equilibration was obtained within a few minutes, then the six-way valve 9 was switched back to include the extract trap loop in the flow line and the extract was then injected into the separation column (13).

RESULTS AND DISCUSSION

Comparison of results obtained by SFC and potentiometry

Peanut oils having different POVs prepared according to the procedure described under Experimental were analysed by SFC. The POVs of these oils were determined by potentiometry prior to SFC analysis. Fig. 2 shows a typical SFC result for peanut oil having a POV of 41.0.

As can be seen in the chromatogram, the retention behaviour of the oil components in both the mobile phase of supercritical carbon dioxide modified with ethanol and the stationary phase of silica gel was similar to the retention behaviour in normal-phase HPLC[6,10].

With regard to controlling the retention in normal-phase chromatography, SFC may prove superior to HPLC. The reason is that the mobile phase strength in SFC can be precisely controlled simply by changing the pressure and temperature of the fluid. Such control cannot be achieved in HPLC by changing the mobile phase composition from a non-polar to a polar solvent.

Glycerides, which are the main constituents of the oil, were eluted at 2.1 min and hydroperoxides were eluted at 3.65 min. The contour plot of this chromatogram (not shown) suggested that the hydroperoxide peak contained at least three components. This corresponds to previous results obtained by HPLC[10].

UV absorption spectra of the peak at 2.10 min containing glycerides and the peak at 3.65 min containing hydroperoxide are shown in Fig. 3. These spectra are in good agreement with those obtained using an ordinary UV spectrometer at wavelengths longer than 215 nm. At shorter wavelengths there is an abrupt fall-off in the spectra owing to UV absorption by ethanol, which is very high in this region, resulting in distortion of the spectra below 215 nm.
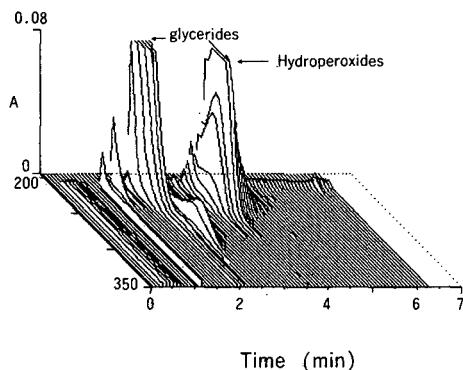
Fig. 2. Chromatogram of peanut oil (POV 41.0) in SFC.
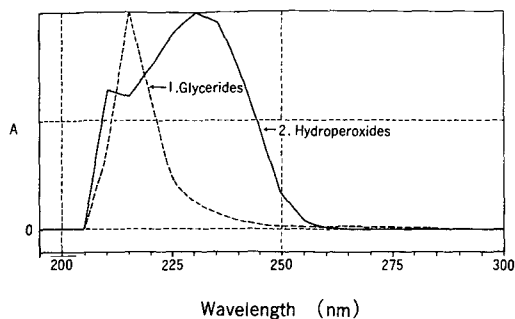
Fig. 3. SFC spectrum for Fig. 2. (1) 2.10 min, 0.2623 a.u.f.s.; (2) 3.65 min, 0.0591 a.u.f.s.

Table I gives quantitative results obtained by SFC and potentiometry. As demonstrated by a linear regression analysis, the correlation between the results obtained by these two methods was excellent. The regression equation was $y = 0.6556x - 0.1031$ and the correlation coefficient was 0.9923.

The reproducibility (relative standard deviation) for SFC and potentiometry for five consecutive measurements of peanut oil having a POV of 53.2 was calculated to be 1.57% ($n = 5$) and 1.63% ($n = 5$), respectively.

Comparison of results obtained by SFE–SFC and potentiometry

Peanut samples for SFE–SFC analysis were exposed to heat for different periods of time as described under Experimental section. The POVs of oils from these samples were determined by potentiometry in the same way as for the SFC analysis. In order to obtain reliable quantitative results in SFE–SFC analysis, it is essential that the compound selected for the internal standard should have the same extraction yield as the target compound. SFC analysis provides useful information for selecting a compound for use as an internal standard. The retention behaviour of a compound is highly dependent on its polarity, as is the extraction yield. Therefore, if the retention times of both the internal standard and the target compounds are similar, it is reasonable to assume that the extraction yield in SFE may also be similar under the same extraction conditions. In practice, a longer extraction time tends to minimize errors related to differences in extraction yields.

TABLE I

COMPARISON OF QUANTITATIVE RESULTS OBTAINED BY SFC AND POTENTIOMETRY

Method	Number of hours of ageing					
	0^a	45	65	112	328	450
SFC: peak area[b]	1.86	2.86	3.16	3.47	4.24	6.31
Potentiometry: POV[c]	19.9	38.4	53.1	60.0	70.2	93.6

[a] Indicates fresh peanuts, tested as supplied without ageing.
[b] Peak areas are given in terms of absorbance (at 230 nm) seconds.
[c] Lipid peroxide values are given in terms of mequiv./kg.
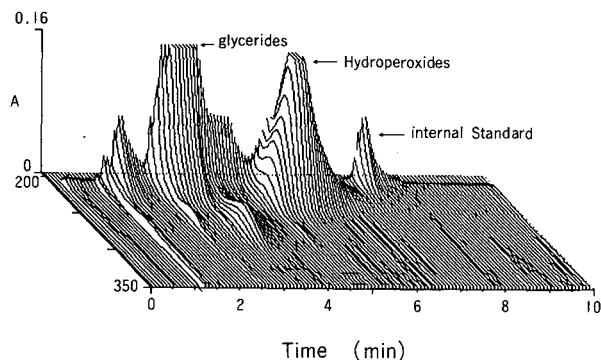
Fig. 4. Chromatrogram obtained by coupled SFE–SFC.

Fig. 4 shows typical SFE–SFC results for oil from a peanut sample containing stigmasterol as the internal standard. The POV of the oil was determined in a separate potentiometric measurement to be 41.0. Glycerides were eluted at 3.12 min, hydroperoxides at 5.54 min and the internal standard at 7.12 min.

The UV adsorption spectrum of each peak component is shown in Fig. 5. Below 215 nm, the absorption curves are distorted for the same reason as given above for Fig. 3.

SFE–SFC analyses were performed on different peanut samples having POVs of 1.95, 40.74 and 89.03. Table II shows the results and reproducibility of the analysis. The peak areas of stigmasterol, the internal standard, were measured at 215 and 220 nm. Hydroperoxide peak areas were measured at 230 nm and were divided by those of the internal standard at 215 and 220 nm to normalize the data for hydroperoxides in the conventional internal standard method. All peak-area data are expressed as absorbance seconds.

The normalized data were then subjected to linear regression analysis to evaluate the correlation between the SFE–SFC results and POV as determined by potentiometry. The correlation coefficients for the 230/215 nm and 230/220 nm ratios were
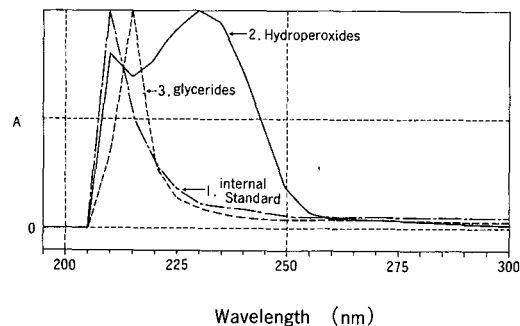
Fig. 5. Spectrum of hydroperoxide compounds and glycerides in peanut oil, together with stigmasterol as the internal standard. (1) 7.12 min, 0.0642 a.u.f.s.; (2) 5.54 min, 0.0875 a.u.f.s.; (3) 3.12 min, 0.2415 a.u.f.s.

TABLE II

COMPARISON OF QUANTITATIVE RESULTS OBTAINED BY COUPLED SFE–SFC AND PO-
TENTIOMETRY

Sample	Stigmasterol		Hydroperoxide		
	Peak area at 215 nm	Peak area at 220 nm	Peak area at 230 nm	Ratio of peak areas	
				230/215 nm	230/220 nm
Sample 1: POV = 1.95[a]	145	0.83	2.19	1.48	2.79
R.S.D. (%)[b]	3.40	5.86	3.20	2.92	6.33
Sample 2: POV = 40.74[a]	1.54	0.84	9.97	6.47	11.89
R.S.D. (%)[b]	3.84	2.58	6.65	4.45	4.49
Sample 3: POV = 89.03[a]	1.43	0.81	15.59	10.90	19.28
R.S.D. (%)[b]	2.08	5.02	5.75	4.13	2.74

[a] POVs were determined by potentiometric analysis of peanut samples employing the same extrac-
tion method for sample preparation described under Procedures.
[b] Relative standard deviation ($n = 5$).

9.890 and 0.9881, respectively. The relationships in the above data can be expressed
linearly as $y = 0.1064x + 1.665$ for 230/215 nm and $y = 0.1894x + 3.188$ for 230/220
nm. Hence the reproducibility of POV determinations by SFE–SFC is as good as that
by potentiometry.

The samples for coupled SFE–SFC were solid samples introduced into the
system without pre-extraction. Therefore, by eliminating the need for pre-extraction
when using solid samples, coupled SFE–SFC can serve as a simple and rapid high-
speed method for extracting and separating hydroperoxide compounds from foods.

CONCLUSION

SFC using a multi-wavelength UV detector appears to be a useful method for
detecting and measuring hydroperoxide compounds in fats and oils. POVs measured
by SFC are in good agreement with those determined by potentiometry.

Coupled SFE–SFC was shown to provide useful qualitative and quantitative
information and can therefore serve as a simple and rapid method for extracting and
separating hydroperoxide compounds. Compared with conventional methods, cou-
pled SFE–SFC offers an advantage with regard to sample preparation by eliminating
the need for pre-extraction when using solid samples.

ACKNOWLEDGEMENTS

REFERENCES

1 *Official and Tentative Methods of the Japan Oil Chemist's Society* (JOCS), Maruzen, Tokyo, 1943, Method 2.4.12-71.
2 S. Hara, O. Washizu and Y. Totani, *Yakugaku*, 31 (1982) 1004.
3 S. Hara and Y. Totani, *J. Am. Oil Chem. Soc.*, 65 (1988) 1948.
4 R. D. Plattner, G. F. Speneer and R. Kleiman, *J. Am. Oil Chem. Soc.*, 54 (1977) 511.
5 R. D. Plattner, *J. Am. Oil Chem. Soc.*, 58 (1981) 638.
6 S. Hara, H. Yamawaki and Y. Totani, *Yukagaku*, 32 (1981) 594.
7 M. W. Dong and J. L. Dicesare, *J. Am. Oil Chem. Soc.*, 60 (1983) 788.
8 D. K. Park, J. Terao and S. Matsushita, *Agric. Biol. Chem.*, 45 (1981) 2443.
9 Y. Totani, *Yukagaku*, 35 (1986) 337.
10 S. Hara, K. Nemoto, H. Yamawaki and Y. Totani, *Yukagaku*, 37 (1988) 541.
11 T. Hoshino, T. Hondo, M. Senda, M. Saito and S. Tohei, *J. Chromatogr.*, 332 (1985) 139.
12 K. Sugiyama, M. Saito, T. Hondo and M. Senda, *J. Chromatogr.*, 332 (1985) 107.
13 K. Sugiyama and M. Saito, *J. Chromatogr.*, 442 (1988) 1213.
14 M. Yoshioka, S. Parvez, T. Miyazaki and H. Parvez, *Progress in HPLC*, Vol. 4, VSP, Utrecht, 1988, p. 101.

CHROMSYMP. 1781

High-performance liquid chromatography of transfer ribonucleic acids on spherical hydroxyapatite beads

II. Effects of pH and sodium chloride on chromatography

YOSHIO YAMAKAWA*

Department of Applied Immunology, National Institute of Health, Kamiosaki 2-10-35, Shinagawa-ku, Tokyo 141 (Japan)

KENJI MIYASAKA and TOSHIHIRO ISHIKAWA

New Venture Business Department, Toa Nenryo Kogyo Co., 1-1Hitotubashi, 1-chome Chiyoda-ku, Tokyo 100 (Japan)

YUKO YAMADA

Laboratory of Chemistry, Jichi Medical School, Minamikawauchi machi, Kawauchi-Gun, Tochigi 329-04 (Japan)

and

TSUNEO OKUYAMA

Department of Chemistry, Faculty of Science, Tokyo Metropolitan University, Fukazawa 2-1-1, Setagaya-ku, Tokyo 158 (Japan)

ABSTRACT

The effects of pH and sodium chloride on the high-performance liquid chromatography of transfer ribonucleic acids (tRNAs) on spherical hydroxyapatite beads were investigated. Binding of tRNAs on the beads was strengthened by increasing the pH of the mobile phase (phosphate buffer, pH 6.4–8.0), a phenomenon which is opposite to the retention of proteins on the beads. By using phosphate buffer of pH 8.0 instead of pH 6.8, the resolution of tRNAs was improved significantly; as many as ten times more theoretical plates were calculated with the use of the former buffer. Addition of sodium chloride to the phosphate buffer has a bifunctional effect on the retention of tRNAs: elution of tRNA$^{f\text{-Met}}$ and tRNA^{Val} was retarded whereas that of tRNA^{Phe} was facilitated.

INTRODUCTION

High-performance liquid chromatography (HPLC) on spherical hydroxyapatite (HAP) beads is a useful method for the purification and analysis of biomacromolecules such as proteins and nucleic acids[1–3]. The beads have been successfully applied to the

purification of mouse monoclonal antibodies from ascitic fluid[4], a protease from the venom of the king cobra[5] and the separation of two isomers of human tumour necrotic factor[6]. Recently, chromatography of tRNAs on HAP beads has been reported[7,8]. Both reports demonstrated that the HPLC of tRNAs on HAP beads gave good resolution and a high recovery of tRNAs (>90%). The column was also useful for the separation of isoacceptors of tRNAs. In an attempt to improve the resolution of tRNAs by HPLC on HAP beads, we examined the effects of pH and NaCl on resolution in comparison with the previously described method in which tRNAs were analysed in a phosphate buffer at pH 6.8.

EXPERIMENTAL

tRNAs

Purified *Escherichia coli* tRNAs (Val, Lot No. 97F-0079-1; f-Met, Lot No. 128F-01371; and Phe, Lot No. 88F-01691) were purchased from Sigma (St. Louis, MO, U.S.A.). Total tRNA (tRNA^{Total}) was prepared from *E. coli* K12 and *Bacillus subtilis* W168 as described by Zubay[9]. Purified tRNA was dissolved in 5 mM phosphate buffer (pH 8.0) at about 0.5 mg/ml and was stored at 5°C. tRNA^{Total} was also dissolved in the same buffer at a concentration of about 1.5–2 mg/ml. The concentration of tRNA was determined spectrophotometrically using $A_{1\,cm}^{1\%} = 20$ at 260 nm.

Determination of amino acid-accepting activity

The preparation of crude *E. coli* aminoacyl-tRNA synthetase and the determination of the amino acid-accepting activity of tRNA with ^{14}C-labelled amino acids were carried out as described by Nishimura *et al.*[10].

Columns

Packed columns (10 × 0.75 cm I.D. and 10 × 2.14 cm I.D.) of spherical beads of HAP were obtained from Toa Nenryo Kogyo (Tokyo, Japan). The small-bore column packed with 2.2-μm HAP beads was used for routine analysis and the larger bore column packed with 5-μm beads for semi-preparative use.

Apparatus

A Shimadzu LC-7A liquid chromatograph with a two-pump gradient system was used for the analytical column. Elution of nucleic acids was monitored at 260 nm with an SPD-6A UV detector and recorded with a Chromatopak C-R4A. Samples were introduced into the column from a SIL-6A automatic sample injector. The semi-preparative column was eluted with a CCPM prep-pump (Tosoh, Tokyo, Japan) and the eluate was monitored with a Model 875-UV detector (JASCO, Tokyo, Japan) with a 1-mm light-path cell.

Elution

Elution of tRNA from the column was performed with a linear gradient of phosphate buffers of various pHs between solvents A (5 mM) and B (300 mM). The gradient was started immediately after sample injection, but its action is delayed by 15 min when the analytical column was eluted at a flow-rate of 0.5 ml/min. The

analytical column was usually elutd at a flow-rate of 0.5 ml/min (back-pressure *ca.* 20 kg/cm^2). The semi-preparative column was eluted at 5.0 ml/min (*ca.* 5 kg/cm^2); 5-ml fractions of eluate were collected by a fraction collector for determination of the respective amino acid-accepting activity. Chromatography was carried out at room temperature.

RESULTS

Effects of pH on the retention of tRNAs on the HAP column
    Fig. 1 shows a comparison of typical elution profiles of a mixture of equal amounts of purified *E. coli* tRNAs (f-Met, Val and Phe) on the HAP column when the column was developed using the same linear gradient (15–78% B in 60 min) of phosphate ion concentrations but at different pHs (6.8 and 8.0). It is evident that binding of tRNAs to the HAP column was greater at the higher pH. All three tRNAs were separately eluted from the column within a narrow range of phosphate ion concentrations (*ca.* 20–40% B; 60–120 mM) at pH 6.8. However, a higher and wider range of phosphate ion concentrations (*ca.* 40–70% B; 120–210 mM) was necessary to elute these tRNAs at pH 8.0. In addition to this finding, tRNA^{Phe}, which was eluted from the column as a single peak at pH 6.8, was completely divided into two distinct peaks, tentatively named Phe-I and Phe-II, at pH 8.0; a peak that eluted just before tRNA^{Val} at pH 6.8 was also split into several minor peaks, which were eluted between
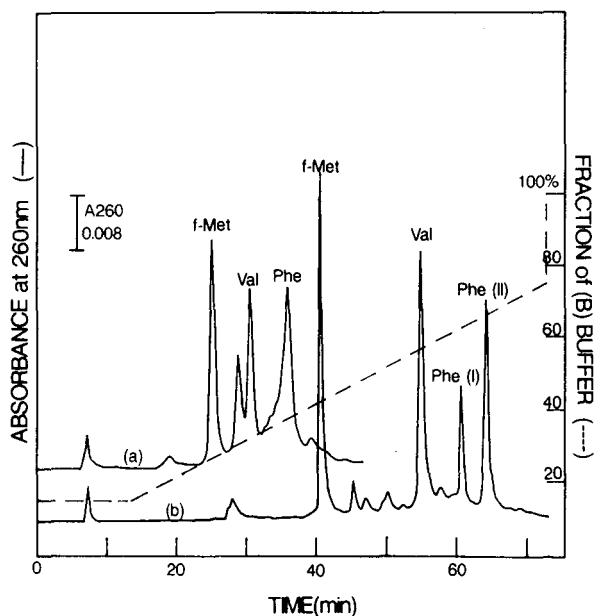
Fig. 1. Chromatography of a mixture of *E. coli* tRNAs on the analytical column (10 cm × 0.75 cm I.D.) of HAP at different pH. A mixture of purified *E. coli* tRNAs (f-Met, Val and Phe; 3.5 μg each) was eluted from the column at a flow-rate of 0.5 ml/min by a gradient of phosphate ion concentration (15–78% B in 60 min) at (a) pH 6.8 and (b) pH 8.0. Buffer A, 5 mM phosphate buffer (pH 6.8 or 8.0); buffer B, 300 mM phosphate buffer (pH 6.8 or 8.0).

the peaks of tRNA$^{\text{f-Met}}$ and tRNA$^{\text{Val}}$ in the analysis at pH 8.0. Moreover, each tRNA was eluted more sharply from the column at the higher pH in spite of the elution with the same gradient of phosphate ion concentrations.

Fig. 2 shows the relationship between the pH of the mobile phase and the retention times of the three tRNAs on the HAP column when a mixture containing equal amounts was eluted with the same gradient of phosphate ion concentrations from 15 to 78% B in 60 min at different pHs. An effect of pH on the retention of tRNAs on HAP beads was evident. The binding of tRNAs on the HAP beads was strengthened with, but not proportionally, to the increase in pH of the eluent. Incidentally, the separation of tRNA$^{\text{Phe-I}}$ and tRNA$^{\text{Phe-II}}$ and the split peak of tRNA$^{\text{Val}}$ mentioned above also became clearer at higher pH. As phosphate buffer possesses a weak buffering action above pH 8.0, experiments above pH 8.0 were not performed.

The efficiency of the HAP chromatography of tRNA between pH 6.8 and 8.0 was determined by comparing the theoretical plate numbers of the column. For this purpose, the gradient of phosphate ion concentration was adjusted so that corresponding tRNA molecules would elute at a similar retention time at both pH values. The resulting chromatograms and theoretical plates (N) of the column are shown in Fig. 3. Regarding the elution of tRNA$^{\text{f-Met}}$ and tRNA$^{\text{Val}}$, as many as ten times more theoretical plates were calculated for the column at pH 8.0 than that at pH 6.8; about six times more theoretical plates were also calculated with the tRNA$^{\text{Phe-II}}$ peak at pH 8.0. The results clearly demonstrate that a higher pH is advantageous for the HPLC of tRNAs on HAP beads.

Chromatography of tRNA$^{\text{Total}}$ of E. coli and B. subtilis

Under the conditions described above, we analysed *E. coli* and *B. subtilis* tRNA$^{\text{Total}}$ on the analytical HAP column in phosphate buffer at pH 8.0. Fig. 4a shows a typical elution profile of *E. coli* tRNA$^{\text{Total}}$ on the analytical HAP column with an optimized linear gradient (40–75% B in 60 min) of phosphate ion concentrations at pH 8.0; the elution profile of the mixture of equal amounts of purified tRNAs (f-Met,
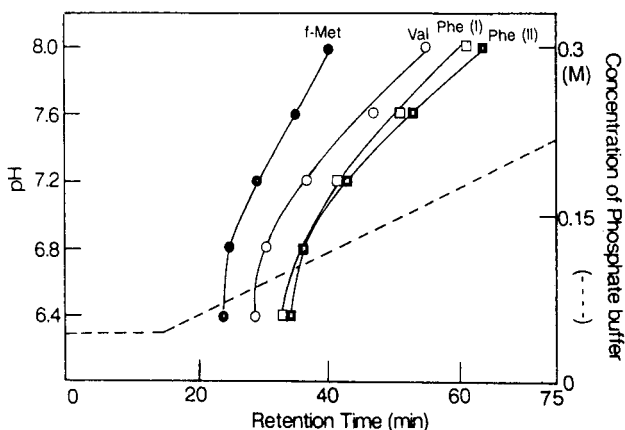
Fig. 2. Effects of pH on the retention of tRNAs on HAP. A mixture of equal amounts of *E. coli* tRNAs was chromatographed on the analytical column with the same linear gradient of phosphate ion concentration as in Fig. 1 at various pHs; retention times of the tRNAs were plotted against pH of the phosphate buffer.
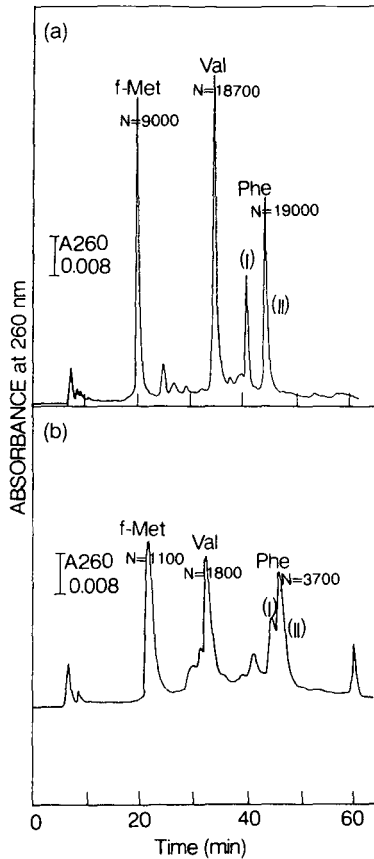
Fig. 3. Comparison of elution profiles of mixtures of equal amounts of *E. coli* tRNAs at pH 8.0 and 6.8. (a) A mixture of *E. coli* tRNAs (the same as in Fig. 1) was eluted from the analytical HAP column at a flow-rate of 0.5 ml/min with a linear gradient of phosphate ion concentration (40–78% B in 45 min, buffer A 5 mM, buffer B 300 mM) at pH 8.0. (b) The same mixture as in (a) was eluted from the HAP column at a flow-rate of 0.5 ml/min with a linear gradient of phosphate ion concentration (23–43% B in 45 min, buffer A 5 mM, buffer B 300 mM) at pH 6.8.

Val and Phe) analysed under the same conditions is shown in Fig. 4b. As expected, the resolution of the tRNA^{Total} on the analytical column was improved considerably by eluting the column at pH 8.0 when compared with the chromatogram shown in the previous paper[7], in which phosphate buffer of pH 6.8 was used for elution. When the tRNA^{Total} was analysed at pH 6.8[7], the elution profile revealed peaks that were widely spread and irregularly shaped, and only ten significant peaks could be recognized; in contrast as many as twenty significant peaks were observed in the chromatography at pH 8.0. Therefore, we analysed tRNA^{Total} of *B. subtilis* under the same conditions. As shown in Fig. 5, the resolution of tRNA^{Total} of *B. subtilis* on the column was also improved by eluting the column with phosphate buffer of pH 8.0.
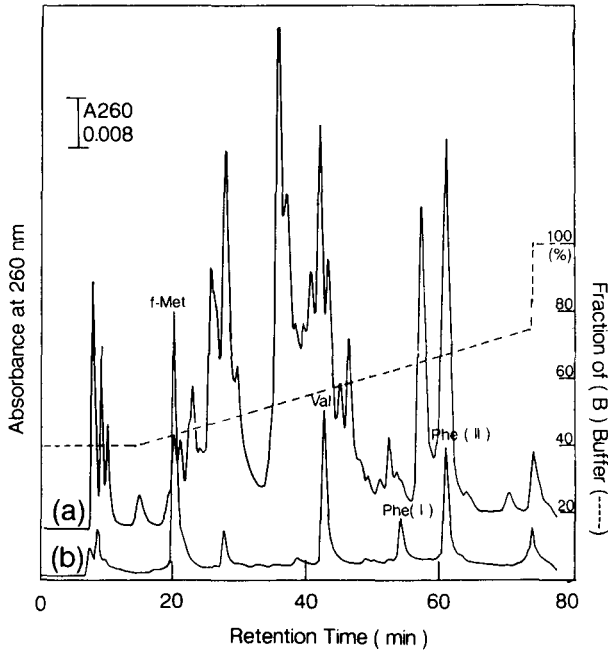
Fig. 4. Chromatography of *E. coli* tRNA[Total] and a mixture of equal amounts of purified *E. coli* tRNAs on the analytical HAP column. (a) 50 μg of *E. coli* tRNA[Total] were applied to the analytical HAP column and eluted with a 60-min linear gradient of phosphate ion concentration from 40 to 75% B (buffer A 5 mM, buffer B 300 mM; pH 8.0) at a flow-rate of 0.5 ml/min. (b) A mixture of equal amounts of *E. coli* tRNAs was chromatographed under the same conditions as in (a).
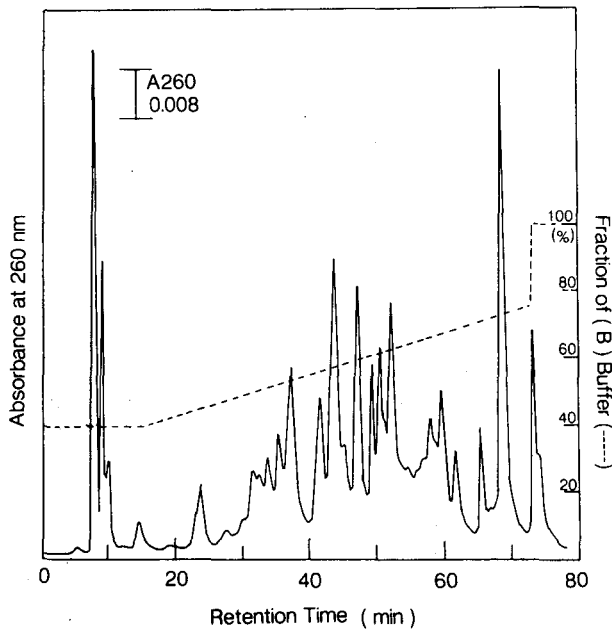
Fig. 5. Chromatography of *B. subtilis* tRNA[Total] on the analytical HAP column. 40 μg of tRNA[Total] of *B. subtilis* were chromatographed under the same conditions as in Fig. 4.

Chromatography of E. coli tRNA^{Total} on the semi-preparative column and determination of amino acid-accepting activity of several tRNAs

Fig. 6 shows typical elution profile of *E. coli* tRNA^{Total} on the semi-preparative column (10 cm × 2.4 cm I.D.) eluted with optimized phosphate ion concentration at pH 8.0. The elution profiles of the accepting activity of six amino acids in the eluate are also shown. The retention of tRNAs on this column was weaker than that on the analytical column and a phosphate ion gradient of 25–55% B at pH 8.0 was optimum for elution of tRNA^{Total}. The elution profile of tRNA^{Total} monitored at 260 nm (top) was not as good as that obtained with the analytical column (see Fig. 4) as the column was packed with 5-μm beads instead of 2.2-μm beads for the analytical column. As expected, the elution of tRNA from the semi-preparative column was also clearly improved in comparison with the previous chromatography performed at pH 6.8. tRNAs such as tRNA^{f-Met}, tRNA^{Val} and tRNA^{Phe} contained in the tRNA^{Total} were eluted from the column separately at the earlier, middle and later parts, respectively, of the gradient, as expected from the results on the analytical column (see Fig. 1).
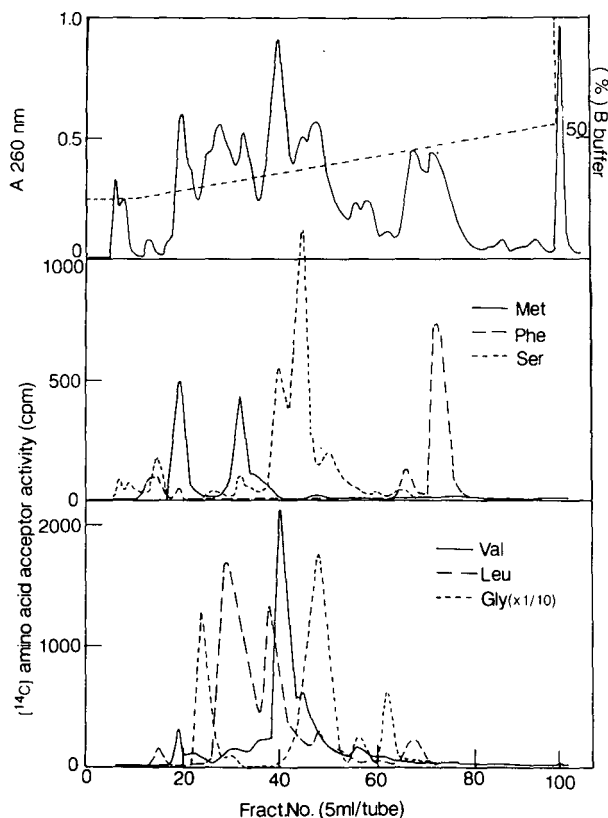
Fig. 6. Chromatography of *E. coli* tRNA^{Total} on the semi-preparative HAP column. *E. coli* tRNA^{Total} (7 mg) was applied to the semi-preparative column (10 cm × 2.14 cm I.D.) of HAP equilibrated with 25% B and eluted with a 90-min linear gradient of phosphate ion concentration from 25 to 55% B (buffer A 5 m*M*, buffer B 300 m*M*; pH 8.0) at a flow-rate of 5 ml/min. Fractions of 5 ml were collected and A_{260} (top) and amino acid acceptor activities of the fractions (middle and bottom) were determined.

Two methionine-accepting activity peaks were eluted from the column, which appears to indicate separation of tRNA^{f-Met} and tRNA^{Met} in the preparation. Judging from the retention times of these peaks, the former methionine-accepting peak was considered to be tRNA^{f-Met}. The elution of two phenylalanine-accepting activities in the later part of the gradient corresponded to the elution of isoacceptors of tRNA^{Phe-I} and tRNA^{Phe-II} observed in the purified preparation of tRNA^{Phe}, as pointed out earlier. In addition, it was noted that two or more peaks were found for some amino acid-accepting activities, which indicates the presence and separation of isoacceptors of each tRNA in the preparation.

Effects of sodium chloride on chromatography at pH 8.0

It has been shown[7,8] that the resolution of tRNAs, and also aminoacyl-tRNAs, can be improved by the inclusion of sodium chloride in the phosphate buffer eluent at pH 6.8. Therefore, we analysed the effect of sodium chloride on the HAP chromatography of tRNAs at pH 8.0. As demonstrated in Figs. 7 and 8, addition of sodium chloride to the phosphate buffers had a significant effect on the retentions of the tRNAs on HAP; elution of tRNA^{Phe-I} and tRNA^{Phe-II} was facilitated by the addition of sodium chloride whereas that of tRNA^{f-Met} and tRNA^{Val} was retarded. No obvious change in the widths of the tRNA peaks was observed either with or without
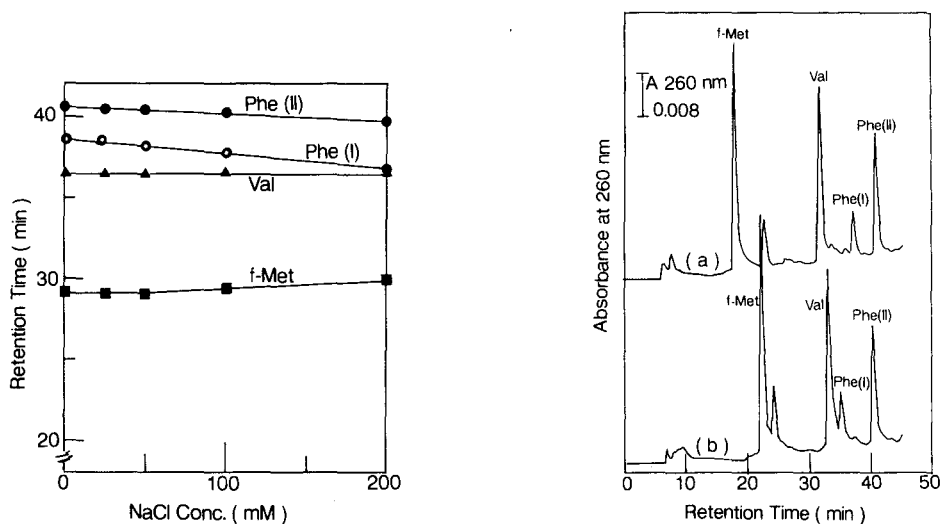
Fig. 7. Effect of NaCl on the retention of tRNAs on hydroxyapatite. A mixture of equal amounts of *E. coli* tRNAs was eluted from the analytical column at a flow-rate of 0.5 ml/min with a 30-min linear gradient of phosphate ion concentration from 15 to 83% B at pH 8.0. Retention times of the tRNA peaks were plotted against the concentration of NaCl included in the buffers. Buffer A, 5 mM phosphate buffer (pH 8.0) containing various concentrations of NaCl (0, 25, 50, 100, 200 mM); buffer B, 300 mM phosphate buffer containing NaCl at the same concentrations as in buffer A.

Fig. 8. Chromatography of a mixture of equal amounts of purified *E. coli* tRNAs (a) without and (b) with 0.2 M NaCl. The mixture of purified tRNAs was eluted from the analytical column at a flow-rate of 0.5 ml/min with a 30-min linear gradient of phosphate ion concentration from 40 to 80% B at pH 8.0 in or absence (a) or presence (b) of 0.2 M NaCl. Buffer A, 5 mM phosphate buffer (pH 8.0) with or without 0.2 M NaCl; buffer B, 300 mM phosphate buffer with or without 0.2 M NaCl.

sodium chloride, as demonstrated in Fig. 8. In this connection, tRNA^{Total} of *B. subtilis* was chromatographed at pH 8.0 in the presence and absence of 0.2 M sodium chloride. The results indicated that there is no advantage in adding sodium chloride to the buffers for the chromatography of tRNAs on spherical HAP beads in phosphate buffer at pH 8.0.

DISCUSSION

tRNAs were retained more strongly on the beads with an increase in the pH of the mobile phase (phosphate buffer), which is opposite to the retention of proteins on the beads[11]. We also observed that λ-phage DNA would bind more strongly to the beads at pH 8.0 than pH 6.8 (unpublished observation). These findings indicate that the interactions between the calcium site of HAP and the phosphate group of tRNAs are strengthened at higher pH, probably owing to the ionization of the phosphate group in tRNAs and/or conformational changes of the tRNA molecules. The improvement in the resolution of tRNAs may be attributed to strong binding of tRNAs to the beads, as chromatography at higher concentrations of phosphate buffer may decrease the non-specific interactions of tRNAs on the beads and aid the selective elution of the individual tRNAs. In addition, the use of a steep phosphate ion gradient also aided the sharp elution of the peaks.

Inclusion of sodium chloride in the phosphate buffer eluent showed bifunctional effects on the retention of tRNAs on the HAP: elution of tRNA^{f-Met} and tRNA^{Val} was retarded whereas that of tRNA^{Phe-I} and tRNA^{Phe-II} was facilitated. In this connection, it is noteworthy that inclusion of sodium chloride in the phosphate buffer also had a bifunctional effect on the retention of proteins on the HAP beads; it weakened the binding of highly basic proteins such as lysozyme and chymotrypsinogen A on the beads whereas it strengthened the retention of highly acidic proteins such as chicken egg albumin[8]. Sodium chloride strengthened the binding of substances that have relatively weak interactions with HAP such as strongly acidic proteins and tRNA^{f-Met}, whereas it reduced the strong interactions between HAP and basic proteins and tRNA^{Phe-I} or tRNA^{Phe-II}. Further investigations are necessary to clarify such bifunctional effects of sodium chloride on the retention of biomacromolecules on HAP. In the expectation of such bifunctional effects, rechromatography in the presence of sodium chloride might be effective for the purification of certain tRNAs.

The semi-preparative column retained tRNAs weakly compared with the retention of tRNAs on the analytical column. This may be due to the difference in the sintering temperature of HAP. Preliminary experiments indicated that protein retention on HAP was also affected by the sintering temperature. HAP prepared at higher temperatures showed a lower binding activity with acidic proteins such as bovine serum albumin, whereas binding of basic proteins such as lysozyme and cytochrome c on the HAP was hardly affected by the sintering temperature. Considering these results, the sintering temperature might have affected the properties of the calcium sites of the HAP. Incidentally, the effects of sintering temperature on the binding capacity of HAP for protein were demonstrated by Inoue and Ohtaki[12] and their results seem to be in agreement with our observations.

REFERENCES

1 T. Kadoya, T. Isobe, M. Ebihara, T. Ogawa, M. Sumita, H. Kuwahara, A. Kobayashi, H. Ishikawa and
   T. Okuyama, *J. Liq. Chromatogr.*, 9 (1986) 3543.
2 T. Kadoya, T. Ogawa, H. Kuwahara and T. Okuyama, *J. Liq. Chromatogr.*, 11 (1988) 2951.
3 S. Hjerten, J. Linderberg and B. Shopova, *J. Chromatogr.*, 440 (1988) 305.
4 Y. Yamakawa and J. Chiba, *J. Liq. Chromatogr.*, 11 (1988) 665.
5 Y. Yamakawa and T. Ohmori-Sato, *Toxicon*, 26 (1988) 1145.
6 K. Inaka, A. Hasegawa, M. Kubota, K. Takeda, R. Kamijo, K. Konno and M. Ikehara, paper presented
   at *the Second International TNF Conference administered by UCLA, Symposia on Molecular and Cellular
   Biology; Tumor Necrotic Factor and Related Cytokines*, Napa Valley, CA, 1989.
7 Y. Yamakawa, K. Miyasaka, T. Ishikawa, Y. Yamada and T. Okuyama, *J. Chromatogr.*, 506 (1990)
   319.
8 J. Linderberg, T. Srichaiyo and S. Hjerten, *J. Chromatogr.*, 499 (1990) 153.
9 G. Zubay, *J. Mol. Biol.*, 4 (1962) 347.
10 S. Nishimura, F. Harada, U. Narushima and T. Seno, *Biochim. Biophys. Acta*, 142 (1967) 133.
11 G. Bernaldi, *Methods Enzymol.*, 22 (1971) 471.
12 S. Inoue and N. Ohtaki, *J. Chromatogr.*, 515 (1990) 193.

Note

Isolation of the insect metabolite trehalose by high-performance liquid chromatography

KATSUMI IIDA and MASAHIRO KAJIWARA*

Department of Medicinal Chemistry, Meiji College of Pharmacy, 1–22–1 Yato-cho, Tanasi-shi, Tokyo 188 (Japan)

Several approaches are used in our laboratory for the preparation of labelled compounds[1,2]. We are interested in a biological process for preparing ^{13}C-labelled compounds. Trehalose, which is a non-reducible disaccharide, was discovered in the blood of *Antheraea polyphemus* by Wyatt and Kalf[3]. Today, it is well known that trehalose is generally the blood sugar of insects. Candy and Kilby[4,5] discovered that trehalose is formed from glucose *in vivo* by insects. [1-^{13}C]-D-Glucose was converted into [1,1'-^{13}C$_2$]-D-trehalose in live *Gryllodes sigillatus*, the Japanese Kamado cricket. The time course of the metabolism of [1-^{13}C]-D-glucose to [1,1'-^{13}C$_2$]-D-trehalose was studied *in vivo* by ^{13}C NMR spectrometry. The isolation[6] of [1,1'-^{13}C$_2$]-D-trehalose was performed by high-performance liquid chromatography (HPLC).

EXPERIMENTAL

Materials

Gryllodes sigillatus were adult males. [1-^{13}C]-D-Glucose (99 atom-% ^{13}C) was supplied by Cambridge Isotope Laboratories. Ethanol and acetonitrile were distilled before use. Water was ion exchanged and distilled before use.

HPLC system

A SSC Flow System 3100J pump, equipped with an Erma ERC-7520 refractive index detector, and a Senshu Pak NH$_2$-1251-N (5 μm) column (25 cm × 0.46 cm I.D.) was used. The mobile phase was acetonitrile–water (70:30). The flow-rate of the mobile phase was maintained at 1 ml/min. The column pressure was 75 kg/cm^2 and the column temperature was kept at 22°C.

Assay of trehalose

^{13}C NMR spectra were recorded on a JEOL GSX-400 (100 MHz) spectrometer and referenced from CDCl$_3$ (77.0 ppm) as an external standard. Fast atom bombardment mass spectrometry (FAB-MS) was performed on a JMS-DX302 spectrometer.
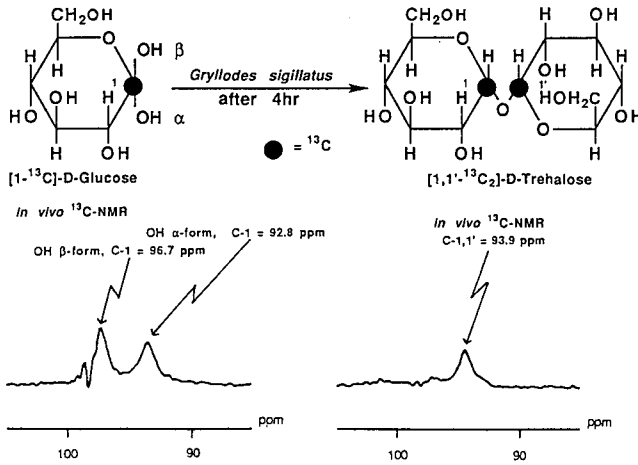
Fig. 1. ^{13}C NMR spectra of the *in vivo* transformation of [1-^{13}C]-D-glucose to [1,1'-^{13}C$_2$]-D-trehalose in *Gryllodes sigillatus*.

RESULTS AND DISCUSSION

[1-^{13}C]-D-Glucose (150 mg) was dissolved in distilled water (500 μl). The solution (10 μl) was injected intra-abdominally into each cricket, *Gryllodes sigillatus* (50 specimens). The metabolism to [1,1'-^{13}C$_2$]-D-trehalose (93.9 ppm)[7] from [1-^{13}C]-D-glucose (OH α-form = 92.8 ppm, OH β-form = 96.7 ppm)[8] was followed *in vivo* by using ^{13}C NMR spectrometry (Fig. 1).

After 4 h, the crickets were immersed in ethanol-saturated dry-ice for instanta-
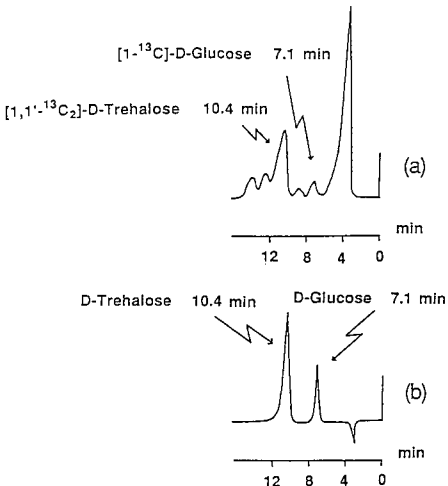
Fig. 2. Purification of extracted [1,1'-^{13}C$_2$]-D-trehalose by HPLC. (a) Separation of extracted [1-^{13}C]-D-glucose and [1,1'-^{13}C$_2$]-D-trehalose using HPLC. (b) Separation of authentic samples of D-glucose and D-trehalose using HPLC.

neous freezing, then homogenized in 70% ethanol. The suspension was centrifuged at 10 000 g for 20 min. The supernatant solution was passed through a cellulose acetate filter (20 μm) before freeze-drying. The residue was dissolved in mobile phase (800 μl) and the solution (20 μl) was injected onto the column. After purification by HPLC (Fig. 2), 20 mg of [1,1'-^{13}C$_2$]-D-trehalose were obtained in 27% yield. ^{12}C$_{10}$^{13}C$_2$H$_{10}$O$_{11}$: mol.wt. = 344.31. FAB-MS: m/z = 343 (M$^+$ − 1, 3%). ^{13}C NMR: 93.9 ppm.

CONCLUSION

Based on the metabolic function of the insects, [1-^{13}C]-D-glucose was converted into [1,1'-^{13}C$_2$]-D-trehalose, which was isolated by HPLC. [1,1'-^{13}C$_2$]-D-Trehalose will be useful in the study of insect sugars.

REFERENCES

1 K. Kurumaya, T. Okazaki, N. Seido, Y. Akasaka, Y. Kawajiri, M. Kondo and M. Kajiwara, *J. Labelled Compd. Radiopharm.*, 27 (1989) 217.
2 K. Kurumaya, T. Okazaki and M. Kajiwara, *Chem. Pharm. Bull.*, 37 (1989) 1151.
3 G. R. Wyatt and G. F. Kalf, *J. Gen. Physiol.*, 40 (1957) 833.
4 D. J. Candy and B. A. Kilby, *Nature (London)*, 183 (1959) 1594.
5 D. J. Candy and B. A. Kilby, *Biochem. J.*, 78 (1961) 531.
6 L. C. Stewart, N. K. Richtmyer and C. S. Hudson, *J. Am. Chem. Soc.*, 72 (1950) 2059.
7 T. Usui, N. Yamaoka, K. Matsuda, K. Tuzimura, H. Sugiyama and S. Seto, *J. Chem. Soc., Perkin Trans. 1*, (1973) 2425.
8 E. Breitmaier and W. Voelter, *Carbon-13 NMR Spectroscopy*, VCH Verlagsgesellschaft, Weinheim, 1987, pp. 27 and 380.

CHROMSYMP. 1936

Sensitive assay system for bile acids and steroids having hydroxyl groups utilizing high-performance liquid chromatography with peroxyoxalate chemiluminescence detection

SAKAE HIGASHIDATE*, KIYOKATSU HIBI and MASAAKI SENDA

JASCO, Japan Spectroscopic Co., Ltd., 2967–5 Ishikawa-cho, Hachioji City, Tokyo 192 (Japan)

and

SUSUMU KANDA and KAZUHIRO IMAI

Branch Hospital Pharmacy, University of Tokyo, 3–28–6 Mejirodai, Bunkyo-ku, Tokyo 112 (Japan)

ABSTRACT

3α- or 3β-hydroxysteroids, such as bile acids (free and glycine and taurine conjugates), 3β-hydroxy-5-cholenic acid, pregnanediol, 5-pregnene-3β,20β-diol and 5-pregnene-3β,20α-diol, were converted to 3-oxosteroids by enzymatic reaction using immobilized hydroxysteroid dehydrogenase, derivatized with dansylhydrazine to the corresponding dansyl hydrazones and purified by gel permeation chromatography. The dansyl hydrazones were chromatographed on a C_{18} column with a tetrahydrofuran-containing eluent and detected at the level of a few femtomoles by a peroxyoxalate chemiluminescence post-column reaction using bis[4-nitro-2-(3,6,9-trioxadecyloxycarbonyl)phenyl] oxalate as a chemilumigenic reagent. The dansyl hydrazones of chenodeoxycholic acid and deoxycholic acid (free and glycine and taurine conjugates) in particular, which coeluted under the chromatographic conditions above, were separated using an eluent including acetonitrile and 2,6-di-O-methyl-β-cyclodextrin and detected in the same way.

INTRODUCTION

Bile acids, produced from cholesterol in the liver, have one, two or three hydroxyl groups at the C-3, C-7 or C-12 position in the steroid ring. One or two such hydroxyl groups occur in other steroids, steroid hormones and metabolites, such as cholesterol, testosterone and pregnanediol. For the sensitive detection of these steroids, the hydroxyl group has been effectively used. For example, Okuyama *et al.*[1] reported the detection of bile acids by means of post-column derivatization using an immobilized hydroxysteroid dehydrogenase (HSD) column reactor, in which fluorescence detection of NADH [reduced form of nicotinamide adenine dinucleotide (NAD)] produced in the reactor was utilized. Kawasaki *et al.*[2] used an HSD reactor for

the precolumn derivatization of bile acids; the 3-oxo-bile acids thus produced were derivatized with dansylhydrazine to the corresponding dansyl hydrazones, separated and detected fluorimetrically.

Although these fluorimetric methods provided high sensitivity, the detection limits were in the picomole to sub-picomole range. Recently, we reported the sensitive detection of oxosteroids by derivatization of the oxosteroids with dansylhydrazine followed by high-performance liquid chromatographic (HPLC) separation and peroxyoxalate chemiluminescence detection[3,4]. The detection limits were in the femtomole range. Therefore, all hydroxysteroids could be sensitively detected according to the above procedures combined, provide that they can be converted to oxosteroids by the corresponding HSDs.

In this work, 3α- or 3β-hydroxy-bile acids and 3α- or 3β-hydroxysteroids were converted to the corresponding 3-oxosteroids by using co-immobilized 3α- and 3β-HSD, derivatized with dansylhydrazine to the corresponding dansyl hydrazones, separated on a C_{18} column and detected by peroxyoxalate chemiluminescence detection using bis[4-nitro-2-(3,6,9-trioxadecyloxycarbonyl)phenyl] oxalate (TDPO) as a chemilumigenic reagent.

EXPERIMENTAL

Materials

Fifteen bile acids (cholic acid, deoxycholic acid, chenodeoxycholic acid, lithocholic acid and ursodeoxycholic acid and their glycine and taurine conjugates) were purchased from Technochemical (Tokyo, Japan). 5β-Pregnane-3α,20α-diol (pregnanediol), 5-pregnene-3β,20α-diol and 5-pregnene-3β,20β-diol were obtained from Sigma (St. Louis, MO, U.S.A.) and 3β-hydroxy-5-cholenic acid from Steraloids (Wilton, NH, U.S.A.). Dansylhydrazine, nicotinamide adenine dinucleotide (NAD) and hydroxysteroid dehydrogenase (HSD, grade II) were purchased from Sigma. Aminopropyl-CPG (120–200 mesh, 500 Å) was obtained from Electro-Nucleonics (Fairfield, NJ, U.S.A.). Bond Elut C_{18} cartridges were purchased from Analytichem (Harbor City, CA, U.S.A.). Bis[4-nitro-2-(3,6,9-trioxadecyloxycarbonyl)phenyl] oxalate (TDPO) and 2,6-di-O-methyl-β-cyclodextrin were purchased from Wako (Osaka, Japan) and imidazole (zone refined) was a gift from Tokyo Kasei Kogyo (Tokyo, Japan). The other reagents were of analytical-reagent or HPLC grade.

An immobilized enzyme was prepared by immobilizing HSD on aminopropyl-CPG with glutaraldehyde as a coupling reagent[1]. This immobilized enzyme was packed into an open glass column (60 mm × 8 mm I.D.); the height of the packed material was 20 mm.

NAD solution was prepared by dissolving NAD in 0.1 M tris(hydroxymethyl)aminomethane buffer (chloride, pH 9.00)–methanol (9:1) to give a 0.5 mM solution. Dansylhydrazine solution was prepared by dissolving 2 mg of dansylhydrazine in 10 ml of ethanol. Hydrochloric acid (0.022 M) was prepared by dissolving 0.45 ml of 36% hydrochloric acid in 250 ml of ethanol.

Preparation of dansyl hydrazones of hydroxysteroids

A 20-nmol amount of each hydroxysteroid dissolved in 100 μl of methanol was applied to the immobilized enzyme column, then three 1-ml portions (for bile acids) or

five 1-ml portions (for other steroids) of the NAD solution were added to elute the oxosteroid produced on the column. The column eluate was mixed with 3 ml (for bile acids) or 5 ml (for other steroids) of water. The mixed solution was then applied to a Bond Elut C_{18} cartridge which had been preconditioned with water. The cartridge was washed with three 3-ml portions of water and then evacuated with an aspirator to remove water in the column. The oxosteroid remaining in the cartridge was eluted with 3 ml of ethanol. The ethanol solution obtained was evaporated to dryness *in vacuo* at room temperature and the residue was dissolved in 1 ml of ethanol. To one tenth of this solution were added 200 μl of the dansylhydrazine solution and 2 ml of the 0.022 M ethanolic hydrochloric acid solution. The mixture was allowed to stand overnight at room temperature and evaporated to dryness *in vacuo*. The residue was dissolved in 100 μl of chloroform and a 80-μl portion of the chloroform solution was injected into a Finepak GEL 101 gel permeation column (500 mm × 7.2 mm I.D.) (JASCO). Chloroform was used as the eluent at a flow-rate of 0.7 ml/min.

The column eluate was monitored with a fluorimetric detector (JASCO Model 820-FP) at an excitation wavelength of 350 nm and an emission wavelength of 505 nm. The fraction from 14.2 to 15.2 min (for bile acids) or that from 14.8 to 16.1 min (for other steroids) was collected and evaporated to dryness *in vacuo*. The residue was dissolved in 1 ml of acetonitrile. A portion of the solution was diluted 100-fold with the corresponding eluent and a 10-μl aliquot was injected into the HPLC system.

HPLC conditions

The HPLC system consisted of an eluent delivery pump (JASCO Model 880-PU), a column oven (JASCO Model 860-CO), a reagent delivery pump (JASCO Model 880-PU), a chemiluminescence detector (JASCO Model 825-CL) and a mixing device (Kyowa Seimitsu Model KZU-1). The column eluate was mixed at the mixing device with the chemilumigenic reagent solution. The mixture was introduced into the detector, having a PTFE spiral-type flow cell with a volume of 93 μl. The analytical columns were a Finepak SIL C_{18} S (5 μm) (150 mm × 4.6 mm I.D.) (JASCO) and a phenyl-bonded silica gel column packed with Develosil PhA (5 μm) (150 mm × 4.6 mm I.D.) (Nomura Chemical, Aichi, Japan) and the column temperature was 40°C. The eluent was 50 mM imidazole buffer (nitrate, pH 6.00)–tetrahydrofuran [95:105 (v/v) for the separation of bile acids or 105:95 (v/v) for that of other steroids] and was delivered at a flow-rate of 1.0 ml/min. In particular, a 25:75 (v/v) mixture of the same imidazole buffer and acetonitrile containing 7.5 mM 2,6-di-O-methyl-β-cyclodextrin was used as an eluent to separate chenodeoxycholic acid and deoxycholic acid (free and glycine and taurine conjugates).

The chemilumigenic reagent solution was prepared by dissolving 0.25 mM TDPO and 12.5 mM hydrogen peroxide in acetonitrile–ethyl acetate (1:1) and was delivered at a flow-rate of 1.7 ml/min.

RESULTS AND DISCUSSION

Hydroxysteroids are converted to oxosteroids in accordance with the oxidation selectivity of HSDs. For example, 7α-HSD converts 7α-hydroxysteroids to 7-oxo-steroids. In this way, selection of suitable HSDs permits the formation of different

kinds of oxosteroids. The oxosteroids obtained are derivatized with dansylhydrazine to the corresponding dansyl hydrazones.

Among several kinds of HSDs, we selected an HSD from Sigma which converts both 3α- and 3β-hydroxysteroids to 3-oxosteroids in the presence of NAD. The enzyme immobilized on aminopropyl-CPG was used repeatedly in the form of an enzyme column reactor to produce 3-oxosteroids. During this experiment, it was found that three times the reactor volume of NAD solution was required to elute 3-oxo-bile acids and five times the reactor volume to elute other 3-oxosteroids, probably because of the greater affinity of the latter to the reactor column.

Compounds derivatized with dansylhydrazine have a higher molecular weight than dansylhydrazine; the former elute faster than the latter in gel permeation chromatography (GPC). Thus, as reported previously[5], dansyl hydrazones of oxosteroids in a reaction mixture were separated from the excess of dansylhydrazine and purified. Fig. 1 shows a gel permeation chromatogram obtained from a reaction mixture of 7α,12α-dihydroxy-3-oxo-5βcholanic acid (an oxidation product of cholic acid) and dansylhydrazine. Peak 1 eluting at 14.7 min corresponds to the dansyl hydrazone of the above oxo-bile acid; the amount corresponds to 1.6 nmol.

A compound derivatized with dansylhydrazine forms *anti* and *syn* conformers; this results in the appearance of two peaks corresponding to these conformers with the
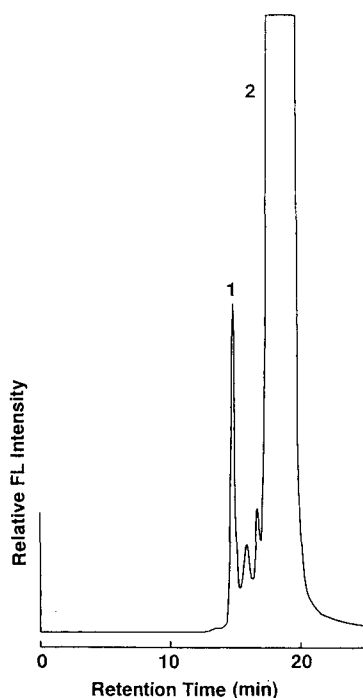
Fig. 1. GPC of a reaction mixture of 7α,12α-dihydroxy-3-oxo-5β-cholanic acid and dansylhydrazine. Peaks: 1 = dansyl hydrazone of cholic acid (1.6 nmol); 2 = dansylhydrazine. Conditions: column, Finepak GEL 101 (500 mm × 7.2 mm I.D.); eluent, chloroform; flow-rate, 0.7 ml/min; detector, 820-FP (excitation wavelength 350 nm, emission wavelength 505 nm).

usual organic constituents such as methanol and acetonitrile in the eluent[6]. As we reported previously[5], the use of tetrahydrofuran as an organic constituent in the eluent caused these two conformers to elute as a single peak with a C_{18} column. This effect of tetrahydrofuran was also demonstrated in this work on the separation of bile acids and other steroids. Fig. 2 shows a chromatogram obtained from a mixture of derivatized bile acids (free form, 160 fmol each). Although chenodeoxycholic and deoxycholic acid remained unresolved, each bile acid exhibited a single peak. In the same way, derivatized glycine- and taurine-conjugated bile acids gave the corresponding single peaks. The detection limits at a signal-to-noise ratio of 2 were between 3 and 8 fmol for all the bile acids. The difference in the detection limits could be due to the difference in reactivity of immobilized HSD with individual bile acids. These detection limits were about 100 times lower than those obtained with fluorescence detection[2].

On the C_{18} column, the separation of the dansyl hydrazone of chenodeoxycholic acid from that of deoxycholic acid was not successful. Another kind of reversed-phase column with phenyl-bonded silica gel was used with tetrahydrofuran as an organic constituent. However, the separation was not achieved. We then investigated the effect of β-cyclodextrins on the separation between the dansyl hydrazones of these two bile acids, as the addition of β-cyclodextrin to the eluent (phosphate buffer–acetonitrile) improved the separation of bile acids according to Shimada et al.[7]. Addition of
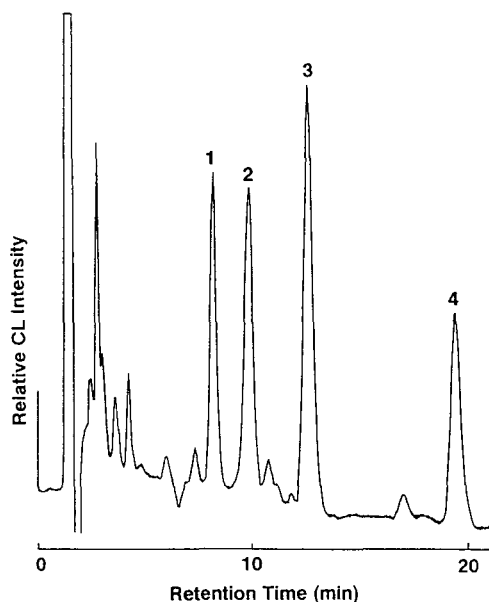
Fig. 2. HPLC of a mixture of bile acids (free form) derivatized with dansylhydrazine. Peaks (160 fmol each): dansyl hydrazones of (1) cholic acid, (2) ursodeoxycholic acid, (3) chenodeoxycholic acid and deoxycholic acid and (4) lithocholic acid. Conditions: column, Finepak SIL C_{18} S (5 μm) (150 mm × 4.6 mm I.D.); column temperature, 40°C; eluent, 50 mM imidazole buffer (nitrate, pH 6.00)–tetrahydrofuran (95:105, v/v); flow-rate, 1.0 ml/min; chemilumigenic reagent, 0.25 mM TDPO and 12.5 mM hydrogen peroxide in acetonitrile–ethyl acetate (1:1, v/v); reagent flow-rate, 1.7 ml/min.

β-cyclodextrin to the eluent containing 52.5% tetrahydrofuran for the C_{18} column resulted in precipitation of β-cyclodextrin owing to its low solubility in tetrahydrofuran. Instead, more soluble cyclodextrins such as 2,6-di-O-methyl- and 2,3,6-tri-O-methyl-β-cyclodextrin were examined. However, the separation between the dansyl hydrazones of the two bile acids was not successful. Next, tetrahydrofuran was replacd with acetonitrile. As shown in Fig. 3, derivatized chenodeoxycholic acid and deoxycholic acid were separated by using an eluent containing 2,6-di-O-methyl-β-cyclodextrin, acetonitrile and the imidazole buffer, although the peaks were broader than those obtained with an eluent containing tetrahydrofuran without cyclodextrin. The reason why the effect of the cyclodextrin disappeared on addition of tetrahydrofuran is not clear.

In the same way, glycine and taurine conjugates of these two bile acids were separated. The detection limits at a signal-to-noise ratio of 2 were between 8 and 15 fmol. Hence a combination of these two kinds of eluent permits the separation of all fifteen bile acids.

As shown in Fig. 4, derivatized 3β-hydroxy-5-cholenic acid (a bile acid having a 3β-hydroxyl group, 160 fmol) was also detected sensitively by the present system. The detection limit at a signal-to-noise ratio of 2 was 4 fmol.
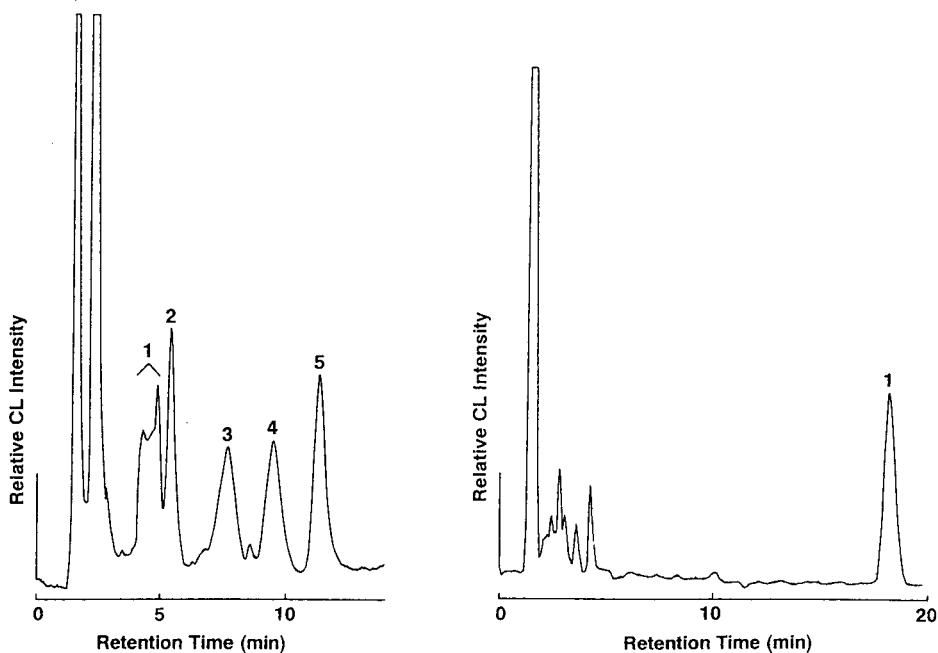
Fig. 3. HPLC of a mixture of bile acids (free form) derivatized with dansylhydrazine. Peaks (160 fmol each): dansyl hydrazones of (1) ursodeoxycholic acid, (2) cholic acid, (3) chenodeoxycholic acid, (4) deoxycholic acid and (5) lithocholic acid. Eluent, 50 mM imidazole buffer (nitrate, pH 6.00)–acetonitrile (25:75, v/v) containing 7.5 mM 2,6-di-O-methyl-β-cyclodextrin; other conditions as in Fig. 2.

Fig. 4. HPLC of 3β-hydroxy-5-cholenic acid derivatized with dansylhydrazine. Peak 1 = dansyl hydrazone of 3β-hydroxy-5-cholenic acid (160 fmol). Conditions as given in Fig. 2.
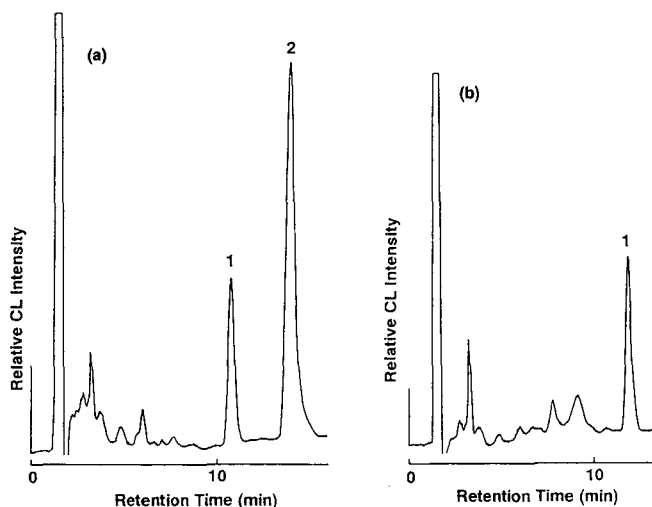
Fig. 5. HPLC of 3β-hydroxysteroids and pregnanediol derivatized with dansylhydrazine. (a) Peaks (160 fmol each): dansyl hydrazones of (1) 5-pregnene-3β,20α-diol and (2) 5-pregnene-3β,20β-diol. (b) Peak 1 = dansyl hydrazone of pregnanediol (160 fmol). Eluent, 50 mM imidazole buffer (nitrate, pH 6.00)–tetrahydrofuran (105:95, v/v); other conditions in Fig. 2.

Fig. 5 shows chromatograms obtained from two derivatized 3β-hydroxysteroids (5-pregnene-3β,20α-diol ad 5-pregnene-3β,20β-diol) and from derivatized pregnanediol (5β-pregnane-3α,20α-diol). It can be seen that steroids that have a 3β- or 3α-hydroxyl group were also detected sensitively by the present system. The detection limits at a signal-to-noise ratio of 2 were between 2 and 4 fmol.

We are now trying to apply this detection method to the determination of bile acids in biological fluids such as serum and urine. After bile acids have been separated into three groups, namely free, glycine-conjugated and taurine-conjugated, with a piperidinohydroxypropyl-Sephadex LH-20 column[8], each group of bile acids would be analysed by the present detection method.

An immobilized 3α- or 3β-HSD column reactor provides better selectivity than the HSD reactor used in this work and should be used in analysis of bile acids in biological fluids. In the similar way, as in this work, the use of immobilized 7α-HSD would permit the analysis of chenodeoxycholic acid and cholic acid and immobilized 12α-HSD that of deoxycholic acid and cholic acid.

In the present assay system, oxosteroids present in the biological specimens would affect the selectivity. Therefore, steroids having an oxo group should be converted to N-hydroximes with hydroxylamine and removed with a Bond Elut SCX cartridge (strong cation-exchange type) (Analytichem)[9] before the enzymatic conversion of hydroxysteroids. In this way, the hydroxysteroids remaining in the specimens can be subjected to the present assay system.

REFERENCES

1 S. Okuyama, N. Kokubun, S. Higashidate, D. Uemura and Y. Hirata, *Chem. Lett.*, (1979) 1443.
2 T. Kawasaki, M. Maeda and A. Tsuji, *J. Chromatogr.*, 272 (1983) 261.
3 S. Kobayashi and K. Imai, *Anal. Chem.*, 52 (1980) 424.
4 K. Imai, S. Higashidate, A. Nishitani, Y. Tsukamoto, M. Ishibashi, J. Shoda and T. Osuga, *Anal. Chim. Acta*, 227 (1989) 21.
5 K. Imai, S. Higashidate, Y. Tsukamoto, S. Uzu and S. Kanda, *Anal. Chim. Acta*, 225 (1989) 421.
6 R. Weinberger, T. Koziol and G. Millington, *Chromatographia*, 19 (1984) 452.
7 K. Shimada, Y. Komine and T. Oe, *J. Liq. Chromatogr.*, 12 (1989) 501.
8 J. Goto, M. Hasegawa, H. Kato and T. Nambara, *Clin. Chim. Acta*, 87 (1978) 141.
9 J. Shoda, Y. Matsuzaki, K. Mitsumura, T. Osuga, T. Aikawa, S. Yamazaki, M. Ito, M. Ishibashi and H. Miyazaki, *KANZO*, 106 (1984) 1618.

CHROMSYMP. 1930

Determination of α-tocopherol, free cholesterol, esterified cholesterols and triacylglycerols in human lipoproteins by high-performance liquid chromatography

KAZUO SETA*[,a]

Analytical Instrument Division, Yokogawa Electric Corporation, 2-9-32, Naka-cho, Musashino-shi, Tokyo 180 (Japan)

HARUO NAKAMURA

Internal Medicine, National Defence Medical College, 3-2, Namiki, Tokorozawa-shi, Saitama 359 (Japan)

and

TSUNEO OKUYAMA

Biochemistry, Department of Chemistry, Faculty of Science, Tokyo Metropolitan University, 2-1-1, Fukasawa, Setagaya-ku, Tokyo 158 (Japan)

ABSTRACT

The determination of α-tocopherol, free cholesterol, esterified cholesterols and triacylglycerols in human plasma and in fractions containing individual lipoproteins was achieved by reversed-phase high-performance liquid chromatography (HPLC). The lipoprotein fractions, such as chylomicron, VLDL, LDL, HDL_2 and HDL_3, were collected by ultracentrifugation of human plasma. The chromatographic separation was accomplished with a column packed with Hitachi Gel 3057, which is a spherical octadecylsilica of particle size 3 μm. The mobile phase was acetonitrile–2-propanol (75:25, v/v), and the eluate was monitored with ultraviolet absorption and fluorescence detectors connected in series. Qualitative analysis of the main chromatographic peaks collected during the HPLC of a plasma sample was done with the use of field-desorption mass spectrometry. The determination analysis of α-tocopherol, free cholesterol and esterified cholesterols was effected with a single chromatographic run with *n*-hexane extracts of plasma or lipoprotein fraction. The separation and determination of these fat-soluble components required as little as 5 μl of plasma or lipoprotein fraction.

---

[a] Present address: Biochemistry, Department of Chemistry, Faculty of Science, Tokyo Metropolitan University, 2-1-1, Fukasawa, Setagaya-ku, Tokyo 158, Japan.

INTRODUCTION

The lipids of the living body are a heterogeneous group of compounds related, either actually or potentially, to the fatty acids. They have the common property of being relatively insoluble in water and soluble in non-polar solvents. Fat serves as an insulating material in the subcutaneous tissues and around certain organs. Combinations of lipids and protein (lipoprotein) are important cellular constituents, occurring both in the cell membrane and in the mitochondria within the cytoplasma, and serving also as the means of transporting lipids in the blood[1].

Pure fat is less dense than water; it follows that as the proportion of lipid to protein in lipoproteins creases, the density decreases. Use is made if this property in separating the various lipoproteins in plasma by ultracentrifugation[2,3]. By this separation method, lipoproteins are classified as chylomicron, very-low-density lipoprotein (VLDL), low-density lipoprotein (LDL) and high-density lipoproteins (HDL$_2$ and HDL$_3$). Lipoproteins are known to be composed of free cholesterol (FC), esterified cholesterols (cholesteryl esters, CE), triacylglycerols (triglycerides, TG), phospholipids, apoproteins, tocopherols and others[4,5]. Nevertheless, the distribution and the behaviour of these components in lipoproteins and the steric structure of lipoproteins are not yet clear[6]. Further, these components are correlated with the states of various diseases such as atherosclerosis and hyperlipaemia[7].

Numerous analytical procedures are used for the measurement of these lipids because of their clinical significance. The most commonly used method is spectrophotometry, which is based on the colour reactions of these components with acid reagents[8,9]. However, this method can be used for the determination of only one component or the total homologues in plasma. Chromatographic methods are capable of determining fat-soluble components; gas–liquid[10], thin-layer[11], and high-performance liquid chromatography (HPLC)[12–16] have been applied. HPLC is useful for the determination of various types and numbers of components of plasma[14,15] and TG[14] in plasma. Various HPLC methods have been reported for determining tocopherols[6,12–16], FC[6,14,15], CE[14,15] and TG[14] in plasma. Unfortunately, the separation of these components in fractions containing individual proteins has not yet been achieved.

In this paper, we report an HPLC method for the determination of these fat-soluble components in human plasma and in individual lipoprotein fractions.

EXPERIMENTAL

Chemicals
n-Hexane, acetonitrile, 2-propanol and ethanol of liquid chromatography grade were purchased from Wako (Osaka, Japan). Cholesterol and cholesteryl benzoate, caprylate, linoleate, oleate, palmitate and stearate were purchased from Nacalai Tesque (Kyoto, Japan), cholesteryl arachidonate and cholesteryl heptadecanoate from Sigma (St. Louis, MO, U.S.A.), cholesteryl myristate from Tokyo Kasei (Tokyo, Japan), triolein, trilinolein, 1,2-dioleoylstearin, 1,2-dipalmitoylolein, 1,3-dipalmitoylolein and 1,2-dipalmitoylstearin from P. L. Biochemicals (Milwaukee, WI, U.S.A.) and pig liver triglycerides from Serdary Research Labs. (London, Canada).

Preparation of samples

Plasma samples from individual normal healthy adult male volunteers were obtained from the National Defence Medical College (Saitama, Japan). All centrifugations of samples were carried out in a Hitachi Model 55P-7 ultracentrifuge at 4°C.

Lipoprotein fractions of human plasma were prepared by the standard method of flotation ultracentrifugation[2,6] using potassium bromide to adjust the density (d) of the plasma. The plasma was centrifuged sequentially at densities of 1.006, 1.063, 1.125 and 1.21 to separate plasma lipoproteins. The first fraction ($d < 1.006$), obtained by centrifugation for 30 min at 27 000 rpm (60 000 g) contains chylomicrons, the second fraction ($1.006 > d > 1.063$), obtained by centrifugation for 18 h at 39 000 rpm (120 000 g) contains VLDL, the third ($1.063 < d < 1.125$) contains LDL, the fourth ($1.125 < d < 1.21$) contains HDL$_2$ and the fifth ($d > 1.21$) contains HDL$_3$ and plasma proteins.

Preparation of sample extracts

A 100-μl plasma or lipoprotein sample was pipetted into a 115 mm $\times$ 23 mm I.D. glass test tube and 1 ml of water and 1 ml of ethanol were added and mixed on a vortex mixer for 2 min. Then 5 ml of *n*-hexane (containing 15 μg of cholesteryl benzoate or heptadecanoate as an internal standard) was added, and the tube was shaken mechanically for 10 min. A 4-ml aliquot of the *n*-hexane layer was pipetted into a 110 mm $\times$ 16 mm I.D. glass test-tube and evaporated to dryness in a water-bath at 45°C under reduced pressure using a rotary evaporator. The residue was then dissolved in 100 μl of ethanol and the extract was used for sampling for injection (usually 20 μl) onto the chromatographic column.

Apparatus

A Toyo Soda Model 803-B liquid chromatograph with a Schoeffel Model 770 UV detector and a Schoeffel Model 970 fluorescence detector connected in series was used. A 150 mm $\times$ 4 mm I.D. stainless-steel column packed with Hitachi Gel 3057 (octadecylsilica) of particle size 3 μm was used for the reversed-phase HPLC of lipids.

For routine plasma and lipoprotein analyses, an isocratic system was used with a mobile phase of acetonitrile–2-propanol (75:25, v/v). The eluent flow-rate was 1 ml/min with UV monitoring at 205 nm (0.04 a.u.f.s.) and with fluorescence monitoring at $\lambda_{ex.}$ 215 and $\lambda_{em.}$ 320 nm. The column temperature was maintained at 50°C. Field-desorption mass spectrometry (FD-MS) of cholesteryl esters and triglycerides collected during the HPLC of individual samples was carried out with a Hitachi Model M80-A mass spectrometer.

RESULTS AND DISCUSSION

Fig. 1 shows typical chromatograms obtained from (A) the HPLC separation of a standard solution containing α-tocopherol, FC and individual CE and (B) the HPLC separation of a standard solution containing pig liver TG. A chromatographic run was completed in *ca.* 20 min. As shown by the solid line, CE with saturated fatty acids, cholesteryl caprylate ($C_{8:0}$), myristate ($C_{14:0}$), palmitate ($C_{16:0}$), heptadecanoate ($C_{17:0}$) and stearate ($C_{18:0}$) were eluted in that order owing to the differences in partitioning of the fatty acid chain length on the column. On the other hand, CE with
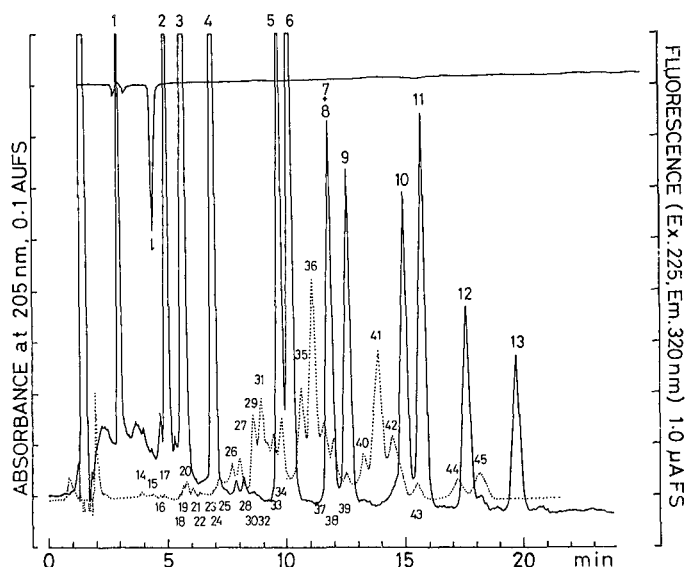
Fig. 1. Chromatograms of standard compounds. Conditions: column, stainless steel (15 × 0.4 cm I.D.) packed with Hitachi Gel 3057; eluent, acetonitrile–isopropanol (75:25, v/v); flow-rate, 1 ml/min; temperature, 50°C; pressure, 10.3 MPa; sample, (a) standard solution containing α-tocopherol (145 ng), cholesterol (2.23 μg) and cholesteryl esters (1.5–6.85 μg) (solid line) and (b) standard pig liver triglyceride (10 μg) (dotted line). For identification of individual peaks, see Table 1.

unsaturated fatty acids, cholesteryl linolenate ($C_{18:3}$), arachidonate ($C_{20:4}$), linoleate ($C_{18:2}$) and oleate ($C_{18:1}$) were eluted in that order owing to the differences in the number of double bonds in the fatty acid chain. The peak for cholesteryl palmitoleate was eluted between those for cholesteryl myristate and linoleate.

TABLE I

CAPACITY FACTORS (k') OF MAIN FAT-SOLUBLE COMPOUNDS ON THE HITACHI GEL 3057 COLUMN

No.	Compound	k'	No.	Compound	k'
1	α-Tocopherol	1.25	23	Trilinolein (LLL)	4.35
2	Cholesterol	3.01	39	Triolein (OOO)	8.59
3	Cholesteryl benzoate	3.22	41	1,2- or 1,3-Dipalmitoylolein	9.59
4	Cholesteryl caprylate ($C_{8:0}$)	4.16		(PPO or POP)	
5	Cholesteryl linolenate ($C_{18:3}$)	6.18	43	Tripalmitin (PPP)	10.61
6	Cholesteryl arachidonate ($C_{20:4}$)	6.51	44	1,2-Dioleoylstearin (OOS)	11.44
7	Cholesteryl linoleate ($C_{18:2}$)	7.72			
8	Cholesteryl palmitoleate ($C_{16:1}$)	7.72			
9	Cholesteryl myristate ($C_{14:0}$)	8.34			
10	Cholesteryl oleate ($C_{18:1}$)	10.06			
11	Cholesteryl palmitate ($C_{16:0}$)	10.68			
12	Cholesteryl heptadecanoate ($C_{17:0}$)	12.08			
13	Cholesteryl stearate ($C_{18:0}$)	13.65			

Similarly, as shown by the dotted line, standard pig liver TG were also separated under the same conditions as standard cholesteryl esters. From the chromatogram, it is clear that the sample contains about 30 kinds of individual TG. As the TG consist of three fatty acids and glycerol, the chromatographic behaviour of TG is more complicated than that of CE. However, as a rule, the retention of TG depends on the structure of the three fatty acids as with CE.

The retention characteristics of these standard compounds are given in Table I as capacity factors (k'). The HPLC separation of some CE and a few TG have been reported by other investigators[14,15] using columns packed with 10-μm reversed-phase octadecylsilica packings, but the resolutions of individual CE and/or TG were not satisfactory. With regard to the mobile phase, we chose acetonitrile–2-propanol (75:25, v/v) to measure fat-soluble components in blood at low UV wavelengths. The fluorescence detector was also employed for the sensitive measurement of α-tocopherol. Fig. 2 shows a chromatogram of a plasma extract corresponding to 8 μl of original human plasma. The completeness of extraction of α-tocopherol, FC and CE from plasma was investigated by the use of an internal standard. The recoveries of each component were also excellent when known amounts of standard compounds were added to plasma together with the internal standards before the extraction. The use of antioxidants was not necessary for the determination of α-tocopherol and other constituents.

With regard to plasma determination, the values obtained for α-tocopherol, FC and individual cholesteryl esters are given in Table II. These values are in agreement with those reported in the literature for α-tocopherol[13,16] and FC and CE[14,15]. In order to ascertain the identity of the chromatographic peaks of CE, each peak fraction was collected during a run with plasma, and then analysed by FD-MS. The mass
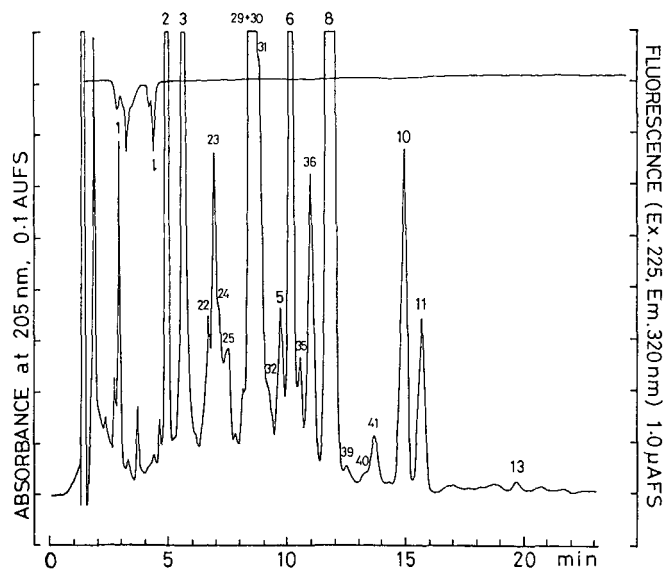
Fig. 2. Chromatogram of fat-soluble components of human plasma extracts. Conditions as in Fig. 1.

TABLE II

CONCENTRATIONS OF α-TOCOPHEROL, FREE CHOLESTEROL, INDIVIDUAL CHOLESTERYL ESTERS AND TOTAL CHOLESTEROL IN HUMAN PLASMA AND IN INDIVIDUAL LIPOPROTEIN FRACTIONS DETERMINED BY HPLC

| Compound | Concentration (mg/dl plasma) (mean ± S.D., n=5) | | | | | |
| | Plasma | Lipoprotein | | | | |
		Chylomicron	VLDL	LDL	HDL_2	HDL_3
α-Tocopherol	0.93 ± 1.6	0.39 ± 0.33	0.20 ± 0.14	0.35 ± 0.21	0.14 ± 0.1	0.02 ± 0.02
Free cholesterol[a]	40.9 ± 4.7	5.50 ± 2.4	4.7 ± 2.6	19.7 ± 4.0	3.2 ± 0.6	1.7 ± 0.4
Cholesteryl linolenate[b]	4.2 ± 1.4	0.5 ± 0.2	0	3.2 ± 1.4	1.0 ± 0.1	0.5 ± 0.2
	2.5[a]	0.3[a]	0[a]	1.9[a]	0.6[a]	0.3[a]
Cholesteryl arachidonate[b]	34.2 ± 9.0	3.4 ± 1.6	2.8 ± 2.6	22.0 ± 9.9	7.4 ± 1.4	4.7 ± 1.1
	19.6[a]	2.0[a]	1.6[a]	12.6[a]	4.3[a]	2.7[a]
Cholesteryl linoleate[b] }	191.2 ± 36.6	19.4 ± 6.8	11.8 ± 8.6	123.2 ± 34.0	40.0 ± 8.7	26.2 ± 2.6
Cholesteryl palmitoleate[b] }	113.9[a]	11.6[a]	7.0[a]	73.4[a]	23.8[a]	15.6[a]
Cholesteryl oleate[b]	27.7 ± 5.6	2.6 ± 1.4	1.8 ± 1.4	21.5 ± 7.7	5.5 ± 0.6	3.2 ± 1.0
	16.4[a]	1.5[a]	1.1[a]	12.8[a]	3.3[a]	1.9[a]
Cholesteryl palmitate[b]	11.9 ± 2.3	1.6 ± 0.6	0.7 ± 0.6	10.1 ± 3.9	2.6 ± 0.3	2.2 ± 0.9
	7.4[a]	1.0[a]	0.4[a]	6.2[a]	1.6[a]	1.4[a]
Cholesteryl stearate[b]	1.7 ± 0.9	0	0	0	0	0
	1.0[a]	0[a]	0[a]	0[a]	0[a]	0[a]
Cholesteryl ester[b]	270.9 ± 55.8	27.5 ± 10.6	17.1 ± 13.2	180.0 ± 56.9	56.5 ± 11.1	36.8 ± 5.8
Cholesteryl ester[a]	160.8	16.4	10.1	106.9	33.6	21.9
Total cholesterol[a]	201.7	21.9	14.8	126.6	36.8	23.6

[a] Value as free cholesterol.
[b] Value as individual cholesteryl estr.
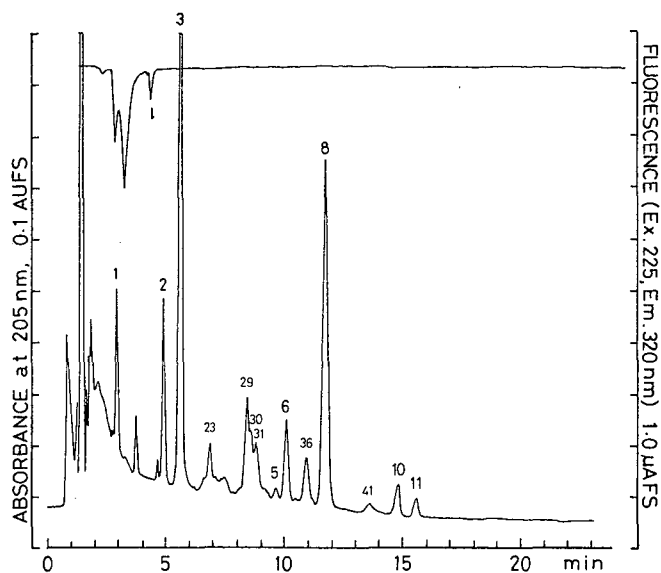
Fig. 3. Chromatogram of fat-soluble components of extracts from chylomicron. Conditions as in Fig. 1.

spectra of each peak of CE showed the molecular ion of each CE and fragment ions of cholesterol.

As Fig. 2 shows, not only tocopherols, FC and CE, but also many other peaks are separated and detected. These peaks from 22 to 41 were assigned as individual
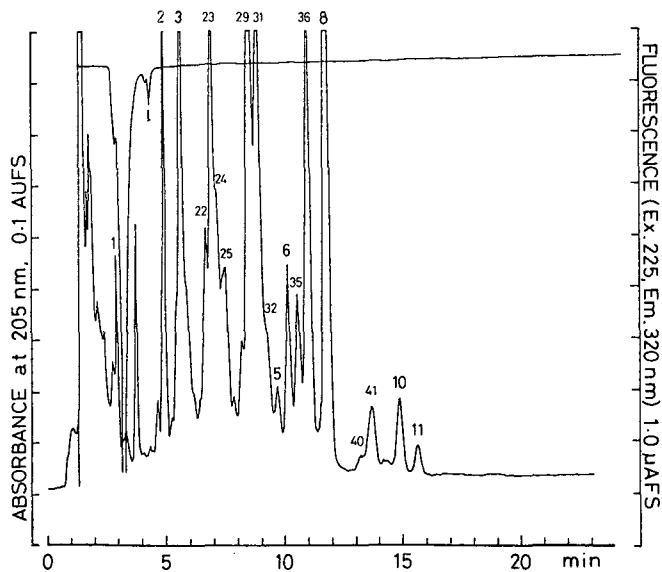
Fig. 4. Chromatogram of fat-soluble components of extract from VLDL. Conditions as in Fig. 1.

glycerols by FD-MS. Of these glycerol peaks, 23 and 41 were assigned as trilinolein and triolein, respectively. From the chromatogram, the profile of human plasma TG is apparently different from that of pig liver TG, as shown in Fig. 1. Unsaturated fatty acids have larger UV absorption coefficients than saturated fatty acids. Fatty acids of glycerols are combined with one, two or three fatty acids. Therefore, it is necessary to identify the TG peak and to prepare the individual TG standard compounds for the determination of these components in plasma.

Each lipoprotein fraction was chromatographed under the same conditions as for plasma extracts. A series chromatograms of fractions of chylomicron, VLDL, LDL, HDL$_2$ and HDL$_3$ from the same subject are illustrated in Figs. 3–7.

Fig. 3 shows a chromatogràm of the chylomicron fraction, corresponding to 25 μl of original plasma. Chylomicron is derived from the intestinal absorption of TG and has a molecular weight of several hundred million, but its concentration in plasma is low compared with those of other lipoproteins. Chylomicron is also characterized by relatively large amounts of TG and by small amounts of FC, phospholipids and apoprotein. As expected, the peaks of α-tocopherol and TG in the chromatogram of chylomicron are larger than those of plasma or other lipoproteins. In particularly, chylomicron has 35% of the total α-tocopherol in plasma.

Figs. 4 and 5 show chromatograms of VLDL and LDL, respectively. VLDL and LDL have higher contents of FC and CE than chylomicron, but less TG. These two chromatograms resemble that of the original plasma as shown in Fig. 2. However, the contents of α-tocopherol, FC and CE of LDL are apparently higher than those of VLDL. Therefore, it is confirmed that almost all of the lipids in plasma are involved in the LDL. It is known that VLDL is formed to a lesser extent from dietary lipids but is mainly derived from the liver for the export of TG. The bulk of plasma VLDL is of
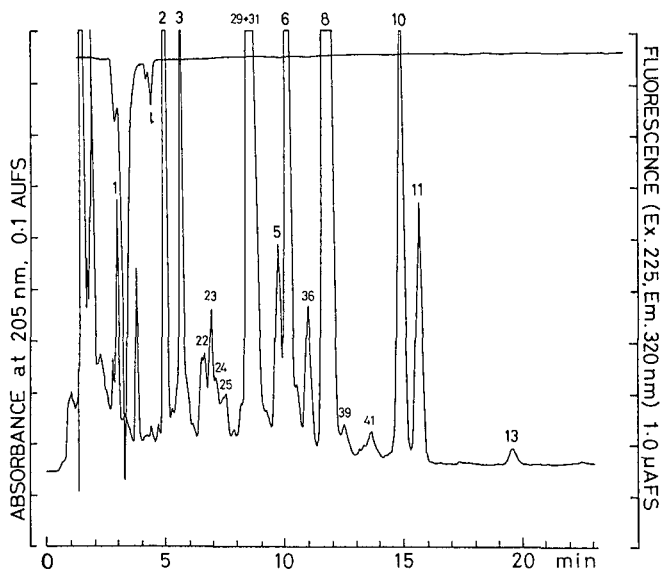
Fig. 5. Chromatogram of fat-soluble components of extract from LDL. Conditions as in Fig. 1.
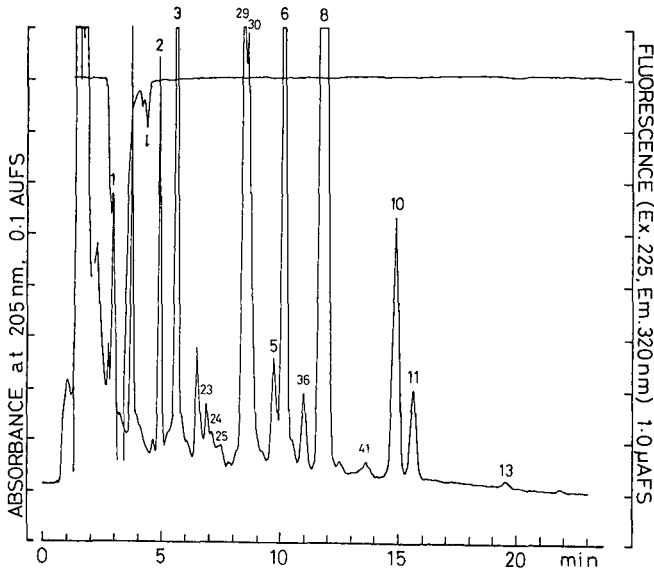
Fig. 6. Chromatogram of fat-soluble components of extract from HDL₂. Conditions as in Fig. 1.
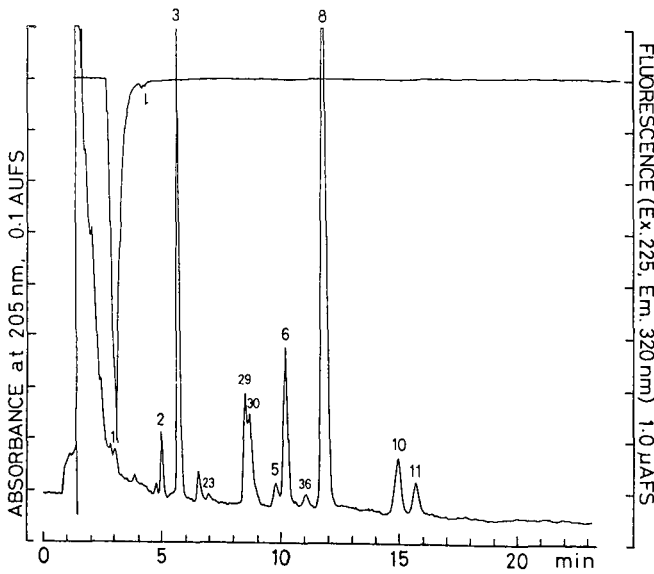
Fig. 7. Chromatogram of fat-soluble components of extract from HDL₃. Conditions as in Fig. 1.

hepatic origin, being the vehicle for transportation of TG from the liver to the extrahepatic tissues. This suggests a high content of TG in VLDL and it agrees with the results presented here. On the other hand, LDL represents the final stage in the catabolism of VLDL and possibly chylomicron.

Figs. 6 and 7 show chromatograms of HDL_2 and HDL_3, corresponding to 32 and 17 μl of original plasma, respectively. The characteristic profiles of these two chromatograms show a relatively high content of CE and low contents of FC and TG. In particular, HDL_3 has more small peaks of TG than other lipoproteins. This result is in agreement with the result for the chemical composition of HDL reported in the literature[17].

The results of the determination of α-tocopherol, FC and CE in plasma or individual lipoprotein fractions are listed in Table II. In the plasma lipoprotein, the FC value averaged 15.8% for chylomicron, 13.5% for VLDL, 56.6% for LDL, 9.2% for HDL_2 and 4.9% for HDL_3. Similarly, the α-tocopherol values averaged 35.5% for chylomicron, 18.2% for VLDL, 31.8% for LDL, 12.7% for HDL_2 and 1.8% for HDL_3. The total value of α-tocopherol, FC, individual CE and total cholesterol of five lipoprotein fractions are almost equal to the values for plasma. These results demonstrate that the present HPLC method is applicable to the determination of fat-soluble components in plasma and lipoprotein fractions.

The data obtained by the HPLC method were compared with those obtained by other HPLC or spectrophotometric methods. It was found that the plasma levels of α-tocopherol and FC are similar to those obtained by the other methods[14,16], but the plasma levels of individual CE are different[14,15]. These differences were considered to be due to the use of plasma samples from different human races.

Lipoproteins from human plasma have been isolated in narrow size ranges, and their chemical compositions have been determined[6,17]. Calulations based on these results were consistent with a model having FC, apoproteins and phospholipids present in a thin film around an inner core of CE and TG. The results from the analyses of lipoprotein fractions by HPLC method appear to be compatible with this model.

CONCLUSION

The physiological importance of the physical exchange of α-tocopherol and free cholesterol between lipoproteins and tissues is not yet clear although cholesterol[18] and α-tocopherol[19] are rapidly taken up by tissues from plasma lipoproteins. Glomset[17] reported a scheme for cholesterol transport involving the physical exchange of free cholesterol between the membrane of tissues and plasma lipoprotein (particularly HDL) which is mediated by the action of lecithin–cholesterol acyltransferase (LCAT). By the use of the present HPLC method, physical exchange of fat-soluble components may be analysed clearly.

The use of HPLC made it possible to increase the separability of analytical procedures for many compounds contained in body fluids and tissues[20–22]. The HPLC method reported here was developed to determine many components not only of plasma but also of individual lipoprotein fractions. The HPLC method provides results that compare favourably with those obtained with widely used methods and yields important information about many fat-soluble components from one easily prepared extract. An additional advantage is that with even as little as 5 μl of plasma,

serum or lipoprotein fraction, it is possible to measure the content of the main fat-soluble components. Further, the HPLC method is applicable to the diagnosis of the state of many diseases which relate to the content of marker components in the body, and to the evaluation of the effects of the treatment of diseases with drugs[23].

REFERENCES

1 P. A. Mayes, in H. A. Harper, V. W. Rodwell and P. A. Mayes (Editors), *Reviews of Physiological Chemistry,* Lange Medical Publications, 16th ed., 1977, pp. 108–121 and 280–320.
2 R. J. Havel, H. A. Eder and J. H. Bragdon, *J. Clin. Invest.,* 34 (1955) 1345.
3 J. H. Bragdon, R. J. Havel and E. Boyle, *J. Lab. Clin. Med.,* 48 (1956) 36.
4 R. L. Hamilton, *Adv. Exp. Med. Biol.,* 26 (1971) 7.
5 T. Sata, R. J. Havel and A. L. Jones, *J. Lipid Res.,* 13 (1972) 757.
6 L. K. Bjornson, C. Gniewkowski and H. J. Kayden, *J. Lipid Res.,* 16 (1975) 39.
7 J. R. Sabine, *Cholesterol,* Marcel Dekker, New York, 1977, pp.245–276.
8 L. L. Abell, B. B. Levy, B. B. Bradie and F. E. Kendall, *Standard Methods of Clinical Chemistry,* Vol. 2, Academic Press, New York, 1958, p. 26.
9 R. D. Ellefson and W. T. Caraway, in N. W. Tiezt (Editor), *Fundamentals of Clinical Chemistry,* Saunders, Philadelphia, PA, 1976, pp. 506–516.
10 T. T. Ishikawa, J. B. Brajier, L. E. Stewart, R. W. Fallat and C. J. Glueck, *J. Lab. Clin. Med.,* 87 (1976) 345.
11 D. Kritchevsky, L. M. Davidson, H. K. Kim and S. Malhotra, *Clin. Chim. Acta,* 46 (1973) 63.
12 K. Abe, M. Ohmae and G. Katsui, *Vitamins,* 49 (1975) 259.
13 L. Hatam and H. J. Kayden, *J. Lipid Res.,* 20 (1979) 639.
14 I. W. Dunkan, P. H. Culbreth and C. A. Burtis, *J. Chromatogr.,* 162 (1979) 281.
15 J. C. Kuo and E. S. Yeung, *J. Chromatogr.,* 229 (1982) 293.
16 C. C. Tangney, H. M. McNair and J. A. Driskell, *J. Chromatogr.,* 224 (1981) 389.
17 J. A. Glomset, *J. Lipid Res.,* 9 (1968) 155.
18 J. Avigan, D. Steinberg and M. Berman, *J. Lipid Res.,* 3 (1962) 216.
19 I. R. Peake, H. G. Windmuller and J. G. Bieri, *Biochim. Biophys. Acta,* 260 (1972) 679.
20 K. Seta, M. Washitake, T. Anmo, N. Takai and T. Okuyama, *J. Chromatogr.,* 181 (1980) 311.
21 K. Seta, M. Washitake, I. Tanaka, N. Takai and T. Okuyama, *J. Chromatogr.,* 221 (1980) 215.
22 K. Seta, M. Washitake, T. Anmo, N. Takai and T. Okuyama, *J. Liq. Chromatogr.,* 4 (1981) 129.
23 H. Nakamura, *Medical Digest,* 27 (1978) 11.

Direct determination of the antihypertensive agent Cromakalim and its major metabolites in human urine by high-performance liquid chromatography

SHINOBU KUDOH

Laboratory of Beecham Yakuhin Co., Ltd., 3–51–4 Bubai-cho, Fuchu-shi, Tokyo 183 (Japan)

and

HIROSHI NAKAMURA*

Department of Analytical Chemistry, Faculty of Pharmaceutical Sciences, University of Tokyo, 7–3–1 Hongo, Bunkyo-ku, Tokyo 113 (Japan)

ABSTRACT

A high-performance liquid chromatographic (HPLC) method has been developed for the simultaneous determination of Cromakalim, a novel antihypertensive agent, and its urinary metabolites including diastereomeric glucuronides. The HPLC system employed a strong cation-exchange precolumn (Senshu Pak SCX-2051-N) to allow direct injection of urine samples. The unchanged drug and its three major metabolites were simultaneously separated on a reversed-phase column (Develosil ODS-5) and fluorometrically detected (excitation, 254 nm; emission, 306 nm) by the aid of their native fluorescence. The calibration curves for Cromakalim and a metabolite were linear in the range from 10 to 200 ng ml^{-1}, while those for the diastereomeric glucuronides were linear in the range from 20 to 400 ng ml^{-1}. The detection limits (signal-to-noise ratio = 3) of these compounds were 0.3 ng ml^{-1} or less in all cases.

INTRODUCTION

Cromakalim, ($\pm$)-*trans*-6-cyano-3,4-dihydro-2,2-dimethyl-4-(2-oxo-1-pyrro-lidinyl)-2*H*-1-benzo[*b*]pyran-3-ol, is a novel antihypertensive agent, discovered by Beecham Pharmaceuticals Research Division (Essex, U.K.), which relaxes vascular smooth muscle by activation of potassium ion channels[1]. In the phase I study, the plasma levels of the parent drug were determined using capillary gas chromatography (GC)[2,3] or high-performance liquid chromatography (HPLC)[4]. Urinary excretion of a drug and its related substances is also an important aspect of a pharmacokinetic study. For this purpose, an HPLC method was developed[5] and used to determine Cromakalim and its three major metabolites, including the diastereomeric glucuronides, in human urine (Fig. 1). However, the method requires a solid-phase extraction
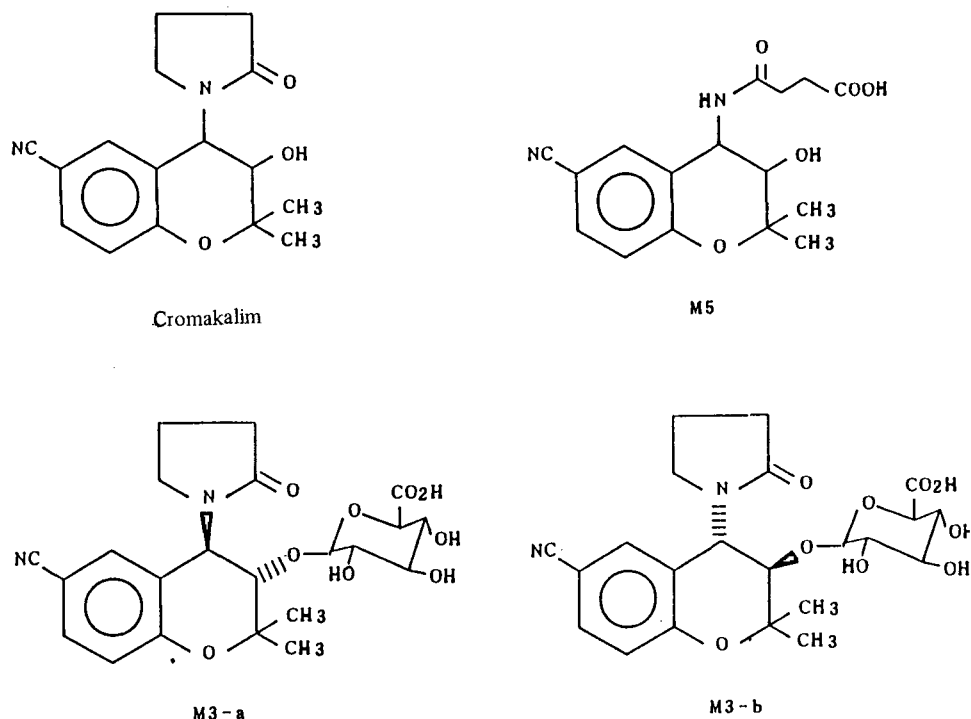
Fig. 1. Structures of Cromakalim and its major metabolites in human urine.

as the pretreatment procedure, which prolongs the time necessary for the assay. It is probable that the number of samples processed would be increased and more information on the metabolism could be obtained if the samples could be analysed without pretreatment.

In this paper, an HPLC method employing two different types of column for the direct determination of Cromakalim and its major metabolites in human urine is described.

EXPERIMENTAL

Reagents

All chemicals and solvents were of analytical-reagent or HPLC grade (Kanto Chemical, Tokyo, Japan), except for physiological saline (Physisalz), purchased from Fuso Yakuhin Kogyo (Osaka, Japan). Distilled water was used to prepare aqueous solutions, and all other chemicals and solvents were used without further purification. Acetate buffers were prepared by mixing the same concentrations of sodium acetate and acetic acid in various proportions. Eluents for HPLC were filtered through an FP-450 membrane filter (0.45 μm) (Gelman Sciences Japan, Tokyo, Japan) before use.

Standard solutions

Standard stock solutions of Cromakalim and its metabolites were prepared by accurately weighing about 10 mg of each reference material. Each sample was dissolved in 5 ml of methanol and then diluted with saline to give concentrations of 40 μg ml^{-1} (M3-a and M3-b) and 20 μg ml^{-1} (Cromakalim and M5). All standard compounds were synthesized and characterized by Beecham Pharmaceuticals Research Division (Essex, U.K.). The solutions were stored in amber-coloured silanized glass bottles at 4°C in the dark until required.

Calibration graphs

Working solutions for construction of the calibration graphs were prepared by diluting each stock solution with saline to give the appropriate concentrations. To 1 ml of blank urine, 100 μl of each working solution were added and a 50-μl aliquot of the spiked urine was subjected to HPLC directly after filtration with an Acro™ LC13 filter assembly (0.2 μm) (Gelman Sciences Japan). Blank urine collected from Japanese male volunteers was pooled and kept at -20°C until used.

HPLC system

The LC-6A HPLC system consisted of two LC-6A pumps, an RF-535 fluorescence detector, a SIL-6A autoinjector, a SCL-6A system controller and a C-R4AX Chromatopac integrator (Shimadzu, Kyoto, Japan). A Develosil ODS-5 (5 μm, 100 Å) column (25 cm × 4.6 mm I.D.) (Nomura Chemical, Seto, Japan) was used as the main analytical column. Either a strong anion-exchange column of Senshu Pak SAX-2051-N (5 μm, 100 Å) or a strong cation-exchange column of Senshu Pak SCX-2051-N (5 μm, 100 Å) (both 50 mm × 6 mm I.D.) (Senshu Scientific, Tokyo, Japan) was used as the precolumn. The columns were maintained at 35°C by an SSC 3520C column oven (Senshu Scientific). Cromakalim and its metabolites were detected by monitoring their inherent fluorescence at excitation and emission wavelengths of 254 and 306 nm, respectively[5].

RESULTS AND DISCUSSION

Selection of precolumn

Initially, a column-switching technique utilizing an ion-exchange column was considered as a possible method for the direct determination of Cromakalim and related substances in human urine. However, experimentation indicated that good separations from urinary endogenous substances could be accomplished even when the urine samples were introduced directly into the system in which an ion-exchange column was connected in series to the C_{18} analytical column. Accordingly, the usefulness of anion-and cation-exchange columns in the separation of urinary substances was investigated. As favourable results were observed when a strong cation-exchange column of Senshu Pak SCX-2051-N was placed before the main C_{18} analytical column as shown in Fig. 2, further experiments were carried out to develop a method involving direct injection via the strong cation-exchange column.

Separation and determination

The separation was optimized based on the analytical conditions of gradient

(a)   (b)

Retention time / min
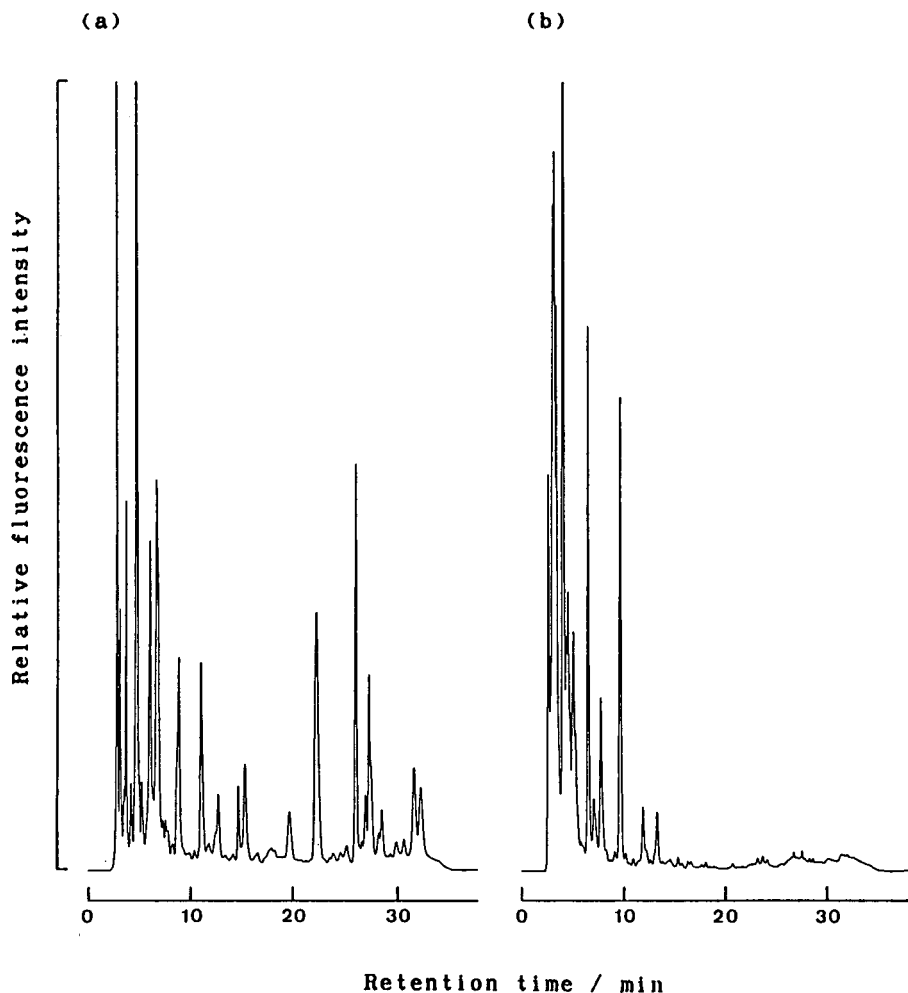
Fig. 2. Effectiveness of Senshu Pak (a) SAX-2051-N and (b) SCX-2051-N precolumn in separation of human blank urine.

elution, on a reversed-phase C_{18} column, with acetate buffer and acetonitrile, established in a previous study[5]. The effects of acetate buffer concentration and its pH on the chromatographic elution were re-examined as the strong cation-exchange column was newly attached to the analytical column being used. Buffer concentrations in the range 50–250 mM at pH 3.2 had little effect on the chromatographic patterns. After consideration of this fact and the variation of the pH of the urine samples, the original concentration, 150 mM, was employed for the study of the effect of pH in the range 3.2–6.2. The results reconfirmed that a pH of 3.2 was suitable for achieving a baseline resolution between the diastereomeric glucuronides M3-a, M3-b. Moreover, the retention times of M3-a, M3-b and M5 tended to be short and their separation from urinary substances became difficult as the pH of the eluent increased. Therefore,
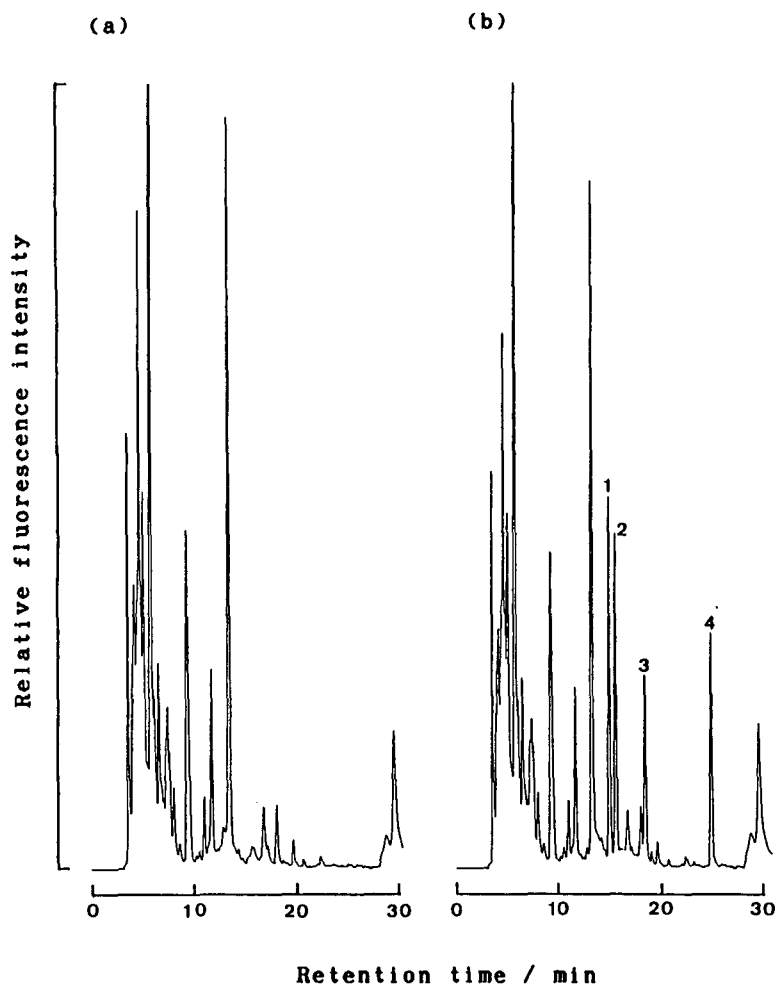
Fig. 3. Typical chromatograms obtained with the proposed HPLC system. (a) Blank urine; (b) working standard solutions added to blank urine. Peaks: 1 = M3-a; 2 = M3-b; 3 = M5; 4 = Cromakalim.

separation was achieved with eluent A [150 mM sodium acetate buffer (pH 3.2)] and eluent B [750 mM sodium acetate buffer (pH 3.2)–acetonitrile (1:4, v/v)], optimum separation being obtained using a linear gradient from 22 to 40% eluent B over 20 min followed by column washing with eluent B for 8 min. The flow-rate was maintained at 1 ml min^{-1} through this work. Representative chromatograms are depicted in Fig. 3.

The calibration graphs were linear ($r \geqslant 0.9995$ each) in the range 10–200 ng ml^{-1} for Cromakalim and M5 and 20–400 ng ml^{-1} for M3-a and M3-b. The detection limits (signal-to-noise ratio = 3) for Cromakalim, M5, M3-a and M3-b were 0.21, 0.25, 0.29 and 0.26 ng ml^{-1}, respectively. The reproducibility and accuracy were also satisfactory, as shown in Table I. Hence the method can be applied to the assay of real

TABLE I

RECOVERIES OF CROMAKALIM AND ITS URINARY METABOLITES

Compound	Concentration (ng/ml)			
	Added	Determined	Recovery (%)[a]	Relative standard deviation (%)[a]
M3-a	50	46.79	93.59	3.73
	200	197.9	98.95	1.91
M3-b	50	50.92	101.8	1.54
	200	203.1	101.5	0.69
M5	25	26.51	106.1	2.51
	100	101.3	101.3	1.26
Cromakalim	25	23.34	93.36	3.38
	100	96.12	96.12	1.38

[a] $n = 3$.

urine samples from preclinical studies. As described above, the method achieved a direct determination of Cromakalim and its major metabolites, including the diastereomeric glucuronides, simultaneously in human urine. As this is a direct measurement, the urine assay can be carried out as a fully automated procedure. The sample throughput can therefore be increased and also more information on the metabolites possibly obtained. The concept of utilizing an ion-exchange column as a precolumn is of value in the development of drug assays in biological fluids. This study has shown that the direct measurement of cationic drugs in urine is possible with the aid of an SCX-2051-N precolumn.

ACKNOWLEDGEMENTS

REFERENCES

1 T. C. Hamilton, S. W. Weir and A. H. Weston, Br. J. Pharmacol., 88 (1986) 103.
2 B. E. Davies, Br. J. Clin. Pharmacol., 24 (1987) 273.
3 T. S. Gill, G. D. Allen and B. E. Davies, Br. J. Clin. Pharmacol., 26 (1988) 227.
4 S. Kudoh and H. Nakamura, Anal. Sci., 5 (1989) 39.
5 S. Kudoh, H. Okada, K. Nakahira and H. Nakamura, Anal. Sci., 6 (1990) 53.

Formazan derivatives as the precolumn derivatization reagents in a coupled high-performance liquid chromatographic–spectrophotometric system for trace metal determination

HITOSHI HOSHINO*, KOUJI NAKANO[a] and TAKAO YOTSUYANAGI

Department of Molecular Chemistry and Engineering, Tohoku University, Aoba, Aramaki, Aoba-ku, Sendai 980 (Japan)

ABSTRACT

As precolumn chelating reagents for use in high-performance liquid chromatographic (HPLC) determinations of ultratrace metal ions, several kinds of 3-phenyl- and 3-cyanoformazans were examined and the reagent structure is discussed in connection with the HPLC selectivity for metal ions. These zincon-type formazans, functioning as quadridentate ligands, provide excellent ability in the precolumn derivatization scheme for spectrophotometric detection. The coplanarity and the chelate-cage effect of the reagent skeleton are probably responsible for the unique selectivity for Cu^{II} and Zn^{II} ions, respectively. The formazans possessing oxygen donors give a good resolution of trivalent metal ions, which seems to be ascribable to the hard-base character produced by the oxygen atoms. Detectability for the Ni^{II} ion is only shown with a reagent that provides an α-diimine-like coordination environment consisting of a four-N donor assembly. The limits of detection for most of the metal ions tested are down to the nanomoles per litre level (sub-picomole amounts). Highly sensitive HPLC methods for metal ions at sub-ppb to ppb (10^{-9} g/g) levels are suggested.

INTRODUCTION

Although many formazan compounds have been investigated as photometric reagents for metal ions[1–5], in fact only three, diphenylcarbazone, diphenylthiocarbazone (dithizone) and zincon, have so far been used in practical applications[6]. Dithizone, which has N,S donor functions, was one of the reagents employed in the high-performance liquid chromatography (HPLC) of metal chelates in its earlier developmental stage[7–9]. In contrast to dithizone, zincon behaves as a potentially

---

[a] Present address: Department of Synthetic Chemistry, Kyushu University, Hakozaki, Higashi-ku, Fukuoka 812, Japan.

planar ligand with quadridentate O,O,N,N donor sites[5]. The coordination environment provided by zincon-type analogues was thus thought to be fairly suitable for HPLC applications by analogy with quadridentate Schiff base ligands derived from 1,2-phenylenediamine[10]. This idea led us to the present detailed examination of a wide variety of 3-phenyl- and 3-cyanoformazans as precolumn derivatization reagents for metal ions in a reversed-phase (RP) HPLC system.

On the basis of the results of our systematic studies, we have concluded that the unique selectivity as a result of on-column kinetic differentiation of inert from labile chelates is the key feature of the precolumn derivatization system in conjunction with an RP-HPLC separation[10-15]. Additionally, the precolumn technique allows the utilization of the great sensitivity of modern absorbance detectors (the 0.001 a.u.f.s. range is now available), with freedom from the increased baseline noise caused by the added reagent in an eluent stream. The molar absorption coefficients of the formazan chelates, $> 10^4 \, l \, mol^{-1} \, cm^{-1}$, are sufficient to ensure the nanomolar detection of metal ions. Formazans designed to possess two five-membered and one six-membered chelate rings are a highly promising choice for HPLC work because they are the most capable of forming the kinetically inert chelates with many metal ions owing to their strong "chelate effect"[1]. Indeed, formazan chelates of typically labile cations such as Cu^{II} and Zn^{II} ions sometimes exhibit well resolved peaks even when working with an eluent with no added reagent.

TABLE I

FORMULAE OF THE FORMAZAN REAGENTS EMPLOYED

No.	Reagent	Source of preparation
1		
2		2 CNCH$_2$COOH
3		2 CNCH$_2$COOH
4		2 CNCH$_2$COOH

In this paper the excellent suitability of formazan compounds for metal ions is described in relation to information concerning the HPLC selectivity principle.

EXPERIMENTAL

Apparatus

Absorption spectra and absorbances were recorded on a Shimadzu Model UV-365 recording spectrophotometer. A Hitachi-Horiba F-5 pH meter was used. The HPLC set-up used consisted of a TWINCLE pump unit, a UVIDEC 100-IV UV–VIS spectrophotometric detector and a VL 611 injector with a 100-μl loop from JASCO (Hachioji, Japan). Analytical columns used were a LiChroCart RP-18 (150 mm × 4 mm I.D.) from Cica-Merck Japan and a Zorbax CN (150 mm × 4.6 mm I.D.) from Shimadzu.

Preparation of the formazan reagents

The formazans employed, the structures of which are given in Table I, were (1) 1-(2-pyridyl)-3-phenyl-5-(2-carboxyphenyl)formazan, (2) 1,5-bis(2-hydroxyphenyl)-3-cyanoformazan, (3) 1,5-bis(3-chloro-5-sulpho-6-hydroxyphenyl)-3-cyanoformazan and (4) 1,5-bis(8-quinolyl)-3-cyanoformazan. They were prepared by ordinary coupling reactions of the corresponding diazonium ions to benzaldehyde 2-pyridyl-hydrazone or cyanoacetic acid[1–5]. The recrystallized products (from ethanol) were HPLC pure and their absorption spectra were identical with those found in the literature[1–5].

Reagents and solutions

Metal ion standard solutions (each 0.01 M) were prepared from the chlorides or the nitrates. Solutions of V^V and Mo^{VI} ions were prepared from ammonium metavanadate and sodium molybdate, respectively. All the metal salts used were of the highest purity available.

The concentration of each formazan solution was 0.01 M. Reagents 1 and 3 were dissolved in 0.01 M sodium hydroxide solution. For reagent 2, a non-ionic surfactant, polyoxyethylene 4-nonylphenoxy ether with 20 oxyethylene units (PONPE-20), was added (2%, w/w) to enhance dissolution. Reagent 4 was dissolved in 2% PONPE-20 solution containing a few drops of concentrated nitric acid.

The mobile phase solutions were acetonitrile–doubly distilled water mixtures containing a pH buffer, disodium EDTA for masking metal interferences and tetrabutylammonium bromide (TBABr) for ion pairing as well as for surface modifying of the RP packings. The detailed eluent conditions are specified for each reagent in the figure captions.

All other reagents and solvents were of analytical-reagent grade.

Procedures

A mixed metal ion solution containing Al^{III}, Be^{II}, Cd^{II}, Co^{II}, Cu^{II}, Fe^{III}, Ga^{III}, Mn^{II}, Mo^{VI}, Ni^{II}, Pb^{II}, V^V and Zn^{II} ions was used for a screening test for the optimization of the complexation conditions and the HPLC parameters.

The complexation reactions were in general carried out in an acetate buffer solution (0.04 M, pH 4.5–5.0) or in the presence of a Tris–HCl buffer (0.01 M,

pH 7.0–8.5). The solution was heated at 90°C for 10 min on a water-bath before diluting to volume. An aliquot of the final solution was loaded on a 100-μl loop. The detection wavelengths and sensitivity settings used are given in the captions of the figures.

RESULTS AND DISCUSSION

Absorption spectra and complexation reactions
     The absorption spectra of some metal chelates of reagents 3 and 4 are shown in Figs. 1 and 2. As the formazan chelates were assumed to have a 1:1 stoichiometry (metal-to-ligand ratio), the absorption spectra were recorded for equimolar solutions of metal ion and the reagent. The molar absorptivity (ε) values are 3.2 · 10^4 1 mol^{-1} cm^{-1} at 680 nm and 2.6 · 10^4 1 mol^{-1} cm^{-1} at 645 nm for the reagent 3 chelates of Al^{III} and Zn^{II} ions, respectively. The ε value of the reagent 4 chelate of Ni^{II} is small, 5.9 · 10^3 1 mol^{-1} cm^{-1} at 650 nm, compared with that of the Zn^{II} chelate of 1.5 · 10^4 1 mol^{-1} cm^{-1} at 545 nm. The spectral properties of the chelates seem to be unattractive for the usual spectrophotometric applications, but the data in Figs. 1 and 2 show promise for the excellent ability for the sensitive detection of metal ions at sub-ppb to ppb (10^{-9} g/g) levels using HPLC–spectrophotometry. Spectral overlapping no longer causes a serious problem in the precolumn derivatization technique.
     As the complexation reactions of the formazans are often slow at room temperature, the reaction mixture was heated at 90°C for 10 min. Two pH ranges for the precolumn derivatization studies were employed, 4.5–5.0 with acetate buffer for reagents 1 and 3 and 7.0–8.5 with Tris–HCl buffer for reagents 2 and 4. The criteria for the choice of the pH conditions were the stability and height of the peak signals. A sufficient excess of the reagent, finally established as 10^{-4} M, was added in the precolumn derivatization protocol.
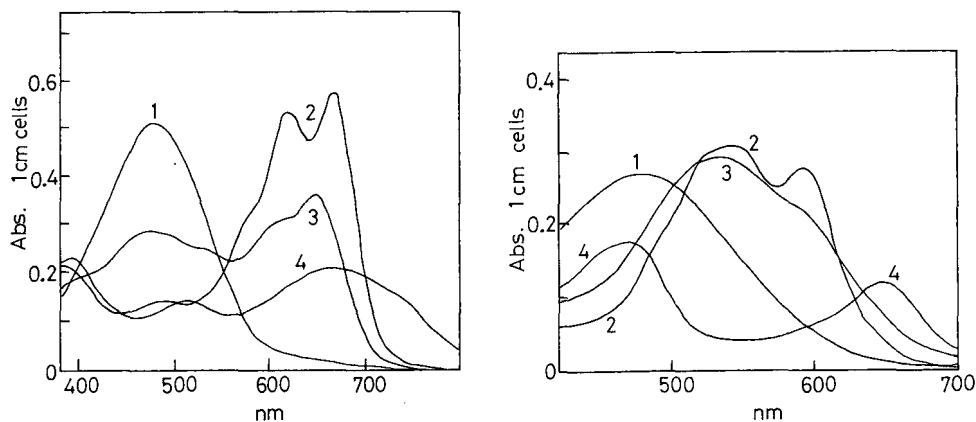
Fig. 1. Absorption spectra of reagent 3 and the chelates in slightly acidic aqueous solution. 1 = Reagent 3, 1.84 · 10^{-5} M; 2 = Al^{III}, 2.00 · 10^{-5} M; 3 = Zn^{II}, 2.05 · 10^{-5} M; 4 = Co^{II}, 1.96 · 10^{-5} M. pH 5.0 acetate buffer solution (0.04 M).

Fig. 2. Absorption spectra of reagent 4 and the metal chelates in aqueous 0.16 wt.-% PONPE-20 solution at pH 7.0. 1 = Reagent 4, 2.0 · 10^{-5} M; 2 = Zn^{II}, 2.05 · 10^{-5} M; 3 = Cd^{II}, 2.40 · 10^{-5} M; 4 = Ni^{II}, 2.03 · 10^{-5} M. pH 7.0 phosphate buffer solution (0.01 M).

Equilibrium stability data for the chelate formation reaction of 3-cyano-formazans were reported by Budesinsky and Svec[1]. They pointed out that the coplanarity and the chelate cage effect of the ligands are responsible for the unusual stability of the chelates with Zn^{II}, Cu^{II} and Pd^{II} ions. However, little quantitative information is available on the chelate formation reactions of hard metal ions such as Al^{III}, Ga^{III} and V^{V}. Additionally, no kinetic data have yet been given for the complexation reactions of the formazans.

HPLC separation studies

A preliminary experiment using commercially available zincon showed that it was almost useless because a number of unknown peaks due to impurities appeared. Therefore, even though zincon gave peaks for Co^{II}, Cu^{II} and V^{V} ions, a more detailed investigation was not attempted.

Acetonitrile–water as the eluent was more suitable for the resolution of the formazan chelates than methanol–water. The (apparent) pH of the mobile phase was maintained at 7–7.5 with sodium acetate. Better resolution was often achieved using a relatively polar Zorbax CN packing. The addition of TBABr was found to be a very important factor influencing the retention and the resolution of the chelates. When anionic chelates are predominant in the RP-HPLC process (all the chelates of reagent 3 and the reagent $2-V^{V}$ chelate), the TBA^{+} cation undoubtedly enhances their retention by ion-pair formation. In contrast, even in the separation of neutral or cationic chelates (most of the chelates of reagents 1, 2 and 4), this onium ion probably controls their retention and resolution, adsorbing both on the bonded phase and on the residual ionized silanol groups present in the surface. The further addition of sodium bromide was very effective in resolving the Cu^{II} and Ni^{II} chelates of reagent 4. The optimum concentrations of TBABr dissolved in the mobile phase are given in captions of the figures.

Typical chromatograms for the reagent systems are shown in Figs. 3–5. Most of the metal chelates which did not give peaks possibly decomposed on the HPLC column, because the free concentration of the reagent in the vicinity of the chelate bands was extremely low. This phenomenon is probably based on the difference in the kinetics of the chelate dissociation processes in an HPLC column (typically, the aquation reactions). In our continuing studies, emphasis has been placed on this "kinetic differentiation" of metal chelates which results in the unique selectivity acquired in the HPLC approach[10–15].

It is thus noteworthy that the Zn^{II} ion appears in the reagent systems 2 and 3. The formazan ligand structure may contribute to the stabilization of this "labile cation" chelate, seemingly in accordance with the considerations of Budesinsky and Svec[1]. Additionally, the Cu^{II} gives the peaks in all the systems examined. The coplanarity of the formazan ligands again seems to be favourable for this ion in the RP-HPLC separation. Co^{II} ion gives peaks in reagent systems 1 and 2, in which the oxidation state of cobalt is presumed to be the trivalent judging from its inert nature.

Advantages were found with reagent 3. In addition to Cu^{II} and Zn^{II} ions, this reagent is compatible with the detectability of several trivalent cations such as Al^{III}, Ga^{III} and Mn^{III}. The most likely reason is the hard-base nature of the reagent resulting from the donor assembly with two oxygen atoms. The added form of manganese was the Mn^{II}, but oxidation readily occurred to give the Mn^{III} chelate. As shown in Fig. 4A,

the peaks for Al^{III} and Mn^{III} ions are seriously overlapped, but this was effectively circumvented by adding sodium fluoride $(1 \cdot 10^{-3} M)$ to masking Al^{III} at the derivatization stage. As can be seen in Fig. 4B, the peak due to Al^{III} ion disappears in the presence of fluoride.

On the other hand, only with reagent system 4 was Ni^{II} ion detected. This can be explained in terms of its α-diimine-like structure; bi-, tri- and quadridentate ligands which have five-membered conjugated N,N-coordination (2,2'-bipyridyl-like moiety) probably show selectivity for Ni^{II} ion[10,16,17]. The discussion of this aspect will be presented elsewhere[15].

As this work was basically undertaken to develop the potential utility of formazan compounds in RP-HPLC, the practical applicability to real samples was not been studied in detail. The estimated limits of detection (LOD) of major metal ions are listed in Table II. As the baseline stability of the detector used here is about $2 \cdot 10^{-5}$ absorbance, the LOD is defined as the concentration which gives a signal three times the baseline noise, $1 \cdot 10^{-4}$ absorbance. It is striking that the LODs of most of the metal ions examined are down to the nanomolar range (sub-ppb to ppb level). These data suggest that spectrophotometric methods coupled with RP-HPLC would be complementary to atomic absorption or emission spectrometric techniques. The development
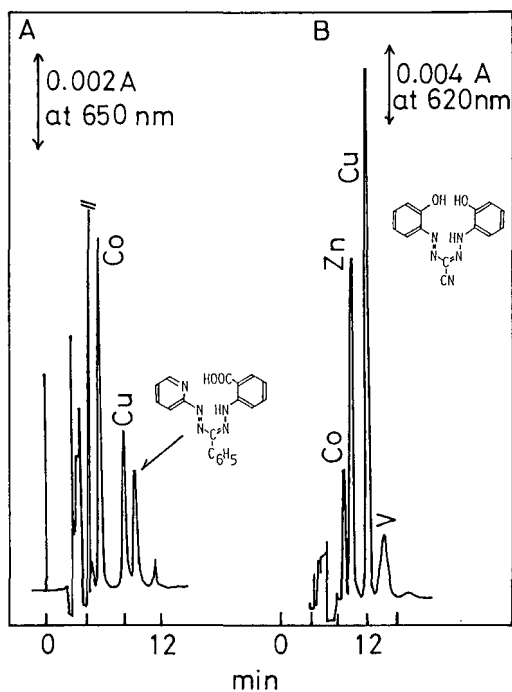
Fig. 3. Typical chromatograms for the formazan reagents 1 (left) and 2 (right). Metal ion concentrations $(10^{-6} M)$: Al 1.00, Be 1.03, Mn 0.990, Ga 0.989, Co 1.09, Cu 1.01, V 1.00, Ni 1.02, Zn 1.02, Cd 1.20, Pb 1.0 and Mo 1.0. Reagent concentrations each $1 \cdot 10^{-4} M$. pH 5.0 (acetate) for 1 and 7.5 (Tris–HCl) for 2. (A) Column, Zorbax CN; mobile phase, 38.1% (w/w) acetonitrile–water, 7.76 mM TBABr, 5 mM sodium acetate, 0.1 mM Na$_2$EDTA; flow-rate, 0.5 ml/min. (B) Column, Zorbax CN; mobile phase, 39.0% (w/w) acetonitrile–water, 3.1 mM TBABr, sodium acetate and Na$_2$EDTA added as in (A); flow-rate, 0.3 ml/min.
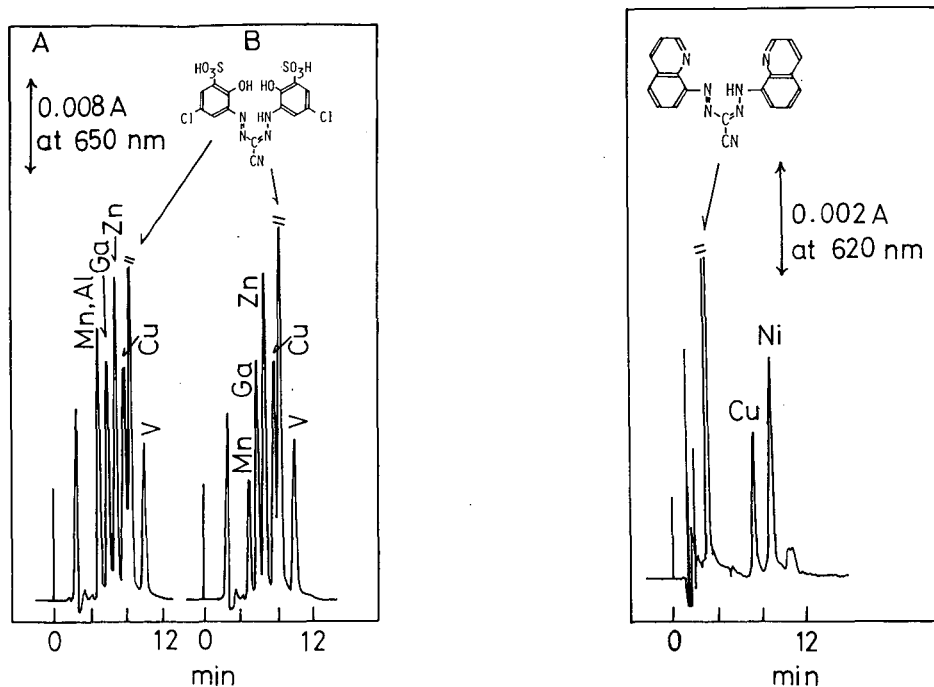
Fig. 4. Chromatograms for the formazan reagent 3 in the absence (left) and presence (right) of sodium fluoride in the sample solution. Concentrations of metal ions and reagent 3 as in Fig. 3; $1 \cdot 10^{-3}$ M NaF added in the final solution; pH 5.0 (acetate). Column, LiChroCart RP-18; mobile phase, 39.0% (w/w) acetonitrile–water, 3.1 mm TBABr, concentrations of sodium acetate and Na$_2$EDTA as in Fig. 3; flow-rate, 0.5 ml/min.

Fig. 5. Typical chromatogram for the formazan reagent 4. Concentrations of metal ions and reagent 4 as in Fig. 3; pH 7.5 (Tris–HCl). Column, Zorbax CN; mobile phase, 60.0% (w/w) acetonitrile–water, 1.86 mm TBABr, 55.8 mm sodium bromide, concentrations of sodium acetate and Na$_2$EDTA as in Fig. 3; flow-rate, 1.0 ml/min.

TABLE II

LIMITS OF DETECTION (LOD)^a FOR METAL IONS

Reagent	LOD (nM)^b						
	V	Mn	Co	Ni	Cu	Zn	Ga
1			15 (0.89)				
2					4.2 (0.27)	6.4 (0.42)	
3	7.8 (0.40)	11 (0.58)				4.2 (0.27)	6.2 (0.43)
4				25 (1.4)			

^{a} LOD is defined as the concentration which gives an absorbance signal of 10^{-4}.
^{b} LOD in ppb in parentheses.

of RP-HPLC–spectrophotometric methods using formazan reagents is therefore worthy of investigation in future trace metal analysis.

REFERENCES

1 B. W. Budesinsky and J. Svec, *Inorg. Chem.*, 10 (1971) 313.
2 A. Kawase, *Bunseki Kagaku*, 16 (1967) 1364; 21 (1972) 578.
3 H. Ishii, T. Mizoguchi and T. Odashima, *Bunseki Kagaku*, 26 (1977) 540.
4 M. I. Ermakova, N. L. Vasil'eva and I. Ya. Postovskii, *Zh. Anal. Khim., Engl. Transl.*, 16 (1961) 6.
5 R. M. Rush and J. H. Yoe, *Anal. Chem.*, 26 (1954) 1345.
6 K. L. Cheng, K. Ueno and T. Imamura, *CRC Handbook of Organic Analytical Reagents*, CRC Press, Boca Raton, FL, 1982.
7 M. Lohmuller, P. Heizmann and K. Ballschmiter, *J. Chromatogr.*, 137 (1977) 165.
8 D. E. Henderson, R. Chaffee and F. P. Novak, *J. Chromatogr. Sci.*, 19 (1981) 79.
9 E. B. Edward-Inatimi, *J. Chromatogr.*, 256 (1983) 253.
10 M. Kanbayashi, H. Hoshino and T. Yotsuyanagi, *J. Chromatogr.*, 386 (1987) 191.
11 H. Hoshino and T. Yotsuyanagi, *Chem. Lett.*, (1984) 1445.
12 H. Hoshino and T. Yotsuyanagi, *Anal. Chem.*, 57 (1985) 625.
13 N. Uehara, M. Kanbayashi, H. Hoshino and T. Yotsuyanagi, *Talanta*, 36 (1989) 1031.
14 H. Hoshino, K. Nakano and T. Yotsuyanagi, *Analyst (London)*, 115 (1990) 133.
15 N. Iki, H. Hoshino and T. Yotsuyanagi, *Analyst (London)*, submitted for publication.
16 J. W. O'Laughlin, *Anal. Chem.*, 54 (1982) 178.
17 M. Mangia and M. T. Lugari, *J. Liq. Chromatogr.*, 6 (1983) 1073.

CHROMSYMP. 1724

Separation of high-molecular mass RNAs by high-performance liquid chromatography on hydroxyapatite

SHINICHIRO HORI* and SACHIKO OHTANI

Department of Neurochemistry, Tokyo Metropolitan Institute for Neurosciences, 2-6 Musashidai, Fuchu-city, Tokyo 183 (Japan)

KENJI MIYASAKA and TOSHIHIRO ISHIKAWA

New Business Development Department, Tonen Corporation, 1-1-1 Hitotsubashi, Chiyoda-ku, Tokyo 100 (Japan)

and

HITOSHI TANABE

Tokyo Metropolitan Neurological Hospital, 2-6-1 Musashidai, Fuchu-city, Tokyo 183 (Japan)

ABSTRACT

High-molecular-mass RNAs [transfer-(t-), 5S-, 18S- and 28S-RNA] in 25 mM sodium acetate buffer (pH 6.0) were separated by high-performance liquid chromatography (HPLC) on hydroxyapatite using a linear gradient (120 min–duration) from 0.03 to 0.147 M of phosphate buffer (pH 7.0) containing 0.3 M potassium chloride and 1 mM sodium azide with a slope of 2 mM/ml at a flow-rate of 0.5 ml/min. When the RNAs were dissolved in 4 M guanidine isothiocyanate–25 mM sodium acetate buffer (pH 6.0)–0.1 M β-mercaptoethanol (4 M GIT), t-, 5S- and 18S- or 28S-RNAs but not 18S- and 28S-RNAs were separated. RNAs extracted from rat superior cervical ganglia with 4 M GIT could be separated. Thus, HPLC on hydroxyapatite is a rapid and accurate means of quantifying and/or preparing high-molecular-mass RNAs such as t- and ribosomal RNAs.

INTRODUCTION

To separate and analyse RNAs of higher molecular mass than transfer RNA (tRNA), agarose or polyacrylamide gel electrophoresis is often used[1]. These methods are simple, but time consuming, and quantification can be difficult. The ceramic-type hydroxyapatite resin, which has a spherical and rigid structure with uniform quality, has been developed[2]. This resin for high-performance liquid chromatography (HPLC) has been used to purify mouse monoclonal antibodies[3] and to separate tRNAs from *Escherichia coli* and *Bacillus subtilis*[4]. HPLC on hydroxyapatite has been used to separate single- and double-stranded DNAs[5] and also RNA and DNA[6]. We now report the separation of t- and ribosomal RNAs and a procedure applicable

to the quantitative analysis of t- and ribosomal RNAs in the superior cervical ganglion (SCG), using HPLC on hydroxyapatite.

EXPERIMENTAL

Materials

   Ribosomal RNAs (18S and 28S) of calf liver (100 absorbance units at 260 nm) were purchased from Pharmacia (Tokyo, Japan), 16S- and 23S-ribosomal RNAs (100 absorbance units at 260 nm), 5S-ribosomal RNA (20 absorbance units at 260 nm) and tRNA of *E. coli* MRE 600 from Boehringer Mannheim Yamanouchi (Tokyo, Japan), [5,6-^{3}H]uridine (38.3–42.0 Ci/mmol) from New England Nuclear (Boston, MA, U.S.A.), Dulbecco's modified Eagle medium, high glucose (DME medium) in powder form from GIBCO (OH, U.S.A.) and a Millex-GV (0.22 μm) filter from Japan Millipore (Yamagata, Japan). Other reagents were obtained from commercial sources.

High-performance liquid chromatography

   A packed column (10 cm × 7.5 mm I.D.) of hydroxyapatite (2 or 5 μm) was obtained from Tonen (Tokyo, Japan). A guard column (1 cm × 7.5 mm I.D.) was installed. A Hitachi (Tokyo, Japan) L-6200 intelligent pump with a low pressure gradient system was used. The elution pattern was monitored at 260 nm using a Hitachi L-4200 UV–VIS detector and recordings were made with a Hitachi D-2500 chromato-integrator. To dissolve the RNAs we used 25 mM sodium acetate buffer (pH 6.0) or 4 M guanidine isothiocyanate–25 mM sodium acetate buffer (pH 6.0)–0.1 M β-mercaptoethanol (4 M GIT). Injection of the sample (50 μl) onto the column was followed by washing for 2 min with 0.01 M KH$_2$PO$_4$–KOH (pH 7.0) containing 0.3 M potassium chloride and 1 mM sodium azide. Elution of RNAs was done by a linear gradient (120 min–duration) of phosphate buffer (pH 7.0) from 30 to 147 mM with a flow-rate of 0.5 ml/min at ambient temperature (20–25°C), unless stated otherwise.

Electrophoresis in agarose gel

   Fractions of each peak were dialysed against 1 M guanidine isothiocyanate–25 mM sodium acetate buffer (pH 6.0) for 4 h to remove the phosphate, a necessary procedure because a high concentration of phosphate interferes with the ethanol precipitation of RNA. RNAs in each sample were precipitated in 75% ethanol and then dissolved in autoclaved (120°C, 20 min) Milli-Q water. Dissolved RNA samples were denatured with glyoxal and dimethyl sulphoxide, followed by electrophoresis[7] in a 1.5% agarose gel submerged in buffer (0.01 M NaH$_2$PO$_4$–NaOH, pH 7.0) at 3–4 V/cm for 5 h. At the end of the run, the gel was stained with aqueous acridine orange (20 μg/ml)[8] for 30 min and photographed under UV light (λ_{max} = 254 nm) after destaining overnight with Milli-Q water.

Labelling of synthesized RNA and extraction of RNA from rat superior cervical ganglion

   Superior cervical ganglia (SCG) were removed from Wistar albino rats (20 days old). Synthesized RNA was labelled with [^{3}H]uridine, in organ culture in which DME medium was used together with 100 units/ml of penicillin G, 100 μg/ml of streptomycin sulphate and 0.25 μg/ml of amphotericin B (fungizone). Four SCGs were in-

cubated at 37°C under oxygen–carbon dioxide (95:5) in 300 μl of the culture medium with [^{3}H]uridine (20 μCi) for 20 h. At the end of incubation, the SCGs were immediately homogenized in 4 M GIT.

Chromatogram of rat SCG extract

The homogenate was centrifuged at 18 500 g for 25 min and the supernatant was injected onto the hydroxyapatite (5 μm) column (10 cm × 7.5 mm I.D.) after passage through a 0.22-μm filter. The column was washed with 0.01 M KH$_2$PO$_4$–KOH (pH 7.0) containing 0.3 M potassium chloride and 1 mM sodium azide for 5 min with a flow-rate of 2 ml/min at ambient temperature (20–25°C) and 0.2-min fractions were collected. A 100-μl volume of each of fraction in a microvial was mixed with 4 ml of Atomlight. Radioactivity was measured using a Packard Tri-Carb 460C liquid scintillation spectrophotometer.

Determination of RNA content

Absorbance measured in a cuvette with a 1-cm path length was considered to indicate an RNA with a concentration of approximately 40 μg/ml[9].

RESULTS AND DISCUSSION

Chromatogram of tRNA

An appropriate concentration gradient (80 min–duration) of phosphate for chromatography of tRNA was from 0.03 to 0.11 M with a slope of 2 mM/ml at a flow-rate of 0.5 ml/min (Figs. 1A and 2A). tRNA dissolved in 25 mM sodium acetate buffer (pH 6.0) (Fig. 1A) or 4 M GIT (Fig. 2A) was separated into several peaks, as noted by Yamakawa et al.[4]. The molecular mass of each peak corresponded to that of tRNA on agarose gel electrophoresis (lanes 1,2 and 3 in Figs. 1D and 2D). Hence, these multiple peaks presumably indicate the heterogeneity of tRNA corresponding to each amino acid.

Chromatogram of 5S-RNA

An appropriate concentration gradient (80 min–duration) of phosphate for chromatography of 5S-RNA was the same as that for tRNA (Figs. 1B and 2B). 5S-RNA dissolved in 25 mM sodium acetate buffer (pH 6.0) (Fig. 1B) was separated into one major peak and one minor peak, but 5S-RNA dissolved in 4 M GIT (Fig. 2B) separated into one major and two minor peaks. The molecular mass of each peak corresponded to that of 5S-RNA on agarose gel electrophoresis (lanes 1 and 2 in Figs. 1E and 2E). Hence these multiple peaks are indicative of contamination, multiplicity of 5S-RNA or minor degradation of native 5S-RNA. Four variants of 5S-RNA have been found in E. coli A19[10]. The multiple peaks may correspond to these variants of 5S-RNA.

Chromatogram of 18S- and 28S-RNA

An appropriate concentration gradient (80 min–duration) of phosphate for the separation of 18S- and 28S-RNAs dissolved in 25 mM sodium acetate buffer (pH 6.0) was from 0.07 to 0.15 M with a slope of 2 mM/ml at a flow-rate of 0.5 ml/min (Fig. 1C). 18S- and 28S-RNAs each gave single symmetrical peaks. Elution of 28S-RNA
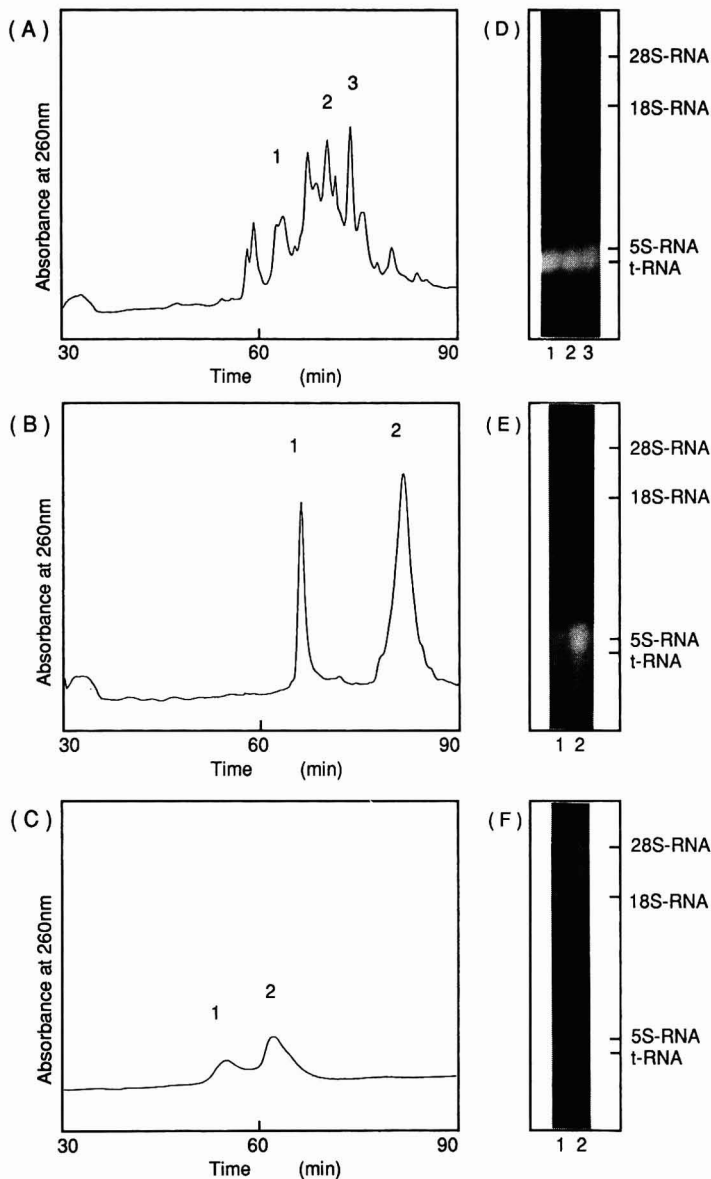
Fig. 1. Chromatograms of t-, 5S-, 18S- and 28S-RNAs on hydroxyapatite. A packed column (10 cm × 7.5 mm I.D.) of hydroxyapatite (2 μm) was used. Washing buffer at sample application was 0.01 M KH_2PO_4–KOH (pH 7.0) containing 0.3 M KCl and 1 mM NaN_3. Elution of RNA was done by a linear gradient (80 min–duration) of phosphate buffer (pH 7.0) containing 0.3 M KCl and 1 mM NaN_3 at a flow-rate of 0.5 ml/min at ambient temperature (20–25°C). The concentration gradient was varied as described below. RNAs were dissolved in 25 mM sodium acetate buffer (pH 6.0). (A) Chromatogram of tRNA from E. coli MRE 600. tRNA (1.2 μg) was injected onto the column and eluted by a linear gradient from 0.03 to 0.11 M of phosphate buffer (pH 7.0). (B) Chromatogram of 5S-RNA from E. coli MRE 600. 5S-RNA (0.1 μg) was injected onto the column and eluted by a linear gradient from 0.03 to 0.11 M of phosphate buffer (pH 7.0). (C) Chromatogram of 18S- and 28S-RNAs. 18S- and 28S-RNA mixture (0.5 μg) was injected onto the column and eluted by a linear gradient from 0.07 to 0.15 M of phosphate buffer (pH 7.0). (D) Electrophoresis in agarose gel of tRNA. Peak fractions 1, 2 and 3 from tRNA chromatogram A were electrophoresed in 1.5% agarose gel. The gel was stained with acridine orange and photographed under UV light ($\lambda_{max} = 254$ nm). (E) Electrophoresis in agarose gel of 5S-RNA. Peak fractions 1 and 2 from 5S-RNA chromatogram B were electrophoresed in 1.5% agarose gel. The gel was stained with acridine orange and photographed under UV light ($\lambda_{max} = 254$ nm). (F) Electrophoresis in agarose gel of 18S- and 28S-RNAs. Peak fractions 1 and 2 from 18S- and 28S-RNA chromatogram C were electrophoresed in 1.5% agarose gel. The gel was stained with acridine orange and photographed under UV light ($\lambda_{max} = 254$ nm).
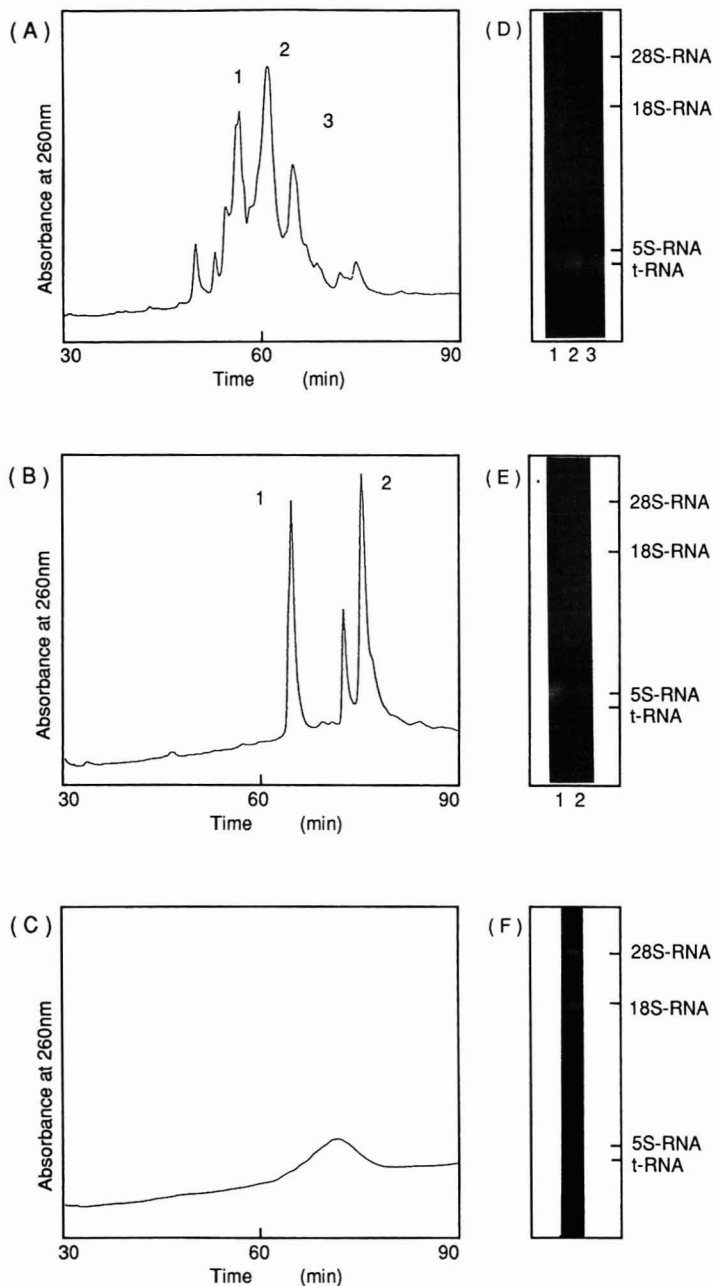
Fig. 2. Chromatograms of t-, 5S-, 18S- and 28S-RNAs on hydroxyapatite. RNAs were dissolved in 4 *M* GIT. (A) Chromatogram of tRNA from *E. coli* MRE 600. (B) Chromatogram of 5S-RNA from *E. coli* MRE 600. (C) Chromatogram of 18S- and 28S-RNAs. (D) Electrophoresis in agarose gel of tRNA. Peak fractions 1, 2 and 3 from tRNA chromatogram A were electrophoresed in 1.5% agarose gel. (E) Electrophoresis in agarose gel of 5S-RNA. Peak fractions 1 and 2 from 5S-RNA chromatogram B were electrophoresed in 1.5% agarose gel. (F) Electrophoresis in agarose gel of 18S- and 28S-RNAs. Peak fraction of 18S- and 28S-RNA chromatogram C was electrophoresed in 1.5% agarose gel. Other conditions in Fig. 1.

followed that of 18S-RNA (Fig. 1F). However, when the 18S- and 28S-RNA mixture was dissolved in 4 *M* GIT, separation was not feasible (Fig. 2C and F). 16S- and 23S-RNAs dissolved in 25 m*M* sodium acetate buffer (pH 6.0) were also separated using a linear gradient (80 min–duration) from 0.07 to 0.15 *M* of phosphate buffer (pH 7.0) with a slope of 2 m*M*/ml at a flow-rate of 0.5 ml/min (data not shown). However, when the mixture was dissolved in 4 *M* GIT, they could not be separated. A mixture of 16S-, 18S-, 23S- and 28S-RNAs in 25 m*M* sodium acetate buffer (pH 6.0) could not be separated using our experimental procedures; only a single broad peak appeared (data not shown).

Separation of t-, 5S-, 18S- and 28S-RNAs

5S-RNA was separated from tRNA using a linear gradient of phosphate from 0.03 to 0.11 *M* (Fig. 3B), that is, 5S-RNA was eluted following tRNA. For the separation of t- and 5S-RNAs, the addition of a salt such as potassium chloride or sodium chloride was essential (Fig. 3A and B). The first minor peak of 5S-RNA
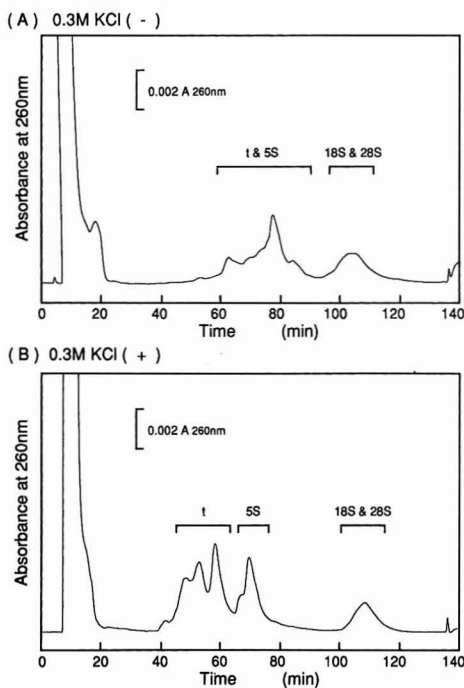
Fig. 3. Effect of salt on separation of t-, 5S-, 18S- and 28S-RNAs on hydroxyapatite. A packed column (10 cm × 7.5 mm I.D.) of hydroxyapatite (2 μm) was used. RNAs were dissolved in 4 *M* GIT. (A) Washing buffer at sample application was 0.01 *M* KH$_2$PO$_4$–KOH (pH 7.0) containing 1 m*M* NaN$_3$. Elution of RNA was done by a linear gradient (120 min–duration) from 0.03 to 0.147 *M* of phosphate buffer (pH 7.0) containing 1 m*M* NaN$_3$ at a flow-rate of 0.5 ml/min at ambient temperature (20–25°C). (B) Washing buffer at sample application was 0.01 *M* KH$_2$PO$_4$–KOH (pH 7.0) containing 0.3 *M* KCl and 1 m*M* NaN$_3$. Elution of RNA was done by a linear gradient (120 min–duration) from 0.03 to 0.147 *M* of phosphate buffer (pH 7.0) containing 0.3 *M* KCl and 1 m*M* NaN$_3$ at a flow-rate of 0.5 ml/min at ambient temperature (20–25°C).
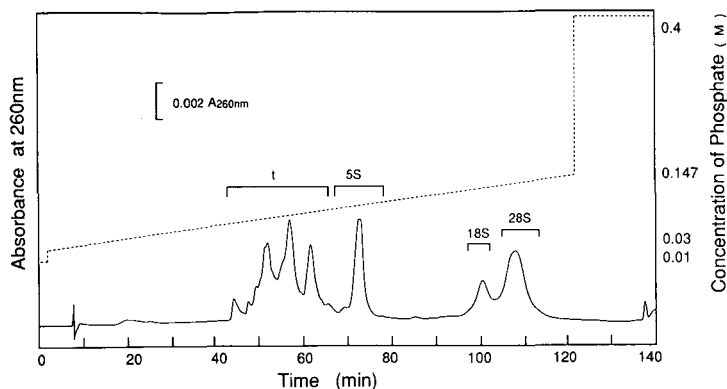
Fig. 4. Separation of t-, 5S-, 18S- and 28S-RNAs on hydroxyapatite. A packed column (10 cm × 7.5 mm I.D.) of hydroxyapatite (2 μm) was used. Washing buffer at sample application was 0.01 M KH$_2$PO$_4$–KOH (pH 7.0) containing 0.3 M KCl and 1 mM NaN$_3$. Elution of RNA was done by a linear gradient (120 min–duration) from 0.03 to 0.147 M of phosphate buffer (pH 7.0) containing 0.3 M KCl and 1 mM NaN$_3$ at a flow-rate of 0.5 ml/min at ambient temperature (20–25°C). RNAs were dissolved in 25 mM sodium acetate buffer (pH 6.0).

overlapped with the later peak of tRNA, even in the presence of 0.3 M potassium chloride (Fig. 3B). The mixture of t-, 5S-, 18S- and 28S-RNAs in 25 mM sodium acetate buffer (pH 6.0) was separated using a linear gradient (120 min–duration) from 0.03 to 0.147 M of phosphate buffer (pH 7.0) with a slope of 2 mM/ml at a flow-rate of 0.5 ml/min (Fig. 4), except that a minor peak of 5S-RNA overlapped with that of tRNA, as described above. When the mixture of t-, 5S-, 18S- and 28S-RNAs dissolved in 4 M GIT was chromatographed on hydroxyapatite using a linear gradient (120 min–duration) from 0.03 to 0.147 M of phosphate buffer (pH 7.0) with a slope of 2 mM/ml at a flow-rate of 0.5 ml/min, 18S- and 28S-RNAs could not be separated, but t- and 5S-RNAs could be separated (Fig. 5), except for a partial overlap, as described above. The elution sequence of t-, 5S-, 18S- and 28S-RNAs was from a
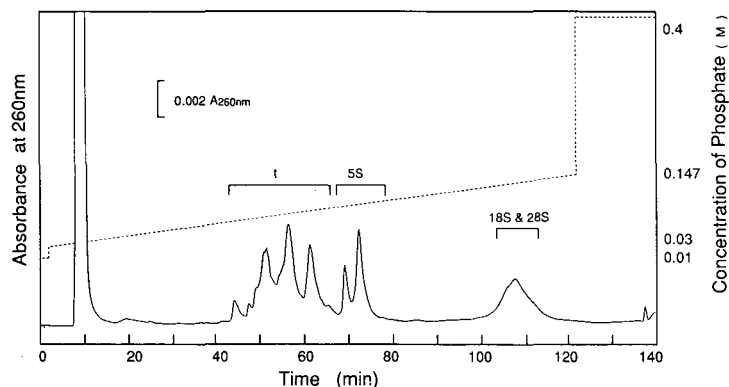
Fig. 5. Separation of t-, 5S-, 18S- and 28S-RNAs on hydroxyapatite. RNAs were dissolved in 4 M GIT. Other experimental conditions in Fig. 4.
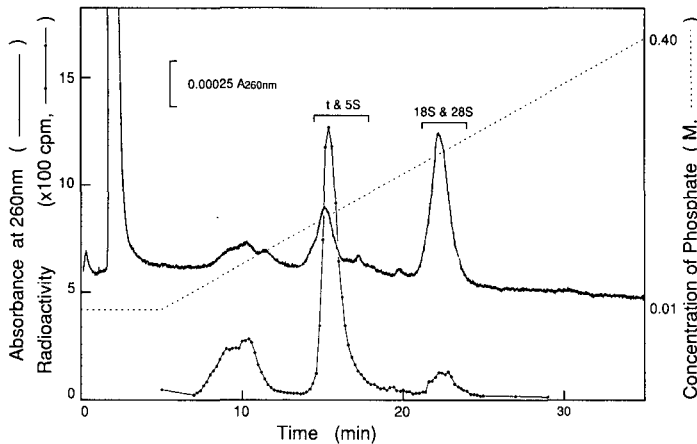
Fig. 6. Chromatogram of rat SCG extract. SCGs from 20-day-old rats were incubated with [³H]uridine for 20 h. The extract of SCG with 4 *M* GIT was injected onto a hydroxyapatite (5 μm) column (10 cm × 7.5 mm I.D.). The column was washed with 0.01 *M* KH₂PO₄–KOH (pH 7.0) containing 0.3 *M* KCl and 1 m*M* NaN₃ for 5 min at a flow-rate of 2 ml/min. Elution of RNA was done by a linear gradient (30 min– duration) from 0.01 to 0.4 *M* of phosphate buffer (pH 7.0) containing 0.3 *M* KCl and 1 m*M* NaN₃ at a flow-rate of 2 ml/min at ambient temperature (20–25°C); 0.2 min fractions were collected. The radioactivity in each of these fractions was determined using a liquid scintillation spectrophotometer.

lower to a higher molecular mass, that is, a higher concentration of phosphate was necessary to elute the higher molecular mass of RNA, presumably because the phosphate moiety in nucleic acid interacts with the Ca²⁺ moiety in hydroxyapatite, and the interaction is strengthened, depending on the amount of nucleic acid in RNA.

Separation of t- and ribosomal RNAs in rat SCG

GIT 4 *M* is useful for the complete inhibition of endogenous nucleases and deproteinization from RNA[11]. Thus, extraction of RNAs in rat SCG was effected using 4 *M* GIT and the extracted RNAs were used for hydroxyapatite column chromatography with a linear gradient (30 min–duration) from 0.01 to 0.4 *M* of phosphate buffer (pH 7.0) with a slope of 6.5 m*M*/ml at a flow-rate of 2 ml/min (Fig. 6). The t- and 5S-RNAs were completely separated from 18S- and 28S-RNAs. The radioactivity of [³H]uridine corresponded to the absorbance at 260 nm. Hence HPLC on hydroxyapatite can be used for the analysis and/or preparation of high-molecular-mass RNAs such as t- and ribosomal RNAs. Separation between t- and 5S-RNAs and between 18S- and 28S-RNAs is in progress.

ACKNOWLEDGEMENTS

REFERENCES

1 R. C. Ogden and D. A. Adams, *Methods Enzymol.*, 152 (1987) 61.
2 T. Kadoya, T. Isobe, M. Ebihara, T. Ogawa, M. Sumita, H. Kuwahara, A. Kobayashi, H. Ishikawa and T. Okuyama, *J. Liq. Chromatogr.*, 9 (1986) 3543.
3 Y. Yamakawa and J. Chiba, *J. Liq. Chromatogr.*, 11 (1988) 665.
4 Y. Yamakawa, K. Miyasaka, T. Ishikawa, Y. Yamada and T. Okuyama, *J. Chromatogr.*, 506 (1990) 319.
5 Y. Yamasaki, A. Yokoyama, A. Ohnaka and Y. Kato, *J. Chromatogr.*, 467 (1989) 299.
6 J. R. Milligan, L. Catz-Biro and M. C. Archer, *J. Chromatogr.*, 411 (1987) 481.
7 T. Maniatis, E. F. Fritsch and J. Sambrook (Editors), *Molecular Cloning, a Laboratory Manual*, Cold Spring Harbor Laboratory, New York, 1982, p. 199.
8 G. K. McMaster and G. G. Carmichael, *Proc. Natl. Acad. Sci. U.S.A.*, 74 (1977) 4835.
9 S. L. Berger, *Methods Enzymol.* 152 (1987) 49.
10 M. Digweed, I. Kumagai, T. Pieler and V. A. Erdmann, *Eur. J. Biochem.*, 127 (1982) 531.
11 R. J. MacDonald, G. H. Swift, A. E. Przybyla and J. M. Chirgwin, *Methods Enzymol.* 152 (1987) 219.

Determination of urinary free noradrenaline by reversed-phase high-performance liquid chromatography with on-line extraction and fluorescence derivatization

OSAMU NOZAKI* and YASUHIRO OHBA

Department of Clinical Pathology, Kinki University School of Medicine, 377–2, Ohno-Higashi, Osaka-Sayama, Osaka 589 (Japan)

ABSTRACT

A fully automated reversed-phase high-performance liquid chromatographic method with fluorimetric detection for the determination of urinary free noradrenaline was developed. Urine samples, diluted with buffer were injected into a boric acid gel column (12 μm, TSK: 10 × 4.6 mm I.D.) without prior extraction. Urinary noradrenaline was simultaneously extracted and derivatized with an alkaline mobile phase of pH 11, containing *o*-phthalaldehyde and 2-mercaptoethanol, in a boric acid gel column. After switching columns, the fluorescent derivatized catecholamines were separated with an ODS-4PW column (TSK) and a mobile phase of pH 2 and the fluorescence was monitored with excitation at 340 and emission at 440 nm. The retention times of noradrenaline and dopamine were 11.0 and 14.2 min, respectively. The detection limits for noadrenaline and dopamine were 0.2 and 20 ng, respectively.

This method has the advantages of not requiring preliminary extraction of urinary catecholamines, high sensitivity and stability of *o*-phthalaldehyde-derivatized catecholamines.

INTRODUCTION

Urinary catecholamines are determined as markers of the adrenal medulla and sympathetic nervous system by high-performance liquid chromatography (HPLC). The method normally requires prior isolation of catecholamines by chromatography on alumina[1,2], an ion-exchange gel[3,4] or a boric acid gel[5-8]. These procedures are time consuming and become impractical when large numbers of samples need to be analysed. The method described here dose not require the extraction of catecholamines, but permits their highly sensitive detection and rapid analysis.

If a hard boric acid gel[9] is used as a precolumn, together with an alkaline mobile phase containing *o*-phthalaldehyde (OPA) and 2-mercaptoethanol (2-ME), extraction and OPA derivatization of catecholamines may be performed simultaneously. Fig. 1 shows the principle of the method. The reaction between catecholamines and a boric

(a)

boric acid gel   catecholamines

(b)

o-phthalaldehyde   noradrenaline   2-mercaptoethanol
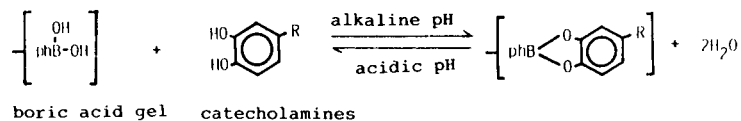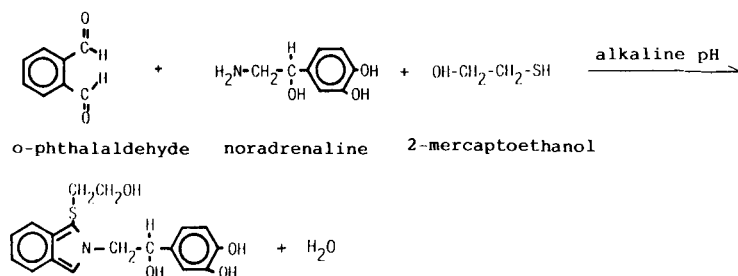
Fig. 1. Principle of the proposed HPLC method for urinary catecholamines (a) Scheme of the adsorption of catecholamines on boric acid gel. (b) Scheme of the fluorescence derivatization of noradrenaline with o-phthalaldehyde and 2-mercaptoethanol.

acid gel[7] and the reaction between catecholamines, OPA and 2-ME[10,11] are commonly carried out in alkaline solution and, after switching columns[12], OPA-derivatized catecholamines are separated with an acidic eluent on an ODS column and monitored by fluorimetry. A fully automated HPLC system was developed, based on a column-switching technique. As a result, urinary free noradrenaline in samples from patients can be determined.

EXPERIMENTAL

Reagents

Noradrenaline and dopamine were obtained from Sigma (St. Louis, MO, U.S.A.), potassium biphthalate from Tokyo Kasei (Tokyo, Japan), disodium hydrogenphosphate, tetrahydrofuran and phosphoric acid from Wako (Osaka, Japan) and 2-mercaptoethanol, acetonitrile, ethanol, 4 M sodium hydroxide solution and 0.1 and 1 M hydrochloric acid from Kantokagaku (Tokyo, Japan). All reagents were of analytical-reagent grade and used without further purification. Distilled water was used after being passed through an ion-exchange column (Milli-Q; Millipore, Bedford, MA, U.S.A.).

Stock standard solutions of noradrenaline and dopamine (1.0 mg/ml in 1 M hydrochloric acid were placed in polypropylene sample cups with caps and stored at $-20°C$. Working standard solutions of noradrenaline and dopamine were prepared by dilution of the stock standard solutions with 0.1 M hydrochloric acid, stored at 4°C and used within 1 day. The OPA solution (3.0 mg/ml in ethanol) was stored at 4°C.

The alkaline mobile phase (pH 11.0) (S_1) for the boric acid gel precolumn was 5 mM disodium hydrogenphosphate–acetonitrile–4 M NaOH–3 mg/ml OPA–2-ME (160:40:0.36:0.40:0.10, v/v) and was prepared just before use. The acidic mobile phase

(pH 2.0) (S$_2$) for the ODS-4PW analytical column was 10 mM potassium biphthalate–acetonitrile–tetrahydrofuran–phosphoric acid (280:120:20:0.33, v/v).

Sample collection

Samples of 0.90 ml were collected from patients in polypropylene sample cups containing 0.1 ml of 1 M hydrochloric acid, capped, stored at 4°C and analysed within 1 day.

Chromatographic system

Fig. 2 shows a block diagram of the HPLC system. This system consisted of two HPLC pumps (880-PU; JASCO, Tokyo, Japan), an autosampler (850-AS, JASCO), a high-pressure switching valve (892-01, JASCO), a fluorimonitor (FS-8000, TSK, Tokyo, Japan), an integrator (805-GI, JASCO), a precolumn (boric acid gel, 12 μm, TSK; 10 × 4.6 mm I.D.), a guard column (ODS-4PW, 8 μm, TSK; 10 × 4.6 mm I.D.) and an analytical column (ODS-4PW, 8 μm, TSK; 250 × 4.6 mm I.D.). The two HPLC pumps, the high-pressure switching valve, the autosampler and the integrator were automatically regulated with a system controller (801-SC, JASCO). All HPLC columns were packed by Tosoh (Yamaguchi, Japan) and were used at room temperature.

Chromatographic separation and fluorimetric determination

Samples of urine (200 μl), diluted with the same volume of 100 mM disodium hydrogenphosphate (pH 8.4) and kept at 4°C, were injected by an autosampler every 25 min, and 3.5 min after sample injection the alkaline mobile phase containing OPA and 2-ME was passed through the boric acid gel precolumn at a flow-rate of 1.3 ml/min to extract and derivatize urinary catecholamines almost simultaneously. Then the high-pressure switching valve was turned and the fluorescent OPA-derivatized catecholamines were eluted from the precolumn, transferred to the ODS-4PW column and separated with the acidic mobile phase at a flow-rate of 1.0 ml/min. The eluate was monitored with a fluorimeter with excitation at 340 nm and emission at 440 nm.
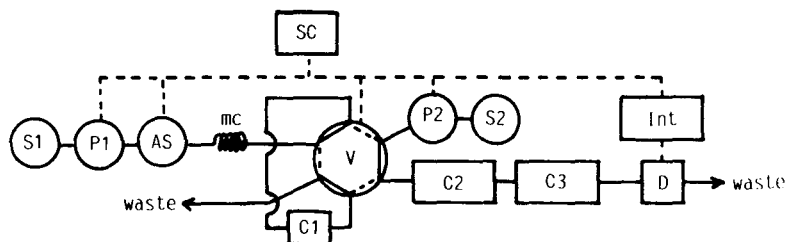
Fig. 2. Block diagram of the HPLC system with column switching. S$_1$ and S$_2$ = solvents; P$_1$ and P$_2$ = HPLC pumps; AS = autosampler; mc = mixing coil (2 m × 0.5 mm I.D.); V = high-pressure switching valve; D = fluorescence monitor; Int = integrator; SC = system controller; C$_1$ = precolumn (boric acid gel, 12 μm, TSK; 10 × 4.6 mm I.D.); C$_2$ = guard column (ODS-4PW, 8 μm, TSK; 10 × 4.6 mm I.D.); C$_3$ = analytical column (ODS-4PW, 8 μm, TSK; 250 × 4.6 mm I.D.). The flow-rate of solvent S$_1$ was 1.3 ml/min and that of solvent S$_2$ 1.0 ml/min both before and after the column switching. Solvents S$_1$ and S$_2$ passed through the solid line of the high-pressure switching valve (V) before turning the valve, and then the broken line of V after turning the valve.

RESULTS

Influence of alkaline mobile phase (S₁) pH on simultaneous extraction and OPA derivatization of noradrenaline and dopamine using a boric acid gel column

Fig. 3 shows changes in the relative peak areas of OPA-derivatized noradrenaline and dopamine standards corresponding to pH 9.27, 10.0, 11.2, 11.7, 11.9 of the mobile phase (S_1). The maximum peak areas of the derivatized noradrenaline and dopamine were both obtained in the pH range 10–11 and a mobile phase (S_1) pH of 11 was adopted.
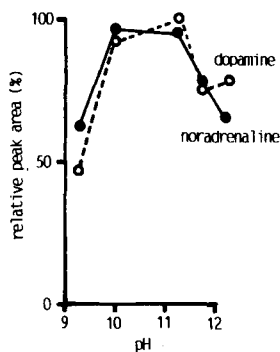
Fig. 3. Influence of mobile phase pH on adsorption and fluorescence derivatization of catecholamines in the boric acid gel column.

Influence of 2-mercaptoethanol concentration in the mobile phase (S₁) on OPA derivatization of noradrenaline and dopamine using a boric acid gel column

Fig. 4 shows changes in the relative peak areas of OPA-derivatized noradrenaline and dopamine standards with variation in the concentration of 2-ME (0.02, 0.04, 0.05, 0.06 and 0.10%) in the mobile phase (S_1). The maximum peak areas were obtained at 2-ME concentrations of 0.04–0.06% and 0.05% was adopted.
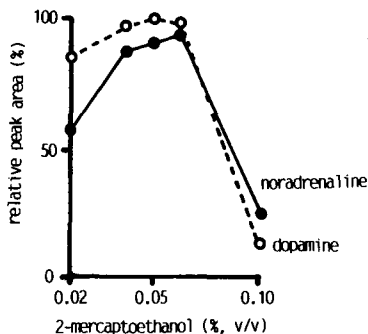
Fig. 4. Influence of 2-mercaptoethanol in the mobile phase on fluorescence derivatization of catecholamines in the boric acid gel column.
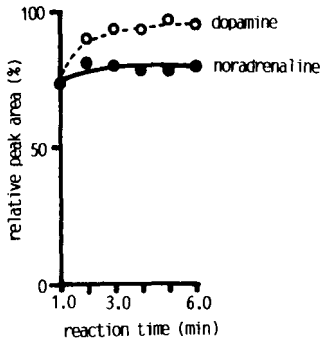
Fig. 5. Reaction time of fluorescence derivatization of catecholamines with o-phthalaldehyde and 2-mercaptoethanol in the boric acid gel column.

Column switching time for the maximum peak areas of OPA-derivatized noradrenaline and dopamine for the boric acid gel column

The column switching time that provided both maximum OPA derivatization and maximum extraction yields of noradrenaline and dopamine on the boric acid gel column was determined between sample injection and the time of column switching at a flow-rate of 1.3 ml/min of the mobile phase (S_1) and at room temperature. Fig. 5 shows the changes in the relative peak areas of OPA-derivatized noradrenaline and dopamine standards each minute from 1.0 to 6.0 min. The optimum column switching time was determined to be 3.5 min, because the maximum relative peak area of OPA-derivatized noradrenaline was observed between 2.0 and 6.0 min and that of OPA-derivatized dopamine between 3.0 and 6.0 min.
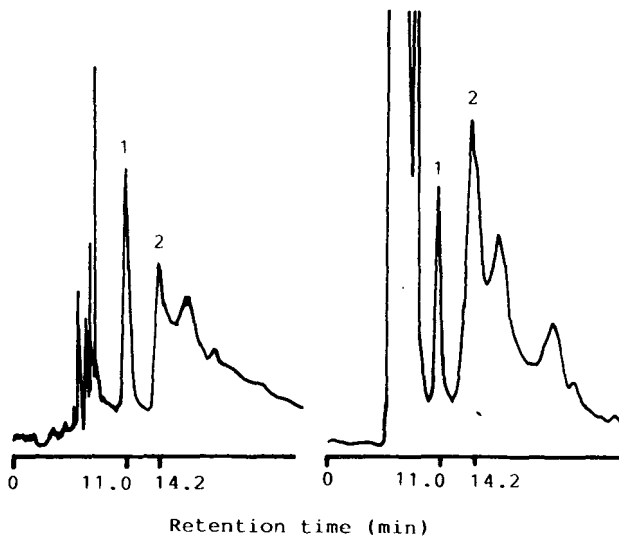
Fig. 6. Chromatograms obtained: left, standard solution containing 40 ng of noradrenaline and dopamine; right, 100 μl of urine from a patient. Peaks: 1 = noradrenaline; 2 = dopamine.

Chromatograms

Fig. 6 shows chromatograms of standard solutions containing 40 ng of noradrenaline and dopamine and a 100-μl urine sample which was diluted to 200 μl with 100 mM disodium hydrogenphosphate. The retention times of OPA-derivatized noradrenaline and dopamine were 11.0 and 14.2 min, respectively. Nevertheless, the peak corresponding to noradrenaline was well separated from the other peaks, even in urine samples. The peaks corresponding to dopamine were sometimes overlapped with other unknown peaks in the standard solutions and in urine samples. The detection limits were about 0.2 and 20 ng for noradrenaline and dopamine, respectively (signal-to-noise ratio = 2).

The intra- and inter-assay relative standard deviations for noradrenaline (120 ng) in urine were 3.4 and 4.8%, respectively (n = 5).

Identification of the peaks corresponding to noradrenaline and dopamine in chromatograms of urine samples was based on coincidence of both the retention times and the maximum fluorescent excitation and emission wavelengths in comparison with noradrenaline and dopamine standards.

DISCUSSION

It is known that boric acid gel can react with the diol groups of catecholamines under alkaline conditions and the reaction is reversible under acidic conditions[5-8]. The soft boric acid gels normally used in the preliminary extraction of urinary catecholamines cannot be packed into HPLC columns. However, the boric acid gel (TSK) used in this study is hard and can withstand high column pressures such as 300 kg/cm^2, so there were no problems in using it in a short column of 10 × 4.6 mm I.D.

The proposed method was successful in extracting urinary catecholamines with the boric acid gel column and an alkaline mobile phase (S$_1$) of pH 11 (Fig. 3).

Although boric acid gel is also known to have affinities for sugars, nucleosides and nucleotides[13,14], these substances are not thought to interfere in the present detection method, because the OPA derivatives were monitored at their maximum excitation and emission wavelengths of 340 and 440 nm, respectively.

The boric acid gel column used in this study tolerated hundreds of injections of crude urine samples, and there was no need to replace the column during this study.

It is well known that a primary amino group reacts rapidly with OPA in the presence of 2-ME and under alkaline conditions at room temperature[10,11]. The derivatization reactions of noradrenaline and dopamine with OPA and 2-ME are thought, from the results in Fig. 5, to have occurred in part in the mixing coil, but mainly in the boric acid gel column, because the peak areas of these catecholamines increased 2 and 3 min after sample injection, respectively. Hence, the boric acid gel column played two roles, as an affinity column and as a solid-phase reactor for OPA derivatization of noradrenaline and dopamine.

There is another advantage of this on-line OPA derivatization method for catecholamines. The usual instability of OPA derivatives of catecholamines after derivatization was eliminated because the derivatives were produced on-line and analysed within 20 min after sample injection.

The pH of the mobile phase (S$_2$) for the ODS-4PW column needed to elute OPA-derivatized catecholamines from the boric acid gel column was below 4. The

peak shapes of the OPA-derivatized catecholamines became sharper, corresponding to changes in the pH of the mobile phase (S_2) from 4 to 2.

We used an ODS-4PW gel column (TSK) for the separation of OPA derivatives of catecholamines because this gel, which is prepared by introducing octadecyl groups into a hydrophyric resin (TSK gel 4000 PW), can be used with mobile phase solutions in the pH range 2–12. ODS-4PW gel can tolerate alkaline solutions eluted from a boric acid gel precolumn to an analytical column when the columns are switched.

Under these conditions, good separation of noradrenaline OPA derivative peaks from other peaks in chromatograms of urine samples was obtained. On the other hand, peaks of OPA-derivatized dopamine often showed interference from peaks of other unknown substances (Fig. 6)[15]. Presumably the boric acid binding does not interfere with the OPA reaction and *vice versa*. We are now making efforts to solve this problem.

ACKNOWLEDGEMENTS

REFERENCES

1 K. Mori, *Tampakushitsu Kakusan Koso*, 26 (1981) 1099.
2 A. H. Anton and D. F. Sayre, *J. Pharmacol Exp. Ther.*, 138 (1962) 360.
3 A. Yamatodani and H. Wada, *Tampakushitsu Kakusan Koso*, 26 (1981) 1108.
4 T. Seki and H. Wada, *J. Chromatogr.*, 14 (1975) 227.
5 C. F. Gelijkens and A. P. De Leenheer, *J. Chromatogr.*, 183 (1980) 78.
6 K. Oka, M. Sekiya, H. Osaka, K. Fujita, T. Kato and T. Nagatsu, *Clin. Chem.*, 28 (1982) 646.
7 S. Higa, T. Suzuki, A. Hayashi, I. Tsuge and Y. Yamamura, *Anal. Biochem.*, 77 (1977) 18.
8 A. J. Speek, J. Odink, J. Schrijver and W. H. P. Schreurs, *Clin. Chim. Acta*, 128 (1983) 103.
9 S. Yamazaki, *Tampakushitsu Kakusan Koso*, 26 (1981) 1076.
10 T. P. Davis, C. W. Gehrke, C. W. Gehrke, Jr., T. D. Cunningham, K. C. Kuo, K. O. Gerhardt, H. D. Johnson and C. H. Williams, *J. Chromatogr.*, 162 (1979) 293.
11 L. D. Mell, Jr., A. R. Dasler and A. B. Gustafson, *J. Liq. Chromatogr.*, 1 (1978) 261.
12 C. J. Little and O. Stahel, *J. Chromatogr.*, 316 (1984) 105.
13 K. Nakano, K. Shindo and T. Yasaka, *J. Chromatogr.*, 332 (1985) 127.
14 M. Glad and S. Ohlson, *J. Chromatogr.*, 200 (1980) 254.
15 T. Seki, Y. Yamaguchi, K. Noguchi and Y. Yanagihara, *J. Chromatogr.*, 332 (1985) 9.

Applications of semi-micro supercritical fluid chromatography with gradient elution to synthetic oligomer separation

MAKOTO TAKEUCHI* and TOSHINORI SAITO

New Project Development Office, JEOL Ltd., Musashino 3-1-2, Akishima City, Tokyo (Japan)

ABSTRACT

A semi-micro supercritical fluid chromatograph which is capable of using carbon dioxide as eluent and a modifier at any concentration, gradient elution and column temperature programming and capable of keeping the column back-pressure at any constant value independent of the eluent flow-rate was applied to oligomer separations. For the separation of low-molecular-weight polymers such as methyl methacrylate, polystyrene and polymethylphenylsiloxane, it was demonstrated that temperature-programmed elution was a valuable technique for the separation of higher-molecular-weight polymers or more polar polymers, and a gradient of eluent composition was useful for obtaining good resolution over the whole range of oligomers.

INTRODUCTION

For high-efficiency separations of polymers by supercritical fluid chromatography (SFC), the use of a gradient method is essential in order to obtain equally spaced peaks[1-3]. There are three methods in gradient elution, two of them involving increasing the solvent strength with increasing mobile phase density, that is, by increasing the column pressure or by decreasing the column temperature, and the other involving changing the eluent composition.

The gradient method with a decreasing temperature gradient is a convenient method and wide applications are to be expected when the eluent composition can be changed and the back pressure can be set at will. However, for a first survey analysis of unknown polymers, the gradient method with changing composition is more powerful if a good solvent for the solute is used as a modifier; by increasing the concentration of the modifier up to 100% under extreme conditions, it is fairly certain that all the injected solute in the column will be removed out.

In this paper we consider elution with a composition gradient and a temperature gradient using a semi-micro packed column of silica-based ODS.

EXPERIMENTAL

Apparatus

Separations were performed using a prototype model JEOL JSF-8800 SFC instrument which is shown schematically in Fig. 1.

Two "intelligent cascade pumps"[4,5] are provided; one is for delivery of carbon dioxide (CAP-G03) with help of a pump-head cooler (CAP-L02) and the other is for delivery of liquid organic solvent as modifier (CAP-C02) with help of a pressurized solvent reservoir (CAP-RP01). Liquid carbon dioxide delivered through a siphon equipped with a high-pressure cylinder (10 l, sufficient for 1 month's work) is supplied through a gas purification unit to the pump CAP-G03.
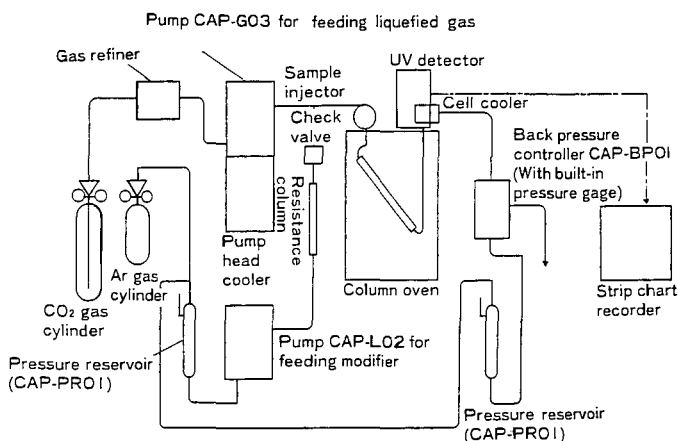
Fig. 1. Flow diagram of JSF-8800 supercritical fluid chromatograph. For explanation, see text.

The gas purification unit consisted of a serially connected silica column, an ODS column and a 0.01-μm particle filter. When "four nines" grade carbon dioxide was employed, this unit could be used for 4 months without a decrease in the purification power; to recover it from used columns, regeneration was possible by washing out the column with 500 ml of methanol delivered from a special valve mounted between the columns and the filter.

The temperature of the pump head of the CAP-G03 was kept constant between $+3$ and $-3°C$ throughout. The mobile phase was carbon dioxide mixed with a second fluid as modifier. The composition of the mobile phase, expressed as the ratio of the carbon dioxide flow-rate to that of the second fluid, can be changed from 100% to 0%, but in most instances we kept the flow-rate of carbon dioxide constant while increasing that of the second fluid. This adjustment was easily made owing to the feature of the intelligent cascade pumps of flow-rate controllability independent of the loaded pressure and the compressibility of the fluid[4,5].

The two fluid lines were mixed at a T-union through a check valve for isolation of each mobile phase. A sample injector (Rheodyne 7520) with a volume of 0.2, 0.5 or 1 μl, depending on the size of the column used, was employed.

The columns employed were SFPAK ODS 05S25 and 05M50 (JEOL), which were 250 mm × 1.7 mm I.D. and 500 mm × 1.0 mm I.D. semi-micro and micro columns packed with 5-μm ODS.

A column oven which had the capability for regulated temperature programming within the range from 300°C to room temperature was fitted to an HP 5890 gas chromatograph (Hewlett-Packard) having no gas inlet and no detector, with necessary modifications for sample injection and a UV detector.

The UV detector (CAP-UV01) employed was equipped with a high-pressure cell for SFC (CAP-CC01) which had a 5-mm light path length and a 1-μl cell volume. A thermo-electric cooling device was used to keep the carbon dioxide liquid.

To control the column bottom pressure, a back-pressure control unit (CAP-BP01) was employed at the outlet of the UV cell, consisting of a digital pressure-measuring device, an in-line filter and a constant-pressure release valve equipped with a temperature controller and a mechanical actuator. The constant-pressure release valve was provided with two lines, one as a pressure-released eluent line and the other as a solvent supply line which extended to the other pressurized solvent reservoir (CAP-RP01).

The solvent contained in the second reservoir should be a good solvent for the solute and miscible with the modifier, which was used for quickly restoring the initial operating conditions by flushing the residual solute from the column at the end of chromatographic run or for preventing precipitation of solute by flowing continuously throughout the running time, this procedure being necessary for stable operation of back-pressure regulation, especially when the solute was soluble in the supercritical phase but not in the modifier itself. The solvent reservoir (CAP-PR01) had a 70-ml capacity and three connection lines, for solvent, gas and drain in addition to the solvent outlet. The gas used was argon at about 7 kg/cm^2.

With a 0.22-μm membrane filter provided in the solvent outlet of the reservoir, tedious processes such as degassing and filtering could be eliminated.

Mobile and stationary phases

Carbon dioxide was the main component of the eluent, to which a second fluid such as methanol, ethanol, *n*-hexane, dichloromethane, tetrahydrofuran, acetonitrile or hexafluoroisopropanol or their binary mixtures was added. The stationary phase was low-polarity end-capped ODS silica gel of particle diameter 5 μm which had been developed for high-performance liquid chromatography (HPLC).

RESULTS AND DISCUSSION

As the experimental parameters of the system, the following four instrumental values can be selected independent of each other: flow-rate of carbon dioxide in the liquid phase, U_1; flow-rate of the second fluid (modifier), U_2; column temperature, T; and back-pressure, P_b.

With column temperature-programmed elution (temperature gradient), T is changed from a certain value T_1 to a lower value T_2 at a rate $-\Delta T/\Delta t$, while the other parameters U_1, U_2 and P_b are kept at constant. The primary effect of a temperature gradient on oligomer separation is to make the solvent strength increase with increasing mobile phase density according to the decrease in the column temperature.

The change in temperature leads to variations in the linear velocity, V, and the other characteristics of the solute, mobile phase and even the stationary phase, but these are minor changes in comparison with the primary effect in most instances.

In gradient elution, the solvent strength is increased with time by changing the composition of the eluent, which can be achieved by increasing U_2 and/or by decreasing U_1, while T and P_b are kept constant. The former elution method in which U_2 is changed will be called the "modifier gradient" method.

Fig. 2 shows a typical example of temperature gradient elution. The sample was a non-ionic surfactant, Triton X-165 (octylphenylpolyoxyethylene). The experimental conditions were as follows; carbon dioxide, U_1 = 150 μl/min; modifier, ethanol, U_2 = 25 μl/min; P_b = 169 kg/cm^2; T_1 = 120°C; T_2 = 70°C; rate, -2.5°C/min; column, 500 × 1.0 mm I.D. ODS-5; detection, UV (210 nm); and sample size, 0.5 μl.
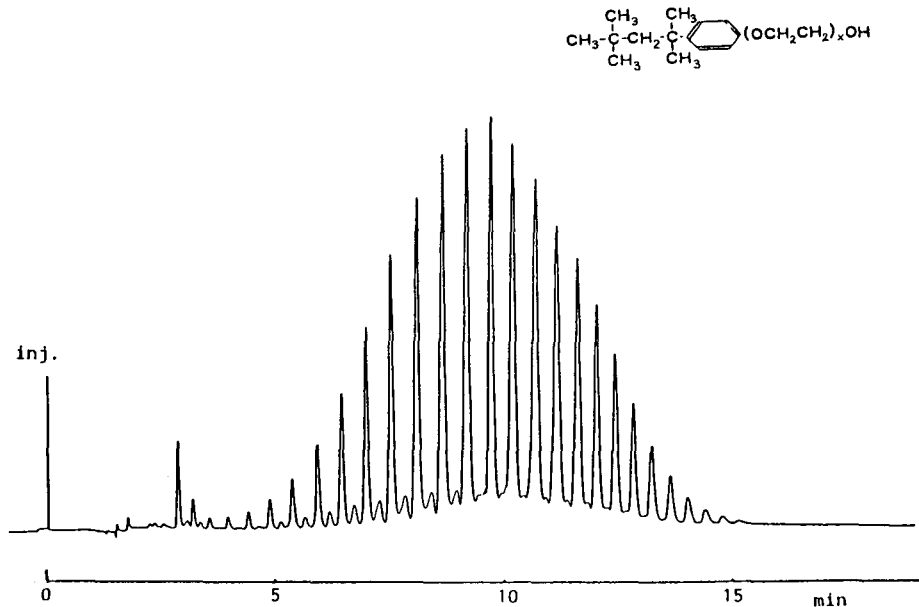
Fig. 2. SFC separation of octylphenylpolyoxyethylene (Triton X-165). Mobile phase, CO$_2$ at 150 μl/min and ethanol at 25 μl/min; pressure at column outlet, P_b (initial) = 169 kg/cm^2; column temperature (initial), 120°C; temperature gradient, -2.5°C/min; column, 500 × 1.0 mm I.D. ODS-5; detection, UV (210 nm); sample size, 0.5 μl.

Another example of temperature gradient elution applied to the analysis of methyl methacrylate (MMA) oligomer is shown in Fig. 3. The pressure dependence of the elution behaviour was also investigated on the same sample. Fig. 4 shows the change in retention time of fourteen arbitrarily selected peaks of oligomers versus the back-pressure change; these results were obtained from four successive chromatographic runs under the same conditions (except for the back-pressure change). The plots for thirteen of the peaks are parallel, which means that they were homologous linear-chain compounds of MMA. The line that was not parallel might indicate a different structure. This unknown peak was fractionated, then investigated with Fourier transform (FT)NMR, FT-IR and field desorption mass spectrometry
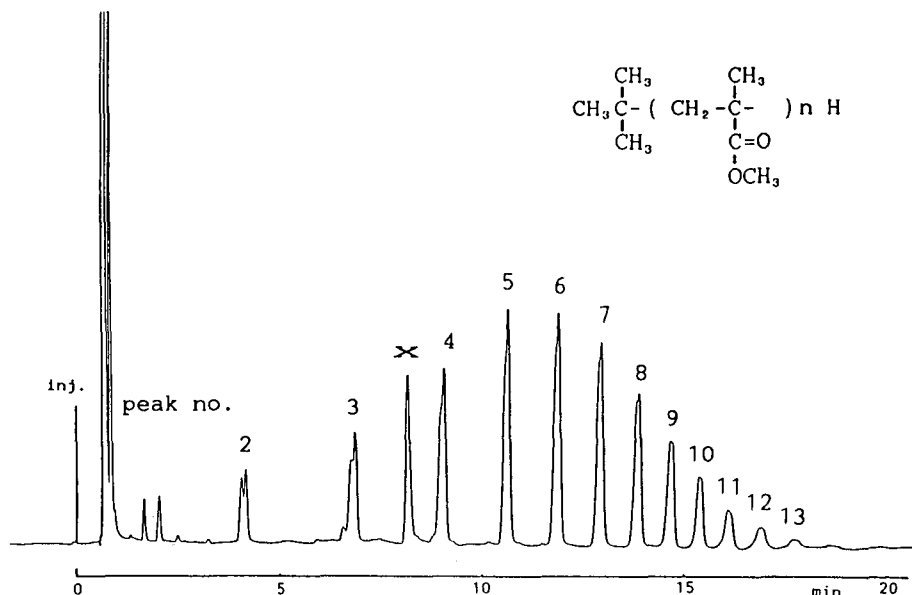
Fig. 3. SFC separation of MMA oligomers with temperature gradient elution. P_b (initial), 150 kg/cm²; eluent, carbon dioxide at 300 μl/min and ethanol at 25 μl/min; column temperature, $T_1 = 120°C$, $T_2 = 70°C$, rate = 3°C/min; detection, UV (210 nm).
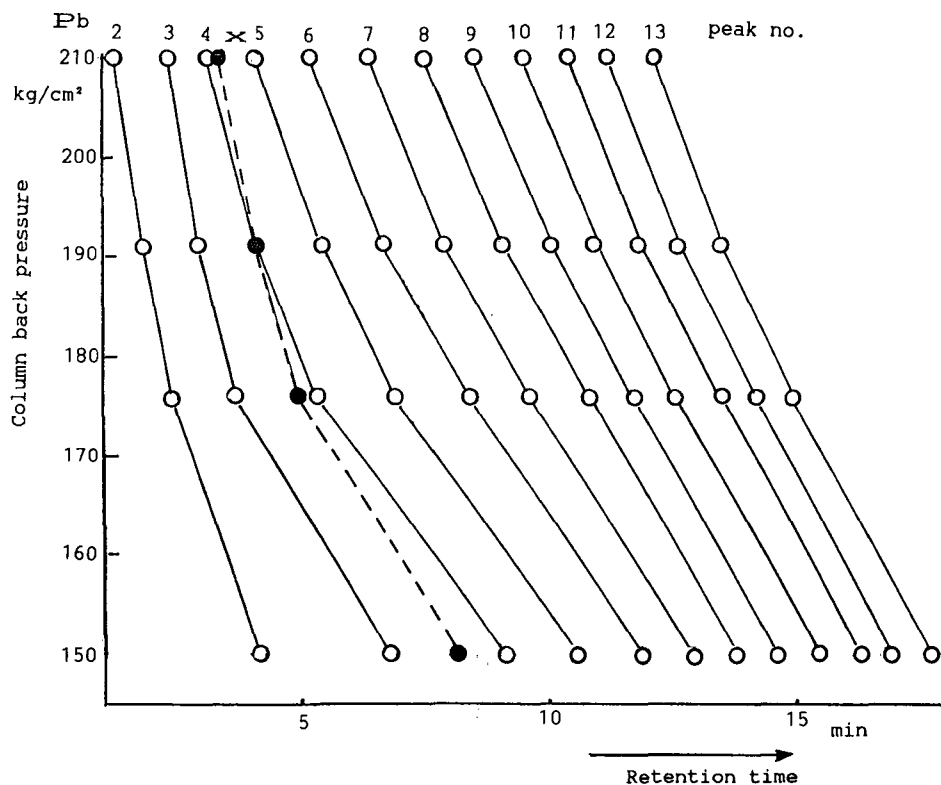
Fig. 4. Change in retention time of fourteen arbitrarily selected peaks in Fig. 3 depending on back-pressure, P_b. Other conditions as in Fig. 3.
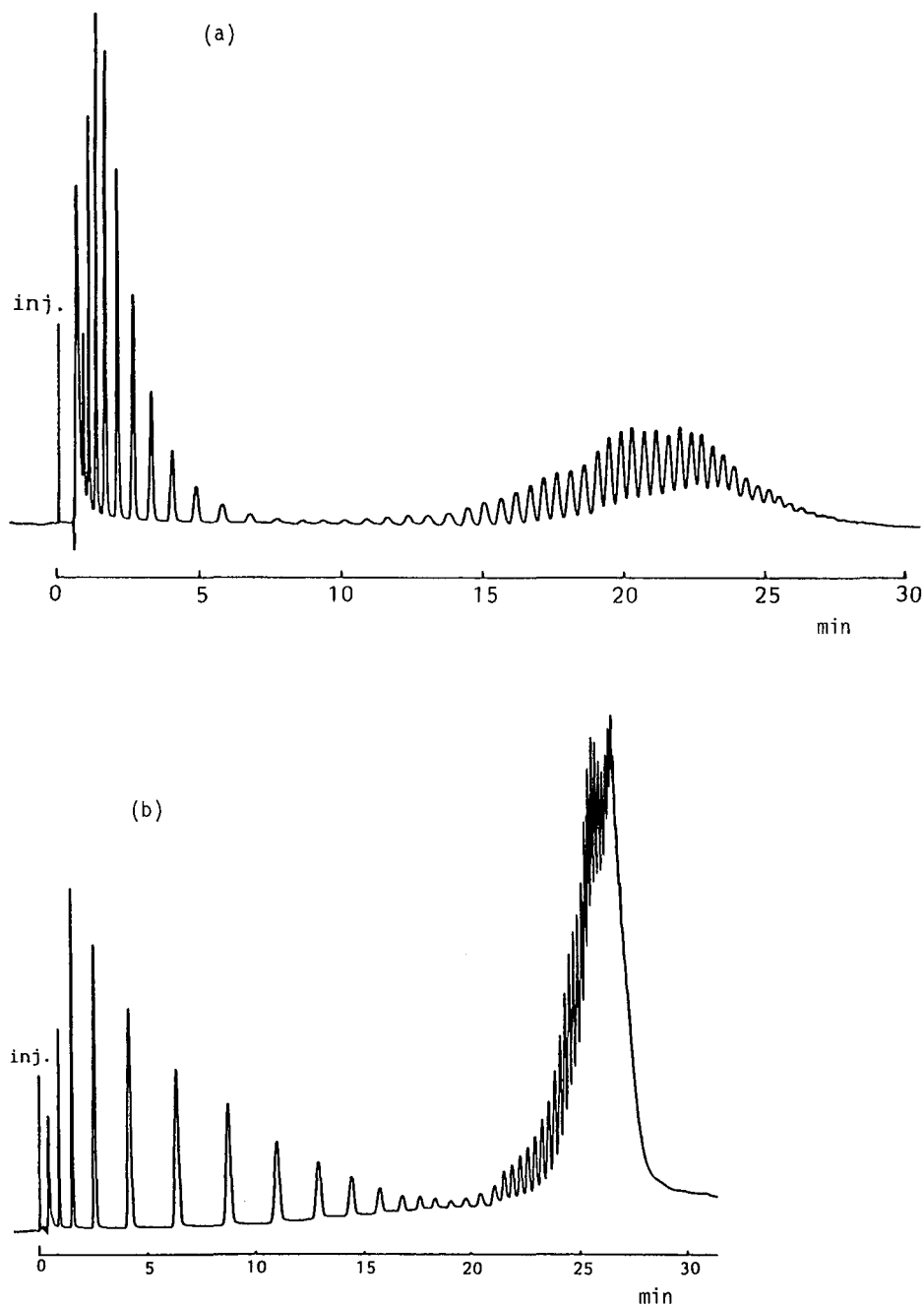
Fig. 5. SFC separation of styrene oligomers prepared by mixing two single dispersive oligomers, three parts of mean molecular weight ($\bar{M}$) = 600 and ten parts of $\bar{M}$ = 4000. (a) With modifier gradient, carbon dioxide constant at 150 μl/min and n-hexane increasing from 75 to 300 μl/min in 30 min; (b) carbon dioxide gradient, decreasing from 300 to 100 μl/min in 25 min, then kept constant, n-hexane increasing from 100 to 300 μl/min in 25 min, then kept constant.

(FD-MS) to determine its structure; these studies are still continuing, but the possibility was confirmed[6]. These results mean that temperature gradient elution has different features to pressure gradient elution, which is feasible for the pressure dependence analysis of oligomers consisting of components with different structures.

As shown in the above example, the temperature gradient method is useful and convenient for the analysis of oligomers that are non-polar or that have a molecular weight distribution that is not too large.

Unlike HPLC, in our SFC experiments column regeneration is rapid in most instances requiring only 3–5 min.

The flow-rates, U_1 and U_2, and the back-pressure, P_b, were kept almost constant during temperature gradient elution. Only the density, ρ, and the linear velocity, v, of the eluent in the column were changed, but not in the cell of the UV detector, because the eluent was cooled quickly outside the oven. Consequently, the baseline movement was kept within a small range.

Fig. 5 shows two examples of composition gradient elution. The separation of styrene oligomers prepared by mixing two single dispersive oligomers, three parts of $\bar{M} = 600$ and ten parts of $\bar{M} = 4000$, were performed by using n-hexane containing 15% of ethanol as a modifier.

Fig. 5a shows the results of modifier gradient elution with the flow-rate of carbon dioxide being kept at constant at 150 μl/min and that of the second fluid was increased from 150 to 300 μl/min, the overall flow-rate of the eluent thus increasing from 300 to 450 μl/min. Correspondingly, if the total flow-rate is kept constant, when U_2 is increased U_1 must be decreased to the same extent.

Fig. 5b shows the results of such gradient elution. The separation of the oligomer component of $\bar{M} = 600$ was good, but not that of the $\bar{M} = 4000$ component; however, the peak height was increased considerably compared with the results in Fig. 5a. As shown in the above example, for a first analytical survey of unknown polymers, this elution method is useful for confirming the maximum elution time of the highest retained component.

We confirmed that the effect of the modifier plays an important role in the high-speed elution of oligomers by maintaining a reasonably good resolution, as suggested by Smith et al.[7] that several fold faster analyses are attainable in some instances than without a modifier. However, it has to be considered that the binary fluid mixture may remain as single phase at the temperature, pressure and composition used during separation. To investigate this aspect, we observed the retention behaviour of non-polar oligomers with a composition gradient at various temperatures over a wide range of compositions. As an example, the separation of methylphenylpoly-siloxane oligomers, obtained at $T = 180, 150, 120, 90$ and $30°C$, is shown in Fig. 6. The content of ethanol relative to the total volume changed from 0.2 to 0.499 (v/v) in 32 min. The initial back-pressure was kept at constant at $ca.$ 212 kg/cm^2 and the pressure drops, ΔP, in the column were also observed.

The binary fluids are liquid at $30°C$ and supercritical at $180°C$ as is clear from the physical constants of each compound: ethanol, $T_c = 243°C$, $P_c = 63$ kg/cm^2; carbon dioxide, $T_c = 31°C$, $P_c = 73$ kg/cm^2. However, the properties under other conditions in the above experiments change from the supercritical to the subcritical liquid phase, depending on the increase in the component of high critical temperature. The chromatograms obtained here show that the mobile phase remained as a single phase
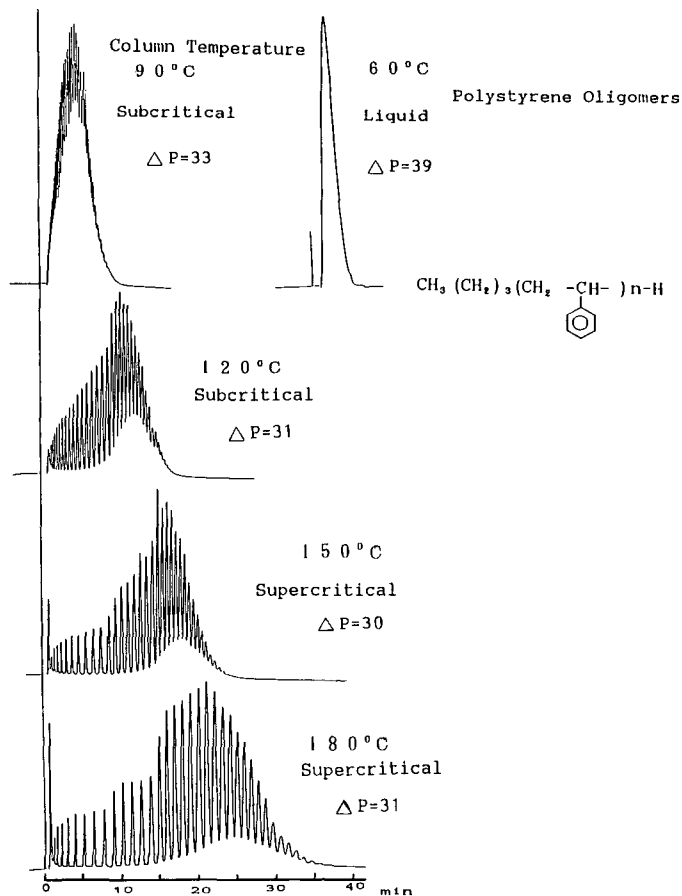
Fig. 6. SFC separation of methylphenylpolysiloxane oligomers with modifier gradient elution at 180, 150, 120, 90 and 30°C. Eluent, carbon dioxide at 300 μl/min, n-hexane increasing from 75 to 299 μl/min in 32 min. ΔP = pressure drop in the column.

under all conditions employed. Moreover, a significant change in the pressure drop in the column was not observed over the whole range of conditions examined here, which means that there was virtually no increase in viscosity.

A similar example for styrene oligomers is shown in Fig. 7, obtained using a ternary fluid system of carbon dioxide, n-hexane and ethanol, the composition of which was changed from 0.5:0.45:0.05 to 0.33:0.60:0.07. The eluent is apparently supercritical at 180°C and liquid at 60°C. The chromatograms obtained show that elution was performed gradually and continuously depending on the changes in temperature and composition. The pressure drop in the column again remained almost constant, with only a small increase at 90°C and 60°C.

Generally, the physical properties of binary fluids can be discussed on the basis of the pressure–temperature–composition (P–T–X) diagram[7], but this is complicated when it is not known if the binary system employed belongs to Type I at the given temperature and pressure.
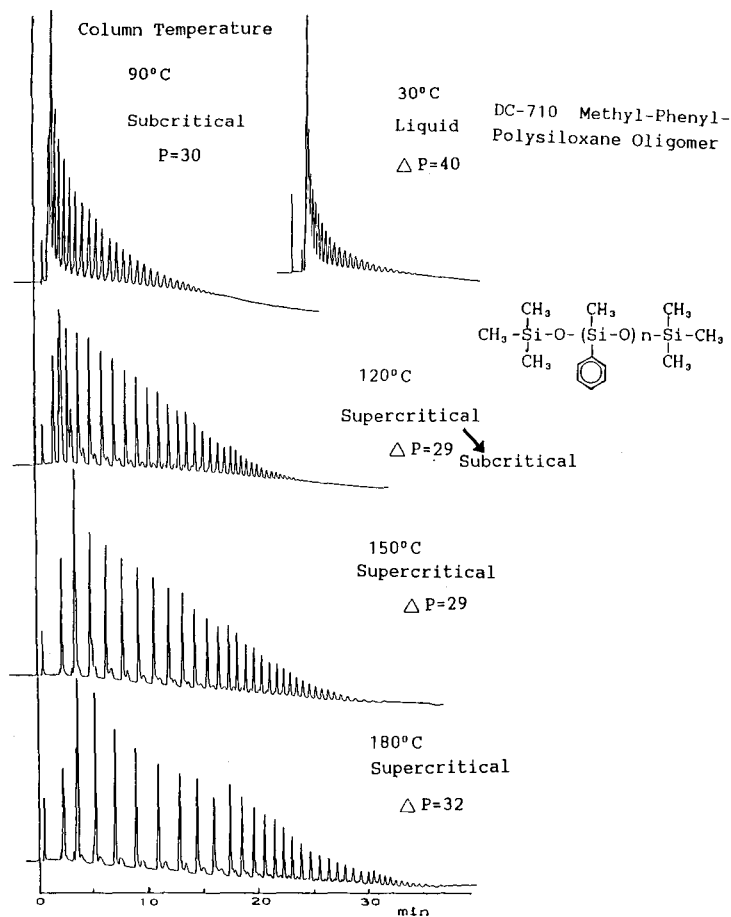
Fig. 7. SFC separation of styrene oligomers (M = 2100) with modifier gradient elution at 180, 150, 120, 90 and 60°C. Eluent, carbon dioxide at 150 μl/min, n-hexane–ethanol (85:15) increasing from 150 to 300 μl/min in 30 min. ΔP = pressure drop in the column.

The confirmation method described in the above example was practical, useful and simple. Also, we can calculate a brief density, ρ, in the column as follows: the linear velocity, v, in the column is given by $(U_1 + U_2)/\rho$, and v is inversely proportional to the retention time, τ, of the void peak, hence ρ can be derived from the equation $\rho = k\tau(U_1 + U_2)$, where k is an instrumental factor that can be determined from the result of using a known fluid such as pure carbon dioxide.

CONCLUSION

A semi-micro packed column SFC instrument was used extensively for the separation of synthetic oligomers by using gradient elution. A temperature gradient is useful and convenient when the eluent composition and back-pressure can be selected freely, to obtain a stable baseline and a fairly high resolution chromatogram in a short

running time with rapid column regeneration. A composition gradient is more powerful for the elution of an unknown polymer in a first trial analysis. By performing separations of known oligomers with composition gradients at various temperatures and pressures, the properties of the binary or ternary fluids can be confirmed.

The system is promising for the fractionation of eluted components for subsequent structure determination by ^{1}H NMR, FT-IR, and FD-MS. Further expansion of applications can be expected by the use of different stationary phases and different modifiers.

REFERENCES

1 F. P. Schmitz and B. Gemmel, in M. Yoshioka, S. Parvez, T. Miazaki and H. Parvez (Editors), *Progress in HPLC*, Vol. 4, VSP, Utrecht, Tokyo, 1989, pp. 74–85.
2 E. Klesper and F. P. Schmitz, in C. M. White (Editor), *Modern Supercritical Fluid Chromatography*, Hüthig, Heidelberg, 1987, pp. 1–13.
3 R. D. Smith, H. T. Kaloinoski and H. R. Udseth, *Mass Spectrom. Rev.*, 6 (1987) 445–496.
4 T. Saito and M. Takeuchi, in Yoshioka *et al.* (Editors), *Progress in HPLC*, Vol. 4, VSP, Utrecht, Tokyo, 1989, pp. 25–51.
5 T. Saito and M. Takeuchi, *JEOL News*, 23A, No. 2 (1987) 15–19.
6 K. Hatada, K. Ute, T. Nishimura, M. Takeuchi and T. Saito, *Polym. Bull.*, 23 (1990) 157–162.
7 R. D. Smith, B. W. Wright and H. T. Kalinoski, in M. Yoshioka, S. Parvez, T. Miazaki and H. Parvez (Editors), *Progress in HPLC*, Vol. 4, VSP, Utrecht, Tokyo, 1989, pp. 111–155.

CHROMSYMP. 1776

Indirect fluorescence detection of sugars separated by capillary zone electrophoresis with visible laser excitation

TOMMY W. GARNER and EDWARD S. YEUNG*

Ames Laboratory–U.S. Department of Energy and Department of Chemistry, Iowa State University, Ames, IA 50011 (U.S.A.)

ABSTRACT

This work extends the use of indirect fluorescence detection for capillary zone electrophoresis to the visible region. Detection is based on charge displacement and is not based upon any absorption or emission properties of the analyte, therefore the need for chemical derivatization is eliminated. Capillary zone electrophoresis–indirect fluorescence detection can separate and detect almost any compound that contains a charge. This was demonstrated by the separation and detection of a mixture of sugars which are only weakly acidic. The mass detection limit of fructose was 2 fmol using a 5-μm diameter capillary. This peak had an efficiency of more than 600 000 theoretical plates.

INTRODUCTION

Capillary zone electrophoresis (CZE) is a new separation technique that separates ionic compounds based on their differential migration rates in an electric field[1]. CZE is known for its high separation efficiencies which can be more than 10^6 theoretical plates[2]. The separation in CZE takes place is small capillaries with internal diameters often less than 50 μm. Detection of the pl injection volumes in this technique is a challenging problem. Fluorescence and electrochemical detection have produced excellent results, but are limited to compounds which have the appropriate physical properties[3,4]. These physical properties can be obtained by chemical derivatization, but derivatization is time consuming and inefficient. There exists a need for an all-purpose detector for CZE.

Indirect fluorescence detection (IFD) for CZE has been applied successfully to many ionic compounds including amino acids[5], proteins, nucleotides[6], tryptic digests[7] and other ionic organic and inorganic compounds[8]. Indirect detection is a universal detection scheme that can detect a wide variety of compounds without the need for chemical derivatization. CZE–IFD is also very sensitive with limits of detection (LOD) in the 50-amol range. Previously, CZE–IFD has been done in the UV region using salicylate as the indirect fluorophore. Fluorophores that fit lasers in the visible region

will aid detection by allowing the use of visible optics and more powerful visible-light sources.

In CZE a buffer is necessary to establish the potential gradient across the capillary tube. This buffer, which is usually inert, can be selected to optimize detection. In indirect fluorescence detection a fluorescing buffer is chosen. This gives a continuously high signal at the detector. When a charged analyte molecule reaches the detector region it displaces the fluorescing buffer ions to maintain constant conductance. Even though the analyte does not absorb or fluoresce it will give a signal by this displacement mechanism. This is unlike indirect detection in liquid chromatography[9], where even neutral analytes can be detected based on changes in partition at the stationary phase.

Sugars present especially challenging separation and detection problems in CZE. Sugars are only weakly acidic and thus the buffer must be made very basic before any ionization will occur. As an example the pK for glucose is 12.35[10]. The sugars can then be separated by their differences in migration velocity. Sugars also show little if any ultraviolet–visible absorption or fluorescence activity. This problem is even more challenging due to the small volumes of analytes injected in CZE.

In this work we will also introduce two new fluorophores that can be used for CZE–IFD. Fluorescein is a highly efficient fluorophore that matches very well with the argon ion 488-nm laser line. Coumarin 343 works very well with the 442-nm line of a helium–cadmium laser.

EXPERIMENTAL

The CZE system is similar to that described previously[5]. A high-voltage power supply (Spellman, Plainview, NY, U.S.A.; Model UHR50PN50 or Glassman, Whitehouse Station, NJ, U.S.A.; Model MJ30P0400-11) was used to supply the electromotive force across the capillary. The anodic high-voltage end of the capillary was isolated in a plexiglass box for operator safety while the cathodic end was held at ground potential.

Capillary columns of various lengths and diameters were used. Lengths ranged from 80 to 100 cm. The outer diameter of the columns was always 150 μm, while the inner diameters ranged from 5 to 22 μm. The polymer coating was burned off 10 cm from the cathodic end of the capillary to form the observation region.

A helium–cadmium Laser (Linconix, Sunnyvale, CA, U.S.A.; Model 4240NB) operating at 442 nm or an argon ion laser (Control Laser Corp., Orlando, CA, U.S.A.; Model 554A) operating at 488 nm was used for excitation. The laser beams (1 mW) were stabilized within 0.04% with a laser power stabilizer (Cambridge Research Institute, Cambridge, MA, U.S.A.; Model LS100). The laser was focused onto the capillary with a 1 or 0.5 cm focal length lens (0.5 cm for the 5-μm capillary). The capillary was mounted at Brewster's angle to reduce scattered radiation.

The fluorescence was collected at 90° with a 20 × microscope objective. The fluorescent image was focused onto a photomultiplier tube (Hamamatsu, Middlesex, NJ, U.S.A.; Model R928). Stray and scattered radiation were rejected by two spatial filters at either end of a blackened tube preceding the photomultiplier tube. The fluorescence was further isolated with two color filters (Corning Glass, Corning, NY, U.S.A.; Model 3-71 and Schott Glass, Duryea, PA, U.S.A.; Model GG475).

The photomultiplier tube current was monitored with a pA meter (Keithly,

Cleveland, OH, U.S.A.; Model 417). The output from the pA-meter was recorded on a chart recorder (Fisher series 5000) or on a personal computer after analog-to-digital conversion (Data Translations, Marlborough, MA, U.S.A.; Model DT 2825 or DT 2827). Digital data were smoothed with a smoothing routine based on the Savitsky–Golay smoothing algorithm[11]. A 1-s time constant was added after the pA meter.

The photomultiplier tube voltage was adjusted to maintain a 1-μA background current. Injections were made for 1 s at 30 kV and the voltage was held at 30 kV throughout the run.

Reagents

All chemicals were reagent grade unless otherwise noted. Fluorescein (Molecular Probes) and Coumarin 343 (Eastman Kodak, Rochester, NY, U.S.A.; laser grade) were prepared in deionized water (Millipore, Bedford, MA, U.S.A.; Milli-Q system) and the pH was adjusted with sodium hydroxide. Buffers were purged with nitrogen to remove carbon dioxide. The pH was checked and adjusted if necessary every 3 h. All quantitative data were obtained with freshly prepared buffer solutions. All analytes were diluted in buffer before injection.

RESULTS AND DISCUSSION

There are several factors involved in the selection of a fluorophore used for CZE–IFD. First, the molecule must have a high molar absorptivity for the excitation wavelengths available. Second, it must have a high fluorescence quantum efficiency. Thirdly, it must be compatible with the solvent system used, *i.e.* it must be soluble and inert. The molecule must also be charged, preferable a charge of one. This will ensure a value as close to unity as possible for the transfer ratio, *TR*. *TR* is defined as the number of fluorophore molecules displaced by one analyte molecule. The molecule also must be well behaved in the system. Some molecules may adsorb to the column walls causing a non-equilibrium state to exist.

The first new fluorophore studied in this work was disodium fluorescein, and is demonstrated by the separation of glutamic acid and aspartic acid. Tris was added to the buffer to increase the buffer capacity. Separation efficiencies were high for this system with plate numbers for each amino acid exceeding 100 000. This allows indirect detection to be implemented with an argon ion laser. No stabilization of the laser power was implemented. Although this system was not optimized for the best LOD high absolute sensitivities were obtained with a LOD for each amino acid of 2 fmol. Lower detection limits should be obtained by lowering the concentration of buffer and stabilization of the laser intensity[6]. As can be seen from these results, fluorescein worked well at pH 7. When the pH was increased to 9, however, the baseline became very erratic. This was believed to be caused by the interaction of fluorescein with the wall of the capillary.

The next fluorophore studied in this work was coumarin 343. Coumarin 343 was selected because of its good solubility in water, high molar absorptivity and high fluorescence yield. Coumarin 343 has a molar absorptivity of $2 \cdot 10^4$ at 442 nm which matches very well with the 442-nm line of the helium–cadmium laser. The high fluorescence yield was evaluated experimentally by injecting coumarin 343 in the direct detection mode. The buffer used was 10 mM sodium bicarbonate at pH 10.7. The
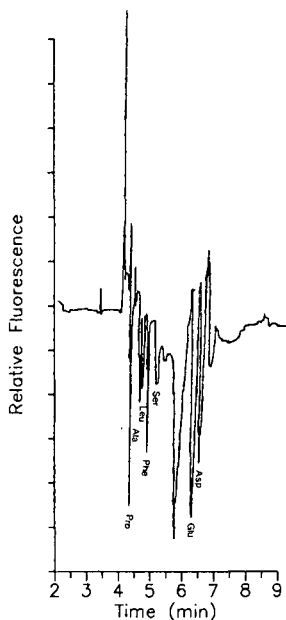
Fig. 1. Indirect detection of an amino acid mixture using coumarin 343 as the fluorophore. The buffer used was 1 mM coumarin 343 at pH 9.5. A 1-s, 30-kV injection of 75 μM each was followed by electrophoresis at 30 kV on a 80 cm $\times$ 18 μm I.D. $\times$ 150 μm O.D. column.

detection limit was $8 \cdot 10^{-10}$ M (signal-to-noise ratio, $S/N = 3$) (column 80 cm, 5 μm diameter, 1 s injection at 30 kV, 30-kV separation).

Coumarin 343 is successfully employed in the separation of a complex mixture of amono acids shown in Fig. 1. The elution order agrees with previous work[5]. The broad peak at 5.5 min is an unknown impurity. The separation efficiency is very good here also, with an average plate number of 270 000. This proves that indirect detection is based on the charge displacement and not specific interaction with the fluorescing ion. Otherwise, the peak heights would have been different from those in previous work.

Sugars have been separated by CZE as their borate complexes[12]. It is shown here that sugars can be separated and detected without any prior derivatization. CZE separates compounds based on their mobility which is related to the pK values and the buffer pH. In indirect detection the sensitivity depends on the fraction of the analyte that is ionized. This means when using indirect detection for the detection of sugars the pH of the running buffer must be approaching 12 to have any substantial fraction, α, in the ionized form. This presents another problem. When the pH of the buffer solution gets this high the concentration of hydroxide ion is no longer negligible relative to the concentration of the fluorophore. This results in a decrease of TR. These effects must be balanced to obtain the best sensitivity possible for the system.

The effect of the hydroxide ion can be approximately described by eqn. 1.

$$TR_{tot} = \frac{\alpha[\text{sugar}]}{[\text{FL}] + [\text{OH}^-]} \qquad (1)$$
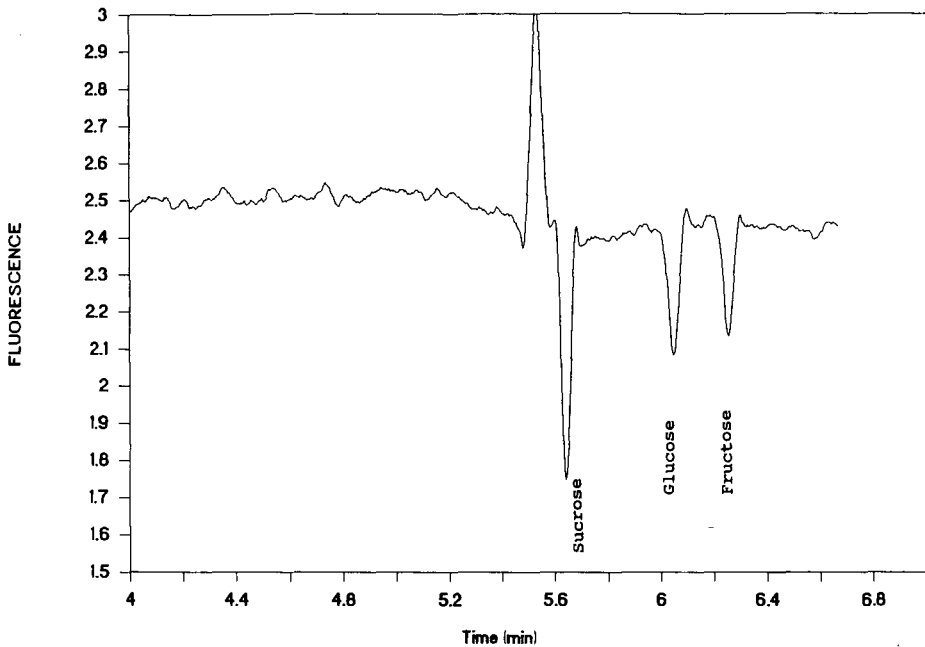
Fig. 2. Separation of a sugar mixture. Indirect detection of 640 fmol of each sugar in 1 mM coumarin at pH 11.5. The column was 90 cm × 18 μm I.D. × 150 μm O.D.

In this equation TR_{tot} is the total transfer ratio. This includes the amount of fluorophore [FL], and the amount of hydroxide ion [OH$^-$], displaced by the sugar molecules that are ionized. Ir can be seen that at constant fluorophore and sugar concentrations α in the numerator and the [OH$^-$] in the denominator are competing functions of pH. TR_{tot} goes through a maximum when it is plotted as a function of pH. The pH at this maximum is the most sensitive pH for detection.

The separation of a three-sugar mixture is shown in Fig. 2. The optimum detection pH was found to be 11.65 based on tabulated literature values of the pK for each sugar[10] and eqn. 1. A pH of 11.5 was used for detection, however, because the rate

TABLE I

SUGARS DETECTED BY INDIRECT FLUORESCENCE DETECTION

Each sugar was injected at a concentration of 1 mM in 1 mM coumarin 343 at pH 11.5. Column was 84 cm × 18 μm I.D. × 150 μm O.D.

Sugar	Migration time (min)
Raffinose	4.98
Sucrose	4.99
Maltose	5.35
Arabinose	5.47
Glucose	5.50
Lactose	5.61
Xylose	5.62
Fructose	5.66

of degradation of fluorophore was decreased without any appreciable decrease of detection efficiency. The capillary columns were found to be stable for many runs at this pH. Table I is a compilation of the sugars detected using CZE–IFD and their corresponding migration times. Each of these sugars were injected at a concentration of 1 mM. This is compared to a previous report where the N-2-pyridylglycamine derivatives of sugars are injected in the 10–100-mM range and detected by UV absorbance[12].

In this analysis of biological compounds there is often a limited supply of sample, such as in the analysis of single cells[13]. The analysis of such small volumes of analytes requires the use of smaller bore capillaries in the CZE system. The use of these smaller bore capillaries, however, requires the absolute detection limit of the detection method to decrease as the dimensions of the capillary decrease. The detection scheme should also be universal to detect the large number of biological compounds that lack analytically useful physical properties. CZE–IFD fulfills the requirements that are demanded by the use of smaller capillaries. This was demonstrated by the detection of fructose after it was injected into a 5-μm diameter capillary. The absolute limit of detection in this system was 2 fmol based on a S/N_{rms} (rms = root mean square) of 3. This is expected based on eqn. 1 and ref. 6. The high separation efficiency offered by this system (over 600 000 theoretical plates) is partially responsible for the low detection limit obtained. The dynamic range is therefore a factor of 100, from the detection limit to saturation of the background signal.

The detection limit of fructose was believed to be limited by the mechanical vibration of the system. This is because the capillary diameters are approaching the diameter of the focused laser beam[14]. Small fluctuations in the capillary relative to the beam will cause large fluctuations in the signal. This can be partially compensated for by slightly defocusing the beam by moving the capillary away from the beam focusing lens. This problem will have to be studied further as capillary dimensions decrease.

ACKNOWLEDGEMENTS

REFERENCES

1 K. D. Lukacs and J. W. Jorgenson, *Science (Washington, D.C.)*, 222 (1983) 266.
2 K. D. Lukacs and J. W. Jorgenson, *J. High Resolut. Chromatogr. Chromatogr. Commun.*, 8 (1985) 407.
3 R. A. Wallingford and A. G. Ewing, *Anal. Chem.*, 60 (1988) 258.
4 J. S. Green and J. W. Jorgenson, *J. High Resolut. Chromatogr. Chromatogr. Commun.*, 7 (1984) 529.
5 W. G. Kuhr and E. S. Yeung, *Anal. Chem.*, 60 (1988) 1832.
6 W. G. Kuhr and E. S. Yeung, *Anal. Chem.*, 60 (1988) 2642.
7 B. L. Hogan and E. S. Yeung, *J. Chromatogr. Sci.*, 28 (1990) 15.
8 L. Gross and E. S. Yeung, *J. Chromatogr.*, 480 (1989) 169.
9 J. E. Parkin, *J. Chromatogr.*, 287 (1984) 457.
10 J. A. Rendle, Jr., in H. S. Isbell (Editor), *Carbohydrates in Solution*, American Chemical Society, Washington, DC, 1973, p. 54.
11 A. Savitsky and M. J. E. Golay, *Anal. Chem.*, 36 (1964) 1627.
12 S. Honda, S. Iwase, A. Makino and S. Fugiwara, *Anal. Biochem.*, 176 (1989) 72.
13 R. A. Wallingford and A. G. Ewing, *Anal. Chem.*, 60 (1988) 1975.
14 E. J. Guthrie, J. W. Jorgenson and P. R. Dluzneski, *J. Chromatogr. Sci.*, 22 (1984) 171.

CHROMSYMP. 1799

Electrochromatography with continuous sample introduction

TAKAO TSUDA* and YOSHIHIKO MURAMATSU

Nagoya Institute of Technology, Gokiso-cho, Showa-ku, Nagoya 466 (Japan)

ABSTRACT

The flow profile and height equivalent to a theoretical plate in electromatography are discussed. Apparatus for continuous injection is proposed. Continuous injection of sample onto the column was accomplished for a period of up to 5 min, and charged solutes were in the column. Typical examples are presented.

INTRODUCTION

Electrochromatography, in which two functions (mobility and sorptive interaction) are used at the same time, is a highly effective separation method[1-4]. Otsuka and Listowsky[1] and O'Farrell[2] separated ferritin subunits by applyling a voltage along a column. As the applied voltages in these experiments were relatively low, such as 12 V/cm, the separation process took more than 10 h. In previous studies[3,4] we demonstrated electrochromatography with a high voltage along a column and obtained effective separations within a few minutes. A theory of band broadening in a column was proposed and the effect of an electric field on the nature of the column support was examined[4].

In this paper we discuss several examples of variations in flow profiles with respect to the time axis due to different values of the linear velocity of pressurized flow, v(pres), and mobility, v(mob).

In electrochromatography, it is possible to retain a solute in a column during operation under pressurized flow if the velocity due to its mobility toward the inlet of the column is higher than that due to pressurized flow toward the outlet of the column. Therefore, we can concentrate a solute in a column during a period of several injections and then elute it after stopping the voltage applied to the column[4]. In this work, we have developed a technique that allows a solute or group of compounds to be concentrated in a column under an applied voltage with continuous injection of the samples.

EXPERIMENTAL

The apparatus is shown in Fig. 1. The glass column (5 cm × 4 mm I.D.) (Kusano Kagaku Seisakusho, Tokyo, Japan) was slurry packed with silica gel bonded with

octadecylsilane of particle diameter 7 μm (Capcell C_{18}; Shiseido, Yokohama, Japan). The injector and connectors (2, 4, 5 and 7 in Fig. 1) were made of PTFE resin (Kusano Kagaku Seisakusho). To exclude bubbles generated at the terminals, fused-silica capillary tubing (20–30 cm $\times$ 50 μm I.D.) (9 and 9′ in Fig. 1) were used. As there was a high voltage gap between the outlet of 9 in Fig. 1 and the air, a side flow of the effluent was electrically sprayed into the air. This side flow was estimated to be less than 0.1 ml/min. Sample was injected by a pump (Microfeeder MF-2; Azuma Denki Kogyo, Tokyo, Japan) at 4–10 μl/min. The sample was stored in the pump in a microsyringe (250 or 500 μl), with the end of the needle directly connected to a fused-silica capillary tube (8′ in Fig. 1) by a short PTFE tip (10 mm $\times$ 0.25 mm I.D.). A UV absorbance detector operated at 254 nm (Uvidec II; Jasco, Tokyo, Japan), a pump for supplying effluent (LC-6A; Shimadzu, Kyoto, Japan) and a high-voltage d.c. power supply (Matsusada Precision, Yokaichi, Shiga, Japan) were used. To avoid high voltages, the pumps (12 and 13 in Fig. 1) were connected to that part of the apparatus which carried the high voltage by long fused-silica capillary tubes (ca. 60 cm $\times$ 50 μm I.D.; 8 and 8′ in Fig. 1), which offered high electrical resistance. In this work, the inlet of the column was kept at high voltage. A positive high voltage means that a positive high voltage is applied at the inlet part of the column.

Reagents of guaranteed grade (Wako, Osaka, Japan) were used. *cis*-N-Methyl-4-β-styrylpyridinium iodide was a gift from K. Takagi, Nagoya University.
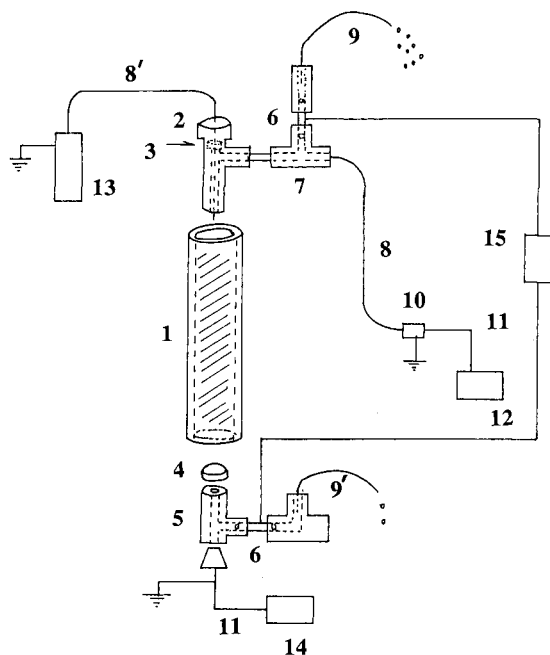
Fig. 1. Schematic diagram of apparatus for continuous injection. 1 = Column (5 cm $\times$ 4 mm I.D.) made of Pyrex glass, packed with silica-ODS; 2 = injector; 3 = silicone-rubber septum; 4 = frit; 5 = connector; 6 = platinum tubing (I.D. 0.5 mm) for terminal; 7 = three-way connector; 8, 8′, 9 and 9′ = fused-silica capillary tubing; 10 = connector; 11 = stainless-steel tubing (O.D. 1/16 in.); 12 = pump for effluent; 13 = pump for sample injection; 14 = UV detector (254 nm); 15 = high-voltage d.c. power supply.

THEORY OF CHROMATOGRAPHIC BEHAVIOUR

In electrochromatography there are two factors, electrophoretic mobility and electroosmotic flow, that do not exist in ordinary liquid chromatography. Therefore, the band broading of a solute in electrochromatography is different from that in ordinary chromatography. The apparent mean linear flow velocity of a solute, $v(\text{app})$, is

$$v(\text{app}) = v(\text{pres}) + v(\text{mob}) + v(\text{osm}) \tag{1}$$

where $v(\text{pres})$, $v(\text{mob})$ and $v(\text{osm})$ are mean linear flow velocities due to pressurized flow, mobility and electroosmosis, respectively. Generally, $v(\text{osm})$ in a slurry-packed capillary column is 10–20% of that in an open-tubular capillary column[5,6]. If $v(\text{osm})$ in a slurry-packed capillary column is considerably lower than $v(\text{mob})$, eqn. 1 becomes

$$v(\text{app}) = v(\text{pres}) + v(\text{mob}) \tag{2}$$

In the process of flow in electrochromatography, the flow of $v(\text{pres})$ is operated with a Poiseuille flow profile, and we assume that the flow pattern of $v(\text{mob})$ would be a plug flow profile. Therefore, the velocity inequality in the radial direction is due only to laminar flow, namely $v(\text{pres})$. The flow pattern in electrochromatography is assumed to be mixed Poiseuille and plug flow.

The assumed flow profiles are shown in Fig. 2; x_0 is the point of injection and the region $x \geqslant 0$ corresponds to the column, but the region $x < 0$ before the column inlet is assumed to exist. The region $x < 0$ is necessary to figure out the retarded solute at the column inlet. At time t_0, solute was introduced as a plug (Fig. 2a). Fig. 2b shows the flow profile at time t_1 under the conditions $v(\text{mob}) = 0$ and $v(\text{pres}) > 0$. Fig. 2c shows the flow profile at time t_1 under the condition $v(\text{pres}) = 0$. Fig. 2d shows the actual net profiles under the condition $v(\text{pres}) > 0$ and $|v(\text{mob})| > 0$.

The sample will remain in the column under the condition $v(\text{pres}) \leqslant -2v(\text{mob})$, shown in Fig. 2d-1-2 and d-1-3, because the highest velocity in laminar flow is twice the mean linear flow velocity. When the inside diameter of the connecting tubing between the injector and the column is extremely small compared with that of the column, $v(\text{pres})$ in the connecting tube will be considerably larger than $-2v(\text{mob})$. Under this condition the solute will be forced to remain just at the inlet of the column when there is an applied voltage.

The plate height, H in general chromatography is[7]

$$H = B/v + C_s v + C_m v + (1/A + 1/C_m v)^{-1} \tag{3}$$

and H in electrochromatography is

$$H = B/v(\text{app}) + C_s v(\text{app}) + H_3 + (1/A + 1/H_3)^{-1} \tag{4}$$

where

$$H_3 = w_\alpha^2 w_\beta^2 \cdot \frac{d_p^2 v(\text{pres})}{2D_m v(\text{app})} \cdot v(\text{pres}) = C_m \cdot \frac{v(\text{pres})^2}{v(\text{app})} \tag{5}$$
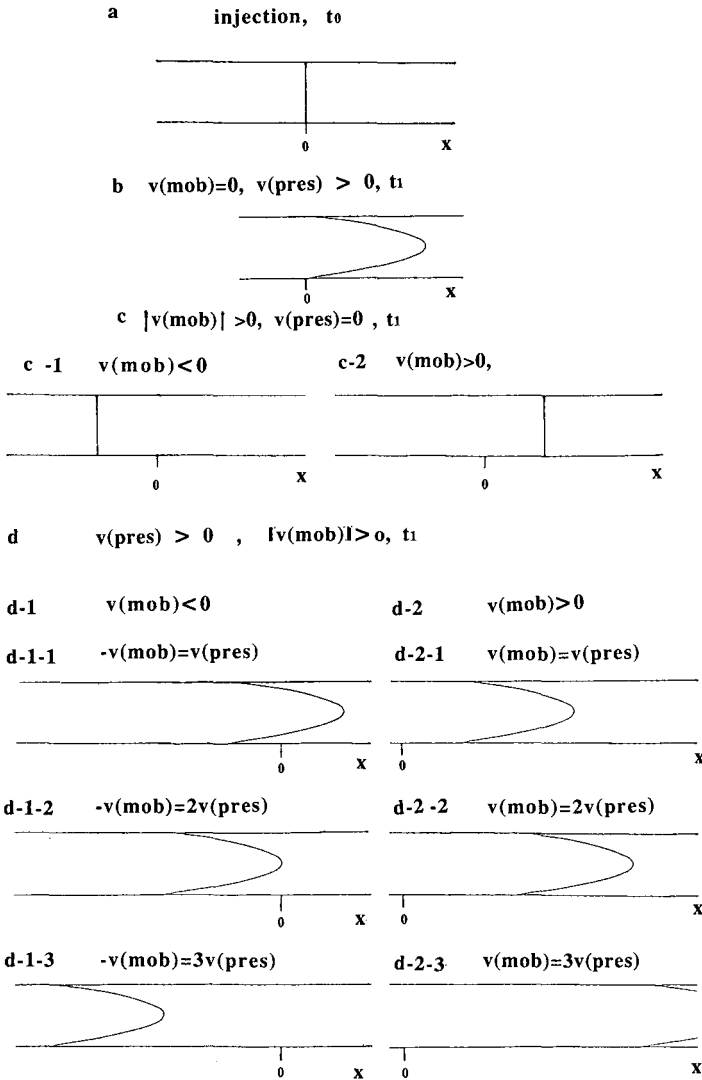
Fig. 2. Assumed flow profile in electrochromatography. t_0, t_1, Time; x, direction of pressurized flow.

In these equations A, B, C_s and C_m are coefficients for eddy diffusion, axial molecular diffusion, resistance to mass transfer in the stationary phase and resistance to mass transfer in the mobile phase, respectively, w_α is a coefficient of a step in molecular diffusion, w_p is equal to $\Delta v(\text{pres})/v(\text{pres})$ and Δv is the difference between the extreme and the mean velocities[4].

Eqn. 4 is valid in the region $v(\text{app}) > 0$. H as given by eqn. 4 is different from H in general chromatography, given by eqn. 3, in the following respects. First, the flow velocity of a solute is equal to $v(\text{pres}) + v(\text{mob})$. Second, H_3 in electrochromatography is completely different from H_3 in general chromatography, given by

$C_m v(pres)$. When $v(mob) > v(pres)$, the contribution of $v(mob)$ to H makes the value of each term less than 1 in general chromatography. When $v(app) < v(pres)$, owing to the negative value of $v(mob)$ the solute will remain in the column longer than in ordinary chromatography. Hence the second term in eqn. 4 becomes smaller and the other terms larger compared with the corresponding terms when $v(mob) = 0$.

The variation of H_3 *with* $v(app)$ for several values of $v(mob)$ is shown in Fig. 3. The H_3 term under the condition $v(mob) > 0$ is always smaller than that when $v(mob) = 0$. Conversely, H_3 under the condition $-v(mob) < v(pres)$ becomes larger than that when $v(mob) = 0$. It is understandable that H become larger, as the solute is retained in the column for a long period of time.

RESULTS AND DISCUSSION

The apparatus for continuous injection is shown in Fig. 1. The sample is injected via a fused-silica capillary tube, the extremity of which is placed on or just into the head of the column packing material. The reproducibility of the sample injection is shown in Fig. 4. The amount of sample injected was proportional to the duration period of injection by the pump (13 in Fig. 1). The amount of sample injected per second was adjusted by setting the flow-rate of the pump. This device may be a very good system for electrochromatography. Because the fused-silica capillary works as an electric insulator, the process of injection is safe. Also, from Fig. 4, no tailing of the peaks is observed. Therefore, the electroosmotic flow in the fused-silica capillary due to applied voltage[8] is not sufficient to cause continuous leakage of sample from sample storage in the pump.

The chromatographic behaviour with continuous injection of sample solution into the column inlet is demonstrated in Figs. 5 and 6. The chromatograms in Figs. 4 and 5 were obtained with continuous operation. In Fig. 5, continuous injection of *cis*-N-methyl-4-β-styrylpyridinium iodide (CIS) for 90 s gave a strong solvent peak (c) and an unknown peak (b). The latter peak has a negative charge. Just after stopping the
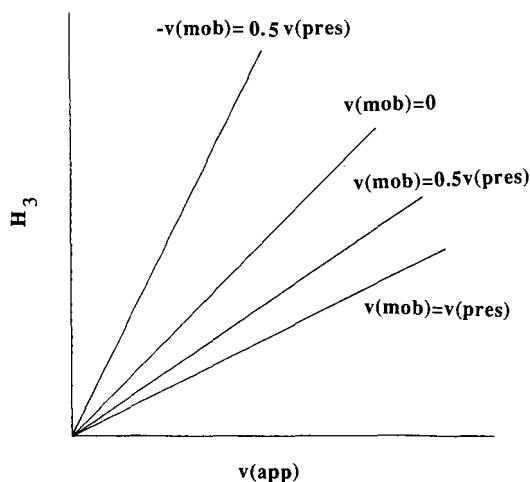
Fig. 3. Relationship between H_3 and $v(app)$ at different values of $v(mob)$.
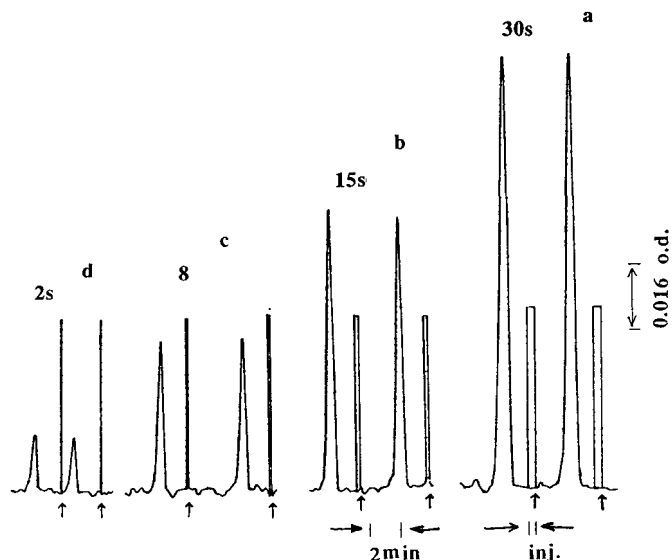
Fig. 4. Reproducibility of continuous injection. Sample, 1% benzene–methanol solution; applied voltage, −5.1 kV (58 μA); detection, UV 254 nm, 0.16 a.u.f.s.; duration of continuous injection for a, b, c and d, 30, 15, 8 and 2 s, respectively; sample injection rate, 10 μl/min; eluent, 2 mM phosphate buffer–methanol (5:95) at a flow-rate of 0.4 ml/min.

electric field at time zero in chromatogram D, two peaks were eluted, which were isomers of CIS. These isomers, having a positive charge, had been retained in the column while the applied voltage was −8.1 kV. Continuous injection for 5 min (total sample amount 50 μl) is shown in Fig. 6. During this period a positive electric field was applied in order to retain sample components of negative charge. In chromatogram c in Fig. 6 there is a large solvent peak due to the relatively long period of sample injection. After stopping the applied voltage, sulphonic acids that had been retained in the column were eluted. As the total length between the two terminals was about 12 cm, the real voltage applied to the column was *ca.* 40% of the actual applied voltage.

We used samples of relatively high concentration, and the sample injection rates were 4–10 μl/min. The latter rate was also increased up to 10% of the flow-rate of effluent. In this instance, we kept the total flow-rate of the eluent and sample solution in the column constant and avoided a reverse flow to the pump at the time when injection began.

Even if a solute has a high mobility, such as $-v$(mob) $\geqslant 2v$(pres), it is possible to retain it in the column. Hence it is possible to concentrate a very minor component of the mixture solution by passing an amount of the mixture through the column under an applied high voltage. Electrochromatography might be a good method for concentrating some types of compounds.
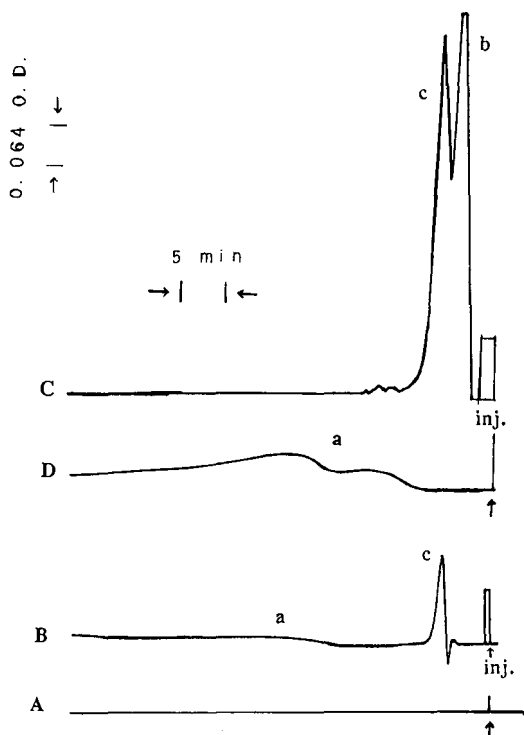
Fig. 5. Chromatogram with continuous injection of a solute having a positive charge. Sample, 10^{-2} M cis-N-methyl-4-β-styrylpyridinium iodide (CIS); sample injection rate, 10 μl/min; eluent, 2 mM phosphate buffer (pH 7)–methanol (5:95); applied voltage, -8.1 kV (80 μA). Peaks a and b belong to the sample and peak c is the solvent peak. A, Applied voltage on, without injection; B, applied voltage off, 0.5-min injection; C, applied voltage on, 1.5-min injection; D, chromatogram obtained just after stopping the applied voltage at time zero.
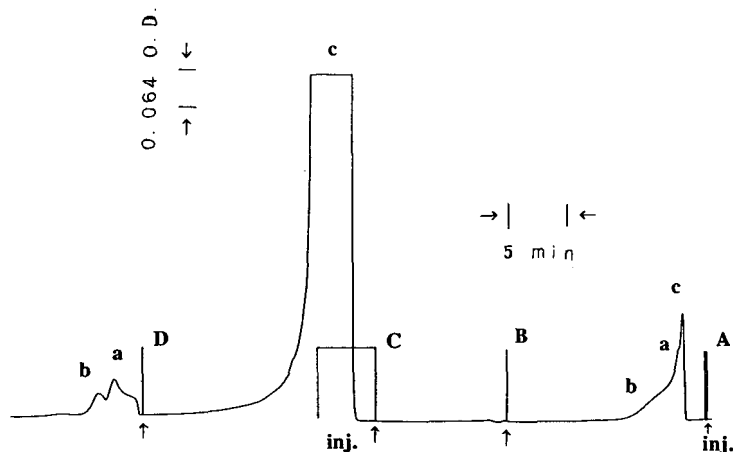
Fig. 6. Chromatogram with continuous injection of a solute having a negative charge. Sample: 10^{-2} M aqueous 1,2,6-naphthalenetrisulphonic acid solution; sample injection rate, 10 μl/min; eluent, 0.1 mM phosphate buffer (pH 7)–methanol (40:60); applied voltage, $+5$ kV (75 μA). Peaks a and b belong to the sample and peak c is the solvent peak. A, Applied voltage off, 15-s injection; B, applied voltage on, without injection; C, applied voltage on, 5-min injection; D, chromatogram obtained just after stopping the applied voltage at time zero.

REFERENCES

1 S. Otsuka and L. Listowsky, *Anal. Biochem.*, 102 (1980) 419–422.
2 P. H. O'Farrell, *Science*, 227 (1987) 1586–1589.
3 T. Tsuda, *Anal. Chem.*, 59 (1987) 521–523.
4 T. Tsuda, *Anal. Chem.*, 60 (1988) 1677–1680.
5 T. S. Stevens and H. J. Cortes, *Anal. Chem.*, 55 (1983) 1365–1370.
6 T. Tsuda, K. Nomura and G. Nakagawa, *J. Chromatogr.*, 248 (1982) 241–247.
7 J. C. Giddings, *Dynamics of Chromatography*, Marcel Dekker, New York, 1965.
8 T. Tsuda, K. Nomura and G. Nakagawa, *J. Chromatogr.*, 264 (1983) 385–392.

Analysis of the components of *Paeonia radix* by capillary zone electrophoresis

SUSUMU HONDA*, KENJI SUZUKI, MAYUMI KATAOKA, AKIKO MAKINO and KAZUAKI KAKEHI

Faculty of Pharmaceutical Sciences, Kinki University, 3-4-1 Kowakae, Higashi-osaka (Japan)

ABSTRACT

The methanol extract of *Paeonia radix* was analysed by capillary zone electrophoresis in 100 mM borate buffer (pH 10.5). Monoterpene glycosides (paeoniflorin and oxypaeoniflorin) were migrated first, well separated from each other, then gallic acid and its derivatives. The monoterpene glycosides were quantified with high reproducibility using 3,4-dimethoxycinnamic acid as an internal standard. The data obtained from various *Paeonia radix* samples were highly correlated to those obtained by high-performance liquid chromatography.

INTRODUCTION

Capillary zone electrophoresis (CZE), introduced by Mikkers *et al.*[1], allows the separation of ionic components of samples in a capillary tube with excellent resolution by the combined effects of electrophoresis and electroosmosis. Electrophoresis separates ions based on differences in charge and size, whereas the flow of carrier induced by electroosmosis drives the separated ions from one end of the tube to the other. As electroosmotic flow is plug flow and heat evolved during analysis is efficiently dissipated from the capillary wall, diffusion of separated components is minimized and a high column efficiency is attainable. This capillary method also allows accurate and reproducible quantification of components by on-tube detection.

CZE has been applied to various ionic compounds, including inorganic anions[1] and cations[2], organic acids[1,2–5], dansylated amino acids[6], ammonium salts[7], pyridinium salts[2], catecholamines[8], nucleosides[9], drug metabolites[10] and proteins[11]. However, there have been no papers dealing with crude drugs. Therefore, we have undertaken a study of the application of this powerful method to the determination of the components of crude drugs. This paper presents some preliminary results obtained for *Paeonia radix*, which has been traditionally used as a sedative, lenitive or antispasmolytic agent.

EXPERIMENTAL

Samples of *Paeonia radix* were gifts from Tochimoto Tenkaido (Suehiro-cho, Kita-ku, Osaka, Japan). The authentic specimens of paeoniflorin and oxypaeoniflorin were isolated by chromatography of the methanol extract of *Paeonia radix* on a column of silica gel with chloroform–methanol as eluent and purified by recrystallization from chloroform. All other chemicals were of the highest grade commercially available.

Extraction of the components
Methanol (10 ml) was addd to thin slices of each crude drug sample (100 mg), and the mixture was heated under reflux for 30 min. The methanol extract was removed and the residue was heated twice more with additional batches (10 ml each) of methanol. The extracts were combined and evaporated to dryness under reduced pressure. The residue was reconstituted with methanol, and the solution was analysed.

Procedure for CZE
Each of two laboratory-made PTFE blocks having hollows of 1.5-ml capacity, in which platinum wires (10 mm × 1 mm O.D.) as electrodes were fixed, was filled with 100 mM borate buffer (pH 10.5) and an 80-cm portion of 50-μm I.D. fused-silica capillary tubing (Scientific Glass Engineering, Melbourne, Australia) newly cut off from a roll, containing the same solution as the carrier, was bridged between these blocks. A Matsusada Precision Devices Model HER-30PI apparatus was used to supply high voltages. The platinum wires were connected to the anode and the cathode (grounded) via shielded cables. Part of the polyethylene coating of the tube was removed by burning at a position 15 cm from the cathode, and the transparent portion was fixed to a slit (50 μm × 700 μm) which was screwed on a specially made PTFE holder. This holder was placed in the cell housing of a JASCO UVIDEC 100-V UV monitor and the absorbance at 254 nm was recorded.

Prior to each run, the tube was rinsed with 0.1 M sodium hydroxide solution, and conditioned by rinsing with the carrier solution using a small injector. The tube was also rinsed with methanol after every five runs. A sample solution was introduced into the tube by moving the anodic end of the tube into the sample solution and its level was maintained for 5 s 5 cm higher than the level of the cathode solution. By this syphonic procedure several nanolitres of the sample solution were introduced into the tube. After introduction of the sample solution the anodic end was quickly returned to the anode solution, and its level was adjusted to that of the cathode solution. Analysis was performed by applying 20 kV in the constant-voltage mode.

RESULTS AND DISCUSSION

In CZE, the main factors affecting separation are the nature of the inner wall of the capillary tube and the composition and pH of the carrier solution. Several kinds of materials are used for such narrow-bore tubes (mostly 25–100 μm), including glass, fluorinated polyethylene (FPE) and fused silica. All of them are negatively charged when in contact with electrolyte. Glass and FPE are advantageous for handling, because capillary tubes made of these materials, especially FPE, are flexible. However,

they absorb UV light strongly, and this causes problems with detection. In contrast, fused silica does not absorb in the UV region, where various organic and inorganic compounds have absorption bands. Fragility is overcome by coating polyimine resin on the surface of the tube, as in gas–liquid chromatography. For these reasons, a fused-silica tube coated with polyimine was used in this work. The high negativity of the inner wall induced rapid electroosmotic flow, which facilitated transportation of the separated components, making the analysis time short.

The composition and pH of the carrier may be varied so that the best separation is obtained for each sample. However, in this preliminary work we used 100 mM borate buffer (pH 10.5), because this carrier permitted the separation of glycosides in addition to anionic components[12].

Fig. 1 shows a typical electropherogram of the methanol extract of *Paeonia radix*. Peaks 1 and 2, appearing at 8.14 and 10.94 min, respectively, were assigned to paeoniflorin and oxypaeoniflorin, based on comparison of their migration times with those of authentic samples. Although paeoniflorin is a neutral compound, its carbohydrate moiety reacts with the borate ion in the carrier to form an anionic complex. This complex was slightly held back by electrophoresis to give a peak at 8.14 min, slightly retarded from the methanol peak (7.21 min), which was driven only by electroosmotic flow.

Oxypaeoniflorin is a derivative of paeoniflorin, having a phenolic hydroxyl
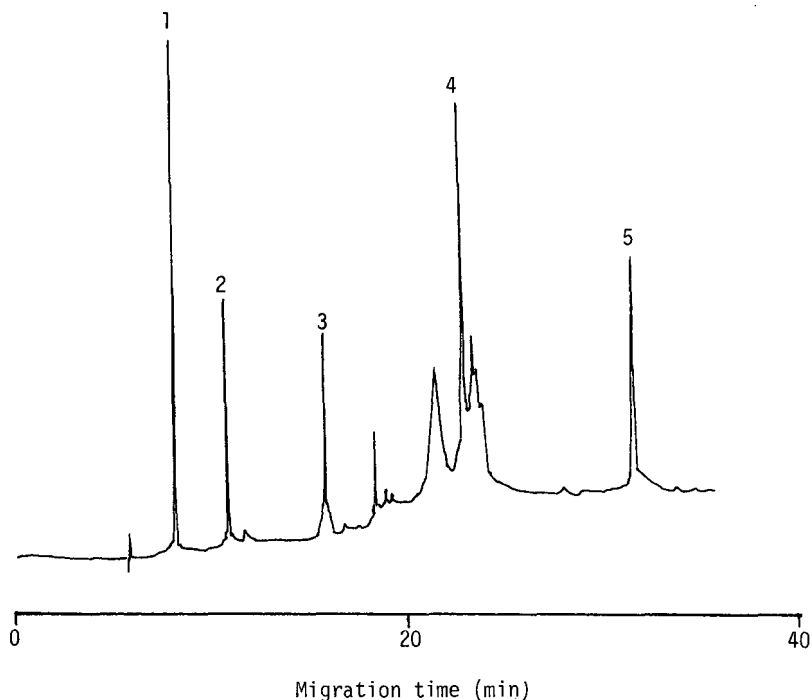
Fig. 1. Typical electropherogram of the methanol extract of *Paeonia radix*. Capillary, fused silica (80 cm × 50 μm I.D.); carrier, 100 mM borate buffer (pH 10.5); applied voltage, 20 kV; detection, UV (254 nm). Peaks: 1 = paeoniflorin; 2 = oxypaeoniflorin; 3 = methyl gallate; 4 = tannic acid; 5 = gallic acid.

group in the *para* position of the benzoyl group in paeoniflorin. Because of the dissociation of the phenolic hydroxyl group, it was more strongly held back by electrophoresis than paeoniflorin. The peaks eluting more slowly than 15 min were those of gallic acid and its derivatives. Among these peaks the fastest (peak 3, 15.57 min) was that of methyl gallate, presumably formed during the extraction process. The broadened multiple peaks in the range 20.5–24.5 min (peak 4 at the centre) were due to tannic acid analogues and the peak at 31.71 min (peak 5) was gallic acid. Analysis of tannic acids suffers from a number of problems arising from its susceptibility to air oxidation. Extensive studies of tannic acid analysis are in progress, using a number of samples from various sources apart from *Paeonia radix*, and the results will appear elsewhere.

As both paeoniflorin and oxypaeoniflorin are considered to be the effective components of this crude drug, they were quantified using 3,4-dimethoxycinnamic acid as an internal standard. For both monoterpene glycosides the plot of the peak response relative to the internal standard (IS) *versus* concentration was a straight line passing through the origin at least in the range 2–20 ng/nl, as shown in Fig. 2.

The relative standard deviations (R.S.D.) for paeoniflorin ($n = 8$) at 5 and 20 ng/nl were 2.2 and 3.0%, respectively. The R.S.D. values for oxypaeoniflorin ($n = 8$)
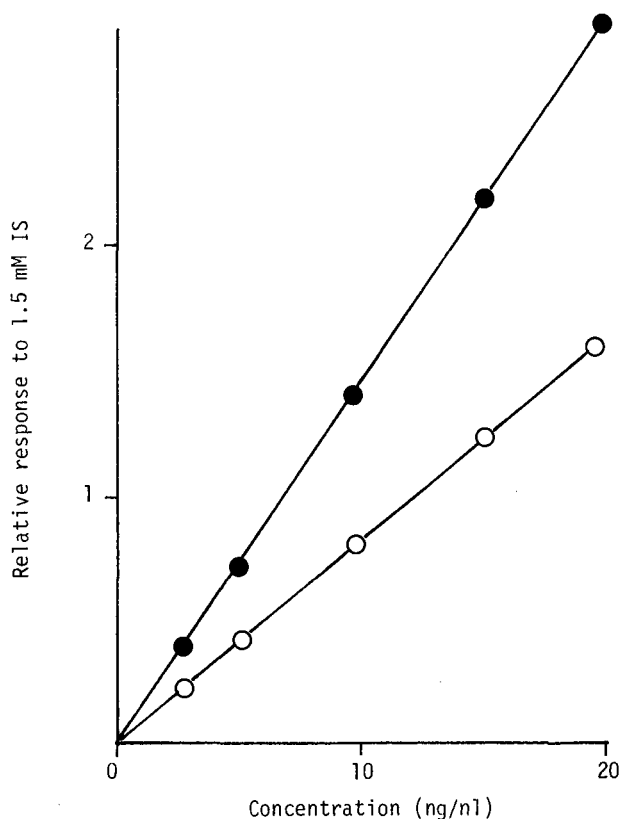
Fig. 2. Calibration graphs for (○) paeoniflorin and (●) oxypaeoniflorin.
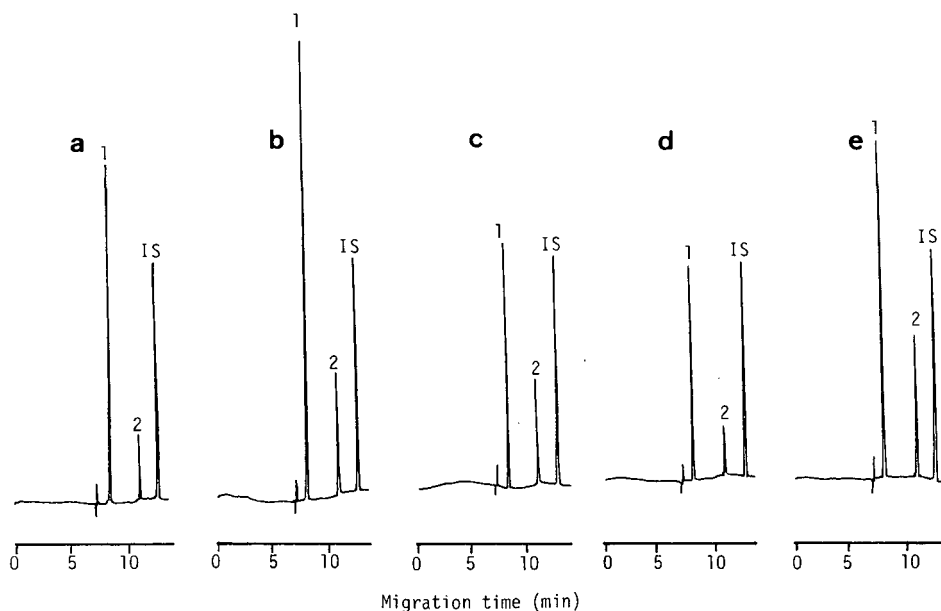
Fig. 3. Comparison of the electropherograms of the methanol extracts of *Paeonia radix* obtained from various habitats (a, Gunma; b, Nara; c, Hokkaido; d, China; e, Korea). Peaks after 15 min are omitted. The extract from each *Paeonia radix* sample (100 mg) was reconstituted with 500 μl of methanol containing 3,4-dimethoxycinnamic acid as an internal standard (IS) to a concentration of 1.5 m*M*. Analytical conditions and assignment of peaks 1 and 2 as in Fig. 1.

were higher (4.2 and 2.8%, respectively), but sufficiently low for practical analysis. The R.S.D. values of the migration times were higher (paeoniflorin 4.6%, oxypaeoniflorin 5.1%), because temperature control was not applied in this work. The use of an efficient thermostat would have made improved the reproducibility of the migration time and hence the peak response. Rinsing with an alkali solution and methanol was essential, otherwise the migration times of paeoniflorin and oxypaeoniflorin became longer on repetition of analysis, owing to the reduction in the rate of electroosmotic

TABLE I

CONTENTS OF PAEONIFLORIN AND OXYPAEONIFLORIN IN *PAEONIA RADIX* SAMPLES FROM VARIOUS HABITATS

Habitat	Content (%)	
	Paeoniflorin[a]	Oxypaeonoflorin
Gunma	3.27 (3.55)	0.16
Nara	4.32 (4.86)	0.28
Hokkaido	2.36 (2.57)	0.24
China	2.11 (2.11)	0.12
Korea	3.29 (3.61)	0.32

[a] Values in parentheses were obtained by HPLC[13].

flow by adsorption of the components on the inner wall of the capillary. By this rinsing the repeatability of analysis were ensured, the change in migration time being less than 5% even after 100 analyses.

Fig. 3 shows electropherograms for several *Paeonia radix* samples obtained from various habitats, and Table I gives the contents of paeoniflorin and oxypaeoniflorin determined by the present method.

We shall not discuss the difference in habitats as these data were obtained from only one sample for each habitat, but it should be noted that the values obtained for paeoniflorin were in good agreement with those determined by high-performance liquid chromatography (HPLC) (column, μBondapak C_{18}; eluent, acetonitrile–water–acetic acid, 15:85:1) according to the literature[13], which is considered to be the standard method.

REFERENCES

1 F. E. P. Mikkers, F. M. Everaerts and Th. P. E. M. Verheggen, *J. Chromatogr.*, 169 (1979) 11.
2 T. Tsuda, K. Nomura and G. Nakagawa, *J. Chromatogr.*, 264 (1983) 385.
3 S. Hjerten, *J. Chromatogr.*, 270 (1983) 1.
4 S. Hjerten, *J. Chromatogr.*, 347 (1985) 191.
5 M. Deml, F. Forel and P. Boček, *J. Chromatogr.*, 320 (1985) 159.
6 J. W. Jorgenson and K. D. Lukacs, *Anal. Chem.*, 53 (1981) 1298.
7 J. A. Olivares, N. T. Nguyen, C. R. Yonker and R. D. Smith, *Anal. Chem.*, 59 (1987) 1230.
8 R. A. Wallingford and A. G. Ewing, *Anal. Chem.*, 59 (1987) 1762.
9 S. Hjerten and M.-D. Zhu, *J. Chromatogr.*, 327 (1985) 157.
10 S. Fujiwara and S. Honda, *Anal. Chem.*, 58 (1986) 1811.
11 H. H. Lauer and D. McManigill, *Anal. Chem.*, 58 (1986) 166.
12 S. Honda, S. Iwase, A. Makino and S. Fujiwara, *Anal. Biochem.*, 176 (1989) 72.
13 N. Asakawa, T. Hattori, M. Ueyama, A. Shinoda and Y. Miyake, *Yakugaku Zasshi*, 99 (1979) 598.

CHROMSYMP. 1746

Apparatus for coupled high-performance liquid chromatography and capillary electrophoresis in the analysis of complex protein mixtures

HIDEKO YAMAMOTO*, TAKASHI MANABE and TSUNEO OKUYAMA

Department of Chemistry, Faculty of Science, Tokyo Metropolitan University, 1-1 Fukazawa, Setagaya-ku, Tokyo 158 (Japan)

ABSTRACT

Apparatus for coupled high-performance gel permeation chromatography (HPLC) and capillary electrophoresis was constructed and applied to the analysis of complex protein mixtures. To avoid electric leakage to the HPLC system, an electromagnetic pinch valve was inserted in the line from the column outlet to the injection port of the capillary electrophoresis apparatus. All the procedures for chromatography and electrophoresis were automated with the aid of a system controller. The apparatus was successfully used for the automatic two-step separation of human serum proteins and water-soluble proteins in bovine brain. Proteins separated by gel permeation HPLC were further analysed by capillary electrophoresis according to their characteristic electrophoretic mobilities.

INTRODUCTION

The techniques of high-performance liquid chromatography (HPLC) and electrophoresis are widely used for the analysis of proteins. However, the resolution of each technique is low with respect to the number of protein species present in tissues or cells. In order to improve the resolution, instruments have been developed that combine two techniques having different separation principles. For example, gel permeation HPLC and reversed-phase HPLC were coupled for the analysis of glycosides in plant extracts[1], ion-exchange HPLC and reversed-phase HPLC for the analysis of polypeptides[2] and reversed-phase HPLC and sodium dodecyl sulphate polyacrylamide gel electrophoreis for the analysis of water-soluble proteins in *E. coli*[3]. Two-dimensional polyacrylamide gel electrophoresis, which offers the highest resolution of proteins at present, is a combination of gel isoelectric focusing and pore-gradient gel electrophoresis[4].

In a preceding paper, we reported on the construction of an apparatus combining low-pressure gel permeation chromatography (GPC) with capillary

electrophoresis for the analysis of proteins with high sensitivity and simple operation[5]. The apparatus was used for the automatic two-step separation of purified proteins. Proteins were separated according to their molecular size in the first step, then separated according to their electrophoretic mobility in the second step.

To improve the resolution of proteins in the GPC step, we have now employed an HPLC system instead of the low-pressure chromatographic system. This apparatus was applied to the analysis of human serum proteins and water-soluble proteins in bovine brain.

EXPERIMENTAL

Apparatus

A schematic diagram of our apparatus is shown in Fig. 1. The HPLC system was
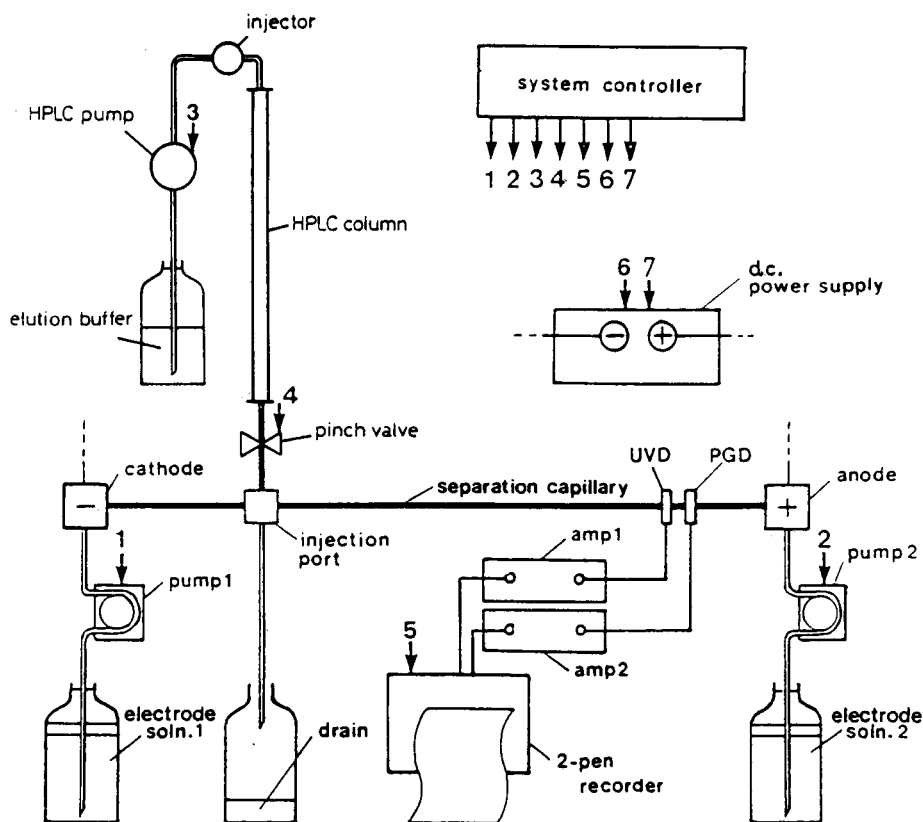
Fig. 1. Apparatus combining HPLC and capillary electrophoresis. The terminating electrolyte (solution 1) and leading electrolyte (solution 2) are pumped by peristaltic pumps (pumps 1 and 2) to wash the electrodes and separation capillary. Elution buffer for GPC is pumped through the HPLC column by a high-pressure pump (HPLC pump) and the effluent from the column is loaded through the injection port. An electromagnetic pinch valve is closed to avoid electric leakage to the HPLC system and then a d.c. high voltage is applied between the electrodes. Protein zones are detected with UV and potential gradient detectors (UVD and PGD) during the analysis. The numbered arrows indicate the output lines connecting the system controller to the equipment.

combined with a capillary electrophoresis apparatus. The HPLC system consisted of a glass column (500 mm × 4.0 mm I.D.), packed with the gel permeation packing Asahipak GS-520 (polyvinyl alcohol-type gel, particle diameter 9 μm, exclusion limit for pullulan 300 000) (Asahi Chemical Industry, Kawasaki, Japan), a Model NP-DX-8 high-pressure pump (Nihon Seimitsu Kagaku, Tokyo, Japan) and a Model KLS-3T line sample injector (Kyowa Seimitsu, Tokyo, Japan).

In order to avoid electric leakage, the outlet of the HPLC column was connected to the sample injection port of the capillary electrophoresis apparatus in the following manner. A perfluorinate ethylene–propylene (PFEP) copolymer tube (50 mm × 0.25 mm I.D.) from the column outlet was connected to a silicone-rubber tube (10 mm × 0.5 mm I.D. × 2.3 mm O.D.), equipped with a Model PM-02 electromagnetic pinch valve (Takasago Electric, Tokyo, Japan) in the middle. The other end of the silicone-rubber tube was connected to a PFEP tube (50 mm × 0.25 mm I.D.). A glass capillary tube (50 mm × 0.24 mm I.D. × 0.35 mm O.D.) was connected to the end of the PFEP tube and the other end was introduced into the injection port through a septum. The column effluent was introduced into the separation capillary through the port and the excess effluent was drained off. A constant volume (*ca.* 5 μl) of the effluent was retained in the separation capillary and was subjected to electrophoresis. The part of the apparatus for capillary electrophoresis is basically the same as that reported previously[5,6].

System controller

For the automatic operation of the apparatus, all the components (the HPLC pump, the electromagnetic pinch valve, peristaltic pumps, a recorder and a high-voltage d.c. power supply) were controlled by a system controller. Construction details have been described fully elsewhere[6].

Computer programs and time schedule for automated operation

After equilibration and sampling, the cycle of HPLC elution and electrophoresis of the effluent was repeated automatically. The microcomputer programs for the automatic operation were written in BASIC. The time schedule of the program is as follows: (1) pump the leading electrolyte solution to rinse the anode and the separation capillary (2 ml in 2 min); (2) pump the termination electrolyte solution to rinse the cathode (0.7 ml in 3 min); (3) open the electromagnetic pinch valve; (4) pump the chromatographic elution buffer into the column to introduce the column effluent into the injection port (70 μl in 30 s); (5) close the pinch valve; (6) turn on the d.c. power supply to start electrophoresis (150 μA constant current); (7) turn on the two-pen recorder and reduce the current to 50 μA; (8) turn off the d.c power supply and the recorder. These procedures are repeated from step 1. The time needed for one cycle of analysis is 23 min.

Preparation of protein samples

Sera from normal human adults were freshly obtained and stored at −20°C. Soluble proteins from bovine brain were prepared in basically the same way as described previously[7]: fresh bovine brain tissue was washed thoroughly with distilled, deionized water to remove clotted blood, then combined with an equal weight of distilled deionized water and homogenized with a Potter–Elvehjem homogenizer in an

ice-bath. The homogenate was centrifuged at 35 000 g for 1 h and the supernatant was stored at $-20°C$.

Reagents

The following reagents were used for the preparation of the electrode solutions without further purification: 2-Amino-2-methyl-1-propanol (Nakarai Chemicals, Kyoto, Japan), tranexamic acid (Daiici Seiyaku, Tokyo, Japan), hydrochloric acid (1 M, special grade for amino acid sequence analysis), potassium hydroxide and hexane (Wako, Osaka, Japan), hydroxypropylmethylcellulose (HPMC) (Aldrich, Milwaukee, WI, U.S.A.), sodium azide (Kanto Pure Chemical, Tokyo, Japan) and ampholyte mixture (Ampholine, pH 3.5–10) (Pharmacia–LKB, Uppsala, Sweden).

Conditions for gel permeation HPLC and capillary electrophoresis

Protein samples (200–600 μg of protein in 30 μl) were applied to the HPLC column. The elution buffer was 0.25% Ampholine (pH 3.5–10)–0.00625% sodium azide. The conditions for capillary electrophoresis were as follows. The leading electrolyte solution was 5 mM HCl–9.3 mM 2-amino-2-methyl-1-propanol (pH 9.9) and the terminating electrolyte solution was 50 mM tranexamic acid–potassium hydroxide (pH 10.8). The solutions were kept in amber-glass bottles and overlayed with a 1-cm layer of hexane to minimize the dissolution of carbon dioxide. A PFEP capillary tube (230 mm × 0.5 mm I.D. × 1.0 mm O.D.), the inner surface of which had been coated with HPMC, was used as the separation tube. Electrophoresis was performed at a constant current of 150 μA for 4.8 min (initial voltage $ca.$ 6 kV) and then at a constant current of 50 μA for about 12 min.

RESULTS AND DISCUSSION

Combination of HPLC system with capillary electrophoresis apparatus

In the preceding study[5] we used an open column packed with Sephadex G-50 and a micro-peristaltic pump for GPC. To improve the resolution of proteins by GPC, we experimented with connecting the HPLC system to the electrophoresis apparatus. When the outlet line (PFEP tubing) of the HPLC column was directly connected to the injection port, malfunction of the computer frequently occurred during electrophoresis and the automatic operation was interrupted. These effects were found to be due to the electric discharge of the high-voltage d.c. through the metallic parts of the HPLC system (the stainless-steel tubing, high-pressure pump and injector). In order to avoid electric leakage, an electromagnetic pinch valve was installed between the column outlet and the injection port, as described under Experimental. The time schedule for automatic operation was reprogrammed so that the pinch valve was closed during electrophoresis. With the aid of these devices, the two-step separation could be performed automatically.

Gel permeation HPLC of human serum proteins

Before the two-step separation, gel permeation HPLC was performed separately. Fig. 2 shows the elution profile of a human serum sample. Human serum (10 μl) was diluted 5-fold with the chromatographic elution buffer (40 μl) and a 30-μl portion was applied to the column and eluted at a flow-rate of 140 μl/min. As Fig. 2 shows, the
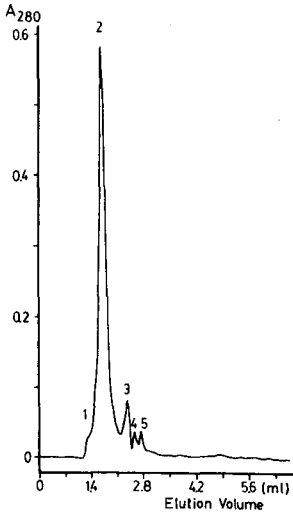
Fig. 2. Elution profile of human serum obtained by gel permeation HPLC. Human serum, diluted 5-fold (30 μl), was applied to the glass column (500 mm × 4 mm I.D.) and eluted with the elution buffer (0.25% Ampholine–0.00625% sodium azide) at a flow-rate of 140 μl/min.
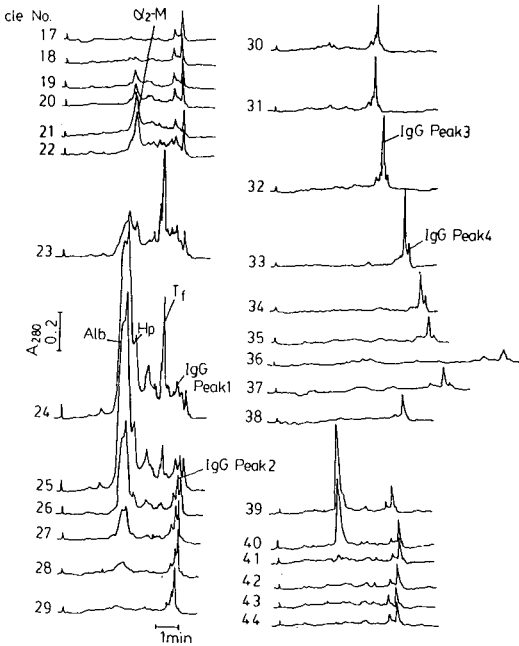
Fig. 3. Separation of serum proteins and other constituents with the combined apparatus. A serum sample solution (30 μl) was applied and the UV patterns of the electropherograms were traced. Serum proteins eluted from the gel permeation HPLC column were further separated with their characteristic electrophoretic mobility. α_2-M = α_2-Macroglobulin; Hp = haptoglobin (type 1-1); Tf = transferrin; Alb = albumin; IgG peak 1, etc. = separated peaks of IgG.

UV-absorbing constituents of human serum were separated into four peaks and one shoulder.

Gel permeation HPLC capillary electrophoresis of serum proteins

The serum sample solution (30 μl) was applied to the column. The column volume was 6.28 ml (500 mm × 4 mm I.D.), the line dead volume from the HPLC column outlet to the injection port was calculated to be 9 μl and the volume of the effluent pumped in one cycle was tentatively set at 70 μl. Then, the cycle of analysis described under Experimental was repeated 90 times without manual intervention.

Of the 90 electropherograms obtained, those from the 1st to the 17th cycle and from the 44th to the 90th cycle were fairly reproducible, showing the UV pattern of Ampholine. The UV- absorbing constituents in human serum appeared from the 18th to the 43th cycles, as shown in Fig. 3. From the elution volumes, the shoulder numbered 1 in Fig. 2 corresponded to cycles 18–20, peak 2 to cycles 21–30, peak 3 to cycles 31–34, peak 4 to cycles 35–38 and peak 5 to cycles 39–43.

Some of the UV peaks in the patterns were identified by analysing either purified serum proteins or the effluent from the HPLC column by micro two-dimensional gel
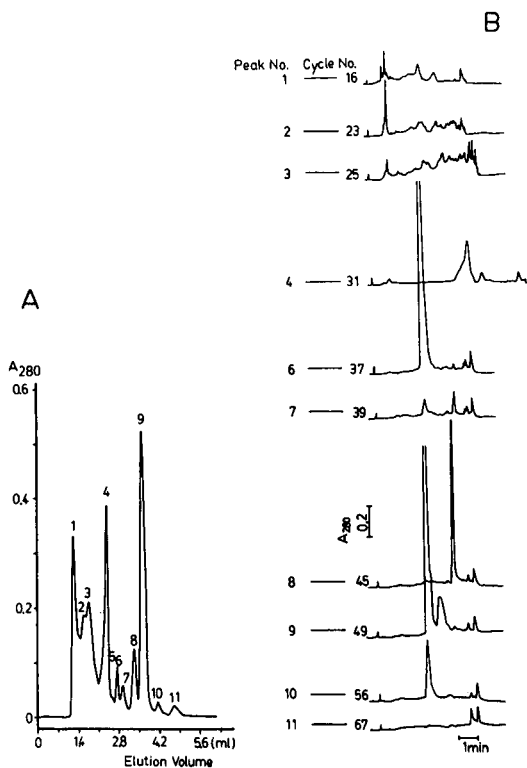
Fig. 4. Examples of the electropherograms obtained with the combined apparatus for a soluble brain fraction. Soluble fraction of bovine brain (30 μl) was applied to the combined apparatus. The electropherograms (UV patterns) corresponding to the UV peak positions of gel permeation HPLC (shown in A) are shown in B.

electrophoresis[8]. The peaks of α_2-macroglobulin (molecular weight estimated by pore-gradient fel electrophoresis, *ca.* 500 000), haptoglobin 1-1 (100 000), transferrin (90 000), albumin (69 000) and immunoglobulin G (IgG) (150 000) were identified as indicated in Fig. 3. The serum proteins were eluted from the HPLC column according to their molecular weight, except IgG, which seemed to be retarded by ionic interaction with the column material. IgG appeared as four peaks in the electropherograms and the peak ratio changed as shown in Fig. 3.

Each identified protein appeared in four or five cycles, corresponding to an effluent volume of *ca.* 300 μl. The plate number of the HPLC column under the conditions employed was calculated to be about 600–1000.

The UV peak appearing in cycles 39–40 (Fig. 3), which corresponded to peak 5 in Fig. 2, was identified as being due to uric acid. The component corresponding to peak 4 in Fig. 2 was not detected in the electropherograms, suggesting that it did not migrate to the anode under the electrophoretic conditions. The potential gradient curves (not shown in Fig. 3) around cycles 33–37 showed much smaller slopes than the others, suggesting the presence of ions with no UV absorbance. These results showed that low-molecular-weight substances appeared after cycle 33 (elution volume *ca.* 2.3 ml).

Analysis of soluble brain proteins

Soluble proteins in bovine brain (280 μg in 30 μl) were injected into the apparatus. The conditions were the same as those for the analysis of human serum proteins. Some of the electropherograms, which corresponded to the UV peak positions in gel permeation HPLC (Fig. 4A), are shown in Fig. 4B. From the elution volumes, peaks 1–4 in Fig. 4A seem to be due to proteins and peaks 5–11
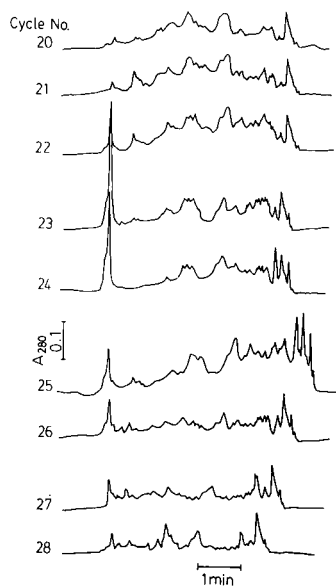
Fig. 5. Examples of sequential electropherograms (UV patterns) representing protein fractions. Electropherograms corresponding to peaks 2 and 3 in Fig. 4A were traced. In each electropherogram, 20–30 peaks or shoulders were observed.

low-molecular-weight substances. The simple UV absorption patterns of the electropherograms also suggested the absence of proteins after *ca.* cycle 37 (elution volume 2.6 ml).

Some of the sequential electropherograms (cycles 20–28), corresponding to parts of peaks 2 and 3 in Fig. 4A, are shown in Fig. 5. In each electropherogram, about 20–30 peaks or shoulders of proteins were observed.

The resolution of proteins with the combined system is determined by the resolution in each separation step. As shown in Figs. 3, 4B and 5, 20–30 protein peaks can be resolved in the capillary electrophoresis step. The HPLC packing used improved the resolution in the gel permeation chromatographic step, but still only a few protein peaks could be obtained. As improvements in the resolution of proteins in gel permeation HPLC may be restricted by the low diffusion constants of proteins and by the upper limit of the capacity factors, an HPLC system based on other separation principles (*e.g.*, reversed-phase HPLC) should also be examined for the high-resolution analysis of proteins.

REFERENCES

1 F. Erni and R. W. Frei, *J. Chromatogr.*, 149 (1978) 410.
2 N. Takahashi, Y. Takahashi and F. W. Putnam, *J. Chromatogr.*, 266 (1983) 511.
3 K. D. Nugent, W. G. Burton, T. K. Slattery, B. F. Johnson and L. R. Snyder, *J. Chromatogr.*, 443 (1988) 381.
4 P. O'Farrell, *J. Biol. Chem.*, 250 (1975) 4007.
5 H. Yamamoto, T. Manabe and T. Okuyama, *J. Chromatogr.*, 480 (1989) 277.
6 T. Manabe, H. Yamamoto and T. Okuyama, *Electrophoresis*, 10 (1989) 172.
7 T. Manabe, S. Jitzukawa, N. Ishioka, T. Isobe and T. Okuyama, *J. Biochem.*, 91 (1982) 1009.
8 T. Manabe, Y. Takahashi, N. Higuchi and T. Okuyama, *Electrophoresis*, 6 (1985) 462.

CHROMSYMP. 1855

Effect of polymer ion concentrations on migration velocities in ion-exchange electrokinetic chromatography

SHIGERU TERABE[*,a] and TSUGUHIDE ISEMURA

Department of Industrial Chemistry, Faculty of Engineering, Kyoto University, Sakyo-ku, Kyoto 606 (Japan)

ABSTRACT

Ion-exchange electrokinetic chromatography was developed for the separation of analyte ions having identical electrophoretic mobilities in capillary electrophoresis. The separation principle is based on the differential ion-pair formation of the analyte ion with a polymer ion. Polybrene and poly(diallyldimethylammonium chloride) were employed as polymer ions and some isomeric acids as analytes. The dependence of the relative migration velocities of the analytes on the concentration of the polymer ions was studied experimentally, and the results are discussed in comparison with a theoretically derived equation.

INTRODUCTION

Electrokinetic chromatography (EKC)[1] is an electrophoretic separation technique based on the separation principle of chromatography. Micellar EKC[2,3] has been developed for the separation of electrically neutral analytes by electrophoresis with an ionic micellar solution as a separation solution. The ionic micelle, which corresponds to the stationary phase in conventional liquid chromatography, incorporates the analyte and migrates with a different velocity from that of the surrounding aqueous medium by electrophoresis. Accordingly, differential partition and differential migration constitute the separation principle of EKC, similar to that of chromatography. All of the advantages of high-performance capillary electrophoresis (HPCE)[4,5] can also be realized for EKC, and plate numbers more than 100 000 are easily obtained[6].

Micellar EKC has become a popular technique in HPCE. Although it is also called micellar electrokinetic capillary chromatography (MECC)[7], EKC techniques other than micellar are available. For example, in cyclodextrin EKC[1,8], cyclodextrin derivatives having ionizable groups are employed instead of a micelle. As inclusion-complex formation is the partition mechanism in cyclodextrin EKC, isomeric aromatic

---

[a] Present address: Department of Material Science, Himeji Institute of Technology, 2167 Shosha, Himeji, Hyogo 671-22, Japan.

compounds and many chiral compounds have been successfully separated. It is noteworthy that ordinary cyclodextrins can modify the electrophoretic mobility of ionic analytes[9], but electrically neutral cyclodextrins themselves do not separate electrically neutral analytes.

HPCE has been proved to be a highly efficient separation method[4,5] and it is still a subject to extensive studies from the viewpoints of instrumentation and separation techniques. A disadvantage of HPCE is that it can separate only charged substances, but this has been overcome by the development of EKC. As the separation principle of HPCE is based on differences in electrophoretic mobilities, it is not effective for the separation of analytes having very similar or identical mobilities. This is often the case with isotopic ions or isomeric ions, such as positional isomers of aromatic compounds. Oxygen isotopic benzoic acids have been successfully resolved by optimizing the experimental conditions, in particular by carefully adjusting the pH of the separation buffer to the calculated optimum value[10]. The choice of pH is thus very important in separate analytes having very similar dissociation constants.

In order to increase its selectivity for isomeric ions, we have developed ion-exchange EKC, in which the separation mechanism is based on differential ion-pair formation of analyte ions with a polymer ion added to the separation solution[1,11]. A successful application of the technique was recently demonstrated with the separation of five isomeric naphthalenedisulphonates, which could not be resolved by HPCE alone[11].

In ion-exchange EKC, a polymer ion having a charge opposite to that of the analyte ion is employed as a modifier of the electrophoretic mobility. Both the analyte and the polymer ions are subject to electrophoresis, but the migration directions differ. Accordingly, an analyte ion bonded to the polymer ion through ion-pair formation migrates in the opposite direction of the free analyte ion, as shown in Fig. 1. It is consequently possible that even analytes having identical electrophoretic mobilities will migrate with different velocities if their ion-pair formation constants are different. The separation principle is based on differences in ion-pair formation constants, but
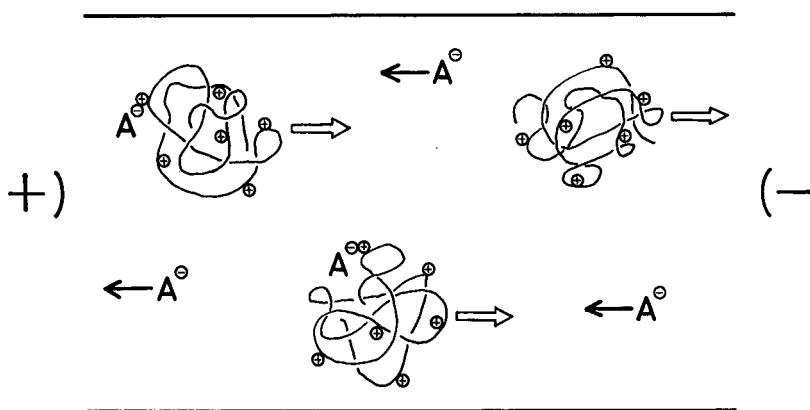
Fig. 1. Schematic diagram of the separation principle of ion-exchange EKC, where polymer cations are used. A^- = analyte ion; open and filled arrows = electrophoretic migration of the polymer ion and that of the analyte ion, respectively.

not on those in electrophoretic mobilities; therefore, the technique should be classified as a chromatographic method.

In this study, two different polymer cations, polybrene and poly(diallyldimethyl-ammonium chloride) (PDDAC), were employed. The effect of the concentration of PDDAC on the relative migration velocities of various analytes was investigated mainly from the viewpoint of selectivity. The experimental data are explained according to a theoretically derived equation.

EXPERIMENTAL

Apparatus and procedures

HPCE equipment similar to that described previously[2,10] was employed. Fused-silica tubing of 50 μm I.D. (Polymicro Technologies, Phoenix, AZ, U.S.A., or Scientific Glass Engineering, Ringwood, Victoria, Australia) was used as separation capillaries. The HPCE instrument consisted of a regulated high-voltage d.c. power supply (LG-40R-3.5, Glassman, Whitehouse Station, NJ, U.S.A.), which delivered up to 40 kV, a variable-wavelength UV detector for high-performance liquid chromato-graphy (HPLC) (Uvidec-100-V, Jasco, Tokyo, Japan), the cell holder of which was modified to accommodate the 50-μm I.D. fused-silica capillary for on-column detection, and a data processor (C-R3A Chromatopac, Shimadzu, Kyoto, Japan). A sample solution was introduced manually into one end of the capillary by the hydrostatic or siphoning method, as described previously[2]. HPCE experiments were performed at ambient temperature (*ca.* 25°C).

Reagents

The two polymer cations employed were commercial products: polybrene (Aldrich, Milwaukee, WI, U.S.A.) and PDDAC as a solution of 15% solid in water (Polyscience, Warrington, PA, U.S.A.) (Fig. 2). Disodium 1,6- and 1,7-napthalene-disulphonates were gifts from Sumitomo (Osaka, Japan). All other reagents were of analytical-reagent grade and purchased from Wako (Osaka, Japan). All the reagents were used as received. Water was purified with a Milli-Q system (Nihon Millipore, Tokyo, Japan).

RESULTS

As the electroosmotic velocity was significantly dependent on the experimental conditions, especially on the concentration of polymer cations, relative velocities were
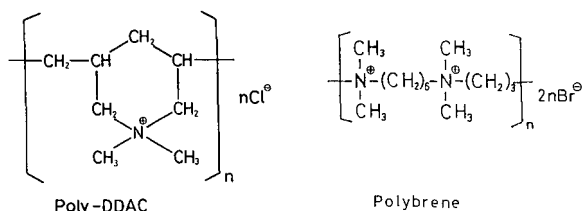
Fig. 2. Molecular structures of PDDAC and polybrene.
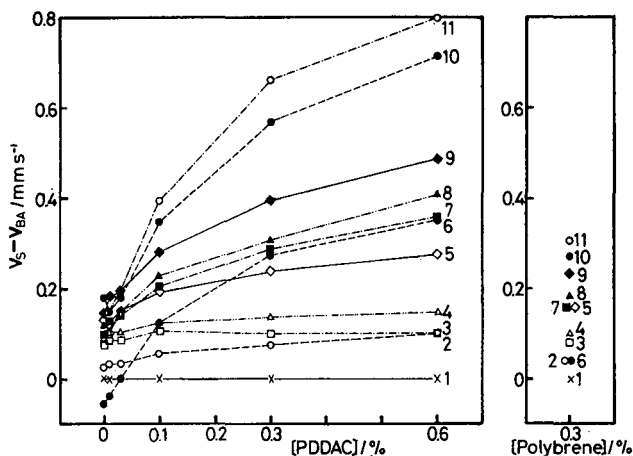
Fig. 3. Dependence of relative migration velocities of monobasic acids on the concentration of PDDAC.
1 = benzoic acid (BA, the standard solute of the migration velocity); 2 = o-; 3 = m-; 4 = p-aminobenzoic
acids; 5 = 1-naphthoic acid; 6 = o-; 7 = m-; 8 = p-hydroxybenzoic acids; 9 = 2-naphthoic acid; 10 = 2-;
11 = 1-naphthalenesulphonic acids. The relative velocities in a 0.3% polybrene solution are also shown.
Capillary, 750 mm × 50 μm I.D., 500 mm to the detector; buffer solution, 50 mM phosphate buffer (pH 7.0);
applied voltage, 20 kV. See text regarding the ordinate.

employed to evaluate the effect of the polymer cations. The variable electroosmotic
velocity was probably due to the change in the surface condition of the capillary wall,
depending on the polymer concentration. The adsorption of the polymer cation on the
negatively charged wall must have changed its zeta potential substantially. The
electroosmotic flow was actually positive or toward the negative electrode in the
absence of the polymer cation, but toward the positive electrode in its presence. We
shall take the velocity to be positive when it is toward the negative electrode.

Benzoic acid was chosen as the standard solute for the migration velocity and
was added to every sample solution. The difference between the migration velocity of
the solute, v_s, and that of benzoic acid, v_{ba}, was measured at different concentrations of
PDDAC, and the results are shown in Fig. 3 for monoanionic and in Fig. 4 for
dianionic solutes. The differential velocity data in the absence of PDDAC and in the
presence of 0.3% polybrene are also given.

The electroosmotic velocity was $ca.$ 0.7 mm s^{-1} in the absence of the polymer
ions, $ca.$ −2.0 mm s^{-1} in 0.01–0.03% PDDAC solutions and $ca.$ −1.7 mm s^{-1} in
a 0.3% polybrene solution. The use of the differential velocity, $v_s - v_{ba}$, eliminates the
effect of the electroosmotic velocity, and hence indicates the effect of just the polymer
addition on the apparent electrophoretic velocity.

Benzoic acid had the highest electrophoretic mobility among the monobasic
acids in this study, except for o-hydroxybenzoic acid, either in the absence or in the
presence of the polymer cation. It is noteworthy that the electrophoretic velocities of
these solutes and their electrophoretic mobilities were all negative, but we shall
consider only the magnitude of these values. The difference in velocities increased with
increase in PDDAC concentration, in particular the naphthalene derivatives showed
significant dependences. The increase in differential velocities suggests that the
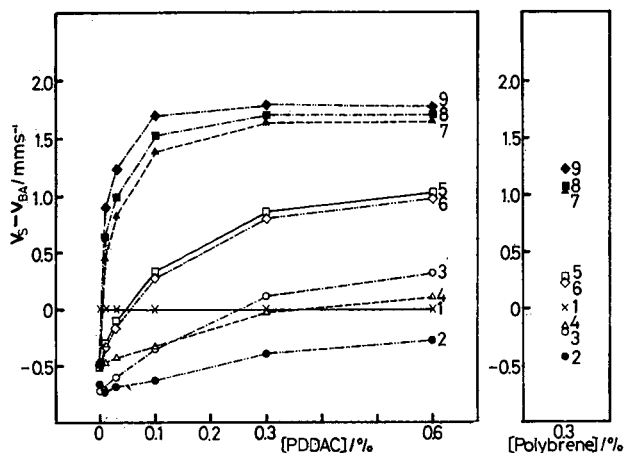
Fig. 4. Dependence of relative velocities of dibasic acids on the concentration of PDDAC. 1 = benzoic acid; 2 = maleic acid; 3 = fumaric acid; 4 = phthalic acid; 5 = isophthalic acid; 6 = terephthalic acid; 7 = 2,6-; 8 = 2,7-; 9 = 1,5-naphthalenedisulphonic acids. Other conditions as in Fig. 3.

naphthalene derivatives, *e.g.*, 1- and 2-naphthalenesulphonate ions, form ion pairs with PDDAC more strongly than benzoic acid. All the solutes employed are considered to be fully ionized at the experimental pH of 7.0. The abnormal behaviour of *o*-hydroxybenzoic acid will be discussed later.

All the dibasic acids employed had electrophoretic mobilities higher than that of benzoic acid in the absence of the polymer cations. This is obvious, because the divalent acids will have charges higher than monobasic benzoic acid at pH 7.0.
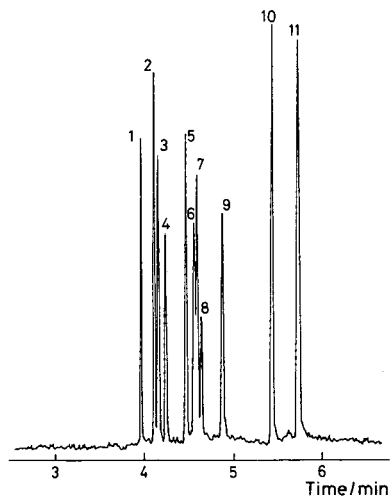
Fig. 5. Ion-exchange electrokinetic chromatogram of monobasic acids. Peak numbers as in Fig. 3. Separation solution, 0.3% PDDAC in 50 mM phosphate buffer (pH 7.0); current, 49 μA. Other conditions as in Fig. 3.

However, in the presence of PDDAC, the electrophoretic mobilities decreased rapidly with increase in the PDDAC concentration, and eventually led to lower values than that of benzoic acid, except for maleic acid. It should be noted that the scales of the ordinates are different between Figs. 3 and 4. In particular, the velocities of the naphthalenedisulphonates were most susceptible to the polymer cation addition.

When a 0.3% polybrene solution was used, the results agreed fairly well with those expected at 0.06% PDDAC, as shown in Figs. 3 and 4. Although the concentration effects of PDDAC and polybrene were not identical, the fact that the relative magnitudes of solute velocities were almost the same between 0.06% PDDAC and 0.3% polybrene strongly suggests that PDDAC and polybrene have very similar selectivity in ion-pair formation.

An ion-exchange electrokinetic chromatogram of the mixture of eleven mono-basic acids employed in Fig. 3 is shown in Fig. 5, which was obtained with a 0.3% PDDAC solution. Although most of the analytes were also separated well in the absence of PDDAC, as judged from Fig. 3, the use of the polymer cations gave better separations. For example, 1- and 2-naphthalenesulphonates could not be resolved by conventional HPCE, but they were easily separated by use of PDDAC, as shown in Fig. 5. The plate numbers of the peaks were about 250 000. Fig. 6 shows an electropherogram of the mixture of nine dibasic acids employed in Fig. 4. As expected from Fig. 4, the resolution of three naphthalenedisulphonates was unsuccessful. Fig. 7 shows an ion-exchange electrokinetic chromatogram of the same mixture of dibasic acids as in Fig. 6. All the solutes were successfully separated with the addition of 0.01% PDDAC, although the peaks of the three naphthalenedisulphonates were broad and tailed. The successful separation of five isomeric naphthalenedisulphonates, including the three isomers shown in Fig. 7, with a 2% diethylaminoethyldextran was illustrated elsewhere[11]. Although no chromatogram is shown, the use of polybrene instead of PDDAC resulted in chromatograms very similar to those in Figs. 5 and 7.
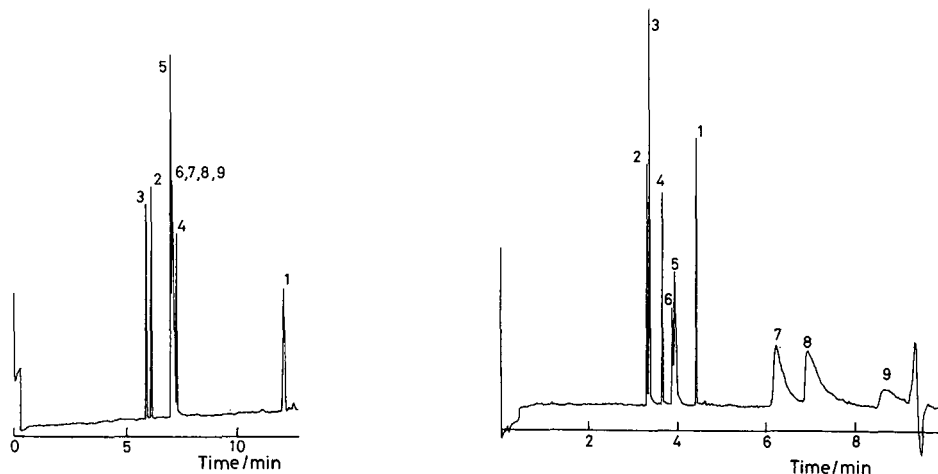
Fig. 6. Capillary electropherogram of dibasic acids. Peak numbers as in Fig. 4. Current, 39 μA; other conditions as in Fig. 3, except for the PDDAC concentration, which was zero in this run.

Fig. 7. Ion-exchange electrokinetic chromatogram of dibasic acids. Peak numbers as in Fig. 4. Separation solution, 0.01% PDDAC in 50 mM phosphate buffer (pH 7.0); current, 49 μA. Other conditions as in Fig. 3.

DISCUSSION

If two ionic solutes have identical electrophoretic mobilities and the polymer ion has the opposite charge to the solutes, the differences in migration velocities, Δv, between the two solutes, 1 and 2, in the presence of the polymer ion is derived as[11]

$$\Delta v = \frac{(K_{ip2} - K_{ip1})[\text{pi}]_0[v_{ep}(\text{free}) - v_{ep}(\text{pi})]}{(1 + K_{ip1}[\text{pi}]_0)(1 + K_{ip2}[\text{pi}]_0)} \tag{1}$$

where $[\text{pi}]_0$ is the total concentration of the polymer ion in the separation solution, $v_{ep}(\text{free})$ and $v_{ep}(\text{pi})$ are the electrophoretic velocities of the solute free from the polymer ion and that of the polymer ion, respectively, and K_{ip1} and K_{ip2} are the ion-pair formation constants of the solutes 1 and 2, as shown in the following equilibrium equation:

$$\text{s} + \text{pi} \rightleftharpoons \text{s} \cdot \text{pi} \tag{2}$$

$$K_{ip} = [\text{s} \cdot \text{pi}]/[\text{s}][\text{pi}] \tag{3}$$

where s and pi are the solute and polymer ion, respectively. In the derivation of eqn. 1, the electrophoretic velocity of the ion pair is assumed to be equal to that of the polymer ion, or the electrophoretic velocity is independent of ion-pair formation; [pi] in eqn. 3 is presumed to be equal to $[\text{pi}]_0$, because [s · pi] may be negligibly low compared with [pi]. Although the polymer ions are considered to have wide distributions of molecular weights, if the equilibrium given in eqn. 2 is rapid in comparison with the migration velocities, the molecular weight distribution may not affect the migration velocities of the solutes.

Eqn. 1 describes the dependence of the differential velocity on the polymer concentration when the solutes have identical electrophoretic velocities in the absence of the polymer ion. Accordingly, some pairs of solutes in Figs. 3 and 4 that are suitable for the evaluation of eqn. 1 are selected and their data are replotted in Fig. 8. Here, Δv for each pair of solutes is zero or close to zero when the polymer ion concentration is zero. Not all the electrophoretic velocities were identical among the solutes shown in Fig. 8, even in the absence of the polymer ion, but the electrophoretic velocities of each pair were identical or nearly equal under such conditions.

The relationship between Δv and $[\text{pi}]_0$ does not seem straightforward and, therefore, in order to simplify eqn. 1 we shall assume that K_{ip1} and K_{ip2} are close to each other. Then, we shall discuss the function of P, which is a $[\text{pi}]_0$-related part extracted from eqn. 1:

$$f(P) = P/(1 + KP)^2 \tag{4}$$

where P means $[\text{pi}]_0$ and K is assumed to be equal to K_{ip1} and K_{ip2} only in the denominator. The dependence of $f(P)$ on P is shown in Fig. 9, where the maximum value of $f(P)$ is obtained at $P = K^{-1}$. The value of $f(P)$ increases from zero to $0.25\,K$ with increase in P from zero to K^{-1}, and then decreases asymptotically to zero with a further increase in P more than K^{-1}.
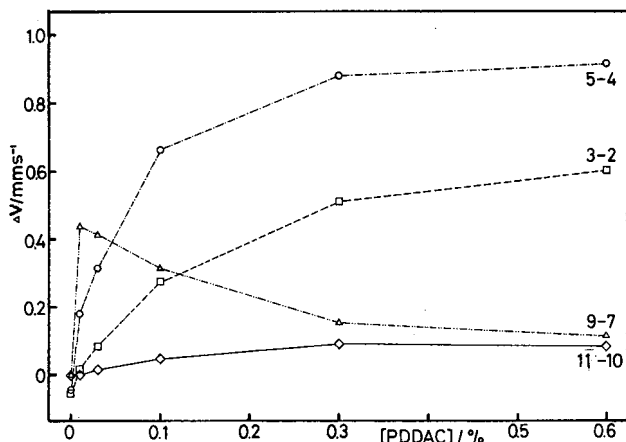
Fig. 8. Dependence of differential velocities between two solutes having identical or very close electrophoretic velocities on the concentration of PDDAC. Each curve was obtained by plotting the differential velocity between the pair of solutes shown on each curve. The numbers are the same as in Fig. 4, except for 10 and 11, which appear in Fig. 3.

The plot denoted 11–10 in Fig. 8 is for 1- and 2-naphthalenesulphonates, and it has the maximum value of Δv at 0.3% PDDAC, although the exact concentration of PDDAC that gives this is not known. If we assume that 0.3% PDDAC gives the maximum Δv, K_{ip} is easily calculated to be 54 l mol^{-1} according to eqn. 4, where [PDDAC] is transformed to the molar concentration of the quaternary ammonium ion in PDDAC. In order to obtain precise K_{ip} values, we have to determine the most appropriate values for K_{ip1} and K_{ip2} that agree best with the observed data of Δv for the pair of solutes.

The maximum value of Δv appears at 0.01% PDDAC fo the pair of 1,5- and 2,6-naphthalenedisulphonates (9–7 in Fig. 8), and this will mean that K_{ip} is much larger
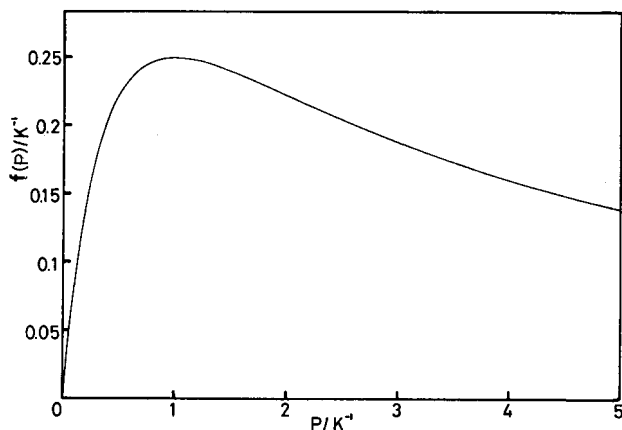
Fig. 9. Dependence of the function f(P) given in eqn. 4 on P.

than that of the naphthalenesulphonates. In the case of the other two pairs denoted 3–2 and 5–4 in Fig. 8, the maximum values of Δv are not realized at concentrations of PDDAC lower than 0.6%. This suggests that the values of K_{ip} for these compounds are smaller than those of the naphthalenesulphonates and that is consistent with the data shown in Fig. 4. However, it should be mentioned that eqn. 4 assumes that $K_{ip1} = K_{ip2}$ in deriving eqn. 1, but the Δv values shown in Fig. 8 seem too large to assume $K_{ip1} = K_{ip2}$ for these pairs of compounds.

Hydrophobic interaction seems to enhance ion-pair formation, because the naphthalenesulphonic and naphthoic acids formed stronger ion pairs than the benzoic acid derivatives, as shown in Fig. 3; this tendency was also observed for the divalent acids in Fig. 4. The sulphonate group may tend to form ion pairs with the quaternary ammonium group more readily than the carboxyl group, as judged by the differences between naphthalenesulphonates and naphthoates, as shown in Fig. 3.

Although we have not extensively explored the use of different polymer cations for ion-exchange EKC, PDDAC and polybrene have very similar selectivities in ion-pair formation. However, diethylaminoethyldextran showed significantly different selectivities, as shown elsewhere[11]. The relationship between selectivity in ion-pair formation and the structure of the polymer ion remains to be extensively studied.

A very different dependence of the differential velocity, $v_s - v_{ba}$, for o-hydroxybenzoic acid shown in Fig. 3 is probably due to the effect of intramolecular hydrogen bonding[12]. The high electrophoretic velocity of this compound in the absence of the polymer ion probably means that it is less hydrated than the other benzoic acids, owing to the intramolecular hydrogen bond. The polymer cation will interfere with the intramolecular hydrogen bonding by forming an ion pair, and at about 0.3% PDDAC the intramolecular hydrogen bond seems to be completely broken.

CONCLUSION

Ion-exchange EKC, which is easily performed by adding a polymer ion having charges opposite to the analyte ions to the separation solution, has been shown to be very effective for the separation of analyte ions that cannot be resolved by HPCE alone, because of identical electrophoretic mobilities. The effect of the polymer ion on the migration velocity has been investigated. In particular, the dependence of the differential velocity between two solutes having identical electrophoretic velocities on the concentration of polymer ions has been theoretically treated on the basis of the ion-pair formation equilibrium. It has been predicted that the concentration of the polymer ion producing the maximum difference in velocity is equal to K_{ip}^{-1}, provided that the ion-pair formation constants of the analyte ions are very close. However, it is difficult at present to obtain the precise values of K_{ip}.

REFERENCES

1 S. Terabe, *Trends Anal. Chem.*, 8 (1989) 129.
2 S. Terabe, K. Otsuka, K. Ichikawa, A. Tsuchiya and T. Ando, *Anal. Chem.*, 56 (1984) 111.
3 S. Terabe, K. Otsuka and T. Ando, *Anal. Chem.*, 57 (1985) 834.
4 M. J. Gordon, X. Huang, S. L. Pentoney, Jr. and R. N. Zare, *Science*, 242 (1988) 224.
5 R. A. Wallingford and A. G. Ewing, *Adv. Chromatogr.*, 30 (1989) 1.
6 S. Terabe, K. Otsuka and T. Ando, *Anal. Chem.*, 61 (1989) 251.
7 D. E. Burton, M. J. Sepaniak and M. P. Mascarinec, *J. Chromatogr. Sci.*, 24 (1986) 211.
8 S. Terabe, H. Ozaki, K. Otsuka and T. Ando, *J. Chromatogr.*, 332 (1985) 211.
9 A. Guttman, A. Paulus, A. S. Cohen, N. Grinberg and B. L. Karger, *J. Chromatogr.*, 448 (1988) 41.
10 S. Terabe, T. Yashima, N. Tanaka and M. Araki, *Anal. Chem.*, 60 (1988) 1673.
11 S. Terabe and T. Isemura, *Anal. Chem.*, 62 (1990) 650.
12 S. Fujiwara and S. Honda, *Anal. Chem.*, 59 (1987) 487.

Author Index

PUBLICATION SCHEDULE FOR 1990

Journal of Chromatography and Journal of Chromatography, Biomedical Applications

MONTH	J	F	M	A	M	J	J	A	S	O	N	Dᵃ
Journal of Chromatography	498/1 498/2 499	500 502/1	502/2 503/1 503/2 504/1	504/2 505/1	505/2 506 507 508/1	508/2 509/1 509/2 510	511 512 513	514/1 514/2 515	516/1 516/2 517 518/1	518/2 519/1	519/2 520 521/1 521/2	
Cumulative Indexes, Vols. 451–500		501										
Bibliography Section		524/1		524/2		524/3		524/4		524/5		
Biomedical Applications	525/1	525/2	526/1	526/2 527/1	527/2	528/1 528/2	529/1	529/2 530/1	530/2	531 532/1	532/2 533	

ᵃ The publication schedule for further issues will be published later.

INFORMATION FOR AUTHORS

(Detailed *Instructions to Authors* were published in Vol. 513, pp. 413–416. A free reprint can be obtained by application to the publisher, Elsevier Science Publishers B.V., P.O. Box 330, 1000 AH Amsterdam, The Netherlands.)

Types of Contributions. The following types of papers are published in the *Journal of Chromatography* and the section on *Biomedical Applications:* Regular research papers (Full-length papers), Notes, Review articles and Letters to the Editor. Notes are usually descriptions of short investigations and reflect the same quality of research as Full-length papers, but should preferably not exceed six printed pages. Letters to the Editor can comment on (parts of) previously published articles, or they can report minor technical improvements of previously published procedures; they should preferably not exceed two printed pages. For review articles, see inside front cover under Submission of Papers.

Submission. Every paper must be accompanied by a letter from the senior author, stating that he is submitting the paper for publication in the *Journal of Chromatography*. Please do not send a letter signed by the director of the institute or the professor unless he is one of the authors.

Manuscripts. Manuscripts should be typed in double spacing on consecutively numbered pages of uniform size. The manuscript should be preceded by a sheet of manuscript paper carrying the title of the paper and the name and full postal address of the person to whom the proofs are to be sent. As a rule, papers should be divided into sections, headed by a caption (*e.g.*, Abstract, Introduction, Experimental, Results, Discussion, etc.). All illustrations, photographs, tables, etc., should be on separate sheets.

Introduction. Every paper must have a concise introduction mentioning what has been done before on the topic described, and stating clearly what is new in the paper now submitted.

Abstract. Full-length papers and Review articles should have an abstract of 50–100 words which clearly and briefly indicates what is new, different and significant. (Notes and Letters to the Editor are published without an abstract.)

Illustrations. The figures should be submitted in a form suitable for reproduction, drawn in Indian ink on drawing or tracing paper. Each illustration should have a legend, all the *legends* being typed (with double spacing) together on a *separate sheet*. If structures are given in the text, the original drawings should be supplied. Coloured illustrations are reproduced at the author's expense, the cost being determined by the number of pages and by the number of colours needed. The written permission of the author and publisher must be obtained for the use of any figure already published. Its source must be indicated in the legend.

References. References should be numbered in the order in which they are cited in the text, and listed in numerical sequence on a separate sheet at the end of the article. Please check a recent issue for the layout of the reference list. Abbreviations for the titles of journals should follow the system used by *Chemical Abstracts*: Articles not yet published should be given as "in press" (journal should be specified), "submitted for publication" (journal should be specified), "in preparation" or "personal communication".

Dispatch. Before sending the manuscript to the Editor please check that the envelope contains four copies of the paper complete with references, legends and figures. One of the sets of figures must be the originals suitable for direct reproduction. Please also ensure that permission to publish has been obtained from your institute.

Proofs. One set of proofs will be sent to the author to be carefully checked for printer's errors. Corrections must be restricted to instances in which the proof is at variance with the manuscript. "Extra corrections" will be inserted at the author's expense.
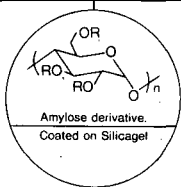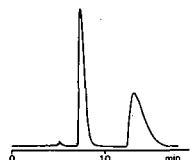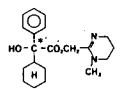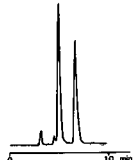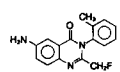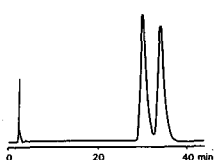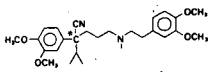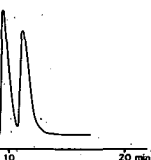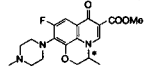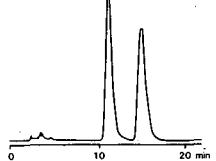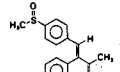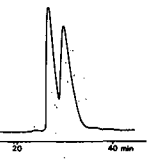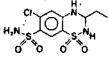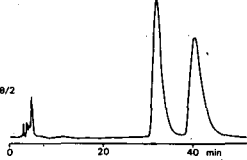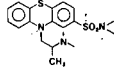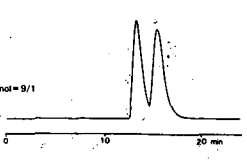
Reprints. Fifty reprints of Full-length papers, Notes and Letters to the Editor will be supplied free of charge. Additional reprints can be ordered by the authors. An order form containing price quotations will be sent to the authors together with the proofs of their article.

Advertisements. Advertisement rates are available from the publisher on request. The Editors of the journal accept no responsibility for the contents of the advertisements.

For Superior Chiral Separation

The finest from DAICEL······

Why look beyond DAICEL? We have developed the finest CHIRALCEL, CHIRALPAK and CROWNPAK with up to 17 types of HPLC columns, all providing superior resolution of racemic compounds.

NEW CHIRALPAK AS	NEW CHIRALPAK AD
•CHIRALPAK AS R: —C—N—C—⬡ 　O H H 　CH₃ * : S体 for β-Lactam antibiotics	•CHIRALPAK AD R: —C—N—⬡—CH₃ 　O H　CH₃

Amylose derivative. Coated on Silicagel

4-Acetoxy-2-azetidine

Eluent : Hexane/Ethanol = 8/2
Flow rate : 1.0mℓ/min
Temperature: r.t.
Detection : UV254nm

Oxyphencyclimine

Eluent : Hexane/2-Propanol = 9/1
Flow rate : 1.0mℓ/min
Temperature: r.t.
Detection : UV254nm

Afloqualone

Eluent : Hexane/EtOH = 95/5
Flow rate : 1.3mℓ/min
Temperature: 50°C
Detection : UV254nm

Verapamil

Eluent : Hexane/2-Propanol = 9/1
Flow rate : 1.0mℓ/min
Temperature: r.t.
Detection : UV254nm

Ofloxacine methyl ester

Eluent : Hexane/EtOH = 8/2
Flow rate : 1.2mℓ/min
Temperature: 40°C
Detection : UV254nm

Sulindac methyl ester

Eluent : Hexane/2-Propanol = 9/1
Flow rate : 1.0mℓ/min
Temperature: r.t.
Detection : UV254nm

Ethiazide

Eluent : Hexane/Ethanol = 8/2
Flow rate : 1.0mℓ/min
Temperature: 40°C
Detection : UV254nm

Dimethotiazine

Eluent : Hexane/2-Propanol = 9/1
Flow rate : 1.0mℓ/min
Temperature: r.t.
Detection : UV254nm

■Separation Service
- A pure enantiomer separation in the amount of 100g~10kg is now available.
- Please contact us for additional information regarding the manner of use and application of our chiral columns and how to procure our separation service.

⧑ DAICEL CHEMICAL INDUSTRIES, LTD.

8-1, Kasumigaseki 3-chome, Chiyoda-ku, Tokyo 100, Japan Phone: 03 (507) 3151 FAX: 03 (507) 3193